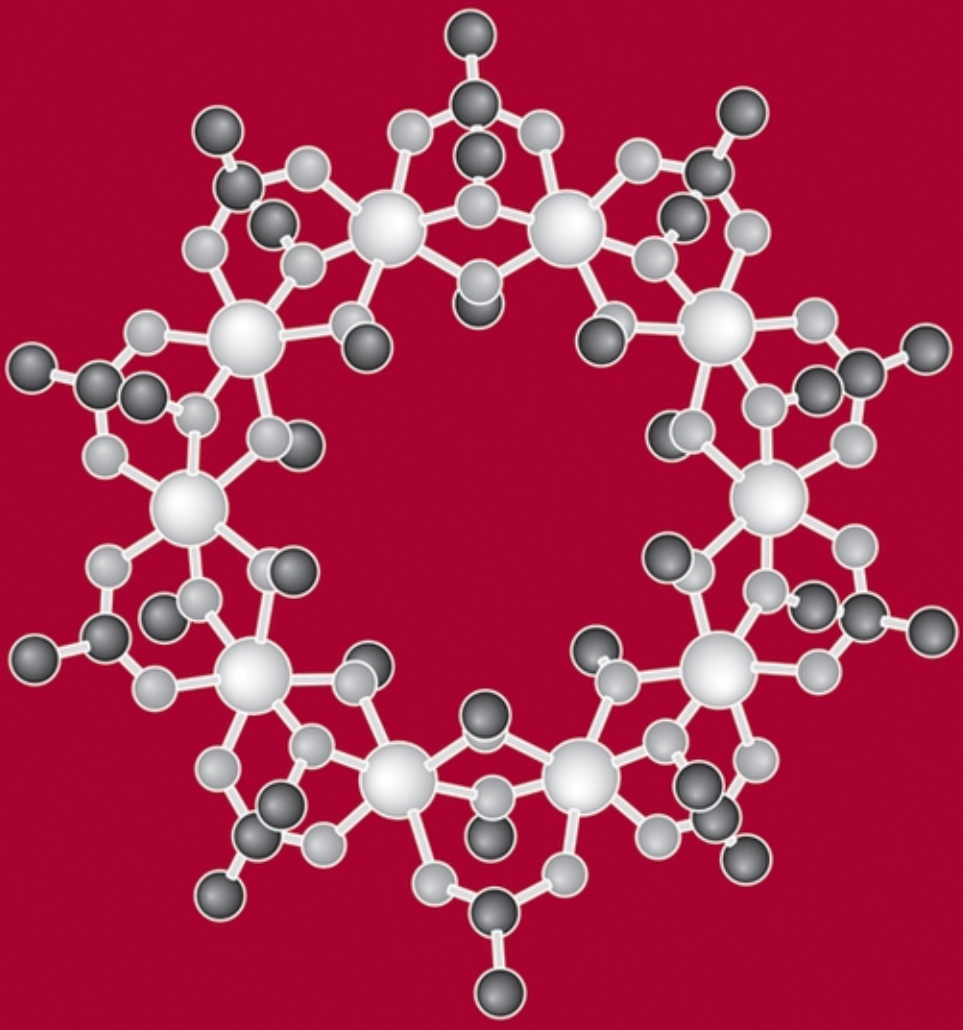

Edited by

KENNETH D. KARLIN

PROGRESS IN INORGANIC CHEMISTRY

VOLUME 53

PROGRESS IN INORGANIC CHEMISTRY

Edited by

KENNETH D. KARLIN

DEPARTMENT OF CHEMISTRY
JOHNS HOPKINS UNIVERSITY
BALTIMORE, MARYLAND

VOLUME 53

AN INTERSCIENCE PUBLICATION
JOHN WILEY & SONS, INC.

Progress in Inorganic Chemistry

Volume 53

Advisory Board

PROGRESS IN INORGANIC CHEMISTRY

Edited by

KENNETH D. KARLIN

DEPARTMENT OF CHEMISTRY
JOHNS HOPKINS UNIVERSITY
BALTIMORE, MARYLAND

VOLUME 53

AN INTERSCIENCE PUBLICATION
JOHN WILEY & SONS, INC.

Cover Illustration or "a molecular ferric wheel" was adapted from Taft. K. L. and Lippard. S. J., *J. Am. Chem. Soc.*, **1990**. 112, 9629.

Published by John Wiley & Sons, Inc., Hoboken, New Jersey.
Published simultaneously in Canada.

Library of Congress Catalog Card Number 59-13035
ISBN 0-471-46370-1

Printed in the United States of America

10 9 8 7 6 5 4 3 2 1

Contents

Progress in Inorganic Chemistry

Volume 53

CHAPTER 1

Main Group Dithiocarbamate Complexes

PETER J. HEARD

School of Biological and Chemical Sciences
Birkbeck University of London
London UK, WC1E 7HX

CONTENTS

Progress in Inorganic Chemistry, Vol. 53 Edited by Kenneth D. Karlin

I. INTRODUCTION

Main group dithiocarbamate complexes find wide-ranging applications in materials and separation science, and have potential use as chemotherapeutics, pesticides, and fungicides. The literature on main group dithiocarbamates as a whole has not been reviewed extensively since the 1970s (1, 2) despite the large number of publications that have appeared subsequently. From an inorganic chemistry stand point, dithiocarbamates are highly versatile ligands toward main group metals. They can stabilize a variety of oxidation states and coordination geometries, and seemingly small modifications to the ligand can lead to significant changes in the structure–behavior of the complexes formed. This chapter focuses primarily on structural aspect of main group dithiocarbamate complexes, covering the essential literature from 1978 to 2003. For the purposes of this chapter, the zinc triad of elements is not considered as being main group: Zinc dithiocarbamate complexes are covered in chapter 2 of this volume on transition metal dithiocarbamates by Hogarth.

The structural parameters of the dithiocarbamate ligands themselves are not modified significantly on coordination to main group elements. Distances (Å) and angles (°) are in the range: C–N(R_2) = 1.24–1.52 (1.33 mean);

C—S = 1.52–1.82 (1.72 mean); SCS = 110.1–128.9 (118.6 mean). The two C—S distances are often slightly different, indicating some charge localization: as one would expect, the shorter C—S are generally associated with the S atom that is least strongly associated with the metal center. The SCS bond angle generally increases in line with the size of the metal to which the dithiocarbamate is coordinated.

Extensive use has also been made of infrared (IR) spectroscopy for the characterization of dithiocarbamate complexes. Particular diagnostic use has been made of the C—N(R_2) and C=S stretching modes, which fall typically in the range 1500 ± 50 and $980 \pm 50\,cm^{-1}$, respectively. The occurrence of more than one C=S stretching band has been used to imply a monodentate or highly anisobidentate bonding mode for the dithiocarbamate ligand; however, this is not unambiguous and should not be relied upon.

II. *s*-BLOCK METALS

The dithiocarbamates of the *s*-block elements, prepared by reaction of the appropriate amine and CS_2 in the presence of the metal cation, are water soluble, ionic compounds. The structures of a number of hydrated compounds have been determined by X-ray crystallography (3–26). Although there are some exceptions (see below), data show that, except for the heavier metal ions, there is generally little or no direct interaction between metal ion and the essentially planar dithiocarbamate anion in the solid state. Structural data show that the C—S bond distances of the free dithiocarbamate moieties lie in the range 1.65–1.81 Å; one C—S bond is often significantly shorter than the other, indicating some localization of the negative charge. The C—N distances and SCS angles lie in the range 1.32–1.43 Å and 117.0–128.9°, respectively. The SCS bond angle generally decreases with increasing steric bulk of the N substituents, as a result of intermolecular S···H—C interactions.

Under anhydrous conditions, dithiocarbamates can coordinate to lighter *s*-block metal ions. Insertion of CS_2 into the Be—N bonds of bis(diisopropylamino)beryllium yields the corresponding bis(diisopropyldithiocarbamate)beryllium compound (27). The four S atoms of the two dithiocarbamate ligands coordinate to Be, giving a distorted tetrahedral geometry at the metal ion. The ^{9}Be nuclear magnetic resonance (NMR) spectrum of [Be(S_2CN*i*-Pr_2)$_2$] in cyclohexane displays a single resonance at δ 1.55, typical of four-coordinate Be, indicating that the solid-state structure is retained in solution. Similarly, lithiation of diphenylamine followed by reaction with CS_2 in tetrahydrofuran (THF) gives $Ph_2NCS_2Li \cdot 2THF$, in which the diphenyldithiocarbamate anion chelates the Li^+ ion (Fig. 1) (28a).

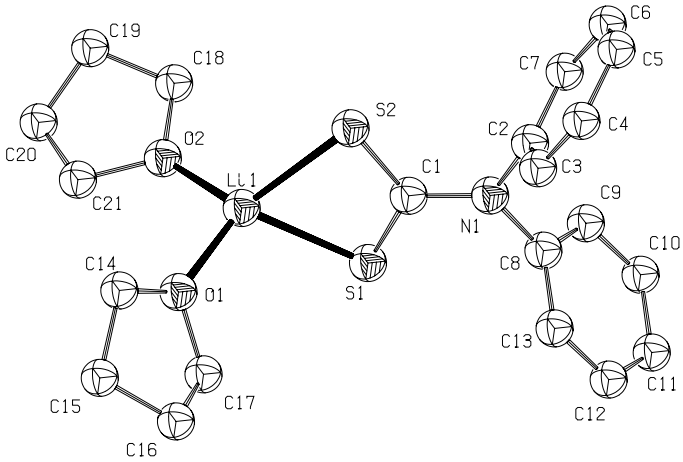

Figure 1. The ORTEP plot of $[Li(S_2CNPh_2)(THF)_2]$. *Note*: ORTEP and PLUTON plots were drawn using the PLATON software, with arbitrary displacement parameters. In all cases hydrogen atoms have been omitted for clarity. (See Refs. 28b and 28c.)

III. GROUP 13 (III A)

A. Boron and Aluminum

Main group dithiocarbamate complexes are generally prepared by reaction of the appropriate metal halide with the parent (hydrated) group 1 (I A) metal or ammonium dithiocarbamate salt. Few dithiocarbamate complexes of boron and aluminum have therefore been reported: aluminum and boron halides are susceptible to hydrolysis, and hydroxide substitution is generally unfavorable.

Aminoboranes react readily with CS_2 to form the dithiocarbamate complexes $[BR(S_2CNR'_2)_2]$ or $[BR(NR_2)(S_2CNR'_2)]$, where R is an organic substituent (29), while the corresponding reactions with diboranes give complexes of the types $[B_2R_2(S_2CNR'_2)_2]$ and $[B_2(S_2CNR_2)_4]$ (30). No detailed structural studies appear to have been carried out on these complexes, but ^{11}B NMR spectra of the diboron complexes each display two signals, indicating that they exist as a mixture of two coordination isomers in solution (30). Reaction of boron trichloride with sodium dimethyldithiocarbamate gives either $[BCl_2(S_2CNMe_2)]$ or $[B(S_2CNMe_2)_3]_2$, depending on the reaction conditions (31). The product of the reaction of $BRCl_2$ with sodium dimethyldithiocarbamate depends on the nature of the R group: if R = butyl or phenyl, the dithiocarbamate complexes $[BRCl(S_2CNR_2)]$ result, but when R = methyl, CS_2 elimination occurs, yielding

the corresponding aminoborane (31). Elimination of CS_2 also occurs on addition of sodium dimethyldithiocarbamate to the dialkyl compounds, BR_2Cl (31).

In the cluster compound [μ-2,7-(S_2CNEt_2)-7-(PMe_2Ph)-*nido*-7-$PtB_{10}H_{11}$], the dithiocarbamate ligand bridges the Pt—B bond, forming an exopolyhedral five-membered PtSCSB ring (32). The B—S bond length (1.90 Å) is comparable to other B—S bonds in boron cluster compounds and indicates a bond order between one and two.

Only five aluminum dithiocarbamate complexes have so far been reported, namely, [$Al(S_2CNR_2)_3$] [R = methyl (Me), ethyl (Et), isopropyl (*i*-Pr), or benzyl (Bz)] (33–35) and [$AlCl(S_2CNEt_2)_2$] (33). The homoleptic tris(dithiocarbamate) complexes are mononuclear, with the hexacoordinated aluminum atom displaying a distorted octahedral geometry, in both the solid state and in solution. The dithiocarbamate ligands are bound in an essentially isobidentate fashion. The unusually long Al—S bond lengths (2.38–2.40 Å), similar to the analogous Ga—S distances, have been attributed to the relative ''hardness'' of Al compared to S. The complex [$AlCl(S_2CNEt_2)_2$] has not been characterized crystallographically, but solution molecular mass measurements and ^{27}Al NMR data indicate the Al atom is hexacoordinate, suggesting a dimeric structure in which the Al atoms are presumed to be chloride bridged (33).

Dithiocarbamates have been shown to inhibit the corrosion of Al in aqueous sodium chloride solution (36), probably via the formation of a dithiocarbamate species at the surface of the metal, and have also been used as complexing agents for the extraction and quantitative determination of Al (37).

B. Gallium, Indium, and Thallium

1. Homoleptic and Mixed Bidentate Ligand Complexes

A large number of monomeric tris(dithiocarbamate) complexes (Table I) is known for the heavier group 13 (III A) elements, Ga(III) (34, 38–44), In(III) (35, 38, 40–43, 45–49), and Tl(III) (50–54), in which the MS_6 core possesses approximate D_3 symmetry rather than O_h symmetry because of the small bite angle of the dithiocarbamate ligands (55). The dithiocarbamate ligands are bound in a quasiisobidentate fashion, with only small, but in some cases chemically significant, differences in the M—S bond lengths. These differences tend to be greater in the Ga complexes than in either the In or Tl complexes.

The ambient temperature solution NMR spectra of the tris(dithiocarbamate) complexes, including those of Al (see above), show the complexes to be fluxional on the NMR chemical shift time scale. The stereodynamics can be quite complex with several different processes possible, namely, (1) a metal-centered rearrangement of the ligand polyhedron, (2) reversible ligand dissociation, (3) restricted rotation about the single N—C bonds of (bulky) N substituents,

TABLE I
Group 13 (III A) Homoleptic Dithiocarbamate Complexes

Complex	M–S (Å)	References
$[B(S_2CNMe_2)_3]$		31
$[B_2(S_2CNMe_2)_4]$		30
$[Al(S_2CNMe_2)_3]$		33
$[Al(S_2CNEt_2)_3]$		34
$[Al(S_2CN\textit{i}\text{-}Pr_2)_3]$		35
$[Al(S_2CNBz_2)_3]$		34
$[Ga(S_2CNH_2)_3]$		38
$[Ga(S_2CNMe_2)_3]$		34, 38, 39, 42
$[Ga(S_2CNEt_2)_3]$	2.40–2.46	34, 38, 40
$[Ga(S_2CN\textit{n}\text{-}Pr_2)_3]$		38
$[Ga(S_2CN\textit{i}\text{-}Pr_2)_3]$		42
$[Ga(S_2CN\textit{n}\text{-}Bu_2)_3]$		38
$[Ga\{S_2CN(Et)Ph\}_3]$		38
$[Ga\{S_2CN(Me)Ph\}_3]$		41
$[Ga(S_2CNBz_2)_3]$		34, 41
$[Ga\{S_2CN(CH_2)_4\}_3]$	2.41–2.47	42
$[Ga\{S_2CN(CH_2)_5\}_3]$		38
$[Ga\{S_2CN(CH_2)_4NMe\}_3]$		43
$[Ga\{S_2CN(CH_2CH_2)_2O\}_3]$	2.42–2.45	43
$[Ga\{S_2CN(Me)Hex\}_3]$		44
$[In(S_2CNH_2)_3]$		38
$[In(S_2CNHMe)_3]$		38
$[In(S_2CNMe_2)_3]$	2.58–2.61	47
$[In(S_2CNEt_2)_3]$	2.58–2.61	38, 40
$[In\{S_2CN(Me)\textit{n}\text{-}Bu\}_3]$		48
$[In(S_2CN(Me)Hex\}_3]$		48
$[In(S_2CN\textit{i}\text{-}Pr_2)_3]$	2.58–2.62	35, 46
$[In\{S_2CN(CH_2)_4\}_3]$	2.58–2.61	46
$[In(S_2CNMePh_2)_3]$		41
$[In(S_2CNBz_2)_3]$		41
$[In\{S_2CN(CH_2)_5\}_3]$	2.58–2.59	45
$[In\{S_2CN(CH_2CH_2)_2O\}_3]$	2.58–2.62	43
$[In\{S_2CN(CH_2CH_2)_2NMe\}_3]$	2.57–2.58	43, 49
$[Tl(S_2CNMe_2)_3]$	2.61–2.68	51, 52, 54[a]
$[Tl(S_2CNEt_2)_3]$	2.67	51, 54[a]
$[Tl(S_2CN\textit{n}\text{-}Pr_2)_3]$		54[a]
$[Tl(S_2CNBu_2)_3]$		54[a]
$[Tl(S_2CNBz_2)_3]$		54[a]
$[Tl\{S_2CN(CH_2)_5\}_3]$		54[a]
$[Tl(S_2CNMe_2)]$	2.99–3.44	56, 57, 60, 64, 65
$[Tl(S_2CNEt_2)]$	3.07–3.62	53, 56, 57, 62, 64, 65
$[Tl(S_2CN\textit{n}\text{-}Pr_2)]$	2.88–4.37	56, 57, 58, 64, 65
$[Tl(S_2CN\textit{i}\text{-}Pr_2)]$	2.98–3.04	57, 59
$[Tl(S_2CN\textit{n}\text{-}Bu_2)]$	2.97–3.16	56, 57, 63, 64, 65
$[Tl(S_2CN\textit{i}\text{-}Bu_2)]$	2.97–3.47	61
$[Tl\{S_2CN(\textit{i}\text{-}C_5H_{11})_2\}]$		57
$[Tl\{S_2CN(Me)Ph\}]$		65

TABLE I (*Continued*)

Complex	M—S (Å)	References
$[Tl(S_2CNBz_2)]$		65
$[Tl\{S_2CN(CH_2)_5\}]$		64
$[Tl\{S_2CN(CH_2)_4O\}]$		65

[a] Reference 54 also reports mixed dithiocarbamate complexes of the type $[Tl(S_2CNR_2)_2(S_2CNR'_2)]$.

or (4) restricted rotation about the $(S_2)C—N$ partial double bond (34, 35, 41, 46, 52). It is not always easy to distinguish between these processes and it is possible that two or more can occur simultaneously. The energy barriers observed (<60 kJ mol^{-1}) are rather low for rotation about the $(S_2)C—N$ partial double bond and Fay and co-worker (35) demonstrated unambiguously that restricted rotation occurs about the N—C(*i*-Pr) single bonds rather than about the $(S_2)C—N$ bond in the $[M(S_2CNi\text{-}Pr_2)_3]$ complexes (M = Al or In) at and below ambient temperatures: Contributions to the measured rate constants from $(S_2)C—N$ bond rotation process are negligible. Synthetic studies of some Tl^{III} complexes (54) indicate that the dithiocarbamate ligands are labile: mixed-ligand complexes, $[Tl(S_2CNR_2)_2(S_2CNR'_2)]$, are rapidly formed on mixing simple, "symmetric" dithiocarbamate complexes. Rates of formation of the mixed-ligand complexes are greater in polar solvents, indicating the formation of a $[Tl(S_2CNR_2)_2]^+$ intermediate, consistent with a ligand dissociation pathway and lending support for a dynamic ligand dissociation–recombination process, at least in the case of Tl(III).

Unlike the lighter members of the group, which only form M(III) dithiocarbamate complexes, a number of homoleptic thallium(I) dithiocarbamates has been reported (56–65). In the solid state, $[Tl_2(S_2CNR_2)_2]$ dimers are linked by intermolecular Tl—S coordination to form polymeric structures (56–63). Although the basic dimeric structure is similar in each case (see below), the way in which they are linked differs, depending on the nature of the N-substituents: The balance between the coordination requirements of Tl and the packing forces determines the precise crystal structure. The dimeric units have a distorted octahedral structure, shown in Fig. 2, with the two Tl atoms axial and the four S atoms, which form an almost planar parallelogram, equatorial. Tl···Tl distances vary between 3.47 and 4.00 Å. When the interdimer Tl···S coordination is considered, the Tl atoms may be five-, six-, or even seven-coordinate, leading to the formation of either extended chains or layers.

The basic dimeric structure of the Tl(I) dithiocarbamates (see Fig. 2) appears to be retained in solution (56, 57); consequently they have lower motilities than their monomeric Tl(III) analogues, enabling mixtures of to be readily separated (65). Dithiocarbamate ligands have thus been used for the separation and extraction of (toxic) Tl(I) from Tl(III), as well as other metal ions (64–70).

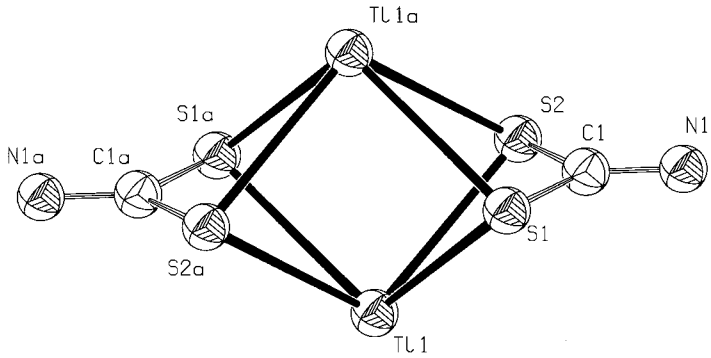

Figure 2. The ORTEP plot of the dimeric unit in the Tl(I) complexes $[Tl_2(S_2CNR_2)_2)]$. The N substituents are omitted for clarity.

The complexes

$[Ga\{S_2CN(CH_2)_4O\}\{S_2P(OR)_2\}_2]$ (R = Et or *i*-Pr)
$[Ga\{S_2CN(CH_2)_4O\}\{SCH_2CH_2)_2O\}]$ and $[Ga\{S_2CN(CH_2)_4NMe\}\{(SCH_2CH_2)_2O\}]$

prepared by adding stoichiometric quantities of the appropriate ligands to $GaCl_3$, appear to be the only complexes in which two different types of bidentate ligand (including a dithiocarbamate) are coordinated to the group 13 (III A) metal center (43).

2. *Nonhomoleptic Complexes*

Complexes of the type $[MCl_2(S_2CNR_2)]$, $[MR_2(S_2CNR'_2)]$, $[MCl(S_2CNR_2)_2]$, and/or $[MR(S_2CNR'_2)_2]$ (R = alkyl, aryl, or Cp) are known for all group 13 (III A) elements (Table II). The most numerous are the diorganometal complexes (51, 71–77), which have found use as single source precursors for the chemical vapor deposition of M_xS_y thin films (75–77). The complexes are generally monomeric in both the solid state and in solution. X-ray crystallographic studies of $[InR_2(S_2CNEt_2)]$ [R = Me (75), Et (75), or *t*-Bu (77)], $[In$*t*$-Bu_2(S_2CNMe_2)]$ (77), and $[TlPh_2(S_2CNEt_2)]$ [Fig. 3(*a*)] (72) show that the metal ions possess a highly distorted tetrahedral geometry. With the exception of $[InMe_2(S_2CNEt_2)]$ and $[In$*t*$-Bu_2(S_2CNMe_2)]$, which show a small but chemically significant difference in the two M—S distances, the dithiocarbamate ligands are bound in an essentially isobidentate fashion. In contrast, the molecular units in $[TlMe_2(S_2CN$*n*$-Pr_2)]$ (74) are linked by two intermolecular Tl···S interactions, giving a well-ordered spiral arrangement, while in

TABLE II
Group 13 (III A) Akyl- and Chlorodithiocarbamate Complexes

Complexes	M–S (Å)	References
$[BMe(S_2CNMe_2)_2]$		31
$[BPh(S_2CNMe_2)_2]$		31
$[B$*n*$\text{-}BuCl(S_2CNMe_2)]$		31
$[BPhCl(S_2CNMe_2)]$		31
$[BCl_2(S_2CNMe_2)]$		31
$[AlCl(S_2CNEt_2)_2]$		33
$[GaMe_2(S_2CNEt_2)]$		75
$[GaEt_2(S_2CNEt_2)]$		75
$[Ga\ t\text{-}Bu_2(S_2CNMe_2)]$		77
$[Ga\ t\text{-}Bu_2(S_2CNEt_2)]$	2.38, 2.43	77
$[Ga\ t\text{-}Bu_2(S_2CN$*n*$\text{-}Pr_2)]$		77
$[Ga(C_5H_{11})_2(S_2CNEt_2)]$		75
$[GaMe_2\{S_2CNMe(CH_2)_3NMe_2\}]$		76
$[GaEt_2\{S_2CNMe(CH_2)_3NMe_2\}]$		76
$[Ga(CH_2CHMe_2)_2\{S_2CNMe(CH_2)_3NMe_2\}]$		76
$[Ga(C_5H_{11})_2\{S_2CNMe(CH_2)_3NMe_2\}]$		76
$[GaCl_2\{S_2CN(CH_2CH_2)_2O\}]$		43
$[GaCl_2(4\text{-}MePy)_2(S_2CNMe_2)]$	2.45, 2.49	80
$[GaCl_2(4\text{-}MePy)_2(S_2CNEt_2)]$	2.48, 2.48	81
$[Ga$*t*$\text{-}Bu(S_2CNMe_2)_2]$		77
$[Ga$*t*$\text{-}Bu(S_2CNEt_2)_2]$		77
$[Ga$*t*$\text{-}Bu(S_2CN$*n*$\text{-}Pr_2)_2]$	2.31–2.60	77, 78
$[Ga(O$*i*$\text{-}Pr)(S_2CN$*n*$\text{-}Pr_2)_2]$	2.31–2.57	78
$[GaCl(S_2CNMe_2)_2]$	2.21–2.43	42
$[GaCl(S_2CN$*i*$\text{-}Pr_2)_2]$		42
$[GaCl\{S_2CN(CH_2)_5\}_2]$		42
$[GaCl\{S_2CN(CH_2CH_2)_2O\}_2]$		43
$[InMe_2(S_2CNMe_2)]$		71
$[InMe_2(S_2CNEt_2)]$		75
$[InEt_2(S_2CNEt_2)]$	2.56, 2.68	75
$[In(C_5H_{11})_2(S_2CNEt_2)]$		75
$[InMe_2\{S_2CNMe(CH_2)_3NMe_2\}]$		75
$[InEt_2\{S_2CNMe(CH_2)_3NMe_2\}]$	2.59, 2.79	75
$[In(CH_2CHMe_2)_2\{S_2CNMe(CH_2)_3NMe_2\}]$		75
$[In(C_5H_{11})_2\{S_2CNMe(CH_2)_3NMe_2\}]$		75
$[InCl_2\{S_2CN(CH_2CH_2)_2O\}]$		43
$[InMe(S_2CNMe_2)_2]$		71
$[InEt(S_2CNMe_2)_2]$		71
$[InCl(S_2CN$*i*$\text{-}Pr_2)_2]$	2.38–2.56	42
$[GaCl\{S_2CN(CH_2CH_2)_2O\}_2]$		43
$[TlMe_2(S_2CNHEt_2)]$		74
$[TlMe_2(S_2CNH$*n*$\text{-}Pr)]$		74
$[TlMe_2(S_2CN$*n*$\text{-}Pr_2)]$	2.70, 2.80	74
$[TlMe_2(S_2CN$*n*$\text{-}Bu_2)]$		74
$TlMe_2(S_2CN$*sec*$\text{-}Bu_2)]$		74
$[TlMe_2\{S_2CNMe(CH_2)_2OH\}]$		74

TABLE II (*Continued*)

Complexes	M–S (Å)	References
$[TlMe_2(S_2CNMe_2)]$		51
$[TlMe_2(S_2CNEt_2)]$		51
$[TlMe_2(S_2CNPh_2)]$		51
$[TlPh_2(S_2CNEt_2)]$	2.72, 7.72	51, 72
$[TlCp_2\{S_2CN(Me)Cy\}]$		73
$[TlCp_2\{S_2CN(Et)Cy\}]$		73
$[TlCp_2\{S_2CN(Me)Cy\}]$		73
$[TlCp_2\{S_2CN(i\text{-}Pr)Cy\}]$		73
$[Tl(C_9H_7)\{S_2CN(Me)Cy\}]$		73
$[Tl(C_9H_7)\{S_2CN(Et)Cy\}]$		71
$[Tl(C_9H_7)\{S_2CN(i\text{-}Pr)Cy\}]$		73
$[Tl(C_{13}H_9)_2\{S_2CN(Me)Cy\}]$		71
$[Tl(C_{13}H_9)_2\{S_2CN(Et)Cy\}]$		71
$[Tl(C_{13}H_9)_2\{S_2CN(i\text{-}Pr)Cy\}]$		73
$[Tl(p\text{-tolyl})(S_2CNEt_2)_2]$	2.55–2.80	79

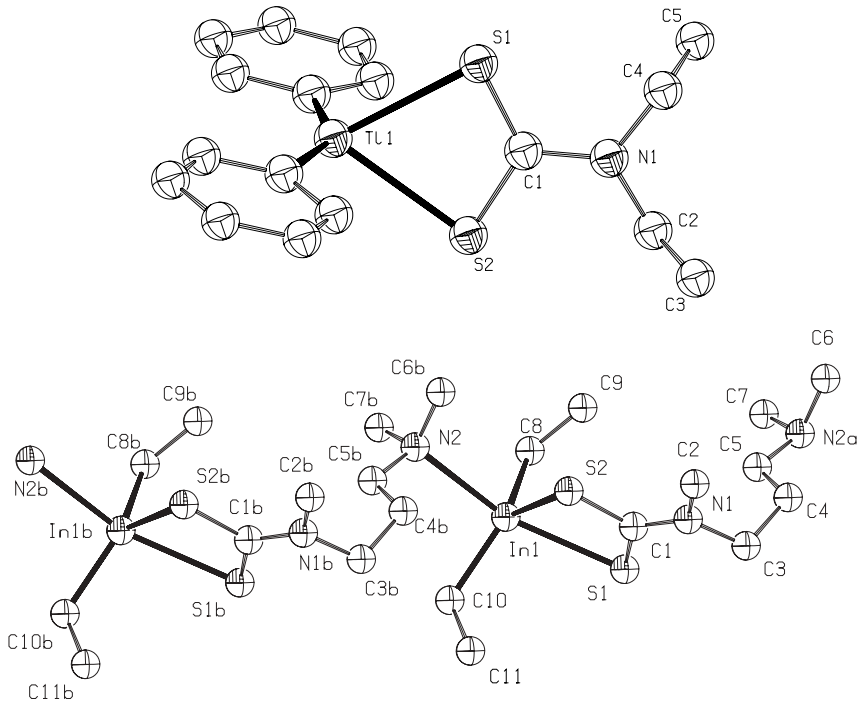

Figure 3. The ORTEP plots of (*a*) $[TlPh_2(S_2CNEt_2)]$ and (*b*) $[InEt_2\{S_2CN(Me)(CH_2)_3NMe_2\}]$, showing a section of the polymeric chain.

$[InEt_2\{S_2CNMe(CH_2)_3NMe_2\}]$ (76) the molecular units are linked by intermolecular In—N bonds (2.66 Å), forming a chain polymer [Fig. 3(*b*)].

Although less common than the dialkylmetal dithiocarbamate complexes, several monoalkyl bis(dithiocarbamate) complexes have been reported (31, 71, 77–79). The complexes $[Ga\textit{t}\text{-}Bu(S_2CNR_2)_2]$ (R = Me, Et, or *n*-Pr), were isolated as minor products during the synthesis of the dialkyl complexes $[Ga\textit{t}\text{-}Bu_2(S_2CNR_2)]$ from the reaction of $[Ga\textit{t}\text{-}Bu_2(\mu\text{-}Cl)]_2$ with sodium dithiocarbamate salts (77). Interestingly, these monoalkyl complexes are only formed during the initial synthesis: The dialkylmetal complexes cannot be converted to the corresponding monoalkyl complexes.

The X-ray molecular structures of $[Ga\textit{t}\text{-}Bu(S_2CN\textit{n}\text{-}Pr_2)_2]$ (78), $[Ga(O\textit{i}\text{-}Pr)(S_2CNEt_2)_2]$ (78) and $[Tl(\textit{p}\text{-tolyl})(S_2CNEt_2)_2]$ (79) show that the metal ions possess a distorted trigonal-bipyramidal geometry, with the alkyl or aryl group occupying an axial position. The dithiocarbamate ligands bind in an anisobidentate fashion. The precise geometry at the metal atom is determined primarily by the steric bulk of the alkyl ligand, as measured by the Tolman cone angles: cone angles $<94^\circ$ favor a square-based pyramidal structure, while cone angles $>94^\circ$ shift the geometry toward trigonal bipyramidal (78). These structures lie on the unusual two-step "Texas" pseudo-rotation pathway between true square-based pyramidal and trigonal-bipyramidal structures rather than the more usual one-step Berry pseudo-rotation pathway.

The monochloro bis(dithiocarbamate) complexes of gallium and indium, $[MCl(S_2CNR_2)_2]$ (42, 43), closely resemble the corresponding monoalkyl complexes; however, the geometry at the metal atom tends toward square pyramidal rather than trigonal bipyramidal, because of the smaller cone angle of Cl. The dichloro complexes, $[MCl_2(S_2CNR_2)]$ (M = Ga or In) (43) have not been well characterized. Solution molecular mass measurements of the corresponding boron complexes, $[BCl_2(S_2CNR_2)]$, indicate that they are monomeric (31): By analogy, the gallium and indium complexes have therefore also been assumed to be monomeric in solution. Reaction of Ga_2Cl_2 with tetramethyl- or tetraethylthiuram disulfide in 4-methylpyridine solvent yields $[GaCl_2(4\text{-}Mepy)_2(S_2CNR_2)]$ [R = Me (80) or Et (81) and py = pyridine (ligand)]. X-ray crystallography shows that the Ga atoms are in a distorted octahedral coordination environment, with chloride ligands cis each other, trans the dithiocarbamate S atoms.

IV. GROUP 14 (IV A)

The carbon compounds of dithiocarbamates, dithiocarbamic acid esters, are generally classified as organic compounds and, as such, fall outside the scope of this chapter.

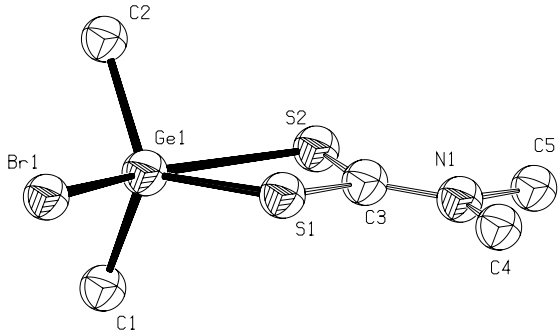

Figure 4. The ORTEP plot of $[GeMe_2Br(S_2CNMe_2)]$.

A. Silicon and Germanium

Although silicon dithiocarbamate complexes remain rare, complexes of the type $[SiR_2(S_2CNR_2)_2]$ (R = Me or Ph) have been reported recently (82). Spectroscopic data for the complexes (IR and NMR) have been interpreted in terms of a tetracoordinate silicon atom, with the two dithiocarbamate ligands monodentate.

The homoleptic germanium dithiocarbamate complex $[Ge\{S_2CN(i\text{-}Pr)Cy)\}_4]$ (cy = cyclohexyl), was reportedly prepared by the reaction of $GeCl_4$ with an excess of the sodium dithiocarbamate salt (83). However, attempts to prepare $[Ge(S_2CNMe_2)_4]$ similarly were unsuccessful (84). The diorganogallium bis(dithiocarbamate) complexes, $[GeR_2(S_2CNR_2)_2]$, have been prepared by reaction of GeR_2Cl_2 with the appropriate sodium dithiocarbamate salt (84, 85); an X-ray crystallographic study of $[GeMe_2(S_2CNMe_2)_2]$ reveals that the Ge atom lies at the center of a distorted octahedron, with the four S atoms in the equatorial plane (84). In the $[GeMe_2X(S_2CNMe_2)]$ complexes (X = Cl, Br, or I) the Ge atom is in a distorted trigonal-bipyramidal coordination environment with the dithiocarbamate ligand bound in an anisobidentate fashion (86–88). The structure of $[GeMe_2Br(S_2CNMe_2)]$ is shown in Fig. 4. Complexes of general formula $[GeR_3(S_2CNR_2)]$ (R = alkyl or phenyl) have also been prepared (84, 89, 90); solution NMR data indicate they are essentially isostructural with the $[GeMe_2X(S_2CNMe_2)]$ complexes.

B. Tin and Lead

1. Homoleptic Complexes

Homoleptic dithiocarbamate complexes are known for tin(II), tin(IV), and lead(II). The tin(II) complexes, $[Sn(S_2CNR_2)_2]$, are best prepared by reaction of

$SnCl_2$ with the sodium salt of the appropriate dithiocarbamic acid (91–93). The complexes are monomeric in the solid state (92), with the dithiocarbamate bound in an anisobidentate fashion, but molecular weight measurements suggest they may be polymeric in solution (93). In the solid state molecular structure, the geometry at Sn is best considered as highly distorted trigonal bipyramid, with the stereochemically active lone pair of electrons equatorial and the two long Sn—S bonds displaced away from the lone pair in pseudo-axial positions.

The tetrakis(dithiocarbamate)tin(IV) complexes are of interest because of the different bonding modes of the dithiocarbamate ligands, which may be monodentate, anisobidentate, or isobidentate (94, 95). The geometry at Sn depends on the binding modes adopted. In $[Sn(S_2CNMe_2)_4]$ the Sn atom is essentially six coordinate, with two of the dithiocarbamate ligands anisobidentate and two monodentate: The nonbonding Sn···S distances are 3.44 and 3.64 Å (94). In contrast, in $[Sn\{S_2CN(CH_2)_4\}_4]$ two of the ligands are essentially isobidentate and two highly anisobidentate (Sn—S = 2.42 and 3.24 Å); if the long Sn—S contacts are included, the tin is best considered as displaying a distorted dodecahedral arrangement (Fig. 5) (95). The very low frequency shift of the ^{119}Sn NMR signal in tetrakis(1-pyrrolidinedithiocarbamate)tin(IV) ($\delta = -729$, relative to $SnMe_4$) indicates that the Sn atom is at least six and possibly seven coordinate in solution. Ambient temperature solution proton NMR (^1H) and ^{13}C NMR spectra indicate that the four ligands are equivalent on the NMR chemical

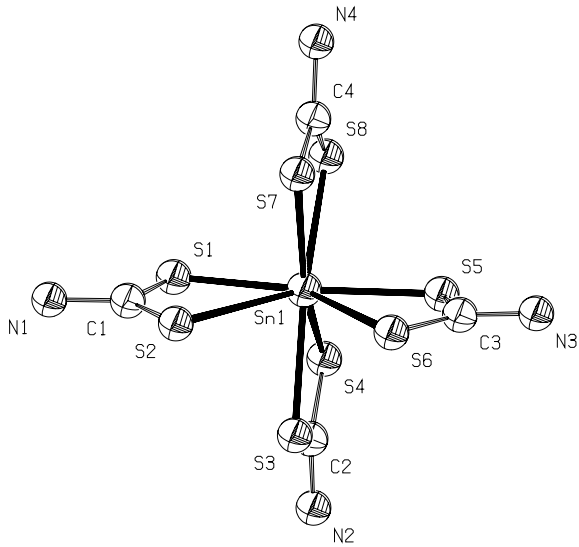

Figure 5. The ORTEP plot of $[Sn\{S_2CN(CH_2)_4\}_4]$, showing dodecahedral arrangement at tin. The N substituents omitted for clarity.

shift time scale, with an effective plane of symmetry bisecting the SCS angle. These observations are consistent with a fluxional process that involves reversible cleavage of the Sn—S bonds.

The bis(dithiocarbamate) complexes of lead(II), $[Pb(S_2CNR_2)_2]$, have been studied quite extensively, revealing a number of interesting structural variations (96–101). The basic molecular geometry at lead is that of a distorted square pyramid, with the four S atoms of the (usually) anisobidentate ligands forming the base and the stereochemically active lone pair of electrons apical, consistent with the results of quantum chemical calculations (102). However, secondary Pb···S intermolecular interactions in the solid state increase the coordination number at lead to between 5 and 8, depending on the number of interactions. The crystal structure of bis(dimethyldithiocarbamate)lead comprises $[Pb(S_2CNMe_2)_2]$ units stacked along the crystallographic *c* axis (96). Within the stack, each Pb atom has a long contact with two S atoms (Pb···S = 3.36 Å) of the unit directly above, giving a pseudo-six-coordinate metal center. The crystal structure of $[Pb\{S_2CN(Et)i\text{-}Pr\}_2]$ comprises polymeric chains of bis(dithiocarbamate)lead units, also linked by bridging S atoms; however, the bridging S atoms are from different monomer units (one above and one below) (98). A rather different situation is found in bis(pyrrolidinedithiocarbamate)lead (99), where all four S atoms form long-range interactions with a second $[Pb\{S_2CN(CH_2)_4\}_2]$ unit. The coordination environment at lead is that of a distorted square antiprism, with staggered faces. The lone-pair points through the square face formed by the four S atoms of the next monomeric unit, toward the lead atom. The Pb···Pb distance is 3.89 Å, suggesting some weak metal–metal bonding (Fig. 6). The bulky N substituents in bis(dipropyldithiocarbamate)lead give rise to a notably different, centrosymmetric tetrameric structure with pentacoordinate Pb atoms (97). The tetramer possesses a $Pb_2(S_2CNn\text{-}Pr_2)_4$ core, in which the two Pb atoms are bridged by S atoms from different

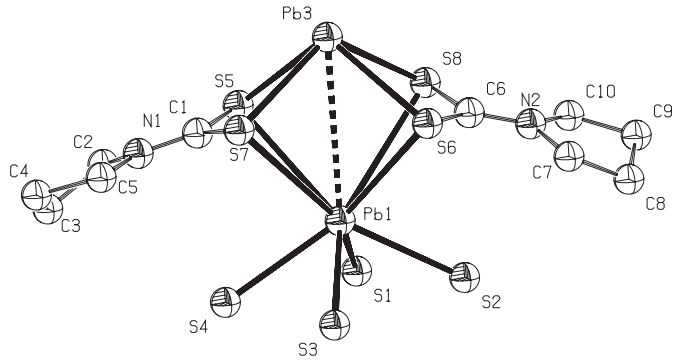

Figure 6. The ORTEP plot of $[Pb\{S_2CN(CH_2)_4\}_2]$, showing a section of the polymeric chain.

dithiocarbamate ligands. Two further [Pb(S_2CNn-Pr_2)$_2$] monomer units bind to the Pb_2S_4 core via single Pb—S bridges, completing the tetrameric structure.

The NMR and molecular mass measurements indicate that, while they retain the same basic molecular structures, the [Pb(S_2CNR_2)$_2$] complexes tend to polymerize in solution (93, 103). The NMR and electrochemical studies also show that the dithiocarbamate ligands are highly labile in solution (103, 104).

The homoleptic dithiocarbamate complexes of both Sn and Pb have been investigated recently as possible single source precursors for the deposition of metal sulfide materials (98, 105, 106) and dithiocarbamates have also been used for the extraction of lead from environmental samples (107).

2. *Nonhomoleptic Complexes*

Although nonhomoleptic complexes of Sn have been extensively studied because of their considerable structural diversity and potential applications, for example, in chemotherapy, those of lead are rare. The complex [Pb(phen)(S_2C-NEt_2)$_2$] (phen = 1,10-phenanthroline) is one of only a few examples of a nonhomoleptic lead(II) dithiocarbamate complex (108). The geometry at Pb (Fig. 7) is best considered as distorted trigonal bipyramidal, with the bridging S atoms occupying axial positions.

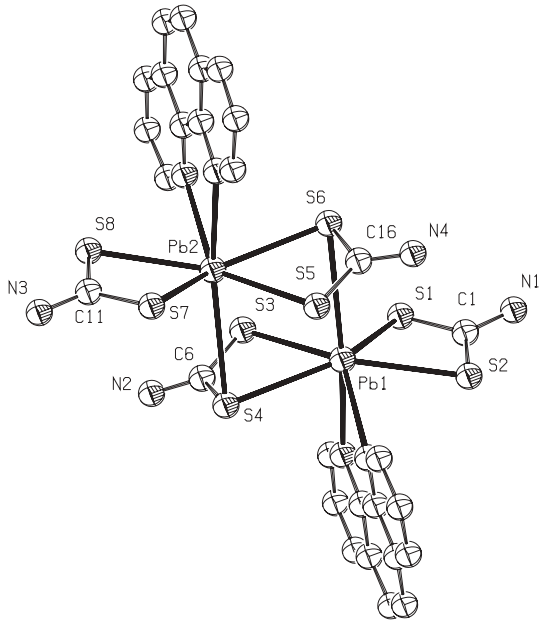

Figure 7. The ORTEP plot showing the dimeric structure of [Pb(phen)(S_2CNEt_2)]. The N substituents of the dithiocarbamates and atom labels of the phen ligands have been omitted for clarity.

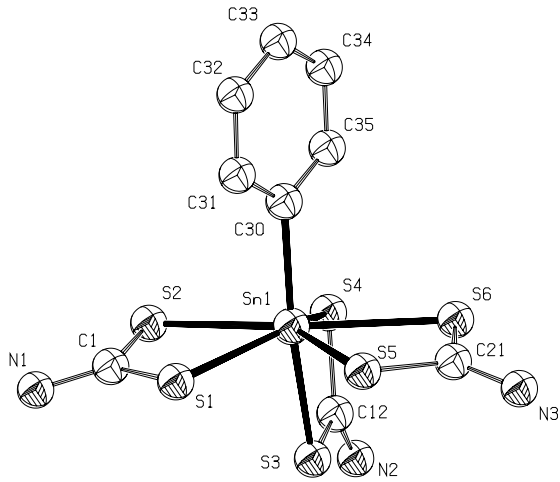

Figure 8. The ORTEP plot of [SnR(S_2CN*i*-Bu_2)$_3$] showing the distorted pentagonal bipyramidal coordination of tin in the complexes [SnR(S_2CNR_2)$_3$] and [SnX(S_2CNR_2)$_3$]. The N substituents are omitted for clarity.

The majority of tin(IV) dithiocarbamate complexes are of the general type [$SnR_{4-n-m}X_n(S_2CNR_2)_m$] (where R = alkyl or aryl; X = halide; $n = 0$, 1, 2, 3; $m = 1$, 2, or 3). In the tris(dithiocarbamate) complexes [SnR(S_2CNR_2)$_3$] and [SnX(S_2CNR_2)$_3$] (109–121), the Sn atom is in a distorted pentagonal bipyramidal coordination environment, with the unidentate ligand axial (Fig. 8). The dithiocarbamate ligand that spans the axial (ax)–equatorial (eq) positions is highly anisobidentate [Sn—S(ax) $\approx$ 2.48 Å; Sn—S(eq) $\approx$ 2.77 Å]; usually the two equatorial dithiocarbamates are also anisobidentate, but to a much lesser degree. The solution ^{119}Sn NMR chemical shift of [SnPh(S_2CNEt_2)$_3$] is strongly temperature dependent: $\delta = -813$ (ambient); $\delta = -888$ (-100°C) (115). Nuclear magnetic resonance data thus indicate a dynamic process, which involves the exchange of dithiocarbamate ligands, leading to a decrease in the effective coordination number of Sn at ambient temperature. Solid-state ^{13}C and ^{119}Sn NMR data (115, 117) are consistent with the X-ray structure (115); it is noteworthy that the ^{119}Sn SSNMR chemical shift (-894 ppm) is to slightly lower frequency of that in solution at -100°C, suggesting that the lower temperature limit of the fluxional process is only a little below -100°C.

A large number of bis(dithiocarbamate)tin(IV) complexes of general formula [$SnR_nX_{2-n}(S_2CNR_2)_2$] (R = alkyl or aryl; X = halogen or pseudo-halogen; $n = 0$, 1, or 2) have been reported (89, 95, 111–115, 117, 119, 122–167). In the majority of cases, the geometry at tin is best described as a highly distorted octahedron or skew-trapezoidal bipyramid, with asymmetrically coordinated

dithiocarbamate ligands. Although the CSnC bond angle in the [$SnR_2(S_2CNR_2)_2$] complexes is highly variable (∼100–150°), there is no obvious trend with respect to the steric bulk of the organic Sn substituents; however, if one or both of the organic groups is substituted for a halogen, the bond angle (RSnX or XSnX) decreases to ∼89–96°, suggesting that the Lewis acidity of the metal center is an important factor.

Three crystalline modifications of [$SnMe_2(S_2CNEt_2)_2$] are known (141, 163), namely, triclinic, monoclinic, and orthorhombic; except for the small variability in the CSnC bond angles the molecular structures are chemically identical in the three forms, and differ little from the other dimethyltin(IV) bis(dithiocarbamate) complexes that have been structurally characterized (95, 125, 143, 152). The *tert*-butyl complexes [Sn*t*-$Bu_2(S_2CNMe_2)_2$] (150), [(Sn*t*-$Bu_2)_2$\{μ-$S_2CN(H)(CH_2)_2N(H)CS_2$\}] (124), and [Sn*t*-$Bu_2(S_2CNEt_2)_2$] (153) show some interesting structural differences. The molecular structure of [Sn*t*-$Bu_2(S_2CNEt_2)_2$] is very similar to that of the dimethyltin(IV) bis(dithiocarbamate) complexes, but in [Sn*t*-$Bu_2(S_2CNMe_2)_2$] one of the dithiocarbamates is essentially monodentate (Sn—S (long) = 3.53 Å) and the geometry at Sn is best described as a distorted trigonal bipyramid, with the two *t*-Bu groups equatorial; in this respect, [Sn*t*-$Bu_2(S_2CNMe_2)_2$] is structurally more akin to the triorganotin(IV) dithiocarbamates. The Sn atoms in the centrosymmetric dimeric complex [(Sn*t*-$Bu_2)_2$ \{μ-$S_2CN(H)(CH_2)_2N(H)CS_2$\}$_2$] (Fig. 9) are also five coordinate: one end of the ligand is bidentate, while the other is monodentate. The chelating dithiocarbamate ligand spans ax/eq positions and is highly anisobidentate (Sn—S = 2.459 and 2.878 Å).

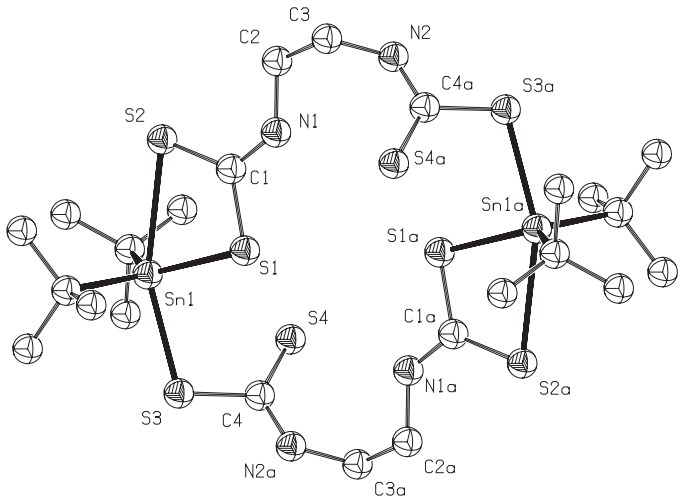

Figure 9. The ORTEP plot of [(Sn*t*-$Bu_2)_2$\{μ-$S_2CN(H)(CH_2)_2N(H)CS_2$\}].

The complex $[SnPh_2(S_2CNEt_2)_2]$ has been shown to exist in at least two polymorphs, namely, monoclinic (122, 152) and tetragonal (117). In the monoclinic form, one dithiocarbamate is anisobidentate and the other almost isobidentate, while in the tetragonal form, both are asymmetrically coordinated; the degree of asymmetry in the tetragonal polymorph is about one-half that observed for the anisobidentate dithiocarbamate in the monoclinic form [ΔSn—S = 0.10 Å (tetragonal) and 0.24 Å (monoclinic)].

The effects of the dithiocarbamate N substituents on the structures of the phenyl and vinyl complexes $[SnPh_2(S_2CNR_2)_2]$ and $[Sn(CHCH_2)_2(S_2CNR_2)_2]$ have been investigated by Tiekink and Hall (159, 160) and appear to be small as far as the tin-dithiocarbamate bonding is concerned. In contrast, the effects of the ancillary organic ligands are quite marked: The greater the electronegativity of the ligands, the more symmetrical the bonding of the dithiocarbamate. The reduction in the asymmetry is presumably due to the increased Lewis acidity of the metal center. The effect of the organic groups on the CSnC bond angle is considerable: The average CSnC angle in the phenyl complexes is 102.4°, which contrasts with 136.2° in the vinyl complexes. The reasons for the difference in the bond angle are not immediately obvious, although it is clear from crystallographic data for other bis(dithiocarbamate)tin(IV) complexes that the CSnC angle generally decreases as the electronegativity of the substituents increases.

The $[SnRCl(S_2CNR'_2)_2]$ complexes are structurally similar to the dialkyl analogues (95, 117, 126, 128–131); the Sn atom is in a highly distorted octahedral coordination environment, with the two dithiocarbamate ligands bidentate. Although the dithiocarbamate ligands are anisobidentate, the asymmetry in the bonding is reduced considerably [ΔSn—S(ave) $\approx$ 0.06 Å], compared to that observed in the dialkyl complexes, because the Lewis acidity of the metal center is increased by the presence of the more electronegative chloride ligand: The CSnX bond angle is also reduced.

Reaction of anhydrous tin(II) chloride with sodium diethyldithiocarbamate under aerobic conditions gives the tin(IV) bis(dithiocarbamate) complex, $[SnCl_2(S_2CNEt_2)_2]$ (157). The mechanism probably involves the initial formation of $[Sn(S_2CNEt_2)_2]$, followed by aerial oxidation to yield tetraethylthiuram disulfide, which then oxidatively adds to another molecule of $SnCl_2$, giving the final product, accounting for the reaction yield (50%, relative to $SnCl_2$). In a separate experiment, it was shown that tetramethylthiuram disulfide reacts directly with $SnCl_2$, yielding $[SnCl_2(S_2CNEt_2)_2]$, providing further evidence in support of the proposed mechanism. Interestingly, reaction of $[SnCl_2(S_2CNEt_2)_2]$ with 2-thiouracil in dimethyl sulfoxide (DMSO) yields the dithioester $CH_2(S_2CNEt_2)_2$ (167). The X-ray structure of $[SnCl_2(S_2CNEt_2)_2]$ reveals that the Sn atom is in a distorted octahedral coordination environment (156, 157), with the two dithiocarbamate ligands chelating in an almost symmetric fashion (ΔSn—S $\approx$ 0.06 Å). The two chloride ligands are cis

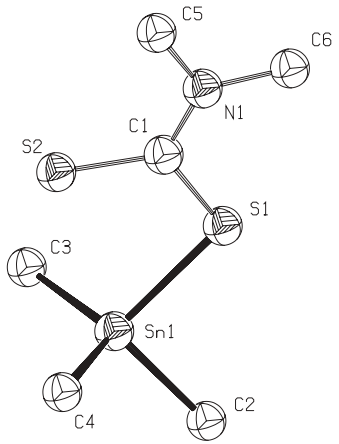

Figure 10. The ORTEP plot of $[SnMe_3(S_2CNMe_2)]$ showing the distorted tetrahedral coordination geometry of tin in the $[SnR_3(S_2CNR_2)]$ complexes.

(ClSnCl = 91.8°). The other dihalide complexes that have been characterized crystallographically are structurally analogous (133, 134, 140, 168).

The mono(dithiocarbamate) complexes $[SnR_{3-n}X_n(S_2CNR_2)]$ (R = alkyl or aryl; X = halide; $n = 0$, 1, 2, or 3) have also been studied extensively (112–114, 116, 117, 119, 131, 140, 153, 169–188). In the triorganyl complexes the dithiocarbamate ligands tend toward monodentate coordination and the geometry at tin is probably best considered as (distorted) tetrahedral rather than pentagonal bipyramidal (Fig. 10); the average Sn—S distances are 2.46 Å (short) and 3.04 Å (long). Substitution of one or more of the organic groups by Cl reduces the asymmetry [Sn—S(short) = 2.46 Å, Sn—S (long) = 2.71 Å], such that the dithiocarbamate should be considered as anisobidentate. The geometry at Sn is thus best described as a highly distorted trigonal bipyramid, with the dithiocarbamate bridging ax–eq positions; the long Sn—S bond is axial. The reduction in the asymmetry of the Sn—S bonding presumably arises because the presence of the electronegative chloride ligand increases the Lewis acidity of the metal center. Although there appears to be some correlation of the Sn dithiocarbamate bonding parameters with both the Lewis acidity of the metal center and the basicity of the dithiocarbamate N substituents in the gas phase, no such correlation is found in the solid state: Crystal packing factors are therefore thought to have a significant effect on the solid-state structures (180).

Molloy et al. (116) prepared a series of triorganotin(IV) dithiocarbamate complexes of general formula $[SnPh_2R(S_2CNR'_2)]$ {R = 2-(2-pyridyl)ethyl, R′ = Me or Et; R = 2-(4-pyridyl)ethyl, R′ = Me; R = 2-(2-oxo-*N*-pyrrolidinyl)ethyl, R′ = Me}, and Das (176) reported the analogous complexes

$[SnMe_2R(S_2CNMe_2)]$ [R = 2-(4,4-dimethyl-2-oxazolinyl)-3-thienyl or 3-(2-pyridyl)-2-thienyl] and $[Sn(p\text{-tolyl})_2R(S_2CNMe_2)]$ [R = 3-(2-pyridyl)-2-thienyl]. In the complexes of 2-(2-pyridyl)ethyl, 2-(4,4-dimethyl-2-oxazolinyl)-3-thienyl and 3-(2-pyridyl)-2-thienyl, the N donor of the organic ligand is coordinated to the metal in both the solid state and in solution. The dithiocarbamate is monodentate (the nonbonding Sn···S distance is ~3.27–3.47 Å). In contrast, the carbonyl oxygen in the 2-(2-oxo-*N*-pyrrolidinyl)ethyl complex does not interact significantly with the metal, and the dithiocarbamate is weakly bidentate.

The N donor of the pyridyl ring of the 2-(4-pyridyl)ethyl ligand, R, in $[SnPh_2R(S_2CNMe_2)]$ cannot coordinate to the metal center in an intramolecular sense: Spectroscopic data suggest that the complex is monomeric in solution and polymeric, with intermolecular coordination of N, in the solid state. The dithiocarbamate appears to be monodentate both in the solid state and in solution.

3. *Mixed-Ligand and Ester Complexes*

Ester tin(IV) dithiocarbamate complexes of general formula $[SnX_{3-n}(ester)(S_2CNR_2)_n]$ and $[SnX_{2-n}(ester)_2(S_2CNR_2)_n]$ (where X = Cl or pseudo-halide; $n = 1$ or 2) have been studied in some detail (151, 189–191). The dithiocarbamate ligands are usually bound in an anisobidentate fashion both in the solid state and solution. The ester may be monodentate (Sn—C coordination only) or bidentate (Sn—C and Sn—O coordination). Solution NMR data (^{119}Sn and ^{1}H) indicate that the Sn atom in the monoester mono(dithiocarbamate) complexes $[Sn(CH_2CH_2COOR)(S_2CNMe_2)\{(XCH_2CH_2)_2Y\}]$ (R = Me or Et, X = O or S, Y = O, S or NMe) (192) is essentially six coordinate in solution: The ester group appears to be monodentate (Sn—C coordination only), irrespective of the $(XCH_2CH_2)_2Y$ ligand, which is always terdentate. X-ray structural data show clearly how the bonding of the dithiocarbamate ligand is influenced by the ancillary ligand, $(XCH_2CH_2)_2Y$; it is isobidentate in $[Sn(CH_2CH_2COOR)(S_2CNMe_2)(OCH_2CH_2)_2NMe]$ (i.e., X = O, Y = NMe), but highly anisobidentate, with one exceptionally long Sn—S contact (3.09 Å), in $[Sn(CH_2CH_2COOR)(S_2CNMe_2)(SCH_2CH_2)_2O]$ (i.e., X = S, Y = O). In the former case, both dithiocarbamate S atoms are trans O, while in the latter, one is trans O and the other trans S; the long Sn—S(dithiocarbamate) contact is trans S and is presumably a consequence of the strong trans influence of S.

Reaction of the diester tin monohalide complex, $[SnCl(CH_2CH_2COOMe)_2(S_2CNMe_2)]$, with sodium sulfide (190) gives the known products $[Sn(CH_2CH_2COOMe_3)_2S]_3$ and $[Sn(CH_2CH_2COOMe)_2(S_2CNMe_2)_2]$. The corresponding reaction of the monoester tin dihalide complexes, $[SnCl_2\{CH_2CH_2COOMe\}(S_2CNMe_2)]$ and $[SnCl_2\{CH_2CH(COOMe)CH_2COOMe\}(S_2CNMe_2)]$ yields the pentacoordinate dimers, $[Sn(ester)(S_2CNMe_2)S]_2$,

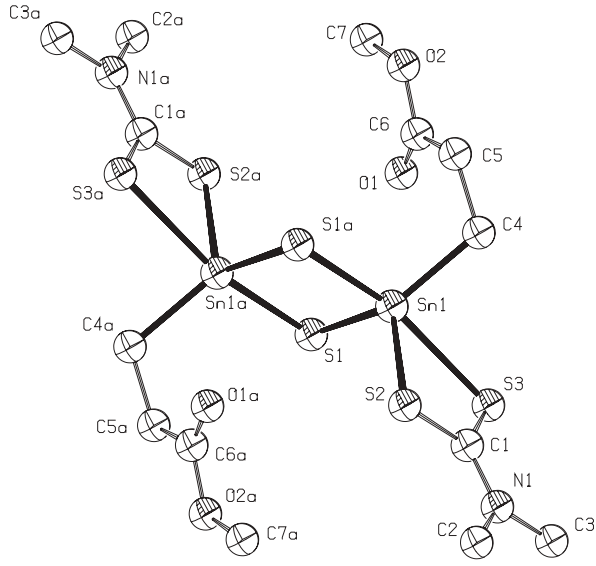

Figure 11. The ORTEP plot of $[Sn\{CH_2CH_2COOMe\}(S_2CNMe_2)S]_2$, showing the Sn_2S_2 ring found in the $[Sn(ester)(S_2CNMe_2)S]_2$ complexes.

which possess a Sn_2S_2 four-membered ring in the solid state and in solution (Fig. 11) (193). Prolonged reflux of tetrakis(4-methylpiperidinedithiocarbamate)tin(IV) in dichloromethane yields $[\{Sn\{S_2CN(CH_2)_4CHMe\}\ S\}_2]$, which also possesses a Sn_2S_2 ring (194), as does $[Sn(S_2CNEt_2)_2S_2]$, which is the initial product of the decomposition of $[Sn(S_2CNEt_2)_4]$ (106). In all three cases, the dithiocarbamate ligands are bound in a bidentate fashion.

Reaction of $[\{SnPh(S_2CNEt_2)\}_2(CH_2)_3]$ with Na_2S gives $[\{SnPh(S_2CNEt_2)\}_2(CH_2)_3(\mu\text{-}S)]$, which possesses a SnC_3SnS six-membered metallocycle (195). The X-ray structure (Fig. 12) reveals that the dithiocarbamate ligands are bound to the tin atoms in an anisobidentate fashion. The phenyl groups are cis. The solid state ^{119}Sn NMR spectrum displays two signals at -149 and -169 ppm, consistent with five-coordinate tin atoms; the two signals are due to the presence of cis and trans isomers in the polycrystalline material, which are also present in solution.

The addition of sodium acetylacetonate to $[SnBr_2(S_2CNEt_2)_2]$ is reported to initially give the expected product, $[SnBr(S_2CNEt_2)_2\{MeC(O)CHC(O)Me\}]$, although it has not been characterized fully. On prolonged standing in solution, orange, crystalline $[Sn(S_2CNEt_2)_2\{OC(Me)CSC(O)Me\}]$, which possesses a five-membered SnOC=CS ring, was isolated (196). The source of the *additional* S atom is not clear, although it has been suggested that it might be derived from

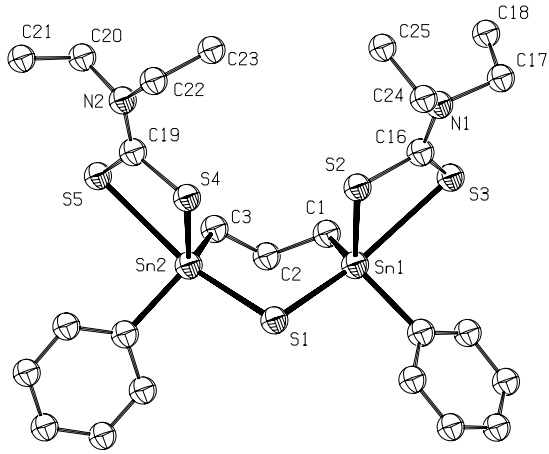

Figure 12. The ORTEP plot of $[\{SnPh(S_2CNEt_2)\}_2(CH_2)_3(\mu\text{-}S)]$. The phenyl C atom labels have been omitted for clarity.

tetraethylthiuram disulfide, which is known to be produced as a side product in the bromination of tin(II) dithiocarbamates (197); the starting material, $[SnBr_2(S_2CNEt_2)_2]$, was prepared by bromination of $[Sn(S_2CNEt_2)_2]$. The closely related catecholate complex, $[Sn(S_2CNEt_2)_2(o\text{-}C_6H_4O_2)]$, which possesses a five-membered SnOC=CO ring, is prepared by oxidative addition of tetraethylthiuram disulfide to $[Sn(o\text{-}C_6H_4O_2)]$ (198). In both complexes, the dithiocarbamate ligands are bound in an essentially isobidentate fashion, with the tin atoms in a distorted octahedral coordination environment.

The complexes 2-*n*-butyl-2-(dimethyldithiocarbamate)-1,3,2-oxathiastannolane (Fig. 13) and 2-*n*-butyl-2-(piperidyldithiocarbamate)-1,3,2-oxathiastannolane (199) are dimeric in the solid state, with the Sn atoms adopting a highly distorted octahedral geometry: Notably, the Sn atoms are O bridged rather than S bridged. However, the ^{119}Sn NMR spectra of the complexes points toward them being monomeric in solution: The ^{119}Sn chemical shifts (-251 and -230, respectively) are consistent with the Sn atom being five coordinate and, importantly, no Sn–Sn scalar couplings are observed.

4. Spectroscopic Studies

As has already been alluded to, the solution-state structures of tin(IV) dithiocarbamate complexes have been studied extensively using ^{119}Sn NMR (95, 106, 111, 112, 115–117, 119, 121, 131, 134, 143, 146–148, 153, 157, 171, 176, 181, 189–193, 198, 199). Although it is often difficult to ascertain the exact coordination of the tin atom unambiguously, because of the anisobidenticity of

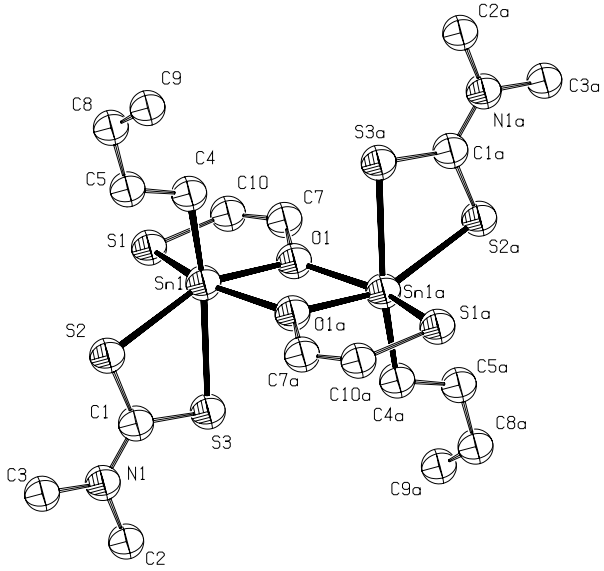

Figure 13. The ORTEP plot of 2-*n*-butyl-2-(dimethyldithiocarbamate)-1,3,2-oxathiastannolane.

the dithiocarbamate ligands and the latent fluxional behavior of many of the complexes, ^{119}Sn chemical shifts give a reasonable guide to the coordination number within a particular series of compounds: the higher the coordination number the lower the resonance frequency (Table III). From Table III, it is also apparent that, as the electronegativity of the tin substituents increases, the asymmetry in the Sn—S(dithiocarbamate) bonding decreases, leading to an increase in the effective coordination number of Sn, causing the chemical shift to move to lower frequency.

Hydrogen-1 and ^{13}C NMR spectroscopy can also be used to probe the structures of the diorganotin(IV) complexes in solution; the magnitudes of the $^{1}J_{SnC}$ and $^{2}J_{SnH}$ scalar coupling constants have been shown empirically to depend on the CSnC bond angle, θ (141, 200).

The ^{119}Sn Mössbauer spectra of a number of tin dithiocarbamate complexes have been reported (89, 91, 94, 108, 118, 147, 178, 180): Data are collected in Table IV. The Mössbauer spectral parameters have been used to infer the coordination number of the Sn atom. The isomer shift (IS) of tin species decreases as the *s*-electron density at the Sn atom decreases; thus the isomer shift would generally be expected to decrease on increasing coordination number or increasing electronegativity of the ligands. These two factors are difficult to separate, since the anisobidenticity of dithiocarbamate ligands generally decreases as the Lewis acidity of the metal moiety increases.

TABLE III
Solution ^{119}Sn NMR Data for Tin Dithiocarbamate Complexes

Complex[a]	δ(^{119}Sn)	References
$[SnI_2(S_2CNEt_2)_2]$	−1861	134
$[SnBr_2(S_2CNEt_2)_2]$	−1092	134
$[SnPh(S_2CNEt_2)_3]$	−813	115
[Sn*n*-Bu{$S_2CN(Me)$*n*-Bu}$_3$]	−807	119
$[SnPh(S_2CNEt_2)_3]$	−807	117
$[Sn(MeO_2CCH_2CH_2)(S_2CNMe_2)_3]$	−804	189
[Sn{$S_2CN(Me)$*n*-Bu}$_4$]	−786	106
$[Sn(S_2CNEt_2)_4]$	−766	106
$[SnMe(S_2CNEt_2)_3]$	−752	115
$[Sn(S_2CNEt_2)_2S]_2]$	−736	106
[Sn{$S_2CN(CH_2)_5$}$_4$]	−729	95
$[SnPhBr(S_2CNEt_2)_2]$	−704	115
$[SnPh(S_2CNMe_2)_3]$	−695	111
$[SnPh\{S_2P(OEt_2)\}(S_2CNEt_2)_2]$	−689	115
$[Sn(PhS)_2(S_2CNEt_2)_2]$	−666	106
$[Sn(CF_3CH_2S)_2(S_2CNEt_2)_2]$	−661	106
[SnPh{$S_2CN(Me)$*n*-Bu}$_3$]	−655	119
$[SnPhCl(S_2CNEt_2)_2]$	−650	117
	−647	115
$[Sn(CyS)_2(S_2CNEt_2)_2]$	−649	106
$[Sn(o\text{-}C_6H_4O_2)(S_2CNEt_2)_2]$	−647	198
$[SnPh(S_2COEt)(S_2CNEt_2)_2]$	−645	115
[SnMe{$S_2CN(Me)$*n*-Bu)$_3$]	−605	119
$[SnCl(MeO_2CCH_2CH_2)(S_2CNMe_2)_2]$	−605	189
$[SnMeCl(S_2CNEt_2)_2]$	−598	115
$[SnCl_2(S_2CNEt_2)_2]$	−519	157
[$SnPh_2${$S_2CN(Me)$*n*-Bu}$_2$]	−505	119
$[SnPh_2(S_2CNEt_2)_2]$	−502	117
	−501	112
	−499	153
$[SnPhBr_2(S_2CNEt_2)]$	−472	115
$[SnMe_2L^1(S_2CNMe_2)]$	−466	147
$[SnMe_2L^1(S_2CNEt_2)]$	−463	147
$[Sn(MeO_2CCH_2CH_2)_2(S_2CNMe_2)_2]$	−439	190
$[SnPhBrCl(S_2CNEt_2)]$	−419	115
$[Sn(CH_2CH_2CO_2Me)\{(OCH_2CH_2)_2NMe\}(S_2CNMe_2)]$	−418	192
$[SnCl_2\{CH_2CH(CO_2Me)CH_2CO_2Me\}(S_2CNMe_2)]$	−405	191
$[SnCl_2(CH_2CH_2CO_2Me)(S_2CNMe_2)]$	−386	189
[SnPh{$S_2CN(CH_2)_4$}$_3$]	−378	121
[SnPhCl{$S_2CN(CH_2)_5$}$_2$]	−378	95
$[SnPhCl(S_2CNMe_2)_2]$	−361	111, 112, 147
$[SnPhCl_2(S_2CNEt_2)]$	−355	115
$[SnPhCl_2\{S_2CN(CH_2)_5\}]$	−354	181
[$SnMe_2${$S_2CN(Me)$*n*-Bu}$_2$]	−349	119
$[SnPhCl_2\{S_2CN(CH_2)_4NMe\}]$	−349	181
$[SnPhCl_2\{S_2CN(CH_2)_4O\}]$	−349	181
$[SnPh_2Br(S_2CNEt_2)]$	−343	153

TABLE III (*continued*)

Complex[a]	δ(^{119}Sn)	References
[Sn*n*-Bu_2{$S_2CN(Me)$*n*-Bu_2}]	−341	119
[$SnMe_2(S_2CNMe_2)_2$]	−338	112, 146, 147
[$SnMe_2${$S_2CN(CH_2)_4CHMe$}$_2$]	−336	143
[$SnMe_2(S_2CNEt_2)_2$]	−336	153
	−333	112, 146, 147
[Sn*n*-$Bu_2(S_2CNEt_2)_2$]	−336	153
[$SnMe_2${$S_2CN(CH_2)_5$}$_2$]	−335	143
[$SnMe_2${$S_2CN(CH_2)_4NMe$}$_2$]	−330	143
[$SnPh_2Cl(S_2CNEt_2)$]	−327	153
	−325; −340	117
[$SnPhCl_2${$S_2CN(CH_2)_4CHMe$}]	−326	181
[$SnMe_2${$S_2CN(CH_2)_4O$}$_2$]	−325	143
[Sn*n*-$BuCl_2${$S_2CN(CH_2)_4CHMe$}]	−299	181
[$SnMeCl_2(S_2CNEt_2)$]	−296	115
[Sn*n*-$BuCl_2${$S_2CN(CH_2)_5$}$_2$]	−293	181
[Sn*n*-$BuCl_2(S_2CNEt_2)$]	−285	131
[Sn*n*-$BuCl_2${$S_2CN(CH_2)_4NMe$}]	−283	181
[Sn*n*-$BuCl_2${$S_2CN(CH_2)_4O$}]	−273	181
[$SnMe_2${$S_2CN(CH_2)_4$}$_2$]	−267	121
[Sn*t*-$Bu_2(S_2CNEt_2)_2$]	−262	148
	−239	153
[$Sn(CH_2CH_2CO_2Me)_2Cl(S_2CNMe_2)$]	−259	190
[Sn*t*-$Bu_2(S_2CNMe_2)_2$]	−255	148
[{Sn*n*-$Bu(SCH_2CH_2O)(S_2CNMe_2)$}$_2$]	−251	199
[{Sn{$CH_2CH(CO_2Me)CH_2CO_2Me$}$(S_2CNMe_2)S$}$_2$]	−246	191
[{$Sn(CH_2CH_2CO_2Me)(S_2CNEt_2)S$}$_2$]	−233; −235	193
[{Sn*n*-$Bu(SCH_2CH_2O)${$S_2CN(CH_2)_5$}$_2$]	−231	199
[$Sn(CH_2CH_2CO_2Me)(S_2CNMe_2)S$}$_2$]	−230; −232	193
[Sn*t*-$Bu_2Cl(S_2CNEt_2)$]	−217	153
[Sn(*p*-tolyl)$_2(L^2)(S_2CNMe_2)$]	−211	176
[$SnPh_2L^3(S_2CNMe_2)$]	−202	116
[$SnMe_2Cl(S_2CNEt_2)$]	−201; −204	112, 153
[Sn*n*-$Bu_2Cl(S_2CNEt_2)$]	−200	153
[$SnPh_2L^4(S_2CNEt_2)$]	−198	116
[Sn{$CH_2CH_2CO_2Me$}{$(OCH_2CH_2)_2S$}(S_2CNMe_2)]	−196	192
[$SnPh_3(S_2CNEt_2)$]	−192	112, 117, 153
[$SnPh_3${$S_2CN(CH_2)_5$}]	−191	171
[$SnPh_3[S_2CN(CH_2)_2CHMe(CH_2)_2$]	−191	171
[$SnPh_3${$S_2CN(Me)$*n*-Bu}]	−190	119
[$SnPh_2L^3(S_2CNEt_2)$]	−183	116
[$SnPh_3${$S_2CN(CH_2)_2O(CH_2)_2$]	−182	171
[$Sn(CH_2CH_2CO_2Me){(SCH_2CH_2)_2O}(S_2CNMe_2)$]	−178	192
[$SnPh_3${$S_2CN(CH_2)_2NMe(CH_2)_2$}]	−176	171
[$SnMe_2(L^3)(S_2CNMe_2)$]	−174	176
[$SnCl_2${$S_2CN(CH_2)_4$}$_2$]	−140	121
[$SnMe_2(L^5)(S_2CNMe_2)$]	−139	176
[$SnPh_3${$S_2CN(CH_2)_4$}]	−131	121
[$SnPh_2L^6(S_2CNMe_2)$]	−128	116

TABLE III (*continued*)

Complex[a]	$\delta(^{119}Sn)$	References
$[SnMe_3\{S_2CN(CH_2)_2CHMe(CH_2)\}]$	17	171
$[SnMe_3\{S_2CN(CH_2)_5\}]$	20	171
$[SnMe_3(S_2CNEt_2)]$	21	153
$[Sn\textit{n}\text{-}Bu_3\{S_2CN(Me)\textit{n}\text{-}Bu\}]$	21	119
$[SnMe_3\{S_2CN(Me)\textit{n}\text{-}Bu\}]$	22	119
$[SnMe_3\{S_2CN(CH_2)_2NMe(CH_2)_2\}]$	23	171
$[SnMe_3(S_2CNMe_2)]$	25	112
$[SnMe_3\{S_2CN(CH_2)_2O(CH_2)_2\}]$	34	171

[a] Chemical shifts reported in ppm relative to $SnMe_4$ as an external standard. Data quoted at ambient temperature. L^1 = 1-(2-pyridylazo)-2-naphtholate. L^2 = 3-(2-pyridyl)-2-thienyl. L^3 = 2-(2-oxo-*N*-pyrrolidinyl)ethyl. L^4 = 2-ethylpyridine. L^5 = 2-(4,4-dimethyl-2-oxazolinyl)-3-thienyl. L^6 = 4-ethylpyridine.

Examination of Table IV shows no reliable correlation of the isomer shift with coordination number in organotin dithiocarbamate complexes.

The magnitude of quadrupole splitting (QS) and the QS/IS ratio (ρ) have also been used as a diagnostic probe for the geometry at tin (higher magnitudes being associated with higher coordination numbers), but again data collected in Table IV show no reliable correlation for the organotin dithiocarbamate complexes. However, for the diorganotin compounds, the QS can be correlated with the CSnC bond angle, provided a point-charge model is applicable and that the contribution of the organic ligands to the electric field-gradient is negligible (89).

V. GROUP 15 (V A)

Homoleptic and mixed-ligand dithiocarbamate complexes of the heavier group 15 (V A) elements have been studied extensively and show considerable structural diversity. The dithiocarbamate ligand tends to act in an unsymmetrical chelating fashion to the smaller members of the group, with one of the two M—S bonds appreciably shorter than the other. As the size of the metal increases, the asymmetry in the M—S bond lengths diminishes and there is an increasing tendency for polynuclear species to form via either halide and/or S bridges; halide bridges are favored whenever possible. The arsenic, antimony and bismuth complexes of dithiocarbamates together with other 1,1-dithiolate ligands have been reviewed previously (201).

A. Nitrogen and Phosphorus

The nitrogen compounds $[N(SiMe_3)_2(S_2CNR_2)]$ (R = Me, Et, *i*-Pr, or Bz) (202–204) have been prepared via three routes, namely, (1) reaction of

TABLE IV
Tin-119 Mössbauer Data for Tin Dithiocarbamate Complexes

Complex[a]	IS	QS	ρ	Reference
[{Sn(S_2CNEt_2)$_2$S}$_2$]	0.97	0.66	0.68	108
[SnPh{S_2CN(Me)*n*-Bu}$_3$]	1.11	1.81	1.63	121
[SnMe{S_2CN(Me)*n*-Bu}$_3$]	1.13	1.92	1.7	121
[Sn(*p*-tolyl)$_2$(L^1)(S_2CNMe_2)]	1.16	2.47	2.13	178
[SnPh$_2${$S_2CN(CH_2)_4$}$_2$]	1.2	1.7	1.42	91
[SnPh$_3${S_2CN(Me)*n*-Bu}]	1.23	1.79	1.46	121
[Sn*n*-Bu{S_2CN(Me)*n*-Bu}$_3$]	1.25	1.84	1.47	121
[SnPh$_2${S_2CN(Me)*n*-Bu}$_2$]	1.26	2.13	1.69	121
[SnPh$_2${2-(2-py)CH_2CH_2}(S_2CNEt_2)]	1.27	2.35	1.85	118
[SnPh$_2${2-(2-py)CH_2CH_2}(S_2CNMe_2)]	1.27	2.55	2.01	118
[SnPh$_2${2-(4-py)CH_2CH_2}(S_2CNMe_2)]	1.27	2.55	2.01	118
[SnMe$_3${S_2CN(Me)*n*-Bu}]	1.27	2.14	1.69	121
[SnMe$_2$(L^2)(S_2CNMe_2)]	1.27	2.59	2.04	178
[SnHex$_2$(S_2CNEt_2)$_2$]	1.29	3.02	2.34	147
[SnPh$_3${$S_2CN(CH_2)_4$}]	1.3	1.9	1.46	91
[SnPh$_2${2-(2-Oxo-*N*-pyr)CH_2CH_2}(S_2CNMe_2)]	1.3	2.18	1.68	118
[SnMe$_2$(L^1)(S_2CNMe_2)]	1.31	2.71	2.07	180
[Sn*n*-Bu$_3${S_2CN(Me)*n*-Bu}]	1.39	2.19	1.58	121
[SnMe$_2${S_2CN(Me)*n*-Bu}$_2$]	1.4	2.89	2.06	121
[SnHex$_2$(S_2CN*i*-Pr$_2$)$_2$]	1.4	2.83	2.02	147
[SnHex$_2${S_2CN(Me)Ph}$_2$]	1.42	2.89	2.04	147
[Sn*n*-Bu$_3${$S_2CN(CH_2)_4$}]	1.44	1.94	1.35	91
[SnMe$_2${$S_2CN(CH_2)_4$}$_2$]	1.44	2.84	1.97	91
[SnHex$_2$(S_2CNMe_2)$_2$]	1.45	2.96	2.04	147
[Sn*n*-Bu$_2$(S_2CNMe_2)$_2$]	1.49	2.93	1.97	147
[SnHex$_2${$S_2CN(CH_2)_2O(CH_2)_2$}$_2$]	1.51	2.89	1.91	147
[Sn*n*-Bu$_2${S_2CN(Me)*n*-Bu}$_2$]	1.52	2.89	1.9	121
[Sn*n*-Bu$_2${S_2CN(Me)Ph}$_2$]	1.55	2.68	1.73	147
[SnBz$_2${$S_2CN(CH_2)_4$}$_2$]	1.58	2.45	1.55	91
[SnOct$_2${$S_2CN(CH_2)_4$}$_2$]	1.58	2.92	1.85	91
[Sn*n*-Bu$_2$(S_2CNEt_2)$_2$]	1.59	2.71	1.7	147
[Sn*n*-Bu$_2${$S_2CN(CH_2)_4$}$_2$]	1.65	2.46	1.49	91
[SnEt$_2${$S_2CN(CH_2)_4$}$_2$]	1.65	2.83	1.72	89
[Sn*n*-Bu$_2$(S_2CN*i*-Pr$_2$)$_2$]	1.66	2.61	1.57	147
[Sn*n*-Bu$_2${$S_2CN(CH_2)_2O(CH_2)_2$}$_2$]	1.69	2.93	1.73	147
[Sn(S_2CNEt_2)$_2$]	1.92	1.05	0.55	94

[a] IS = Isomer shift, QS = quadrupole splitting, ρ = (QS/IS). Data reported in mm s^{-1}. L^1 = 2-(4,4-dimethyl-2-oxazolinyl)-3-thienyl. L^2 = 3-(2-pyridyl)-2-thienyl.

$N(SiMe_3)_2Br$ with the sodium salt of the appropriate dithiocarbamate, (2) reaction of $Na[N(SiMe_3)_2]$ with thiuram disulfides, and (3) reaction of $(SiMe_3)_2NMgBr$ with thiuram disulfides (202). The X-ray molecular structures show that the dithiocarbamates are essentially monodentate [N—S(short) ≈ 1.66 Å; N—S(long) ≈ 3.05 Å] with the amino nitrogen and dithiocarbamate coplanar (203). A variable temperature NMR study of the dimethyldithiocarbamate

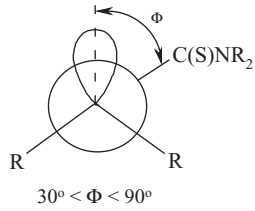

Figure 14. Newman projection showing the *gauche* arrangement of the P–S–C=S moiety in the complexes $[PR_2(S_2CNR'_2)]$.

complex indicates that the barrier to $(S_2)C-N(Me_2)$ bond rotation is 58 kJ mol^{-1} at 371 K (204), which is similar to magnitudes observed in other main group and transition metal complexes.

Although phosphorus dithiocarbamate compounds, which are generally prepared by insertion of CS_2 into P–N bonds or by reaction of dithiocarbamate salts with phosphorus chlorides, have been known for >100 years, they have received relatively little attention recently (205–213). The structures of $[P(S_2CNMe_2)_3]$ (205), $[P(S_2CNEt_2)_3]$ (206), $[PPh(S_2CNEt_2)_2]$ (207, 208), and $[PPh_2(S_2CNEt_2)]$ (207) have been determined crystallographically; in all four cases the dithiocarbamate ligand is essentially monodentate (P–S=2.12–2.18 Å), with only weak secondary interactions between the P atom and the second S(=C) atom (P···S = 2.88–3.18 Å; cf. 3.74 Å for the sum of the van der Waals radii). The P–S–C=S moiety adopts a *gauche* arrangement (Fig. 14) as a consequence of repulsions between the stereochemically active lone pair and the S(–P)atom, and the secondary P···S interactions (207). The ^{31}P NMR spectrum of $[P(S_2CNMe_2)_3]$ shows a single chemical shift at ca. −63 ppm suggesting the phosphorus atom has a coordination number >3 (205); this presumably arises because the P atom undergoes metallotropic shifts between the dithiocarbamate S atoms, via a pseudo-bidentate transition state.

The complex $[P(S)Ph_2(S_2CNEt_2)]$ adopts a similar structure to $[PPh_2(S_2CNEt_2)]$, but the secondary P···S interaction is weaker (3.315 Å) and the angle, ϕ (see Fig. 14), is increased significantly (to 106.4°) as a result of greater steric interactions between the dithiocarbamate and the bulky sulfide ligand attached to the PPh_2 moiety (209). The analogous ethoxide complexes, $[P(S)(OEt)_2(S_2CNR_2)]$ have been shown to display both antifungal and antiviral activity (210), although they are less active than classical organophosphorus reagents.

Bicyclic $P_4S_3I_2$ reacts with $[SnPh_3(S_2CNR_2)]$ or dithiocarbamic acids in the presence of dimethylamine to give $[P_4S_3I(S_2CNR_2)]$ or $[P_4S_3(S_2CNR_2)_2]$, depending on the stoichiometry (211). The dithiocarbamate ligands are bound in an essentially monodentate fashion, but variable temperature ^{31}P NMR

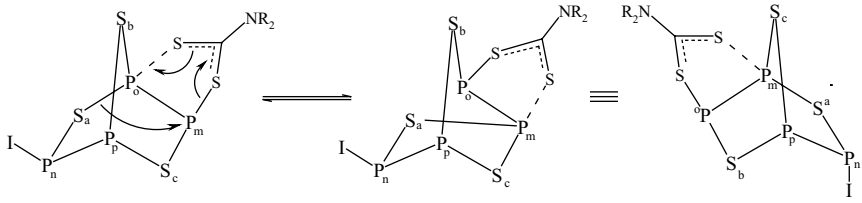

Figure 15. The skeletal rearrangement observed in $[P_4S_3I(S_2CNR_2)]$.

indicates that the P_4S_3 bicyclic skeleton undergoes an unusual rearrangement (Fig. 15) in solution via the formation of a bidentate (bridging) mode in the transition state.

B. Arsenic, Antimony, and Bismuth

1. Homoleptic Complexes

The homoleptic tris(dithiocarbamate) complexes $[M(S_2CNR_2)_3]$ (M = As, Sb, or Bi) have been studied extensively (93, 212–245). The arsenic complexes are mononuclear with three short As—S bonds (As—S = 2.31–2.39 Å) that are essentially cis each other, and three long As—S bonds (As—S = 2.77–2.94 Å). Valence bond sum (VBS) calculations show that the valency of the As atom is, as expected, close to three (224). The geometry at arsenic in the $[As(S_2CNR_2)_3]$ is best described as a distorted octahedron with the stereochemically active lone pair directed along the pseudo threefold axis, capping the triangular face defined by the three weakly coordinated S atoms (Fig. 16) (222–224, 230).

As with other main group homoleptic dithiocarbamate complexes, those of antimony have been prepared traditionally by the reaction of $SbCl_3$ with the appropriate dithiocarbamate salt or by insertion of CS_2 into Sb–amide bonds. However, the condensation of Sb_2O_3 with dithiocarbamic acids has been shown to be a more facile route (221). The complexes are monomeric, nonelectrolytes in solution (213), but may be either monomeric or dimeric, with weak Sb—S···Sb bridges, in the solid state. Thus, for example, while tris(diethanoldithiocarbamate)antimony(III) is monomeric (223), tris(diethydithiocarbamate)antimony(III) is a centrosymmetric dimer in the solid state, with one S from a dithiocarbamate of each $Sb(S_2CNEt_2)_3$ moiety bridging: (Sb)S···Sb = 3.47 Å (217). The reasons for the differences in behavior are not clear; there are no stabilizing interactions between the hydroxyl groups and the metal center in the diethanoldithiocarbamate complex, for example, and there are no obvious steric restrictions to dimerization. In both cases, the lone pair is stereochemically active. The local geometry around Sb is best considered as distorted trigonal

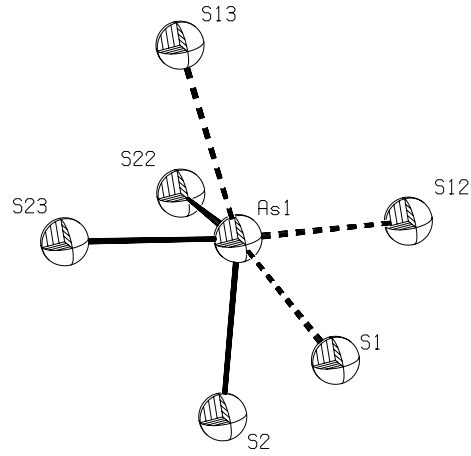

Figure 16. The ORTEP plot of the coordination sphere of As in the tris(dithiocarbamate) complexes $[As(S_2CNR_2)_3]$. The stereochemical active lone-pair caps the triangular face made by the three weakly bound S atoms, which are indicated by the dashed lines.

prismatic and distorted dodecahedral, respectively. The dithiocarbamate ligands are anisobidentate, with the three short Sb—S bonds essentially at right angles to each other: Sb—S(short) = 2.47–2.74 Å; Sb—S(long) = 2.83–3.00 Å. The shortest Sb—S contact is to the apical S atom.

The homoleptic bis(dimethyldithiocarbamate) cations $[Sb(S_2CNMe_2)_2]^+$ and $[M(S_2CN\textit{n}\text{-}Bu_2)_2]^+$ (M = As or Sb) have also been prepared (246–248). The dithiocarbamate ligands are bond in an asymmetric fashion (ΔSb—S $\approx$ 0.16 Å). The metal is in a pyramidal coordination environment with the lone pair of electrons apical. In $[Sb(S_2CNMe_2)_2][CF_3SO_3]$, weak Sb$\cdots$S interactions lead to the cation possessing a dimeric structure, with a center of symmetry, in the solid state: there are also weak interactions between one of the Sb atoms and an oxygen atom of the triflate group (247).

Although $[Bi\{S_2CN(Me)CH_2CH_2OH\}_3]$ (224), $[Bi\{S_2CN(\textit{i}\text{-}Pr)CH_2CH_2OH\}_3]$ (225) and $[Bi\{S_2CN(Me)(Hex)\}_3]$ (240) are monomeric in the solid state, the tris(dithiocarbamate) complexes, $[Bi(S_2CNR_2)_3]$, are generally S-bridged dimers: The Bi—S$\cdots$Bi bridges are appreciably stronger than in the Sb analogues. The coordination environments of the Bi atoms can vary quite appreciably and the exact structure depends on the nature of the dithiocarbamate. In $[Bi_2\{S_2CN(CH_2CH_2OH)_2\}_6]$ the metal atoms are bridged by four S atoms, so that the geometry at the Bi is described best as a distorted square antiprism (Fig. 17) (223, 227), while in $[Bi_2\{S_2CN(Et)\textit{n}\text{-}Bu\}_6]$ (228) the two Bi atoms are bridged by only two S atoms. The bonding of the nonbridging dithiocarbamate ligands to the metal center is considerably less asymmetric than in the corresponding arsenic or antimony complexes.

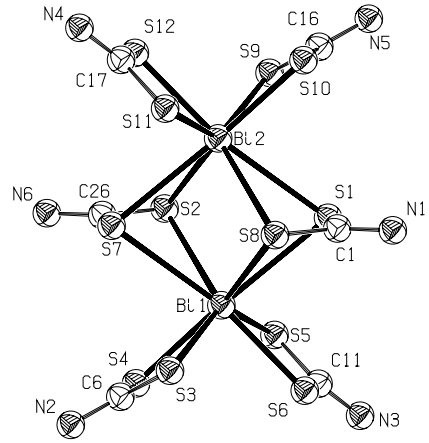

Figure 17. The ORTEP plots of $[Bi_2\{S_2CN(CH_2CH_2OH)_2\}_6]$. The N-substituents omitted for clarity.

The geometries at the two bismuth atoms in the pyrrolidinedithiocarbamate complex $[Bi_2\{S_2CN(CH_2)_4\}_6]$ are quite different (Fig. 18): One Bi atom is trigonal prismatic with a S atom capping one of the rectangular faces, while the other Bi atom lies approximately at the center of a pentagonal pyramid. The Bi···Bi distance is 4.264 Å (244).

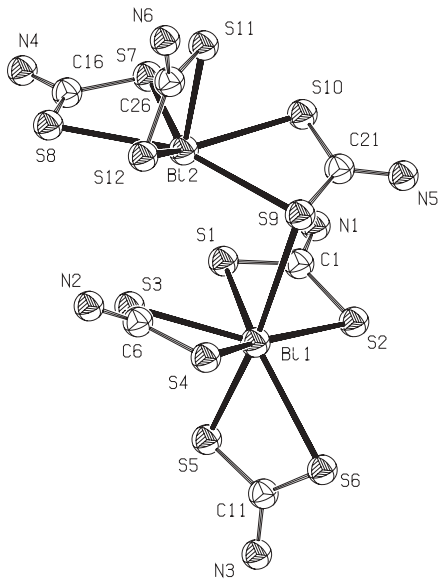

Figure 18. The ORTEP plot of $[Bi_2\{S_2CN(CH_2)_4\}_6]$ showing the two different Bi coordination environments. The N-substituents omitted for clarity.

The mixed tris(dithiocarbamate) complexes, $[Bi(S_2CNR_2)_2(S_2CNR'_2)]$ have been prepared by mixing $[Bi(S_2CNR_2)_3]$ and $[Bi(S_2CNR'_2)_3]$, although the rate of ligand scrambling is sufficiently slow to allow chromatographic separation of the complexes (220, 242). Ligand scrambling probably occurs via a dissociative route: The lability of the dithiocarbamate ligands is evidenced by mass spectrometry (219), in which the highest observable mass peaks in the tris(dithiocarbamate) complexes are due to the species $[M(S_2CNR_2)_2]^+$, and the ease by which the $[M(S_2CNR_2)_2]^+$ cation can be formed chemically (246–248). The same complexes can also be prepared by reaction of the halide complexes $[MX(S_2CNR_2)_2]$ with the appropriate dithiocarbamic acids or their salts (see below) (220, 249, 250).

Thermodynamic measurements on the tris(dithiocarbamate) complexes, $[M(S_2CNR_2)_3]$ (M = P, As, Sb, or Bi), show the M—S bond dissociation enthalpy decreases rapidly from P to As, then reduces more slowly down the group. The greater stability of the P—S bonds has been attributed to participation of $d(\pi)$–$d(\pi)$ bonding between phosphorus and sulfur (231–236). Thermal analytical studies (231, 232, 237–241) indicate that the complexes undergo thermal decomposition to yield various metal sulfides, such as M_2S_3, and the bismuth complexes have been used as single source precursors for the deposition of Bi_2S_3 (237–241). The tris(dithiocarbamate) complexes have also been shown to be useful lubricant additives, with excellent wear resistance properties even under extreme pressures (243). The complexation of dithiocarbamates to trivalent group 15 (V A) metal ions has been shown to be an effective method of preconcentration for the extraction and quantification of the metals in environmental samples (251, 252).

2. *Nonhomoleptic Bis(dithiocarbamate) Complexes*

Bis(dithiocarbamate) complexes of the type $[MR(S_2CNR_2)_2]$ and $[MX(S_2CNR_2)_2]$ (M = As, Sb, or Bi; R = alkyl, aryl, or organometallic group; X = halide) have also been studied extensively (212, 213, 219, 224, 241, 248, 253–270). The organyl complexes are prepared by reaction of the metal dihalides, RMX_2, with the appropriate dithiocarbamate salt (253, 254, 260–263, 266, 268). The As complexes are monomeric (263); the dithiocarbamate ligands are almost monodentate [As—S(short) $\approx$ 2.33 Å; As—S(long) $\approx$ 2.90 Å] and the metal center is thus best considered as possessing a pyramidal geometry, with the stereochemically active lone-pair apical.

The organoantimony and organobismuth bis(dithiocarbamate) complexes are structurally similar, forming dimers in the solid state via intermolecular M—S$\cdots$M bridges. The dimers are formed by the *side-on* docking of the $[MR(S_2CNR_2)_2]$ units (Fig. 19), such that the two metal and eight S atoms are essentially coplanar (255, 260, 261). The dithiocarbamate ligands are best

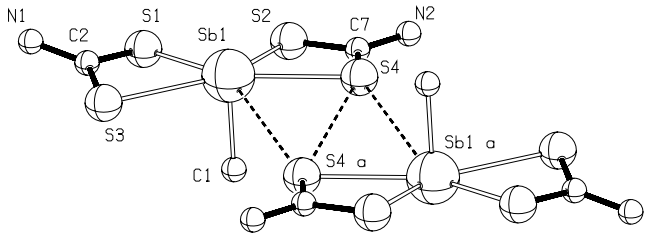

Figure 19. The PLUTON plot of $[SbMe(S_2CNEt_2)_2]$ showing the side-on docking of the molecular units found in the organyl complexes $[MR(S_2CNR_2)_2]$ (M = Sb or Bi). The dashed lines indicate intermolecular interactions. N substituents omitted for clarity.

considered as anisobidentate: The asymmetry in the M—S bonding decreases as the size of the metal increases. The overall geometry at the metal atom is pseudo-pentagonal bipyramidal, with the organyl group and the lone pair of electrons in axial positions.

Although monomeric, the Bi atom in $[BiR(S_2CNEt_2)_2]$ [{R = 2-(2′-pyridyl)-phenyl] is also pentagonal bipyramidal: The N atom of the pyridyl ring coordinates to the metal (Bi—N = 2.55 Å), completing the coordination sphere. The equatorial plane contains the four S atoms plus the nitrogen atom, with the C(phenyl) atom and stereochemically active lone pair in the axial positions (Fig. 20) (261).

The halide complexes $[MX(S_2CNR_2)_2]$ (M = Sb or Bi; X = Cl, Br, or I) have been prepared from both the trihalide, MX_3 (212, 213, 241), and the tris(dithiocarbamate) (219, 248) complexes. Several different structural motifs have been observed but, with the exception of $[SbCl\{S_2CN(CH_2)_4\}_2]$, which is monomeric

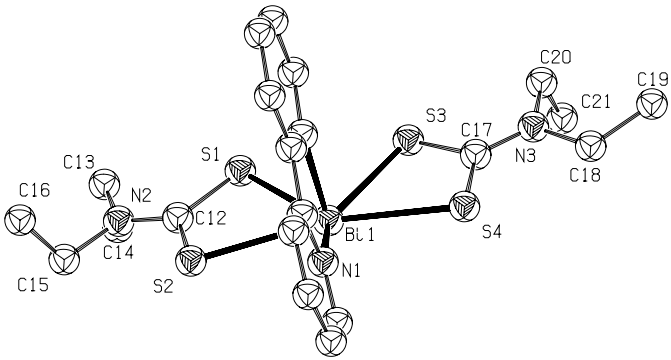

Figure 20. The ORTEP plot of $[BiL(S_2CNEt_2)_2]$; L = 2-(2′-pyridyl)phenyl. Atom labels for the ligand 2-(2′-pyridyl)phenyl omitted for clarity.

(265), all exhibit intermolecular interactions in the solid state. In all cases, the dithiocarbamate ligands are bound in an anisobidentate fashion: The degree of asymmetry is generally lower in the bismuth complexes. In solution, molecular mass measurements indicate the antimony species are monomeric, while the bismuth complexes retain a degree of association (213, 219): Both sets of complexes are non-electrolytes (213).

The iodide complexes, $[SbI(S_2CNEt_2)_2]$ (258), $[SbI\{S_2CN(CH_2)_4\}_2]$ (256) and $[BiI(S_2CNEt_2)_2]$ (257) form *zigzag* polymeric species in which metal moieties are linked by a single halide [Fig. 21(*a*)]. Although structurally similar,

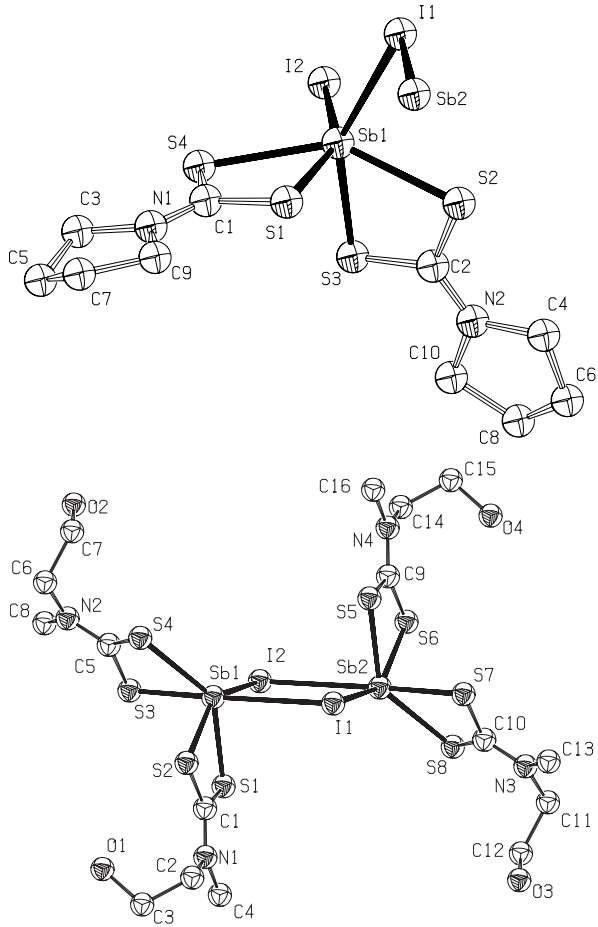

Figure 21. The two structural types observed in the iodide complexes $[MI(S_2CNR_2)_2]$ (M = Sb or Bi), exemplified by the ORTEP plots of (*a*) $[SbI\{S_2CN(CH_2)_4\}_2]$, showing part of the polymeric chain, and (*b*) $[SbI\{S_2CN(Me)CH_2CH_2OH\}_2]$.

there are a number of important differences between the antimony and bismuth diethydithiocarbamate complexes: In particular, the IMI bond angle is reduced from 135.8° in the antimony complex to just 89.7° in the Bi complex.

The complex $[SbI\{S_2CN(Me)CH_2CH_2OH\}_2]$ is structurally quite different (224). It is dinuclear in the solid state with the two $Sb(S_2CNR_2)_2$ units linked by a pair of iodides bridges [Fig. 21(*b*)]. In each of the above cases, the metal atom can be considered as being in a highly distorted octahedral coordination environment, with a stereochemically active lone-pair capping one of the faces.

The complex $[BiCl\{S_2CN(CH_2)_4\}_2]$ is also polymeric; however, both chloride and sulfur bridges are present, giving a pseudo-seven-coordinate metal center (241). The BiSBi and BiClBi bond angles are 90.9 and 97.1°, respectively. The two bridging Bi—S bonds are approximately equal (2.99 and 3.10 Å), as are the two Bi—Cl bonds (2.84 and 2.94 Å). The bromo compound $[BiBr(S_2CNEt_2)_2]$ is tetrameric in the solid state, with two distinctly different pairs of Br and Bi sites. One pair of the bromine atoms bridges two bismuth atoms, while the other bridges three atoms: Two of the Bi atoms are thus best described as being in a capped trigonal-prismatic environment, while the other two may be considered as being in a 5:2:1 pseudo-eight coordinate environment, including the stereochemically active lone pair (Fig. 22) (257). The dithiocarbamate ligands chelate to the metal centers in an asymmetric fashion.

Reaction of $BiCl_3$ with thiourea (tu) and ammonium pyrrolidinedithiocarbamate yields the dimeric Bi(III) complex, $[\{Bi(tu)S_2CN(CH_2)_4\}_2(\mu\text{-}Cl)_2]$ (244). The coordination environment at Bi is essentially pentagonal bipyramidal, with one Cl axial and the other equatorial. The Bi_2Cl_2 metallocycle is planar: The Bi···Bi distance is 4.603 Å.

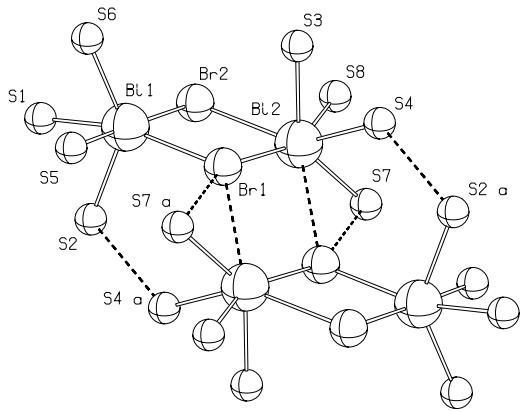

Figure 22. The PLUTON plot showing the different coordination spheres around the Bi atoms in the tetrameric complex $[BiBr(S_2CNEt_2)_2]$. Dashed lines indicate intermolecular interactions.

The halides are easily removed from the $[MX(S_2CNR_2)_2]$ complexes giving the homoleptic bis(dithiocarbamate) cations, $[M(S_2CNR_2)_2]^+$ (247, 248), and can be substituted for other ligands, such as a different dithiocarbamate, thiophosphates, xanthates, or β-diketonates, giving mixed-ligand complexes of the type $[M(S_2CNR_2)_2L]$, in which the metal atom is presumed to be hexacoordinate (220, 249, 250, 264, 270). The analogous mono(dithiocarbamate) complexes, $[M(S_2CNR_2)\{S_2P(OR')_2\}_2]$, can be prepared by reaction of $[MCl\{S_2P(OR)_2\}_2]$ with the appropriate dithiocarbamate salt (271, 272). Reaction of $[SbCl(S_2CNR_2)_2]$ with the sodium salts of either ethane-1,2-dithiolate or 4-methylbenzene-1,2-dithiolate (L) gives the dinuclear complexes $[\{Sb(S_2CNR_2)_2\}_2(\mu\text{-}L)]$ (269), analogous to the methylene bridged $[\{Sb(S_2CNR_2)_2\}_2(\mu\text{-}CH_2)]$ complexes (268). The antimony complexes $[SbCl(S_2CNR_2)_2]$ have also been shown to form stable 1:1 adducts with amines, revealing the metal center to be Lewis acidic (267).

3. *Mono(dithiocarbamate) Complexes*

A number of mono(dithiocarbamate) complexes of general formula $[MX_2(S_2CNR_2)]$ (M = As, Sb or Bi; X = Cl, Br, or I) have been reported (212, 273–279). The bismuth complexes have been the subject of particular interest because they exhibit interesting structural variations (274–279). The solid-state molecular structures adopted depend on the halogen and the conditions under which recrystallization is carried out. The complex $[BiI_2(S_2CNEt_2)]$ crystallizes by slow diffusion of *n*-butanol into a dimethylformamide (DMF) solution as an infinite polymeric array, $[BiI_2(S_2CNEt_2)]_\infty$, in which each pair of Bi atoms is bridged by two iodides and one S atom of the dithiocarbamate, which chelates in a slightly asymmetric fashion (274). Under identical conditions, the chloro- and bromo-analogues crystallize as the pentanuclear species $[Bi_5X_7(S_2CNEt_2)_8]$, in which one of the Bi atoms is bound to six chlorides, giving an octahedral $[BiX_6]^{3-}$ unit at the core of the array (276), but from acetonitrile (277) they crystallize as the polymeric $[BiX_2(S_2CNEt_2)]_\infty$ species, which are isomorphous with the iodo analogue, $[BiI_2(S_2CNEt_2)]_\infty$. Conversely, slow evaporation of a DMF/*n*-butanol solution of $[BiI_2(S_2CNEt_2)]$ gives $[Bi_5I_7(S_2CNEt_2)_8]$ (276).

Crystallization of $[BiI_2(S_2CNEt_2)]$ from DMF with a stoichiometric amount of tetraethylammonium iodide or bromide gives the isostructural complexes $[NEt_4]_2[\{BiI_2(S_2CNEt_2)\}_2(\mu\text{-}I)_2]$ and $[NEt_4]_2[BiI_2(S_2CNEt_2)(\mu\text{-}I)_2BiBrI(S_2CNEt_2)]$ (Fig. 23), respectively: The anions are centrosymmetric with Bi···Bi distances of 4.75 and 4.68 Å (275). Crystallization of $[BiX_2(S_2CNEt_2)]$ (X = Cl, Br, or I) from Py yields the monocular tris(pyridine) adducts, $[BiX_2(S_2CNEt_2)(py)_3]$ (278), while crystallization by slow evaporation of a Py/*n*-butanol solution, gives the tetranuclear $[Bi_4(S_2CNEt_2)_4Br_{10}]^{2-}$ anion as its pyridinium

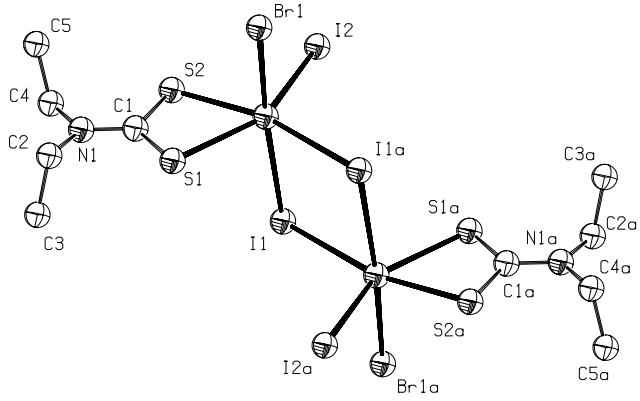

Figure 23. The ORTEP plot of $[NEt_4]_2[BiI_2(S_2CNEt_2)(\mu\text{-}I)_2BiBrI(S_2CNEt_2)]$. Cations omitted for clarity.

salt (276). The three Py adducts (X = Cl, Br, or I) are isomorphous. The Bi atom is in a distorted pentagonal bipyramidal coordination environment, with the two halides axial ($\angle$ XBiX $\approx$ 170–175°): there is no evidence of a stereochemically active lone pair. The pyridines are loosely bound, with the Bi—N distances (2.7–2.8 Å) slightly longer than the Bi—N(py) distance in $[BiL(S_2CNEt_2)_2]$ [L = 2-(2′-pyridyl)phenyl] (261). The 1:1 adducts of $[BiX_2(S_2CNEt_2)]$ with 2,2′-bipyridyl (bpy) and 2,2′:6′,2″-terpyridyl (terpy) have also been prepared (279). The terpy analogue (Fig. 24) is essentially isostructural with the tris(pyridine) adduct, while the bpy adduct crystallizes as the halide bridged dimer, $[\{Bi(S_2CNEt_2)(bpy)\}_2(\mu\text{-}X)_2]$. The geometry at the Bi atom in

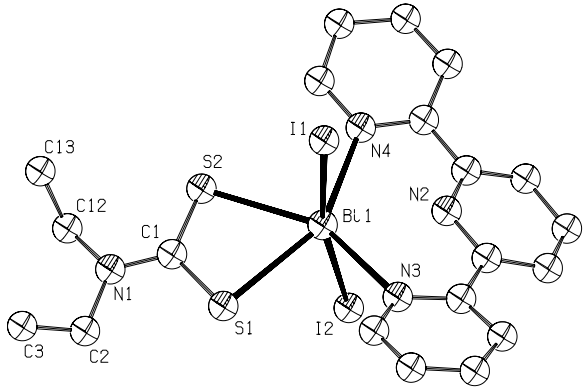

Figure 24. The ORTEP plot of $[BiI_2(S_2CNEt_2)(terpy)]$. Carbon atom labels on 2,2′:6′,2″-terpyridyl ligand have been omitted for clarity.

$[\{Bi(S_2CNEt_2)(bpy)\}_2(\mu\text{-}X)_2]$ is best described as pentagonal bipyramidal, the equatorial plane being defined by the two S atoms of the dithiocarbamate, one N donor of bpy and the two bridging halides. In all cases, the dithiocarbamate ligands are bound in an essentially symmetrical fashion.

Formal substitution of the two halides in the $[MX_2(S_2CNR_2)]$ (M = As or Sb) with a dithiolate ligand gives the mononuclear complexes $[M(S^{\frown}S)(S_2CNR_2)]$ ($S^{\frown}S$ = ethane-1,2-dithiolate, 4-oxaheptan-1,7-dithiolate, or 4-thiaheptan-1,7-dithiolate) (280–283) in which the dithiocarbamate is highly anisobidentate (281). The analogous phenoxyarsinyl complexes $[As\{(C_6H_4)_2O\}(S_2CNR_2)]$, prepared by reaction of $[AsCl\{(C_6H_4)_2O]$ with the sodium salt of the appropriate dithiocarbamic acid, have also been reported (284). The X-ray molecular structure of the pyrrolidinedithiocarbamate complex $[As\{(C_6H_4)_2O\}\{S_2CN(CH_2)_4\}]$ again shows the dithiocarbamate to be highly anisobidentate [As—S(short) = 2.28; As—S(long) = 3.18 Å]. If both S atoms are included in the arsenic coordination sphere, the arsenic atom can be considered as having a highly distorted trigonal-bipyramidal geometry: The equatorial plane is defined by one C atom, one S atom, and the stereochemically active lone pair. The dihedral angle between the arene rings of the phenoxyarsine moiety is 155.2°. Hydrogen-1 and ^{13}C solution NMR data show that the dithiocarbamate N substituents are inequivalent, consistent with the dithiocarbamate ligand being nonlabile on the NMR chemical shift time scale and with restricted rotation about the $(S_2)C—N$ bond.

Few mono(dithiocarbamate) complexes of the type $[MR_2(S_2CNR'_2)]$ and $[MRX(S_2CNR'_2)]$ (M = As or Sb; R = Me or Ph; X = Cl or Br) have been reported (262, 285, 286). The NMR and IR spectroscopy, as well as molecular mass data, are consistent with the species being monomeric in solution and the dithiocarbamate ligand bidentate: The complexes have therefore been assigned as possessing pentagonal-bipyramidal structures (assuming a stereochemically active lone pair) in solution (262, 286). However, ^{121}Sb Mössbauer spectroscopy indicates that the Sb atom is more likely to be pyramidal in the solid state, with the lone pair of electrons apical and the dithiocarbamate ligand essentially monodentate (214). Conductimetry measurements on the arsenic(III) diiodide complex $[AsI_2Me(S_2CNMe_2)]$, which is prepared by the reaction of tetramethylthiuram disulfide with AsI_2Me, show it is ionic in solution, although data are inconsistent with a simple 1:1 electrolyte (285). The X-ray structure reveals a two-dimensional (2D) network (Fig. 25), in which $I—As—I\cdots I_2\cdots I—As—I$ chains are $I\cdots As\cdots I$ cross-linked: The dithiocarbamate ligand is essentially isobidentate (As—S = 2.31–2.35 Å).

The As(III), Sb(III), and Bi(III) complexes $[ML_3XY]$, $[ML_2XY_2]$, and $[M_2LX_5Y_2]$ (L = $S_2CN(H)o\text{-}C_6H_4Me$; X and Y = neutral or anionic ligands) have been screened for their antifungal activities. Although a number of the complexes, and in particular those in which a chloride ligand is present, display some activity, it is, in all cases, limited (287).

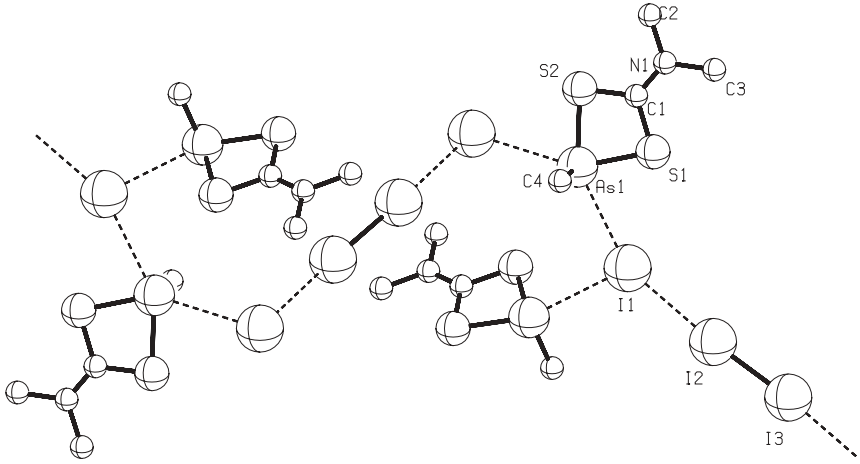

Figure 25. The PLUTON plot of $[AsI_2Me(S_2CNMe_2)]$ showing the 2D network of I···As···I cross-linked I–As–I···I_2···I–As–I chains. Intermolecular interactions are indicated by dashed lines.

4. Antimony(V) Complexes

The antimony(V) complexes $[SbMe_3(S_2CNR_2)_2]$ (288, 289), $[\{SbMe_3(S_2CNR_2)\}_2(\mu\text{-O})]$ (290), and $[SbAr_4(S_2CNR_2)]$ (Ar = phenyl or *p*-tolyl) (291, 292) have been prepared from the reaction of corresponding antimony halides (or dihalides) with the appropriate dithiocarbamate salts, although the reaction of $SbPh_3Cl_2$ with sodium diethyldithiocarbamate gave triphenylantimony(III), $SbPh_3$, and tetraethylthiuram disulfide (291). The dithiocarbamate ligands in $[SbMe_3(S_2CNMe_2)_2]$ are highly anisobidentate [Sb–S(short) = 2.61 (ave); Sb–S(long) = 3.30 Å (av)] (average = av) (289), whereas in $[SbPh_4(S_2CNMe_2)]$ (291) and $[SbAr_4(S_2CNEt_2)]$ (Ar = phenyl or *p*-tolyl) (292) there is little asymmetry. The geometry at Sb in $[SbMe_3(S_2CNMe_2)_2]$ is essentially trigonal bipyramidal, while in $[SbPh_4(S_2CNMe_2)]$ and $[SbAr_4(S_2CNEt_2)]$, it is octahedral.

5. Antimony-121 Mössbauer Spectroscopy

The ^{121}Sb Mössbauer spectra of a number of antimony dithiocarbamate complexes have been recorded (214, 246, 289): Data are reported in Table V. Data are difficult to interpret because subtle changes in the ligands can produce significant changes in the geometry at the metal atom, and examination of Table V does not reveal any clear correlation of the spectral parameters with the known structures.

TABLE V
Antimony-121 Mössbauer Data for Antimony Dithiocarbamate Complexes

Complex[a]	Geometry[b] at Sb	IS	QS	η	ρ	References
$[Sb(S_2CNn\text{-}Bu_2)_2][I_3]$	dtbp	−5.5	9.4	0.5	−1.7	214, 246
$[Sb(S_2CNn\text{-}Bu_2)_2]\cdot 0.5[Cd_2I_6]$	dtbp	−6.4	10.3	0.0	−1.6	214, 246
$[Sb(S_2CNEt_2)_3]$	ddh	−6.9	7.5	0.0	−1.1	214
		−6.8	7.8	0.0	−1.1	
$[Sb(S_2CNn\text{-}Bu_2)_3]$	ddh	−6.4	7.8	0.2	−1.2	214
$[SbCl(S_2CNEt_2)_2]$		−6.0	10.6	0.4	−1.8	214
$[SbBr(S_2CNEt_2)_2]$		−6.2	9.9	0.3	−1.6	214
$[SbI(S_2CNEt_2)_2]$	doh	−5.8	9.3	0.4	−1.6	214
$[SbCl_2(S_2CNEt_2)]$		−5.9	13.3	0.1	−2.3	214
$[SbBr_2(S_2CNEt_2)]$		−7.2	10.6	0.2	−1.5	214
$[SbI_2(S_2CNEt_2)]$		−7.2	8.1	0.0	−1.1	214
$[SbPh(S_2CNEt_2)_2]$	dpby	−4.1	22.2	0.2	−5.4	214
$[SbMe(S_2CNEt_2)_2]$	dpby	−4.0	25.1	0.2	−6.3	214
$[SbPh_2(S_2CNEt_2)]$		−2.5	20.0	1.0	−8.0	214
$[SbMe_3(S_2CNEt_2)_2]$	dtbp	2.7	−17.4	0.4	−6.4	214, 289
$[SbMe_4(S_2CNEt_2)]$	doh[c]	3.0	−2.1		−0.7	214

[a] IS = Isomer shift quoted in millimeters per second (mm s^{-1}) relative to InSb; QS = quadrupole splitting (in mm s^{-1}); η = asymmetry parameter; ρ = (QS/IS).
[b] From X-ray data where available. dtpy = distorted trigonal bipyramidal; ddh = distorted dodecahedral; dpby = distorted pentagonal bipyramidal; doh = distorted octahedral.
[c] Distorted octahedral geometry assumed on the basis that $[SbPh_4(S_2CNEt_2)]$ possesses a distorted octahedral geometry.

VI. GROUP 16 (VI A)

There are no oxygen dithiocarbamate complexes and, although dithiocarbamates do bond to sulfur, forming thiurams, these are considered as a separate class of compound and fall outside the scope of this chapter. While the dithiocarbamate complexes of selenium remain relatively few in number, those of tellurium have been studied more extensively, with particular attention being paid to the different possible coordination numbers and geometries displayed by the metal atom.

A. Homoleptic and Mixed Bidentate Ligand Complexes

Reaction of selenium(IV) dioxide with sodium dithiocarbamate salts yields the homoleptic selenium(II) bis(dithiocarbamate) complexes $[Se(S_2CNR_2)_2]$ (293–297). No selenium(IV) dithiocarbamate complexes appear to have been authenticated and dithiocarbamate ligands have been successfully employed as a method of separating selenites from selenates (298), as well as from other metal

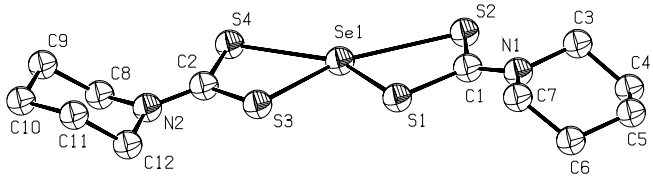

Figure 26. The ORTEP plot of $[Se\{S_2CN(CH_2)_5\}_2]$, showing the planar trapezoidal geometry at the metal center in the $[Se(S_2CNR_2)_2]$ complexes.

ions (299). The two dithiocarbamate ligands in the $[Se(S_2CNR_2)_2]$ complexes coordinate in an anisobidentate fashion [Se—S(av) = 2.31 (short) and 2.77 Å (long)]: The two S atoms with the short Se—S contacts are cis. The geometry at Se is planar trapezoidal (Fig. 26). Molecular mass measurements show that the complexes are monomeric in solution, and conductimetry and magnetic susceptibility measurements show them to be diamagnetic, non-electrolytes (293, 294).

Reaction of $[Se(S_2CNR_2)_2]$ with either bromine or iodine leads to the oxidative displacement of one of the dithiocarbamate ligands, yielding polymeric $[SeX(S_2CNR)]_\infty$, with the halide bridging and the dithiocarbamate bound in an essentially isobidentate fashion (ΔSe—S < 0.05 Å) (300, 301). The geometry at Se is, again, best described as planar trapezoidal (SSeS $\approx 77°$; XSeX $\approx 129°$). In solution, the complexes are only stable in the presence of the appropriate hydrohalic acid, HX (X = Br or I). The stability of the complexes increases as the size of the halogen increases; the corresponding chloro complex, $[SeCl(S_2CNR)]$, undergoes rapid decomposition via CS_2 elimination even in the presence of HCl (300).

Homoleptic dithiocarbamate complexes of both tellurium(II) (215, 293, 294, 296, 302–311) and tellurium(IV) (293, 294, 296, 302, 304–306, 309, 310, 312–315) are well known. The molecular structures of the bis(dithiocarbamate)tellurium(II) compounds, $[Te(S_2CNR_2)_2]$, are analogous to those of the corresponding Se compounds: The Te atom exhibits a planar trapezoidal coordination geometry, with the two dithiocarbamate ligands bound in an anisobidentate fashion [Te—S(ave) = 2.52 (short) and 2.83 Å (long)]. Tellurium(II) has a tendency for pentacoordination and, with the exception of $[Te(S_2CNCy_2)_2]$, which is monomeric (311), there is a short intermolecular Te···S contact (av 3.56 Å; cf. sum of van der Waals radii 3.86 Å) in the solid state, leading to the formation of weakly bound dimers. The geometry at Te atom in these complexes is thus described best as pentagonal bipyramidal with the five S atoms in the equatorial plane and the two, stereochemically active lone pairs axial. The mixed dithiocarbamate–xanthate complex, $[Te(S_2CNEt_2)(S_2COEt)]$ (316), is structurally analogous to the parent bis(dithiocarbamate) complex, $[Te(S_2CNEt_2)_2]$ (317). Like their Se analogues, all complexes are monomeric, diamagnetic, non-electrolytes in solution (293, 294).

The weak intermolecular Te···S interaction in the solid-state structures of the bis(dithiocarbamate)tellurium(II) complexes suggest that other ligands may be able to coordinate to the Te atom: This is indeed the case. The complexes $[Te(S_2CNEt_2)_2]$ and $[Te(S_2CN\textit{i}\text{-}Pr_2)_2]$ have been shown to form hemi-adducts with 4,4′-bipyridyl (4,4′-bpy) (318). The structure of $[\{Te(S_2CNEt_2)\}_2(\mu\text{-}4,4'\text{-bipy})]$ has been determined by X-ray crystallography. The geometry at each Te is pentagonal bipyramidal; the N and four S atoms lie in the equatorial plane and the two stereochemically active lone pairs are axial. The Te—N bonds are weak (2.70 Å) and the complexes are unstable with respect to loss of bpy.

With the exception of perchloric acid media, in which tris(dithiocarbamate)tellurium(IV) perchlorate species are formed (319), TeO_2 reacts with dithiocarbamate salts under acidic conditions to give the intensely colored homoleptic tetrakis(dithiocarbamate)tellurium(IV) complexes, $[Te(S_2CNR_2)_4]$. The intense coloration results form ligand-to-metal charge transfer (LMCT) bands in the visible region (293).

The $[Te(S_2CNR_2)_4]$ complexes are generally unstable. The complexes undergo facile decomposition to the corresponding bis(dithiocarbamate)tellurium(II) complex and thiuram disulfide. It has been suggested (320) that the mechanism of decomposition involves interligand S—S bond formation between the two spatially close S atoms, followed by cleavage of the corresponding Te—S bonds. This mechanism may be the dominant process, but the differences in the relative stabilities of the complexes do not correlate well with the (small) structural variations observed; other factors, such as the reducing ability of the ligand and intermolecular interactions, are also likely to play a role.

Despite their instability, several $[Te(S_2CNR_2)_4]$ complexes have been characterized crystallographically (312–315). In all cases, the Te atom possesses a slightly distorted dodecahedral geometry (Fig. 27), in which all eight S atoms are coordinated and the lone pair is stereochemically inert. A regular dodecahedron can be considered as being comprised of two interleaved, perpendicular trapezoids: The angles between the two planes in the dithiocarbamate complexes are 90° (*N*-2-hydroxyethyl-*N*-methyldithiocarbamate) (312), 86.5° (di-2-hydroxyethyldithiocarbamate) (313), 87.6° (diisopropyldithiocarbamate) (314) and 89.6° (diethyldithiocarbamate) (315). The trapezoidal planes are similar to those observed in the bis(dithiocarbamate)tellurium(II) complexes.

The attempted isolation of the cationic Te(IV) species $[Te(S_2CNEt_2)_3]^+$ by the substitution of the weakly coordinating perchlorate ligand in $[Te(S_2CNEt_2)_3][ClO_4]$ (319) with the hexafluorophosphate anion gave the mixed-valence species $[\{Te^{IV}(S_2CNEt_2)_3\}_2\{Te^{II}(S_2CNEt_2)_2\}][PF_6]_2$ (321), in which the $[Te(S_2CNEt_2)_2]$ moiety is sandwiched between the two $[Te(S_2CNEt_2)_3]^+$ units, held together by weak Te···Te (3.39 Å) and Te···S interactions (Fig. 28): the TeTeTe bond angle is 161.4°. The perchlorate complex, $[\{Te^{IV}(S_2CNEt_2)_3\}\{Te^{II}(S_2CNEt_2)_2\}][ClO_4]$ is also comprised of $[Te(S_2CNEt_2)_2]$ and

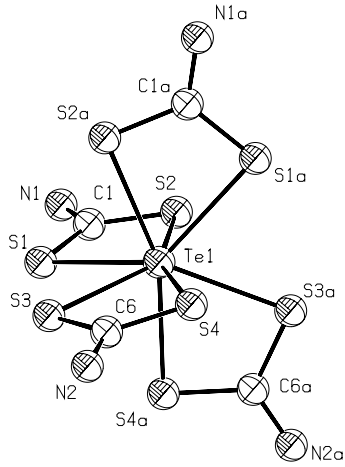

Figure 27. The ORTEP plot of $[Te(S_2CNEt_2)_4]$, showing the distorted dodecahedral geometry at Te in the tetrakis(dithiocarbamate) complexes $[Te(S_2CNR_2)_4]$. The N substituents omitted for clarity.

$[Te(S_2CNEt_2)_3]^+$ units, but in a 1:1 ratio, again held together by secondary Te···Te and Te···S contacts (321).

Dithiocarbamate ligands do not appear to complex tellurium(VI) and have been used successfully to separate aqueous mixtures of Te(IV) and Te(VI) (322).

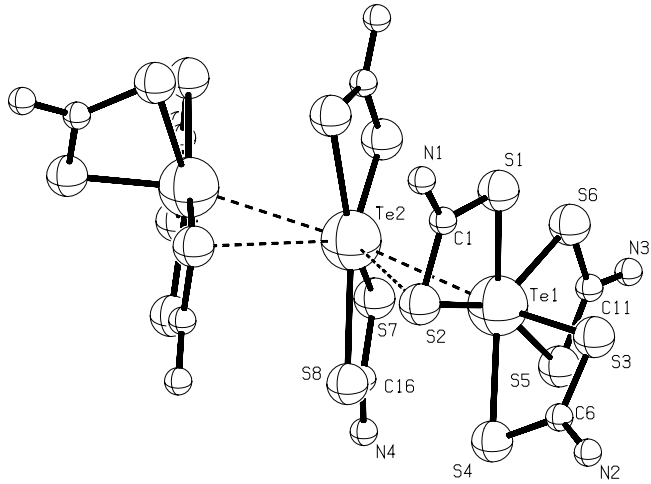

Figure 28. The PLUTON plot of $[\{Te^{IV}(S_2CNEt_2)_3\}_2\{Te^{II}(S_2CNEt_2)_2\}][PF_6]_2$. The PF_6 counterions omitted for clarity. Intermolecular interactions are indicated by dashed lines.

B. Nonhomoleptic Tellurium(II) Complexes

Formation of nonhomoleptic complexes by substitution of one of the dithiocarbamate ligands in the $[Te(S_2CNR_2)_2]$ complexes is generally difficult because of the strength of the Te—S bonds and is often only feasible when electron-withdrawing substituents, such as CH_2CH_2OH, are attached to the dithiocarbamate. However, improvements in synthetic methodologies have enabled organyl, halide and pseudo-halide substituted analogues to be prepared (309, 323–332).

The organic ligands in the $[TeR(S_2CNR'_2)]$ complexes [R = 2-phenylazophenyl, R′ = Me or Bz (323); R = 2-(2-quinolinyl)phenyl, R′ = Et (324); R = 2-(2-pyridyl)phenyl, R′ = Me (325); R = 8-(dimethylamino)-1-naphthyl, R′ = Et (331)] are C,N coordinated in the solid state, with the dithiocarbamate ligand highly anisobidentate: The Te—S distances are in the range 2.52–2.57 (short) and 3.23–3.67 Å (long). Two distinct geometries at Te are apparent (Fig. 29). In

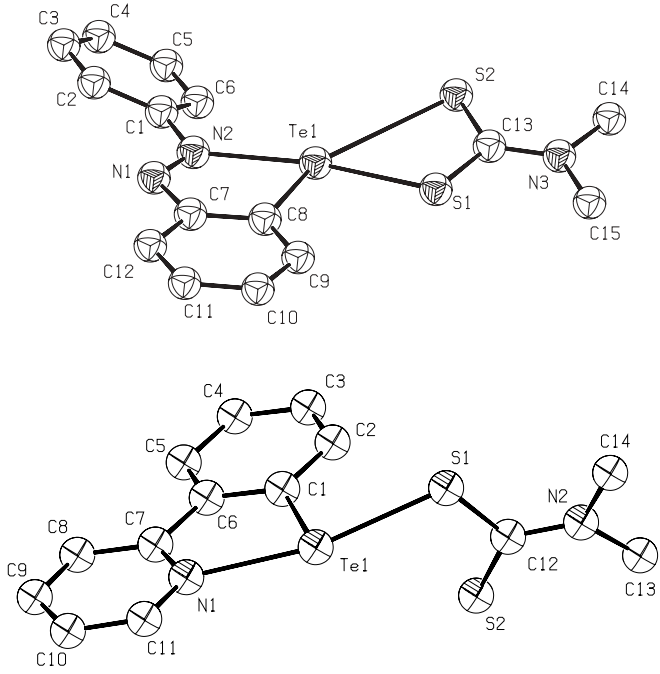

Figure 29. The ORTEP plots of (*a*) $[TeR(S_2CNMe_2)]$ (R = 2-phenylazophenyl) and (*b*) $[TeR(S_2CNMe_2)]$ [R = 2-(2-pyridyl)phenyl], showing the two types of coordination geometry exhibited by Te in the $[TeR(S_2CNR'_2)]$ complexes [R = 2-phenylazophenyl, 2-(2-quinolinyl)phenyl, 2-(2-pyridyl)phenyl or 8-(dimethylamino)-1-naphthyl].

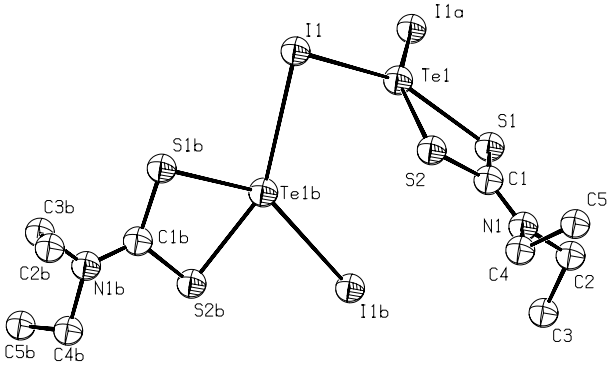

Figure 30. The ORTEP plot of $[TeI(S_2CNEt_2)_2]$, showing a section of the polymeric chain arrangement in the tellurium(II) complexes$[TeI(S_2CNR_2)]$.

the 2-phenylazophenyl and 8-(dimethylamino)-1-naphthyl complexes, the Te atom has a planar-trapezoidal geometry, with the two lone pairs above and below the plane, whereas in the 2-(2-quinolinyl)phenyl and 2-(2-pyridyl)phenyl complexes, in which the dithiocarbamate is essentially monodentate, the geometry is best considered as distorted trigonal planar.

The iodo-complex $[TeI(S_2CNEt_2)]$ can be prepared by reduction of $[TeI_2(S_2CNEt_2)_2]$ with elemental Te (327). The corresponding chloro and bromo complexes, $[TeX(S_2CNEt_2)]$, can be prepared by halide substitution, using AgX (X = Cl or Br) (329). In the solid state the halide bridges two Te atoms, forming a helical polymeric arrangement (Fig. 30). The TeI_2S_2 core is essentially planar, with the dithiocarbamate ligand coordinated in an anisobidentate fashion. There is an intermolecular Te $\cdots$ Te contact [distances vary from 3.88 (I) to 3.65 Å (Cl) (av = 3.76 Å)], indicating a weak bonding interaction (sum of van der Waals radii = 4.12 Å) and a long-range intermolecular Te $\cdots$ S interaction (average 3.74 Å).

The $[TeX(S_2CNEt_2)]$ compounds (X = Br or I) react with tetraethylammonium halide salts or phen, giving $[TeX_2(S_2CNEt_2)][NEt_4]$ and $[TeX_2(S_2CNEt_2)][H(phen)_2]$ (where X = Br or I), respectively; the corresponding chloro complexes are not formed (330). The Te atom in the $[TeX_2(S_2CNEt_2)]^-$ anion displays a planar trapezoidal coordination geometry as a consequence of the small bite angle of the dithiocarbamate ligand (av = 69.9°); the corresponding XTeX angle is (av) 126.7°. The almost isobidentate dithiocarbamate [ΔTe—S(av) = 0.04 Å] exerts a strong trans influence, weakening the Te—X bonds: Te—X(av) = 3.09 Å (I) and 2.95 Å (Br) [cf. sum of covalent radii: 2.70 Å (TeI); 2.43 Å (TeBr)].

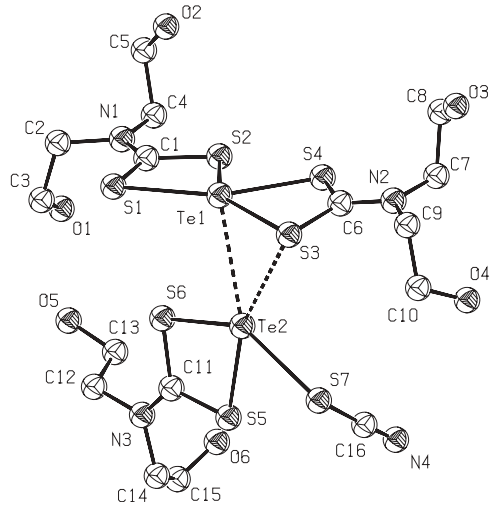

Figure 31. The ORTEP plot of $[Te_2(SCN)(S_2CNR_2)_3]$. Intermolecular contacts are indicated by dashed lines.

Reaction of $[Te\{S_2CN(CH_2CH_2OH)_2\}_2]$ with a large excess of KX (X = Br, I, or SCN) gives complexes of general formula $[Te_2X(S_2CNR_2)_3]$ (328). X-ray crystallography of the thiocyanato complex reveals a 1:1 adduct of $[Te\{S_2CN(CH_2CH_2OH)_2\}_2]$ and $[Te(SCN)\{S_2CN(CH_2CH_2OH)_2\}]$ held together by weak Te···Te (3.22 Å) and Te···S (3.48 Å) intermolecular interactions between the two moieties: Both Te atoms are thus pseudo-five coordinate (Fig. 31). The $[Te\{(S_2CN(CH_2CH_2OH)_2\}_2]$ moiety differs little chemically from that in the pure crystalline material (313). The dithiocarbamate ligand is bound in an isobidentate fashion in the $[Te(SCN)\{S_2CN(CH_2CH_2OH)_2\}]$ unit [Δ(Te–S) < 0.01 Å], which is also essentially planar: The dihedral angle between the TeS_4 and TeS_3 planes is 99.6°. The thiocyanato ligand is S bonded to Te.

Addition of sodium diethyldithiocarbamate or dimethyldithiocarbamate salts to the aryl complexes $[TeRL_2]Cl$ (R = 4-hydroxyphenyl, 4-methoxyphenyl, or 4-ethoxyphenyl; L = benzaldehyde or salicylaldehyde) leads to the displacement of both the chloride and the aldehyde ligand, yielding complexes of general formula $[TeR(S_2CNR'_2)][NaS_2CNR'_2]$ (R′ = Me or Et), in which it has been suggested the sodium dithiocarbamate is closely associated with the $[TeR(S_2CNR'_2)]$ moiety, presumably via an η^1 Te—S bonding mode (326). The structures of these complexes have yet to be confirmed by crystallography.

The complex $[Te_2I_3(S_2CN\textit{i}\text{-}Pr_2)_3]$ is a 1:1 adduct of the Te(IV) complex $[TeI_2(S_2CN\textit{i}\text{-}Pr_2)_2]$ and the Te(II) complex $[TeI(S_2CN\textit{i}\text{-}Pr_2)]$, in which the two Te units are bridged by an iodine atom (Fig. 32) (332). There is a weak Te···Te

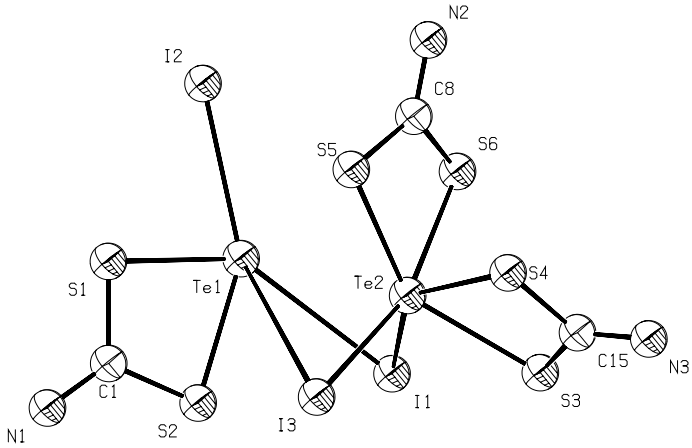

Figure 32. The ORTEP plot of $[Te_2I_3(S_2CN\textit{i}\text{-}Pr_2)_3]$, which is a 1:1 adduct of the tellurium(II) species $[TeI(S_2CN\textit{i}\text{-}Pr_2)]$ and the tellurium(IV) species $[TeI_2(S_2CN\textit{i}\text{-}Pr_2)_2]$. The N substituents omitted for clarity.

interaction (3.542 Å), so that the coordination geometries at both Te(II) and Te(IV) are best considered as distorted pentagonal bipyramidal: The stereochemically active lone pairs on Te(II) are axial. The Te—S bond lengths are 2.44 and 2.56 Å for Te(II) and for Te(IV), the Te—S bond lengths 2.48 and 2.55 (short), and 2.65 and 2.58 Å (long).

C. Nonhomoleptic Tellurium(IV) Complexes

1. Tris(dithiocarbamate) Complexes

Formal substitution of one of the dithiocarbamates in $[Te(S_2CNR_2)_4]$ by a uninegative ligand gives seven coordinate Te(IV) complexes of general formulas $[TeR(S_2CNR_2)_3]$ and $[TeX(S_2CNR_2)_3]$ (R = aryl; X = halide or pseudohalide) (293, 304, 309, 312, 319, 323, 333–342). In all cases the geometry at Te is distorted pentagonal bipyramidal, with the uninegative ligand (R or X) axial and one dithiocarbamate ligand spanning axial and equatorial positions. The bite angle of the dithiocarbamate ligand (mean STeS bond angle is 66.6°) is too small for the S atoms to be simultaneously in truly axial and equatorial positions and, consequently, two structural types can be distinguished (Fig. 33): (1) one of the S atoms is essentially axial (av $R/XTeS_{ax}$ angle = 171.5°) while the other is positioned below the equatorial plane and (2) one of the S atoms is in the equatorial plane, while the other is pulled away from a true axial position, reducing the $R/XTeS_{ax}$ bond angle to ∼144.3° (av). As the electronegativity of

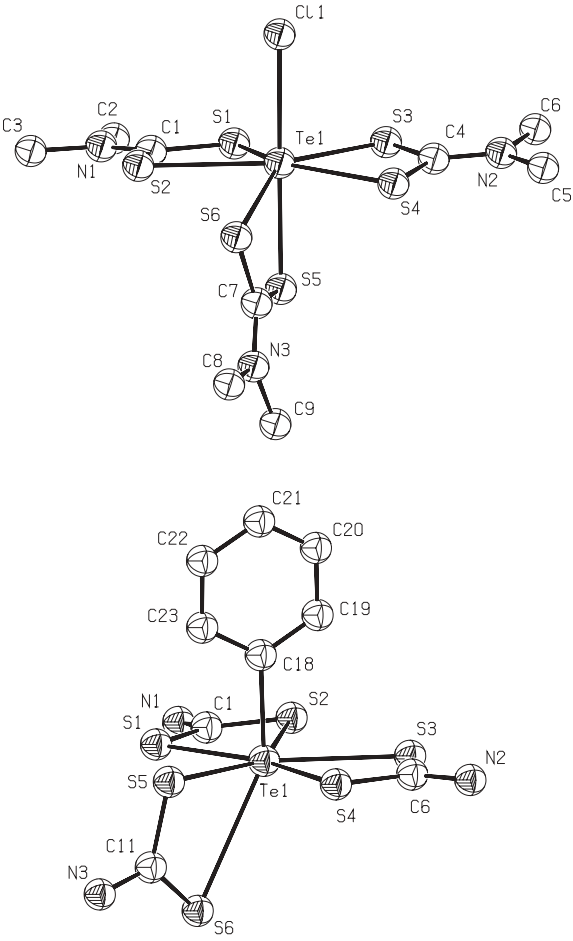

Figure 33. The ORTEP plots of (*a*) [$TeCl(S_2CNMe_2)_3$] and (*b*) [$TePh(S_2CNEt_2)_3$], showing the two structural types found in the [$TeR(S_2CNR_2)_3$] and [$TeX(S_2CNR_2)_3$] complexes (R = aryl; X = halide or pseudo-halide). The N substituents of [$TePh(S_2CNEt_2)_3$] omitted for clarity.

the tellurium substituent increases, so the structures tend toward the former type; thus halide and pseudo-halide complexes fall in category (1), while aryl complexes fall in category (2). In both cases, there is an approximate mirror plane perpendicular to the equatorial plane of the molecule. The unique axial–equatorial dithiocarbamate ligand is highly anisobidentate: The asymmetry in these Te—S bond lengths, which varies considerably (ΔTe—S = 0.15–0.69 Å), is smallest in the halide–pseudo-halide complexes; this is presumably because of the weaker trans influence of the halide–pseudo-halide and/or the increase in

Lewis acidity at the metal center. The long Te—S bond is equatorial in the halide and pseudo-halide complexes [type (1) structure] and axial in the aryl complexes [type (2) structure]. The two equatorial dithiocarbamate ligands, which are coordinated to the Te atom in a trapezoidal fashion, are also anisobidentate, although less so [ΔTe—S(av) $\approx$ 0.13 Å]. The lone pair of electrons on Te, which probably occupies a low-lying, ligand-centered antibonding orbital, is essentially stereochemically inert, although it does exert some influence on the precise geometry adopted at Te.

Tellurium dioxide reacts with sodium dithiocarbamate salts in the presence or perchloric acid to yield the perchlorate complexes $[Te(S_2CNR_2)_3(ClO_4)]$ or $[Te_3(S_2CNR_2)_9(ClO_4)(OH)_2]$, depending on the reaction conditions (319). The X-ray molecular structure of $[Te(S_2CNR_2)_3(ClO_4)]$ reveals that the perchlorate ligand is weakly bound to the metal center via two oxygen atoms (Te—O = 2.87 and 3.12 Å). The Te atom thus adopts a dodecahedral arrangement, formed by two interposing trapezoids. The dihedral angle between the two trapezoidal planes is 88.4°, comparable to that in the tetrakis(dithiocarbamate) complexes.

2. *Bis(dithiocarbamate) Complexes*

Several dihalogeno bis(dithiocarbamate) complexes, $[TeX_2(S_2CNR_2)_2]$ (X = Cl, Br, or I), have been reported (293, 309, 342–346). The complexes that have been analyzed crystallographically display one of two distinct structural types (Fig. 34): The $[TeBr_2(S_2CNEt_2)_2]$ (343) and $[TeI_2(S_2CN$*i*-$Pr_2)_2]$ (345) are monomeric in the solid state, with the halides essentially cis [XTeX(av) = 99.8°], whereas $[TeI_2(S_2CNEt_2)_2]$ (346) and $[TeI_2\{S_2CN(CH_2CH_2OH)_2)_2]$ (344) are centrosymmetric halide-bridged dimers, with the halides essentially trans [XTeX(av) = 173.8°]. The dithiocarbamate ligands are unsymmetrically chelating in both cases, but the anisobidenticity is considerably greater in the dimeric species [ΔTe—S(av) = 0.04 and 0.22 Å, respectively]. The Te atom is thus six coordinate in the monomers and seven coordinate in the halide-bridged dimers. The halogen and three S atoms occupying the equatorial positions in the monomeric species have a trapezoidal arrangement, opening a space in the polyhedron, which may be occupied by the lone pair. It is difficult to determine unambiguously if the lone pair has a stereochemical role, but if it is considered active, then the geometry at Te would best be described as distorted pentagonal bipyramidal in both structural types.

Formal substitution of one of the halides with an alkyl or aryl group gives the complexes $[TeXR(S_2CNR'_2)_2]$ (347–352). The NMR data (347) indicate that the complexes are monomeric in solution, but secondary Te$\cdots$S or Te$\cdots$X interactions in the aryl complexes lead to the formation of centrosymmetric dimers in the solid state. The relative strengths of the secondary interactions are in the order Te$\cdots$I > Te$\cdots$Br > Te$\cdots$S > Te$\cdots$Cl, as expected for the soft Te

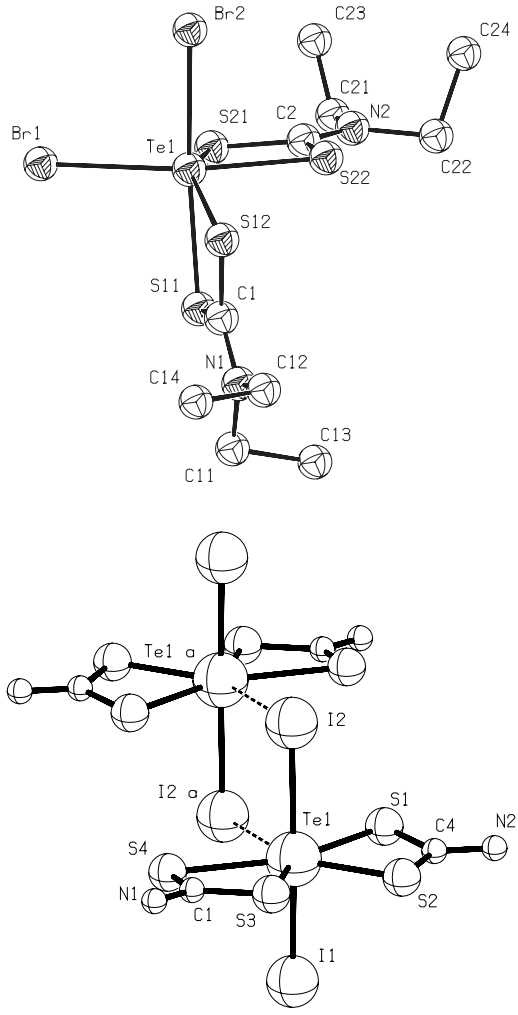

Figure 34. The two structural types exhibited by the $[TeX_2(S_2CNR_2)_2]$ complexes (X = Cl, Br, or I), exemplified by (*a*) the ORTEP plot of $[TeBr_2(S_2CNEt_2)_2]$ and (*b*) PLUTON plot of $[TeI_2(S_2CNEt_2)_2]$. Dashed lines indicate intermolecular contacts. The N substituents of $[TeI_2(S_2CNEt_2)_2]$ omitted for clarity.

atom; the type of secondary interaction appears to be governed by crystal packing effects (349). The halogen and four S atoms of the almost isobidentate dithiocarbamates comprise the equatorial plane, with the C(aryl) axial. The secondary interactions are directed toward the empty (axial) coordination site, indicating that the lone pair is essentially inert stereochemically. The alkyl

complex $[TeIMe(S_2CNEt_2)_2]$ is analogous to the aryl complexes, but there are no significant secondary interactions and it is monomeric both in the solid state and in solution (347).

In the perchlorate complex $[Te(p\text{-}C_6H_4OCH_3)(S_2CNMe_2)_2(ClO_4)]$ (353), an oxygen atom of the perchlorate coordinates to the Te in an equatorial position so that, with the exception that the dithiocarbamate ligands are anisobidentate (ΔTe—S = 0.29 Å), it is structurally similar to the $[TeXR(S_2CNR_2)_2]$ complexes.

The diorganyl complexes, $[TeR_2(S_2CNR_2)_2]$ (R = alkyl or aryl), which are prepared by the reaction of TeR_2Cl_2 with the appropriate sodium dithiocarbamate salt, are structurally very different from the $[TeXR(S_2CNR'_2)_2]$ complexes (152, 354–362). The dithiocarbamate ligands are highly anisobidentate, to the extent that they are often best considered as monodentate. The average Te—S(short) distance is 2.62 Å and varies little. The Te—S(long) bond lengths range between 3.05 and 3.33 Å (cf. sum of van der Waals radii = 4.05 Å); the corresponding normalized Pauling bond orders (360) vary between 0.38 and 0.20. If the dithiocarbamates are considered as monodentate, then the geometry at Te is trigonal bipyramidal; the stereochemically active lone pair and two organic groups are equatorial, and the two S atoms axial. There is some flexibility in the STeS angle, which varies between 162.2 and 179.0° (av = 170.9°), but there is no obvious trend in terms of either the dithiocarbamate or Te substituents.

Although the $[TeR_2(S_2CNR_2)_2]$ complexes undergo slow disproportionation to yield TeR_2 and the corresponding thiuram disulfide, they are sufficiently stable to allow detailed studies to be carried out. In solution, rapid intramolecular exchange occurs between η^1 and η^2 dithiocarbamate bonding modes (i.e., monodentate $\rightleftarrows$ bidentate), so that, on the NMR time scale, the Te atom has a 1:2:2:2 geometry, including the lone pair (355). Although it is slow on the NMR time scale, intermolecular ligand exchange also occurs readily in solution, allowing mixed-ligand complexes of the type $[TeR_2(S_2CNR'_2)L]$ (L = uninegative bidentate ligand) to be prepared (355, 357, 360, 362–365): the complexes are structurally analogous to the parent bis(dithiocarbamates).

3. *Mono(dithiocarbamate) Complexes*

With the exception of the $[TeX_2(aryl)(S_2CNEt_2)]$ complexes (X = Br or I; aryl = C_6H_5 or p-$MeOC_6H_4$) (370), the molecular structures of the mono (dithiocarbamate) species $[TeR_{3-n}X_n(S_2CNR_2)]$ (R = alkyl or aryl, X = Cl, Br or I, and n = 0, 1, 2, or 3) (323, 355, 358–360, 366–374) are all similar.

Although essentially monomeric in solution (366, 367), intermolecular Te$\cdots$S or Te$\cdots$X interactions in the $[TeR_{3-n}X_n(S_2CNR_2)]$ complexes (R = alkyl or aryl, X = Cl, Br, or I, and n = 0, 1, or 3) lead to the formation of dimers or

polymers in the solid state. The basic molecular structures can be considered as being derived from the formal substitution of one of the dithiocarbamate ligands in the bis(dithiocarbamate) complexes, $[TeR_{2-n}X_n(S_2CNR'_2)_2]$ ($n = 0$, 1, or 2), with an additional halide or organic group: Thus the Te atom is best considered as possessing a distorted-trigonal-bipyramidal geometry, with the stereochemically active lone-pair equatorial [Fig. 35(*a*)]. The dithiocarbamate ligands are anisobidentate; the asymmetry decreases essentially in line with increasing electronegativity of the Te substituents (i.e., with increasing Lewis acidity of the metal center). For dialkyl complexes the Te—S distances are in the range 2.43–2.55 Å (short) and 3.10–3.30 Å (long); the normalized Pauling bond order (360) of the latter is ~0.22 (av). The Te—S lengths are considerably longer in the triorganyl complexes [~3.10 (short) and 3.60 Å (long)] (368, 369), indicating a very weak interaction between the dithiocarbamate and the metal moiety. As would be expected, the Te—S bonds are much shorter (2.43 and 2.68 Å) in the triiodo complex, $[TeI_3(S_2CNEt_2)]$ (371).

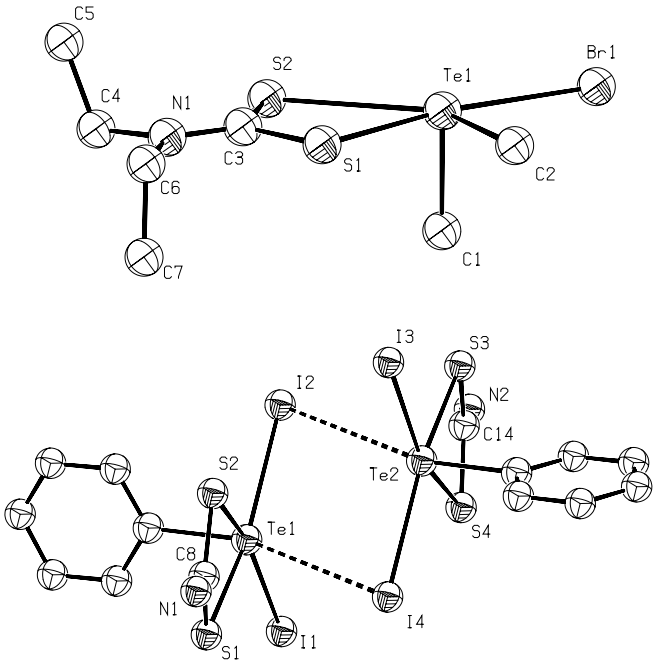

Figure 35. (*a*) The ORTEP plot of $[TeMe_2Br(S_2CNEt_2)]$ showing the basic molecular structure of the $[TeR_{3-n}X_n(S_2CNR_2)]$ complexes (R = alkyl or aryl, X = Cl, Br, or I, and $n = 0$, 1, or 3). (*b*) ORTEP plot of $[TePhI_2(S_2CNEt_2)]$, showing the dimeric solid-state structure of the [Te(aryl)$X_2(S_2CNEt_2)$] complexes (X = Br or I; aryl = C_6H_5 or *p*-$MeOC_6H_4$). The N substituents of $[TePhI_2(S_2CNEt_2)]$ and phenyl ring C atom labels omitted for clarity.

The geometry of the Te atom in the $[Te(aryl)X_2(S_2CNEt_2)]$ complexes (X = Br or I; aryl = C_6H_5 or *p*-$MeOC_6H_4$) (370), is octahedral: The two halogen atoms are cis (XTeX $\approx 110^\circ$) and the aryl group axial. The second axial position is occupied by a weakly bonding halogen atom of a neighboring molecule, giving a quasi-centrosymmetric dimmer [Fig. 35(*b*)]. The lone pair is essentially inert and the dithiocarbamate ligand almost isobidentate (ΔTe—S ≈ 0.02 Å).

The Te atom in the monomeric tetrahalo anions, $[TeX_4(S_2CNR_2)]^-$ (X = Br or I) (342, 375) is also octahedral, and the dithiocarbamate ligand is, again, essentially isobidentate.

The NMR spectra of the mono(dithiocarbamate) complexes are generally difficult to interpret due to ligand exchange reactions, metal-centered rearrangements and reductive elimination reactions occurring quite rapidly on the NMR time scale (358–360): The occurrence of these processes indicates that the dithiocarbamate is only weakly bound to Te. Furthermore, conductimetry measurements show the triphenyl complexes $[TePh_3(S_2CNR_2)]$ are close to 1:1 electrolytes, again indicative of the dithiocarbamate being only weakly associated with the metal moiety in solution (367, 369).

4. Tellurium-125 NMR and Mössbauer Spectroscopy

Tellurium-125 NMR spectroscopy has been applied extensively to the study of Te dithiocarbamate complexes (304, 306, 310, 323, 331, 347, 355, 357–360, 361, 363–366, 372, 374); data are reported in Table VI. Caution should be exercised in data interpretation because of the instability of many of the complexes in solution, and their ability to undergo facile intermolecular ligand-exchange reactions. The chemical-shift range for tellurium dithiocarbamate complexes appears to span just <2000 ppm (ca. -600 to 1240 ppm, relative to $TeMe_2$); the shifts of the Te(II) complexes occur at the high frequency end of the range. Data also reveal that the shifts generally move to higher frequency as the electronegativity of the Te substituents increases, consistent with the shifts being dominated by the contribution of valence orbital populations to the paramagnetic shielding term (304).

Tellurium NMR is particularly well suited to the study of ligand-exchange reactions. Although facile, the rate of exchange is generally comparable to, or slow on the NMR chemical shift time scale (304, 306, 347, 355, 357). Rates of exchange appear to be more rapid in Te(II) species than in Te(IV) (306). The ^{125}Te NMR spectrum of a mixture of $[Te(S_2CNEt_2)_2]$, $(Et_2NCS_2)_2$, and $(i\text{-}Pr_2NCS_2)_2$ displays five signals, assignable to $[Te(S_2CNEt_2)_4]$, $[Te(i\text{-}Pr_2NCS_2)(S_2CNEt_2)_3]$, $[Te(i\text{-}Pr_2NCS_2)_2(S_2CNEt_2)_2]$, $[Te(i\text{-}Pr_2NCS_2)_3(S_2CNEt_2)]$, and $[Te(i\text{-}Pr_2NCS_2)_4]$ (304). The generation of Te(IV) species from Te(II) and the thiuram disulfides shows clearly that the reductive elimination of thiuram disulfide from Te(IV) species is reversible.

TABLE VI
Tellurium-125 NMR[a] Data for Tellurium Dithiocarbamato Complexes

Complex	Solvent[b]	δ (^{125}Te)	References
$[Te(S_2CNEt_2)_4]$	C_6D_6	−600	306
	THF	−577	306
	$CDCl_3$	−561	304
$[Te(S_2CNEt_2)_3\{S_2CN(CH_2)_4O\}]$	THF	−570	306
$[Te(S_2CNEt_2)_2\{S_2CN(CH_2)_4O\}_2]$	THF	−564	306
$[Te(S_2CN\textit{n}\text{-}Pr_2)_4]$	$(CD_3)_2CO$	−561	304
$[Te(S_2CNEt_2)\{S_2CN(CH_2)_4O\}_3]$	THF	−559	306
$[Te\{S_2CN(CH_2)_4O\}_4]$	THF	−555	306
$[Te(S_2CN\textit{i}\text{-}Bu_2)_4]$	$(CD_3)_2CO$	−543	304
$[Te(S_2CN\textit{i}\text{-}Pr_2)_4]$	$(CD_3)_2CO$	−416	304
	$CDCl_3$	−403	304
$[Te(S_2CNBz_2)_4]$	$CDCl_3$	−299	304
$[TeI(S_2CNEt_2)_3]$	$CDCl_3$	−218	304
$[TeMeI(S_2CNEt_2)_2]$	CD_2Cl_2	−160	347
$[TeCl(S_2CNEt_2)_3]$	$CDCl_3$	−155	304
$[Te(SCN)(S_2CNEt_2)_3]$	$CDCl_3$	−129	304
$[TeMe(S_2CNEt_2)_2\{S_2P(OEt)_2\}]$	CD_2Cl_2	−36	347
$[TeMe(S_2CNEt_2)_2(S_2COEt)]$	CD_2Cl_2	10	347
$[TeMe(S_2CNEt_2)_3]$	CD_2Cl_2	59	347
$[TePhCl(S_2CNEt_2)_2]$	THF	110	347
$[TePh(S_2CNEt_2)_2\{S_2P(OEt)_2\}]$	CD_2Cl_2	169	347
$[TePh(S_2CNEt_2)_2(S_2COEt)]$	CD_2Cl_2	222	347
$[TePh(S_2CNEt_2)_3]$	THF	277	347
$[TeMe_2(S_2CNEt_2)_2]$	*c*	463	359
$[TeMe_2\{S_2CN(CH_2)_5\}_2]$	$CDCl_3$	465	360
$[TeMe_2\{S_2CN(CH_2)_4\}\{S_2CN(CH_2)_5\}]$	$CDCl_3$	469	360
$[TeMe_2(S_2CNEt_2)(S_2COMe)]$	$CDCl_3$	474	363
$[TeMe_2(S_2CNMe_2)_2]$	*c*	475	359
$[TeMe_2(S_2CNMe_2)(S_2COEt)]$	$CDCl_3$	488	363
$[TeMe_2(S_2CNMe_2)(S_2COMe)]$	$CDCl_3$	491	363
$[TeMe_2\{S_2CN(CH_2)_4\}_2]$	$CDCl_3$	500	360
$[TeMe_2I\{S_2CN(CH_2)_4\}]$	$CDCl_3$	500	360
$[TeMe_2I(S_2CNEt_2)]$	$CDCl_3$	501	372
$[TeMe_2I\{S_2CN(CH_2)_5\}]$	$CDCl_3$	501	360
$[TeMe_2I(S_2CNMe_2)]$	$CDCl_3$	507	372
$[TeMe_2Br(S_2CNEt_2)]$	$CDCl_3$	527	372
$[TeMe_2Br\{S_2CN(CH_2)_5\}]$	$CDCl_3$	529	360
$[TeMe_2Br\{S_2CN(CH_2)_4\}]$	$CDCl_3$	534	360
$[TeMe_2Br(S_2CNMe_2)]$	$CDCl_3$	536	372
$[TeMe_2Cl(S_2CNEt_2)]$	*c*	545	359
$[TeMe_2Cl\{S_2CN(CH_2)_5\}]$	$CDCl_3$	548	360
$[TeMe_2Cl\{S_2CN(CH_2)_4\}]$	$CDCl_3$	552	360
$[TeMe_2Cl(S_2CNMe_2)]$	*c*	554	359
$[Te(C_8H_8)(S_2CN\textit{i}\text{-}Pr_2)_2]$	CD_2Cl_2	590	355
$[Te(S_2CNEt_2)(S_2CN\textit{i}\text{-}Pr)]$	CD_2Cl_2	601	355
$[Te(C_8H_8)(S_2CNEt_2)_2]$	CD_2Cl_2	611	355

TABLE VI (*continued*)

Complex	Solvent[b]	δ (^{125}Te)	References
		627	362
[$TePhCl_2(S_2CNEt_2)$]	THF; 233 K	634	347
[$Te(C_8H_8)(S_2CNEt_2)(S_2COEt)$]	CD_2Cl_2	634	355
[$Te(C_8H_8)(S_2CN$*i*-$Pr_2)\{S_2P(OEt)_2\}$]	CD_2Cl_2	660	355
[$Te(C_8H_8)(S_2CN$*i*-$Pr_2)\{S_2P(O$*i*-$Pr)_2\}$]	$CDCl_3$	670	355
[$Te(C_8H_8)(S_2CNEt_2)\{S_2P(OEt)_2\}$]	CD_2Cl_2	672	355, 362
[$Te(C_8H_8)(S_2CNEt_2)\{S_2P(O$*i*-$Pr)_2\}$]	CD_2Cl_2	677	355
[$TePh_2(S_2CNEt_2)_2$]	CD_2Cl_2	692	357
[$TePh_2(S_2CN$*n*-$Pr_2)_2$]	*c*	703	358
[$TePh_2(S_2CN$*n*-$Bu_2)_2$]	*c*	704	358
[$Te($*p*-$MeOC_6H_4)(S_2CNEt_2)_2$]	*c*	711	359
[$Te($*p*-$MeOC_6H_4)(S_2CNMe_2)_2$]	*c*	724	359
[$Te(C_8H_8)\{S_2CN(CH_2)_5\}\{(SPPh_2)_2N\}$]	*c*	725	364, 365
[$Te(C_8H_8)I(S_2CNEt_2)$]	DMF; 233 K	726	366
	$CDCl_3$	773	374
[$Te(C_8H_8)(S_2CNEt_2)\{(SPPh_2)_2N\}$]	*c*	728	364, 365
[$TePh_2(S_2CNEt_2)(S_2COEt)$]	THF; 233 K	729	357
[$TePh_2(S_2CNEt_2)\{S_2P(OEt)_2\}$]	DMF; 233 K	736	357
[$Te(C_8H_8)\{S_2CN(CH_2)_4O\}\{(SPPh_2)_2N\}$]	*c*	736	364, 365
[$Te(C_8H_8)\{S_2CN(CH_2)_4S\}\{(SPPh_2)_2N\}$]	*c*	737	364, 365
[$Te(C_8H_8)Br(S_2CNEt_2)$]	DMF; 233 K	750	366
[$TePh_2Br(S_2CN$*i*-$Pr_2)$]	*c*	763	358
[$TePh_2Br(S_2CN$*n*-$Pr_2)$]	*c*	774	358
[$TePh_2Br(S_2CNEt_2)$]	*c*	774	358
[$Te(C_8H_8)I(S_2CNC_4H_6)$]	$CDCl_3$	775	374
[$TePh_2Br(S_2CN$*n*-$Bu_2)$]	*c*	775	358
[$TePh_2Br(S_2CNMe_2)$]	*c*	779	358
[$TePh_2Cl(S_2CN$*n*-$Bu_2)$]	*c*	779	358
[$Te(S_2CNEt_2)\{S_2CN(CH_2)_4O\}$]	CD_2Cl_2; 233 K	786	306
[$Te($*p*-$MeOC_6H_4)Cl(S_2CNEt_2)$]	*c*	788	359
[$TePh_2Cl(S_2CNEt_2)$]	DMF; 233 K	789	357
[$Te($*p*-$MeOC_6H_4)Cl(S_2CNMe_2)$]	*c*	794	359
[$Te(S_2CNEt_2)_2$]	CD_2Cl_2; 275 K	802	306
	$(CD_3)_2CO$	827	304
	$CDCl_3$	838	304
	$CDCl_3$	841	310[d]
[$Te(C_8H_8)(OAc)(S_2CNEt_2)$]	CD_2Cl_2	808	362
[$Te(S_2CN$*n*-$Pr_2)_2$]	$(CD_3)_2CO$	829	304
	$CDCl_3$	836	304
[$Te(S_2CN$*i*-$Pr_2)_2$]	$CDCl_3$	833	304
[$Te(S_2CN$*i*-$Bu_2)_2$]	$(CD_3)_2CO$	845	304
[$Te(S_2CNEt_2)(S_2CNBz_2)$]	$CDCl_3$	852	310[d]
[$Te(C_8H_8)Cl(S_2CNEt_2)$]	DMF; 233 K	863	366
[$Te(S_2CNBz_2)_2$]	$CDCl_3$	865	304
	$CDCl_3$	868	310[d]
[$Te\{S_2CN(CH_2)_4O\}_2$]	CD_2Cl_2	879	306
[$Te\{S_2CN(CH_2)_4\}_2$]	$CDCl_3$	1117	304

TABLE VI (*continued*)

Complex	Solvent[b]	δ (^{125}Te)	References
$TeL^1(S_2CNEt_2)]$	$CDCl_3$	1124	331
$[Te(C_6H_4N_2Ph)(S_2CNMe_2)]$	$CDCl_3$	1229	323
$[Te(C_6H_4N_2Ph)(S_2CNEt_2)]$	$CDCl_3$	1239	323

[a] Chemical shifts reported relative to Me_2Te as an external standard (corrections from other references applied where necessary). L^1 = 8-(dimethylamino)-1-naphthyl.
[b] Data at ambient temperature, unless otherwise stated. THF = tetrahydrofuran. DMF = dimethylformamide.
[c] Solvent not specified.
[d] Incorrectly reported as the tetrakis(dithiocarbamato)tellurium(IV) complex.

Tellurium-125 Mössbauer spectroscopy has not be employed widely in the study of tellurium dithiocarbamate complexes, probably because isomer shifts are subject to substantial errors and are generally quite insensitive to the environment at Te. Generally, however, isomer shifts and quadrupole splittings are expected to be more positive for Te(II) complexes than for Te(IV) (323). The ^{125}Te NMR and Mössbauer spectra of the organotellurium dithiocarbamate complexes $[Te(C_6H_4N_2Ph)(S_2CNMe_2)]$ and $[Te(C_6H_4N_2Ph)(S_2CNMe_2)_3]$ have been reported by McWhinnie and co-workers (323). While NMR data for the two complexes are almost identical, suggesting that the Te(IV) complex has undergone reductive elimination of tetramethylthiuram disulfide in solution, the quadrupole splittings are significantly different, ruling out the possibility that the tris(dithiocarbamate) Te(IV) complex is simply a mixture of $[Te(C_6H_4N_2Ph)(S_2CNMe_2)]$ and $(Me_2NCS_2)_2$ in the solid state: Data tend to suggest a loose charge-transfer complex between the mono(dithiocarbamate) complex and the disulfide.

ACKNOWLEDGMENTS

The author is grateful to Stanley and Margaret Heard and Dr. Howard Carless and Dr. Paul King for helpful discussions. The author would also like to thank the referees for their constructive comments.

ABBREVIATIONS

av	Average
ax	Axial
2D	Two dimensional
Bpy	2,2′-Bipyridyl ($C_{10}H_8N_2$)
Bz	Benzyl ($CH_2C_6H_5$)

Cp	Cyclopentadienyl anion ($C_5H_5^-$)
Cy	Cyclohexyl (C_6H_{11})
ddh	Distorted dodecahedral
DMF	Dimethylformamide
DMSO	Dimethyl sulfoxide
doh	Distorted octahedral
dpby	Distorted pentagonal bipyramidal
dtpy	Distorted trigonal bipyramidal
Et	Ethyl (CH_2CH_3)
eq.	equitorial
^{1}H NMR	Proton NMR
Hex	Hexyl ($CH_2CH_2CH_2CH_2CH_2CH_3$)
i-Bu	isobutyl (CH_2CHMe_2)
i-Pr	isopropyl ($CHMe_2$)
IR	Infrared
IS	Isomer shift
L	Any unspecified ligand
Me	Methyl (CH_3)
MLCT	Metal-to-ligand charge transfer
n-Bu	Normal-Butyl ($CH_2CH_2CH_2CH_3$)
NMR	Nuclear magnetic resonance
n-Pr	Normal-Propyl ($CH_2CH_2CH_3$)
NQR	Nuclear quadruple resonance
phen	1,10-Phenanthroline ($C_{12}H_8N_2$)
py	Pyridine (ligand)
Py	Pyridine (solvent) (C_5H_5N)
QS	Quadrupole splitting
R	Any unspecified alkyl or aryl group
ρ	QS/IS ratio
terpy	4,4′:6′,2″-Terpyridine
thf	Tetrahydrofuran (ligand)
THF	Tetrahydrofuran (solvent)
tu	Tetramethylthiourea
VBS	Valence bond sum
X	Any unspecified halide or pseudohalide

REFERENCES

1. D. Coucouvanis, *Prog. Inorg. Chem.*, *11*, 233 (1970).
2. D. Coucouvanis, *Prog. Inorg. Chem.*, *26*, 301 (1979).
3. I. Ymen, *Acta Crystallogs.*, *37*, C223 (1981).

4. A. Oskarsson and I. Ymen, *Acta Crystallogs., Sect. C*, *39*, 66 (1983).
5. I. Ymen, *Acta Crystallogs., Sect. C*, *39*, 570 (1983).
6. I. Ymen, *Acta Crystallogs., Sect. C*, *39*, 874 (1983).
7. I. Ymen, *Acta Crystallogs., Sect. C*, *40*, 30 (1984).
8. I. Ymen, *Acta Crystallogs., Sect. C*, *40*, 33 (1984).
9. I. Ymen, *Acta Crystallogs., Sect. C*, *40*, 241 (1984).
10. J.-P. Legros, D. Troy, and J. Galy, *Acta Crystallogs., Sect. C*, *40*, 801 (1984).
11. R. Gerner, G. Kiel, and G. Gattow, *Acta Crystallogs., Sect. A*, *40*, C286 (1984).
12. R. Gerner, G. Kiel, and G. Gattow, *Z. Anorg. Allg. Chem*., *523*, 76 (1985).
13. T. C. W. Mark, K. S. Jasim, and C. Chieh, *Can. J. Chem.*, *62*, 808 (1984).
14. V. Vrabel, S. Gergely, J. Lokaj, E. Kello, and J. Garaj, *Acta Crystallogs., Sect. C*, *43*, 2293 (1987).
15. A. Wahlberg, *Acta Chem. Scand.*, *A30*, 433 (1976).
16. U. Aava and R. Hesse, *Ark. Kemi*., *30*, 149 (1969).
17. C. F. Conde, M. Millan, A. Conde, and R. Marquez, *Acta Crystallogs., Sect. C*, *42*, 286 (1986).
18. A. Wahlberg, *Acta Chem. Scand.*, *A30*, 614 (1976).
19. M. Colapietro, A. Domenicano and A. Vaciago, *Chem. Commun.*, 572 (1968).
20. K. Mereiter, A. Preisinger, W. Mikenda, and H. Steidl, *Inorg. Chim. Acta*, *98*, 71 (1985).
21. V. D. Khavryuchenko, A. F. Savost'yanova, A. D. Gorbalyuk, and V. S. Fundamenskii, *Zh. Neorg. Khim*., *36*, 501 (1991).
22. Z. V. Zvonkova, Z. P. Povet'eva, V. M. Vozzhenikov, V. P. Gluskova, V. I. Jakovenko and A. N. Khvatkina, *Acta Crystallogs., Sect. A*, *155*, 21 (1966).
23. I. Ymen, *Acta Crystallogs., Sect. B*, *38*, 2671 (1982).
24. W. Eul, G. Kiel, and G. Gattow, *Z. Anorg. Allg. Chem*., *535*, 167 (1986).
25. A. P. Purdy and C. F. George, *Main Group Chem*., *1*, 229 (1996).
26. D. A. Cook, S. J. Coles, M. B. Hursthouse, and D. J. Price, *Z. Anorg. Allg. Chem*., *629*, 192 (2003).
27. H. Nöth and D. Schlosser, *Chem. Ber.*, *121*, 1711 (1988).
28. (a) S. C. Ball, I. Cragg-Hine, M. C. Davidson, R. P. Davies, A. J. Edwards, I. Lopez-Solera, P. R. Raithby, and R. Snaith, *Angew. Chem. Int. Ed. Engl*., *34*, 921 (1995). (b) A. L. Spek, *PLATON*, A Multipurpose Crystallographic Tool, Utrecht University, Utrecht, The Netherlands, 2004 (c) A. L. Spek, *J. Appl. Crystallogs*., *36*, 7 (2003).
29. R. H. Cragg, M. F. Lappert, H. Nöth, P. Schweitzer, and B. P. Tilley, *Chem. Ber.*, *100*, 2377 (1967).
30. G. Abeler, H. Nöth, and H. Schick, *Chem. Ber.*, *101*, 3981 (1968).
31. H. Nöth and P. Schweizer, *Chem. Ber.*, *102*, 161 (1969).
32. M. A. Beckett, N. N. Greenwood, J. D. Kennedy, and M. Thornton-Pett, *Polyhedron*, *4*, 505 (1985).
33. H. Nöth and P. Konard, *Chem. Ber.*, *116*, 3552 (1983).
34. P. C. Andrews, S. M. Lawrence, C. L. Raston, B. W. Skelton, V.-A. Tolhurst, and A. H. White, *Inorg. Chim. Acta*, *300*, 56 (2000).
35. A. F. Lindmark and R. C. Fay, *Inorg. Chem*., *22*, 2000 (1983).
36. A. Ma and A. A. Alsuhybani, *Indian J. Chem. Tech*., *2*, 25 (1995).

37. I. Karadjova, G. Zachariadis, G. Boskou, and J. Stratis, *J. Anal. Atom. Spectrom.*, *13*, 201 (1998).
38. M. Delphine, *Ann. Chim.*, *6*, 633 (1951).
39. N. Nöth and P. Konard, *Z. Naturforsch*, *30b*, 681 (1975).
40. K. Dymock, G. J. Palenik, J. Slezak, C. L. Raston, and A. H. White, *J. Chem. Soc., Dalton Trans.*, *28* (1976).
41. L. Que and L. H. Pignolet, *Inorg. Chem.*, *13*, 351 (1974).
42. S. Bhattacharya, N. Seth, D. K. Srivastava, V. D. Gupta, H. Nöth, and M. Thomann-Albach, *J. Chem. Soc., Dalton Trans.*, 2815 (1996).
43. D. P. Gutta, V. K. Jain, A. Knoedler, and W. Kaim, *Polyhedron*, *21*, 239 (2002).
44. M. R. Lazell, P. O'Brien, D. J. Otway, and J.-H. Park, *Chem. Mater.*, *11*, 3430 (1999).
45. P. J. Hauser, J. Bordner, and A. F. Schreiner, *Inorg. Chem.*, *12*, 1347 (1973).
46. S. Bhattacharya, N. Seth, V. D. Gupta, H. Nöth, and M. Thomann, *Z. Naturforsch*, *49b*, 193 (1994).
47. E. B. Clark, M. L. Breen, P. E. Fanwick, A. F. Hepp, and S. A. Duraj, *J. Coord. Chem.*, *52*, 111 (2000).
48. P. O'Brien, D. J. Otway, and J. R. Walsh, *Thin Solid Films*, *315*, 57 (1998).
49. D. Pahari Dutta, V. K. Jain, S. Chaudhury, and E. R. T. Tiekink, *Main Group Met. Chem.*, *24*, 405 (2001).
50. F. A. Cotton, B. F. G. Johnson, and R. M. Wing, *Inorg. Chem.*, *4*, 502 (1965).
51. F. Bonati, C. Cemini, and R. Ugo, *J. Organomet. Chem.*, *9*, 395 (1967).
52. H. Abrahamson, J. R. Heiman, and L. H. Pignolet, *Inorg. Chem.*, *14*, 2070 (1975).
53. D. L. Kepert, C. L. Raston, N. K. Roberts, and A. H. White, *Aust. J. Chem.*, *31*, 1927 (1978).
54. G. Soundararajan and M. Subbaiyan, *Bull. Chem. Soc. Jpn.*, *57*, 2299 (1984).
55. L. Silaghi-Dumitrescu, I. Silaghi-Dumitrescu, I. Haiduc, R.-A. Toscano, V. Garcia-Montalvo, and R. Cae-Olivares, *Z. Anorg. Allg. Chem.*, *625*, 347 (1999).
56. S. Akerström, *Acta Chem. Scand.*, *18*, 824 (1964).
57. S. Akerström, *Arkiv. Kemi.*, *24*, 495 (1965).
58. L. Nilson and R. Hesse, *Acta Chem. Scand.*, *23*, 1951 (1969).
59. P. Jennische, Å. Olin, and R. Hesse, *Acta Chem. Scand.*, *26*, 2799 (1972).
60. P. Jennische and R. Hesse, *Acta. Chem. Scand.*, *27*, 3531 (1973).
61. H. Anacker-Eickhoff, P. Jennische, and R. Hesse, *Acta Chem. Scand.*, *A29*, 51 (1975).
62. H. Pritzkow and P. Jennische, *Acta Chem. Scand.*, *A29*, 60 (1975).
63. E. Elfwing, H. Anacker-Eickhoff, P. Jennische, and R. Hesse, *Acta Chem. Scand.*, *A30*, 335 (1976).
64. G. Soundararajan and M. Subbalyan, *Anal. Chem.*, *55*, 910 (1983).
65. G. Soundararajan and M. Subbalyan, *Separ. Sci. Technol.*, *18*, 645 (1983).
66. J. C. Yu and C. M. Wai, *Anal. Chem.*, *56*, 1689 (1984).
67. J. Stary and K. Kratzer, *J. Radioanal. Nuc. Chem. Lett.*, *165*, 137 (1992).
68. R. K. Dubey, S. Puri, M. K. Gupta, and B. K. Puri, *Anal. Lett.*, *31*, 2729 (1998).
69. B. Wen, X. Q. Liu, R. X. Liu, and H. X. Tang, *Fresenius J. Anal. Chem.*, *363*, 251 (1999).
70. Z. Todorovic, P. Polic, T. Sabo, and M. Cakic, *J. Serbian Chem. Soc.*, *67*, 879 (2002).
71. T. Maeda and R. Okawara, *J. Organomet. Chem.*, *39*, 87 (1972).

72. R. T. Griffin, K. Henrick, R. W. Matthews, and M. McPartlin, *J. Chem. Soc., Dalton Trans.*, 1550 (1980)
73. B. Khera, A. K. Sharma, and N. K. Kaushik, *Synth. React. Inorg. Met.-Org. Chem.*, *12*, 583 (1982).
74. J. S. Casas, M. V. Castaño, C. Freire, A. Sánchez, J. Sordo, E. E. Castellano, and J. Zukerman-Schpector, *Inorg. Chim. Acta*, *216*, 15 (1994).
75. S. W. Haggata, M. Azad Malik, M. Motevalli, P. O'Brien, and J. C. Knowles, *Chem. Mater.*, *7*, 716 (1995).
76. S. W. Haggata, M. Azad Malik, M. Motevalli, and P. O'Brien, *J. Organomet. Chem.*, *511*, 199 (1996).
77. A. Keys, S. G. Bott, and A. R. Barron, *Chem. Mater.*, *11*, 3578 (1999).
78. A. Keys, S. G. Bott, and A. R. Barron, *J. Chem. Crystallogs.*, *28*, 629 (1998).
79. V. Ch. Burschka, *Z. Anorg. Allg. Chem.*, *485*, 217 (1982).
80. X. Zhou, M. L. Breen, S. A. Duraj, and A. F. Hepp, *Main Group Met. Chem.*, *22*, 35 (1999).
81. E. M. Gordon, A. F. Hepp, S. A. Duraj, T. S. Habash, P. E. Fanwick, J. D. Schupp, W. E. Eckles, and S. Long., *Inorg. Chim. Acta*, *257*, 247 (1997).
82. J. Sharma, Y. P. Singh, and A. K. Rai, *Main Group Met. Chem.*, *22*, 595 (1999).
83. N. Gandhi, R. Jain, and N. K. Kaushik, *Thermochim Acta*, *282/283*, 501 (1996).
84. R. K. Chadha, J. E. Drake, and A. B. Sarkar, *Inorg. Chem.*, *25*, 2201 (1986).
85. R.-F. Zhang, D.-Z. Zhu, H.-D. Yin, and C.-L. Ma, *Chin. J. Inorg. Chem.*, *18*, 386 (2002).
86. R. K. Chadha, J. E. Drake, and A. B. Sarkar, *Inorg. Chem.*, *23*, 4769 (1984).
87. N. Gandhi and N. K. Kaushik, *Indian J. Chem., Sect. A*, *34*, 154 (1995).
88. R. K. Chadha, J. E. Drake, A. B. Sarkar, and M. L. Wong, *Acta Crystallogs., Sect. C*, *45*, 37 (1989).
89. E. M. Holt, F. A. K. Nasser, A. Wilson, Jr., and J. J. Zuckerman, *Organometallics*, *4*, 2073 (1985).
90. H.-D. Yin, R.-F. Zhang, L.-Y. Zhang, and C.-L. Ma, *ACH-Model Chem.*, *137*, 43 (2000).
91. C. Preti, G. Tosi, and P. Zannini, *J. Mol. Struct.*, *65*, 283 (1980).
92. B. F. Hoskins, R. L. Martin, and N. M. Rohde, *Aust. J. Chem.*, *29*, 213 (1976).
93. A. C. Fabretti, A. Giusti, C. Preti, G. Tosi, and P. Zannini, *Polyhedron*, *5*, 871 (1986).
94. J. Potenza, R. J. Johnson, and D. Mastropaolo, *Acta Crystallogs., Sect. B*, *32*, 941 (1976).
95. N. Seth, V. D. Gupta, H, Nöth, and M. Thomann, *Chem. Ber.*, *125*, 1523 (1992).
96. H. Iwasaki, *Acta Crystallogs., Sect. B*, *36*, 2138 (1980).
97. P. K. Bharadwaj, B. W. Arbuckle, and W. K. Musker, *Inorg. Chim. Acta*, *142*, 243 (1988).
98. T. Trindade, P. O'Brien, X.-M. Zhang, and M. Motevalli, *J. Mater. Chem.*, *7*, 1011 (1997).
99. F. Caruso, M.-L. Chan, and M. Rossi, *Inorg. Chem.*, *36*, 3609 (1997).
100. M. Ito and H. Iwasaki, *Acta Crystallogs., Sect. B*, *36*, 443 (1980).
101. I. Baba, Y. Farina, A. H. Othman, I. A. Razak, H.-K. Fun, and S. W. Ng, *Acta Crystallogs., Sect. E*, *57*, m35 (2001).
102. G. Bauer, G. St. Nikolov, and N. Trendafilova, *J. Mol. Struct.*, *415*, 123 (1997).
103. A. M. Bond, R. Colton, and A. F. Hollenkamp, *Inorg. Chem.*, *29*, 1991 (1990).
104. A. Ichimura, Y. Morimoto, H. Kitamura, and T. Kitagawa, *Bunseki Kagaku*, *33*, E503 (1984).
105. T. Trindade and P. O'Brien, *Chem. Vapor Deposition*, *3*, 75 (1997).

106. G. Barone, T. Chaplin, T. G. Hibbert, A. T. Kana, M. F. Hahon, K. C. Molloy, I. D. Worsley, I. P. Parkin, and L. S. Price, *J. Chem. Soc., Dalton Trans*., 1085 (2002).
107. A. R. K. Dapaah, N. Takano, and A. Ayame, *Anal. Chim. Acta*, *386*, 281 (1999).
108. J. D. Zubkowski, T. Hall, E. J. Valente, D. L. Perry, L. A. Fleiu, and J. Garmon, *J. Chem. Crystallogr.*, *27*, 251 (1997).
109. J. S. Morris and E. O. Schlemper, *J. Cryst. Mol. Struct*., *8*, 295 (1978).
110. J. S. Morris and E. O. Schlemper, *J. Cryst. Mol. Struct*., *9*, 1 (1979).
111. J. Otera, T. Hinoshi, and R. Okawara, *J. Organomet. Chem*., *202*, C93 (1980).
112. J. Otera, *Organomet. Chem*., *221*, 57 (1981).
113. S. S. Gupta and N. K. Kaushik, *Thermochim. Acta*, *106*, 233 (1986).
114. S. S. Gupta and N. K. Kaushik, *Indian J. Chem*., *26*, 175 (1987).
115. D. Dakternieks, H. Zhu, D. Masi, and C. Mealli, *Inorg. Chim. Acta*, *211*, 155 (1993).
116. M. F. Mahon, K. C. Molloy, and P. C. Waterfield, *Organometallics*, *12*, 769 (1993).
117. J. M. Hook, B. M. Linahan, R. L. Taylor, E. R. T. Tiekink, L. van Gorkom, and L. K. Webster, *Main Group Met. Chem*., *17*, 293 (1994).
118. E. Kellö, V. Vrábel, and I. Skačáni, *Acta Crystallogs., Sect. C*, *51*, 408 (1995).
119. A. T. Kana, T. G. Hibbert, M. F. Mahon, K. C. Molloy, I. P. Parkin, and L. S. Price, *Polyhedron*, *20*, 2989 (2001).
120. D. J. Clarke, D. Dakternieks, and E. R. T. Tiekink, *Main Group Met. Chem*., *24*, 305 (2001).
121. N. Seth, A. K. Mishra, and V. D. Gupta, *Synth. React. Inorg. Met.-Org. Chem*., *20*, 1001 (1990).
122. P. F. Lindley and P. Carr, *J. Chem. Cryst. Mol. Struct*., *4*, 173 (1974).
123. J. Lokaj, E. Kellö, V. Kettmann, V. Vrabel, and V. Rattay, *Collect. Czech. Chem. Comm*., *51*, 2521 (1986).
124. O.-S. Jung, Y. S. Sohn, and J. A. Ibers, *Inorg. Chem*., *25*, 2273 (1986).
125. K. M. A. Malik, P. F. Lindley, and J. W. Jeffery, *J. Bangladesh Acad. Sci*., *5*, 53 (1981).
126. P. G. Harrison and A. Mangia, *J. Organomet. Chem*., *120*, 211 (1976).
127. O.-K. Jung, M. J. Kim, J. H. Jeong, and Y. S. Sohn, *Bull. Korean Chem. Soc*., *10*, 343 (1989).
128. D. J. Clarke, D. Dakternieks, and E. R. T. Tiekink, *Main Group Met. Chem*., *24*, 303 (2001).
129. D. J. Clarke, D. Dakternieks, and E. R. T. Tiekink, *Main Group Met. Chem*., *24*, 305 (2001).
130. D. J. Clarke, D. Dakternieks, and E. R. T. Tiekink, *Main Group Met. Chem*., *24*, 385 (2001).
131. T. G. Hibbert, M. F. Mahon, and K. C. Molloy, *Main Group Met. Chem*., *22*, 235 (1999).
132. Y. Farina, I. Baba, A. H. Othman, and S. W. Ng, *Main Group Met. Chem*., *23*, 795 (2000).
133. P. Laavanya, R. Selvaraju, S. Thenmozhi, and K. Panchanatheswaran, *J. Chem. Res. (S)*, *93*, 354 (2001).
134. R. Selvaraju, M. Manoharan, P. Laavanya, K. Panchanatheswaran, and P. Venuvanalingam, *J. Chem. Res. (M)*, *82*, 419 (1999).
135. Y. Farina, A. H. Othman, I. Baba, S. W. Ng, and H.-K. Fun, *Main Group Met. Chem*., *25*, 67 (2002).
136. Y. Farina, A. H. Othman, I. A. Razak, H.-K. Fun, S. W. Ng, and I. Baba, *Acta Crystallogs., Sect. E*, *57*, m46 (2001).
137. Y. A. A. Farina, A. H. Othman, I. Baba, K. Sivakumar, H.-K. Fun, and S. W. Ng, *Acta Crystallogs., Sect. C*, *56*, 84 (2000).
138. Y. Farina, I. Baba, A. H. Othman, I. A. Razak, H.-K. Fun, and S. W. Ng, *Acta Crystallogs., Sect. E*, *57*, m41 (2001).

139. N. Seth, A. K. Mishra, and V. D. Gupta, *Synth. React. Inorg. Met.-Org. Chem.*, *20*, 1001 (1990).
140. H.-D. Yin, G.-F. He, C.-H. Wang, and C.-L. Ma, *Chinese J. Inorg. Chem.*, *19*, 1019 (2003).
141. T. P. Lockhart, W. E. Manders, E. O. Schlemper, and J. J. Zuckerman, *J. Am. Chem. Soc.*, *108*, 4074 (1986).
142. S. W. Ng, C. Wei, and V. G. K. Das, *J. Organomet. Chem.*, *365*, 75 (1989).
143. J. Sharma, Y. Sing, R. Bohra, and A. K. Rai, *Polyhedron*, *15*, 1097 (1996).
144. Y.-I. Takeda, N. Watanabe, and T. Tanaka, *Spectrochim. Acta*, *32A*, 1553 (1976).
145. C. P. Sharma, N. Kumar, M. C. Khandpal, S. Chandra, and V. G. Bhide, *J. Inorg. Nucl. Chem.*, *43*, 923 (1981).
146. J. Otera, T. Hinoishi, Y. Kawabe, and R. Okawara, *Chem. Lett.*, *273* (1981).
147. J. Otera, A. Kusaba, T. Hinoishi, and Y. Kawasaki, *J. Organomet. Chem.*, *228*, 223 (1982).
148. J. Otera, T. Yano, and K. Kusakabe, *Bull. Chem. Soc. Jpn.*, *56*, 1057 (1983).
149. T. P. Lockhart, W. F. Manders, and E. O. Schlemper, *J. Am. Chem. Soc.*, *107*, 7451 (1985).
150. K. Kim, J. A. Ibers, O.-S. Jung, and Y. S. Sohn, *Acta Crystallogs., Sect. C*, *43*, 2317 (1987).
151. O.-K. Jung, J. H. Jeong, and Y. S. Sohn, *Acta Crystallogs., Sect. C*, *46*, 31 (1990).
152. N. W. Alcock, J. Culver, and S. M. Roe, *J. Chem. Soc., Dalton Trans.*, 1477 (1992).
153. D. Dakternieks, H. Zhu, D. Masi, and C. Mealli, *Inorg. Chem.*, *31*, 3601 (1992).
154. V. Vrábel, J. Lokaj, E. Kellö, V. Rattay, A. C. Batsanov, and Y. T. Struchkov, *Acta Crystallogs., Sect. C*, *48*, 627 (1992).
155. V. Vrábel and E. Kellö, *Acta Crystallogs., Sect. C*, *49*, 873 (1993).
156. R. Bohra, S. Sharma and A. Dhammani, *Acta Crystallogs., Sect. C*, *50*, 1447 (1994).
157. R. Selvaraju, K. Panchanatheswaran, and K. Venkatasubramanian, *Polyhedron*, *13*, 903 (1994).
158. V. Vrábel, E. Kellö, J. Holeček, J. Sivy, and J. Lokaj, *Acta Crystallogs., Sect. C*, *51*, 70 (1995).
159. V. J. Hall and E. R. T. Tiekink, *Main Group Met. Chem.*, *18*, 611 (1995).
160. V. J. Hall and E. R. T. Tiekink, *Main Group Met. Chem.*, *21*, 245 (1998).
161. H.-D. Yin, C.-H. Wang, Y. Wang, and C.-L. Ma, *Chinese J. Chem.*, *21*, 356 (2003).
162. D. J. Clarke, D. Dakternieks, and E. R. T. Tiekink, *Main Group Met. Chem.*, *24*, 307 (2001).
163. J. S. Morris and E. O. Schlemper, *J. Cryst. Mol. Struct.*, *9*, 13 (1979).
164. V. J. Hall and E. R. T. Tiekink, *Z. Kristallogr. New Cryst. Struct.*, *213*, 535 (1998).
165. V. Vrábel, J. Lokaj, E. Kellö, J. Garaj, A. C. Batsanov, and Y. T. Struchkov, *Acta Crystallogs., Sect. C*, *48*, 633 (1992).
166. H.-D. Yin, C.-H. Wang, Y. Wang, R.-F. Zhang, and C.-L. Ma, *Chinese J. Inorg. Chem.*, *18*, 201 (2002).
167. A. Marzotto, D. A. Clemente, and G. Valle, *Acta Crystallogs., Sect. C*, *54*, 1040 (1998).
168. M. J. Cox, M. I. Mohamed-Ibrahim, and E. R. T. Tiekink, *Z. Kristallogr. New Cryst. Struct.*, *213*, 531 (1998).
169. V. K. G. Das, C. Wei, and E. Sinn, *J. Organomet. Chem.*, *290*, 291 (1985).
170. D.-Z. Zhu, R.-F. Zhang, C.-L. Ma, and H.-D. Yin, *Indian J. Chem. Sect. A*, *41*, 1634 (2002).
171. J. Sharma, Y. Singh, and A. K. Rai, *Phosphorus, Sulfur, Silicon*, *112*, 19 (1996).
172. S. Chandra, B. D. James, R. J. Magee, W. C. Patalinghug, B. W. Ske lton, and A. H. White, *J. Organomet. Chem.*, *346*, 7 (1998).
173. H.-D. Yin, R.-F. Zhang, and C.-L. Ma, *Chinese J. Org. Chem.*, *19*, 413 (1999).

174. H.-D. Yin, C.-H. Wang, C.-L. Ma, Y. Wang, and R.-F. Zhang, *Chinese J. Inorg. Chem.*, *18*, 347 (2002).
175. C. Wei, K. Das, and E. Sinn, *Inorg. Chim. Acta*, *100*, 245 (1985).
176. K. M. Lo, S. Selvaratnam, S. W. Ng, C. Wei, and V. G. K. Das, *J. Organomet. Chem.*, *430*, 149 (1992).
177. T. S. Basu Baul and E. R. T. Tiekink, *Main Group Met. Chem.*, *16*, 201 (1993).
178. V. J. Hall and E. R. T. Tiekink, *Main Group Met. Chem.*, *18*, 217 (1995).
179. A. H. Othman, H.-K. Fun, and B. H. Yamin, *Acta Crystallogs., Sect. C*, *53*, 1228 (1997).
180. E. R. T. Tiekink, V. J. Hall, and M. A. Buntine, *Z. Kristallogr.*, *214*, 124 (1999).
181. J. Sharma, Y. P. Singh, and A. K. Rai, *Main Group Met. Chem.*, *23*, 317 (2000).
182. L.-J. Tian, Z.-C. Shang, Q.-S. Yu, W.-N. Zhao, Z.-Y. Zhou, and W.-T. Yu, *Chinese J. Inorg. Chem.*, *19*, 685 (2003).
183. J. Sharma, Y. Singh, and A. K. Rai, *Indian J. Chem., Sect. A*, *36*, 602 (1997).
184. H.-D. Yin, C.-L. Ma, and Y. Wang, *Indian J. Chem., Sect. A*, *41*, 342 (2002).
185. H.-D. Yin, C.-H. Wang, C.-L. Ma, Y. Wang, and R.-F. Zhang, *Chinese J. Org. Chem.*, *21*, 1117 (2001).
186. M. A. Buntine, V. J. Hall, F. J. Kosovel, and E. R. T. Tiekink, *J. Phys. Chem. A*, *102*, 2472 (1998).
187. X. Song, C. Cahill, and G. Eng, *Main Group Met. Chem.*, *25*, 13 (2002).
188. H.-D. Yin, C.-L. Ma, Y. Wang, H.-X. Fang, and J.-X. Shao, *Acta Chim. Sinica*, *60*, 897 (2002).
189. O.-S. Jung, J. H. Jeong, and Y. S. Sohn, *Polyhedron*, *8*, 1413 (1989).
190. O.-S. Jung, J. H. Jeong, and Y. S. Sohn, *Organometallics*, *10*, 2217 (1991).
191. O.-S. Jung, J. H. Jeong, and Y. S. Sohn, *J. Organomet. Chem.*, *439*, 23 (1992).
192. O.-S. Jung, J. H. Jeong, and Y. S. Sohn, *Organometallics*, *10*, 761 (1991).
193. O.-S. Jung, J. H. Jeong, and Y. S. Sohn, *Polyhedron*, *8*, 2557 (1989).
194. A. C. Fabretti and C. Preti, *J. Crystallogs. Spectrosc. Res.*, *19*, 957 (1989).
195. D. Dakternieks, K. Jurkschat, D. Schollmeyer, and H. Wu, *J. Organomet. Chem.*, *492*, 145 (1995).
196. S. Sharma, R. Bohra, and R. C. Mehrotra, *Polyhedron*, *15*, 1525 (1996).
197. E. Romani, *Giorn. Chim. Ind. Appl.*, *3*, 197 (1921).
198. R. Selvaraju, P. Laavsaya, K. Panchanatheswaran, L. Pellerito, and G. La Manna, *J. Chem. Res. (M)*, 2925 (1998).
199. L. A. Gómez-Ortiz, R. Cea-Olivares, V. García-Montalvo, and S. Hernández-Ortega, *J. Organomet. Chem.*, *654*, 51 (2002).
200. T. P. Lockhart and W. F. Manders, *Inorg. Chem.*, *25*, 892 (1986).
201. S. S. Garje and V. K. Jain, *Coord. Chem. Rev.*, *236*, 35 (2003).
202. G. Schubert and G. Gattow, *Z. Anorg. Allg. Chem.*, *572*, 126 (1989).
203. G. Schubert, G. Kiel, and G. Gattow, *Z. Anorg. Allg. Chem.*, *574*, 153 (1989).
204. G. Schubert and G. Gattow, *Z. Anorg. Allg. Chem.*, *573*, 75 (1989).
205. R. W. Light, L. D. Hutchins, R. T. Paine, and C. F. Campana, *Inorg. Chem.*, *19*, 3579 (1980).
206. D. S. Yufit, Yu. T. Struchkov, M. A. Pudovik, L. K. Kibardina, I. A. Aleksandrova, V. K. Khairullin, and A. N. Pudovik, *Dokl. Akad. Nauk SSSR*, *255*, 1190 (1980).
207. I. A. Litvinov, M. B. Zuez, O. N. Kataeva, and V. A. Naumov, *Russ. J. Gen. Chem.*, *61*, 1017 (1991).

208. M. Wieber, C. Burschka, and B. Bauer, *Phosphorus, Sulfur, Silicon*, *42*, 157 (1989).
209. V. A. Al'fonsov, I. A. Litinov, O. N. Kataeva, D. A. Pudovik, and S. A. Katsyuba, *Russ. Chem. Bull*., *44*, 1987 (1995).
210. K. Chaturvedi, A. K. Jaiswal, O. P. Pandy, and S. K. Sengupta, *Synth. React. Inorg. Met.-Org. Chem*., *25*, 1581 (1995).
211. R. Blachnik, K. Hackmann, and U. Peukert, *Z. Anorg. Allg. Chem*., *621*, 1211 (1995).
212. T. N. Srivastava and A. Bhargava, *J. Indian Chem. Soc*., *62*, 103 (1979).
213. C. Preti, G. Tosi, and P. Zannini, *J. Mol. Struct*., *53*, 35 (1979).
214. J. G. Stevens and J. M. Trooster, *J. Chem. Soc., Dalton Trans*., 740 (1979).
215. K. A. Uvarova, *Zh. Anal. Khim*., *35*, 1910 (1980).
216. C. A. Kavounis, S. C. Kokkou, and P. J. Rentzeperis, *Acta Crystallogs., Sect. B*, *36*, 2954 (1980).
217. C. A. Kavounis, S. C. Kokkou, P. J. Rentzeperis, and P. Karagiannidis, *Acta Crystallogs., Sect. B*, *38*, 2686 (1982).
218. M. Meula-Žigon, J. R. Dias, and S. Gomišček, *Vestn. Slov. Kem. Drus*., *29*, 23 (1982).
219. A. Benedetti, C. Preti, and G. Tosi, *J. Mol. Struct*., *98*, 155 (1983).
220. G. Soundararajan and M. Subbaiyan, *J. Indian Chem. Soc*., *60*, 1182 (1983).
221. R. Nomura, A. Takabe, and H. Matsuda, *Polyhedron*, *6*, 411 (1987).
222. V. Venkatachalam, K. Ramalingam, T. C. W. Mak, and B.-S. Luo, *J. Chem. Cryst*., *26*, 467 (1996).
223. V. Venkatachalam, K. Ramalingam, U. Casellato, and R. Graziani, *Polyhedron*, *16*, 1211 (1997).
224. V. Venkatachalam, K. Ramalingam, C. Bocelli, and A. Cantoni, *Inorg. Chim. Acta*, *261*, 23 (1997).
225. K. Y. Low, I. Baba, Y. Farina, A. H. Othman, A. R. Ibrahim, H.-K. Fun, and S. W. Ng, *Main Group Met. Chem*., *24*, 451 (2001).
226. I. Baba, S. Ibrahim, Y. Farina, A. H. Othman, I. A. Razak, H.-K. Fun, and S. W. Ng, *Acta Crystallogs., Sect. E*, *57*, m39 (2001).
227. M.-H. Zeng, H. Liang, R.-X. Hu, X.-H. Liu, Y.-C. Deng, and S.-Q. Huang, *Chin. J. Appl. Chem*., *18*, 837 (2001).
228. I. Baba, K. Karimah, Y. Farina, A. H. Othman, A. R. Ibrahim, A. Usman, H.-K. Fun, and S. W. Ng, *Acta Crystallogs., Sect. E*, *58*, m756 (2002).
229. I. bin Baba, B. W. Skelton, and A. H. White, *Aust. J. Chem*., *56*, 27 (2003).
230. B. W. Wenclawiak, S. Uttich, H. J. Deisroth, and D. Schmitz, *Inorg. Chim. Acta*, *348*, 1 (2003).
231. S. Kumar and N. K. Kaushik, *Thermochim. Acta*, *41*, 19 (1980).
232. H. B. Singh, S. Maheshwari, and H. Tomer. *Thermochim. Acta*, *64*, 47 (1983).
233. C. Airoldi and A. G. de Souza, *J. Chem. Soc., Dalton Trans*., 2955 (1987).
234. A. G. de Souza and C. Airoldi, *Thermochim. Acta*, *130*, 95 (1988).
235. C. Airoldi and A. G. de Souza, *J. Chem. Thermo*., *21*, 283 (1989).
236. A. G. de Souza, F. de Souza Neto, J. H. de Souza, R. O. Macedo, J. B. L. de Oliveira, and C. D. Pinheiro, *J. Therm. Anal*., *49*, 679 (1997).
237. R. Nomura, K. Kanaya, and H. Matsuda, *Bull. Chem. Soc. Jpn*., *62*, 939 (1989).
238. O. C. Monteiro, T. Trindade, J. H. Park, and P. O'Brien, *Chem. Vapor Deposition*, *6*, 230 (2000).
239. C. O. Monteiro and T. Trindade, *J. Mater. Sci. Lett*., *19*, 859 (2000).
240. O. C. Monteiro, H. I. S. Nogueira, T. Trindade, and M. Motevalli, *Chem. Mater*., *13*, 2103 (2001).

241. Y. W. Koh, C. S. Lai, A. Y. Du, E. R. T. Tiekink, and K. P. Loh, *Chem. Mater.*, *15*, 4544 (2003).
242. G. Soundararjan and M. Subbaiyan, *Indian J. Chem., Sect. A*, *22*, 311 (1983).
243. L. Li, K.-L. Huang, L. Qu, and W.-Y. Shu, *Trans. Nonferrous Met. Soc., China*, *11*, 946 (2001).
244. L. P. Battaglia and A. B. Corradi, *J. Chem. Soc., Dalton Trans*., 1513 (1986).
245. D. Chen, C. S. Lai, and E. R. T. Tiekink, *Appl. Organomet. Chem*., *17*, 813 (2003).
246. P. J. H. A. M. van de Leemput, J. A. Cras, and J. Willemse, *Recl. Trav. Chim. Pays-Bas*, *96*, 288 (1977).
247. R. Egle, W. Klinkhammer, and A. Schmidt, *Z. Anorg. Allg. Chem*., *617*, 72 (1992).
248. R. Egle and A.Schmidt, *Z. Anorg. Allg. Chem.*, *620*, 539 (1994).
249. F. M.-N. Kheiri, C. A. Tsipis, and G. E. Manoussakis, *Inorg. Chim. Acta*, *25*, 223 (1977).
250. F. M.-N. Kheiri, C. A. Tsipis, C. L. Tsiamis, and G. E. Manoussakis, *Can. J. Chem*., *57*, 767 (1979).
251. L. Vuchkova and S. Arpadjan, *Talanta*, *43*, 479 (1996).
252. S. Garboś, M. Rzepecka, E. Bulska, and A. Hulanicki, *Spectrochim. Acta*, *B54*, 873 (1999).
253. V. M. Wieber and A. Basel, *Z. Anorg. Allg. Chem*., *448*, 89 (1979).
254. H. L. M. van Gaal, J. W. Diesveld, F. W. Pijpers, and J. G. M. van der Linden, *Inorg. Chem*., *18*, 3251 (1979).
255. C. Burschka and M. Wieber, *Z. Naturforsch*., *34b*, 1037 (1979).
256. E. Kellö, V. Kettman, and J. Garaj, *Acta Crystallogs., Sect. C*, *41*, 520 (1985).
257. C. L. Raston, G. L. Rowbottom, and A. H. White, *J. Chem. Soc., Dalton Trans*., 1352 (1981).
258. G. McKie, C. L. Raston, G. L. Rowbottom, and A. H. White, *J. Chem. Soc., Dalton Trans*., 1360 (1981).
259. M. Wieber, D. Wirth, and C. Burschka, *Z. Naturforsch*., *40b*, 258 (1985).
260. M. Wieber, D. Wirth, J. Metter, and Ch. Burschka, *Z. Anorg. Allg. Chem*., *520*, 65 (1985).
261. M. Ali, W. R. McWhinnie, A. A. West, and T. A. Hamor, *J. Chem. Soc., Dalton Trans*, 899 (1990).
262. J. Sharma, Y. Singh, and A. K. Rai, *Phosphorus, Sulfur, Silicon*, *107*, 13 (1995).
263. S. S. Garje, V. K. Jain, and E. R. T. Tiekink, *J. Organomet. Chem*., *538*, 129 (1997).
264. H. P. S. Chauhan, B. Nahar, and R. K. Singh*, Synth. React. Inorg. Met.-Org. Chem*., *28*, 1541 (1998).
265. C. S. Lai and E. R. T. Tiekink, *Appl. Organomet. Chem*., *17*, 195 (2003).
266. A. Gupta, R. K. Sharma, R. Bohra, V. K. Jain, J. E. Drake, M. B. Hursthouse, and M. E. Light, *J. Organomet. Chem*., *678*, 122 (2003).
267. S. Sharma, R. Bohra, and R. C. Mehrotra, *J. Indian Chem. Soc*., *67*, 945 (1990).
268. S. Kraft and M. Wieber, *Z. Anorg. Allg. Chem*., *607*, 164 (1992).
269. S. Chourasia, B. Nahar, and H. P. S. Chauhan, *Phosphorus, Sulfur, Silicon*, *119*, 77 (1996).
270. S. Sharma, R. Bohra, and R. C. Mehrotra, *Indian J. Chem. Sect. A*, *32*, 59 (1993).
271. H. P. S. Chauhan, R. K. Singh, and K. Kori, *Main Group Met. Chem*., *25*, 511 (2002).
272. H. P. S. Chauhan and B. Nahar, *Phosphorus, Sulfur, Silicon*, *128*, 119 (1997).
273. J. A. Cras, P. J. H. A. M. van de Leemput, J. Willemse, and W. P. Bosman, *Recl. Trav. Chim. Pays-Bas*, *96*, 78 (1977).
274. C. L. Raston, G. L. Rowbottom, and A. H. White, *J. Chem. Soc., Dalton Trans*., 1366 (1981).
275. C. L. Raston, G. L. Rowbottom, and A. H. White, *J. Chem. Soc., Dalton Trans*., 1369 (1981).

276. C. L. Raston, G. L. Rowbottom, and A. H. White, *J. Chem. Soc., Dalton Trans*., 1372 (1981).

277. P. K. Bharadwaj, A. M. Lee, B. W. Skelton, B. R. Srinivasan, and A. H. White, *Aust. J. Chem*., *47*, 405 (1994).

278. C. L. Raston, G. L. Rowbottom, and A. H. White, *J. Chem. Soc., Dalton Trans*., 1379 (1981).

279. C. L. Raston, G. L. Rowbottom, and A. H. White, *J. Chem. Soc., Dalton Trans*., 1383 (1981).

280. R. Cea-Olivares, J. Wingartz, E. Rios, and J. Valdés-Martinez, *Monatsh. Chem*., *121*, 377 (1990).

281. R. Cea-Olivares, R. A. Toscano, and P. Garcia, *Monatsh. Chem*., *124*, 177 (1993).

282. R. Cea-Olivares, M. R. Estrada, G. Espinosa Perez, I. Haiduc, P. G. Y. Garcia, M. López Cardoso, M. López Vaca, and A. M. Cotero Villegas, *Main Group Chem*., *1*, 159 (1995).

283. R. Cea-Olivares, R. A. Toscano, M. López, and P. García, *Heteroatom Chem*., *4*, 313 (1993).

284. R. Cea-Olivares, R.-A. Toscano, C. Silestru, P. Garcia-García, M. López-Cardoso, G. Blass-Amador, and H. Nöth, *J. Organomet. Chem*., *493*, 61 (1995).

285. G. Beurskens, P. T. Beurskens, J. H. Noordik, and J. Willemse, *Recl. Trav. Chim. Pays-Bas*, *98*, 416 (1979).

286. J. Sharma, Y. P. Singh, and A. K. Rai, *Phosphor., Sulfur, Silicon*, *86*, 197 (1994).

287. R. N. Sharma, A. Kumar, A. Kumari, H. R. Singh, and R. Kumar, *Asian J. Chem*., *15*, 57 (2003).

288. A. Ouchi, M. Shimoi, F. Bbina, T. Uehiro, and Y. Yoshino, *Bull. Chem. Soc. Jpn*., *51*, 3511 (1978).

289. J. A. Cras and J. Willemse, *Recl. Trav. Chim. Pays-Bas*, *97*, 28 (1978).

290. S. Kraft and M. Wieber, *Z. Anorg. Allg. Chem*., *607*, 153 (1992).

291. (a) V. V. Sharutin, O. K. Sharutina, T. P. Platonova, A. P. Pakusina, D. B. Krivolapov, A. T. Gubaidullin, and I. A. Litvinov, *Russ. J. Gen. Chem*., *72*, 1379 (2002). (b) V. V. Sharutin, O. K. Sharutina, T. P. Platonova, A. P. Pakusina, D. B. Krivolapov, A. T. Gubaidullin, and I. A. Litvinov, *Zh. Obshchei Khim*., *72*, 1465 (2002).

292. V. V. Sharutin, O. K. Sharutina, T. P. Platonova, A. P. Pakusina, A. V. Gerasimenko, E. A. Gerasimenko, B. V. Bukvetskii, and D. Yu. Popov, *Russ. J. Coord. Chem*., *29*, 11 (2003).

293. B. G. Sejekan, C. J. Janakiram, and G. Aravamudan, *J. Inorg. Nucl. Chem*., *40*, 211 (1978).

294. G Aramudan, C. Janarkiram, and G. Sejekan, *Phosphorus Sulfur*, *5*, 185 (1978).

295. A. Sugihara, *Kagaku Kogyo (Osaka)*, *59*, 319 (1985).

296. S. Husebye, *Phosphorus Sulfur*, *38*, 271 (1988).

297. S. P. Chidambaram, G. Aravamudan, and M. Seshasayee, *Z. Kristallogr*., *187*, 231 (1989).

298. X. P. Yan, M. Sperling, and W. Welz, *Anal. Chem*., *71*, 4353 (1999).

299. M.-L. Kiekkola, *Mikrochim. Acta*, *1*, 327 (1982).

300. S. Rajashree, R. K. Kumar, M. R. Udupa, G. Aravamudan, and M. Seshasayee, *Phosphorus, Sulfur, Silicon*, *108*, 85 (1996).

301. S. Rajashree, R. K. Kumar, G. Aravamudan, M. R. Udupa, K. Sivakumar, and H-K Fun, *Acta Crystallogs., Sect. C*, *55*, 1320 (1999).

302. N. Zumbulyadis and H. J. Gysling, *Inorg. Chem*., *21*, 564 (1982).

303. G. C. Rout, M. Seshasayee, K. Radha, and G. Aravamudan, *Acta Crystallogs., Sect. C*, *39*, 1021 (1983).

304. W. Mazurek and A. G. Moritz, *Inorg. Chim. Acta*, *154*, 71 (1988).

305. W. Mazurek, *Inorg. Chim. Acta*., *160*, 11 (1989).

306. A. M. Bond, D. Dakternieks, R. Di Giacomo, and A. F. Hollenkamp, *Inorg. Chem.*, *28*, 1510 (1989).
307. V.Ganesh, M. Seshasayee, Sp. Chidambaram, G. Aravamudan, K. Goubitz, and H. Schenk, *Acta Crystallogs., Sect. C*, *45*, 1506 (1989).
308. V. Kumar, G. Aravamudan, M. Seshasayee, P. Selvam, and K. Yvon, *Acta Crystallogs., Sect. C*, *46*, 2081 (1990).
309. R. K. Kumar, G. Aravamudan, and M. R. Udupa, *Phosphorus, Sulfur, Silicon*, *114*, 39 (1996).
310. M. A. K. Ahmed and W. R. McWhinnie, *Polyhedron*, *5*, 859 (1986).
311. M. J. Cox and E. R. T. Tiekink, *Z. Kristallogr.*, *214*, 584 (1999).
312. S. Husebye, *Acta Chem. Scand.*, *A33*, 485 (1979).
313. G. C. Rout, M. Seshasayee, G. Aravamudan, and K. Radha, *Acta Crystallogs., Sect. C*, *40*, 1142 (1984).
314. V. Kumar, G. Aravamudan, M. Seshasayee, P. Selvam, and K. Yvon, *Acta Crystallogs., Sect. C*, *46*, 2100 (1990).
315. A. V. Virovets, I. V. Kalinna, V. P. Fedin, and D. Fenske, *Acta Crystallogs., Sect. C*, *56*, E589 (2000).
316. B. F. Hoskins, E. R. T. Tiekink, and G. Winter, *Inorg. Chim. Acta*, *105*, 171 (1985).
317. C. Fabiani, R. Spagna, A. Vaciago, and L. Zambonelli, *Acta Crystallogs., Sect. B*, *27*, 1499 (1971).
318. S. Rajashree, R. K. Kumar, M. R. Udupa, M. Seshasayee, and G. Aravamudan, *Acta Crystallogs., Sect. C*, *52*, 707 (1996).
319. S. Chidambaram, G. Aravamudan, M. Seshasayee, T. A. Shibanova, and V. I. Simonov, *Polyhedron*, *7*, 1267 (1988).
320. S. Husebye and S. E. Svaeren, *Acta Chem. Scand.*, *27*, 763 (1973).
321. R. K. Kumar, G. Aravamudan, M. Seshasayee, K. Sivakumar, H-K. Fun, and I. Goldberg, *Polyhedron*, *17*, 1659 (1998).
322. C. H. Yu, Q. T. Cai, Z. X. Guo, Z. G. Yang, and S. B. Khoo, *Anal. Bioanal. Chem.*, *376*, 236 (2003).
323. M. A. K. Ahmed, A. E. McCarthy W. R. McWhinnie, and F. J. Berry, *J. Chem. Soc., Dalton Trans.*, 771 (1986).
324. A. A. West, W. R. McWhinnie, and T. A. Hamor, *J. Organomet. Chem.*, *356*, 159 (1988).
325. N Al-Salim, A. A. West, and W. R. McWhinnie, *J. Chem. Soc., Dalton Trans.*, 2363 (1988).
326. A. K. Singh and K. M. M. S. Prakash, *Polyhedron*, *11*, 1225 (1992).
327. R. K. Kumar, G. Aravamudan, M. R. Udupa, M. Seshasayee, and T. A. Hamor, *Polyhedron*, *12*, 2201 (1993).
328. K. Radha, G. Aravamudan, A. Rajalakshmi, G. C. Rout, and M. Seshasayee, *Aust. J. Chem.*, *39*, 847 (1986).
329. R. K. Kumar, G. Aravamudan, M. R. Udupa, and M. Seshasayee, *Polyhedron*, *15*, 3123 (1996).
330. R. K. Kumar, G. Aravamudan, M. R. Udupa, M. Seshasayee, and T. A. Hamor, *J. Chem. Soc., Dalton Trans.*, 2253 (1996).
331. A. Panda, G. Mugesh, H. B. Singh, and R. J. Butcher, *Organometallics*, *18*, 1986 (1999).
332. V. Ganesh, M. Seshasayee, V. Kumar, S. Chidambaram, G. Aravamudan, K. Goubitz, and H. Schenk, *J. Crystallogr. Spectrosc. Res.*, *19*, 745 (1989).
333. K. von Deuten, W. Schnabel, and G. Klar, *Phosphorus Sulfur*, *9*, 93 (1980).

334. S. Husebye and A. Thowsen, *Acta Chem. Scand*., *A35*, 386 (1981).
335. S. Husebye and A. G. Thowsen, *Acta Chem. Scand*., *A35*, 443 (1981).
336. G. V. N. A. Rao, M. Seshasayee, G. Aravamudan, and K. Radha, *Inorg. Chem*., *22*, 2590 (1983).
337. G. C. Rout, M. Seshasayee, G. Aravamudan, and K. Radha, *J. Crystallogr. Spectrosc. Res*., *14*, 193 (1984).
338. S. Chidambaram, G. Aravamudan, M.Seshasayee, M. R. Snow, and E. R. T. Tiekink, *Aust. J. Chem*., *42*, 969 (1989).
339. S. Husebye, K. Maartmann-Moe, and W.Steffensen, *Acta Chem. Scand*., *44*, 579 (1990).
340. S. Husebye and S. V. Lindeman, *Acta Crystallogs., Sect. C*, *51*, 2152 (1995).
341. M. J. Cox and E. R. T. Tiekink, *Z. Kristallogr. New Cryst. Struct*., *214*, 49 (1999).
342. W. Schnabel, K.von Deuten, and G. Klar, *Phosphours Sulfur*, *13*, 345 (1982).
343. W. Schnabel, K.von Deuten, and G. Klar, *Cryst. Struct. Commun.*, *10*, 1405 (1981).
344. G. V. N. Appa Rao, M. Seshasayee, G. Aravamudan, and K. Radha, *Acta Crystallogs., Sect. C*, *39*, 1018 (1983).
345. V. Kumar, G. Aravamudan, and M. Seshasayee, *J. Crystallogr. Spectrosc. Res*., *21*, 65 (1991).
346. R. K. Kumar, G. Aravamudan, M. R. Udupa, M. Seshasayee, and T. A. Hamor, *Acta Crystallogs., Sect. C*, *49*, 1328 (1993).
347. D. Dakternieks, R. Di Giacomo, R. W. Gable, and B. F. Hoskins, *J. Am. Chem. Soc*., *110*, 6762 (1988).
348. S. Husebye, K. Maartmann-Moe, and W. Steffensen, *Acta Chem. Scand*., *44*, 139 (1990).
349. S. Husebye and K. Maartmann-Moe, *Acta Chem. Scand*., *49*, 834 (1995).
350. S. Husebye, S. Kudis, and S. V. Lindeman, *Acta Crystallogs., Sect. C*, *52*, 424 (1996).
351. S. Husebye, S. Kudis, and S. V. Lindeman, *Acta Crystallogs., Sect. C*, *52*, 429 (1996).
352. S. Husebye, T. Engebretsen, M. D. Rudd, and S. V. Lindeman, *Acta Crystallogs., Sect. C*, *52*, 2022 (1996).
353. D. S. Yufit, Yu. T. Struchkov, L. Yu. Ukhin, Z. S. Morkovnik, A. A. Maksimenko, I. D. Sadekov, M. M. Levkovich, S. I. Tesgoedova, and V. D. Stebletsova, *Koord. Khim*., *13*, 1702 (1987).
354. D. Dakternieks, R. Di Giacomo, R. W. Gable, and B. F. Hoskins, *J. Organomet. Chem.*, *349*, 305 (1988).
355. D. Dakternieks, R. Di Giacomo, R. W. Gable, and B. F. Hoskins, *J. Am. Chem. Soc*., *110*, 6753 (1988).
356. J. H. E. Bailey, J. E. Drake, A. B. Sarkar, and M. L. Y. Wong, *Can. J. Chem*., *67*, 1735 (1989).
357. A. M. Bond, D. Dakternieks, R. Di Giacomo, and A. F. Hollenkamp, *Organometallics*, *10*, 3310 (1991).
358. J. H. E. Bailey, J. E. Drake, and M. L. Y. Wong, *Can. J. Chem*., *69*, 1948 (1991).
359. J. H. E. Bailey and J. E. Drake, *Can. J. Chem*., *71*, 42 (1993).
360. J. E. Drake and J. Yang, *Inorg. Chem*., *36*, 1890 (1997).
361. V. García-Montalvo, R. A. Toscano, A. Badillo-Delgado, and R. Cea-Olivares, *Polyhedron*, *20*, 203 (2001).
362. J. O. Bogason, D. Dakternieks, S. Husebye, K. Maartmann-Moe, and H. Zhu, *Phosphorus, Sulfur, Silicon*, *71*, 13 (1992).
363. J. E. Drake, L. N. Khasrou, A. G. Misiankar, and R. Ratnani, *Can. J. Chem*., *77*, 1262 (1999).
364. G. Canseco-Melchor, V. García-Montalvo, R. A. Toscano, and R. Cea-Olivares, *Z. Anorg. Allg. Chem*., *627*, 2391 (2001).

365. G. Canseco-Melchor, V. García-Montalvo, R. A. Toscano, and R. Cea-Olivares, *J. Organomet. Chem*., *631*, 99 (2001).

366. D. Dakternieks, R. Di Giacomo, R. W. Gable, and B. F. Hoskins, *J. Organomet. Chem*., *353*, 35 (1988).

367. A. K. Singh and J. K. Basumatary, *J. Organomet. Chem*., *364*, 73 (1989).

368. J. E. Drake and M. L. Y. Wong, *J. Organomet. Chem*., *377*, 43 (1989).

369. A. K. Singh, V. Srivastava, J. K. Basumatary, T. P. Singh, and A. K. Saxena, *Phosphorus, Sulfur, Silicon*, *89*, 31 (1994).

370. S. Husebye, S. Kudis, S. V. Lindeman, and P. Strauch, *Acta Crystallogs., Sect. C*, *51*, 1870 (1995).

371. R. K. Kumar, G. Aravamudan, M. R. Udupa, M. Seshasayee, P. Selvam, and K. Yvon, *Polyhedron*, *15*, 1453 (1996).

372. J. E. Drake, L. N. Khasrou, A. G. Mislankar, and R. Ratnani, *Inorg. Chem*., *38*, 3994 (1999).

373. J. G. Alvarado-Rodrígues, Y. M. C. G. Gutiérrez, and R. Cea-Olivares, *Rev. Mex. Fis*, *46* (Suppl. 2), 44 (2000).

374. V. García-Montalvo, A. Marcelo-Polo, R. Montoya, R. A. Alfredo, S. Hernández-Ortega, and R. Cea-Olivares, *J. Organomet. Chem*., *623*, 74 (2001).

375. R. K. Kumar, G. Aravamudan, K. Sivakumar, and H-K. Fun, *Acta Crystallogs., Sect. C*, *55*, 1121 (1999).

CHAPTER 2

Transition Metal Dithiocarbamates: 1978–2003

GRAEME HOGARTH

Department of Chemistry
University College London
London, UK

CONTENTS

Progress in Inorganic Chemistry, Vol. 53 Edited by Kenneth D. Karlin

I. INTRODUCTION

Dithiocarbamates ($R_2CNS_2^-$) are a versatile class of monoanionic 1,1-dithio ligands (Fig. 1) and as they are easily prepared, a wide range of chemistry has been developed around them. Indeed, they rank alongside such ligands as phosphines and cyclopentadienyls in their versatility and abundance.[1]

[1] The term ''dithiocarbamate'' rather than ''dithiocarbamato'' is used throughout this chapter.

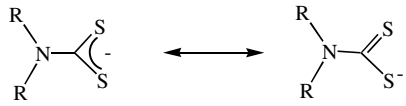

Figure 1. The dithiocarbamate ligand.

It is not clear when dithiocarbamates were first prepared, but certainly they have been known for at least 150 years, since as early as 1850 Debus reported the synthesis of dithiocarbamic acids (1). The first synthesis of a transition metal dithiocarbamate complex is also unclear, however, in a seminal paper in 1907, Delépine (2) reported on the synthesis of a range of aliphatic dithiocarbamates and also the salts of di-*iso*-butyldithiocarbamate with transition metals including; chromium, molybdenum, iron, manganese, cobalt, nickel, copper, zinc, platinum, cadmium, mercury, silver, and gold. He also noted that while dithiocarbamate salts of the alkali and alkali earth elements were water soluble, those of the transition metals and also the *p*-block metals and lanthanides were precipitated from water, to give salts soluble in ether and chloroform, and even in some cases, in benzene and carbon disulfide.

From these early studies, dithiocarbamates and their transition metal complexes soon found a host of applications. For example, as a result of their insoluble nature they are widely used in inorganic analysis (3, 4). They can also be used to separate different metal ions by high-performance liquid chromatography (HPLC) (5–10) and capillary gas chromatography (GC) (11, 12), and find use as rubber vulcanization accelerators (13), fungicides (14), and pesticides (15). Concomitant with the development of these applications came a burgeoning interest in their general transition metal chemistry and the characteristics and properties of the complexes formed.

This chapter focuses on the development of transition metal dithiocarbamate chemistry between 1978–2003. As such, it follows from two previous reviews of the area by Coucouvanis, which appeared in this series and covered work published up to and including 1977 (16, 17). However, a major difference with these predecessors is its scope. While Coucouvanis reviewed dithiocarbamates along with other 1,1-dithio ligands, and also sought to include their chemistry when bound to main group elements, this chapter is limited solely to transition metal dithiocarbamate chemistry. This coverage has been necessitated by the tremendous expansion of this area of chemistry, and also the author's attempt to make this chapter as comprehensive as possible. The latter is a major challenge even in today's electronic publishing world (a Web of Science search for dithiocarbamate or dithiocarbamato gives >3500 hits while SciFinder gives 13,000 hits!), and sincere apologies are offered to anyone whose work has been missed. It also means that there is less of a critical evaluation; apologies once again.

While the work covered is primarily that between 1978 and 2003, some examples of earlier work have been included, either in the form of an historical background, or in order to put recent contributions in context. The introductory section also briefly includes some older material, as it is inappropriate for the reader to refer back continuously to the earlier reviews.

It should be acknowledged that both before and after Coucouvanis's reviews (16, 17) others also reviewed aspects of transition metal dithiocarbamate chemistry (18–31). Notably, in 1984 Bond and Martin reviewed the electrochemical and redox behavior of transition metal dithiocarbamate complexes (20), and as such less emphasis is placed here on electrochemical properties. Further, as early as 1965, Thorn and Ludwig produced an excellent book *The Dithiocarbamates and Related Compounds* (32), which is still well worth a read, especially for the newcomer to the area.

Given the limitations of this chapter, related ligands such as selenothiocarbamates, diselenocarbamates, xanthates, and others illustrated in Fig. 2, are not covered here. Some key references to more recent contributions in these areas are given in order to aid the reader further.

This chapter is aimed at inorganic chemists and as such it focuses on the synthesis, properties, and reactivity of transition metal dithiocarbamate complexes. A flavor of the established and potential applications of each metal type is given in Section IV, but space restrictions nessetate that their applications in analytical chemistry and the agricultural industry (27), together with their widespread biological applications (45–48) are not fully developed.

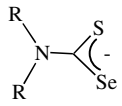

Selenothiocarbamate [33]

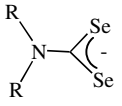

Diselenocarbamate [33–35]

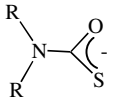

Thiocarbamate [36]

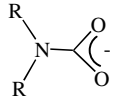

Carbamate [37]

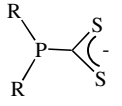

Phosphino-dithioformate [38]

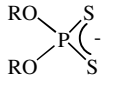

Dithiophosphate [39]

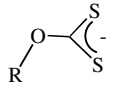

Xanthate [40, 41]

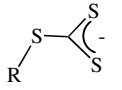

Thioxanthate [42, 43]

Dithiocarboxylate [44]

Figure 2. Monoanionic, small bite-angle, bidentate ligands related to dithiocarbamates.

II. SYNTHESIS AND PROPERTIES OF DITHIOCARBAMATES

Dithiocarbamates are generally easily prepared, resulting from the reaction of carbon disulfide with a secondary amine in the presence of base (Eq. 1). Reactions are usually carried out in water, methanol or ethanol, and sodium or potassium hydroxides typically serve as the base. Some preparations recommend that the reaction be carried out at low temperature, but in most cases room temperature suffices. Reactions are typically rapid and proceed cleanly and in high yield.

$$R_2NH + CS_2 + MOH \longrightarrow R_2NCS_2M + H_2O \qquad (1)$$

Virtually all secondary dialkylamines react in this manner. Most are water soluble, and are used as prepared, although if required, the sodium and potassium salts can often be isolated. Indeed, NaS_2CNR_2 (R = Me, Et) are available commercially and are sold as the tris(aqua) salts, $NaS_2CNR_2.3H_2O$, which if required can easily be dehydrated in a vacuum oven. In some instances the salts can precipitate upon formation, generally as white solids, and are stored for later use. Recrystallization from methanol or other alcohols can often be carried out, and in this manner the sodium salts of dithiocarbamates derived from succinimide (**1**) and phthalimide (**2**) (Fig. 3) have been successfully prepared and isolated in 55–60% yields (49), as has that from aza-15-crown-5 (**3**) (Fig. 3) (50). Figure 4 gives a range of some novel dithiocarbamates prepared.

The sodium and potassium salts of dithiocarbamates, while often displaying good solubility in water, are only very poorly soluble (if at all) in common organic solvents. In contrast, the corresponding ammonium salts, $[R_2NH_2][S_2CNR_2]$, generally show much better solubility in organic media. The latter are very easily prepared from the reaction of carbon disulfide and secondary amines in the absence of base (Eq. 2).

$$2\,R_2NH + CS_2 \rightleftharpoons [R_2NCS_2][R_2NH_2] \qquad (2)$$

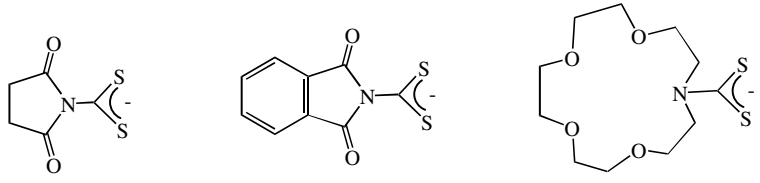

1 **2** **3**

Figure 3. Examples of dithiocarbamates crystallized from alcohols.

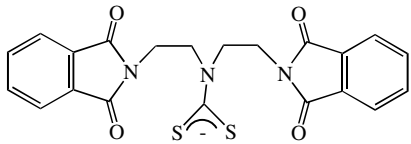

(51)

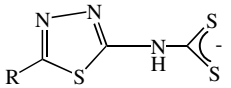

(52, 53)

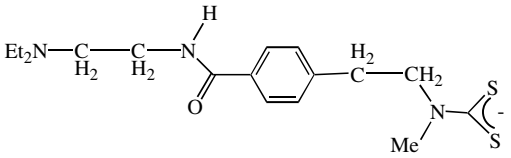

(54)

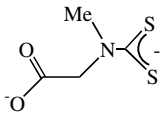

(55)

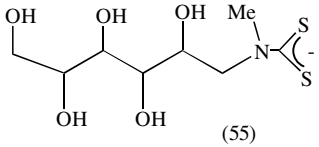

(55)

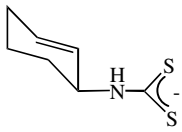

(56)

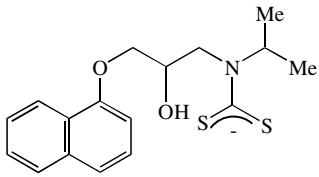

(57)

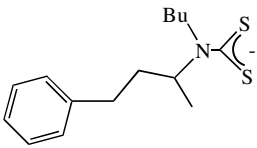

(58)

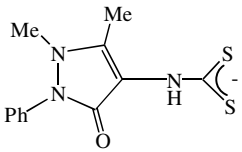

(59, 60)

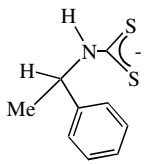

(61)

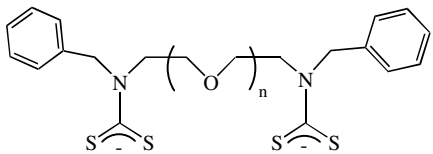

(62)

Figure 4. A selection of unusual dithiocarbamate ligands.

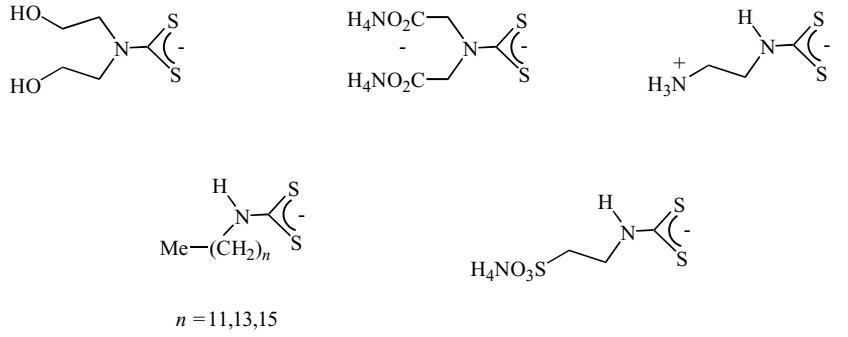

Figure 5. Water soluble ammonium dithiocarbamates prepared by Jones et al. (67).

Calderazzo et al. (63, 64) followed these reactions in toluene by infrared (IR) spectroscopy. They noted that the equilibrium was rapidly established, and was shifted almost completely to the salt as surmised from the disappearance of the 2160-cm^{-1} vibration of carbon disulfide within a few minutes. Cavell et al. (65) also noted the rapid formation of these salts in acetone at $<10°C$. All are virtually nonelectrolytes in this solvent suggesting that they are strongly ion paired, the molar conductance of $[Et_2NH_2][S_2CNEt_2]$ (4.4 Ω cm^{-1} mol^{-1}) being significantly less than the sodium salt (21.0 $\Omega\,cm^{-1}$ mol^{-1}). They have also calculated heats of formation of $[Et_2NH_2][S_2CNEt_2]$ as -81.1 ± 3.2 and -87.0 ± 4.6 kJ mol^{-1} for solid and gaseous states, respectively (66).

Jones et al. (67) also prepared a wide range of water soluble ammonium dithiocarbamate salts, $[NH_4][S_2CNR_2]$ (Fig. 5). They result from the initial reaction of the amine with concentrated aqueous ammonia in ethanol, followed by later addition of carbon disulfide at low temperatures. For example, diethanolamine, $HN(CH_2CH_2OH)_2$, forms a yellow precipitate in 65% yield. Castro et al. (68) studied the kinetics and mechanism of the reactions of piperidine, pyrrolidine, morpholine, and benzylamine (69) with carbon disulfide in ethanol (Fig. 6). They proceed via a dithiocarbamic acid intermediate (**4**), which in turn yields the dithiocarbamate anion (**5**) upon proton loss to the amine. While for pyrrolidine, formation of the dithiocarbamic acid is rate determining and proceeds to the dithiocarbamate irreversibly, for both morpholine and benzylamine, the transformation is reversible. Further, in these cases the ethoxide anion is found to catalyze the transformations. They have also determined that pyrrolidine is $\sim$200 times more nucleophilic toward carbon disulfide than piperidine, despite the later being only slightly more basic, a feature that may relate to the irreversible nature of the formation of pyrrolidine dithiocarbamate.

Dithiocarbamates with two aryl substituents are far less common and the sodium and potassium salts cannot be prepared as simply as those of

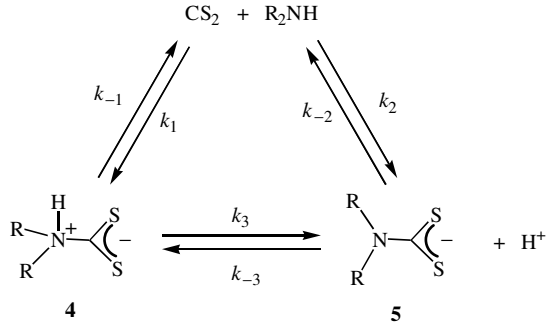

Figure 6. Mechanism of the reaction of secondary amines with carbon disulfide.

dialkylamines. Vella and Zubieta (70, 71) described the synthesis of NaS_2CNPh_2, via the initial generation of sodium diphenylamide, upon refluxing Ph_2NH with excess sodium hydride in tetrahydrofuran (THF) under nitrogen, followed by later addition of excess (XS) carbon disulfide (Eq. 3).

$$Ph_2NH + CS_2 + NaH \longrightarrow Ph_2NCS_2Na + H_2 \qquad (3)$$

Bereman and Nalewajek (72) described the synthesis of dithiocarbamates derived from indole, indoline, carbazole, and imidazole (Fig. 7). Again, the amides are initially generated in dry THF upon addition of potassium metal, and later addition of excess carbon disulfide at $-78°C$ leads to generation of the potassium salts of the dithiocarbamates (Eq. 4). While the indoline and imidazole derivatives are relatively air stable, the others are extremely air sensitive decomposing in a matter of minutes. The potassium salt of the dithiocarbamate derived from 2,2′-dipyridylamine (Fig. 7) has been prepared in a similar fashion, and while air stable, it is extremely hygroscopic (73).

$$R_2NH + CS_2 + K \longrightarrow R_2NCS_2K + 0.5\,H_2 \qquad (4)$$

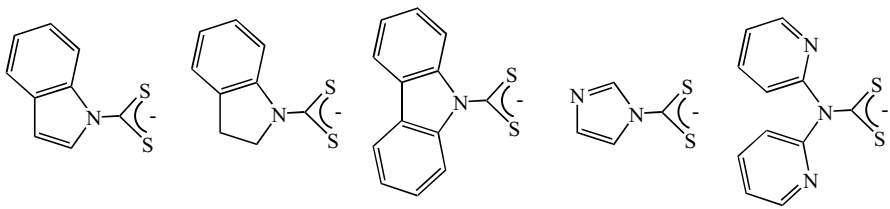

Figure 7. Some dithiocarbamates prepared by Bereman and co-workers.

The bis(2,2,2-trifluoroethyl) dithiocarbamate salt, $NaS_2CN(CH_2CF_3)_2$, is a valuable precursor to a range of complexes that find widespread uses in analytical chemistry (74–82). It can be readily prepared from the amine using sodium amide as the base in the presence of carbon disulfide (Eq. 5) (76, 75), and a synthesis of the lithium salt has also been reported (83, 84).

$$(CF_3CH_2)_2NH + CS_2 + NaNH_2 \longrightarrow (CF_3CH_2)_2NCS_2Na + NH_3 \quad (5)$$

Dithiocarbamates generated from primary amines are generally less stable than their secondary amine counterparts, and can decompose to give the corresponding isothiocyanate (Eq. 6).

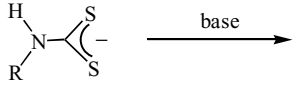

(6)

Indeed, this transformation has been developed into a procedure for the preparation of isothiocyanates from primary amines using hydrogen peroxide as the dehydrosulfurization reagent. It proceeds via the thiuram disulfide, although concentrations of the latter are always kept low (Fig. 8) (85).

Ammonium salts, $[NH_4][S_2CNHR]$ (R = Bu, Cy), have been prepared in high yields upon addition of carbon disulfide to an ice cold mixture of the amine in the presence of concentrated aqueous ammonia (Fig. 9) (86). As expected, they are not very stable and decompose upon heating. Nevertheless, they have still been used to prepare a wide range of group 10 bis(dithiocarbamate) complexes. The primary amine $CF_3CH_2NH_2$ also reacts directly with carbon disulfide to

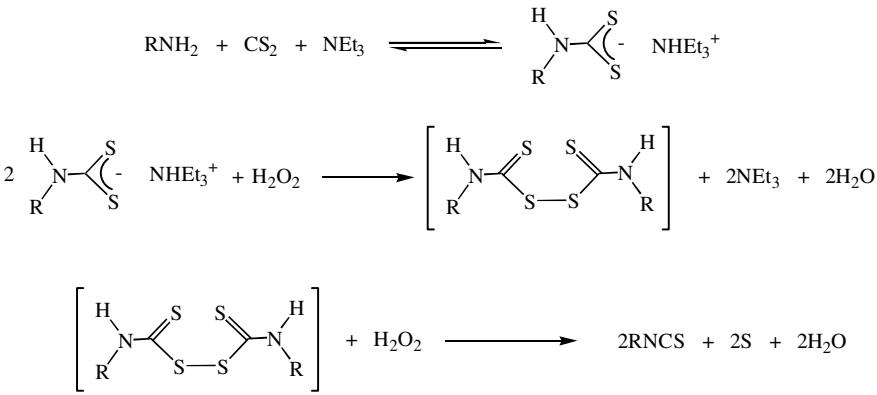

Figure 8. Proposed route for the preparation of isothiocyanates from primary amines.

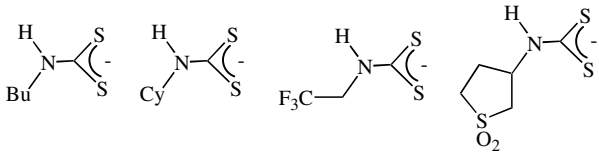

Figure 9. Some dithiocarbamates derived from primary amines.

presumably produce the salt $[CF_3CH_2NH_3][S_2CNHCH_2CF_3]$, which has been used *in situ* to prepare a nickel complex (76), while Vasiliev and Polackov have prepared potassium 1,1-dioxothiolan-3-yl dithiocarbamate upon addition of potassium hydroxide to the amine in the presence of carbon disulfide (87).

In a series of publications, George and Weiss (88–90) reported the preparation of dithiocarbamate salts, $[H(CH_2)_nNHCS_2][H(CH_2)_nNH_3]$ ($n = 3$, 10, 18), upon addition of carbon disulfide to the relevant amines. All behave as low-molecular-mass organic gelators (LMOGs), forming microheterogeneous phases in which they self-assemble in three dimensional (3D) fibrillar networks as a result of the organization of hydrophobic alkyl chains and charged end-groups (Fig. 10). As expected, salts with longer alkyl chains are better gelators than their shorter homologues. They also show a much greater tendency to aggregate in chloroform than do the corresponding carbamates, and also display no tendency to undergo CS_2 scrambling under conditions where the exchange of CO_2 in the carbamates is very fast.

Aniline-derived dithiocarbamates (Fig. 11) have been prepared either as the sodium or ammonium salts, with the latter being the most common (91–94). For

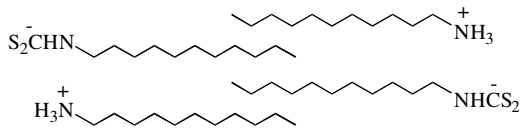

Figure 10. Dithiocarbamate salts acting as LMOGs.

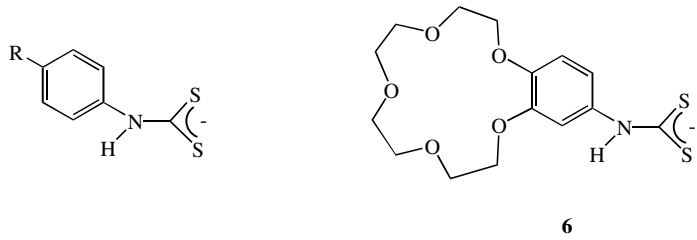

6

Figure 11. Examples of aniline-derived dithiocarbamates.

example, Kaul and Pandeya (95) prepared a large range of substituted aniline-derived dithiocarbamate salts, $[ArNHCS_2][NH_4]$, upon addition of the aniline to an ice-cold mixture of carbon disulfide and aqueous ammonia (Fig. 11). They precipitate from solution as white solids, but tend to become yellow and decompose within a few days. Consequently, they are best used as prepared. Green and co-workers (50) reported the preparation of the sodium salt of the dithiocarbamate derived from 4-aminobenzo-15-crown-5 (**6**) (Fig. 11) from the simple addition of carbon disulfide to 4-aminobenzo-15-crown-5 in water in the presence of sodium hydroxide. However, repeated attempts to purify it failed and attempts to oxidize it to the thiuram disulfide lead only to formation of the isothiocyanate. Nevertheless, analytically pure nickel and copper bis(dithiocarbamate) complexes were still prepared. The parent dithiocarbamate, $H_2NCS_2^-$, can be prepared as its ammonium salt and the 1939 synthesis of Booth is still widely utilized (96).

Dithiocarbamates can also be prepared from diamines. For example, as early as 1872, Hofmann (97) reported the reaction of carbon disulfide with 1,2-diaminoethane. Later in the 1960s, addition of 2 equiv of sodium hydroxide and carbon disulfide to 1,2-diaminoethane was shown to afford the bis(dithiocarbamate) compound in an exothermic reaction (98–102); 1,6-diaminohexane behaving in a similar manner (98). A wide range of polymeric transition metal complexes have been prepared using these salts (98). All are insoluble in water and common organic solvents, and some examples have been developed as fungicides (14, 31).

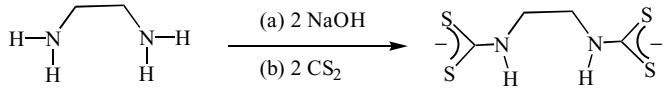

(7)

Fabretti et al. (103) showed that a similar transformation can be effected with piperazine and again a wide range of polymeric transition metal complexes have been prepared, as have related derivatives of the dithiocarbamate derived from homopiperazine (Fig. 12) (104).

Triethylammonium salts of bis(dithiocarbamates) can also be prepared using NEt_3 as the base, and in this way Lorcy and co-workers (105) prepared examples derived from 1,2-diaminoethane and 2,2-(ethylenedioxy)bis(ethylamine) (106) in near quantitative yields. Further, Jones et al. (67) prepared the

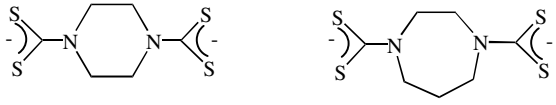

Figure 12. Bis(dithiocarbamtes) derived from piperazine and homopiperazine.

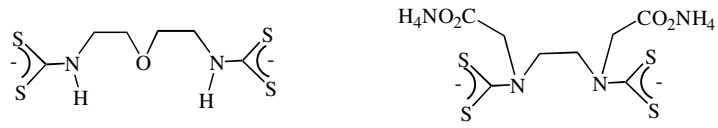

Figure 13. Further examples of bis(dithiocarbamates).

bis(dithiocarbamate) derived from ethylenediaminediacetic acid in 95% yield using concentrated aqueous ammonia as the base (Fig. 13).

Zagidullin (107) reported the synthesis of bis- and tris(dithiocarbamates) from acyclic di- and polyamines (**7**–**9**) (Fig. 14). Although the precise nature of the dithiocarbamates formed is not clear, all are reported to form complexes upon addition of MCl_2 (M = Mn, Fe, Co, Ni, Cu, Zn, Cd), which show fungicidal activity. Similarly, bis(dithiocarbamates) have been prepared from *N*-(β-aminoethyl)piperazine (**10**) as well as and some derivatives such as (**11**) (Fig. 14) (108).

In one contribution, Siddiqi et al. (109) suggest that addition of 2 equiv of sodium hydroxide and carbon disulfide to 1,3-diaminopropane affords only the monodithiocarbamate salt, although this seems unlikely given the work discussed earlier.

It is possible to prepare monodithiocarbamates from diamines simply upon addition of carbon disulfide, one of the amines acting as the base and the second as the nucleophile. For example, addition of carbon disulfide to homopiperazine yields $H_2NC_5H_{10}CS_2$ (Eq. 8) (104).

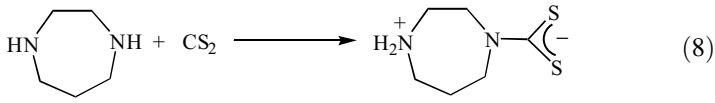

(8)

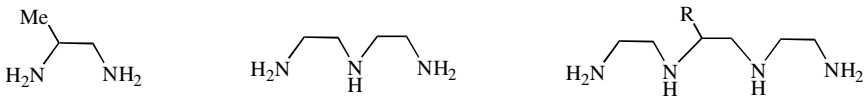

7 **8** **9**

R = H, Me

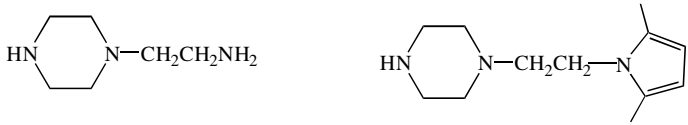

10 **11**

Figure 14. Amines used to prepare bis- and tris(dithiocarbamates).

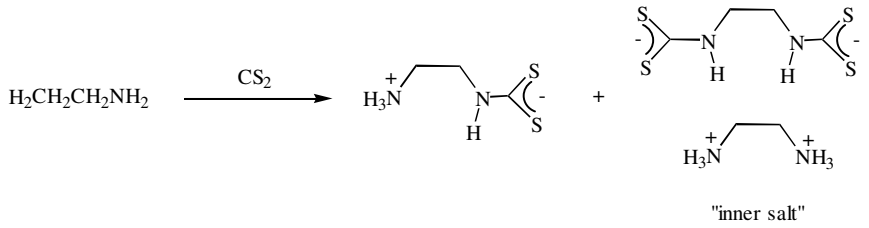

Figure 15. The competing formation of monodithiocarbamate and ''inner salts''.

Formation of zwitterions in this manner a well-known process that has previously been studied in detail for 1,2-diaminoethane (110) and piperazine (111,112). Reactions are, however, generally not clean and $\sim$ 20–30 % of the ''inner salt'' is usually generated as well (Fig. 15). Further, if the reaction is carried out in a solvent in which the inner salt is insoluble, then the product of the reaction is mainly the latter (113). Frank (114) used (proton nuclear magnetic resonance) ^{1}H NMR measurements in D_2O to determine the mono- and bis(dithiocarbamate) ratios generated from 1,2-diaminoethane. When there is more than one inequiv amine site in a compound, it is normally the least basic of them, which initially reacts with carbon disulfide to form the dithiocarbamate, the more basic site acting as the proton acceptor.

Phenylene diamines do not always behave in the same way as aliphatic diamines. Addition of carbon disulfide to 1,2-diaminobenzene in the presence of base is proposed to initially afford the bis(dithiocarbamate), but this exhibits only limited stability, rapidly undergoing cyclization to give the thione (Fig. 16) (102).

Monodithiocarbamates can be prepared from phenylene diamines in the presence of a second, more basic amine. For example, addition of carbon disulfide and NEt_3 to 1,2-diaminobenzene affords the yellow triethylammonium dithiocarbamate salt in high yield (115). The latter can then be reacted with various α-halogenated carbonyl derivatives resulting in cyclization and dehydration to give the new amines. These in turn react with carbon disulfide and

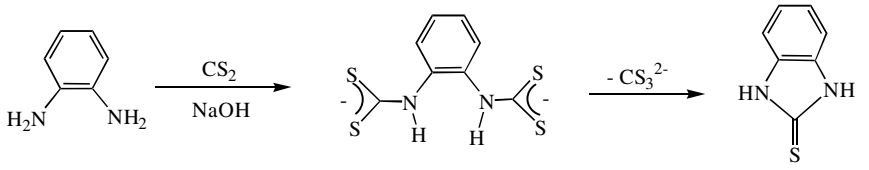

Figure 16. Formation of the bis(dithiocarbamate) derived from 1,2-diaminobenzene and later rearrangement to yield the corresponding thione.

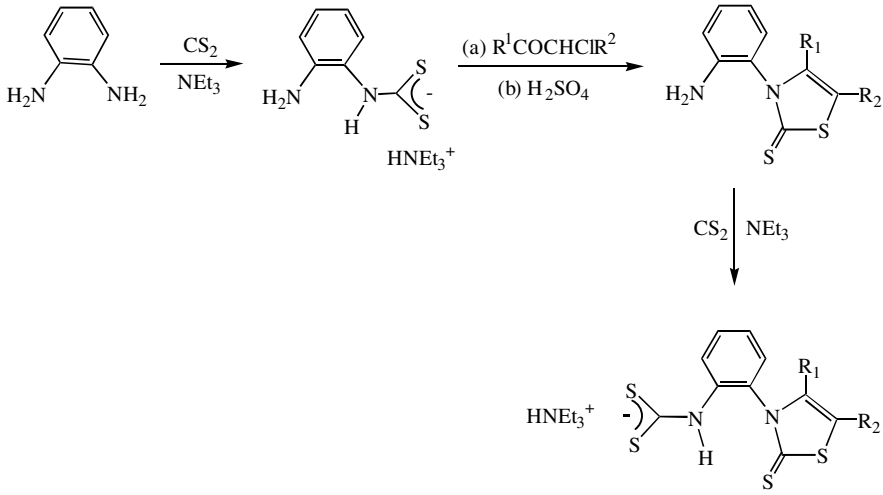

Figure 17. The stepwise formation of monodithiocarbamates derived from 1,2-diaminobenzene.

NEt_3 to form a second dithiocarbamate, although this transformation is far slower than the first and only occurs after 10 days (Fig. 17) (115). You and co-workers (116) also reported the preparation of the monodithiocarbamate derived from 1,4-diamoinobenzene, formed upon addition of carbon disulfide to the amine at low temperature (Eq. 9).

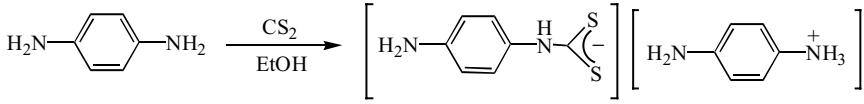

(9)

Dithiocarbamates can also be prepared from hydrazines (Fig. 18). Hydrazine itself reacts with carbon disulfide in the presence of base to afford the dithiocarbamate salt, NaS_2CNHNH_2 (117), although if more carbon disulfide and base are used a second product, $Na_3S_2CNHCS_2$ can result (118). Substituted

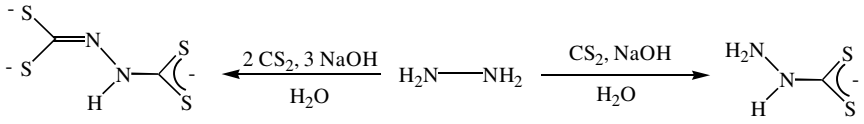

Figure 18. Reaction of hydrazine with carbon disulfide in the presence of base.

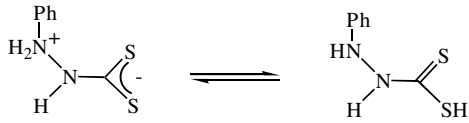

Figure 19. Possible resonance forms for the dithiocarbamate derived from phenylhydrazine.

hydrazines also react with carbon disulfide alone, although the products can exist in the dithiocarbazic acid form, as shown below for phenylhydrazine (Fig. 19) (92).

Dithiocarbamates have been prepared from a wide range of amino acids (Fig. 20) (119–123). They are usually generated as the barium salts upon addition of barium hydroxide to the amino acid in the presence of carbon disulfide. Macías et al. (124) measured the ionization energies of various α-amino acid dithiocarbamates by X-ray photoelectron spectroscopy (XPS) and find that they increase as the side chain becomes longer; probably being related to the change in donor ability. They react with transition metal salts to afford complexes in much the same way as simple dithiocarbamates (122, 125–138), although in some instances metal coordination of the carboxylate moiety is also proposed (119).

A number of polymers have been prepared bearing pendant dithiocarbamate groups and these have been used extensively for the removal of heavy ions from aqueous solutions (139–145). For example, Fish and co-workers (139) prepared a *N*-sulfonylethylene bis(dithiocarbamate) ligand anchored on macroporous polystyrene-divinylbenzene beads (Fig. 21), which is selective for the removal of Ag^{+}, Hg^{2+}, Cu^{2+}, Pb^{2+}, and Cd^{2+} ions from aqueous solutions.

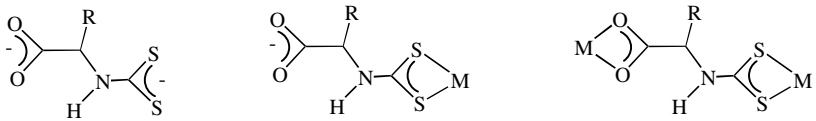

Figure 20. Some examples of dithiocarbamates derived from amino acids.

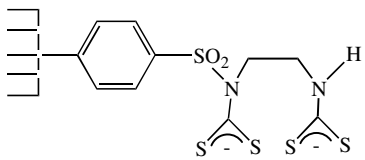

Figure 21. Schematic of the bis(dithiocarbamate) ligand derived from *N*-sulfonyletylene diamine anchored on macroporous polystyrene–divinylbenzene beads.

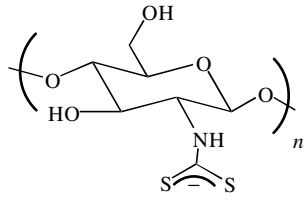

Figure 22. Schematic of the dithiocarbamate derived from chitosan.

Other dithiocarbamates have been prepared from naturally occurring polymers such as chitosan, a linear polymer of β-(1-4)-linked 2-amino-2-deoxy-D-glucopyranose (Fig. 22). The degree of dithiocarbamate substitution (defined as the number of dithiocarbamate units generated per 100 groups of 2-amino-2-deoxyglucopyranoside) has been assessed using both solid-state ^{13}C CP/MAS (MAS = magic-angle spinning)–TOSS (TOSS = total sideband suppression) NMR and microanalysis (sulfur content); both methods giving a value close to 22 (146).

The structural chemistry of alkali metal and ammonium dithiocarbamate salts was detailed in Coucouvanis's 1979 review (17) and relatively few new examples have been crystallographically characterized (147–151). In $LiS_2CNMe_2.4H_2O$, each lithium ion coordinates to four water molecules and there are no lithium–sulfur bonds, although the dithiocarbamates are linked by O—H···S hydrogen bonds (147). In contrast, the sodium ion in $NaS_2CNMe_2.2H_2O$ coordinates four water molecules and two sulfur atoms in a distorted octahedral arrangement that share edges and corners to form layers parallel to the ab plane, while each sulfur atom accepts two O—H···S hydrogen bonds (148).

A number of bis(dithiocarbamate) salts have also been crystallographically characterized (102, 152–154), including the disodium hexaaqua salts derived from 1,2-diaminoethane (102,154) and piperazine (153), and $K_2[S_2CN(R)CH_2CH_2N(R)CS_2].2EtOH$ (R = Me, *i*-Pr) (152). They generally consist of a polymeric chain in which the bis(dithiocarbamate) units are linked through the alkali metal ions. In all cases, the S_2CNC_2 unit(s) are approximately planar.

With the exception of those derived from primary amines, most dithiocarbamates are stable under neutral and basic conditions. However, under acidic conditions they rapidly decompose to give the free amine and carbon disulfide (Eq. 10).

$$R_2NCS_2^- \xrightarrow{H^+} R_2NH + CS_2 \qquad (10)$$

Jencks and co-workers (155) and Humeres et al. (91, 156, 157) studied in some detail the acid cleavage of dithiocarbamates (Eq. 11). The breakdown of

aryldithiocarbamates occurs much faster than that of alkyldithiocarbamates, being $> 10^4$-fold faster at similar pK_N values, the acid dissociation constant of the parent amine (91, 156, 157). A water molecule acting as an acid–base catalyst catalyzes the reaction. For alkyldithiocarbamates, two mechanisms have been proposed, the pathway taken being dependent on pK_N. At $pK_N < 10.5$, they decompose via slow intermolecular N-protonation to form a zwitterion, which is followed by rapid carbon–nitrogen bond cleavage; a pathway also observed for aryldithiocarbamates. In contrast, at $pK_N > 10.5$ a concerted intramolecular proton transfer and cleavage of the carbon–nitrogen bond is proposed.

$$RNHCS_2^- + H^+ \rightleftharpoons \overset{+}{R}NH_2CS_2^- \rightleftharpoons RNH_2 + CS_2 \qquad (11)$$

Given the propensity of dithiocarbamates to decompose upon protonation, the determination of the pK_a of dithiocarbamic acids is necessarily nontrivial. Cavalheiro and co-workers (158, 159) adopted a spectrophotometric method based on the rapid acquisition of data using a diode-array spectrophotometer to determine pK_a values for a number of cyclic dithiocarbamic acids at 25°C (Fig. 23).

Dithiocarbamates are nucleophiles and undergo substitution reactions with simple organic halides to produce new organosulfur compounds (31). For example, addition of NaS_2CNMe_2 to 1,2-dichloroethane (160), and chloroform (31) affords the compounds (**12** and **13**), respectively, while the same concept can be used to prepare more elaborate organosulfur compounds such as (**14** and **15**) (106, 161).

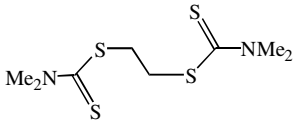

12

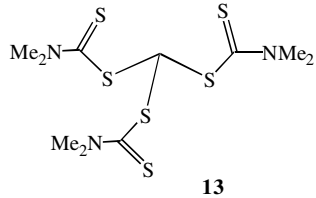

13

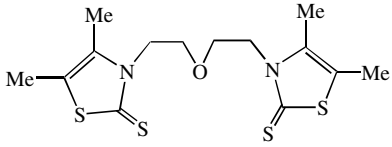

14

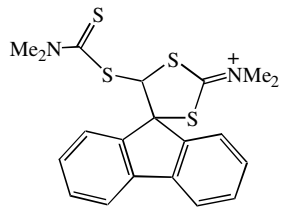

15

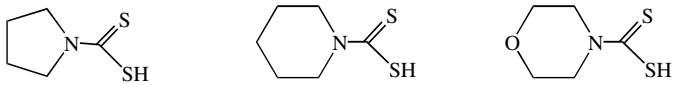

pK_a	3.10	3.51	3.56

Figure 23. The pK_a values for various dithiocarbamic acids.

Dithiocarbamates are easily oxidized to give the corresponding radicals that combine at almost the diffusion rate to yield thiuram disulfides (Eq. 12) (162). Thus, the voltammetric oxidation of $Et_2NCS_2^-$ gives an irreversible response at 0.09 V versus Ag/AgCl (ca. −0.4 V vs Cp_2Fe^+/Cp_2Fe) corresponding to the formation of tetraethylthiuram disulfide (163). At a synthetic level, iodine is often used as the oxidizing agent, the thiuram disulfides being generated in high yields. The dithiocarbamic acids also yield dithiocarbamate radicals upon photolysis, although here the radical cleavage of the thiol unit is a competing process (164).

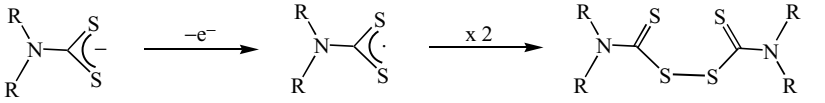

(12)

In very recent work, Lieder (165) calculated standard potentials of the dithiocarbamate–thiuram disulfide redox system via thermochemical cycles and computational electrochemistry. A pathway proceeding via a single electron detachment is predicted to be the most favorable mechanism for dithiocarbamate oxidation, while thiuram disulfide reduction can proceed via two pathways. In the gas phase, reduction followed by sulfur–sulfur bond cleavage is energetically preferred, while in solution a concerted bond-breaking electron-transfer mechanism is predicted to be equally probable.

Dithiocarbamate salts have a number of characterizing features. They exhibit strong ν(C—N) bands in the IR spectrum, together with other vibrations. For example, the ν(C—N) band in NaS_2CNEt_2 is reported at 1477 cm^{-1} in the solid state (CsI), while same band in the ammonium salt, $[NBu_4][S_2CNEt_2]$, is seen at 1485 cm^{-1} in the solid state (CsI) and 1467 cm^{-1} in solution ($CHCl_3$). In contrast, the ν(C—N) band in NaS_2CNPh_2 appears at 1325 cm^{-1} in the solid-state CsI (166).

Pandeya and co-workers (167) compared the IR spectra of benzyldithiocarbamate salts, $Bz(R)NCS_2^-$ (R = H, Me, Et, *i*-Pr, Bz), with those of dialkyl and phenyldithiocarbamates. As expected the ν(C—N) bands for the benzyl compounds (1470–1432 cm^{-1}) are slightly lower in frequency than the dialkyldithiocarbamates, and much higher than the phenyldithiocarbamates.

Surface-enhanced Raman scattering (SERS) spectra of NaS_2CNR_2 (R = Me, Et) have been obtained and compared with normal Raman spectra in both solid and solution. Dimethyldithiocarbamate has 30 fundamental modes of vibration in the C_{2v} point group, all being Raman active. In the 1400–1520-cm^{-1} region, three bands are seen in the SERS spectrum at 1446, 1492, and 1510 cm^{-1}, corresponding bands appearing at 1438, 1488, and 1493 cm^{-1} in the normal solid-state Raman spectrum. Mylrajan (168) has assigned these to δ (CH_3) modes, while broad bands at 564 and 442 cm^{-1} in the SERS spectrum are assigned to δ (CNC) and ν (CNC) modes, respectively.

Dithiocarbamate salts also show characteristic NMR features, the most pertinent being the low-field ^{13}C NMR resonance assigned to the backbone carbon atom, $\delta(N^{13}CS_2)$. This appears at 207.3 ppm for NaS_2CNEt_2 in D_2O and 212.0 ppm for $[NBu_4][S_2CNEt_2]$ in $CDCl_3$. As expected, in aromatic dithiocarbamates it is shifted to even lower field, appearing at 219.4 ppm for $[NBu_4][S_2CNPh_2]$ in $CDCl_3$ (166).

In comparison to the related transition metal complexes (see Section III.E), the free dithiocarbamate salts have extremely low ν(C—N) values, together with relatively high $\delta(N^{13}CS_2)$ values. Interestingly, lower ν(C—N) bands are seen for hydrated with respect to anhydrous ions, an effect attributed to hydrogen bonding that leads to a weakening of the carbon–sulfur bonds and concomitant strengthening of the carbon–nitrogen bond. These effects may also contribute to the lowering of the $\delta(N^{13}CS_2)$ values (166).

III. TRANSITION METAL DITHIOCARBAMATE COMPLEXES

Transition metal dithiocarbamate complexes were probably first prepared in 1907 by Delépine (2) and over the following century, dithiocarbamate complexes of all the transition elements have been prepared and in a wide range of different oxidation states (Table I). Perhaps most impressive is their ability to stabilize molybdenum in seven oxidation states ranging from +6 to 0 (Fig. 24).

A. Synthesis

While transition metal dithiocarbamate complexes can be prepared in a wide variety of ways, by far the most common is the direct ligand addition, which often, but not necessarily, results in loss of a coordinated anionic ligand, and sometimes a second neutral ligand also (Eq. 13). This route has few limitations and complexes of all the transition metals have been prepared using it.

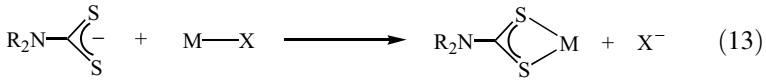

(13)

TABLE I
Range of Oxidation States Stabilized by Dithiocarbamates

Ti	+4	**V**	+3	**Cr**	0	**Mn**	+1	**Fe**	+2	**Co**	+1	**Ni**	+1?	**Cu**	+1	**Zn**	+2
	+3?		+4		+2		+2		+3		+2		+3		+2		
			+5		+3		+3		+4		+3		+3		+3		
					+4		+4				+4		+4				
Zr	+4	**Nb**	+3	**Mo**	0	**Tc**	+1	**Ru**	+2	**Rh**	+1	**Pd**	+2	**Ag**	+1	**Cd**	+2
			+4		+1		+2		+3		+2?		+4		+2?		
			+5		+2		+3		+4		+3						
					+3		+4										
					+4		+5										
					+5												
					+6												
Hf	+4	**Ta**	+3	**W**	0	**Re**	+1	**Os**	+2	**Ir**	+1	**Pt**	+2	**Au**	+1	**Hg**	+2
			+4		+2		+2		+3		+3		+3		+2		
			+5		+3		+3		+4				+4		+3		
					+4		+4		+6?								
					+5		+5										
					+6												

For example, addition of 2 equiv of NaS_2CNEt_2 to all *trans*-$[RuCl_2(CO)_2(PEt_3)_2]$ initially affords *trans*-$[RuCl(CO)(PEt_3)_2(S_2CNEt_2)]$ and later *cis*-$[Ru(CO)(PEt_3)(S_2CNEt_2)_2]$ (Eq. 14), while successive addition of NaS_2CNEt_2 and NaS_2CNMe_2 yields *cis*-$[Ru(CO)(PEt_3)(S_2CNMe_2)(S_2CNEt_2)]$ (169).

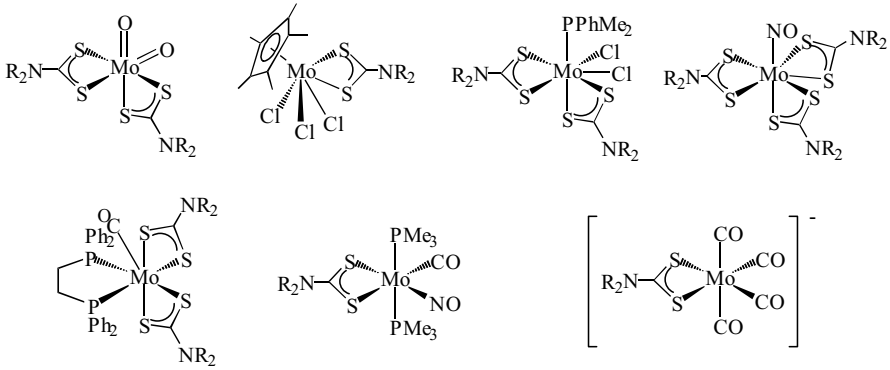

Figure 24. A selection of molybdenum dithiocarbamate complexes in oxidation states +6 to 0.

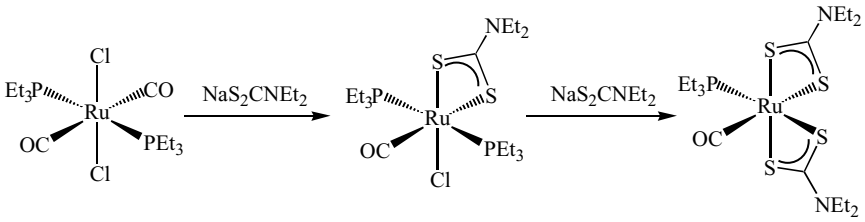

(14)

Another widely utilized method involves the oxidative–addition of thiuram disulfides to metal centers (Eq. 15); a reaction that has been reviewed by Victoriano (25, 170). Dithiocarbamate complexes of a number of transition metals can be prepared via this method, with examples at vanadium (171–173), molybdenum (174–180) and tungsten (181–183) being particularly prevalent.

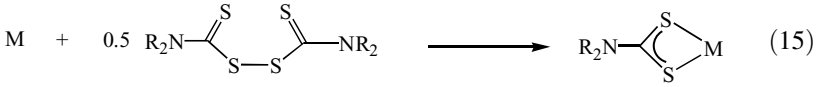

(15)

For example, addition of a range of thiuram disulfides to the vandium(II) complex, $[VCl_2(thf)_2]$, yields vanadium(IV) bis(dithiocarbamate) complexes, $[VCl_2(S_2CNR_2)_2]$ (R = Me, Et; $R_2 = C_5H_{10}$, C_4H_8O) (Eq. 16) (173).

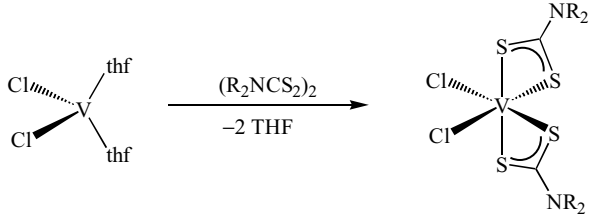

(16)

The transformation may occur via initial coordination of the thiuram disulfide complex followed by later addition of the sulfur–sulfur bond to the metal center. A limitation would appear to be the ability of the metal center to undergo a two-electron oxidation. However, Stiefel and co-workers (184, 185) reported unusual examples, whereby addition of thiuram disulfides (R = Me, Et, *i*-Bu) to the rhenium(VII) complex, $[Et_4N][ReS_4]$, results in the *reduction* of the metal center. Thus, addition of 1.5 equiv of thiuram disulfide affords dimeric rhenium(IV) complexes, $[Re(\mu\text{-}S)(S_2CNR_2)_2]_2$, while with 3 equiv rhenium(V)

complexes, $[Re(S_2CNR_2)_4]^+$, result (Eq. 17). While it seems counterintuitive that the addition of an oxidant leads to reduction of the metal center, the situation becomes clearer when it is realized that some of the metal-bound sulfido groups (S^{2-}) are oxidized to disulfide (S_2^{2-}) or elemental sulfur.

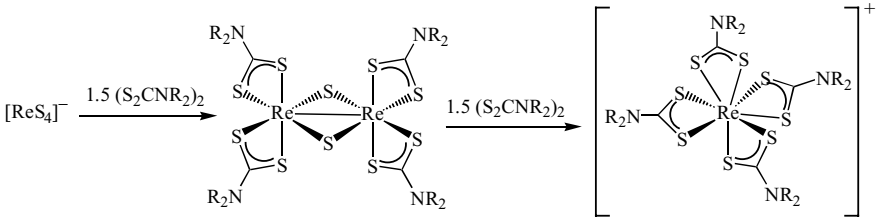

(17)

Casey and Vecchio (186,187) developed the oxidative–addition of thiuram disulfides to metals in order to produce a one-step preparation of a wide range of transition metal dithiocarbamate complexes. In this way, $[Ni(S_2CNMe_2)_2]$ and $[Zn(S_2CNMe_2)_2]$ can be prepared in near quantitative yields. With copper, only the copper(II) species are seen, and this is in keeping with Åkerström's (188) earlier observation that copper(I) species react instantaneously with thiuram disulfides to generate the analogous copper(II) complexes.

In a somewhat related manner, Tetsumi et al. (189) reported that dithiocarbamate salts, NaS_2CNR_2 (R = Me, Et), react readily with iron, nickel, chromium, and copper present in the ion source of a mass spectrometer to give their metal complexes. Here it would appear that the dithiocarbamate is first oxidized to the thiuram disulfide, which in turn reacts with metal; although the nature of the oxidizing agent is unclear. The reaction of metals with dithiocarbamate salts has been developed into a synthetic route to copper and nickel bis(dithiocarbamate) complexes. Thus, addition of the NaS_2CNR_2 to copper or nickel powders in chloroform yields $[M(S_2CNR_2)_2]$ (M = Cu, Ni; R = Me, Et, Pr, Bu; $R_2 = C_4H_8$). These reactions also work in ethanol or dimethyl sulfoxide (DMSO) and their rates are dependent on both the nature of the metal (Cu > Ni) and alkyl substituents (Bu > Pr > E > Me) (190). In related work, the direct synthesis of $[Cu(S_2CNMe_2)_2]$ from metallic copper has been shown to be accelerated by ultrasonic treatment (191).

Addition of tetraethylthiuram disulfide to silver(I) and cadmium(II) complexes, [AgR] and $[CdR_2]$ ($R = CF_3$, C_2F_5, C_4F_9, C_6F_5), generates the diethyldithiocarbamate complexes, $[Ag(S_2CNEt_2)]_6$ and $[Cd(S_2CNEt_2)_2]$, respectively, together with perfluoroorgano esters of diethyldithiocarbamic acid, Et_2NCS_2R (Eq. 18) (192).

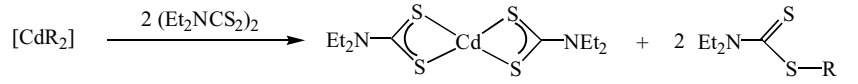

(18)

Although not now as widely utilized, an important historical synthesis was the insertion of carbon disulfide into a metal-amide (Eq. 19). In this way Bradley and Gitlitz (193) first prepared the eight-coordinate group 4 (IV B) complexes, $[M(S_2CNR_2)_4]$ (M = Ti, Zr, Hf; R = Me, Et, Pr) by utilizing $[M(NR_2)_4]$. It is limited to those metals that form stable amide complexes, generally being the early transition metals and some others in higher oxidation states, as the amide group is a good π-donor ligand.

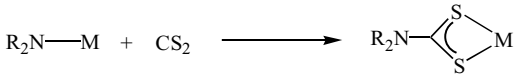

(19)

Examples of this behavior at late transition metal centers are also known, when the amide is stabilized, for example, by coordination to a ring. Thus, the dicarbonyl complex, $[Re(CO)_2(PPh_3)_2\{S_2CN(Me)CNSC_2H_2\}]$, has been prepared in low yield from the thermolysis of $[Re(CO)_2(PPh_3)_2(mat)]$ (mat = 2-methylaminothiazole) with excess carbon disulfide (Eq. 20) (194).

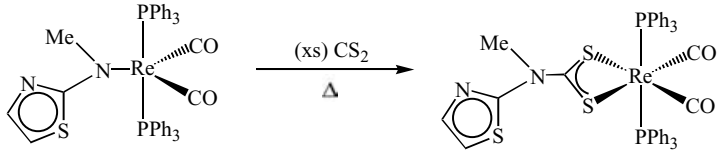

(20)

Copper complexes of bis(2,2′-dipyridyl)dithiocarbamate have been prepared upon insertion of carbon disulfide into the copper–nitrogen bonds of the corresponding 2,2′-dipyridylamine (dpa) complexes (195, 196). Kumar and Tuck (195) initially noted this behavior for $[Cu(dpa)]_n$, $[Cu(dpa)_2]$, and [Cu(dpa)(dppe)] [dppe = 1,2-bis(diphenylphosphino)ethane], but characterization was made only on the basis of the presence of characteristic ν(C—S) and ν(C—N) bands in their IR spectra. Later, this was confirmed by the X-ray crystal structure of $[Cu(S_2Cdpa)_2]$, formed upon slow evaporation of a carbon disulfide solution of $[Cu(dpa)_2]$ (Eq. 21) (196). The transformation is actually quite complex as in the dpa complex, metal coordination is through the nitrogen atoms of the pyridyl rings (197), and thus a rearrangement to the amide form must occur prior to carbon disulfide insertion.

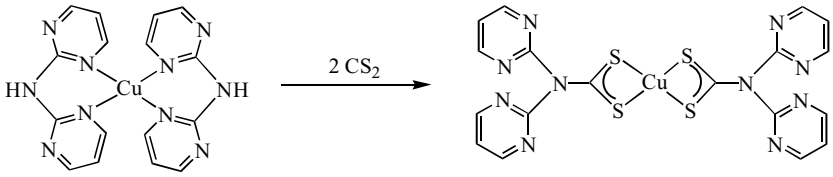

(21)

A variation on this theme is the addition of carbon disulfide to a metal bound amine in the presence of base, the amide presumably being generated *in situ*. Thus, addition of carbon disulfide to $[ReBr(CO)_3(HNMe_2)]$ in the presence of more dimethylamine yields $[Re(CO)_3(HNMe_2)(S_2CNMe_2)]$ (63), while addition of carbon disulfide to *cis*-$[Cr(CO)_4(NHC_5H_{10})_2]$ in the presence of *n*-butyllithium yields $[Cr(CO)_4(S_2CNC_5H_{10})][NEt_4]$ (Eq. 22), the latter being inaccessible from the direct reaction of the dithiocarbamate salt with $Cr(CO)_6$ (198).

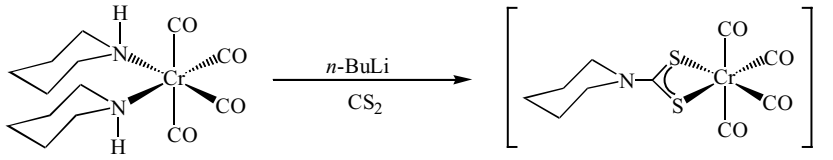

(22)

Similarly, insertion of carbon disulfide into the nickel–nitrogen bonds of $[Ni\{S(CH_2)_3NH_2\}_2]$ results in proton transfer from nitrogen to sulfur, being proposed to afford $[Ni\{S_2CNH(CH_2)_3SH\}_2]$ (Eq. 23) (199).

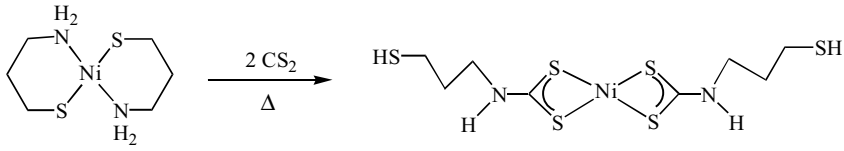

(23)

A related insertion into an *N*,*N*′-formamidine ligand has been reported; carbon disulfide addition to $[Pd(C_6F_5)_2(\eta^2\text{-tolNCHNtol})]^-$ (tol = tolyl) resulting in formation of $[Pd(C_6F_5)_2\{S_2CN(tol)CHNtol\}]^-$ (Eq. 24) (200).

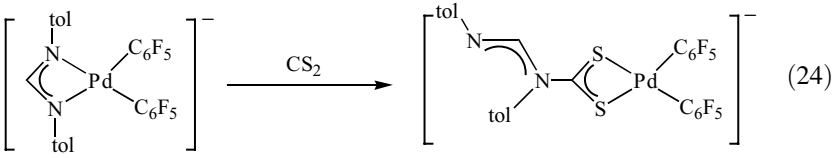

(24)

A synthetic route developed by Tsipis co-workers (201) involves the addition of electrophiles to anionic dithiocarbimato complexes of the group 10 (VIII) elements; the latter being prepared upon deprotonation of the corresponding primary amine derived dithiocarbamate complexes. In this way, Schwarz and Rauchfuss (202) also prepared the rhenium complexes [ReS(η^2-S_4)(S_2CNMeR)] (Eq. 25).

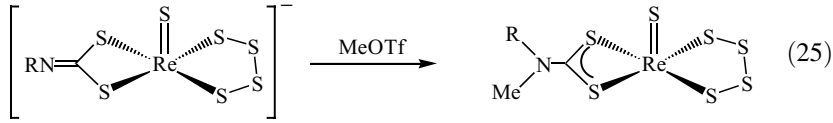

(25)

In a number of instances dithiocarbamates can be exchanged between a *p*-block and a transition metal center. For example, reaction of [$P(S_2CNMe_2)_3$] (203) with $CuCl_2$ (Eq. 26), $CoCl_2$, or $Hg(SCN)_2$ in each case results in dimethyldithiocarbamate transfer yielding [$Cu(S_2CNMe_2)_2$], [$Co(S_2CNMe_2)_3$], and [$Hg(SCN)(S_2CNMe_2)$], respectively (204). Redistribution of dithiocarbamates between a *p*-block and transition metal center is also possible, as shown recently from the reaction of [$Fe(S_2CNR_2)_3$] with [$In(S_2CNR'_2)_3$], which results in some instances in a nonstatistical redistribution of the dithiocarbamate ligands (205).

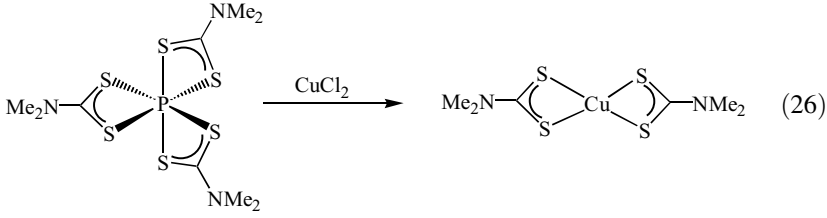

(26)

A number of synthetic approaches involve the cleavage of a sulfur-element bond in order to generate the dithiocarbamate. Faraglia and co-workers (206, 207) developed a route to certain palladium and platinum dithiocarbamate from the thermolysis of dithiocarbamic ester complexes, upon loss of methyl halide (Eq. 27).

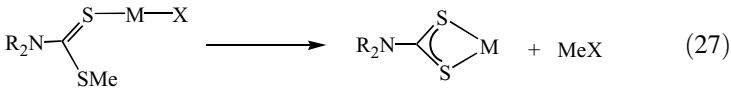

(27)

For example, heating $[MX_2(MeS_2CNMe_2)]$ (M = Pd, Pt; X = Cl, Br) in DMSO affords the dimethyldithiocarbamate complexes, $[MX(dmso)(S_2CNMe_2)]$ (207), while heating $[PtCl(MeS_2CNMe_2)(S_2CNMe_2)]$ affords the mixed dithiocarbamate product, $[Pt(S_2CNEt_2)(S_2CNMe_2)]$ (Eq. 28) (206).

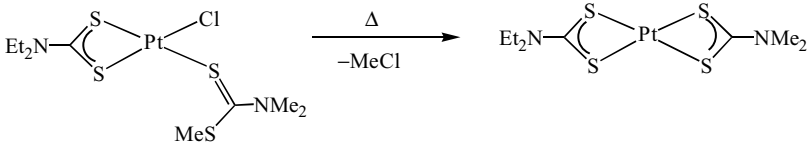

(28)

Related to this is the cleavage of other groups from sulfur. For example, both zirconium and hafnium tetrachlorides react with $Me_2NC(S)SN(SiMe_3)_2$ to give $[MCl_3(S_2CNMe_2)]$ (the precise structures of which are unknown), which in the presence of excess pyridine (Py) yield *fac*-$[MCl_3(py)_2(S_2CNMe_2)]$ (Eq. 29) (208). Here, loss of the sulfur–nitrogen bond has occurred, although it is noteworthy that the analogous reaction with titanium tetrachlorides leads instead to cleavage of both silicon–nitrogen bonds with generation of a nitrogen-inserted dithiocarbamate ligand (see Section V.E) (209).

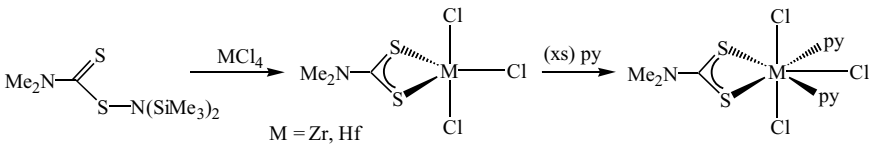

(29)

Loss of Me_3SiCl from $Me_3SiS_2CNR_2$ (R = Me, Et) can also drive the formation of dithiocarbamates. Thus, a wide range of imido complexes, $[M(NR')(S_2CNR_2)_3]$ (M = Nb, Ta; R′ = Me, Pr, *i*-Pr, *t*-Bu, Ph, *p*-tol, *p*-C_6H_4OMe), have been prepared in this way from the reaction of group 5 (VB) pentahalides with $Me_3SiS_2CNR_2$ (R = Me, Et) in the presence of an excess of the relevant primary amine (210). Further, carrying out the same synthetic procedure in the presence of 1,1-disubstituted hydrazines yields related hydrazido(2−) complexes, $[M(NNR_2)(S_2CNR_2)_3]$ (Eq. 30) (210).

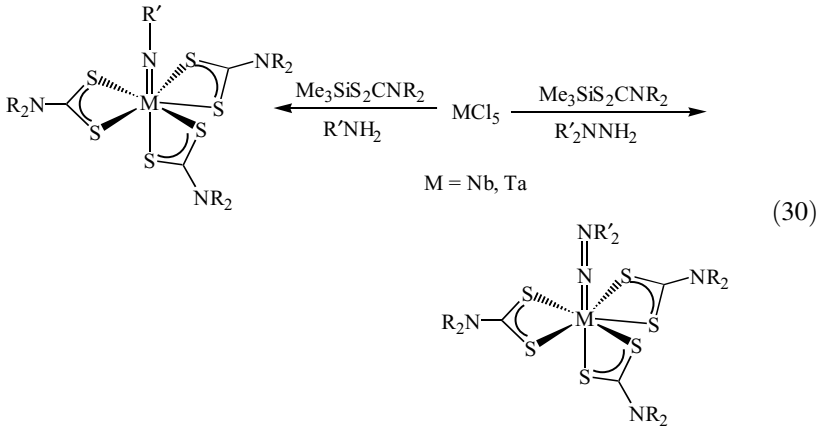

(30)

Adams and Huang (211) showed that S-[(ethoxycarbonyl)amino]-1,2,4-dithiazole-3-one (**16**) acts as a dithiocarbamate source. Reaction with $[Re_2(CO)_9(MeCN)]$ gives a number of rhenium(I) products including **17**, **18**, and isomeric **19**. All three have been characterized crystallographically and the based-catalyzed interconversion of the two isomers has been shown upon addition of pyridine (Fig. 25).

Adams and Huang (212) also showed that the manganese(I) complex $[Mn(CO)_4(S_2CNHCO_2Et)]$ can be prepared from $[Mn_2(CO)_9(MeCN)]$ and $[EtO_2CN{=}CS_2CNHCO_2Et][S_2CNHCO_2Et]$ (**20**) (Eq. 31). The latter results from the reaction of water with ethoxycarbonylisothiocyanate and can be viewed as an adduct of the dithiocarbamate EtO_2CNHCS_2. Thus, cleavage of a sulfur–carbon bond and displacement of the metal-bound acetonitrile ligand leads to the observed product.

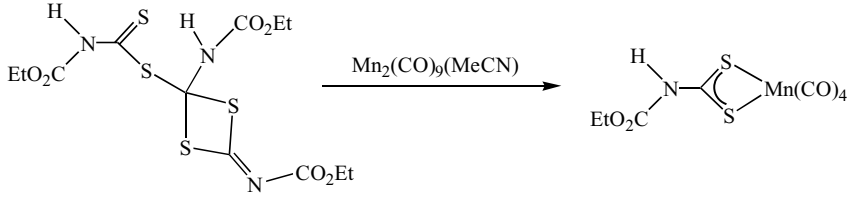

20

(31)

The addition of dithiocarbomyl chlorides, $R_2NC(S)Cl$, to anionic metal centers is a well-utilized synthetic route toward thiocarboxamide complexes.

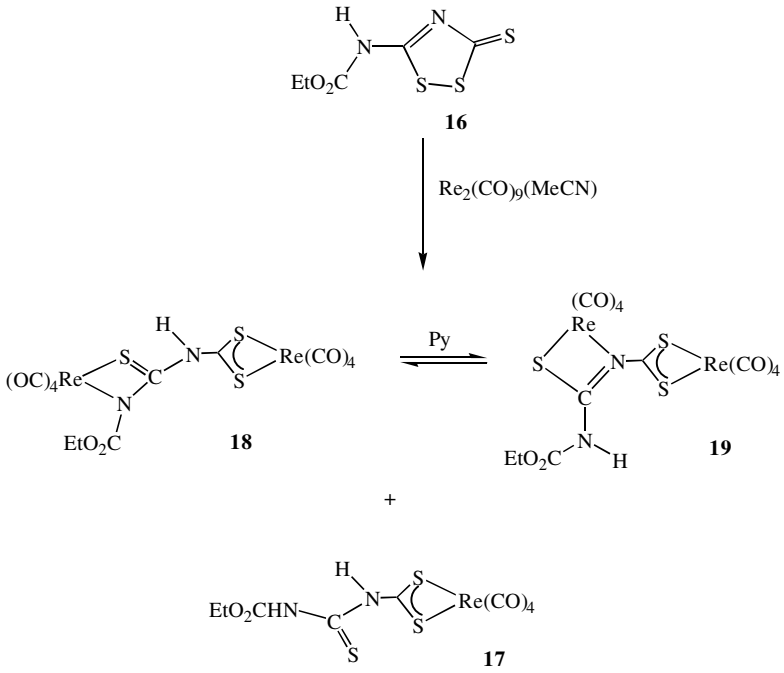

Figure 25. Products of the reaction of $[Re_2(CO)_9(MeCN)]$ with S-[(ethoxycarbonyl)amino]-1,2,4-dithiazole-3-one.

In theory, it should also be possible to prepare dithiocarbamate complexes in this manner from anionic metal sulfides, upon nucleophilic attack of the sulfide at the electrophilic carbon center (Eq. 32).

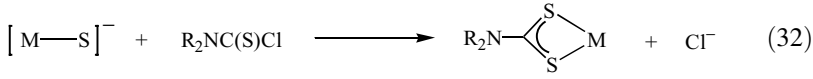

(32)

Indeed, very recently Miguel et al. (213) achieved this result. Addition of dimethyldithiocarbomyl chloride to $[MnRe(CO)_6(\mu\text{-}S)\{\mu\text{-}SC(PR_3)\}]^{2-}$ (R = Cy, *i*-Pr) affords bridging dithiocarbamate complexes, $[MnRe(CO)_6(\mu\text{-}S_2CNMe_2)\{\mu\text{-}SCH(PR_3)\}]$, protonation of the second bridging ligand also occurring (Eq. 33).

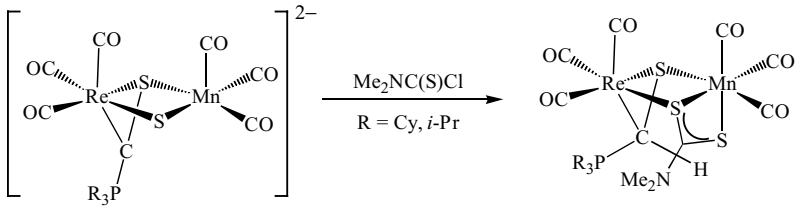

(33)

In a number of instances, organic isothiocyanates have been used as dithiocarbamate sources. The most logical approach to using these reagents would be their insertion into the sulfur–carbon bond of metal-bound thiolates (Eq. 34), and indeed this has been achieved in a number of instances.

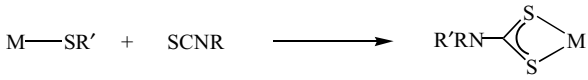

(34)

Early examples were restricted to the insertion into sulfur–hydrogen bonds (214–216). For example, addition of phenylisothiocyanate to $[Au(SH)_2]^-$ affords the bis(dithiocarbamate) complex $[Au(S_2CNHPh)_2]^-$ (216). More recently, Shaver and co-workers (217) demonstrated a similar insertion into the sulfur–silicon bond of $[CpRu(PPh_3)_2(SSi\text{-}i\text{-}Pr_3)]$, yielding unusual silicon-substituted dithiocarbamate ligands (Eq. 35).

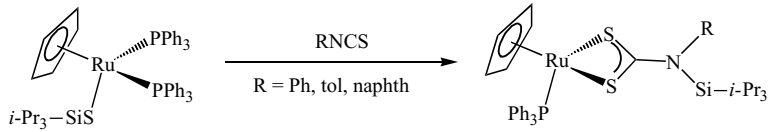

(35)

(naphth = naphth Line)

The nature of these insertion reactions is not fully understood. In the case of the silyl thiols, they are believed to proceed via precoordination of the isothiocyanate to ruthenium, while with thiol itself, direct nucleophilic insertion is proposed. In support of this, $[CpRu(dppe)(SSi\text{—}i\text{-}Pr_3)]$ does not react with isothiocyanates, while [CpRu(dppe)(SH)] does, giving monodentate products, $[CpRu(dppe)(\eta^1\text{-}S_2CNHR)]$ (R = Ph, 1-naphth), a reaction that is reversible in one case (R = 1-naphth) (Eq. 36) (217).

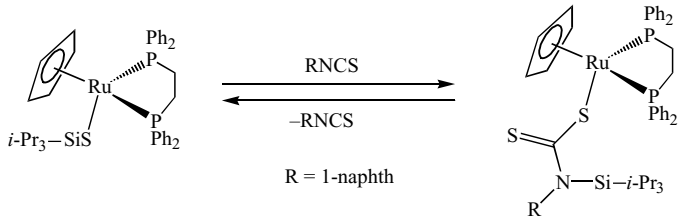

(36)

A second route to dithiocarbamates that utilizes organic isothiocyanates involves the transfer of a sulfur atom between two of them, and also the addition of a proton to nitrogen, generally from a metal hydride (Eq. 37).

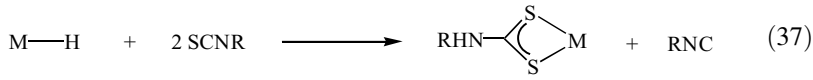

(37)

In this way, Bianchini et al. (218, 219) prepared copper(I) phosphine complexes, $[Cu(PR_3)_2(S_2CNHPh)]$ (R = Ph, Cy), in high yields from phenylisothiocyanate and $[Cu(PR_3)_2(\eta^2\text{-}BH_4)]$, borohydride ligand acting as the hydrogen source with benzonitrile being eliminated (Eq. 38). Somewhat similarly, the borane complex, $[Rh(B_{10}H_{10}Te)(PPh_3)(S_2CNHPh)]$, results from the addition of phenylisothiocyanate to $[2,2\text{-}(PPh_3)_2\text{-}2\text{-}H\text{-}1,2\text{-}TeRhB_{10}H_{10}]$ in dichloromethane (220).

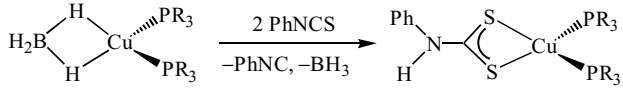

(38)

In other instances, it is less obvious as to how an isothiocyanate has been converted into a dithiocarbamate. For example, the novel technetium(I) complex, $[Tc(CO)_2(PPh_3)_2(S_2CNHPh)]$, results upon heating $[Tc(CO)_2(PPh_3)_2(\eta^2\text{-}OCH\text{-}N\text{-}p\text{-}tol)]$ with phenylisothiocyanate in wet benzene (Eq. 39). It plausibly arises by abstraction of sulfur from the isothiocyanate with concomitant generation of phenylisocyanate (221). Analogous chemistry has also been shown to occur at rhenium, with $[Re(CO)_2(PPh_3)_2(S_2CNHPh)]$ being prepared in a similar manner (222).

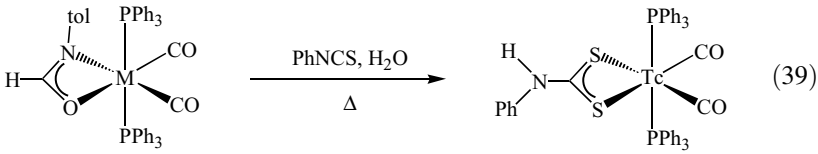

(39)

Fackler et al. (223, 224) previously explored the transformation of metal-bound xanthates into dithiocarbamates upon reaction with secondary and primary amines (Eq. 40). Indeed, a detailed study of the reaction of $[Pt(S_2COEt)_2]$ and piperidine revealed that formation of $[Pt(S_2CNC_5H_{10})_2]$ took place in a step-wise fashion and was reversible (223).

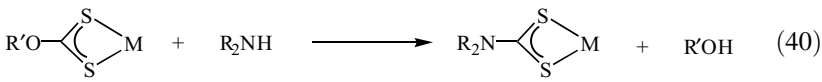

(40)

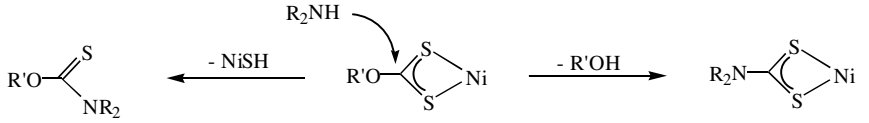

Figure 26. Competing routes upon addition of secondary amine to nickel xanthate complexes.

Later work on the reactions of nickel xanthate complexes, $[Ni(S_2COR')_2]$, with secondary amines revealed the formation of thiourethanes, $R_2NC(S)OR'$, together with nickel bis(dithiocarbamate) complexes (Fig. 26). Both are product of nucleophilic attack of the amine at the sp^2-hybridized carbon, the difference between the two pathways being whether the alkoxide or metal–sulfide moieties act as the leaving group (225).

In a similar fashion, alkyl trithiocarbonate complexes react with secondary amines to yield dithiocarbamates with concomitant elimination of the thiol (Eq. 41) (224, 226–228).

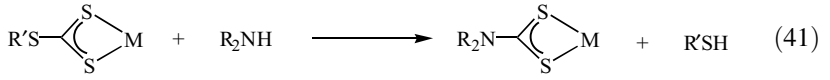

(41)

For example, Bianchini et al. (226) used this as a route toward cobalt(II) dithiocarbamate complexes (Eq. 42).

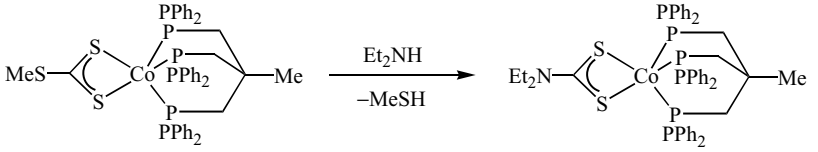

(42)

One report details the unusual transformation of an η^1-bound dithiophosphinate moiety in $[W(CO)_5\{\eta^1\text{-}P(Ph)_2CS_2\}]^-$ into dithiocarbamate and secondary phosphine ligands upon addition of *cis*-$[W(CO)_4(pip)_2]$ (pip = piperidine) (Eq. 43) (229). It is not obvious how this transformation proceeds, but it may involve a binuclear intermediate.

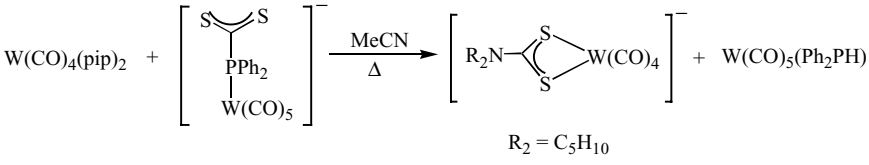

(43)

B. Binding Modes

Dithiocarbamates can bind to between one and four transition metal atoms in a variety of different ways as illustrated in Fig. 27. By far, the most common of these is the simple chelating mode A. Here, the two metal sulfur interactions are approximately equal and the ligand can be considered as a net four-electron donor. (For electron-counting purposes it is often considered as a three-electron donor radical.) This mode of bonding is found for all the transition metals in all accessible oxidation states.

In a number of instances the dithiocarbamate acts as a monodentate ligand B (178, 179, 230–245). This often results when the demands of the other coordinated ligands dictate that there is not room for bidentate coordination of the dithiocarbamate, while in other instances the monodentate coordination mode is isolated en route to further ligand loss and bidentate complexation.

Recent examples include a series of ruthenium(III) complexes, $[Ru(tacn)(S_2CNR_2)(\eta^1\text{-}S_2CNR_2)][PF_6]$ (tacn = 1,4,7-triazacyclononane) (**21**) (Fig. 28), formed upon addition of 2 equiv of dithiocarbamate salt to $[Ru(tacn)(dmso)_2Cl]Cl$ (233). The triazacyclononane ligand is tightly bound and cannot be displaced by the second sulfur atom of one dithiocarbamate. Interestingly, it is the monodentate dithiocarbamate that is the most easily lost, for example upon addition of nitric oxide. Lai and Tiekink (235) isolated the mercury–chloride complex $[HgCl(\eta^1\text{-}S_2CNEt_2)(4,7\text{-}Me_2\text{-}1,10\text{-}phen)]$ (**22**) (Fig. 28) from the reaction of $[Hg(S_2CNEt_2)_2]$ and 4,7-dimethyl-1,10-phenantroline ($4,7\text{-}Me_2$-1,10-phen), which is presumed to result from the loss of a dithiocarbamate and chloride abstraction from the chloroform solvent. An X-ray crystal structure

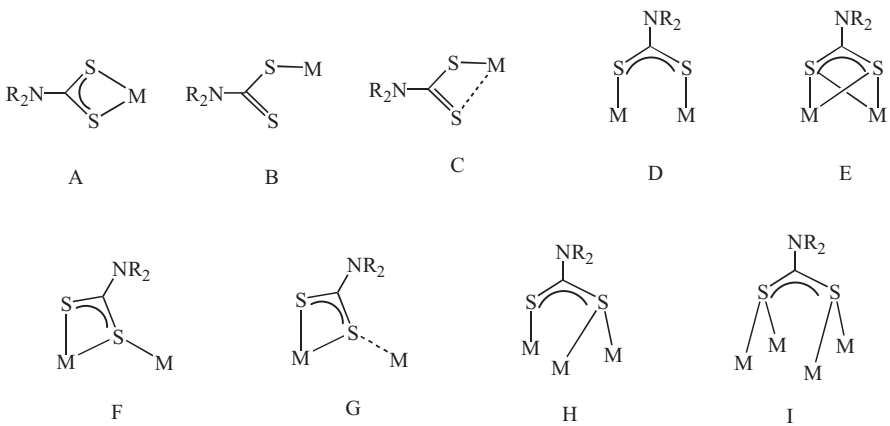

Figure 27. Dithiocarbamate coordination modes.

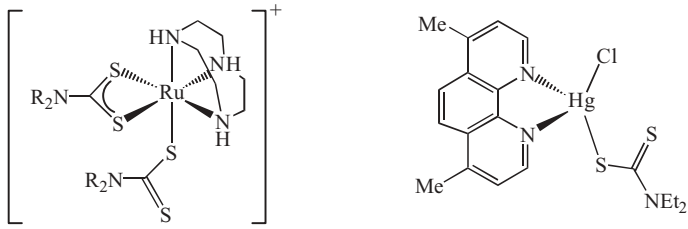

21 22

Figure 28. Examples of terminally bound dithiocarbamate complexes.

shows that the dithiocarbamate binds in a monodentate fashion, allowing the mercury center to adopt a highly distorted tetrahedral coordination geometry.

As mentioned above, in a number of instances monodentate dithiocarbamate complexes are formed en route to bidentate complexes. This finding is illustrated by the reaction of thiuram disulfides with $[CpCr(CO)_3]_2$ (Cp = cyclopentadienyl) (240, 246, 247). At room temperature, chromium(II) dicarbonyl complexes $[CpCr(CO)_2(S_2CNR_2)]$ (R = Me, Et, *i*-Pr) are formed in high yields, however, if the reactions are monitored carefully the monodentate tricarbonyl intermediates, $[CpCr(CO)_3(\eta^1\text{-}S_2CNR_2)]$, can be detected (Eq. 44). Crystallographic studies have been carried out on both dimethyldithiocarbamate complexes, the chromium–sulfur bond length decreasing slightly upon chelation [Cr—S 2.4406(5) and 2.4237(6) Å (av)] (240).

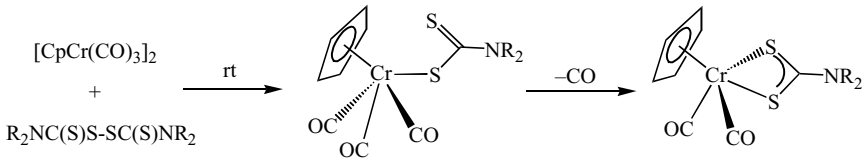

rt = room temperature

(44)

Monodentate dithiocarbamate coordination is quite common in gold chemistry (236–239, 244, 245, 248–250). For example, gold(III) tris(dithiocarbamate) complexes, $[Au(S_2CNR_2)_3]$, which result from addition of 3 equiv of dithiocarbamate salts to $NaAuCl_4$ or from the reaction of gold(I) dimers with thiuram disulfides (Fig. 29) (249–252), contain a square-planar arrangement with one chelating and two monodentate dithiocarbamates, as found crystallographically for $[Au(S_2CNEt_2)_3]$ (249).

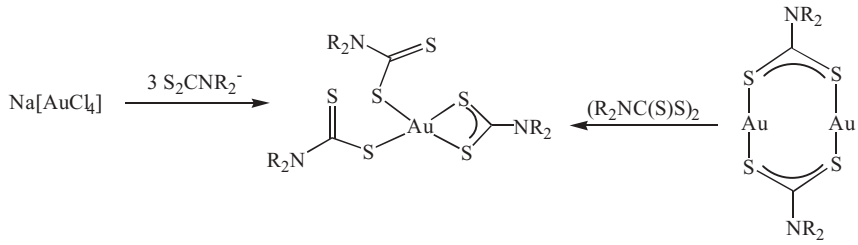

Figure 29. Formation and structure of gold(III) tris(dithiocarbamate) complexes.

In a number of instances, the interconversion of mono- and bidentate dithiocarbamate ligands has been proposed to occur in solution. This is highlighted by $[Au(S_2CNEt_2)_2(\eta^1\text{-}C_6H_4CH_2NMe_2)]$, a crystal structure revealing that in the solid-state one dithiocarbamate chelates, while the second is monodentate (244). In solution, however, the dithiocarbamates are equivalent, being attributed to the rapid interconversion of mono- and bidentate binding modes (Fig. 30). A similar situation is also found for $[Au(S_2CNEt_2)_2\{\eta^1\text{-}CH_2P(S)PPh_2\}]$ (248).

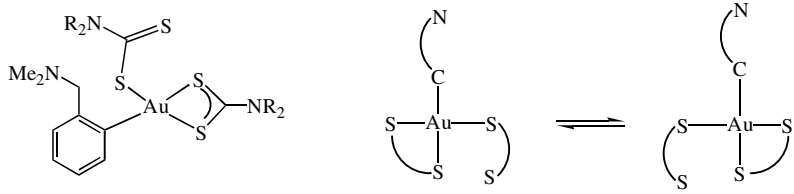

Figure 30. Interconversion of mono and bidentate dithiocarbamate ligands at a gold(III) center.

Further, utilizing $[CpCoI(S_2CNEt_2)]$ is possible to prepare the mixed-ligand complex, $[CpCo(S_2CNMe_2)(S_2CNEt_2)]$, which exits as two isomers in solution with $[CpCo(S_2CNEt_2)(\eta^1\text{-}S_2CNMe_2)]$ being favored at higher temperatures (Fig. 31) (253).

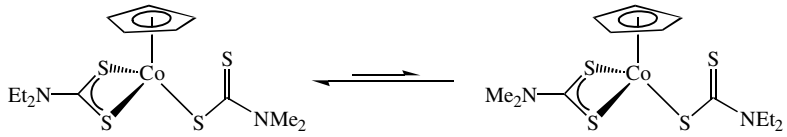

Figure 31. Equilibrium between isomers of $[CpCo(S_2CNMe_2)(S_2CNEt_2)]$.

In some instances, the binding of the dithiocarbamate to the metal center is highly asymmetric and can be best described by mode (C), sometimes termed *anisobidentate*. For example, a crystallographic study of $[Pt(\eta^3\text{-triphos})(\eta^1\text{-}S_2CNEt_2)]^+$ [tripos = 1,1,1-tris(diphenylphosphino)methane] (**23**) (Fig. 32)

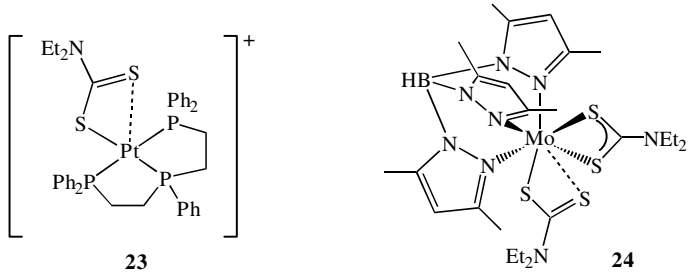

Figure 32. Examples of asymmetrically bound dithiocarbamate ligands.

reveals a distorted square-planar primary coordination geometry [Pt—S 2.396(3) Å], the second sulfur of the dithiocarbamate being only weakly bound [Pt—S 2.754(3) Å]. This type of coordination mode leads to long and short carbon–sulfur bonds [C—S 1.727(9) and 1.707(9) Å] (254). Sometimes it is not easy to distinguish between modes B and C. For example, the molybdenum(III) complex [Tp*Mo(S_2CNEt_2)$_2$] [Tp* = hydridotris(3,5-dimethylpyrazolyl)borate] (**24**) (Fig. 32) contains one bidentate dithiocarbamate, while the second is bound in a highly asymmetric fashion, the long molybdenum–sulfur interaction of 3.820(2) Å being extremely weak (178,179).

Asymmetric binding mode C is quite common at gold and mercury centers that favor a linear two-coordinate geometry. For example, Laguna and co-workers (230) prepared 1,1-bis(diphenylphosphino)ethane-bridged complexes, [$Au_2(\eta^1$-$S_2CNR_2)_2\{\mu$-$Ph_2PC(=CH_2)PPh_2\}$] (R = Me, Et, Bz) (**25**) (Fig. 33). Coordination at gold is linear [S—Au—P 174.4(1)°] and short and long gold–sulfur interactions are seen [Au—S 2.319(4) and 2.949(4) Å], the asymmetric ligand binding again leading to long and short carbon–sulfur bonds [C—S 1.658(13) and 1.765(13) Å]. Related behavior is seen in dimeric mercury(II) complexes, [$ArHg(S_2CNR_2)]_2$ (255–259). For example, in [$PhHg(S_2CNPr_2)]_2$ (**26**) (Fig. 33) each mercury center is bound in an approximately linear fashion [C—Hg—S 166.76(10)°] to the phenyl group and one sulfur atom of the dithiocarbamate. The second sulfur binds less strongly [Hg—S 2.4033(9) and

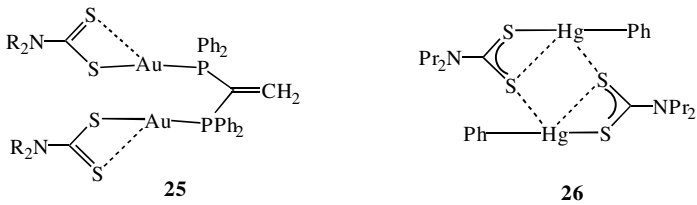

Figure 33. Examples of anisobidentate dithiocarbamate complexes.

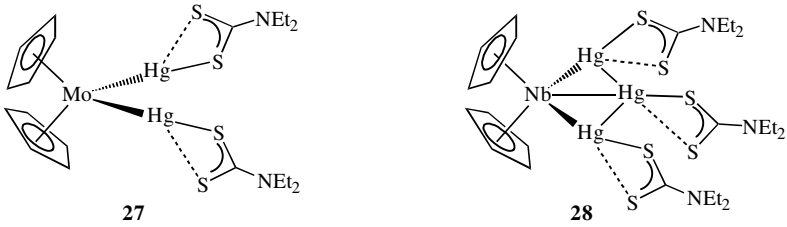

27 **28**

Figure 34. Examples of anisobidentate dithiocarbamate complexes containing metal–metal bonds.

2.9093(10) Å] and also forms a bridge to the second mercury center [Hg—S 3.1809(10) Å] (258).

Anisobidentate binding of dithiocarbamates to mercury is also observed in complexes with metal–metal bonds, such as $[Cp_2Mo\{Hg(S_2CNEt_2)\}_2]$ (**27**) (Fig. 34) [Hg—S 2.94(3) Å and 2.50(2) Å] (260), and $[Cp_2Nb\{Hg(S_2CNEt_2)\}_3]$ (**28**) (Fig. 34) (261). In the latter, the short mercury–sulfur bonds [2.513(8)–2.526(8) Å] lie in the plane of the metal atoms, while the longer interactions [2.75(3)–2.919(10) Å] lie approximately perpendicular to it.

Monomeric gold(I) phosphine complexes $[Au(PPh_3)_2(S_2CNC_5H_{10})]$ (263) (**30**) (Fig. 35) and $[Au(PPh_3)_2(S_2CN—i\text{-}Pr_2)].C_4H_{10}$ (**29**) (Fig. 35) (262) have both been crystallographically characterized, the metal adopting a distorted tetrahedral coordination environment. Interestingly, while gold–sulfur interactions are similar in the latter [Au—S 2.714(2) and 2.681(2) Å], in $[Au(PPh_3)_2(S_2CNC_5H_{10})]$ they differ by almost 0.3 Å [Au—S 2.561(2) and 2.858(3) Å], and could be considered to be anisobidentate. This difference is reflected to a lesser extent in the carbon–sulfur bond lengths and has been attributed to an ''allyl-like'' interaction within the dithiocarbamate (Fig. 35) (263).

Dithiocarbamates can bridge two metal atoms in a number of ways (D–G). In mode D, each sulfur atom binds to a single metal center, in an η^1,η^1-manner. It is not particularly common, although a significant number of complexes containing this binding mode have now been crystallographically characterized

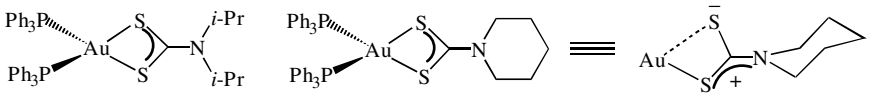

29 **30**

Figure 35. Gold(I) bis(phosphine) complexes highlighting the ''allyl-like'' binding of the dithiocarbamate ligand in $[Au(PPh_3)_2(S_2CNC_5H_{10})]$.

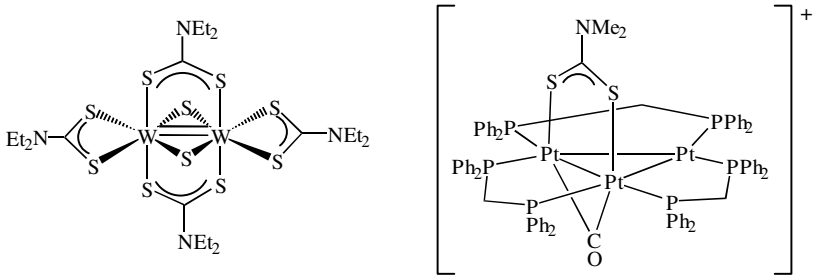

31 **32**

Figure 36. Examples of complexes containing η^1,η^1-bridging dithiocarbamate ligands.

(264–267). Examples include, dimeric tungsten(IV) complex, $[W(\mu\text{-}S)(\mu\text{-}S_2CNEt_2)(S_2CNEt_2)]_2$ (**31**) (Fig. 36) (265), a range of cubane-type cluster complexes (268–274), and $[Pt_3(\mu\text{-}CO)(\mu\text{-}S_2CNMe_2)(\mu\text{-dppm})_3]^+$ (dppm = bis (diphenylphosphino)ethane) (**32**) (Fig. 36) (267). Interesting in the latter, while in the solid state all three diphosphines are inequivalent, a single phosphorus environment is observed by NMR at room temperature, an observation attributed to a fluxional process involving migration of the dithiocarbamate ligand around the platinum triangle.

Binding mode D is particularly common at gold(I) and gold(II) centers (239,275–284). For example, gold(I) complexes $[Au(\mu\text{-}S_2CNR_2)]_2$ (Fig. 37), are dimeric the gold–gold vector being bridged by two dithiocarbamate ligands and crystallize to form linear chains, characterized by alternating short, $\sim$ 2.5–2.8 Å, and long, $\sim$ 3.0–3.1 Å, gold–gold interactions.

In binding mode E, each sulfur atom binds to each metal atom. Only a few examples of this mode of binding have been found, and seem to be restricted to dirhodium complexes. In binuclear complexes, $[Rh_2L_2(cod)(\mu\text{-}S_2CNMePh)]^+$ (L = CO; L_2 = cod), the dithiocarbamate binds in a $\mu\text{-}\eta^2,\eta^2$ fashion as confirmed crystallographically (L_2 = cod) (cod = cyclooctadiene) (**33**). However,

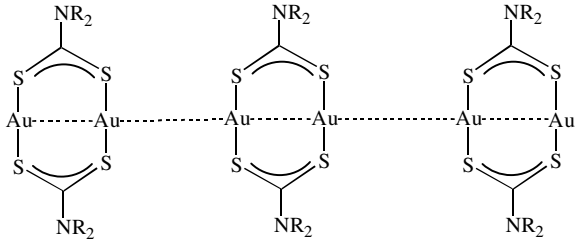

Figure 37. Dimeric gold(I) complexes that form linear chains in the solid state.

solution NMR measurements on $[Rh_2(cod)_2(\mu\text{-}S_2CNMePh)]^+$ show that the two metal centers are equivalent even at $-60°$ C, suggesting a rapid oscillation of the dithiocarbamate CNR_2 moiety between both sides of an idealized plane containing the midpoint of the metal-metal bond and the two sulfur atoms (285). The bis(dithiocarbamate) complex, $[Rh_2(CO)_2(\mu\text{-}S_2CNEt_2)_2]$, is also believed to have bridging $\mu\text{-}\eta^2,\eta^2$ dithiocarbamate ligands and a rhodium dicarbonyl unit, however, precise structural details remain unknown (286).

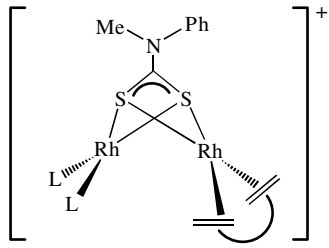

33

In binding mode F, one sulfur atom bridges the metal–metal vector and all three metal–sulfur interactions are of similar length. This mode of binding is quite common, with a large number of examples being found at ruthenium (287–294), osmium (295, 296), and other late transition metal centers (297–301). Thus, the ruthenium(II) dimer $[Ru_2I(CO)_2(PPh_3)_2(S_2CNEt_2)(\mu\text{-}I)(\mu\text{-}S_2CNEt_2)]$ (**34**) (Fig. 38) is the product of iodine addition to $[Ru(CO)(PPh_3)_2(NHSO_2Ar)(S_2CNEt_2)]$ ($Ar = 2,4,6\text{-}i\text{-}Pr_3C_6H_2$) (292). The bridging sulfur atom binds approximately symmetrically to both ruthenium centers [Ru-S 2.448(4) and 2.395(4) Å], and at distances comparable to the binding of the second sulfur atom of this ligand [Ru-S 2.482(4) Å] and also the chelating dithiocarbamate [Ru—S 2.367(4) and 2.486(4) Å]. This mode of binding is capable of spanning both long and short metal–metal vectors as exemplified by trinuclear

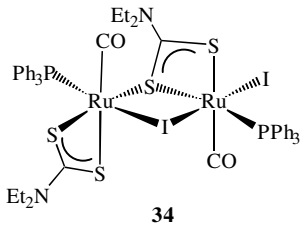

34

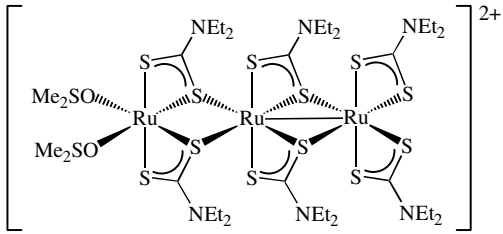

35

Figure 38. Examples of complexes containing η^1,η^2-bridging dithiocarbamate ligands.

$[Ru_3(dmso)_2(S_2CNEt_2)_2(\mu\text{-}S_2CNEt_2)_4][I_3]_2$ (**35**) (Fig. 38), which contains two ruthenium(III) centers in close proximity [Ru-Ru 2.826(2) Å] and a single ruthenium(III) center, which is not metal–metal bonded (287).

Other common species with this mode of coordination are the binuclear group 9 (VIII) complexes $[M_2(S_2CNR_2)_5]^+$, formed upon oxidation of tris(-dithiocarbamate) complexes, $[M(S_2CNR_2)_3]$ (M = Co, Rh) (Eq. 45) (302–311).

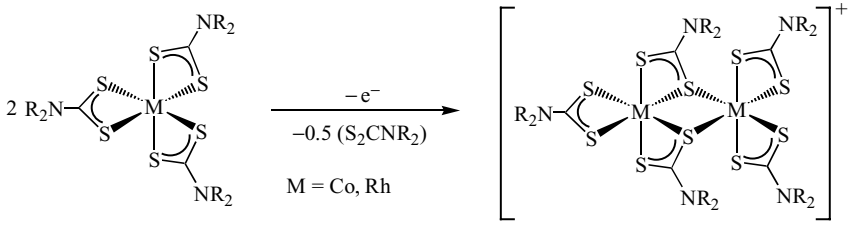

(45)

Here, the bridging dithiocarbamate ligands have resulted upon addition of a second metal center to terminal dithiocarbamates. Indeed, this is a relatively common feature and the sulfur atoms in a range of mononuclear dithiocarbamate complexes can bind to other Lewis acidic metal centers.

For example, varying amounts of copper(I) iodide can be added to $[Cr(S_2CNR_2)_3]$ in acetonitrile to yield complexes in which sulfur atoms bridge two copper ions (**36**) (Fig. 39). Such species have been characterized crystallographically, and consist of polymeric chains in the bridging dithiocarbamate groups link together the metal centers (312). Other examples include $[Co_2Ag(\mu\text{-}S_2CNR_2)_4(S_2CNR_2)_2]^+$ (**37**) (Fig. 39) formed upon addition of 1 equiv of $AgBF_4$ to $[Co(S_2CNR_2)_3]$ (313).

Binding mode G is similar to that discussed above, but the bridging interaction is not symmetrical. It is commonly seen in the solid state, being

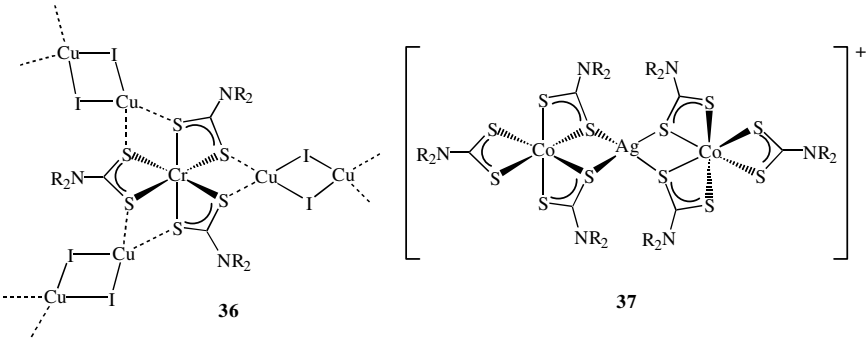

36 **37**

Figure 39. Examples of dithiocarbamate ligands bridging between two different metal centers.

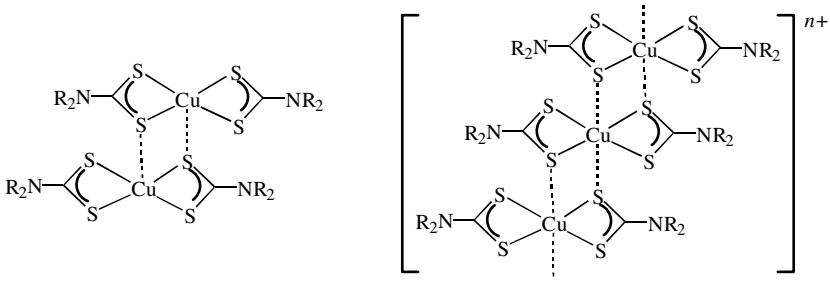

Figure 40. Examples of copper(II) and (III) complexes with briding dithiocarbamates.

lost upon dissolution. This is exemplified by the structural chemistry of copper(II) and copper(III) bis(dithiocarbamate) complexes, $[Cu(S_2CNR_2)_2]$ (104, 196, 314–317), $[Cu(S_2CNR_2)_2]^+$ (104,318–326) (Fig. 40), and related mixed-valence species (see Section IV.H.1.d). Here the copper bis(dithiocarbamate) units are held together by secondary copper–sulfur interactions. For example in $[Cu(S_2CNPr_2)_2]_2$ the intramolecular copper–sulfur interactions [Cu—S(av) 2.325 Å] are significantly shorter than the intermolecular contact [Cu···S 2.666(1) Å] (104,317). In copper(III) complexes such as $[Cu(S_2CNPr_2)_2][ClO_4]$, as expected the intramolecular copper–sulfur contacts [Cu-S(av) 2.272 Å] are slightly shorter than those in the copper(II) species, while the intermolecular contacts [Cu···S(av) 2.868 Å] are slightly longer (104).

Binding modes H and I, in which the dithiocarbamate caps three and four metal atoms respectively, are uncommon and limited to the late transition metals (Fig. 41). The classic example of mode H is found in copper(I) complexes, $[Cu(S_2CNR_2)]_4$. A recent crystallographic study of $[Cu(S_2CNBu_2)]_4$ confirms the expected tetrahedral arrangement of copper atoms, each triangular face being capped by a dithiocarbamate binding in an η^1,η^2-manner (327). Early crystallographic studies on related silver(I) species revealed their hexameric nature (R = Et, Pr) (328,329), although in solution they are believed to be in

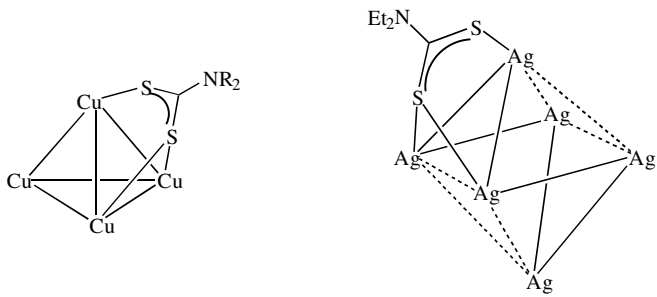

Figure 41. Examples of dithiocarbamates capping a triangular metal unit.

equilibrium with monomers (329). More recently, the diethyldithiocarbamate complex has been further characterized crystallographically (330, 331). Delgado and Diez (331) used powder data to characterize the previously known (329) monoclinic α-modification, which is hexameric and consists of a distorted octahedron of silver atoms, with six comparatively short and long silver–silver interactions. The dithiocarbamates cap six of the faces in an η^1,η^2-fashion (H), the remaining two faces, characterized by the long metal interactions, remaining uncapped (329).

Interestingly, a single-crystal study of the new β-modification of [Ag(S_2C-NEt_2)] shows that it adopts a polymeric chain structure. Each metal ion is bound to three dithiocarbamate ligands, one acting as a chelate (A) and the other two in a bridging fashion (D), the overall coordination geometry being a distorted tetrahedron (330). Clearly, in some cases the energy differences between the different binding modes is only small.

Binding mode I, in which the dithiocarbamate binds four metal atoms, is extremely rare. A recent example is the copper cube [Cu_8(μ_4-$S_2CNPr_2)_6$][ClO_4]$_2$, isolated from the reaction of [Cu($S_2CNPr_2)_2$] and copper(II) perchlorate, and crystallographically characterized (104). Each copper face is capped by a dithiocarbamate (Fig. 42), and overall the molecule consists of a cube of copper atoms, surrounded by an icosahedron of sulfurs, further surrounded by an octahedral array of carbon–nitrogen bonds. The copper–copper distances of 2.8038(6)–2.8087(6) Å are similar to those of 2.6368(4)–2.8119(5) Å found in [Cu(μ_3-S_2CNBu_2)]$_4$ (327).

At this stage, it is worth commenting that the assignment of bridging dithiocarbamate binding modes is not always straightforward. For example, a number of workers have reported the synthesis of a series of tri- and polynuclear dithiocarbamate-bridged complexes [$M_2M'(S_2CNR_2)$(μ-$S_2CNR_2)_2$]$_2$ and [MM'(μ-$S_2CNR_2)_2$]$_n$ (332–335), which later studies showed were probably just mixtures of homonuclear complexes (336). In the absence of crystallographic data, it is difficult to unambiguously assign the bonding mode of

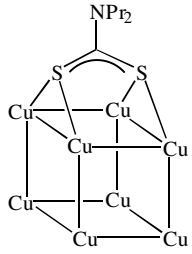

Figure 42. A schematic of the binding of a dithiocarbamate ligand to the square face in [Cu_8(μ_4-$S_2CNPr_2)_6$][ClO_4]$_2$.

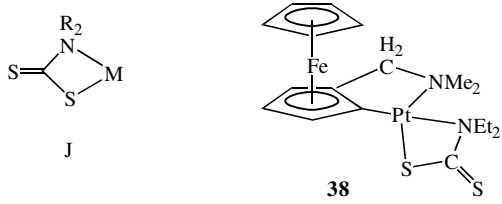

Figure 43. Proposed S,N-binding mode of a dithiocarbamate.

the dithiocarbamate, although some information can be gleaned from the IR spectrum (see Section III.E).

Bonding modes A–I are all well characterized and can be found for a range of substituents. Other modes are theoretically possible, but have not been authenticated. For example, the dithiocarbamate could act as a chelate with metal–sulfur and metal–nitrogen interactions (J), although this results in a localization of π character. In one instance, this mode of binding has been postulated. Thus, the ferrocenyl–platinum complex $[Pt(S_2CNEt_2)(\eta^2\text{-}Me_2NCH_2\text{-}\eta^5\text{-}C_5H_4Fe)]_2$ has been prepared, together with a related mononuclear derivative **38** (Fig. 43). On the basis of the nonequivalence of the alkyl substituents in the ^{1}H NMR spectrum and the low-field shift (δ 211 ppm) of the central dithiocarbamate carbon resonance in the ^{13}C NMR spectrum, both are believed to contain N,S-chelating dithiocarbamate ligands (J), although this seems unlikely and no structural data was forthcoming (337).

In some instances, the substituents can play a noninnocent role and other binding modes can be achieved. For example, addition of the bis(2-diethylamino)ethyl dithiocarbamate to $[AuCl_4]^-$ affords a product that shows four ν(C=N) thiocyanate bands in the IR spectrum (Fig. 44). This observation has been attributed to a unique linkage isomerization between a neutral dithiocarbamate complex, $[Au(SCN)_2\{S_2CN(CH_2CH_2NEt_2)_2\}]$ (**39**), and ionic $[Au(NCS)\{\eta^3\text{-}N(CH_2CH_2NEt_2)_2CS_2\}][SCN]$ (**40**), although this has not been confirmed (338).

The potassium dithiocarbamate salt generated from 3,5-dimethylpyrazole has been reported (339) and used to prepare copper (339–341) and nickel (342) complexes. In theory, the ligand can bind in two ways, **41** and **42** (Fig. 45). A crystallographic study on **43** (Fig. 45) reveals that the ligand binds not through

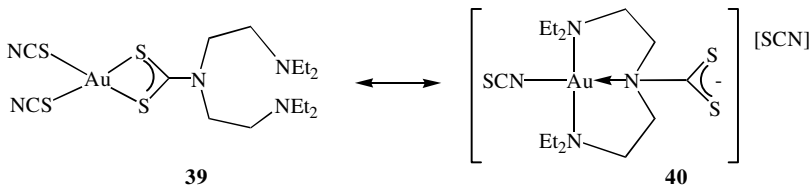

Figure 44. Proposed linkage isomerization in $[Au(SCN)_2\{S_2CN(CH_2CH_2NEt_2)_2\}]$.

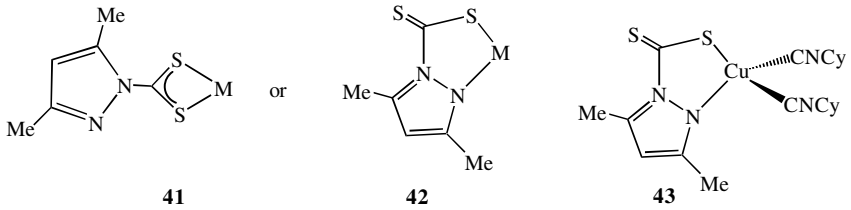

41 **42** **43**

Figure 45. Possible binding modes for 3,5-dimethylpyrazole dithiocarbamate.

the two sulfur atoms, but rather through sulfur and nitrogen. This may account for the relatively facile loss of carbon disulfide from both the free dithiocarbamate (340, 339) and its complexes (341, 342).

In a similar manner, the dithiocarbamate salts derived from 2,2′-dipyridylamine (73, 195, 196) and substituted hydrazines (92, 343) form complexes with a range of metal centers, and it is not always clear whether these bind through two sulfurs or one sulfur and one nitrogen (Fig. 46). In the case of hydrazines, it is thought probable that the dithiocarbamate bonding mode is adopted (92,343).

In the case of the dpa derived ligand, the situation is less clear (Fig. 47) (73, 195), although the crystallographic characterization of $[Cu(S_2Cdpa)_2]$ shows clearly that in this instance it binds as a dithiocarbamate (196).

Gogoi and Phukan (344, 345) prepared the bis(dithiocarbamate) salt of diethylenetriamine, utilizing it toward the synthesis of a wide range of transition metal complexes. The precise binding mode of the ligand is unknown. The authors' propose a quadridenate binding mode yielding monomeric complexes, although it seems more likely that it bridges metal centers to yield oligomers or polymers (Fig. 48).

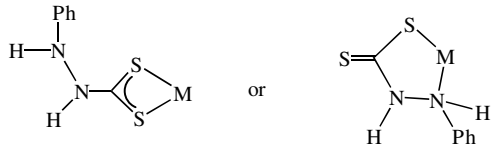

Figure 46. Possible binding modes for the dithiocarbamate derived from phenylhydrazine.

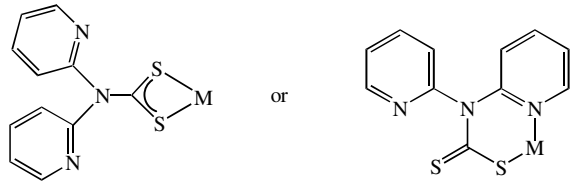

Figure 47. Possible binding modes for 2,2′-dipyridyl dithiocarbamate.

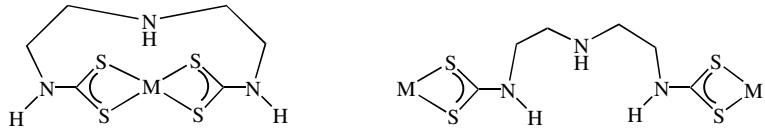

Figure 48. Possible binding modes the bis(dithiocarbamate) salt of diethylenetriamine.

C. Ligand Characteristics

A key characteristic of dithiocarbamate ligands is their ability to stabilize metals in a wide range of oxidation states (Table I). This stabilization is widely attributed to their ability to adopt a resonance form in which the nitrogen carries a positive charge, with each sulfur carrying a negative charge; often termed the *thioureide* form (Fig. 49). Its adoption helps to explain why dithiocarbamates are capable of stabilizing metals in high oxidation states, being far better in this sense than the related xanthate ligands, for which the development of positive charge at the more electronegative oxygen atom is relatively unfavorable.

In certain instances, other resonance forms of the dithiocarbamate are possible. For example, the X-ray crystal structure of $[Ni\{S_2CN(Bz)C(O)Me\}_2]$ (Bz = benzyl) reveals some double-bond character in the N–C(acetyl) unit, which together with the coplanarity of the dithiocarbamate and acetyl groups, suggests that some contribution from a resonance hybrid with negative charge localized on oxygen may be important (346) (Fig. 50).

Dithiocarbamates can be both *strong-* and *weak-field* ligands, a consideration of the resonance forms above (Fig. 49) providing insight into this flexibility. Thus, if the dithiocarbamate resonance form dominates then it would be

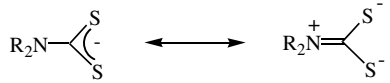

Dithiocarbamate Thioureide

Figure 49. Resonance forms of the dithiocarbamate ligand.

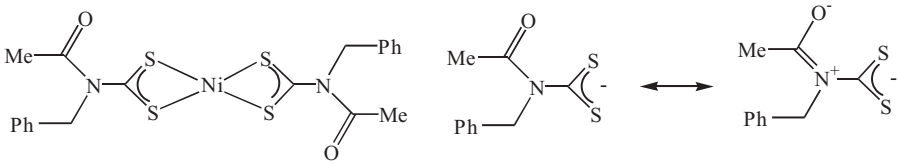

Figure 50. The complex $[Ni\{S_2CN(Bz)C(O)Me\}_2]$ showing proposed dithiocarbamate resonance forms.

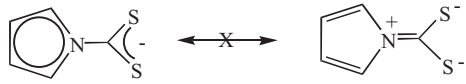

Figure 51. Pyrrole dithiocarbamate in which the thioureide resonance is inaccessible.

considered a *strong-field* ligand, a significant contribution from the thioureide resonance hybrid would suggest it is more likely to be a *weak-field* ligand. One probe of the relative importance of the thioureide form comes from studies of pyrrole-dithiocarbamate complexes (Fig. 51), which cannot adopt this form and therefore should behave as *strong-field* ligands (72, 347–356).

Compelling evidence for the *strong-field* nature of this dithiocarbamate comes from the observation that the iron(III) complex $[Fe(S_2CNC_4H_4)_3]$ remains a low-spin (*strong-field*) species throughout the temperature range 4–400 K, while in contrast the related pyrrolidine complex $[Fe(S_2CNC_4H_8)_3]$ displays high-spin (*weak-field*) behavior (348,351) (Fig. 52).

Other evidence for the reluctance of the pyrrole ring to provide π-electron density to the CS_2 fragment comes from the observation that pyrrole–dithiocarbamate is a poor electron donor relative to other dialkyldithiocarbamates. This difference leads to a number of effects, for example, the far greater lability of the carbonyl group in $[Mo(CO)(RC_2R)(S_2CNC_4H_4)_2]$ (350), and the facile reduction of $[Fe(S_2CNC_4H_4)_3]$ (356), when compared to related dialkyl derivatives.

It is noteworthy, however, that a study by Ymén and Stahl (357) suggested that for iron tris(dithiocarbamate) complexes with only aliphatic hydrocarbon substituents, the most important influence in determining their spin state (and

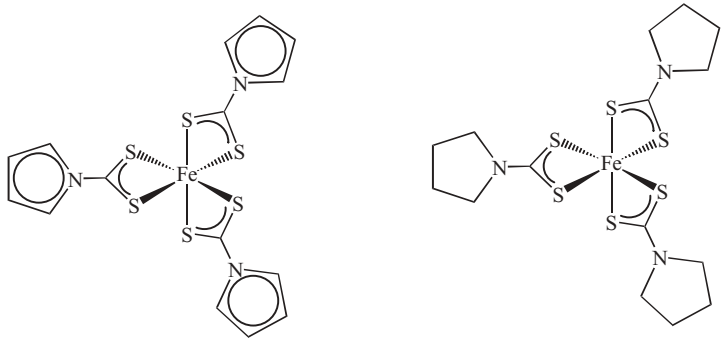

Low-spin *strong field* High-spin *weak field*

Figure 52. Different magnetic behavior of iron(III) pyrrole and pyrrolidene dithiocarbamate complexes.

thus the ligand-field strength) was the intraligand S···H—C interactions. These increase with increasing steric bulk of the substituent atoms, and not their electronic interaction with the sulfur atoms through the π-bonding network of the S_2CN moiety. In related work, White and co-workers (358) also probed the effects of different alkyl substituents on the structures of cobalt tris(dithiocarbamate) complexes, $[Co(S_2CNR_2)_3]$, their results supporting those of Ymén and Stahl.

A second study by White's group utilized both solution and solid-state ^{13}C NMR spectroscopy and solution ^{59}Co NMR measurements to show that the increase in ligand-field strength associated with phenyl substituents is due to a combination of steric and electronic effects (359). Cobalt-59 NMR chemical shifts have also be used to compare the ligand-field strength of dithiocarbamates with related species, the results suggesting the following series (360);

$$R_2NCSO^- < R_2CNS_2^- < R_2CNSSe^- < R_2NCSe_2^-$$

However, while results from various studies involving iron(III) complexes also support the hypothesis that monothiocarbamates are weaker field ligands than dithiocarbamates, the differentiation between dithiocarbamates and their selenium-containing analogues is less clear (33–35).

In a number of contributions, Juranic (361,362) has developed a magnetochemical series of ligands, ordering them according to the increased magnetic shielding of a metal nucleus that they are bound to, which has been found to be closely comparable to the ligand-field strength series (363). At the cobalt(III) center, for example, the following magnetochemical series is found;

$$P(OMe)_3 > CN^- > bpy > R_2NCS_2^- > en > NO_2^- > NH_3 > I^- > Br^- > Cl^- > H_2O > F^-$$

en = ethylenediamine bpy = $2,2'-$ bipyridine or $4,4'$-bipyridine

A feature of metal-bound dithiocarbamates is the restricted rotation about the carbon–nitrogen bond, often being attributed to the importance of the thioureide resonance hybrid, although it should be pointed that in purely organic systems a similar restricted rotation is also observed. A large number of NMR studies have been carried out in order to probe the barrier to carbon–nitrogen bond rotation (232, 364–377). In dimeric *fac*-$[PtMe_3(\mu\text{-}S_2CNR_2)]_2$ (R = H, Me, Et; R_2 = HMe, HEt, HPh, PhMe) (**44**) (Fig. 53) two distinct processes have been identified; the independent rotation about each carbon–nitrogen bond and a correlated rotation about both. Free energies of activation range between 65 and 88 kJ mol^{-1}, are highly dependent on the nature of the substituents; the complex derived from aniline having the lowest, and that from diethylamine the highest, barrier to rotation (364).

Fay and co-workers (366, 367) used variable temperature NMR studies to probe the stereochemical nonrigidity of seven-coordinate pentagonal

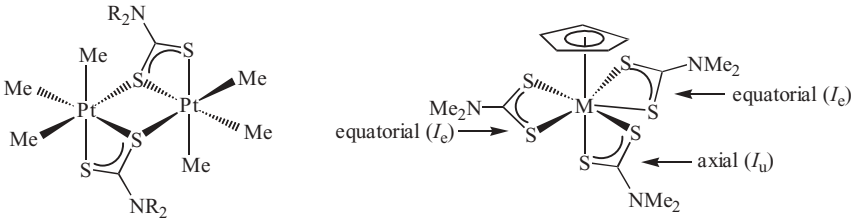

44 **45**

Figure 53. Examples of dithiocarbamate complexes in which restricted rotation occurs about the backbone carbon–nitrogen bond(s).

bipyramidal complexes $[CpM(S_2CNMe_2)_3]$ (M = Ti, Zr, Hf) (**45**) (Fig. 53). Each undergoes a metal-centered rearrangement, which is slow on the NMR time scale, together with three other fluxional processes; (1) methyl group exchange in the equatorial dithiocarbamates (I_e); (2) methyl group exchange in the unique dithiocarbamate (I_u); (3) exchange of dithiocarbamate ligands (366). On titanium, exchange of the methyl groups on the equatorial dithiocarbamate ligands (I_e) ($\Delta G^{\#} \sim 59$ kJ mol^{-1}) is $\sim 10^2$–10^3 times faster than exchange of the methyl groups in the unique dithiocarbamate (I_u), and also $\sim 10^3$ times faster than equatorial exchange (I_e) for zirconium and hafnium ($\Delta G^{\#} \sim 80$ kJ mol^{-1}). For zirconium and hafnium, the exchange rates are similar $(I_e - I_u)$, while the exchange of the equatorial and unique dithiocarbamates at titanium has a similar activation barrier ($\Delta G^{\#} \sim 75$–80 kJ mol^{-1}). It is believed that $I_e < I_u$ at titanium is a result of the relatively long titanium–sulfur distances to the equatorial ligands, while dithiocarbamate exchange is proposed to occur via a double-facial twist mechanism involving a capped trigonal-prismatic transition state.

Restricted carbon–nitrogen bond rotation has also been studied in unsymmetrical palladium bis(dithiocarbamate) complexes by HPLC (Fig. 54). At high temperature, there is rapid rotation and a single peak is observed, however, at lower temperatures two peaks can be separated. For $[Pd(S_2CNHCH_2CH_2Ph)_2]$, $\Delta H^{\#}$ was found to be 83 ± 5 kJ mol^{-1} (372).

Monajjemi et al. (373) carried out theoretical studies on the rotational barriers in square-planar rhodium(I) and iridium(I) systems using density functional theory. Their results suggest that in the transition state (90° rotation) significant changes occur to both the carbon–sulfur and carbon–nitrogen bond lengths, being shortened and lengthened, respectively, as a result of the loss of carbon–nitrogen double bond character. Rotational barriers are also effected by the ancillary ligands, increasing for those with π-acceptor ability and decreasing with increasing σ-donor ability; being attributed to the development of greater carbon–nitrogen π-bond character by π-acceptor ligands.

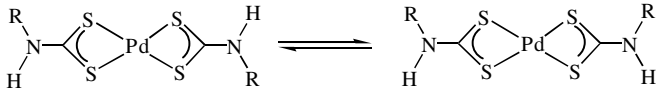

Figure 54. Rotomers of asymmetric palladium bis(dithiocarbamate) complexes being interconverted via rotation about the backbone carbon–nitrogen bonds.

Free dithiocarbamate salts generated from secondary amines, while stable under basic conditions, are generally unstable to acids rapidly decomposing to afford the amine and carbon disulfide (Eq. 10). In contrast, those derived from primary amines are unstable under both acidic and basic conditions, deprotonation occurring in the case of the latter to afford isothiocyanates (Eq. 6). When bound to a metal center, however, the stability of all dithiocarbamates toward acids is greatly enhanced, as is the stability of those derived from primary amines toward bases. Thus, Katsoulos and co-workers (86, 201, 374–381) prepared a wide range of group 10 (VIII) complexes derived from primary amines. Generally, they behave like analogous complexes derived from secondary amines, although their chemical behavior toward tertiary phosphines is more similar to that of the isoelectronic xanthate complexes rather than dialkyldithiocarbamates (376, 380, 381). They are, however, easily deprotonated to afford related dithiocarbimato complexes, a process that can be reversed upon addition of nucleophiles, providing a convenient synthesis of asymmetrically substituted dithiocarbamate complexes (Eq. 46) (201).

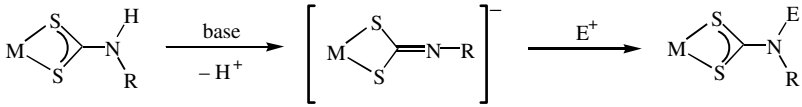

(46)

A feature of the dithiocarbimato complexes is their relatively short carbon–nitrogen bonds. For example, in $[Pd(S_2CNC_6H_4NH_2)_2]^{2-}$, the backbone carbon–nitrogen bond is 1.280(4) Å as compared to the average value of $\sim$ 1.35 Å in dithiocarbamate complexes (see below). This is also reflected in the ν(C—N) vibration that appears at 1508 cm^{-1} as compared to 1390 cm^{-1} in the analogous bis(dithiocarbamate) complex (116).

D. Structural Studies

The first crystallographic study of a dithiocarbamate complex was carried out by Simonsen and Ho in 1953 (382), whereby they reported the space group and unit-cell parameters of the zinc complex $[Zn(S_2CNEt_2)_2]$. In the proceeding 50 years, a massive amount of structural data has been amassed for dithiocarbamate

complexes. Data given in Table II is based on the work of Orpen et al. (383) and centers on examples retrieved from the Cambridge Structural Database in September 1985. It generally considers only the chelating bonding mode (A), although in some instances anisobidentate coordination (C) is included. Some entries have been updated since there was a paucity of structural information on these elements at that time and it is noteworthy that no structural data for hafnium dithiocarbamate complexes has yet been reported.

TABLE II
Interatomic Distances (Å) for Dithiocarbamate Complexes[a,b]

	d	m	σ	q_l	q_u	n
S–C[c]	1.714	1.715	0.018	1.704	1.726	539
C–N[c]	1.324	1.322	0.021	1.313	1.334	269
N–R[c]	1.473	1.475	0.030	1.462	1.487	537
Ti–S	2.576	2.592	0.048	2.527	2.609	22
V–S	2.466	2.467	0.042	2.434	2.497	134
Cr–S	2.416	2.407	0.026	2.396	2.441	24
Mn–S	2.459	2.465	0.078	2.385	2.529	12
Fe–S[d]	2.354	2.336	0.060	2.307	2.422	112
<2.375	2.319	2.313	0.026	2.299	2.340	78
>2.390	2.436	2.434	0.020	2.428	2.449	34
Co–S	2.267	2.270	0.013	2.255	2.277	32
Ni–S	2.207	2.206	0.017	2.196	2.218	18
Cu–S	2.250	2.222	0.044	2.214	2.286	14
Zn–S	2.436	2.452	0.056	2.406	2.466	16
Zr–S	2.685	2.676	0.050	2.644	2.717	20
Nb–S	2.580	2.578	0.042	2.561	2.599	100
Mo–S	2.513	2.507	0.059	2.478	2.530	164
Tc–S	2.457	2.476	0.043	2.405	2.490	14
Ru–S	2.379	2.392	0.039	2.345	2.400	20
Rh–S	2.367	2.363	0.024	2.352	2.378	38
Pd–S	2.323	2.319	0.031	2.315	2.323	18
Ag–S	2.613	2.569	0.078	2.563	2.708	7
Cd–S	2.681	2.654	0.107	2.615	2.716	58
Ta–S	2.560	2.561	0.036	2.529	2.580	36
W–S	2.522	2.523	0.052	2.490	2.548	120
Re–S	2.442	2.441	0.040	2.410	2.474	20
Os–S	2.410	2.417	0.021	2.405	2.424	20
Ir–S	2.377	2.373	0.020	2.365	2.390	20
Pt–S	2.350	2.350	0.033	2.323	2.372	60
Au–S	2.349	2.336	0.033	2.330	2.381	12
Hg–S	2.631	2.539	0.212	2.422	2.725	54

[a]Based on Table 9.6.1.2 in (383). Values for titanium and silver have been added. Data for vanadium, zirconium, rhodium, cadmium, tantalum, tungsten, iridium, platinum, and mercury have been updated.
[b]Unweighted sample mean = d; sample median = m; standard deviation = σ; lower quartile (25%) = q_l; upper quartile (75%) = q_u; number of observations = n.
[c]These values do not include the newly added data (see above).
[d]Distribution is bimodal.

Currently, the Cambridge Structural Database contains data for ~1500 chelating dithiocarbamate ligands. Table III provides structural data for simple diethyldithiocarbamate complexes of all the transition metals (where available).

Both carbon–nitrogen and carbon–sulfur bonds lie between values expected for single and double carbon-element bonds and vary only slightly over all dithiocarbamate complexes. The mean carbon–nitrogen bond length is 1.324 Å (Table II) with >95% of all measured lengths falling between 1.28 and 1.40 Å. Likewise, the mean carbon–sulfur bond length is 1.714–1.715 Å (Table II), the overall range again being small, varying between 1.65 and 1.80 Å.

Metal–sulfur bonds are comparable to those in related disulfur ligands, and generally decrease across the periodic table and increase on going down a group, in line with the expected decrease and increase, respectively, of the metal ion size. Values for the groups 11 (I B) and 12 (II B) elements seem to be unexpectedly high, however, it is here where anisobidentate binding becomes common (especially for cadmium and mercury) and low oxidation states dominate (silver).

A key feature of crystallographic studies on metal-bound dithiocarbamates is the planarity of the MS_2CNC_2 unit; that is, all seven atoms lie approximately in a plane and thus dithiocarbamates are generally considered to be sterically nondemanding. From a survey of structural data on a range of bis(dithiocarbamate) complexes, $[M(S_2CNR_2)_2]$ (M = Fe, Ni, Cu, Zn, Cd, Hg), Nikolov (425) concluded that the ligand remains essentially unchanged upon coordination and is best considered as being stereochemically rigid.

Dithiocarbamates are small-bite angle ligands, S–M–S bite angles varying between 64 and 80° in the simple complexes listed in Table III, and over a slightly wider range for all chelating complexes. The S–C–S angle is close to that expected for a carbon atom with both sp^3 and sp^2 character, varying between 100 and 133°, although the vast majority of examples cover a narrower range (108–122°), the mean value being 113.18°.

The lengthening of a single bond trans to a multiple bond in six- and seven-coordinate transition metal complexes is a well-known phenomenon, being ascribed to a trans-influence, whereby the increasing strength of the σ component of the metal–ligand multiple bond reduces the potential for bonding of the σ orbital trans to it. The effect is seen quite clearly for dithiocarbamate ligands in seven- (Table IV) and six- (Table V) coordinate complexes.

The greatest effect is seen with nitride (Δ 0.390–0.330 Å) and is slightly greater in six versus seven coordination. It can also be seen (Table V) that addition of Lewis acids to the nitride results in a reduction in the trans influence, while as seen from the niobium complexes, $[NbE(S_2CNEt_2)_3]$ (Table IV) the effect diminishes in the order; O > S > NAr. In a number of instances, two

TABLE III
Structural Parameters for Selected Dithiocarbamate Complexes

Complex	M–S (range; Å)	M–S (av; Å)	S–M–S (range;°)	S–M–S (av;°)	References
$[Ti(S_2CNEt_2)_4]$	2.500–2.620	2.564	66.46–67.93	67.26	384
$[V(S_2CNEt_2)_3]$	2.422–2.445	2.434	72.61–73.01	72.77	385
$[Cr(S_2CNEt_2)_3]$	2.393–2.399	2.396	73.78–74.19	74.03	386
$[Mn(S_2CNEt_2)_3]^a$	2.370–2.582	2.450	74.15–71.91	72.73	387, 388
$[Fe(S_2CNEt_2)_3]^b$	2.351–2.362	2.357	74.09–74.39	74.24	389
$[Fe(S_2CNEt_2)_3]^c$	2.301–2.310	2.307	75.85–75.86	75.85	389
$[Co(S_2CNEt_2)_3]$	2.249–2.274	2.265	75.90–76.82	76.46	358, 390, 391, 392, 393
$[Ni(S_2CNEt_2)_2]^d$	2.193–2.207	2.200	79.19–79.57	79.39	394, 395, 396
$[Ni(S_2CNEt_2)_3]$	2.268–2.272	2.270	76.47–76.71	76.59	397
$[Cu(S_2CNEt_2)_2]$	2.301–2.338	2.315	76.04–77.31	76.61	398,399
$[Zn(S_2CNMeEt)_2]^e$	2.322–2.472	2.376	68.99–75.58	72.41	400
$[Zn(S_2CNMe_2)_3]^{-f}$	2.299–3.151	2.626	64.05–73.71	67.31	401
$[CpZr(S_2CNMe_2)_3]$	2.654–2.717	2.690	64.37–66.09	65.02	402
$[Nb(S_2CNEt_2)_4]Br$	2.512–2.594	2.554	66.97–67.65	67.39	403
$[Mo(S_2CNEt_2)_4]$	2.521–2.538	2.530	67.53–67.69	67.61	404
$[Tc(CO)(S_2CNEt_2)_3]$	2.442–2.521	2.482	68.10–70.98	69.20	405
$[Ru(S_2CNEt_2)_3]$	2.367–2.379	2.377	72.86–73.21	72.98	406
$[Rh(S_2CNEt_2)_3]^g$	2.351–2.378	2.360	73.43–74.11	73.69	286, 407
$[Pd(S_2CNEt_2)_2]^h$	2.314–2.330	2.321	75.09–75.56	75.37	393, 408, 409
$[Ag(S_2CNEt_2)]^i$	2.539–2.950	2.722	64.42–66.60	65.51	330
$[Cd(S_2CNEt_2)_2]^j$	2.536–2.594	2.560	67.30–70.94	69.14	410,411
$[Cd(S_2CNEt_2)_3]^{-k}$	2.518–3.068	2.728	63.48–66.91	65.11	412–415
$[Ta(S_2CNMe_2)_4]Cl$	2.512–2.591	2.555	67.37–67.77	67.57	416
$[W(S_2CNEt_2)_4]Br$	2.480–2.535	2.509	67.44–68.18	67.78	417
$[Re(CO)(S_2CNEt_2)_3]$	2.433–2.518	2.480	68.01–70.96	69.02	418
$[Os(S_2CNEt_2)_3]^{+l}$	2.363–2.444	2.411	69.01–72.74	70.57	296
$[Ir(S_2CNEt_2)_3]$	2.365–2.394	2.372	73.12–73.32	73.25	419
$[Pt(S_2CNEt_2)_2]$	2.314–2.321	2.318	75.22	75.22	420
$[Au(S_2CNEt_2)_2]^{+m}$	2.318–2.334	2.326	74.98–75.75	75.38	421, 422
$[Hg(S_2CNEt_2)_2]^n$	2.394–2.992	2.687	66.43–66.43	66.43	423, 424

[a] Averaged over two polymorphs.
[b] At room temperature.
[c] At −194°C.
[d] Averaged over two polymorphs.
[e] Molecule is dimeric—the bridging sulfur has a long Zn–S bond of 2.851(av) Å.
[f] Contains two ambidentate dithiocarbamates.
[g] Averaged over two polymorphs.
[h] Includes data from a benzene solvated structure (409).
[i] Polymeric—values include terminal and bridging dithiocarbamates.
[j] Molecule is dimeric—the bridging sulfur has a long Cd–S bond of 2.806(av) Å.
[k] Average of five structures with different cations.
[l] Molecule is dimeric—the bridging sulfurs have Os–S bonds of 2.421(av) Å.
[m] Average of three structures with different anions.
[n] Both dithiocarbamates are ambidentate.

TABLE IV
Trans Influence on the Metal–Sulfur Bond in Seven-Coordinate Dithiocarbamate Complexes

Complex	M–S_{equ}(range)	M–S_{equ}(av)	M–S_{trans}	Δ	Reference
$[VO(S_2CNEt_2)_3]$	2.460–2.503	2.478	2.630	0.152	426
$[V(N\text{-}2,6\text{-}i\text{-}Pr_2C_6H_3)(S_2CNC_4H_4)_3]$	2.494–2.500	2.499	2.564	0.065	427
$[NbO(S_2CNEt_2)_3]$	2.545–2.581	2.569	2.765	0.196	426
$[NbS(S_2CNEt_2)_3]$[a]	2.550–2.598	2.566	2.716	0.150	428
	2.558–2.614	2.580	2.706	0.126	428
$[Nb(N\text{-}4\text{-}MeC_6H_4)(S_2CNEt_2)_3]$	2.556–2.607	2.581	2.707	0.126	210
$[\{Nb(S_2CNEt_2)_3\}_2(\mu\text{-}N_2)]$[a]	2.561–2.583	2.572	2.670	0.098	429
	2.566–2.589	2.579	2.632	0.053	429
$[NbS_2(S_2CNEt_2)_3]$	2.557–2.616	2.581	2.568	−0.013	430
$[TaS(S_2CNEt_2)_3]$	2.537–2.590	2.556	2.682	0.126	431
$[TaS_2(S_2CNEt_2)_3]$	2.506–2.594	2.552	2.580	0.028	432
$[MoN(S_2CNEt_2)_3]$	2.508–2.539	2.522	2.852	0.330	433
$[Mo(NTpOs)(S_2CNEt_2)_3]$	2.480–2.528	2.509	2.664	0.155	434
$[MoO(S_2CNR_2)_3]^+$	2.459–2.509	2.486	2.630	0.144	435
$[MoO(S_2CNEt_2)_3][TCNQ]$	2.463–2.503	2.483	2.616	0.133	436
$[Mo(NCPh_3)(S_2CNMe_2)_3]^+$	2.488–2.508	2.500	2.604	0.104	437
$[Mo(N\text{-}2,4\text{-}Me_2C_6H_3)(S_2CNEt_2)_3]^+$	2.486–2.520	2.498	2.587	0.089	438
$[Mo(NPh)(S_2CNEt_2)_3]^+$	2.486–2.516	2.499	2.585	0.086	439
$[Mo(N\text{-}2,4,6\text{-}Me_3C_6H_2)(S_2CNEt_2)_3]^+$	2.481–2.519	2.499	2.580	0.081	438
$[Mo(N\text{-}2,6\text{-}Me_2C_6H_3)(S_2CNEt_2)_3]^+$	2.493–2.519	2.501	2.577	0.075	438
$[Mo(NSO_2Ph)(S_2CNEt_2)_3]^+$	2.467–2.500	2.480	2.525	0.045	437
$[Mo(N_2Ph)(S_2CNMe_2)_3]$	2.479–2.531	2.514	2.611	0.097	440
$[Mo(N_2\text{-}4\text{-}NO_2C_6H_4)(S_2CNEt_2)_3]$	2.490–2.531	2.517	2.576	0.059	441
$[Mo(N_2\text{-}3\text{-}NO_2C_6H_4)(S_2CNMe_2)_3]$	2.482–2.529	2.516	2.569	0.053	440
$[Mo(NS)(S_2CNEt_2)_3]$	2.482–2.532	2.510	2.608	0.098	442
$[Mo(NS)(S_2CNMe_2)_3]$	2.487–2.530	2.515	2.601	0.087	433
$[Mo(NO)(S_2CNBu_2)_3]$	2.465–2.529	2.509	2.570	0.060	443
$[Mo(S_2)(S_2CNEt_2)_3]$	2.496–2.552	2.524	2.507	−0.017	180
$[Mo(SO_2)(S_2CNEt_2)_3]$	2.499–2.511	2.503	2.462	−0.046	444
$[Mo(S_2O)(S_2CNEt_2)_3]$	2.492–2.539	2.514	2.496	−0.018	445
$[Mo(SH)(S_2CNEt_2)_3]$	2.486–2.523	2.505	2.467	−0.038	446
$[Mo(PhPMe_2)(S_2CNEt_2)_3]$[a]	2.481–2.506	2.492	2.485	−0.007	434
	2.484–2.504	2.494	2.484	−0.010	434

[a]Two molecules in the asymmetric unit.

molecules are observed in the asymmetric unit (Table IV) and this can lead to quite different values of Δ, suggesting that all the bonds are quite *soft*.

It is not possible make a clear differentiation between chelating modes A and C, but based on the maximum lengthening of a metal–sulfur bond as a result of a trans-influence effect (Tables IV and V) at ∼ 0.4 Å observed in $[TcN(S_2CNEt_2)(PMe_2Ph)]$ (447), then this would seem to be a sensible break point. For example, in the β-polymorph of $[Hg(S_2CNEt_2)_2]$ (423, 424), the short and

TABLE V
Trans influence on the Metal–Sulfur Bond in Group 7 (VII B) Dithiocarbamate Complexes

Complex	M–S_{equ}(range)	M–S_{equ}(av)	M–S_{trans}	Δ	Reference
$[TcN(S_2CNEt_2)_2(PMe_2Ph)]$	2.411–2.460	2.435	2.826	0.390	447
$[ReN(S_2CNEt_2)_2(PMe_2Ph)]$	2.396–2.449	2.427	2.793	0.366	448
$[Re_4(\mu\text{-}N)_4(S_2CNEt_2)_6(MeOH)_2(PPh_3)_2]^{2+}$	2.397–2.450	2.429	2.626	0.197	449
$[Re\{NB(C_6F_5)_3\}(S_2CNMe_2)_2(PMe_2Ph)]$	2.377–2.461	2.424	2.609	0.185	450
$[Re(NBPh_3)(S_2CNEt_2)_2(PMe_2Ph)]$	2.364–2.433	2.408	2.579	0.171	451
$[Re(NBCl_2Ph)(S_2CNEt_2)_2(PMe_2Ph)]$	2.390–2.460	2.425	2.593	0.168	452
$[Re(NGaCl_3)(S_2CNEt_2)_2(PMe_2Ph)]$	2.377–2.449	2.419	2.581	0.162	453
$[Re(NBCl_3)(S_2CNEt_2)_2(PMe_2Ph)]$	2.376–2.455	2.421	2.565	0.144	453
$[Re(NCPh_3)(S_2CNEt_2)_2(PMe_2Ph)]^+$	2.356–2.467	2.418	2.555	0.137	454
	2.372–2.461	2.417	2.553	0.136	454
$[Tc(N_2\text{-}4\text{-}C_6H_4Cl)(S_2CNMe_2)_2(PPh_3)]$	2.412–2.478	2.447	2.537	0.090	455
$[Re(CS)(S_2CNEt_2)_3]$	2.415–2.489	2.467	2.595	0.128	456
$[Tc(CO)(S_2CNEt_2)_3]$	2.442–2.488	2.474	2.521	0.047	457
$[Re(CO)(S_2CNEt_2)_3]$	2.433–2.481	2.473	2.518	0.045	418

long mercury–sulfur bonds differ by an average of 0.582 Å, and this coordination would be considered as anisobidentate (C).

Precise variations of structural parameters as a function of the nature of the dithiocarbamate substituents can be difficult to assess. The most widely studied dithiocarbamate complexes by X-ray crystallographically are the tris(dithiocarbamate), $[M(S_2CNR_2)_3]$ (M = Fe, Co), and bis(dithiocarbamates), $[Ni(S_2CNR_2)_2]$, complexes. As can be seen from Table II, for the iron complexes a bimodal distribution of iron–sulfur bonds is seen, resulting from the well-characterized $^6A_1$–$^2T_2$ spin-state cross-over. Thus, in the high-spin $^6A_1$ state, the partial filling of the e_g level, which is metal–ligand antibonding in nature, leads to an elongation of the iron–sulfur bonds. Hence, simple systematic variations in the nature of the substituents cannot easily be assessed. For cobalt (Table VI) the situation is simpler as all adopt a low-spin d^6 configuration, while for similarly, all nickel bis(dithiocarbamate) complexes (Table VII) adopt a square-planar coordination geometry.

In light of supposed difference between pyrrolyl and pyrrolidine dithiocarbamates (see above) it is interesting to look at some comparative structural data for these two ligand types (Table VIII). The most direct comparisons are between the cobalt and iron tris(dithiocarbamate) complexes. For cobalt, the cobalt–sulfur bonds do not differ significantly. There is, however, a significant shortening of the carbon–nitrogen bond (−0.072 Å) in the pyrrolidine complex, and lengthening of the carbon–sulfur bonds (+0.035 Å) consistent with a greater degree of thioureide bonding in the saturated ring. For iron, similar though less

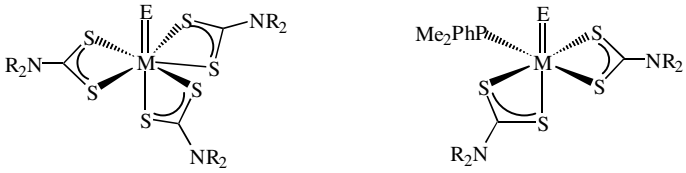

Figure 55. Seven- and six-coordinate dithiocarbamate complexes that display a trans influence with respect to a lengthening of the metal–sulfur bond trans to E as compared to those in the equatorial (eqv) plane.

pronounced effects are seen on the carbon–nitrogen (−0.57 Å) and carbon–sulfur (+0.032 Å) bonds. Now the iron–sulfur bonds vary significantly, the lengthening of 0.155 Å in the pyrrolidine relative to the pyrrolyl complex being a function of the high-spin nature of the former and low-spin nature of the latter (Fig. 52). It seems that at the copper(II) center the dithiocarbamate resonance form is primarily adopted in both instances and structural variations are small and nonconsistent. A comparison of the copper(II) and (III) pyrrolyl complexes is interesting, since given the inability of this ligand to adopt the thioureide resonance form, observed differences are purely a result of the increasing charge on the metal center. Thus as expected, the copper–sulfur bond gets shorter upon oxidation (−0.082 Å) while other bond lengths vary only slightly.

For monodentate dithiocarbamates (B), as expected the angle at carbon is more open ranging between 115 and 128°, the largest angle being 127.28° found in [Au(η^1-S_2CNEt_2)(S_2CNEt_2)(η^1-C_6H_4—*o*-CH_2NMe_2)] (**46**) (244). The mean carbon–nitrogen bond length at 1.335 Å is slightly greater than that found for chelating dithiocarbamates. As expected, the biggest difference is in the carbon–sulfur bonds; that bound to the metal averaging at 1.746 Å, while the uncoordinated bond averages at 1.679 Å, some 0.67 Å shorter. The biggest difference of 0.108 Å comes in the 1,1-bis(diphenylphosphino)ethane-bridged complex, [$Au_2(\eta^1$-$S_2CNEt_2)_2$\{μ-$Ph_2PC(=CH_2)PPh_2$\}] (**47**) (C—S 1.766 and 1.658 Å) (230).

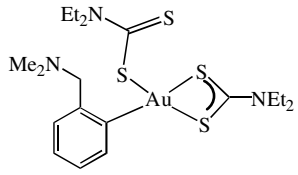

46

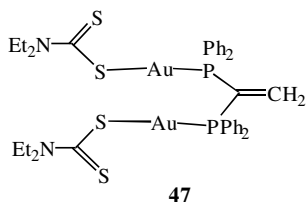

47

Structurally, bridging dithiocarbamate complexes fall into three types, which can be broadly distinguished on the basis of the angles subtended at carbon. Type D typically range between 122 and 129° as typified by one polymorph of [Au(μ-S_2CNEt_2)]$_2$ (**48**) in which the S–C–S angle is 128.92° (277). Type G

TABLE VI
Structural Parameters for $[Co(S_2CNR_2)_3]$[a]

R	Co–S Å	Co–S (av; Å)	S–Co–S°	S–Co–S (av;°)	References
H	2.258, 2.292	2.276	76.32	76.45	458
	2.267, 2.279		76.67		
	2.276, 2.284		76.38		
Me	2.254, 2.269	2.264	76.32	76.35	459
	2.255, 2.274		76.46		
	2.264, 2.270		76.25		
Me[b]	2.260, 2.279	2.270	76.49	76.62	460
	2.271		76.87		
Et	2.249, 2.263	2.261	76.82	76.72	390
	2.270		76.51		
	2.258, 2.260	2.258	75.90	76.47	391
	2.255		76.76		
	2.265, 2.267	2.267	76.32	76.38	358
	2.268		76.49		
	2.269, 2.274	2.271	76.36	76.37	392
	2.269		76.40		
	2.267, 2.268	2.268	76.41	76.48	393
	2.269		76.61		
Pr	2.266, 2.266	2.266	76.35	76.35	393
i-Pr	2.255, 2.261	2.258	75.68	75.68	358
i-Pr (120 K)	2.249, 2.274	2.262	75.98	75.98	358
Bz^3	2.250, 2.299	2.269	76.27	76.47	358
	2.258, 2.283		76.46		
	2.269, 2.271		76.51		
	2.251, 2.287		76.45		
	2.255, 2.273		76.75		
	2.261, 2.274		76.38		
$CH_2CH{=}CH_2$	2.259, 2.279	2.268	76.08	76.25	461
	2.266		76.60		
C_4H_8[c]	2.255, 2.284	2.272	76.16	76.47	358, 462
	2.269, 2.277		76.46		
	2.272, 2.274		76.65		
	2.255, 2.191		76.57		
	2.272		76.42		
C_4H_4	2.249, 2.278	2.267	76.54	76.31	463
	2.255, 2.273		76.37		
	2.268, 2.280		76.02		
C_4H_8O[d]	2.257, 2.287	2.273	76.41	76.25	464
	2.263, 2.282		76.12		
	2.273, 2.277		76.20		
C_4H_8O[e]	2.269, 2.277	2.273	76.59	76.56	465
	2.272		76.49		
C_4H_8O[f]	2.260, 2.284	2.275	76.11	76.10	466
	2.264, 2.287		76.10		
	2.277, 2.277		76.10		
Macrocycle[g]	2.252, 2.295	2.269	76.17	76.35	50

TABLE VI (*Continued*)

R	Co–S Å	Co–S (av; Å)	S–Co–S°	S–Co–S (av;°)	References
	2.256, 2.278		76.35		
	2.265, 2.267		76.54		
Ph	2.236, 2.294	2.268	76.37	76.39	359
	2.256, 2.286		76.47		
	2.261, 2.276		76.32		
Me/Ph	2.251, 2.284	2.270	76.15	76.27	359
	2.259, 2.282		76.23		
	2.263, 2.278		76.42		
Et/Ph	2.255, 2.267	2.263	76.09	76.22	467
	2.256, 2.263		76.43		
	2.256, 2.279		76.14		

[a] At room temperature unless otherwise stated.
[b] Cocrystallizes with two molecules of I_2.
[c] Two molecules in the asymmetric unit.
[d] Cocrystallizes with MeCN.
[e] Cocrystallizes with C_6H_6.
[f] Cocrystallizes with CH_2Cl_2.
[g] Macrocyclic complex **308**.

complexes subtend angles between 113 and 121° as exemplified by a polymorph of $[Cu(S_2CNEt_2)_2]_2$ (**49**) (S–C–S 117.0°) (411), while type F complexes subtend angles of between 105 and 112°, a typical example being $[CoCu(\mu\text{-}S_2CNR_2)_2(S_2CNR_2)(\mu\text{-Br})]$ (**50**) (S–C–S 109.84°) (498).

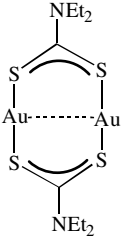

48

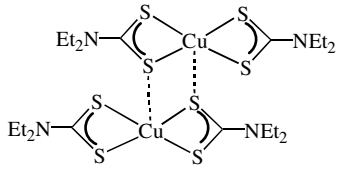

49

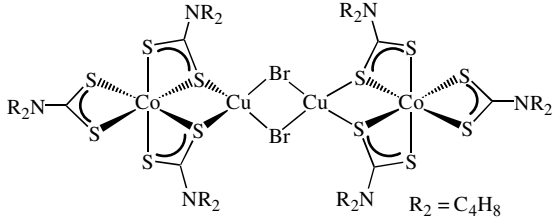

50

TABLE VII
Structural Parameters for $[Ni(S_2CNR_2)_2]$[a]

R	Ni–S (Å)	Ni–S (av; Å)	S–Ni–S(°)	S–M–S (av; °)	References
H	2.207, 2.224	2.214	78.6	78.5	468
	2.210, 2.218		78.4		
H (at 100 K)	2.208, 2.212	2.210	79.44	79.61	469
	2.208, 2.211		79.71		
H/Me	2.184, 2.198	2.191	79.55		470
H/Pr	2.192, 2.201	2.197	79.92		471
H/*i*-Pr	2.203, 2.222	2.213	78.89		472
Me	2.197, 2.220	2.209	79.22		473
Et (monoclinic)	2.195, 2.207	2.201	79.19		394
	2.196, 2.202	2.199	79.43		396
Et (tetragonal)	2.193, 2.204	2.199	79.57		395
Pr (triclinic)	2.197, 2.209	2.203	79.11		474, 475
Pr (rhombohedral)[b]	2.197, 2.203	2.200	79.42	79.41	476
	2.201, 2.207	2.204	79.39		
Pr (triclinic)[b]	2.198, 2.202	2.200	79.36	79.35	477
	2.203, 2.207	2.205	79.35		
Pr (at 173 K)[b]	2.202, 2.206	2.204	79.48	79.48	477
	2.203, 2.212	2.208	79.44		
i-Pr[b]	2.183, 2.183	2.183	79.01	79.15	358
	2.183, 2.189	2.186	79.30		
Bu	2.197, 2.210	2.204	79.19		478
i-Bu[b]	2.192, 2.204	2.198	79.29	79.35	479
	2.204, 2.205	2.205	79.42		
C_5H_{12}	2.179, 2.190	2.185			480
Cy	2.182, 2.203	2.193	79.05	79.05	481
	2.185, 2.196	2.191	79.05		
CH_2CH_2OH	2.193, 2.209	2.201	79.29		482
CH_2CF_3	2.197, 2.200	2.199	79.07		483
$CH_2CH{=}CH_2$	2.198, 2.210	2.204	79.16		484
C_4H_8	2.200, 2.217	2.209	79.51		485
	2.197, 2.214	2.206	79.33		486
C_5H_{10}	2.201, 2.212	2.207	78.98		487
	2.196, 2.207	2.202	79.41		488
C_6H_{12}[b]	2.191, 2.203	2.197	80.09	79.85	489
	2.200, 2.201	2.201	79.61		
C_4H_8O	2.206, 2.211	2.209	79.01		490
	2.200, 2.201	2.201	78.85		491
Et/Cy	2.196, 2.197	2.197	79.58		481
$Bz/CH_2C_4H_3N$	2.202, 2.207	2.205	79.47		492
Me/C_4H_3S	2.198, 2.201	2.200	79.59		493
Me/Ph	2.217, 2.217	2.217	79.09		494
Bz/acetyl[b]	2.196, 2.206	2.201	78.60	78.70	346
	2.198, 2.200	2.199	78.80		
Macrocycle[c]	2.164, 2.221	2.193	79.86	79.65	492
	2.171, 2.201	2.186	78.99		

TABLE VII (*Continued*)

R	Ni–S (Å)	Ni–S (av; Å)	S–Ni–S(°)	S–M–S (av; °)	References
	2.201, 2.224	2.213	79.69		
	2.206, 2.210	2.208	80.07		

[a] At room temperature unless otherwise stated.
[b] Two molecules in the asymmetric unit.
[c] Macrocyclic complex **350** with two crystallographically independent metal centers.

X-ray absorption fine structure (XAFS) studies have been carried out on a range of dithiocarbamate complexes. Young and co-workers (499) point out that while spin equilibria in iron tris(dithiocarbamate) complexes has been extensively studied by single-crystal X-ray crystallography, the latter gives only a weighted average of the high- and low-spin forms even when data has been collected at different temperatures (357, 500–503). Using a combination of Fe K-edge XAFS and advanced data analysis they have determined the iron–sulfur distances and spin state populations in $[Fe(S_2CNEtPh)_3]$ and $[Fe(S_2CNC_4H_8O)_3]$; iron–sulfur distances of 2.44(2) Å and 2.30(2) Å being determined for high- and low-spin isomers, respectively (479), as opposed to an average value previously measured (504).

The structures of dithiocarbamate complexes in solution have also been investigated by extended X-ray absorption spectroscopy (EXAFS) and X-ray

TABLE VIII
Structural Parameters for Pyrrolyl and Pyrrolidine Dithiocarbamate Complexes

Complex	M–S (av)	C–N (av)	C–S (av)	S–C–S (av)	References
$[Co(S_2CNC_4H_4)_3]$	2.267	1.382	1.675	113.44	463
$[V(NAr)(S_2CNC_4H_4)_3]$[a]	2.499	1.381	1.685	113.15	427
$[FeI(S_2CNC_4H_4)_2]$[b]	2.288	1.291	1.726	110.97	495
$[Fe(S_2CNC_4H_4)_3]$[c]	2.301	1.368	1.688	113.17	351
$[Cu(S_2CNC_4H_4)_2]$	2.297	1.310	1.713	114.35	496
$[Cu(S_2CNC_4H_4)_2]^+$	2.215	1.301	1.716	110.27	323
$[Co(S_2CNC_4H_8)_3]$	2.272	1.310	1.710	110.57	358
$[Cu(S_2CNC_4H_8)_2]$[d]	2.310	1.330	1.707	115.36	470, 486
$[Fe(S_2CNC_4H_8)_3]$	2.456	1.311	1.720	115.56	497

[a] Ar = 2,6-*i*-$Pr_2C_6H_3$; parameters due to trans-elongated V–S bond excluded.
[b] Cocrystallizes with 0.5 I_2.
[c] Cocrystallizes with 0.5 CH_2Cl_2.
[d] Averaged over two structures.

absorption near edge spectroscopy (XANES) using synchrotron radiation (505). The EXAFS data suggest that both $[Ni(S_2CNEt_2)_2]$ and $[Co(S_2CNEt_2)_3]$ are monomeric in benzene, while for $[Cd(S_2CNR_2)_2]$ (R = Et, Bu) monomers and dimers coexit. Most interestingly, the EXAFS data for $[Zn(S_2CNEt_2)_2]$ have been interpreted in terms of the dimeric structure being maintained upon dissolution. The XANES spectra of both $[Cd(S_2CNEt_2)_2]$ and $[Zn(S_2CNEt_2)_2]$ have been recorded in the solid state as well as in pyridine and tributylphosphine, the main features of the solid-state spectra being maintained upon dissolution.

Both EXAFS and XANES studies have also been carried out on cobalt(II) and (III) complexes (506) and molybdenum (V) and (VI) complexes with proline dithiocarbamate (125). EXAFS measurements have also been made on the gold(I) complex, $[Au_2\{\mu\text{-}S_2CN(C_2H_4OMe)_2\}_2]$, allowing a comparison with crystallographic data. In the latter, the polymeric chain consists of alternating short (2.790 Å) and long (3.157 Å) gold–gold interactions, and analogous separations of 2.775 and 3.271 Å are found from the EXAFS data (280).

Few neutron diffraction studies of dithiocarbamate complexes appear to have been carried out, examples including a single-crystal study of $[Zn(S_2CNEt_2)_2]_2$ (507), and two reports centered on the molecular ferromagnet, $[FeCl(S_2CNEt_2)_2]$ (508, 509). For the latter, high-resolution data on a deuterated sample between 50 and 300 K reveal a structural transition associated with a disorder of one of the ethyl groups over two positions at room temperature, which are frozen out into a single position in the low-temperature phase (508). Other workers have also carried out neutron diffraction experiments on both powder and single-crystal samples of $[FeCl(S_2CNEt_2)_2]$; Mössbauer simulations in conjunction with these results allowing the authors to conclude that the system is a noncollinear ferromagnet (509).

Deformation density maps and DFT calculations have been used to study the electron-density distribution about $[Co(S_2CNMe_2)_3]$. A spherical distribution about the cobalt(III) ion is seen, displaying a linear relationship between electron density at the bond critical point and bond length, suggesting that the former is a good indicator of bond strength (510).

E. Other Characterization Techniques

Perhaps the most characteristic feature of transition metal dithiocarbamate complexes are their IR spectra (16, 17, 511). Three regions can be identified; (1) the backbone ν(C—N) vibration at between 1450 and 1550 cm^{-1}, (2) the ν(C—S) vibrations between 950 and 1050 cm^{-1}, (3) ν(M—S) vibrations between 300 and 400 cm^{-1}. Variations in ν(C—N) and ν(C—S) as a function of the substituents are generally quite consistent within a particular class of complex. Some typical values for nickel bis(dithiocarbamate) complexes are given in Table IX.

TABLE IX
Some IR Data for Nickel Bis(dithiocarbamate) Complexes (cm^{-1}) (512)

R	ν(C—N)	ν(C—S)
Me	1532	974
Et	1522	993
Pr	1516	976
Bu	1511	972
Pentyl	1516	974
Hexyl	1515	977
Heptyl	1510	977
Octyl	1506	976
i-Pr	1503	945
i-Bu	1508	985
C_5H_{10}	1518	1000
C_4H_8O	1501	1015/1025

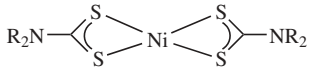

The ν(C—N) band is generally strong and its position is suggestive of a significant degree of double-bond character, consistent with a significant contribution from the thioureide resonance form. In support of this, it is noted that pyrrole dithiocarbamate complexes typically show intense bands in the 1300 cm^{-1} region of the IR spectrum being shifted ~150 cm^{-1} to higher wavenumbers than the corresponding pyrrolidine analogues, in line with their decreased thioureide character (346).

Kellner and St. Nikolov (513) studied the far-IR spectra of a range of simple dithiocarbamate complexes $[M(S_2CNR_2)_2]$ (M = Ni, Cu, Zn, Cd, Hg) and $[M(S_2CNR_2)_3]$ (M = Mn, Fe, Co). They note that the ν(M—S) vibrations lie in a surprisingly narrow frequency range (320–400 cm^{-1}) and also observe δ(SCN), δ_{as}(SCN), and δ_s(SMS) bands (as = asymmetric, s = symmetric). Interestingly, the ν(M—S) vibrations correlate with a number of structural parameters including the M—S bond length and S–M–S bond angle.

While several physical methods have been used toward the differentiation of chelating and monodentate dithiocarbamate bonding modes (binding modes A and B in Fig. 27, respectively), the Bonati and Ugo (514) criterion based on the number and splitting of ν(C—S) bands in the 950–1050 cm^{-1} is generally utilized. More recently, however, using group theoretical predications, Kellner et al. (515) challenged this criterion. By comparing the ν_{as}(C—S) bands for dithiocarbamate complexes containing different substituents, they suggest that the splittings are due to interligand coupling of the CS ligand modes. Further, a

comparison with X-ray diffraction data shows that the dithiocarbamate ligands, irrespective of the metal they bind to or the ligand-bonding type, are at sites of C_1 symmetry, thus ruling out the possibility of detecting the ligand bonding type from the solid-state vibrational spectra.

In recent work, ruthenium(III) complexes, $[Ru(tacn)(S_2CNR_2)(\eta^1\text{-}S_2CNR_2)][PF_6]$ (**21**) (Fig. 28), containing both monodentate and bidentate dithiocarbamate ligands, exhibited two ν(C—N) bands in their IR spectra. On the basis that the monodentate dithiocarbamate should have less C—N double-bond character, a band in the 1460 cm^{-1} region is assigned to this ligand, a second band at $\sim$ 1550 cm^{-1} being associated with the bidentate dithiocarbamate (233). The differentiation of monodentate and bidentate binding modes is, however, not always possible by IR spectroscopy. For example, a number of complexes of the type $[CpRu(PR_3)_2(\eta^1\text{-}S_2CNR'_2)]$ and $[CpRu(PR_3)(S_2CNR'_2)]$ are known, and while IR spectra of both show characteristic ν(C—S) and ν(C—N) bands, they are too similar to allow unequivocal distinction between η^1- and η^2-coordination (234).

Cavell et al. (76) compared ν(C—N) and ν(C—S) bands in a range of nickel(II) bis(dithiocarbamate) complexes, $[Ni(S_2CNR^1R^2)_2]$, with ethyl and 2,2,2-trifluoroethyl dithiocarbamate ligands. Upon introduction of more fluorine atoms, there is a relative lowering of the ν(C—N) stretch consistent with a significant decrease in the carbon–nitrogen bond order, being attributable to the inductive effect of the CF_3 groups. In contrast, fluorination has little effect on the ν(C—S) stretch (Fig. 56).

The IR and Raman spectra of a number of zinc and cadmium dithiocarbamate complexes and their deutero derivatives have been reported, and a complete vibrational assignment proposed (516). Isotopic labeling has also been used to assign the ν(C—S) and δ(S–M–S) modes in a wide range of nickel(II) and copper(II) heterocyclic dithiocarbamate complexes. The same study makes a comparison between the ν(C—N) bands in both types of complexes, being generally observed at higher frequency in the nickel versus the copper complexes, the higher value been accompanied by a lower ν(C—S) mode (517). The ν(C—N) bands in related zinc bis(dithiocarbamate) complexes tend to be at slightly lower wavenumbers again than the analogous copper complexes (Fig. 57) (512).

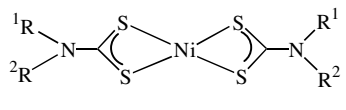

$R^1 = R^2 =$ Et; C-N 1508; C-S 985
R^1 = Et, R^2 = H; C-N 1522; C-S 960
$R^1 = CF_3CH_2$, R^2 = H; C-N 1535; C-S 993
$R^1 = R^2 = CF_3CH_2$; C-N 1465; C-S 988

Figure 56. Infrared data (cm^{-1}) for some nickel bis(dithiocarbamate) complexes.

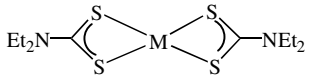

	ν(C-N)	ν(C-S)	ν(M-S)
M = Ni	1522	993	384
M = Cu	1508	995	356
M = Zn	1505	995	379

Figure 57. Infrared data (cm^{-1}) for some bis(diethyldithiocarbamate) complexes (3800–400 cm^{-1} in KBr; 600–1200 cm^{-1} in nujol).

Fourier transform infrared (FT–IR) attenuated total reflectance spectra of single crystals of $[Cd(S_2CNEt_2)_2]$ have been reported and dichrotic measurements of vibrational bands made (518). From their different dichrotic ratios, assignments of the A_u and B_u bands (C_{2h} symmetry) was possible, being verified by force constant refinement calculations.

Vibrational spectroscopy, as well as proving a useful characterization tool, has also been widely used in the study of the structure and reactivity of dithiocarbamate complexes. For example, Ramadevi and co-workers used IR spectroscopy to follow isotopic exchange for both $[Cu(S_2CNEt_2)_2]$ (519) and $[Cr(S_2CNEt_2)_3]$ (520) and their free metal ions in solution. As expected, increasing both the temperature and concentration of the metal complexes results in an increased reaction rate.

St. Nikolov and Atanasov recorded vibrational spectra for a number of diethyldithiocarbamate complexes, $[M(S_2CNEt_2)_2]$ (M = Ni, Cu, Cd, Zn), both in solution and the solid state, a comparison allowing structural changes that may occur upon dissolution to be assessed (521, 522). In all cases, enhanced symmetry was seen upon dissolution, consistent with the removal of intermolecular contacts found in the solid state.

In other work, vibrational shifts for nickel and copper dithiocarbamate complexes have been correlated with those observed for atomic core levels in the X-ray photoelectron spectra (523), and an experimental procedure is detailed for the collection of high-quality IR spectra from metal dithiocarbamate single-crystal surfaces using polarized radiation and attenuated total reflectance (524).

The dithiocarbamate ligand contains three NMR nuclei and thus diamagnetic transition metal complexes especially can be characterized by ^1H, ^{13}C, and ^{15}N NMR spectroscopy. In practice, it is generally the ^{13}C NMR spectra that prove most useful, and specifically the low-field quaternary carbon resonance that is most characteristic. In a seminal study, van der Linden and co-workers (166, 525) reported the ^{13}C NMR spectra of >70 dithiocarbamate-containing compounds. All show the characteristic quaternary carbon resonance in the region 190–220 ppm. The substituents seem to have little effect on the chemical shift, although diphenyldithiocarbamates tend to appear $\sim$8 ppm downfield of analogous dialkyldithiocarbamate compounds, while solvent effects also appear to be minimal. Most interestingly, the chemical shift of the backbone carbon can be correlated to the π-bonding in the NCS_2 fragment via the ν(C—N) stretching

frequency. Using pattern recognition techniques, five classes of compounds can be distinguished; (1) the free ligands, (2) normal oxidation state transition metal complexes, (3) normal main group compounds and organic dithiocarbamates, (4) high oxidation state transition metal complexes, (5) low coordination number main group compounds. In the context of this chapter, it is classes (2) and (4) that are significant. Van der Linden defines a term the *fractional oxidation number* (FON), the ratio of the oxidation number and coordination number. For *normal* complexes (2) this is 0.5; examples include the homoleptic complexes, $[M(S_2CNR_2)_n]$ ($n = 2, 3, 4$). In contrast, high oxidation state complexes have high FON values; the molybdenum(VI) complexes, $[MoO_2(S_2CNR_2)_2]$, having an FON of 1. Typically, for class (2) complexes the backbone carbon appears at between 202 and 213 ppm in the ^{13}C NMR spectrum and ν(C—N) at 1485–1515 cm^{-1} in the IR spectrum, while for class (4) complexes, the carbon resonance appears upfield between 190 and 200 ppm with ν(C—N) at 1520–1575 cm^{-1}.

Another feature of the ^{13}C NMR spectra of dialkyldithiocarbamate complexes are the resonances from the alkyl substituents. The nitrogen-bound α-carbon is shifted downfield with respect to the other signals, being typically found between 43 and 57 ppm. Further methylene groups appear between 20 and 30 ppm, being shifted to higher field upon increasing distance from the nitrogen center, while the end methyl groups are typically found between 14 and 10 ppm.

Proton NMR spectra are often characteristic of the alkyl substituent(s) used, but otherwise often convey little further information. In diethyldithiocarbamate complexes, the nature of the methylene proton signals can give valuable information regarding the coordination geometry at the metal center, asymmetry being reflected in their diastereotopic nature. For example, in $[MoO(S_2)(S_2CNEt_2)_2]$, the room temperature stereochemical rigidity of the seven-coordinate pentagonal bipyramid is easily seen by the inequivalence of all eight methylene protons (and the four methyl groups) (526). Further, while six of the methylene protons lie in the region δ 3.75–3.95 and overlap to such an extent that individual assignments cannot be made from the one-dimensional (1D) spectrum, two of the methylene protons are considerably shielded, lying between δ 3.35 and 3.55 (Fig. 58). This shielding is also seen in one of the methyl groups and is assigned to the ethyl moiety, which lies close to the Mo=O vector. The effect is not limited to the oxo ligand, and has also been noted for related imido complexes (527, 528).

Proton NMR can provide a useful tool to follow reactions. These include dithiocarbamate exchange, and for which it has been used extensively in the study of paramagnetic iron(III) complexes (529–531). Indeed, on the basis of their results it appears that a report on the preparation of mixed-ligand spin-crossover complexes, $[Fe(S_2CNR_2)_2(S_2CNR')]$, upon addition of $NaS_2CNR'_2$ to

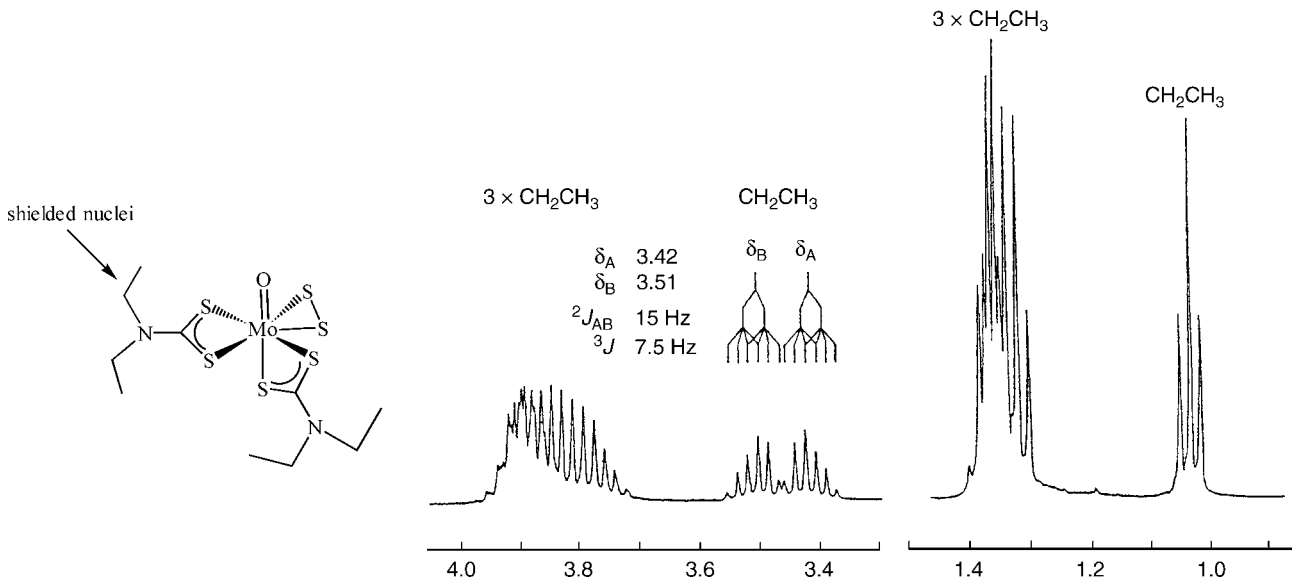

Figure 58. A 400-MHz ^{1}H NMR spectrum of $[MoO(S_2)(S_2CNEt_2)_2]$.

$[Fe(S_2CNR_2)_2Cl]$ is probably incorrect (532), since facile ligand exchange gives equilibrium mixtures of mixed-ligand complexes.

The third NMR nucleus of a dithiocarbamate is nitrogen, and a number of ^{15}N NMR studies have been carried out both in solution and the solid state (533–538). For example, the natural abundance ^{15}N NMR spectrum of *cis*-$[Fe(CO)_2(S_2CNEt_2)_2]$ shows a single sharp line at 213.35 ppm, a region indicative of substantial carbon–nitrogen double-bond character (534, 535), while the stereochemical rigidity of *cis*-$[FeI(NO)(S_2CNEt_2)_2]$ is shown by the observation of two peaks associated with the inequivalent dithiocarbamate ligands at 210.92 and 209.09 ppm (534). The ^{15}N chemical shift may also relate to the magnitude of the rotational barrier about the carbon–nitrogen bond; a more positive value corresponding to greater partial double-bond character and thus a larger rotational energy barrier. In this context, Duffy and co-workers (534) suggested that rotational barriers in a series of compounds increase in the order; $[Co(S_2CNEt_2)_3] < (S_2CNEt_2)_2 <$ *cis*-$[Fe(CO)_2(S_2CNEt_2)_2] <$ *cis*-$[FeI(NO)(S_2CNEt_2)_2]$.

Natural abundance ^{14}N NMR spectroscopy has also been utilized, but to a far lesser extent. Sachinidis and Grant (539) used it to measure the rate of pyridine exchange in bis(pyridine) adducts of $[Ni(S_2CNR_2)_2]$.

Electrospray mass spectrometry (ESMS) has been applied quite widely to the characterization of dithiocarbamate complexes (231, 303, 313, 540–548). For example, mass spectra of diethyldithiocarbamate complexes of iron(III), manganese(III), copper(II), nickel(II), and cobalt(III) were obtained at low source offset voltages. All showed molecular ions of the oxidized complexes in addition to ions due to loss of a dithiocarbamate ligand (542). Bond et al. (547) also used electrospray MS to study the constitution of mercury and mixed mercury–cadmium dithiocarbamate complexes in dichloromethane–methanol solutions, leading to the observation of a range of ions $[M(S_2CNR_2)]^+ + n[M(S_2CNR_2)_2]$ ($n = 1$–3; M = Hg, Cd), with addition of $[M(S_2CNR_2)_2]$ resulting in the formation of higher oligomers.

X-ray photoelectron spectroscopy (XPS) has been carried out on a wide range of dithiocarbamate complexes (270, 271, 521, 523, 549–558), aspects of this work being reviewed (559). For example, He(I) and He(II) photoelectron spectra for $[M(S_2CNR_2)_2]$ (M = Ni, Pd, Pt) have been recorded; the very low photoionization He(II) cross-section of the sulfur based, when compared to the metal-based orbitals, allowing the efficient identification of a complicated spectral pattern. Further, comparing spectra for different metals suggests an increase in the π-donor capability along the series; Ni > Pd > Pt (550). Liesegang and co-workers (523) investigated the different electron-donor properties of ethyl and butyl dithiocarbamate ligands from the XPS spectra of $[Ni(S_2CNR_2)_2]$ (R = Et, Bu). The Ni $2p_{3/2}$, S $2p$, and N $1s$ XPS binding energies were found to increase by 0.46, 0.53, and 0.44 eV, respectively, upon

replacing butyl for ethyl groups, suggesting that diethyldithiocarbamate is a better electron-donor ligand than dibutyldithiocarbamate.

X-ray photoelectron spectra for a number of copper(II) bis(dithiocarbamate) complexes have been recorded (521, 556, 558, 560). Early work on [$Cu(S_2CNEt_2)_2$] seemed to suggest that the nitrogen was directly bound to the copper center (556), but subsequent studies on [$Cu(S_2CNBz_2)_2$] refuted this (558). The XPS spectra for a range of heterocyclic derivatives, [$Cu(S_2CNC_4H_8X)_2$] (X = O, S, NH, NMe, CH_2) have been recorded (560), and it is noted that the Cu $2p_{3/2}$ peaks are particularly narrow (1.0–2.1 eV).

Liesegang and Lee (561) showed that vibrational or absorption shifts in the IR spectra of copper and nickel bis(dithiocarbamate) complexes correlate with shifts observed for atomic core levels in their XPS spectra. In a quite different application, the decomposition during XPS experiments of gold(III) complexes, [$AuMe_2(S_2CNMe_2)$] and [$AuBr_2(S_2CNPr_2)$], has been found to be a function of temperature and X-ray intensity; decomposition being an order of magnitude slower on graphite than silver (549).

F. Thermochemical Properties

The thermochemistry of dithiocarbamate complexes is of considerable interest, primarily since they can be used as molecular precursors for the synthesis of a range of technologically important metal sulfides, especially those of copper and zinc (see Sections III.H.1.g.ii and III.I.1.h.i). The successful application of this approach relies on the volatility of the metal complexes and the strength of the metal–sulfur and metal–carbon bonds; since the latter must be cleaved, while the former is retained (at least to some extent). Consequently, a large number of studies have focused on the thermochemical properties of transition metal dithiocarbamate complexes and Hill and co-workers (22, 562, 563) and others (23, 564) reviewed aspects of these.

The first quantitative data on the volatility of dithiocarbamate complexes was obtained by D'Ascenzo and Wiendlant (565, 566) who used an isoteniscope to obtain the vapor pressure of [$Fe(S_2CNEt_2)_3$] and some other diethyldithiocarbamate complexes as a function of temperature. Later, Magee and co-workers obtained enthalpies of sublimation for [$Ni(S_2CNEt_2)_2$], [$Cu(S_2CNEt_2)_2$], and [$Co(S_2CNEt_2)_3$] from vacuum DSC (DSC = differential scanning calorimetry) data (567, 568). Heats of sublimation for [$Ni(S_2CNEt_2)_2$] (102.6 ± 1.5 kJ mol^{-1}) and [$Cu(S_2CNEt_2)_2$] (116.2 ± 1.3 kJ mol^{-1}) from this latter method (567) were significantly higher than those determined earlier, the difference being attributed to the low volatility of the complexes leading to resulting uncertainties with the isoteniscope measurements (566).

The standard molar enthalpies of formation and enthalpies of sublimation have been determined for a number of dithiocarbamate complexes and this has

allowed the mean molar bond dissociation energies to be derived (569–578), others being estimated from ligand exchange reactions (579–581). Homolytic metal–sulfur bond scission is far more favorable than heterolytic cleavage. For example, homolytic and heterolytic scission in $[Cu(S_2CNEt_2)_2]$ is estimated at 143 and 678 kJ mol^{-1}, respectively (580). Some values for the homolytic cleavage of metal–sulfur bonds are given in Table X. Comparing the diethyldithiocarbamate complexes of each of the metals listed, the following trends appear; M(III): Cr > Co > Mn ≅ Fe; M(II): Ni > Cu > Zn > Pd > Cd. Mean bond dissociation enthalpies also vary as a function of alkyl substituents in the order; Me < Et < Pr < Bu. Similar thermal stability sequences have been found from the decomposition kinetics of dithiocarbamate complexes (583).

Melting points of homoleptic diethyldithiocarbamate complexes vary as a function of the metal; Zn (177°C) < Cu (198°C) < Fe (234°C) ≅ Ru (235°C) ≅ Ni (236°C) ≅ Pd (240°C) < Cd (251°C) < Cr (257°C) ≅ Rh (260°C) < Ir (265°C) < Pt (275°C) (584, 585), while a somewhat similar trend is seen in their sublimation temperatures; Zn (217°C) < Cu (229°C) < Fe (246°C) < Co (267°C) < Ni (286°C) (586).

Although there are no clear trends on the volatility of dithiocarbamate complexes, it appears that volatility increases upon increasing length of the alkyl substituents. For example, the melting points of nickel bis(dithiocarbamate) complexes decrease with increasing alkyl chain length (587, 588); Me (275°C dec) > Et (234°C) > Pr (134°C) > Bu (95°C) > pentyl (80°C) > octyl (30°C). The introduction of fluorine atoms also generally decreases the melting point as compared to analogous alkyl dithiocarbamate complexes. For example, the melting point of $[Ni\{S_2CN(CH_2CF_3)_2\}_2]$ at 143°C (75) is some 90°C below that of $[Ni(S_2CNEt_2)_2]$.

Riekkola has investigated a wide range of dithiocarbamate complexes using electron impact MS (589). Their gas-phase stability varies as a function of the metal ion in the following manner; M(II): Ni > Pd > Cu > Zn > Cd > Hg; M(III): Rh > Cr > Co > Fe. Stability also varies as a function of the alkyl substituents: Et > Pr > *i*-Bu ≅ Bu. Riekkola also found that while fluorination of the alkyl backbone increased volatility, it also leads to a decrease in gas-phase stability. Thus, 2,2,2-trifluoroethyldithiocarbamate complexes, while more volatile than the corresponding ethyl analogues, were also significantly less stable (589) an observation that may have important consequences on the design of new MOCVD (MOCVD = molecular chemical vapor deposition) precursors. In light of the latter, thermogravimetric analysis (TGA) studies have been carried out using 2,2,2-trifluoroethyldithiocarbamate complexes as MOCVD precursors (75).

The thermal properties of dithiocarbamate complexes have been investigated in great detail using TGA and DSC (23, 27, 159, 564, 590–592). For example,

TABLE X
Mean Molar Bond Dissociation Enthalpies (kJ mol^{-1}) for Dithiocarbamate Complexes

Complex	Value	Reference
$[Cr(S_2CNMe_2)_3]$	202 ± 5	582
$[Cr(S_2CNEt_2)_3]$	214 ± 6	571
$[Cr(S_2CNPr_2)_3]$	215 ± 6	571
$[Cr(S_2CN{-}i\text{-}Pr_2)_3]$	205 ± 6	571
$[Cr(S_2CNBu_2)_3]$	222 ± 6	571
$[Cr(S_2CN{-}i\text{-}Bu_2)_3]$	227 ± 6	571
$[Mn(S_2CNEt_2)_3]$	185 ± 6	571
$[Mn(S_2CNPr_2)_3]$	185 ± 6	571
$[Mn(S_2CN{-}i\text{-}Pr_2)_3]$	180 ± 6	571
$[Mn(S_2CNBu_2)_3]$	196 ± 6	571
$[Mn(S_2CN{-}i\text{-}Bu_2)_3]$	198 ± 6	571
$[Fe(S_2CNMe_2)_3]$	183 ± 5	582
$[Fe(S_2CNEt_2)_3]$	182 ± 6	571
$[Fe(S_2CNPr_2)_3]$	183 ± 6	571
$[Fe(S_2CN{-}i\text{-}Pr_2)_3]$	174 ± 6	571
$[Fe(S_2CNBu_2)_3]$	186 ± 6	571
$[Fe(S_2CN{-}i\text{-}Bu_2)_3]$	191 ± 6	571
$[Co(S_2CNEt_2)_3]$	200 ± 6	571
	200 ± 25	581
$[Co(S_2CNPr_2)_3]$	200 ± 6	571
$[Co(S_2CN{-}i\text{-}Pr_2)_3]$	186 ± 6	571
$[Co(S_2CNBu_2)_3]$	214 ± 6	571
$[Co(S_2CN{-}i\text{-}Bu_2)_3]$	210 ± 6	571
$[Ni(S_2CNMe_2)_2]$	222 ± 4	573
$[Ni(S_2CNEt_2)_2]$	227 ± 2	570
	193	579
$[Ni(S_2CNPr_2)_2]$	232 ± 3	570
$[Ni(S_2CN{-}i\text{-}Pr_2)_2]$	221 ± 3	570
$[Ni(S_2CNBu_2)_2]$	242 ± 3	570
$[Ni(S_2CN{-}i\text{-}Bu_2)_2]$	238 ± 3	570
$[Pd(S_2CNEt_2)_2]$	172 ± 4	577
$[Pd(S_2CNPr_2)_2]$	183 ± 3	577
$[Pd(S_2CNBu_2)_2]$	151 ± 3	577
$[Pd(S_2CN{-}i\text{-}Bu_2)_2]$	163 ± 3	577
$[Cu(S_2CNMe_2)_2]$	183 ± 4	573
$[Cu(S_2CNEt_2)_2]$	187 ± 3	569
	143	580
$[Cu(S_2CNPr_2)_2]$	197 ± 3	569
$[Cu(S_2CN{-}i\text{-}Pr_2)_2]$	193 ± 3	569
$[Cu(S_2CNBu_2)_2]$	205 ± 3	569
$[Cu(S_2CN{-}i\text{-}Bu_2)_2]$	200 ± 3	569

TABLE X (*Continued*)

Complex	Value	Reference
$[Zn(S_2CNEt_2)_2]$	177 ± 3	578
$[Zn(S_2CNPr_2)_2]$	182 ± 3	574
$[Zn(S_2CNBu_2)_2]$	183 ± 3	575
$[Zn(S_2CN{-}i\text{-}Bu_2)_2]$	137 ± 4	576
$[Cd(S_2CNEt_2)_2]$	167 ± 4	572
$[Cd(S_2CNPr_2)_2]$	154 ± 3	574
$[Cd(S_2CNBu_2)_2]$	168 ± 3	575
$[Cd(S_2CN{-}i\text{-}Bu_2)_2]$	118 ± 4	576
$[Hg(S_2CNEt_2)_2]$	75 ± 4	572
$[Hg(S_2CNPr_2)_2]$	102 ± 3	574
$[Hg(S_2CNBu_2)_2]$	105 ± 3	575
$[Hg(S_2CN{-}i\text{-}Bu_2)_2]$	75 ± 4	576

Cavalheiro et al. (593, 594) investigated the thermal decomposition of a range of cyclic dithiocarbamate complexes and find a correlation between their IR spectra and thermal decomposition pathways. A correlation between the thermal decomposition and ionic radius of the metal ion is also noted (592, 595); the smaller the metallic ionic radius, the greater the thermal stability, suggesting that high valent complexes are more stable than their low-valent counterparts. In other work, the thermal properties of rubber vulcanization catalysts, $[M(S_2CNEtPh)_n]$ ($n = 2$, M = Ni, Cu, Zn; $n = 3$, M = Co) were studied by DSC. The curing reaction order and rate constants follow the order; Co > Ni > Cu > Zn (568).

G. Stability Constants and Dithiocarbamate Exchange

Stability constants have been measured for a wide range of dithiocarbamate complexes from ultraviolet (UV)–visible spectroscopy (316,392,596,597), pH (598), and potentiometric (599,600) titrations, electron spin resonance (ESR) spectroscopy (601), and HPLC (602–605). They are determined typically from exchange studies between a free metal salt and its dithiocarbamate complex (Eq. 47). Sachinidis and Grant (597) identified two pathways for ligand transfer; the first involves dissociation of a dithiocarbamate followed by substitution at the metal ion, while the second results from direct electrophilic attack by the metal ion on the dithiocarbamate complex.

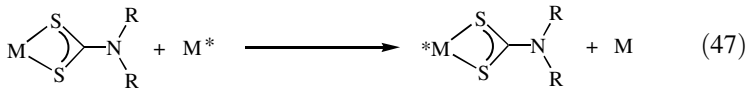

(47)

From these studies it was not possible to determine a single order of stability as a function of the metal (and oxidation state). Sachinidis and Grant (597) placed the stability of dithiocarbamate complexes in DMSO in the following order; Hg > Cu > Ni > Cd > Zn, while in an ethanol–water mixture the order; Zn < Cu > Ni > Co > Fe > Mn was determined (598). Moriyasu and co-workers (602–605) utilized HPLC to study dithiocarbamate exchange at a number of late transition metal centers. They noted that the rate of ligand exchange is >10 times faster than that of ternary complex formation, and concluded the following series of increasing stability constants at a nickel(II) center in chloroform; $Bu_2 > Pr_2 > C_6H_{12} > Et_2 > C_5H_{10} > Me_2 > C_4H_8$.

By using electrochemical methods, Bond and Schultz (606) also derived a considerable number of stability constants (β_2) for mercury bis(dithiocarbamate) complexes in water (Eq. 48). They found no correlation between them and the Taft substituent constants for the dithiocarbamate substituents. There is, however, a linear correlation between log β_2 and the molecular weight (M_w) of the complexes, which can be represented by the empirical equation; log $\beta_2 = 29.95 + 0.03301\ M_w$.

$$Hg^{2+} + 2\,R_2NCS_2^- \overset{\beta_n}{\rightleftharpoons} [Hg(S_2CNR_2)_2] \tag{48}$$

Bond and co-workers (303, 540,541) also utilized (ESMS) to study ligand-exchange reactions. For example, while cobalt(III) tris(dithiocarbamate) complexes are inert to substitution and exchange reactions, they do undergo ligand exchange at elevated temperatures and upon controlled-potential oxidation and reduction (Fig. 59) (541).

Also, while addition of silver(I) alone does not lead to dithiocarbamate exchange at cobalt(III) centers, further addition of $[Hg(S_2CNR_2)_2]$ leads to fast global exchange of the dithiocarbamates on both cobalt and mercury. Similar global dithiocarbamate exchange does not result with analogous rhodium or iridium tris(dithiocarbamate) complexes, but is seen with $[Pt(S_2CNR_2)_2]$. It is

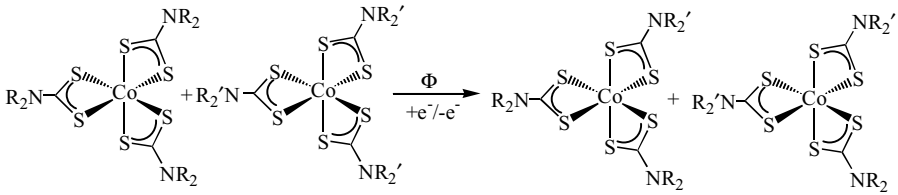

Figure 59. Thermally and electrochemically activated dithiocarbamate exchange in coblat(III) complexes.

not clear precisely how exchange occurs, but reactions are catalytic in silver(I) and probably proceed via the intermediate formation of cationic mixed-metal clusters (540). The same group have also shown that dithiocarbamate exchange at mercury(II) and cadmium(II) centers is facile, probably occurring via the intermediate formation of dimeric species (547, 607).

IV. TRANSITION METAL COMPLEXES: GROUP SURVEY

A. Group 4 (IV B): Titanium, Zirconium, and Hafnium

1. Titanium, Zirconium, and Hafnium

Group 4 (IV B) dithiocarbamate chemistry is constrained to the +4 oxidation state. The first reported example was the eight-coordinate tetrakis(dithiocarbamate) titanium complex, $[Ti(S_2CNBz_2)_4]$, prepared by Dermer and Fernelius in 1934 (608), while the heavier zirconium and hafnium analogues were first prepared by Bradley and Gitlitz (193) from the reaction of metal amides, $[M(NR_2)_4]$ (M = Ti, Zr, Hf), with carbon disulfide.

An earlier report on paramagnetic titanium(III) complexes, $[Cp_2Ti(S_2CNR_2)]$, appears to be erroneous (609). More recently, the synthesis of the yellow-green, air-sensitive, titanium(III) complexes, $[Ti(S_2CNR_2)_3]$ (R = Me, Et, Pr, Bu), has been claimed. They supposedly result from the addition of dithiocarbamate salts to $TiCl_3$ in ethanol and have been characterized by IR spectral data and magnetic measurements, the latter appearing to show that the d^1 state is retained (610, 611). There appears to have been no further reports of these complexes and their true identity may require further consideration.

a. Simple Dithiocarbamate Complexes. A number of procedures can be used for the synthesis of simple halide–dithiocarbamate and eight-coordinate tetrakis(dithiocarbamate) complexes. Metal tetrachlorides, MCl_4 (M = Ti, Zr, Hf), react directly with dithiocarbamate salts the precise product being dependent on the reaction stoichiometry. In this way, a range of new derivatives $[MCl_{4-x}(S_2CNR_2)_x]$ (R = Et, R′ = tolyl; R = H, R′ = C_5H_9, C_7H_{13}; x = 1–4) have been prepared (612). All are susceptible to hydrolysis, resistance increasing with the number of dithiocarbamate ligands, while the titanium complexes are more hydrolytically sensitive than their zirconium counterparts (612, 613). Likewise, heating metal tetrachlorides (M = Ti, Zr) with the $[NH_4][S_2CNC_4H_4]$ affords either $[MCl_2(S_2CNC_4H_4)_2]$ or $[M(S_2CNC_4H_4)_4]$ depending on the stoichiometry used (614). In a further contribution, the salmon pink bis(dithiocarbamate) complex $[TiCl_2(S_2CNEt_2)_2]$ has been prepared upon addition of 2 equiv of NaS_2CNEt_2 to $[TiCl_3(CN\text{-}t\text{-}Bu)\{\mu\text{-}C(Cl)=N\text{—}t\text{-}Bu\}]_2$, while

$[Hf(S_2CNEt_2)_4]$ has been prepared from the analogous hafnium *tert*-butyl isocyanide complex (615).

Siddiqi et al. (109) prepared a number of tetrakis(dithiocarbamate) complexes, $[M(S_2CNHR)_4]$ (M = Ti, Zr), derived from primary amines. These can be accessed from the reaction of the pre-formed dithiocarbamate salt, as is the case for propanediamine dithiocarbamate complexes ($R = CH_2CH_2CH_2NH_2$), or from their *in situ* generation in the presence of the metal tetrachloride (R = *N*-phenyl-α-naphthylamines, 2-amino-benzothiazole, benzidine, 2,4-tolylenediamine) (616).

There is little structural data for these complexes, being limited to earlier crystallographic characterization of $[Ti(S_2CNEt_2)_4]$ (384) and $[TiCl(S_2CNMe_2)_3]$ (368, 416, 617), which adopt dodecahedral and pentagonal bipyramidal metal coordination environments, respectively.

Both zirconium and hafnium tetrachlorides also react with $Me_2NC(S)SN(SiMe_3)_2$ to give $[MCl_3(S_2CNMe_2)]$, which in the presence of excess pyridine yield *fac*-$[MCl_3(Py)_2(S_2CNMe_2)]$ (Eq. 29). The zirconium complex has been crystallographically characterized. It shows a distorted pentagonal bipyramidal coordination geometry, the dithiocarbamate lying in the equatorial plane (208). The precise structures of $[MCl_3(S_2CNR_2)]$ remain unknown. In one report, on the basis of the observation of two M—Cl bands in the IR spectrum, $[MCl_3(S_2CNR_2)]$ (M = Ti, Zr; R = Me, Et), have been proposed to be dimeric (618).

Fay (365) showed that the titanium complex, $[TiCl(S_2CNMe_2)_3]$ (**51**), is stereochemically nonrigid on the NMR time scale at temperatures down to −90°C. The low-temperature spectrum shows four methyl resonances (1:2:2:1) consistent with a pentagonal bipyramidal structure (368). Upon warming, line shape changes indicate the onset of two distinct fluxional processes; (1) a low-temperature intramolecular metal-centered rearrangement that exchanges the unique dithiocarbamate ligand with those in the equatorial plane, and (2) a higher temperature process involving rotation about the carbon–nitrogen bonds ($\Delta G^{\#} = 84$ kJ mol^{-1}).

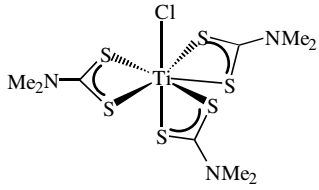

51

A number of reports focus on the synthesis and structure of aryloxide complexes. For example, heating $[M(OPh)_2Cl_2]$ with 2 equiv of NaS_2CNRR' (R = R′ = Me, Et, *i*-Pr; R = Me, Et, *i*-Pr, R′ = Cy) affords complexes

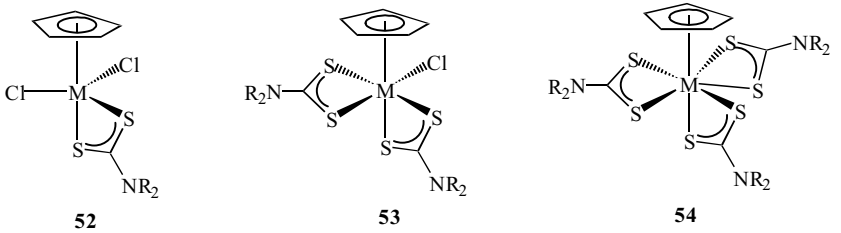

Figure 60. Monocyclopentadienyl complexes of the group 4 (IV B) metals.

$[M(OPh)_2(S_2CNRR')_2]$ (M = Ti, Zr) (619). Related methylsalicylato complexes, $[Ti(OC_6H_4CO_2Me)_2(S_2CNR_2)Cl]$ and $[Ti(OC_6H_4CO_2Me)_2(S_2CNR_2)_2]$ (R = Et, Pr, Bu; $R_2 = C_4H_8$, C_5H_{10}), have also been prepared from $[Ti(OC_6H_4CO_2Me)_2Cl_2]$. Spectroscopic data suggest that they are seven and eight coordinate, respectively, although the precise binding mode of the bidentate methylsalicylato group is unknown (620).

b. Cyclopentadienyl Complexes. A large number of publications concern cyclopentadienyl complexes. Monocyclopentadienyl complexes $[CpMCl_3]$ react with 1–3 equiv of dithiocarbamate salt to produce $[CpMCl_2(S_2CNR_2)]$ (**52**), $[CpMCl(S_2CNR_2)_2]$ (**53**), and $[CpM(S_2CNR_2)_3]$ (**54**), respectively (Fig. 60) (52, 621–630).

Titanium and hafnium complexes $[CpMCl_2(S_2CNR_2)]$ and $[CpMCl(S_2CNR_2)_2]$, in which the dithiocarbamate derives from substituted thiadiazoles (Fig. 4) have also been prepared (52, 631). For the titanium complexes, on the basis of IR data in which two ν(C—S) bands are observed, it is postulated that each dithiocarbamate and the nitrogen of the thiadiazole ring is metal bound to produce six-membered chelate rings, however, this has not been confirmed crystallographically (52).

Tris(dithiocarbamate) complexes, $[(\eta^5\text{-}C_5H_4R')M(S_2CNR_2)_3]$ (M = Ti, Zr, Hf; R = Me, Et, Bz; R′ = H, Me), have also been prepared from addition of 3 equiv of dithiocarbamate salt to $[(\eta^5\text{-}C_5H_4R')_2MCl_2]$ (Eq. 49), one of the cyclopentadienyl ligands is displaced (627–629, 632–634). For example, heating $[Cp_2HfCl_2]$ and dithiocarbamate salts in dichloromethane affords $[CpHf(S_2CNR_2)_3]$ (R = Me, Et) in >90% yield (634).

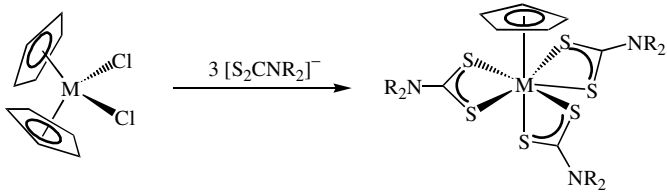

(49)

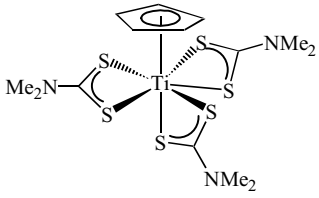

55

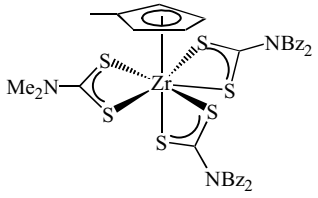

56

Figure 61. Crystallographically characterized examples of seven-coordinate cyclopentadienyl tris(dithiocarbamate) complexes.

Based on IR studies, $[CpM(S_2CNBz_2)_3]$ (M = Ti, Zr, Hf) are proposed to be seven-coordinate (629, 632) and this is confirmed crystallographically for $[CpTi(S_2CNMe_2)_3]$ (**55**) (635) and $[(\eta^5\text{-}C_5H_4Me)Zr(S_2CNBz_2)_3]$ (**56**) (636, 637) (Fig. 61). Both have a distorted trigonal-bipyramidal geometry with the cyclopentadienyl ligand occupying an axial site and one dithiocarbamate spanning axial–equatorial (ax–eq) sites. In $[CpTi(S_2CNMe_2)_3]$ (635), unusually long titanium–sulfur distances [Ti-S(av) 2.611 Å] are found, being attributed to steric crowding. For $[(\eta^5\text{-}C_5H_4Me)Zr(S_2CNBz_2)_3]$, there are two independent molecules in the asymmetric unit, the difference between them relating to the relative orientation of the cyclopentadienyl ligand and five equatorial sulfur atoms being either staggered or eclipsed (636, 637). Less is known about the structure of the hafnium complexes, and on the basis of NMR measurements, it has been suggested that $[CpHf(S_2CNMePh)_3]$ adopts a capped octahedral configuration (628).

In two papers, Fay et al. (366, 367) used variable temperature NMR studies to probe the stereochemical nonrigidity of seven-coordinate pentagonal bipyramidal complexes $[CpM(S_2CNMe_2)_3]$ (M = Ti, Zr, Hf). They undergo a metal-centered rearrangement that is slow on the NMR time scale, together with three other fluxional processes: (1) exchange of the methyl groups on the equatorial dithiocarbamate ligands (I_e); (2) exchange of the methyl groups in the unique dithiocarbamate (I_u); (3) exchange of the equatorial and unique dithiocarbamate ligands (see Section III.C) (366). The complex $[Cp^*Zr(S_2CNMe_2)_3]$ (Cp^* = pentamethylcyclopentadienyl) displays similar fluxional properties to its unsubstituted analogue, although the interconversion of dithiocarbamates is appreciably slower due to the greater steric crowding (367), while $[CpHf(S_2CNR_2)_3]$ (R = Me, Et) also show metal-centered rearrangements and hindered rotation about the carbon–nitrogen bonds, all of which are slow on the NMR time scale (634).

The relative stability of a number of mono(cyclopentadienyl) complexes has been assessed. Hafnium complexes are stable to 160–180°C, but hydrolyze slowly in air (625), while titanium complexes, which are stable up to 150°C, are also air stable, but hydrolyze slowly in solution (626).

A wide range of bis(cyclopentadienyl) complexes $[Cp_2MCl(S_2CNR_2)]$ (M = Ti, Zr) have been prepared by Kaushik and co-workers (619, 621, 622, 633, 638–643) and others (627, 644, 645). They result upon thermolysis of 1 equiv of dithiocarbamate salt with $[Cp_2MCl_2]$ in dichloromethane (Eq. 50), while a large range of related fluorenyl complexes $[(\eta^5\text{-}C_{13}H_9)_2ZrCl(S_2CNHAr)]$ (R = Ph, *o*-tolyl, *p*-tolyl, *o*,*m*,*p*-C_6H_4Cl, *p*-C_6H_4X; X = Cl, Br, I, OMe) has also been prepared in a similar fashion (646). Suzuki et al. (644) also prepared $[Cp_2Zr(Me)(S_2CNR_2)]$ (R = Me, Et) via similar methods but utilizing thallium dithiocarbamates.

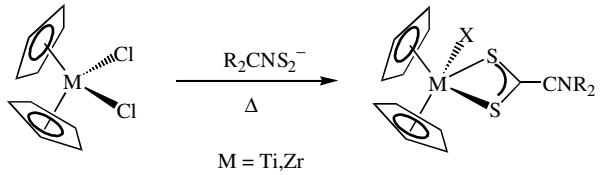

(50)

A number of mono(dithiocarbamate) complexes $[Cp_2ZrCl(S_2CNR_2)]$ have been crystallographically characterized (623, 624, 647–649) as has $[Cp_2Zr(SiMe_3)(S_2CNEt_2)]$, formed like its hafnium analogue, from $[Cp_2M(SiMe_3)Cl]$ (M = Zr, Hf) (650). All show a five-coordinate bent metallocene structure and, as a result of steric crowding, unusually long zirconium–sulfur and zirconium–element bonds. In each the dithiocarbamate is bound asymmetrically with one long zirconium–sulfur contact of >2.7 Å.

Three papers describe cyclopentadienyl zirconium phenoxide complexes (623, 651, 652). Addition of phenols to $[Cp_2Zr(S_2CNC_4H_4)Cl]$ in the presence of triethylamine yields aryloxides, $[Cp_2Zr(S_2CNC_4H_4)(O\text{-}p\text{-}C_6H_4X)]$ (X = H, Me, NH_2, NO_2, Cl, *o*-NO_2) (623), while analogous dimethyldithiocarbamate complexes have also been prepared (652). One example, $[Cp_2Zr(OPh)(S_2CNMe_2)]$, has been crystallographically characterized (651). The two zirconium–sulfur bond lengths differ by 0.13 Å, that at 2.789(4) Å being among the longest terminal zirconium–sulfur bonds known.

Bis(cyclopentadienyl) complexes, $[Cp_2ZrX(S_2CNR_2)]$, have been extensively studied by variable temperature (VT) NMR (647, 649, 652), the dithiocarbamate substituents undergoing exchange. For example, a ^1H NMR study of $[Cp_2ZrCl(S_2CNMe_2)]$ shows that the methyl groups undergo facile exchange (647). Exchange rates are shown to be independent of X for halide or alkyl groups, but a dramatic increase in the rate is seen as the π-donor ability of X varies; Cl < OPy < OPh (652). Possible mechanisms have been analyzed, and on the basis of kinetic and structural data, reinforced by EHMO (EHMO = extended Hückel molecular orbital) calculations, a restricted rotation about the carbon–nitrogen bond is proposed for simple halide and alkyl complexes (647). For aryloxide derivatives, however, methyl group exchange

may occur via a zirconium–sulfur bond rupture mechanism that is promoted by the π-donor properties of these ligands (652).

An early paper describes the synthesis of yellow-brown $[Cp_2Ti(S_2CNHAr)_2]$, formed upon addition of 2 equiv of ammonium dithiocarbamate salts to $[Cp_2TiCl_2]$ in water (653). In light of the later work described above, it would appear that this formulation is incorrect, and interestingly the authors state that attempts to prepare the same materials in organic solvents such as THF or acetone gave only impure products.

c. Other Complexes. In two papers, Shukla and Srivastava make claim to the synthesis of oxo titanium and zirconium complexes, $[MO(S_2CNR_2)_2]$ (654, 655), which are inert to oxygen and water and insoluble in common organic solvents. They result from the reaction of titanyl hydroxide or hydrated oxozirconium hydroxide with 2 equiv of carbon disulfide and amine and are assigned on the basis of IR stretches attributed to the M=O vibration at 1040 ± 5 and 980 ± 2 cm^{-1}, respectively. They are reported to react further with 2 equiv of HgX_2, and although the nature of the products is not clear, it is proposed that mixed-metal complexes result with the dithiocarbamate acting in a bridging capacity. Similarly, Kumar and Kaushik (656) reported the synthesis of related complexes, $[MO(S_2CNR_2)_2].2H_2O$ (M = Zr, Hf), upon addition of 2 equiv of dithiocarbamate salts to the appropriate metal oxychlorides. The IR and magnetic data suggest that they are five-coordinate complexes (656).

In a large number of papers, cationic titanium and zirconium complexes $[CpM_2L]Cl$ (L = monoanionic chelating oxygen or nitrogen bound ligand) have been reacted with dithiocarbamate salts to produce $[CpM_2L][S_2CNR_2]$, with no evidence for metal coordination of the dithiocarbamate (657–665).

d. Applications. In the presence of sodium hydride, $[Cp_2TiCl(S_2CNBz_2)]$ has been shown to display high catalytic activity for the hydrogenation of hex-1-ene under mild conditions [20°C 1 atm^{-1}; TON(max) 1939 mol H_2/ mol Ti s^{-1}, 3522 mol H_2 mol^{-1} Ti in 2 h], however, just like $[Cp_2TiCl_2]$, the activity quickly decays (648).

Toxicity studies of these same tetrakis(dithiocarbamate) complexes toward houseflies and cockroaches have been carried out, showing that the titanium complexes are slightly more toxic than the analogous sodium salts (616).

B. Group 5 (V B): Vanadium, Niobium, and Tantalum

1. Vanadium

The first examples of vanadium dithiocarbamate complexes were the eight-coordinate vanadium(IV) species $[V(S_2CNR_2)_4]$ prepared in the late 1960s by

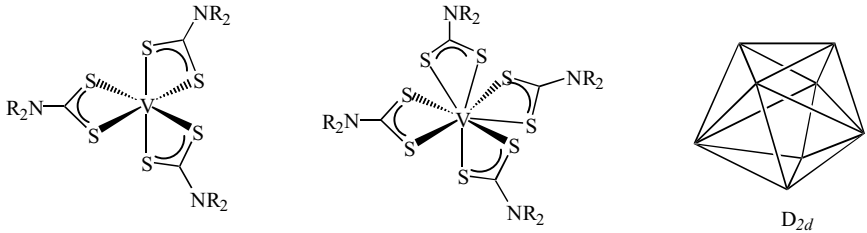

Figure 62. Structural representations of vanadium tris- and tetrakis(dithiocarbamate) complexes.

Bradley and Gitlitz (193, 666) via the insertion of carbon disulfide into metal amides, $[V(NR_2)_4]$. Dithiocarbamates are now known to stabilize vanadium in oxidation states ranging from +3 to +5.

a. Simple Dithiocarbamate Complexes. Vanadium(III) complexes, $[V(S_2CNR_2)_3]$ (**57**) (Fig. 62), can be prepared from the direct reaction of VCl_3 and 3 equiv of anhydrous dithiocarbamate salts (667), while other examples have been prepared from $VBr_2.6H_2O$ (668). Complexes $[V(S_2CNR_2)_3]$ (R = Me, Et, Pr, *i*-Bu) are orange-brown and paramagnetic (μ_{eff} 2.60–2.76 BM), and all change color on exposure to air, with $[V(S_2CNMe_2)_3]$ being pyrophoric (668). Three tris(dithiocarbamate) complexes, $[V(S_2CNEt_2)_3]$ (385), $[V(S_2CN{-}i\text{-}Bu_2)_3]$ (669), and $[V(S_2CNC_5H_{10})_3]$ (670) have been characterized crystallographically, with $[V(S_2CN{-}i\text{-}Bu_2)_3]$ (669) containing two independent molecules in the asymmetric unit. All display a coordination geometry intermediate between an octahedral and trigonal prismatic, the distortion from a pure octahedron being attributed to a Jahn–Teller effect (669).

Few mixed halide–dithiocarbamate complexes appear to be known, the only report in this area suggesting that addition of 2 equiv of dithiocarbamate salts to VCl_3 affords complexes of the form $[VCl(S_2CNC_4H_8X)_2]$ (X = O, S, NMe, CH_2), the structures of which are unknown (667).

Tetrakis(dithiocarbamate) vanadium(IV) complexes, $[V(S_2CNR_2)_4]$ (**58**) (Fig. 62), can also be prepared (615, 671–673). For example, addition of 10 equiv of NaS_2CNBz_2 to vanadyl sulfate affords $[V(S_2CNBz_2)_4]$, which, can be stored at room temperature for 1 week as a solid (671). Pyrrole-, indole-, indoline-, and carbazole-derived dithiocarbamate complexes have all been prepared in a similar manner from their respective potassium salts (672). Single-crystal and powder ESR studies on $[V(S_2CNEt_2)_4]$ have been used to probe the coordination geometry, and confirm that the discrete eight-coordinate geometry is close to an ideal triangular dodecahedron (D_{2d}) (**59**) (Fig. 62) (673).

Vanadium(IV) cyclopentadienyl complexes, $[Cp_2V(S_2CNR_2)]^+$, have previously been prepared and studied (674, 675), and more recently a crystallographic and ESR study of $[Cp_2V(S_2CNEt_2)][BF_4]$ has been carried out (676).

b. Oxo and Imido Complexes. A number of vanadium dithiocarbamate complexes have been studied with strong π donors such as oxo or imido as supporting ligands. A range of vanadium(V) complexes, $[VOCl_2(S_2CNR_2)]$, $[VOCl(S_2CNR_2)_2]$, and $[VO(S_2CNR_2)_3]$ ($R^1 = H$, $R^2 = C_5H_9$, $C_7H_{13;}$ $R_2 = C_4H_8X$; $X = O$, S, NMe, CH_2), are reported to be formed upon addition of between 1 and 3 equiv of dithiocarbamate salts to $VOCl_3$ (667, 677), although their structures remain unknown.

A number of reports detail the synthesis of vanadyl dithiocarbamate complexes of the general formula $[VO(S_2CNR_2)_2]$ (**60**) (53,345,351,667–683). They are generally prepared upon addition of dithiocarbamate salts to vanadyl sulfate. For example, Preti and co-workers (667) reported that addition of 2 equiv of cyclic dithiocarbamate salts to vanadyl sulfate affords $[VO(S_2CNC_4H_8X)_2]$ ($X = O$, S, NMe, CH_2), and the dithiocarbamate salt derived from 2-methylpiperazine gives a similar product (345). Sakurai et al. (678) prepared a number of these complexes including those with *N*-methyl, *N*′-D-glucamine and sarcosine dithiocarbamate, while Bereman and Nalewajek (352) prepared gray pyrrole, indole, indoline, and carbazole-derived dithiocarbamate complexes. The latter are prepared under almost identical conditions to the red-brown tetrakis(dithiocarbamate) complexes described above, the only difference being the solvent used; ethanol for vanadyl complexes versus acetonitrile for the latter.

All are proposed to have five-coordinate square-based pyramidal structure, similar to that found previously in $[VO(S_2CNEt_2)_2]$ (684). Doadrio et al. (681) looked in some detail at the vibrational and electronic spectra of a range of these complexes. In the IR, a number of distinct bands are observed, most notably the ν(V=O), which appears between 950 and 1000 cm^{-1}, varying as a function of the dithiocarbamate substituents and being correlated with the $b_2 \Rightarrow e\pi^*$ absorption in the electronic spectrum.

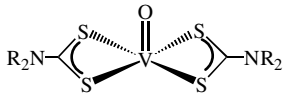

60

The six-coordinate vanadyl dithiocarbamate complex, $[VO(S_2CNEt_2)_2(py)]$, results from addition of NaS_2CNEt_2 to vanadyl sulfate in the presence of pyridine. In contrast, addition of piperidine to $[VO(S_2CNR_2)_2]$ (R = Et, Pr, *i*-Pr,

Bu, *i*-Bu) in water reportedly affords ionic compounds formulated as $[VO(OH)_2(S_2CNR_2)(pip)_2].3H_2O$ (685). More recently, the same group have reported somewhat similar results from reactions of pyridine with a range of vanadyl bis(dithiocarbamate) complexes (679). In some instances simple adducts, $[VO(S_2CNR_2)_2(py)]$ (R = Pr, *i*-Bu, Cy; R_2 = PhH), are formed, however, for others, ionic products, $[VO(OH)(S_2CNR_2)(py)_2][OH].H_2O$ (R = *i*-Pr; $R_2 = C_4H_8O$, C_5H_{10}), result.

One of the dithiocarbamate ligands in $[VO(S_2CNR_2)_2]$ (R = *i*-Pr; $R_2 = C_4H_8$) can be replaced by quinoline or thiourea ligands (L) producing mixed-ligand vanadyl complexes, $[VO(S_2CNR_2)L]$, which have been characterized by ESR spectroscopy (682). In a series of papers, Ivanov et al. (686–688) has probed the products of the reaction of $[VO(S_2CNR_2)_2]$ with varying amounts of thallium dithiocarbamates by ESR spectroscopy. While definitive structural assignments are difficult to arrive at, it seems that addition of 1 and 2 equiv of TlS_2CNR_2 is possible, with dithiocarbamates bridging between metal centers.

Shukla and Srivastava (683) reported that vanadyl complexes $[VO(S_2CNR_2)_2]$ react with a range of soft acceptors, such as AgX, HgX_2, and CdX_2 (X = Cl, SCN, CO_2CF_3, ClO_4), to form heterobimetallic adducts, $[VO(S_2CNR_2)_2.2MX]$. The structures of these are unknown, with the authors proposing that they contain dithiocarbamates bridging the two metal centers.

Acetyl halides have been used to replace the oxo group in $[VO(S_2CNR_2)_2]$ (R = Me, Et; $R_2 = C_4H_4$) yielding $[VX_2(S_2CNR_2)_2]$ (X = Cl, Br) (Eq. 51). Both diethyldithiocarbamate complexes have been crystallographically characterized and show a distorted octahedral coordination geometry with cis halides (689, 690). The dichlorides, $[VCl_2(S_2CNR_2)_2]$ (R = Me, Et; $R_2 = C_5H_{10}$, C_4H_8O), have also been prepared from the reaction of $[VCl_2(thf)_2]$ with thiuram disulfides (Eq. 51) (173).

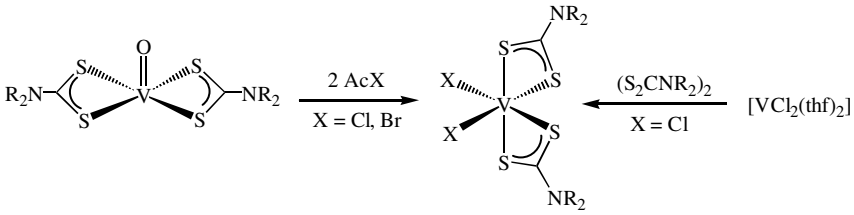

(51)

The synthesis and crystal structure of the tris pyrazolylborate complex [Tp*VO(S_2CNPr_2)] (**61**) has been reported. It adopts a distorted octahedral geometry with approximate C_s symmetry, and a short V=O bond [1.589(4) Å] (691), which is similar to that found in [Tp*VO(acac)] (acac = acetylacetonato). The ESR studies have been carried out on [Tp*VO(S_2CNR_2)] (R = Et, Pr), and

the ESR parameters and molecular geometries, in conjunction with a parameterized angular overlap model, are used to analyze the electronic structures in both molecules. A similar analysis has been carried out on $[VO(S_2CNEt_2)_2]$ for comparison (692).

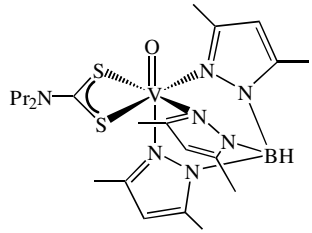

61

Vanadium imido complexes feature in a number of reports. Addition of 3 equiv of dithiocarbamate salts to $[V(NAr)Cl_3(dme)]$ (dme = 1,2-dimethoxyethane) (Ar = 2,6-*i*-$Pr_2C_6H_3$) affords $[V(NAr)(S_2CNR_2)_3]$ (R = *i*-Pr; $R_2 = C_4H_4$) (**62**) (Fig. 63) (427). A crystallographic study ($R_2 = C_4H_4$) reveals a distorted pentagonal bipyramidal coordination geometry, the imido group occupying an axial site. The trans-influence of the latter is apparent from the lengthening of the unique axial vanadium–sulfur bond [2.564(3) Å] as compared to those in equatorial positions [2.494(3)–2.504(3) Å]. Maatta and co-workers (693) have also prepared a series of imido–dithiocarbamate complexes, $[V(NAr)Cl_{3-x}(S_2CNR_2)_x]$ (Ar = *p*-tolyl; R = Me, Et; $x = 1$–3), from $[V(NAr)Cl_3]$, together with imido-bridged $[(R_2NCS_2)_3V{=}N\text{-}p\text{-}C_6H_4N{=}V(S_2CNR_2)_3]$ (**63**) (Fig. 63), prepared in an analogous way.

Further reduction of $[V(NAr)Cl(S_2CNR_2)_2]$ with zinc affords $[V(NAr)(S_2CNR_2)_2]$ (Eq. 52). A large number of ^{51}V NMR spectra have been measured and

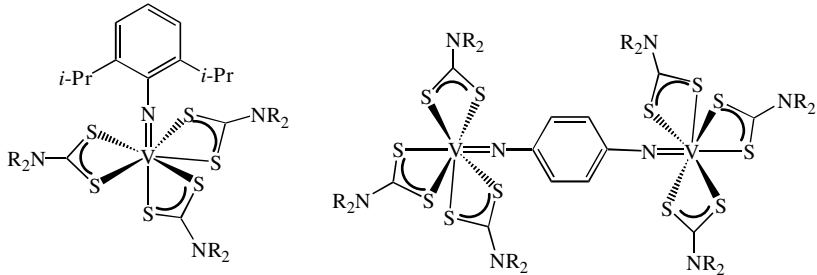

62 **63**

Figure 63. Examples of vanadium(V) tris(dithiocarbamate) imido complexes.

it is found that $\delta^{51}V$ correlates with λ_{max} from the visible region of the electronic spectrum (693).

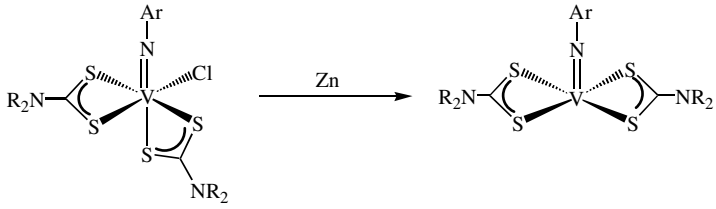

(52)

c. Bi- and Polynuclear Complexes. Dimeric vanadium(IV) complexes, $[V_2(\mu\text{-}S_2)_2(S_2CNR_2)_4]$, readily form from the reaction of $[VS_4]^{3-}$ and thiuram disulfides (171, 172, 694, 695). Two examples (R = Et, Bu) have also been prepared from the nucleophilic substitution of the alkyl trithiocarbonate ligands in $[V_2(\mu\text{-}S_2)_2(S_2CSMe)_4]$ upon reaction with the corresponding secondary amines (227). Recently, a further synthetic procedure has also been developed from commercially available starting materials; involving the slow acidification of an aqueous solution of $[VO_4]^{3-}$ and NaS_2CNR_2. The resulting precipitate, presumed to be $[VO(S_2CNR_2)_3]$, is then reacted with hydrogen sulfide in air and in this manner a number of complexes (R = Et, Bu; $R_2 = C_4H_8$) have been prepared in good yields (696).

Depending on the crystallization conditions, solvated or unsolvated structures result and the configurations at vanadium varies (Fig. 64). In all structures, vanadium–vanadium and sulfur–sulfur distances are $\sim$ 2.9 and 2.0 Å, respectively, and the structural unit has been compared to that of the mineral patronite (VS_4), which consists of linear chains of vanadium(IV) ions bridged by S_2^{2-} ligands (172). Molecules generally possess a center of inversion and thus are the meso diastereoisomers (172, 696), the exception is $[V_2(\mu\text{-}S_2)_2(S_2CN\text{—}i\text{-}Bu_2)_4]$, which adopts the rac form, possibly in order to ease the steric crowding caused by the bulky isopropyl substituents (695).

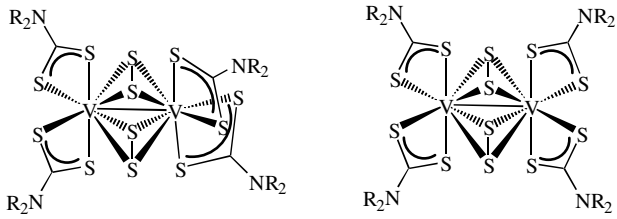

Figure 64. Optical isomers of $[V_2(\mu\text{-}S)_2(S_2CNR_2)_4]$.

A wide range of sulfido-capped tri- and tetranuclear clusters have been prepared and crystallographically characterized, mainly by Liu and co-workers (697–699). The general synthetic strategy adopted is to react $[NH_4]_3[VS_4]$ with a reducing agent and a dithiocarbamate salt in acetonitrile. A number of monoanionic trinuclear clusters, $[V_3(\mu^3\text{-}S)(\mu\text{-}S_2)_3(S_2CNR_2)_3]^-$ (**64**), have been prepared in this fashion (697–699); mononuclear tris(dithiocarbamate) complexes, $[V(S_2CNR_2)_3]$, often being coproducts (385). The cluster core has approximate C_{3v} symmetry, with one sulfur atom capping all three vanadium atoms. The S_2^{2-} units bridge vanadium–vanadium vectors, one sulfur lying in the V_3 plane and the second below it. This arrangement is similar to that found in related molybdenum and tungsten clusters discussed later (see Sections IV.C.2.c and IV.C.3.i).

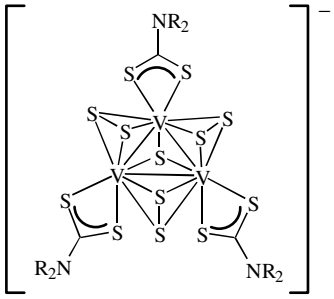

64

Although the trinuclear core formally contains vanadium(III) and vanadium (IV) ions, all are equivalent suggesting that the unpaired electron(s) are delocalized. The paramagnetic trimetallic center also has an unusual effect on the chemical shifts of α-protons of the dithiocarbamate ligands in the ^{1}H NMR spectrum, which can be shifted downfield as far as δ 10.7 ppm. The clusters are redox active and undergo reversible one-electron reduction and oxidation processes (697).

The cubane cluster, $[V_4(\mu^3\text{-}S)_4(S_2CNC_4H_8)_4(\mu\text{-}S_2CNC_4H_8)_2]^-$ (**65**), has been prepared from $[VS_4]^{3-}$ utilizing PPh_3 as the reductant (268). Again, there is electronic delocalization over the V_4S_4 core, with two reversible one-electron redox couples are seen by cyclic voltammetry. Variable-temperature magnetic susceptibility studies also reveal the presence of intermolecular antiferromagnetic exchange interactions even at room temperature, while when dissolved in DMSO, one of the terminal dithiocarbamate ligands is exchanged reversibly yielding $[V_4(\mu^3\text{-}S)_4(S_2CNC_4H_8)_3(dmso)_2(\mu\text{-}S_2CNC_4H_8)_2]$.

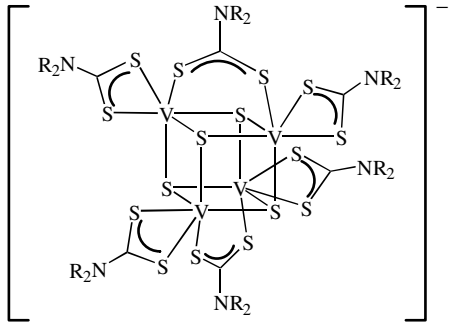

65

Carrying out the reduction of $[VS_4]^{3-}$ in the presence of a second metal salt leads to the generation of a wide-range heterocubane clusters (269, 700–706) many of which have been characterized crystallographically. These include $[V_2M_2(\mu^3\text{-}S)_4(S_2CNR_2)_2(SPh)_2]^{2-}$ (M = Cu, Ag) (**66**) (Fig. 65) (700, 704–706), $[VFe_3(\mu^3\text{-}S)_4(S_2CNR_2)_4]^-$ (**67**) (Fig. 65) (701, 702), $[V_2Fe_2(\mu^3\text{-}S)_4(S_2CNR_2)_2\text{-}(\mu\text{-}S_2CNR_2)]^-$ (269), and $[V_2Ag_2(\mu^3\text{-}S)_4(S_2CNR_2)_2(PPh_3)]^-$ (703). Crystallographic, Mössbauer, and electrochemical data suggest that all display a high degree of electronic delocalization within the cubane core. For example, in $[VFe_3(\mu^3\text{-}S)_4(S_2CNR_2)_4]^-$ (701, 702), metal sites are crystallographically indistinguishable, and all three iron sites are equivalent by Mössbauer spectroscopy. Clusters are redox active, for example, $[VFe_3(\mu^3\text{-}S)_4(S_2CNR_2)_4]^-$ shows two reversible one-electron reduction processes together with a reversible one-electron oxidation (701).

An incomplete cubane cluster, $[V_2Ag(\mu^3\text{-}S)(\mu\text{-}S)_3(S_2CNMe_2)_2(PPh_3)]^-$ (**68**) (Fig. 66), has also been synthesized in low yield using $[Ag(PPh_3)_2Cl]$ as both the silver source and reductant (703). Both vanadium ions possess identical coordination environments and all metal–metal distances are shorter than found

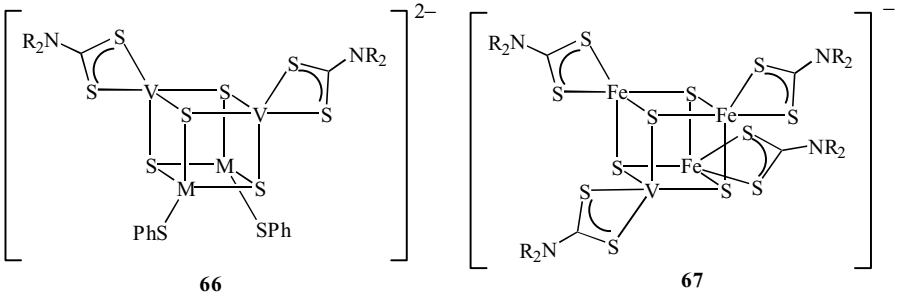

66 **67**

Figure 65. Examples of heterocubane clusters containing vanadium dithiocarbamate groups.

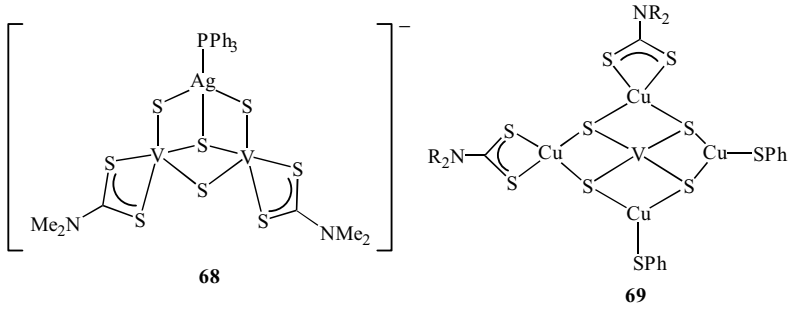

Figure 66. Further examples of vanadium-containing dithiocarbamate clusters.

in related cubane clusters. Open pentanuclear clusters $[VCu_4(\mu\text{-}S)_4(S_2CNR_2)_n(SPh)_{4-n}]^{3-}$ ($n = 0$–2) (**69**) (Fig. 66) have also been isolated along with heterometallic cubanes from the reaction of $[NH_4]_3[VS_4]$, CuCl, NaS_2CNR_2, and NaSPh in dimethylsulfoxide (DMF) (706). They contain a tetrahedral VS_4 core and almost planar VCu_4 array, each copper ion supporting either a dithiocarbamate or thiolate ligand. Spectroscopic and magnetic data suggest that the vanadium is in the +5 oxidation state, being surrounded by four copper(I) centers, while ^{51}V NMR spectroscopy has been utilized in order to probe cluster assembly.

Garner and co-workers (707) reported the synthesis of trinuclear $[V_3O(\mu\text{-}O)_2(\mu\text{-}S)_2(S_2CNEt_2)_3]^-$ (**70**) (Fig. 67) from VCl_3, Li_2S, Et_4NBr, and $NaS_2CNEt_2.3H_2O$ in acetonitrile. Lui and co-workers (703) also prepared this as a side product of the reaction of $[NH_4]_3[VS_4]$, $[Ag(PPh_3)_2Cl]$, Et_4NCl, and $NaS_2CNEt_2.3H_2O$. Both groups have crystallographically characterized the complex. An ESR study (707) suggests that the paramagnetism is associated with the vanadyl ion, the other two vanadium (IV) ions are spin coupled by the vanadium–vanadium interaction over 2.715(3) Å. Cyclic voltammetry in DMF shows a series of redox processes that have been interpreted to result from a dissociation of the trimer into $[V_2O_2(\mu\text{-}S)_2(S_2CNEt_2)_2]^{2-}$ (**71**) (Fig. 67) and $[VO(S_2CNEt_2)(dmf)_2]^+$ fragments (703).

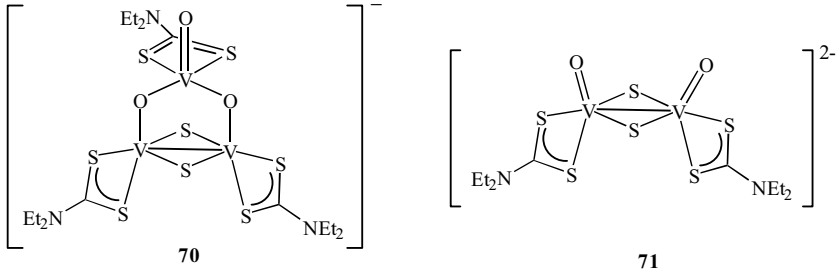

Figure 67. Sulfido-bridged vanadium oxo complexes.

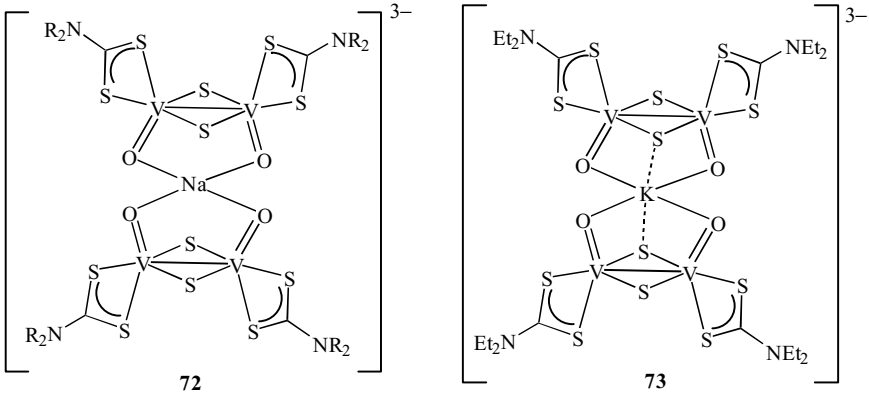

Figure 68. Examples of clusters containing $V_2O_2(\mu\text{-}S)_2(S_2CNR_2)_2$ units linked by alkali metal ions.

In support of this hypothesis, Liu and co-workers (703) prepared and crystallographically characterized $[NEt_4]_3[Na\{V_2O_2(\mu\text{-}S)_2(S_2CNEt_2)_2\}_2]$, which contains two *cis*-$[V_2O_2(\mu\text{-}S)_2(S_2CNEt_2)_2]^{2-}$ anions linked through all four oxygens to the sodium cation, and shows some common redox properties with $[V_3O(\mu\text{-}O)_2(\mu\text{-}S)_2(S_2CNEt_2)_3]^-$.

The $V_2O_2(\mu\text{-}S_2)(S_2CNR_2)_2$ unit seen above is quite common. Reaction of $M(S_2CNR_2)$ (M = Na, K), $[NH_4]_3[VS_4]$, PPh_3, and Et_4NCl in acetonitrile leads to three complexes of this type, which have been crystallographically characterized, namely, $[NEt_4]_3[K\{V_2O_2(\mu\text{-}S)_2(S_2CNEt_2)_2\}_2]$, $[NEt_4]_2[NH_4][Na\{V_2O_2(\mu\text{-}S)_2(S_2CNC_5H_{10})_2\}_2]$ (**72**) (Fig. 68), and $[NEt_4]_3[Na_3(H_2O)\{V_2O_2(\mu\text{-}S)_2(S_2CNMe_2)_2\}_3]$ (**73**) (Fig. 68) (670). In the latter, each of the three sodium ions links to two vanadyl oxygen atoms of different $V_2O_2(\mu\text{-}S_2)$ units and are further held together via a central water molecule.

d. Other Complexes. Other reports include the reaction of vanadyl sulfate and ammonium molybdate in the presence of dithiocarbamate salts, which is proposed to afford heterobimetallic complexes, $[MoVO_4(S_2CNR_2)_2]$. The dithiocarbamates probably act in a bridging capacity, although precise structural details remain unknown (708). Addition of barium salts of dithiocarbamates derived from amino acids to $[VO(acac)_2]$ and other acetylacetenoate salts is believed to yield complexes of the type, $[\{M(acac)\}_2(\mu\text{-}S_2CNR_2)]$ (M = V, Fe, Co, Ni, Cu), whereby the dithiocarbamate is bound to one metal ion through the two sulfurs, and to the second through the carboxylic acid functionality (709).

e. Applications. Vanadium dithiocarbamate complexes have found a range of applications, some being quite unusual. Vanadocene complexes, $[Cp_2V(S_2CNR_2)][X]$ (**74**), are effective spermicidal agents (676,710–713), with the BF_4 (676) and SO_3CF_3 (712) salts being the most potent in the inhibition of

human sperm motility. By using ESR spectroscopy, $[Cp_2V(S_2CNEt_2)][BF_4]$ has been shown to retain its structural integrity at physiologic pH, while cyclic voltammetry reveals a quasi-reversible one-electron reduction process (676).

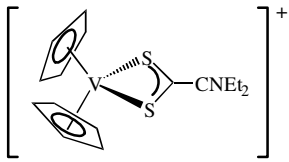

74

A range of vanadyl complexes, $[VO(S_2CNR_2)_2]$, have been investigated as insulin mimics as they inhibit the release of fatty acid from rat apidocytes, similar to the action of insulin (678, 680). Sakurai and co-workers (678) found that complexes derived from piperidine and sarcosine proved the most effective, while the piperidine complex also promoted the incorporation of glucose in rat L6 muscle cells and may be a good agent to treat insulin-dependent diabetes in experimental animals. In very recent work, Conconi et al. (680) found that $[VO(S_2CNC_4H_8)_2]$ exerted insulin secretagogue action within concentration levels of 0.1–1.0 m*M*, enhancing both basal and glucose-stimulated insulin release, and as such it may be considered a potential elective pharmaceutical tool in the therapy of diabetes.

The vanadium(V) oxo complex, $[VO(S_2CNMe_2)_3]$ (714), has been shown to sensitize the polymerization of styrene when irradiated at λ 365 nm (715). A spectroscopic analysis shows that initiation occurs primarily through loss of a dithiocarbamate radical via an intramolecular photoredox reaction, with $[VO(S_2CNMe_2)_2]$ being the final photoproduct. The rate of polymerization is proportional to the square root of $[VO(S_2CNMe_2)_3]$ concentration.

The yellow vanadium(III) complex, $[V(S_2CNEt_2)_3]$, has been utilized as a spectrophotometric reagent for the determination of vanadium concentrations; vanadium(V) being first reduced with dithionite, and after addition of NaS_2CNEt_2, the absorption maxima of $[V(S_2CNEt_2)_3]$ at 350 nm is measured (716).

2. *Niobium and Tantalum*

The development of niobium and tantalum dithiocarbamate chemistry is relatively recent, the first well authenticated examples coming from the insertion of carbon disulfide into metal amide complexes to give $[M(S_2CNR_2)_4]$ (193, 666). Dithiocarbamates are now known to stabilize niobium and tantalum in the +3 to +5 oxidation states.

a. Simple Dithiocarbamate Complexes. Simple niobium(V) complexes include $[NbCl_3(S_2CNEt_2)_2]$ (**75**) (Fig. 69), which has been characterized crystallographically (717, 718). It contains a pentagonal bipyramidal coordination

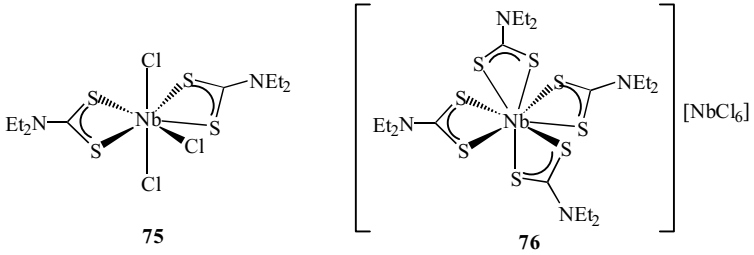

Figure 69. Examples of niobium(V) dithiocarbamate complexes.

geometry, with two chlorides occupying the axial sites. It can be prepared upon addition of tetraethylthiuram disulfide to $[Nb_2Cl_6(SMe_2)_3]$ (718) or from the reaction of $NbCl_5$ with $Me_3SiS_2CNEt_2$ (717). Interestingly, from the latter, a coordination isomer, $[Nb(S_2CNEt_2)_4][NbCl_6]$ (**76**) (Fig. 69), also results, the two being easily distinguished by ^{93}Nb NMR spectroscopy. Somewhat similarly, attempts to crystallize $[NbCl_2(S_2CNEt_2)_3]$ gave $[Nb(S_2CNEt_2)_4]_2[NbCl_5S]$, which contains two independent cations each with a dodecahedral (D_{2d}) coordination environment (428).

A range of other cationic niobium and tantalum tetrakis(dithiocarbamate) complexes, $[M(S_2CNR^1R^2)_4]X$ (M = Nb, Ta; $R^1 = R^2 =$ Me, *i*-Bu; $R^1 =$ Me, $R^2 =$ *i*-Pr, Ph, Cy, Bz), have been prepared from the metal pentachlorides and anhydrous dithiocarbamate salts (719). They are fluxional on the NMR time scale, a polytopal mechanism being proposed via a cubic or square antiprismatic transition state. The kinetics of this process has been studied by total line shape analysis, giving $\Delta G^{\#}$ values of 42–50 kJ mol^{-1}.

Tantalum halide complexes have not been so widely studied as their niobium analogues. Richards and co-workers (615) reported the synthesis of $[TaBr_3(S_2CNEt_2)_2]$ upon addition of NaS_2CNEt_2 to Ta_2Br_{10}. They suggest that it is a seven-coordinate complex, and may have a structure similar to $[NbCl_3(S_2CNEt_2)_2]$ (discussed above). However, there is some suggestion that in solution partial dissociation of a bromide occurs, in a similar fashion to that previously proposed for the analogous chloride, $[TaCl_3(S_2CNEt_2)_2]$ (720). The tris(dithiocarbamate) tantalum bromide complex, $[TaBr_2(S_2CNEt_2)_3]$, is molecular as shown by a crystallographic study. It adopts a dodecahedral geometry, the bromides occupying sites trans to one another (429).

In other work, a new high-yield synthesis of the known alkoxide complexes, $[NbCl(OR)_2(S_2CNR_2)_2]$, has been reported from $[NbCl_3(OR)_2]$ and 4 equiv of dithiocarbamate salt in THF. All are soluble in polar solvents, but insoluble in alkanes (721).

b. Oxo and Sulfido Complexes. Oxo complexes of niobium and tantalum supported by dithiocarbamate ligands are rare and unknown, respectively. Holm and co-workers (722) prepared $[NbO(S_2CNEt_2)_3]$ from $[Nb_6O_{19}]^{8-}$ and

NaS_2CNEt_2 at pH $\sim$ 5. Addition of $(Me_3Si)_2S$ (722) or boron sulfide (430) affords the analogous sulfido complex, $[NbS(S_2CNEt_2)_3]$ (Eq. 53), while with boron sulfide, small amounts of $[Nb(\eta^2\text{-}S_2)(S_2CNEt_2)_3]$ and $[Nb_2(\mu\text{-}S_2)_2(S_2CNEt_2)_4]$ also result (430).

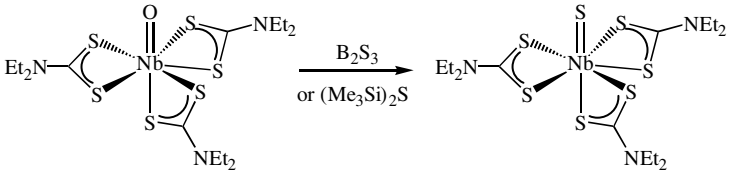

(53)

A numbers of other publications focus on complexes supporting sulfido ligands. Products from the addition of 5 equiv of NaS_2CNEt_2 to niobium pentahalides are halide dependent. The sulfido complex, $[NbS(S_2CNEt_2)_3]$, results from the chloride, while in contrast $[Nb(S_2CNEt_2)_4]Br$ is formed in high yield when the bromide is used (403). Both structures have been elucidated crystallographically. The coordination sphere in $[NbS(S_2CNEt_2)_3]$ is a distorted pentagonal bipyramid, the sulfido ligand occupying an axial site (402, 428). Interestingly, there are two molecules in the asymmetric unit that differ as a result of the ethyl group orientations and this is manifested in the somewhat different niobium–sulfido bond lengths of 2.164(3) and 2.112(3) Å (403). Addition of 5 equiv of NaS_2CNEt_2 to $TaCl_5$ yields both yellow $[TaS(S_2CNEt_2)_3]$ (**77**) and green $[TaS_2(S_2CNEt_2)_3]$ (**78**) (Fig. 70), as does the reaction of $TaBr_3S$ with 3 equiv of dithiocarbamate salt in carbon disulfide (403, 431, 723). Both have also been characterized crystallographically and show distorted pentagonal bipyramidal (723) and dodecahedral (403, 432) coordination geometries, respectively.

Niobium complexes with sulfido and disulfur ligands behave quite differently toward the activated alkyne, dimethylacetylene dicarboxylate ($R = CO_2Me$) (724). Thus, while $[NbS(S_2CNEt_2)_3]$ is unreactive, even under forcing conditions, a clean reaction occurs with $[NbS_2(S_2CNEt_2)_3]$ giving $[Nb\{\eta^2\text{-}SC(R)=C(R)S\}(S_2CNEt_2)_3]$ (Eq. 54). The latter, which results from alkyne addition across the disulfur unit, has been characterized crystallographically and shows a

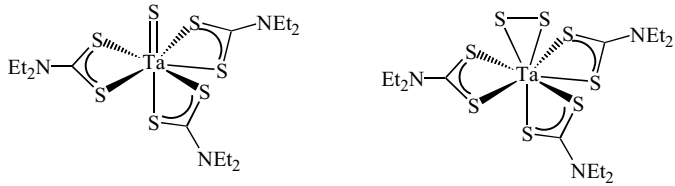

77 **78**

Figure 70. Tantalum(V) tris(dithiocarbamate) sulfido and disulfido complexes.

distorted dodecahedral coordination geometry.

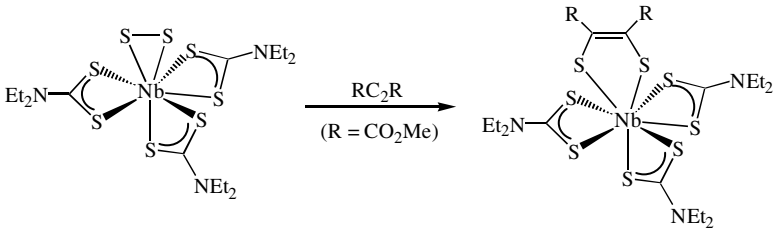

(54)

c. Complexes with Nitrogen Donor Ligands. A wide range of niobium and tantalum imido complexes, $[M(NR')(S_2CNR_2)_3]$ (M = Nb, Ta; R′ = Me, Pr, *i*-Pr, *t*-Bu, Ph, *p*-tol, *p*-C_6H_4OMe), have been prepared from the reaction of metal pentahalides with $Me_3SiS_2CNR_2$ (R = Me, Et) in the presence of an excess of the relevant primary amine (210). Crystallographic characterization of $[Nb(N\text{-}p\text{-tolyl})(S_2CNEt_2)_3]$ confirms that the π-donor ligand occupies an axial site, while carrying out the same synthetic procedure in the presence of 1,1-disubstituted hydrazines yields related hydrazido(2−) complexes $[M(NNR_2)(S_2CNR_2)_3]$ (Eq. 30) (210).

In a series of contributions, Henderson and co-workers (429, 725–728) focused on the chemistry of niobium and tantalum dithiocarbamate complexes with a variety of dinitrogen-containing ligands. Complexes containing dinitrogen itself, $[\{M(S_2CNEt_2)_3\}_2(\mu\text{-}N_2)]$ (M = Nb, Ta), are formed from $[\{MCl_3(thf)_2\}_2(\mu\text{-}N_2)]$ and $Me_3SiS_2CNEt_2$ (429). They are the first dinitrogen complexes in which the coligands are exclusively sulfurous. A crystallographic study (M = Nb) shows that each nitrogen occupies an axial site, the nitrogen–nitrogen distance of 1.25(2) Å suggesting some double-bond character. Addition of excess anhydrous acids (HX) results in the stoichiometric release of hydrazine with formation of $[MX_2(S_2CNEt_2)_3]$ (Eq. 55).

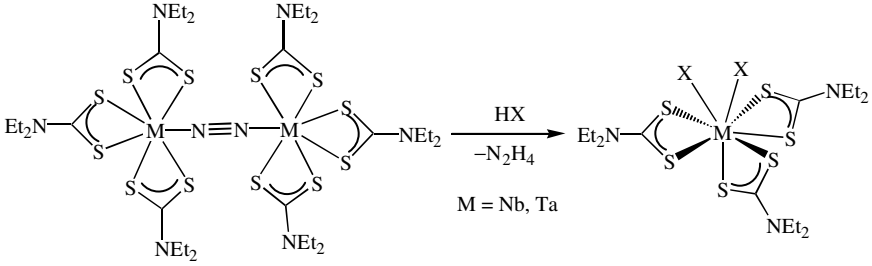

(55)

The kinetics of this reaction have been determined and a multistep reaction scheme proposed (727), in which the rate-limiting step is the protonation of the bridging nitrogen atoms (Fig. 71). In the case of tantalum, the monoprotonated

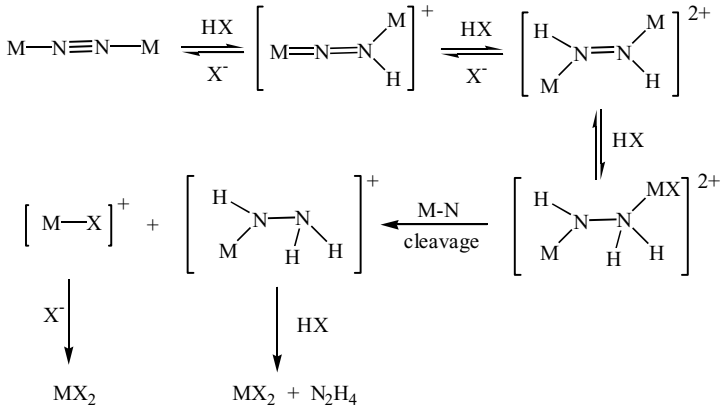

Figure 71. A proposed mechanistic pathway for the generation of hydrazine upon protonation of tantalum dinitrogen complexes.

species, $[\{Ta(S_2CNEt_2)_3\}_2(\mu\text{-}N_2H)]^+$, was detected spectrophotometrically and cleavage of the nitrogen–nitrogen bond occurs only after addition of at least two protons. Addition of HBr in MeCN to $[\{Ta(S_2CNEt_2)_3\}_2(\mu\text{-}N_2)]$ resulted in the rapid formation of $[(Et_2NCS_2)_3Ta(\mu\text{-}NHNH_2)TaBr(S_2CNEt_2)_3]^{2+}$ from which tantalum–nitrogen cleavage was rate limiting, leading to the formation of $[TaBr(S_2CNEt_2)_3]^+$ and $[Ta(S_2CNEt_2)_3(NHNH_2)]^+$. The latter reacts further with HBr to give hydrazine and $[TaBr_2(S_2CNEt_2)_3]$ (728).

In related studies designed to gain further insight into the role of hydrazido ligands in the process, hydrazido(2−) $[Nb(NNMeR)(S_2CNEt_2)_3]$ (R = Me, Ph) (**79**) (Fig. 72) (726), hydrazido(1−) $[TaCl_3(MeNNMe_2)(S_2CNEt_2)]$ (**80**) (Fig. 72), and $[Ta(MeNNMe_2)(S_2CNEt_2)_3]Br$ (**81**) (Fig. 72) (725) complexes have been prepared and investigated. Addition of excess anhydrous HBr to

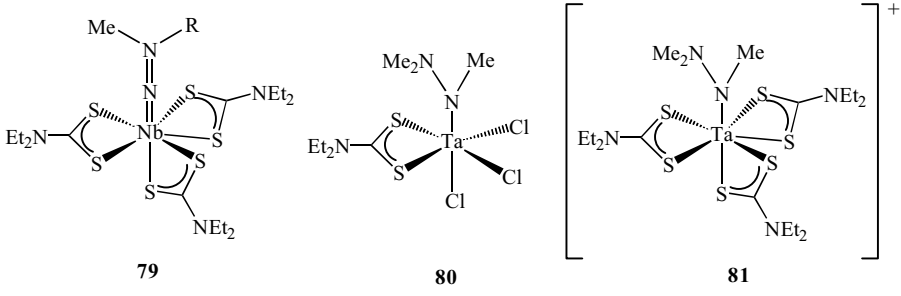

Figure 72. Examples of niobium and tantalum hydrazido complexes.

$[Ta(MeNNMe_2)(S_2CNEt_2)_3]Br$ yields an equivalent of substituted hydrazine salt together with $[TaBr_2(S_2CNEt_2)_3]$ (725), while under the same conditions $[Nb(NNMeR)(S_2CNEt_2)_3]$ behaves analogously generating $[NbBr_2(S_2CNEt_2)_3]$ (726). The latter reaction has been studied in some depth and occurs in two stages; a rapid initial double protonation to yield $[Nb(NHNHMeR)(S_2C\text{-}NEt_2)_3]^{2+}$, which then slowly decomposes to the observed products.

d. Other Complexes. Dimeric niobium(IV) complexes, $[Nb_2(\mu\text{-}S_2)_2(S_2CNR_2)_4]$, analogous to those discussed earlier for vanadium, have been prepared (729–731) and bridging ligand substitution reactions studied (732). For example, addition of $NaS_2CNEt_2.3H_2O$ to $[Et_4N]_4[Nb_2(\mu\text{-}S_2)_2(NCS)_8]$ gives $[Nb_2(\mu\text{-}S_2)_2(S_2CNEt_2)_4]$ in 73% yield (Eq. 56) (731). An initial X-ray diffraction study appeared to show an unusually long sulfur–sulfur interaction of 2.282 Å (729), but subsequent refinement assuming a disordered S_2^{2-} ligand with respect to a mirror plane corrected this anomaly [S-S 2.027 Å] (730).

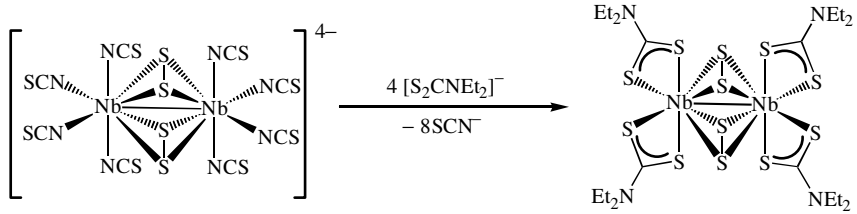

(56)

Reactions of $[Nb_2(\mu\text{-}S_2)_2(S_2CNEt_2)_4]$ with chalcogen transfer reagents, $Et_3P{=}Y$ (Y = Se, Te), have been studied (732). With $Et_3P{=}Se$, $[Nb_2(\mu\text{-}Se_2)_2(S_2CNEt_2)_4]$ (**82**) (Fig. 73) results when a catalytic amount of free PEt_3 is present. This complex has also been crystallographically characterized [Se—Se 2.303(2) Å] and undergoes a reversible one-electron oxidation to yield

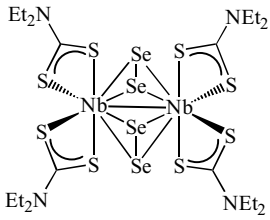

82

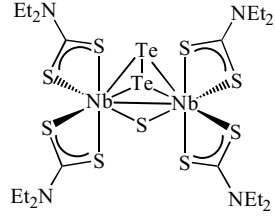

83

Figure 73. Dimeric niobium(V) complexes with bridging dichalcogenide units.

a blue ESR active cation. In contrast, the phosphine telluride reacts to give $[Nb_2(\mu\text{-}S)(\mu\text{-}Te_2)(S_2CNEt_2)_4]$ [Te-Te 2.648(3) Å] (**83**) (Fig. 73) (732), while a mixed sulfur–selenium complex, analytically characterized as $[Nb_2(\mu\text{-}S_{1.72}Se_{2.28})(S_2CNEt_2)_4]$, results from addition of dithiocarbamate salt to $NbSe_2Cl_2$ and KNCS in a fusion cake (730).

Addition of $[Cp_2Fe][PF_6]$ to $[Nb_2(\mu\text{-}S_2)_2(S_2CNEt_2)_4]$ results in an immediate color change from light-brown to deep violet, which is supposed to result from a one-electron oxidation giving $[Nb_2(\mu\text{-}S_2)_2(S_2CNEt_2)_4]^+$ (731). The resulting solution has been characterized by ESR spectroscopy that shows a 19 line pattern arising from the interaction of the lone electron with the two equivalent niobium nuclei $(I = \frac{9}{2})$. Upon cooling the spectrum changes, but this is associated with the slowing down of molecular motion and not the localization of the electron on a single niobium atom.

A few further publications focus on niobium and tantalum dithiocarbamate complexes in the +4 oxidation state. Insertion of carbon disulfide into all three amides of $[(\eta^5\text{-}C_2B_9H_{11})M(NMe_2)_3]$ (M = Nb, Ta) yields $[(\eta^5\text{-}C_2B_9H_{11})M(S_2CNMe_2)_3]$ (**84**) (733) and Richards and co-workers (615) studied the reactions of the unusual organometallic complexes, $[MX_4(CN\text{—}t\text{-}Bu)\{\mu\text{-}C(X)N\text{-}t\text{-}Bu\}]_2$ (M = Nb, Ta; X = Cl, Br), with NaS_2CNEt_2. The tantalum complexes react to give dimeric products, $[TaX_3(S_2CNEt_2)\{\mu\text{-}C(X)N\text{—}t\text{-}Bu\}]_2$, whereby a halide and an isocyanide have been displaced from each metal center. In contrast, monomeric niobium complexes, $[NbX_2(S_2CNEt_2)_2\{C(X)N\text{—}t\text{-}Bu\}]$ result, the structures of which are unknown.

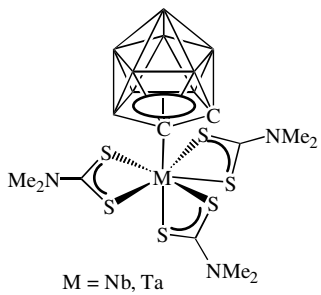

84

Addition of thiuram disulfides to the niobium(IV) dimethyl complex $[Cp_2NbMe_2]$ results in cleavage of the sulfur–sulfur bond and addition to the metal center (734). The nature of the final product is dependent on the alkyl substituents. With tetraethylthiuram disulfide, the molecular niobium(V) dithiocarbamate complex $[Cp_2NbMe_2(\eta^1\text{-}S_2CNEt_2)_2]$ results, which is believed to contain a monodentate dithiocarbamate ligand. In contrast, tetramethylthiuram disulfide affords a 1:1 electrolyte, believed to be $[Cp_2NbMe(S_2CN\text{-}$

Me_2)][S_2CNMe_2], the metal-bound dithiocarbamate binding in a chelating fashion.

The +3 oxidation state has also been explored. Addition of 3 equiv of dithiocarbamate salt to [$NbCl_3$(dme)(RC_2R')] yields alkyne complexes, [$Nb(S_2CNR_2)_3(R'C_2R'')$] (735) (R = Me, Et). One (R = Me; R′ = Me, R″ = Ph) Ph) (**85**) has been characterized crystallographically, the symmetrically bound alkyne occupying an axial site. Their dynamic behavior has also been followed by NMR spectroscopy; all three dithiocarbamates are equivalent at higher temperatures, and even at 188 K, alkyne rotation is not frozen out.

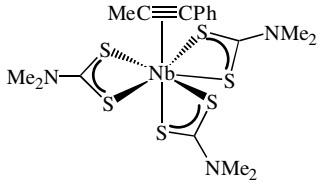

85

e. Applications. Virtually no applications of niobium or tantalum dithiocarbamate complexes have been reported. Sokolov et al. (736) measured the vapor pressure of some sulfur-rich niobium(IV) dimers, [$Nb_2(\mu\text{-}S_2)_2(S_2CNR_2)_4$], using the Knudsen method, finding that they are quite volatile. In this respect, they have carried out differential thermal analysis and thermal gravimetric studies in attempting to utilize them toward the preparation of niobium-containing thin films.

C. Group 6 (VI B): Chromium, Molybdenum, and Tungsten

1. Chromium

Chromium(III) tris(dithiocarbamate) complexes, [$Cr(S_2CNR_2)_3$], were first prepared by Delépine (2). Now a large number of chromium(III) complexes are known, while other oxidation states are also accessible, including zero, +2 and +4.

a. Chromium(III) Tris(dithiocarbamate) Complexes. Simple chromium tris(dithiocarbamate) complexes, [$Cr(S_2CNR_2)_3$], continue to attract attention. A range of violet or blue-violet benzyl complexes, [$Cr(S_2CNBzR)_3$] (R = H, Me, Et, *i*-Pr), have been prepared (737), as have light green [$Cr(S_2CNC_4H_8S)_3$] and pale blue [$Cr(S_2CNC_4H_8NR)_3$] (R = H, Me, Ph) (738, 739). All are paramagnetic (μ_{eff} 3.82–4.12 BM) and have been characterized by ESR spectroscopy, *g*

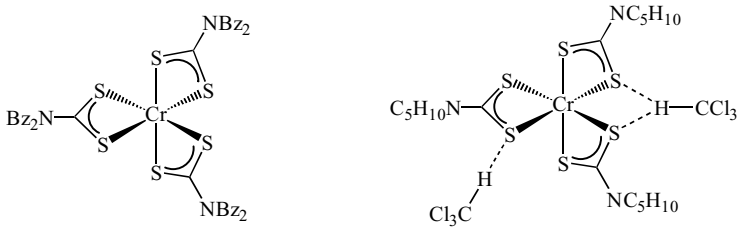

Figure 74. Crystallographically characterized chromium tris(dithiocarbamate) complexes.

values ranging from 1.991–1.999, while nephelauxetic parameters are indicative of appreciable metal–ligand covalency (739). Electronic and ESR spectra of the poorly soluble, $[Cr\{S_2CN(CH_2CH_2OH)_2\}_3]$, also show that the chromium–sulfur bonds have strong covalent character (740), while the dithiocarbamate ligands in $[Cr(S_2CNEt_2)_3]$ have been shown to be kinetically labile, exchanging readily with $CrCl_3$ (520).

Two examples, $[Cr(S_2CNR_2)_3]$ ($R = Bz$; $R_2 = C_5H_{10}$) (Fig. 74), have been characterized crystallographically and display the expected octahedral coordination geometry (741, 742). The latter also contains two molecules of chloroform, which are hydrogen bonded via the proton to sulfurs through a $p\pi$ orbital.

The redox chemistry of tris(dithiocarbamate) complexes has been studied in some detail, although reports are somewhat contradictory. Complexes $[Cr(S_2CNR_2)_3]$ ($R = Et$; $R_2 = C_4H_8$, C_5H_{10}) show a two-step process reduction process; the first one-electron reduction resulting in liberation of a dithiocarbamate ligand, while a second two-electron process leads to chromium(0) and complete decomposition of the coordination sphere. Oxidation is also possible, but is followed by an intramolecular redox process, the metal reverting back to the +3 state, while the ligand is oxidized to the thiuram disulfide (743). Vella and Zubieta (744) also studied a range of complexes ($R = Me$, Et, Pr, *i*-Pr, Ph; $R_2 = EtPh$). Again they observe an irreversible one-electron reduction, which results in loss of a dithiocarbamate ligand. However, they also report that all exhibit a reversible one-electron oxidation, although attempts to isolate the oxidized salts $[Cr(S_2CNEt_2)_3][X]$ ($X = BF_4$, PF_6) were unsuccessful. Further, from a comparison of electrochemical data for a series of chromium(III) dithioacid derivatives, they deduced that the ease of oxidation at this center follows the order;

$$S_2CNR_2^- > S_2COR^- > S_2CSR^- > S_2CR^-$$

The sulfur atoms in tris(dithiocarbamate) complexes can bind to Lewis acidic metal centers. For example, varying amounts of copper(I) iodide can be added to $[Cr(S_2CNR_2)_3]$ in acetonitrile to yield complexes in which sulfur atoms bridge

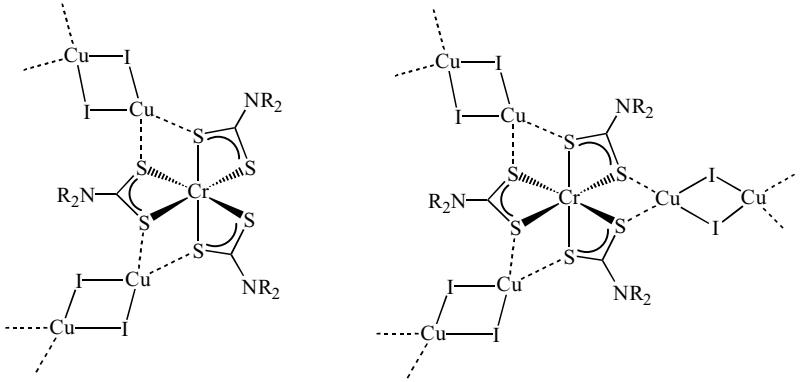

Figure 75. Schematic representations of polymers formed via the linking of chromium tris(dithiocarbamate) units by Cu_2I_2 moieties.

two copper ions. Two of these, namely, $[Cr(S_2CNEt_2)_3].2CuI.2MeCN$ and $[Cr(S_2CNC_4H_4)_3].3CuI.MeCN$ (Fig. 75), have been characterized crystallographically, and consist of polymeric chains in which $Cu_2(\mu\text{-}I)_2$ units link together chromium dithiocarbamate groups (312).

Tris(dithiocarbamate) complexes, $[Cr(S_2CNR_2)_3]$ ($R = Et$, Bz; $R_2 = C_4H_8O$), react with iodine in dichloromethane to form 1:1 complexes, as shown by spectrophotometric studies. The interaction results in charge transfer between the iodine and a sulfur atom (745).

Related to the tris(dithiocarbamate) species are the oxygen-expanded complexes, $[Cr(S_2CNR_2)_2\{OSC(NR_2)S\}]$, formed along with $[Cr(S_2CNR_2)_3]$ from the reaction of dichromate and dithiocarbamate salts (746), although a report that this reaction produces a dimeric oxo-bridged complex would appear to be erroneous (747). A new refinement of the structure of $[Cr(S_2CNEt_2)_2\{OSC(NEt_2)S\}]$ shows that the O,S-chelate is disordered over three sites (748). An extensive electrochemical comparison of $[Cr(S_2CNR_2)_3]$ and $[Cr(S_2CNR_2)_2\{OSC(NR_2)S\}]$ (Fig. 76) has been carried out in order to examine the influence

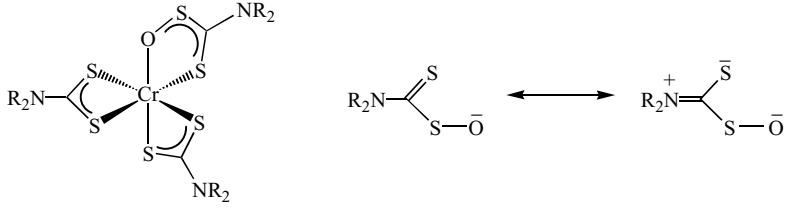

Figure 76. Oxygen-expanded chromium dithiocarbamate complexes together with representations of possible resonance hybrids for the expanded ligand.

of oxygen insertion (746). Oxygen-expanded complexes are more easily oxidized and the generated cations exhibit enhanced stability, believed to result from the increased importance of the resonance state, $R_2N^+{=}CS(SO)^{2-}$.

Larin et al. (749) reported that addition of NaS_2CNEt_2 to CrO_3 in concentrated HCl gives $[CrOCl_2(S_2CNEt_2)]$, while in 3% HCl or below, the same reaction yields $[CrOCl(S_2CNEt_2)_2]$. Both are postulated as chromium(V) complexes and on the basis of ESR data are proposed to adopt square-based pyramidal and octahedral coordination geometries, respectively. Little further data is given, and attempts to replace the final chloride with a dithiocarbamate were unsuccessful. If these are truly chromium(V) complexes they warrant further study, however, it cannot be ruled out that they contain oxygen-expanded dithiocarbamate ligands.

b. Other Chromium(III) Complexes. Mixed-ligand chromium(III) complexes, $[Cr(S_2CNR_2)X_2]$ and $[Cr(S_2CNR_2)_2X]$, containing acac (**86**), oxine or glycine ligands have been prepared. All are paramagnetic with magnetic moments of 3.5–4.2 BM (750). Paramagnetic nitrosyl complexes, $[Cr(S_2CNR_2)_3(NO)]$ ($R = Me$, Et; $R_2 = C_4H_4$) (**87**), have also been prepared (751, 752) and crystallographically characterized ($R = Et$) (752). The nitrosyl occupies an axial site and the trans chromium–sulfur bond is the shortest in the molecule [Cr—S(ax) 2.449(1) Å; Cr—S(eq) av. 2.459 Å]. This finding is in contrast to the situation found in the analogous molybdenum complex $[Mo(NO)(S_2CNBu_2)_3]$ (753), where the axial interaction is significantly longer than all others. Indeed, all chromium–sulfur bonds in $[Cr(S_2CNEt_2)_3(NO)]$ are longer than those found in $[Cr(S_2CNEt_2)_3]$ [av. Cr—S 2.396 Å] (386), leading the authors to speculate that this is a result of steric crowding in the seven-coordinate complex.

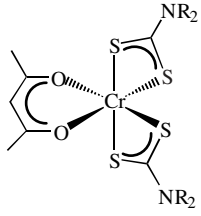

86

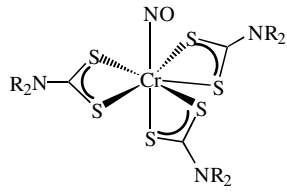

87

Chromium nitrosyl complexes, $[Cr(S_2CNR_2)_3(NO)]$, are somewhat less thermally stable than their molybdenum and tungsten counterparts; heating $[Cr(S_2CNMe_2)_3(NO)]$ in toluene for 3 h leads to the formation of *cis*-$[Cr(NO)_2(S_2CNMe_2)_2]$ and $[Cr(S_2CNMe_2)_3]$ (752). Somewhat contradictory reports surround the electrochemical behavior of $[Cr(S_2CNR_2)_3(NO)]$. Connelly and co-workers (752) report that they show no redox chemistry between ± 1.5 V,

while others suggest that reduction is possible, the presence of the nitrosyl group simply shifting the reduction process to a higher potential as compared to $[Cr(S_2CNR_2)_3]$ (751).

c. Chromium(II) and Organometallic Complexes. The yellow-green chromium(II) bis(dithiocarbamate) complex $[Cr(S_2CNEt_2)_2]$ was first reported in 1965 by Fackler and Holah (754). The precise structure remains unknown and little further work has been carried out in this area. Lancashire and Smith (755) report that when the thermolysis of $[Hg(S_2CNEt_2)_2]$ and $Cr(CO)_6$ is carried out in rigorously dried and degassed toluene, mercury is deposited and a green solution is generated that has an identical electronic spectrum to $[Cr(S_2CNEt_2)_2]$. Further, in keeping with the earlier report, exposure of this solution to oxygen results in rapid formation of dark blue, $[Cr(S_2CNEt_2)_3]$.

More recently, a series of well-defined cyclopentadienyl chromium(II) complexes, $[CpCr(CO)_n(S_2CNR_2)]$ ($n = 2, 3$) have been prepared (Eq. 57). In three papers, Goh et al. (240, 246, 247) describe the reaction of thiuram disulfides with $[CpCr(CO)_3]_2$. At room temperature, chromium(II) complexes, $[CpCr(CO)_2(S_2CNR_2)]$ (R = Me, Et, *i*-Pr), are formed in high yields, and if the reactions are monitored carefully the monodentate intermediates $[CpCr(CO)_3(\eta^1\text{-}S_2CNR_2)]$ can be detected. Crystallographic studies have been carried out on both dimethyldithiocarbamate complexes, the chromium–sulfur bond lengths decreasing slightly upon chelation [Cr—S 2.4406(5) and 2.4237(6) Å (av)] (240).

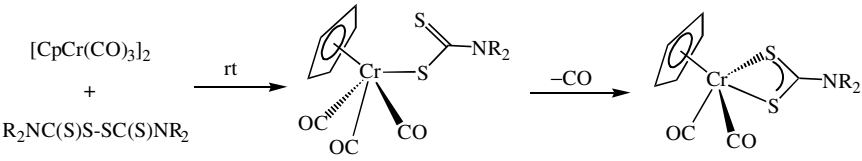

(57)

When the reactions are carried out at 90°C a number of other products are also isolated, namely, $[Cp_6Cr_8S_8\{\eta^2\text{:}\eta^4\text{-}S_2(CNR_2)_2\}]$, $[Cp_6Cr_8S_8(\eta^1\text{:}\eta^2\text{-}S_2CNR_2)_2]$, $[Cr(S_2CNR_2)_3]$, $[Cp_2Cr_2(CO)_4(\mu\text{-}S)]$, and $[CpCr(\mu^3\text{-}S)]_4$, and these are discussed more fully later (see Section V.B).

A series of chromium(II) nitrosyl complexes, $[Cr(NO)(S_2CNR_2)_2L]$ ($L = H_2O$, thiourea), have been prepared, the thiourea resulting from dithiocarbamate degradation (756). They are characterized by ESR spectroscopy, which suggests that the thiourea lies trans to the nitrosyl.

An early report detailed the IR characterization of the chromium(0) complex, $Na[Cr(CO)_4(S_2CNEt_2)]$, formed upon thermolysis of $Cr(CO)_6$ and NaS_2CNEt_2 in DMSO at 60–65°C (757). Although this complex was not isolated, an

analogue, $[Cr(CO)_4(S_2CNC_5H_{10})][NEt_4]$, has been prepared from cis-$[Cr(CO)_4(NHC_5H_{10})_2]$ and carbon disulfide in the presence of *n*-butyl lithium (Eq. 58); the latter initiating the reaction by proton abstraction (198). A crystallographic study showed the expected distorted octahedral coordination environment (758). Interestingly, this complex is inaccessible from the direct reaction of $Cr(CO)_6$ and the piperidine dithiocarbamate salt.

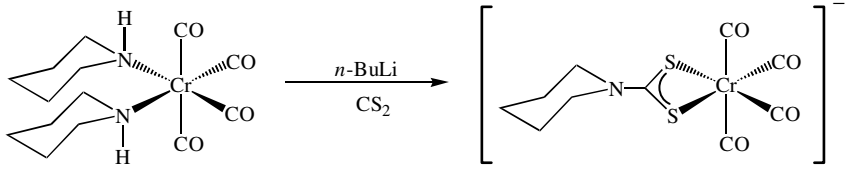

(58)

d. Applications. Dithiocarbamates find extensive use in the analytical determination of chromium ion concentrations. For example, using a dithiocarbamate salt as complexing agent affords a rapid, sensitive, and selective method for the differential determination of chromium(III) and chromium(VI) in natural waters (759, 760). Since chromium(VI) reacts to give $[Cr(S_2CNR_2)_3]$, but chromium(III) is substitutionally inert, the amount of the former can be measured, for example, after preconcentration by electrothermal atomic absorption spectroscopy, the chromium(III) concentration being determined by difference after oxidation of all chromium by potassium peroxydisulfate.

Fluorinated dithiocarbamates have been used as part of a supercritical fluid extraction (761), while pyrrolidene (762, 763), and benzyl (741, 764) dithiocarbamates and poly(dithiocarbamate) chelating resin (765) have also been utilized, as has detection by XRF (764) and inductively coupled plasma atomic emission spectroscopy (765). Related to this, the determination of chromium levels in urine has been achieved using lithium bis(trifluoroethyl)dithiocarbamate as the complexing agent with detection via an isotopic dilution GC and mass spectral method (766).

2. *Molybdenum*

The chemistry of molybdenum dithiocarbamate complexes has come a long way since the early work of Malatesta (767), and between 1978 and 2003 there were over 300 publications in this area, accessible oxidation states ranging from 0 to +6.

a. Tetrakis(dithiocarbamate) Complexes. Molybdenum tetrakis(dithiocarbamate) complexes have been synthesized in the +4 and +5 oxidation states

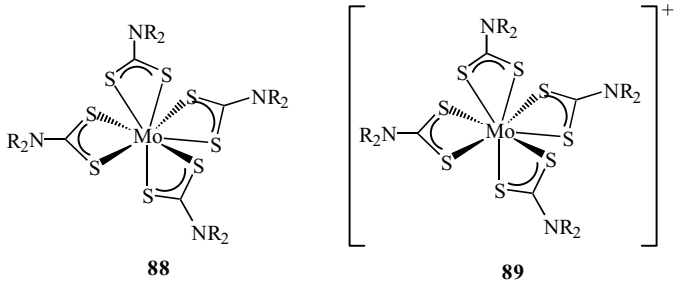

Figure 77. Molybdenum tetrakis(dithiocarbamate) complexes.

(Fig. 77), the latter being most common. Molybdenum(IV) complexes (**88**) were first prepared from the insertion of carbon disulfide into the corresponding metal amides (768), and later from the addition of dithiocarbamate salts to $MoCl_4$ in acetonitrile (769). More recently, addition of the pyrrole dithiocarbamate to $MoCl_5$ in aqueous solution has been shown to afford $[Mo(S_2CNC_4H_4)_4]$; a crystallographic study revealing the D_{2d} symmetry in the solid state, the sulfur atoms lying on the vertices of a dodecahedron (354).

Cationic molybdenum(V) complexes (**89**) (Fig. 77) have been prepared in a number of ways (441, 770–778). Most result from simple metathesis reactions, with $[Mo(S_2CNR_2)_4]Cl$ being commonly used (773), and in this way lanthanide salts $[Mo(S_2CNR_2)_4][Er(S_2CNR_2)_4]$ (779) and $[Mo(S_2CNR_2)_4][Sm(S_2CNR_2)_4]$ (774,780) have been prepared. Redox reactions have also been utilized, metal oxidation being most common. For example, addition of TCNQ (TCNQ = 7,7,8,8-tetracyano-*p*-quinodimethane) or TCNE (TCNE = tetracyanoethylene) to molybdenum(IV) complexes, $[Mo(S_2CNR_2)_4]$ (R = Me, Et), leads to metal-centered oxidation (as shown by ESR spectroscopy) giving $[Mo(S_2CNR_2)_4][X]$ (X = TCNE, TCNQ) (772), while oxidation of the molybdenum(III) dimer, $[Mo_2(S_2CNEt_2)_6]$, by oxygen in chloroform affords a mixture of $[Mo(S_2CNR_2)_4]Cl$ and $[Mo(S_2CNR_2)_4]_2[Mo_6O_{19}]$ (778,781,782). More unusually, irradiation of the low-valent carbonyl complex, $[Mo(CO)_5I][NH_4]$, with excess dithiocarbamate salt affords $[Mo(S_2CNC_4H_8)_4]I_3$, the metal being oxidized from the zero oxidation state (770). In contrast, $[Mo(S_2CNR_2)_4]BF_4$ have been prepared by metal-centered reduction, upon addition of boron sulfide to the molybdenum(VI) oxo complexes, $[MoO(S_2CNR_2)_3]BF_4$ (775).

A considerable number of molybdenum(V) complexes, $[Mo(S_2CNR_2)_4]X$, have been characterised crystallographically, anions including; $FeCl_4^-$ (783–785), $MoCl_4^-$ > (773), $MoCl_6^-$ (786), $[MoCl_4(OMe)_2]^-$ (441), Cl^- (776,781,782), I_3^- (770,787), $Mo_6O_{19}^{2-}$ (438,776,778,788), $[Ln(S_2CNR_2)_4]^-$ (Ln = Er, Sm) (771,774,780), and $TCNQ^-$ (772,779). In all, the cations adopt a distorted dodecahedral structure with approximate D_{2d} symmetry. A number are formed

as clathrates (779,783,784), and in $[Mo(S_2CNEt_2)_4][TCNQ].MeCN$, the TCNQ radical anions are dimerized and exhibit an usual slipped conformation (779). Further addition of TCNQ results in formation of $[Mo(S_2CNEt_2)_4][TCNQ]_2$ which, however, still contains a molybdenum(V) radical cation (772).

b. Molybdenum(VI) Dioxo Complexes. Molybdenum(VI) dioxo complexes $[MoO_2(S_2CNR_2)_2]$ have been known since the 1930s (767) and prior to 1978 a large number of examples had been prepared (789,790). Their synthesis is simple, and generally involves the addition of 2 equiv of dithiocarbamate salt to Na_2MoO_4 under acidic conditions (Eq. 59). The product readily precipitates, generally as a yellow solid. Indeed, Young has described a preparation of $[MoO_2(S_2CNEt_2)_2]$ together with a series of its subsequent reactions which form the basis of an excellent undergraduate laboratory experiment (791).

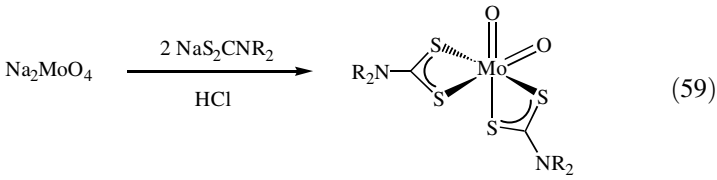

(59)

Over the period of this chapter, a number of further examples have been reported including $[MoO_2(S_2CNR_2)_2]$ ($R = Cy$, Ph, CH_2CH_2OH, CH_2CF_3) (84, 792), $[MoO_2(S_2CNR_2)_2]$ ($R_2 = C_4H_8O$, C_5H_{10}, C_5H_9Me, $C_6H_6Me_4$) (84, 792, 793), $[MoO_2(S_2CNBzR)_2]$ ($R = Bz$, Me, Et, *i*-Pr) (794), $[MoO_2(S_2CNMePh)_2]$ (795), $[MoO_2(S_2CNHR)_2]$ ($R = Ar$, C_5H_9, Cy, C_7H_{13}, *l*-neomenthyl) (677, 792, 795), and a range of α-amino acid (glycine, alanine, α-amino-butyric acid, valine, norleucine, leucine, isoleucine) derivatives (126). The dialkyl complexes show high stability, however, those derived from primary amines or with aryl substituents are markedly less stable. Here, loss of an oxygen atom and concomitant formation of the molybdenum(V) dimers, $[Mo_2O_2(\mu\text{-}O)(S_2CNR_2)_4]$, is often facile. This behavior is exemplified by yellow $[MoO_2(S_2CNPhMe)_2]$, which turns purple upon standing with generation of $[Mo_2O_2(\mu\text{-}O)(S_2CNPhMe_2)_4]$ (795).

The structure of $[MoO_2(S_2CNEt_2)_2]$ has been redetermined (796) the data being substantially different to that found in an earlier investigation (797). The molecule has a distorted octahedral geometry, the oxo groups lying cis to one another [O—Mo—O 105.61(12)°]. The short molybdenum–oxygen distance [Mo=O 1.703(2) Å] leads to a significant trans influence as highlighted by the differing molybdenum–sulfur distances [Mo-S 2.450(1) and 2.639(1) Å] those trans to the oxo moieties being elongated. The X-ray structure of $[MoO_2(S_2CNC_4H_8S)_2]$ has also been determined (798) and an EXAFS study

has been carried out on the proline derivative, for which IR spectroscopy shows that the carboxylic acid group is in the acidic form and not coordinated to the molybdenum cations (125).

Quite recently, Unoura et al. (799) reported the synthesis and structure of $[MoO_2\{\mu\text{-}S_2CN(Bz)CH_2CH_2N(Bz)CS_2\}]_2$ (**90**) in which the molybdenum centers are bridged by the bidentate dithiocarbamate ligands.

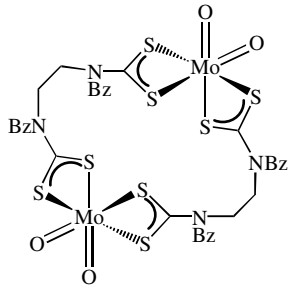

90

The same group have also carried out detailed electrochemical studies (798, 799) utilizing semiinfinite cyclic voltammetry, thin-layer voltammetry, and coulometry at low temperature. Most derivatives undergo a quasi-reversible one-electron reduction to give free dithiocarbamate salt and oxo bridged, $[Mo_2O_2(\mu\text{-}O)(S_2CNR_2)_4]^+$, the equilibrium constant for the formation of the latter decreasing with increasing electron-donor ability of the dithiocarbamate (800). Interestingly, the potential for this process correlates well with the second-order rate constants for their oxo-transfer reactions to PPh_3 (see below) (798,800).

Dioxo complexes, $[MoO_2(S_2CNR_2)_2]$, exhibit a wide range of reactivity. Peterson and Richman (801) showed that irradiation at 380 nm into the lowest energy charge-transfer band of $[MoO_2(S_2CNEt_2)_2]$ affords $[MoO_2(S_2CNEt_2)]$, identified by its solvent independent ESR spectrum, and a dithiocarbamate radical with a quantum yield of 0.0207. In the dark, a subsequent radical chain reaction occurs leading ultimately to molybdenum oxide and tetraethylthiuram disulfide, and a mechanism for this process has been proposed (Fig. 78).

Dioxo complexes have been widely studied as oxo-transfer agents to phosphines (Eq. 60) (795, 798, 800, 802–804). Electrochemical and oxo-transfer properties to PPh_3 have been systematically investigated, a good correlation being found between the log of the second-order rate constant of oxo transfer and the reduction potential (798, 800). A departure from linearity is seen for a number of phenyl and benzyl derivatives, which is postulated to result from increased steric effects hindering the approach of PPh_3; a negative $\Delta S^{\#}$ of -114 J mol^{-1} K^{-1} for $[MoO_2(S_2CNEt_2)_2]$ confirming that the reaction is

$$MoO_2(S_2CNEt_2)_2 \underset{}{\overset{h\nu}{\rightleftharpoons}} MoO_2(S_2CNEt_2)_2^*$$

$$MoO_2(S_2CNEt_2)_2^* \longrightarrow MoO_2(S_2CNEt_2) + S_2CNEt_2^{\bullet}$$

$$S_2CNEt_2^{\bullet} + MoO_2(S_2CNEt_2)_2 \longrightarrow MoO_2(S_2CNEt_2) + (Et_2NCS_2)_2$$

$$S_2CNEt_2^{\bullet} + MoO_2(S_2CNEt_2) \longrightarrow MoO_2(S_2CNEt_2)_2$$

$$S_2CNEt_2^{\bullet} + MoO_2(S_2CNEt_2) \longrightarrow MoO_2 + (Et_2NCS_2)_2$$

$$S_2CNEt_2^{\bullet} + S_2CNEt_2^{\bullet} \longrightarrow (Et_2NCS_2)_2$$

Figure 78. Proposed mechanism for the photochemically induced decomposition of $[MoO_2(S_2CNEt_2)_2]$.

associative in nature. Unoura et al. (798,802) also systematically analyzed IR, ^{13}C, and ^{95}Mo NMR parameters as a function of their oxo-transfer ability. For the latter, chemical shifts range from δ 151 (R = Me) to 216 (R = *i*-Pr) and show a good correlation with the rate constant for oxo transfer to PPh_3 in 1,2-dichloroethane (802). Further work on the oxo transfer of $[MoO_2(S_2CNEt_2)_2]$ to PPh_3 in nonaqueous solvents has shown that the rate constants and activation energies follow linear relationships as a function of the refractive index, supporting a one-step mechanism in which the lone pair on phosphorus enters directly into the π^*-anti-bonding Mo=O orbital, which results in bond cleavage (803).

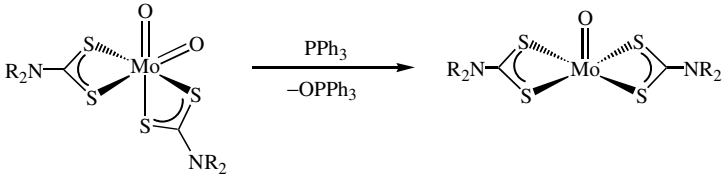

(60)

In contrast to the facile oxo transfer to phosphines, related transfer to Ph_3As and Ph_3Sb is poor, with only small amounts of the relevant group 15 (V A) oxides being generated. On the basis of a comparative study of the ease of stoichiometric oxo transfer from $[MoO_2(S_2CNEt_2)_2]$ to Ph_3E and Et_3N, the following relative reactivity series has been deduced (804);

$$Ph_3P \gg Et_3N \cong Ph_3As > Ph_3Sb > Ph_3Bi > Ph_3N$$

Reaction of $[MoO_2(S_2CNEt_2)_2]$ with Me_3SiX (X = Cl, Br, I) and Me_3SiNCS yields $[MoOX_2(S_2CNEt_2)_2]$ and $[MoO(NCS)_2(S_2CNEt_2)_2]$, respectively

(805,806), while in contrast the silicon–carbon bond in Me_3SiCN adds to give $[MoO(CN)(OSiMe_3)(S_2CNEt_2)_2]$ (Eq. 61) (807). Like $[MoO_2(S_2CNEt_2)_2]$, the latter also acts as an oxo-transfer agent to PPh_3, but at a much lower rate than the analogous cis dioxo complex.

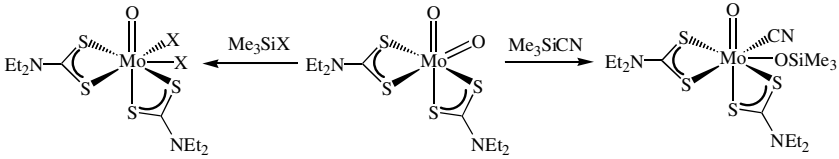

X = Cl, Br, I, NCS

(61)

In an interesting communication, Nicholas and co-workers (808) reported that $[MoO_2(S_2CNR_2)_2]$ catalyze the allylic amination of alkenes by phenylhydroxylamine, the reaction proceeding with high regioselectivity resulting from double-bond migration (Eq. 62). A nitrosobenzene complex has been detected in the reaction, suggesting that it may proceed via an ene reaction between PhN=O and the alkene.

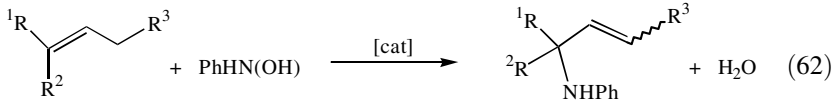

[cat] = $[MoO_2(S_2CNR_2)_2]$ (62)

A wide variety of other reactions of $[MoO_2(S_2CNR_2)_2]$ have been reported and these are detailed throughout the following sections.

c. Other Monomeric Oxo Complexes. A number of publications deal with other monomeric molybdenum oxide complexes. Molybdenum(VI) bis(oxo) complexes, $[MoO_2Cl(S_2CNR_2)L]$ ($R = Et$, *i*-Pr; $R_2 = C_4H_8$, C_5H_{10}; $L = dmso$, Ph_3PO) (**91**) (Fig. 79), have been prepared from $[MoO_2Cl_2L_2]$ and dithiocarbamate salts in dichloromethane, and also via a ligand redistribution reaction upon mixing $[MoO_2(S_2CNEt_2)_2]$ and $[MoO_2Cl_2(Ph_3PO)_2]$ (809).

Molybdenum(VI) mono(oxo) complexes, $[MoO(S_2CNR_2)_3]X$ **92** (Fig. 79), were first synthesized from the decomposition of $[MoO_2(S_2CNR_2)_2]$ and $[MoOF_2(S_2CNR_2)_2]$ (435) and more recently, a large number have been prepared. For example, charge-transfer salts, $[MoO(S_2CNR_2)_3][TCNQ]$ ($R = Me$, Et, Pr), result from the reaction of TCNQ with $[Mo_2O_3(S_2CNR_2)_4]$, LiTCNQ, and $[MoO(S_2CNEt_2)_3][BF_4]$, and addition of TCNQ to $[MoO(S_2CNEt_2)_2]$ in the

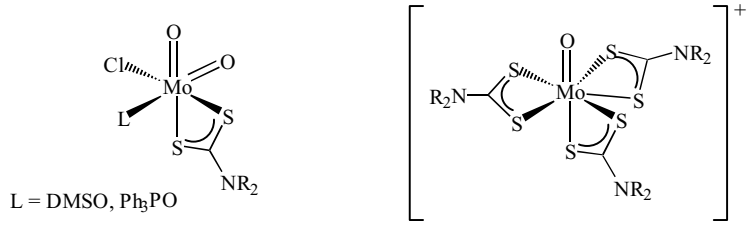

91 **92**

Figure 79. Further examples of molybdenum(VI) oxo complexes.

presence of tetraethylthiuram disulfide (436). An X-ray crystal structure of $[MoO(S_2CNEt_2)_3][TCNQ].THF$ shows a seven-coordinate molybdenum center with the usual trans influence of the oxo group [Mo—S_{ax} 2.626(1); Mo—S_{eq} 2.466(1)–2.503(1) Å], together with an unusual, almost perfectly eclipsed, $TCNTCNQ_2^{2-}$ dimer (436). Other orange diamagnetic tris(dithiocarbamate) complexes, $[MoO(S_2CNR_2)_3][X]$ (R = Me, Et, *i*-Pr; X = BF_4, PF_6, ClO_4), have been prepared from reactions of $[MoO_2(S_2CNR_2)_2]$ with HX in acetone. They have been analyzed in detail by ^1H and ^{13}C NMR spectroscopy and some examples have been shown to catalytically convert PPh_3 to its oxide in air (810).

Related to the latter, abstraction of an oxo ligand from $[MoO(S_2CNR_2)_3]$-$[BF_4]$ (R = Me, Et) by PPh_3 yields the dimeric mixed oxidation state [Mo(IV)/Mo(V)] complexes, $[Mo_2(S_2CNR_2)_6(\mu\text{-}O)]^+$ (Eq. 63). The equivalence of the molybdenum–oxygen bonds [Mo—O 1.848(2) Å] leads to their classification as class IIIa compounds on the Robin and Day scheme (436,811,812). Cyclic voltammetry shows that they undergo a reversible one-electron reduction, however, oxidation results in irreversible cleavage of the oxo bridge.

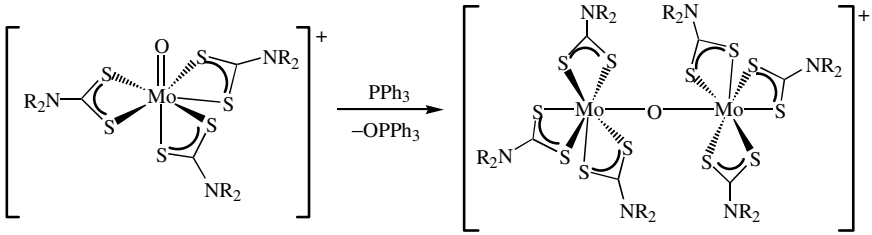

(63)

Reduction of molybdenum(VI) complexes, $[MoOX_2(S_2CNR_2)_2]$ (X = Cl, Br; R = Me, Et; $R_2 = C_5H_{10}$), by phosphines is dependent on both the phosphine and solvent (Eq. 64). With $PhPMe_2$ in THF, neutral molybdenum(IV)

complexes, $[MoX_2(S_2CNR_2)_2(PMe_2Ph)]$ result, while in methanol a range of phosphines yield ionic, $[MoX(S_2CNR_2)_2L_2]Y$ ($L = PMe_2Ph$, $PMePh_2$, PEt_2Ph; $L_2 =$ dppe; $Y = BF_4$, PF_6). The latter have been shown crystallographically to adopt a distorted pentagonal bipyramidal geometry with either trans phosphines ($R = Et$, $L = PMe_2Ph$, $X = Cl$, $Y = PF_6$) or with a halide trans to phosphorus ($R = Et$, $L_2 =$ dppe, $X = Cl$, $Y = BF_4$) (813).

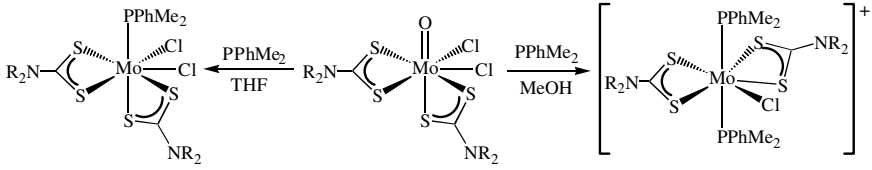

(64)

The molybdenum(VI) oxo complex $[MoOCl_2(S_2CNEt_2)_2]$ reacts with 6, 7-dimethyl-5,6,7,8-tetrahydropterin (H_4dmp) to give $[MoOCl_2(S_2CNEt_2)(H_3dmp)]Cl$ (**93**). A crystallographic study reveals a reduced pterin ligand coordinated through the carbonyl oxygen and pyrazine nitrogen. Most interestingly, in DMSO, a net five-electron oxidation of the complex occurs, 0.5 equiv of thiuram disulfide and 1 equiv of dimethylpterin (814).

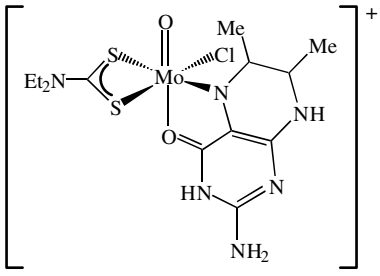

93

Molybdenum(V) oxo complexes are also common. Addition of NaS_2CNEt_2 to MoO_3 in concentrated HCl affords $[MoOCl(S_2CNEt_2)_2]$, while when the acid concentration is reduced, $[MoO(S_2CNEt_2)_3]$ is the major product (Eq. 65) (749). The same tris(dithiocarbamate) complex also results from the thermal reaction of $Mo(CO)_6$ with $[Hg(S_2CNEt_2)_2]$ (755). Other paramagnetic molybdenum(V) complexes, $[MoO(NCS)(S_2CNR_2)_2]$ ($R = Et$, Bz; $R_2 = C_5H_{10}$, C_4H_8O), have been prepared in good yields from MoO_3 after reduction and addition of

ammonium thiocyanate. All are red with magnetic moments of 1.6–1.7 BM and the expected six line pattern in the ESR spectrum (815).

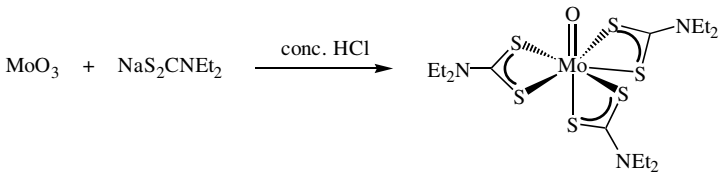

(65)

Molybdenum(IV) complexes, $[MoO(S_2CNR_2)_2]$, are formed upon oxo abstraction from $[MoO_2(S_2CNR_2)_2]$, and a number of reactions have been have been carried out on these coordinately unsaturated species. The (formally) molybdenum(IV) alkyne complexes, $[MoO(S_2CNR_2)_2(RC_2R)]$, result upon addition of alkynes (816–819), the alkyne lying perpendicular to the molybdenum-oxo group (Eq. 66). Wentworth and co-workers (817) showed that ethyne addition is reversible, while in contrast ethylene does not bind. Addition of other alkynes such as diphenylethyne, affords more stable complexes (818), while cylooctyne complexes, $[MoO(C_8H_{12})(S_2CNR_2)_2]$ (R = Me, Et), show no propensity to lose the alkyne at all (819). In related work, addition of an industrial mixture of C_4 hydrocarbons to $[MoO(S_2CNEt_2)_2]$ has been carried out, and it is only the alkyne components, HC_2R (R = Et, $CH{=}CH_2$) that react, and even then when the solvent is removed the alkynes are lost (820).

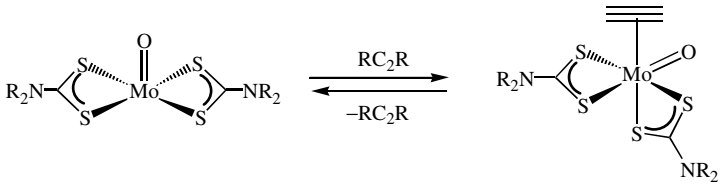

(66)

The NMR studies revealed that these complexes are fluxional and also that there is a significant alkyne to metal π donation. On the basis of the latter and IR data, it was concluded that they are best considered as molybdenum(VI) complexes, the alkyne competing for π donation with the oxo group (816, 819). Templeton et al. (821) carried out a molecular orbital study on the model complex, $[MoO(HC_2H)(S_2CNH_2)_2]$. This study confirms that the lowest energy form is that in which the alkyne lies perpendicular to the oxo moiety, which is some 81 kJ mol^{-1} lower in energy than the parallel configuration, and accounts for the relatively high barrier to alkyne rotation in complexes of this type (Fig. 80).

Interaction of alkylammonium azides with $[MoO(S_2CNEt_2)_2]$ partitioned between water and chloroform leads to the slow formation of nitrogen,

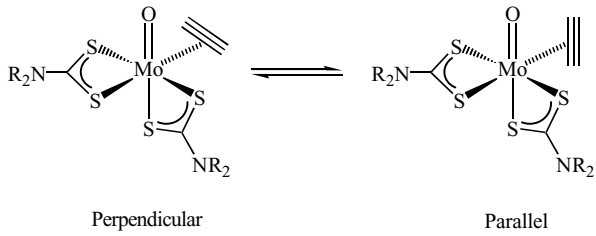

Figure 80. Possible orientations of the alkyne in $[MoO(alkyne)(S_2CNR_2)_2]$—that perpendicular to the molybdenum–oxo bond being favored.

ammonia, and $[MoO_2(S_2CNEt_2)_2]$; a significant rate enhancement being observed if the aqueous layer is acidified (822). Schwartz et al. (823) also reported that diazoalkanes add to $[MoO(S_2CNR_2)_2]$ (R = Me, Et) to afford metalloazines, $[MoO(NN{=}CCR_2')(S_2CNR_2)_2]$, which in turn react with amines and ylides in a Wittig-type reaction to afford imines and alkenes, respectively (Eq. 67).

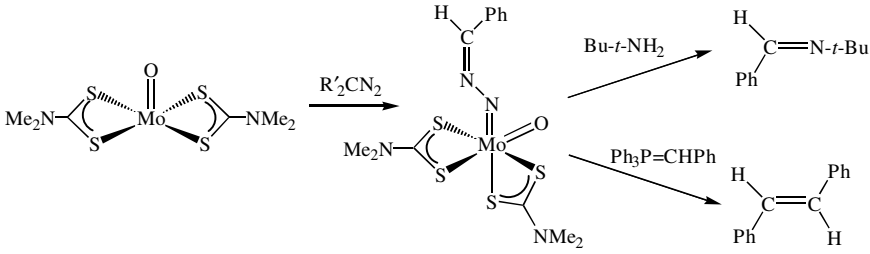

(67)

In a series of papers, oxo-bridged heterobimetallic complexes containing the $MoO(S_2CNR_2)_2$ unit have been prepared and studied by IR spectroscopy and other physical techniques (824–828). Structural studies have not, however, been possible and precise structural characteristics remain largely unknown. For example, reaction of iron(III)molybdate and sodium dithiocarbamates in 7*M* HCl affords purple complexes, $[FeMoO_2(S_2CNR_2)_4(H_2O)]$, which lose water upon heating. Magnetic moments of 2.88–2.95 BM have been interpreted as resulting from low-spin iron(III) and molybdenum(V) ions being linked via an oxo bridge (828).

d. Mononuclear Imido Complexes. Around 30 papers concern the chemistry of monomeric imido (NR) complexes. They include molybdenum(VI) complexes, $[MoO(NR)(S_2CNR_2)_2]$ (829–835), $[Mo(NR)_2(S_2CNR_2)_2]$ (538, 831, 832, 836, 837), $[Mo(NR)(S_2)(S_2CNR_2)_2]$ (527, 528, 838, 839), $[MoX_2(NR)$-

$(S_2CNR_2)_2]$ (832, 833, 839–843), and $[Mo(NR)(S_2CNR_2)_3]^+$ (437, 439, 810, 832); as well as molybdenum(IV) complexes, $[Mo(alkyne)(NR)(S_2CNR_2)_2]$ (830, 833), and $[Mo(NR)(S_2CNR_2)_2]$ (831, 833).

Bis(imido) complexes, $[Mo(NR)_2(S_2CNR_2)_2]$, were first prepared by Maatta and co-workers (837) upon oxidation of $[Mo(CO)_2(S_2CNEt_2)_2]$ with aryl azides. In this manner, the phenyl and *p*-tolyl derivatives were prepared, the former being shown crystallographically to contain one linear [Mo—N—C 169.4(4)°] and one bent [Mo—N—C 139.4(4)°] imido ligand. Subsequently, Harlem and Holm (831) prepared the tosylimido derivative in a similar manner, while Hogarth and co-workers (538,836) showed that bulky aryl derivatives could be prepared from the thermal reaction between $[MoO_2(S_2CNR_2)_2]$ (R = Me, Et) and organic isocyanates; similar products also being obtained from $[MoO_2(S_2CNMe_2)_2]$ and ortho-substituted N-sulfinylanilines (Ar = 2,4,6-$X_3C_6H_2$; X = Cl, Br, Me) (844). These latter approaches are somewhat limited to complexes with tertiary butyl or bulky aryl substituents, a more general synthetic method involving the room temperature addition of dithiocarbamate salts to $[MoCl_2(NR)_2(dme)]$ (538) (Fig. 81).

Crystallographic studies on a number of bis(imido) complexes (538, 831, 836) reveal that the two imido ligands are close to linearity (Mo—N—C > 160°). Indeed it has proved possible to correlate the difference in bond angles at

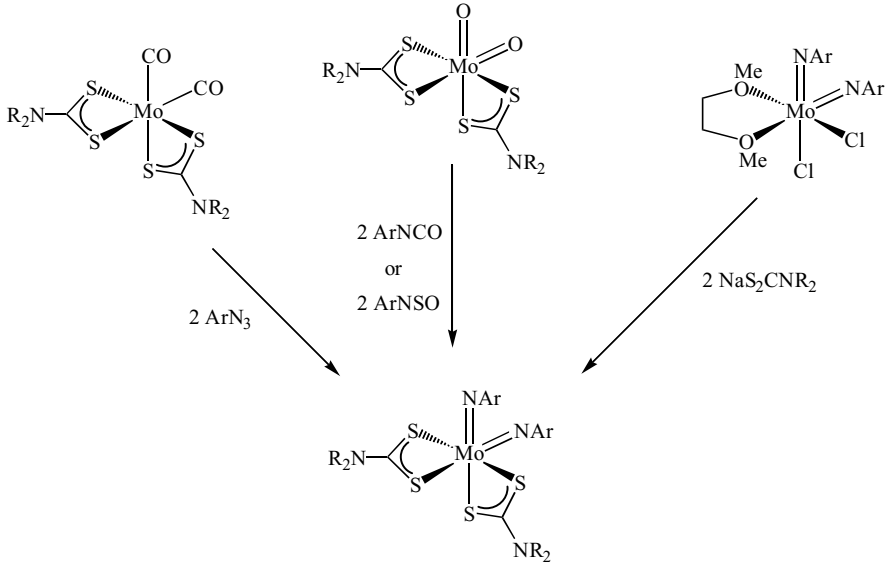

Figure 81. Synthetic routes to $[Mo(NAr)_2(S_2CNR_2)_2]$.

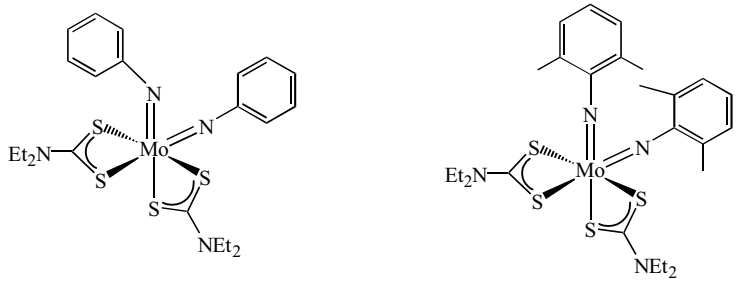

Figure 82. Examples of bent and linear forms of $[Mo(NAr)_2(S_2CNEt_2)_2]$ complexes.

nitrogen (Δ°) to the difference in chemical shift of the ipso imido carbon atoms ($\Delta\delta$) in the solid-state ^{13}C CPMAS spectra (538). In solution, however, both imido ligands in $[Mo(NPh)_2(S_2CNEt_2)_2]$ are equivalent even at low temperatures, suggesting a rapid interchange between bent and linear coordination modes (Fig. 82) (538, 832).

Reactions of bis(imido) complexes include the acid-induced hydrolysis of $[Mo(NAr)_2(S_2CNEt_2)_2]$ (Ar = 2,6-*i*-$Pr_2C_6H_3$), which results in imido loss and formation of an unusual molybdate-bridged complex, $[Mo(S_2CNEt_2)_2(NAr)(\mu\text{-}MoO_4)]_2$ (**94**), which has been crystallographically characterized (845). Similar molybdate-bridged complexes are also accessible from the slow hydrolysis of bis(imido) complexes, $[Mo(NPh)_2(S_2CNR_2)_2]$ (R = Me, Et), although their insolubility hampers full characterization (439).

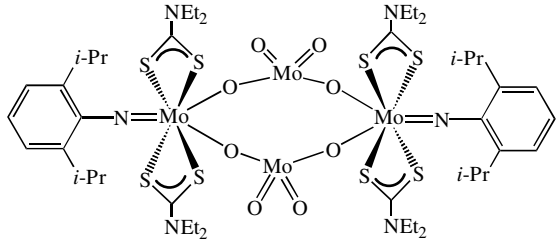

94

Oxo–imido complexes, $[MoO(NAr)(S_2CNR_2)_2]$, were first prepared upon addition of aryl azides to $[MoO(S_2CNEt_2)_2]$ (832), which has since been shown to react with a range of a range of *N*-tosyl (Ts) reagents, TsNX (X = py, PhMeS, Ph_3Sb, PhI, N_2), to give crystallographically characterized $[MoO(NTs)(S_2CNEt_2)_2]$ (831). More recently, a number of mesityl–imido complexes, $[MoO(NMes)(S_2CNR_2)_2]$ (R = *i*-Pr; $R_2 = C_4H_4$, C_5H_{10}), have been prepared

upon addition of dithiocarbamate salts to $[MoO(NMes)Cl_2(dme)]$ (Eq. 68) (829), while the low-yield preparations of $[MoO(NAr)(S_2CNMe_2)_2]$ (Ar = 2,6-*i*-$Pr_2C_6H_3$, 2,4,6-$Me_3C_6H_2$) have also been reported (844).

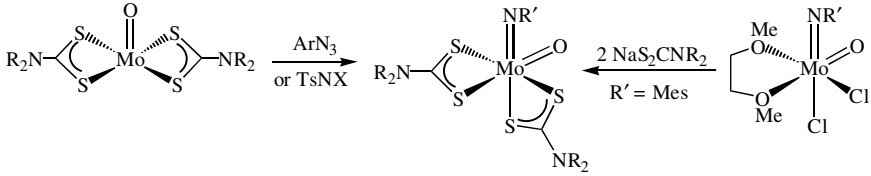

(68)

Variable-temperature NMR studies on $[MoO(NMes)(S_2CNR_2)_2]$ are consistent with the rapid equilibration of the two dithiocarbamate ligands and a process that proceeds via an η^1-bound dithiocarbamate intermediate has been proposed (Fig. 83); its facile nature relating to the strong trans influence of oxo and imido ligands (829).

Addition of PPh_3 to $[MoO(N\text{-}p\text{-tol})(S_2CNR_2)_2]$ (R = Et; $R_2 = C_4H_8$) results in clean abstraction of the oxo ligand to afford orange, $[M(N\text{-}p\text{-tol})(S_2CNR_2)_2]$, which in turn react with a chromium(IV) oxo porphyrin complex to afford oxo-bridged, $[(porphrin)Cr(\mu\text{-}O)Mo(N\text{-}p\text{-tol})(S_2CNR_2)_2]$ (835). The related molybdenum–oxo complexes have also been prepared, upon addition of the chromium oxide to $[MoO_2(S_2CNR_2)_2]$, and all are proposed to contain chromium(III) and molybdenum(V) centers; the variation of magnetic susceptibiliy with temperature providing evidence for a strong antiferromagnet coupling between them.

In further work, Maatta and Wentworth (846) reported a valence isomer of the oxo–imido complex $[MoO(NPh)(S_2CNEt_2)_2]$, namely, $[Mo(ONPh)(S_2CNEt_2)_2]$, formed upon addition of nitrosobenzene to $[Mo(CO)_2(S_2CNEt_2)_2]$ (Eq. 69). The NMR evidence points toward an η^2-coordination of nitrosobenzene, however, all attempts to bring about an isomerization to the oxo–imido

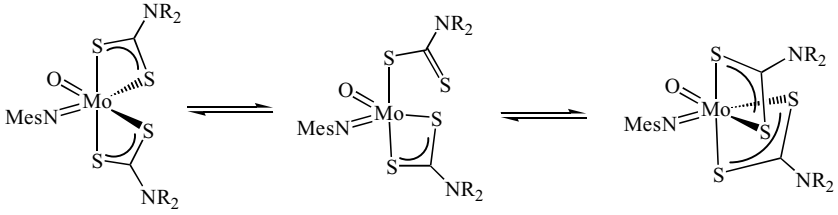

Figure 83. Proposed mechanism for dithiocarbamate exchange in $[MoO(NMes)(S_2CNR_2)_2]$.

complex, and visa versa, failed.

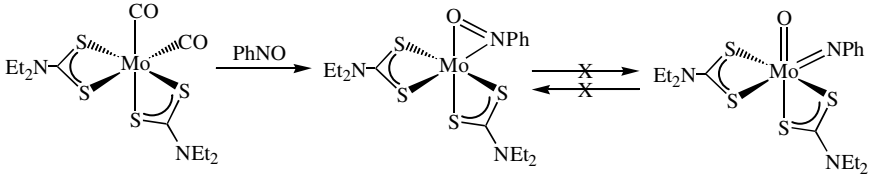

(69)

The synthesis of seven-coordinate imido molybdenum(VI) complexes, $[Mo(NR')X_2(S_2CNR_2)_2]$, often utilizes the analogous oxo compounds $[MoOX_2(S_2CNR_2)_2]$. For example, addition of substituted anilines in the presence of a base affords $[Mo(NAr)Cl_2(S_2CNR_2)_2]$ (438, 839, 841), while reaction with phenylisocyanate and $PhNPPh_3$ yield $[Mo(NPh)Cl_2(S_2CNEt_2)_2]$ (843). Interestingly, when aryl diamines are used, generally only one of the amine groups reacts, the second being deactivated via coordination to the electron-deficient molybdenum(VI) center (Eq. 70) (839, 841).

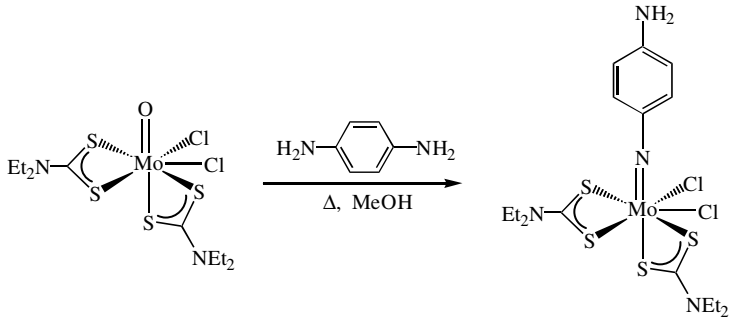

(70)

Naphthalene-1,5-diamine behaves somewhat differently, products from the reaction of one and both amine functionalities being generated, with binuclear $[\{Mo(S_2CNEt_2)_2Cl_2\}_2(\mu\text{-}1,5\text{-}NC_{10}H_6N)]$ (**95**) (Fig. 84) being the major product (839). Using a similar preparative method and employing 2-aminothiophenol, Minelli et al. (840,842) prepared a number of chelating bent imido complexes, $[Mo(N\text{-}o\text{-}C_6H_4S)X(S_2CNEt_2)_2]$ (X = F, Cl, OMe) (**96**) (Fig. 84). Crystallographic studies show a seven-coordinate distorted pentagonal bipyramidal geometry, with imido and halide occupying axial sites. The chelating nature of the imido ligand also leads to extreme bending (Mo–N–C $\sim 140°$] (840,842), while in contrast, nonchelating complexes with similar coordination geometries have linear imido linkages (841,843).

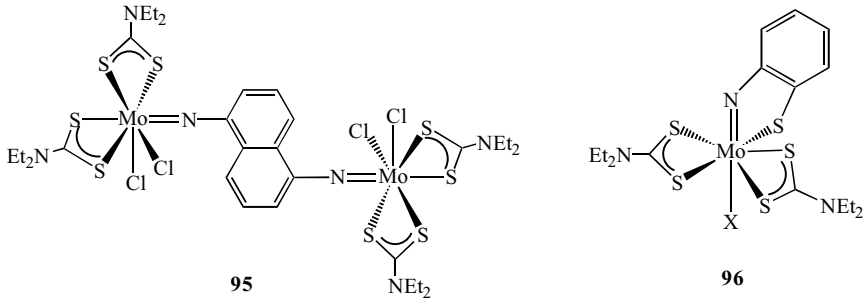

Figure 84. Examples of molybdenum (VI) imido bis(dithiocarbamate) complexes.

Other synthetic methods used to generate imido–dihalide complexes, $[Mo(NR)X_2(S_2CNR_2)_2]$, include reactions of $[Mo(NAr)_2(S_2CNR_2)_2]$ and $[MoO(NAr)(S_2CNR_2)_2]$ with HCl or CH_3Br, giving the chloride and bromide, respectively (832,843). Minelli et al. (438) correlated ^{95}Mo NMR chemical shifts with the Mo–N–C angle in dichloride complexes, $[Mo(NAr)Cl_2(S_2CNEt_2)_2]$, the position of the substituents on the aryl group influencing both. Thus, alkyl groups in the 2,6 and 2,4,6-positions have the greatest deshielding effect on the ^{95}Mo nucleus, which have bond angles close to 180°. Electrochemical studies have been carried out on the bent imido complex, $[Mo(N\text{–}o\text{–}C_6H_4S)Cl(S_2CNEt_2)_2]$, an irreversible one-electron reduction leading to a molybdenum(V) complex, which has been detected by ESR spectroscopy (842).

Cationic tris(dithiocarbamate) complexes, $[Mo(NR')(S_2CNR_2)_3]^+$, can be prepared in a number of ways (Fig. 85). For example, they result from addition of dithiocarbamate salts to $[Mo(NR')Cl_2(S_2CNR_2)_2]$ (832), thermolysis of $[MoO(S_2CNR_2)_3]^+$ with phenylisocyanate (810) and thermolysis of $[MoO_2(S_2CNEt_2)_2]$ with aryl isocyanates in air (439). Recently, they have also been prepared from the reactions of $[MoOX_2(S_2CNEt_2)_2]$ with functionalized anilines in methanol in the presence of 2 equiv of triethylamine (438), while a further route involves the addition of electrophilic reagents (PhCOCl, $PhSO_2Cl$, ArSCl, ArCl, Ph_3CBF_4, R_3OBF_4) to the nitride, $[MoN(S_2CNR_2)_3]$ (R = Me, Et) (437). A number have been crystallographically characterized. All show a distorted pentagonal bipyramidal metal coordination, with the linear imido ligand occupying an axial site (437–439). The trans-influence of the imido group is reflected in the molybdenum–sulfur bonds [Ar = Ph; Mo—S_{ax} 2.585(1); Mo—S_{eq} 2.486(1)–2.516(1) Å] (439).

Imido–disulfur complexes, $[Mo(NR')(S_2)(S_2CNR_2)_2]$, are quite common and have been prepared in a number of ways (Fig. 86). For example, $[Mo(NPh)(S_2)(S_2CNEt_2)_2]$ results from the thermolysis of phenylisocyanate with

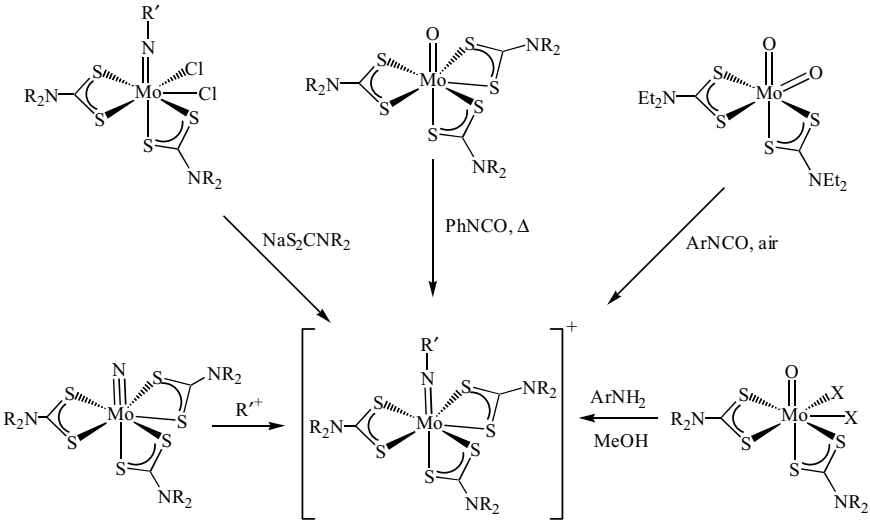

Figure 85. Synthetic routes to $[Mo(NR')(S_2CNR_2)_3]^+$.

$[MoO(S_2)(S_2CNEt_2)_2]$, although this reaction fails for *t*-BuNCO (527). A more general route to these complexes is via the thermal reaction of organic isocyanates with $[MoO_2(S_2CNR_2)_2]$, which lead to a formal double sulfur–carbon bond cleavage reaction (527,528,839), while addition of hydrogen

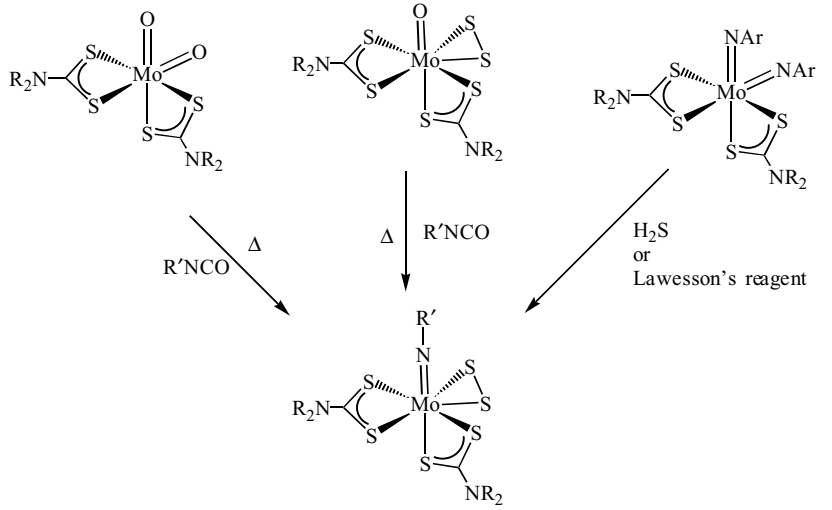

Figure 86. Synthetic routes to $[Mo(NR')(S_2)(S_2CNR_2)_3]$.

sulfide or Lawesson's reagent to bis(imido) complexes, $[Mo(NAr)_2(S_2CNEt_2)_2]$, also yields the same complexes (838). A number of crystallographic studies have been carried out. All show a distorted pentagonal bipyramidal metal coordination, the imido occupying an axial site and the disulfur ligand lying in the equatorial plane (527,528).

The reactivity of a number of molybdenum(VI) imido complexes has been investigated. Harlan and Holm (831) investigated tosyl–imido complexes as imido group-transfer agents. Addition of 5 equiv of PPh_3 to $[Mo(NTs)_2(S_2CNEt_2)_2]$ gave only 5% conversion to the phosphorus imine. In contrast, reaction with 1 equiv of the more basic PPh_2Me gave quantitative imine formation after 5 h, while treatment of $[MoO(NTs)(S_2CNEt_2)_2]$ with the same phosphine gave a 2:1 mixture of Ph_2MePO and $Ph_2MePNTs$. In both cases, several molybdenum containing species were seen by NMR spectroscopy, being postulated to result from an equilibrium between the expected molybdenum(IV) complexes and molybdenum(VI) starting materials. Catalytic imido transfer to Ph_2MeP was successful utilizing PhMeSNTs or Ph_3SbNTs as the stoichiometric nitrene sources, and systems are reported to be robust. Devore and co-workers (833,834) noted similar behavior for tolyl imido complexes, however, they found that addition of Ph_2EtP to $[MoO(N\text{-}p\text{-tol})(S_2CNEt_2)_2]$ proceeded via $[Mo_2(N\text{-}p\text{-tol})_2(\mu\text{-}O)(S_2CNEt_2)_2]$ (834) to give the reactive molybdenum(IV) species, $[Mo(N\text{-}p\text{-tol})(S_2CNEt_2)_2]$. While this could not be isolated pure, it was trapped with dimethylacetylenedicarboxylate (dmad) giving $[Mo(N\text{-}p\text{-tol})(dmad)(S_2CNEt_2)_2]$ (833). The latter has been crystallographically characterized, the average molybdenum–carbon bond length of 2.12 Å being slightly longer than found for other two-electron donor alkynes (830).

e. Hydrazido, Diazenido, and Other Nitrogen-Based Ligands. A wide range of hydrazido, diazenido, and related nitrogen based ligands can be stabilized at molybdenum dithiocarbamate centers.

Mo–N=N–R	Mo=N–NR_2	Mo=NR–NR_2	Mo=N–N=C(R)O
Diazenido(1−)	Hydrazido(2−)	Hydrazido(1−)	Diazenido(3−)

Hydrazido(2−) complexes, $[MoO(NNR_2)(S_2CNR_2)_2]$ (847–850) and $[Mo(NNR_2)_2(S_2CNR_2)_2]$ (848,851–855], have been prepared via addition of disubstituted hydrazines with $[MoO_2(S_2CNR_2)_2]$. The basicity of the hydrazine plays a crucial role in dictating the reaction pathway. For example, $[MoO(NNMe_2)(S_2CNMe_2)_2]$ reacts with $PhMeNNH_2$ via a diazenido–hydrazido intermediate to give $[Mo(NNMePh)_2(S_2CNMe_2)_2]$, while hydrazine itself is unreactive. Further, $[MoO(NNMePh)(S_2CNMe_2)_2]$ reacts with Me_2NNH_2 to give the mixed-complex $[Mo(NNMe_2)(NNMePh)(S_2CNMe_2)_2]$ (Eq. 71) (848).

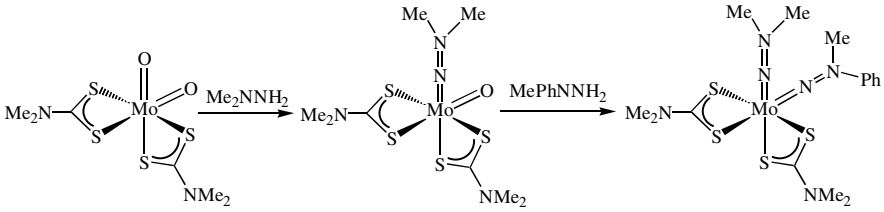

(71)

A number of crystallographic studies have been carried out (847–849,851,855). All show nearly linear hydrazido ligands and, while substitution at nitrogen has little effect on either the molybdenum–nitrogen bond length or hydrazido linearity, the nature of the dithiocarbamate can have a strong effect on both (847). Interestingly, as found for the related oxo–imido complexes (829), both dithiocarbamates are seen to be equivalent in solution (by NMR spectroscopy), suggesting the possibility of a related interconversion process in these oxo–hydrazido complexes (849), possibly via an η^1-bound dithiocarbamate.

A number of reactions of bis(hydrazido) complexes have been carried out, protonation being studied in some detail (Fig. 87) (852–854). Initial protonation leads to the formation of $[Mo(NNR'_2)(\eta^2\text{-}NHNR'_2)(S_2CNR_2)_2]^+$, containing a side-on hydrazido(1−) ligand, while addition of a second proton fleetingly affords $[Mo(\eta^2\text{-}NHNR'_2)_2(S_2CNR_2)_2]^{2+}$. Rapid solvent attack, followed by halide substitution, then leads to further protonation and loss of hydrazinium salt with formation of $[MoX_2(NNR'_2)(S_2CNR_2)_2]$. Interestingly, upon deprotonation of $[Mo(NNR_2)(\eta^2\text{-}NHNR_2)(S_2CNR_2)_2]^+$ by a variety of bases, kinetic studies suggest the formation of a transient side-bound hydrazido(2−) complex prior to regeneration of the terminal ligand.

Reaction of $[MoO_2(S_2CNR_2)_2]$ with functionalized hydrazines, $H_2NNHC(E)X$ (E = O, S; X = OMe, SR), yields complexes, $[Mo(N_2CEX)(\eta^2\text{-}NH_2NCEX)(S_2CNR_2)_2]$, containing both side-on hydrazido and linear diazenido ligands (856–860). For the sulfides (E = S), the sulfur of the hydrazido ligand is also metal-bound generating a chelating ligand. Further, when crystallized in air (858) or upon addition of HCl (856,857,861), novel dimeric complexes $[Mo_2O(S_2CNR_2)_2\{\mu\text{-}NNC(R)S\}_2]$ result in which the nitrogens bridge the dimolybdenum(V) vector, while both sulfurs are bound to a single metal center (Fig. 88).

Related dimeric benzoyldiazenido and thiobenzoyldiazenido complexes, $[Mo_2O(S_2CNR_2)_2\{\mu\text{-}NNC(Ar)O\}_2]$ (**97**) and $[Mo_2O(S_2CNR_2)_2\{\mu\text{-}NNC(Ar)S\}_2]$ (**98**) (Fig. 89), have been prepared from $[MoO_2(S_2CNR_2)_2]$ (R = Me, Et) and benzoyl or thiobenzoylhydrazines in refluxing methanol in the presence of PPh_3 (862). Two examples have been crystallographically characterized, namely, $[Mo_2O(S_2CNEt_2)_2\{\mu\text{-}NNC(Ph)O\}_2]$ and $[Mo_2O(S_2CNEt_2)_2\{\mu\text{-}NNC$

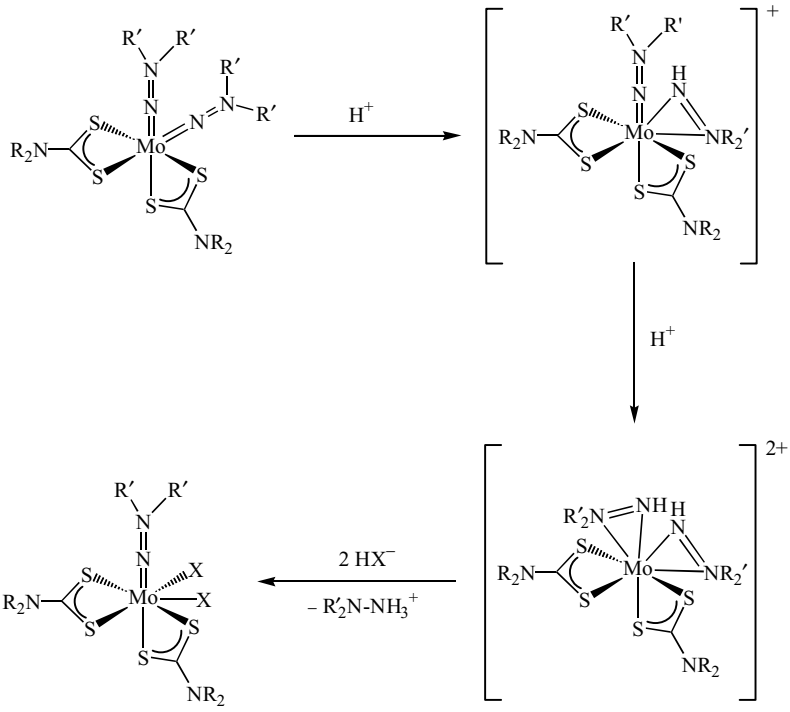

Figure 87. Protonation of bis(hydrazido) complexes, $[Mo(NNR'_2)(S_2CNR_2)_2]$.

$(Ar)S\}_2]$ ($Ar = p\text{-}ClC_6H_4$), their nonplanar Mo_2N_2 cores being almost identical. Cyclic voltammetry studies have also been carried out, each showing a reversible one-electron reduction followed by an irreversible cathodic process at more negative potentials.

In a further contribution, the previously prepared molybdenum(VI) dibenzoyldiazene complex, $[MoO(S_2CNMe_2)_2\{\eta^2\text{-}N(COPh){=}NC(Ph)O\}]$ (**99**), has been crystallographically characterized and contains a pentagonal bipyramidal coordination sphere, the oxygen atom of the diazene ligand lying trans to the molybdenum–oxo group [O–Mo–O 166.0(3)°] (863).

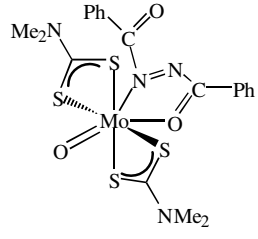

99

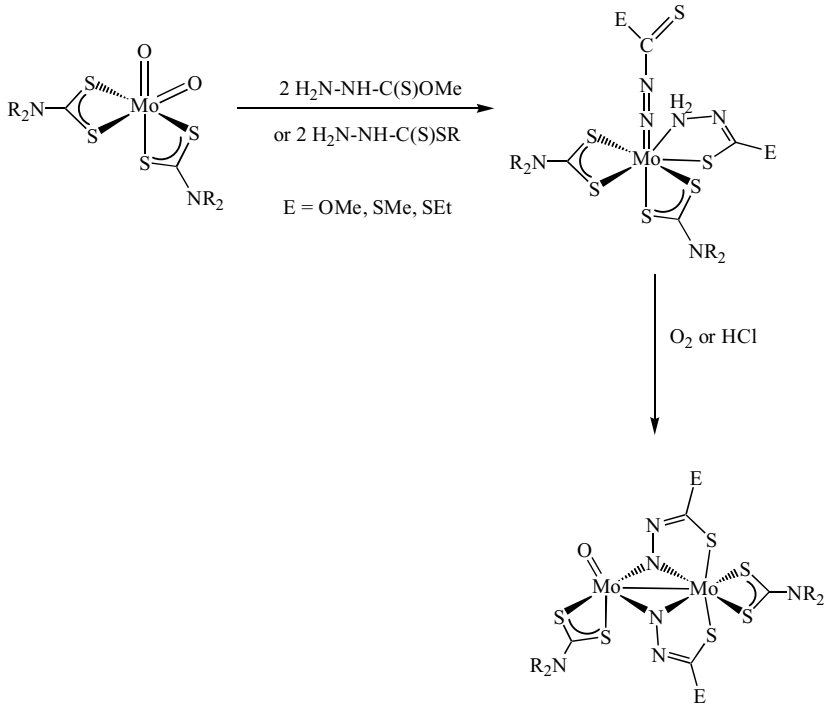

Figure 88. Generation of diazenido–hydrazido complexes from $[MoO_2(S_2CNR_2)_2]$ and their subsequent rearrangement to give binuclear diazenido-bridged complexes.

Molybdenum(V) tris(dithiocarbamate) diazenido complexes, $[Mo(NNR')(S_2CNR_2)_3]$, have been known since the early 1970s (864,865). They can be prepared in high yields from $[MoO_2(S_2CNR_2)_2]$ and hydrazines, NH_2NHR', in refluxing methanol in the presence of a further equivalent of dithiocarbamate salt (Eq. 72) (866). More recently, Poveda and co-workers (441) prepared

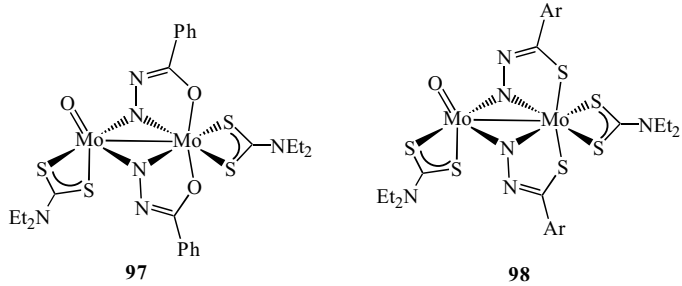

97 **98**

Figure 89. Examples of benzoyl and thiobenzoyldiazenido complexes.

further examples, $[Mo\{NNC(O)Ar\}(S_2CNR_2)_3]$ ($Ar = p\text{-}C_6H_4NO_2$), together with related hydrazido(2-) complexes, $[Mo\{NNH(CO)Ph\}(S_2CNR_2)_3]$, via the same synthetic proceedure.

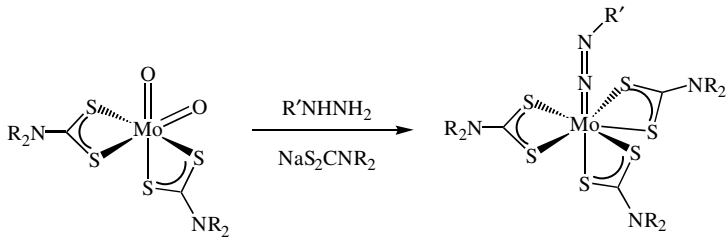

(72)

In solution the complexes are fluxional, exchange of the methyl groups in $[Mo(NN\text{-}p\text{-}C_6H_4X)(S_2CNMe_2)_3]$ ($X = H$, Cl, NO_2, OMe, Me) being observed by NMR spectroscopy, a process that is attributed to a polytopal rearrangement.

The crystal structures of two previously prepared (867) aryl diazenido complexes, $[Mo(NNAr)(S_2CNMe_2)_3]$ ($Ar = Ph$, $m\text{-}C_6H_4NO_2$), have been reported (440,868). The metal center adopts a pentagonal bipyramidal coordination geometry, the diazenido ligand occupying an axial site, while the linear nature of the latter suggests that it acts as a three-electron donor ligand. Interestingly in the nitro complex, the substituent further interacts with the nitrogen of one of the dithiocarbamate ligands (440).

Crystal structures of $[Mo\{NNC(O)Ar\}(S_2CNEt_2)_3]$ ($Ar = p\text{-}C_6H_4NO_2$) (441) and $[Mo\{NNC(O)Et\}(S_2CNMe_2)_3]$ (869) have also been carried out, the same gross structural features being observed. Refluxing both ($R = Et$) with HCl in methanol affords $[Mo(S_2CNEt_2)_4]$, while over longer periods the oxidation product, $[Mo(S_2CNEt_2)_4][MoCl_4(OMe)_2]$, was isolated (441).

Yamanouchi and Enemark (870) crystallographically characterized the molybdenum(III) bis(amide) complex, $[Mo(S_2CNEt_2)(\eta^2\text{-}o\text{-}SC_6H_4NH)_2]$ (**100**), formed from the reaction of $[MoO(\mu\text{-}O)(S_2CNEt_2)]_2$ and 2-aminobenzenethiol. The coordination polyhedron is found to be midway between a trigonal prism and octahedron, the nitrogens lying approximately trans to one another [N—Mo—N 157.5(1)°].

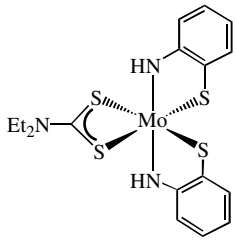

100

The nitride complex, $[MoN(S_2CNEt_2)_3]$, first prepared by Chatt and Dilworth (871), contains a relatively nucleophilic nitride moiety as a result of the electron-releasing nature of the dithiocarbamate ligands. As such, it reacts with a range of organic and nonorganic electrophiles as detailed above (437,872). Very recently, Seymore and Brown (873) showed that it also reacts with the electrophilic nitride complex $[TpOsNCl_2]$ at 50°C to give dinitrogen together with nitride-bridged $[TpCl_2OsNMo(S_2CNEt_2)_3]$ (**101**); labeling studies showing that the nitride derives primarily from osmium.

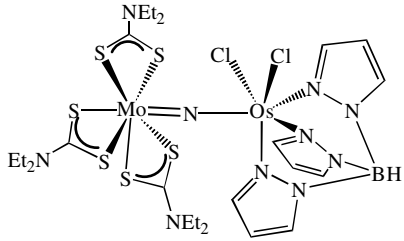

101

f. Mononuclear Disulfide and Related Chalcogenide Complexes. Molybdenum disulfide complexes have been prepared in a number of ways. Addition of thiuram disulfides to $[MoS_4]^{2-}$ and $[MoO_2S_2]^{2-}$ affords molybdenum(V) and (VI) complexes, $[Mo(S_2)(S_2CNR_2)_3]$ (**102**), and $[MoO(S_2)(S_2CNR_2)_2]$ (**103**) (R = Me, Et) (Fig. 90), respectively; as a result of induced internal electron-transfer and ligand electron-transfer processes (180). Oxo complexes, $[MoO(S_2)(S_2CNR_2)_2]$, have also been prepared by a number of other methods (810, 874, 875). These include the addition of sodium sulfide to $[MoO_2(S_2CNR_2)_2]$ (874), but the most convenient method appears to be from addition of propylene sulfide to $[MoO(S_2CNR_2)_2]$ (526). Analogous imido complexes, $[Mo(NR')(S_2)(S_2CNR_2)_2]$ (**104**) (Fig. 90) have also been prepared

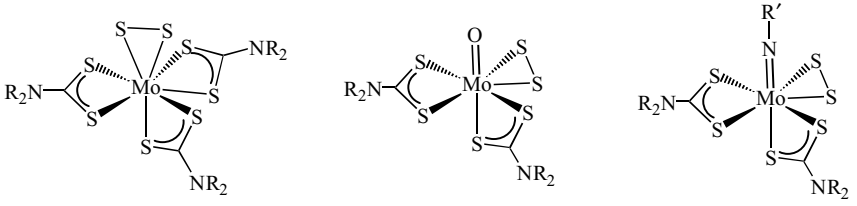

102 **103** **104**

Figure 90. Examples of disulfide (S_2^{2-}) complexes.

via an unusual double sulfur–carbon bond-cleavage process upon thermolysis of $[MoO_2(S_2CNR_2)_2]$ with organic isocyanates (527,528), from thermolysis of $[MoO(S_2)(S_2CNEt_2)_2]$ with phenyl isocyanate (527), and from the reaction of H_2S with $[Mo(NAr)_2(S_2CNEt_2)_2]$ (838,876).

A number of crystallographic studies have been carried out, the S_2^{2-} ligand generally being approximately symmetrically bound with a sulfur–sulfur bond length of just over 2Å (180,527,528,838,874). Yan and Young have studied the NMR characteristics of $[MoO(S_2)(S_2CNR_2)_2]$ (R = Me, Et, Pr, Bu) in some detail, the methyl resonance close to the Mo=O vector being considerably shielded relative to the other three (526) and a similar effect is seen in imido analogues (527).

A number of reactivity studies have been reported on oxo–disulfide complexes, $[MoO(S_2)(S_2CNR_2)_2]$. A key feature is the ease of removal of the disulfide group. Dubois and co-workers (874) also showed that it is readily removed upon addition of nucleophiles (PPh_3, MeNC, CN^-,SO_3^{2-}), for example, addition of 2 equiv of phosphine resulting in the generation of $[MoO(S_2CNR_2)_2]$ and phosphine sulfide. By using PPh_3 in 1,2-dichloroethane, the transformation has been studied kinetically by stop-flow methods, and has been shown to be an irreversible second-order reaction, the rate constant varying as a function of the alkyl substituents; Me > Et > Pr (877,878).

Electrochemical studies (R = Me, Et) reveal irreversible one-electron oxidation and reduction processes, the disulfide unit being lost in both instances. Controlled electrolysis or oxidation with $[NO]PF_6$ is postulated to yield the mixed-valence complex, $[Mo_2O(\mu\text{-}O)(S_2CNR_2)_4]^+$, which in turn is reduced to $[MoO(S_2CNR_2)_2]$ (879). Sulfur is also partially lost upon heating $[MoO(S_2)(S_2CNR_2)_2]$ at >160°C. Here, dinuclear $[MoO(\mu\text{-}S)(S_2CNR_2)]_2$ results (526), which is also formed upon addition of thiophenol (874). The imido–disulfide complex, $[Mo(NPh)(S_2)(S_2CNEt_2)_2]$, behaves in a somewhat similar manner to its oxo analogue. Addition of triethylphosphite followed by oxidation by air affords dimeric $[Mo_2O_2(\mu\text{-}S)(\mu\text{-}NPh)(S_2CNEt_2)_2]$ (Eq. 73), postulated to result from abstraction of a single sulfur atom of one molecule and the disulfide unit of a second (527).

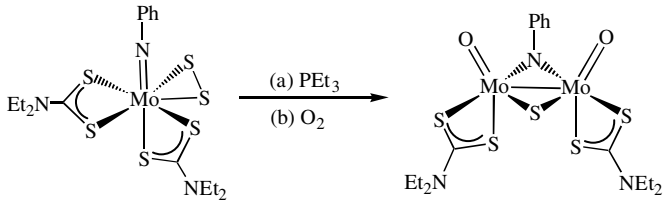

(73)

Bargon and co-workers utilized the reversible removal addition of sulfur in $[MoO(S_2)(S_2CNEt_2)_2]$ to employ it as a catalyst for the conversion of isonitriles

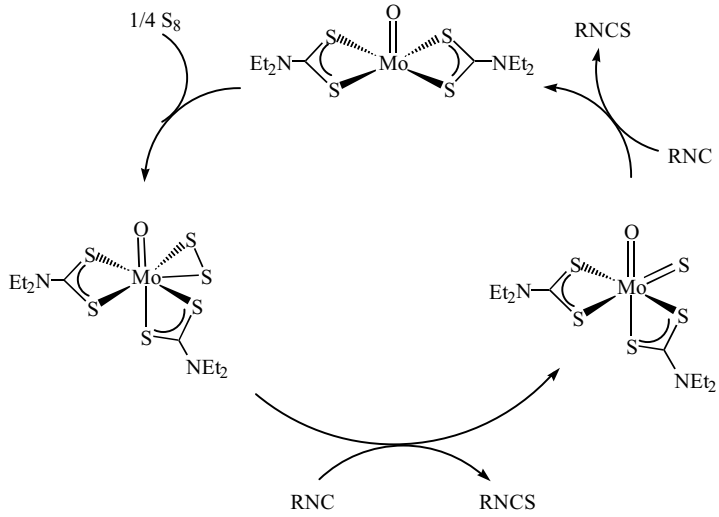

Figure 91. Proposed mechanistic scheme for the sulfuration of isonitriles catalyzed by $[MoO(S_2)(S_2CNEt_2)_2]$.

into isothiocyanates (880) and the direct episulfidation of alkenes and allenes with elemental sulfur (881,882). Both transformations occur in good yields and under mild conditions. Sulfuration of isonitriles is believed to occur via a catalytic cycle shown in Fig. 91, involving the unknown oxo–sulfido complex, $[MoOS(S_2CNEt_2)_2]$. Further, in a secondary reaction the isonitrile binds to coordinately unsaturated $[MoO(S_2CNEt_2)_2]$, one example $[MoO(t\text{-BuNC})(S_2C\text{-}NEt_2)_2]$ being characterized crystallographically (880).

The episulfidation of alkenes and allenes is believed to proceed in a similar manner (881,882). Here there is also a secondary reaction, but in this instance it is noninnocent, in that the molybdenum(V) dimer, $[MoO(\mu\text{-}S)(S_2CNEt_2)]_2$, and tetraethylthiuram disulfide are formed. This is especially noticeable when less reactive (Z)-cycloalkanes are used, and the authors suggest that while initial sulfur transfer is facile, transfer from $[MoOS(S_2CNEt_2)_2]$ proceeds at a slower rate, allowing the internal redox reaction to become a dominant pathway.

The disulfide unit is retained upon addition of methyl iodide to $[MoO(S_2)(S_2CNR_2)_2]$, the salts $[MoO(S_2Me)(S_2CNR_2)_2]I$ being produced (874). Disulfides can also be oxidized; addition of *m*-chloroperoxybenzoic acid to $[MoO(S_2)(S_2CNR_2)_2]$ and $[Mo(S_2)(S_2CNR_2)_3]$ yielding the S_2O complexes, $[MoO(\eta^2\text{-}S_2O)(S_2CNR_2)_2]$ and $[Mo(\eta^2\text{-}S_2O)(S_2CNR_2)_3]$, respectively (Fig. 92) (445,883). The latter are also formed in low yield from the reaction of $[MoS_4]^{2-}$ with $[VCl_2(S_2CNR_2)_2]$ (445).

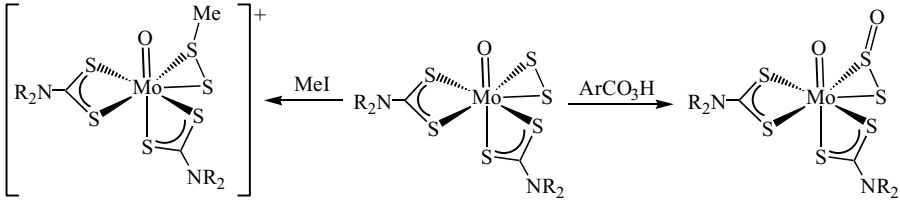

Figure 92. Reactions of $[MoO(S_2)(S_2CNR_2)_2]$ that result in modification of the disulfide moiety.

The EHMO calculations have shown that the S_2^{2-} and S_2O^{2-} ligands bind to molybdenum(V) in a similar fashion, the S_2O group being both a weaker π acid and base (445). Both types of complex show similar cyclic voltammetric properties, undergoing a reversible one-electron reduction and a quasi-reversible one-electron oxidation, while chemical oxidation of $[Mo(\eta^2\text{-}S_2O)(S_2CNR_2)_3]$ by ferrocenium affords $[Mo(S_2CNR_2)_4]^+$. Loss of the S_2O ligand from $[MoO(S_2O)(S_2CNR_2)_2]$ also occurs upon addition of PPh_3, generating Ph_3PS and $[Mo_2O_3(S_2CNR_2)_4]$ (883).

Upon reduction of $[MoCl(S_2CNEt_2)_3]$ in SO_2, $[Mo(\eta^2\text{-}SO_2)(S_2CNEt_2)_3]$ (Eq. 74), is formed along with what is proposed to be the novel thionyl chloride complex, $[Mo(SOCl_2)(S_2CNEt_2)_3]$. The latter has not been structurally characterized, and hence the precise binding mode remains unknown. The S—O coordination of the SO_2 ligand has, however, been confirmed by a crystallographic study, which shows that it occupies an axial site in a pentagonal prismatic arrangement (444).

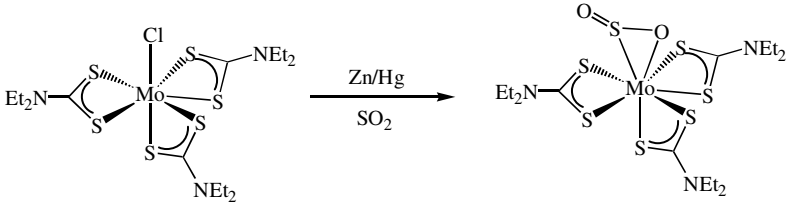

(74)

g. Nitrosyl and Thionitrosyl Complexes. A wide range of molybdenum dithiocarbamate nitrosyl complexes are known, while in contrast the related thionitrosyl complexes are relatively scarce. Reductive nitrosylation of $[MoO_2(S_2CNEt_2)_2]$ by hydroxylamine results in the formation of the molybdenum(III) nitrosyl complex $[Mo(NO)(S_2CNEt_2)_3]$ (884), while the corresponding thionitrosyl results from the reaction of the molybdenum(VI) nitride, [MoN-

$(S_2CNEt_2)_3]$, with sulfur of propene sulfide (Eq. 75) (872).

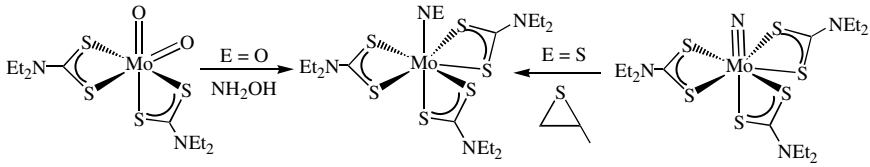

(75)

Johnson et al. (885) showed that nitrosyl complexes, $[Mo(NO)(S_2CNR_2)_3]$ (R = Me, Et, Bu), also result almost quantitatively upon photolysis of $[Mo(NO)_2(S_2CNR_2)_2]$, dinitrogen oxide also being detected (Eq. 76).

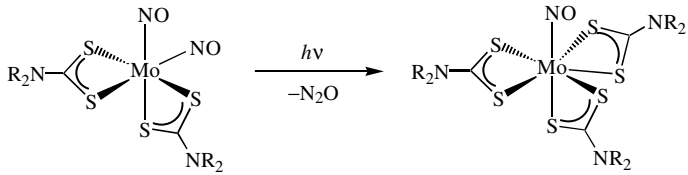

(76)

The nitride (433), nitrosyl (884), and thionitrosyl (442) have all been crystallographically characterized. Each displays a pentagonal bipyramidal coordination sphere, the nitrogen occupying an axial site. This leads to an elongation of the molybdenum–sulfur vector trans to nitrogen as a result of the trans-influence of the ligands, such that; N > NS > NO [trans Mo–S; NO 2.561(2), NS 2.608(1), N 2.852(3) Å] (Table IV).

Previous workers have noted the unexpectedly high barrier to dithiocarbamate exchange in $[Mo(NO)(S_2CNMe_2)_3]$ and this has been confirmed by Johnson et al. (885). It is unusual since related seven-coordinate tris(dithiocarbamate) complexes such as $[TiCl(S_2CNMe_2)_3]$ and $[Re(CO)(S_2CNMe_2)_3]$ have relatively low barriers to dithiocarbamate exchange. In order to further probe this anomalous behavior at molybdenum (and tungsten), attempted exchange reactions were carried out between $[Mo(NO)(S_2CNMe_2)_3]$ and NaS_2CNEt_2. However, under both photochemical and thermal conditions no intermolecular dithiocarbamate exchange was noted, suggesting that intramolecular exchange in $[Mo(NO)(S_2CNMe_2)_3]$ cannot proceed via a dissociative process, which may account for the high-activation barrier.

A number of other molybdenum(III) nitrosyl complexes have been reported. Addition of dithiocarbamate salt to $[MoBr_2(CO)_4]_2$ in the presence of *o*-phenylene-bis(dimethylarsine) (diars) yields, $[Mo(CO)(S_2CNR_2)_2(diars)]$ (R = Me, Et), which in turn are oxidized by $[NO]BF_4$ to nitrosyls, $[Mo(NO)(S_2CNR_2)_2(diars)]BF_4$ (Eq. 77) (886). A crystallographic study (R = Et) reveals

that the nitrogen and one sulfur atom occupy axial sites in a distorted pentagonal bipyramidal geometry (887).

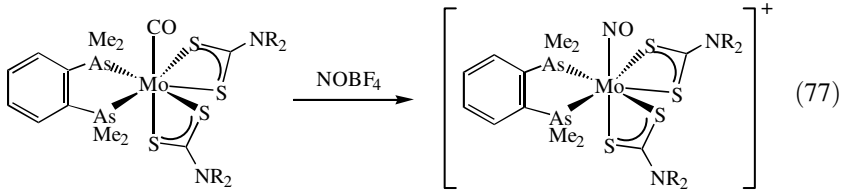

(77)

Broomhead and Budge (888) prepared a further molybdenum(III) nitrosyl complex, $[Mo(NO)(NCO)(dmso)(S_2CNEt_2)_2]$, and investigated its chemistry (Fig. 93). A crystal structure shows that the metal center adopts a pentagonal bipyramidal geometry, both dithiocarbamate ligands lying in the equatorial plane, along with the isocyanate. The dimethylsulfoxide ligand is readily lost upon addition of ammonia, pyridine, and hydrazine, the latter generating a binuclear complex. Addition of anions also results in a similar reaction to generate $[MoX(NO)(NCO)(S_2CNEt_2)_2]^-$ (X = Cl, N_3, NCO, NCS); a preliminary X-ray structure of the bis(isocyanate) complex suggesting that the nitrosyl now occupies the final equatorial site.

Further molybdenum(III) nitrosyl complexes include $[CpMo(NO)(S_2CNR_2)\{\eta^1\text{-}S_2P(OR')_2\}]$ (R = Me, Et; R′ = Et, *i*-Pr), formed upon addition of dithiocarbamate salts to $[CpMo(NO)I\{S_2P(OR')_2\}]$ (889). Interestingly, the ^{31}P NMR spectra show only a sharp singlet resonance at all temperatures up to 330 K suggesting the absence of any scrambling between the unidentate dithiophosphinate and bidentate dithiocarbamate ligands, the stronger tendency of the dithiocarbamate to act as a bidentate is a reflection of its higher nucleophilicity.

Molydenum(II) bis(nitrosyl) complexes are well known. For example, $[Mo(NO)_2(S_2CNEt_2)_2]$ results cleanly from addition of NO to $[Mo(CO)_2(S_2CNEt_2)_2]$, itself prepared from $[Mo(CO)_4Br_2]$ and 2 equiv of dithiocarbamate salt (890). An alternative synthesis of these nitrosyl complexes involves the *in situ* generation of $[Mo(NO)_2]^{2+}$, upon heating ammonium heptamolybdate and

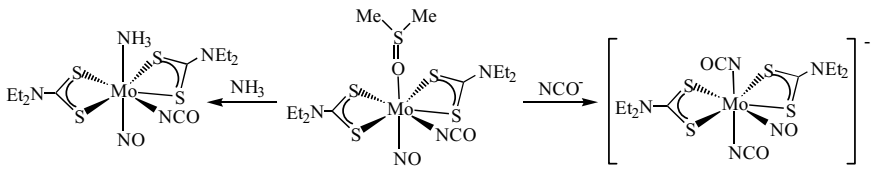

Figure 93. Some reactions of $[Mo(NO)(NCO)(dmso)(S_2CNEt_2)_2]$.

hydroxylamine in DMF, followed by addition of 2 equiv of dithiocarbamate salts (891, 892). Broomhead and co-workers (893) studied the electrochemistry of a range of bis(nitrosyl) complexes (R = Me, Et, *i*-Pr, Bu, Bz; $R_2 = C_4H_4$). They undergo a reversible one-electron reduction to give radical anions, $[Mo(NO)_2(S_2CNR_2)_2]^-$, ESR studies showing that the unpaired electron is delocalized over both nitrosyl groups, while the angle between the nitrosyl ligands remains unchanged upon reduction.

Addition of NaS_2CNEt_2 to $[Mo(NO)_2(S_2CNMe_2)_2]$ results in dithiocarbamate exchange, presumably via initial monodentate coordination of the new dithiocarbamate ligand (885). Similarly, reactions of $[Mo(NO)_2(S_2CNEt_2)_2]$ toward azide, cyanate and diethyldithiocarbamate anions have been studied in hot DMSO. All are initiated by anion coordination, which leads to nitrosyl activation, and elimination of dinitrogen oxide (894). Mechanistic studies, together with earlier work on the characterization of final products, $[MoX_2(NO)(S_2CNEt_2)_2]^-$ (X = N_3, NCO) (895), have lead to the proposal of a mechanistic scheme for these transformations (Fig. 94) (894).

Further examples of molybdenum(II) nitrosyl complexes are $[Mo(NO)(Ph_3PO)(S_2CNR_2)_2]$ (R = Me, Et), prepared upon addition of NO to $[Mo(CO)_2(PPh_3)(S_2CNR_2)_2]$. Here the dithiocarbamates are retained and the phosphine is oxidized. In contrast, addition of NOBr to $[Mo(NO)(Ph_3PO)(S_2CNR_2)_2]$ results in both phosphine oxidation and dithiocarbamate loss generating $[MoBr_2(NO)_2(Ph_3PO)_2]$ (896).

Dimeric molybdenum(I) nitrosyl complexes, $[Mo(CO)_2(NO)(\mu\text{-}S_2CNR_2)]_2$ (R = Me, Et; $R_2 = C_4H_8$), have been prepared that contain bridging dithiocarbamate ligands (897). Addition of a range of neutral or ionic ligands results in cleavage to give neutral monomeric, $[Mo(NO)(CO)(S_2CNR_2)L_2]$ [L = PPh_3, PMe_3, $P(OMe)_3$, Py; L_2 = dppe], or anionic, $[Mo(NO)(CO)_2(S_2CNR_2)X]^-$ (X = SCN, NO_3, N_3, Br, Cl), complexes (Fig. 95) (898). Crystallographic studies have shown that the latter contain cis carbonyls and trans NO and X ligands, while for the neutral complexes, phosphorus ligands lie trans to one another, except for the dppe complex in which NO lies trans to phosphorus and CO trans to sulfur.

$$Mo(NO)_2(S_2CNEt_2)_2 + X^- \longrightarrow [MoX(NO)_2(S_2CNEt_2)_2]^-$$

$$2\ [MoX(NO)_2(S_2CNEt_2)_2]^- \longrightarrow [\{MoX(S_2CNEt_2)_2NO\}_2(\mu\text{-}N_2O_2)]^{2-}$$

$$[\{MoX(S_2CNEt_2)_2NO\}_2(\mu\text{-}N_2O_2)]^{2-} + DMSO \longrightarrow MoX(S_2CNEt_2)(dmso)_2.NO + N_2O$$

$$MoX(S_2CNEt_2)(dmso)_2.NO + X^- \longrightarrow [MoX_2(NO)(S_2CNEt_2)_2]^- + DMSO$$

Figure 94. Proposed mechanistic scheme for the reactions of $[Mo(NO)_2(S_2CNEt_2)_2]$ with anions.

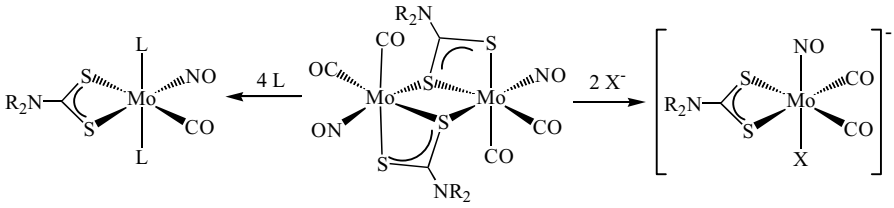

Figure 95. Reactions of $[Mo(CO)_2(NO)(\mu\text{-}S_2CNR_2)_2]_2$ with neutral and charged two-electron ligands.

Carmona et al. (899) prepared another monomeric molybdenum(I) nitrosyl complex, *mer*-$[Mo(NO)(PMe_3)_3(S_2CNMe_2)]$, from $[MoCl(NO)(PMe_3)_4]$. Further reaction with carbon monoxide yields *trans*-$[Mo(NO)(CO)(S_2CNMe_2)(PMe_3)_2]$ via replacement of the phosphine trans to a molybdenum–sulfur bond (Eq. 78).

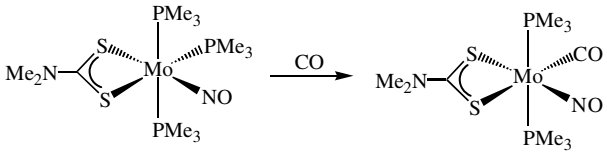

(78)

The same group also described the synthesis and characterization of $[Mo(NO)(PMe_3)(S_2CNMe_2)(\eta^3\text{-}S_2CPMe_3)]$ (**105**), containing an allyl-type, zwitterionic, phosphonium dithiocarboxylate ligand and formed from $[MoCl(NO)(PMe_3)_2(\eta^3\text{-}S_2CPMe_3)]$ and NaS_2CNMe_2 (899).

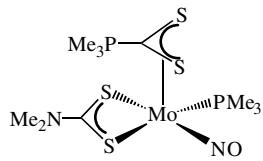

105

h. Cyclopentadienyl, Tris(pyrazolyl)borate, and Related Ligands. Cyclopentadienyl complexes, $[CpMo(CO)_2(S_2CNR_2)]$, have been prepared via addition of thiuram disulfides to the triple-bonded dimers, $[CpMo(CO)_2]_2$ (900,901), and from the thermal reaction of $[CpMo(CO)_3]_2$ and diethylamine in the presence of carbon disulfide (902). Two examples of complexes of this type, namely, $[CpMo(CO)_2(S_2CNMe_2)]$ and $[CpMo(CO)_2(S_2CN{-}i\text{-}Pr_2)]$ have been crystallographically characterized (900,901). Brunner and Wachter (903) also isolated some unusual examples, namely, $[CpMo(CO)_2(S_2CNRH)]$

Figure 96. Some products of the reactions of $[CpMoCl(CO)_3]$ with $Li[RN{=}C(Ph)NR]$.

(R = Me) and $[CpMo(CO)_2\{S_2CN(R)C(Ph){=}NR\}]$ (R = *i*-Pr, Bz), prepared from the reactions of $[CpMo(CO)_3Cl]$ and $Li[RN{=}C(Ph)NR]$ in the presence of carbon disulfide (Fig. 96). Formation of the latter iminoacyl dithiocarbamate complexes is what might be expected upon initial formation of the dithiocarbamate, while the former results formally from a carbon–nitrogen bond cleavage process, which only occurs for the methyl derivative.

Davidson and Sence (904) investigated the chemistry of a number of molybdenum(II) alkyne complexes. For example, addition of NaS_2CNMe_2 to $[CpMoCl(CO)(PhC_2Ph)]$ yields $[CpMo(PhC_2Ph)(S_2CNMe_2)]$, which contains a four-electron alkyne ligand (Eq. 79).

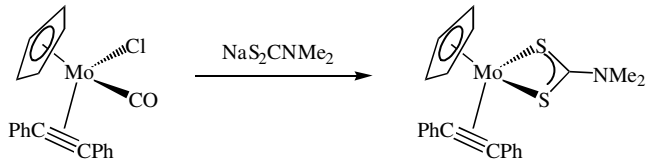

(79)

The bis(alkyne) complexes, $[CpMo(CF_3C_2CF_3)_2(S_2CNR_2)]$ (R = Me, Et), result from addition of dithiocarbamate salts to $[CpMoCl(CF_3C_2CF_3)_2]$ (Eq. 80); each hexafluorobut-2-yne ligand acting as a two-electron donor (905). Interesting, upon heating the latter in hexane at 100°C, clean carbon–carbon bond formation results giving the butadiene complexes, $[CpMo\{\eta^4\text{-}C_4(CF_3)_4\}(S_2CNR_2)]$, which can also be prepared directly from $[CpMo(CO)X\{\eta^4\text{-}C_4(CF_3)_4\}]$ upon addition of dithiocarbamate salts (906).

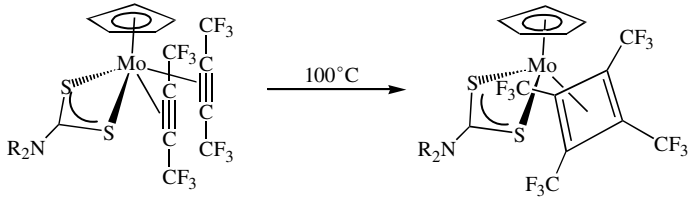

(80)

Molybdenum(II) tris(pyrazolyl)borate and tris(1,2,4-triazolyl)borate (Tp^t) dicarbonyl complexes, $[TpMo(CO)_2(S_2CNEt_2)]$ and $[Tp^tMo(CO)_2(S_2CNEt_2)]$,

can be generated from reactions of the respective tricarbonyl–iodide complexes with $[Ag(S_2CNEt_2)]_6$, with both being crystallographically characterized (907). In related work, the thermal addition of thiuram disulfides to $[Tp^*Mo(CO)_3]$ is shown to afford molybdenum(III) complexes, $[Tp^*Mo(S_2CNR_2)_2]$ (R = Me, Et) (178,179). A crystallographic study (R = Et) (**106**) reveals that one of the dithiocarbamates is essentially monodentate, the second molybdenum–sulfur interaction of 3.820(2) Å, being only weak. A similar addition of tetraethylthiuram disulfide to $[(\eta^5\text{-}C_2B_9H_{11})Mo(CO)_3]^{2-}$ yields the molybdenum(II) complex, $[(\eta^5\text{-}C_2B_9H_{11})Mo(CO)(S_2CNEt_2)]^-$; shown to have a psuedo pyramidal coordination geometry (908).

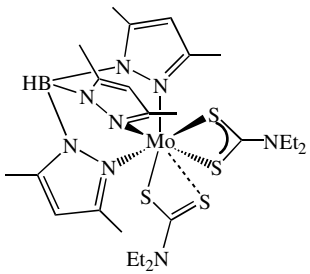

106

Molybdenum(III) and (V) pentamethylcyclopentadienyl complexes, $[Cp^*MoI(NO)(S_2CNR_2)]$ (R = Me, Et) (909) and $[Cp^*MoCl_3(S_2CNEt_2)]$ (910) respectively, have been prepared. The latter reacts further with hydrogen peroxide to give $[Cp^*MoO(\eta^2\text{-}O_2)Cl]$, while reduction with sodium amalgam affords what is believed to be $[Cp^*MoCl_2(S_2CNEt_2)]$ (Eq. 81), albeit in low yield (910). In contrast, related cyclopentadienyl and indenyl complexes, $[CpMoCl_2(S_2CNEt_2)]$ and $[(\eta^5\text{-}C_9H_7)MoCl_2(S_2CNEt_2)]$, are prepared in high yields upon addition of NaS_2CNEt_2 to $[(ring)MoCl_3]$ (911).

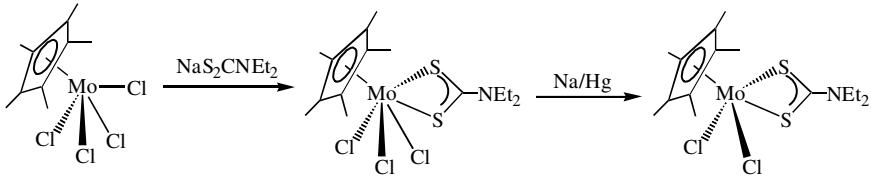

(81)

In a series of papers, McCleverty and co-workers (912–914) reported on the synthesis, structure, and reactivity of $[CpMo(NO)(\eta^1\text{-}C_5H_5)(S_2CNR_2)]$ (R = Me, Bu), which contain both η^5- and η^1-cyclopentadienyl ligands. They

are prepared upon addition of dithiocarbamate salts to [$Cp_2MoI(NO)$] (912), and related molybdenum(III) nitrosyl complexes, [$CpMoX(NO)(S_2CNMe_2)$] (X = Cl, Br), are also reported from the addition of NaS_2CNMe_2 to [$CpMoX_2(\mu\text{-}NO)]_2$. The η^1-cyclopentadienyl complexes have been studied by variable temperature NMR, and display three independent fluxional processes; (1) 1,2-shifts of the η^1-cyclopentadienyl ring; (2) η^1-η^5-cyclopentadienyl ring exchange, (3) restricted rotation about the carbon–nitrogen bonds.

A number of reactivity studies have been carried out on [$CpMo(NO)(\eta^1\text{-}C_5H_5)(S_2CNMe_2)$] (**107**) (Fig. 97). Addition of trifluoroacetic acid results in replacement of the η^1-cyclopentadienyl ligand affording [$CpMo(NO)(\eta^1\text{-}OCOCF_3)(S_2CNMe_2)$] (**108**) (913), but most interesting is its reactions with electron-deficient alkenes and alkynes (914). These result in 2 + 4 Diels–Alder addition reactions to afford molybdenum(III) complexes with elaborate organic alkyl ligands. For example, addition of hexafluorobut-2-yne leads after a day to the formation of [$CpMo(NO)(S_2CNMe_2)\{\eta^1\text{-}C_7H_5(CF_3)_2\}$] (**109**), while with maleic anhydride, [$CpMo(NO)(S_2CNMe_2)\{\eta^1\text{-}C_7H_7(C_2O_3)\}$] (**110**) results.

The molybdenum(IV) bis(indenyl) complex, $[(\eta^5\text{-}C_9H_7)_2Mo(S_2CNEt_2)]BF_4$, is formed in high yield from $[(\eta^5\text{-}C_9H_7)_2Mo(MeCN)_2]^{2+}$ and NaS_2CNEt_2. A crystallographic study reveals that the dithiocarbamate is bidentate and both

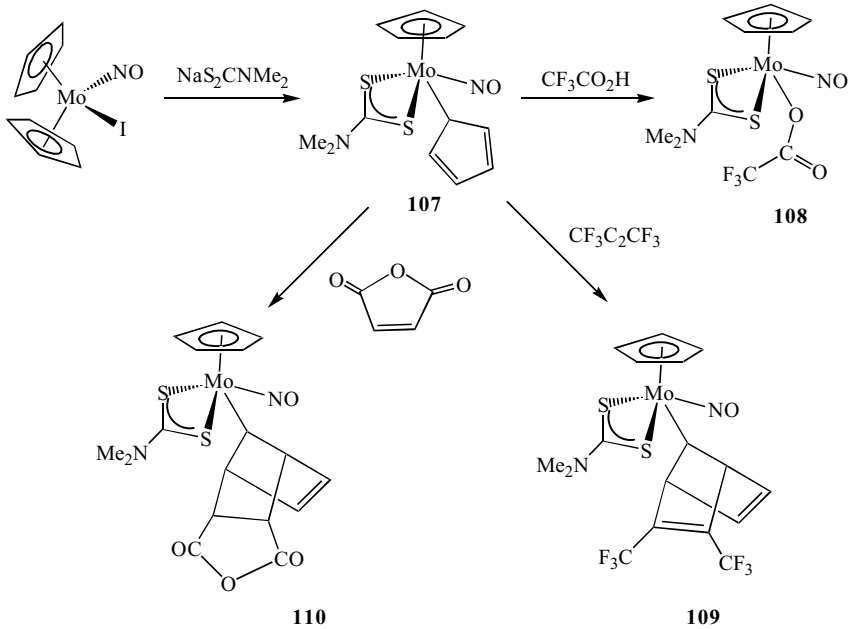

Figure 97. Synthesis and reactivity of the η^1-cyclopentadienyl complex, [$CpMo(NO)(\eta^1\text{-}C_5H_5)(S_2CNMe_2)$].

indenyl rings are η^5-bound (915). Related molybdenum(IV) cyclopentadienyl complexes, $[Cp_2Mo(S_2CNR_2)]^+$, can be generated from $[Cp_2MoCl_2]$ and dithiocarbamate salts, examples including a complex generated from 1,4,7,10-tetraoxo-13-azacyclopentadecane (50).

Tris(pyrazolyl)borate complexes containing strong π-donor oxo and sulfido ligands have been prepared. Addition of KTp* to $[MoO(S_2CNR_2)_2]$ yields $[Tp^*MoO(S_2CNR_2)]$ (R = Me, Et, Pr, Bu) (916), two examples of which (R = Et, Pr) have been crystallographically characterized (916,917). A few reactions have also been explored. With boron sulfide, the oxo group is replaced to give $[Tp^*MoS(S_2CNR_2)]$ (916), along with the dimeric side product *trans*-$[Tp^*MoS(\mu\text{-}S)]_2$ (918). The monomeric oxo complexes undergo a quasi-reversible one-electron oxidation, a process that is irreversible for the sulfides (916). Addition of $B(C_6F_5)_3$ to $[Tp^*MoO(S_2CNMe_2)]$ results in formation of $[Tp^*Mo\{OB(C_6F_5)_3\}(S_2CNMe_2)]$, which has been crystallographically characterized (919). The boron–oxygen interaction of 1.531(2) Å is typical of a single bond, while the molybdenum–oxygen bond of 1.767(1) Å is ∼ 0.1 Å longer than in simple oxo complexes.

i. Organometallic Molybdenum(II) Complexes. In the vast majority of organometallic molybdenum dithiocarbamate complexes, the metal is in the +2 oxidation state, although as seen in Section IV.C.2.h, cyclopentadienyl and related complexes are found for molybdenum(V)–(III), while molybdenum(0) carbonyl complexes can also be prepared (see Section IV.C.2.j).

Seven-coordinate tricarbonyl complexes, $[Mo(CO)_3(S_2CNR_2)_2]$, were first prepared by Colton and Scollary (921) from the reaction of $[MoX_2(CO)_2(PPh_3)_2]$ (X = Cl, Br) (920) or $[MoX_2(CO)_4]_2$ (921) with 2 equiv of dithiocarbamate salt. The latter method is the most widely utilized and has been adopted by others (353,922). For example, Herrick and Templeton (353) used this to prepare the pyrrole complex, $[Mo(CO)_3(S_2CNC_4H_4)_2]$. All are easily oxidized by air, and readily lose a carbonyl under vacuum to afford the related 16-electron dicarbonyl complexes, $[Mo(CO)_2(S_2CNR_2)_2]$, a process that is reversible (Eq. 82). The rate of loss of CO is a function of the dithiocarbamate substituents, such that; Bz > Et > Me ≫ C_4H_4, the latter losing CO only very slowly (353,921).

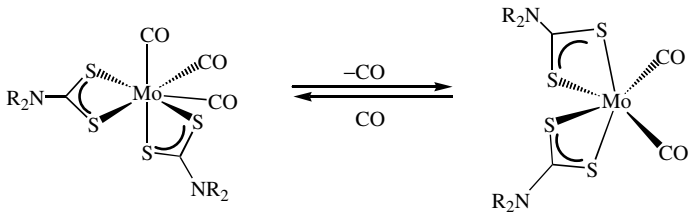

(82)

These 16-electron complexes dicarbonyl have been studied in some detail (369,446,770,832,923,924). A general synthesis is that described above, while in a similar manner, $[Mo(CO)_2(S_2CNC_4H_8)_2]$ results from addition of iodine to $[Mo(CO)_5I]^-$ followed by reaction with 2 equiv of dithiocarbamate salt (770). Crystallographic characterization of $[Mo(CO)_2(S_2CN\text{-}i\text{-}Pr_2)_2]$ reveals a trigonal-prismatic coordination geometry, C–Mo–C 74.3(3)°, which is unprecedented in metal carbonyl chemistry (924). This is believed to result from the planar nature of the dithiocarbamate ligands, which fixes the orientation of the filled π orbitals perpendicular to the bite angle of the ligand and limits overlap of the dπ-LUMO with filled sulfur π-type orbitals in the octahedral coordination mode. Thus, in order to effectively interact with the single vacant $d\pi$ -level a trigonal-prismatic core is imposed (924).

A wide range of reactions of both $[Mo(CO)_3(S_2CNR_2)_2]$ and $[Mo(CO)_2(S_2CNR_2)_2]$ have been explored. The moderate electrophilic nature of the dicarbonyl complexes has been established by following a series of ligand addition reactions, and the prediction from molecular orbital theory that initial ligand attack occurs trans to a carbonyl, is confirmed in a crystallographic structure of a tetrahydrothiophene (THT) adduct, $[Mo(CO)_2(tht)(S_2CNEt_2)_2]$ (923).

Templeton et al. (925) reported the formation of the vinylketene complexes, $[Mo(CO)\{\eta^2,\eta^2\text{-}H_2C{=}CH{=}C(R){=}CO\}(S_2CNEt_2)_2$ (R = H, Me), produced rapidly upon addition of cylcopropene and its methyl derivative to $[Mo(CO)_2(S_2CNEt_2)_2]$ (Eq. 83). The reaction involves both the ring opening of a cyclopropene and carbonyl insertion, although precise mechanistic details are unknown.

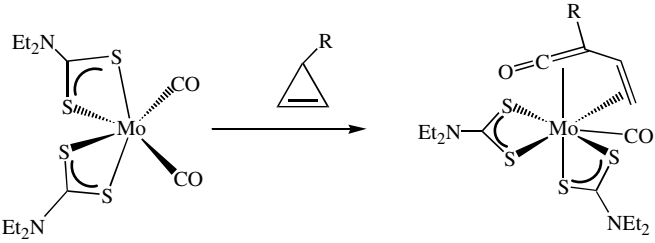

(83)

The dicarbonyls react with other two-electron donor ligands (L) such as phosphines and phosphites to give 18-electron complexes, $[Mo(CO)_2L\text{-}(S_2CNR_2)_2]$, examples of which can also be prepared by other methods (353). For example, Baker et al. (926) prepared $[Mo(CO)_2(SbPh_3)(S_2CNBz_2)_2]$ from the addition of 2 equiv of dithiocarbamate salt to $[MoI_2(CO)_3(MeCN)(SbPh_3)]$. Likewise, Carmona et al. (927) reported the synthesis of mono and bis(phosphine) complexes, $[Mo(CO)_n(PMe_3)_{3-n}(S_2CNR_2)_2]$ (n = 1,2; R = Me, Et, *i*-Pr), from dithiocarbamate addition to $[MoCl_2(CO)_2(PMe_3)_3]$. Interestingly, in a

similar manner to the tri- and dicarbonyl complexes, they can be interconverted upon addition of CO and heating in the presence of phosphine, respectively, (Eq. 84).

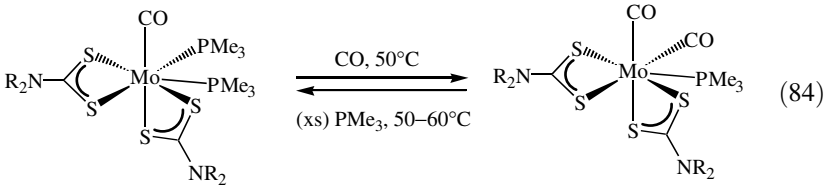

(84)

Addition of halides or azide to $[Mo(CO)_3(S_2CNEt_2)_2]$ affords $[Mo(CO)_2X(S_2CNEt_2)_2]^-$ (353,928); the fluoride (**111**) being shown by X-ray crystallography to have a capped trigonal-prismatic geometry. The halide occupys the capping site, with an acute angle of (67.4°) between the carbonyl groups (928).

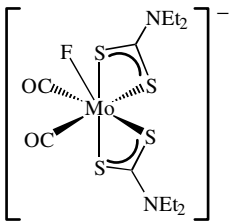

111

Reduction of the molybdenum(IV) complexes, $[MoX(dppe)(S_2CNR_2)_2]X$ ($X = Cl$, Br; $R = Me$, Et; $R_2 = C_5H_{10}$), by tin in the presence of carbon monoxide affords the related diphosphine complexes, $[Mo(CO)(dppe)(S_2CNR_2)_2]$ (813), also prepared upon heating $[Mo(CO)_3(S_2CNEt_2)_2]$ and dppe in methanol (929). In contrast, reduction of $[MoX(dppe)(S_2CNR_2)_2]X$ in a nitrogen or argon atmosphere affords dimeric molybdenum(III) complexes, $[\{Mo(dppe)(S_2CNR_2)_2\}_2]^{2+}$ (813).

The 18-electron monocarbonyl complexes, $[Mo(CO)L_2(S_2CNEt_2)_2]$ ($L = PMe_2Ph$, $PMePh_2$; $L_2 =$ dppe), have been probed electrochemically (929). They undergo two successive one-electron oxidations, the primary process being reversible, while reversibility of the latter is only seen for the dppe complexes at high scan rates (Eq. 85). The reversible generation of molybdenum(III) species is in contrast to that found for $[Mo(CO)_2(PPh_3)(S_2CNEt_2)_2]$, which oxidizes irreversibly. Interestingly, a solution of the molybdenum(III) carbonyl, $[Mo(CO)(dppe)(S_2CNEt_2)_2]^+$, can be prepared at 0°C by

controlled-potential electrolysis, the IR band of the molybdenum(II) carbonyl at 1930 cm^{-1}, being replaced by a new absorption at 1790 cm^{-1}.

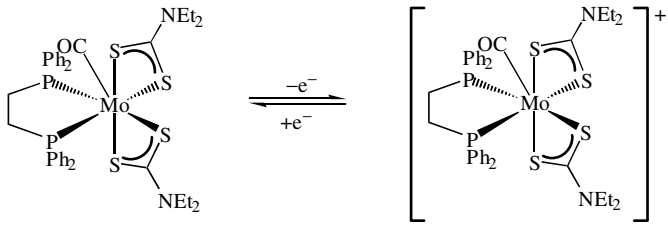

(85)

Oxidation of the molybdenum(II) center with external reagents is often facile. For example, addition of bromine to $[Mo(CO)_3(S_2CNMe_2)_2]$ gives the known molybdenum(IV) complex, $[MoBr_2(S_2CNMe_2)_2]$, which can subsequently be converted into $[Mo(S_2CNMe_2)_4]$ and $[MoOBr_2(S_2CNMe_2)_2]$ upon addition of TlS_2CNMe_2 and Br_2/H_2O, respectively (922). Addition of aryl azides to $[Mo(CO)_2(S_2CNEt_2)_2]$ leads to the molybdenum(VI) bis(imido) complexes, $[Mo(NAr)_2(S_2CNEt_2)_2]$ (Ar = Ph, *p*-tolyl) (832), while with $[Cp_4Fe_4(\mu^3\text{-}S)_4]$ a slow reaction occurs to give the molybdenum(IV) thiol complex, $[Mo(SH)(S_2CNEt_2)_3]$. The latter has been crystallographically characterized, and also shown by magnetic susceptibility measurements to be paramagnetic (μ 2.45 BM at 250 K); adopting a singlet ground state as the temperature is lowered (446).

A range of alkyne complexes, $[Mo(CO)(RC_2R)(S_2CNR_2)_2]$ and $[Mo(RC_2R)_2(S_2CNR_2)_2]$, have been extensively studied. The former are prepared from the addition of a slight excess of alkyne to $[Mo(CO)_n(S_2CNR_2)_2]$ ($n = 2, 3$) or *via* alkyne exchange reactions with $[Mo(CO)(HC_2H)(S_2CNEt_2)_2]$ (930), the latter providing a good synthetic route to complexes, which do not chromatograph well (931). Bennett and Boyd (819) also prepared the cyclooctyne derivatives, $[Mo(CO)(C_8H_{12})(S_2CNR_2)_2]$ (R = Me, Et), upon addition of cyclooctyne to $[Mo(CO)_2(PPh_3)(S_2CNR_2)_2]$.

Addition of excess alkyne to $[Mo(CO)_2(S_2CNR_2)_2]$ (350,369,932) or $[Mo(CO)(RC_2R)(S_2CNR_2)_2]$ (933) affords bis(alkyne) complexes, $[Mo(RC_2R)_2(S_2CNR_2)_2]$ (350). Templeton and co-workers (933) studied the kinetics of the conversion of mono to bis(alkyne) complexes, which they propose proceeds via carbonyl loss, the relative rate of substitution corresponding to the relative electron-withdrawing ability of the bound alkyne. Further, when the free alkyne differs from the bound alkyne, exchange occurs, the second order rate expression found being consistent with an associative mechanism. Due to the alkyne exchange it has proved difficult to prepare mixed-alkyne complexes, although the synthesis of $[Mo(PhC_2H)(EtC_2Et)(S_2CNMe_2)_2]$ has been achieved from

$[Mo(CO)(PhC_2H)(S_2CNMe_2)_2]$ (Eq. 86) (933).

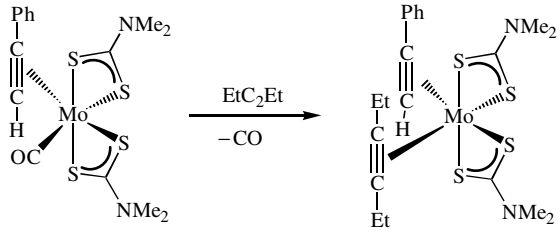

(86)

The parent bis(alkyne) complexes, $[Mo(HC_2H)_2(S_2CNR_2)_2]$ (R = Me, Et), have remained somewhat elusive, although trace amounts have been prepared from $[Mo(CO)(HC_2H)(S_2CNR_2)_2]$ and acetylene in an autoclave (369). With pyrrole dithiocarbamate, the bis(alkyne) complexes form far more readily that with dialkyl dithiocarbamates, an effect that is attributed to the decreased electron density at the metal center in the former. In support of this hypothesis, both solid state and solution data for $[Mo(CO)_3(S_2CNC_4H_4)_2]$ reflect the reluctance of the pyrrole nitrogen to provide π-electron density to the CS_2 fragment. This difference is also reflected in the synthesis of $[Mo(HC_2H)_2(S_2CNC_4H_4)_2]$, albeit in low (10%) yield (350).

The crystal structure of $[Mo(MeC_2Me)_2(S_2CNC_4H_4)_2]$ has been reported. The geometry of the molecule is a distorted octahedron, the two alkynes residing cis to one another, each adopting a bent geometry with the methyl groups directed away from the metal center (350). In solution, the bis(alkyne) complexes are fluxional and two independent fluxional processes have been identified (350,369); (1) a low-energy rotation about the carbon–nitrogen bonds of the dithiocarbamates, and (2) a higher energy rotation of the alkynes, an activation barrier of 64 kJ mol^{-1} being estimated for $[Mo(EtC_2Et)_2(S_2CNMe_2)_2]$ (369). Went and co-workers (931) prepared the bis(1,4,7-trithiacycloundec-9-yne) complex, $[Mo(RC_2R)_2(S_2CNMe_2)_2]$, and on the basis of the ^{13}C NMR shifts for the alkyne carbons (δ181.4 and 178.5) suggest that each acts as a three-electron donor.

A number of further reactions of $[Mo(CO)(RC_2R)(S_2CNR_2)_2]$ have been probed. With electron-deficient olefins, mixed alkyne–olefin complexes are generated upon carbonyl loss (934), while addition of nucleophiles to $[Mo(CO)(RC_2R)(S_2CNMe_2)_2]$ results in rapid alkyne loss even at room temperature affording $[Mo(CO)L_2(S_2CNMe_2)_2]$ [L = CO, PEt_3, $P(OMe)_3$] (933). In further work, Bennett and Boyd (818) showed that addition of halides to the cyclooctyne complexes, $[Mo(CO)(C_8H_{12})(S_2CNR_2)_2]$ (R = Me, Et) affords molybdenum(IV) complexes, $[MoX_2(C_8H_{12})(S_2CNR_2)_2]$ (X = Br, I), in which the carbonyl is lost, but the alkyne retained.

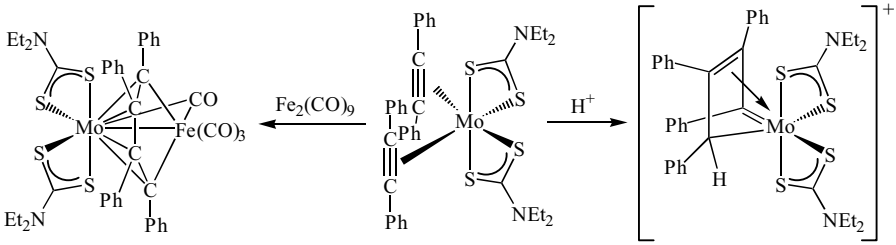

112

Figure 98. Selected reactions of $[Mo(PhC_2Ph)_2(S_2CNEt_2)_2]$.

Molecular orbital calculations have been used to rationalize the relative inertness of 16-electron bis(alkyne) complexes, which is due to destabilization of the vacant $d\pi$–LUMO resulting from alkyne $\pi_\perp$ donation (369,821). They do, however, still undergo a number of reactions (Fig. 98). Addition of $Fe_2(CO)_9$ to $[Mo(PhC_2Ph)_2(S_2CNEt_2)_2]$ gives heterobimetallic $[MoFe(CO)_3(S_2CNEt_2)(\mu\text{-}CO)(\mu\text{-}\eta^1,\eta^2,\eta^2,\eta^1\text{-}C_4Ph_4)]$ (**112**), in which the two alkynes have coupled (935), while protonation with HBF_4 leads to a similar carbon–carbon coupling to give the butadienyl cation, $[Mo(\eta^4\text{-}C_4Ph_4H)(S_2CNEt_2)_2]^+$ (936) (see Section IV.C.3.g).

In other contributions, Baker et al. (926,937) detailed the preparation of seven-coordinate group 15 (VA) compounds, $[MoI(CO)_3(EPh_3)(S_2CNR_2)]$ ($R = Et$, Bz; $E = P$, As, Sb) and $[Mo(CO)_3(S_2CNBz_2)(\mu\text{-}I)]_2$, together with related alkyne complexes, $[MoI(CO)(EtC_2Et)\{P(OPh)_3\}(S_2CNR_2)]$ ($R = Me$, Et) (**113**), prepared upon addition of dithiocarbamate salts to $[MoI_2(CO)(MeCN)(EtC_2Et)\{P(OPh)_3\}]$ (938).

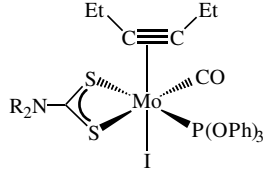

113

Molybdenum(II) allyl complexes, $[Mo(CO)_2(\eta^3\text{-}C_3H_5)(MeCN)(S_2CNR_2)]$ ($R = Et$; $R_2 = C_4H_8$) (**114**), can be prepared upon addition of allyl bromide to $[Mo(CO)_4(S_2CNR_2)]^-$, or dithiocarbamate salts to $[Mo(CO)_2(\eta^3\text{-}C_3H_5)(MeCN)_2Br]$ (939,940). A number of reactions have been carried out (Fig. 99). Addition of pyridine gives $[Mo(CO)_2(py)(\eta^3\text{-}C_3H_5)(S_2CNR_2)]$ (**115**) (939), which is also formed upon addition of dithiocarbamate salts to $[Mo(CO)_2(\eta^3\text{-}C_3H_5)(py)_2Br]$ (940). The pyridine complexes are useful synthetic intermediates

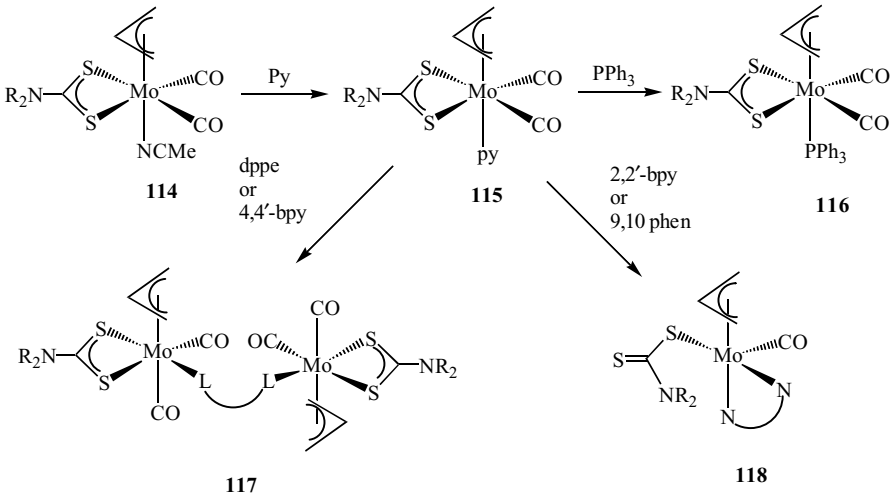

Figure 99. Synthesis and reactivity of $[Mo(CO)_2(py)(\eta^3\text{-}C_3H_5)(S_2CNR_2)]$.

as pyridine is readily lost, for example, upon addition of PPh_3, affording $[Mo(CO)_2(PPh_3)(\eta^3\text{-}C_3H_5)(S_2CNR_2)]$ (**116**). With 4,4′-bpy and dppe (L_2), binuclear complexes (**117**) result with either bridging carbonyls, $[Mo_2(\eta^3\text{-}C_3H_5)_2(S_2CNEtR)_2(dppe)_2(\mu\text{-}CO)_2]$ or bridging ligands $[Mo_2(\eta^3\text{-}C_3H_5)_2(S_2CNEtR)_2(CO)_2(\mu\text{-}L_2)]$, while addition of 1,10-phenanthroline (phen) or 2,2′-bpy leads to chelate complexes in which the dithiocarbamate is now monodentate (**118**) (241). Related monodentate dithiocarbamate complexes, $[Mo(\eta^1\text{-}S_2CNHR)(\eta^3\text{-}C_3H_5)(CO)_2(2,2'\text{-bpy})]$ (R = Me, Et), have also been prepared from the reaction of $[MoBr(\eta^3\text{-}C_3H_5)(CO)_2(2,2'\text{-bpy})]$ with dithiocarbamate salts (242).

The acetonitrile complexes, $[Mo(CO)_2(NCMe)(\eta^3\text{-}C_3H_5)(S_2CNR_2)]$ (R = Et; $R_2 = C_4H_8$) (**114**), are also versatile synthetic intermediates, reacting with diphosphines at reflux to give $[Mo(CO)(\eta^3\text{-}C_3H_5)(Ph_2XPPh_2)(S_2CNR_2)]$ (X = CH_2, CH_2CH_2, NH) (939, 941, 942). They exist as mixtures of *endo*-**119** and *exo*-**120** isomers (Fig. 100) that interconvert in solution, as shown by NMR spectroscopy. The dppm ligand (X = CH_2) favors the formation of the exo products, while with dppe (X = CH_2CH_2) endo isomers dominate, and are the only product with dppa (X = NH). Activation barriers to exo–endo interconversion are somewhat greater for dppm versus dppe complexes, being attributed to the smaller bite angle of the former.

Carmona and co-workers (943–945) detailed the synthesis and structure of molybdenum(II) complexes bearing an agostic acyl ligand. Thus, addition of dithiocarbamate salts to $[MoCl(CO)(PMe_3)_3\{\eta^2\text{-}C(O)CH_2X\}]$ (X = H, $SiMe_3$)

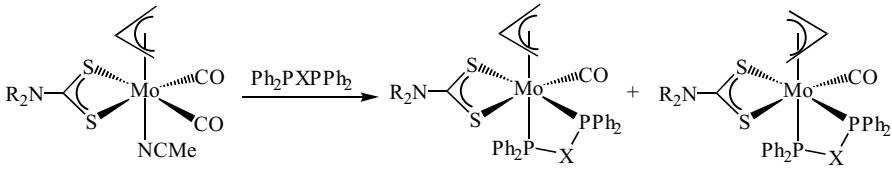

114 *endo* **119** *exo* **120**

Figure 100. Generation of exo and endo isomers of $[Mo(CO)(\eta^3\text{-}C_3H_5)(Ph_2PXPPh_2)(S_2CNR_2)]$.

affords agostic acyl complexes $[Mo(CO)(PMe_3)_2(S_2CNR_2)\{\eta^1\text{-}C(O)CH_2X\}]$ ($R = Me$, *i*-Pr; $R_2 = C_5H_{10}$), which attain an 18-electron configuration through a β-carbon–hydrogen bond rather than dihapto coordination of the acyl group. In contrast, addition of the pyrrole dithiocarbamate salt gives complexes $[Mo(CO)(PMe_3)_2(S_2CNC_4H_4)\{\eta^2\text{-}C(O)Me\}]$, with a dihapto acyl ligand. This different behavior has been ascribed to the weaker donor ability of pyrrole dithiocarbamate (which is more similar to a xanthate) relative to dialkyl dithiocarbamates (943), although small steric and electronic changes about the metal center may also be important. Interestingly, in more recent work complexes $[Mo(CO)(PMe_3)_2(S_2CNMe_2)\{\eta^2\text{-}C(O)CH_2SiMe_2R\}]$ ($R = Me$, Ph) have been shown to exist as an isomeric mixture of β-agostic **121** and η^2-acyl **122** forms in solution (Fig. 101), the agostic form of $[Mo(CO)(PMe_3)_2(S_2CNMe_2)\{\eta^2\text{-}C(O)CH_2SiMe_3\}]$ being the subject of a crystallographic study (946) (Fig. 101).

j. Zero-Valent Complexes. A number of zero-valent complexes, $[Mo(CO)_4(S_2CNR_2)]^-$, have been prepared (198,757,947–950) and some preliminary reactivity studies have been carried out (948,951). Synthetic methods include heating dithiocarbamate salts and $Mo(CO)_6$ (757,948–950) or $[Mo(CO)_4(bpy)]$ (950), reaction of *cis*-$[Mo(CO)_4(piperidine)_2]$ with dithiocarbamate

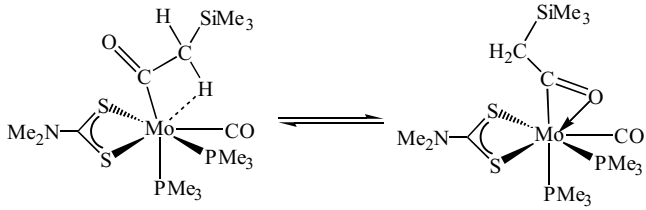

121 **122**

Figure 101. β-Agostic (**121**) and η^2-acyl (**122**) forms of $[Mo(CO)(PMe_3)_2(S_2CNMe_2)\{C(O)CH_2SiMe_3\}]$.

salts ($R_2 = C_4H_8$, C_5H_{10}) (947), and deprotonation of *cis*-[$Mo(CO)_4$(piperidine)$_2$] by *n*-BuLi in the presence of carbon disulfide ($R_2 = C_5H_{10}$) (198). All are easily characterized by IR spectroscopy with the observation of four bands in the carbonyl region of the spectrum. The X-ray structure of [NEt_4][$Mo(CO)_4(S_2CNEt_2)$] (**123**) has been carried out and reveals the expected distorted octahedral geometry, and electrochemical studies show that dithiocarbamate is lost upon oxidation (948). Interestingly, when the thermal reaction of dithiocarbamate salts with $Mo(CO)_6$ is carried out in acetone, pentacarbonyl anions $[Mo(CO)_5(S_2CNR_2)]^-$ are seen by IR spectroscopy ($R = Et$; $R_2 = C_4H_8$) and in one instance, this is the major product, namely, $[Mo(CO)_5(S_2CNHMe)]^-$ (950). The instability of these compounds has precluded their full characterization, but the dithiocarbamate probably binds in a monodentate fashion.

The reactivity of the tetracarbonyl complexes has been briefly explored (Fig. 102). Oxidation of [NEt_4][$Mo(CO)_4(S_2CNEt_2)$] (**123**) by iodine gives [$Mo(CO)_2(S_2CNEt_2)_2$] (**124**), aerobic oxidation affords [$MoO(S_2CNEt_2)_2$] (**125**), and exposure to iodine in air gives [$Mo_2O_2(\mu\text{-}O)(S_2CNEt_2)_4$] and [$MoO(\mu\text{-}O)(S_2CNEt_2)_2]_2$ (948). Addition of $[MoS_4]^{2-}$ to [NEt_4][$Mo(CO)_4(S_2CNEt_2)$] results in the clean loss of the dithiocarbamate ligand affording $[(CO)_4Mo(\mu\text{-}S)_2Mo(\mu\text{-}S)_2Mo(CO)_4]^{2-}$ (951), while reaction with $Li_2[Fe_2(CO)_6(\mu\text{-}S_2)]$ yields a novel diamagnetic trinuclear cluster, $[MoFe_2(\mu^3\text{-}S)_2(CO)_8(S_2CNEt_2)][NEt_4]$, shown by crystallography to contain a distorted tetragonal-pyramidal core and a molybdenum(0) dithiocarbamate center with trans carbonyls (952).

k. Binuclear Complexes. A wide-range of dimolybdenum dithiocarbamate complexes have been reported, including an extensive series of oxo-, sulfido-, and imido-containing species. The vast majority contain two molybdenum(V) ions, although the +2 and +3 states are also accessible. There has been a continuing debate about the identity of complexes of the formula [$Mo_2(S_2CNR_2)_4$] (953). As early as 1973, Ricard et al. (954,955) showed that a complex of this stoichiometry, formed from the reaction of [$Mo_2(\mu\text{-}OAc)_4$] and 4 equiv of dithiocarbamate salt, was in fact the molybdenum(IV) dimer [$Mo(\mu\text{-}S)(S_2CNPr_2)(\eta^2\text{-}SCNPr_2)]_2$ (see Section V).

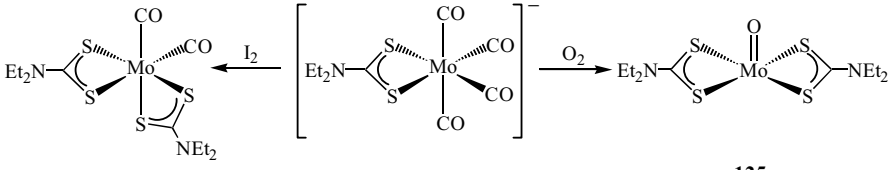

Figure 102. Selected reactions of $[Mo(CO)_4(S_2CNEt_2)]^-$.

More recently, addition of 2 equiv of NaS_2CNEt_2 to $[Mo_2(\mu\text{-}OAc)_4]$ in methanol has been reported to give the green molybdenum(II) dimer, $[Mo_2(S_2CNEt)_4]$ (**126**) (70,909), which in turn reacts slowly with air generating purple $[Mo_2O_3(S_2CNEt_2)_4]$ (909). Green $[Mo_2(S_2CNEt)_4]$ also results from dithiocarbamate addition to $MoCl_5$ followed by zinc reduction. A crystallographic study reveals that two of the dithiocarbamates bridge the dimolybdenum center in a μ,η^1-fashion, with two normal ($\sim$ 2.4 Å) and one long [2.826(2) Å] molybdenum–sulfur bonds, while the metal–metal distance of 3.85(1) Å suggests that there is no direct bond (956).

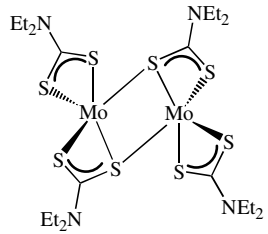

126

Addition of excess $KS_2CNC_4H_4$ to $[Mo_2(\mu\text{-}OAc)_4]$ in THF is reported to yield purple $[Mo_2(S_2CNC_4H_4)_4].2THF$ (952). The structure is unknown, although the electronic spectrum has been interpreted in terms of a molybdenum–molybdenum quadruple bond. Addition of 4 equiv of dithiocarbamate salt to $[Mo_2(\mu\text{-}OAc)_4]$, followed by addition of Ph_3PO affords *cis*-$[Mo_2(\mu\text{-}OAc)_2(\mu\text{-}S_2CNC_4H_4)_2.OPPh_3]$ (**127**), which has been crystallographically characterized (355). This confirms the cis coordination of the bridging dithiocarbamates and also coordination of a single $OPPh_3$ group despite addition of 2 equiv. Further, the molybdenum–molybdenum bond length of 2.134(1) Å suggests multiple bond character (355). The precise reason for the different behavior of diethyl and pyrrole dithiocarbamates has been suggested to result from the enhanced stability of the dithioacid resonance structure for the latter (355).

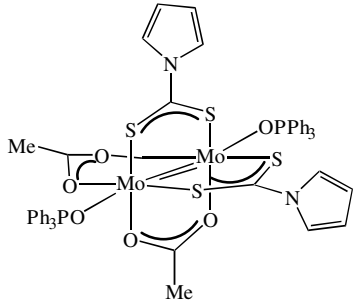

127

A range of pyridine adducts, $[Mo_2(S_2CNR_2)_4(py)_2]$, have also been claimed, with DSC and TGA studies showing that the bases are lost upon heating, activation energies ranging from 155 to 565 kJ mol^{-1} (957).

There also remains some debate regarding the precise nature of dimeric molybdenum(III) complexes, $[Mo_2(S_2CNR_2)_6]$, formed from reactions of thiuram disulfides with $[Mo(CO)_6]$ and $[Mo(CO)_3(\eta^6\text{-}C_7H_8)]$ (174,175,177). Brown et al. (174) reported that heating $[Mo(CO)_3(\eta^6\text{-}C_7H_8)]$ and tetraethylthiuram disulfide in toluene for 15 min affords red-brown $[Mo_2(S_2CNEt_2)_6]$, while when the same reaction is carried out in the dark the black mononuclear molybdenum(IV) complex, $[Mo(S_2CNEt_2)_4]$, is the sole product. The dimeric complexes are sensitive to oxidation, $[Mo_2(S_2CNEt_2)_6]$ generating $[Mo(S_2CNEt_2)_4]X$ ($X = Cl$, 0.5 Mo_6O_{19}) and $[Mo_2(\mu\text{-}S)(S_2CNR_2)_6]$ (Eq. 87) in aerated chloroform and toluene, respectively (781,782,788). The source of sulfur in the latter is unknown, but a crystallographic study shows that it is approximately symmetrically bound with a Mo–S–Mo angle of 157.2° (788). Oxidation can also be carried out by iodine affording $[Mo(S_2CNEt_2)_4]I$ (787).

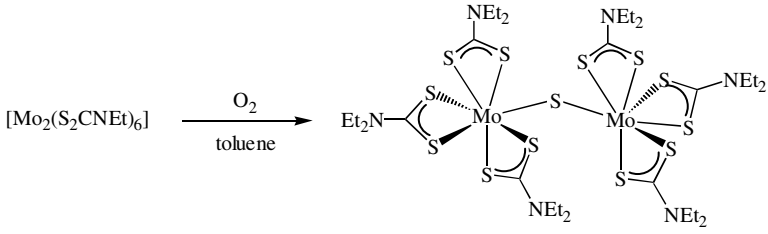

(87)

Seymore and Brown (434) recently prepared dimeric molybdenum(IV) complexes, $[Mo_2(S_2CNR_2)_4(\mu\text{-}S_2CNR_2)_2][OTf]_2$ ($R = Me$, Et), via halide abstraction from $[Mo(S_2CNR_2)_3Cl]$ by silver triflate (Eq. 88). A crystallographic study ($R = Et$) shows that the cation consists of two pentagonal bipyramids sharing an axial site, a motif previously seen in $[Os_2(S_2CNEt_2)_4(\mu\text{-}S_2CNEt_2)_2][PF_6]_2$ (296). The molybdenum–molybdenum bond length of 2.8462(8) Å is suggestive of a significant degree of metal–metal bonding, and molecular orbital calculations and their diamagnetic nature substantiate this. Nevertheless, it is readily cleaved upon addition of donor ligands, providing a useful synthetic route to molybdenum(IV) dithiocarbamate complexes. For example, addition of phosphines quantitatively gives paramagnetic adducts, $[Mo(S_2CNEt_2)_3(PR_3)][OTf]$, while reaction with sodium azide initially yields, $[Mo(S_2CNEt_2)_3(N_3)]$. The latter loses nitrogen slowly to afford the known nitride complex, $[MoN(S_2CNEt_2)_3]$, which reacts with more molybdenum(IV) dimer to produce nitride-bridged $[Mo_2(S_2CNEt_2)_6(\mu\text{-}N)][OTf]$, as shown by NMR and fast atom

bombardment mass spectrometry (FABMS).

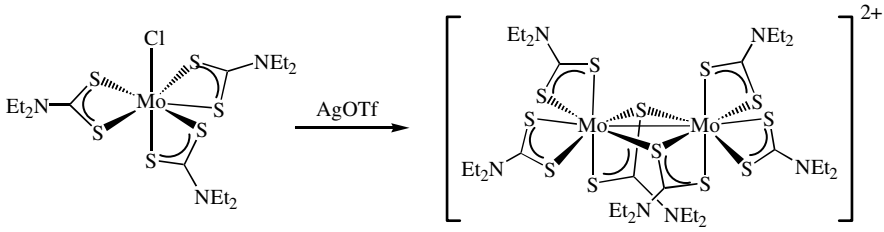

(88)

i. *Molybdenum(V) Oxo and Sulfido Complexes.* A wide-range of dimeric molybdenum(V) complexes have been reported, supported primarily by strong π-donor oxo, sulfido, and imido ligands. In a number of instances, metal coordination is entirely by sulfur. For example, bis(disulfide)-bridged complexes, $[Mo_2(\mu\text{-}S_2)_2(S_2CNR_2)_4][BF_4]_2$ (R = Et, *i*-Pr, *i*-Bu), have been prepared from the reaction of $[MoO(S_2CNR_2)_3][BF_4]$ with boron sulfide under anaerobic conditions (Eq. 89), a transformation that overall represents a coupled redox and dithiocarbamate ligand redistribution process (181,775,958). A crystallographic study (R = Et) shows that it is the ΔΛ (meso) diastereomer that predominates, the molybdenum–molybdenum vector [Mo—Mo 2.808(1) Å] being bridged by two noninteracting disulfide units [av. S–S 2.01(2) Å] (181,958). Addition of LiTCNQ in methanol affords $[Mo_2(\mu\text{-}S_2)_2(S_2CNR_2)_4][TCNQ]_n$ (R = Me, Et; $n = 2$), while further addition of TCNQ gives a second complex ($n = 3$). The ESR spectra reveal the existence of a TCNQ radical anion, and an X-ray structure ($n = 3$) shows that the trication is centrosymmetric [Mo-Mo 2.817(2); S-S 2.001(2) Å], while TCNQ forms centrosymmetric trimers with a slipped conformation (959).

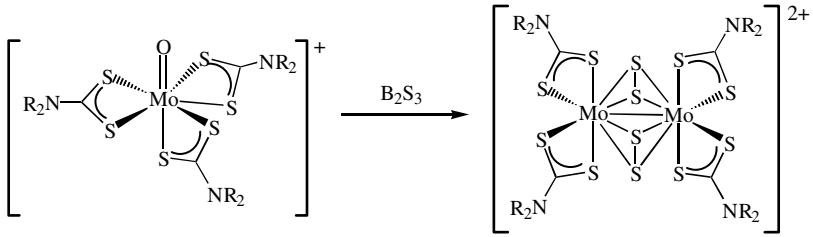

(89)

More common fully sulfur-ligated complexes are red $[MoS(\mu\text{-}S)(S_2CNR_2)]_2$ (**128**) (Fig. 103). A variety of synthetic methods have been adopted to generate

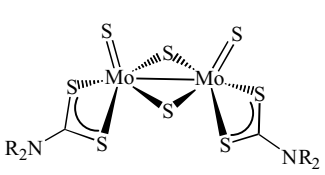

128

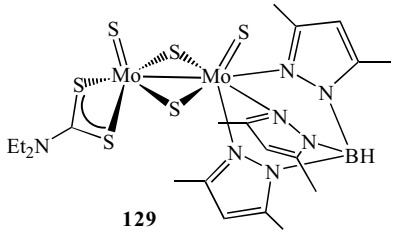

129

Figure 103. Dithiocarbamate complexes with the $Mo_2S_2(\mu\text{-}S)_2$ core.

these species including; substitution using P_2S_5 of oxo ligands in $[MoO(\mu\text{-}O)(S_2CNR_2)]_2$ (960) or $[MoO_2(S_2CNR_2)_2]$ (961), reaction of $[MoS_4]^{2-}$ with dithiocarbamate salts (961) including those derived from α-amino acids (128), and reactions of $[Mo_2(S_2)_6]^{2-}$ with excess dithiocarbamate salt in ethanol (962), or with 4 equiv of dithiocarbamate salt in the presence of PPh_3, the phosphine sulfide being generated quantitatively in the latter reaction (963,964). The related selenide species, $[MoSe(\mu\text{-}Se)(S_2CNR_2)]_2$, have also been prepared from the reaction of $[MoO_2(S_2CNR_2)_2]$ with aluminum selenide (965).

A number of crystallographic studies have been carried out (962,963,966). All show a syn configuration of dithiocarbamate ligands and molybdenum–molybdenum single bonds [R = Et, Mo—Mo 2.817(2) Å]. A related complex, $[Tp^*Mo_2S_2(\mu\text{-}S)_2(S_2CNEt_2)]$ (**129**) (Fig. 103), a byproduct of the reaction of $[Tp^*MoO(S_2CNEt_2)]$ with boron sulfide, adopts a similar structure [Mo—Mo 2.829(2) Å] (918).

Mixed oxo–sulfido complexes are common. In a series of papers, Musha et al. (960,967–969) reported the separation and interconversion of complexes, $[Mo_2O_nS_{4-n}(S_2CNR_2)_2]$ (R = Bu; R_2 = EtHex), prepared from reactions of dithiocarbamate salts with $MoCl_5$ in water or MoO_3 and sodium hydrogen sulfide. Thus, oxidation of $[MoS(\mu\text{-}S)(S_2CNEtHex)]_2$ affords sequentially the tris- and bis(sulfido) complexes, in which the terminal sites are replaced, but even under forcing conditions the bridging sulfides remain intact (Fig. 104) (968).

Similarly, addition of PPh_3 or cyanide to $[Mo_2OS(\mu\text{-}S)_2(S_2CNR_2)_2]$ affords $[MoO(\mu\text{-}S)(S_2CNR_2)]_2$, however, heating mixtures of $[MoO(\mu\text{-}S)(S_2CNR_2)]_2$ and $[MoS(\mu\text{-}S)(S_2CNR_2)]_2$ does not lead to any ligand exchange, while $[MoO(\mu\text{-}S)(S_2CNR_2)]_2$ also fails to react with elemental sulfur (970). Other synthetic methods to complexes $[MoO(\mu\text{-}S)(S_2CNR_2)]_2$ include the slow reduction of $[MoO_4]^{2-}$ by dithiocarbamate salt (R = Et) (962), addition of dithiocarbamate salts (R = Me, Bz) to $[NH_4]_2[MoO_2S_2]$ (971), and reduction of $[MoO(S_2)(S_2CNR_2)_2]$ (R = Me, Et, Pr) by thiophenol (874). The pyrrolidine dithiocarbamate complex ($R_2 = C_4H_8$) has been prepared by three methods: oxidation of the tetrasulfide by Cu^{2+} or Ni^{2+} (963), addition of Na_2S_5 to

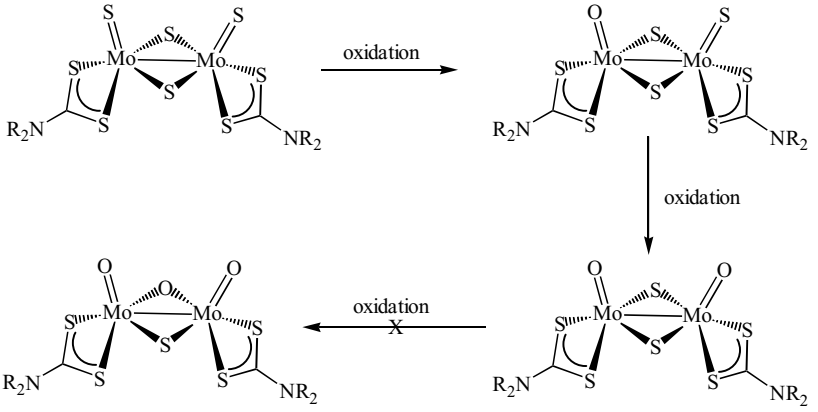

Figure 104. Oxidation of $[MoS(\mu\text{-}S)(S_2CNR_2)]_2$.

$[Mo(CO)_5I]^-$ in the presence of dithiocarbamate salt (770); and in very low yield upon heating $[Mo(CO)_6]$ with dithiocarbamate salt in DMSO (972). Trisulfide complexes, $[Mo_2OS(\mu\text{-}S)_2(S_2CNR_2)_2]$, can be prepared in high yields upon reduction of $[MoS_4]^{2-}$ by sodium dithionate in the presence of dithiocarbamate salts (970,973) or upon addition of hydrogen sulfide to either $[MoO_2(S_2CNR_2)_2]$ (Eq. 90) or $[MoO(\mu\text{-}O)(S_2CNR_2)]_2$ (R = Me, Et, Bu; $R_2 = C_4H_8$, C_5H_{10}) (970).

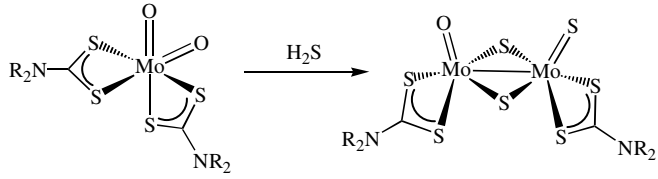

(90)

A large number of crystallographic studies have been carried out. All show the syn arrangement of dithiocarbamate ligands and molybdenum–molybdenum distances indicative of a single bond (770,874,963,967,970,972–975). These include the unsubstituted dithiocarbamate complex, *syn*-$[MoO(\mu\text{-}S)(S_2CNH_2)]_2$ [Mo—Mo 2.820(1) Å], generated from ammonium molybdate and ammonium dithiocarbamate (974), which undergoes an irreversible two-electron reduction, being associated with dithiocarbamate loss.

A number of publications detail dimeric molybdenum(V) complexes with three bridging ligands. Thiolate-bridged, $[Mo_2O_2(\mu\text{-}O)(\mu\text{-}SPh)_2(S_2CNMe_2)_2]$, is prepared upon addition of thiophenol to $[MoO_2(S_2CNMe_2)_2]$ in methanol (Eq. 91), and contains a short metal–metal interaction [Mo—Mo 2.649(1) Å]

(976) as do $[Mo_2O_2(\mu\text{-}S)(\mu\text{-}SCH_2CH_2O)(S_2CNEt_2)_2]$ [Mo—Mo 2.628(1) Å] (977) and $[Mo_2O_2(\mu\text{-}S)(\mu\text{-}SCH_2CH_2O)(S_2CN\text{—}i\text{-}Bu_2)_2]$ [Mo—Mo 2.595(2) Å] (978). Some of these triply bridged complexes have been investigated extensively by cyclic voltammetry (CV) and ^{95}Mo NMR spectroscopy (978). In the former, two successive one-electron reductions are observed, potentials correlating well with the Taft polar substituent constants for the dithiocarbamates, while ^{95}Mo chemical shifts vary between δ 329 (R = Me) and 354 (R = *i*-Pr), the line width increasing as a function of dithiocarbamate steric bulk.

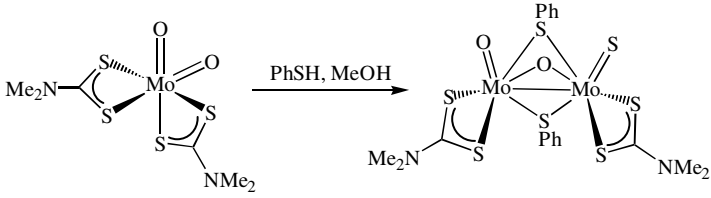

(91)

Dimeric molybdenum(V) dithiocarbamate complexes with only oxo ligands fall into two general types; (1) $[MoO(\mu\text{-}O)(S_2CNR_2)]_2$ (**130**) with metal–metal bonds being analogous to sulfido and oxo–sulfido complexes described above, and (2) $[Mo_2O_2(\mu\text{-}O)(S_2CNR_2)_4]$ (**131**), containing an approximately linear oxo bridge (Fig. 105).

A large number of complexes, $[MoO(\mu\text{-}O)(S_2CNR_2)]_2$, have been prepared from dithiocarbamate salts and $[MoO_4]^{2-}$ upon varying the pH from 8 to 4 (979), while dithiocarbamate derivatives of α-amino acids have been synthesized from $MoCl_5$ in water under an inert atmosphere (125,127). IR spectra are diagnostic; terminal Mo=O absorptions appearing between 930 and 910 cm^{-1}, and bridging Mo–O–Mo bands between 790 and 720 cm^{-1} (979).

Linear oxo-bridged complexes, $[Mo_2O_2(\mu\text{-}O)(S_2CNR_2)_4]$, have also been prepared in a number of ways (59,126,792,794,926,980). Generally, $MoCl_5$ and $[MoO_4]^{2-}$ are again the starting materials, but more unusually, Baker et al. (926) showed that addition of dithiocarbamate salts to molybdenum(II) complexes $[MoI_2(CO)_3(MeCN)(EPh_3)]$ (E = P, As) provides a synthetic route, while

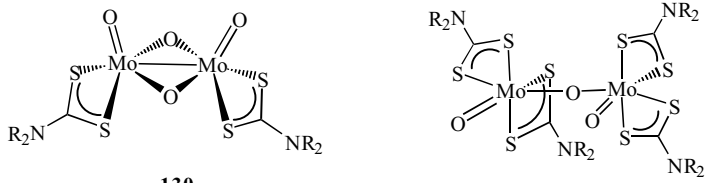

130 **131**

Figure 105. Different types of oxo-bridged dimolybdenum (V) oxo complexes.

complexes $[Mo_2O_2(\mu\text{-}O)(S_2CNR_2)_2(S_2CNR'_2)_2]$ with two different dithiocarbamate ligands have been prepared from $[MoI(CO)_3(EPh_3)(S_2CNR_2)]$. Similar mixed dithiophosphate–dithiocarbamate complexes, $[Mo_2O_2(\mu\text{-}O)(S_2CNEt_2)_2\{S_2P(OR)_2\}_2]$ (R = Et, Pr, *i*-Pr, *i*-Bu), have been prepared via two routes; addition of $[MoO_2(S_2CNEt_2)_2]$ to $[MoO\{S_2P(OR)_2\}_2]$ and the reaction of $[MoO(\mu\text{-}O)(S_2CNEt_2)]_2$ with dithiophosphoric acids (981). Both methods afford the same products, characterized by a singlet resonance in the ^{31}P NMR spectrum, suggesting the intramolecular interchange of ligands (981).

Cooper and co-workers (980) explored the interchange of dithiocarbamate ligands in labeled $[Mo_2O_2(\mu\text{-}O)(S_2{}^{13}CNBz_2)_4]$ by VT ^{13}C NMR spectroscopy. All dithiocarbamate ligands are rendered equivalent by exchange of terminal and bridging oxo groups and a transition state is proposed with two bent oxo bridges (Fig. 106). Interestingly, a crystallographic study shows an anti arrangement of the terminal oxo ligands, which contrasts with the syn arrangement found in $[Mo_2O_2(\mu\text{-}O)(S_2CNEt_2)_4]$ (982). Further, in solution (R = Bz) a mixture of syn and anti isomers is observed suggesting that there is a small free energy difference between the two forms (980).

A number of reactions of these oxo-bridged dimers have been reported. In organic solvents α-amino acid derivatives can be oxidized to $[MoO_2(S_2CNR_2)_2]$, a transformation shown by UV/vis spectroscopy to involve a multistep mechanism (126). Further, from the reaction of $[MoOCl_3]$ and 3 equiv of dithiocarbamate salt in dichloromethane, two types of crystals result, namely, $[Mo_2O_2(\mu\text{-}O)(S_2CNEt_2)_4]$ and $[Mo_2O_2(\mu\text{-}O)(S_2CNEt_2)_4]_3[H_5O_2]$. The latter is formulated as $[Mo_2O_2(\mu\text{-}O)(S_2CNEt_2)_4][H_5O_2].2[Mo_2O_2(\mu\text{-}O)(S_2CNEt_2)_4]$, the ESR spectrum showing two distinct paramagnetic molybdenum centers associated with the $[Mo_2O_2(\mu\text{-}O)(S_2CNEt_2)_4]^-$ anion (982).

In other work, addition of TCNQ to $[Mo_2O_2(\mu\text{-}O)(S_2CNR_2)_4]$ (R = Me, Et, Pr) initially gives $[MoO(S_2CNR_2)_3][TCNQ]$. In one case (R = Et), this is further reduced by PPh_3 to the mixed-valence Mo(V)/Mo(IV) complex, $[Mo_2(\mu\text{-}O)(S_2CNEt_2)_6][TCNQ]$, the presence of a bridging oxo group being supported by IR measurements (436).

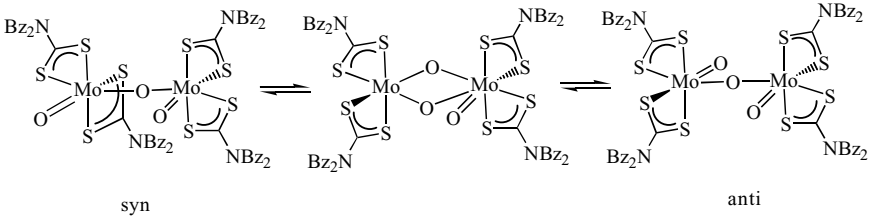

Figure 106. Proposed interconversion of syn and anti isomers of $[Mo_2O_2(\mu\text{-}O)(S_2CNBz_2)_4]$.

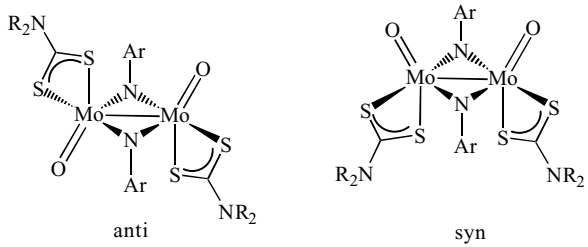

Figure 107. The anti and syn isomers of $[MoO(\mu\text{-}NAr)(S_2CNR_2)]_2$.

ii. *Binuclear Imido Complexes.* A range of binuclear molybdenum(V) imido complexes have been prepared (439,528,840,876,983–986). Mixed oxo–imido complexes $[MoO(\mu\text{-}NAr)(S_2CNR_2)]_2$ are side products of the reaction of $[MoO_2(S_2CNR_2)_2]$ with organic isocyanates (528,983), as are the related sulfido-bridged complexes $[Mo_2O(NR)(\mu\text{-}S)_2(\mu\text{-}S_2CNEt_2)_2]$ (R = *t*-Bu, 2,6-$Me_2C_6H_3$, adamantyl) (983). The former exist as both syn and anti isomers, with the *syn* isomer predominating (Fig. 107) (439).

These react further with organic isocyanates, the nature of the products being dependent on the steric bulk on the isocyanate. Bulky *o*-tolyl isocyanate yields the tetraimido complex, $[Mo(NAr)(\mu\text{-}NAr)(S_2CNEt_2)]_2$ (Ar = *o*-tol), which has been crystallographically characterized (986), and exhibits restricted rotation about the carbon–nitrogen bonds of the imido groups in solution (983). In contrast, the less sterically bulky phenyl and *p*-tolyl isocyanates yield ureato complexes, $[Mo_2(NAr)_2(\mu\text{-}NAr)\{\mu\text{-}ArNC(O)NAr\}(S_2CNR_2)_2]$ (Ar = Ph, *p*-tolyl) (**132**), as a result of the formal addition of 1 equiv of isocyanate to the tetraimido complex (439,806,983,985). Indeed, this is the case. Heating $[Mo_2(NPh)_2(\mu\text{-}NPh)\{\mu\text{-}PhNC(O)NPh\}(S_2CNEt_2)_2]$ in toluene affords $[Mo(NPh)(\mu\text{-}NPh)(S_2CNEt_2)]_2$, which rapidly adds phenylisocyanate to regenerate the ureato bridge (Eq. 92) (439,983,985).

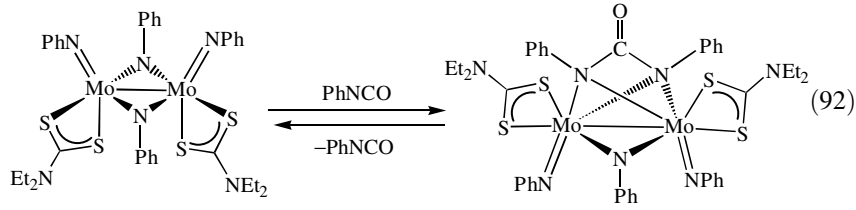

(92)

A crystal structure of $[Mo_2(NPh)_2(\mu\text{-}NPh)\{\mu\text{-}PhNC(O)NPh\}(S_2CNEt_2)_2]$ lends more insight into this process, as the ureato nitrogens are not symmetrically bound to the dimolybdenum center; molybdenum–nitrogen bonds trans [Mo–N(av) 2.158 Å] to the bridging imido ligand being significantly shorter than those cis [Mo–N(av) 2.367 Å] (806,983). Indeed, by NMR spectroscopy

the regioselective loss of one isocyanate from the ureato complex upon heating is clearly seen, and that it is the cis isocyanate that is lost is shown unequivocally by an X-ray crystal structure of $[Mo_2(NAr)_2(\mu\text{-}NAr)\{\mu\text{-}PhNC(O)NAr\}(S_2CNEt_2)_2]$ (Ar = *p*-tol) formed from the reaction of $[Mo_2(NAr)_2(\mu\text{-}NAr)\{\mu\text{-}ArNC(O)NAr\}(S_2CNEt_2)_2]$ with phenyl isocyanate (Eq. 93) (439).

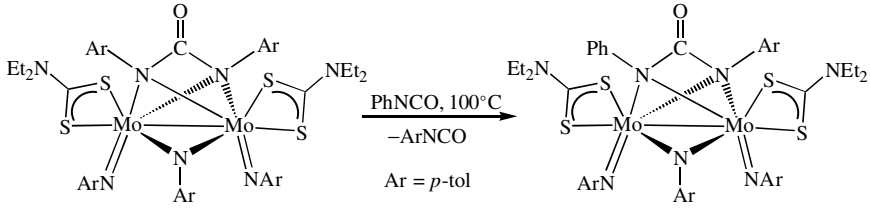

(93)

The ureato complexes (**132**) react with phenyl isothiocyanate to initially afford $[Mo_2(NAr)_2(\mu\text{-}S)\{\mu\text{-}ArNC(O)NAr\}(S_2CNR_2)_2]$ (**133**) (983) resulting from displacement of the bridging-imido ligand, and later $[Mo(NAr)(\mu\text{-}S)(S_2CNR_2)]_n$ [$n = 2$ (**134**), 4 (**135**)] (Fig. 108) (439). The latter have also been prepared from the reaction of dithiocarbamate salts with $[Mo(NAr)(\mu^3\text{-}S)\{S_2P(OEt)_2\}]_4$ (Ar = *p*-tol) and exist as an equilibrium mixture of yellow dimeric, $[Mo(NAr)(\mu\text{-}S)(S_2CNR_2)]_2$, and red cubane-like tetrameric, $[Mo(NAr)(\mu^3\text{-}S)(S_2CNR_2)]_4$, complexes in solution (984). Interestingly, the mono-imido complexes, $[Mo_2O(NR)(\mu\text{-}S)_2(\mu\text{-}S_2CNEt_2)_2]$, show no such tendency to dimerize, suggesting that the stronger π-donor ability of the imido ligand is responsible for making the bridging sulfur atoms nucleophilic. Crystal structures of both forms of $[Mo(N\text{-}p\text{-tol})(\mu\text{-}S)(S_2CN{-}i\text{-}Pr_2)]_n$ ($n = 2$, 4) have been carried out and no significant structural differences are seen between dimeric units, molybdenum–sulfur bonds between dimeric units being about 0.3 Å longer than those within them (439,984).

Related to the bis(sulfido)-bridged complexes are tris(sulfido)-bridged $[Mo_2(NAr)_2(\mu\text{-}S)(\mu\text{-}S_2)(S_2CNEt_2)_2]$ (Ar = 2,6-*i*-$Pr_2C_6H_3$, *p*-tol) (**136**) (439,876), low-yield products of the addition of H_2S to $[Mo(NAr)_2(S_2CNEt_2)_2]$, and phenyl isothiocyanate to $[Mo_2(NAr)_2(\mu\text{-}S)\{\mu\text{-}ArNC(O)NAr\}(S_2CNEt_2)_2]$ (Ar = *p*-tol). These trisulfide complexes show the essential features of the proposed Mo_2S_9 unit in molybdenum trisulfide.

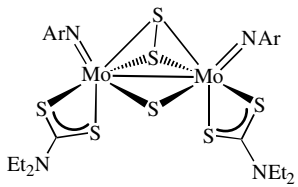

136

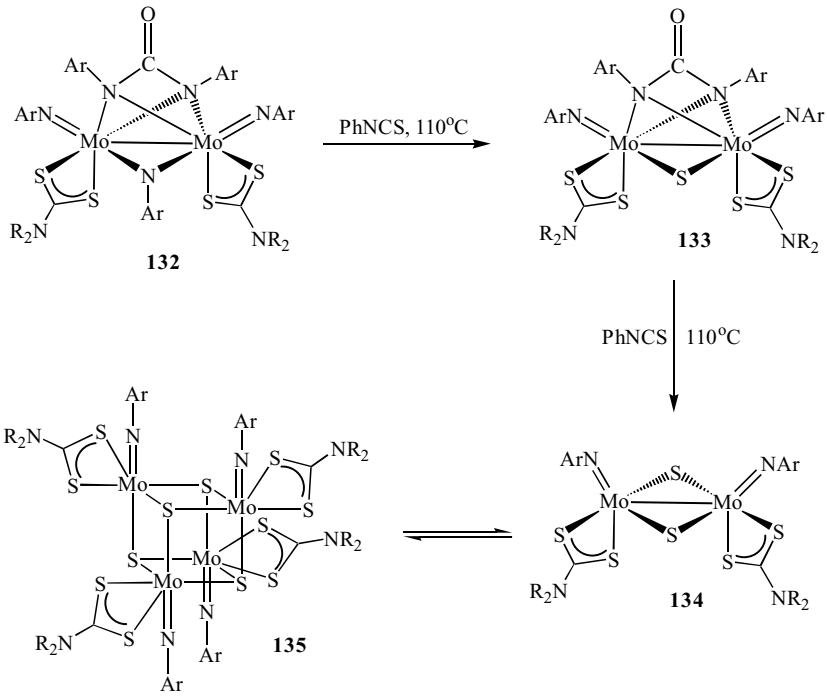

Figure 108. Formation of sulfido-bridge dimolybdenum complexes and the equilibrium between dimeric and cubane forms of $[Mo(NAr)(\mu\text{-}S)(S_2CNR_2)]_{2,4}$.

When oxo complexes $[MoOX_2(S_2CNEt_2)_2]$ ($X = F$, Br; $X_2 = O$) or $[Mo_2O_2(\mu\text{-}O)(S_2CNEt_2)_2]$ are reacted with 2-aminothiophenol, bis(imido)-bridged $[Mo_2O(S_2CNEt_2)_2(\mu\text{-}N\text{-}o\text{-}C_6H_4S)_2]$ (**137**) (Fig. 109) results, which has been crystallographically characterized. This complex has also been shown to undergo a quasi-reversible two-electron reduction by cyclic voltammetry,

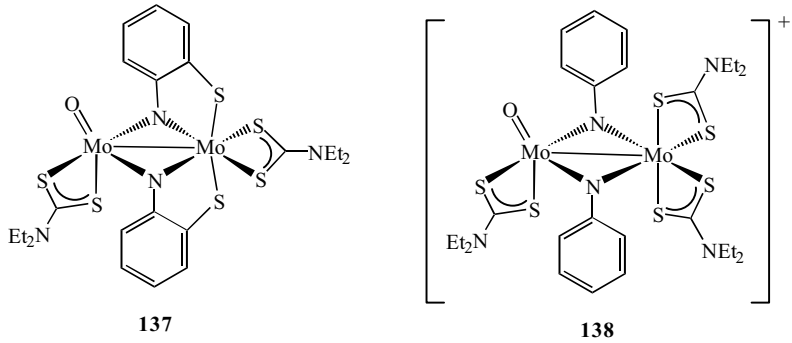

Figure 109. Structurally related imido-bridged dimolybdenum complexes.

presumably generating a molybdenum(IV) dimer (840). A somewhat similar binuclear unit is found in $[Mo_2O(\mu\text{-}NPh)_2(S_2CNEt_2)_3][BF_4]$ (**138**) (Fig. 109), the major product of the reaction of $[MoO(\mu\text{-}NPh)(S_2CNEt_2)]_2$ with HBF_4 (983).

In contrast, protonation of $[MoO(\mu\text{-}N\text{-}o\text{-}tol)(S_2CNEt_2)]_2$ with CF_3CO_2H yields tetrameric, $[\{Mo_2O(S_2CNEt_2)(\mu\text{-}N\text{-}o\text{-}tol)_2(\eta^1\text{-}O_2CCF_3)\}_2(\mu\text{-}O)(\mu\text{-}O_2CCF_3)_2]$ (**139**), through loss of a dithiocarbamate from one molybdenum center (439).

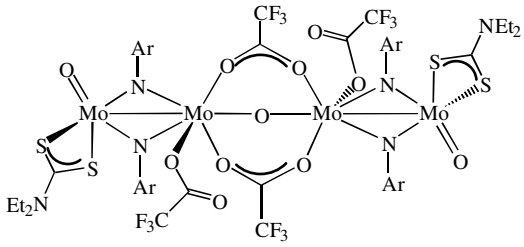

139

l. Tri- and Tetranuclear Clusters. A large number of cationic trimolybdenum clusters of the type $[Mo_3(\mu^3\text{-}S)(\mu\text{-}S_2)_3(S_2CNR_2)_3]X$ (962,987,998) and related seleno (987,999–1002) and mixed-sulfido–seleno (1003,1004) complexes have been reported (Fig. 110).

Synthesis of the sulfides has been achieved in a number of ways. Mixtures of $[MoS_4]^{2-}$, a copper or silver halide, ammonium and dithiocarbamate salts have been utilized (989, 990, 992), as has addition of dithiocarbamate salts to preformed clusters, $[Mo_3(\mu^3\text{-}S)(\mu\text{-}S_2)_3(oxq)_3]^+$ (Hoxq = 8-hydroxyquinoline) (988), $[Mo_3(\mu^3\text{-}S)(\mu\text{-}S_2)_3Br_6]^{2-}$ (994,997,1001), and thiuram disulfides to $[Mo_3(\mu^3\text{-}S)(\mu\text{-}S_2)_3Br_6]^{2-}$ (994). Novelly, $[Mo_3(\mu^3\text{-}S)(\mu\text{-}S_2)_3(S_2CNEt_2)_3][S_2CNEt_2]$, has been prepared from $[Mo_3(\mu^3\text{-}S)(\mu\text{-}S_2)_3Br_6][NEt_4]_2$ in a mechanoactivated solid-state reaction involving the addition of the reagents in a vacuum ball mill (1001). Metathesis reactions have been widely used to extend the range

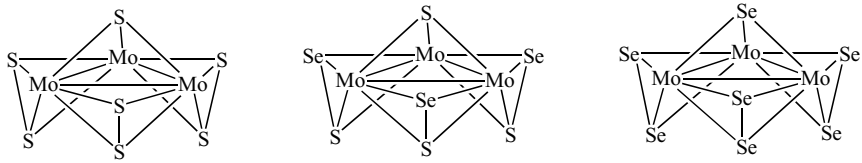

Figure 110. Cluster core geometries in $[Mo_3(\mu^3\text{-}E)(E_2)_3(S_2CNR_2)_3]^+$ cations.

of cations (987,993,995–997), while one example ($R_2 = C_4H_8$, X = I) has been isolated from the reduction of $[MoS(\mu\text{-}S)(S_2CNC_4H_8)]_2$ by Cu^{2+} or Ni^{2+} (963).

Selenium analogues, $[Mo_3(\mu^3\text{-}Se)(\mu\text{-}Se_2)_3(S_2CNR_2)_3]X$, have also been prepared from $[Mo_3Se_7X_4]$ (X = Cl, Br) upon addition of dithiocarbamate salts (999,1000) and via metathesis reactions (987). Mixed-sulfur–selenium compounds, $[Mo_3(\mu^3\text{-}S)(\mu\text{-}SSe)_3(S_2CNR_2)_3]^+$, have been synthesized upon reduction of $[Mo_3(\mu^3\text{-}S)(\mu\text{-}S_2)_3Br_6]^{2-}$ by PPh_3 in the presence of $Se(S_2CNR_2)_2$ (1004), and from the reaction of $[Mo_3(\mu^3\text{-}S)(\mu\text{-}S_2)_3(S_2CNR_2)_3][S_2CNR_2]$ with KSeCN (1003). Very recently, Almond et al. (1002) reported a simple high-yielding synthesis of $[Mo_3(\mu^3\text{-}Se)(\mu\text{-}Se_2)_3(S_2CNEt_2)_3]_2Se$, being formed upon thermolysis of $Mo(CO)_6$, tetraethylthiuram disulfide and selenium in refluxing 1,2-dichloromethane.

In one instance, a related tellurium complex has been reported. Reaction of $KS_2CN(CH_2CH_2OH)_2$ with a mixture of the elements, molybdenum, tellurium, and iodine at high temperature leads to the isolation of $[Mo_3(\mu^3\text{-}Te)(\mu\text{-}Te_2)_3\{S_2CN(CH_2CH_2OH)_2\}_3]I$ (1005).

A large amount of crystallographic data has been amassed, all molecules having essentially the same core. A single chalcogen atom caps the approximately symmetrical trimolybdenum unit (Mo—Mo $\sim$ 2.7 Å), while dichalcogenide ligands bridge each edge of the triangle in an η^2,η^2 manner (S–S $\sim$ 2.0 Å). In the latter, one chalcogen lies in the plane of the metal atoms, while the second lies below the plane, that is away from the sulfido cap. In all mixed-sulfur–selenium complexes, it is the sulfur that occupies this lower axial site (1003,1004).

Perhaps the most interesting solid-state characteristic of these complexes is the short anion–cation contacts to the axial chalcogen atoms that are invariably present (Fig. 111). For example, two polymorphs of $[Mo_3(\mu^3\text{-}S)(\mu\text{-}S_2)_3(S_2CNEt_2)_3]I$ have been crystallographically characterized, both showing weak binding of iodide to the axial sulfur atoms (S—I 3.25 and 3.30 Å) (994). A Raman study on a range of complexes $[Mo_3(\mu^3\text{-}S)(\mu\text{-}S_2)_3(S_2CNEt_2)_3]^+$

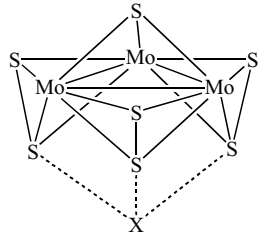

Figure 111. Cluster core of $[Mo_3(\mu^3\text{-}S)(\mu\text{-}S_2)_3(S_2CNR_2)_3]^+$ showing interactions with the anion, X^-.

with different anions showed a significant decrease in the sulfur–sulfur resonance in an order that parallels a slight increase in the sulfur–sulfur bond length and a significant shortening of the S—X distance.

Calculations carried out suggest that for hard anions such as nitrate and perchlorate the interaction is electrostatic in nature, while for softer anions such as iodide and sulfide there is a significant degree of covalent character (993). Generally, each metal ion in the clusters is formally molybdenum(IV), although in $[Mo_3(\mu^3\text{-}S)(\mu\text{-}S_2)_3(S_2CNEt_2)_3]_2Cl$, the chloride lies between two clusters, making six contacts with axial sulfur atoms, and a $[Mo_3(\mu^3\text{-}S)(\mu\text{-}S_2)_3]^{3.5+}$ state is assigned (992).

A number of related trimolybdenum–chalcogenide complexes have been reported, including the mixed-ligand cluster $[Mo_3(\mu^3\text{-}S)(\mu\text{-}S_2)_3(S_2CNEt_2)(tpy)_2]I$ (tpyH = *o*-pyridinethiol) (994). The selenium complex, $[Mo_3(\mu^3\text{-}Se)(\mu\text{-}Se)_3(S_2CNEt_2)_3][S_2CNEt_2]$, reacts with 4 equiv of PPh_3 to give $[Mo_3(\mu^3\text{-}Se)(\mu\text{-}Se)_3(PPh_3)(S_2CNEt_2)_3(\mu\text{-}S_2CNEt_2)]$, in which it is proposed that one metal ion bears a phosphine ligand, and a dithiocarbamate bridges between the other two (999,1000).

Analogous sulfido complexes, $[Mo_3(\mu^3\text{-}S)(\mu\text{-}S)_3L(S_2CNEt_2)_3(\mu\text{-}S_2CNEt_2)]$ (L = py, dmf), have been prepared from $[Mo_3(\mu^3\text{-}S)(\mu\text{-}S)_3(H_2O)\{S_2P(OEt)_2\}_4]$ and dithiocarbamate salts in the presence of Py and DMF, respectively (1006). The thiophosphinate complex also reacts with sodium acetate in the presence of dithiocarbamate salt to give $[Mo_3O_2(\mu^3\text{-}S)(\mu\text{-}S)_2(S_2CNC_4H_8)_3(\mu\text{-}O_2CMe)]$. This has been crystallographically characterized and contains two short [av. 2.808(1) Å] and one long [3.374(2) Å] molybdenum–molybdenum contacts (1007).

In one contribution, the synthesis and X-ray crystal structure of the heterotrimetallic cluster $[Et_4N][\{MoO(S_2CNMe_2)(\mu\text{-}S)_2\}_2Fe]$ (**140**) has been reported (1008). It results from the reaction of $FeCl_2$, NaS_2CNMe_2, Et_4NCl, and $[NH_4]_2[MoO_2S_2]$ in DMF and consists of an approximately linear trinuclear core containing two molybdenum(V) and one iron(III) ions. It can be reversibly reduced to the dianion, but while it also undergoes a one-electron oxidation, the latter is irreversible.

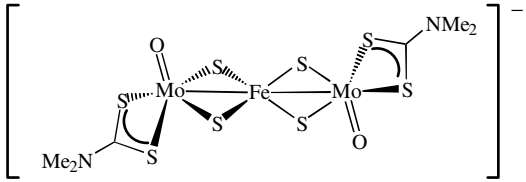

140

In a further report, the synthesis and X-ray crystal structure of $[MoO_2(S_2CNEt_2)(\mu\text{-}S)_2Fe(\mu\text{-}S)_2Fe(\mu\text{-}S)_2Mo(S_2CNEt_2)O_2]$ (**141**) is detailed, in

which molybdenum(VI) centers are linked via an Fe_2S_6 unit (1009). Unusually, the oxo ligands are reported to be trans to one another [O—Mo—O 177(1)°], however, the structure is poor and may be erroneous (oxygen site occupancies are only 0.5).

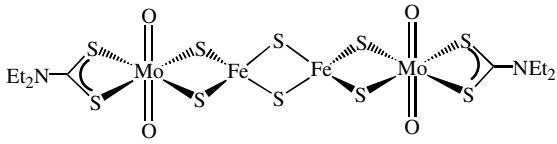

141

Tetranuclear, $[Mo_4(\mu^3\text{-}S)_2(\mu\text{-}S)_4(S_2CNEt_2)_2(PMe_3)_4]$ (**142**), has been prepared from $[Mo_4Br_2(\mu^3\text{-}S)_2(\mu\text{-}S)_4(PMe_3)_6]$ and 2 equiv of dithiocarbamate salt (1010). The average metal oxidation state is +3.5 and, primarily on the basis of short [av. 2.814(1) Å] and long (hinge) [2.838(1) Å] molybdenum–molybdenum contacts, the authors suggest a localized bonding model with equal numbers of molybdenum(IV) and molybdenum(III) ions.

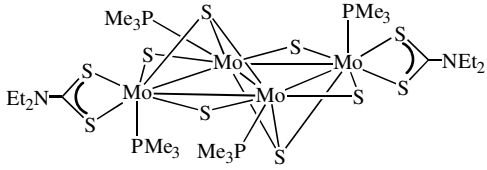

142

A significant number of cubane-type clusters containing both tetramolybdenum and mixed-metal cores have been prepared. Prolonged heating of $[Mo_2(S_2CNEt_2)_6]$ in toluene affords the black diamagnetic tetramolybdenum cluster, $[Mo_4(\mu^3\text{-}S)_4(S_2CNEt_2)_4(\mu\text{-}S_2CNEt_2)_2]$ (**143**), in moderate yield (174,176,177). A crystallographic study reveals bridging dithiocarbamates on opposite sides of the cube and an average molybdenum–molybdenum distance of 2.818 Å. The latter is longer than generally found for single molybdenum–molybdenum bonds, and a molecular orbital analysis suggests that in the 58-electron cluster, there are only 10 electrons available for the six metal–metal bonding orbitals (177). Related tetramolybdenum clusters are $[Mo(N\text{-}Ar)(\mu^3\text{-}S)(S_2CNR_2)]_4$ discussed in more detail above (439,984). They are characterized by EANs of 68-electrons and contain two molybdenum–molybdenum bonds.

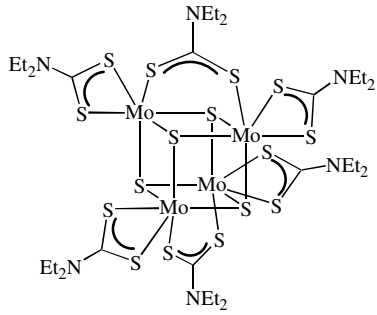

143

Paramagnetic molybdenum–iron complexes $[MoFe_3(\mu^3\text{-}S)_4(S_2CNR_2)_4(\mu\text{-}S_2CNR_2)]$ can be prepared in a one-step spontaneous self-assembly process from $FeCl_2$ and $[MoS_4]^{2-}$ in the presence of dithiocarbamate salts (274,1011–1016). They are characterized by an EAN (EAN = equivalent atomic number) of 61 electrons. Crystallographic studies show that each metal ion carries a chelating dithiocarbamate ligand, with one further ligand bridging between iron and molybdenum centers. In some instances clusters, $[MoFe_3(\mu^3\text{-}S)_4(S_2CNR_2)_4(\mu\text{-}S_2CNR_2)_2]$, can be isolated with a second bridging dithiocarbamate lying on the opposite side of the cube (274,1016). A related cubane-type cluster, $[Mo_2Fe_2(\mu^3\text{-}S)_4(S_2CNEt_2)_4(\mu\text{-}S_2CNEt_2)]$, is formed under similar conditions described above, but employing $FeCl_3$ as the iron source (270,271). A magnetic susceptibility measurement shows that it is paramagnetic (μ 4.27 BM), while XPS and Mössbauer studies show that the two iron atoms are in different oxidation states.

Further cubane-type clusters, $[Mo_3CuI(Py)(\mu^3\text{-}S)_4(S_2CNR_2)_3(\mu\text{-}S_2CNR_2)]$, can be prepared upon addition of copper(I) iodide to $[Mo_3(\mu^3\text{-}S)(\mu\text{-}S)_3(S_2CNR_2)_3(\mu\text{-}S_2CNR_2)].H_2O$ (R = Et; $R_2 = C_4H_8$) in the presence of pyridine (272). Interestingly, when ethyl acetate is added ($R_2 = C_4H_4$), the oxidized cluster $[Mo_3CuO_2(\mu^3\text{-}S)_4(S_2CNC_4H_4)_3(\mu\text{-}S_2CNC_4H_4)(\mu\text{-}I)(py)]$ results (Eq. 94). The latter is shown by X-ray crystallography to contain only molybdenum–molybdenum bonds, the formal oxidation states of molybdenum being +5 (272).

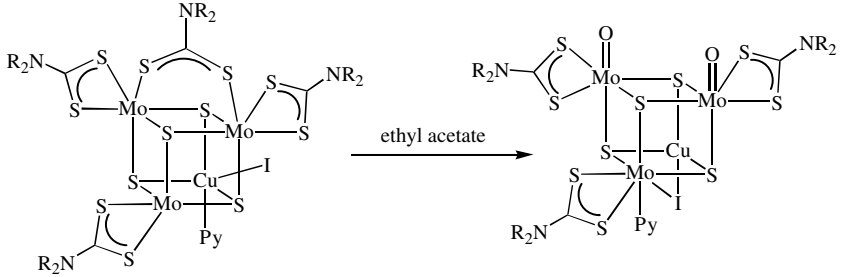

(94)

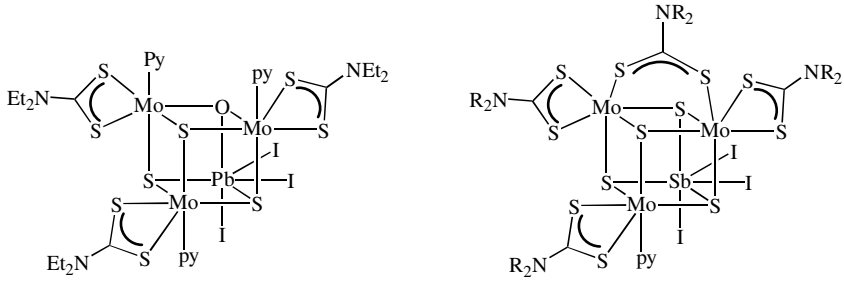

Figure 112. Examples of cubane-type clusters containing a main group element.

Some *p*-block metals can also be incorporated into molybdenum dithiocarbamate cubane-type clusters. Reaction of $K[PbI_3]$ with $[Mo_3(\mu\text{-}S)_3(\mu^3\text{-}O)(S_2CNEt_2)_4(H_2O)]$ (1017) in pyridine yields $[Mo_3PbI_3(\mu^3\text{-}S)_3(\mu^3\text{-}O)(S_2CNEt_2)_3(py)_3]$ (**144**) (Fig. 112), a cubane-type cluster with a PbI_3 unit at one corner, while reaction of SbI_3 with $[Mo_3(\mu\text{-}S)_4(S_2CNC_4H_8)_4(H_2O)]$ (1018) gives the related antimony cluster $[Mo_3SbI_3(\mu^3\text{-}S)_4(\mu\text{-}S_2CNC_4H_8)(S_2CNC_4H_8)_3(py)]$ (**145**) (Fig. 112) (264).

A more complex cluster, $[Mo_2Cu_5(\mu^3\text{-}S)_6(\mu^3\text{-}O)_2(\mu\text{-}S_2CNEt_2)_2(S_2CNEt_2)]^{2-}$, has been prepared from a mixture of $[MoO_2S_2]^{2-}$, CuCl, and NaS_2CNEt_2 in DMF (266). It consists of two defective cube-like units, $OMoS_3Cu_2$ and $OMoS_3Cu_3$, linked by two weak copper–sulfur interactions and two bridging dithiocarbamate ligands.

Like its tungsten analogue, binuclear *syn*-$[MoS(\mu\text{-}S)(S_2CNEt_2)]_2$ is a useful precursor to a range of trinuclear and cubane-type clusters (1019,1020). For example, reaction with $[RhCl(PPh_2R)_3]$ (R = Ph, Me) yields $[Mo_2Rh(PPh_2R)_2(S_2CNEt_2)_2(\mu\text{-}Cl)(\mu\text{-}S)_3(\mu^3\text{-}S)]$ (1019). The latter in turn reacts with excess phenylethyne at room temperature to afford $[Mo_2Rh(PPh_2R)Cl(S_2CNEt_2)_2(\mu\text{-}SCPh{=}CH)_2(\mu\text{-}SCPh{=}CHS)]$ (Eq. 95) resulting from insertion of three alkyne moieties into and across the bridging sulfides (1021).

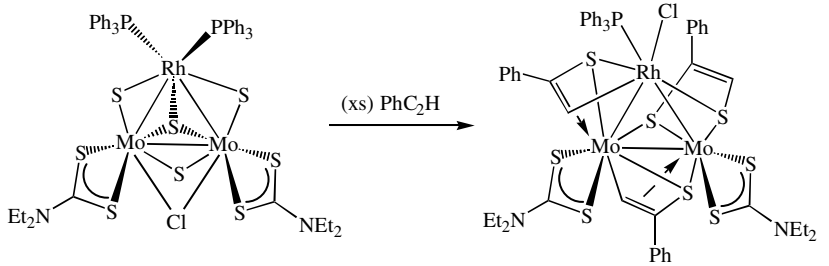

(95)

Reaction of *syn*-[MoS(μ-S)(S_2CNEt_2)]$_2$ (**146**) with [$Co_2(CO)_8$] in acetonitrile gives the cubane-type cluster, [$Mo_2Co_2(\mu^3$-S)$_4$(MeCN)$_2$(CO)$_2$(S_2CNEt_2)$_2$] (**147**) (1022). Low-valent group 9 (VIII) and 10 (VIII) complexes, [M(cod)(μ-Cl)]$_2$ (M = Rh, Ir) (1023) and [Pd(PPh_3)$_4$] (1024), yield similar clusters, [$Mo_2M_2(\mu^3$-S)$_4Cl_2$(cod)$_2$(S_2CNEt_2)$_2$] (**148**) and [$Mo_2Pd_2(\mu^3$-S)$_4$(PPh_3)$_2$(S_2CNEt_2)$_2$] (**149**), respectively (Fig. 113). Some insight into the cluster build-up is gleaned from the reaction with 1 equiv of [Pd(PPh_3)$_4$], which yields the trinuclear, incomplete cubane-type cluster, [$Mo_2Pd(\mu$-S)$_4$(PPh_3)$_2$(S_2CNEt_2)$_2$] on-route to the cubane, related trinuclear species being isolated with [Pt(PPh_3)$_4$] and [M$Cl(PPh_3)_3$] (M = Rh, Ir) (1023,1024).

m. Applications. As detailed earlier, dioxo complexes, [$MoO_2(S_2CNR_2)_2$], can act as stoichiometric and catalytic oxo-transfer agents (795,798,800,802, 804), and are also active in the catalytic allylic amination of alkenes (808). The bis(imido) complex, [Mo(NTs)$_2$(S_2CNEt_2)$_2$], has been used in catalytic imido group transfer to phosphines (831), and [$MoO(S_2)(S_2CNEt_2)_2$] has been shown to be a good catalyst for the conversion of isonitriles into isothiocyanates (880) and the direct episulfidation of alkenes and allenes (881,882) using elemental sulfur.

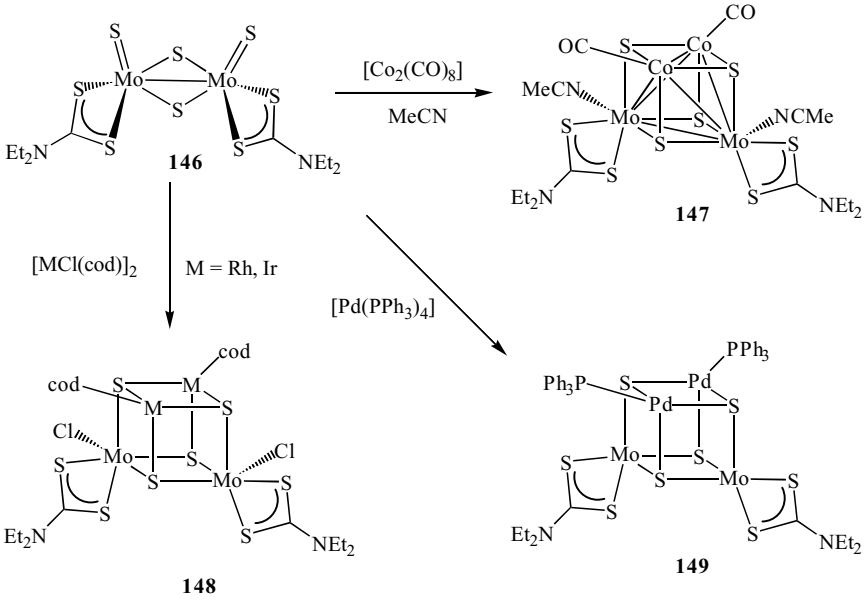

Figure 113. Some examples of the synthesis of cubane-type clusters from *syn*-[MoS(μ-S)(S_2CNEt_2)]$_2$.

Molybdenum(VI) dioxo complexes have also been used for the catalytic conversion of 1,2-diphenylhydrazine to azobenzene (795), and the oxidation of 2-hydroxy-2-phenylacetophenone (benzoin) to benzil (1025). In the latter, however, the reaction is rapidly deactivated as the catalyst $[MoO_2(S_2CNEt_2)_2]$ is converted into the inactive molybdenum(V) dimer, $[MoO(\mu\text{-}O)(S_2CNEt_2)]_2$. Attempts to oxidize aldehydes using these catalysts have generally been unsuccessful (795).

Molybdenum(VI) dioxo complexes do not oxidize alkenes to epoxides, thermochemical data suggesting that alkene epoxidation by $[MoO_2(S_2CNEt_2)_2]$ leading to the formation of $[MoO(S_2CNEt_2)_2]$ is endothermic by ~ 35 kJ mol^{-1} (1026). Moloy (84) instead has developed the back reaction; namely, the deoxygenation of epoxides by $[MoO(S_2CNEt_2)_2]$. Treating a variety of epoxides with $[MoO(S_2CNEt_2)_2]$ in toluene at high temperatures leads to the selective formation of alkenes; no other oxygenates being observed. Although selective, the reactions are not quantitative as a good deal of complex decomposition occurs. Reactions do, however, occur with $>98\%$ retention of symmetry indicating that deoxygenation proceeds via a concerted reaction or through a cyclic intermediate.

A wide range of other possible applications of molybdenum dithiocarbamate complexes has also been explored. Dimeric $[Mo_2O_2(\mu\text{-}O)(S_2CNEt_2)_4]$ anchored on functionalized cross-linked polystyrene has been used as a catalyst for the conversion of Me_2SO to Me_2SO_2 and cyclohexene to its oxide, using *t*-BuO_2H as the stoichiometric oxidant. While slow loss of metal ions from the polymer support is observed, this heterogeneous system still performs better than the homogeneous counterpart (1027).

The photoreduction of acetylene to ethylene and ethane can be catalyzed by $[MoO(\mu\text{-}O)(S_2CNEt_2)]_2$ in the presence of 5–8-nm diameter colloidal TiO_2. The optimum activity was found at pH 6 with a loading of 30 catalyst molecules per titania particle, and the overall efficiency is 1.3% at full lamp intensity. The authors suggest that the molybdenum(V) dimer becomes attached to the TiO_2 surface and serves to transfer electrons or hydrogen atoms to bound substrates (1028).

Drew et al. (1029) prepared samples of molybdenum dithiocarbamates in the Linde A zeolite, which is achieved by first stirring the zeolite with an aqueous solution of sodium molybdate followed, after drying, by addition of NaS_2CNEt_2 in dilute HCl. After washing to remove surface molybdenum dithiocarbamates, the blue solids were characterized by their strong paramagnetism, being characteristic of monomeric molybdenum(V) species. In order to probe the nature of the later they have used molecular graphics, which suggest that dimerization of molybdenum(V) dithiocarbamate species cannot occur within the zeolite cages, which is in keeping with the experimental observations.

The effects of a number of molybdenum dithiocarbamate complexes, most notably $[MoO(\mu\text{-}S)(S_2CNR_2)]_2$, on the friction and wear properties between aluminum alloy and steel have been investigated (1030–1039). Friction reduction via boundary lubrication occurs as a result of the formation of MoS_2, a well-known lamellar solid lubricant, shown to form by electron-transfer mechanisms activated by the friction process (1031,1032). Somewhat complementary to this work are thermal gravimetric studies showing that between 200 and 400°C, $[Mo(NO)_2(S_2CNEt_2)_2]$, $[MoO(NCS)(S_2CNEt_2)_2]$, and $[MoS(\mu\text{-}S)(S_2CNEt_2)]_2$, break down to give MoS_3, MoS_2, and "Mo_2S_8", respectively (1040).

Isotopically enriched $^{95,97,98}[MoO(S_2CNEt_2)_3]$ has been characterized by ESR spectroscopy in frozen benzene solutions. A comparison of experimental and calculated parameters shows that the axial symmetry of the magnetic tensors does not contradict the low symmetry of the complex (1041). Finally, in a quite different application, the dithiocarbamate salt derived from piperidine has been utilized for determination of the molybdenum content in soils, the dioxo complex $[MoO_2(S_2CNC_5H_{10})_2]$ generated, being measured by its absorbance at 460 nm (1042).

3. Tungsten

In many respects, tungsten dithiocarbamate chemistry follows on closely to that of molybdenum, although far less ground has been covered; the first reported examples being the tetrakis(dithiocarbamate) complexes, $[W(S_2CNR_2)_4]$, prepared in the early 1970s (769,1043). A major difference between the dithiocarbamate chemistry of molybdenum and tungsten, is that while cis dioxo complexes $[WO_2(S_2CNR_2)_2]$ are known (1044,1045), they are far less common and their chemistry has not been developed. Another difference is that the organometallic chemistry of low-valent tungsten dithiocarbamate complexes has been developed to a somewhat greater extent than that of molybdenum.

a. Tetrakis(dithiocarbamate) and Related Complexes. Both tungsten (IV) and (V) tetrakis(dithiocarbamate) complexes are known, being prepared in a number of different ways. The tungsten(IV) complexes, $[W(S_2CNR_2)_4]$ (**150**) (Fig. 114), are typically prepared upon addition of dithiocarbamate salts to WCl_4 in acetonitrile (1046) and can also be prepared from $W(CO)_6$ and thiuram disulfides (1047). More recently, irradiation of $[W(CO)_3(\eta^6\text{-}C_6H_5Me)]$ with thiuram disulfides has been shown to afford mixtures of tungsten(III) and (IV) complexes, $[W_2(S_2CNR_2)_6]$ and $[W(S_2CNR_2)_4]$ (R = Et, Pr, Bu; $R_2 = C_5H_{10}$), respectively (1048).

Tungsten(V) complexes, $[W(S_2CNR_2)_4]X$ (**151**) (Fig. 114), can be prepared in a similar manner to the tungsten(IV) complexes detailed above, however, the

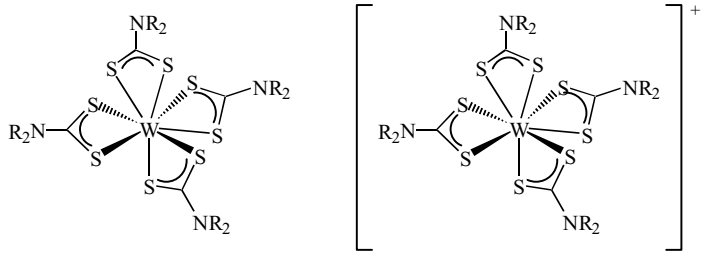

150 **151**

Figure 114. Tungsten tetrakis(dithiocarbamate) complexes.

reactions are carried out in air in the presence of Bu_4NX (X = Cl, Br, I) (1047). A number of other synthetic procedures have also been adopted, including the reaction of $W(CO)_6$ with $(Et_2NCS_2)_2Te$ (R = Et, X = 0.5 W_6O_{19}) (1049); hydrolysis of the product of PPh_3 reduction of $[WS(S_2)(S_2CNMe_2)_2]$ (R = Me, X = 0.5 W_6O_{19}) (1050); and prolonged heating of $[Tp^*W(CO)_3]^-$ and tetraethylthiuram disulfide (R = Et, X = Cl), the latter giving only low yields (182). Addition of LiTCNQ to $[W(S_2CNR_2)_4]I$ (R = Me, Et) in DMF/H_2O gives $[W(S_2CNR_2)_4][TCNQ]$, while further addition of TCNQ in acetonitrile yields $[W(S_2CNR_2)_4][TCNQ]_2$, in which the TCNQ is in mixed-valence states (779). A number of crystallographic studies have been carried out (779,1049,1050), and in all the tungsten cation shows a dodecahedral coordination geometry.

Tungsten(III) tris(dithiocarbamate) complexes are not known. However, in one report a related tungsten(III) complex, $[W(S_2CH)(S_2CNMe_2)_2]$ (**152**), has been reported; prepared as a side product of the addition of carbon disulfide and sulfur to $[W_2(NMe_2)_6]$ (1051).

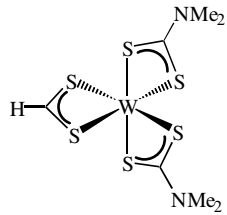

152

b. Tungsten Oxo Complexes. As seen in the previous sections, much of the high-valent dithiocarbamate chemistry of molybdenum centers on the cis dioxo complexes, $[MoO_2(S_2CNR_2)_2]$, which are easily prepared and generally

stable. In contrast, analogous tungsten(IV) dioxo complexes, $[WO_2(S_2CNR_2)_2]$, remain virtually unexplored, primarily as a result of their relative instability.

They were first prepared by McDonald and co-workers (1044) via an oxo-transfer reaction between $[W(CO)_3(S_2CNR_2)_2]$ (R = Me, Et, Pr) and $[Mo_2O_2(\mu\text{-}O)\{S_2P(OEt)_2\}_4]$, but characterization was poor, being based mainly on the observation of W=O bands in the IR spectrum between 890 and 935 cm^{-1}. Later, Yu and Holm (1052) developed this route, and also gave further details of their relative instability; being highly sensitive to water and oxygen, while even in dry organic solvents slow decomposition took place. They noted that the off-white piperidine dithiocarbamate complex, $[WO_2(S_2CNC_5H_{10})_2]$, displayed a greater stability than simple alkyl derivatives, showing some stability for short periods in dichloromethane and 1,2-dichloroethane, while unstable in DMF or DMSO.

Cooper and co-workers (1053) later described a more direct route to one of these complexes, yellow $[WO_2(S_2CNBz_2)_2]$ being prepared in high yield when oxygen saturated THF was bubbled through a solution of $[W(CO)_3(S_2CNBz_2)_2]$ in the absence of light (Eq. 96). It was characterized by strong W=O vibrations at 939 and 893 cm^{-1} in the IR spectrum. This reaction probably proceeds via the initial formation of dimeric $[W_2O_2(\mu\text{-}O)(S_2CNBz_2)_4]$, and indeed when carried out in dichloromethane, the latter was isolated in high yield, a crystal structure revealing the anti orientation of the terminal oxo ligands (1053).

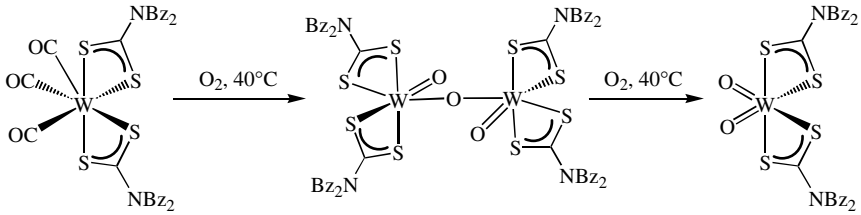

(96)

Very recently, Unoura et al. (1045) reported the synthesis of $[WO_2(S_2CN{-}i\text{-}Bu_2)_2]$, which shows surprising stability for this class of complex. It is formed in $\sim$ 20% yield from the reaction of $Na_2WO_4.2H_2O$ with $NaS_2CN{-}i\text{-}Bu_2$ in aqueous solution in air; conditions that fail to yield tractable products for a range of other dithiocarbamates (R = Me, Et, *i*-Pr, Cy, Bz, Ph). Precise reasons for the surprising stability of $[WO_2(S_2CN{-}i\text{-}Bu_2)_2]$ remain unknown. A structural study reveals similar features to analogous molybdenum complexes, [W=O(av) 1.719 Å, O–W–O 104.7°]. Cyclic voltammetry has also been carried out; two irreversible reduction waves being observed. The reversibility of the first reduction increases with increasing scan rates, and controlled-potential electrolysis at a potential just after this reduction leads to the formation of a deep violet solution suggesting the formation of $[W_2O_2(\mu\text{-}O)(S_2CN{-}i\text{-}Bu_2)_4]$.

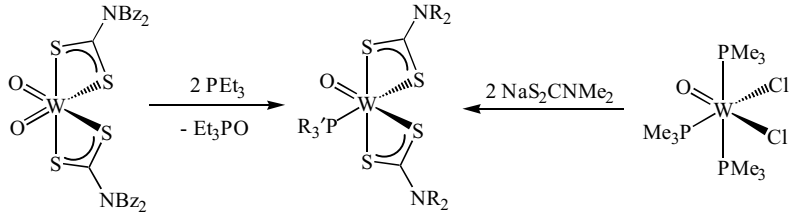

Figure 115. Synthetic routes to tungsten(IV) oxo complexes $[WO(PR'_3)(S_2CNR_2)_2]$.

The dioxo complexes have been tested as oxo-transfer reagents (1052,1053). The piperidine complex $[WO_2(S_2CNC_5H_{10})_2]$ does not react with PPh_3 and reacts only slowly with alkyl phosphines, however, upon addition of $P(OMe)_3$, oxo-transfer does occur relatively rapidly to give the oxide and $[W_2O_2(\mu\text{-}O)(S_2CNC_5H_{10})_4]$ (1052). In contrast, $[WO_2(S_2CNBz_2)_2]$ is reduced by PPh_3, $PPhMe_2$, and PEt_3, the latter being studied in some detail. Thus, addition of excess phosphine gave the red tungsten(IV) phosphine adduct $[WO(PEt_3)(S_2CNBz_2)_2]$ (Fig. 115) (1053). Carmona et al. (1054) prepared a similar phosphine adduct, $[WO(PMe_3)(S_2CNMe_2)_2]$, from the reaction of NaS_2CNMe_2 with $[WOCl_2(PMe_3)_3]$, the temperature dependence of its ^1H NMR spectrum being suggested to result from an η^1-dithiocarbamate intermediate.

Thus it is clear that the relative lack of chemistry developed from $[WO_2(S_2CNR_2)_2]$ stems primarily from their instability, although the variation of this as a function of dithiocarbamate substituents suggests that more work is justified in this area. Holm and co-worker (1052) noted that their poor oxo-transfer behavior, as compared to analogous molybdenum systems, is associated with the difficulty in reducing the tungsten(VI) center, and thus related tungsten(IV) complexes may be good oxo acceptors.

Other tungsten(VI) oxo complexes have been prepared. For example, bis(indenyl) complexes, $[(\eta^5\text{-}C_9H_7)_2WOCl(S_2CNR_2)]$ ($R = Me$, Et, *i*-Pr; $R_1 = Cy$, $R_2 = Me$, Et, *i*-Pr), are reported to result from addition of dithiocarbamate salts to $[(\eta^5\text{-}C_9H_7)_2WOCl_2]$ (639). A further class of tungsten(VI) oxides are the disulfide complexes, $[WO(S_2)(S_2CNR_2)_2]$, and these are discussed more fully in Section (IV.C.3.c).

Oxo-bridged tungsten(V) dimers, $[W_2O_2(\mu\text{-}O)(S_2CNR_2)_4]$, an example of which was detailed above, have been prepared by a number of groups, including those of Lozano et al. (1055,1056) and Brown et al. (1048); although there is some suggestion that these reports may be partially incorrect (1053). Monomeric tungsten(V) oxo complexes have also been prepared. For example, oxidation of $[W(S_2CNR_2)_4]$ ($R = Et$, Pr, Bu; $R_2 = C_5H_{10}$) by pyridine *N*-oxide is reported to give, $[WO(S_2CNR_2)_3]$ (1048).

A number of reports deal with tungsten(IV) oxo complexes. As detailed above, phosphine complexes of the type, $[WO(PR_3)(S_2CNR'_2)_2]$, have been prepared in a number of ways (1053,1054). A further report suggests that addition of dithiocarbamate salts to $[CpWOCl_2]$, and the related indenyl complex, leads to the formation of tungsten(IV) complexes, $[CpWO(S_2CNR_2)]$ (R = Me, Et) (1057), reduction of the metal center presumably resulting from oxidation of some of the dithiocarbamate salt to the thiuram disulfide. Since their report in 1980, however, no further details of these complexes have been given. In other work, a range of alkyne complexes, $[WO(RC_2R)(S_2CNR'_2)_2]$ (821,1058), have been prepared from the controlled oxidation of $[W(CO)(RC_2R)(S_2CNR'_2)_2]$ and their properties and structures probed (see Section IV.C.3.f).

c. Chalcogenide Complexes. A number of tungsten(V) and (VI) complexes containing the disulfide (S_2^{2-}) ligand have been prepared and studied, as have related diselenide complexes. Tungsten(VI) complexes, $[WE(S_2)(S_2CNR_2)_2]$ (E = S, O), are particularly common (180, 370, 879, 1051, 1059–1062), a wide range of synthetic methods being adopted. Addition of thiuram disulfides to $[WS_4]^{2-}$ (180) or related selenium compounds, $(R_2NCS_2)_2Se$ (R = Me, Et), to $[WS_4]^{2-}$ or $[W_3S_9]^{2-}$ (1061) affords $[WS(S_2)(S_2CNR_2)_2]$, as does addition of sulfur or selenium to $[W_2(NMe_2)_6]$ in carbon disulfide (1051). Reaction of sulfur dioxide with $[W(CO)_3(S_2CNR_2)_2]$ (R = Me, Et, *i*-Pr, Bz; $R_2 = C_4H_4$) affords both oxo and sulfido complexes, $[WE(S_2)(S_2CNR_2)_2]$ (E = O, S), via a complex process in which $(Et_2NCS_2)_2CH_2$ is also generated (1059), and reaction of $Me_3SiS_2CNR_2$ (R = Me, Et) with $[WSCl_4]$ yields $[WS(S_2)(S_2CNR_2)_2]$ together with cationic $[WS(S_2CNR_2)_3]^+$ (Eq. 97) (370, 1060, 1062).

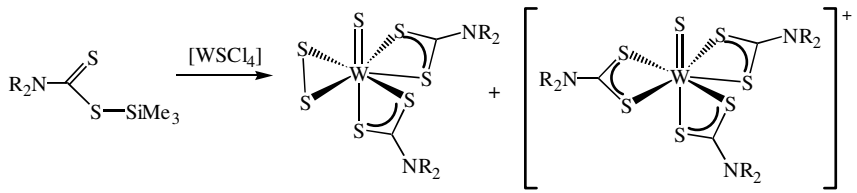

(97)

Crystallographic studies have been carried out on a number of complexes of the type $[WE(S_2)(S_2CNR_2)_2]$ (180,1051,1059). The metal center adopts a distorted trigonal-bipyramidal coordination sphere, the disulfide ligand lying in the equatorial plane and the π-donor ligand taking up an axial site.

Electrochemical studies on $[WE(S_2)(S_2CNR_2)_2]$ (E = O, S; R = Me, Et) reveal an irreversible one-electron ligand-based oxidation process involving the disulfide ligand, and a one-electron reduction generating radical anions that are inherently unstable and decay to unidentified products (879).

Russian workers have shown that $[WS(S_2)(S_2CNR_2)_2]$ (R = Me, Et) react with acids (HX) in acetonitrile generating, $[WSX_2(S_2CNR_2)_2]$ (X = Cl, Br), an example of which has been crystallographically characterized (R = Me, X = Cl). Interestingly, this reacts further with labeled $[t\text{-}Bu_4N]_2[^{34}S_6]$ to give a mixture of isotopomers of $[WS(S_2)(S_2CNMe_2)_2]$ containing two ^{34}S atoms and one ^{32}S atom (Eq. 98), and it is proposed that this occurs via a WS_3 metallacyclic intermediate (1061).

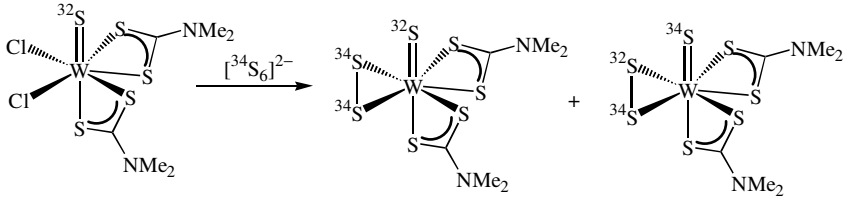

(98)

As mentioned above, when $[WSCl_4]$ reacts with $Me_3SiS_2CNEt_2$ in methanol, tungsten(VI) cations, $[WS(S_2CNR_2)_3]^+$, are among the products (370,1060, 1062). A crystal structure of $[WS(S_2CNEt_2)_3][BF_4]$ reveals that the metal adopts a distorted trigonal-bipyramidal ligand sphere, the sulfido ligand occupying an axial site and displaying a significant trans-influence as measured by the elongation of the trans tungsten–sulfur bond by ~ 0.07 Å as compared to those in the equatorial plane (370,1060). These molecules are fluxional in solution as shown by VT NMR studies. For example in $[WS(S_2CNMe_2)_3][BPh_4]$, rotation about the backbone carbon–nitrogen bond of the dithiocarbamates leads to a single methyl environment at 25°C, while upon cooling to −50°C the expected four signal pattern for a static C_s structure is seen. The two-site exchange has activation barriers of 57 ± 1 and 54 ± 1 kJ mol^{-1} for the equatorial and unique dithiocarbamates, respectively. Averaging of all methyl groups requires a metal-centered polytopal rearrangement, and a double facial twist mechanism involving a trigonal-prismatic transition state is proposed (370).

Oxidation of $[Tp^*W(CO)_2(S_2CNEt_2)]$ by cyclohexene sulfide at 85°C yields the tungsten(IV) sulfido complex, $[Tp^*WS(S_2CNEt_2)]$ (**153**), which is also the major product upon prolonged heating of $[Tp^*W(CO)_3]^-$ and tetraethylthiuram disulfide. Crystallographic characterization reveals a distorted octahedral coordination geometry and a W=S distance of 2.153(2) Å (183).

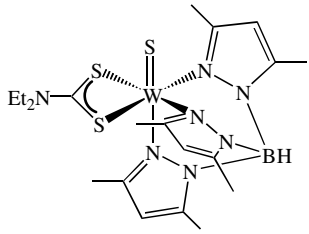

153

Three reports have appeared concerning tungsten diselenide (Se_2^{2-}) complexes (1049,1063,1064). Tungsten(V) complexes, $[W(Se_2)(S_2CNR_2)_3]$ (R = Et, *i*-Bu), can be prepared via oxidation of $[W(CO)_5(MeCN)]$ by $(Et_2NCS_2)_2Se$ (1049), or from thiuram disulfides and $[WSe_4]^{2-}$; the latter resulting from an induced internal electron-transfer process (1063). Interestingly, this appears to be time dependent, extended reaction times (7 days) leading instead to tungsten (VI) complexes, $[WE(Se_2)(S_2CNEt_2)_2]$ (E = O, S) (1064). Crystallographic studies reveal selenium–selenium bond lengths of 2.23 Å at tungsten(V) and 2.31 Å at tungsten(VI), both being less that in elemental selenium (2.37 Å), but greater than found in Se_2 (2.19 Å).

d. Cyclopentadienyl and Tris(pyrazolyl)borate Complexes. Mononuclear tungsten complexes are known with cyclopentadienyl ligands in oxidation states +2 to +5 (Fig. 116). A number of pentamethylcyclopentadienyl complexes have been reported. For example, tungsten(III) complexes, $[Cp^*WI(NO)(S_2CNR_2)]$ (R = Me, Et) (1065) (**154**), have been prepared, while addition of dithiocarbamate salt to $[Cp^*WCl_4]$ gives the tungsten(V) complex, $[Cp^*WCl_3(S_2CNEt_2)]$ (**155**); this in turn is oxidized by hydrogen peroxide to $[Cp^*WO(\eta^2\text{-}O_2)Cl]$ with loss of the dithiocarbamate ligand (910).

As detailed above, tungsten(IV) oxo complexes, $[CpWO(S_2CNR_2)]$ and $[(C_9H_7)WO(S_2CNR_2)]$ (R = Me, Et), have been briefly reported (1057). One

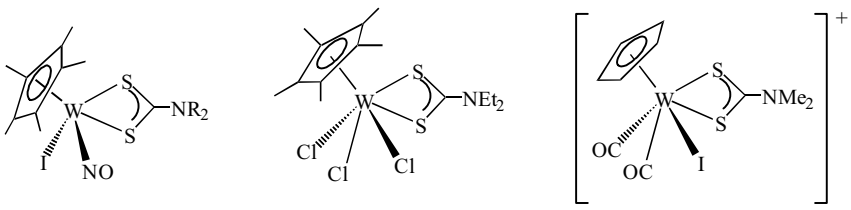

154 **155** **156**

Figure 116. Examples of tungsten cyclopentadienyl complexes.

further example of a tungsten(IV) cyclopentadienyl complex has been reported; addition of iodine to $[CpW(CO)_3(\eta^1\text{-}S_2CNMe_2)]$ affording the salt, $[CpWI(CO)_2(S_2CNMe_2)]I$ (**156**) (1066), along with a thiocarboxamide complex resulting from carbon–sulfur bond cleavage (see Section V.A)

A number of tungsten(II) cyclopentadienyl and tris(pyrazolyl)borate complexes have been prepared. Photolysis of $[CpW(CO)_3]_2$ and tetramethylthiuram disulfide affords $[CpW(CO)_3(\eta^1\text{-}S_2CNMe_2)]$ in good yield, which upon further photolysis or heating loses carbon monoxide giving $[CpW(CO)_2(S_2CNMe_2)]$ (1066,1067). A crystal structure of $[CpW(CO)_3(\eta^1\text{-}S_2CNMe_2)]$ confirms that the dithiocarbamate is monodentate, the two carbon–sulfur bonds as expected being quite different [C–S 1.769(3), C=S 1.676(3) Å] (1066). The uncoordinated sulfur atom may be able to bind to a second metal center. Thus, reaction with $[W(CO)_5(thf)]$ affords a new complex, which is only stable at low temperatures and thus has not been fully characterized, but on the basis of limited spectroscopic data the authors propose that this is $[CpW(CO)_3(\mu\text{-}S_2CNMe_2)W(CO)_5]$.

The tris(pyrazolyl)borate complex $[Tp^*W(CO)_2(S_2CNEt_2)]$, prepared upon thermolysis of $[Tp^*W(CO)_3]^-$ and tetraethylthiuram disulfide, has been structurally characterized (182). It reacts with alkynes to give a variety of products, being highly dependent on the nature of the alkyne substituents (1068). With phenyl ethyne, $[Tp^*W(CO)(PhC_2H)(\eta^1\text{-}S_2CNEt_2)]$ results. Here again the dithiocarbamate is monodentate, their being only a very weak interaction of the second sulfur atom with the tungsten center [W—S 2.397(2) and 3.999(2) Å], the carbon–sulfur bonds also differing [C—S 1.798(7), C=S 1.668(6) Å].

Further tungsten(II) alkyne complexes, $[CpW(PhC_2Ph)(S_2CNMe_2)]$ (904) and $[CpW(RC_2R)_2(S_2CNEt_2)]$ ($R = CF_3$) (905), have been prepared from the addition of dithiocarbamate salts to $[CpWCl(CO)(PhC_2Ph)]$ and $[CpWCl(RC_2R)_2]$, respectively; the barrier to alkyne rotation in the hexafluorobut-2-yne complex is estimated as 56 kJ mol^{-1} (905).

e. Carbonyl and Nitrosyl Complexes. A number of zero-valent tungsten complexes, $[W(CO)_4(S_2CNR_2)]^-$, have been reported, being similar to the chromium and molybdenum analogues (discussed earlier). Synthetic routes include the addition of a dithiocarbamate salt to $[W(CO)_6]$ ($R = Et$; $R_2 = C_4H_8$) (757,1069,1070) or pyridine analogues (1070); insertion of carbon disulfide into a metal amide prepared *in situ* from *n*-BuLi and *cis*-$[W(CO)_4(NHR_2)_2]$ [$R_2 = C_5H_{10}$, C_4H_4) (198)]; and reaction of *cis*-$[W(CO)_4(NHC_5H_{10})_2]$ with $[W(CO)_5(\eta^1\text{-}Ph_2PCS_2)]^-$, which also gives $[W(CO)_5(PPh_2H)]$ (Eq. 43) (229). Crystallographic studies reveal a distorted octahedral coordination environment resulting from the small dithiocarbamate bite angle (198).

A few reactions have been carried out. Addition of $[Fe_2(\mu\text{-}S_2)(CO)_6]^{2-}$ yields trinuclear $[WFe_2(\mu^3\text{-}S)(CO)_8(S_2CNEt_2)]^-$ (952), while with $[WS_4]^{2-}$

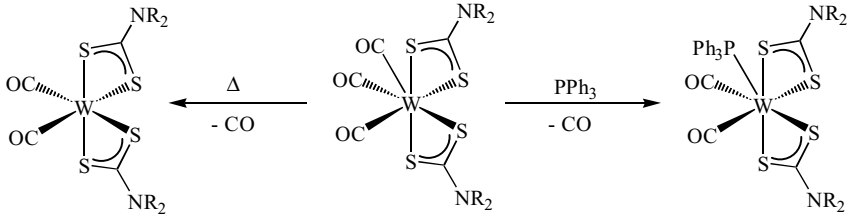

158 **157** **159**

Figure 117. Examples of the reactivity of $[W(CO)_3(S_2CNR_2)_2]$.

the dithiocarbamate is lost to yield $[WS_2(\mu\text{-}S)_2W(CO)_4]^{2-}$ (1069). A cyclic voltammetric study has been carried out on $[W(CO)_4(S_2CNEt_2)]^-$, three irreversible oxidation waves were observed with behavior similar to that found for the molybdenum analogue (1069).

Tungsten(II) tricarbonyl complexes, $[W(CO)_3(S_2CNR_2)_2]$ (**157**) (Fig. 117), have been studied widely and in many respects their chemistry is similar to that described previously for the analogous molybdenum species. Preparative routes include the addition of 2 equiv of dithiocarbamate salt to $[WX_2(CO)_4]_2$ (X = I, Br; R = Me, Et, Bz) (353,922,1053,1071,1072) or $[W(CO)_5I][NEt_4]$ (928). A crystal structure (R = Me) reveals that the carbonyls adopt a facial arrangement, the coordination polyhedron at tungsten were best described as a 4:3 tetragonal–trigonal base (1071). In solution, they are fluxional with two distinct intramolecular rearrangement processes observed by VT ^{13}C NMR spectroscopy; the first averaging two carbonyls and the second, all three. A twisting of the trigonal plane (which contains two carbonyls) relative to the tetragonal base and an internal trigonal rotation have been suggested to account for these observations (353,1071,1073).

Like the molybdenum analogues, they lose CO to give 16-electron complexes, $[W(CO)_2(S_2CNR_2)_2]$ (**158**) (Fig. 117), however, this generally proceeds more slowly and often requires thermal activation, the process being more rapid for the larger ethyl versus methyl derivative (1072). Addition of nitrogen-donor ligands results in weak coordination, although hydrazine and ethylenediamine bind more strongly to give bridged complexes, $[\{W(CO)_2(S_2CNR_2)_2\}(\mu\text{-}L)]$ (1072). In contrast, phosphines and phosphites bind much more strongly (353,1072,1073). A crystal structure of one such adduct, $[W(CO)_2(PPh_3)(S_2CNEt_2)_2]$ (**159**) (Fig. 117), reveals a similar 4:3 tetragonal–trigonal base geometry, the phosphine lying in the tetragonal plane (1073).

Phosphine substituted complexes also undergo a facile intramolecular rearrangement at low temperatures. Two distinct carbonyl signals are seen in the ^{13}C NMR spectrum, which interconvert even at 0°C via a process believed to involve a capped trigonal-prismatic intermediate (1073). Related phosphine

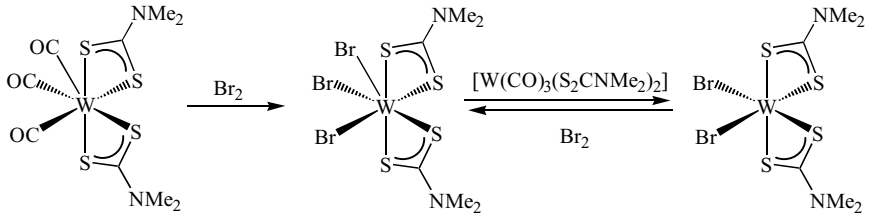

160 **161** **162**

Figure 118. Synthesis of $[WBr_3(S_2CNMe_2)_2]$ and interconversion with $[WBr_2(S_2CNMe_2)_2]$.

complexes, $[W(CO)_n(PMe_3)_{3-n}(S_2CNR_2)_2]$ (n = 1, 2; R = Me, Et, *i*-Pr), can be prepared upon addition of 2 equiv of dithiocarbamate salt to $[WCl_2(CO)_2(PMe_3)_3]$, and can be interconverted upon addition of CO and PMe_3, respectively, although the latter does not go to completion (927). In a similar manner the bis(phosphite) complex, $[W(CO)\{P(OMe)_3\}_2(S_2CNC_4H_4)_2]$, has also been prepared upon addition of 2 equiv of $KS_2CNC_4H_4$ to $[WCl_2(CO)_2\{P(OMe)_3\}_2]$ (353).

A number of further reactions have been carried out, those with alkynes being discussed later. Oxidation of $[W(CO)_3(S_2CNMe_2)_2]$ (**160**) by bromine occurs at room temperature giving the tungsten(V) complex $[WBr_3(S_2CNMe_2)_2]$ (**161**) (Fig. 118). The latter in turn is converted into the corresponding tungsten(IV) dihalide, $[WBr_2(S_2CNMe_2)_2]$ (**162**), upon heating with further $[W(CO)_3(S_2CNMe_2)_2]$ in dichloromethane, a transformation that is reversed upon addition of more bromine (922).

Addition of either $[NEt_4]F$ or $[PPN]N_3$ to $[W(CO)_3(S_2CNR_2)_2]$ (R = Me, Et) gives seven-coordinate anions, $[WX(CO)_2(S_2CNR_2)_2]^-$ (X = F, N_3) (**163**) (Fig. 119) (928). Lappert and co-workers have shown that a carbonyl can be replaced by the stannylene, SnR_2 [R = $CH(SiMe_3)_2$], to give $[W(CO)_2(SnR_2)$

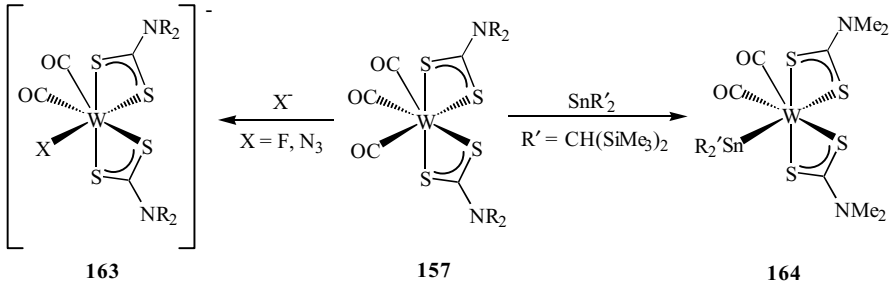

163 **157** **164**

Figure 119. Further reactions of $[W(CO)_3(S_2CNR_2)_2]$.

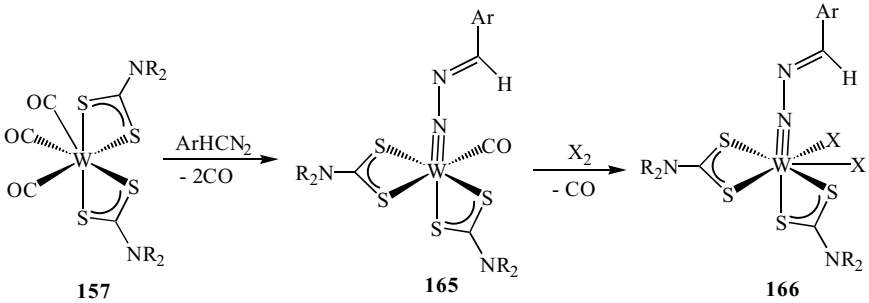

157 **165** **166**

Figure 120. Formation of diazoalkane complexes from $[W(CO)_3(S_2CNR_2)_2]$ and their subsequent oxidation.

$(S_2CNMe_2)_2]$ (**164**) (Fig. 119), which in turn reacts slowly with diphenylethyne affording $[W(CO)_2(PhC_2Ph)(S_2CNMe_2)_2]$ (1074). More unusually, prolonged thermolysis in benzene affords novel dimeric complexes as detailed later (see Section V.B) (1074,1075).

Hillhouse and Haymore (922) described the formation of diazoalkane complexes, $[W(CO)(N_2CHAr)(S_2CNR_2)_2]$ ($R = Me$, Et, $R_2 = C_4H_8$; $Ar = Ph$, *p*-tol) (**165**) (Fig. 120), from the room temperature reaction of diazoalkanes with $[W(CO)_3(S_2CNR_2)_2]$, together with some analogous molybdenum complexes that are less stable. They react further with halogens to give tungsten(IV) complexes, $[WX_2(N_2CHAr)(S_2CNR_2)_2]$ ($X = Cl$, Br), while addition of HBr affords what is believed to be $[WBr_2(NH{-}NH{=}CHAr)(S_2CNR_2)_2]$ (**166**) (Fig. 120), resulting from the addition of two hydrogen atoms to the diazoalkane moiety.

In other work, Baker et al. (926,937) shown that addition of NaS_2CNBz_2 to $[WI_2(CO)_3(MeCN)_2]$ yields dimeric $[\{W(\mu\text{-}I)(CO)_3(S_2CNBz_2)\}_2]$, while related monomeric complexes, $[WI(CO)_3(EPPh_3)(S_2CNR_2)]$ ($R = Et$, Bz; $E = P$, As, Sb), result from $[WI_2(CO)_3(MeCN)(EPPh_3)]$.

The nitrosyl chemistry of tungsten is not as well developed as that of molybdenum. Broomhead and co-workers (893–895) investigated the reactivity of tungsten(II) nitrosyl complexes, $[W(NO)_2(S_2CNR_2)_2]$. Their behavior is generally analogous to their molybdenum counterparts (see earlier). However, the reaction of $[W(NO)_2(S_2CNEt_2)_2]$ with anions ($X = N_3$, NCO or NCS) in DMSO, which results in loss of N_2O and formation of $[WX_2(NO)(S_2CNEt_2)_2]^-$, is photochemically (888,895), rather than thermally activated, and proceeds at a slower rate than the molybdenum analogue (893). This has been attributed, in part, to the greater energy required to transfer an electron pair from the metal *d* orbitals to the π^*-$(NO)_2$ orbital upon formation of the postulated, reactive seven-coordinate intermediate.

Johnson et al. (885) shown that, in a similar manner to the analogous molybdenum complexes, photolysis of $[W(NO)_2(S_2CNR_2)_2]$ (R = Me, Et, Pr) affords tungsten(III) nitrosyl complexes, $[W(NO)(S_2CNR_2)_3]$, in high yields. The latter are rigid at room temperature on the NMR time scale, and it is only upon heating to 130°C when all three dithiocarbamate ligands become equivalent.

f. Alkyne Complexes. Alkynes bind to a range of tungsten dithiocarbamate centers, being most common for tungsten(II). The first example of a tungsten(II) alkyne–carbonyl complex, namely, $[W(CO)(HC_2H)(S_2CNEt_2)_2]$, was prepared upon displacement of the phosphine from $[W(CO)_2(PPh_3)(S_2CNEt_2)_2]$ (1076,1077). Further examples of complexes of this type have more recently been prepared from $[W(CO)_3(S_2CNR_2)_2]$ and alkynes (819, 820, 931, 1078). Carlton and Davidson (1079) also prepared examples, $[W(CO)(MeC_2R)(S_2CNMe_2)_2]$ (R = Me, Ph), upon addition of 2 equiv of NaS_2CNMe_2 to $[WBr_2(CO)(MeC_2R)_2]_2$, while Baker and Flower (1080), have prepared $[W(CO)(MeC_2Me)(S_2CNC_4H_8)(S_2CNR_2)]$ (R = Me, Et, Bz; $R_2 = C_4H_8$) upon addition of a second dithiocarbamate salt to $[W(CO)(MeCN)(MeC_2Me)_2(S_2CNC_4H_8)][BF_4]$ (Fig. 121).

Crystallographic studies show that the alkyne and carbonyl are nearly coplanar, and although the metal center may be considered as pseudo-octahedral, a better description seems to be one in which the carbonyl and a sulfur of one dithiocarbamate ligand occupy the axial sites of a pentagonal bipyramid (820,1078).

In solution, complexes are fluxional, being attributed to an alkyne rotation, activation barriers being in the region of 45–50 kJ mol^{-1} (1078,1079). Molecular orbital calculations have been carried out on the model complexes, $[M(CO)(HC_2H)(S_2CNH_2)_2]$ (M = Mo, W), and satisfyingly (but possibly fortuitously) the calculated barrier to alkyne rotation is very close to those measured (821). For the asymmetric alkyne complexes, $[W(CO)(MeC_2Ph)(S_2CNMe_2)_2]$, two isomers might be expected, but in both instances, as is the case with $[W(CO)(HC_2Ph)(S_2CNEt_2)_2]$, only one is observed at low temperature (1079). This effect is attributed to the propensity of the bulky phenyl group to adopt a position distal to the carbonyl ligand (931).

Electrochemical studies have also been carried out and reveal reversible reduction behavior but irreversible oxidation chemistry as expected for unsaturated species (931). However, ^{13}C NMR studies suggest that the alkyne acts as a four-electron donor, chemical shifts of $\sim$ 206 ppm being noted for the alkyne carbons, and thus the complexes are best considered as 18-electron species (819,1081).

The hydrid phosphine–alkyne, bis(diphenylphosphino)ethyne, reacts with $[W(CO)_3(S_2CNEt_2)_2]$ to give orange $[W(CO)_2(Ph_2PC_2PPh_2)(S_2CNEt_2)_2]$,

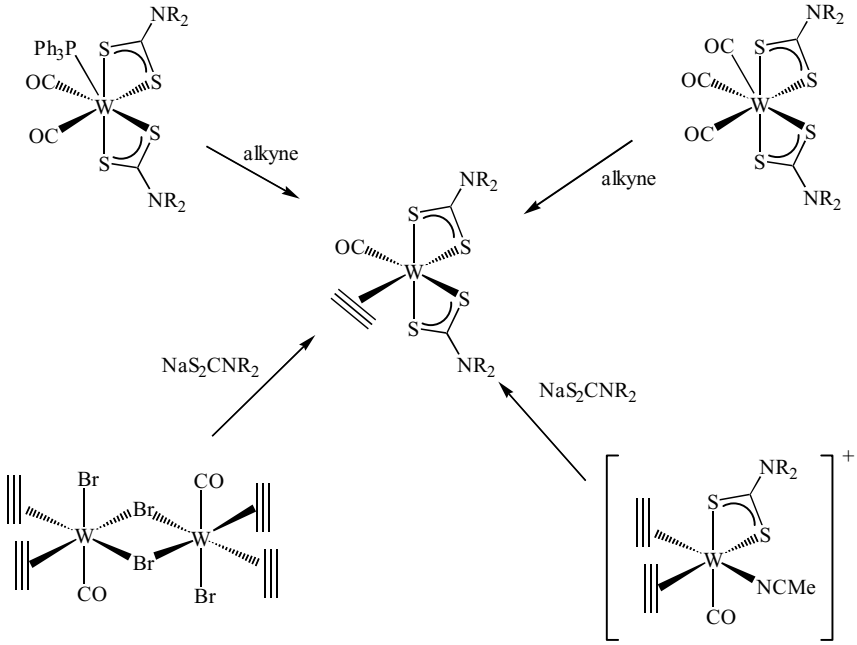

Figure 121. Schematic representations of synthetic routes to $[W(CO)_2(alkyne)(S_2CNR_2)_2]$.

whereby the ligand coordinates as a phosphine. Upon sitting in acetone for 10 h, the solution turns green as a result of carbonyl loss and the formation of the alkyne complex, $[W(CO)(Ph_2PC_2PPh_2)(S_2CNEt_2)_2]$ (1078). This then reacts further with a range of metal carbonyl via coordination of the two phosphorus atoms. For example, addition of *cis*-$[M(CO)_4(NHC_5H_{10})_2]$ (M = Cr, Mo, W) yields $[W(CO)(Ph_2PC_2PPh_2)(S_2CNEt_2)_2M(CO)_4]$ (Eq. 99), in which the diphosphine binds to tungsten via the alkyne moiety and chelates the second group 6 (VIB) metal center through phosphorus (1082). Incorporation of the phosphine centers has the advantage that barriers to alkyne rotation can be conveniently measured by ^{31}P NMR spectroscopy.

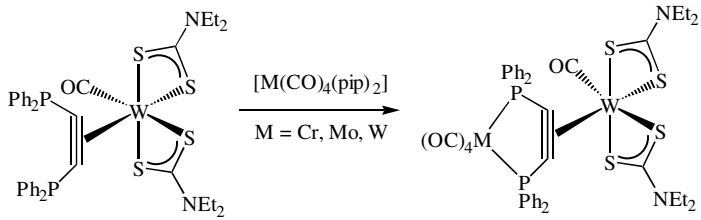

(99)

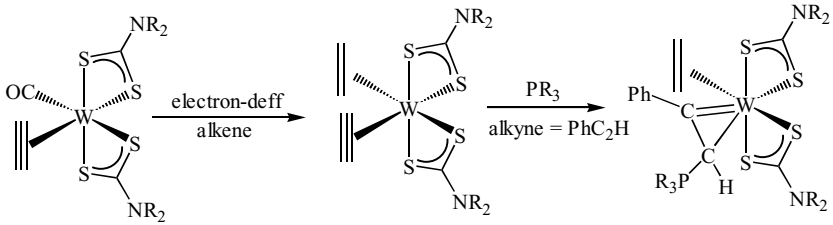

Figure 122. Formation of $[W(alkene)(alkyne)(S_2CNR_2)_2]$ and their subsequent reaction with phosphines.

A number of other reactions of $[W(CO)(alkyne)(S_2CNR_2)_2]$ complexes have been carried out, which broadly mirror the chemistry of the molybdenum analogues. Addition of electron-deficient alkenes yields mixed alkene–alkyne complexes, $[W(alkene)(alkyne)(S_2CNR_2)_2]$ (**167**) (Fig. 122) (934). A crystal structure of the maleic anhydride derivative, $[W(alkene)(PhC_2H)(S_2CNMe_2)_2]$, reveals the expected cis arrangement of the organic ligands. These mixed-alkene–alkyne complexes react further with phosphites and phosphines. The site of attack is the terminal carbon of the alkyne, which yields a range of cyclic alkylidene complexes, such as $[W(alkene)\{\eta^2\text{-}C(Ph)CH(PR_3)\}(S_2CNR_2)_2]$ (**168**) (Fig. 122) (934).

Controlled oxidation of $[W(CO)(HC_2R')(S_2CNR)_2]$ ($R' = H$, Ph; $R = Me$, Et) by the dimeric oxo-transfer reagent, $[Mo_2O_2(\mu\text{-}O)\{S_2P(OEt)_2\}_4]$, affords the tungsten(IV) oxo complexes, $[WO(HC_2R')(S_2CNR)_2]$ (1058). Variable temperature NMR studies suggest that alkyne rotation does not occur for these complexes (on the NMR time scale). There is, however, a fluxional process that interconverts the two dithiocarbamate ligands at higher temperatures. This behavior has been interpreted in terms of an intermediate involving a monodentate dithiocarbamate, the sulfur trans to the oxo moiety is labilized by the trans-influence of the π-donor ligand.

Similar fluxional behavior is found for the analogous sulfido complexes, $[WS(PhC_2Ph)(S_2CNR_2)_2]$ (**170**), formed upon addition of cyclohexene sulfide to $[W(CO)(PhC_2Ph)(S_2CNR_2)_2]$ ($R = Et$, Me) (**169**) (Eq. 100). A second product of this reaction is the thiocarboxamide complex $[WS(PhC_2Ph)(S_2CNR_2)(SCNR_2)]$ (**171**) (1083), formed from a carbon–sulfur bond cleavage reaction, and also resulting from addition of PEt_3 to $[WS(PhC_2Ph)(S_2CNR_2)_2]$ (1084) (see Section V.A). Variable temperature NMR studies on **171** also reveal a dynamic process that equilibrates the alkyl substituents on the dithiocarbamate. Here it is proposed to involve dechelation of the thiocarboxamide group

followed by rearrangement of the five-coordinate intermediate (1084).

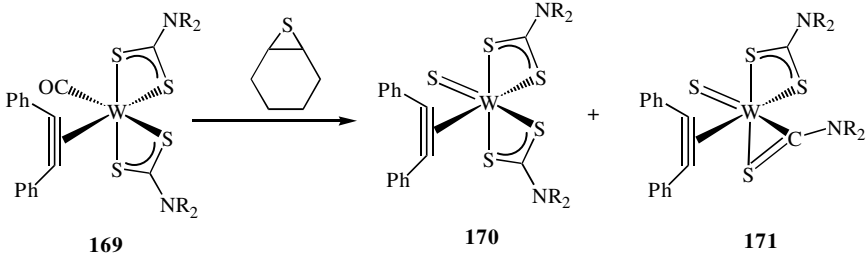

169 **170** **171**

(100)

Bis(alkyne) complexes, $[W(R'C_2R')_2(S_2CNR_2)_2]$, have been prepared from $[W(CO)(RC_2R)(S_2CNR_2)_2]$ (369,936,1085) and also upon addition of 2 equiv of dithiocarbamate salts to $[WI_2(PhC_2Ph)_2(MeCN)_2]$ (Fig. 123); dimeric $[W(\mu\text{-}I)(PhC_2Ph)_2(S_2CNR_2)]_2$ being an intermediate in the latter process (1086).

In a recent publication, Curran et al. (1085) described the synthesis of bis(alkyne) complexes, $[W(HC_2R)_2(S_2CNMe_2)_2]$, in which the alkyne is part of an amino acid derivative. From ^{1}H NMR data, it is clear that three conformations about the metal center exist simultaneously in solution, namely, cis, trans', and trans'' (Fig. 124). This situation is similar to the one found for other unsymmetrical alkynes (369).

In a series of publications, Baker and co-workers(1087–1091) investigated the synthesis, structure, and reactivity of cationic tungsten(II) alkyne complexes. They are formed via neutral bis(alkyne) complexes, $[WI(CO)(R^1C_2R^1)_2(S_2CNR_2)]$ ($R^1 = Me$, Ph) (**173**), being prepared from $[WI_2(CO)(MeCN)(R^1C_2R^1)_2]$ (**172**) (1089), and in turn react with $NaBPh_4$ or $AgBF_4$ in acetonitrile to give $[W(CO)(MeCN)(R^1C_2R^1)_2(S_2CNR_2)]^+$ (**174**) (Fig. 125) (1087,1088, 1090). Crystallographic studies reveal a pseudo-octahedral coordination sphere

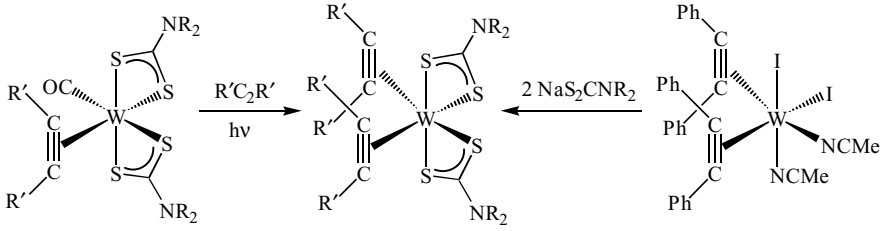

Figure 123. Synthetic routes to $[W(alkyne)_2(S_2CNR_2)_2]$.

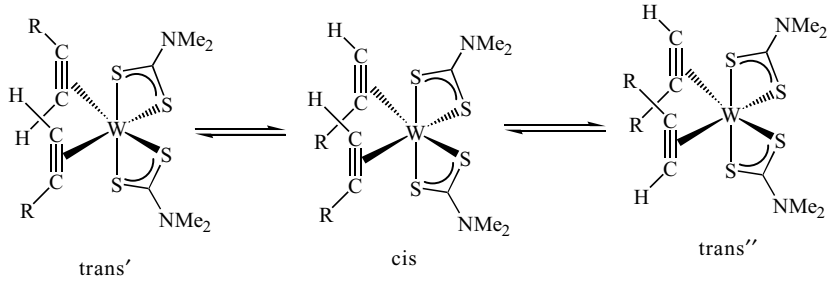

Figure 124. Isomeric forms of unsymmetrical bis(alkyne) complexes, $[W(RC_2H)(S_2CNMe_2)_2]$.

with a trans arrangement of carbonyl and acetonitrile ligands (1090), and ^{13}C NMR data suggest that each alkyne acts as a three-electron donor (1089).

The reactivity of but-2-yne complexes has been probed, incorporation of a wide variety of monodentate ligands including phosphines, phosphites, isonitriles (1087), and neutral and anionic chelating ligands are reported (1087,1088). Monodentate ligands tend to displace the acetonitrile readily (1087), while with bidentate ligands loss of an alkyne and acetonitrile occurs (1088). For example, bis(diphenylphosphino)methane (dppm), reacts with $[W(CO)(MeCN)(S_2CNC_4H_8)(MeC_2Me)_2]^+$ to give the monoalkyne complex, $[W(CO)(S_2CNC_4H_8)(MeC_2Me)(\eta^2\text{-dppm})]^+$ (Eq. 101), which has been crystallographically characterized. Analogous diphosphine complexes, $[W(CO)(S_2CNR_2)(MeC_2Me)(\eta^2\text{-dppm})]I$ ($R = Me$, Et, Bz; $R_2 = C_4H_8$), have also been prepared upon addition of dithiocarbamate salts to $[WI(CO)(MeCN)(MeC_2Me)(dppm)][BF_4]$ or $[WI_2(CO)(MeC_2Me)(dppm)]$; reactions proposed to occur via an intermediate containing a monodentate dithiocarbamate. Incorporation of the diphosphine again also allows the rotational barrier of the alkyne to be easily measured

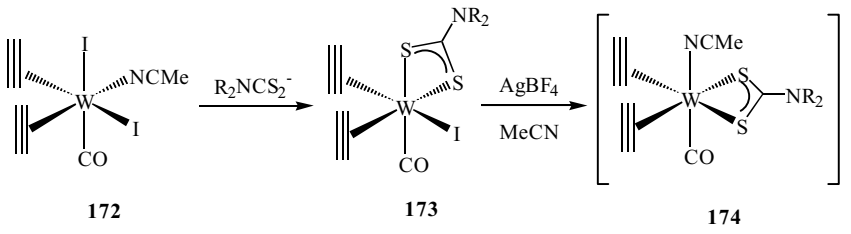

Figure 125. Synthesis of tungsten(II) bis(alkyne) complexes.

(50 ± 1 kJ mol^{-1}) by ^{31}P NMR spectroscopy (1091).

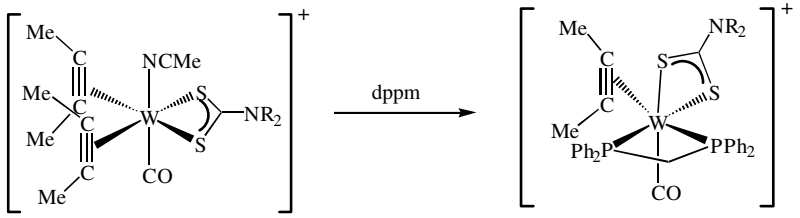

(101)

g. Other Organic Ligands and Transformations. A wide range of different organic ligands have been prepared at the dithiocarbamate-stabilized tungsten center. These include tungsten(IV) alkylidyne complexes, [W(CPh)$(CO)_2(PPh_3)(S_2CNMe_2)$] and [W(CPh)$(CO)(PMe_3)_2(S_2CNEt_2)$] (**176**), formed upon addition of dithiocarbamate salts to *cis*-[WCl(CPh)-$(CO)_2(PPh_3)_2$] and [WCl(CPh)$(CO)(PMe_3)_3$] (**175**), respectively. Interestingly, (**176**) reacts further with carbon monoxide in both the solid state and in solution to give the ketenyl complex [W{PhCC(O)}$(CO)(PMe_3)_2(S_2CNEt_2)$] (**177**), a process that can be reversed at 100°C (Fig. 126) (1092).

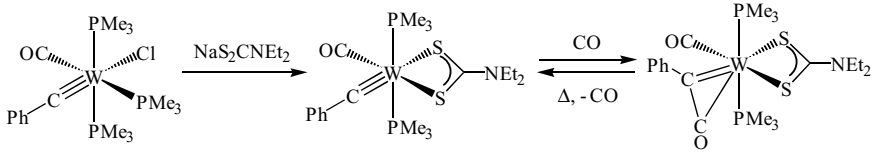

175 **176** **177**

Figure 126. Synthesis of [W(CPh)$(CO)(PMe_3)_2(S_2CNEt_2)$] and subsequent reversible formation of a ketenyl complex.

The alkylidyne complex, $[W(CO)_2(CCH_2Ph)(dppe)]^+$, also reacts with dithiocarbamate salts to give ketenyl products, $[W(CO)_2\{PhCH_2CC(O)\}(dppe)(S_2CNR_2)]$ (R = Me, Et), formed via an intermediate containing a monodentate dithiocarbamate. The nucleophilic nature of the ketenyl ligand is shown by facile reactions with acids and $[Me_3O][BF_4]$ (Eq. 102) yielding alkyne complexes, $[W(CO)(PhCH_2C_2OX)(dppe)(S_2CNR_2)]$ (X = H, Me) (1093).

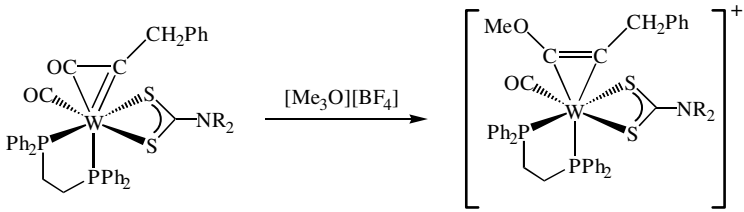

(102)

Facile dithiocarbamate-induced carbonyl-alkylidyne coupling is also observed upon addition of dithiocarbamate salts (R = Me, Et) to cyclic alkylidyne complexes $[W(CO)_2(MeCN)(dppe)\{CCH{=}(CH_2)_n\}]$ ($n = 4$, 7) (Eq. 103), a monodentate dithiocarbamate intermediate being proposed (1094).

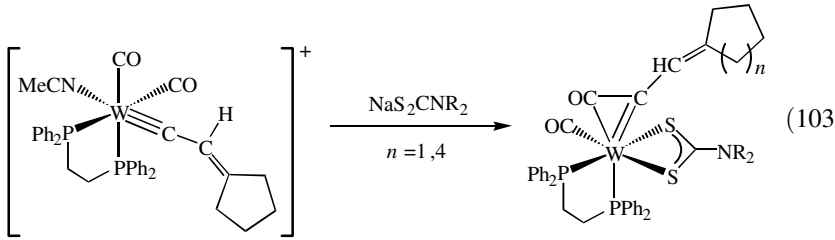

(103)

Addition of 2 equiv of dithiocarbamate salts to $[WCl(CPh)(CO)_2(py)_2]$ (**178**) also affords ketenyl complexes, $[W(CO)\{PhCC(O)\}(S_2CNR_2)_2]^-$ (**179**). With $[H_2NEt_2][S_2CNEt_2]$, however, a quite different reaction occurs; the thioaldehyde complex, $[W(CO)(SCHPh)(SCNEt_2)(S_2CNEt_2)]$ (**180**), being formed in 96% yield (Fig. 127). Mechanistic details are unclear, but it is proposed that an intermediate bearing two dithiocarbamates (one monodentate) may have an alkylidyne ligand, the latter being sufficiently basic to deprotonate the ammonium salt and give an alkylidene. The alkylidene then interacts with a dithiocarbamate to give thioaldehyde and thiocarboxamide ligands (1095).

Related to this ketenyl chemistry is the formation of vinylketenes, $[W(CO)(S_2CNR_2)_2\{\eta^2,\eta^2\text{-}O{=}C{=}C(Ph)CH{=}CHMe\}]$ (R = Me, Et, Ph) (**183**), from the allylidene complex $[W(CO)_2Br_2\{\eta^1,\eta^2\text{-}C(Ph)CH{=}CHMe\}(4\text{-picolene})]$ (**181**) and dithiocarbamate salts at 50°C (1096–1098). At lower temperatures four intermediates are observed, spectroscopic studies indicating that each contains an η^1,η^3-allyldithiocarbamate ligand generated by dithiocarbamate addition to the tungsten–alkylidene bond. Indeed, in one case such a complex,

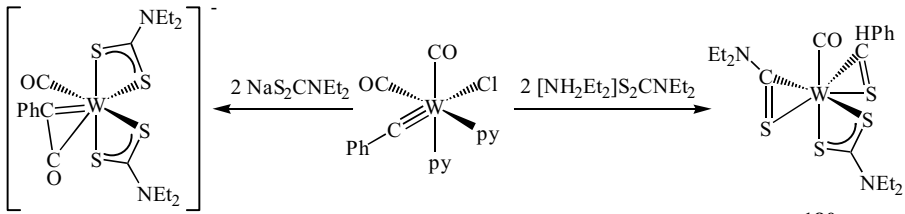

179 **178** **180**

Figure 127. Reactions of $[WCl(CPh)(CO)_2(py)_2]$ with different diethyldithiocarbamate salts.

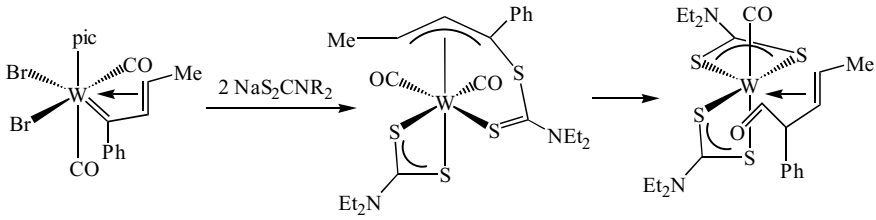

181 **182** **183**

Figure 128. Formation of vinylketene complexes via an allyldithiocarbamate intermediate.

namely, $[W(CO)_2(S_2CNEt_2)\{\eta^1,\eta^3\text{-}SC(NEt_2)SCPhCH{=}CHMe\}]$ (**182**), was isolated and crystallographically characterized (Fig. 128) (1096).

Vinyl ketene complexes, $[W(CO)(S_2CNR_2)_2\{\eta^2,\eta^2\text{-}O{=}C{=}C(R')CH{=}CH_2\}]$ ($R' = H$, Me; $R = Me$, Et, Ph; $R_2 = C_4H_4$), are also formed upon addition of cyclopropene or methyl cyclopropene to $[W(CO)_2(S_2CNR_2)_2]$ in an analogous fashion to that described for the molybdenum analogues (see Section IV.C.2.i). Two carbonyl bands are seen in the IR spectrum, that between 1960 and 1933 cm^{-1} being attributed to the metal bound carbonyl, while a second band between 1780 and 1734 cm^{-1} is associated with the ketenyl carbonyl (925).

Carmona et al. (1099) reported that addition of NaS_2CNMe_2 to monodentate acyl complexes, $[WCl(CO)\{C(O)R\}(PMe_3)_3]$ ($R = CH_2{-}t\text{-}Bu$, CH_2CMe_2Ph), yields $[W(CO)(PMe_3)_2\{\eta^2\text{-}C(O)R\}(S_2CNMe_2)]$. In one case ($R = CH_2SiMe_3$), a mixture of acyl and alkyl complexes results, the $SiMe_3$ group also being extremely susceptible to hydrolytic cleavage. A related acyl complex, $[W(CO)_2(PMe_3)\{\eta^2\text{-}C(O)Me\}(S_2CNMe_2)]$ (**185**), results from carbonylation of $[W(CH_3)(CO)_2(PMe_3)_2(S_2CNMe_2)]$ (**184**). It reversibly adds a further equivalent of phosphine to yield $[W(CO)_2(PMe_3)_2\{\eta^2\text{-}C(O)Me\}(\eta^1\text{-}S_2CNMe_2)]$ (**186**), proposed on the basis of spectroscopic data to contain a monodentate dithiocarbamate ligand (Fig. 129) (243).

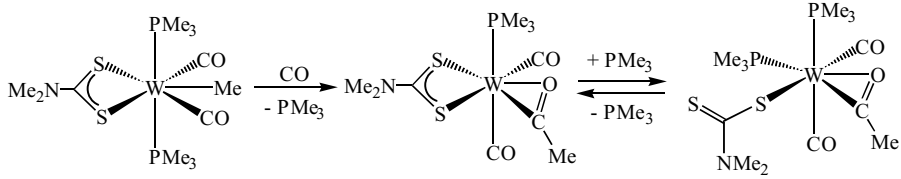

184 **185** **186**

Figure 129. Synthesis of $[W(CO)_2(PMe_3)\{\eta^2\text{-}C(O)Me\}(S_2CNMe_2)]$ and subsequent reversible reaction with PMe_3.

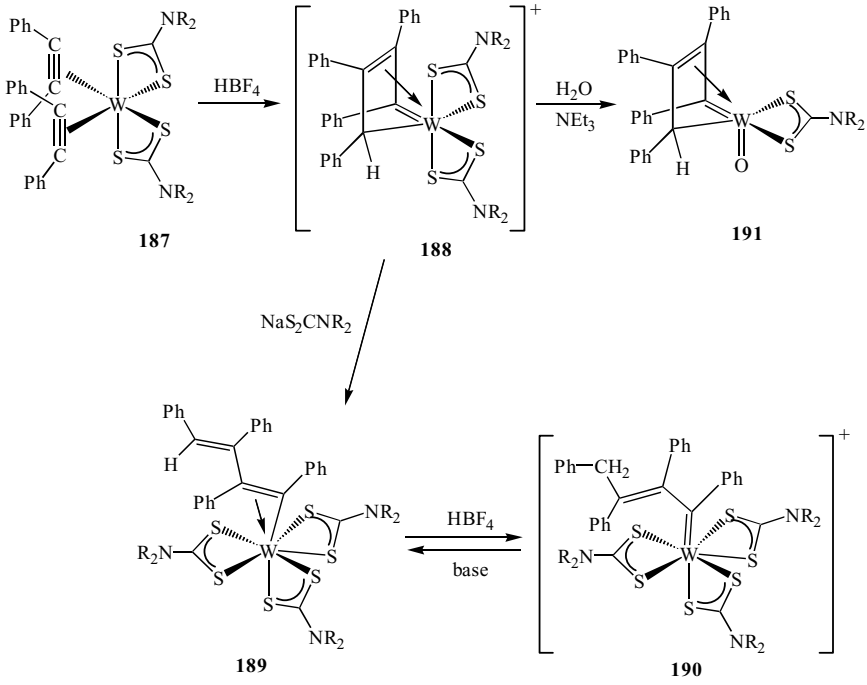

Figure 130. Synthesis of $[W(\eta^4\text{-}C_4Ph_4H)(S_2CNR_2)_2]$ and examples of its reactivity.

Templeton and co-workers (936) reported that coupling of alkynes in $[W(PhC_2Ph)_2(S_2CNR_2)_2]$ (R = Me, Et) (**187**) upon protonation with HBF_4 yields η^4-butadienyl complexes $[W(\eta^4\text{-}C_4Ph_4H)(S_2CNR_2)_2][BF_4]$ (**188**) (Fig. 130). These in turn react with more dithiocarbamate salt to give η^2-vinyl complexes, $[W(\eta^2\text{-}CPh{=}CPhCPh{=}CHPh)(S_2CNR_2)_3]$ (**189**). Further protonation then occurs reversibly at the terminal olefin carbon yielding vinylcarbene products $[W\{{=}CPhCPh{=}CPh(CH_2Ph)\}(S_2CNR_2)_3]^+$ (**190**) (1100). The butadienyl complex, $[W(\eta^4\text{-}C_4Ph_4H)(S_2CNEt_2)_2][BF_4]$, also reacts with $LiBHEt_3$ giving $[W(\eta^4\text{-}C_4Ph_4H)(S_2CNEt_2)_3]$ and $[WS(\eta^4\text{-}C_4Ph_4H)(S_2CNEt_2)]$ (1100), while with water in the presence of triethylamine, the oxo analogue, $[WO(\eta^4\text{-}C_4Ph_4H)(S_2CNEt_2)]$ (**191**), results (936). Crystallographic studies of the latter (936,1100) reveal delocalization within the ring π-system as evidenced from an inspection of the carbon–carbon bond lengths.

In related work, coupling of two alkynes and carbon monoxide has been achieved at a tungsten(II) center. Thus, reaction of $[W(CO)_2L(S_2CNMe_2)_2]$ (L = CO, PPh_3) with an excess of cyclooctyne results in two products; $[W(CO)(S_2CNMe_2)_2(\eta^2,\eta^2\text{-}C_4R_4CO)]$ and $[W(\eta^2\text{-}RC_2R)(S_2CNMe_2)_2(\eta^2,\eta^2\text{-}C_4R_4CO)]$ (RC_2R = cyclooctyne), both containing a cyclopentadienone ligand

(Eq. 104). Crystallographic characterization of the former reveals that the carbonyl and organic ligands lie cis to one another (1101).

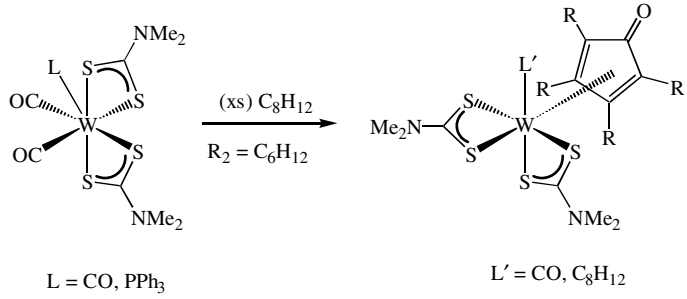

(104)

L = CO, PPh_3 L′ = CO, C_8H_{12}

h. Binuclear Complexes. A significant number of binuclear tungsten complexes have been reported, predominantly supported by oxo and sulfido ligands and containing tungsten(V) centers, although tungsten(III) complexes are also known. Of the tungsten(V) complexes, those with the general formula, $[WE(\mu\text{-}E)(S_2CNR_2)]_2$ (E = O, S), are most common (183, 1055, 1056, 1059, 1062, 1102–1109). Oxo complexes (E = O) have been prepared from addition of dithiocarbamate salts to $[WO_4]^{2-}$, which in turn react with hydrogen sulfide to give $[WO(\mu\text{-}S)(S_2CNR_2)]_2$; the sulfur atoms taking up bridging sites (1105, 1110). The latter have also been prepared from reduction of $[WO(S_2)\text{-}(S_2CNR_2)_2]$ by sulfur dioxide (1059).

Tetrasulfide complexes, $[WS(\mu\text{-}S)(S_2CNR_2)]_2$, can be prepared in a number of ways. Stiefel and co-worker (1111) showed that reduction of $[NEt_4]_2$ $[W_2S_2(\mu\text{-}S)_2(S_4)_2]$ by PPh_3 in the presence of dithiocarbamate salts affords an elegant route (R = Et, *i*-Bu); the mono-oxo complex, $[W_2OS(\mu\text{-}S)_2(S_2CN{-}i\text{-}Bu_2)_2]$, being a side product in one instance. In a similar manner, tetrasulfide complexes (R = Me, Ph) have also been reported from addition of dithiocarbamate salts to $[NH_4]_2[WS_4]$ (1109). Other preparative methods have also been used, including the displacement of dithiophosphate ligands from $[WS(\mu\text{-}S)\{S_2P(OEt)_2\}]_2$ (1106), reactions of thiuram disulfides with $W(CO)_6$ (1106) or $[Tp^*W(CO)_3]^-$ (183), and the replacement of the terminal oxo groups of $[WO(\mu\text{-}S)(S_2CNR_2)]_2$ upon reaction with P_4S_{10} (Eq. 105) (1103,1104,1107).

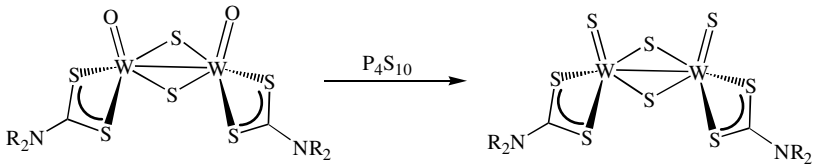

(105)

Crystallographic studies on $[WE(\mu\text{-}S)(S_2CNEt_2)]_2$ (E = O, S) reveal tungsten–tungsten interactions indicative of a single bond and a syn coordination of dithiocarbamate ligands (1106,1062). Related complexes are believed to display similar characteristics.

Few reactions of $[WS(\mu\text{-}S)(S_2CNEt_2)]_2$ have been reported. Addition of a range of substituted pyridines (L) is proposed to reversibly yield $[WS(\mu\text{-}S)(S_2CNEt_2)L]_2$, although their precise nature has not been determined (1102), while tetrasulfides have also been used as synthons to a range of trinuclear and cubane-type tetranuclear clusters (see below) (1023,1024).

Dimeric tungsten(V) sulfido-bridged diazoalkane complexes, $[W_2S(NNCR^1R^2)(PPhMe_2)(\mu\text{-}S)_2(S_2CNR_2)_2]$ (R = Et, *i*-Pr; $R^1 = R^2 = Me$; R^1 = Me, R^2 = Ph; R^1 = H, R^2 = *p*-tol), have been prepared upon addition of thiuram disulfides to $[W_2S_2Cl(NNCR^1R^2)(PPhMe_2)_2(\mu\text{-}S)_2]^+$ at 0°C (Eq. 106), and the pyrrolyl imido complexes $[W_2S(NNC_4H_4)(PPhMe_2)(\mu\text{-}S)_2(S_2CNR_2)_2]$ have been prepared via a similar method (1112).

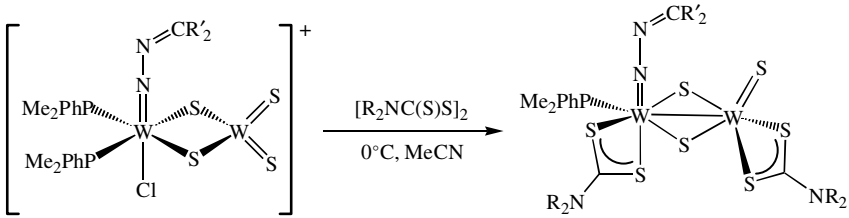

(106)

Tungsten(III) dimers, $[W_2(S_2CNR_2)_6]$ (R = Et, Pr, Bu; $R_2 = C_5H_{10}$), result upon irradiation of $[W(CO)_3(\eta^6\text{-}C_6H_5Me)]$ with thiuram disulfides. They reportedly react further (R = Et) with pyridine *N*-oxide and $[Et_4N]NO_3$ to give $[W_2O_2(\mu\text{-}O)(S_2CNEt_2)_4]$ and $[W_2(\mu\text{-}O)\{\mu\text{-}N(=O)O\}(S_2CNEt_2)_4(\eta^1\text{-}S_2CNEt_2)_2]$, respectively, although precise details regarding the nature of the latter are not clear (1048). A further tungsten(III) complex, $[W(np)(S_2CNEt_2)(\mu\text{-}O_2CMe)]_2$ (np = neopentyl), results from addition of 2 equiv of dithiocarbamate salt to $[W(np)(\mu\text{-}O_2CMe)_2]_2$ (1113). Both complexes contain tungsten–tungsten triple bonds, but the transformation leads to a change in electronic structure from $\pi^4\delta^2$ to $\sigma^2\pi^4$ and is shown to have no electronic barrier.

i. Clusters. In a similar manner to the molybdenum analogue (see Section IV.3.C.l), s*yn*-$[WS(\mu\text{-}S)(S_2CNEt_2)]_2$ (**192**) has been used as a synthon toward trinuclear and tetranuclear cubane-type clusters (1020,1023,1024). For example, addition of $[M(PPh_3)_4]$ (M = Pd, Pt) or $[MCl(PPh_3)_3]$ (M = Rh, Ir) affords trinuclear clusters $[W_2M(PPh_3)(\mu\text{-}S)_4(S_2CNEt_2)_2]$ (**193**) and $[W_2M(PPh_3)_2(\mu\text{-}Cl)(\mu\text{-}S)_3(\mu^3\text{-}S)(S_2CNEt_2)_2]$ (**194**), respectively, while with $[MCl(cod)]_2$

(M = Rh, Ir) cubane-type clusters $[W_2M_2Cl_2(cod)_2(\mu\text{-}S)_4(S_2CNEt_2)_2]$ (**195**) result. A related tetranuclear cluster $[W_2Co_2(CO)_2(MeCN)_2(\mu\text{-}S)_4(S_2CNEt_2)_2]$ is proposed to result from addition of $[Co_2(CO)_8]$ to *syn*-$[WS(\mu\text{-}S)(S_2CNEt_2)]_2$ followed by extraction with acetonitrile (1022).

Trinuclear $[W_3(\mu^3\text{-}Se)(\mu\text{-}Se_2)_3(S_2CNEt_2)_3][S_2CNEt_2]$ results from addition of NaS_2CNEt_2 to $[W_3X_4(\mu^3\text{-}Se)(\mu\text{-}Se_2)_3]$ (X = Cl, Br) (1000), while the analogous complex $[W_3(\mu^3\text{-}Se)(\mu\text{-}Se_2)_3(S_2CNEt_2)_3]Se$ has been prepared in low yields from the addition of tetraethylthiuram disulfide to $W(CO)_6$ in the presence of selenium (1002). The crystal structure of the latter has been carried out and shows the same cluster core arrangement **196** as the well-known molybdenum analogues, two trinuclear units being linked together by interactions with the selenide anion.

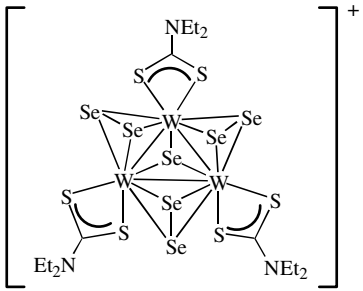

196

In further work, the mixed-metal trinuclear complex, $[WFe_2(\mu^3\text{-}S)_2(CO)_8(S_2CNEt_2)]^-$ (**197**), has been prepared from $[W(CO)_4(S_2CNEt_2)]^-$ and $[Fe_2(\mu\text{-}S_2)(CO)_6]^{2-}$. It has been crystallographically characterized and shows no direct metal–metal interactions (952).

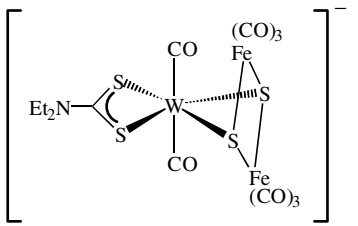

197

Tetranuclear cubane clusters $[WFe_3(\mu^3\text{-}S)_4(S_2CNR_2)_4(\mu\text{-}S_2CNR_2)]$ (R = Me; $R_2 = C_4H_8$) have been prepared from $[WS_4]^{2-}$, $FeCl_2$, and dithiocarbamate salts

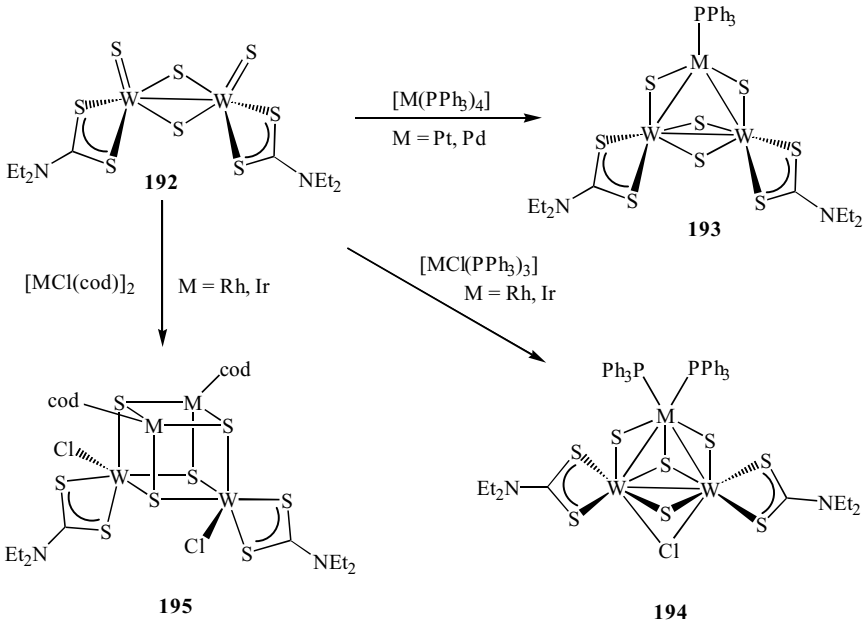

Figure 131. A selection of cluster building reactions utilizing *syn*-[WS(μ-S)(S_2CNEt_2)]$_2$.

in DMF (273,274). Crystallographic studies show that, like their molybdenum analogues, one dithiocarbamate bridges between tungsten and iron centers, and this is confirmed with the observation of two iron environments by ^{57}Fe Mössbauer spectroscopy (273).

D. Group 7: Manganese, Technetium, and Rhenium

1. Manganese

Dark violet manganese(III) dithiocarbamate complexes, [Mn(S_2CNR_2)$_3$], were first detailed in 1907 (2). In 1931, the synthesis of yellow manganese(II) complexes [Mn(S_2CNR_2)$_2$] was reported, which were shown to readily oxidize to their manganese(III) counterparts (1114). Now, manganese dithiocarbamate complexes are known for all oxidation states +1 to +4, although the nature of manganese(II) complexes, [Mn(S_2CNR_2)$_2$], still remains a topic of some debate.

a. Manganese (III) Complexes. Tris(dithiocarbamate) manganese(III) complexes [Mn(S_2CNR_2)$_3$] are well known and easily prepared. For example,

addition of 3 equiv of dithiocarbamate salts to $MnCl_2$ affords brown $[Mn(S_2CNC_5H_{10})_3]$ (1115), and violet $[Mn(S_2CNC_4H_8X)_3]$ (X = S, NMe, CH_2) (738), while a series of related methyl-substituted piperidine derivatives have also been prepared by this method (1116).

The crystal structure of a monoclinic polymorph of $[Mn(S_2CNEt_2)_3]$ has been determined and shows the same tetragonally distorted octahedron as seen in other compounds of this type with long axial [Mn—S_{ax} 2.582(1) Å] and short equatorial [Mn—S_{eq} 2.382(1), 2.389(1) Å] bonds (387). An electron-impact MS study of $[Mn(S_2CNR_2)_3]$ (R = Et; $R_2 = C_5H_{10}$, C_4H_8O) shows that molecular ions are not observed, the heaviest ions being those associated with loss of one dithiocarbamate (1117). Transfer of dithiocarbamate from manganese to copper is possible. Thus, interaction of $[Mn(S_2CNR_2)_3]$ (R = Et, Bz; $R_2 = C_4H_8$, MePh) and $[Cu(BF_4)_2]$ leads to the formation of $[Cu(S_2CNR_2)_2][BF_4]$, which results from dithiocarbamate transfer and oxidation to copper(III); the manganese(II) product being spontaneously oxidized in the nondeaerated solvent (1118).

Indian workers have described the synthesis of pentacoordinate complexes, $[MnCl(S_2CNR_2)_2]$ (R = Et; $R_2 = C_4H_8O$, C_5H_{10}) (1119). They result from the addition of HCl to the tris(dithiocarbamate) complexes, $[Mn(S_2CNR_2)_3]$, in dichloromethane. Structural characteristics are not known. They are nonelectrolytes, and thus presumed to be molecular, with the authors' favoring a square-based pyramidal metal coordination environment. Jezierski (1120) reported the synthesis of nitrosyl derivatives, $[MnCl(NO)(S_2CNR_2)_2]$. They are formed upon addition of NO to $[Mn(S_2CNR_2)_2]$ in the presence of chloride; no reaction is observed in the absence of the latter. The thiourea complexes $[Mn(NO)\{R_2NC(S)NR_2\}(S_2CNR_2)_2]^+$ are also formed in this reaction; the thiourea resulting from dithiocarbamate degradation (756). On the basis of ESR data, both types of complex are believed to be octahedral, the dithiocarbamates being mutually cis.

A number of mixed-ligand manganese(III) complexes have been prepared. For example, acetylacetenoate (acac) and glycine (gly) complexes, $[Mn(S_2CNR_2)_{3-n}(acac)_n]$ and $[Mn(S_2CNR_2)_{3-n}(gly)_n]$ ($R_2 = C_5H_{10}$, C_4H_8O; $n = 1, 2$), result from reactions of $MnCl_2$ with mixtures of the respective sodium salts (1115). The ESR measurements show that all are six coordinate with magnetic moments of 4.5–5.3 BM. One report also gives details of the synthesis of mixed-dithiocarbamate complexes, $[Mn(OH)(S_2CNH_2)(S_2CNR_2)]$, in which the substituted dithiocarbamates are Schiff-base derivatives of diethyldithiocarbamates, although structural details are not given (1121). Oxo-bridged, mixed-metal complexes, $[MnMoO(H_2O)(\mu\text{-}O)(S_2CNR_2)_4]$ (R = Et; $R_2 = C_5H_{10}$, C_4H_8O), are reportedly prepared from $Mn[MoO_4]$ and dithiocarbamate salts in acidic DMF. On the basis of magnetic susceptibility measurements (μ_{eff} 6.02–6.24 BM) they are proposed to contain manganese(III) and molybdenum(V) centers, although again precise structural details are not known (827).

b. Manganese (IV) Complexes. Manganese(IV) complexes $[Mn(S_2CNR_2)_3]^+$ are easily prepared upon oxidation of the corresponding manganese(III) species (Eq. 107). For example, oxidation of $[Mn(S_2CNC_4H_8O)_3]$ by iodine gives dark brown $[Mn(S_2CNC_4H_8O)_3]I_5$, which has been characterized crystallographically (1122). The anions form chains and the octahedral coordination environment of the cation is again tetragonally distorted, but to a much lesser extent than found in manganese(III) complexes [Mn—S 2.305(9)–2.351(7) Å]. Other workers report that addition of dilute solutions of halides to $[Mn(S_2CNR_2)_3]$ ($R = Et$; $R_2 = C_4H_8O$) yields manganese(IV) species, $[Mn(S_2CNR_2)_2X_2]$ ($X = Cl$, Br), with effective magnetic moments of 3.91–4.09 BM (1123). Oxidation $[Mn(S_2CNR_2)_3]$ can also be effected by copper(III) complexes such as $[Cu(S_2CNEt_2)_2][BF_4]$ (1124).

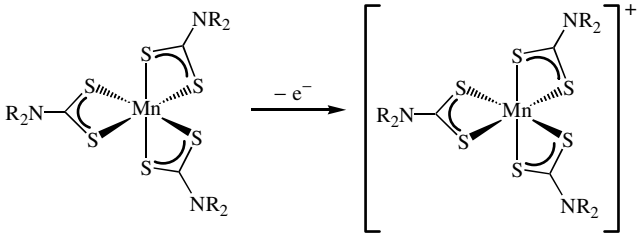

(107)

c. Manganese (II) Complexes. The authenticity and structure of highly air-sensitive manganese(II) complexes $[Mn(S_2CNR_2)_2]$ has been debated previously. A few new reports have appeared in this area and structural data is still absent. Siddiqi et al. (1125) reported a gray complex derived from β-naphthylamine under dry, nonaqueous conditions and propose manganese(II) on the basis of a magnetic susceptibility measurement (μ_{eff} 5.73 BM) and ESR spectra; the latter supporting a tetrahedral coordination environment. The same group also report manganese(II) dithiocarbamate complexes generated from succinimide and phthalimide (49). Jezierskii (1120) gives details of ESR measurements on bis(dithiocarbamate) complexes, analyzing the ^{55}Mn hyperfine interaction as a high-spin ($S = 5/2$) system.

The manganese(II) complex of benzylpiperazine dithiocarbamate is reported to be pink, with a magnetic moment of 3.71 BM (1126), while $[Mn(S_2CNR_2)_2]$ ($R_2 = C_4H_8$, C_5H_{10}), generated from $MnCl_2.4H_2O$, are reported decompose on heating under nitrogen to MnS, as monitored by TGA and DSC measurements (590).

Pandeya et al. (1127) reported the synthesis and characterization of red-brown manganese(II) complexes, $[Mn(S_2CNR_2)_2(L)]$ ($R = Et$; $R_2 = C_5H_{10}$, C_4H_8O; L = 2,2′-bpy, 1,10-phen), prepared by first adding the neutral bidentate

ligand to $MnCl_2$ followed by later addition of dithiocarbamate salts. The complexes are air stable and display magnetic moments of 5.8 ± 0.3 BM. The ESR measurements have been carried out, the results being comparable to those calculated for; $D = 0.19\ cm^{-1}$, $l = 0.04$, and $g_{iso} = 2.00$, and for magnetic field directions parallel to the principal D-tensor axes. Thus, it appears that addition of neutral bidentate ligands may stabilize the manganese(II) dithiocarbamate centers, and further work is warranted.

Doherty and Manning prepared authentic manganese(II) dithiocarbamate complexes, $[(\eta^5\text{-}C_5H_4Me)Mn(NO)(S_2CNR_2)]$, from the addition of dithiocarbamate salts to $[(\eta^5\text{-}C_5H_4Me)Mn(CO)_2(NO)][PF_6]$ (Eq. 108), although this interesting class of complexes appears not to have been studied further (1128).

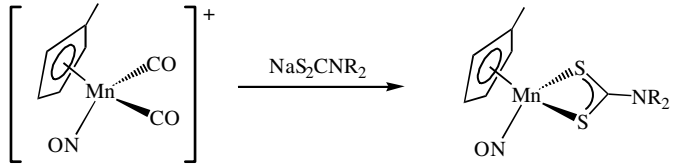

(108)

d. Manganese (I) Complexes. Adams and Huang (212) reported the synthesis of a manganese(I) complex, $[Mn(CO)_4(S_2CNHCO_2Et)]$, from the reaction of $[Mn_2(CO)_9(MeCN)]$ and $[EtO_2CN{=}CS_2CNHCO_2Et][S_2CNHCO_2Et]$. Heating the tetracarbonyl with $PhPMe_2$ at 68°C gives $[Mn(CO)_3(PPhMe_2)(S_2CNHCO_2Et)]$ (Eq. 109), in which the phosphine lies cis to the dithiocarbamate [Mn—S 2.38882(8), 2.3851(9) Å], while in the ^1H NMR spectrum the unique proton appears as a broad singlet at δ 8.05 (212).

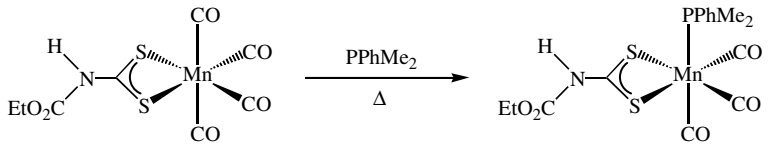

(109)

A second synthesis of a manganese(I) tetracarbonyl complex, namely, $[Mn(CO)_4(S_2CNHMe)]$, involves the addition of carbon disulfide to $[Mn(CO)_4(NH_2Me)\{\eta^1\text{-}C(O)NHMe\}]$ (1129).

e. Applications. A number of potential applications of manganese dithiocarbamate complexes have been suggested. Manganese-doped electroluminescent zinc sulfide films have been prepared by chemical vapor deposition and upon simultaneous pyrolysis of zinc and manganese dithiocarbamate complexes (1130,1131). These films show high luminance and luminous efficiency (1130),

while ESR measurements show that at manganese concentrations of 1% or less, the dopant is incorporated into the ZnS lattice as single noninteracting ions (1131).

A manganese(III) dithiocarbamate complex has been shown to display photoredox behavior (1132) and in this context has been investigated as a potential solar energy conversion system (1133). Thus, wet DMF solutions of the purported oxo-bridged manganese(III)–molybdenum(V) complex [MnMoO(H_2O)(μ-O)(S_2CNEt_2)$_4$] (827), turn from brown to green upon exposure to sunlight with the generation of a potential of 0.243 V (vs. SCE) and a maximum current of 7.0 μA. When studied under nitrogen the reversibility of the system is lost, while cross-over experiments show that [Mn(S_2CNEt_2)$_3$] is not active, and [Mo_2O_2(μ-O)(S_2CNEt_2)$_4$] showed only irreversible behavior. The authors suggest that photoreduction of Mo(V) to Mo(IV) occurs and the latter is reoxidized by Mn(III), which in turn is reduced to Mn(II), and subsequently returned to Mn(III) by aerial oxidation (1132,1133).

The manganese ethylene bis(dithiocarbamate) complex MANEB is used as a fungicide (15). Manganese is a well-known toxin for Parkinsonism in humans, while dithiocarbamates can induce extra-pyramidal syndromes. One publication details the development of permanent Parkinsonism in a 37-year old man exposed to MANEB for only 2 years (1134), and follows a previous report of the same symptoms developed after 10 years exposure (1135).

2. *Technetium*

Prior to 1980, dithiocarbamate complexes of technetium were unknown. However, over the past 20 years considerable developments have been made, driven mainly by the application of technetium(V) nitride complexes in radiopharmaceuticals. More recently, dithiocarbamate chemistry of technetium has been more fully explored with diphosphine, carbonyl, oxo, imido, and other ligand combinations.

a. Technetium(V) Nitride Complexes. The first technetium dithiocarbamate complex [TcN(S_2CNEt_2)$_2$] (**198**) was prepared in 1981 (457). In the preceding 20 years a wide range of other technetium(V) nitride complexes have also been synthesized, and some examples have found applications in nuclear medicine (see the preceding section). Addition of a fivefold excess of NaS_2CNEt_2 to [$TcNX_2L_2$] (X = Cl, Br; L = PPh_3, $AsPPh_3$) or [$TcNX_2(PPhMe_2)_3$] affords **198** in yields of 80–90% (1136). The reaction with [$TcNCl_2(PMe_2Ph)_3$] (**199**) has been shown to occur in a stepwise fashion (Fig. 132) generating [TcNCl(S_2CNEt_2)(PMe_2Ph)$_2$] (**200**) and [TcN(S_2CNEt_2)$_2$(PMe_2Ph)] (**201**) sequentially (447). The latter has been crystallographically characterized, the technetium–sulfur bond trans to the nitride being elongated by nearly 0.4 Å

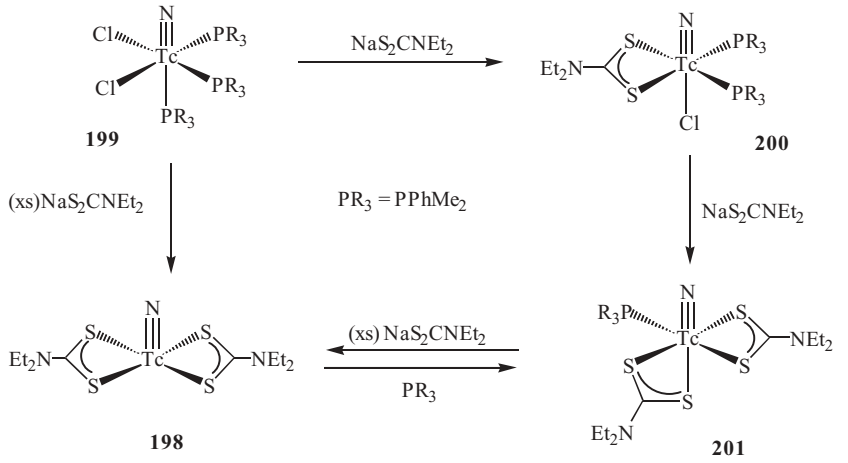

Figure 132. Stepwise formation of $[TcN(S_2CNEt_2)_2]$ upon addition of NaS_2CNEt_2 to $[TcNCl_2(PMe_2Ph)_2]$.

(447). Addition of excess dithiocarbamate salt to $[TcN(S_2CNEt_2)_2(PMe_2Ph)]$ leads to phosphine loss and generation of five-coordinate **198**, a process that can be reversed upon addition of more phosphine.

Reduction of $Cs[TcNCl_5]$ or $[TcN(H_2O)_3(\mu\text{-}O)]_2^{2+}$ in the presence of dithiocarbamate salts leads to dimeric technetium(VI) nitrides, $[TcN(S_2CNR_2)(\mu\text{-}O)]_2$ ($R = Et$; $R_2 = C_4H_8$) (**202**) (Fig. 133). They are shown by X-ray crystallography to contain edge-sharing square-pyramidal technetium centers [R = Et, Tc-Tc 2.543(1) Å]; a dihedral angle of 151° being subtended between

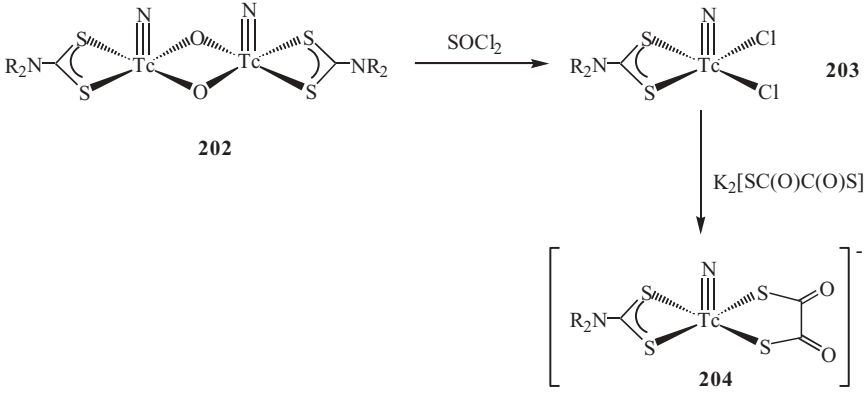

Figure 133. Synthesis of $[TcNCl_2(S_2CNR_2)]$ and subsequent reaction with $K_2[SC(O)C(O)S]$.

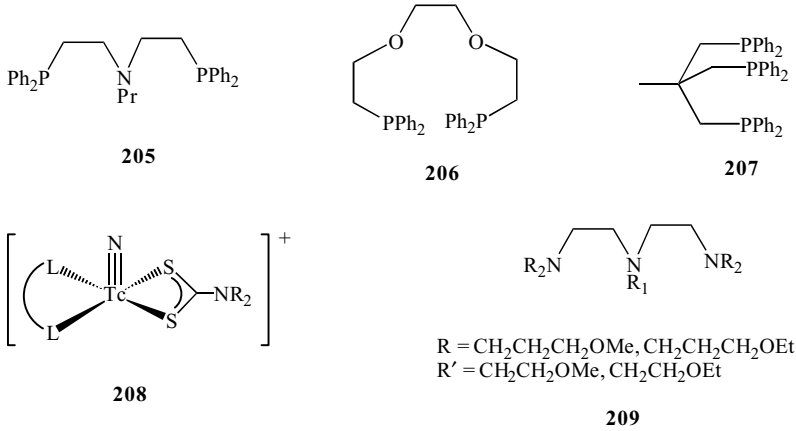

Figure 134. Structural representation of $[TcNL_2(S_2CNR_2)]^+$ and examples of L_2 ligands.

TcO_2 planes (1137). Attempts to run ESR spectra in $SOCl_2$ in the presence of $[AsPh_4]Cl.HCl$ resulted in cleavage giving $[TcNCl_2(S_2CNR_2)]$ (**203**), which subsequently reacts (R = Et) with $K_2[SC(O)C(O)S]$ to give the technetium(V) complex, $[TcN(S_2CNEt_2)\{\eta^2\text{- }SC(O)C(O)S\}]^-$ (**204**) (Fig. 133) (1137,1138).

Cationic technetium nitride complexes $[TcNL_2(S_2CNEt_2)]^+$, containing multidentate phosphine ligands (L_2), have been prepared in good yields upon addition of KS_2CNEt_2 to $[TcNCl_2L_2]$ (1139). Precise structural characteristics have not been determined, although in other nitride complexes, phosphines **205** and **206** have been shown to be bidentate, while **207** is tridentate. Very recently, Duatti and co-workers (1140,1141) prepared further cationic nitride complexes $[TcNL(S_2CNR_2)]^+$ (**208**), containing PNP ligands (**209**) and a wide range of dithiocarbamates from the reaction of $[TcNCl_2(PPh_3)_2]$ with the free ligands. These have been shown to contain a square-based pyramidal coordination geometry, the neutral ligands acting in a bidentate capacity, and it seems reasonable to assume that all complexes of this general type behave similarly (Fig. 134).

b. Application of Technetium(V) Nitrides in Medicine. In the same year as their discovery, the first application in radiopharmaceuticals was also detailed; being based on the long half-life (2.14×10^5 years) of ^{99}Tc, which provides a practically invariant source of β^- radiation (1142). Over the past 20 years, technetium(V) nitride complexes, $[TcN(S_2CNR_2)_2]$ (**210**), have been extensively investigated as radiopharmaceuticals, while a radiochemical method for the detection of ^{99}Tc in low-level radioactive waste, involving extraction with dithiocarbamate salts at low pH, has also been developed (1143).

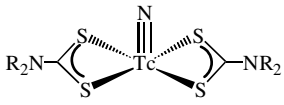

210

Baldas et al. (457) first prepared $[TcN(S_2CNEt_2)_2]$ from $[TcO_4][NH_4]$ and the dithiocarbamate salt, using hydrazine as the reducing agent. Crystallographic characterization revealed a square-based pyramidal coordination sphere, the dithiocarbamates occupying the basal plane. Since this report a large number of related complexes have been prepared by the same general method (54,1144–1154). They include those with simple alkyl substituents (R = *i*-Pr, Bu, *i*-Bu; $R_2 = C_5H_{10}$, C_4H_8O) (1144–1147,1149,1152,1153), amine-containing derivatives (1144), and a range of lipophilic complexes (54,1146,1148,1154). The latter include those derived from spiperone (1154) and $NaS_2CNMe(CH_2)_2C_6H_4$-$C(O)NH(CH_2)_2NEt_2$ (**211**) (54), which is prepared via a seven-step synthesis.

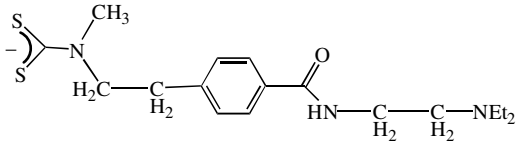

211

Their potential as radiopharmaceuticals has also been thoroughly tested in mice, rats, rabbits, and dogs (1144,1149–1160). In general, nonpolar complexes are readily extracted by the liver and then only slowly excreted, while polar compounds are cleared more slowly from the blood with concurrent rapid hepatobiliary excretion (1155). Further, lipophilic complexes generally show high uptake in tumor cell lines, with most of the bound activity being retained by cells after removal of an unbound tracer, and suggesting an application for *in vivo* tumor imaging and characterization (1146). A tandem MS study has detected $[^{99m}TcN(S_2CNEt_2)_2]$ in liver tissue, showing that it does not undergo ligand exchange reactions with plasma proteins (1161).

An early analysis of the cerebral perfusion imaging (CPI) ability of $[^{99m}TcN(S_2CNEt_2)_2]$ as compared with the widely used reagent $[^{201}Tl(S_2CNEt_2)]$ came to the conclusion that it was not suitable for CPI in its present form (1162). Of all the compounds prepared and tested to date, that which seems most promising is the ethoxy-ethyl derivative, $[^{99m}TcN\{S_2CNEt(OEt)\}_2]$ (**212**), commonly termed ^{99m}TcN(NOET) (NOET = *N*-ethyl-*N*-ethoxydithiocarbamate) (1148). Detailed physiological studies have been carried out on TcN(NOET) (1156,1160,1163–1174). It has an extremely high uptake and

retention in normal myocardin, which is not significantly effected by ongoing myocardinal ischemia or reperfusion injury (1163,1165,1166), although extraction and retention are decreased by severe ischemic injury (1169). The kinetics of uptake and retention has also been closely looked at (1166,1167); a comparison with ^{201}Tl images showing that it is of comparable utility in the detection of coronary artery disease (1164). Recent work has shown that it binds to L-type calcium channels in the open configuration without entering cardiomyocytes (1168), the optimal timing for acquiring initial and delayed images to maximize its sensitivity as a myocardial profusion agent being assessed as 10 min and 2 h respectively (1171). Further, the bio-distribution, safety, and dosimetry have been studied in 10 healthy volunteers. It shows a high cardiac uptake and an estimated effective dose comparable to other ^{99}Tc-labeled compounds used in myocardial perfusion imaging (1170). More studies are required to precisely define the place ^{99m}TcN(NOET) will take among currently available cardiac perfusion tracers, as it is not an analogue of ^{201}Tl, nor is it the equivalent of ^{99m}Tc sestamibi or ^{99m}Tc tetrofosmin.

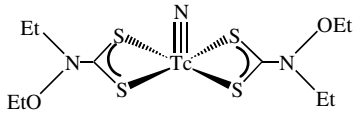

212

Technetium(III) complexes, [^{99m}Tc(CO)(S_2CNR_2)$_3$] (R = Et, CH_2CH_2OH, $CH_2CHOHMe$), have also been shown to be extremely stable and their biological behavior in mice has been compared to that of nitride complexes (1175). They were found to be efficient hepatobility reagents and cleared more rapidly than corresponding nitride and dithionite complexes.

Very recently, cationic nitride complexes, [TcN(S_2CNR_2)L_2]Cl, containing diphosphine ligands (L_2) (**205**) (Fig. 134), have also been tested as heart imaging agents (1140,1141). They show high myocardial uptake in rats and dramatically high heart/lung and heart/liver ratios, suggesting that they may be employed to obtain heart images with superior imaging quality.

c. Other High-Valent Technetium Complexes. The technetium(V) tetrakis(dithiocarbamate) complex [Tc($S_2CNC_5H_{10}$)$_4$]Br has been prepared in 67% yield upon addition of dicyclopentamethylenethiuram disulfide to [NBu_4][$TcOCl_4$] in the presence of [NBu_4]Br. The coordination geometry about the metal ion is best described as a distorted square antiprism and metal–sulfur bonds range from 2.463(2)–2.494(2) Å (1176). A single report details the synthesis of a technetium(V) oxo complex, namely, [TcO(S_2CNMe_2){S=C(NMe_2)$_2$}$_2$][PF_6]$_2$ (**213**) prepared from [TcO{S=C(NMe_2)$_2$}$_4$][PF_6]$_3$ upon

addition of dppe in DMF (1177). The dithiocarbamate is clearly a degradation product of tetramethylthiourea, although precise details remain unknown.

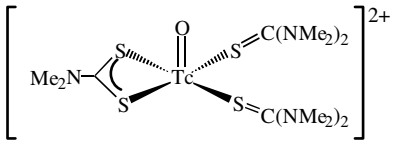

213

A thionitrosyl ligand is generated upon reaction of $[TcN(S_2CNEt_2)_2]$ with either $SOCl_2$ or S_2Cl_2. The technetium(IV) product, $[Tc(NS)Cl_2(S_2CNEt_2)_2]$ **214**, contains a pentagonal bipyramidal metal coordination sphere, the thionitrosyl and one chloride occupying the axial sites (1178). This appears to be the only example of a technetium(IV) dithiocarbamate complex.

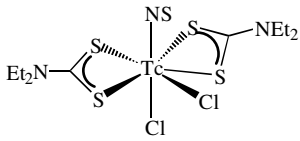

214

d. Technetium(III) and (II) Complexes. Technetium(II) and (III) complexes have been prepared. A second product of the addition of dppe to $[TcO(S_2CNMe_2)\{S{=}C(NMe_2)_2\}_2][PF_6]_2$ in DMF (see above) is the technetium(II) diphosphine complex, $[Tc(dppe)_2(S_2CNMe_2)][PF_6]$ (**215**) (1177), which has also been prepared (as have analogues) upon reduction of $[TcO(OH)(dppe)_2][PF_6]_2$ by formamidine sulfuric acid in alkali solution in the presence of dithiocarbamate salts ($R = Et$; $R_2 = C_5H_{10}$) (1179). Crystallographic characterization reveals a distorted octahedral coordination geometry, while cyclic voltammetry shows that reversible one-electron reduction and oxidation processes are accessible (1179). The latter leads to a technetium(III) species, and although not isolated in this case, a number of such complexes are known.

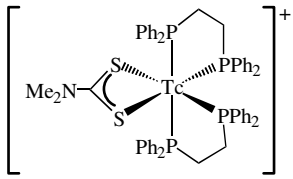

215

The diazenido complex, $[Tc(N{=}NAr)(S_2CNMe_2)_2(PPh_3)]$ ($Ar = p\text{-}C_6H_4Cl$) (**216**), results from addition of NaS_2CNMe_2 to $[TcCl(N{=}NAr)_2(PPh_3)_2]$ in methanol. It contains a cis orientation of phosphine and diazenido groups in the solid state (455).

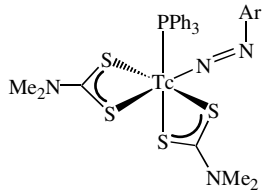

216

Technetium(III) carbonyl complexes, $[Tc(CO)(S_2CNR_2)_3]$ (**217**) (Fig. 135), have been prepared. Baldas et al. (405) first made $[Tc(CO)(S_2CNEt_2)_3]$ from $[TcO_4][NH_4]$ and NaS_2CNEt_2 using aminoiminomethane sulfinic acid as the reducing agent. Subsequently, a range of these complexes has been prepared via the same method ($R = i$-Pr, Bu, i-Bu; $R_2 = C_5H_{10}$, C_4H_8O) (1145). A crystallographic study of $[Tc(CO)(S_2CNEt_2)_3]$ shows that the carbonyl occupies an axial site in a distorted pentagonal bipyramidal array (405). While direct substitution of a carbonyl for a phosphine is not possible, related phosphine complexes can be prepared by other routes. Thus, addition of 3 equiv of NaS_2CNEt_2 to $[TcCl_3(PPMe_2)_3]$ gives $[Tc(S_2CNEt_2)_3(PPhMe_2)]$ (**218**) (Fig. 135), which also has a distorted pentagonal-bipyramidal coordination sphere, the phosphine occupying an axial site (1180).

e. Technetium(I) Complexes. The novel technetium(I) complex $[Tc(CO)_2(PPh_3)_2(S_2CNHPh)]$ (**219**) results upon heating $[Tc(CO)_2(PPh_3)_2(O{=}CH{-}N{-}p\text{-tol})]$ with phenylisothiocyanate in wet benzene. It plausibly arises by abstraction of sulfur from the isothiocyanate with concomitant generation of phenylisocyanate. A crystallographic study shows an octahedral coordination environment with cis carbonyls and trans phosphines (221). Analogous chemistry has also

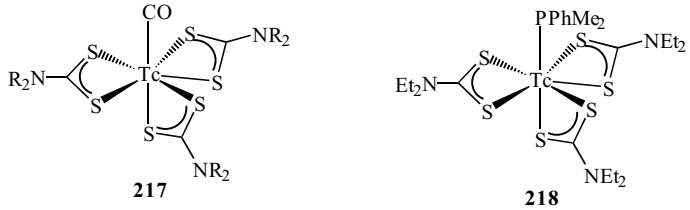

217 **218**

Figure 135. Examples of seven-coordinate technetium(III) tris(dithiocarbamate) complexes.

been shown to occur for rhenium, with $[Re(CO)_2(PPh_3)_2(S_2CNHPh)]$ also being crystallographically characterized (222).

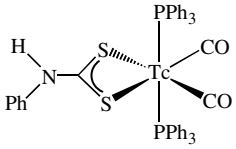

219

3. Rhenium

The first rhenium dithiocarbamate complexes, $[ReCl_2(S_2CNR_2)]$, were not reported until 1960 (1181), and even then, it was not until the 1970s that substantial inroads were made. Now, dithiocarbamates are known to stabilize rhenium in oxidation states +1 to +5, with the latter being the most common, and the chemistry is dominated by strong π-donor ligands such as oxo and imido, and especially prevalent are nitride complexes.

a. Rhenium(V) Nitrides. Diamagnetic rhenium(V) nitride complexes, $[ReN(S_2CNR_2)_2]$, have been known for some time (1182), and like their technetium analogues they adopt a distorted square-pyramidal structure. They can be prepared from $[ReNCl_2(PR_3)_n]$ ($n = 2, 3$) and dithiocarbamate salts (448,1183), but quite recently a new one-pot synthesis has also been developed. This synthesis involves the reduction of $KReO_4$ by $SnCl_2$ in the presence of *N*-methyl-*S*-methyldithiocarbazate, followed by addition of 2 equiv of dithiocarbamate salt. In this way, a range of complexes can be prepared (R = Me, Et, Pr, Ph; $R_2 = C_5H_{10}$) in moderate yields (1183,1184). By using this method, a number of radioactive ^{188}Re derivatives have been made and biodistribution studies carried out on rats (1183).

The electrochemical properties of a number of nitride complexes, $[ReN(S_2CNR_2)_2]$, have been studied by cyclic voltammetry, however, in a range of organic solvents all show only an irreversible reduction wave (1185).

Reactions of $[ReNCl_2(PR_3)_n]$ ($n = 2, 3$) and dithiocarbamate salts, which ultimately afford $[ReN(S_2CNR_2)_2]$, occur like their technetium counterparts, occur in a step-wise manner. Thus, addition of 1 equiv of dithiocarbamate to $[ReNCl_2(PPhMe_2)_3]$ affords $[ReNCl(PPhMe_2)_2(S_2CNR_2)]$, while under controlled conditions the second equivalent initially gives $[ReN(PPhMe_2)(S_2CNR_2)_2]$ (448). Crystal structures have been carried out on both product types. In the first (R = Me) the nitride ligand lies trans to chloride, and cis to the phosphines, while in the second (R = Et) the nitride and phosphine are again

mutually cis. The latter leads to a significant lengthening of the trans rhenium–sulfur bond [Re–S_{trans} 2.7983(2) Å] with respect to those cis [Re–S_{cis} 2.396(1)–2.449(1) Å], a manifestation of the strong trans-influence of the nitride ligand. A cationic mixed-dithiocarbamate nitride complex, [ReN(S_2CNEt_2){S_2CN(Me)$CH_2CH_2NMe_3$}($PPhMe_2$)][BPh_4] (**220**), has been prepared in this manner from [ReNCl($PPhMe_2$)$_2$(S_2CNEt_2)] and 1 equiv of the second dithiocarbamate salt (449).

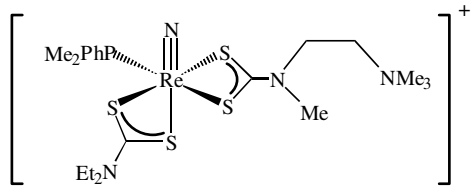

220

Terminal nitride complexes are known to readily undergo reactions with electrophilic reagents, and this behavior has been explored extensively for [ReN(S_2CNR_2)$_2$($PPhMe_2$)] and to a lesser extent [ReN(S_2CNR_2)$_2$] and [ReNCl(S_2CNR_2)($PPhMe_2$)] (R = Me, Et). All add $B(C_6F_5)_3$ to give new complexes containing the N-$B(C_6F_5)_3$ unit (450,1186). For the phosphine complexes these are monomeric (see Fig. 137), however, with [ReN(S_2CNEt_2)$_2$], dimeric [Re{$NB(C_6F_5)_3$}(S_2CNEt_2)$_2$]$_2$ results (Eq. 110); monomeric units being weakly held together by long range rhenium–sulfur interactions [Re—S 2.835(6) and 2.856(6) Å] (1186).

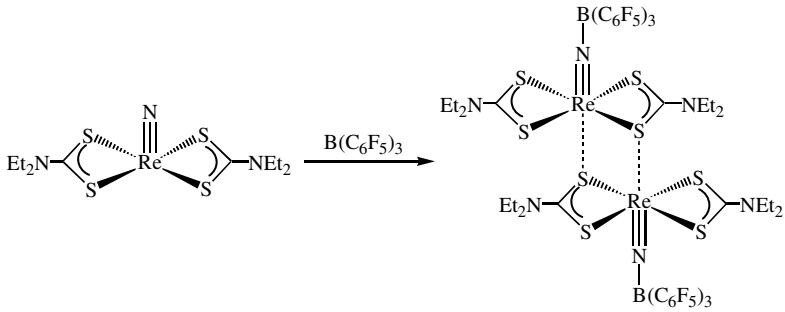

(110)

Addition of $NaBPh_4$ to an acidic solution of [ReN(S_2CNEt_2)$_2$($PPhMe_2$)] (**221**) in acetone yields the related complex [Re($NBPh_3$)(S_2CNEt_2)$_2$($PPhMe_2$)] (**222**) (Fig. 136). The solvent plays a key role in this reaction as it proceeds via the imido intermediate, [Re{$NC(Me_2)CH_2C(O)Me$}(S_2CNEt_2)$_2$($PPhMe_2$)]$^+$

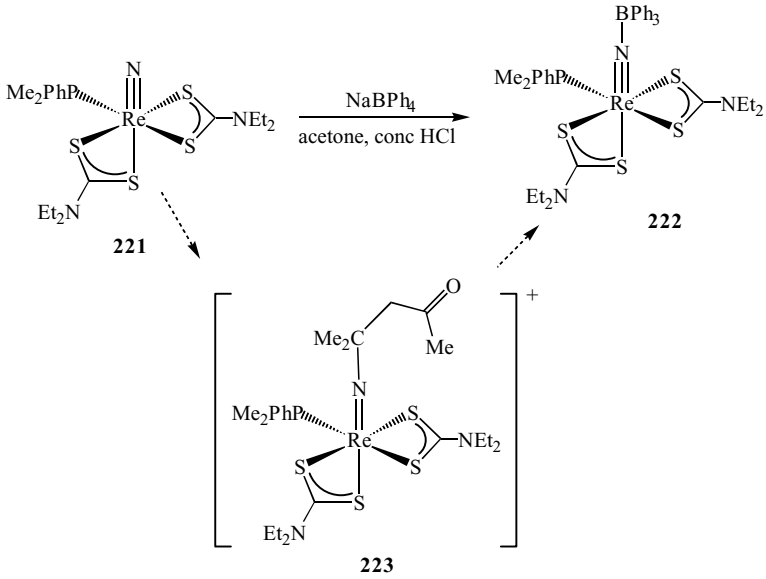

Figure 136. Formation of $[Re(NBPh_3)(S_2CNEt_2)_2(PPhMe_2)]$ via an imido intermediate.

(**223**) (451). A crystal structure of $[Re(NBPh_3)(S_2CNEt_2)_2(PPhMe_2)]$ shows that the cis arrangement of phosphine and nitrogen ligands is retained. Further, the rhenium–sulfur bond trans to the N-BPh_3 ligand at 2.579(4) Å is some 0.214 Å shorter than in the nitride complex, an indication of the weakening trans-influence. The related complex, $[Re(NBCl_2Ph)(S_2CNEt_2)_2(PPhMe_2)]$, prepared from $[ReN(S_2CNEt_2)_2(PPhMe_2)]$ and BCl_2Ph, shows similar structural features (452).

Nitride complexes react with a wide range of other Lewis acids (Fig. 137). Addition of BCl_3 and $GaCl_3$ to $[ReN(S_2CNEt_2)_2(PPhMe_2)]$ (**224**), affords $[Re(NECl_3)(S_2CNEt_2)_2(PPhMe_2)]$ (E = B, Ga) (**225**) the rhenium–sulfur bonds trans to nitrogen again being shortened with respect to that found in the nitride [E = B; 2.565(2) and E = Ga; 2.581(2) Å] (453). Similar addition of $B(C_6F_5)_3$ to **224** affords $[Re\{NB(C_6F_5)_3\}(S_2CNEt_2)_2(PPhMe_2)]$ (**226**). Addition of S_2Cl_2 proceeds in a slightly different manner to give the thionitrosyl complex, $[ReCl(NS)(S_2CNEt_2)(PPhMe_2)_2]$ (**227**), in which a dithiocarbamate has also been replaced by a phosphine and chloride. The latter lies trans to the thionitrosyl, two crystallographically independent molecules being characterized by rhenium–nitrogen bond lengths of 1.795(6) and 1.72(1) Å (453).

The triphenylcarbonium cation adds to **224** giving the blue imido cation, $[Re(NCPh_3)(S_2CNEt_2)_2(PPhMe_2)]^+$ (**228**). This complex has a rhenium–

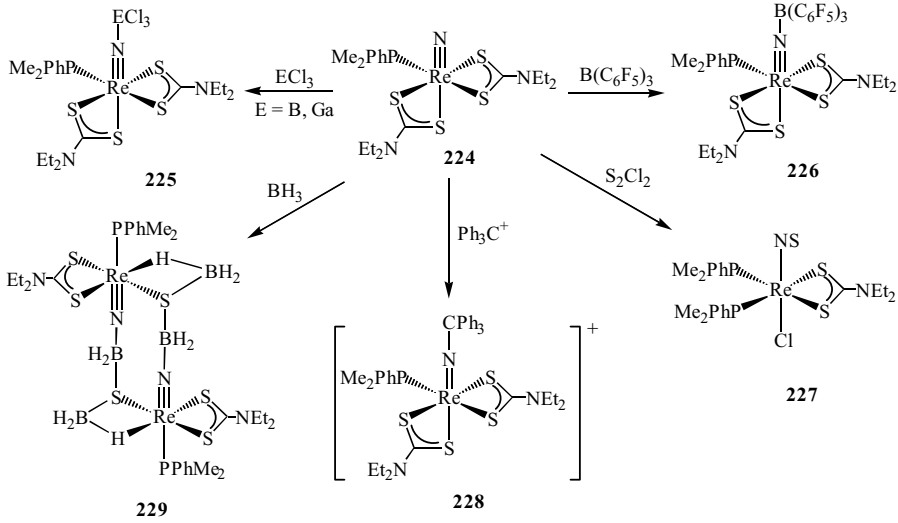

Figure 137. Examples of the reactivity of $[ReN(S_2CNEt_2)(PPhMe_2)]$ toward Lewis acids.

nitrogen bond length of 1.706(6) Å, and a decrease in the elongation of the trans rhenium–sulfur bond by 0.24 Å [Re—S_{trans} 2.552(2) Å] (454). Addition of excess BH_3 in THF results in formation of dimeric $[Re(\mu\text{-}NBH_2SBH_3)(S_2CNEt_2)(PPhMe_2)]_2$ (**229**), in which the unusual $[NBH_2SBH_3]^{4-}$ ligands bridge between rhenium(V) centers (1187). The mode of formation of this anion is unclear but it may result from electrophilic attack of BH_3 at one of the sulfur atoms of a dithiocarbamate, generating thioformic acid, diethylamide and $[BH_2—S—BH_3]^-$, the latter then attacking the nitride ligand.

Addition of TlCl and $Pr(O_3SCF_3)_3$ to **224** results in formation of novel trinuclear complexes, containing a Re≡N-Re(≡N)-N≡Re backbone (Fig. 138) (1188). Thus, reaction with 4 equiv of thallium chloride gives $[\{ReCl(S_2CNEt_2)(PPhMe_2)_2(\mu\text{-}N)\}_2(ReNCl_2(PPhMe_2)]$ (**230**), in a complex ligand redistribution reaction, while with $Pr(O_3SCF_3)_3$ the related ionic complex $[\{Re(S_2CNEt_2)_2(PPhMe_2)(\mu\text{-}N)\}_2(ReN(S_2CNEt_2)(PPhMe_2)][CF_3SO_3]$ (**231**) results. A crystal structure of the neutral complex shows an approximately linear Re_3N_2 backbone, characterized by short interactions to the terminal metal atoms [Re_{term}–N 1.69(2) and 1.72(2) Å] and long interactions to the central atom [Re_{cent}—N 2.07(2) and 2.04(2) Å] (1188).

A number of related cyclic tetranuclear complexes have been prepared that contain an Re_4N_4 core. Thus, $[ReNCl_2(PPh_3)_2]$ reacts with 1.5 equiv of

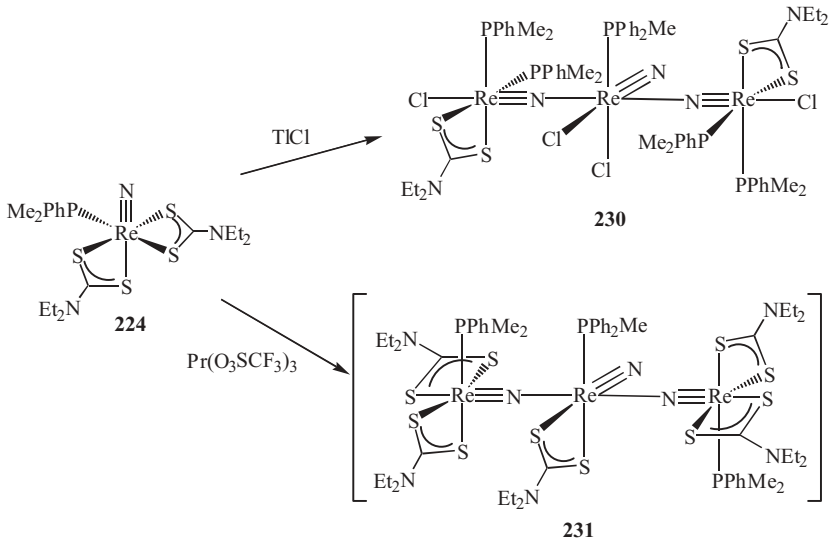

Figure 138. Addition of further Lewis acids to $[ReN(S_2CNEt_2)(PPhMe_2)]$.

KS_2CNEt_2 in methanol to give the cyclic tetranuclear complex $[Re_4(\mu\text{-}N)_4(S_2CNEt_2)_6(MeOH)_2(PPh_3)_2]^{2+}$, and a very similar complex $[Re_4(\mu\text{-}N)_4(S_2CNEt_2)_4Cl_4(PPhMe_2)_2]$ (**232**) is formed upon addition of Al_2Cl_6 to $[ReN(S_2CNEt_2)_2(PPhMe_2)]$ (449). Both contain a nonplanar cyclic $Re_4(\mu\text{-}N)_4$ core, with asymmetric Re≡N—Re bridges (average Re—N bonds of 1.69 and 2.03 Å, respectively). Cyclic voltammetry has been carried out on the cationic complex; a quasi-reversible one-electron oxidation being followed by two further irreversible one-electron oxidation processes, while two reversible and one irreversible one-electron reduction waves are also observed. These results indicate that $Re(V)_3Re(VI)$ and $Re(V)_2Re(IV)_2$ cyclic units have some stability (449).

In a similar manner, reaction of $[ReN(S_2CNEt_2)_2(PPhMe_2)]$ (**224**) with $SbCl_3$ affords $[\{ReN(S_2CNEt_2)Cl(PPhMe_2)\}_2\{ReN(S_2CNEt_2)_2\}\{SbCl_3\}_2]$ (**233**), which contains an almost planar Re_4N_4 ring. Again the nitride linkages are asymmetric, with two edges of the ring being spanned by $SbCl_3$ units, each binding to the metal bound chloride and sulfur atoms of the dithiocarbamates (1189). This complex is unstable at higher temperatures, decomposing in acetonitrile to give $[ReN(S_2CNEt_2)_2]$ and a further tetrameric complex, $[ReN(S_2CNEt_2)Cl(PPhMe_2)]_4$. The latter also contains an eight-membered Re_4N_4 ring, but this is now severely distorted from planarity; a dihedral angle of 47.88(2)° being found between Re_3N_3 planes.

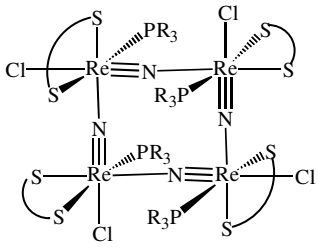

232

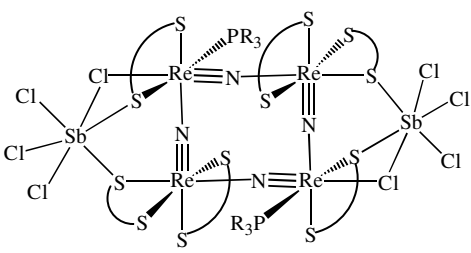

233

$PR_3 = PPhMe_2$ $\overset{S}{\underset{S}{\frown}} = S_2CNEt_2$

b. Other Rhenium(V) Complexes. A range of other rhenium(V) dithiocarbamate complexes are known especially those with oxo ligands. Dimeric oxo-bridged complexes $[Re_2O_2(\mu\text{-}O)(S_2CNR_2)_4]$ are well known, and contain a linear Re_2O_3 unit and octahedral rhenium centers. Cyclic voltammetry studies have shown that one-electron oxidation, while reversible at fast scan rates, leads to a cation that dissociates rapidly into $[ReO(S_2CNR_2)_2]^+$ and $[ReO_2(S_2CNR_2)_2]$ (1185). Similarly, the reversible one-electron reduction product also decomposes to give $[ReO(S_2CNR_2)_2]$, dithiocarbamate salt and other rhenium-containing species. The couples and anion stability are strongly dependent on the nature of the dithiocarbamate substituents and the solvent used (1190).

A number of reactions of $[Re_2O_2(\mu\text{-}O)(S_2CNEt_2)_4]$ (**234**) have been explored (Fig. 139). Addition of excess S-methyldithiocarbazate, $H_2NNHC(S)SMe$, gives $[ReO(S_2CNEt_2)\{\eta^2\text{-}SC(SMe)NNH\}]$ (**235**), which has a distorted square-pyramidal structure (1191), while with catechol and 2-amino-4-methyl-phenol, octahedral complexes $[ReO(S_2CNEt_2)_2(\eta^1\text{-}OAr)]$ (**236**) result, the dithiocarbamates lying in the equatorial plane (1192). Closely related to the latter is dimeric $[\{ReO(S_2CNEt_2)_2\}_2(\mu\text{-}OC_6H_4O)]$ (**237**), formed from 1,4-dihydroxybenzene. Reactions with thiols take a quite different course. Thus, dithiolates (HSXSH) give $[ReO(\eta^2\text{-}SXS)_2][NEt_2H_2]$, the cation resulting from dithiocarbamate degradation, while reaction with $PhP(o\text{-}C_6H_4SH)_2$ yields octahedral, $[ReO(S_2CNEt_2)\{\eta^3\text{-}PhP(o\text{-}C_6H_4S)_2\}]$ (**238**) (1192).

Rhenium(V) oxo-halide complexes $[ReOX(S_2CNR_2)_2]$ (X = Cl, Br) have previously been prepared from reactions of thiuram disulfides with $[ReOX_3(PPh_3)_2]$ (1182). More recent work suggests that in solution they exist in equilibrium with $[ReO(S_2CNR_2)_2]^+$ and X^-, the position of the equilibrium depending critically on the nature of X (1185).

Rhenium imido-dithiocarbamate complexes were first prepared by Rowbottom and Wilkinson in 1972 (1182) and considerable recent progress has been made in this area. Reaction of $[ReCl_3(NAr)(PPh_3)_2]$ (Ar = Ph, *p*-tol, Me) (**240**) with either $Me_3SiS_2CNR_2$ or TlS_2CNR_2 (R = Me, Et) gives [Re(NAr)-

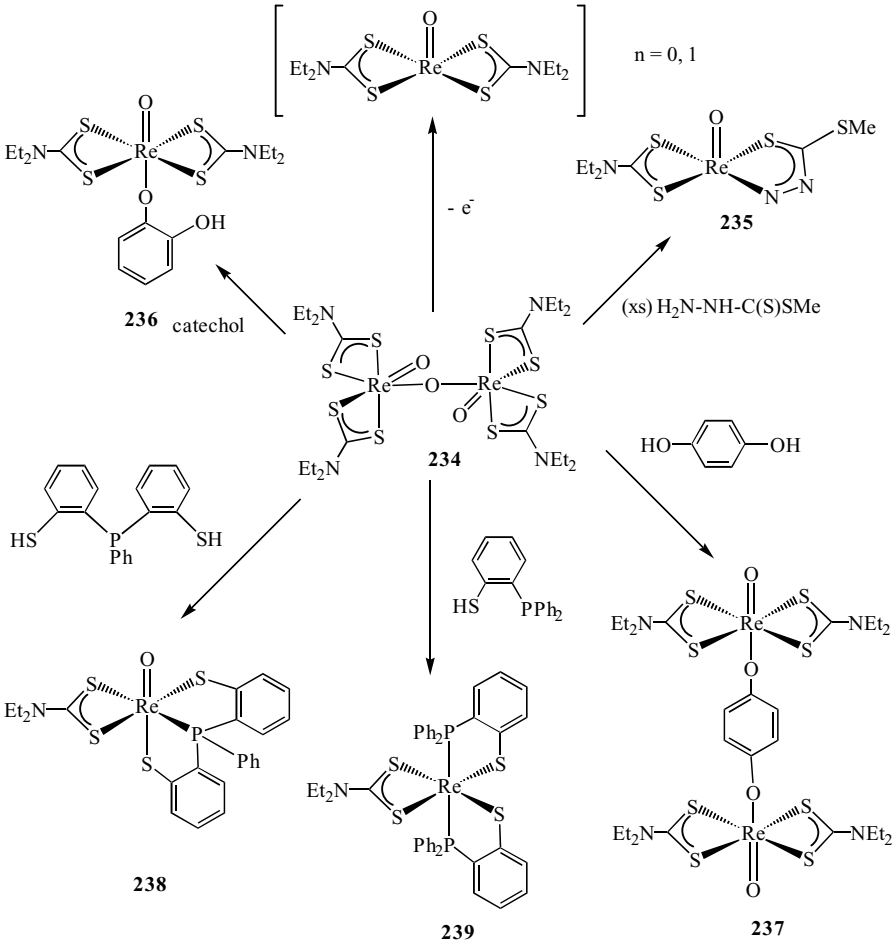

Figure 139. Examples of the reactivity of $[Re_2O_2(\mu\text{-}O)(S_2CNEt_2)_4]$.

$(S_2CNR_2)_3]$, while with thiuram disulfides, bis(dithiocarbamate) complexes, $[ReCl(NAr)(S_2CNR_2)_2]$ (**241**) (Fig. 140), result. The structure of the tris(dithiocarbamate) complexes $[Re(NAr)(S_2CNR_2)_3]$ is unknown. On the basis of IR and ^{1}H NMR data, Goeden and Haymore (1193) proposed a cis six-coordinate geometry with one monodentate dithiocarbamate, although in light of the seven-coordinate nature of analogous molybdenum and tungsten complexes, a pentagonal-bipyramidal geometry appears more probable. The chloro complexes, $[ReCl(NAr)(S_2CNR_2)_2]$ (**241**), react further with sodium methoxide or ethoxide to give $[Re(OR^1)(NAr)(S_2CNR_2)_2]$ ($R^1 = Me$, Et) (**242**); a process that is

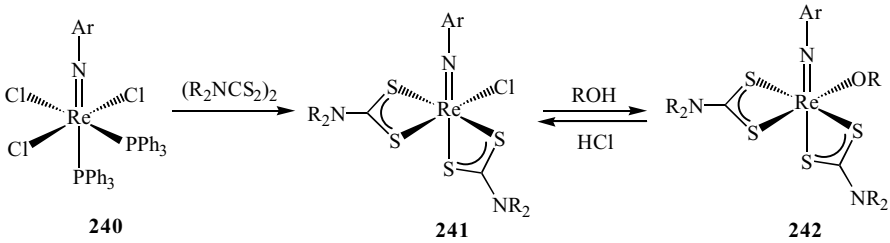

Figure 140. Formation of $[ReCl(NAr)(S_2CNR_2)_2]$ and its reversible reaction to give related alkoxides.

reversed with HCl (Fig. 140) (1193). A crystallographic study of brown $[Re(OEt)(N\text{-}p\text{-tol})(S_2CNMe_2)_2]$ reveals an octahedral metal center with trans imido and ethoxide ligands. The rhenium–nitrogen bond at 1.745(5) Å is quite long, and there is significant bending at the nitrogen [Re—N—C 155.5(5)°] (1193).

A related *N*-succinimidyl ester complex, $[ReCl\{N\text{-}p\text{-}C_6H_4C(O)ON(CO)_2\text{-}C_2H_4\}(S_2CNEt_2)_2]$ (**243**), has been prepared as part of a program to identify potential radiopharmaceuticals. However, it was found to be unsuitable due to the facile hydrolysis of the imido groups in basic aqueous solutions (1194). This is a general characteristic of this class of complex and leads to the formation of dimeric species $[Re_2(NAr)_2(\mu\text{-}O)(S_2CNR_2)_4]$ (**244**) (Eq. 111), related to the oxo complexes described above (1193). The transformation can be reversed upon addition of HCl, while reaction with alcohols and $Me_3SiS_2CNR_2$ also regenerates mononuclear complexes.

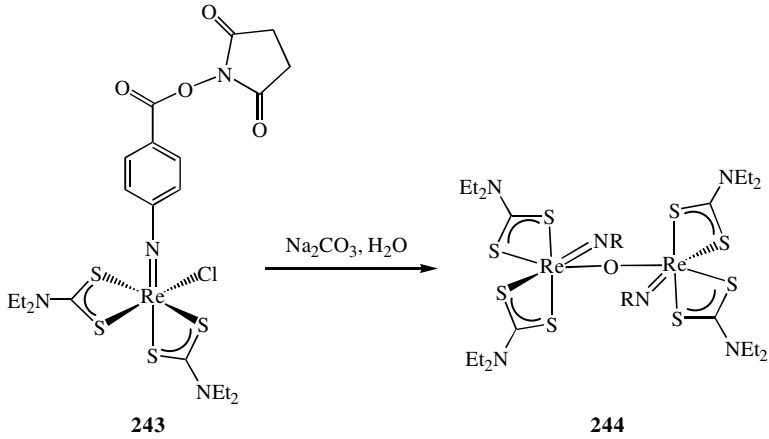

(111)

Electrochemical measurements have been made on $[Re_2(N\text{-}p\text{-}C_6H_4X)_2(\mu\text{-}O)(S_2CNR_2)_4]$ (R = Et, Ph; X = H, Me, Cl, OMe) (1195). They undergo a quasi-reversible one-electron reduction, which is followed by cleavage of the oxo-bridge and loss of one dithiocarbamate. The redox potential and stability of the anion depend on the nature of both R and X. The diphenyldithiocarbamate complexes are easiest to reduce by some 170 mV, but all are harder to reduce than the corresponding oxo complexes. They also undergo an irreversible one-electron oxidation, while the oxo analogues exhibit ill-defined oxidative behavior.

Maatta and Kim (1196) prepared a number of linked bis(imido) complexes. For example, reaction of tetraethylthiuram disulfide with $[\{ReCl_3(PPh_3)_2\}_2(\mu\text{-}N\text{-}p\text{-}C_6H_4{-}N)]$ yields $[\{ReCl(S_2CNEt_2)_2\}_2(\mu\text{-}N\text{-}p\text{-}C_6H_4\text{-}N)]$ (**245**). Here the remaining chlorides lie trans to the imido ligand and are readily replaced, for example, by ethoxide. Black tetranuclear chains (**246**) (Eq. 112) result upon heating in acetone with NaOH, however, these were completely insoluble, and attempts to enhance solubility by using dicyclohexyldithiocarbamate analogues were unsuccessful (1190).

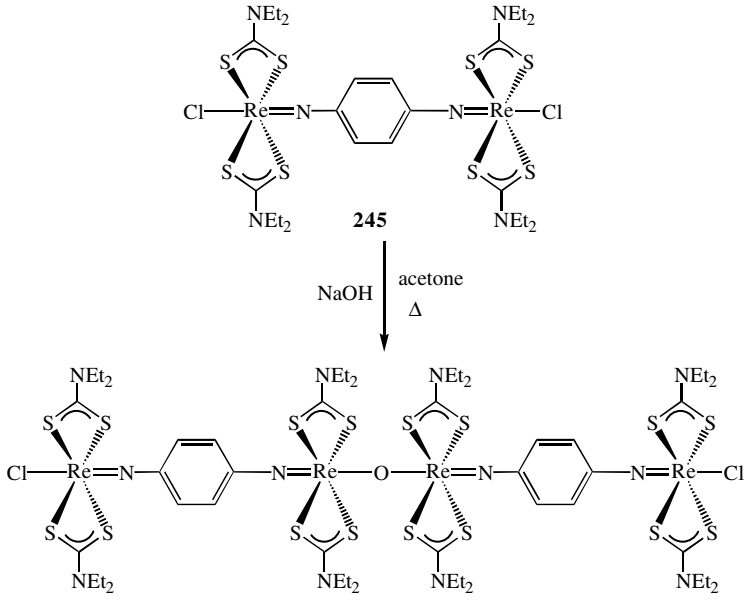

(112)

246

Related to the imido complexes are hydrazido(−2) complexes $[Re(NNMePh)_2(S_2CNR_2)_2][BPh_4]$ (R = Me, Et), generated from $[ReCl_2(NNMePh)_2$

$(PPh_3)][BPh_4]$ and 2 equiv of dithiocarbamate salt. A crystallographic study provides evidence of rhenium–nitrogen π-bonding as shown by the lengthening of the rhenium–sulfur bonds trans to nitrogen by >0.05 Å with respect to the others (1197).

Only one report has appeared on related sulfido complexes; reaction of $[ReS(\eta^2\text{-}S_4)(S_2C{=}NMe)]^-$ with MeOTf giving the dithiocarbamate complex $[ReS(\eta^2\text{-}S_4)(S_2CNMe_2)]$ (202). The latter appears to be quite stable and it is somewhat surprising that other terminal sulfido complexes have not been reported. Stiefel and co-workers (184,185) reported the synthesis of a range of dimeric rhenium(IV) complexes with bridging sulfido ligands and these are discussed further below.

A number of other rhenium(V) complexes have been reported. Addition of 3 equiv of thiuram disulfides to $[ReS_4]^-$ gives $[Re(S_2CNR_2)_4]Cl$ in high yields. One example (R = Me) has been crystallographically characterized. It shows the expected, slightly distorted D_{2d} dodecahedaral coordination environment, which is common for tetrakis(dithiocarbamate) complexes (185). A further cationic rhenium(V) complex, $[ReCl_2(S_2CNEt_2)_2][BPh_4]$, has been prepared upon reaction of $[Re_2O_2(\mu\text{-}O)(S_2CNEt_2)_4]$ with Me_3SiCl. It provides a potential route into non-oxo rhenium(V) dithiocarbamate chemistry, but the precise structural form has not yet been elucidated (1192).

c. Rhenium (IV) and (III) Complexes. Dimeric rhenium(IV) complexes $[Re(\mu\text{-}S)(S_2CNR_2)_2]_2$ (R = Me, Et, *i*-Bu) (**247**) have been prepared upon addition of 1.5 equiv of thiuram disulfides to $[ReS_4]^-$ in acetonitrile (184,185). They are diamagnetic and crystallographic characterization (R = *i*-Bu) reveals a centrosymmetric structure containing distorted edge-shared bioctahedra. The dithiocarbamate ligands are in a ΔΛ conformation, and the short rhenium–rhenium distance of 2.546(1) Å is indicative of some multiple-bonding character.

All undergo a reversible one-electron oxidation that in the presence of further thiuram disulfide gives rhenium(III) complexes $[Re_2(\mu\text{-}SS_2CNR_2)_2(S_2CNR_2)_3]^+$ (**248**) (Fig. 141), the two trithiocarbamate ligands being generated from sulfur–sulfur bond formation. Crystallographic characterization (R = *i*-Bu) again shows a short rhenium–rhenium bond of 2.573(2) Å. Reaction with $LiEt_3BH$ or H_2 results in regeneration of the starting material. The regioselectivity of this interconversion process has been investigated by labeling studies. These show that during trithiocarbamate formation, one dithiocarbamate unit from the thiuram disulfide ends up as either the trithiocarbamate or one of the equivalent pair of dithiocarbamates. In the back-reaction, the same dithiocarbamate unit (or its symmetry equivalent) is eliminated and the authors favor the trithiocarbamate ligand as the reactive entity. The oxidized complexes $[Re_2(\mu\text{-}S)_2(S_2CNR_2)_4]^+$ also react with excess sulfur giving $[\{Re_2(\mu\text{-}S)(S_2CNR_2)_4\}_2(\mu\text{-}S_4)]^{2+}$. A crystal

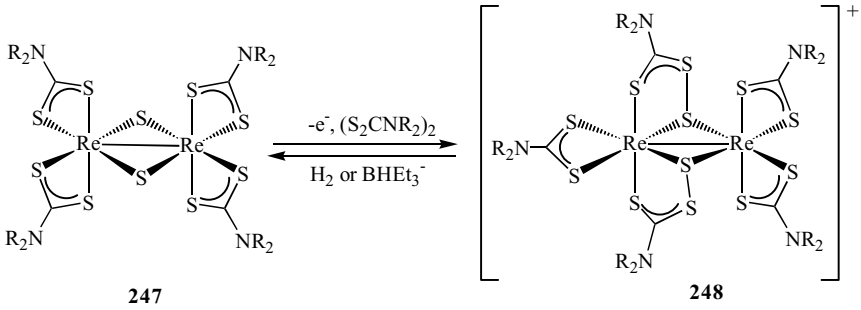

Figure 141. Interconversion of di- and trithiocarbamate ligands at a binuclear rhenium.

structure (R = *i*-Bu) shows that the tetrasulfide ligand links the dirhenium centers, the two central sulfur atoms remaining uncoordinated (185).

Mononuclear rhenium(III) complexes are well known. Tris(dithiocarbamate) complexes $[Re(S_2CNR_2)_3]$ are formed from the reaction of $[ReOCl_3(PPh_3)_2]$ and dithiocarbamate salts. Cyclic voltammetric studies reveal a reversible one-electron oxidation process, followed by a second irreversible process (1185). Other rhenium(III) complexes can also be prepared via reduction of rhenium(V) oxo complexes. For example, addition of bidentate phosphines to $[Re-O(S_2CNEt_2)_2(\eta^1\text{-O-}o\text{-}C_6H_4OH)]$ yields $[Re(S_2CNEt_2)_2(R_2PCH_2CH_2PR_2)]^+$ (R = Me, Ph), while $[Re_2O_2(\mu\text{-O})(S_2CNEt_2)_4]$ (**232**) reacts with $o\text{-}Ph_2PC_6H_4SH$ to give $[Re(S_2CNEt_2)(\eta^2\text{-}Ph_2PC_6H_4S)_2]$ (**239**) (Fig. 139). The latter has a distorted octahedral coordination geometry with the sulfur atoms lying cis to one another. It shows two reversible and one irreversible oxidation processes by cyclic voltammetry (1192).

d. Rhenium(II) and (I) Complexes. A number of publications deal with rhenium(I) carbonyl and thiocarbonyl complexes. Following the reaction of $[Re_2(CO)_6(\mu\text{-OH})_3]^-$ with dithiocarbamate salt by negative-ion ESMS leads to the suggestion that initial substitution of one or two of the hydroxide groups occurs giving dimers $[Re_2(OH)_2(S_2CNR_2)(CO)_6]^-$ and $[Re_2(OH)(S_2CNR_2)_2(CO)_6]^-$ respectively, which upon standing yield $[Re(S_2CNR_2)_2(CO)_3]^-$ (R = Et, $R_2 = C_4H_8$) (545).

Rhenium(I) tetracarbonyl complexes $[Re(CO)_4(S_2CNR_2)]$ (R = Me, Et) have been prepared from dimeric $[Re(CO)_4(\mu\text{-Br})]_2$ upon addition of dialkylammonium dithiocarbamates, or carbonylation of $[Re(CO)_3(NHMe_2)(S_2CNMe_2)]$, the latter being prepared from $[ReBr(CO)_3(NHMe_2)_2]$ and carbon disulfide (63). The related dicarbonyl complex $[Re(CO)_2(PPh_3)_2\{S_2CN(Me)CNSC_2H_2\}]$ has been prepared in a similar fashion, being isolated in low yield from the thermolysis of $[Re(CO)_2(PPh_3)_2(mat)]$ with excess carbon disulfide (Eq. 20).

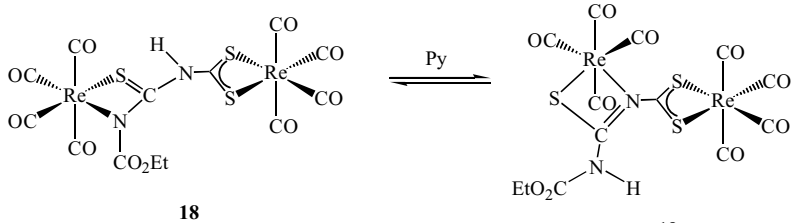

18 **19**

Figure 142. Base-catalyzed interconversion of rhenium(I) dithiocarbamate complexes.

A crystal structure shows a trans disposition of phosphines that lie cis to the dithiocarbamate (194).

Adams and Huang (211) showed that S-((ethoxycarbonyl)amino)-1,2,4-dithiazole-3-one acts as a dithiocarbamate source. Reaction with $[Re_2(CO)_9(MeCN)]$ gives a number of rhenium(I) products including $[Re(CO)_4\{S_2CNHC(S)NHCO_2Et\}]$, $[Re(CO)_4\{S_2CNHC(S)NCO_2Et\}Re(CO)_4]$ (**18**) and its isomer $[Re(CO)_4\{S_2CN{=}C(NHCO_2Et)S\}Re(CO)_4]$ (**19**) (Fig. 142). All three complexes have been characterized crystallographically and the based-catalyzed inter conversion of the two isomers (Fig. 142) has been shown upon addition of pyridine.

In an analogous fashion to the related manganese complexes (see Section IV.D.1.d), the rhenium(I) carbonyl complex $[Re(CO)_4(S_2CNHMe)]$ results from the addition of carbon disulfide to $[Re(CO)_4(NH_2Me)\{\eta^1\text{-}C(O)NHMe\}]$ (1129). The precise reaction pathway is not clear, but the dithiocarbamate probably results from initial attack of the iminoacyl on carbon disulfide, followed by carbonyl loss and ligand rearrangement. This pathway (Fig. 143) is favored over that involving the coordinated amine, since the rhenium(II) complex $[CpRe(CO)(NO)(S_2CNHMe)]$ (**250**) has been prepared in an analogous fashion from $[CpRe(CO)(NO)\{\eta^1\text{-}C(O)NHMe\}]$ (**249**) (Fig. 143). The former appears to be the only example of a rhenium(II) dithiocarbamate complex.

In a recent publication, the reaction of $[Re_2(CO)_8(\mu\text{-}Br)(\mu\text{-}PCy_2)]$ with NaS_2CNEt_2 was shown to give a moderate yield of yellow $[Re_2(CO)_8(\mu\text{-}S_2CNEt_2)(\mu\text{-}PCy_2)]$ (**251**), which has been crystallographically characterized (1198). The dithiocarbamate bridges the non-metal–metal bonded dirhenium center, the angle subtended at the backbone carbon being 123.7(1)°.

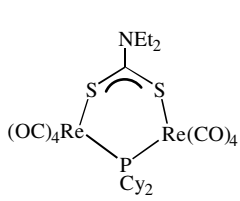

251

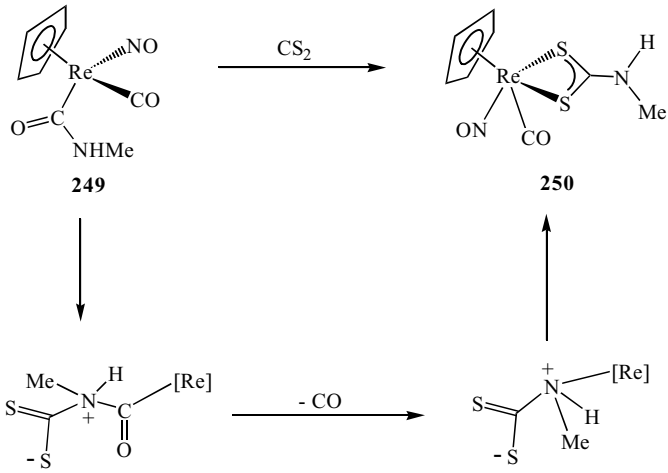

Figure 143. Synthesis of [CpRe(CO)(NO)(S_2CNHMe)] upon addition of carbon disulfide to [CpRe (CO)(NO){η^1-C(O)NHMe}] together with a proposed pathway for the transformation.

e. Applications. The only applications of rhenium dithiocarbamate complexes focus on their potential use in radiopharmaceuticals, in a similar manner to that discussed for technetium (Section IV.D.2.b). Thus, ^{188}Re is a β-emitter ($t_{1/2} = 16.9$ h), which can be produced from ^{188}W through a transport generator system, similar to the ^{99}Mo/^{99m}Tc generator. Demaimay et al. (1172) prepared [^{188}ReN{S_2CNEt(OEt)}$_2$] using a kit method and observe the subcellular localization of ^{188}Re and ^{99m}Tc in granulocytes using microautoradiography. Uptake was found to be independent of the radionuclide and predominantly nuclear, HPLC being used to show that the ^{99m}Tc complex was the same before and after blood cell labeling. Duatti and co-workers (1183) prepared [^{188}ReN(S_2CNR$_2$)$_2$] (R = Me, Et, Pr) and carried out biodistribution studies in rats. They are found to exhibit similar biological behavior to the related ^{99m}Tc complexes and may have potential utilization in nuclear medicine as therapeutic agents.

E. Group 8 (VIII B): Iron, Ruthenium, and Osmium

1. Iron

The first report of iron dithiocarbamate chemistry was in 1907, when Delépine (2) detailed the synthesis of the iron(III) tris(dithiocarbamate) complex [Fe(S_2CN—*i*-Bu$_2$)$_3$]. Later the dimethyldithiocarbamate complex [Fe(S_2-CNMe$_2$)$_3$] (Ferbam) found widespread use as a fungicide (14). Iron(II)

dithiocarbamate species were first described by Gleu and Schwarb in 1950 (29), and some 20 years later iron(IV) complexes were prepared (1199). More recent work has focused on the development of iron(III) chemistry, and the use of iron(II) nitrosyl complexes as endogenous NO trapping agents.

a. Iron(III) Tris(dithiocarbamate) Complexes. Since first reported in 1907, a wide range of tris(dithiocarbamate) complexes [$Fe(S_2CNR_2)_3$] have been prepared and studied, primarily in relation to the well-known $^6A_1$–$^2T_2$ spin-state cross-over that they exhibit (Fig. 144); a phenomenon first observed in 1931 (1114,1200). It has been established that changes to the ligand substituents, temperature, and pressure, together with other factors, can result in a change in the position of the spin-state equilibrium. Here is not the place to review this area fully, as it would require a detailed survey of past findings to bring the nonexpert up to speed with developments, and thus only a summary of key contributions will be given. For more information, Coucouvanis (17) provides an excellent summary of the area up until 1978. In the preceding years, more than 30 further contributions have been made, many being included in a recent review (1201).

Key contributions have centered on utilizing a variety of experimental techniques including Mössbauer spectroscopy, magnetic susceptibility measurements (1202), X-ray crystallography, EXAFS, ESR, IR, and NMR spectroscopy. Others workers have addressed steric effects (357), vibrational parameters (1203) and passed comment (1204).

In 1982, Duffy and Uhrich (1205) first proposed that the inductive effects of the dithiocarbamate substituents influence the spin-crossover behavior. However, a more detailed later study by Stahl and Ymén (357) found that there was no correlation between the pK_a of secondary amines and the room temperature magnetic moments of their complexes, suggesting that both steric and electronic effects are important. Solvent incorporation into the crystal lattice can also effect the magnetic properties considerably, through interactions with the sulfur atoms (1206,1207). Those capable of hydrogen bonding (e.g., H_2O, $CHCl_3$, CH_2Cl_2) tend to favor the high-spin conformation, although this is not always

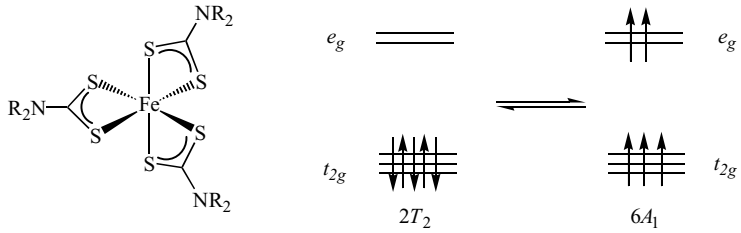

Figure 144. Schematic showing the low- and high-spin configurations of [$Fe(S_2CNR_2)_3$].

the case. For example, Pandeya et al. (1208) found that the water of crystallization in $[Fe\{S_2CN(CH_2CH_2OH)_2\}_3].3H_2O$ favors a low-spin state over the anhydrous compound. Doping iron complexes with cobalt(III) can also have a significant effect on the spin state. In $[Fe\{S_2CN(CH_2CH_2OH)_2\}_3]$, this leads to a gradual move from high to low spin, becoming exclusively low spin at <20 K (1209).

Mössbauer spectroscopy is widely used to study these systems (55,532,1208–1216). Generally, only a single quadrupole doublet is seen; the splitting value increasing with decreasing temperature. This finding suggests a population weighted average as the electronic relaxation rate between the two spin states is smaller than the ^{57}Fe Mössbauer lifetime. The reason for the relatively fast interconversion rate is believed to be the increased covalency and spin–orbit interactions present in the FeS_6 core. Interestingly, in recent work symmetric $[Fe(S_2CNR_2)_3]$ (R = Me, Et, Pr, *i*-Pr, Bu, *i*-Bu) (1214) and asymmetric $[Fe\{S_2CNR(CH_2CH_2OH)\}_3]$ (R = Me, Et, Pr, Bu) (1213) complexes are reported to show an asymmetric doublet that could be resolved into two doublets corresponding to high- and low-spin states.

Ganguli (1217) investigated the spin equilibrium by ^1H NMR spectroscopy in different solvents; observations being interpreted in terms of preferential solvation or second coordination sphere reorganization effects. This work also suggests that neglect of pseudo-contact shift can lead to erroneous conclusions about spin delocalization mechanisms, which occur in these systems by direct π delocalization along the alkyl chain.

The far-IR spectra of iron tris(dithiocarbamate) complexes in various spin states has been measured and Fe—S vibrations assigned using ^{54}Fe and ^{57}Fe isotopes. High-spin complexes show vibrations between 205 and 250 cm^{-1}, and for low spin between 305 and 350 cm^{-1} (1218); assignments that differ from those made earlier (1219).

The ESR spectra of iron(III) tris(dithiocarbamate) complexes have been studied in some detail (1216,1220–1225). At one stage, a narrow line at $g = 2$ with considerable structure was ascribed to a limiting resonance structure involving a low-spin iron(II) species and an unpaired electron on a radical ligand (1223,1224), however, this was later shown to be due to the presence of $[Fe(NO)(S_2CNR_2)_2]$ as an impurity (1222). Pandeya and Singh (1220) studied the ESR spectrum of $[Fe\{S_2CN(CH_2CH_2OH)_2\}_3]$ between 4.2 and 298 K, their results favoring a solid solution over a domain model.

A large number of X-ray studies have been carried out, often at variable temperatures (55,351,357,461,500–503,1226,1227). For example, $[Fe\{S_2CN(CH_2CH_2OH)_2\}_3]$ has been studied at 150 and 298 K, the decrease in the average iron–sulfur distance upon cooling [Fe–S(av) 2.390(3) Å at 295 K; 2.331(3) Å at 150 K] corresponding to a decrease in magnetic moment (μ_{eff} 4.20 and 2.40 BM) (1228). Stahl and Ymén (357) studied the possible correlation

between 10 mean geometric parameters and magnetic moments, concluding that the only parameters significantly correlated to μ_{eff} are the S—C—S and C—N—C bond angles. They postulated that this is probably due to steric effects; the resulting smaller bite angle associated with bulky substituents leading to a strong ligand field and thus favoring the low-spin configuration.

Single-crystal X-ray crystallography gives only a weighted average of the high- and low-spin forms. Young and co-workers used a combination of Fe K-edge XAFS and advanced data analysis to determine spin-state populations and parameters for high- and low-spin forms of $[Fe(S_2CNEtPh)_3]$ and $[Fe(S_2CNC_4H_8O)_3]$ simultaneously. Thus for $[Fe(S_2CNEtPh)_3]$, iron–sulfur distances of 2.44(2) Å and 2.30(2) Å have been determined for high- and low-spin isomers, respectively (499).

Tris(dithiocarbamate) complexes have also been also been prepared from unusual amines such as succinimide, phthalimide (49), 1,4,7,10-tetraoxa-13-azacyclopentadecane (50), and a range of amino acids (138). Very recently, Beer et al. (62) prepared a number of novel tris(dithiocarbamate) complexes in which two iron(III) centers are linked via the dithiocarbamate ligands (Fig. 145).

Mixed-dithiocarbamate complexes $[Fe(S_2CNR_2)_2(S_2CNR'_2)]$ have also been reported. They result from the addition of 1 equiv of a dithiocarbamate salt to either $[Fe(S_2CNR_2)_3]$, $[Fe(S_2CNR_2)_2Cl]$, or $[Fe(S_2CNR_2)_2(NCS)]$; or upon mixing $[Fe(S_2CNR_2)_3]$ and $[Fe(S_2CNR'_2)_3]$ (529–532). In all cases, however, mixtures are formed as a result of ligand scrambling, which is rapid at the substitutionally labile iron(III) center, and suggests that an earlier report may be incorrect (1229).

The addition of ammonium bis(2-hydroxyethyl)dithiocarbamate to iron(III) salts appears to have an equivalence point at a metal/ligand ratio of 2:1 rather than the expected value of 3:1 for the preparation of the tris(dithiocarbamate) complex $[Fe\{S_2CN(CH_2CH_2OH)_2\}_3]$ (599). Cavalheiro and co-workers (599) investigated this phenomenon and proposed that the anomaly results from a fast electron-transfer reaction. This occurs upon addition of a third equivalent of dithiocarbamate salt to $[Fe\{S_2CN(CH_2CH_2OH)_2\}_2]^+$, leading to the formation of the thiuram disulfide and iron(II), simple ligand addition occurring at a much slower rate.

Iron(III) dithiocarbamate complexes with other ligands have also been prepared (1230–1233) and the spin states investigated (1230,1231). These include; oxine, glycine, acac, 8-hydroxyquinoline, phenylalanine, thiomalic acid, phen, and Schiff bases. A number of examples in which two iron(III) centers are linked via the bis(dithiocarbamate) ligand derived from piperazine, namely, $[S_2CNC_4H_8NCS_2]^{2-}$, have also been detailed (1233,1234).

A number of reactions of tris(dithiocarbamate) complexes have been investigated. Reduction of $[Fe(S_2CNR_2)_3]$ ($R = Me$, Et; $R_2 = C_4H_8O$, MePh) by oxalic acid in methanol–benzene proceeds with a first-order dependence on the

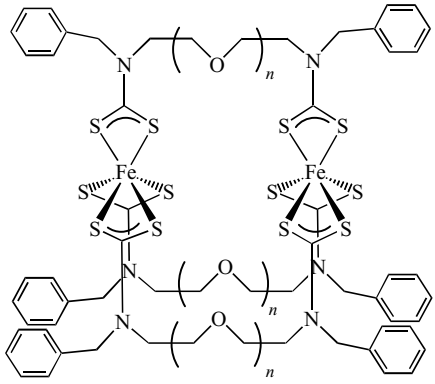

$n = 1, 2, 3$

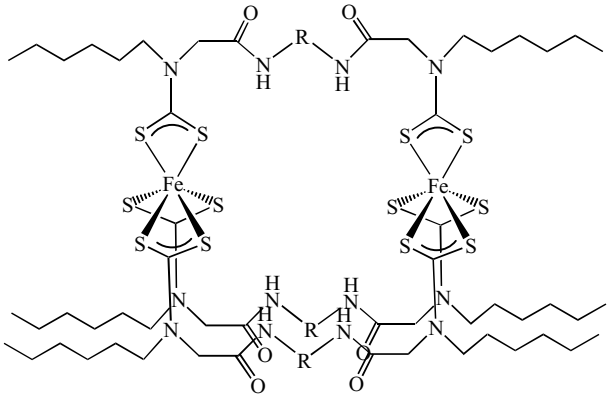

R = Et, *o*-Ph, *m*-Ph

Figure 145. Examples of linked tris(dithiocarbamate) complexes prepared by Beer et al. (62).

concentration of complex. The rate depends on the substituents (MePh > $C_4H_8O \sim$ Me > Et) and added dithiocarbamate, and it is proposed that the initially formed anions $[Fe(S_2CNR_2)_3]^-$, rapidly dissociate to $[Fe(S_2CNR_2)_2]$ and $S_2CNR_2^-$ [1235]. Addition of sodium thiocyanate to tris(dithiocarbamate) complexes results in the formation of green $[Fe(NCS)(S_2CNR_2)_2]$ for a wide range of dithiocarbamates, but fails in a number of cases (R = Ph, Bz) (1205).

Recently, Martin and co-workers (1236) reported the facile abstraction of one of the dithiocarbamate ligands in the morpholine dithiocarbamate complex

$[Fe(S_2CNC_4H_8O)_3]$ upon addition of silver triflate (Eq. 113). The reaction results in the formation of red-black $[Fe(H_2O)(S_2CNC_4H_8O)_2][CF_3SO_3]$ (**252**) in moderate yields, together with $[Ag(S_2CNC_4H_8O)]_n$. A crystal structure of **252** reveals a square-pyramidal coordination environment, with water occupying the axial site.

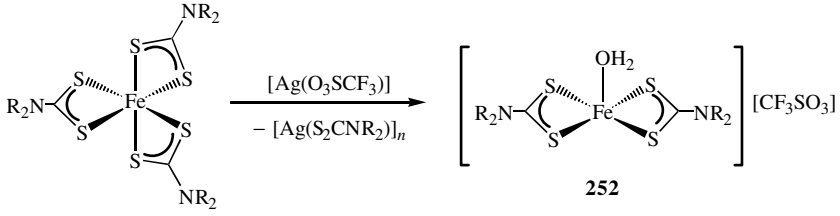

252

$R = C_4H_8O$ (113)

Iron(III) tris(dithiocarbamate) complexes display practically no photochemical activity in solutions free of halogenated hydrocarbons, however, the addition of even small quantities of chlorocarbons results in an increase for the quantum yield of initial product disappearance. Pignolet and co-workers (1237) showed that photolysis of tris(dithiocarbamate) complexes in chlorinated solvents yields $[FeCl(S_2CNR_2)_2]$. The reaction is thought to occur via electron transfer from an excited iron complex to the chlorocarbon with subsequent steps as shown below (Fig. 146) (24).

Photolysis of $[Fe(S_2CNEt_2)_3]$ in chloroform at 313 nm has been shown to afford an excited-state complex, which in turn generates $[FeCl(S_2CNEt_2)_2]$; while at 254 nm a solvent-initiated reaction in which radicals formed after absorption of light by chloroform react thermally to give the same product

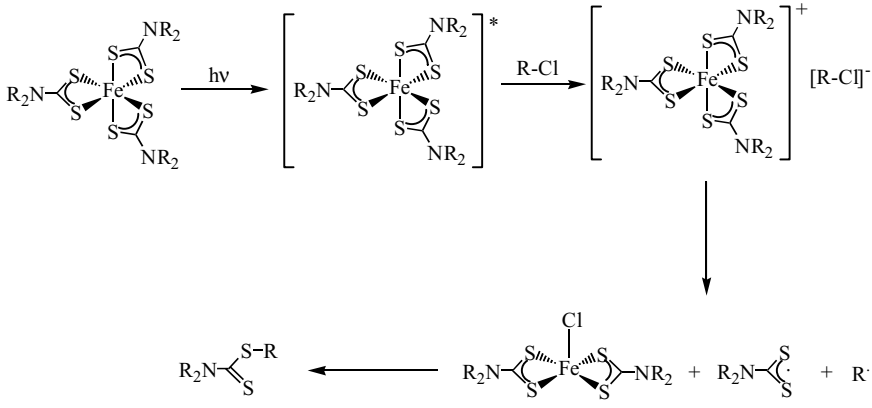

Figure 146. Photochemical transformations of $[Fe(S_2CNR_2)_3]$ in chlorinated solvents.

(1238). Interestingly, photolysis of $[Fe(S_2CNR_2)_2\{SC(CF_3)=C(CF_3)S\}]$ results in selective dissociation of the neutral dithietene ligand rather than a dithiocarbamate (1237).

Reactions of tris(dithiocarbamate) complexes with iodine have been studied in some detail and lead to a range of products, being dependent on the conditions utilized and substituents on the dithiocarbamate ligands, as discussed more fully in Section IV.E.1.b.

b. Iron(III) Halide and Related Complexes. Iron(III) halide complexes $[FeCl(S_2CNR_2)_2]$ were first reported by Tamminen and Hjelt (1239) from the reaction of $FeCl_3$ and thiuram disulfides. A wide range of such complexes, $[FeX(S_2CNR_2)_2]$ (X = Cl, Br, I) (**253**) are now known and can be prepared via a number of different routes (1121,1238,1240–1242); although the addition of concentrated acids, HX, to benzene solutions of $[Fe(S_2CNR_2)_3]$, as developed by Martin and White (1243), remains the most widely applicable.

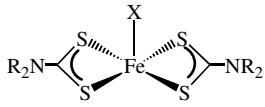

253

As eluded to above, reactions of tris(dithiocarbamate) complexes with iodine have previously been shown to generate a variety of products (1199). Petridis et al. (1244) showed that in dichloromethane, $[Fe(S_2CNMe_2)_3]$ yields a product of the formula, $[Fe(S_2CNMe_2)_2I_2]$, while in contrast, $[Fe(S_2CNEt_2)_3]$ affords $[Fe(S_2CNEt_2)_2I_3]$ (**254**) (Fig. 147). Mössbauer parameters for the latter suggest a

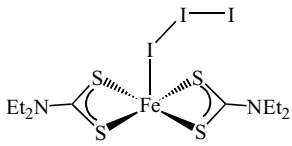

254

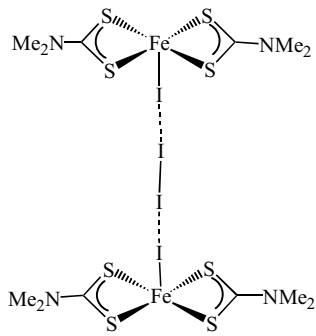

255

Figure 147. Examples of complexes obtained from the reaction of $[Fe(S_2CNR_2)_3]$ with iodine.

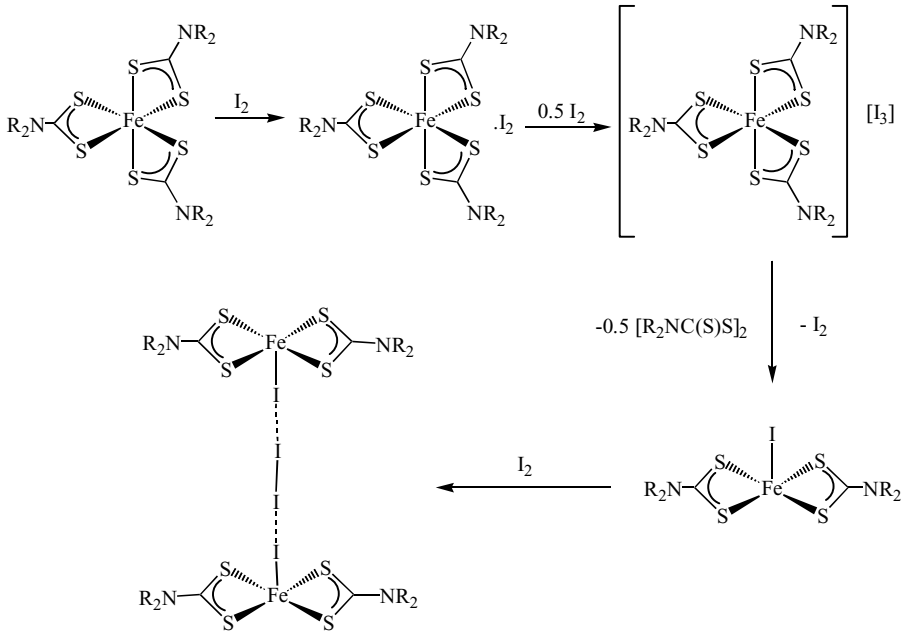

Figure 148. Proposed mechanism of the reaction of $[Fe(S_2CNR_2)_3]$ with iodine.

single paramagnetic iron(III) center with a terminally bound I_3^- ligand, while $[Fe(S_2CNMe_2)_2I_2]$ consists of two iron(III) halide centers bridged by an iodine unit, being best described as $[\{FeI(S_2CNMe_2)_2\}_2(\mu\text{-}I_2)]$ (**255**).

In an attempt to understand mechanistic features of these transformations (Fig. 148), Crisponi et al. (1242) followed reactions of $[Fe(S_2CNR_2)_3]$ (R = Et, Bz; $R_2 = C_4H_8O$) with iodine by spectrophotometric methods. They find that an iodine adduct, $[Fe(S_2CNR_2)_3].I_2$ is initially formed, which reacts further with more iodine to give an iron(IV) complex, $[Fe(S_2CNR_2)_3][I_3]$. The latter then undergoes an internal redox reaction generating $[FeI(S_2CNR_2)_2]$, iodine, and one-half of an equivalent of thiuram disulfide (1242). Later work (see below) has shown that $[FeI(S_2CNR_2)_2]$ can form an adduct of the type **254** with further iodine (1241).

Crystal structures of a number of complexes, $[FeX(S_2CNR_2)_2]$ (X = Cl, Br, I, NCS), have been reported (1245–1252). All have a square-based pyramidal iron center, the halide occupying the axial position. Two modifications of $[FeBr(S_2CNEt_2)_2]$ have been published (1249,1250). They differ in the relative arrangements of the ethyl groups (up–down or down–down) which leads to different magnetic properties (see below). This finding correlates with results from other workers who found that the magnetic properties of $[FeX(S_2CNEt_2)_2]$ (X = Cl,

Br, I) at low temperature depended markedly upon sample preparation (1251). One crystal modification shows a ferromagnetic ordering at 1.347 K, while the second shows a Schottky-type anomaly, which is correlated with the formation of dimeric units in the lattice.

When crystals of $[FeCl(S_2CNC_5H_{10})_2]$ are grown from chloroform an adduct results in which chloroform is hydrogen bonded to two adjacent sulfur atoms of different dithiocarbamate ligands (S···H 2.72–2.88 Å) (1246). In concentrated iodine solutions, $[FeI(S_2CNR_2)_2]$ forms adducts of the type, $[FeI(S_2CNR_2)_2].0.5I_2$ (1241). The structure of one of these ($R_2 = C_4H_8$) has been studied crystallographically and reveals dimeric units in which individual molecules are linked via an approximately linear I_4 unit with two long [I···I 3.516(3) Å] and one short [I–I 2.779(3) Å] interaction (495). More recent work has shown that analogous complexes containing a Br_4 unit can also be prepared (1240).

As early as 1967, the chloride complex $[FeCl(S_2CNEt_2)_2]$ was shown to be a molecular ferromagnet (1253). Over the past 20 years a number of further studies have been carried out on the magnetism of this system (and the related bromide), most notably by De Fotis et al. (1254–1258). It has a ferromagnetic transition temperature of 2.457 K, while mixtures of $[FeCl(S_2CNEt_2)_2]$ and $[FeBr(S_2CNEt_2)_2]$ are characterized by transition temperatures of between 2.213 and 1.613 K (1255).

High-resolution netutron diffraction data on a deuterated sample of $[FeCl(S_2CNEt_2)_2]$ have been carried out between 50 and 300 K. They reveal a structural transition associated with a disorder of one of the ethyl groups over two positions at room temperature, being frozen out into a single position in the low-temperature phase (508). Other workers have also carried out neutron diffraction experiments on both powder and single-crystal samples; Mössbauer simulations in conjunction with the neutron results allowing the authors to conclude that the system is a noncollinear ferromagnet (509).

In complexes of the type $[\{FeI(S_2CNR_2)_2\}_2(\mu\text{-}I_2)]$ (**255**), detailed above, the two iron(III) centers are coupled antiferromagnetically through the bridging halide unit. For example, $[\{FeI(S_2CNMe_2)_2\}_2(\mu\text{-}I_2)]$ shows magnetic-ordering transition at <1.6 K, and quantum mechanical calculations have been used to provide give insight into the possible superexchange process (1240,1259).

Reactions of $[FeX(S_2CNR_2)_2]$ with some Lewis bases (B) has been studied, including those with pyridine and γ-picoline (1260). Ligand exchange via a SN_2 mechanism occurs with the generation of two distinct adducts, $[FeB(S_2CNR_2)_2]X$ and $[FeB_2(S_2CNR_2)_2]X$, in dynamic equilibrium. As they have different spin states ($S = 3/2$ and 5/2, respectively), a parallel spin crossover in the iron(III) ion also occurs.

Iron(III) nitrosyl complexes $[FeX(NO)(S_2CNR_2)_2]$ (X = Br, I) (**256**) have been prepared from both the addition of halogens to $[Fe(NO)(S_2CNR_2)_2]$ (X = Br, I) (**257**) (1261), and from the reaction of $[FeI(S_2CNR_2)_2]$ with NO

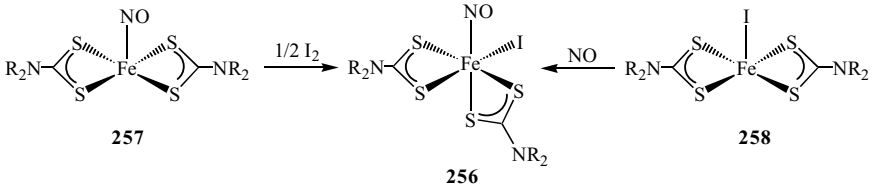

Figure 149. Synthetic routes to $[FeI(NO)(S_2CNR_2)_2]$.

(**258**) (Fig. 149) (534). Attempts to make the analogous chloride complexes upon addition of chlorine to $[Fe(NO)(S_2CNR_2)_2]$, however, failed (1261). The ν(NO) vibration in the IR spectrum lies between 1804 and 1829 cm^{-1}, being shifted some 100–120 cm^{-1} to higher wavenumbers than in the iron(II) nitrosyls (see below).

Mössbauer data have been recorded for a number of these complexes (1261) as have natural abundance ^{15}N NMR spectra (534). For example, the ^{15}N NMR spectrum of $[FeI(NO)(S_2CNEt_2)_2]$ shows three peaks; two assigned to the inequivalent dithiocarbamate ligands at 210.92 and 209.09 ppm, together with a third at 29.28 ppm assigned to the nitrosyl moiety.

c. Iron(II) Nitrosyl Complexes: Endogenous NO Trapping Agents. Iron(II) dithiocarbamate complexes $[Fe(NO)(S_2CNR_2)_2]$ have been known since the late 1960s, being easily prepared from the addition of sodium nitrite to an acidic solution of iron(II) sulfate, followed by addition of the appropriate dithiocarbamate salt (1261,1262).

They contain a square-pyramidal metal center and a linear nitrosyl ligand, as shown crystallographically for $[Fe(NO)(S_2CN{-}i\text{-}Pr_2)_2]$ (1263). Infrared spectra are very characteristic, the ν(NO) absorption being seen between 1693 and 1724 cm^{-1}. The precise value is highly dependent on the nature of the substituents on nitrogen and correlate closely with corrected pK_a values for the parent amines (1262). Indeed, other parameters such as ^{57}Fe Mössbauer isomer shifts and quadrupole splitting (1261,1262), the g_{eff} value, and ^{14}N hyperfine splitting values in the ESR spectra also correlate closely with corrected pK_a values, being explained in terms of the strong mesomeric electron-releasing effect of the NR_2 units (1262).

Iron(II) nitrosyl complexes display a characteristic three-line ESR spectrum ($g_{av} = 2.04$) at room temperature and a spectrum with axial symmetry ($g_{\perp} = 2.037$, $g_{//} = 2.015$) at low temperature, the unpaired electron occupying an orbital comprised of $Fe(d_{z^2})$ and $NO(\sigma^*)$ contributions (1263–1265).

Since iron(II) bis(dithiocarbamate) center binds NO very strongly, and the resultant nitrosyl complexes display a characteristic ESR signal, then quite

recently they have come to the fore as endogenous NO trapping agents (1266–1272). In 1991, Vanin and co-workers (1273) first used iron dithiocarbamates as trapping agents for the physiologically important molecule, NO. Both iron(II) and iron(III) dithiocarbamate complexes, $[Fe(S_2CNR_2)_2]$ and $[Fe(S_2CNR_2)_3]$, react with NO to produce $[Fe(NO)(S_2CNR_2)_2]$. As the latter can be easily detected by ESR spectroscopy, this provides a powerful approach to NO detection that has been developed as an *in vivo* invasive measurement. A recent review provides a good summary of this area (26). Here, only pertinent chemical features, mechanistic considerations, and some key contributions will be considered.

Reactions of NO with iron(II) complexes are simple addition reactions, but those with $[Fe(S_2CNR_2)_3]$ require more consideration, a coproduct being one-half of an equivalent of thiuram disulfide. Studies by Fujii et al. (1274) suggest that two transient intermediates are involved. The first is proposed to be $[Fe(NO)(S_2CNR_2)_2(\eta^1\text{-}S_2CNR_2)]$, which in turn undergoes a disproportionation and ligand redistribution reaction with more $[Fe(S_2CNR_2)_3]$ giving $[Fe(NO)(S_2CNR_2)_2]$, $[Fe(S_2CNR_2)_3]^+$, and free dithiocarbamate. The latter then undergo further electron-transfer regenerating $[Fe(S_2CNR_2)_3]$ and giving one-half of an equivalent of thiuram disulfide (Fig. 150).

In further work on iron(II) nitrosyl complexes, Iliev and Shopov (1275) reported that a ligand redistribution reaction occurs between $[Fe(NO)(S_2CNEt_2)_2]$ and $[Ni\{S_2P(O\text{—}i\text{-}Pr)_2\}_2]$ when mixed in chloroform, the product,

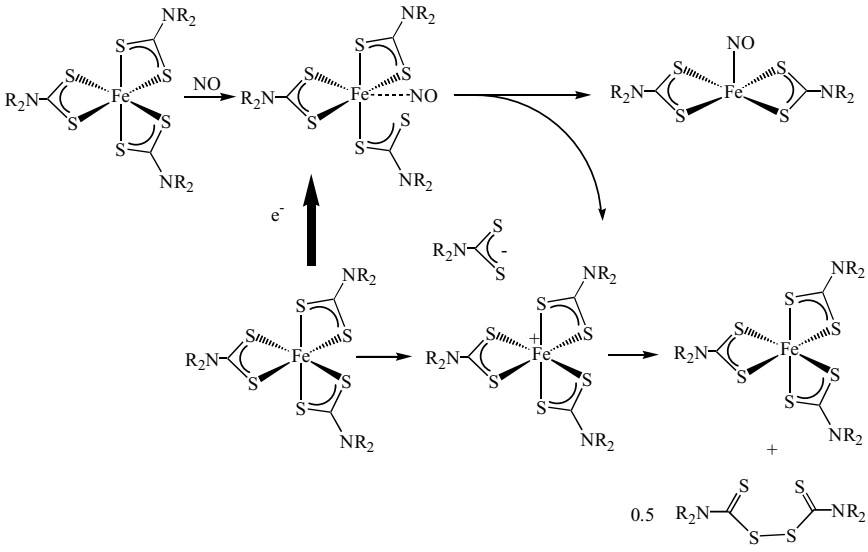

Figure 150. Proposed mechanism for reductive nitrosylation of $[Fe(S_2CNR_2)_3]$.

$[Fe(NO)(S_2CNEt_2)\{S_2P(O{-}i\text{-}Pr)_2\}]$, being detected by ESR spectroscopy. Glidewell and Johnson (1234) reported that addition of the bis(dithiocarbamate) salt derived from piperizine, $Na_2[(S_2CNC_4H_4NCS_2)]$, to Roussin's methyl ester, $[Fe(NO)_2(\mu\text{-}SMe)]_2$, in DMF gives a mixture of mono- and bis(nitrosyl) products as shown by ESR spectroscopy. Their precise nature (monomeric or oligiomeric) was not determined, but the mononitrosyl product was of the type $[Fe(NO)(S_2CNR_2)_2]$. Interestingly, when the same reaction was carried out in acetone it took a completely different course and no simple products were isolated.

d. Cyclopentadienyl Complexes. Astruc and co-workers have made detailed studies on iron(II) cyclopentadienyl complexes of the types, $[(\eta^5\text{-}C_5R'_5)Fe(CO)_2(\eta^1\text{-}S_2CNR_2)]$ and $[(\eta^5\text{-}C_5R'_5)Fe(CO)(S_2CNR_2)]$ ($R = Me$, Et; $R' = H$, Me) (902,1276–1284). A number of synthetic routes to $[CpFe(CO)_2(\eta^1\text{-}S_2CNR_2)]$ have been developed, including the insertion of carbon disulfide into *in situ* generated metal amides (902) and halide displacement (1277), but the most convenient involves the addition of dithiocarbamate salts to $[CpFe(CO)_3][PF_6]$ in acetone (1283).

The reactivity of these monodentate dithiocarbamate complexes has been assessed (Fig. 151) (1283). Transmetalation occurs upon addition of $[Fe_2(CO)_9]$ or $[CpMo(CO)_3]_2$ giving *cis*-$[Fe(CO)_2(S_2CNR_2)_2]$ and $[CpMo(CO)_2(S_2CNR_2)]$, respectively, while reaction with $[NO][PF_6]$ yields $[CpFe(NO)(S_2CNR_2)]$. The

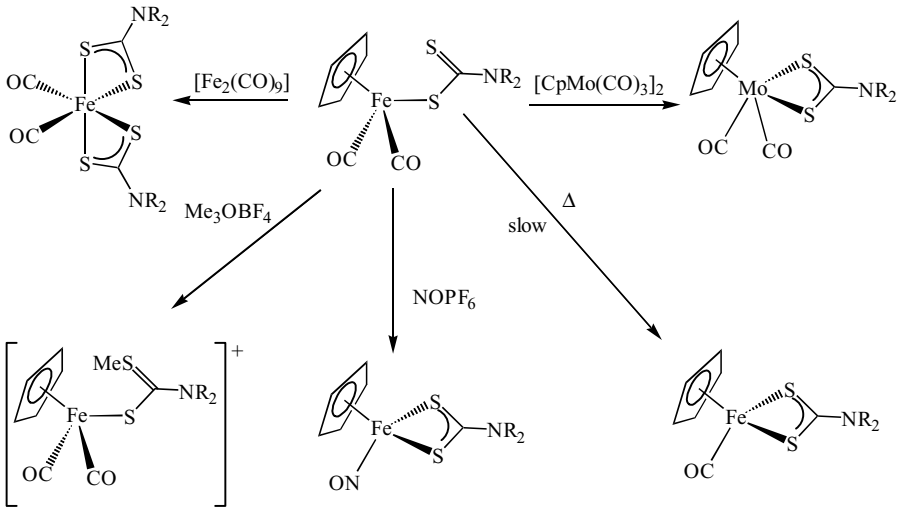

Figure 151. Examples of the reactivity of $[CpFe(CO)_2(\eta^1\text{-}S_2CNR_2)]$.

uncoordinated sulfur atom is electrophilic and addition of $[Me_3O]BF_4$ yields $[CpFe(CO)_2\{\eta^1\text{-}S{=}C(NMe_2)SMe\}][BF_4]$. With methyl iodide, however, methylation and subsequent displacement of the thioester $MeSC(S)NMe_2$ gives $[CpFe(CO)_2I]$.

The thermal conversion of $[(\eta^5\text{-}C_5R'_5)Fe(CO)_2(\eta^1\text{-}S_2CNR_2)]$ to $[(\eta^5\text{-}C_5R'_5)Fe(CO)(S_2CNR_2)]$ is a slow process, which proceeds only at elevated temperatures and with considerable complex decomposition (902,1283,1285). The process can be photochemically induced (1276) and Astruc and co-workers (1283) also found that the rate of chelation could be enhanced considerably upon addition of PPh_3/CS_2, $[Mo(CO)_6]$, or $[Cp_2TiCl_2]$. However, the most efficient method is via an electrocatalytic process catalyzed by $[Cp_2Fe]X$ (1276,1279,1282,1284). Thus, oxidation of $[(\eta^5\text{-}C_5R'_5)Fe(CO)_2(\eta^1\text{-}S_2CNR_2)]$ gives a 17-electron radical cation, which then loses CO giving $[(\eta^5\text{-}C_5R'_5)Fe(CO)(\eta^2\text{-}S_2CNR_2)]^+$ (Fig. 152). The key step is an endergonic ($\Delta G^\circ > 50$ kJ mol^{-1}) cross-electron-transfer propagation process between this species and $[(\eta^5\text{-}C_5R'_5)Fe(CO)_2(\eta^1\text{-}S_2CNR_2)]$, which yields the desired product $[(\eta^5\text{-}C_5R'_5)Fe(CO)(S_2CNR_2)]$ and regenerates $[(\eta^5\text{-}C_5R'_5)Fe(CO)_2(\eta^1\text{-}S_2CNR_2)]^+$. The fact that the overall process works with this key endergonic step suggests that the other propagation step must be exergonic and fast.

On a preparative scale, the conversion yield depends on the nature of the counterion. This observation is related to the precipitation rate of $[(\eta^5\text{-}C_5R'_5)Fe(CO)(\eta^2\text{-}S_2CNR_2)]X$, being faster when the 17-electron cation is not stabilized by a large anion. Interestingly, the chelation process can also be induced by reduction (1282). By this route, yields and efficiencies of the

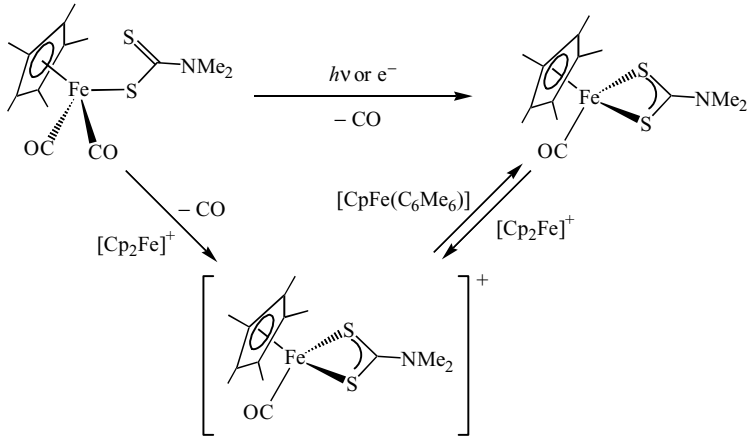

Figure 152. Conversion of $[Cp^*Fe(CO)_2(\eta^1\text{-}S_2CNMe_2)]$ into $[Cp^*Fe(CO)(S_2CNMe_2)]$.

electrocatalytic cycle are better than those induced oxidatively, but a limitation is the instability of the 19-electron radical anions $[(\eta^5\text{-}C_5R'_5)Fe(CO)_2(\eta^1\text{-}S_2CNR_2)]^-$, which readily lose dithiocarbamate.

The electrogenerated 17-electron complexes $[(\eta^5\text{-}C_5R'_5)Fe(CO)(\eta^2\text{-}S_2CNR_2)]^+$ readily lose CO in the presence of a variety of two-electron donor ligands giving $[(\eta^5\text{-}C_5R'_5)FeL(\eta^2\text{-}S_2CNR_2)]^+$ (R = Me, Et; R′ = H, Me, Bz; L = PPh_3, MeCN, Me_2CO, thf, CH_2Cl_2) (1276–1281). Triphenylphosphine derivatives $[(\eta^5\text{-}C_5R'_5)Fe(PPh_3)(\eta^2\text{-}S_2CNR_2)]^+$ can be reversibly reduced to 18-electron species $[(\eta^5\text{-}C_5R'_5)Fe(PPh_3)(\eta^2\text{-}S_2CNR_2)]$ (1280,1281), while weakly coordinating ligands are displaced by anions giving $[(\eta^5\text{-}C_5R'_5)FeX(S_2CNR_2)]$ (X = CN, SCN, Cl) (1281). The latter are believed to proceed via 19-electron intermediates, and depending on the ligand sphere, they can be very electron rich and act as reducing agents. Thus, addition of $NaS_2CNR_2.nH_2O$ gives 18-electron, iron(IV) complexes $[(\eta^5\text{-}C_5R'_5)Fe(S_2CNR_2)_2]^+$, one example of which has been crystallographically characterized (R = Bz, R′ = Me) (1281). Use of anhydrous dithiocarbamate salt or oxidation of the iron(IV) species by $[CpFe(C_6Me_6)]$ yields 19-electron species, $[(\eta^5\text{-}C_5R'_5)Fe(S_2CNR_2)_2]$, which have been characterized by ESR spectroscopy (Fig. 153). In the solid state they slowly transform to 17-electron complexes, $[(\eta^5\text{-}C_5R'_5)Fe(\eta^1\text{-}S_2CNR_2)(S_2CNR_2)]$, a process that is rapid in acetonitrile but surprisingly slow in toluene. Molecular orbital calculations have been performed on both 17- and 19-electron bis(dithiocarbamate) complexes, and suggest that in the 19-electron species the odd electron is in an antibonding metal-centered orbital, while the 17-electron species have significant sulfur spin density.

e. Other Iron(II) Complexes. Simple iron(II) dithiocarbamate complexes $[Fe(S_2CNR_2)_2]$ are known, being formed from the reaction of dithiocarbamate salts and ferrous sulfate heptahydrate (754,1286). They are extremely air-sensitive, chocolate brown solids, the ethyl analogue being shown to be dimeric in the solid-state **259**; the iron centers coupling antiferromagnetically (1287). More recently, the syntheses of $[Fe(S_2CNC_4H_8)_2]$ and $[Fe(S_2CNC_5H_{10})_2]$ have been claimed, but with little supporting data (590).

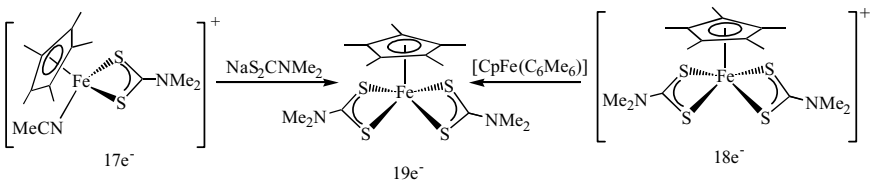

Figure 153. Synthetic routes to $[Cp^*Fe(S_2CNMe_2)_2]$.

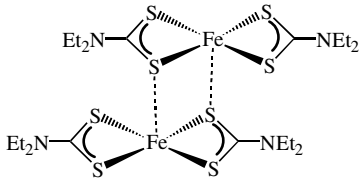

259

A related iron(II) adduct, $[Fe(S_2CNC_4H_8O)_2(O{=}CHNMe_2)]$ (**260**), has been prepared and crystallographically characterized (1288). The metal coordination environment is square-based pyramidal, similar to that found in nitrosyl complexes. The average iron–sulfur distance of 2.460(3) Å is close to that of 2.425 Å found in $[Fe(S_2CNEt_2)_2]_2$ (1287), but longer than those of 2.28–2.30 and 2.15–2.19 Å found in iron(III) and (IV) complexes, respectively. In the Mössbauer spectrum, a large quadrupole splitting of 4.10 mm s^{-1} is seen, being associated with an asymmetric $3d^6$ $(t_{2g}^4 e_g^2)$ electronic configuration.

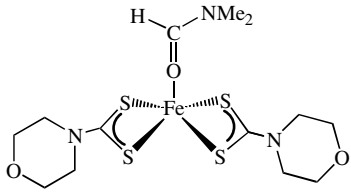

260

Photolysis of $[Fe(S_2CNEt_2)_3]$ in the presence of dppe, affords $[Fe(S_2CNEt_2)_2$ (dppe)] and tetraethylthiuram disulfide. The reaction is initiated by ligand-to-metal charge-transfer (LMCT) excitation, generating $[Fe(S_2CNEt_2)_2]$ and a dithiocarbamate radical in the primary photochemical step, the former being trapped by the diphosphine (Fig. 154) (1289).

Connelly and co-workers (1290) reported that $[Fe(CO)_2(PPh_3)_2(S_2CNMe_2)]^+$ can be obtained from $[Fe(CO)_3(PPh_3)_2]^+$ and NaS_2CNMe_2, although higher yields are found when tetramethylthiuram disulfide is used (Eq. 114); the latter being consistent with a one-electron oxidation of the metal center. The complex is air-stable and shows two carbonyl resonances at 2024 and 1983 cm^{-1}, from which a cis carbonyl and trans phosphine conformation is proposed.

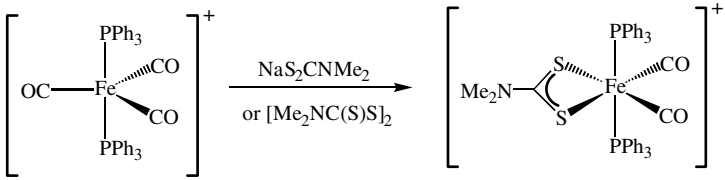

(114)

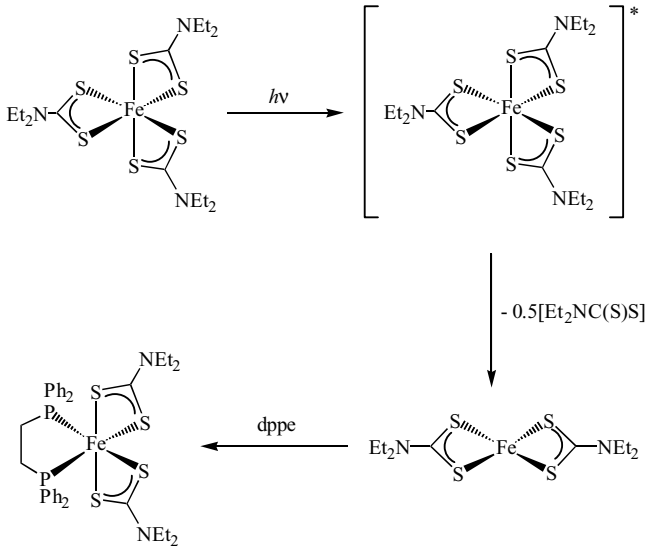

Figure 154. Photolytic synthesis of $[Fe(S_2CNEt_2)_2(dppe)]$ from $[Fe(S_2CNEt_2)_3]$ and dppe.

A number of further carbonyl complexes have been prepared. Addition of 1 equiv of dithiocarbamate salt to *cis*-$[FeI_2(CO)_4]$ yields *fac*-$[FeI(CO)_3(S_2CNR_2)]$ ($R = Et$; $R_2 = PhH$); the geometry being assigned on the basis of the observation of three carbonyl bands in the IR spectrum (1291). Dean (1292) has shown that with 2 equiv of $[NMe_2H_2][S_2CNMe_2]$, brown *cis*-$[Fe(CO)_2(S_2CNMe_2)_2]$ results, the latter also being prepared upon photolysis of $Fe(CO)_5$ and dimethylthiocarbamyl chloride (Fig. 155).

Mathur and co-workers (1293) report that photolysis of $[CpW(CO)_3(\eta^1\text{-}S_2CNMe_2)]$ with either $[Fe_2(CO)_9]$ or $[Fe_3(CO)_{12}]$ gives *cis*-$[Fe(CO)_2(S_2CNMe_2)_2]$ and $[Fe(S_2CNMe_2)_2]$ in 60 and 30% yields, respectively, after chromatography; similar amounts of each coming from the reaction of tetramethylthiuram disulfide and these iron carbonyls. The authors further claim that prolonged photolysis of *cis*-$[Fe(CO)_2(S_2CNMe_2)_2]$ gives $[Fe(S_2CNMe_2)_2]$ quantitatively, and the latter can be converted back to the dicarbonyl when CO was bubbled through a solution for 1 h. The latter is true, as others have shown that $[Fe(S_2CNEt_2)_2]$ in DMF reacts rapidly with CO to give *cis*-$[Fe(CO)_2(S_2CNEt_2)_2]$ (1294). However, the reverse reaction (loss of CO) seems unfounded as isolation of the extremely air-sensitive $[Fe(S_2CNMe_2)_2]$ (754,1286,1287) under these conditions seems unlikely. Further, in a recent paper the photooxidation of *cis*-$[Fe(CO)_2(S_2CNEt_2)_2]$ in chloroform has been shown to give $[FeCl(S_2CNEt_2)_2]$ with a quantum yield of 0.0015 at 366 nm (Eq. 115) (1295), while the

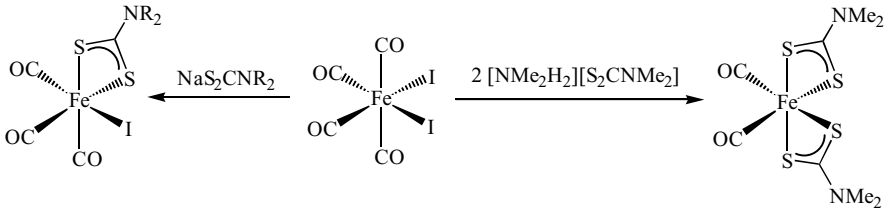

Figure 155. Synthesis of dithiocarbamate complexes utilizing *cis*-$[FeI_2(CO)_4]$.

dicarbonyl will not react with pyridine even under forcing conditions (1294).

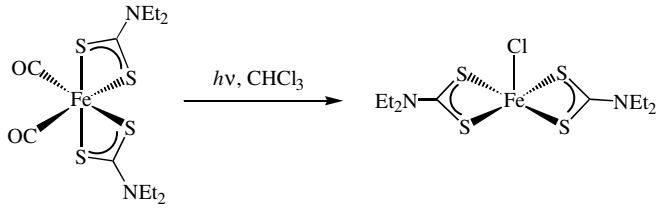

(115)

A wide-range of bis(carbonyl) complexes, *cis*-$[Fe(CO)_2(S_2CNR_2)_2]$, have been studied by ^{13}C and ^{15}N NMR spectroscopy (535). The former provides evidence of hindered rotation about the carbon–nitrogen bonds in complexes with high pK_a(corr) values, while natural abundance ^{15}N NMR spectra are sharp, indicating substantial carbon–nitrogen double-bond character.

In contrast to the reaction of dimethylthiocarbamyl chloride with $Fe(CO)_5$ described above, with either $[Fe_2(CO)_9]$ or $[Fe_3(CO)_{12}]$ the orange thiocarboxamide complex, *cis*-$[Fe(CO)_2(S_2CNMe_2)(\eta^2\text{-}SCNMe_2)]$, is formed exclusively (Eq. 116) (1292). This is confirmed crystallographically (1296), the iron–sulfur bond of the thiocarboxamido group at 2.387(2) Å being somewhat longer than those to the dithiocarbamate [Fe–S(av) 2.325(2) Å] and associated differences also being seen in the carbon–sulfur [1.653(7) vs (av)1.708(7) Å] and carbon–nitrogen [1.302(8) vs 1.321(8) Å] bond lengths. The same product also results from the reaction of $[Fe_2(CO)_9]$ with tetramethylthiuram monosulfide (1296) and displays fluxional behavior associated with the exchange of the methyl groups on the dithiocarbamate via a Bailer-twist type process (1292).

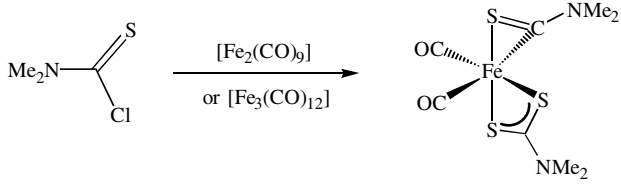

(116)

Addition of [PPN][S_2CNEt_2] to [Fe(NO)$(CO)_2(\eta^4$-$C_4Ph_4)$]$^+$ results in carbonyl loss to give [Fe(NO)$(S_2CNEt_2)(\eta^4$-$C_4Ph_4)$] (**261**) in 62% yield, which has been crystallographically characterized (1297). The oxidation state of the iron center is unclear. The author's suggest that parameters within the cyclobutadiene ring are comparable with those of other iron(0) complexes of this ligand, but the iron–sulfur bonds of 2.316(1) and 2.317(1) Å are similar to those found for iron(II) complexes. The ν(NO) vibration is seen at 1735 cm^{-1} in the IR spectrum is, however, more consistent with binding to an iron(III) rather than an iron(II) center.

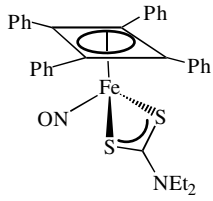

261

f. Iron (IV) Complexes. As mentioned earlier, iron(IV) complexes were first prepared by Pasek and Straub in 1972 (1199), being obtained from air oxidation of tris(dithiocarbamate) complexes in the presence of BF_3 (Eq. 117). More recently, oxidation of [Fe$(S_2CNR_2)_3$] by copper(III) dithiocarbamate complexes has been shown to afford a simple preparative route (R = Me, Et; R_2 = MePh, C_5H_{10}) (1124), while as detailed earlier, addition of iodine to [Fe$(S_2CNEt_2)_3$] in dichloromethane initially yields [Fe$(S_2CNEt_2)_3$][I_5], which has been crystallographically characterized (1298). The iron–sulfur bonds at 2.291(4)–2.314(4) Å are slightly shorter than in the analogous iron(III) complex as are the carbon–nitrogen bonds of 1.295(15)–1.291(16) Å, indicating a greater contribution from the thioureide form of the dithiocarbamate.

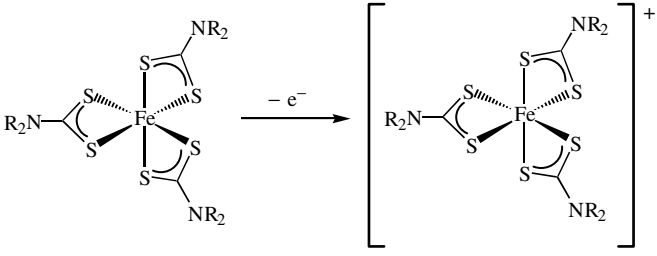

(117)

Oxidation of [Fe$(S_2CNR_2)_3$] by $NOBF_4$ in dichloromethane has been followed by ESMS (303). Peaks associated with [Fe$(S_2CNR_2)_3$]$^+$ are seen, however, at higher source energies ions [Fe$(S_2CNR_2)_2$]$^+$ and [Fe(NO)-$(S_2CNR_2)_2$]$^+$ are also detected, suggesting that dithiocarbamates are labile when bound to both iron(III) and iron(IV). More recently, Astruc and

co-workers (1277, 1280, 1281) detailed the synthesis and properties of iron(IV) cyclopentadienyl complexes, $[(\eta^5\text{-}C_5R'_5)Fe(S_2CNR_2)_2]^+$ (as detailed earlier).

g. Clusters. Over the past 10 years, a wide range of sulfido-capped tetra-iron and heterobimetallic cubane-type clusters have been prepared with valence electron counts ranging from 58 to 64 electrons, and iron in oxidation states +2 or +3. For example, tetra-iron clusters $[Fe_4(\mu^3\text{-}S)_4Cl_{4-n}(S_2CNEt_2)_n]^{2-}$ and $[Fe_4(\mu^3\text{-}S)_4(SPh)_{4-n}(S_2CNEt_2)_n]^{2-}$ $(n = 1, 2)$ (**262**) result from addition of dithiocarbamate salt to $[Fe_4(\mu^3\text{-}S)_4Cl_4][PPh_4]_2$ and $[Fe_4(\mu^3\text{-}S)_4(SPh)_4][PPh_4]_2$, respectively (1299,1300). All have 62 valence electron counts and Mössbauer spectra reveal two distinct iron sites. This finding is confirmed crystallographically with X-ray studies showing those bound with dithiocarbamate to be five coordinate, others being four coordinate; observations interpreted in terms of mixed-valence iron(II) and iron(III) centers.

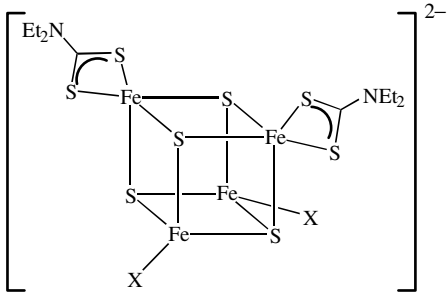

262

The 60-electron iron(III) clusters $[Fe_4(\mu^3\text{-}S)_4(S_2CNR_2)_4]$ $(R = Et;\ R_2 = C_5H_{10})$ are reportedly formed upon addition of dithiocarbamate salts to $[Mg(dmf)_6][Fe_2Cl_4(\mu\text{-}S)_2]$. Both have been crystallographically characterized (1301), as has the one electron-oxidation product, $[Fe_4(\mu^3\text{-}S)_4(S_2CNEt_2)_4][NEt_4]$ (Eq. 118) (1302).

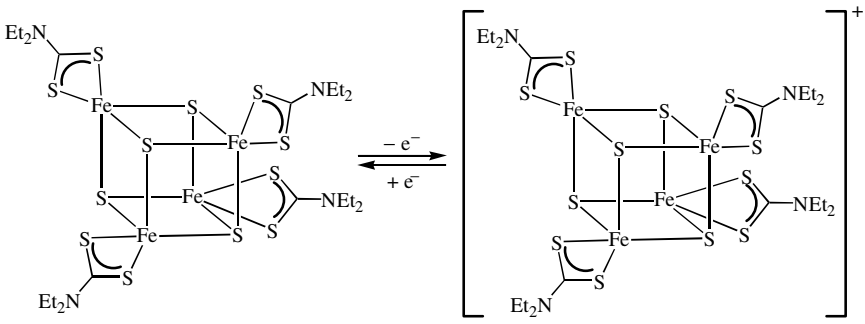

(118)

A wide range of iron-containing heterobimetallic clusters have been prepared with valence electron (VE) counts ranging from 58 to 64. All are generally formed from a self-assembly reaction system of $[MS_4]^{n-}$, $FeCl_2$, $[S_2CNR_2]^-$, and $[SPh]^-$, or from $[Fe(dmf)_6][(FeCl_2)_2MoS_4]$ and $[S_2CNR_2]^-$. Examples include $[VFe_3(\mu^3\text{-}S)_4(S_2CNR_2)_4]^-$ (58 VE) (701,1303), $[V_2Fe_2(\mu^3\text{-}S)_4(S_2CNMe_2)_4(\mu\text{-}S_2CNMe_2)]^-$ (58 VE) (269), $[Mo_2Fe_2(\mu^3\text{-}S)_4(S_2CNEt_2)_4(\mu\text{-}S_2CNEt_2)]$ (59 VE) (270,271), $[MoFe_3(\mu^3\text{-}S)_4(S_2CNR_2)_4(\mu\text{-}S_2CNR_2)]$ (61 VE) (274,1011, 1012,1015,1304), $[WFe_3(\mu^3\text{-}S)_4(S_2CNR_2)_4(\mu\text{-}S_2CNR_2)]$ (61 VE) (273,274,1304), $[MoFe_3(\mu^3\text{-}S)_4(S_2CNEt_2)_4(\mu\text{-}S_2CNEt_2)]^-$ (62 VE) (1013,1014) and $[MoFe_3(\mu^3\text{-}S)_4(S_2CNMe_2)_4(\mu\text{-}S_2CNMe_2)_2]$ (64 VE) (1016).

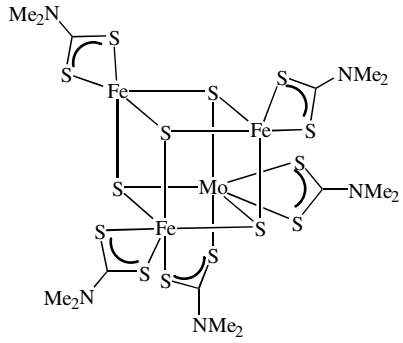

263

Many of these clusters show interesting electrochemical and magnetic properties. For example, in $[MoFe_3(\mu^3\text{-}S)_4(S_2CNMe_2)_4(\mu\text{-}S_2CNMe_2)]$ (**263**), each iron atom is shown by Mössbauer spectroscopy to be in the +3 oxidation state, and interacts with the other metal atoms in the $[MoFe_3S_4]^{5+}$ core, while in the reduced $[MoFe_3S_4]^{4+}$ core, the extra electron is delocalized over all four metal atoms. A recent paper provides a useful summary of the area to-date (701).

h. Applications. As detailed earlier, $[Fe(S_2CNMe_2)_3]$ is a well-known fungicide sold commercially under the name Ferbam. In a series of papers, Malik and co-workers (1305–1314) developed analytical methods for the detection of Ferbam in commercial samples and wheat grains. Most selective is the conversion to an iron(II) 4,7-diphenyl-1,10-phenanthroline complex, detected by an absorbance at 534 nm (1310–1312). In somewhat related work, the tris(dithiocarbamate) complex $[Fe(S_2CNC_5H_{10})_3]$ has been used to determine the iron(III) content in green leafy vegetables via its absorption at 350 nm (1315).

A well-known adverse effect of thiuram di- and monosulfides is their ability to induce allergic contact dermatitis, mainly from rubber products such as gloves. In a recent report, the spontaneous oxidation of $[Fe(S_2CNMe_2)_3]$ is shown to yield tetramethylthiuram disulfide, while iron(III) chloride can also

react with NaS_2CNEt_2 or $[Zn(S_2CNEt_2)_2]$ to generate tetraethylthiuram disulfide (1316).

Tris(dithiocarbamate) complexes $[Fe(S_2CNR_2)_3]$ can be oxidized by $FeCl_3$. This reaction is believed to occur via initial formation of $[FeCl(S_2CNR_2)_2]$, which reacts with further $FeCl_3$ to give mixed-valence complexes $[Fe(S_2CNR_2)_3][FeCl_4]$ and $FeCl_2$. However, the final product is a bis(dialkylimonium)trithiolane (bitt-3) complex, $[bitt\text{-}3][FeCl_5]$ (1317,1318).

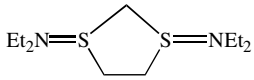

bitt-3

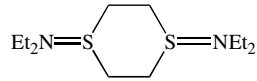

bitt-4

Chen and Qiu (1319) recently developed a novel living atom-transfer radical polymerization (ATRP) system based on this chemistry, utilizing a mixture of $[Fe(S_2CNEt_2)_3]$, $FeCl_3$ and PPh_3 to polymerize methylmethacrylate (MMA). Control experiments reveal that all three components are essential and that $[bitt\text{-}4][FeCl_5]$ is generated; which subsequently decomposes to $Et_2NC(S)SCl$ and $FeCl_2$. Addition of PPh_3 to the latter gives $[FeCl_2(PPh_3)_2]$, which in turn reacts with $Et_2NC(S)SCl$ affording $[FeCl_2(PPh_3)_2]$ and Et_2NCS_2, and it is this radical that initiates polymerization (Fig. 156).

Well-defined polymethylmethacrylate (PMMA) with very low polydispersity and α-S_2CNEt_2 and ω-Cl end groups has been prepared using this method (1320). The same group have also used $[Fe(S_2CNEt_2)_3]$ alone as a catalyst for the reverse ATRP polymerization of vinyl monomers, including MMA and styrene, using diethyl 2,3-dicyano-2,3-diphenylsuccinate as a radical initiator (1321). High molecular weights and low polydispersities are also achieved, the latter getting as low as 1.09 for polystyrene.

Thermal gravimetric analysis of a number of tris(dithiocarbamate) complexes reveals a rapid decomposition between 200 and 300°C to give $[Fe(SCN)_3]$ (1210), while mixed-ligand complexes with dithiocarbamates and oxygen-containing coligands such as oxine, glycine, and acac decompose in one step to give Fe_2O_3 (1230). A number of other tris(dithiocarbamate) complexes have

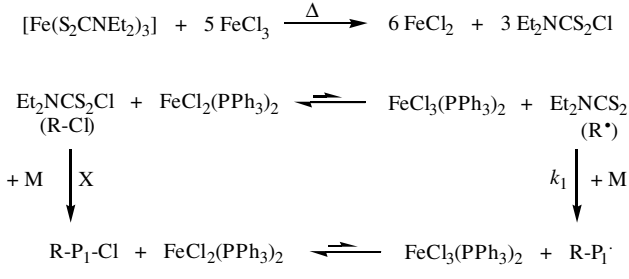

Figure 156. Proposed mode of action of $[Fe(S_2CNEt_2)_3]/FeCl_3/PPh_3$ mixture in ATRP.

been shown to decompose to Fe_2O_3 upon heating in the presence of oxygen (590,1213,1322), in one case the thermal decomposition being followed by Mössbauer spectroscopy (1322).

Liu and Chang (1323) used carboxymethyl (**264**) and bis(carboxymethyl) (**265**) dithiocarbamate salts in conjunction with iron(II) salts for the removal of NO from a simulated flue gas mixture at pH 3–10. The authors suggest that most of the absorbed NO is reduced to nitrogen in conjunction with the oxidative coupling of dithiocarbamate to the thiuram disulfides.

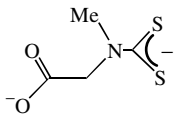

264

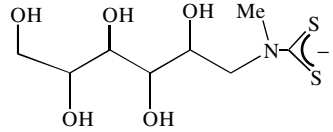

265

2. *Ruthenium and Osmium*

Tris(dithiocarbamate) complexes of ruthenium were first prepared and studied by Malatesta in the 1930s (1324,1325). It was not until some 40 years later that analogous osmium complexes were reported (1326), although prior to this dithiocarbamate ligands had been used for the analytical determination of osmium, a violet color resulting when OsO_4 is added to an aqueous solution of sodium diethyldithiocarbamate (29,1327). More recently, dithiocarbamate chemistry of these elements in low oxidation states (+1 and +2) has been well developed, and while dithiocarbamates can also stabilize the +3 and +4 states, it would appear that an early report of the high-valent complexes $[OsO_2(S_2CNR_2)_2]$ is incorrect (1328).

a. Tris(dithiocarbamate) Complexes and Related Tri- and Tetravalent Complexes. Ruthenium tris(dithiocarbamate) complexes $[Ru(S_2CNR_2)_3]$ have been prepared upon addition of dithiocarbamate salts to aqueous solutions of ruthenium halides (1329–1333); for example, insoluble $[Ru(S_2CNPh_2)_3]$ is generated from $RuCl_3$ at pH 5 (1330). All adopt a low-spin electronic configuration, with effective magnetic moments of $\sim$ 1.8 BM (1329).

Electrochemical studies have been carried out on $[Ru(S_2CNEt_2)_3]$ (1334). It displays a reversible one-electron reduction affording $[Ru(S_2CNEt_2)_3]^-$, together with an irreversible one-electron oxidation. Carrying out the latter in acetonitrile affords the diamagnetic seven-coordinate ruthenium(IV) complex $[Ru(MeCN)(S_2CNEt_2)_3]^+$, which has been isolated in good yield from the reaction of $[RuCl(S_2CNEt_2)_3]$ with $AgBF_4$ in acetonitrile.

Other octahedral ruthenium(III) complexes, $[RuX_2(EPh_3)_2(S_2CNR_2)]$ ($X = Cl,\ Br;\ E = P,\ As;\ R_2 = C_5H_{10},\ C_4H_8O,\ C_4H_8NH$), have been prepared

upon addition of dithiocarbamate salts to $[RuX_3(EPh_3)_3]$ or $[RuBr_3(PPh_3)_2(MeOH)]$ (1335). In the absence of crystallographic data, precise coordination geometries remain unknown, but all have low-spin d^5-electronic configurations and have been characterized by ESR spectroscopy. Cyclic voltammetry measurements show that they undergo fully reversible one-electron oxidation and reduction processes.

Both ruthenium and osmium(III) dithiolate complexes, $[M(SAr)_2(PPhMe_2)_2(S_2CNEt_2)]$ ($M = Ru$, Os; $Ar = C_6F_5$, p-C_6F_4H), have been prepared upon addition of NaS_2CNEt_2 to $[M(SAr)_3(PPhMe_2)_2]$ (Eq. 119) (1336). All are paramagnetic as expected, and an X-ray crystal structure of $[Os(SC_6F_5)_2(PPhMe_2)_2(S_2CNEt_2)]$ reveals that the fluorinated thiolates adopt a relative trans disposition.

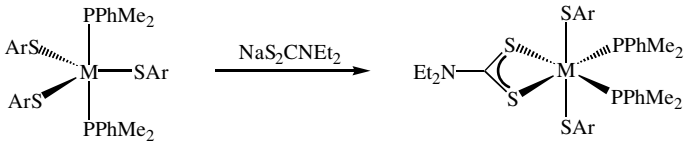

(119)

Cameron and et al. (233) prepared a series of ruthenium(III) complexes, $[Ru(tacn)(S_2CNR_2)(\eta^1\text{-}S_2CNR_2)][PF_6]$ (tacn = 1,4,7-triazacyclononane), upon addition of 2 equiv of dithiocarbamate salt to $[Ru(tacn)(dmso)_2Cl]Cl$ (Eq. 120). These octahedral complexes contain one bidentate and one monodentate dithiocarbamate ligand, being characterized by two CN stretching vibrations at $\sim$1550 and 1460 cm^{-1} in the IR spectrum. The monodentate ligand in $[Ru(tacn)(S_2CNMe_2)(\eta^1\text{-}S_2CNMe_2)][PF_6]$ is easily lost upon addition of NO affording $[Ru(NO)(tacn)(S_2CNMe_2)][PF_6]_2$. In light of this, the biological scavenging ability of the bis(dithiocarbamate) complexes was evaluated, being comparable with established ruthenium(III) polyaminocarboxylates in an *in vitro* assay.

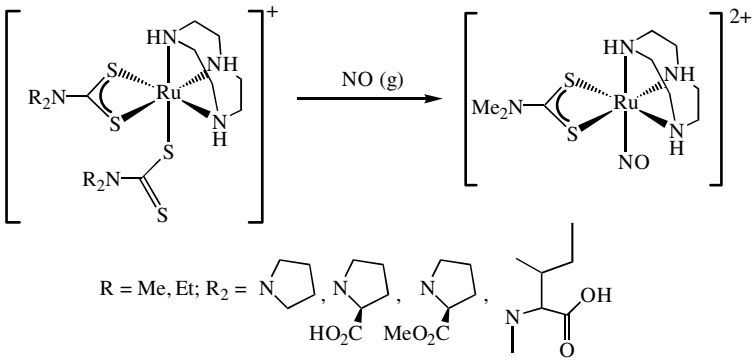

(120)

Toma and co-workers (1337) reported the synthesis of red $Na_2[Ru(edta)(S_2CNEt_2)].2H_2O$ (edta = ethylenediaminetetraacetic acid) from the metathesis of $[Ru(Hedta)(H_2O)]$ and NaS_2CNEt_2 in a minimum amount of water; a reaction proposed to proceed via a monodentate dithiocarbamate intermediate. The ruthenium(III) dithiocarbamate complex undergoes a reversible one-electron reduction. The process has been monitored by spectroelectrochemistry; the reduced species exhibiting a broad absorption band at 438 nm, being assigned to a charge transfer from the filled ruthenium $d\pi$ orbitals to the π^* orbital of edta.

Baird et al. (1338) prepared ruthenium(III) bis(β-diketonate) complexes, $[Ru\{OC(R')CHC(R')O\}_2(S_2CNMe_2)]$ (R′ = Me, Ph), together with others in which the dithiocarbamate is derived from an amino acid (L-proline, L-isoleucine). They are derived from $[Ru\{OC(R')CHC(R')O\}_2(MeCN)_2][CF_3SO_3]$ upon addition of dithiocarbamate salts in air. When the reactions with NaS_2CNMe_2 were carried out under argon, the thiuram disulfide was detected, suggesting that it proceeds via an electron-transfer process. Further, reactions were not clean and in some instances a second product was isolated as a result of carbon disulfide loss. For example, addition of proline (prol-H_2) derived dithiocarbamate to $[Ru(acac)_2(MeCN)_2][CF_3SO_3]$ afforded both the expected dithiocarbamate product $[Ru(acac)_2(S_2Cprol)]$ (**266**), together with a chelated imino prolinato complex, $[Ru(acac)_2(prol\text{-}H_2)]$ (**267**) (Eq. 121). Further work suggests that once the dithiocarbamate is chelated to the ruthenium(III) center it does not undergo carbon disulfide loss, the precise mode of its formation remaining unknown.

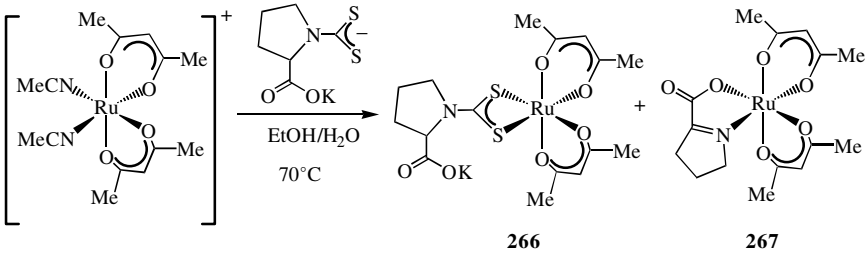

266 **267**

(121)

By utilizing $[Ru(NO)Cl_3]$ as a starting material, Dubrawski and Feltham (232) prepared a range of ruthenium(III) nitrosyl complexes, including; *trans*-$[RuCl(NO)(S_2CNR_2)_2]$, *trans*-$[RuX(NO)(S_2CNMe_2)_2]$ (X = F, Br, I, NO_2), *cis*-$[RuX(NO)(S_2CNEtR)_2]$ (X = Br, I; R = Me, Et), *cis*- and *trans*-$[RuX(NO)(S_2CNMe_2)_2]$ (X = N_3, SCN, NCO), *trans*-$[Ru(OH)(NO)(S_2CNMe_2)_2]$, and *trans*-$[RuL(NO)(S_2CNMe_2)_2]$ (L = H_2O, MeOH). The trans-isomers are generally thermodynamically favored. For example, the conversion of kinetically formed *cis*-$[RuX(NO)(S_2CNMe_2)_2]$ (X = N_3, NCO, NCS) to the

trans-isomer occurs upon heating (Eq. 122).

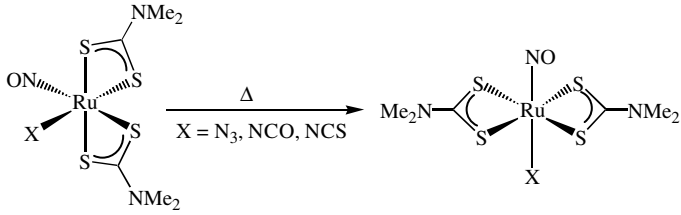

(122)

The same workers have also carried out VT NMR experiments on the known tris(dithiocarbamate) complex *cis*-[Ru(NO)(η^1-S_2CNMe_2)(S_2CNMe_2)$_2$], which is prepared upon addition of NO to [Ru(S_2CNMe_2)$_3$] or excess NaS_2CNMe_2 to ruthenium nitrosyl trichloride. In the solid state, two of the dithiocarbamates are bidentate and the third unidentate. The NMR studies show that the latter has a lower barrier to rotation ($\sim$ 59 kJ mol^{-1}) about the carbon–nitrogen bond than the bidentate ligands, and that there is no exchange between the two over the temperature range studied (−40–150°C) (232).

The known seven-coordinate ruthenium(IV) complex [RuCl(S_2CNEt_2)$_3$] (1339) has been the subject of an electrochemical and reactivity study (1334). Dissolution in acetonitrile affords the ionic complex [Ru(MeCN)(S_2CNEt_2)$_3$]Cl; the weakly bound solvent molecule being readily displaced by PPh_3 to give [Ru(PPh_3)(S_2CNEt_2)$_3$]Cl, which is isolated as a BF_4 salt (Fig. 157).

A further ruthenium(IV) complex, [Ru(η^2-TsN–N=N-NTs)(S_2CNEt_2)$_2$] (**270**), has been prepared in 35% yield from the reaction of excess tosylazide and *cis*-[Ru(PPh_3)$_2$(S_2CNEt_2)$_2$] (**268**) (287). The structure is confirmed crystallographically and the authors speculate that it results from initial formation of a ruthenium(IV) imido complex, [Ru(NTs)(S_2CNEt_2)$_2$] (**269**), which reacts further with a second equivalent of azide (Eq. 123).

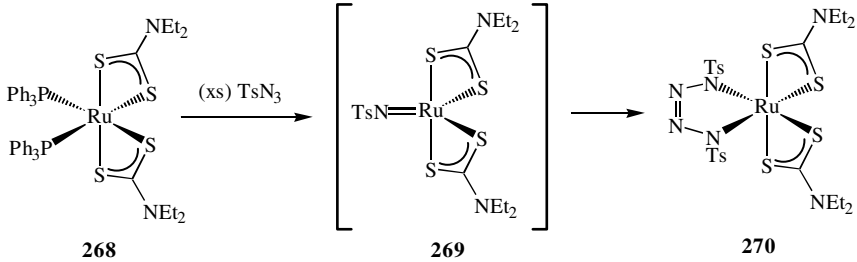

268 **269** **270**

(123)

Osmium tris(dithiocarbamate) complexes [Os(S_2CNR_2)$_3$] were only authentically detailed in the early 1980s (295,296). They can be prepared upon addition

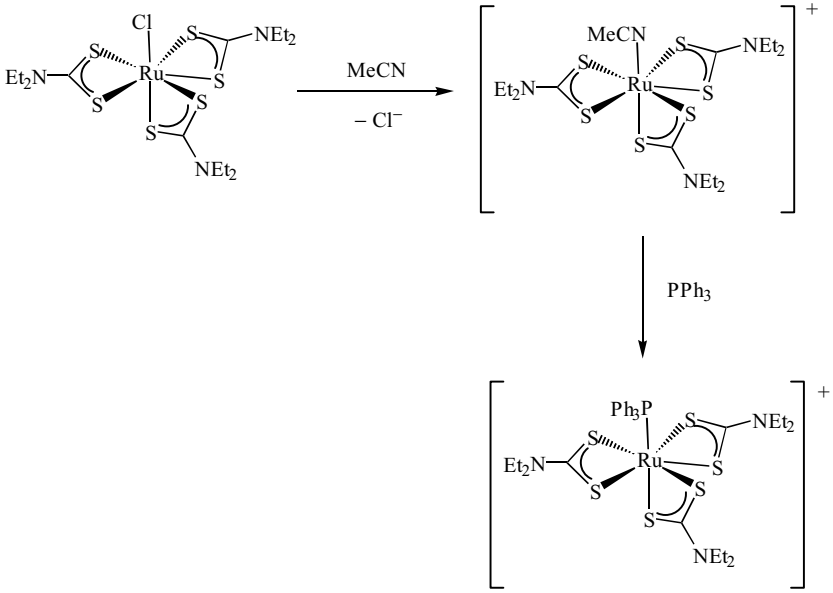

Figure 157. Formation of $[Ru(MeCN)(S_2CNEt_2)_3]^+$ and subsequent reaction with PPh_3.

of an excess of dithiocarbamate salt to $[OsCl_6]^{2-}$ in aqueous methanol (R = Me, Et, Bz; R_2 = MePh) [295, 1331, 1340]. A number of reports suggest that this synthetic method yields diamagnetic osmium(IV) complexes, $[Os(S_2CNR_2)_4]$, although this seems unlikely (1329–1333). Preti et al. (1340) reported the preparation of a series of red-brown complexes, $[Os(S_2CNC_4H_8X)_3]$ (X = O, S, NMe, CH_2), via this method. In contrast, the room temperature reaction between the same dithiocarbamate salts and $OsCl_3$ in water is postulated to yield diamagnetic osmium(II) complexes, $[Os(S_2CNC_4H_8X)_2(H_2O)_2]$; although no further work appears to have been carried out in this area.

Variable temperature NMR studies have shown that tris(dithiocarbamate) complexes are stereochemically nonrigid. A trigonal-twist mechanism is proposed, activation parameters being similar to those found in ruthenium analogues (295). Addition of BF_3 to $[Os(S_2CNEt_2)_3]$ in the presence of $[Et_4N][PF_6]$ for 30 s yields the purple oxidation product $[Os(S_2CNEt_2)_3][PF_6]$ (μ_{eff} 1.4 BM), which reacts rapidly with chloride or acetonitrile giving $[OsCl(S_2CNEt_2)_3]$ and $[Os(MeCN)(S_2CNEt_2)_3]^+$, respectively. The former is partially dissociated into $[Os(S_2CNEt_2)_3]Cl$ in propylene carbonate solution (296). Further, in the free state and even at low temperature, the purple color of $[Os(S_2CNEt_2)_3]^+$ is slowly

replaced by the orange-brown of dimeric $[Os_2(S_2CNEt_2)_4(\mu\text{-}S_2CNEt_2)_2]^{2+}$ (Eq. 124). The latter has been crystallographically characterized, the structure consisting of dimers of $[Os(S_2CNEt_2)_3]^+$, with each osmium adopting a distorted bipyramidal coordination geometry. The osmium–osmium distance of 3.682(1) Å indicates the lack of a direct osmium–osmium interaction.

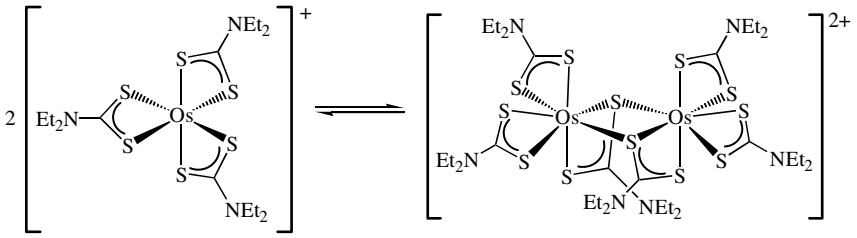

(124)

b. Divalent Mononuclear Complexes. By far, the most common oxidation state for dithiocarbamate complexes of both ruthenium and osmium is +2, and carbon monoxide is often a coligand. Mono(dithiocarbamate) complexes of ruthenium(II) include; the 2-pyrrolyl complex, $[Ru(CO)(PPh_3)\{\eta^2\text{-}O{=}S(O)PhNC_4H_3\}(S_2CNMe_2)]$ (**271**) (1341), and hydrides $[RuH(CO)(PPh_3)\text{-}L(S_2CNR_2)]$($L = PPh_3$, py, piperidine, 4-morphylene; $R_2 = C_4H_4$, C_5H_{10}, C_4H_8O) (1342–1344).

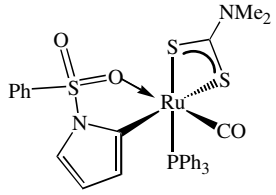

271

The reactivity of a number of these hydrides has been assessed. Addition of hydrogen sulfide to *trans*-$[RuH(CO)(PPh_3)_2(S_2CNMe_2)]$ (**272**) at 50°C yields *trans*-$[Ru(SH)(CO)(PPh_3)_2(S_2CNMe_2)]$ (**273**) (Fig. 158). It has been characterized crystallographically and is also shown to undergo irreversible one-electron oxidation and reduction by cyclic voltammetry (1345). Reaction of *trans*-$[RuH(CO)(PPh_3)_2(S_2CNEt_2)]$ with tosylazides gives amide complexes *cis*-$[Ru(CO)(PPh_3)_2(NHSO_2Ar)(S_2CNMe_2)]$ ($Ar = p$-tol, $p\text{-}C_6H_4\text{-}t\text{-}Bu$, 2,4,6-$Pr_3\text{-}i\text{-}C_6H_2$) (**274**) (Fig. 158) (292), carbonylation of which yields $[Ru(CO)_2(PPh_3)$

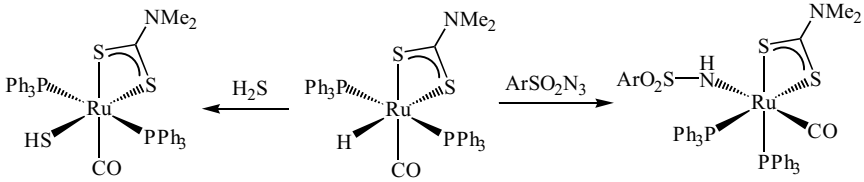

Figure 158. Selected reactions of *trans*-[RuH(CO)$(PPh_3)_2(S_2CNMe_2)$].

$(NHSO_2Ar)(S_2CNMe_2)]$ (Ar = *p*-C_6H_4-*t*-Bu), while addition of HCl gives $[RuCl(CO)(PPh_3)_2(S_2CNEt_2)]$.

Leung and co-workers (1346) showed that addition of triflic acid to *cis*-$[RuH(CO)(PPh_3)_2(S_2CNEt_2)]$ (**275**) gives *cis*-$[Ru(OTf)(CO)(PPh_3)_2(S_2CNEt_2)]$ (**276**), the triflate (Tf) ligand of which is readily replaced (Fig. 159). For example, amines react to give *trans*-$[RuL(CO)(PPh_3)_2(S_2CNEt_2)]$ (L = NH_2OH,

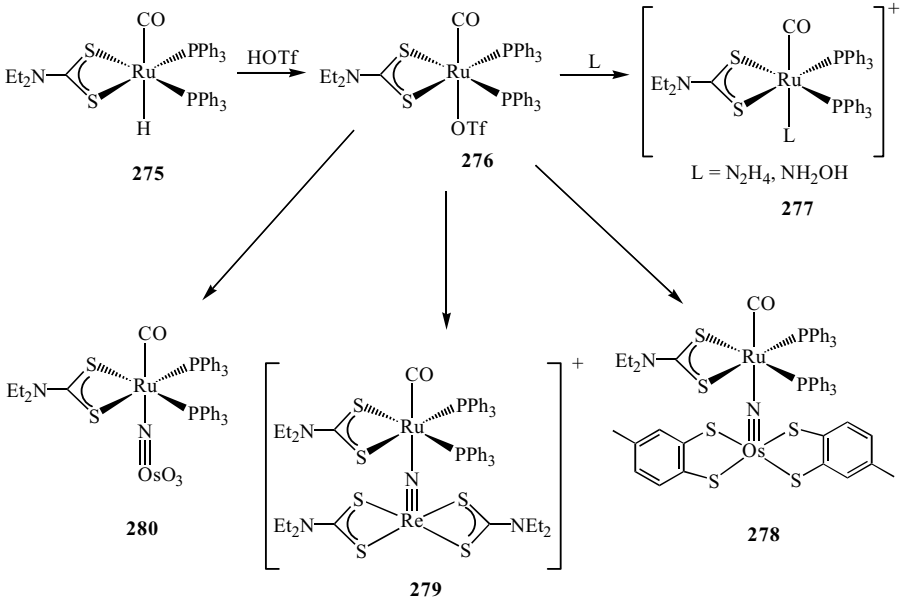

Figure 159. Synthesis and reactivity of *cis*-$[Ru(OTf)(CO)(PPh_3)_2(S_2CNEt_2)]$.

N_2H_4) (**277**). Most interestingly, addition of metal nitrides yields heterobimetallic μ-nitride complexes, *trans*-[Ru(CO)$(PPh_3)_2(S_2CNEt_2)$(μ-N)ML_n] [ML_n = OsO_3, $Os(S_2C_7H_6)_2$, $Re(S_2CNEt_2)_2^+$] (**278–280**). An analysis of bond lengths and angles from crystallographic studies suggest that they are best represented as M≡N→Ru(II) (1346). A further heterobimetallic nitride complex, [Ru(CO)-$(PPh_3)(H_2O)(S_2CNEt_2)$(μ-N)ML_n] (ML_n = ReCl$(PPh_3)\{PO(OEt)_2\}_3$CoCp), has also been reported by the same group (1347).

Robinson and co-workers (1348) showed that bis(dithiocarbamate) complexes [$M(S_2CNEt_2)_2$] (M = Zn, Cd, Hg, Pb) react with *cis*-[$RuCl_2(dppm)_2$] in refluxing acetonitrile to give high yields of salts of the form [$Ru(S_2C-NEt_2)(dppm)_2]_2[MCl_4$] (**281**) (Fig. 160), while [$Ru(S_2CNEt_2)(PPh_3)_2(\eta^2$-taiMe)][$ClO_4$] (taiMe = 1-methyl-2-*p*-tolylazoimidazole) (**282**) (Fig. 160) has been prepared from [$RuCl_2(PPh_3)_2(\eta^2$-taiMe)], NaS_2CNEt_2, and silver chloride upon addition of sodium perchlorate (1349).

A number of ionic complexes containing bidentate nitrogen donor ligands have been prepared. For example, [$RuL_2(S_2CNR_2)$][ClO_4] (L_2 = 2,2′-bpy, 1,10-phen; R = Et, Pr), result from addition of dithiocarbamate salts to [$RuCl_2L_2$] in the presence of silver perchlorate (1350). They undergo a reversible one-electron oxidation generating analogous ruthenium(III) complexes, however, a further one-electron oxidation that gives a ruthenium(IV) species is irreversible. Related functionalized bpy complexes, [Ru(dcbH)$(dcbH_2)(S_2CNR_2)$] (dcbH = 4-CO_2H-4′-CO_2-2,2′bpy; R = Et, Bz; $R_2 = C_4H_8$), have also been prepared and shown to be efficient in the conversion of light to electrical energy (see Section IV.E.2.e) (1351).

Del Zotto et al. (1352) prepared the octahedral ruthenium(II) cation $[Ru(Ph_2PCH_2CH_2py)_2(S_2CNMe_2)]^+$, which exists as an equilibrium mixture of two isomers, the trans-isomer being initially generated slowly equilibrating

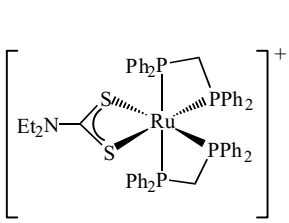

281

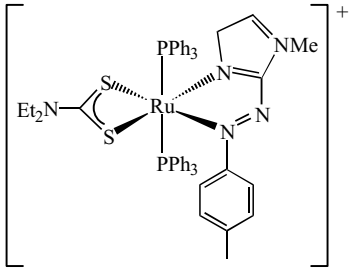

282

Figure 160. Examples of cationic ruthenium(II) dithiocarbamate complexes.

with the cis-isomer, as monitored by ^{31}P NMR spectroscopy (Eq. 125).

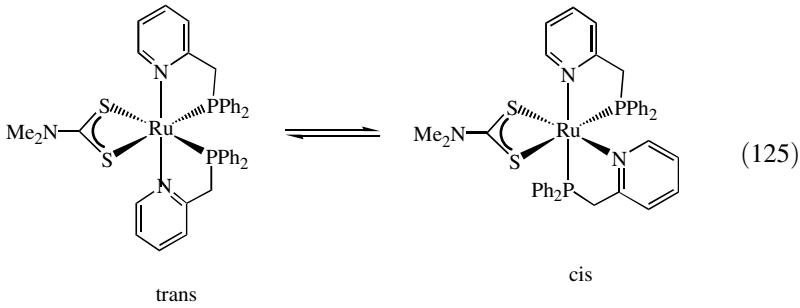

(125)

Roper co-workers prepared a series of ruthenium and osmium(II) dithiocarbamate complexes bearing chelating monoanionic metalated multiaromatic ligands (LX). These include $[M(CO)(PPh_3)(\eta^2\text{-LX})(S_2CNMe_2)]$ (Fig. 161) (1353,1354) and trans-$[Os(CO)(PPh_3)_2(\eta^1\text{-8-quinolinyl})(S_2CNMe_2)]$ (1355).

The same group also prepared osmium(II) boryl and stannyl complexes *trans*-$[Os(CO)(PPh_3)_2(Bcat)(S_2CNEt_2)]$ (Bcat = pyrocatecholatoboryl) (1356) and *trans*-$[Os(CO)(PPh_3)_2(SnMe_3)(S_2CNMe_2)]$ (1357,1358), respectively. A crystal structure of the former reveals the strong trans-influence of the boryl ligand, the osmium–sulfur interaction being lengthened by 0.05 Å. Reaction of trans-$[Os(CO)(PPh_3)_2(SnMe_3)(S_2CNMe_2)]$ with SnI_4 affords *trans*-$[Os(CO)(PPh_3)_2(SnMeI_2)(S_2CNMe_2)]$ which is transformed into *trans*-$[Os(CO)(PPh_3)_2(SnI_3)(S_2CNMe_2)]$ (**283**) (Fig. 162) upon addition of iodine. Both of these complexes undergo facile nucleophilic substitution at the tin(IV) center affording a wide range of functionalized osmium–tin complexes. These include *trans*-$[Os(CO)(PPh_3)_2\{Sn(OH)_3\}(S_2CNMe_2)]$ (**284**) and the first stannatrane complex, *trans*-$[Os(CO)(PPh_3)_2\{Sn(OCH_2CH_2)_3N\}(S_2CNMe_2)]$ (**285**) (Fig. 162) (1357). In the latter, there is a dative tin–nitrogen interaction as shown by X-ray crystallography. In the analogous silatrane complex, a silicon–nitrogen interaction is almost totally absent, reflecting the greater ability of tin to form hypervalent complexes.

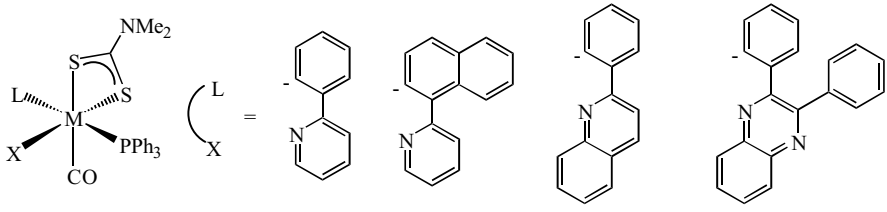

Figure 161. Ruthenium and osmium(II) dithiocarbamate complexes bearing chelating LX-type ligands.

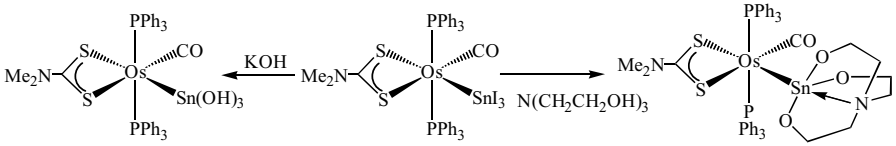

Figure 162. Selected reactions of *trans*-[Os(CO)(PPh_3)$_2$(SnI_3)(S_2CNMe_2)].

A number of bis(dithiocarbamate) ruthenium(II) complexes have been reported. Heating thiuram disulfides with [$Ru_3(CO)_{12}$] in heptane yields *cis*-[$Ru(CO)_2(S_2CNR_2)_2$] (R = Me, Et) (169, 1359). Other routes have also been reported to these cis dicarbonyl complexes. For example, addition of 2 equiv of dithiocarbamate salt to [$Ru_2(CO)_4(MeCN)_6$][BF_4]$_2$, [$Ru_2(CO)_4(\mu\text{-}O_2CMe)_2(\text{-}MeCN)_2$] (1360), or [$Ru(CO)_2Cl_2$]$_n$ (169), while an earlier preparation involves addition of NaS_2CNMe_2 to *cis*-[$RuCl_2(CO)_2(PPh_3)_2$] (1361).

Crystal structures of both *cis*-[$Ru(CO)_2(S_2CNR_2)_2$] (R = Me, Et) (169,1360) and *cis*-[$Ru(CO)_2(S_2CNMe_2)_2$].0.5I_2 (287) have been carried out; all revealing the expected distorted octahedral coordination environment. The iodine in the latter shows no significant intermolecular interactions with the ruthenium complex, suggesting that there is little charge transfer. In accord with this, carbonyl stretching frequencies (2026 and 1956 cm^{-1}) are virtually identical to those in the free complex (2028 and 1952 cm^{-1}) (287).

When NaS_2CNMe_2 was added to [$Ru_2(CO)_4(MeCN)_6$][BF_4]$_2$, a mixture of *cis*-[$Ru(CO)_2(S_2CNMe_2)_2$] and [$Ru(CO)(S_2CNMe_2)(\mu\text{-}S_2CNMe_2)$]$_2$ resulted (1360). The latter has been characterized crystallographically. It shows two trans disposed chelating dithiocarbamate ligands as opposed to their cis disposition in [$Ru(CO)_2(S_2CNMe_2)_2$], while carbon–nitrogen distances in the backbone of the dithiocarbamate ligands do not vary significantly between the two. A rational synthesis of dimeric [$Ru(CO)(S_2CNR_2)(\mu\text{-}S_2CNR_2)$]$_2$ (R = Me, Et) (**286**) involves decarbonylation of *cis*-[$Ru(CO)_2(S_2CNR_2)_2$] (**287**) by trimethylamine *N*-oxide (Fig. 163). The dimer can be cleaved by neural two-electron donor ligands; for example, *cis*-[$Ru(CO)_2(S_2CNMe_2)_2$] reacts with benzyl isocyanide at room temperature to give *cis*-[$Ru(CO)(CNBz)(S_2\text{-}CNMe_2)_2$] (**288**) (Fig. 163).

Critchlow and Robinson (1343) prepared a mixed-carbonyl–phosphine complex *cis*-[$Ru(CO)(PPh_3)(S_2CNMe_2)_2$] by a different route, namely, upon addition of 2 equiv of dithiocarbamate salt to [$Ru(NO_3)_2(CO)(PPh_3)_2$]. Further, all *trans*-[$RuCl_2(CO)_2(PEt_3)_2$] (**289**) affords *cis*-[$Ru(CO)(PEt_3)(S_2CNR_2)_2$] (R = Me, Et) (**291**) in a similar process, which proceeds via *trans*-[$RuCl(CO)(PEt_3)_2(S_2CNR_2)$] (**290**) (Fig. 164), successive addition of NaS_2CNEt_2 and NaS_2CNMe_2 yielding *cis*-[$Ru(CO)(PEt_3)(S_2CNMe_2)(S_2CNEt_2)$]. The latter

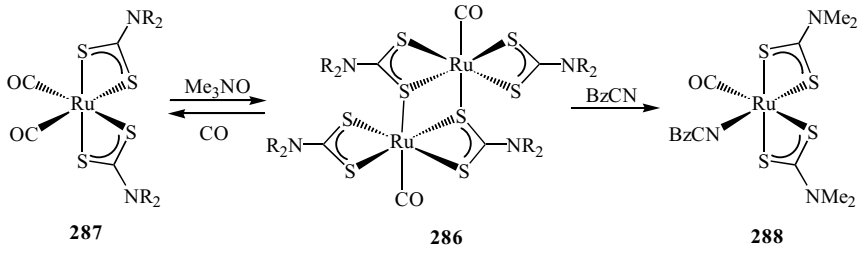

Figure 163. Selected reactions of $[Ru(CO)(S_2CNR_2)(\mu\text{-}S_2CNR_2)]_2$.

exists as two noninterconverting isomers (~1:1 ratio) in solution (169). A crystallographic study of *cis*-$[Ru(CO)(PEt_3)(S_2CNMe_2)_2]$ reveals little variation from the analogous dicarbonyl complex.

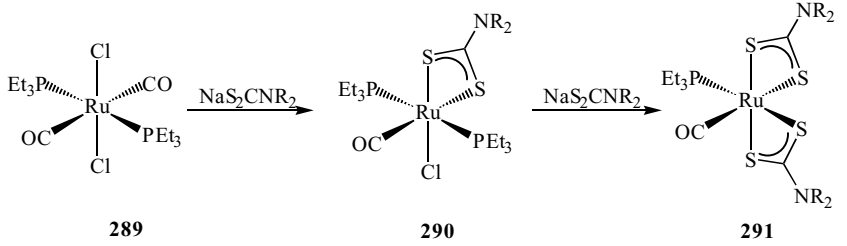

Figure 164. Stepwise formation of *cis*-$[Ru(CO)(PEt_3)(S_2CNR_2)_2]$ from all *trans*-$[RuCl_2(CO)_2(PEt_3)_2]$.

A number of other ruthenium(II) bis(dithiocarbamate) have been reported. Addition of NaS_2CNEt_2 to $[RuCl_2(diene)]_n$ (diene = cod, NBD) affords *cis*-$[Ru(diene)(S_2CNEt_2)_2]$, while reaction of CN—*t*-Bu with *cis*-$[Ru(Me_2SO)_2(S_2CNEt_2)_2]$ gives *trans*-$[Ru(CN—t\text{-}Bu)_2(S_2CNEt_2)_2]$ (Eq. 126) (287). Oxidation potentials of all these species have been determined by cyclic voltammetry and compared with that for *cis*-$[Ru(PPh_3)_2(S_2CNEt_2)_2]$ (1362). Data suggest that the ability to stabilize the Ru(II) state decreases in the order; DMSO > CN—*t*-Bu ~ NBD > PPh_3 [287]. In other work, addition of 2 equiv of dithiocarbamate salt to [CpRuCl(dppe)] has been shown to give $[Ru(dppe)(S_2CNEt_2)_2]$ resulting from loss of the cyclopentadienyl ligand (1363).

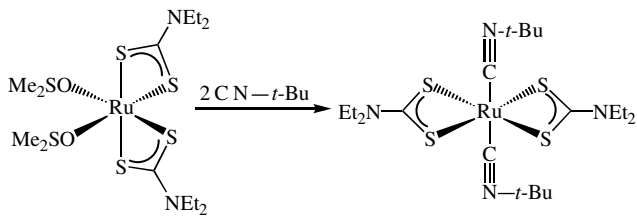

(126)

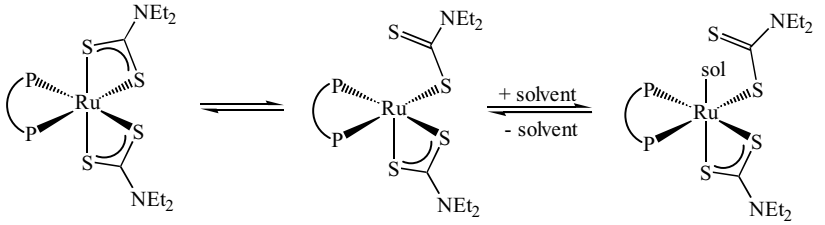

Figure 165. Proposed interconversion of five- and six-coordinate species in $[Ru(dppf)(S_2CNEt_2)_2]$.

A further diphosphine complex, $[Ru(dppf)(S_2CNEt_2)_2]$ (dppf = 1,1′-bis(diphenylphosphino)ferrocene), has been prepared in high yields upon addition of the diphosphine to *cis*-$[Ru(PPh_3)_2(S_2CNEt_2)_2]$ (1364). The NMR spectra are temperature dependent being associated with a fluxional process that results from dechelation of one of the dithiocarbamates, and the authors suggest that at low temperatures in chloroform, the molecule exists completely in a form with one monodentate dithiocarbamate ligand (Fig. 165).

In an early report, the synthesis of a number of ruthenium(II) bis(aqua) complexes, $[Ru(S_2CNC_4H_8X)_2(H_2O)_2]$ (X = O, S, NMe, CH_2), was claimed. Heating $RuCl_3.3H_2O$ in ethanol for 1 day, followed by addition of 2 equiv of dithiocarbamate salts was reported to yield a series of diamagnetic complexes, characterized by ν(C=N) vibrations between 1470 and 1481 cm^{-1} in the IR spectrum, while in one instance, the proposed product $[Ru(S_2CNC_4H_8NH)_2]$ did not contain coordinated water (1365). In the same contribution, 3 equiv of dithiocarbamate reportedly react with $RuCl_3.3H_2O$ at room temperature to yield brown, paramagnetic, ruthenium(I) complexes, $[Ru(S_2CNC_4H_8X)]$ [ν(C=N) 1480–1495 cm^{-1}]. Magnetic moments of 0.6–1.4 BM are very low, which the authors suggest may be due to an exchange interaction between neighboring d^7 ions in a polymeric structure, the latter resulting from heteroatom coordination to ruthenium. No further work appears to have been carried out in this area and thus the authenticity of this report and the structural types remain unclear.

Chakravorty and co-workers (1362,1366) studied bis(dithiocarbamate) complexes, *cis*-$[M(PPh_3)_2(S_2CNEt_2)_2]$ (M = Ru, Os). Addition of 2 equiv of NaS_2CNEt_2 to $[OsBr_2(PPh_3)_3]$ affords the known complex *cis*-$[Os(PPh_3)_2(S_2CNEt_2)_2]$ (**292**). This complex is oxidized by cerium(IV) to the osmium(III) complex *trans*-$[Os(PPh_3)_2(S_2CNEt_2)_2]^+$ (**293**), which is in turn reduced by hydrazine to *trans*-$[Os(PPh_3)_2(S_2CNEt_2)_2]$ (**294**) (Fig. 166). As *cis*-$[Os(PPh_3)_2(S_2CNEt_2)_2]^+$ is never seen, the authors suggest that upon oxidation, isomerization must be rapid (1366). Related redox chemistry has also been studied at the ruthenium center, being quantitatively similar to that described above (1362). All three osmium complexes have been crystallographically characterized and show a progressive decrease in the osmium–phosphorus

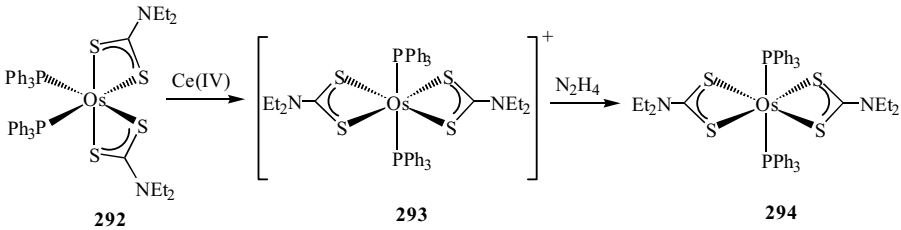

Figure 166. Conversion of *cis*-[Os(PPh$_3$)$_2$(S$_2$CNEt$_2$)$_2$] to the trans isomer via successive oxidation and reduction.

bond lengths; *trans*-[Os(PPh$_3$)$_2$(S$_2$CNEt$_2$)$_2$]$^+$ > *trans*-[Os(PPh$_3$)$_2$(S$_2$CNEt$_2$)$_2$] > *cis*-[Os(PPh$_3$)$_2$(S$_2$CNEt$_2$)$_2$]. The total range is 0.15 Å and the lengthening correlates with the decreasing 5*d*π–3*d*π back-bonding.

A number of cyclopentadienyl and tris(pyrazolyl)borate complexes have been reported. Cyclopentadienyl complexes, [CpRu(PR$'_3$)(S$_2$CNR$_2$)] (**295**) (Fig. 167), are easily prepared from [CpRuCl(PR$'_3$)$_2$] and the relevant dithiocarbamate salt (104,234,1367–1369); related complexes [CpRu(SbPh$_3$)(S$_2$C-NEt$_2$)] (1370), and [CpOs(PPh$_3$)(S$_2$NC$_4$H$_8$)] (1371) being prepared in an analogous fashion. Addition of 2 equiv of [CpRuCl(PPh$_3$)$_2$] to homopiperazine in the presence of carbon disulfide and excess base yields [(CpRuPPh$_3$)$_2$(μ-S$_2$CNC$_5$H$_{10}$NCS$_2$)] (**296**) (Fig. 167), while with 1,4,7-triazacyclononane, NMR evidence supports the formation of a triruthenium complex (104).

A number of crystallographic studies have been carried out including [CpRu(PPh$_3$)(S$_2$CNPr$_2$)] (104) and [CpRu(PPh$_3$)(S$_2$CNMe$_2$)] (1369, 1372). Two polymorphs of the latter have been characterized, and show only minimal differences. In one instance, following this route leads to a monodentate dithiocarbamate complex. Thus, heating [CpRuCl(PEt$_3$)$_2$] with NaS$_2$CNEt$_2$ in acetone yields [CpRu(PEt$_3$)$_2$(η^1-S$_2$CNEt$_2$)] (**297**), while under similar conditions analogous complexes with bulkier cyclopentadienyl or phosphine ligands yield only bidentate dithiocarbamate complexes (234). While IR spectra of both monodentate and bidentate complexes show characteristic ν(CS) and ν(CN) bands, they are too similar to allow unequivocal distinction between η^1- and η^2-coordination. Related xanthate complexes are easily distinguished by ^{13}C NMR

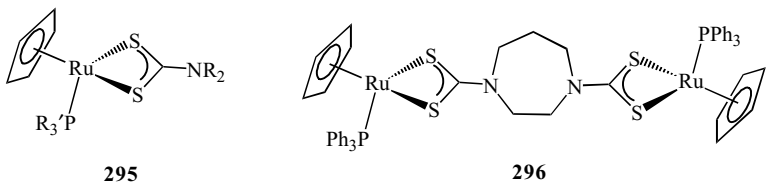

Figure 167. Examples of complexes of the type [CpRu(PR$'_3$)(S$_2$CNR$_2$)].

spectroscopy, the central carbon resonance appearing as virtual triplet or doublet resonance, respectively. For dithiocarbamate complexes, however, this is not always observed and is attributed to the effect of the quadrupolar ^{14}N nucleus (217,234).

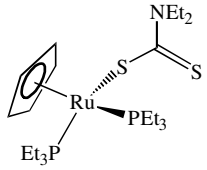

297

Takahashi and co-workers (1373) prepared the 1,3,5-trisubstituted cyclopentadienyl complex [{η^5-C_5H_2-1-Me-3-Ph-5-C(O)$OCH_2CH_2PPh_2$}Ru(S_2CNMe_2)] (**298**) (Fig. 168), with a pendant phosphine moiety. The dithiocarbamate lies in a chiral environment constructed by the substituents on the cyclopentadienyl ligand and the phenyl groups bound to phosphorus. In another interesting report, Shaver and co-workers (217) give details of the synthesis of dithiocarbamate complexes [CpRu(PPh_3)($S_2CNR^1R^2$)] (R^1 = Si—*i*-Pr_3, R^2 = Ph, *p*-tol, 1-naphth; R^1 = H, R^2 = Ph, 1-naphth), formed upon insertion of arylisothiocyanates into the ruthenium–sulfur bonds of [CpRu(PPh_3)$_2$(SSi—*i*-Pr_3)] and [CpRu(PPh_3)$_2$(-SH)], respectively. With the former, reactions are believed to proceed via precoordination of the isothiocyanate to ruthenium, while with the latter, direct nucleophilic insertion is proposed. In support of this, [CpRu(dppe)(SSi—*i*-Pr_3)] does not react with isothiocyanates, while [CpRu(dppe)(SH)] does, giving monodentate products, [CpRu(dppe)(η^1-S_2CNHR)] (R = Ph, 1-naphth); a reaction that is reversible in one case (R = 1-naphth). A further development reported in this paper is the reaction of 1,4-phenylenediisothiocyanate with 2 equiv of [CpRu(PPh_3)$_2$(SH)] leading to a dithiocarbamate-bridged product 1,4-[{CpRu(PPh_3)}$_2$(μ-$S_2CNHC_6H_4NHCS_2$)] (**299**) (Fig. 168), which has been crystallographically characterized.

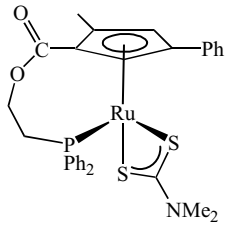

298

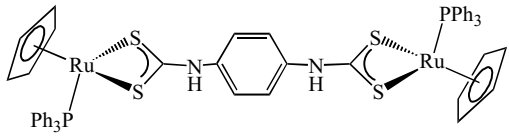

299

Figure 168. Further examples of complexes of the type [CpRu(PR'_3)(S_2CNR_2)].

In two cases, the cyclopentadienyl ligand is lost upon addition of dithiocarbamate salts. As previously noted, addition of 2 equiv of NaS_2CNEt_2 to [CpRuCl(dppe)] affords *cis*-[Ru(dppe)(S_2CNEt_2)$_2$] (1363), while the same reaction with [(η^5-C_5H_4OMe)RuCl(PPh_3)$_2$] in refluxing methanol gives *cis*-[Ru(PPh_3)$_2$(S_2CNEt_2)$_2$] (1368). The latter is particularly interesting as analogous cyclopentadienyl and methylcyclopentadienyl ligands are not removed in a similar manner. Cyclopentadienyl loss can be reversed. Thus, reaction of *cis*-[Ru(PPh_3)$_2$($S_2CNC_4H_8$)$_2$] with thallium cyclopentadienide affords another route to [CpRu(PPh_3)($S_2CNC_4H_8$)] (1368). Few reactions of these complexes have been carried out, although [CpRu(PPh_3)(S_2CNPr_2)] has been shown to react with [$Ru_3(CO)_{12}$] to give the related carbonyl complex [CpRu(CO)(S_2CNPr_2)] (169).

Two groups have independently prepared the tris(pyrazolyl)borate complex [TpRu(PPh_3)(S_2CNMe_2)] from [TpRuCl(PPh_3)$_2$] and dithiocarbamate salt (1374,1375); a crystallographic study revealing the expected distorted octahedral coordination sphere (1374). Similarly, [TpRu(CO)(S_2CNR_2)] (R = Me, Et) have been prepared from [TpRuI(CO)(MeCN)] and the relevant dithiocarbamate salt (1376).

c. Binuclear Complexes. A wide range of binuclear ruthenium dithiocarbamate complexes are known, many with bridging dithiocarbamate ligands (287–292). The ruthenium(II) dimer [$Ru_2I(CO)_2(PPh_3)_2(S_2CNEt_2)$(μ-I)(μ-$S_2CNEt_2$)] (**300**) (Fig. 169) is the product of iodine addition to [Ru(CO)-(PPh_3)$_2$($NHSO_2Ar$)(S_2CNEt_2)] (Ar = 2,4,6-*i*-$Pr_3C_6H_2$) (292). It has been crystallographically characterized and possibly results via the initial formation of [RuI(CO)(PPh_3)(S_2CNEt_2)], followed by dimerization. Since it adopts both terminal and bridging iodide and dithiocarbamate ligands, this suggests these ligands have similar bridging capabilities. A second dimeric ruthenium(II) complex, [Ru([9]aneS_3)(μ-S_2CNMe_2)]$_2^{2+}$, has been prepared upon addition of 2 equiv of NaS_2CNMe_2 to [Ru([9]aneS_3)$(MeCN)_3]^{2+}$ (**301**) (Fig. 169) (289). A crystallographic study reveals quite different carbon–sulfur bonds in the

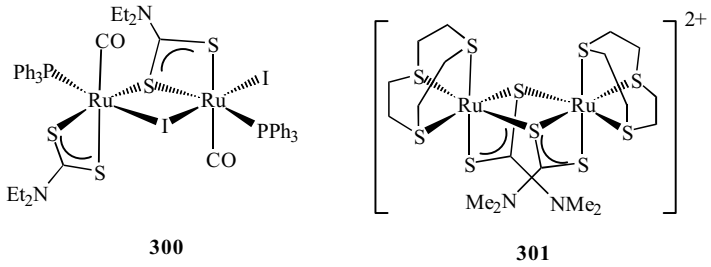

300 **301**

Figure 169. Selected examples of diruthenium complexes with bridging dithiocarbamate ligands.

four-membered S—C—S-Ru rings [C-μ-S 1.773(5), C-η^1-S 1.703(3) Å] indicative of pronounced strain.

Heating elemental sulfur and $[RuH(CO)(PPh_3)_2(S_2CNMe_2)]$ for prolonged periods yields $[Ru_2(CO)_2(PPh_3)_2(S_2CNMe_2)(\mu\text{-}S_{2+n})(\mu\text{-}S_2CNMe_2)]$ ($n = 3, 4$), shown to contain a mixture bridging S_5 and S_6 ligands in an $\sim$ 4:1 ratio (291). Further reactions of this mixture with amines have been studied (290). In all cases the bridging dithiocarbamate ligand converts to a terminal coordination mode upon amine binding. With ammonia, a reversible reaction occurs generating $[\{Ru(CO)(PPh_3)(NH_3)(S_2CNMe_2)\}_2(\mu\text{-}S_6)]$ (Eq. 127), while with pyridine, the pentasulfide displays similar behavior. In contrast, addition of hydrazine forms $[\{Ru(CO)(PPh_3)(S_2CNMe_2)\}_2(\mu\text{-}S_4)(\mu\text{-}N_2H_4)]$ irreversibly.

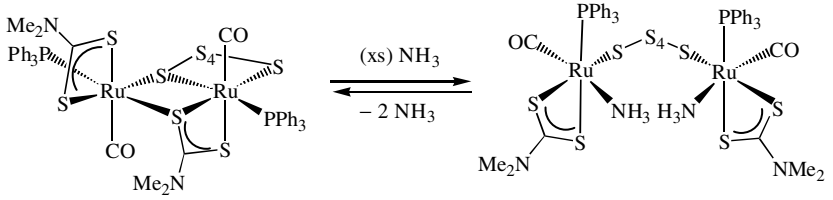

(127)

Mixed-valence ruthenium(II)–ruthenium(III) complexes have been prepared. Controlled-potential oxidation of the ruthenium(II) dimer $[Ru(CO)(S_2CNEt_2)(\mu\text{-}S_2CNEt_2)]_2$, in which each ruthenium carries one carbonyl, yields $[Ru(CO)(S_2CNEt_2)(\mu\text{-}S_2CNEt_2)]_2^+$ (Eq. 128), whereby both carbonyls are bound in a cis fashion to a single metal center (288). The molecule contains a long ruthenium–ruthenium interaction [Ru–Ru 3.614(1) Å] and the sulfurs bridge approximately symmetrically. The authors were not able to determine if the molecule contained separate ruthenium(II) and ruthenium(III) centers or a delocalized state.

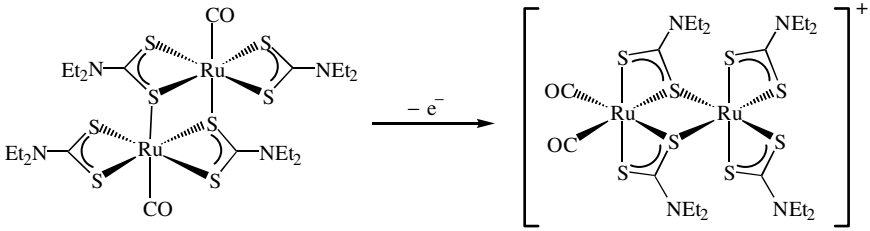

(128)

In contrast, oxidation of *cis*-$[Ru(dmso)_2(S_2CNEt_2)_2]$ by iodine generates trinuclear $[Ru_3(dmso)_2(S_2CNEt_2)_2(\mu\text{-}S_2CNEt_2)_4][I_3]_2$ (Eq. 129), which contains

two ruthenium(III) centers in close proximity [Ru—Ru 2.826(2) Å] and single ruthenium(III) center, which is not metal–metal bonded (287).

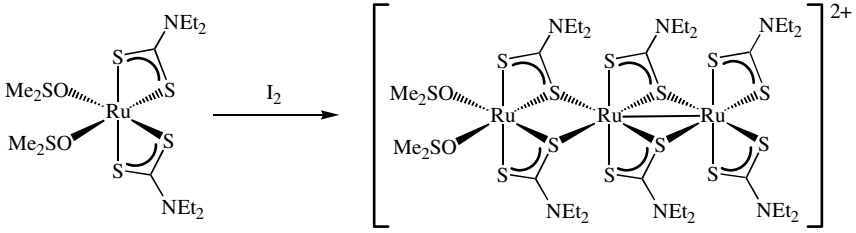

(129)

As early as 1966, Wilkinson and co-worker (293) reported that oxidation of $[Ru(S_2CNR_2)_3]$ by boron trifluoride gave dimeric $[Ru_2(S_2CNR_2)_5]BF_4$, which exists in two forms having either two (α-isomer) or three (β-isomer) bridging dithiocarbamate ligands (294). As discussed above, Pignolet and co-worker (296) later showed that bubbling boron trifluoride through $[Os(S_2CNEt_2)_3]$ at low temperature initially gave purple $[Os(S_2CNEt_2)_3]BF_4$, while upon standing the color was slowly replaced by that of the orange-brown dimer $[Os_2(S_2CNEt_2)_4(\mu\text{-}S_2CNEt_2)_2]^{2+}$. The osmium(III) complex $[Os_2(S_2CNMe_2)_5]Cl$, analogous to the ruthenium complexes described above, has been prepared upon refluxing 4 equiv of NaS_2CNMe_2 and $[OsCl_6][NH_4]_2$ (1377). It has not been possible to unambiguously determine the isomeric form adopted, although later studies did reveal an isomerization process, believed to result from conversion of the initially formed α-isomer to the thermodynamically more stable β-isomer (295).

Pignolet and co-workers (1377) also detailed a rational synthesis of the known nitride-bridged osmium(IV) complexes $[Os_2(S_2CNR_2)_4(\mu\text{-}N)(\mu\text{-}S_2CNR_2)]$ (R = Me, Et), prepared in high yield from the reaction of $[Os(S_2CNR_2)_3]$ and $K_2[OsNCl_5]$ in methanol in the presence of excess dithiocarbamate salt (Eq. 130). The ethyl analogue shows a well-defined reversible one-electron oxidation, followed by a second irreversible process, suggesting that mixed-valence osmium(IV)–osmium(V) complexes may be accessible.

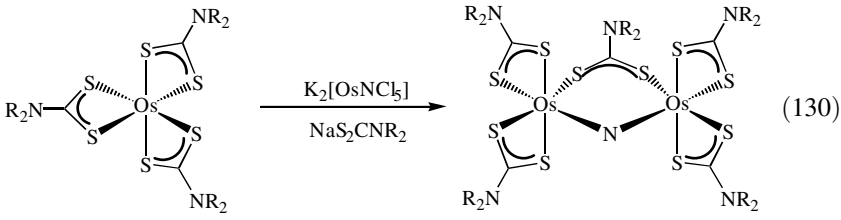

(130)

The examples detailed above generally contain bridging dithiocarbamate ligands, yet there are a number of diruthenium and diosmium dithiocarbamate complexes in which the latter are bound exclusively in a terminal fashion (290,295,1345,1378–1380). Thiolate-bridged $[Ru(CO)(PPh_3)(S_2CNMe_2)(\mu\text{-}SH)]_2$ results from loss of a phosphine upon heating *trans*-$[Ru(CO)(PPh_3)_2(S_2CNMe_2)(SH)]$ at 80°C (1345); the thiolate ligands bridging in preference to dithiocarbamates. Analogues $[Ru(CO)(PPh_3)(S_2CNMe_2)(\mu\text{-}SR)]_2$ (R = Et, Ph) have also been prepared upon reaction of *trans*-$[RuH(CO)(PPh_3)_2(S_2CNMe_2)]$ with excess thiol (1378). All of these complexes have planar Ru_2S_2 cores with long ruthenium–ruthenium interactions of $\sim$ 3.3–3.7 Å. In contrast, addition of nitric acid (R = Ph) results in a unique four-electron oxidation to give $[Ru(CO)(PPh_3)(S_2CNMe_2)(\mu\text{-}SPh)]_2^{4+}$ (Eq. 131), a 32-electron complex with a short ruthenium–ruthenium bond [Ru–Ru 2.876(2) Å]. Concomitant with this oxidation process, the carbonyl vibration in the IR shifts from 1940 to 2020 cm^{-1}. This appears to be the first example in which a four-electron oxidation is followed by metal–metal bond formation. Electrochemical studies further reveal that the ethanethiol analogue behaves slightly differently, displaying two consecutive and fully reversible two-electron oxidation waves.

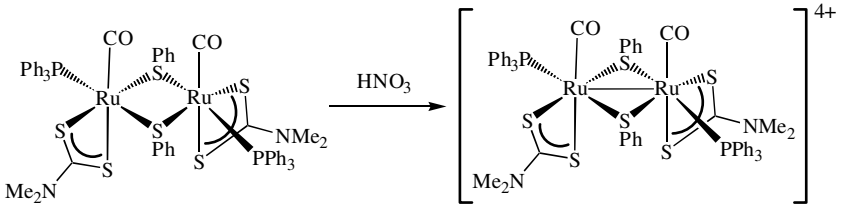

(131)

d. Divalent Organometallic Complexes. Ruthenium(II) and osmium(II) dithiocarbamate complexes have been prepared with a wide range of supporting organic ligands. For example, addition of NaS_2CNEt_2 to $[Ru(\eta^3\text{:}\eta^3\text{-}C_{10}H_{16})Cl(\mu\text{-}Cl)]_2$ yields $[Ru(\eta^3\text{:}\eta^3\text{-}C_{10}H_{16})Cl(S_2CNEt_2)]$ (1381), while the related *p*-cymene complexes $[(\eta^6\text{-}p\text{-cymene})RuCl(S_2CNR_2)]$ (R = Me, Et) have been prepared from $[(\eta^6\text{-}p\text{-cymene})RuCl(\mu\text{-}Cl)]_2$ and NaS_2CNR_2 (1369,1382).

A wide range of unsaturated hydrocarbyl ligands have been studied in conjunction with dithiocarbamates. Hill and co-workers (1383,1384) prepared ruthenium(II) and osmium(II) alkenyl and alkynyl complexes, *trans*-$[M(CO)(PPh_3)_2(HC{=}CHR)(S_2CNMe_2)]$ and *trans*-$[M(CO)(PPh_3)_2(C{\equiv}CR)(S_2CNMe_2)]$, respectively; the phosphines adopting a trans disposition. For example, the alkenyl complex, *trans*-$[Ru(CO)(PPh_3)_2(CH{=}CHCPh_2OH)(S_2CNMe_2)]$ (**302**) reacts with the propargyl alcohol, HC_2CPh_2OH, to afford an alkynyl complex,

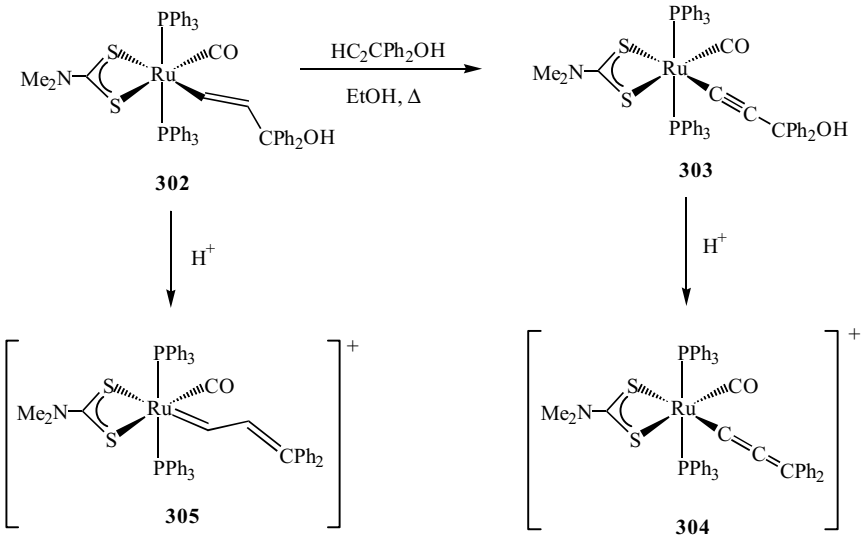

Figure 170. Ruthenium(II) dithiocarbamate complexes bearing a range of unsaturated hydrocarbyl ligands.

trans-[Ru(CO)(PPh_3)$_2$(C≡$CCPh_2OH$)(S_2CNMe_2)] (**303**), protonation of which affords an allenylidene complex, *trans*-[Ru(CO)(PPh_3)$_2$(C=C=CPh_2)-(S_2CNMe_2)]$^+$ (**304**) (1384), while protonation of **302** itself yields the vinyl carbene *trans*-[Ru(CO)(PPh_3)$_2$(CHCH=$CCPh_2$)(S_2CNMe_2)]$^+$ (**305**) (Fig. 170) (1385). The latter reacts with a range of simple nucleophiles, attack being directed at the γ-carbon and giving [Ru(CO)(PPh_3)$_2$(CH=$CHCPh_2X$)(S_2CNMe_2)] (X = H, OH, F, OEt) (1385).

e. Applications. A number of quite diverse applications have been considered for ruthenium dithiocarbamate complexes. For example, ruthenium(III) complexes [$RuX_2(EPh_3)_2(S_2CNR_2)$] have been studied for their antifungal activity, showing higher activity than the free dithiocarbamate ligands (1335), while insoluble [$Ru(S_2CNPh_2)_3$] has been used to modify a graphite electrode via the abrasive method, electrocatalytic oxidation of ascorbic acid being carried out at the modified electrode (1330,1386).

Violet ruthenium(II) complexes, [Ru(dcbH)($dcbH_2$)(S_2CNR_2)] (**306**), carrying a 4,4′-dicarboxy-2,2′-bpy ligand have been shown to be an efficient sensitizers of titanium dioxide anatase nanocrystalline powders, although photophysical studies have shown that the photocurrent is limited by iodide oxidation (1387).

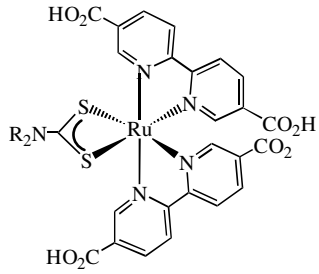

306

Welton and co-workers (1369) prepared zeroth- and first-generation poly(-amido)dendrimers functionalized with ruthenium dithiocarbamate end-groups carrying $CpRu(PPh_3)$ or (*p*-cymene)RuCl functionalities, with FAB and ESMS being used as characterization tools.

Thermal gravimetric analysis studies have been carried out on tris(dithiocarbamate) complexes $[Ru(S_2CNR_2)_3]$. Decomposition to Ru_2S_3 occurs between 448 and 553 K, while at higher temperatures nonstoichiometric sulfides of ruthenium are generated. Purported osmium(IV) complexes $[Os(S_2CNR_2)_4]$ similarly convert to Os_2S_3 at slightly higher temperatures (424–673 K), but decompose above this upper limit (1332).

F. Group 9 (VIII B): Cobalt, Rhodium, and Iridium

1. Cobalt

Cobalt dithiocarbamate complexes are now known in oxidation states +1 to +4, the first reported examples being the tris(dithiocarbamate) complexes $[Co(S_2CNR_2)_3]$, which were prepared in 1920 (1388).

a. Tris(dithiocarbamate) Complexes. Cobalt(III) tris(dithiocarbamate) complexes are easily prepared from the reaction of cobalt(III) and dithiocarbamate salts (58, 130, 358, 357, 392, 459, 462, 463, 1389, 1390). Examples include those derived from diallylamine (1389), α-amino acids (130), 1,4,7,10-tetraoxo-13-azacyclopentadecane, 15-aminobenzo-1,4,7,10,13-pentaoxacyclopentadecane (50), and with aryl substituents (1390). In quite recent work, Beer et al. (62) prepared a number of novel cryptand complexes in which two cobalt(III) centers are linked via three dithiocarbamate ligands, which have been used for the electrochemical recognition of group 1(IA) metal cations (see below). Further, an undergraduate laboratory preparation of $[Co(S_2CNEt_2)_3]$ has been reported from NaS_2CNEt_2 and cobaltous chloride, including its characterization by IR, NMR spectroscopy, and cyclic voltammetry (1391).

The nature of the formation of cobalt(III) tris(dithiocarbamate) complexes has been the focus of a number of publications. A kinetic study of the reaction of $[Co(NH_3)_6]^{3+}$ with 3 equiv of 4-morpholine dithiocarbamate under isothermal conditions showed that an intralattice reaction occur via a phase-boundary reaction mechanism (1392). The photoreaction of $[Co(en)_3]^{3+}$ with the bis(2-hydroxyethyl) dithiocarbamate ion in aqueous solution, leading to $[Co(S_2CNR_2)_3]$ ($R = CH_2CH_2OH$), has also been studied in some detail (1393). The quantum yield depends on the wavelength of light used, and the concentrations of ligand, and complex. A quantum yield of greater than unity in one case suggests that the primary photoredox process is followed by a chain reaction involving cobalt(II) species, and other cobalt amine complexes show similar behavior.

O'Conner and co-workers (1394) prepared a series of optically active examples of $[Co(S_2CNR_2)_3]$ (R = Me, Et, *i*-Pr, Bu, *i*-Bu, Bz, Ph, *t*-Bu, CH_2CH_2OH; $R_2 = C_4H_8$, C_4H_8O) via ligand displacement reactions of $(+)_{546}$-$K[Co(edta)].2H_2O$ and related chiral amine complexes; partially resolved complexes being precipitated in high yields. They have assigned absolute configurations from the sign of the $^1A_1 \rightarrow {}^1E_a$ visible transition in the circular dichroism (CD) spectra. These vary both as a function of the substituents on the dithiocarbamate and the chiral cobalt(III) starting material utilized. In related work, Haines and Chan (61) prepared single diastereoisomers of $[Co(S_2CNHCH MePh)_3]$ starting from optically pure α-phenylethylamines; the (−) ligand affording Λ-$[Co(+)(S_2CNHCHMePh)_3]$ and the (+) form yielding Δ-$[Co(+)(S_2CNHCHMePh)_3]$ (Fig. 171). In nonpolar or weakly polar solvents, however, inversion occurs yielding a second diastereoisomer, which can also be isolated in pure form. This observation suggests that in the original synthesis, the

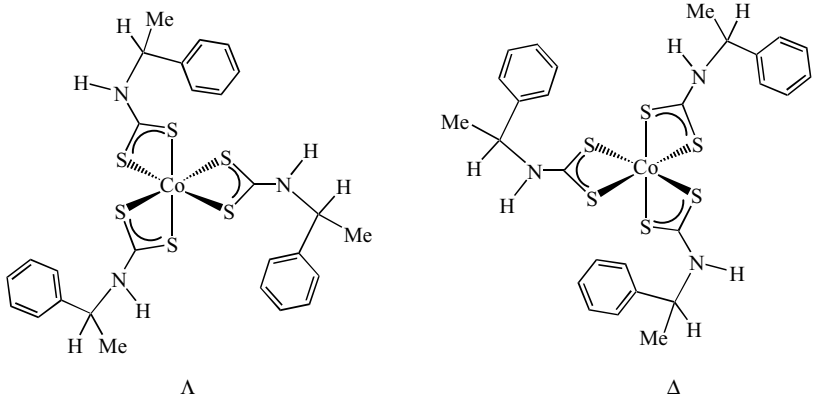

Figure 171. Optical isomers of $[Co(+)(S_2CNHCHMePh)_3]$.

stereoselective precipitation of one isomer occurs, reverting to the thermodynamically most stable form in solution.

All tris(dithiocarbamate) complexes are diamagnetic and a number of crystallographic studies have been carried out (50, 358, 359, 392, 393, 459, 462, 463, 501, 1389), the results of which are summarized in Table VI. In all cases, the metal adopts a distorted octahedral coordination environment. Cobalt–sulfur bonds of ~ 2.26 Å remain approximately constant as the nature of the dithiocarbamate substituents is changed, while carbon–sulfur and carbon–nitrogen bonds do not show any systematic variation (358). Thus, White and coworkers (358) probed the effects of different alkyl substituents on the structures of $[Co(S_2CNR_2)_3]$. Their results suggested that the influence on the ligand-field strength at sulfur is not through the π-bonding network of the S_2CN moiety, but rather results from intraligand S···H—C interactions that increase with increasing steric bulk.

Deformation density maps and DFT calculations have been used to study the electron density distribution about $[Co(S_2CNMe_2)_3]$. A spherical distribution is seen around the cobalt(III) ion, displaying a linear relationship between electron density at the bond critical point and bond length. This result suggest that the former is a good indicator of bond strength (510).

Cobalt-59 NMR data has been recorded for a wide range of complexes (305,362,541,1395,1396), many examples of which are included in a review of this topic (1397). Since ^{59}Co NMR chemical shifts cover a wide range, this allows identification of mixed-ligand species. Bond et al. (541) noted that ^{59}Co NMR chemical shifts do not correlate in a simple fashion with electrochemical data (see below), suggesting that steric effects influence the two techniques in a different way. A second study by the same group used both solution and solid-state ^{13}C NMR spectroscopy and solution ^{59}Co NMR measurements to show that the increase in ligand-field strength associated with phenyl substituents is due to a combination of steric and electronic effects (359).

Stability constants for a number of simple alkyl dithiocarbamate complexes have been assessed by UV–vis data, showing a decrease in the order; Et > *i*-Pr > *n*-Pr > Me (393). Mixed-ligand tris(dithiocarbamate) complexes can also be prepared upon heating mixtures of homoleptic complexes together at elevated temperatures, either in solution or the solid state as monitored by ^{59}Co NMR spectroscopy and MS (541). A second route to these species involves the controlled potential oxidation or reduction of the homoleptic compounds. Here, on a short time scale, no ligand scrambling is seen at cobalt(IV) or (II), suggesting that these species undergo only slow dithiocarbamate exchange (541).

Tris(dithiocarbamate) complexes are readily oxidized (see below), however, upon addition of iodine only simple adducts, $[Co(S_2CNR_2)_3].2I_2$ (R = Me, Et; $R_2 = C_5H_{10}$, C_4H_8O), result. The dimethyldithiocarbamate complex has been

crystallographically characterized, revealing a layered structure with intermolecular iodine–sulfur distances of 3.82 Å within the layers and 3.14 Å between them (460).

b. Oxidation of Tris(dithiocarbamate) Complexes: Generation of $[Co(S_2CNR_2)_3]^+$ and $[Co_2(S_2CNR_2)_5]^+$. The stability and nature of products generated upon one-electron oxidation of cobalt(III) tris(dithiocarbamate) complexes has been a topic of some debate, which has attracted the attention of a number of researchers (302–308), and it is only very recently that a study by Webster et al. (309) has appeared to clarify this area. By using voltammetric, ESR, and UV–vis–NIR data, they showed that one-electron oxidation of $[Co(S_2CNR_2)_3]$ (R = Et, Cy) in dichloromethane generates cobalt(IV) cations, $[Co(S_2CNR_2)_3]^+$, which are stable for several hours at 233 K. The ESR data (at <50 K) showed that the unpaired electron resides mainly on the metal center and displays a high degree of anisotropy attributed to a distorted octahedral structure, while UV–vis–NIR data reveal LMCT excitations to the unfilled t_{2g} orbital on the metal (309). Earlier studies had shown that the stability of these cobalt(IV) cations is dependent on the nature of the substituents, with bulky groups such as cyclohexyl conferring enhanced lifetimes (305).

The instability of cations, $[Co(S_2CNR_2)_3]^+$, stems from their propensity to undergo an internal redox reaction resulting in the generation of dimeric cobalt(III) cations, $[Co_2(S_2CNR_2)_5]^+$ (Fig. 172). Formation of the latter is again sensitive to substituent effects and is also concentration dependent; increased stability being seen in dilute solutions (305). These cations probably result from initial dimerization of $[Co(S_2CNR_2)_3]^+$ to give $[Co_2(S_2CNR_2)_6]^{2+}$, followed by loss of a ligand that is in turn oxidized. At low temperatures, further oxidation to give $[Co_2(S_2CNR_2)_5]^{2+}$ is possible, but the dications decompose at room temperature (305).

Contrary to one report (306), cobalt(IV) cations are unstable in acetone (305, 307), while in acetonitrile, $[Co_2(S_2CNR_2)_5]^+$ is cleaved to give $[Co(S_2$

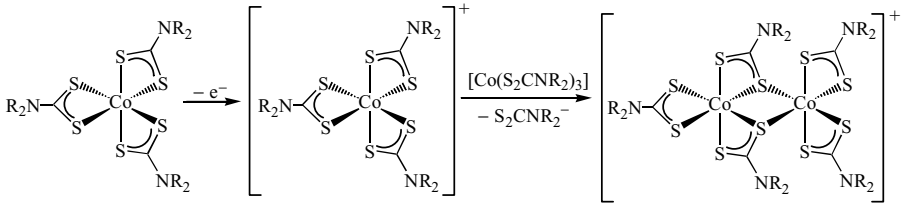

Figure 172. Oxidation of $[Co(S_2CNR_2)_3]$ leading to the formation of $[Co_2(S_2CNR_2)_3(\mu\text{-}S_2CNR_2)_2]^+$.

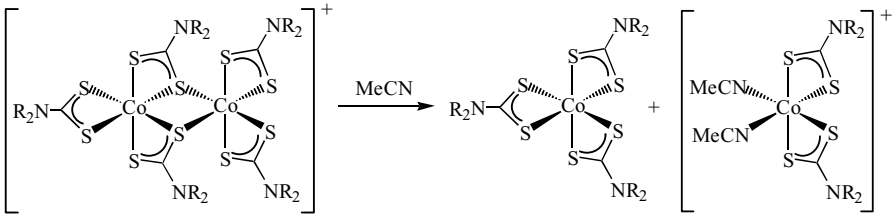

Figure 173. Decomposition of $[Co_2(S_2CNR_2)_3(\mu\text{-}S_2CNR_2)_2]^+$ in acetonitrile.

$CNR_2)_2(MeCN)_2]^+$ and $[Co(S_2CNR_2)_3]$ (Fig. 173) (302). As the latter can be reoxidized, then the overall reaction proceeds via a EC_2C mechanism, which has been successfully simulated. The calculated dimerization rate constant is the same in acetonitrile and dichloromethane, showing that it is solvent independent.

Interestingly, oxidation of $[Co(S_2CNMe_2)_3]$ in acetonitrile in the presence of light (300–600 nm) has been shown to give rise to appreciable photocurrents. These photocurrents are believed to result from generation of $[Co(S_2CNMe_2)_3]^+$ followed by an internal redox reaction to give $[Co(S_2CNMe_2)_2]$ and oxidized dithiocarbamate (1398). Mixed-ligand dithiocarbamate complexes $[Co(S_2CNR_2)(S_2CNR'_2)_2]$ have also been probed electrochemically. Even after repetitive scanning, no evidence for ligand exchange was observed (541).

As noted earlier, Beer et al. (62) prepared a number of cryptand complexes **307** and **308** (Fig. 174). Electrochemical recognition studies using cyclic and square-wave voltammetry showed that these complexes differ from simple derivatives, in that they exhibit broad overlapping redox waves, the addition of alkali metal cations leading to significant anodic shifts in the oxidation potential. Further, for **307** there is a complementary metal cation to cryptand cavity size correlation; the smallest cryptand (**307**, $n = 1$) binding sodium most strongly, while (**307**, $n = 2$) shows the highest shift for potassium, and (**307**, n=3) for caesium. Similarly, amide complexes (**308**, $n = 2,3$) show electrochemical recognition of anions; cathodic perturbations of up to 125 mV being noted with $H_2PO_4^-$ in dichloromethane.

Reactions of $[Co(S_2CNR_2)_3]$ with chemical oxidants gives rise to a range of products, being highly dependent on the nature of the oxidant. An ESMS study of the products generated upon oxidation by $NOBF_4$ revealed ions associated with the unknown species $[Co_2(S_2CNR_2)_5S]^+$ and $[Co_2(S_2CNR_2)_5S_2]^+$. Neither the nature of sulfur coordination nor its source is known, although the authors suggest that the latter may result from thiuram disulfide oxidation by NO^+ (303).

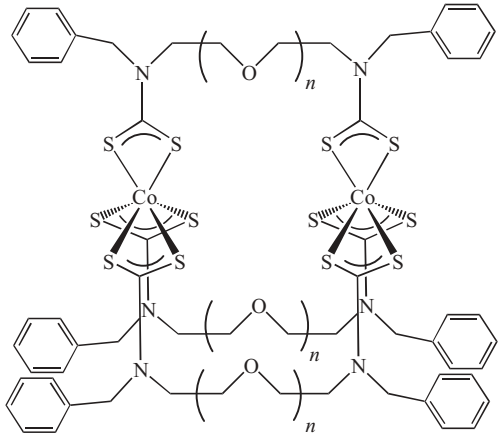

$n = 1, 2, 3$

307

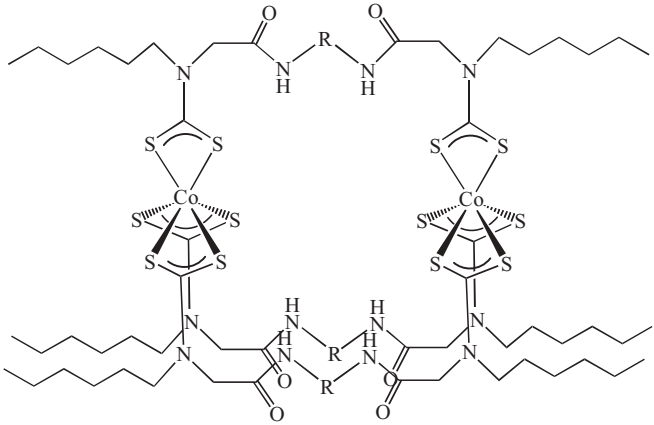

R = Et, *o*-Ph, *m*-Ph

308

Figure 174. Examples of linked cobalt(III) tris(dithiocarbamate) complexes.

While adducts form with iodine (see Section IV.F.1.a), chlorine and bromine both oxidize the cobalt center, although products appear to be substituent sensitive. In most cases (R = Me, Et; $R_2 = C_4H_8$, C_5H_{10}, C_4H_8O), complete loss of dithiocarbamate occurs giving $[CoX_4]$[bitt-4] [bitt-4 = bis(dialkylimonium)tetrathiolane] (Eq. 132), however, this product is not observed in

certain other cases (R = Pr, Bu) (1399).

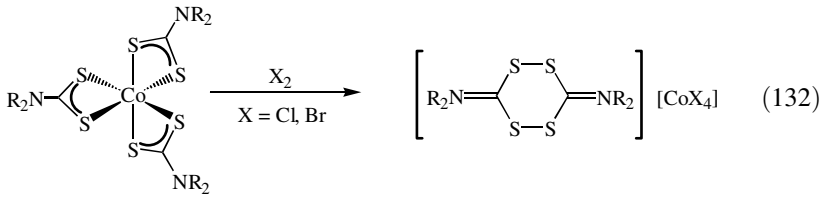

(132)

Bond et al. (313) demonstrated the delicate balance between the oxidizing and coordinating ability of silver(I). Addition of 2 equiv of silver tetrafluoroborate gives dimeric oxidation products, $[Co_2(S_2CNR_2)_5]^+$, while in contrast with 1 equiv, stable coordination complexes, $[Co_2Ag(\mu\text{-}S_2CNR_2)_4(S_2CNR_2)_2]^{2+}$ (**309**), result. A crystallographic study (R = *i*-Pr) shows the absence of any direct metal–metal interaction [Co···Ag ~ 3.4 Å], with four of the dithiocarbamates bridging between the metal centers. Cyclic voltammetric and ESMS studies show that these cations retain their identity in solution, although ^{59}Co NMR spectra showed that they are kinetically labile, addition of further Ag^+ resulting in a considerable broadening and shifting to higher frequency of the signals.

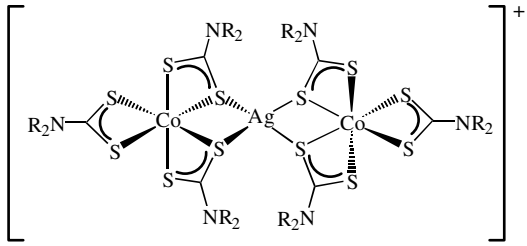

309

The same group also showed that tris(dithiocarbamate) complexes react with a range of copper(I) salts in acetonitrile giving 1:1, 2:1 and 3:1 heterobimetallic adducts together with polymeric species (Fig. 175), the latter being linked and cross-linked into a novel double-stranded polymer by centrosymmetric displaced step CuI_6 units (498,1400,1401). In contrast, reaction with $[Cu(BF_4)_2]$ simply yields $[Co_2(S_2CNR_2)_5][BF_4]$ and $[Cu(S_2CNR_2)_2][BF_4]$ (1118).

c. Other Cobalt(III) Complexes. A wide range of cobalt(III) dithiocarbamate complexes containing other ligands such as phosphines (1402–1405), phosphites (1406,1407), amines (1408–1412), and cyclopentadienyl (253), have been prepared and studied. Cyclam (1,4,8,11-tetraazacyclotetradecane)

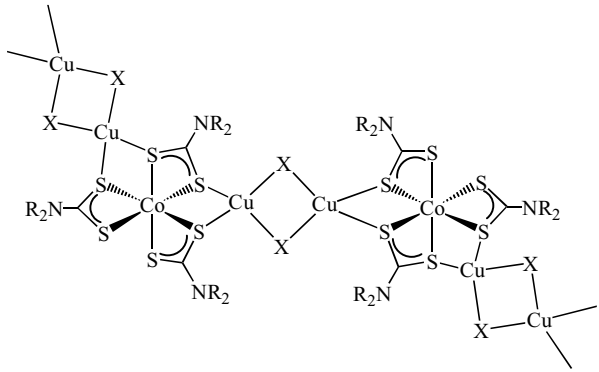

Figure 175. Part of the polymeric unit of a 2:1 adduct of $[Co(S_2CNR_2)_3]$ and a copper(I) halide.

complexes, $[Co(S_2CNR_2)(cyclam)]^{2+}$ (**310**), have been prepared with cyclic dithiocarbamates generated from piperidines, morpholines (morph), and piperazines (1409,1410,1412). The coordination environment at the metal center is octahedral and the cyclam ligand is folded. The trans-influence of the dithiocarbamate has been studied by NMR in DMSO-d^6; pip > morph > Mepip (1410), while the position of the methyl group in monosubstituted piperidine derivatives influences both the positions of ν(C—N) and ν(C—S) and the thermal stability; 2Me > 3Me > 4Me (1409). These complexes have also been studied electrochemically, showing a reversible one-electron reduction in aqueous solution, while in other solvents reduction does not occur (1413).

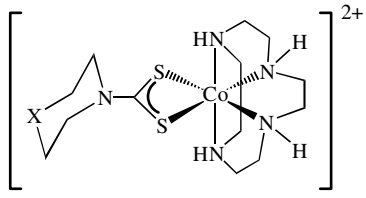

310

The ethylenediamine complex, $[Co(S_2CNEt_2)_2(en)][BF_4]$, and other substituted analogues can be easily prepared upon addition of the diamine to $[Co_2(S_2CNEt_2)_5][BF_4]$ (1414), while further diamine complexes $[Co(S_2CNMe_2)_{3-n}(diamine)_n]^{n+}$ ($n = 1, 2$) (Fig. 176) have been prepared from $[Co(ClO_4)_2]$ and tetramethylthiuram disulfide in the presence of the diamines, and characterized by CD and magnetic circular dichroism (MCD) spectra (1408).

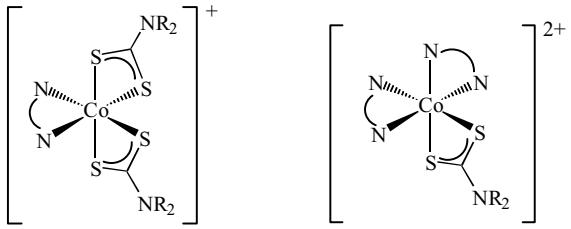

Figure 176. Schematic representations of octahedral mixed-diamine-dithiocarbamate cations.

Dithiocarbamates are suggested to be the best ligands in stabilizing the Co(III)-P bond due to their steric compactness and electronic softness. Developing this, Kashiwabara and co-workers (1402–1407,1415–1418) prepared a range of octahedral phosphine and phosphite complexes, often utilizing the oxidation of cobalt(II) salts by thiuram disulfides for their synthesis. For example, with the monodentate phosphite, 4-Et-2,6,7-trioxa-1-phosphabicyclo[2.2.2]octane (etpb), two products result, $[Co(S_2CNR_2)(etpb)_4][BF_4]_2$ and $[Co(S_2CNR_2)_2(etpb)_2][BF_4]$ (R = Me, Et; $R_2 = C_5H_{10}$) (Fig. 177), while related trimethyl and triethyl phosphite complexes have also been prepared (1407). A crystallographic study of $[Co(S_2CNMe_2)_2(etpb)_2][BF_4]$ reveals a cis disposition of phosphites, however, upon photolysis the less soluble trans isomer is generated almost quantitatively. Complexes have also been prepared with the bidentate phosphite, $(MeO)_2PCH_2CH_2P(OMe)_2$, via oxidation of $Co(BF_4)_2$ or from the tris(dithiocarbamate) complexes upon reduction with activated charcoal (1406).

In recent work, a range of phosphine complexes $[Co(S_2CNMe_2)_2(PMe_{3-n}Ph_n)_2][BF_4]$ ($n = 0$–3) (1415) and $[Co(S_2CNMe_2)_2(PHPh_2)_2][BF_4]$ (1416) have been prepared from $[Co(H_2O)_6][BF_4]_2$, 2 equiv of phosphine and 1 equiv of dithiocarbamate salt or thiuram disulfide, and factors affecting the adoption and relative stability of cis and trans isomers has been assessed using X-ray crystallography. Reactions often give mixtures of cis and trans-isomers, and for $[Co(S_2CNMe_2)_2(PHPh_2)_2][BF_4]$, the cis-isomer is converted into the trans upon photolysis (Eq. 133), a process that can be reversed thermally

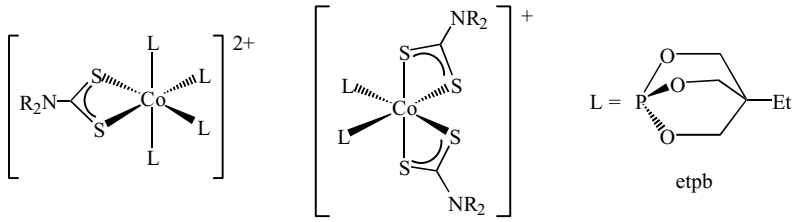

Figure 177. Schematic representations of cobalt(III) dithiocarbamate etpb (L) complexes.

(1415,1416,1418). Mixed-phosphine–phosphite complexes behave in a similar manner (1417).

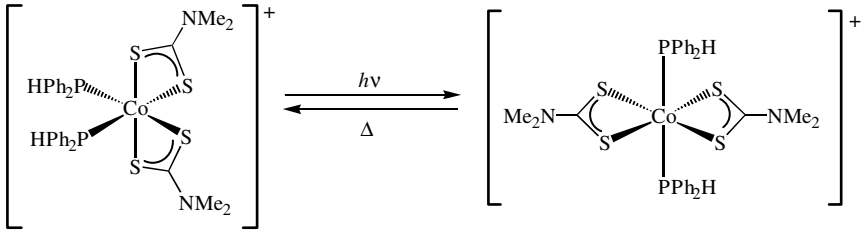

(133)

Crystallographic studies also reveal that the cobalt–sulfur and cobalt–phosphorus bond lengths vary as a function of both the steric and electronic effects of the phosphorus ligands. In the cis-isomers, there is significant steric interaction between the phosphine groups, and π–π stacking interactions also occur between the dithiocarbamate plane and one of the phenyl rings of the phosphine. These effects are largely absent in the trans forms and here it appears to be the electronic trans-influence of the phosphine (as measured by the σ-donicity), which is competitive with its steric requirement and leads to an elongation of the mutually trans cobalt–phosphorus bonds (1415,1417,1418).

Bidentate phosphine complexes are prepared in the same way and display similar properties and structural characteristics. Examples include $Me_2P(CH_2)_n$-PMe_2 ($n = 1$–3), $Ph_2P(CH_2)_nPPh_2$ ($n = 1$–4) (1401), and $[(\eta^5\text{-}C_5H_4PR_2)_2Fe]$ (R = Me, Ph) (1405). Most interesting is $[Co(S_2CNMe_2)_2(313\text{-NPPN})][ClO_4]_3$ (313-NPPN = 4,6-diphenyl-4,6-diphosphanonane-1,9-diamine) being formed as *rac* and *meso* isomers. The latter has been crystallographically characterized, coordination of the ligand occurring through the phosphorus atoms (1403). A byproduct of this synthesis, $[Co(S_2CNMe_2)_2(\eta^2\text{-}H_2NCH_2CH_2PPhCH_2OH)]^+$ (**311**), has also been crystallographically characterized, with the cobalt center being bound through nitrogen and phosphorus.

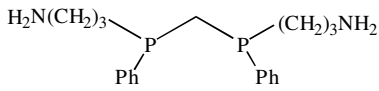

313-NPPN

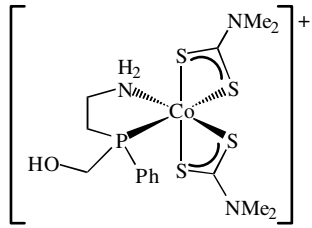

311

When mixed-phosphine–sulfide ligands are used, it is the phosphorus center that preferentially binds to cobalt(III). For example, with $Me_2PCH_2CH_2SR$

(R = Me, Et), *cis*-$[Co(S_2CNMe_2)_2(\eta^1\text{-}Me_2PCH_2CH_2SR)_2]^+$ (**312**) result (1404).

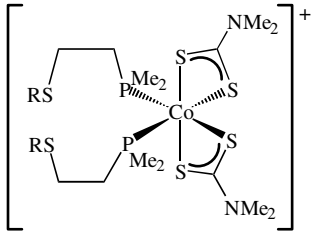

312

Electrochemical studies have been carried out on a wide range of mono- and bis(dithiocarbamate) complexes, $[Co(S_2CNEt_2)(bidentate)_2]^{2+}$, and $[Co(S_2CNEt_2)_2(bidentate)]^+$, respectively, with bidentate phosphorus and nitrogen donor ligands. A good linear relationship is found between the potential difference, $\Delta E = E_{1/2}(\text{ox}) - E_{1/2}(\text{red})$, and the first *d–d* transition energy for these and tris(dithiocarbamate) complexes (308).

Robinson and co-workers (1348) showed that cobalt(II) halides $[CoX_2(dppe)]$ react with dithiocarbamate complexes $[M(S_2CNEt_2)_2]$ (M = Cd, Hg, Zn) in the presence of tetraethylthiuram disulfide to give cobalt(III) products, $[Co(S_2CNEt_2)_2(dppe)]_2[MX_4]$ (Eq. 134). The zinc salt was not quite as expected, being shown crystallographically to be $[Co(S_2CNEt_2)_2(dppe)]_2[Cl_3ZnO(dppe)OZnCl_3]$, containing an unusual anion, but the anticipated cobalt(III) cation.

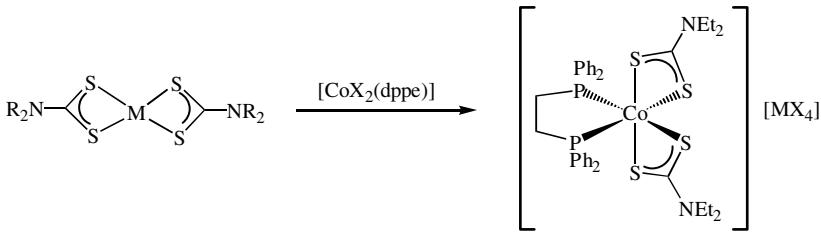

(134)

While dithiocarbamates generally bind strongly to cobalt(III), it is not always possible for them to displace other ligands. Thus, addition of 3 equiv of dithiocarbamate salts to $[Co(diNOsar)]Cl_3$ (diNOsar = 1,8-dinitro-3,6,9,13,16,19-hexaazabicyclo[6.6.6]isosane) gives complexes $[Co(diNOsar)]\text{-}[S_2CNR_2]_3$ (R = Et, *i*-Pr; $R_2 = C_4H_4$), in which the dithiocarbamates simply act as anions; the cobalt(III) center remains bound to the nitrogen atoms of the macrocyclic ligand (1419). Likewise, addition of 3 equiv of NaS_2CNEt_2 to the cryptate complex $[Co(AMMEsarH)]Cl_4$ (AMMEsar = 8-Me-3,6,10,13,16,19-hexaazabicyclo[6.6.6]icosan-1-aminium), yields $[Co(AMMEsar)][S_2CNEt_2]_3$, in which the three dithiocarbamate ligands hydrogen bond through the sulfurs to the cryptate (1420).

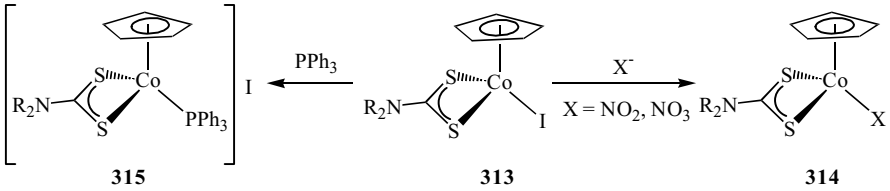

Figure 178. Selected reactions of $[CpCoI(S_2CNR_2)]$.

As might be expected, dithiocarbamates do not readily displace cyclopentadienyl ligands; addition of thiuram disulfides to $[CpCo(CO)_2]$ and its methyl-substituted analogue giving $[CpCo(S_2CNR_2)(\eta^1\text{-}S_2CNR_2)]$ (R = Me, Et) (253). These pseudo-octahedral complexes are fluxional in solution, three processes being identified; rotation about the carbon–nitrogen bonds of inequivalent dithiocarbamates, and η^1 and η^2 dithiocarbamate exchange.

A wide range of cobalt(III) cyclopentadienyl complexes, $[CpCoX(S_2CNR_2)]$ (X = I, CN, NCS) and $[CpCoL(S_2CNR_2)]I$ (L = H_2O, py, phosphine, phosphite, stibine, organoisocyanide), can be prepared upon addition of dithiocarbamate salts to $[CpCo(CO)I_2]$ and $[CpCoLI_2]$, respectively (1128,1421). For example, Miller and co-workers (1421) prepared $[CpCoI(S_2CNR_2)]$ (R = Me, Et) (**313**) from $[CpCo(CO)I_2]$. Further addition of nitrite or nitrate give $[CpCo(NO_2)(S_2CNR_2)]$ and $[CpCo(NO_3)(S_2CNR_2)]$ (**314**), respectively, while the iodide reacts with PPh_3 in acetonitrile to afford $[CpCo(PPh_3)(S_2CNR_2)]I$ (**315**) (Fig. 178).

The fluorinated alkyl complex $[CpCo(C_3F_7)(S_2CNMe_2)]$ is prepared from $[CpCo(CO)I(C_3F_7)]$ upon addition of NaS_2CNMe_2, while addition of MeI or $MeSO_3F$ to $[CpCo(CN)(S_2CNMe_2)]$ yields $[CpCo(CNMe)(S_2CNMe_2)]^+$ (1128). A crystallographic study has been carried out on $[CpCoI(S_2CNEt_2)]$, and shows the expected piano-stool geometry (253). By utilizing the latter, it is possible to prepare the mixed-ligand complex $[CpCo(S_2CNMe_2)(S_2CNEt_2)]$. This complex exits as two isomers with $[CpCo(S_2CNEt_2)(\eta^1\text{-}S_2CNMe_2)]$ being favored at higher temperatures (Eq. 135) (253).

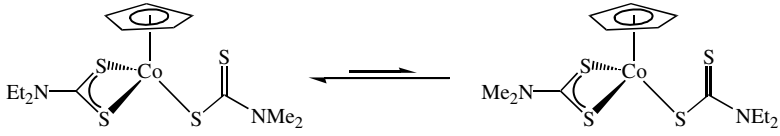

(135)

d. Cobalt(II) Complexes. Cobalt(II) bis(dithiocarbamate) complexes, $[Co(S_2CNR_2)_2]$, have been claimed for many years (754), and are reported to spontaneously oxidize to cobalt(III) complexes in air. To date no

crystallographic evidence has been presented and spectroscopic and other characterization data are often inconclusive. Hoa and Magee (1422) studied the reduction of cobalt(III) tris(dithiocarbamate) complexes $[Co(S_2CNR_2)_3]$ at a mercury electrode in DMSO. The one-electron reduction process to generate $[Co(S_2CNR_2)_3]^-$ is quasi-reversible, and this is followed by an irreversible two-electron reduction. Rate constants for the one-electron processes were found to decrease in the following order: $C_4H_8O < C_5H_{10} < Me_2 < Et_2 < Bu_2 < i\text{-}Bu_2$.

In a series of papers, Siddiqi et al. detail the synthesis of purported cobalt(II) complexes, $[Co(S_2CNR_2)_2]$, derived from a range of amines including; succinimide and phthalimide (49), β-naphthylamine (1125), and chloroanilines (1423). Others have claimed the preparation of those containing benzyl (506) and benzylpiperazine (1126), substituted piperidines (1116,1424,1425), and 1,3,4-thiaxolyl dithiocarbamate (1426). In none of this work was oxygen rigorously excluded.

Some measurements have been made, such as magnetic moments for the black β-naphthylamine (2.58 BM) (1125), green benzylpiperazine (2.09 BM) (1126), and substituted piperidine (2.04–2.31 BM) (1116,1424) derived complexes. ESR studies have been carried out on the green, air, and moisture stable, methyl-substituted piperidine dithiocarbamate complexes $[Co(S_2CNC_5H_{9-}Me)_2].0.5H_2O$; the authors interpreting the results in terms of a distorted square-planar CoS_4 coordination environment (1116). The XPS studies have been carried out (557), as have EXAFS and K-absorption spectral studies (506). The latter compares analogous cobalt(II) and (III) complexes and shows that going from the +2 to +3 state results in only small chemical shifts (0.8–1.6 eV). Certainly, if neutral cobalt(II) complexes $[Co(S_2CNR_2)_2]$ do exist, then they are very susceptible to oxidation and their synthesis and manipulation must be carried out with rigorous exclusion of air and water.

Indirect evidence for their existence comes from their trapping with the nitrene source, PhI=NTs (Ts = *p*-tosyl) (1427). This reagent does not react with cobalt(III) complexes, however, upon reduction with zinc amalgam, a color change from brown to slate-blue occurs and addition of excess PhI=NTs at this stage affords $[Co\{\eta^2\text{-}TsNSC(NR_2)SNTs\}_2]$ (R = Me, Et, Pr, Bu) (Eq. 136). These cobalt(II) products result from insertion of four nitrene (NTs) groups into the cobalt-sulfur bonds of the *in situ* generated $[Co(S_2CNR_2)_2]$.

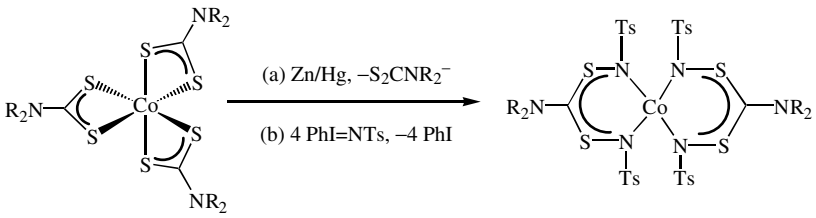

(136)

Bianchini et al. (226) have prepared the cobalt(II) complex $[Co(S_2CNEt_2)\{\eta^3\text{-}(Ph_2PCH_2)_3CMe\}]^+$ upon addition of diethylamine to $[Co(S_2CSMe)\{\eta^3\text{-}(Ph_2PCH_2)_3CMe\}]^+$ (Eq. 42). Cobalt(II) nitrosyl complexes are also well known. For example, addition of 2 equiv of $NaS_2CN{-}i\text{-}Pr_2$ to $[Co(en)_2(NO)]^{2+}$ affords $[Co(NO)(S_2CN{-}i\text{-}Pr)_2]$ (**316**), which has been crystallographically characterized. The nitrosyl is bent [Co–N–O 129.2(9)°], the metal coordination geometry being square-based pyramidal, with the dithiocarbamate ligands forming the base (1264). Mason and co-workers (1428) recorded ^{15}N and ^{59}Co NMR data for three complexes of this type (R = Me, Et, *i*-Pr); ^{59}Co chemical shifts being quite similar to those for the analogous tris(dithiocarbamate) complexes, supporting the description of NO as a weak-field ligand.

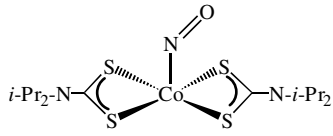

316

e. Analytical Chemistry and Other Applications. Dithiocarbamate complexation has been utilized in a number of analytical tests to determine cobalt levels, often in the presence of other metal ions. Ensafi and Abbasi (56) reported a sensitive stripping voltammetric determination of cobalt(II) based on the selective accumulation of its complex with the ammonium salt of 2-aminocyclohexene dithiocarbamate (**317**). This process is very sensitive and has been applied to the determination of cobalt levels in natural water and serum samples. The same dithiocarbamate salt has been utilized for the simultaneous spectrophotometric determination of cobalt(II), nickel(II), and copper(II), detection limits being 0.072, 0.021, and 0.063 μg mL^{-1} (1429). In a similar manner, the spectrophotometric determination of the β-adrenergic blocking drug, propranolol has been carried out based on the supposed formation of dithiocarbamate (**318**) complexes of cobalt(II), nickel(II), and copper(II) (57).

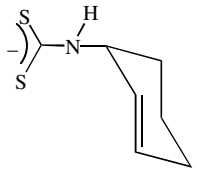

317

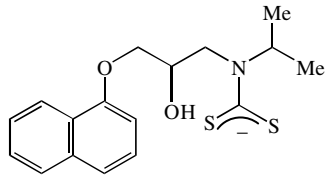

318

Bis(2-hydroxyethyl)dithiocarbamate complexes of a range of metals including cobalt, chromium, nickel, copper, and platinum have been separated by

miceller electrokinetic capillary chromatography with direct photometric detection (1430), while the same complex formation has been utilized for the determination of cobalt, nickel, copper, and mercury levels by HPLC (1431). The HPLC separation of pyrrolidine dithiocarbamate complexes of cobalt, nickel, copper, and palladium has been reported (1432), as has the simultaneous determination of cobalt, iron, nickel, copper, mercury, and lead by energy-dispersive X-ray fluorescence spectroscopy after precipitation as their polymeric piperazino-1,4-bis(dithiocarbamate) complexes (1433).

The simultaneous determination of cobalt and nickel in aqueous solutions as trifluoroethyl dithiocarbamate complexes is possible down to 10 ppb in the presence of a 10-fold excess of iron, copper, cadmium, and zinc (1434), while the same dithiocarbamate is used for the determination of cobalt in urine samples by GC and MS (1435).

Bis(dithiocarbamate) complexes, $[Co(S_2CNR_2)_2L]^+$ ($R = Me$, Et; $R_2 = C_4H_4$), of bidentate nitrogen mustards such as *N*,*N*′-bis(2-chloroethyl)ethylenediamine (DCE) have been prepared from $[Co_2(S_2CNR_2)_5]^+$ and assessed as potential hypoxia-selective cytotoxins (1411). Cyclic voltammetry studies show that upon reduction in water, ligand loss is rapid, and it appears to be the free dithiocarbamate ligands that are responsible for growth inhibition, although released DCE does contribute to clonogenic cell killing. However, the latter is not appreciably enhanced under hypoxic conditions suggesting that they are probably not suited as bioreductive anticancer drugs.

Tsipis and co-workers (1436) reported that reaction of a cobalt-loaded zeolite with NaS_2CNEt_2 results in the crystallization of $[Co(S_2CNEt_2)_3]$ on the surface of the zeolite, forming an inhomogeneous layer patterned on the zeolite.

Miller and co-workers (1421) reported that mixtures of $[CpCo(NO_2)(S_2CNMe_2)]$ and $BF_3.Et_2O$ act as oxidants for the conversion of benzyl alcohol to benzaldehyde. In the absence of oxygen the reaction is stoichiometric, but in the presence of oxygen it is catalytic (Eq. 137). Mechanistic aspects have been probed, a process involving metal-bound nitrogen oxide ester intermediates being ruled out in favor of one in which nitrite reacts with BF_3 to give the actual oxidant. In the stoichiometric transformation, a cobalt product of the form $[CpCo(S_2CNMe_2)(BF_4)]_n$ is isolated. Its precise structure is unknown, but it does react with PPh_3 to give $[CpCo(PPh_3)(S_2CNMe_2)][BF_4]$.

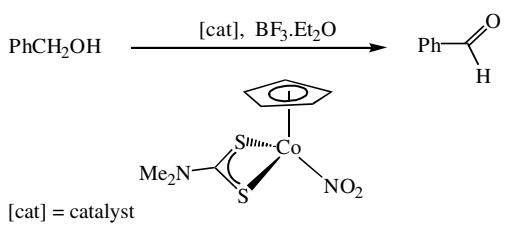

(137)

Decomposition of $[Co(S_2CNEt_2)_3]$ in the presence of hydrogen sulfide occurs below its melting point affording Co_9S_8 in a single phase, as characterized by X-ray and magnetic susceptibility measurements, although the product still contains undesired carbon impurity (1437).

2. *Rhodium and Iridium*

Rhodium(I) and (III) complexes are well known, although there is still some debate about the existence and nature of compounds formulated to contain rhodium(II) dithiocarbamate centers. Relatively little work has been carried out on iridium complexes, although again the $+1$ and $+3$ states are both accessible. The $+4$ oxidation states can also be generated for both metals, and somewhat unusually, rhodium(IV) complexes show far greater stability than their iridium analogues.

a. Trivalent Complexes. Rhodium(III) tris(dithiocarbamate) complexes were first reported by Malatesta in 1938 (767). Like their iridium analogues, they are easily prepared from the metal(III) halides (1329,1331–1333,1438), while iridium complexes can also be prepared utilizing the iridium(IV) starting material Na_2IrCl_6, the metal center being reduced by 1 equiv of dithiocarbamate (1439).

All are diamagnetic and have a distorted octahedral coordination geometry, as confirmed by the crystallographic characterization of a new polymorph of $[Rh(S_2CNEt_2)_3]$ (286). They are also fluxional in solution, a variable temperature NMR study of $[Rh(S_2CNMePh)_3]$ giving a value 61.5 ± 4.2 kJ mol^{-1} for the free energy of activation of rotation about the carbon–nitrogen bonds (371). This value is similar to those found for cobalt(III), but relatively large compared to iron(II) and iron(III) centers. The study also shows that metal-centered optical rotation is slow between 239–324 K.

In a similar manner to the analogous chromium complexes, oxidative controlled-potential electrolysis of $[Rh(S_2CNR_2)_3]$ yields $[Rh_2(S_2CNR_2)_5]^+$ (Fig. 179), presumably via $[Rh(S_2CNR_2)_3]^+$ and $[Rh_2(S_2CNR_2)_6]^{2+}$, with dimerization rate constants being $\sim$1000 times greater than for cobalt (310,311). Analogous iridium complexes can also be oxidized, but now the iridium(IV) cations $[Ir(S_2CNR_2)_3]^+$ (Fig. 179) show remarkable stability, being stable in solution for days (1439). Further, in acetonitrile a second, irreversible, oxidation wave is seen, having a half wave potential of $+1.5$V versus Ag/AgCl, and suggesting that the iridium(V) species, $[Ir(S_2CNR_2)_3]^{2+}$, are accessible as short-lived species. Bond et al. (1439) compared the one-electron oxidation potentials for the $[M(S_2CNR_2)_3]$ and find the unusual order; Rh $>$ Co $>$ Ir.

The iridium(IV) cations are strongly oxidizing, addition of a further equivalent of dithiocarbamate salt leading to the formation of thiuram disulfide

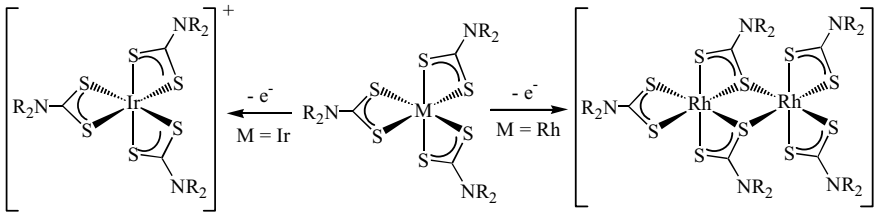

Figure 179. Products of the one-electron oxidation of $[M(S_2CNR_2)_3]$ (M = Rh, Ir).

and $[Ir(S_2CNR_2)_3]$, while oxidation of mercury at an electrode gives rise to the formation of the heterotrimetallic complexes, $[\{Ir(S_2CNR_2)(\mu\text{-}S_2CNR_2)_2\}_2Hg]^{2+}$ (Eq. 138).

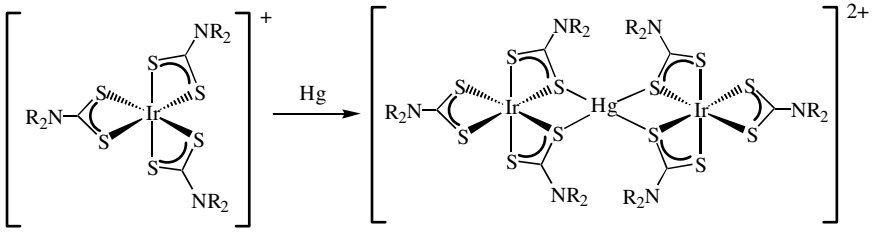

(138)

Dimeric $[Rh_2(S_2CNR_2)_5]^+$ can also be oxidized and reduced, but the species generated have no inherent stability. The oxidation products $[Rh_2(S_2CNR_2)_5]^{2+}$ have been detected as transient intermediates, but the reduction products $[Rh_2(S_2CNR_2)_5]$ have no inherent stability and decompose to $[Rh(S_2CNR_2)_3]$ and $[Rh(S_2CNR_2)_2]$.

Oxidation of $[Rh(S_2CNBu_2)_3]$ in the presence of CO is believed to be a two-electron process initially affording $[Rh(CO)_2(S_2CNBu_2)]$, which is itself immediately reduced to $[Rh(CO)_4]^-$ (311).

The reduction of tris(dithiocarbamate) complexes has not been studied in such detail (1440,1441). Reduction of $[Rh(S_2CNR_2)_3]$ in DMSO for short electrolysis times ($t < 1$ s) is believed to be a two-electron process, but at longer times ($t < 2$ s) three electrons are involved. In both cases, cyclic voltammetry showed that there was loss of free dithiocarbamate anion (1440).

Both $[M(S_2CNR_2)_3]$ (M = Rh, Ir) react with silver tetrafluoroborate to give trinuclear cations $[Ag\{M(S_2CNR_2)_3\}_2]^+$ in the same way as the analogous cobalt complexes (313). In a similar manner, $[Rh(S_2CNC_4H_8)_3]$ reacts with copper(I) iodide in the dark to give $[Rh(S_2CNC_4H_8)_3].3CuI$. The latter is a 3D polymer comprising a pair of interpenetrating uncorrected networks of opposed

chirality, formed by cross-linking of the parent species by $Cu(\mu\text{-}I)_2Cu$ units, which is isostructural with the analogous cobalt complex (312).

The groups of both Stephenson (1442) and Maitlis and co-workers (1443) independently prepared pentamethylcyclopentadienyl complexes $[Cp^*M(S_2CNR_2)_2]$ (M = Rh, Ir; R =Me, Et) upon addition of 2 equiv of dithiocarbamate salt to $[Cp^*MCl(\mu\text{-}Cl)]_2$. Like the analogous cobalt cyclopentadienyl complexes, they contain both a monodentate and a bidentate dithiocarbamate; $[Cp^*Rh(S_2CNMe_2)_2]$ (**319**) (Fig. 180) is characterized by the ν(C—N) vibrations spectrum at 1392 and 1530 cm^{-1}, respectively, in the IR spectrum. In solution, interconversion of the two dithiocarbamates occurs (Fig. 180). The NMR line shape analysis suggests that it occurs via a dissociatively controlled intramolecular mechanism.

Stephenson's group also prepared $[Cp^*RhCl(S_2CNMe_2)]$ (**320**) (Fig. 180) on addition of 1 equiv of NaS_2CNMe_2 to $[Cp^*RhCl(\mu\text{-}Cl)]_2$. This complex has been utilized toward the synthesis of mixed-ligand complexes $[Cp^*Rh(S_2CNMe_2)(\eta^1\text{-}S_2X)]$ (X = OMe, PPh_2, PMe_2) (**321**). The IR spectra suggests that it is the

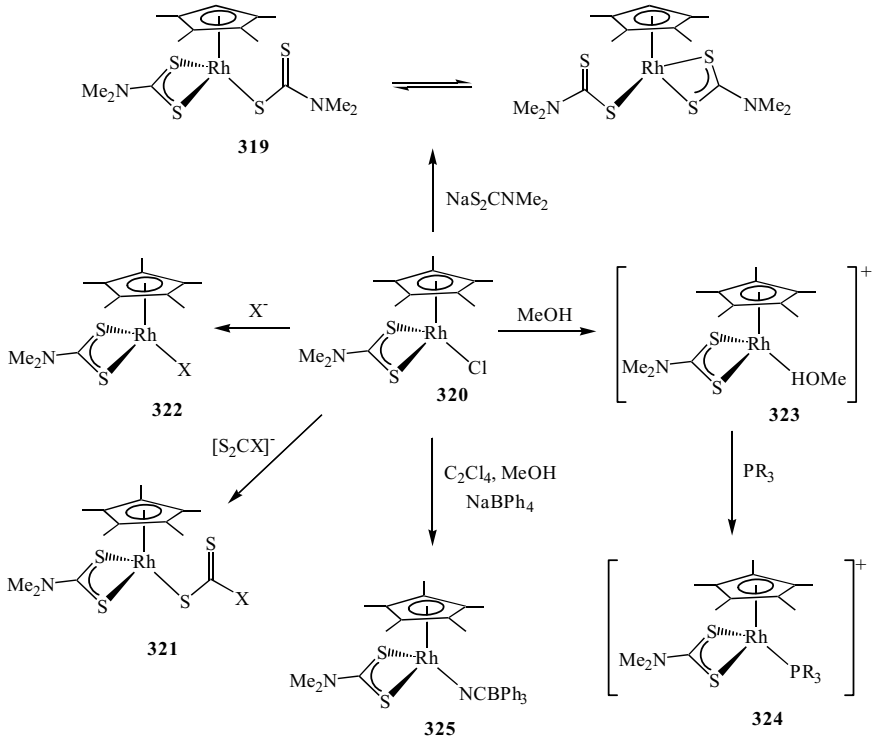

Figure 180. Reactivity of $[Cp^*RhCl(S_2CNMe_2)]$.

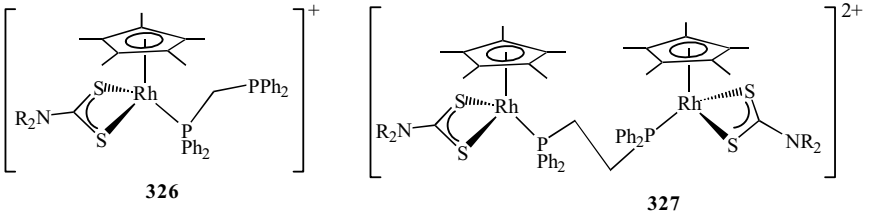

326 **327**

Figure 181. Cationic, pentamethylcyclopentadienyl diphosphine complexes.

dithiocarbamate that is bound in a bidentate manner (1442). The chloride can also be replaced by other anions (Br, I, SCN) (**322**) and dissolves in methanol to afford [Cp*Rh(MeOH)(S_2CNMe_2)]Cl (**323**), which in turn reacts with a wide range of Lewis bases to displace the weakly bound methanol. These include phosphines (**324**), $AsPh_3$, and Py.

The analogous diethyldithiocarbamate complex [Cp*RhCl(S_2CNEt_2)] has also been prepared. Like the dimethyldithiocarbamate complex it reacts with diphosphines leading to the synthesis of $[Cp^*Rh(S_2CNR_2)(\eta^1\text{-dppm})]^+$ (**326**) and $[\{Cp^*Rh(S_2CNR_2)\}_2(\mu\text{-dppe})]^{2+}$ (**327**) (Fig. 181). The latter is formed via an η^1-intermediate, as shown by NMR (1444,1445). Both of the diethyldithiocarbamate complexes have been characterized crystallographically as their BPh_4 salts. Similar phosphine adducts have been prepared in a different way; addition of NaS_2CNEt_2 to $[Cp^*RhCl_2(Ph_2PC_6F_5)]$ in the presence of $NaBF_4$ affords $[Cp^*Rh(S_2CNEt_2)(Ph_2PC_6F_5)][BF_4]$ (1446).

Attempts to bind tetracyanoethylene (TCNE) to the rhodium(III) center, by treating [Cp*RhCl(S_2CNMe_2)] with the alkene in methanol, followed by addition of $NaBPh_4$, were unsuccessful. Instead, a yellow nonconducting solid proposed to be $[Cp^*Rh(S_2CNMe_2)(NCBPh_3)]$ (**325**) (Fig. 180) was isolated. Characterization of the unusual cyanotriphenylborate ion is based on IR and mass spectral data, together with a preliminary crystallographic study of a related complex (1442).

Rhodium(III) dioxygen complexes $[Rh(S_2CNMe_2)(\eta^2\text{-}O_2)L_2]$ ($L = PPh_3$; L_2 = dppe) (**329**) can be prepared from the rhodium(I) complex $[Rh(S_2CNMe_2)L_2]$ (**328**) and oxygen in the presence of the phosphine (Fig. 182) (1447). The monodentate phosphine complex $[Rh(S_2CNMe_2)(\eta^2\text{-}O_2)(PPh_3)_2]$ undergoes a rapid reaction with carboxylic acids to give *trans*-$[Rh(S_2CNMe_2)(PPh_3)_2(\eta^1\text{-}O_2CR)_2]$ (**330**), an example of which ($R = CH{=}CHCO_2H$) has been crystallographically characterized (1448). When carbon dioxide is added to $[Rh(S_2CNMe_2)L_2]$ in the presence of PPh_3, novel peroxycarbonato complexes $[Rh(S_2CNMe_2)(\eta^2\text{-}CO_4)L_2]$ (**331**) result, which in turn yield *trans*-$[Rh(S_2CNMe_2)(\eta^2\text{-}CO_3)L_2]$ (**332**) after oxygen removal by PPh_3. The crystallographically characterized trans-isomer ($L = PPh_3$) is the kinetic product, while heating leads to generation of the thermodynamic cis-isomer (**333**) (1447).

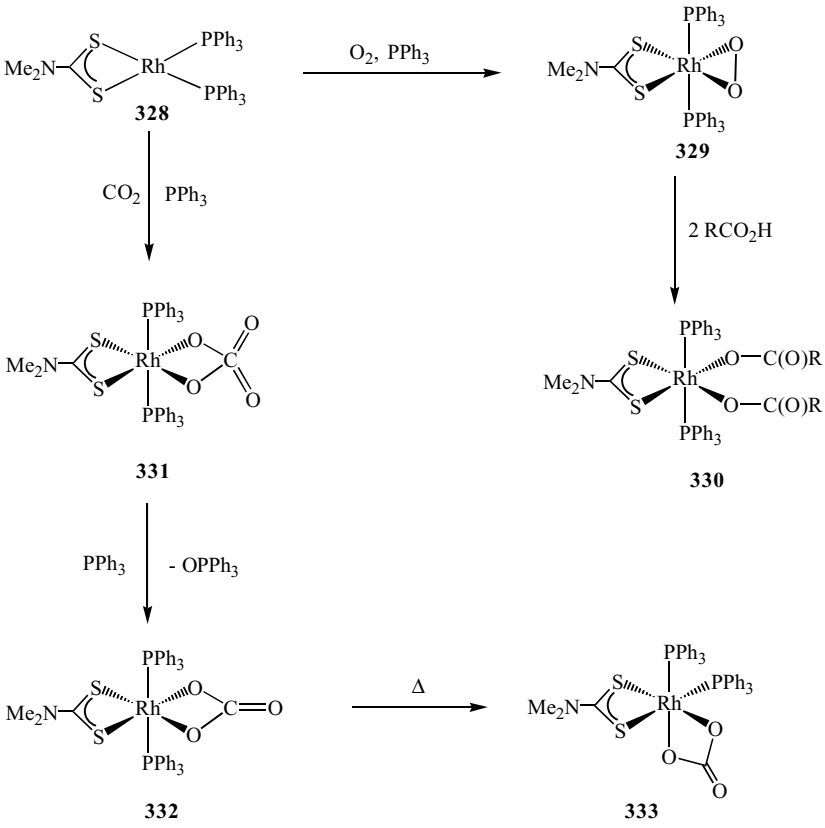

Figure 182. Synthesis and reactivity of octahedral rhodium(III) complexes with oxygen-containing ligands.

Brandt and Sheldrick (1449) reported the synthesis of the macrocycle complex $[RhCl(S_2CNEt_2)(9aneS_3)]^+$ ($9aneS_3 = 1,4,7$-trithiacyclononane), prepared from $[RhCl(MeCN)(9aneS_3)]^{2+}$ and 1 equiv of dithiocarbamate salt. Interestingly, with 2 equiv of dithiocarbamate in methanol, dimeric $[Rh(S_2CNEt_2)_2(\mu\text{-}SR)]_2$ ($R = CH_2CH_2SCH_2CH_2SCH{=}CH_2$) result, which are products of the base-induced ring-opening of the thia-macrocycle.

The same workers also give details of rhodium(III) triphos complexes (1450). Addition of NaS_2CNR_2 to $[RhCl_3(triphos)]$ (triphos = 1,1,1-tris(diphenylphosphino)methane) yields the stereochemically rigid $[RhCl(S_2CNR_2)(triphos)]Cl$ (R = Et, Bz), while addition to $[Rh(MeCN)_3(triphos)]^{3+}$ gives $[Rh(MeCN)(S_2CNR_2)(triphos)]^{2+}$, which in contrast show rapid exchange of phosphorus environments. This result is attributed to an η^3-η^2 interconversion. Isolable bidentate triphos complexes $[Rh(S_2CNR_2)_2(\eta^2\text{-triphos})]^+$ result upon

addition of 2 equiv of dithiocarbamate salts to $[Rh(MeCN)_3(triphos)]^{3+}$, as confirmed crystallographically (R = Et). The uncoordinated phosphorus is further oxidized in solution (Eq. 139).

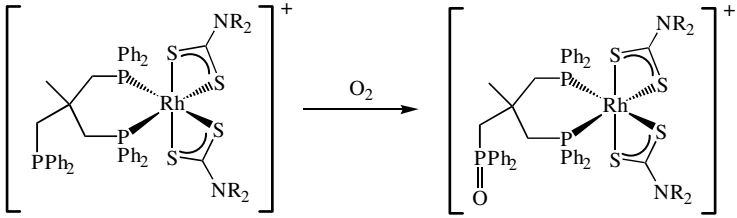

(139)

The borane complex $[Rh(B_{10}H_{10}Te)(PPh_3)(S_2CNHPh)]$ (**334**), resulting from the addition of phenylisothiocyanate to [2,2-$(PPh_3)_2$-2-*H*-1,2-$TeRhB_{10}H_{10}$] in dichloromethane, has been crystallographically characterized, although its precise mode of formation is unknown (220).

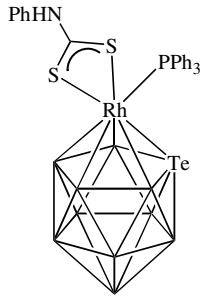

334

Besides the synthesis of tris(dithiocarbamate) complexes, very little further iridium(III) chemistry has been carried out (1451). Addition of NaS_2CNEt_2 to *trans*-$[IrHCl(N_2)(PPh_3)_2(FBF_3)]$ results in the facile loss of the tetrafluoroborate anion and dinitrogen generating *trans*-$[IrHCl(PPh_3)_2(S_2CNEt_2)]$ (1452). Dean has reported the crystal structure of the thiocarboxamido complex $[Ir(CO)(PPh_3)(S_2CNMe_2)(CSNMe_2)][PF_6]$ (**335**) (1453), comparing it with the related rhodium(III) complex $[RhCl(PPh_3)(S_2CNMe_2)(SCNMe_2)]$ (**336**) (Fig. 183) (1454,1455). The major difference between the two is that in the iridium complex a sulfur of the dithiocarbamate ligand lies trans to the thiocarboxamido carbon, while at rhodium, the chloride occupies this position.

b. Monovalent Complexes. A number of rhodium(I) dithiocarbamate complexes are known, all being square planar. For example, the bis(phosphine)

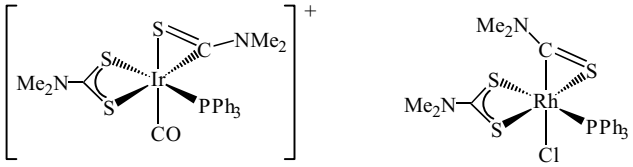

335 **336**

Figure 183. Iridium(III) and rhodium(III) dithiocarboxamido complexes.

complex $[Rh(S_2CNMe_2)(PPh_3)_2]$ is easily prepared from $[RhCl(PPh_3)_3]$ and NaS_2CNEt_2 in the presence of more phosphine (1447). A number of diolefin complexes, $[Rh(S_2CNR_2)(diolefin)]$, can be prepared in a similar fashion from chloro-bridged dimers, $[Rh(diolefin)(\mu\text{-}Cl)]_2$ (285,1456). For example, addition of $[Et_3NH][S_2CNMePh]$ yields $[Rh(S_2CNMePh)(diolefin)]$ (diolefin = cod, NBD). The diolefin is readily replaced, for example, by carbon monoxide and phosphines to give $[Rh(S_2CNR_2)(CO)_2]$ (285,1456) and $[Rh(S_2CNR_2)(PAr_3)_2]$ (1457). Sequential carbonyl substitution can also be carried out on the former to give $[Rh(S_2CNR_2)(CO)(PAr_3)]$ (1456) (Fig. 184).

A number of crystallographic studies have been carried out. The expected square-planar nature of the rhodium(I) center and cis disposition of carbonyl and phosphine is confirmed in isolated molecules of $[Rh(S_2CNEt_2)(CO)(PAr_3)]$ (Ar = *p*-C_6H_4Me) (1457), while in contrast, $[Rh(S_2CNMePh)(CO)_2]$ (**337**) exhibits columnar stacking of the square-planar rhodium(I) units to give almost perfect linear chains [Rh···Rh···Rh 179.47(1)°] with long rhodium–rhodium contacts [Rh···Rh 3.2528(7) Å] (Fig. 185) (285).

A number of binuclear rhodium(I) complexes are known. When carbon monoxide is bubbled through a diethyl ether suspension of [Rh(S_2CN MePh)(NBD)], dimeric $[Rh_2(CO)_2(NBD)(\mu\text{-}S_2CNMePh)_2]$ (**338**) (Fig. 186) results, which is believed to contain two $\mu\text{-}\eta^1,\eta^1$ dithiocarbamates (285). Related binuclear complexes $[Rh_2L_2(cod)(\mu\text{-}S_2CNMePh)]^+$ (L = CO; L_2 = cod) result from reaction of $[Rh(S_2CNMePh)L_2]$ with $[Rh(cod)(acetone)_n]^+$, but here the dithiocarbamate binds in a $\mu\text{-}\eta^2,\eta^2$ fashion as confirmed crystallographically (L_2 = cod) (**339**) (Fig. 186). Solution NMR measurements on $[Rh_2(cod)_2(\mu\text{-}S_2CNMePh)]^+$ show that the two metal centers are equivalent even at −60°C, suggesting a rapid oscillation of the dithiocarbamate CNR_2

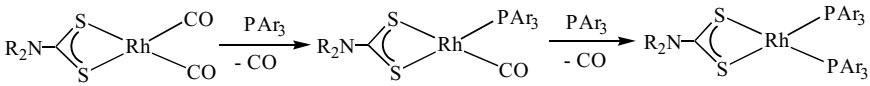

Figure 184. Sequential addition of triaryl phosphines to $[Rh(CO)_2(S_2CNR_2)]$.

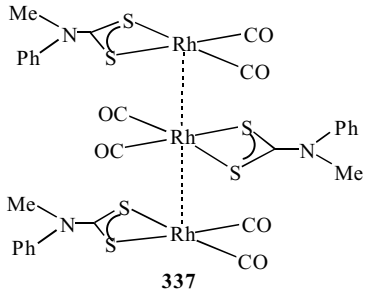

337

Figure 185. Diagramatical representation of the columnar stacking of $[Rh(CO)_2(S_2CNMePh)]$.

moiety between both sides of an idealized plane containing the midpoint of the metal–metal bond and the two sulfur atoms (285).

Reaction of $[Rh(S_2CNEt_2)(CO)_2]$ with 3(5)-*p*-methoxyphenylpyrazole (Hpz^{An}) [Hpz^{An}=3(5)-*p*-methoxyphenylpyrazole] forms dimeric $[Rh(S_2CNEt_2)(CO)(\mu\text{-}pz^{An})]_2$, which can also be prepared from $[RhCl(CO)_2(Hpz^{An})]$ and dithiocarbamate salt (286). Here the dithiocarbamate is not bridging, but interestingly, heating $[Rh(S_2CNEt_2)(CO)_2]$ alone in acetone for 2 h, or upon standing at room temperature for 9 days, generates black $[Rh_2(CO)_2(\mu\text{-}S_2CNEt_2)_2]$, together with amounts of the oxidation product $[Rh(S_2CNEt_2)_3]$. The dimer is believed to have bridging $\mu\text{-}\eta^1,\eta^2$ dithiocarbamate ligands and a rhodium dicarbonyl unit, however, precise structural details remain unknown (286).

Rhodium(I) dithiocarbamate complexes undergo oxidative–addition giving octahedral rhodium(III) products, as discussed with dioxygen earlier (1447). In a similar manner, iodine adds to $[Rh(S_2CNEt_2)(CO)(PAr_3)]$ to give $[RhI_2(S_2CNEt_2)(CO)(PAr_3)]$. With excess methyl iodide, acyl complexes $[RhI(S_2CNR_2)(OCCH_3)(PAr_3)]$ are proposed to result, although precise structural details are unknown (1458).

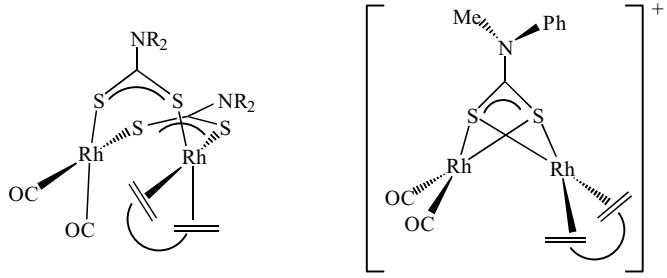

338 **339**

Figure 186. Examples of binuclear rhodium complexes with bridging dithiocarbamate ligands.

Iridium(I) dithiocarbamate complexes have been the subject of a paper by Duckett and co-workers (1451). Reaction of NaS_2CNEt_2 with $[Ir(cod)(\mu\text{-}Cl)]_2$ gives $[Ir(S_2CNEt_2)(cod)]$ from which a range of carbonyl, phosphine, and phosphite complexes are readily prepared via displacement of the diolefin, some of which exhibit luminescence in fluid solution at room temperature. Benzene solutions of $[Ir(S_2CNEt_2)\{P(OPh)_3\}_2]$ are unstable and result in slow formation of the ortho-metalated iridium(III) hydride, $[IrH(S_2CNEt_2)\{P(OPh)_3\}\{P(OPh)_2OC_6H_4\}]$ (Eq. 140), characterized by a hydride resonance at δ −16.02.

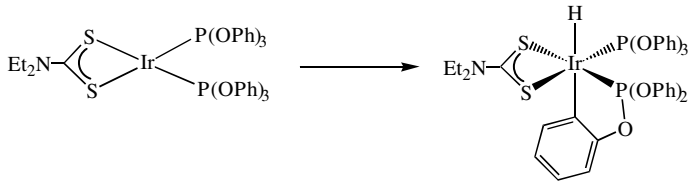

(140)

Further iridium(III) hydride complexes result from addition of hydrogen to $[Ir(CO)(PPh_3)(S_2CNEt_2)]$ (three isomers), $[Ir(PPh_3)_2(S_2CNEt_2)]$ (two isomers), and $[Ir(Ar_2PCH_2CH_2PAr_2)(S_2CNEt_2)]$ ($Ar = C_6F_5$) (one isomer), and ligand exchange in *p*-hydrogen active isomers has been examined. Oxidative–addition of methyl iodide to $[Ir(CO)(PPh_3)(S_2CNEt_2)]$ affords the trans addition product $[IrI(CH_3)(CO)(PPh_3)(S_2CNEt_2)]$ exclusively, while both $[Ir(CO)(PPh_3)(S_2CNEt_2)]$ and $[Ir(dppe)(S_2CNEt_2)]$ add oxygen reversibly, albeit with considerable decomposition upon UV mediated loss of oxygen (Fig. 187).

In another contribution, addition of NaS_2CNMe_2 to $[Ir(cot)(\mu\text{-}Cl)]_2$ (cot = cyclooctene) is reported to afford orange $[Ir(S_2CNMe_2)(cot)_2]$ in 62% yield, a crystal structure showing that the coordinated double bonds lie almost perpendicular to the square plane (1459).

c. Rhodium(II) Complexes. Some uncertainty surrounds the existence of rhodium(II) dithiocarbamate complexes. One group has claimed the preparation of $[Rh(S_2CNR_2)_2(PPh_3)]$ and $[Rh(S_2CNR_2)_2]$ (R = Me, Et) from reactions of dithiocarbamate salts with $[RhCl_2(NO)(PPh_3)_2]$ (1460). Later workers were, however, unable to confirm this and attempts to reproduce the experiments

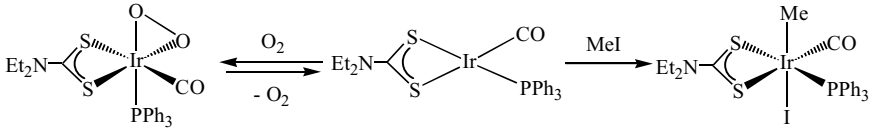

Figure 187. Selected reactions of $[Ir(CO)(PPh_3)(S_2CNEt_2)]$.

lead only to the isolation of mixtures of rhodium(III) complexes including $[Rh(S_2CNEt_2)_3]$ (1461). In the same article, a second attempt was made to prepare a dimeric rhodium(II) dithiocarbamate complex from the reaction of NaS_2CNEt_2 with $[NBu_4][Rh\{S_2C_2(CN)_2\}_2]$, however, again, only $[Rh(S_2CNEt_2)_3]$ resulted.

One further contribution relates to the stabilization of rhodium(II). Addition of TCNQ to $[Rh(S_2CNR_2)(CNPh)_2]$ (R = Me, Et) in hot methanol affords products formulated as $[Rh(S_2CNR_2)(CNPh)_2][TCNQ]$, which on the basis of ESR spectra are believed to contain rhodium(II) and a TCNQ radical anion. Further, it is proposed that the rhodium(II) species is dimeric in the solid state, being bound by a rhodium–rhodium bond (1462).

d. Applications. Few potential applications of rhodium and iridium dithiocarbamate complexes have been developed. The TGA studies have been carried out on both rhodium and iridium complexes (1329,1332,1333). At temperatures up to $\sim$ 553–603 K, tris(dithiocarbamate) complexes decompose to give metal sulfides M_2S_3; which at higher temperatures convert to rhodium metal or nonstoichiometric sulfides of iridium, respectively (1332).

Craciunescu et al. (1463,1464) examined the antitumor activity of a range of rhodium and iridium tris(dithiocarbamate) complexes. Iridium complexes showed low activity against various tumors and there was also a correlation between this activity and their trypanosomicidal activity against various trypanosoma species in rats. Rhodium complexes showed similar behavior with $[Rh(S_2CNHPh)_3]$ being most promising. As a result the nephrotoxic effects of the latter were studied by optical and electron microscopy.

G. Group 10 (VIII B): Nickel, Palladium, and Platinum

1. Nickel

Nickel(II) dithiocarbamate complexes have been known for nearly a century, while since the late 1960s, nickel(IV) complexes have been prepared. These were soon followed by the discovery of nickel(III) complexes, the first crystallographically characterized example coming only in 1990 (1465). Most recent work has served to expand these areas, while electrochemical generation of unstable nickel(I) species has also been documented (1466); and the synthesis of a nickel(I) nitrosyl complex has been claimed (379).

a. Nickel(II) Bis(dithiocarbamate) Complexes. Nickel(II) bis(dithiocarbamate) complexes, $[Ni(S_2CNR_2)_2]$ (**340**), were first prepared by Delépine as early as 1907 (2), and to date a large number have been prepared and studied. Very recently some exciting developments have been documented including the

preparation of complexes bearing ferrocenyl subunits (1467,1468), their use in metal-directed self-assembly reactions (62,1469), and as anion and cation receptors (492,1470,1471).

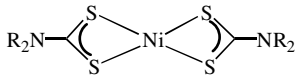

340

They are easily prepared from dithiocarbamate and nickel(II) salts, and examples including those derived from simple amines (587,1472); fluorinated amines (76); amines with ω-hydroxyl groups (1473); indole (**341**); indoline, carbazole, and imidazole (**342**) (72); together with those with heterocyclic (72,1116,1126,1424,1474); benzyl (346,1475); and aryl (95,1423,1425,1476, 1477) substituents. Others include examples prepared from Schiff bases (1121), 2-aryldecahydroquinolin-4-ones (1478), tetrahydroquinoline and tetrahydroisoquinoline (1479), succinimide and phthalimide (49), 1,4,7,10-tetraoxa-13-azacyclopetadecane (50), 1,3,4-thiazolyl (1426), and 3-dithiocarboxy-3-aza-5-aminopentanoate (**343**) (1480,1481). A wide range of amino acid derivatives have also been prepared (122,133–137), as have derivatives of glycine, DL-alanine and DL-valine peptide bonded to ethyl esters of α-amino acids (134).

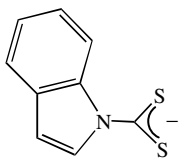

341

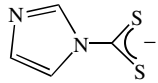

342

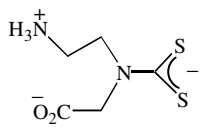

343

In two papers, Grant and co-worker (1482,1483) investigated the kinetics of formation of $[Ni(S_2CNEt_2)_2]$ from $[Ni(dmso)_6]^{2+}$ and NaS_2CNEt_2 in DMSO. When relatively low concentrations of the dithiocarbamate salts are used, $[Ni(S_2CNEt_2)]^+$ is kinetically stabilized, allowing its electronic spectrum to be recorded. It reverts to the bis(dithiocarbamate) by two independent pathways; the first involving direct addition of further dithiocarbamate salt, and the second following a dimerization pathway resulting in formation of $[Ni(S_2CNEt_2)_2]$ and Ni^{2+}.

Nickel(II) complexes with two different dithiocarbamate ligands, $[Ni(S_2CNR_2)(S_2CNR'_2)]$, can be prepared via ligand exchange between pairs of homoleptic complexes (1484). These reactions have been followed HPLC; activation parameters suggest an S_N2 mechanism. While the steric properties of the

substituents affect the rate of ligand exchange, statistical factors seem to determine the position of the equilibrium. Related ligand exchange occurs upon heating $[Ni(S_2CNEt_2)_2]$ and the bis(phenyldithiocabazato) complex $[Ni(S_2CNHNHPh_2)_2]$ in chloroform, resulting in formation of $[Ni(S_2CNEt_2)(S_2CNHNHPh_2)]$ (**344**) (1476).

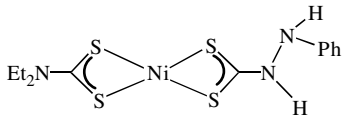

344

Fayyaz and Grant (1477) studied the displacement of a range of monoanionic chelating ligands from the nickel(II) center upon addition of 2 equiv of NaS_2CNEt_2. These include $[Ni\{S_2P(OR)_2\}_2]$, $[Ni(S_2COEt)_2]$, and $[Ni\{SC(Me)CHC(Me)O\}_2]$, while the diphenyldithiocarbamate ligands are also readily displaced from $[Ni(S_2CNPh_2)_2]$. These reactions have been studied kinetically and generally show a second-order dependence with no intermediates being observed. With $[Ni\{SC(Me)CHC(Me)O\}_2]$, however, clear spectrophotometric evidence is seen for a mixed-ligand intermediate, and indeed when the reaction of 1 equiv of NaS_2CNEt_2 was carried out in acetone, the mixed-ligand complex $[Ni(S_2CNEt_2)\{SC(Me)CHC(Me)O\}]$ was isolated (1477).

The melting points of alkyl substituted complexes decrease as the alkyl group length increases, the dioctylamine derivative, $[Ni\{S_2CN\{(CH_2)_7Me\}_2\}_2]$, being prepared as a brown-green wax, which is highly soluble in hydrocarbons (587). Fluorinated derivatives, $[Ni\{S_2CN(CH_2CF_3)_2\}_2]$ and $[Ni\{S_2CNH(CH_2CF_3)\}_2]$, also show high volatility, both subliming when heated at 10^{-2} Torr with volatilization ranges of 75–125°C and 80–120°C, respectively (76).

Both Bruce (1485) and Hoshino-Miyajima (1486) and co-workers prepared bis(dithiocarbamate) complexes with long-chain substituents as potential liquid crystals. Most are derived from four-substituted piperazines with flexible alkoxy tails (**345**), and are mesomorphic, showing smectic phases S_c and crystal B mesophases (1485). Palladium, copper, and zinc bis(dithiocarbamate) complexes of the same ligands showed similar behavior, but nickel piperazine complexes with 4-phenyl, alkyl, and 3-alkoxy tails are non-mesomorphic (1485).

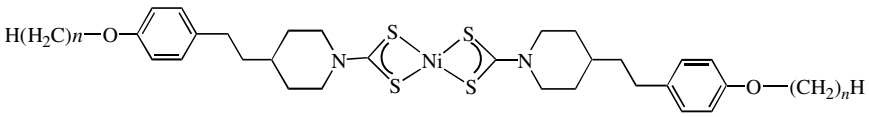

345

Thompson and Moyer have previously shown that reaction of ethylenebis (dithiocarbamate), Na_2(ebdtc).$6H_2O$ with nickel(II) salts affords the coordination polymer [Ni(ebdtc)]$_n$.nH_2O (**346**) (98), which is believed to contain bridging dithiocarbamate ligands. Alonso and Reventós (1487) found that the same polymer was also the major product of the reaction with [$NiCl_2(PPh_3)_2$], while Barrientos et al. (1488) deduced that it has a mean length of 75 units. A similar reaction of [$PPh_4]_2$[ebdtc] with hydrated nickel chloride affords [Ni$_n$(ebdtc)$_{n+1}$] [$PPh_4]_2$ with an average of 3.5 nickel atoms (1487).

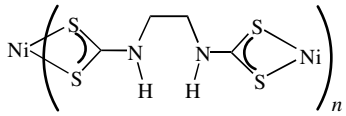

346

Other methods have also been used to prepared nickel(II) bis(dithiocarbamate) complexes. Reactions of primary or secondary amines with metal xanthate complexes have previously been shown to afford a synthetic route to dithiocarbamate complexes, proceeding via nucleophilic attack at the sp^2 carbon (223,224). More recently, the reactions of secondary amines with nickel xanthate complexes [Ni(S_2COR')$_2$] have also been shown to yield [Ni(S_2CNR_2)$_2$]; although yields are highly variable. The reason for this is clear, since thiourethanes, $R_2N{-}C(S)OR'$, are generated in a competing reaction pathway (225). The reaction of carbon disulfide with [Ni{$S(CH_2)_3NH_2$}] is also proposed to yield [Ni{$S_2CNH(CH_2)_3SH$}$_2$], resulting from insertion into the nitrogen–hydrogen bond, although this has not been confirmed crystallographically (199).

In a number of papers, bis(dithiocarbamate) complexes derived from primary amines, [Ni(S_2CNHR)$_2$] (R = Me, *i*-Bu, Bu, Ph, Bz), have been prepared and their chemistry investigated (201,377,379). The amino protons are relatively acidic and can be removed upon addition of triethylamine to give dithiocarbimato complexes. These complexes in turn add a range of electrophiles (E) including acetyl chloride, benzoyl chloride, substituted ureas, carbamic esters, and sulfonamides to give a range of new complexes, [Ni{$S_2CN(E)R$}$_2$] (Fig. 188).

An exciting development in dithiocarbamate chemistry is the synthesis by Beer and co-workers (325,1489) of a range of supramolecular complexes containing nickel(II), zinc(II), and copper(II) bis(dithiocarbamate) centers. These include the preparation of nano-sized resorcarene-based polymetallic assemblies, copper(II) dithiocarbamate macrocycles (62,326,1469,1470), crown-ether derivatives (1471), cryptands (492), and catenanes (544). Details of this work are given in this section and also within the copper and zinc sections (Section IV.H.1 and IV.I.1).

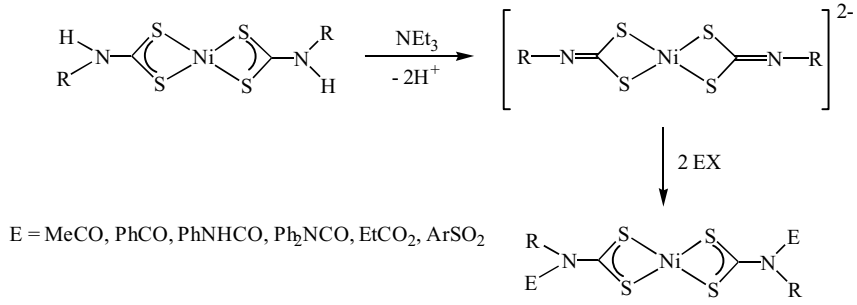

Figure 188. Synthesis of asymmetric nickel bis(dithiocarbamate) complexes from $[Ni(S_2CNHR)_2]$.

A number of dithiocarbamates derived from diamines have been prepared, including those based on a terphenyl backbone, which have utilized these ligands toward the self-assembly of large metal-containing macrocycles upon addition of metal acetates (1468,1469). For example, macrocyclic complexes (**347**) have been prepared in this manner.

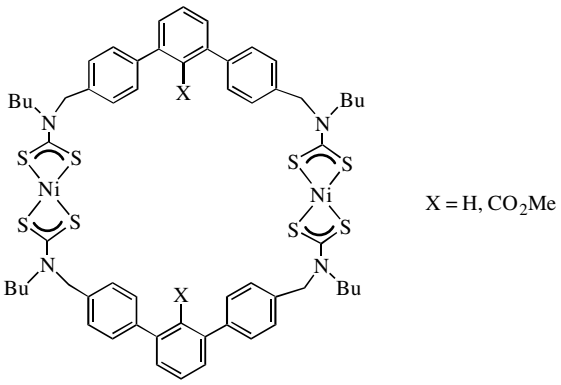

347

Related pyrrole-based metallomacrocycles (**348**) have also been prepared based on a similar principle, as have a range of metallocryptands (**349**) (Fig. 189) (492). The palladium analogue of **348** has also been synthesized.

A number of these complexes have been used as anion receptors (492,1470,1471). These include cyclic (**350**) and acyclic (**351**) dithiocarbamate-based anion receptors (Fig. 190) incorporating thiourea and amide hydrogen-bond donor groups (1470). The NMR titrations with **351** in DMSO-d^6 resulted in significant downshield shifts, particularly for the amide protons, while UV–vis titrations with both **350** and **351** in DMSO show that **350**

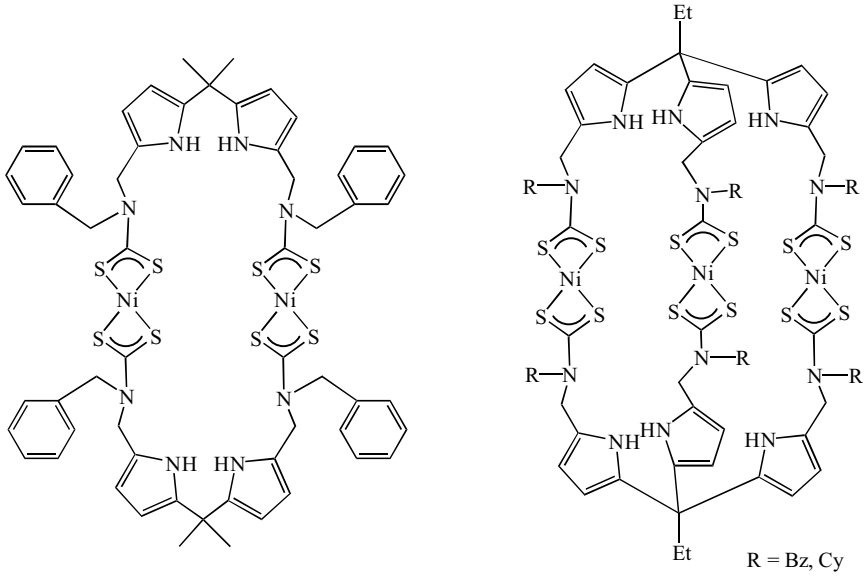

348 **349**

Figure 189. Pyrrole-based nickel(II)-containing macrocycles and crytands.

complexes acetate in a 1:1 stoichiometry, whereas $H_2PO_4^-$ is bound in a 2:1 anion/receptor ratio, while **351** forms strong complexes with carboxylate anions.

Receptor **352** incorporates the well-studied $[Ru(bpy)_3]^{2+}$ subunit. It shows selective downfield shifts in the ^1H NMR spectrum upon addition of anions, displaying the selectivity trend $Cl^- \sim OAc^- > Br^- \gg I^-$, forming stronger complexes with chloride and acetate than its acyclic analogues (1470).

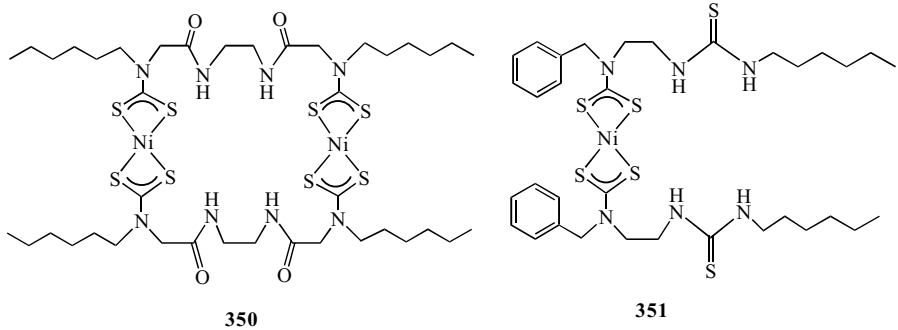

350 **351**

Figure 190. Examples of nickel(II) complexes that can act as anion receptors.

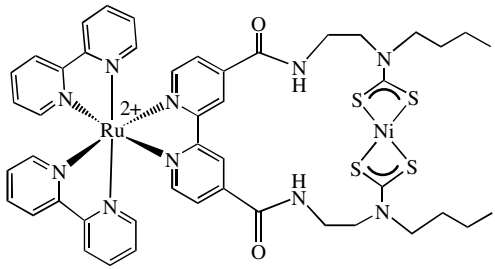

352

Related to this, a crown-ether containing nickel(II) bis(dithiocarbamate) complex **353** has been prepared (1471). As a multisite system, it is capable of exhibiting cooperative complexation of anion–cation pairs. Thus, a sixfold enhancement of the stability constant for acetate results when potassium is cobound at the crown-ether moiety in **353**.

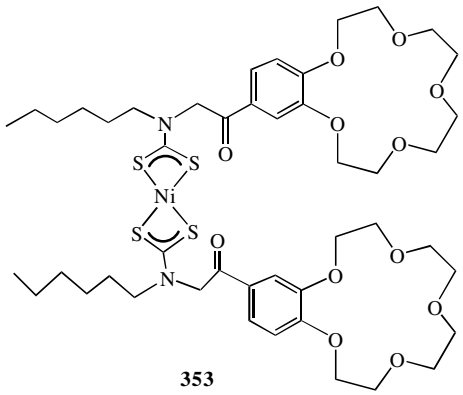

353

In 1999, Tsuchida and co-workers (1467) detailed the first synthesis of nickel(II) bis(dithiocarbamate) complexes bearing ferrocenyl subunits (**354**). These complexes are prepared in three steps from ferrocenecarboxaldehyde.

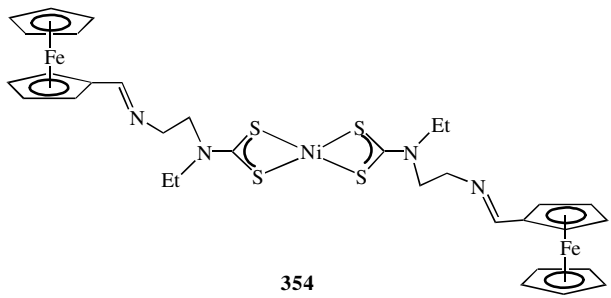

354

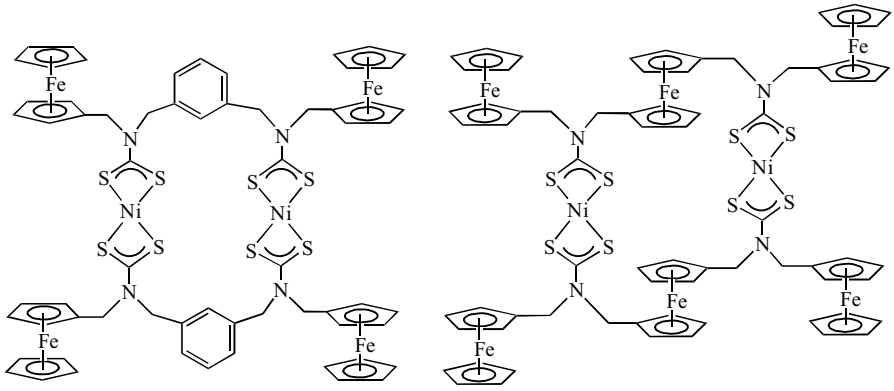

355 **356**

Figure 191. Ferrocene-containing nickel(II) macrocyclic complexes.

Following from this work, Beer and co-workers (1468) developed similar chemistry to incorporate ferrocenyl groups and nickel(II) centers into macrocyclic arrays, such as those found in **355** and **356** (Fig. 191).

A large number of crystallographic studies have been carried out (Table VII). Without exception, all show a square-planar coordination environment bite angles at nickel ranging from 78 to 80°. Nickel–sulfur bonds range between 2.16 and 2.23 Å, being on average the shortest with iso-propyl substituents (393); although interestingly macrocyclic **350** (Fig. 190), with eight crystallographically inequivalent nickel–sulfur bonds (2.164–2.224 Å), shows the full range of bond lengths displayed by this class of complex (492). Structural analyses of $[Ni\{S_2CNMe(CH_2CH_2OH)\}_2]$ and $[Ni\{S_2CN(CH_2CH_2OH)_2\}_2]$ shows that they adopt microchanneled structures formed by networks of hydrogen bonds, the sizes of these channels are estimated at 0.8×0.8 and 0.8×0.3 nm, respectively, while in contrast, for $[Ni(S_2CNC_5H_9OH)_2]$ no such assembly was noted (1473).

Bis(dithiocarbamate) complexes have been studied by a variety of other techniques including XPS (523,550,553–555,1490); polarized optical spectra (1491); the electron spin-echo envelope modulation technique (1492); deformation density maps (510); extended Hückel (1492), quantum mechanical (554), NDDO (1493), and DFT (510) calculations; IR spectroscopy (517); and a normal coordinate analysis using Gibov's fragmentation procedure (1494).

Nickel(II) bis(dithiocarbamate) complexes typically show a maximum absorption at $\sim$ 330 nm in their UV-vis absorption spectra, which is attributed to MLCT, while bands near 220 and 245 nm are assigned to absorptions localized primarily on the dithiocarbamates. Oktavec et al. (1495) studied a wide range of complexes by this technique. Those with longer alkyl chains show an increase in the intensity of λ_{max}, together with a red shift. The polarity of the solvent used also has a significant effect on the spectrum; a blue shift is noted with increasing

solvent polarity. Stability constants for a range of nickel bis(dithiocarbamate) complexes have also been determined by UV–vis spectroscopy (393,1496). The effect of alkyl group stability increases in the order; Me < Et < *n*-Pr < *i*-Pr, a similar trend is found for palladium. This order is partly attributed to changes in the residual positive charge and also to steric effects in branched alkyl groups.

Anderson and Baird (349) carried out a comparative study of the electronic structures of $[Ni(S_2CNEt_2)_2]$ and $[Ni(S_2CNC_4H_4)_2]$. Their calculations confirm that the former is the more readily oxidized of the two, and that neither complex will be susceptible to electrophilic decomposition. Thus, the highest occupied molecular orbitals (HOMOs) of $[Ni(S_2CNEt_2)_2]$ contain appreciable nickel–sulfur antibonding character, and thus electrophilic attack should strengthen these bonds, while for $[Ni(S_2CNC_4H_4)_2]$ the HOMOs are composed primarily of p_z orbitals on the carbon atoms of the pyrrole ring. Attack of a nucleophile on $[Ni(S_2CNEt_2)_2]$ is proposed to lead to a weakening of the carbon–nitrogen backbone bond, since the lowest unoccupied molecular orbitals (LUMOs) are comprised primarily of carbon–nitrogen p_z antibonding character, while $[Ni(S_2CNC_4H_4)_2]$ is predicted to be unaffected.

A number of reactivity studies have been carried out. Some behave as Lewis acids forming adducts, $[Ni(S_2CNR_2)_2B_2]$, although their ability to do this depends markedly upon the nature of the substituents (1497,1498), with adduct forming ability being linked to the electron-withdrawing ability of the substituents. For example, Ramalingham et al. (1499) reported that while no change in the absorption spectrum of $[Ni(S_2CNEt_2)_2]$ occurs upon addition of pyridine, a splitting of λ_{max} does occur for $[Ni\{S_2CN(CH_2CH_2OH)_2\}_2]$, indicative of adduct formation. Similarly, $[Ni\{S_2CN(CH_2CF_3)_2\}_2]$, with strongly electron-withdrawing substituents, forms a stable crystalline adduct with 4-methylpyridine (1500). Sachinidis and Grant (539) used ^{14}N NMR spectroscopy to study pyridine exchange in $[Ni(S_2CNR_2)_2(Py)_2]$ (R = Bz; $R_2 = C_4H_4$), finding it to be more rapid for the pyrrole complex.

Emmenegger (1501) isolated a 1,10-phen adduct $[Ni(S_2CNEt_2)_2(1,10\text{-phen})]$ upon slow cooling of an acetone solution of $[Ni(S_2CNEt_2)_2]$ and a slight excess of 1,10-phen (Eq. 141). The reaction has also been studied spectrophotometrically, the rate of formation being second order and the stability of the complex depending strongly on the organic solvent used, which is attributed to the relative solvation enthalpies and entropies.

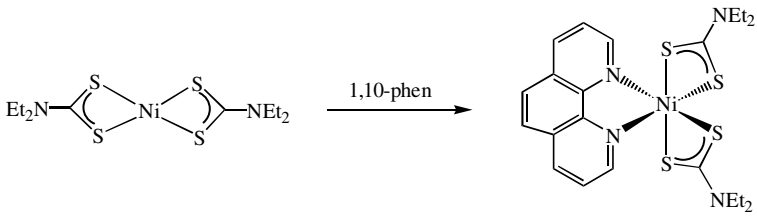

(141)

Preti et al. (1502) showed that cyclic dithiocarbamates complexes $[Ni(S_2CNC_4H_8X)_2]$ (X = O, S, NH, NMe, CH_2) react with 3 equiv of en to give diamagnetic products, $[Ni(S_2CNC_4H_8X)_2(en)_3]$. Their structures are unknown, but formation of salts, $[Ni(en)_3][S_2CNC_4H_8X]_2$, have been ruled out. The authors favor a penta coordinate, high-spin, nickel(II) center with monodentate ethylenediamine and dithiocarbamate ligands.

Addition of metal–sulfide salts $[MS_4]^{2-}$ (M = Mo, W), to $[Ni(S_2CNEt_2)_2]$ results in displacement of one dithiocarbamate and formation of $[Ni(S_2CNEt_2)(\mu\text{-}S)_2MS_2]^-$ (1503). Somewhat related is the addition of $Ph_2P(S)CH_2PPh_2(S)$ ($dppmS_2$) to $[Ni(S_2CNEt_2)_2]$ and $[Ni(S_2CNHAr)_2]$ (Ar = Ph, *p*-tol, α-naphthyl) (1476). Here, adducts of the form $[Ni(S_2CNR_2)_2(dppmS_2)]$ result, although their structural characteristics are unclear.

Interestingly, $[Ni(S_2CNEt_2)_2]$ has also been shown to add Lewis acids. Thus, addition of AsI_3 results in a color change from green to purple and formation of the octahedral bis(adduct), *trans*-$[Ni(AsI_3)_2(S_2CNEt_2)_2]$ (Eq. 142). A related adduct is also formed with SbI_3, but other Lewis acids including $AsBr_3$, $SbCl_3$, and $SbBr_3$ do not bind. The complexes are diamagnetic and are somewhat unstable, especially when heated (1504).

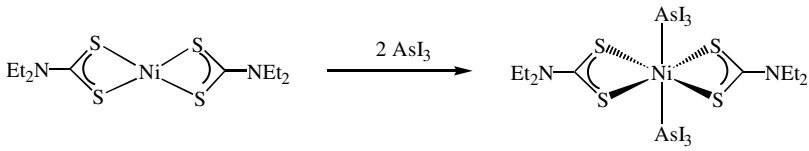

(142)

b. Nickel(II) Mono(dithiocarbamate) Complexes. Nickel(II) mono(dithiocarbamate) complexes fall into four basic types (Fig. 192): (1) neutral complexes, $[NiXL(S_2CNR_2)](K)$; (2) neutral bis(chelate) complexes, $[Ni(S_2CNR_2)(chelate)](L)$; (3) cationic, $[NiL_2(S_2CNR_2)]^+(M)$, and (4) anionic, $[NiX_2(S_2CNR_2)]^-(N)$. All have been extensively studied, each containing a diamagnetic square-planar nickel center.

Neutral complexes of the type $[NiXL(S_2CNR_2)]$ are very common (378,379,1505–1519) and are found for a wide range of monoanionic (e.g.,

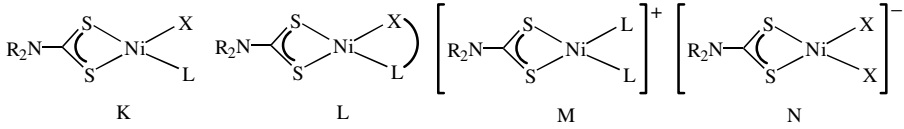

Figure 192. Different types of square planar nickel(II) mono(dithiodithiocarbamate) complexes.

X = Cl, Br, I, NCS, NO_2, SAr, alkyl, C_6F_5) ligands, while the neutral ligand (L) is always a phosphine. They can be prepared in a number of ways, most commonly from a ligand redistribution reaction between $[Ni(S_2CNR_2)_2]$ and $[NiX_2L_2]$ (Eq. 143), while anion metathesis is also widely employed to prepare further derivatives. For example, $[NiCl(PPh_3)(S_2CNHR)]$ (R = Bz, CH_2CO_2Et) can be prepared from $[NiCl_2(PPh_3)_2]$ and the dithiocarbamate salts that are generated *in situ* (1520).

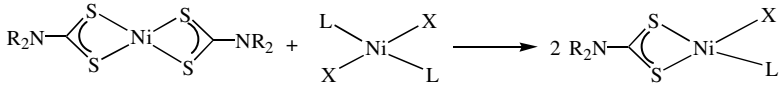

(143)

Organometallic compounds $[Ni(C_6F_5)L(S_2CNR_2)]$ (L = PEt_3, Ph_2PMe, $PhPMe_2$; R = Et, *i*-Pr; R_2 = C_4H_8, C_5H_{10}) result from the addition of dithiocarbamates to *trans*-$[NiClL_2(C_6F_5)]$ (Eq. 144) (1513), while a range of related alkyl complexes, $[Ni(CH_2R)(PMe_3)(S_2CNR'_2)]$ (R = $SiMe_3$, CMe_2Ph; R′ = Me, Et, *i*-Pr), have also been prepared (1519). All complexes of this type are nonelectrolytes, although slightly increased values of molar conductivities have been measured. This observation is considered to result from a partial dissociation of the anion (1511,1513).

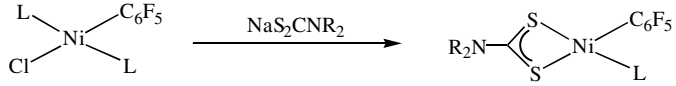

(144)

Like the related bis(dithiocarbamate) complexes, species derived from primary amines $[NiX(PR'_3)(S_2CNHR)]$ (X = Cl, Br, NO_2; R = Me, Et, *i*-Pr, *t*-Bu, Ar; R′ = Bu, Ph) can be deprotonated to give dithiocarbimato complexes, although interestingly a ligand redistribution also occurs such that the isolated products are the bis(phosphine) complexes $[Ni(PR'_3)_2(S_2CNR)]$ (Eq. 145) (378).

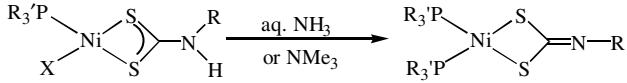

(145)

Neutral bis(chelate) complexes $[Ni(S_2CNR_2)(chelate)]$ are far less common and until recently were limited to dithioacetylacetenoate, $[Ni(S_2CN{-}i\text{-}Pr_2)\{\eta^2\text{-}SC(R)CHC(R)S\}]$ (R = Ph, C_6F_5) (**357**) (Fig. 193) (1521,1522), monothioacetylacetenoate, $[Ni(S_2CNEt_2)\{\eta^2\text{-}SC(Me)CHC(Me)O\}]$ (1477), and thiophosphate, $[Ni(S_2CNMe_2)\{S_2P(OMe)_2\}]$ (1523), complexes. Very recently a number of new complexes of this type have been prepared. Dimethylglyoxime (dmg)

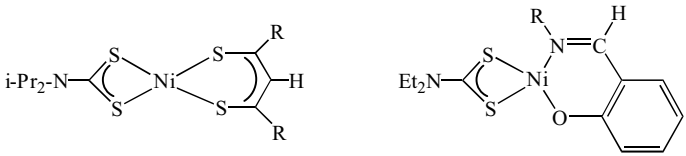

357 **358**

Figure 193. Examples of complexes of the type $[Ni(S_2CNR_2)(chelate)]$.

complexes, $[Ni(S_2CNR_2)(dmg)]$ ($R = Et$; $R_2 = C_5H_{10}$), result from the reaction of $[Ni(S_2CNR_2)_2]$ and dmg in ethanol at 60°C in the presence of ammonia, although with $[Ni\{S_2CN(CH_2CH_2OH)_2\}_2]$ only $[Ni(dmg)_2]$ is formed (1524). Alkylsalicylaldiminate (Rsal) complexes $[Ni(S_2CNEt_2)(Rsal)]$ ($R = Et$, *i*-Pr, *i*-Bu) (**358**) (Fig. 193) have also been prepared starting from $[Ni(Rsal)_2]$ (1525), as have monomeric, $[NiL(S_2CNC_4H_8)]$, and dimeric, $[Ni_2L_2(S_2CNC_4H_8NCS_2)]$, containing tridentate monoanionic N_2O ligands, although their structures have not been determined (1526).

Two types of charged nickel(II) mono(dithiocarbamate) complexes can be identified: cationic $[NiL_2(S_2CNR_2)]^+$ and anionic $[NiX_2(S_2CNR_2)]^-$. The former are by far the more prevalent and can be stabilized by a range of monodentate (**359**) or bidentate (**360**) (Fig. 194) phosphine ligands (132,1348,1490,1509,1527–1540). While a number of synthetic routes have been adopted, most common is the thermolysis of $[Ni(S_2CNR_2)_2]$ and the relevant phosphine in the presence of an anion source, with monodentate phosphines often requiring addition of nickel chloride. The phosphines utilized generally carry aryl substituents, but $[Ni(i\text{-}Pr_2PCH_2CH_2P\text{-}i\text{-}Pr_2)(S_2CNR_2)]Br$ (**360**) (Fig. 194) have been prepared from $[NiBr_2(i\text{-}Pr_2PCH_2CH_2P{-}i\text{-}Pr_2)]$ upon addition of dithiocarbamate salt (1529). Pastorek et al. (1532,1533) detailed the synthesis of a large number of cationic complexes with a range of diphosphine ligands including ferrocenyl diphosphine. In these reports they also detail the formation of dimeric materials, $[Ni_2(S_2CNR_2)_2(NCS)_2(diphosphine)]$, when $[Ni(NCS)_2.6H_2O]$ is utilized, although their precise nature remains as yet unclear.

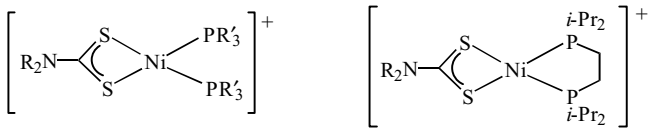

359 **360**

Figure 194. Examples of cationic nickel(II) phosphine complexes.

Serrano et al. (1541) recently prepared a series of complexes of the type, $[Ni(S_2CNR_2)(o\text{-}Ph_2PC_6H_4CH{=}NR')][ClO_4]$ (R = *i*-Pr, *i*-Bu; R′ = Me, Et, *i*-Pr, *t*-Bu) (**361**), containing chelating iminophosphine ligands. They result from the direct reaction between $[Ni(S_2CNR_2)_2]$, nickel perchlorate, and the iminophosphine in ethanol. Two examples have been crystallographically characterized: relatively large dihedral angles of ~9–10° were found between the two chelating ligands, as compared to values of <5° for the majority of compounds of this general type.

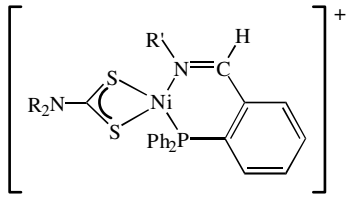

361

Two types of anionic complexes, $[NiX_2(S_2CNR_2)]^-$, have been detailed (1503,1542,1543). Organometallic complexes $[Ni(C_6F_5)_2(S_2CNR_2)][NBu_4]$ (R = Me, Et; R_2 = HEt, HPr, C_4H_8, C_5H_{10}, C_4H_8O) (**362**) (Fig. 195) result from the reaction of $[Ni(C_6F_5)_2(\mu\text{-}OH)]_2[NBu_4]_2$ with 2 equiv of amine in the presence of carbon disulfide (1543), while as detailed earlier, metal–sulfide salts, $[MS_4]^{2-}$ (M = Mo, W), react with $[Ni(S_2CNR_2)_2]$ (R = Et, Bu; $R_2 = C_4H_8$) to give $[Ni(S_2CNR_2)(\mu\text{-}S)_2MS_2]^-$ (1503,1542). One example of the latter, namely, $[Ni(S_2CNC_4H_8)WS_4][NEt_4]$ (**363**) (Fig. 195), has been crystallographically characterized (1542). It contains a square-planar nickel(II) center linked via two sulfido bridges to a distorted tetrahedral tungsten(VI) ion. Electrochemical reduction of $[Ni(S_2CNBu_2)MoS_4]^-$ results in the formation of the corresponding dianion, which has been probed using ESR spectroscopy. A large anisotropy seen in the observed *g* values appears to be inconsistent with the formation of a molybdenum(V) center, but a molecular orbital analysis of $[Ni(S_2CNH_2)\text{-}MoS_4]^{2-}$ that the singly occupied molecular orbital (SOMO) is molybdenum based (1544).

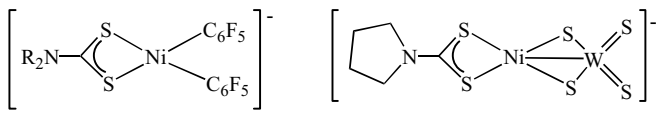

362 **363**

Figure 195. Examples of anionic nickel(II) mono(dithiocarbamate) complexes.

X-ray photoelectron spectra have been measured for a range of nickel(II) complexes including $[Ni(S_2CNEt_2)_2]$, $[Ni(PPh_3)_2(S_2CNR_2)]ClO_4$, and $[NiCl(PPh_3)(S_2CNR_2)]$ (553,1490). Alkyl substituents do not significantly effect the spectra and all show similar binding energies (853.0–853.4 eV) except for the NiS_2P_2 chromophores, $[Ni(PPh_3)_2(S_2CNR_2)]ClO_4$, which are higher (854.1 eV). This difference is proposed to result from the location of excessive positive charge on nickel, and electrochemical measurements appear to support this as they have the lowest one-electron reduction potentials (553). Thus, the relative reduction potentials of nickel(II) dithiocarbamate complexes follow the order: $[NiCl(PPh_3)(S_2CNR_2)] > [Ni(S_2CNR_2)_2] > [Ni(PPh_3)_2(S_2CNR_2)]^+$. Similarly, a change in the value of ν(CN) in the order: $[Ni(PPh_3)_2(S_2CNR_2)]^+ > [NiCl(PPh_3)(S_2CNR_2)] > [Ni(S_2CNR_2)_2]$ suggests that in the cationic complexes there is a greater degree of the thioureide resonance form in the dithiocarbamate.

Alonso and Reventós have described the reactivity of ethylenebis(dithiocarbamate), $Na_2(ebdtc).6H_2O$ (98,1545), toward nickel(II) phosphine complexes (1487). With $[NiCl_2(PPh_3)_2]$, the major product is polymeric $[Ni(ebdtc)]_n.nH_2O$ (see earlier), with dimeric $[\{NiCl(PPh_3)\}_2(\mu\text{-ebdtc})]$ (**364**), also being formed in small amounts. With $[NiCl_2(dppe)]$, a second polymeric species is generated, believed to be $[Ni(\eta^1\text{-dppe})(ebdtc)]_n$, containing a five-coordinate nickel(II) center. Interestingly, the same group have also reported that addition of 2 equiv of NaS_2CNEt_2 to $[NiCl_2(dppe)]$ yields orange $[Ni(dppe)(S_2CNEt_2)_2]$ (**365**), shown by IR spectroscopy to contain only bidentate dithiocarbamates, and postulated on the basis of its magnetic moment (μ 2.85 BM) to be octahedral.

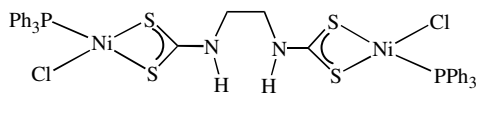

364

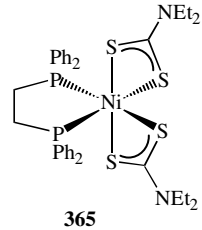

365

c. Other Nickel(II) Dithiocarbamate Complexes. A number of further octahedral nickel(II) dithiocarbamate complexes have been prepared. Addition of dithiocarbamate salts to tetraazamacrocyclic complexes [Ni(DL-CTH)] $[ClO_4]_2$ (DL-CTH = *rac*-5,5,7,12,12,14-hexamethyl-1,4,8,11-tetraazacyclotetradecane] and [Ni(cyclam)]$[ClO_4]_2$ (cyclam = 1,4,8,11-tetraazacyclotetradecane) yields octahedral complexes $[Ni(DL\text{-}CTH)(S_2CNR_2)][ClO_4]$ and $[Ni(cyclam)(S_2CNR_2)][ClO_4]$ (R = Me, Et; $R_2 = C_4H_4$), respectively, with $[Ni(DL\text{-}CTH)(S_2CNEt_2)][ClO_4]$ being crystallographically characterized (1546). Attempts to generate nickel(III) complexes upon oxidation lead only to decomposition.

Further reports on other octahedral nickel(II) mono(dithiocarbamate) species include the synthesis of a range of 1,10-phen complexes $[Ni(phen)_2(S_2CNR_2)]^+$, in which the dithiocarbamates are derived from α-amino acids. Here, on the basis of IR and electronic spectroscopy, molecular association is proposed to occur as a result of hydrogen bonding between the NH and carboxylate groups (119).

Nickel(II) cyclopentadienyl complexes $[(\eta^5\text{-}C_5Ph_5)Ni(S_2CNMe_2)]$ (1464) and $[(\eta^5\text{-}C_5Me_5)Ni(S_2CNEt_2)]$ (1547) have been prepared, the latter from an unusual reaction between $[(\eta^5\text{-}C_5Me_5)Ni(CO)]^-$ and $Te(S_2CNEt_2)_2$ (Eq. 146) (1547).

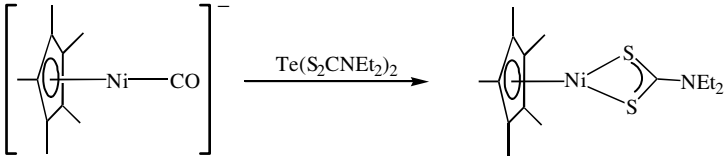

(146)

Binuclear nickel(II) thiolate- and selenolate-bridged dithiocarbamate complexes have also been prepared. Addition of aryl thiolates to $[NiX(PPh_3)(S_2CNR_2)]$ (X = Cl, Br) in the presence of triethylamine affords $[Ni(S_2CNR_2)(\mu\text{-}SAr)]_2$ (1512,1548); related selenolate species $[Ni(S_2CNEt_2)(\mu\text{-}SeR)]_2$ (R = Me, Bz) result from $[NiCl(PPh_3)(S_2CNEt_2)]$ and RSe^- (1549). Interestingly, with aryl selenolates the first product formed is mononuclear, $[Ni(SeAr)(PPh_3)(S_2CNEt_2)]$ (Ar = Ph, $p\text{-}C_6H_4Cl$) (**366**), however, the phosphine can later be removed as the sulfide upon reaction with elemental sulfur to yield binuclear complexes $[Ni(S_2CNEt_2)(\mu\text{-}SeAr)]_2$ (**367**) (Fig. 196) (1549).

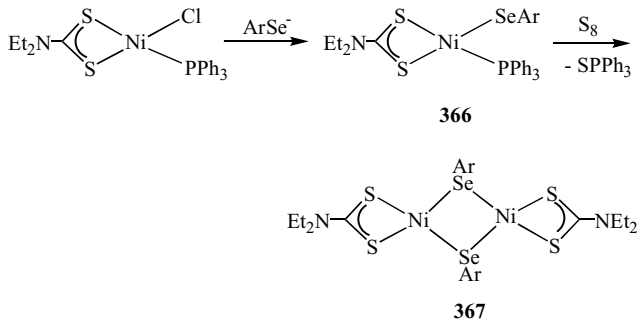

Figure 196. Generation of $[Ni(SeAr)(PPh_3)(S_2CNEt_2)]$ and subsequent conversion to binuclear complexes.

Schulbert and Mattes (1550) reported the synthesis of $[Ni(S_2CNHMe)(\mu\text{-}SMe)]_2$ (**368**), formed from nickel acetate and the dithiocarbamic acid ester MeHNC(S)SMe in a degradation reaction. A crystallographic study shows that in the solid-state two dimeric units are held together by weak Ni···S interactions [3.512(6)–3.709(6) Å] to give a tetramer [Ni···Ni 2.761(4) and 2.831(4) Å].

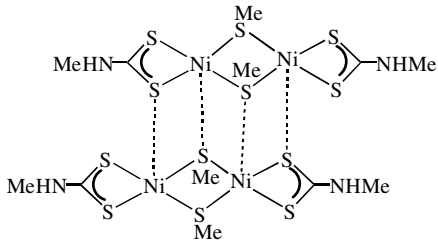

368

Somewhat related to these chalcogenide-bridged complexes are trinuclear $[\{Ni(S_2CN\text{—}i\text{-}Pr_2)(\mu\text{-}Ph_2PO)_2\}_2Pd]$ and tetranuclear $[\{Ni(S_2CN\text{—}i\text{-}Pr_2)(\mu\text{-}Ph_2PO)_2\}_3M]$ (M = Ga, In, Al), formed in the same way as their palladium and platinum counterparts upon refluxing $[\{Ni(S_2CN\text{—}i\text{-}Pr_2)(Ph_2PO)_2H]$ with various metal acetates in toluene (1551).

A single contribution describes the synthesis of trinuclear nickel(II) complexes, $[Ni_3(PR_3)_2(S_2CNEt_2)_2(\mu^3\text{-}S)_2]$ (R = Me, Et) (**369**), formed upon reaction of NaS_2CNEt_2 with $[Ni_3(PR_3)_6(\mu^3\text{-}S)_2][BPh_4]_2$. A crystallographic study (R = Et) shows the nickel triangle contains two short [2.853(2) Å] and one long [2.950(2) Å] nickel–nickel contact, the latter between the dithiocarbamate-carrying nickel centers (1552).

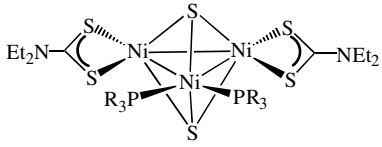

369

d. Nickel(III) and Nickel(IV) Complexes. Nickel(III) and (IV) dithiocarbamate complexes were both known prior to 1978. A wide range of brown nickel(IV) tris(dithiocarbamate) complexes, $[Ni(S_2CNR_2)_3]X$, have been prepared upon addition of halogens to $[Ni(S_2CNR_2)_2]$ (1553–1555), while nickel(III) complexes, $[Ni(S_2CNR_2)_2I]$, have been prepared in a similar manner upon

addition of iodine at low temperatures (1556).

(147)

More recently, other oxidizing reagents have been used (Eq. 147). Oxidation of $[Ni(S_2CNEt_2)_2]$ by $NOBF_4$ has been shown by ESMS to yield both $[Ni(S_2CNEt_2)_2]^+$ and $[Ni(S_2CNEt_2)_3]^+$. When a mixture of $[Ni(S_2CNEt_2)_2]$ and $[Ni(S_2CNBz_2)_2]$ was used, all possible mixed tris(dithiocarbamate) cations were observed indicating that ligand exchange is rapid at the nickel(IV) center (303). In a similar manner, oxidation of $[Ni(S_2CNR_2)_2]$ by iron(III) salts provides a convenient route to nickel(IV) complexes, $[Ni(S_2CNR_2)_3]X$ ($X = ClO_4$, $FeCl_4$) (1557,1558). Eckstein and Hoyer (1559) also prepared a wide range of nickel(IV) salts ($R = Me$, Et, Pr, Bu, *i*-Bu, Cy; $R_2 = C_5H_{10}$; $X = Br$, BF_4, ClO_4, NO_3, PF_6) using a number of different synthetic routes.

The product of the oxidation of $[Ni\{S_2CN(CH_2CH_2OH)_2\}_2]$ is medium dependent. When carried out in neutral or alkaline solution, the thiuram disulfide results, while under acidic conditions, the nickel(IV) tris(dithiocarbamate) cation is the major product (1560). Controlled potential electrolysis of $[Ni(S_2CNEt_2)_2]$ in acetonitrile at the first oxidation potential has been monitored by UV–vis spectroscopy. A nickel(III) intermediate is observed, but decomposes to give nickel(II) and tetraethylthiuram disulfide (1561). In contrast, oxidation of $[Ni(S_2CNEt_2)_2]$ by TCNE yields the isolable nickel(IV) complex $[Ni(S_2CNEt_2)_3][C_3(CN)_5]$, which has been crystallographically characterized. The coordination geometry about nickel is octahedral as expected, with nickel–sulfur bonds varying between 2.246(2) and 2.257(2) Å (1562).

Recently, Beer et al. (62) prepared the novel nickel(IV) complex **371**, in which two metal centers are linked via three bis(dithiocarbamate) ligands, upon oxidation of the related macrocyclic complex **370** by *N*-bromosuccinimide (NBS) (Fig. 197). The nickel(IV) dication **371** binds both chloride and nitrate anions as shown by cathodic shifts of the Ni(IV)/Ni(III) wave of 70 and 15 mV, respectively.

Electrochemical and spectroelectrochemical investigations by Tsucida have shown that oxidation of $[Ni\{S_2CN(Et)CH_2CH_2N{=}CHFc\}_2]$ (**354**) ($Fc = CpFeC_5H_4$) affords the nickel(IV) cation $[Ni\{S_2CN(Et)CH_2CH_2N{=}CHFc\}_3]^+$

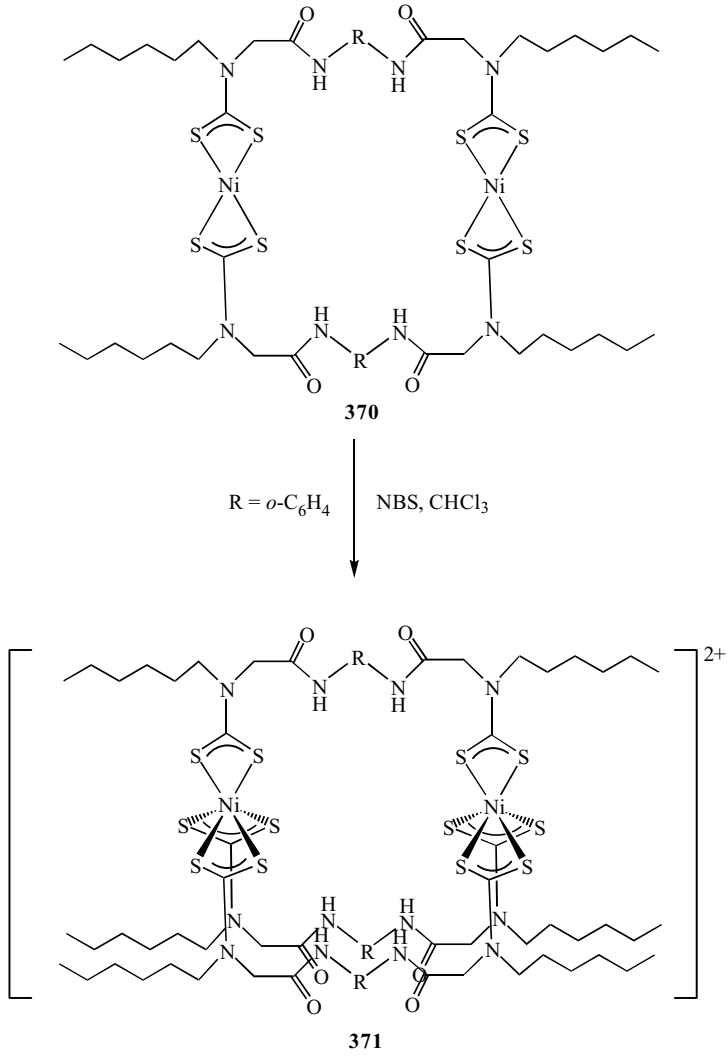

370

371

Figure 197. Oxidative synthesis of linked tris(dithiocarbamate)nickel(IV) complex.

in a four-electron process. The latter then undergoes a further three-electron oxidation in two steps, resulting in one and then all three of the iron centers being oxidized. These two processes are separated ($\Delta E = 250$ mV), which is related to the comproportionation equilibrium (Eq. 148), and despite the chemical equivalence of the three ferrocenyl groups, the mixed-valence state

$[Ni^{IV}Fe^{III}(Fe^{II})_2]^{2+}$ persists for some time in solution (1467).

$$[Ni^{IV}(Fe^{II})_3]^{+} + [Ni^{IV}(Fe^{III})_2Fe^{II}]^{3+} \rightleftharpoons 2\,[Ni^{IV}Fe^{III}(Fe^{II})_2]^{2+} \qquad (148)$$

Fackler et al. (1563) previously showed that the brown color of $[Ni(S_2CNBu_2)_3]^{+}$ can be photochemically and thermally bleached in acetonitrile. Thiuram disulfide and $[Ni(S_2CNBu_2)_2]$ are the products and the process reversible. Eckstein and Hoyer (1559) studied this photochromic behavior in some detail measuring rate constants and quantum yields as a function of the dithiocarbamate substituents and anions (Fig. 198).

Photoreduction study of $[Ni(S_2CNEt_2)_3][BF_4]$ also occurs upon exposure to soft X-rays, generating $[Ni(S_2CNEt_2)_2]$; the rate of the photochemical transformation for a range of complexes, $[Ni(S_2CNR_2)_3][BF_4]$, is proportional to the photon flux, and is also sensitive to the nature of the substituents (1564). Plyusnin and co-workers (24,1565,1566) studied the photolysis of $[Ni(S_2CNR_2)_3]^{+}$ in solution, in a frozen matrix, and on laser flash photolysis (1565), showing that all phototransformations occur within the coordination sphere of the complex. While using ESR spectroscopy, Eckstein et al. (1567) detected intermediate nickel(III) complexes after irradiation of $[Ni(S_2CNR_2)_3]^{+}$ in frozen acetonitrile at 120 K.

A number of nickel(III) dithiocarbamate complexes have been prepared. Oxidation of $[Ni(S_2CNR_2)_2]$ ($R = CH_2CH_2OH$; $R_2 = C_4H_8$, C_5H_{10}) by halogens, nitric acid, or $NO[ClO_4]$ is reported to yield $[Ni(S_2CNR_2)_2]X$ (X = Cl, Br, I, NO_3, ClO_4) (**372**) (Fig. 199). Most are paramagnetic with magnetic moments of 1.37–2.25 BM (1472,1567), although interestingly $[Ni(S_2CNC_5H_{10})_2]X$ ($X = NO_3$, ClO_4) are reported to be diamagnetic (1568). Nickel(III) complexes supported by a single dithiocarbamate ligand have also been reported. Oxidation of $[NiX(PPh_3)(S_2CNR_2)]$ (X = Br, NCS; R = Et, Bu; R_2 = HEt, HBu, C_4H_8O, C_5H_{10}) by bromine yields paramagnetic $[NiX(PPh_3)(S_2CNR_2)]Br$ (μ_{eff} 1.61–2.04 BM) (**373**) (Fig. 199) (1505,1515).

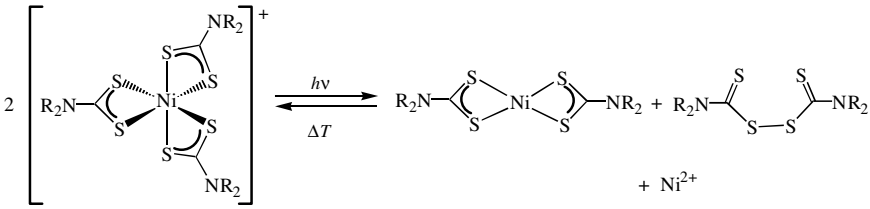

Figure 198. Reversible photobleaching of brown $[Ni(S_2CNR_2)_3]^{+}$.

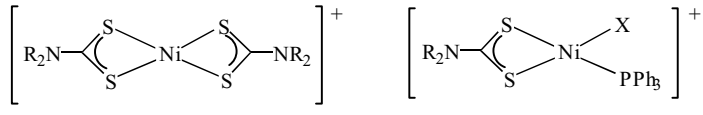

372 373

Figure 199. Examples of nickel(III) dithiocarbamate complexes.

The photochemical addition of tetraethylthiuram disulfide to $[Ni(S_2CNEt_2)_2]$ has been studied in some detail (1569–1571). It results in a color change from green to brown, and the gradual growth of an ESR signal believed to result from initial formation of $[Ni(S_2CNEt_2)_3]$ and a dithiocarbamate radical, with the latter reacting with more $[Ni(S_2CNEt_2)_2]$ (1569). Kinetic studies support the idea of a two component formation of nickel(III). The equilibrium constant is found to be dependent on the solvent polarity. The photochemically generated nickel(III) complex $[Ni(S_2CNEt_2)_3]$ has been characterized by UV–vis spectroscopy (1571), but decays over a few seconds. Accordingly, precise structural characteristics remain unknown, with Ivanov favoring a five-coordinate square-based pyramidal array (Fig. 200) (1571). Given the instability of this nickel(III) complex it is very surprising that a recent report details the crystal structure of octahedral $[Ni(S_2CNEt_2)_3]$ (397). This is surely a mistake (being most probably the cobalt complex).

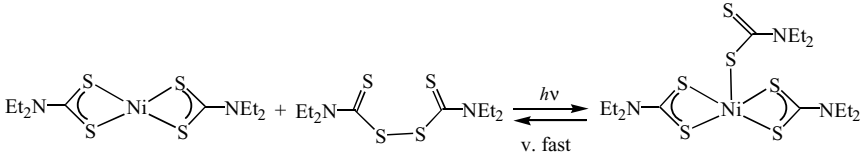

Figure 200. Proposed formation and rapid decay of five-coordinate $[Ni(S_2CNEt_2)_3]$.

The nickel(II) complex, $[(\eta^5\text{-}C_5Ph_5)Ni(MeCN)_2]BF_4$, has been shown to react with tetramethylthiuram di- or monosulfide giving $[(\eta^5\text{-}C_5Ph_5)Ni(S_2CNMe_2)]BF_4$ (1465). The latter has an effective magnetic moment of 1.77 BM and has become the first 17-electron, nickel(III) complex to be structurally characterized. The cation can also been prepared electrochemically from $[(\eta^5\text{-}C_5Ph_5)Ni(S_2CNMe_2)]$, a process that is reversible (Eq. 149). A one-electron reduction of the neutral complex also occurs at -1.43 V to give an unstable nickel(I) complex $[(\eta^5\text{-}C_5Ph_5)Ni(S_2CNMe_2)]^-$ (see below).

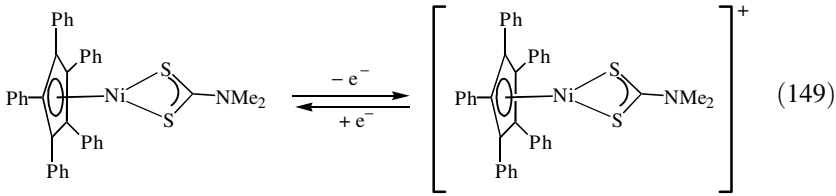

(149)

e. Nickel(I) Complexes. Stable nickel(I) dithiocarbamate complexes remain elusive. Boyd and co-workers (1466) attempted to generate such species electrochemically. Reduction of $[Ni(S_2CNR_2)_2]$ at a platinum electrode in dichloromethane yields $[Ni(S_2CNR_2)_2]^-$, which are also prepared by γ-irradiation of frozen solutions of $[Ni(S_2CNR_2)_2]$. The ESR measurements suggest that they contain a square-planar nickel(I) center, but they show poor stability decomposing to new nickel(I) species with "reversed" *g* values. Reduction of cations $[Ni(dppe)(S_2CNR_2)][PF_6]$ have also been studied in an attempt to generate nickel(I) complexes. Such species can be formed at a platinum electrode, with ESR spectra suggesting equivalent phosphorus environments. However, they are unstable with respect to disproportionation to $[Ni(S_2CNR_2)_2]$ and $[Ni(dppe)_2]$ (1466).

Given the instability of the electrogenerated nickel(I) complexes described above, the generation of a stable nickel(I) nitrosyl complex seems unlikely. However, it has been reported that reduction of $[Ni(NO_2)(PBu_3)(S_2CNHR)]$ by CO affords such complexes, namely, $[Ni(NO)(PBu_3)(S_2CNHR)]$, a transformation that is reversed upon exposure to oxygen (Eq. 150) (379).

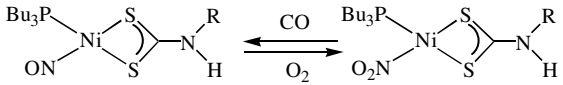

(150)

e. Applications. Relatively few applications of nickel dithiocarbamate complexes have been reported. As detailed above, some bis(dithiocarbamate) complexes display mesomorphic liquid-crystal properties (1485,1486), while others have been found to be efficient, and somewhat selective, anion receptors (492,1470,1471).

Nickel sulfide has a band gap of 0.5 eV, which confers potential for use as a thermophotovoltaic converter. In light of this, nickel(II) bis(dithiocarbamate) complexes have been used as molecular precursors. For example, Noumura and Hayata (1572) used $[Ni(S_2CNEt_2)_2]$ to deposit $NiS_{1.03}$ onto a Si(111) surface by low-pressure MOCVD, while O'Brien (1573) used the same diethyldithiocarbamate complex as well as $[Ni(S_2CNMeR)_2]$ (R = Et, Bu, hexyl) to deposit NiS and $NiS_{1.03}$ films on glass. Katsoulos and co-workers (1574) also report TGA studies on $[Ni(S_2CNHR)_2]$, weight losses being indicative of the formation of nickel sulfides. Interestingly, one report suggests that decomposition of $[Ni(S_2CNEt_2)_2]$ in the presence of H_2S affords the sulfur-deficient material Ni_3S_2 [1437], and in light of this, further work in this area may be warranted.

Bis(dithiocarbamate) complexes have also been shown to be very efficient singlet oxygen quenchers (1575,1576). Recently a series of complexes, $[Ni(S_2CNR^1R^2{}_2)_2]$, (R^1 = H, R^2 = Bu, CH_2CH_2OH; $R^1 = R^2$ = Bu, CH_2CH_2OH), were shown to be efficient oxygen quenchers in solution in the presence of an

acid activated clay, while on dry clay only the hydroxyl-containing complexes were active (1576). Related to this, $[Ni(S_2CNBu_2)_2]$ has been shown to strongly inhibit the light-induced fading of crystal violet lactone dye, an oxidative process involving peroxides. Allan et al. (1577) investigated reactions of $[Ni(S_2CNBu_2)_2]$ with organic peroxides, the main transformation products being organosulfites and sulfur oxides.

2. *Palladium and Platinum*

Palladium and platinum dithiocarbamate complexes are known for the +2 and +4 oxidation states, although the former is by far the more prevalent. Stable complexes are not known in either the +1 or +3 oxidation states, although some evidence has been found for the generation of both in electrochemical experiments (231,1561,1578).

a. Bis(dithiocarbamate) Complexes. Bis(dithiocarbamate) complexes $[Pd(S_2CNR_2)_2]$ (**374**) and $[Pt(S_2CNR_2)_2]$ (**375**) were first reported by Malatesta (1325) and Delépine (2), respectively, and to date a large number have been prepared. Synthesis is generally straightforward from a range of metal(II) complexes and dithiocarbamate salts, although oxidative–addition of tetraethylthiuram disulfide to $[MCl_4]^{2-}$ salts affords a further synthetic route to the diethyldithiocarbamate complexes (1579). All complexes of this type are air stable and diamagnetic.

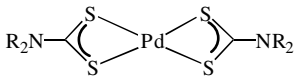

374

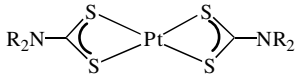

375

Examples include those with simple alkyl substituents (1329,1332,1333, 1580–1583), together with compounds derived from cyclic amines (1331, 1438,1584,1585), quinolines (1479), and anilines (116,1423). More exotic examples of bis(dithiocarbamate) complexes include a platinum complexes derived from aza-15-crown-5 (**376**) (1586) and 4-aminophenazone (**377**) (59), palladium complexes derived from substituted piperidines with long-chain substituents (1485,1486), and a range of platinum and palladium complexes with hydroxy-substitents, including **378** (1587). A number of α-amino acid derivatives of both metals have been prepared (1588,1589). For example, addition of barium dithiocarbamate salts of various amino acids to $[PtCl_4]^{2-}$ affords orange bis(dithiocarbamate) complexes $[Pt\{S_2CNHCH(R)CO_2H\}_2]$ (R = H, Me, *i*-Pr, CH_2-*i*-Pr) after washing with 0.1 *M* HCl (1589).

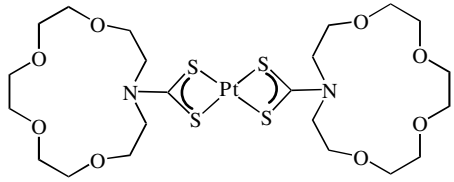

376

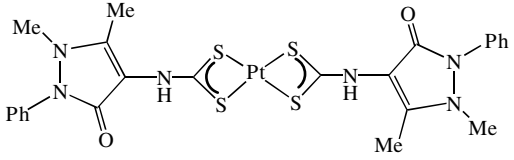

377

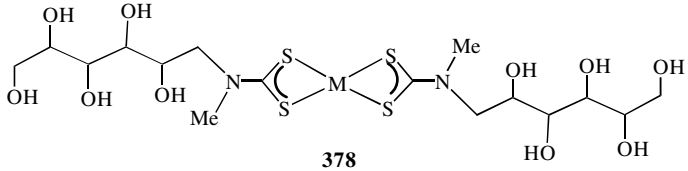

378

Some unusual syntheses of bis(dithiocarbamate) complexes have been reported. Addition of 2 equiv of NaS_2CNEt_2 to dimeric $[Pt(2,2'\text{-bpy})(\mu\text{-SR})]_2$ (SR = acetyl-L-cysteinato) affords $[Pt(S_2CNEt_2)_2]$ in <3 min (1590), while heating the thioester complexes, *trans*-$[MX_2(MeSCSNMeR)_2]$ ($R = CH_2CO_2Et$; X = Cl, Br, I), at 140–214°C in solution or the solid state gives $[M(S_2CNMeR)_2]$ resulting from loss of MeX (1591,1592). At palladium, this transformation occurs via $[PdX(S_2CNMeR)(MeSCSNMeR)]$, which can also be prepared upon addition of the thioester to $[PdX(S_2CNMeR)]_n$ (1592). In a similar fashion, heating $[PtCl(S_2CNEt_2)(MeS_2CNR_2)]$ (R = Me, Et) results in loss of CH_3Cl, in one case (R = Me) giving the mixed-ligand dithiocarbamate product $[Pt(S_2CNMe_2)(S_2CNEt_2)]$ (206).

Fayyaz and Grant (1477) studied the displacement of ethyl xanthate and dithiophosphate ligands by diethyldithiocarbamate. While with dithiophosphate complexes no intermediates are observed, in reactions of NaS_2CNEt_2 with $[M(S_2COEt)_2]$ two have been spectrophotometrically detected, proposed to be $[M(S_2COEt)_2(S_2CNEt_2)]^-$ and $[M(S_2COEt)(S_2CNEt_2)]$.

Crystallographic studies have been carried out on a number of palladium (393,409,1580,1582,1593) and platinum (420,1586,1594) complexes. As expected, all are square planar, with the α-carbons of the substituents generally

lying in the plane. In $[Pt(S_2CNC_7H_{14})_2]$ (**379**), however, which contains the largest carbocyclic ring characterized in a dithiocarbamate complex, there is a twist angle of 12° between the PtS_2C plane and that of the nitrogen and the α-carbons (1594), which contrasts with related angles of 4° in $[Pt(S_2CNEt_2)_2]$ and 2° in $[Pt\{S_2CN(CH_2CH_2OH)_2\}_2]$ (420).

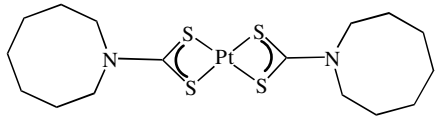

379

Riekkola et al. (1580) crystallographically characterized four palladium complexes (R = *i*-Pr, Bu, *i*-Bu, CF_3CH_2) all in the $P2_{1/c}$ space group, and also compared their volatility and melting points. Both vary significantly with the nature of the substituents, the trifluoroethyl derivative being the most volatile, while the butyl complex has the lowest (109°C) and the ethyl the highest (243°C) melting points.

Stability constants for palladium complexes, $[Pd(S_2CNR_2)_2]$ (R = Me, Et, Pr, *i*-Pr), have been measured in ethanol using UV-vis spectroscopy (393). Their stability varies in the order *i*-Pr > Pr > Et > Me being the same as that found for the analogous nickel complexes. Further, a comparison with related nickel and cobalt complexes showed the palladium complexes to be the most stable: Pd > Ni > Co (393).

Ligand exchange reactions have been studied at palladium by HPLC. Rate constants remain almost unchanged in ethylacetate for a range of substituents, but are strongly effected by the solvent: $BuOH > MeCO_2Et > CS_2 > CCl_4 > CH_2Cl_2$. In contrast, equilibrium constants vary with both the size and structure of the substituents, and an S_N2 mechanism is proposed for the exchange on the basis of a negative entropy of activation (1595).

The restricted rotation about the carbon–nitrogen bonds has also been studied in unsymmetrical palladium bis(dithiocarbamate) complexes by HPLC. At high temperature, there is rapid rotation and a single peak is observed, however, at lower temperatures two peaks can be separated (372).

Polarized optical spectra have been recorded for $[Pd(S_2CNEt_2)_2]$, spectral bands correlating with those for the nickel analogue based on a *d*-level ordering of $d_{xy} > d_{yz} > d_{x^2-y^2} \sim d_{xz} > d_{z^2}$ (1491). Photoelectron spectra He(I) and He(II) have also been recorded for both $[Pd(S_2CNEt_2)_2]$ and $[Pt(S_2CNEt_2)_2]$, as well as the nickel analogue, an increase in the π-bonding capability being observed along the series Ni > Pd >Pt (550).

Few reactions of bis(dithiocarbamate) complexes have been reported, aside from those with other metal salts that are described later. The platinum

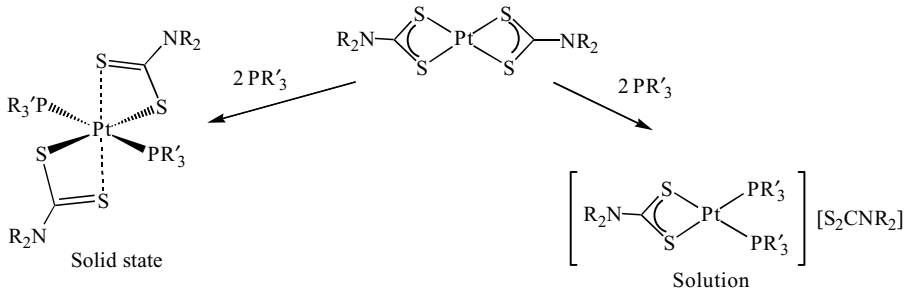

Figure 201. Products of the addition of 2 equiv of phosphines to $[Pt(S_2CNR_2)_2]$.

complexes are known to react with a range of phosphines and also certain amines, although the precise nature of the products has been the subject of some uncertainty. In 1973, Stephenson and Alison (1596) reported that addition of monodentate phosphines afforded ionic complexes of the type $[Pt(S_2CNR_2)(PR'_3)_2][S_2CNR_2]$, whereby one dithiocarbamate was displaced from the platinum center. Earlier, Fackler and Seidel (224) had studied the reactions with PMe_2Ph in more detail, showing that in solution at low temperatures the ionic complexes $[Pt(S_2CNR_2)(PMe_2Ph)_2][S_2CNR_2]$ were the dominant species, while at higher temperatures both dithiocarbamate and phosphine exchange occurred. Most interestingly, in the solid-state, neutral complexes *trans*-$[Pt(PMe_2Ph)_2(\eta^1\text{-}S_2CNR_2)_2]$ are the dominant species (Fig. 201).

The latter is shown by the crystal structure of the di-*i*-butyldithiocarbamate complex *trans*-$[Pt(PMe_2Ph)_2(\eta^1\text{-}S_2CN\text{—}i\text{-}Bu_2)_2]$ (**380**) (Fig. 202). Here, the dithiocarbamates bind in an ambidentate fashion, with short, 2.335(2) Å, and long, 3.392(3) Å, platinum–sulfur interactions. Addition of more bulky phosphines leads to the formation of adducts, $[Pt(S_2CNR_2)_2(PR'_3)]$, as confirmed by the crystallographic characterization of $[Pt(PPh_3)(S_2CNEt_2)(\eta^1\text{-}S_2CNEt_2)]$ (**381**) (Fig. 202) (1597). Here again, while one dithiocarbamate acts as a simple

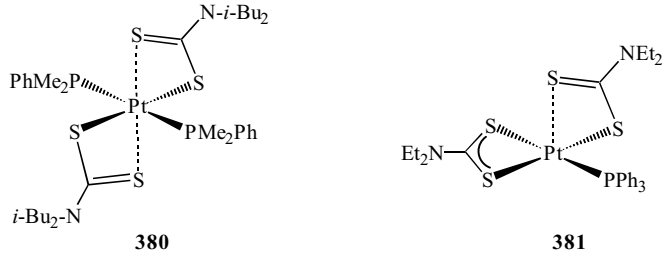

380 **381**

Figure 202. Crystallographically characterized phosphine adducts of $[Pt(S_2CNR_2)_2]$ with ambidentate dithiocarbamate ligands.

chelate, the second coordinates in an ambidentate fashion, having short, 2.331(3) Å, and long, 3.457 Å, interactions with the platinum center.

Platinum complexes derived from primary amines exhibit similar behavior toward bulky phosphines, although addition of 2 equiv of less bulky phosphines can lead to dithiocarbimato complexes (see below). The platinum complex $[Pt(S_2CNHBz)_2]$ adds PCy_3 to give $[Pt(PCy_3)(S_2CNHBz)_2]$ and γ-picoline (γ-pic) to yield $[Pt(\gamma\text{-pic})(S_2CNHBz)_2]$; the latter in turn reacting with iodine to afford $[PtI(PCy_3)(S_2CNHBz)_2]$ (375,376). The inequivalence of the two dithiocarbamate ligands in $[Pt(PCy_3)(S_2CNHBz)_2]$ in the solid state is shown by IR spectroscopy: two ν(C=N) bands appearing at 1535 and 1490 cm^{-1}, as compared with a single band at 1540 cm^{-1} for $[Pt(S_2CNHBz)_2]$ (375). The inequavalence of the dithiocarbamate ligands has been confirmed by a crystallographic study of $[Pt(PCy_3)(S_2CNH\text{—}t\text{-Bu})(\eta^1\text{-}S_2CNH\text{—}t\text{-Bu})]$ (380).

Colton and co-workers (231,254,548,1598–1600) carried out reactions of $[Pt(S_2CNEt_2)_2]$ (**382**) with a range of polydentate phosphines. With stoichiometric amounts of bidentate phosphines and $Ph_2PCH_2CH_2AsPh_2$ (L_2), the final products in all cases are $[Pt(\eta^2\text{-}L_2)(S_2CNEt_2)]^+$, for example, **385**; although the rates of reaction vary enormously. Thus with dppe, the reaction is fast and no intermediates are observed. In contrast, with dppm the reaction is slow and two intermediates are observed, $[Pt(S_2CNEt_2)(\eta^1\text{-}S_2CNEt_2)(\eta^1\text{-dppm})]$ (**383**) and *cis,cis*-$[Pt_2(S_2CNEt_2)_2(\mu\text{-dppm})_2]^{2+}$ (**384**), allowing an overall pathway to be established (Fig. 203). Addition of 2 equiv of these ligands generally affords complexes $[Pt(\eta^1\text{-}L_2)_2(S_2CNEt_2)]^+$, as shown in Fig. 203 for dppm (**386**). No further reaction is seen with dppe (1600).

Potentially tridentate phosphines $PhP(CH_2CH_2PPh_2)_2$ (P_2P') and $MeC(CH_2PPh_2)_3$ (triphos) react in different ways. The former gives $[Pt(\eta^3\text{-}P_2P')(S_2CNEt_2)]^+$ (**387**) (Fig. 204) in which the phosphine binds in a tridentate fashion. A crystallographic study revealed a distorted square-planar PtP_3S geometry [Pt-S 2.396(3) Å], the second sulfur being only weakly bound [Pt—S 2.754(3) Å]; a coordination mode that leads to long and short carbon–sulfur bonds [C—S 1.727(9) and 1.707(9) Å]. The complex undergoes a reversible one-electron oxidation; the platinum(III) species, $[Pt(\eta^3\text{-triphos})(S_2CNEt_2)]^{2+}$, generated by chemical oxidation or bulk electrolysis being moderately stable, allowing characterization by ESR spectroscopy and ESMS (231). The well-known ligand triphos reacts with $[Pt(S_2CNEt_2)_2]$ to give **388** (Fig. 204) in which the phosphine binds only through two phosphorus nuclei; allowing various reactions to be carried out on the unbound phosphorus(III) center (1598).

The chemistry of potentially tetradentate phosphines $P(CH_2CH_2PPh_2)_3$ (P_3P') and $[Ph_2PCH_2CH_2P(Ph)CH_2]_2$ ($P_2P'_2$) have also been investigated (548). On the basis of multinuclear NMR measurements, it is proposed that the former gives a temperature-dependent mixture of isomers, $[Pt(\eta^1\text{-}S_2CNEt_2)(\eta^4\text{-}P_3P')]^+$ and

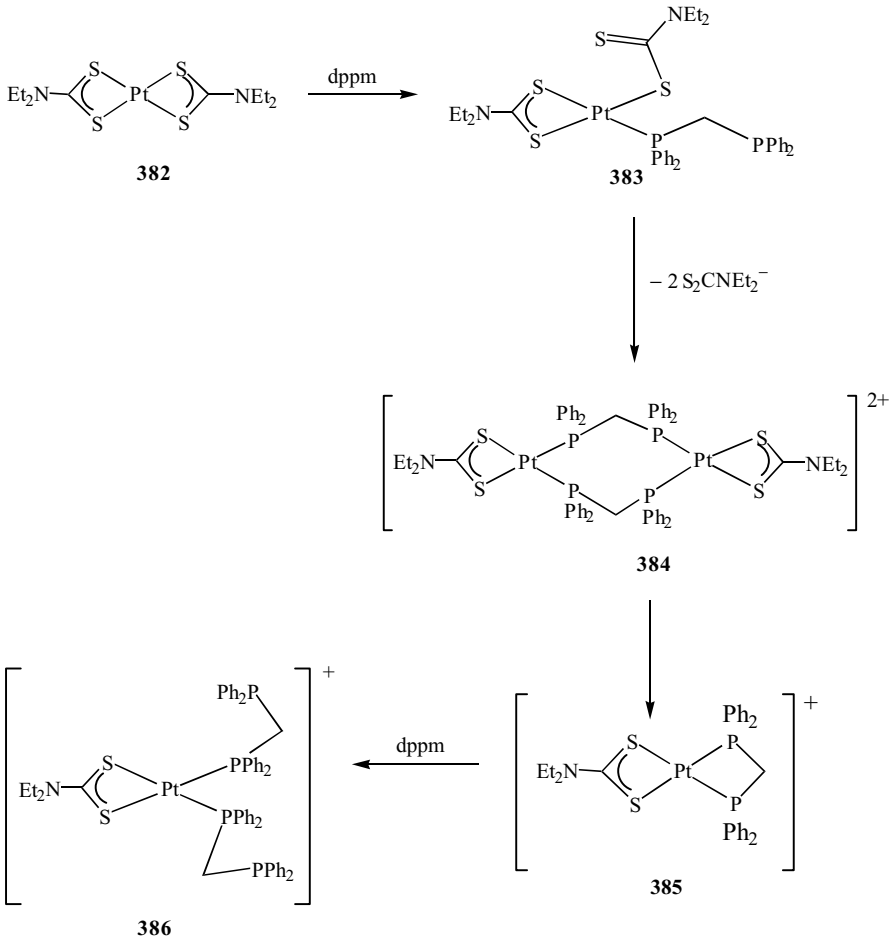

Figure 203. Products of the addition of dppm to $[Pt(S_2CNEt_2)_2]$.

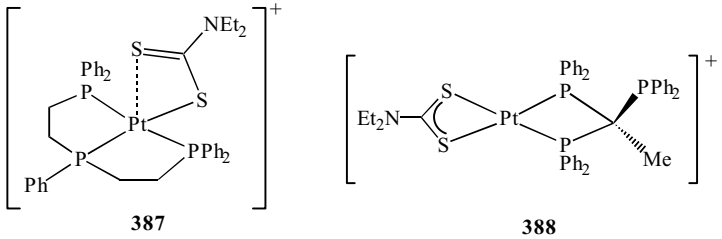

Figure 204. Products of the addition of tridentate phosphines to $[Pt(S_2CNEt_2)_2]$.

$[Pt(S_2CNEt_2)(\eta^3\text{-}P_3P')]^+$, although precise structural characteristics are unknown. With the later a single product is observed, believed to be $[Pt(\eta^1\text{-}S_2CNEt_2)(\eta^3\text{-}P_2P_2')]^+$; presumed to adopt a square-planar structure.

Extended Hückel calculations have been used to analyze the electronic structure of platinum complexes and also to rationalize their reactivity with various nucleophiles. Their inability to form four coordinate species of the type $[Pt(S_2CNR_2)(\eta^1\text{-}S_2CNR_2)_2]^-$ has been ascribed to the lower charge on platinum (when compared with xanthate complexes), strong platinum–sulfur bonds and a repulsive interaction between the platinum 3*d* electrons and the incoming ligand (1601).

Both platinum and palladium complexes, $[M(S_2CNH\text{-}p\text{-}C_6H_4NH_2)_2]$, can be deprotonated by NaOH giving dithiocarbimato complexes, $[M(S_2CN\text{-}p\text{-}C_6H_4NH_2)_2]^{2-}$ (Eq. 151) (116).

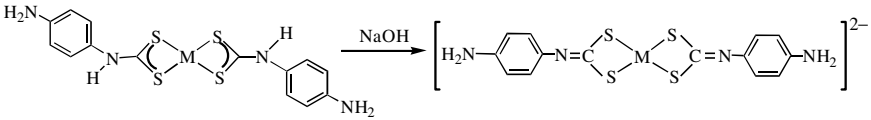

(151)

Interestingly, the process can also be carried out in some instances upon addition of 2 equiv of phosphine to $[M(S_2CNHR)_2]$ (M = Pd, Pt; R = Bz, *t*-Bu), leading to dithiocarbimato complexes $[M(PR'_3)_2(S_2CNR)]$ ($PR'_3 = PMe_2Ph$; $2PR'_3$ = dppe) (Eq. 152) (381). The precise nature of the transformation remains unknown, but the authors suggest the initial formation of a cationic complex upon addition of the phosphine(s) and dithiocarbamate loss; the latter serving as a base to deprotonate the remaining dithiocarbamate ligand.

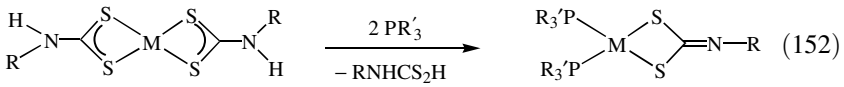

(152)

The electrochemical properties of bis(dithiocarbamate) complexes have been the focus of a number of publications. Bond et al. (231) reported that oxidation of $[Pt(S_2CNR_2)_2]$ does not result in observable platinum(III) species even at $-70°C$ and scan rates of 10,000 Vs^{-1}. In contrast, two other reports suggest that oxidation of both palladium and platinum bis(dithiocarbamate) complexes results in the generation of tris(dithiocarbamate) cations, $[M(S_2CNR_2)_3]^+$, via an irreversible process (1561,1578). In the case of platinum, one study suggests that these further undergo an irreversible two-electron reduction generating $[Pt(S_2CNR_2)_3]^-$, which rapidly revert to $[Pt(S_2CNR_2)_2]$ upon loss of one dithiocarbamate ligand (1578). The reductive chemistry of $[M(S_2CNR_2)_2]$

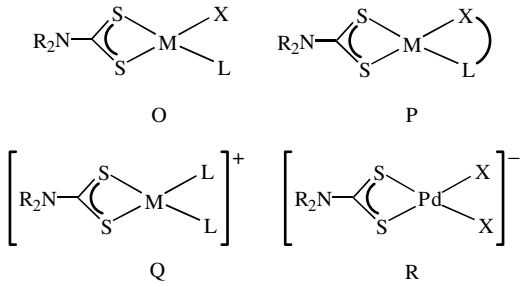

Figure 205. Different types of square-planar palladium and platinum(II) mono(dithiocarbamate) complexes.

complexes has not been well explored, but one group suggested that the unstable M(I) complexes $[M(S_2CNR_2)_2]^-$ result (1578).

b. Mono(dithiocarbamate) Complexes. As for nickel, four general types (Fig. 205) of mono(dithiocarbamate) complexes are seen for palladium and platinum in the +2 oxidation state: (1) neutral complexes $[MXL(S_2CNR_2)]$(O); (2) neutral bis(chelate) complexes $[M(S_2CNR_2)$(chelate)](P); (3) cations $[ML_2(S_2CNR_2)]^+$(Q); and (4) anions $[MX_2(S_2CNR_2)]^-$(R), although the latter are only known for palladium.

Neutral complexes of the type $[MXL(S_2CNR_2)]$ are common for both palladium and platinum. The neutral ligand L is generally a phosphine (1507,1602–1608), while amine (1609,1610), arsine (1606,1611), and thioether (1612) complexes are also known. Anionic ligands (X) range from simple halides (1609,1612,1613), alkoxides, and thiolates (1607,1614) to a wide range of organic groups (1602–1608).

Phosphine complexes are the most common and a number of synthetic pathways have been developed. Chloride complexes, $[MCl(PR'_3)(S_2CNR_2)]$, can be prepared from ligand redistribution reactions between $[MCl_2(PR'_3)_2]$ and $[M(S_2CNR_2)_2]$ in refluxing benzene (1507), and can undergo further metathesis reactions (Fig. 206). In this way, $[PdCl(PEt_3)(S_2CNMe_2)]$ has been utilized toward the synthesis of alkoxide and thiolate complexes $[PdX(PEt_3)(S_2CNMe_2)]$ (X = OPh, SMe, S-*p*-tol) (1607), together with a number of simple alkyl derivatives generated from alkyl lithium or Grignard reagents (1603).

Jain and co-workers (1614) recently reported the pyridine-2-chalcogenate complexes $[Pd(Epy)(PPh_3)(S_2CNEt_2)]$ (E = S, Se), which were prepared in high yields from $[PdCl(PPh_3)(S_2CNEt_2)]$. The NMR data suggest that two species coexist in solution, one predominating (~95%) with a chelating dithiocarbamate, while a second isomer contains a monodentate dithiocarbamate and chelating pyridine-2-chalcogenate ligand (Fig. 207).

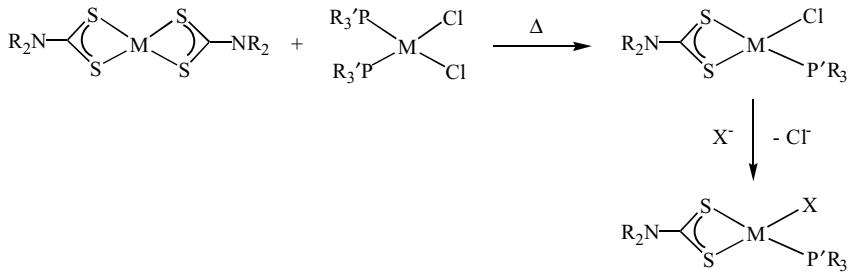

Figure 206. Synthesis of neutral complexes $[MX(PR'_3)(S_2CNR_2)]$.

Halide-bridged dimers also provide a convenient entry into this chemistry (206,207,543,1602,1606,1611,1612). For example, methyl complexes $[PdMe(PPh_2Me)(S_2CNEt_2)]$ and $[PdMe(EPPh_3)(S_2CNR_2)]$ (R = Me, Et; E = P, As) have been prepared from $[PdMe(PPh_2Me)(\mu\text{-}Cl)]_2$ and $[PdMe(cod)(\mu\text{-}Cl)]_2$, respectively, upon addition of dithiocarbamate salts (1606). In a similar manner, amine complexes $[MX(amine)(S_2CNMe_2)]$ (X = Cl, Br; amine = py, $PrNH_2$, cyclobutylamine) and $[MCl(amine)(S_2CNMeR)]$ ($R = CH_2CO_2Et$) are generated from $[M(S_2CNMe_2)(\mu\text{-}X)]_n$ (1609,1610) and organometallic complexes $[Pd(C_6X_5)(PPh_3)(S_2CNR_2)]$ (R = Me, Et; X = Cl, F) from $[Pd(C_6X_5)(PPh_3)(\mu\text{-}OH)]_2$ (1602). Addition of L-methioninol (L-mol) to $[MCl(S_2CNMeR)]_n$ (M = Pd, Pt) affords [M(L-mol)(S_2CNMeR)]Cl (543), while the arsine complex $[PdCl(AsBz_3)(S_2CNEt_2)]$ results from $[Pd(S_2CNEt_2)(\mu\text{-}Cl)]$ or addition of dithiocarbamate salts to $[PdCl_2(AsBz_3)_2]$; metathesis is used to generate further complexes, $[PdCl(AsBz_3)(S_2CNEt_2)]$ (X = Cl, Br, I, NO_2) (Fig. 208) (1611).

Addition of iodine to $[M(S_2CNHR)_2(PR'_3)]$ (M = Pd, Pt; R = Bz, *t*-Bu; R′ = Ph, Cy) results in loss of a dithiocarbamate ligand and formation of $[MI(S_2CNHR)(PR'_3)]$. The halide can in turn be replaced by isothiocyanate, while addition of $SnCl_2$ results in insertion into the metal–iodide bond to give the tin derivatives $[M(SnCl_2I)(S_2CNHR)(PR'_3)]$ (Fig. 209) (376).

All complexes of this type are diamagnetic and show the expected square-planar coordination environment. The crystal structure of $[Pd(SMe)(PEt_3)(S_2CNMe_2)]$ reveals the strong *trans*-influence of the thiolate ligand, being

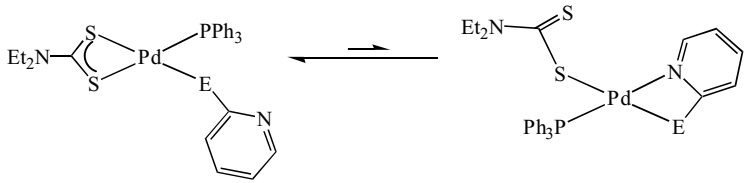

Figure 207. Proposed isomers of $[Pd(o\text{-}EC_5H_4N)(PPh_3)(S_2CNEt_2)]$ (E = S, Se).

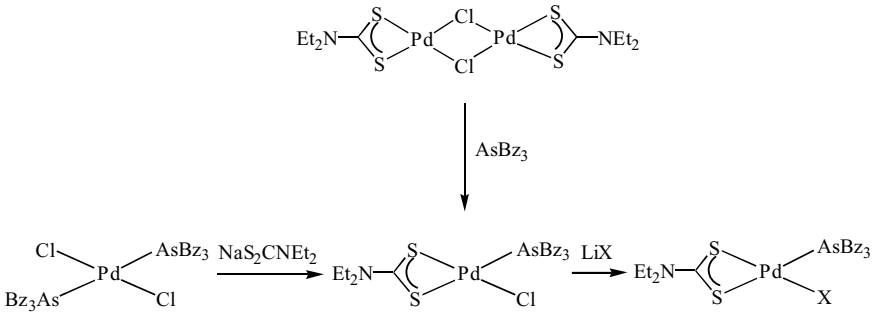

Figure 208. Synthetic routes to $[PdCl(AsBz_3)(S_2CNEt_2)]$ and subsequent metathesis reactions.

comparable to that of the phosphine [Pd—S_{trans} 2.333(2), Pd—S_{cis} 2.347(1) Å] (1607). Palladium and platinum complexes $[MCl(PPh_3)(S_2CNEt_2)]$ have also been characterized crystallographically. In solution they are fluxional, NMR changes being attributed to a hindered rotation about the carbon–nitrogen bond (1507).

In a series of papers, Reger et al. (1603–1605,1615) extensively explored the organometallic chemistry of the palladium(II) center, and to a lesser extent, related platinum(II) chemistry (1608); aspects of the palladium chemistry developed from $[PdCl(PEt_3)(S_2CNMe_2)]$ (**389**) being detailed in Figure 210. Thus, a wide range of alkyl complexes, $[PdR(PEt_3)(S_2CNMe_2)]$ (**390**), can be easily prepared (1603,1604), while others such as **392** are accessible from $[PdH(PEt_3)(S_2CNMe_2)]$ (**391**) (generated *in situ* using super hydride) and alkenes (1604). Alkynyl and alkenyl complexes can also be prepared from the chloride, while the latter further result upon alkyne insertion into the palladium–hydrogen bond of **391**; a process with little regioselectivity (1605). More elaborate organic moieties can also be generated from $[PdMe(PEt_3)(S_2CNMe_2)]$. Insertion of *t*-BuNC into the methyl group giving $[Pd\{\eta^1\text{-}C(Me)=N\text{-}t\text{-}Bu\}(PEt_3)(S_2CNMe_2)]$ (**393**), which in turn is a precursor to $[Pd\{\eta^1\text{-}C(Me)=N(R)\text{-}t\text{-}Bu\}(PEt_3)(S_2CNMe_2)]^+$ (R = H, Me) (**394**) and $[Pd\{\eta^1\text{-}C(=CH_2)=NMe\text{-}t\text{-}Bu\}(PEt_3)(S_2CNMe_2)]$ (**395**) (1605).

Alkyl complexes show good thermal stability, some examples being stable up to 100°C. Interestingly, heating unsubstituted isomers results in some isomerization. Thus, $[Pd(n\text{-}Pr)(PEt_3)(S_2CNMe_2)]$ and $[Pd(i\text{-}Pr)(PEt_3)(S_2CNMe_2)]$ exist

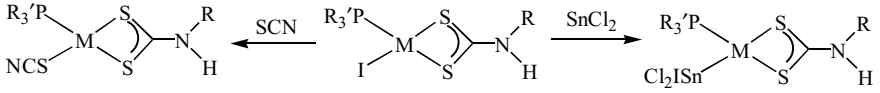

Figure 209. Selected reactions of $[MI(PR'_3)(S_2CNHR)]$.

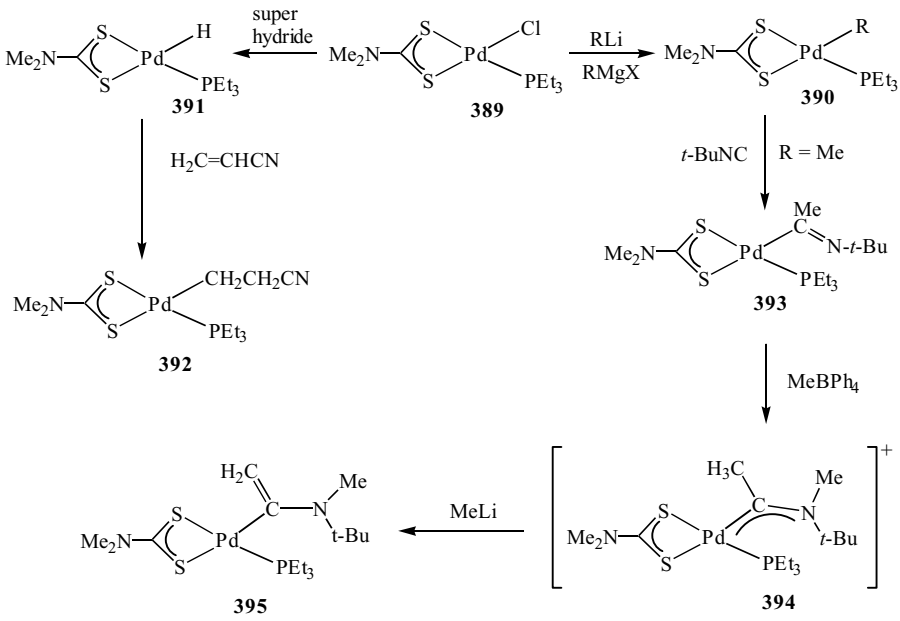

Figure 210. Examples of organometallic palladium(II) complexes prepared from [PdCl(PEt_3)(S_2CNEt_2)].

in a 10:1 ratio (Eq. 153) at 75°C, the 6.9 kJ mol^{-1} energy difference between them being proposed to be that between primary and secondary alkyl metal complexes in the absence of steric constraints. Alkyl exchange reactions also occur; heating [Pd(*i*-Pr)(PEt_3)(S_2CNMe_2)] in the presence of 1-hexane giving a mixture of all three hexyl isomers.

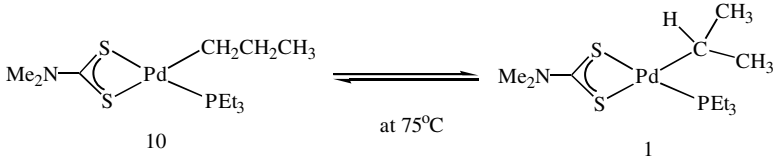

(153)

Alkyl isomerization is a first-order process, being slowed by the presence of Lewis bases and is proposed to proceed via phosphine dissociation (1604). A range of platinum–alkyl complexes, [PtR(PR'_3)(S_2CNMe_2)] (R′ = Et, Bu, Ph, Cy), have also been prepared and display similar properties, which are stable to 100°C, but undergo slow isomerization at 125°C (1608). The effect of different

phosphines on the linear-branched equilibrium has been assessed; bulky groups shift the equilibrium toward linear isomers.

All complexes are square planar and the strong trans-influence of the alkyl substituent has been observed crystallographically, and varies between isomers. Thus, for $[PdR(PEt_3)(S_2CNC_4H_8)]$ (R = *n*-Pr, *i*-Pr), the stronger trans-influence of the isopropyl ligand is apparent [Pd—S(*i*-Pr) 2.384(2) and 2.406(1) Å; Pd—S(*n*-Pr) 2.395(1) and 2.439(1) Å] (1603). The platinum complex, [Pt(*s*-Bu)$(PCy_3)(S_2CNMe_2)$] has also been crystallographically characterized (1608).

Neutral bis(chelate) complexes, $[M(S_2CNR_2)(chelate)]$, are generally prepared from chloro-bridged dimers, $[M(chelate)(\mu\text{-}Cl)]_2$, upon addition of 2 equiv of dithiocarbamate salts. Examples prepared in this way include (Fig. 211); $[Pd(\eta^3\text{-allyl})(S_2CNR_2)]$ (**396**) (1582), $[Pd\{\eta^2\text{-}SC(NMe_2)C_6H_4\}(S_2CNMe_2)]$ (**397**) (1616), $[Pd(\eta^2\text{-}PhN{=}NC_6H_4)(S_2CNR_2)]$ (**398**) (1617), and $[Pt(\eta^2\text{-}o\text{-}tol_2PC_6H_4CH_2)(S_2CNMe_2)]$ (**399**) (1618). The cyclometalated 2-phenylpyridine complex $[Pt(\eta^2\text{-}NC_5H_4C_6H_4)(S_2CNEt_2)]$ (**400**) has been prepared and shown to luminesce at room temperature in solution, but in contrast to related cationic phenanthroline complexes (see below), it shows a single excited state, being assigned to a MLCT involving the 2-phenylpyridine chelate (1619).

Two examples of allyl complexes, $[Pd(\eta^3\text{-allyl})(S_2CNR_2)]$ (**396**), namely, $[Pd(\eta^3\text{-}2\text{-}MeC_3H_4)(S_2CNR_2)]$ (R = Me, Pr) have been crystallographically characterized (1582). As expected, the methyl group lies out of the plane of the palladium dithiocarbamate unit, the palladium–sulfur bonds (2.352–2.380 Å) being slightly longer than those found in bis(dithiocarbamate) complexes.

Maitlis and co-workers (1620,1621) reported the synthesis of a number of novel palladium(II) organometallic complexes formed from ring-opening reactions of pentaaryl cyclobutenyl complexes (Fig. 212). Thus, addition of

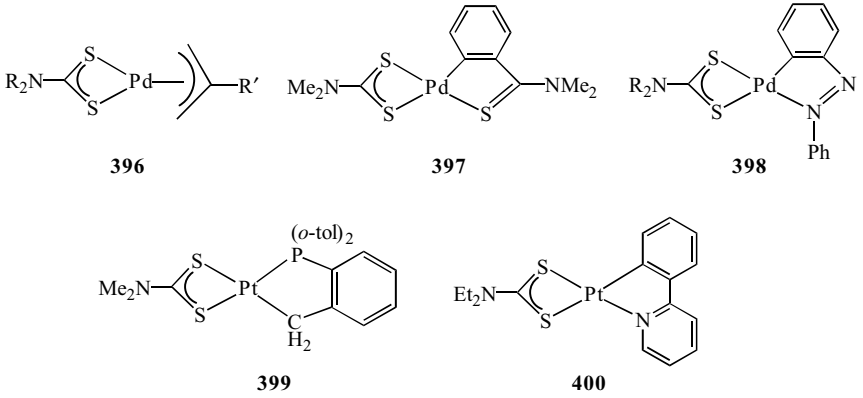

Figure 211. Examples of neutral bis(chelate) of the type $[M(chelate)(S_2CNR_2)]$.

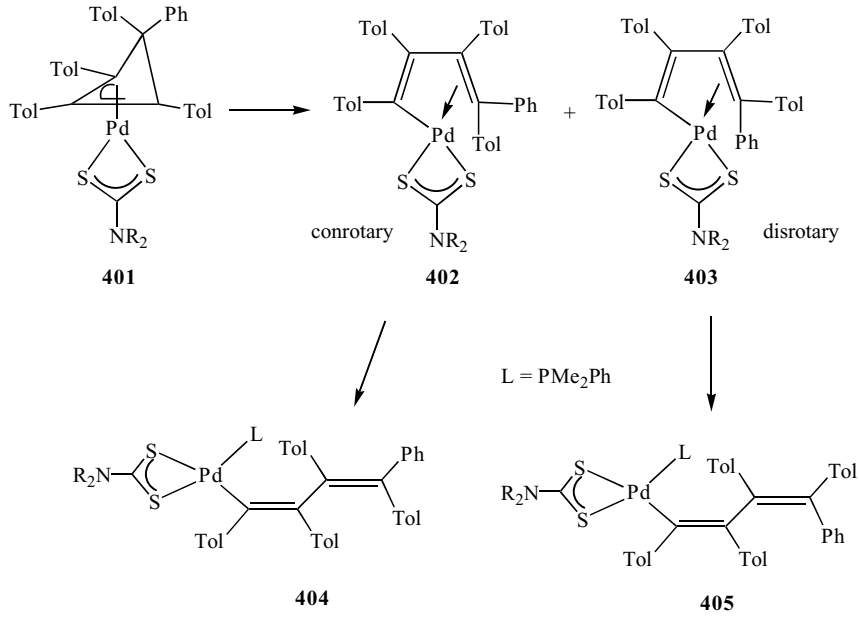

Figure 212. Formation of σ,π-butadienyl complexes from ring-opening reactions and their subsequent conversion to σ-butadienyl complexes.

dithiocarbamate salts to the chloro-bridged dimer, $[Pd(\eta^3\text{-}C_4Phtol_4)(\mu\text{-}Cl)]_2$, affords allyl-type complexes, $[Pd(\eta^3\text{-}C_4Phtol_4)(S_2CNR_2)]$ (R = Me, Et, *i*-Pr) (**401**). The cyclobutenyl ring undergoes a conrotary ring opening upon standing or heating in chloroform to give σ,π-butadienyl complexes **402**, although amounts of the unexpected disrotary isomers **403** are also observed. Both σ,π-butadienyl isomers react further with phosphines and phosphites to give related σ-butadienyl products **404**–**405**. Mechanistic details have been probed and a radical pathway is ruled out in favor of a conrotary ring opening to give **402** followed by an isomerization to **403** via a metallocyclopentenyl intermediate.

Stephenson and co-workers (1622) previously described the synthesis of phosphine–oxide complexes $[M(S_2CNEt_2)(\eta^2\text{-}Ph_2POHOPPh_2)]$ (**406**), from $[M(S_2CNEt_2)_2]$ (M = Pd, Pt) and $Ph_2P(O)H$ (or prehydrolyzed Ph_2PCl). The analogous reaction of $[Pt(S_2CNR_2)_2]$ with $Ph_2P(S)H$ in alcohols gives a variety of products (Fig. 213), which are dependent on the amount of sulfide used, the reaction time and the amount of water present (1623). From the reaction of $[Pt(S_2CNR_2)_2]$ (R = Et, *i*-Pr) with $Ph_2P(S)H$ in wet solvents, an analogous mixed oxo–sulfido complex $[Pt(S_2CNR_2)(\eta^2\text{-}Ph_2POHSPPh_2)]$ (**407**) has been generated (1623,1624), while with $Ph_2P(Se)H$ and $[Pt(S_2CNEt_2)_2]$ in dry

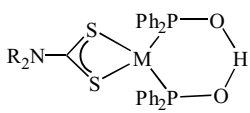

406

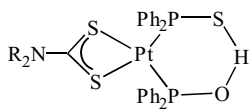

407

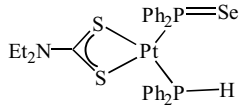

408

Figure 213. Examples of complexes with Ph_2P–E ligands.

solvents, a somewhat different product results, namely, $[Pt(S_2CNEt_2)(Ph_2PH)(Ph_2PSe)]$ (**408**) (1623).

Addition of alkyl halides (RCH_2X) to a range of pyridyl complexes, $[ML(o\text{-}C_5H_4N)(S_2CNMe_2)]$ (L = phosphine), to give $[ML(o\text{-}C_5H_4NCH_2R)(S_2CNMe_2)]X$ has been studied kinetically. A second-order rate law is found suggesting an S_N2 substitution reaction at the saturated carbon (1625).

Cationic complexes $[ML_2(S_2CNR_2)]^+$ are known for both palladium and platinum, with neutral ligands being phosphines (231,254,1520,1626,1627) and amines (1609,1619,1628,1629). Robinson and co-workers (1348,1626,1627) prepared a wide range of diphosphine complexes, $[Pd\{Ph_2P(CH_2)_nPPh_2\}(S_2CNEt_2)][MX_m]$ (n = 1–4) (**409**), from reactions of $[PdX_2\{Ph_2P(CH_2)_nPPh_2\}]$ and $[M(S_2CNEt_2)_2]$ (M = Ni, Cu, VO, MoO_2, Pb, Zn, Cd, Hg) and $[Mn(S_2CNEt_2)_3]$ dispelling earlier reports that such reactions gave molecular heterobimetallic species (332–336).

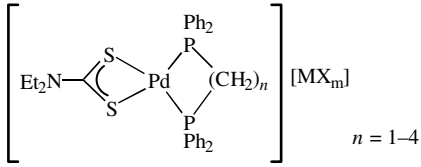

409

Organic isothiocyanates generally insert into metal–hydride bonds to give thioformamide complexes. In contrast, however, Werner and Bertleff (1630) noted that addition of 2 equiv of methyl isothiocyanate to $[PdH(PMe_3)_3][BPh_4]$ affords the dithiocarbamate complex $[Pd(PMe_3)_2(S_2CNMeH)][BPh_4]$ and MeNC, representing an unusual synthetic approach to dithiocarbamates (Eq. 154).

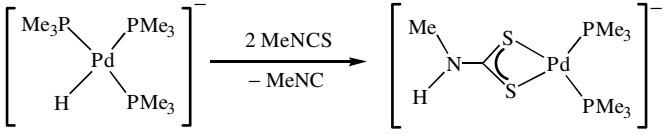

(154)

Monodentate phosphine complexes have also been reported. Dithiocarbimato complexes $[M(PR'_3)_2(S_2CNR)]$ of palladium and platinum have been prepared from $[MCl_2(PR'_3)_2]$, primary amines, and carbon disulfide and can be reversibly protonated to give dithiocarbamate complexes $[M(PR'_3)_2(S_2CNHR)]^+$ (Eq. 155) (1520).

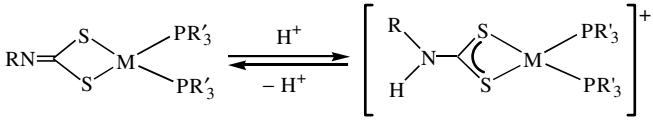

(155)

Both monodentate and bidentate amines form cationic complexes. Reactions of $[MX(S_2CNMe_2)]_n$ (X = Cl, Br) with a wide range of amines has been carried out, the nature of the product being sensitive to the stoichiometry of the reaction. Neutral products, $[MX(amine)(S_2CNMe_2)]$, are obtained when 1 equiv of amine is added, while cations, $[M(amine)_2(S_2CNMe_2)]X$, result upon addition of 2–3 equiv. With the bidentate amines, ethylenediamine and 1,3-diaminopropane, cationic products $[M(diamine)(S_2CNMe_2)]X$ always ensue (1609,1610).

López and co-workers (1631) prepared tetramethylethylenediamine (tmeda) complexes, $[Pd(tmeda)(S_2CNR_2)][BPh_4]$ (R = Me, Et; $R_2 = C_5H_{10}$), upon addition of carbon disulfide and secondary amines to $[Pd(tmeda)(\mu\text{-}OH)]_2[BPh_4]_2$, while related platinum complexes supported by 1,10-phen and 2,2′-bpy ligands have also been prepared (1619). The emission properties of one of these, $[Pt(4,4'\text{-}Me_2\text{-}1,10\text{-}phen)(S_2CNEt_2)]^+$ (**410**), has been investigated. At 77 K, an emission band is seen at 590 nm, together with two higher energy bands at 474 and 506 nm and a low-energy band at 564 nm (1619). Palladium bpy complexes, $[Pd(2,2'\text{-}bpy)(S_2CNBu_2)]_2[MX_4]$ (M = Zn, Cd, Hg, Pb; X = Cl, Br), have also been prepared from the reaction of $[PdX_2(2,2'\text{-}bpy)]$ and $[M(S_2CNBu_2)_2]$ (1348).

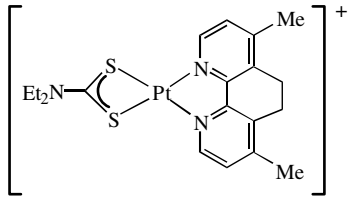

410

Das and Sinha (1632) prepared a range of cationic arylazoimidazole (R′aaiX) complexes $[(R'aaiX)Pd(S_2CNR_2)][ClO_4]$ (R = Et; $R_2 = C_4H_8O$) (**411**), upon addition of dithiocarbamate salts to the dichoride in the presence of $AgNO_3$ and perchlorate. When the reaction is carried out in the absence of the silver salt,

these ternary complexes are not isolated, but rather the bis(dithiocarbamate) complexes result, suggesting that $[(R'aaiX)Pd(S_2CNR_2)][ClO_4]$ are kinetic products.

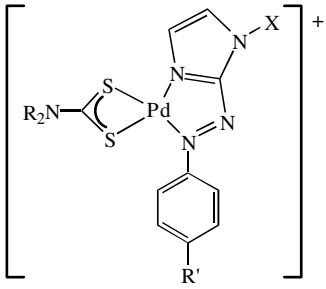

X = Me, Et; R' = H, Me, Cl

411

Relatively few examples of anionic complexes of the type $[MX_2(S_2CNR_2)]^-$ have been reported. Pale yellow $[Pd(C_6F_5)_2(S_2CNHPh)]^-$ (**412**) is formed in 94% yield upon addition of carbon disulfide to $[Pd(C_6F_5)_2(\mu\text{-NHPh})]_2^{2-}$, the unique proton appearing as a broad singlet at δ 10.52 ppm in the ^1H NMR spectrum (1633). Interestingly, carbon disulfide addition to the *N*,*N*′-ditolyformamidine complex $[Pd(C_6F_5)_2(\eta^2\text{-tolNCHNtol})]^-$ results in formation of $[Pd(C_6F_5)_2\{S_2CN(tol)CHNtol\}]^-$ (200).

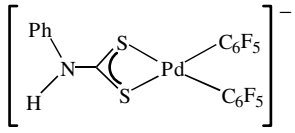

412

Stephenson and co-workers (1623,1624,1634) described the synthesis of $[M(S_2CNR_2)(\eta^1\text{-}Ph_2PS)_2]^-$ (**413**). They are formed upon addition of excess $Ph_2P(S)H$ to $[M(S_2CNR_2)_2]$ (M = Pd, Pt; R = Et, *i*-Pr) in dry solvents; the platinum complex being crystallographically characterized.

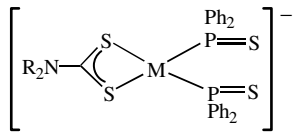

413

c. Bi- and Polynuclear Complexes. A large number of polynuclear homo- and heterometallic complexes have been prepared, the vast majority being characterized crystallographically. A wide range of structural types is observed, many containing bridging dithiocarbamate groups.

The known chloro-bridged dimers $[Pd(S_2CNR_2)(\mu\text{-}Cl)]$ (R = Et, Bu) (1634), have been generated in high yields upon reaction of $[PdCl_2(PhCN)_2]$ (Eq. 156) with a range of bis(dithiocarbamate) complexes $[M(S_2CNR_2)_2]$ (M = Pb, Zn, Cd, Hg, Cu, Ni, MoO_2, VO) in refluxing dichloromethane (1626). The butyl complex is crystallographically characterized (1636).

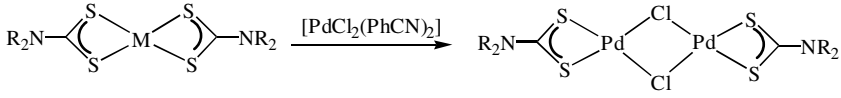

(156)

Related phosphine–sulfide complexes $[M(S_2CNR_2)(\mu\text{-}Ph_2PS)]_2$ (R = Et, *i*-Pr) are likewise prepared upon reaction of equal quantities of $[M(S_2CNR_2)_2]$ and $Ph_2P(S)H$ (Eq. 157) (1623,1624). A crystallographic study on $[Pt(S_2CN\text{—}i\text{-}Pr_2)(\mu\text{-}Ph_2PS)]_2$ reveals a centrosymmetric arrangement of the bridging ligands (1623).

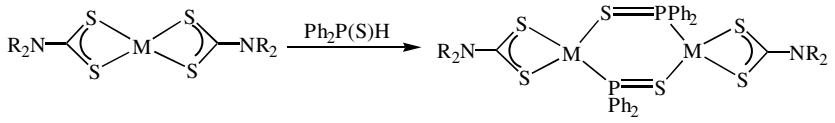

(157)

Base hydrolysis of $[Pt(S_2CNEt_2)(Ph_2PCH_2PPh_2)]Cl$ under phase-transfer catalytic conditions followed by anion exchange affords the novel binuclear platinum complex $[\{Pt(S_2CNEt_2)(Ph_2PMe)\}_2(\mu\text{-}Ph_2POHOPPh_2)][PF_6]$ (**414**). This complex has been crystallographically characterized (1637). The diphosphine has undergone phosphorus–carbon bond cleavage, and the bridging ligand contains a very short hydrogen bond [O···O 2.434(6) Å; O—H—O 174(14)°].

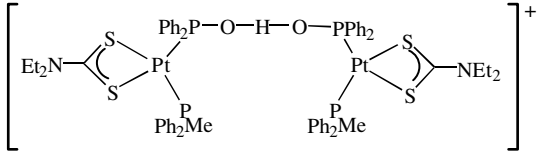

414

A further diplatinum complex $[Pt_2Cl_3(PEt_3)_2(\mu\text{-}S_2CNMe_2)]$ (**415**) is formed upon addition of NaS_2CNMe_2 to $[Pt_2Cl_4(PEt_3)_2]$ and features a bridging dithiocarbamate ligand. This arrangement is maintained in solution as evidenced by the observation of two methyl signals in the ^1H NMR spectrum (1638).

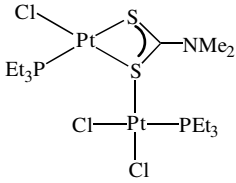

415

Other binuclear complexes include those bound to ferrocenyl groups. The *meso* and *rac* isomers of $[Pd_2(fdt)(S_2CNR_2)_2]$ (R = Et, *i*-Pr; $fdtH_2$ = ferrocene-1,1′-tetramethyldicarbothioamide) (**416**) have been separated by silica gel chromatography, a crystal structure of a *rac* isomer (R = *i*-Pr) revealing a twist angle of 19.1(8)° between the cyclopentadienyl ligands (1639).

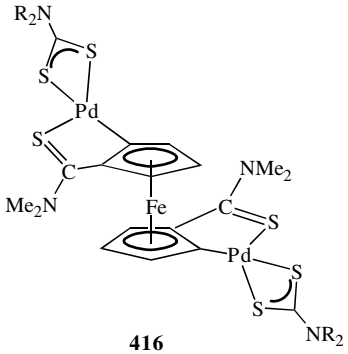

416

Three trinuclear palladium complexes have been synthesized and crystallographically characterized. A minor product from the oxidation of $[Pd(S_2CNEt_2)_2]$ by bromine is yellow $[Pd_3Br_2(S_2CNEt_2)_2(\mu\text{-}S_2CNEt_2)_2]$ (**417**) (1640), while the analogous orange chloride complex has been isolated from an unusual reaction between $[PdCl_2(PhCN)_2]$ and $[Nb_2(S_2CNEt_2)_4(\mu\text{-}S_2)_2]$ (1641). Both are centrosymmetric, the central palladium bis(dithiocarbamate) unit being bound to $Pd(S_2CNEt_2)X$ groups through bridging dithiocarbamates. The palladium–sulfur bonds fall into three groups (X = Br); those to the outer [Pd—S 2.279(1) and 2.291(1) Å] and central [Pd—S 2.313(1) and 2.321(1) Å] palladium ions, and the bridging interaction [Pd—S 2.346(1) Å] (1641).

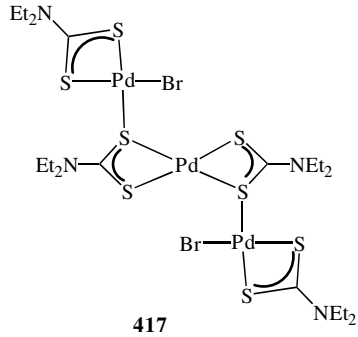

417

In the two complexes described above, the palladium(II) centers are quite distant. In contrast, in diamagnetic $[Pd_3(PPh_3)_2(S_2CNEt_2)_2(\mu^3\text{-}Cl)_2]$ (**418**) (Fig. 214), formed in 60% yield from $[PdCl_2(PhCN)_2]$, PPh_3, and NaS_2CNEt_2, followed by addition of $NaBH_4$, the palladium centers form a triangular array with two long [3.129(1) and 3.162(1) Å] and one shorter [3.016(1) Å] metal–metal interaction (1642). Puddephatt and co-workers (267) also reported triplatinum dithiocarbamate complexes; addition of dithiocarbamate salts to $[Pt_3(\mu^3\text{-}CO)(\mu\text{-}dppm)_3]^{2+}$ give $[Pt_3(\mu\text{-}CO)(\mu\text{-}S_2CNR_2)(\mu\text{-}dppm)_3]^{+}$ (**419**) (Fig. 214). A crystallographic study (R = Me) shows that the dithiocarbamate spans a platinum–platinum bond, lying trans to the carbonyl, while in solution it migrates around the platinum triangle.

Stephenson and co-workers (1551,1643–1647) utilized diphenylphosphine-oxide and sulfide complexes, $[M(S_2CNEt_2)(Ph_2PEHEPPh_2)]$ (E = O, S), toward the synthesis of heterometallic complexes (Fig. 215). For example, $[Pd(S_2CNEt_2)(Ph_2POHOPPh_2)]$ reacts with a range of metal acetylacetate complexes giving trinuclear $[\{Pd(S_2CNEt_2)(\mu\text{-}Ph_2PO)_2\}_2M]$ (M = VO, Co, Ni, Cu, Pd) (**420**) and tetranuclear $[\{Pd(S_2CNEt_2)(\mu\text{-}Ph_2PO)_2\}_3M]$ (M = Mn, Ga, In, Al) products (1551). Lanthanide and actinide complexes have also been

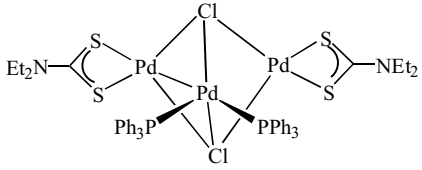

418

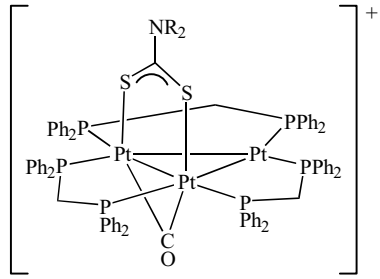

419

Figure 214. Examples of trinuclear group 10 (VIII) dithiocarbamate complexes.

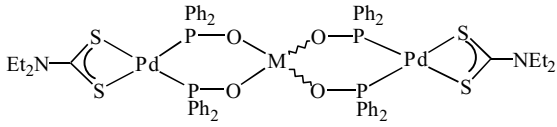

420

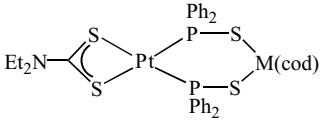

421

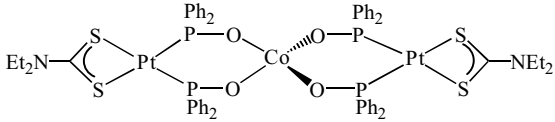

422

Figure 215. Examples of Ph_2PE-bridged heterometallic complexes.

prepared in this way (1646,1647). Closely related platinum complexes such as $[Pt(S_2CNR_2)(\mu\text{-}Ph_2PS)_2M(cod)]$ (M = Rh, Ir; R = Et, *i*-Pr) (**421**) (1645), $[\{Pt(S_2CNEt_2)(\mu\text{-}Ph_2PO)_2\}_2Co]$ (**422**) (1643), and $[\{Pt(S_2CN{-}i\text{-}Pr_2)(\mu\text{-}Ph_2PO)(\mu\text{-}Ph_2PE)\}_2Co]$ (1644), have also been prepared by the same method, and crystallographically characterized.

Bis(dithiocarbamate) complexes, $[Pd(S_2CNR_2)_2]$, have been widely utilized in the synthesis of heterobimetallic complexes. Addition of $[MS_4]^{2-}$ (M = Mo, W) to $[Pd(S_2CNEt_2)_2]$ yields $[PdWS_2(S_2CNEt_2)(\mu\text{-}S)_2]^-$. Interestingly, analogous reactions with $[Pt(S_2CNEt_2)_2]$ do not give the desired product (1503). From the reaction of $[WS_4]^{2-}$ and $[Pd(S_2CNC_4H_8)_2]$, dimeric $[PdWS_2(S_2CNC_4H_8)_2(\mu\text{-}S)_2]^-$ (Eq. 158) has been crystallographically characterized. It has a short tungsten–palladium vector [2.8669(7) Å], which is bridged by two sulfido groups (1648,1649). Interestingly, the nonlinear optical effects have been assessed. While the complex exhibits optical self-defocusing with negligible nonlinear absorption, it is inferior to most group 6 (VI B) group 11 (I B) sulfido cluster compounds previously tested (1648).

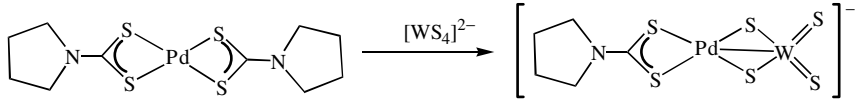

(158)

In a series of papers, Kawamura and co-workers (297–299,1650) report the synthesis of a number of mixed-metal complexes of the type $[M_3(S_2CNR_2)_6M'_2]^{2+}$ (M′ = Ag, Cu), formed upon addition of stoichiometric amounts of $[M(S_2CNR_2)_2]$ (M = Pd, Pt; R = Et, Pr, *i*-Pr, Bu, Cy) to Ag^+ or

$[Cu(MeCN)_4]^+$. Bond et al. (540) observed the same species by ESMS. Crystal structures of nine complexes of this type have been examined. All are held together by bridging dithiocarbamate ligands and fall into three basic types: (1) polymeric, (2) discrete ions with a pseudo-threefold axis through the coinage metal atoms, and (3) discrete ions without a threefold axis. A comparison of the structures shows the existence of a bonding interaction between the heterometal centers, which is greater for platinum than palladium, and for silver over copper. The existence of a strong bonding interaction between platinum and silver in $[Pt_3(S_2CNBu_2)_6Ag_2]^{2+}$ (**423**) is shown by a $^{195}Pt—^{107,109}Ag$ coupling constant of 194 Hz (297). The same group also report the reaction of copper(I) halides with $[Pt(S_2CNEt_2)_2]$, which generate helical polymers linked together by $Cu_2(\mu\text{-}X)_2$ units and bridging dithiocarbamate ligands (1650).

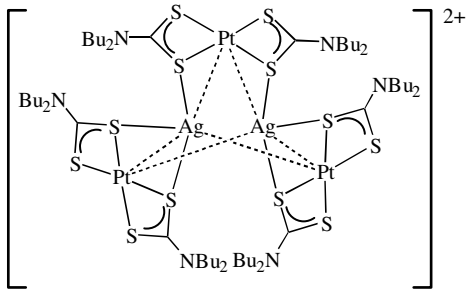

423

Forniés et al. reported somewhat similar chemistry centered upon the reactions of $[M(S_2CNMe_2)(\eta^2\text{-}CH_2C_6H_4PAr_2)]$ (Ar = *o*-tol) (1618) with silver, gold, and mercury salts (301,1651,1652). Both binuclear and tetranuclear complexes have been isolated with silver and gold, all containing bridging dithiocarbamate ligands and short heterometal distances, indicative of a substantial bonding interaction. For example, addition of $AgClO_4$ to $[M(S_2CNMe_2)(\eta^2\text{-}CH_2C_6H_4PAr_2)]$ (**424**) gives tetranuclear $[M_2(\eta^2\text{-}CH_2C_6H_4PAr_2)_2(\mu\text{-}S_2CNMe_2)Ag(AgOClO_3)]ClO_4$ (**425**), which reacts with further PPh_3 to yield binuclear $[M(\eta^2\text{-}CH_2C_6H_4PAr_2)(\mu\text{-}S_2CNMe_2)Ag(PPh_3)]$ (**426**) (Fig. 216) (301).

With mercuric acetates, the products formed depend critically on the nature of the group 10 (VIII) metal, but in all cases the dithiocarbamates remain as simple chelating ligands (Fig. 217). The platinum complex **427** reacts with $[Hg(O_2CR)_2]$ (R = Me, CF_3) to give octahedral complexes $[(\eta^1\text{-}O_2CR)Hg—Pt(S_2CNMe_2)(\eta^2\text{-}CH_2C_6H_4PAr_2)(\eta^1\text{-}O_2CR)]$ (**428**). These react further with hydrobromic acid yielding tetranuclear $[BrHg(\mu\text{-}Br)Pt(S_2CNMe_2)(\eta^2\text{-}CH_2C_6H_4PAr_2)]_2$ (**429**), containing a five-coordinate platinum ion. Short, unsupported, platinum–mercury bonds characterize all of these compounds.

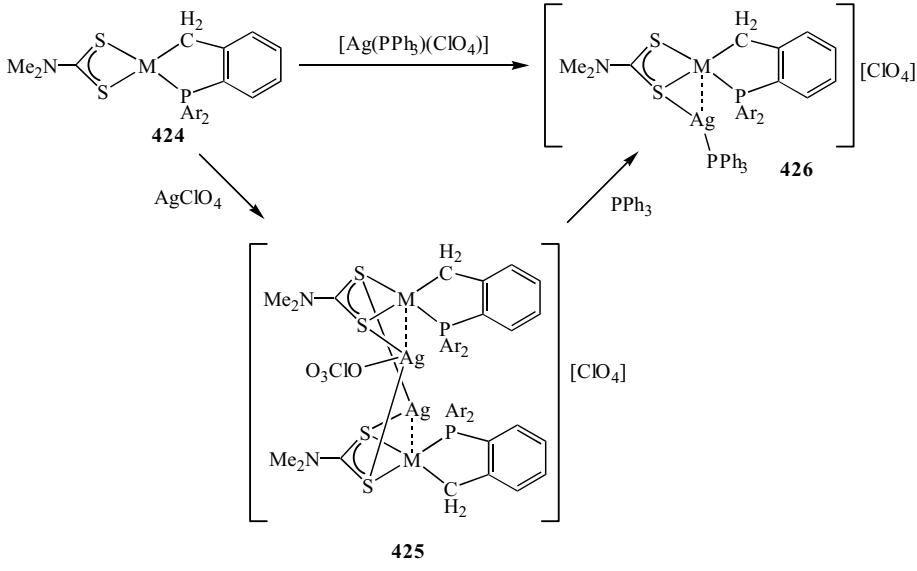

Figure 216. Addition of a silver(I) salt to $[M(S_2CNMe_2)(\eta^2\text{-}CH_2C_6H_4PAr_2)]$.

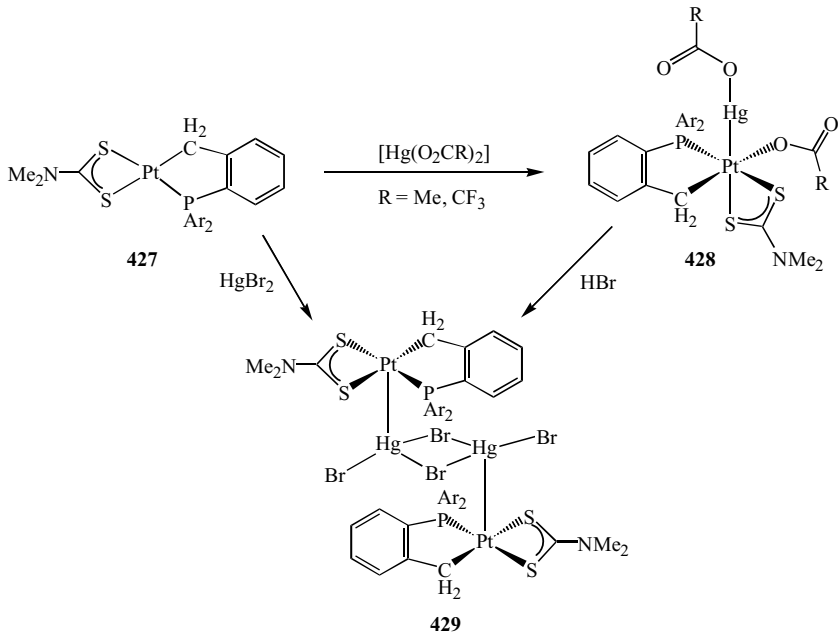

Figure 217. Addition of mercury(II) salts to $[Pt(S_2CNMe_2)(\eta^2\text{-}CH_2C_6H_4PAr_2)]$.

In contrast, reaction of $[Pd(S_2CNMe_2)(\eta^2\text{-}CH_2C_6H_4PAr_2)]$ with mercuric acetates affords binuclear $[(\eta^1\text{-}O_2CR)HgPd(S_2CNMe_2)(\mu\text{-}O_2CR)(\mu\text{-}CH_2C_6H_4PAr_2)]$ (**430**), resulting from an incomplete transmetalation reaction; distant metal centers are bridged by both acetate and ortho-metalated phosphine ligands (1651).

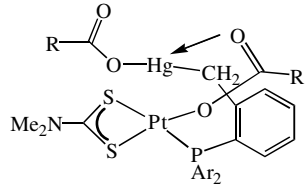

430

d. Tetravalent Complexes. Oxidation of bis(dithiocarbamate) complexes $[M(S_2CNR_2)_2]$ by halogens to give *cis*-$[MX_2(S_2CNR_2)_2]$ is a well-established process (1653). More recently, Blake et al. (1640) crystallographically characterized, *cis*-$[PdBr_2(S_2CNEt_2)_2]$ (**431**), while *cis*-$[PtCl_2(S_2CNBz_2)_2]$ has been prepared from K_2PtCl_6, dibenzylamine, and carbon disulfide (1519). Reaction of $[Pt(S_2CNMe_2)(\eta^2\text{-}CH_2C_6H_4PAr_2)]$ with halogens affords related platinum(IV) complexes, *cis*-$[PtX_2(S_2CNMe_2)(\eta^2\text{-}CH_2C_6H_4PAr_2)]$ (X = Cl, Br, I) (**432**), with the iodide crystallographically characterized (1618). Cyclic voltammetry has been carried out on platinum(IV) complexes, *cis*-$[PtX_2(S_2CNR_2)_2]$. Reduction leads to halide loss and no evidence was found for the formation of platinum(III) complexes (231).

Addition of dithiocarbamate salts to trimethylplatinum(IV) sulfate affords dimeric complexes *fac*-$[PtMe_3(\mu\text{-}S_2CNR_2)]_2$ (R = H, Me, Et; R_2 = HMe, HEt, HPh, PhMe) (**433**) in which the dithiocarbamate acts as a bridging ligand. The crystal structures of two examples have been carried out (R = Me; R_2 = HPh), as has extensive NMR studies aimed at measuring the barriers to rotation about the carbon–nitrogen bonds. Free energies of activation ranging between 65 and 88 kJ mol^{-1} have been found, and are highly dependent on the nature of the

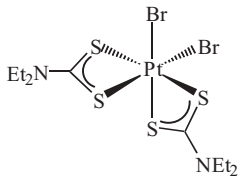

431

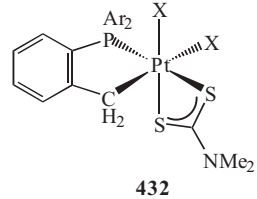

432

Figure 218. Examples of platinum(IV) complexes.

substituents; the complex derived from aniline having the lowest, and that from diethylamine, the highest, barrier to rotation (364).

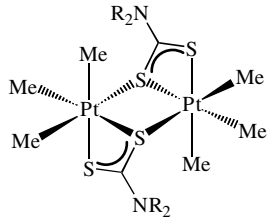

433

e. Applications. A number of potential applications and uses have been explored for both palladium and platinum dithiocarbamate complexes. The bis(dithiocarbamate) complex $[Pd(S_2CNC_5H_{10})_2]$ has been used in the spectrophotometric determination of Pd(II) at pH 6.5 (1654), while zinc silicate-bonded diethyldithiocarbamate also shows a high selectivity for palladium(II) and can be used in its preconcentration (1655). Related to these is a spectrophotometric determination of the fungicide, $[Zn(S_2CNMe_2)_2]$, which relies on precipitating the dithiocarbamate as $[Pd(S_2CNMe_2)_2]$ or $[Cu(S_2CNMe_2)_2]$, which absorb strongly at 395 and 430 nm, respectively (1656).

Palladium bis(dithiocarbamate) complexes derived from 4-(4′-alkyloxyphenylethyl)piperidines (**434**) display mesomorphic liquid-crystalline properties (1485), while in contrast, related complexes lacking the alkyl chains such as $[Pd(S_2CNC_4H_8NPh)_2]$ and $[Pd\{S_2C\{N(CH_2)_nMe\}_2\}_2]$ ($n = 6,8$) (1486) showed no mesomorphism as the chain length was not sufficiently long to depress the melting point enough (1486).

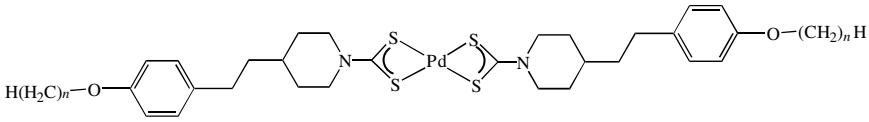

434

Bis(dithiocarbamate) complexes, $[M(S_2CNC_4H_8X)_2]$ ($M = Pd, Pt$; $X = O, S, CH_2$), have been tested for cyclostatic activity on KB cells, but show low activity at best (1585), as do a range of cationic amine complexes (1609). In contrast, related diamine complexes $[M(diamine)(S_2CNR_2)][NO_3]$ (diamine = 2,2′-bpy, 1,10-phen) show antitumor activity against leucemic cells (1628,1629,1657). Further, administration of various dithiocarbamates at a low dose level with cisplatin has been found to afford almost complete protection against cisplatin induced renal toxicity and body weight loss without

significant loss of activity, with *N*-*p*-carboxybenzyl-D-glucaminedithiocarbamate being particularly promising (1658).

Fregona and co-workers (1659,1660) reported the synthesis of palladium and platinum complexes $[Pd\{S_2CN(Me)CH_2CO_2R\}Cl]_n$ (R = Et, Bu) and $[PtCl(Py)\{S_2CN(Me)CH_2C(O)OEt\}]$ (1661), respectively, containing the dithiocarbamate generated from the esters of methylamino acetic acid. The former were examined for their cytotoxic properties in human cell lines and on the kidney, effects after a single injection being found to be similar to those of cisplatin. Further, biochemical and histopathological findings show the complex affects the pars recta and pars convoluta, while cisplatin affects only the pars recta. Toxicity tests on the kidney were also carried out for $[PtCl(Py)\{S_2CN(Me)CH_2C(O)OEt\}]$ (**435**) by means of a renal cortical slice model. It showed very low renal toxicity when compared to cisplatin, and also appeared to be more effective *in vitro* than the latter when tested on sensitive and resistant cisplatin tumor cell lines (1661). Very recently, a number of palladium and platinum amine complexes containing this dithiocarbamate have been tested for *in vitro* cytostatic activity against human leukemic HL-60 and HeLa cells. Those with Py ligands such as $[MCl(Py)\{S_2CN(Me)CH_2C(O)OEt\}]$ and $[M(Py)_2\{S_2CN(Me)CH_2C(O)OEt\}]Cl$ show remarkable activity, which are better than cisplatin (1610).

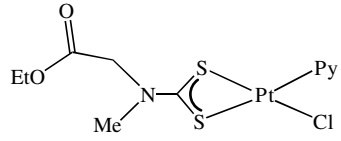

435

Palladium and platinum dithiocarbamate complexes are potential precursors toward technologically important metal sulfides. In this regard, TGA and DSC measurements have been made on a number of bis(dithiocarbamate) complexes. Palladium α-amino acid derivatives tend not to be volatile and PdO simply results (1588). With more volatile derivatives, such as those derived from methyl piperidines, heating to ~400°C yields palladium polysulfides (Pd_xS_y) (1438,1584), which slowly yield PdO at higher temperatures. With $[Pd(S_2CNMeCy)_2]$, heating to between 463 and 618°C affords $Pd(SCN)_2$, which transforms to PdS between 673 and 748°C (1332). Platinum complexes appear to be less stable, and often decompose to platinum sponge at >400°C (1438,1585). However, $[Pt(S_2CNMeCy)_2]$ is reported to give $Pt(SCN)_2$ at 463–658°C, PtS between 673 and 728°C and platinum metal at higher temperatures (1332).

Very recently, O'Brien and co-workers (1581) prepared more volatile bis(dithiocarbamate) complexes $[M(S_2CNMeHex)_2]_2$ (**436**) (Fig. 219) with

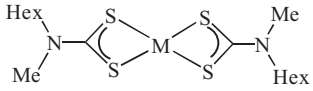

436

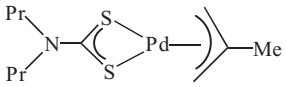

437

Figure 219. Group 10 (VIII) dithiocarbamate complexes utilized as precursors to metal–sulfide films.

melting pints of 80–85°C, and these have been utilized toward the growth of thin films of PdS and PtS by low-pressure MOCVD. They have also been used as precursors to TOPO-capped nanoparticles (TOPO = trioctylphosphine) with diameters of ~5 and 3 nm, respectively. Allyl–dithiocarbamate complexes, $[Pd(S_2CNR_2)(allyl)]$, display relatively high volatility as compared to analogous bis(dithiocarbamate) complexes, and as such they have been used in the preparation of thin films of various palladium sulfides. A particularly good precursor is $[Pd(S_2CNPr_2)(\eta^2\text{-}2\text{-}MeC_3H_4)]$ (**437**) (Fig. 219) (1582).

H. Group 11 (I B): Copper, Silver, and Gold

1. Copper

Dithiocarbamates stabilize copper in the +1, +2, and +3 oxidation states, with copper(II) bis(dithiocarbamate) complexes, first reported by Delépine (2) being most common. Later, Cambi and Coriselli (1662) detailed the synthesis of a range of these and also copper(I) dithiocarbamate complexes, and in the 1960s copper(III) complexes were prepared (1663). Over the past 20 years, some significant new developments have been made and a wide range of applications has been established.

a. Copper(II) Bis(dithiocarbamate) Complexes. Copper(II) bis(dithiocarbamate) complexes $[Cu(S_2CNR_2)_2]$ (**438**) are easily prepared from a range of copper(II) salts and in this way examples have been generated from a large number of amines including dialkylamines (317, 1663), piperidines and piperazines (739, 1126, 1424, 1425, 1474, 1486, 1665, 1666), anilines (1667), β-naphthylamine (1125), α-amino acids (121, 129, 137, 136), indole, indoline, carbazole, imidazole (72), aryldecahydroquinolin-4-ones (1478), Schiff bases derived from ethylenetriamine (1121), succinimide and phthalimide (49), 1,4,7,10-tetraoxz-13-azacyclopentadecane, 1,5-aminobenzo-1,4,7,10,13-pentaoxacyclopentadecane (50) and 3-dithiocarboxy-3-aza-5-aminopentanoate (1481). Complexes derived from para-substituted piperidines with long organic chains have also been prepared and show liquid-crystal properties (see Section IV.H.1.g.v) (1485, 1486, 1668).

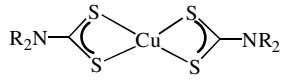

438

In an exciting development, Beer and co-workers prepared a range of novel compounds incorporating copper(II) bis(dithiocarbamate) units (Fig. 220). These include macrocyclic complexes based on terphenyl diamines (**439**–**442**) (326, 1468, 1469) and ferrocenyl amines (**443**) (1468), pyrrole-based metallocryptands (**444**) (492), cyclic amide complexes (**445**), and monometallic complexes with crown-ether substituents (**446**) (492), a number of which have been

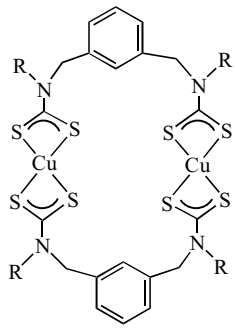

R = Pr, Bu, Hex

439

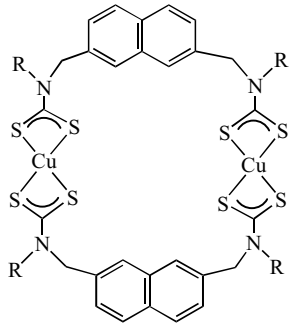

R = Bu, Hex

440

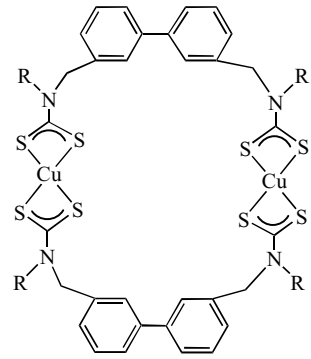

R = Pr, Bu

441

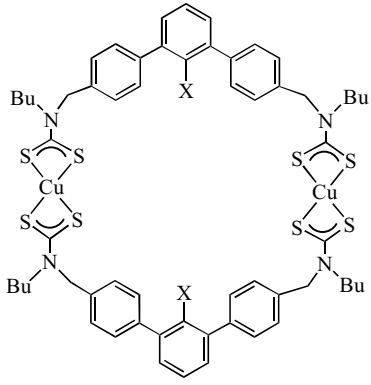

X = H, CO_2Me

442

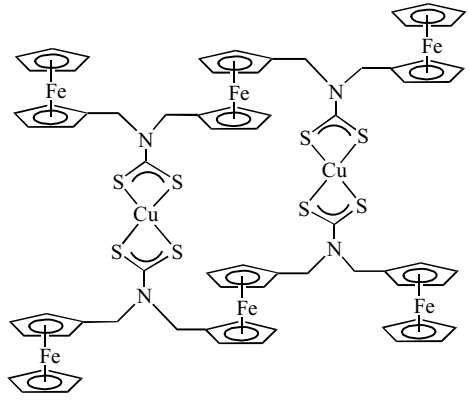

443

Figure 220. Copper(II) bis(dithiocarbamate) complexes prepared by Beer and co-workers.

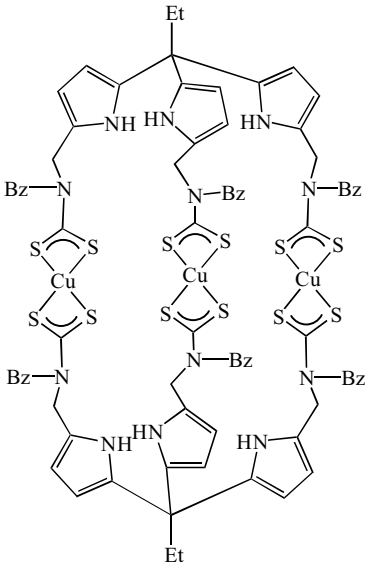

444

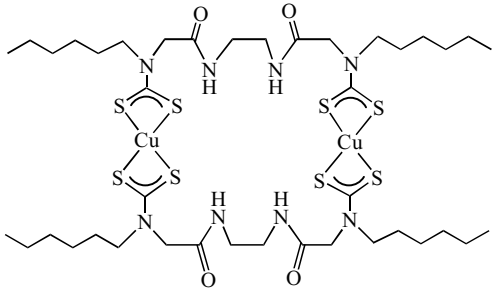

445

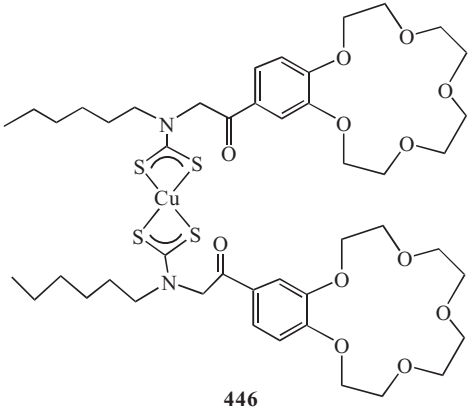

446

Figure 220. (*Continued*)

used as anion receptors (492, 1470, 1471). Many of these are analogous to the nickel and zinc complexes prepared by the same group. Further, the oxidation of some of these to the analogous copper(III) complexes has been studied in some detail and will be discussed later.

A number of other synthetic routes have also been developed toward copper bis(dithiocarbamate) complexes. Two groups have prepared the bis(2,2′-dipyridyl)dithiocarbamate complex **447** (Fig. 221) upon insertion of carbon disulfide

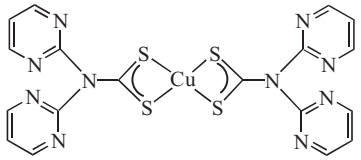

447

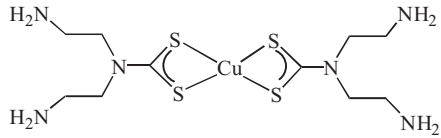

448

Figure 221. Copper(II) bis(dithiocarbamate) complexes with nitrogen-based substituents.

into the copper–nitrogen bonds of the corresponding 2,2′-dipyridyl complex (195, 196), while Klein et al. (204) prepared $[Cu(S_2CNMe_2)_2]$ from the reaction of copper(II) chloride with $P(S_2CNMe_2)_3$. The latter group also report the synthesis of $[Cu\{S_2CN(CH_2CH_2NH_2)_2\}_2]$ (**448**) (Fig. 221) from copper(I) chloride and diethylenetriamine in the presence of carbon disulfide. The structure is unknown, and it may be a polymer.

The oxidative–addition of thiuram disulfides to copper metal affords the bis(dithiocarbamate) complexes in good yields (170, 186, 187). This transformation may occur via initial formation of the copper(I) complexes, since Åkerström's has previously shown that the latter react instantaneously with thiuram disulfides to generate the analogous copper(II) complexes (188). Addition of the dithiocarbamate salts, NaS_2CNR_2, to copper powders in chloroform also yields $[Cu(S_2CNR_2)_2]$ ($R = Me$, Et, Pr, Bu; $R_2 = C_4H_8$). These reactions also work in ethanol or DMSO and their rates are dependent on the nature of the alkyl substituents (Bu > Pr > Et > Me) (190). Further, synthesis of $[Cu(S_2CNMe_2)_2]$ from metallic copper has been shown to accelerated by ultrasonic treatment (191).

All copper(II) bis(dithiocarbamate) complexes contain a square-planar copper(II) center as shown by a large number of crystallographic studies (121, 314–317, 325, 326, 486, 488, 496, 1666, 1669–1672). This arrangement is attributed to the crystal field stabilization energy being greater than the repulsive energy of the steric interactions imposed by the metal upon adoption of a square-planar configuration. Two general structural types are found (Fig. 222): simple monomeric units (**438**) (121, 316, 317, 325, 326, 488, 496, 1666, 1669–1672) and dimeric structures held together by intermolecular copper–sulfur interactions (**449**) (196, 314–317). Monomeric complexes include those with isopropyl, piperidine, and large cyclic substituents, while dimeric structures are observed for ethyl, propyl, allyl, 2-hydroxyethyl, and 2,2′-dipyridyl. In the dimeric structures, each copper center is five coordinate with intermolecular copper–copper and copper–sulfur interactions being ~3.4–3.8 and 2.7–2.9 Å, respectively. These secondary interactions also lead to a substantial deviation from planarity of the CuS_4 moiety, a point that has been addressed using NDDO calculations (1493). The structure of $[Cu(S_2CNMe_2)_2]$ (**450**), carried out in

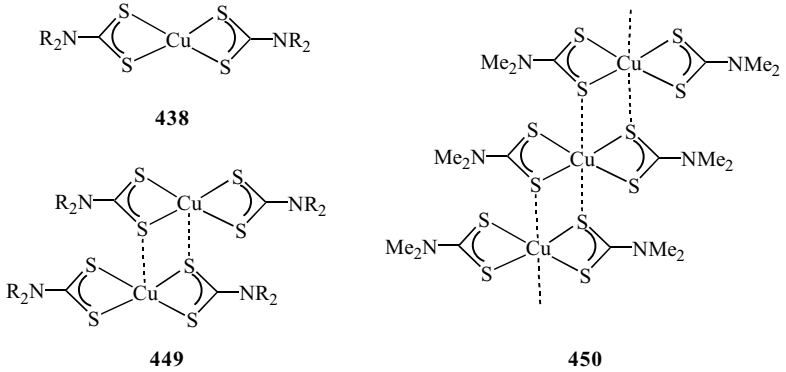

Figure 222. Solid-state structures of copper(II) bis(dithiocarbamate) complexes.

1974, is different from all others in that the long-range copper–sulfur interactions persist throughout, such that the copper center adopts a pseudo-octahedral coordination environment (1673).

The structure of the benzyl derivative $[Cu(S_2CNBz_2)_2]$ (Fig. 223) is also somewhat unusual in that the two independent molecules in the asymmetric unit are linked via one copper–sulfur and a second sulfur–sulfur interaction. The adoption of this configuration presumably arises from the steric requirements of the benzyl substituents (104, 317).

Rice and co-workers (1674) carried out a gas-phase electron diffraction study of $[Cu(S_2CNMe_2)_2]$, for which long-range copper–sulfur interactions are seen in the solid state (1673). They found that it is monomeric in the gas phase, adopting the expected square-planar coordination geometry. Confirmation of the monomeric nature of copper(II) bis(dithiocarbamate) complexes in the gas-phase also comes from mass spectroscopic studies (589). Further, while in the solid state,

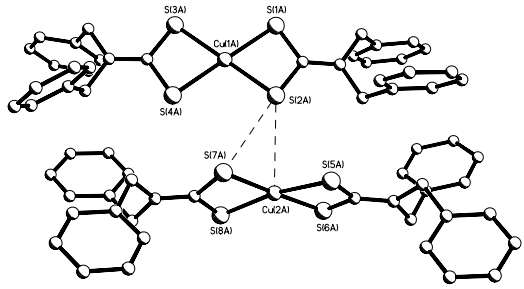

Figure 223. Crystal structure of $[Cu(S_2CNBz_2)_2]$.

$[Cu(S_2CNEt_2)_2]$ adopts a dimeric structure with a nonplanar CuS_4 unit, a ^{13}C and ^{14}N electron–nuclear double resonance (ENDOR) study of this complex substituted into single crystals of $[Ni(S_2CNEt_2)_2]$ revealed that the centrosymmetric structure of the nickel host had been adopted by the guest (1675).

The physical properties of copper(II) bis(dithiocarbamate) complexes have been investigated in some detail. Jian et al. (316) determined equilibrium constants of formation (K_{eq}) from copper(II) chloride in ethanol for a number of simple alkyl derivatives, $[Cu(S_2CNR_2)_2]$, by UV–vis spectroscopy. They range from 3.03×10^7 to 1.40×10^8, showing a dependence on the nature of the alkyl substituents in the order: *i*-Pr > *n*-Pr ≅ Et > Me. The metal-binding properties of other bis(dithiocarbamates), $[Cu(S_2CNR^1R^2)_2]$ ($R^1 = R^2 = Et$, Bu; $R^1 = Et$; $R^2 = Bu$, Hex), have been determined spectrophotometrically on the basis of the competition for these ligands (K_c) with 8-hydroxyquiniloine in 75% aqueous tertiary butanol. All are >1, but that for $[Cu(S_2CNBu_2)_2]$ $(K_c = 33.11 \times 10^2)$ is two orders of magnitude greater than $[Cu(S_2CNEt_2)_2]$ $(K_c = 0.34 \times 10^2)$ (596, 1676). The same authors also assess the relative stability of $[Cu(S_2CNEtHex)_2]$ over $[Fe(S_2CNEtHex)_3]$ by visible spectroscopy, showing that complete transfer of the dithiocarbamate ligand from iron(III) to copper(II) occurs, thus demonstrating the selectivity of the amphiphilic dithiocarbamate for copper over iron.

X-ray photoelectron spectra of $[Cu(S_2CNEt_2)_2]$ (556) and $[Cu(S_2CNC_4H_8X)_2]$ (X = O, S, NH, NMe, CH_2) (560) have been recorded, and for the latter, the Cu2$p_{3/2}$ peaks have been found to be particularly narrow (1.9–2.1 eV). St. Nikolov and Atanasov (521) recorded the electronic spectrum of $[Cu(S_2CNEt_2)_2]$ alone and when doped into a $[Zn(S_2CNEt_2)_2]$ matrix. They also studied these systems theoretically using the angular overlap model and crystal-field theory, finding that while the latter is unsuccessful in interpreting both the photoelectron spectrum and *d–d* transitions, the angular overlap model provides a good interpretation.

A detailed far-IR study of heterocyclic dithiocarbamate complexes with ^{63}Cu and ^{65}Cu isotopes has been carried out allowing the ν(Cu—S) and δ(S—Cu—S) vibrations to be assigned at 339–382 and 188–194 cm^{-1}, respectively (517), while a normal coordinate analysis of $[Cu(S_2CNEt_2)_2]$ has allowed a detailed assignment of the observed frequencies, revealing that a high degree of mixing occurs between different parts of the molecule (1494).

All copper(II) bis(dithiocarbamate) complexes are paramagnetic with magnetic moments of the order of 1.6–1.9 BM (1125, 1126, 1474). White and co-workers (1677) measured the magnetic susceptibilities of a number (R = Me, Et, *i*-Pr, Bu) between 4 and 290 K. Weak antiferromagnetic interactions are generally observed. Interestingly, when the *n*-butyl complex was crystallized from chloroform–light petroleum it gave a material, α-$[Cu(S_2CNBu_2)_2]$, with a strong antiferromagnetic exchange coupling. This material was absent from β-$[Cu(S_2CNBu_2)_2]$, which was crystallized from chloroform–ethanol. In order

to shed light on these magnetic differences, the crystal structures of both have been carried out. The β-form consists of isolated monomer molecules, while in the α-form a dimeric structure is adopted. The authors conclude that the strong antiferromagnetic coupling in the latter results either from the bridging nature of the sulfur atoms altering the efficiency of the antiferromagnetic superexchange pathway, or from an intermolecular coupling via pathways of the type Cu—S···S—Cu. However, based on the available experimental data, they were not able to distinguish between the two (1677). In marked contrast to the work described above, an earlier report suggested that $[Cu(S_2CNEt_2)_2]$ displays a strong ferromagnetic interaction (1678). This work was, however, later shown to be incorrect, a second study showing that weakly interacting pairs of exchange-coupled copper(II) centers in dimeric $[Cu(S_2CNEt_2)_2]$ give rise to a ferromagnetic intrapair-exchange constant of only 0.9 K, and an antiferromagnetic interpair interaction of -0.007 K (1679).

The ESR spectra of copper(II) bis(dithiocarbamate) complexes has been widely discussed in previous reviews (16, 17). A number of more recent contributions have been made (72, 121, 129, 316, 477, 1680–1683). These include work by Bereman and Nalewajek (72), who have analyzed the ESR spectra of indole, indoline, and carbazole-derived dithiocarbamate complexes. Their results suggest a strong covalency in the in-plane σ-bonding and moderate covalency for the in-plane and out-of-plane π-bonding. The latter indicates that these dithiocarbamate complexes exhibit a strong predominance of the non-thioureide resonance form, and it is this which is the strong-field form for dithiocarbamates (see Section III.C). The covalent nature of the copper–sulfur bonds has been confirmed by calculations, which also reveal that the odd electron is delocalized over the CuS_4 unit, and lead to theoretical values for the *g*-tensor and copper and sulfur hyperfine tensors (1684).

Suzuki et al. (1680) reported that ESR spectra of bis(dithiocarbamate) complexes in various media at $-196°C$ show a typical spectrum with narrow hyperfine splittings. However, spectral differences between water soluble and insoluble complexes are seen, which leads them to suggest they differ both structurally and in their interaction with solvents in frozen solution. Further, the water-soluble complexes are permeable in tissues and this has allowed their ESR spectra to be measured for the first time in this medium.

Yordanov and co-workers (1682) reported that no changes were observed to the ESR signal of $[Cu(S_2CNEt_2)_2]$ when studied in a wide range of solvents, indicating its high stability. However, in DMSO the spectrum shifts to low field after several days with two new ESR spectra appearing; changes being rationalized in terms of the formation of a DMSO adduct. Related to this, Sarova and Jeliazkova (1683) reported that photolysis of $[Cu(S_2CNR_2)_2]$ in chloromethane–ethanol mixtures results in the generation of $[Cu(\mu\text{-}Cl)(S_2CNR_2)]_2$, as shown by ESR and visible spectra. The steady-state concentration was found to depend on

the nature of the substituents and the ethanol content. Further, the primary photochemical reaction is an intramolecular electron transfer from an equatorially bound sulfur to the copper(II) center, yielding the corresponding copper(I) complex and a dithiocarbamate radical. Similar charge-transfer photochemistry has been studied in the mixed-ligand complex $[Cu(S_2CNEt_2)(Se_2CNEt_2)]$, with homolytic copper–sulfur bond cleavage believed to be the primary photoprocess (1685).

In a series of papers, Ivanov and co-workers (533,1686–1699) studied the ESR spectra of copper(II) bis(dithiocarbamate) complexes and their adducts with bases while magnetically diluted with other bis(dithiocarbamate) complexes, $[M(S_2CNR_2)_2]$ (M = Ni, Cd, Zn, Hg), as well as with antimony(III) and thallium(I). As other bis(dithiocarbamate) complexes can adopt mononuclear square-planar (M = Ni) or dimeric nonplanar (M = Zn, Cd, Hg) configurations, then depending on the sample preparation, a number of different structural organizations are possible in these magnetically dilute systems. Indeed, they have found that in some cases a new structural type results, the two components crystallizing separately to form local spatial domains with a homogeneous molecular composition. The lack of crystallographic information, however, has meant that structural elucidation has not been possible. In an attempt to gain more insight, solid-state ^{13}C and ^{15}N CP/MAS NMR studies have been carried out on non-copper containing diamagnetic systems (533). These studies allow the third structural type to be tentatively identified as polynuclear $[M_2(S_2CNR_2)_4 \cdot nNi(S_2CNR_2)_2]$ (n = 1–4; M = Zn, Cd, Hg), with the simultaneous presence of mono- and binuclear dithiocarbamate units. Kirmse et al. (1700) also showed by using ^{13}C ENDOR spectra, that incorporation of $[Cu(S_2CNEt_2)_2]$ into single crystals of $[Zn(S_2CNEt_2)_2]$ results in an unexpectedly large isotropic coupling that can be understood in terms of a transannular overlap mechanism.

The electrochemical properties of $[Cu(S_2CNR_2)_2]$ have been widely studied previously (Fig. 224). In complexes undergoing reversible one-electron oxidation and reduction to copper(III) and copper(I) species, respectively (1701), similar findings were reported in a more recent paper (1702).

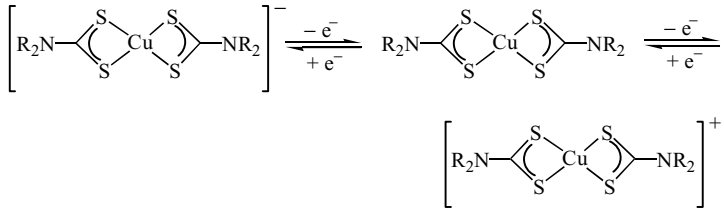

Figure 224. Electrochemical properties of copper(II) bis(dithiocarbamate) complexes.

As detailed earlier, Beer et al. (326) prepared a number of macrocyclic complexes containing copper(II) bis(dithiocarbamate) centers, and some instances electrochemical studies have been carried out. For example, cyclic voltammetry studies of $[Cu\{S_2CN(Bu)CH_2{-}m\text{-}C_6H_4CH_2N(Bu)CS_2\}_2]_2$ (**439**-Bu) show two one-electron oxidation processes separated by 0.14 V, indicating an electrochemical coupling between the two proximal metal centers. Interestingly, when the oxidation of the naphthyl-based complex $[Cu\{S_2CN(Bu)CH_2C_{10}H_6CH_2N(Bu)CS_2\}_2]_2$ (**440**-Bu) (Fig. 220) was carried out in the presence of anions (ReO_4^-, $H_2PO_4^-$, Cl^-,Br^-, NO_3^-), substantial cathodic shifts in the oxidation potential were seen (85 mV for ReO_4^- and $H_2PO_4^-$), while no shift was observed for other anions. In contrast, the smaller xylyl-based macrocycles (**439**) (Fig. 220) exhibited a small shift for chloride (20 mV), but negligible changes for the other anions. The interaction of perrhenate with the naphthyl-based complex (**440**-Bu) was further studied by UV–vis spectroscopy. A bathochromic shift of 10 nm was observed in the absorption maximum upon addition to $[Cu\{S_2CN(Bu)CH_2C_{10}H_6CH_2N(Bu)CS_2\}_2]_2[BF_4]_2$. This shift is interpreted as a result of the inclusion of ReO_4^- into the macrocycle cavity. Related xylyl-based macrocyles (**439**) are too big, and biphenyl-based macrocycles **441** (Fig. 220) are too small for anion inclusion.

Beer and co-workers (1471) also prepared a bis(dithiocarbamate) complex (**446**) (Fig. 220) with crown-ether appendages. Electrochemical studies show that it can sense various anions and cations. Significant cathodic and anodic perturbations of the Cu(II)–Cu(III) couple are observed.

The photochemical properties of $[Cu(S_2CNR_2)_2]$ (R = Et, *i*-Pr) have been investigated, and are characterized by a strongly allowed LMCT in the visible region. It results in reduction of the metal center and proceeds via an intramolecular electron transfer from an equatorially bonded sulfur. When irradiation is carried out in chloroform–ethanol mixtures, $[CuCl(S_2CNR_2)]$ initially results, on route to $CuCl_2$ (1703). Sarova and Jeliazkova (1683) further investigated the role of the solvent in the photochemical reactivity of a range of cyclic bis(dithiocarbamate) complexes, $[Cu(S_2CNC_4H_8X)_2]$ (X = O, NH, NPh, CH_2), and also report formation of $[CuCl(S_2CNR_2)]_n$ in chloromethane–ethanol mixtures. They suggest that monomeric $[CuCl(S_2CNR_2)]$ is in equilibrium with a chloro-bridged dimer $[Cu(\mu\text{-}Cl)(S_2CNR_2)]_2$ (1704) (Fig. 225). In support of

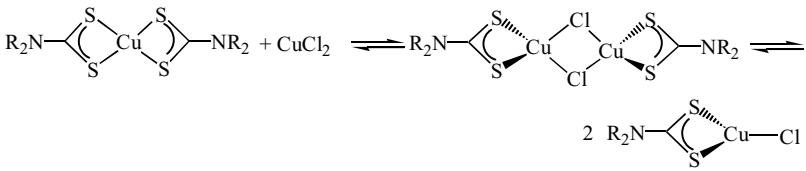

Figure 225. Proposed equilibrium upon addition of $CuCl_2$ to copper(II) bis(dithiocarbamate) complexes.

this finding, isotopic exchange between ^{63}Cu and ^{65}Cu has been noted between $[Cu(S_2CNEt_2)_2]$ and $CuCl_2$ in chloroform–DMSO solutions (519). Further, in either chloroform or ethanol, addition of a number of copper(II) halides is found to destroy the ESR signal of $[Cu(S_2CNR_2)_2]$, generating a new spectrum associated with $[CuX(S_2CNR_2)]_n$ (X = Cl, Br) (1681). This ligand-exchange process has been studied by ESR spectroscopy for a range of copper(II) salts (X = Cl, NO_3, ClO_4); equilibrium constants were calculated (601).

In a number of contributions, Iliev et al. (1705) focused on the reactivity of bis(dithiocarbamate) complexes. They combine with haloalkanes to give $[Cu(S_2CNR_2)X_n]$ (X = Cl, Br; $n = 1$ or 2), which in turn react with weak Lewis bases resulting in complete dithiocarbamate loss and formation of $[CuX_2B_n]$ ($n = 1, 2, 4$). Reactions also occur with Lewis acids, some being followed by ESR spectroscopy. In nonpolar and noncoordinating solvents, mercury(II) and germanium(IV) compounds formed adducts, while in polar coordinating solvents, mixed-ligand complexes resulted. Their reactivity toward Lewis acids such as $CoCl_2$, HgX_2, $GeCl_4$, $AsBr_3$, and $SbCl_3$ has also been investigated by ESR spectroscopy. Both in nonpolar and noncoordinating solvents, HgX_2 (X = Br, I) and $GeCl_4$ form adducts, whereas in polar coordinating solvents salts of the type $[Cu(S_2CNR_2)][HgX_3]$ result. Reactions of $[Cu(S_2CNR_2)_2]$ with $CoCl_2$, $AsBr_3$, and $SbCl_3$ result in halide transfer giving $[CuX(S_2CNR_2)]_n$ (1706).

In contrast to the addition of copper(II) halides, addition of copper(I) chloride to $[Cu(S_2CNR_2)_2]$ (R = Me, Et, *i*-Pr; $R_2 = C_4H_4$, C_4H_8O, C_5H_{10}) is proposed to afford mixed-valence complexes $[Cu(S_2CNR_2)_2(CuCl)_2]$. While their structures are unknown, they are paramagnetic (μ 2.2 BM per structural unit), probably containing both copper(I) and (II) centers bridged by the dithiocarbamates (1707). Addition of halides to $[Cu(S_2CNEt_2)_2]$ in DMSO has been reported to result in complete dissociation of the dithiocarbamates, which are oxidized to give tetraethylthiuram disulfide and the corresponding copper(II) halide (X = Cl, Br, I) (1708).

Addition of aliphatic amines (L) to $[Cu(S_2CNEt_2)_2]$ has been studied by ESR spectroscopy (1697). Initial formation of five-coordinate adducts is proposed, while over longer periods addition of more base affords complexes of the type $[Cu(S_2CNEt_2)_2L_2]$, which are believed to contain four coordinate, square-planar, copper centers, with a trans disposition of monodentate dithiocarbamate ligands.

Mederos et al. (1666) experimentally and theoretically studied the reaction of $[Cu\{S_2CN(CH_2CH_2OH)_2\}_2]$ with NO in water. Their calculations suggest that 2 mol of NO add in a stepwise fashion affording *trans*-$[Cu(NO)_2\{S_2CN(CH_2CH_2OH)_2\}_2]$ as the final product via an aquated intermediate $[Cu(NO)(H_2O)\{S_2CN(CH_2CH_2OH)_2\}_2]$ (Fig. 226). When followed experimentally by UV–vis spectroscopy, an isosbestic point was observed leading to the generation

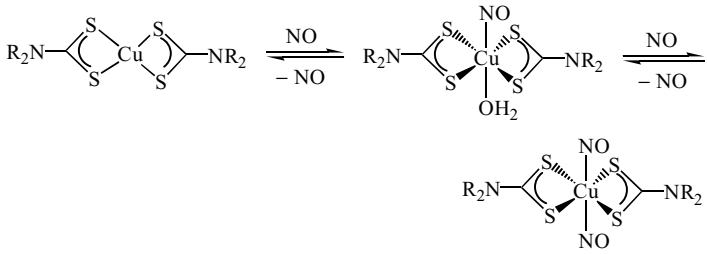

Figure 226. Proposed stepwise formation of a dinitrosyl complex upon addition of NO to $[Cu\{S_2CN(CH_2CH_2OH)_2\}_2]$.

of stability constants. These showed that the 1:1 complex is thermodynamically more stable than the 1:2 complex, which is in agreement with the theoretical studies.

Most recently, the same group reported the actual isolation and characterization of $[Cu(NO)(S_2CNC_4H_8O)_2].3H_2O$. The ν(NO) vibration appears at 1682 cm^{-1} in the IR spectrum and the complex adds a second nitrosyl to give $[Cu(NO)_2(S_2CNC_4H_8O)_2]$, which was not isolated. The mononitrosyl complex shows good stability, remaining unchanged when a solution is purged with either air or argon, while NO only begins to be lost upon heating to 333 K. Even at 373 K a weak nitrosyl band is still observed in the IR spectrum. The authors' also note that the mononitrosyl complex is ESR silent and is attributed to an electron–transfer, generating a reduced copper(I) center (1709).

b. Other Copper(II) Complexes. Dimeric copper(II) halide complexes, $[Cu(\mu\text{-}X)(S_2CNR_2)]_2$, have previously been prepared and crystallographically characterized (1710). More recently, a number of further publications have dealt with their synthesis and properties (1703,1704,1711,1712). In a series of papers, Jeliazkova and co-workers (1713–1716) probed the photochemistry of $[Cu(\mu\text{-}X)(S_2CNEt_2)]_2$ ($X = Cl$, Br) and related copper(II) complexes, $[Cu(S_2CNEt_2)][Y]$ ($Y = ClO_4$, NO_3), proposed to be formed as detailed earlier from reactions of $[Cu(S_2CNEt_2)_2]$ with CuX_2 and CuY_2, respectively. All have a strongly allowed LMCT transition in the visible region, leading to reduction of the metal via an intramolecular electron transfer from an equatorially bound sulfur. Irradiation of $[Cu(S_2CNEt_2)][Y]$ in solvent mixtures containing chlorocarbons affords $[Cu(\mu\text{-}Cl)(S_2CNEt_2)]_2$ enroute to $CuCl_2$ (1713), while photolysis of $[Cu(\mu\text{-}Br)(S_2CNEt_2)]_2$ in chloroform gives the corresponding chloride-bridged dimer and visa versa (1716). Other workers have shown that addition of pyridines or picolines (L) to $[Cu(\mu\text{-}Cl)(S_2CNEt_2)]_2$ gives monomeric, tetrahe-

dral, copper(II) dithiocarbamate complexes, $[CuCl(S_2CNEt_2)L]$ (Eq. 159), with magnetic moments of 1.09–2.09 BM (1717).

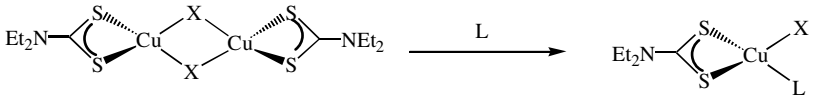

(159)

A number of related monomeric mixed-ligand complexes of the type $[Cu(S_2CNR_2)(chelate)]$ have been reported. They have been prepared with acac, oxime, dithiophosphate, and bis(8-quinoline-thiolato-5-SO_3H) coligands upon mixing bis(dithiocarbamates) with the corresponding bis(chelate) complexes (1718,1719), or from $CuCl_2$ and equimolar amounts of the sodium salts of the corresponding ligands. The latter has been used to prepare a series of 2-hydroxyaryloxime complexes, $[Cu(S_2CNR_2)(\eta^2\text{-}OC_6H_4CR'{=}NOH)]$ ($R = Et$, Bz; $R_2 = C_5H_{10}$; $R' = H$, Me, Et) (**451**) (Fig. 227), shown by ESR spectroscopy to contain a square-planar copper center (1720). Jeliazkova (1721,1722), Iliev (1523,1719), and their co-workers have studied the photochemical properties of mixed-ligand dithiocarbamate–dithiophosphate complexes using ESR spectroscopy as a probe. For example, photolysis of $[Cu(S_2CNEt_2)\{S_2P(O{-}i\text{-}Pr)_2\}]$ (**452**) (Fig. 227) results in generation of an equilibrium mixture with the bis(ligand) complexes; homolytic cleavage of the copper–sulfur bonds to the dithiophosphate ligand being shown to be the primary photoprocess (1719).

Very recently, Esmadi and Irshiadat (1526) reported the synthesis of Schiff base complexes of the stoichiometry $[Cu_2L(S_2CNC_4H_8)_3]$ and $[Cu_4L_2(S_2CNC_4H_8NCS_2)_3]_n$ ($L = OC_6H_4CH{=}NAr$; $Ar = 7$-naphthyl). In the absence of crystallographic data, it is not possible to ascertain precise structural details, but the latter is believed to be polymeric. El-Said et al. (119) detailed the reaction of the dithiocarbamate salt generated from phenylalanine with 2 equiv of $[Cu(1,10\text{-phen})_3]Br_2$ in water, proposing the formation of a binuclear

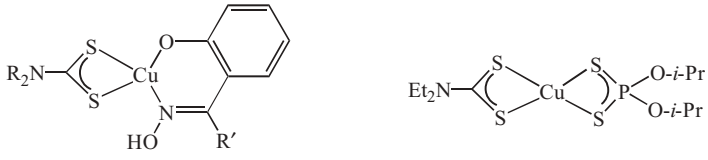

451 **452**

Figure 227. Examples of mixed-ligand complexes of the type $[Cu(S_2CNR_2)(chelate)]$.

complex, $[Cu_2Br_2(1,10\text{-phen})_2(H_2O)_2\{\mu\text{-}S_2CNHCH(Bz)CO_2\}]$ (**453**), with the functionalized dithiocarbamate bridging metal centers in an unusual manner.

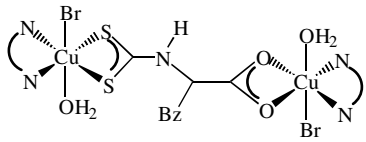

453

c. Copper(III) Complexes. Copper(III) bis(dithiocarbamate)complexes, $[Cu(S_2CNR_2)_2]X$, are readily prepared upon oxidation of the corresponding copper(II) complexes, with oxidizing agents including $[CuClO_4]$ (319, 323, 1723), $[Cu(BF_4)_2]$ (1558), $FeCl_3$ (104, 319, 326, 1558), and iodine (318, 323–325, 586, 1718). Direct reaction of $[Cu(ClO_4)_2.6H_2O]$ with thiuram disulfides also gives a route to $[Cu(S_2CNR_2)_2][ClO_4]$ ($R = Cy$; $R_2 = C_4H_8O$), although copper(III) salts could not be obtained with the smaller anions, such as chloride, bromide, or nitrate (1724). Bond et al. (303) studied the oxidation by $NOBF_4$ using ESMS, and noted that mixing of different copper(III) cations leads to global exchange of the dithiocarbamate ligands. Interestingly, with $[Cu(S_2CNC_5H_{10})_2]$, ions $[CuS(S_2CNC_5H_{10})_2]^+$ and $[CuS(S_2CNC_5H_{10})]^+$ were also observed and this is believed to result from sulfur extrusion from the thiuram disulfide.

Crystallographic studies have been carried out on a number of examples (104, 318–326). All contain square-planar copper(III) centers, which attain an overall distorted octahedral coordination via intermolecular interactions. Six structural types can be differentiated (Fig. 228); (1) polymeric chains with secondary copper–sulfur interactions in which anions and cations are quite separate (104, 319–322) (S); (2) polymeric chains with secondary anion–cation interactions (T); (3) dimeric units with secondary copper–sulfur interactions, but with separate anions and cations (323) (U); (4) dimeric units with secondary interactions to the anions (319) (V); (5) monomeric units with two secondary anion interactions (318, 324, 325) (W); (6) monomeric centers with a single anion interaction (X) (326).

By taking into account the secondary interactions, for structural types (S and T) and (V and W) the coordination geometry at the metal center is pseudo-octahedral, and in (U) and (X), square-based pyramidal. The intramolecular copper–sulfur bonds of ~2.2 Å are some 0.1 Å shorter than those in $[Cu(S_2CNR_2)_2]$, although the intermolecular copper–sulfur interactions are considerably longer (3.1–3.7 Å as compared with 2.7–2.9 Å).

Iron tetrachloride salts display a number of these structural types. Thus, $[Cu(S_2CNEt_2)_2][FeCl_4]$ adopts the structure (S) with discrete anions and cations

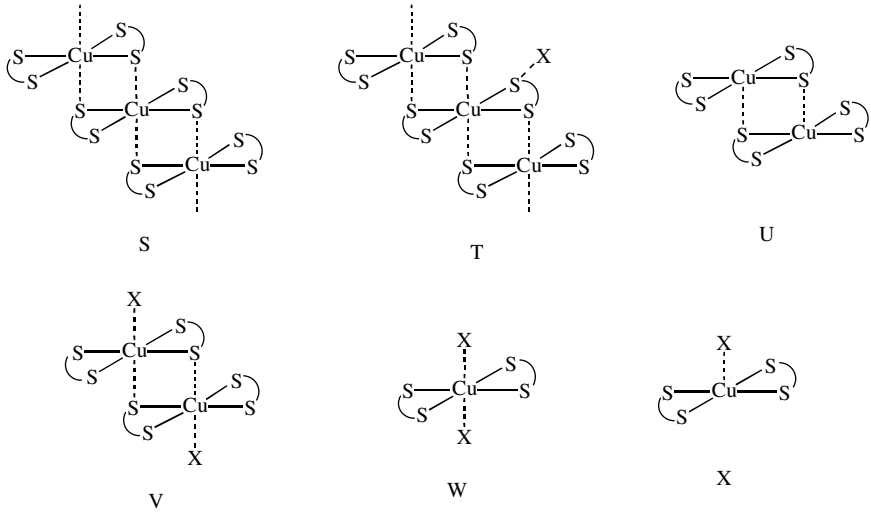

Figure 228. Structural forms adopted by copper(III) bis(dithiocarbamate) complexes.

(319), while in other examples (R = Pr; R^1 = Me, R^2 = Bu) (104) the polymeric cation chain (T) is supplemented with weak Cl···S interactions, typically of ~3.6 Å. Oxidation of $[Cu\{S_2CN(Pr)CH_2{-}m\text{-}C_6H_4CH_2N(Pr)CS_2\}_2]_2$ (**439**-Pr) (Fig. 220) by iron trichloride yields the analogous copper(III) complex in which an $[FeCl_4]^-$ anion binds to each copper center via a chlorine atom [Cu–Cl 3.00 Å] (326), while the benzyl complex $[Cu(S_2CNBz_2)_2][FeCl_4]$ (Fig. 229) exhibits both copper–chlorine and copper–sulfur anion–cation interactions (104).

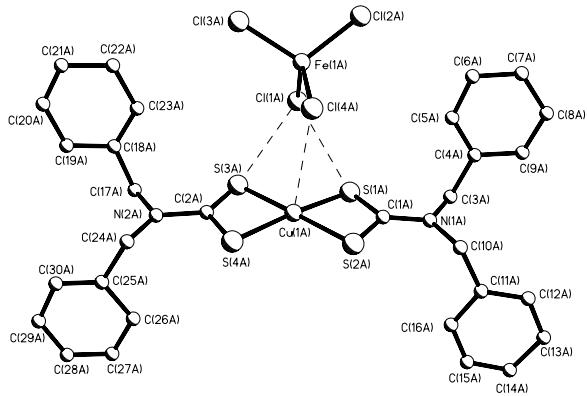

Figure 229. Crystal structure of $[Cu(S_2CNBz_2)_2][FeCl_4]$.

Perchlorate salts also show a range of structural types. For example, $[Cu(S_2CNC_4H_8)_2][ClO_4]$ (323) adopts structural type (U), while $[Cu(S_2CNPr_2)_2][ClO_4]$ is polymeric (S), but also does not show anion–cation contacts (104). In contrast, $[Cu(S_2CNMe_2)_2][ClO_4]$ adopts a type (V) structure with the sixth coordination site on each metal atom being taken up with a Cu···O interaction of 2.753(3) Å (319).

Iodide complexes also adopt different structural types. The $[Cu(S_2CNBu_2)_2][I_3]$ complex polymeric with no anion–cation interactions (S) (320), while $[Cu(S_2CNEt_2)_2][I_3]$ is also polymeric, but adopts structural type (W) to form infinite ladder chains in which bis(dithiocarbamate) units are separated by I_3^- anions (324). In contrast, $[Cu(S_2CNPr_2)_2][I_5]$ adopts a type (X) structure in which the copper center is five coordinate, an is bound to the central atom of the I_5^- anion [Cu···I 3.665(4) Å] (318).

Very recently, Beer and co-workers (325) reported the synthesis and structure of the resorcarene-based complex $[Cu_8(L_1)_4][I_3]_7[I].6H_2O$ (Fig. 230), which is

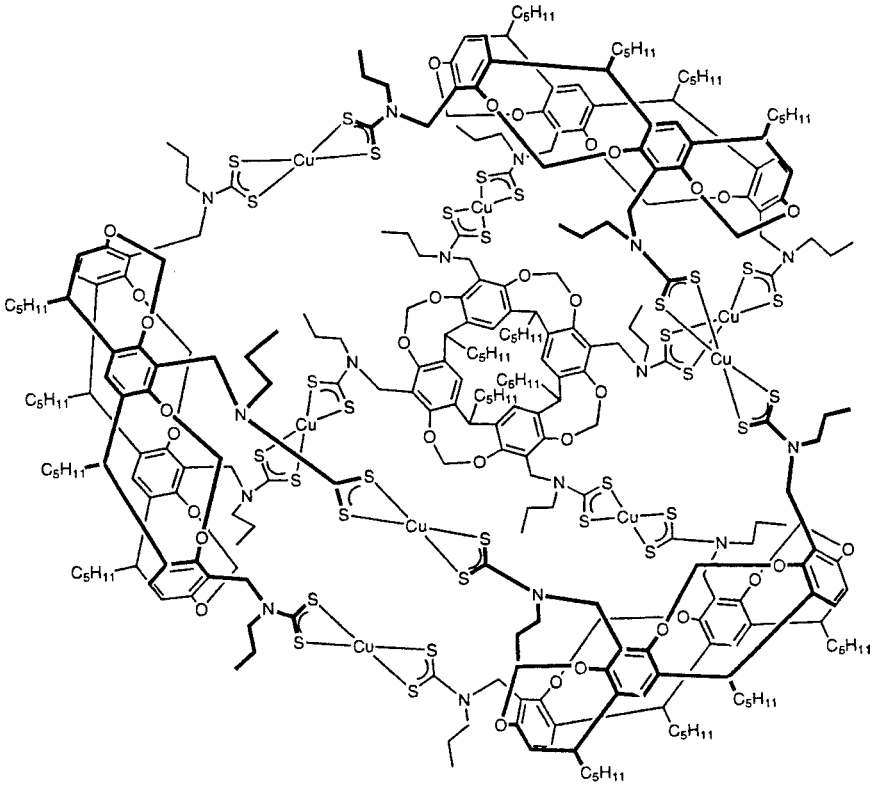

Figure 230. Structural representations of the resorcarene-based complex $[Cu_8(L_1)_4][I_3]_7[I].6H_2O$.

formed upon treatment of the *in situ* generated copper(II) analogue with iodine. Here, the four resorcarene ligands lie at the apices of a distorted tetrahedron, and are connected to each other by the eight copper(III) centers, which fall into two crystallographically unique types. There is a strong variance in the copper–sulfur bond lengths [2.11(2)–2.47(2) Å], probably resulting from stress forces imposed by the overall structure, and each copper center is also bound to a triiodide anion [Cu···I 3.19–3.26 Å]. Thus, the overall structure is that of (X), with the added feature that for one of the types of copper center, this links to a copper ion in a second tetrahedron.

The resorcarene-based complex $[Cu_8(L_1)_4][I_3]_7[I].6H_2O$ is insoluble in nonpolar solvents and upon dissolution in polar or protic solvents is reduced back to the copper(II) species (325). A similar spontaneous reduction of $[Cu(S_2CNEt_2)_2][I_3]$ was reported earlier (324). Interestingly, in this case, monitoring the process by ESR spectroscopy showed that the spectral parameters of the reduced species were dependent on the nature of the solvent, and also were not those associated with $[Cu(S_2CNEt_2)_2]$. The authors attributed these observations to the concomitant oxidation of dithiocarbamate to thiuram disulfide, and generation of a $[Cu(S_2CNEt_2)]^+$ fragment, which is stabilized by coordination of two molecules of solvent (such as pyr or dmso), yielding $[Cu(S_2CNEt_2)_2]$ upon addition of a further equivalent of dithiocarbamate salt (Fig. 231).

Other copper(III) bis(dithiocarbamate) complexes that have been crystallographically characterized include $[Cu(S_2CNBu_2)_2]_2[Hg_2Br_6]$, which adopts the polymeric structure (S) with no significant anion–cation interactions (321,322). This structure is interesting as it exhibits a reversible transition point ca. −50°C, and has been studied at room temperature (321) and at −40°C (322). The two structures are essentially isomorphous apart from a significant change from trans to gauche about the β—γ bond of one butyl substituent.

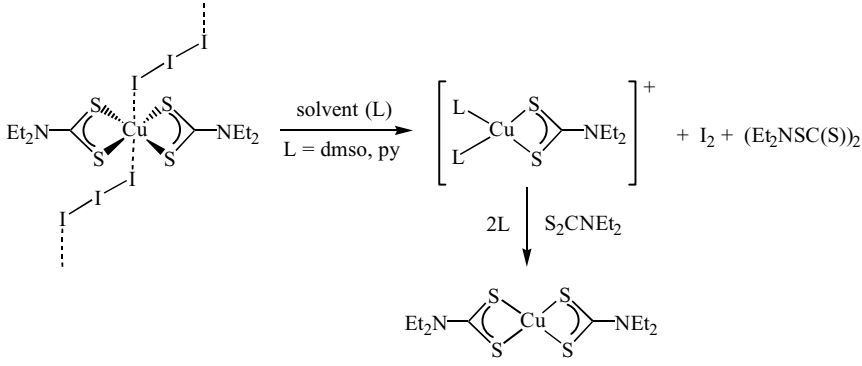

Figure 231. Proposed spontaneous reduction of $[Cu(S_2CNEt_2)_2][I_3]$ upon dissolution.

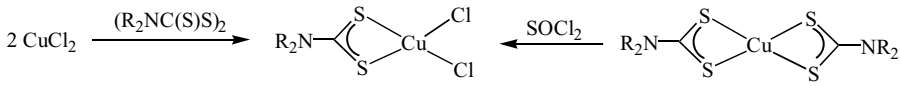

Figure 232. Synthetic routes to $[CuCl_2(S_2CNR_2)]$.

Copper(III) bis(halide) complexes, $[CuCl_2(S_2CNR_2)]$, have been prepared in 80–90% yield upon oxidation of $[Cu(S_2CNR_2)_2]$ (R = Et; $R_2 = C_4H_4$, C_4H_8O, C_5H_{10}) by thionyl chloride (1725), and can also be prepared (R = Me, Et, *i*-Pr) in high yields, along with their bromide analogues, upon addition of thiuram disulfides to copper(II) halides in THF (Fig. 232) (170,1726,1727). These routes provide an alternative synthesis to the direct addition of chlorine to bis(dithiocarbamates).

A related copper(III) complex, $[Cu(CF_3)_2(S_2CNEt_2)]$, prepared from $[CuBr_2(S_2CNEt_2)]$ and $[Cd(CF_3)_2]$ at −30°C (Eq. 160), has been crystallographically characterized. It is stable in DMF to 70°C, but rapidly decomposes at 110°C. At these elevated temperatures, the release of the trifluoromethyl groups has lead to it being used as a reagent for the substitution of halides by CF_3 in aromatic systems (1728).

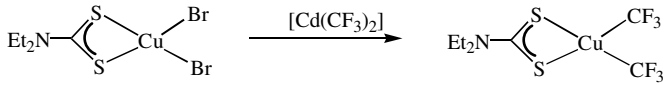

(160)

In further contributions, the kinetics of the reaction of $[Cu(S_2CNR_2)_2]$ (R = Me, Et; R_2 = MePh) with periodate have been studied. Oxidation is shown to be first order with respect to the complex and periodate (1729), while copper(III) complexes, $[Cu(S_2CNR_2)_2][BF_4]$ (R = Me, Et), have been found to oxidize iron and manganese(III) tris(dithiocarbamate) complexes to give $[M(S_2CNR_2)_3][BF_4]$ (M = Fe, Mn) (1124).

d. Mixed-Valence Copper(II)–Copper(III) Complexes. Mixed-valence copper(II)–copper(III) complexes of the type $[Cu_3(S_2CNR_2)_6]^{2+}$ (**454**) previously have been studied extensively (1730,1731). They consist of a copper(II) bis(dithiocarbamate) unit sandwiched between two copper(III) bis(dithiocarbamate) moieties, being linked by weak copper–sulfur interactions such that the copper(II) center is pseudo-octahedral. More recently, complexes of this type

have been prepared from the reaction of mixed benzoic dithiocarbamic anhydrides with copper(II) bromide in ether (1732).

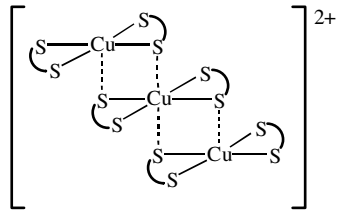

454

Beer and co-workers (544) noted some interesting chemistry upon oxidation of the macrocycle **440**-Bu (Fig. 220) by iron trichloride, which when followed by addition of excess sodium perrhenate affords a novel tetranuclear copper catenane (**455**), with discrete anions and cations. All four copper centers are independent, copper–sulfur bond lengths of 2.233–2.300 Å falling between the expected mean copper(II)–sulfur and copper(III)–sulfur bond lengths of 2.306 and 2.210 Å, respectively. This finding suggest a disorder between copper(II) and copper(III) centers. Further, each copper center also shows axial copper–sulfur interactions. Magnetic susceptibility data (5–300 K) are consistent with two magnetically isolated copper(II) centers, suggesting a formulation $Cu^{(II)}Cu^{(III)}Cu^{(II)}Cu^{(III)}$.

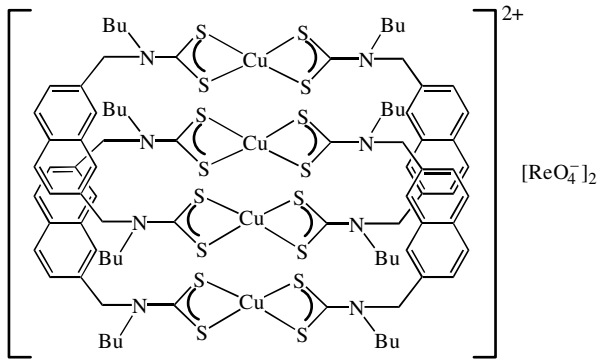

455

Victoriano et al. (1711,1712) reported that addition of thiuram disulfides to copper(I) halides gives mixed-valence complexes $[Cu(S_2CNR_2)_2][CuX(S_2CNR_2)]$ (R = Me, Et; X = Cl, Br) containing one copper(III) and a second copper(II) center. Upon thermolysis (R = Me), electron transfer occurs generating the black copper(II) dimer $[Cu(S_2CNMe_2)(\mu\text{-}Cl)]_2$ (μ_{eff} 1.81 BM) and one-half of an equivalent of tetramethylthiuram disulfide.

e. Copper(I) Complexes. Copper(I) bis(dithiocarbamate) complexes $[Cu(S_2CNR_2)_2]^-$ can be generated electrochemically from the analogous copper(II) species, however, all attempts to isolate them have proved unsuccessful, with loss of a dithiocarbamate ligand occurring to give tetrahedral clusters $[Cu(S_2CNR_2)]_4$ (329). Relatively little work appears to have been published in this area since 1978. Victoriano and Cortes (1733) reported that they can be prepared from the reaction of $[Cu(S_2CNR_2)_2]$ (R = Me, Et) with excess copper powder in carbon disulfide, or more directly from a large excess of the thiuram disulfide (R = Me, Et, *i*-Pr) and electrolytic purity copper powder in the same medium. Zhang et al. (1734) also report the synthesis of $[Cu(S_2CNC_4H_8)]_n$ from the reaction of $[NH_4][S_2CNC_4H_8]$ with copper(I) chloride. Copper(I) complexes, $[Cu(S_2CNR_2)]_n$ and $[Cu(S_2CNR_2)(dppe)]$ (R = *o*-NC_6H_4), have been proposed to result from the insertion of carbon disulfide into the respective copper(I) amine complexes; although characterization was made only on the basis of their IR spectra (195).

By utilizing the conproportionation reaction detailed above, a number of new derivatives have been prepared (R = Pr, Bu, Bz) and the X-ray crystal structure of $[Cu(\mu^3\text{-}S_2CNBu_2)]_4$ (Fig. 233) has been carried out. This structure reveals the

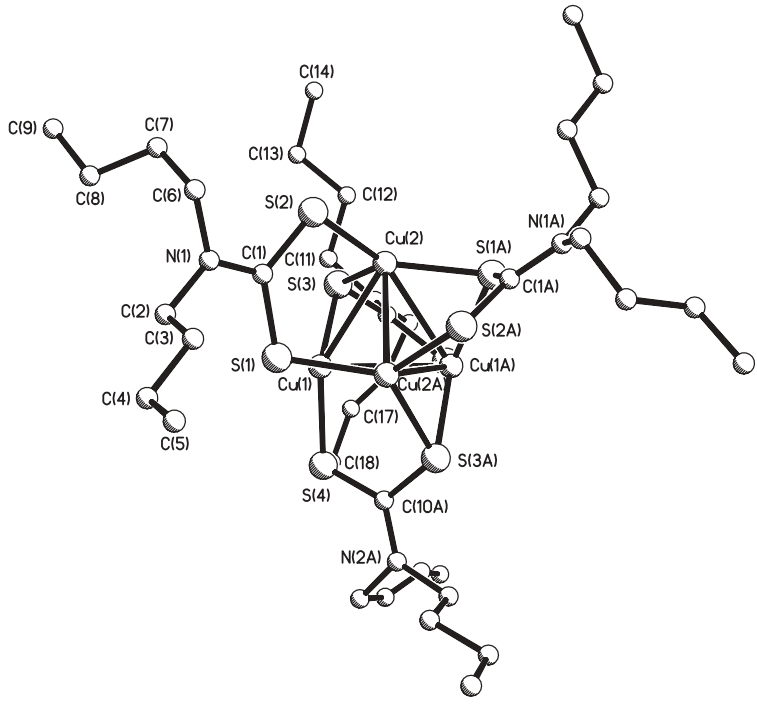

Figure 233. Crystal structure of $[Cu(\mu^3\text{-}S_2CNBu_2)]_4$.

expected tetrahedral arrangement of copper atoms, each triangular face being capped by a dithiocarbamate binding in an η^1,η^2-manner (327).

The disproportionation reaction between $[Cu(S_2CNR_2)_2]$ and copper(II) perchlorate is known to afford copper(III) complexes $[Cu(S_2CNR_2)_2][ClO_4]$ (see above), however, until now the nature of the copper(I) product was unclear (319,323,1723). Very recently, from the reaction with $[Cu(S_2CNPr_2)_2]$, the copper cube $[Cu_8(\mu^4\text{-}S_2CNPr_2)_6][ClO_4]_2$ has been isolated and crystallographically characterized (Fig. 234) (104). Since each copper face is capped by a dithiocarbamate, then the molecule consists of a cube of copper atoms, surrounded by an icosahedron of sulfurs, further surrounded by an octahedral array of carbon–nitrogen bonds. The copper–copper distances of 2.8038(6)–2.8087(6) Å are similar to those of 2.6368(4)–2.8119(5) Å found in $[Cu(\mu^3\text{-}S_2CNBu_2)]_4$ (327).

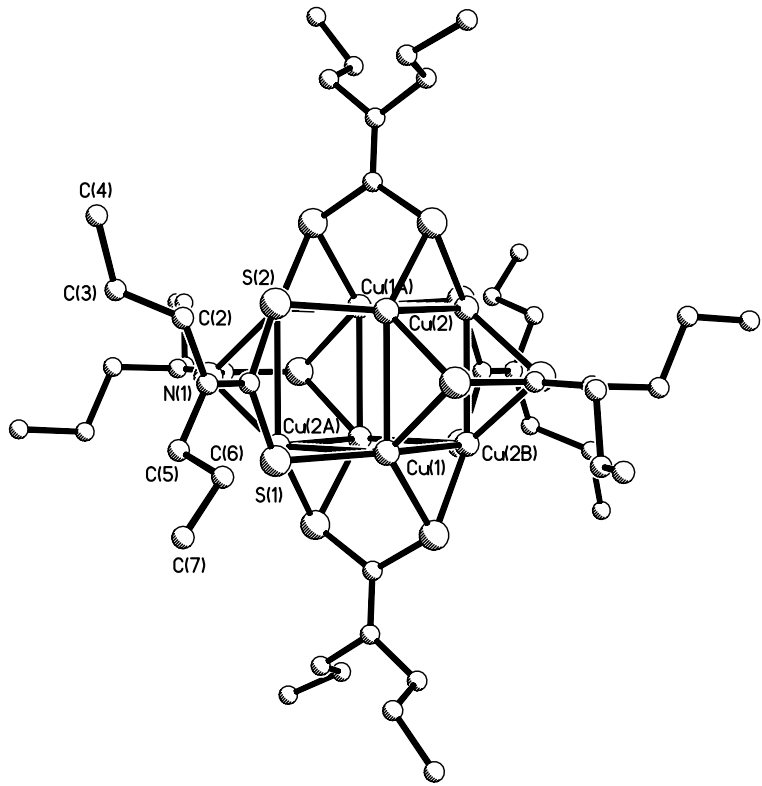

Figure 234. Crystal structure of the cation in $[Cu_8(\mu^4\text{-}S_2CNPr_2)_6][ClO_4]_2$.

A number of reactions of copper(I) complexes, $[Cu(S_2CNR_2)]_4$, have been reported. Those with haloalkanes have been studied by ESR spectroscopy and yield $[Cu(\mu\text{-}X)(S_2CNR_2)]_2$, with free radicals also being detected (1705). Very recently, Odom and Cummins (1735) reported that $[Cu(S_2CNEt_2)]_4$ reacts with the chromium(VI) nitride, [CrN(S—*t*-Bu)$_3$], to give [CrN(S—*t*-Bu)(μ-S—*t*-Bu)$_2$-Cu(S_2CNEt_2)] (Eq. 161), which contains a distorted tetrahedral copper(I) center.

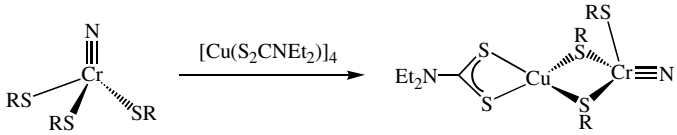

(161)

Addition of PPh_3 to $[Cu(S_2CNR_2)]_4$ in acetonitrile affords bis(phosphine) adducts $[Cu(PPh_3)_2(S_2CNR_2)]$ (1733). They are labile in solution and attempts to crystallize them often leads to rearrangements, nevertheless, the *n*-propyl derivative has been characterized crystallographically and shows the expected distorted tetrahedral coordination geometry (1736). Bianchini et al. (218,219) prepared analogous bis(phosphine) complexes $[Cu(PR_3)_2(S_2CNHPh)]$ (R = Ph, Cy) from the reaction of $[Cu(PR_3)_2(\eta^2\text{-}BH_4)]$ with 2 equiv of phenylisothiocyanate, with benzonitrile being the second product (Eq. 162). One example (R = Ph) has been crystallographically characterized, its unique dithiocarbamate proton being clearly observed in the ^{1}H NMR spectrum at δ 8.99–9.05.

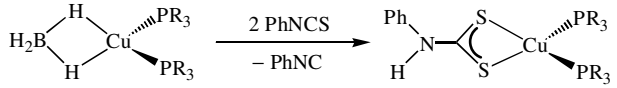

(162)

Reactions of isothiocyanates with the triphosphine complexes $[Cu\{\eta^3\text{-}(Ph_2PCH_2)_3CMe\}(\eta^1\text{-}BH_4)]$ and $[Cu\{\eta^3\text{-}(Ph_2PCH_2CH_2)_3N\}(\eta^1\text{-}BH_4)]$ proceed in a similar manner generating what are believed to be monodentate dithiocarbamate complexes. Spectroscopic data for these complexes is very similar to the bis(phosphine) complexes (219).

A further diphosphine complex, $[Cu_2(\mu\text{-}S_2CNEt_2)(\mu\text{-dppm})_2][ClO_4]$, has been prepared and crystallographically characterized (Fig. 235) (1737). It consists of two copper(I) centers in close proximity [Cu—Cu 2.711(1) Å] bridged by mutually trans diphosphines and a dithiocarbamate that lies at right angles to both.

f. Mixed-Metal Clusters. Three distinct types of copper-containing, mixed-metal, dithiocarbamate clusters can be identified. The first are complexes

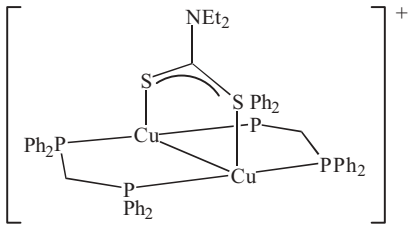

Figure 235. Structure of dicopper cation $[Cu_2(\mu\text{-}S_2CNEt_2)(\mu\text{-}dppm)_2]^+$.

in which copper(I) halide centers are linked via a bridging dithiocarbamate to other metal centers. They are formed upon addition of the copper(I) halides to $[M(S_2CNR_2)_2]$ (M = Pt, Pd) (297,1650) and $[M(S_2CNR_2)_3]$ (M = Cr, Co, Rh, Ir) (312,1400,1401,1738) and have been discussed previously (see Sections IV.C.1.a, IV.F.1.c, and IV.G.2.a). The ratio of copper to heterometal varies, usually being between 1:1 and 3:1, and molecular and polymeric structures can result. For example, addition of 2 equiv of copper(I) iodide to $[Co(S_2CNPr_2)_3]$ in acetonitrile yields tetranuclear, $[Co(S_2CNPr_2)(\mu\text{-}S_2CNPr_2)_2Cu(\mu\text{-}I)]_2$ (**456**), in which two dithiocarbamates form a bridge between cobalt and copper centers. The latter is held together by the iodides (1738).

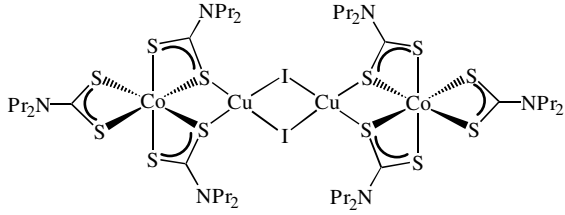

456

In the second type of mixed-metal cluster, copper(I) dithiocarbamate centers are linked to group 6 (VI B) metals via sulfido or selenido bridges (1734, 1739–1746). They are formed from mixtures of copper(I) halides, dithiocarbamate salts, and $[ME_4]^{2-}$ (M = Mo, W; E = S, Se). The ratio of copper heterometal varys between 1:1 and 4:1. All are molecular and each metal ions adopts a distorted tetrahedral geometry. Metal–metal interactions are also found. For example, $[MoCu_3(\mu\text{-}S)_2(\mu^3\text{-}S)_2(S_2CNEt_2)_3][NEt_4]_2$ (**457**) has been shown crystallographically to contain strong copper–molybdenum interactions [Mo—Cu(av) 2.665 Å] (1743).

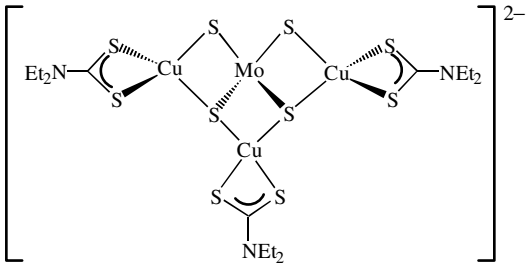

457

Electrochemical studies have been carried out on clusters of this type. For example, $[Mo(\mu\text{-}S)_4\{Cu(S_2CNMe_2)\}_2][NEt_4]_2$ shows two irreversible one-electron oxidation waves together with an irreversible one-electron reduction. Oxidation is believed to occur at copper, with the copper(II) fragment, $[Cu(S_2CNMe_2)]^+$, undergoing rapid dissociation from molybdenum (1742).

Closely related are vanadium–copper complexes $[VCu_4(\mu^3\text{-}S)_4(S_2CNC_4H_8O)_{4-n}(SPh)_n]^{3-}$ ($n = 1$–3) (Fig. 236), in which copper centers are linked by sulfido bridges to vanadium, and each copper carries either a dithiocarbamate or thiolate ligand (700,1747,1748). Vanadium-51 NMR studies suggest that in solution the different complexes are in equilibrium with one another.

A third type of mixed-metal cluster are those with the general formula $[M_2Cu_5S_6E_2(S_2CNR_2)_3]^{2-}$ (M = Mo, W; E = O, S), containing cubane-type cores held together by oxo and sulfido ligands (266,1749–1753). They are formed from reactions of metal sulfides, $[MS_2E_2]^{2-}$, copper(I) chloride, and dithiocarbamate salts in DMF in the presence of Ph_4PBr or Et_4NBr. X-ray crystallographic studies reveal a structure in which two defective cubane-type units, EMS_3Cu_2 and EMS_3Cu_3, are linked by two weak copper–sulfur bonds and

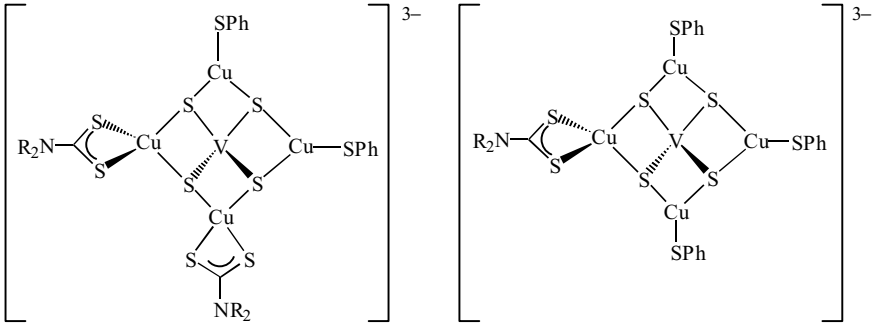

Figure 236. Examples of $[VCu_4(\mu^3\text{-}S)_4(S_2CNC_4H_8O)_{4-n}(SPh)_n]^{3-}$ ($n = 2$, 3).

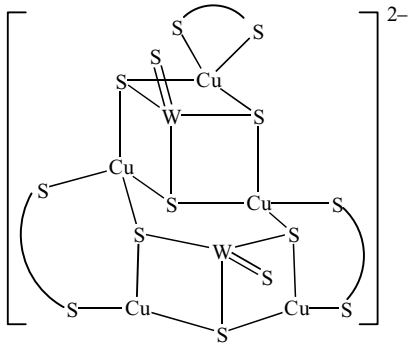

Figure 237. Representation of the cluster core in $[W_2Cu_5(\mu^3\text{-}S)_6S_2(S_2CNMe_2)(\mu\text{-}S_2CNMe_2)_2]^{2-}$.

two bridging dithiocarbamate ligands, as exemplified by $[W_2Cu_5(\mu^3\text{-}S)_6S_2(S_2CNMe_2)(\mu\text{-}S_2CNMe_2)_2][NEt_4]_2$ (Fig. 237) (1750). Here, each group 6 (VI B) ion carries a terminal chalcogenide ligand, which can be oxygen or sulfur, while the other six sulfur ligands are triply bridging, binding to two copper and one group 6 (VI B) ion.

g. Applications. A wide range of applications have been found for copper dithiocarbamate complexes, especially the copper(II) bis(dithiocarbamate) series, which find uses in analytical chemistry as molecular precursors to copper sulfides and as homogeneous catalysts.

i. Analytical Chemistry. Copper(II) bis(dithiocarbamate) complexes find extensive use in the determination of copper(II) concentrations. For example, a gravimetric determination and separation from nickel(II) has being reported (1754,1755), while water-soluble $[Cu\{S_2CN(CH_2CH_2OH)_2\}_2]$ (1756) and other complexes (1757) have been used for copper(II) extraction and spectrophotometric detection (1757). Further, reaction of copper(II) in solution with NaS_2CNEt_2 results in the precipitation of $[Cu(S_2CNEt_2)_2]$, which then absorbs onto the quartz plate in an electrode-separated piezoelectric quartz crystal assembly. The observed frequency change is proportional to the concentration of copper(II) in solution over the range 0.3–5.0 μM, although both silver(I) and mercury(II) interfere (1758).

Bond and Wallace (1759) utilized the well-documented electrochemical behavior of $[Cu(S_2CNEt_2)_2]$ to develop a reverse-phase liquid chromatographic detection of copper(II) with electrochemical detection. Bond has also developed a method for the detection of copper in water-saturated toluene using microdisk electrodes; the absorption or precipitation of electrogenerated $[Cu(S_2CNEt_2)_2]^+$

on the electrode surface leads to the development of a cathodic stripping method for the determination of copper that is not available in dry toluene (1760).

The bis(dithiocarbamate) complex derived from the alkaloid emetine (Eq. 163) can be detected at 10^{-10}–10^{-6} mol dm^{-3} by flow injection analysis using the electrogenerated chemiluminescence detection of $[Ru(bpy)_3]^{2+}$ (1761). Further, the copper, nickel, and cobalt emetine-derived complexes have been successfully separated and detected to a limit of 50 n*M* by using this method (1762).

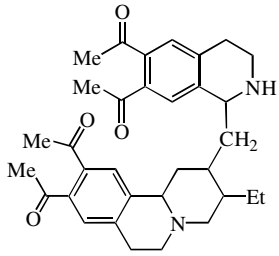

Emetine

$$\text{Emetine} + CS_2 + M^{(II)} \longrightarrow [M(S_2CNR_2)_2] \quad (163)$$

M = Cu, Ni, Co

Copper(II) bis(dithiocarbamate) groups have been bound to macroporous polystyrene resins (139,1763) and other polymeric sorbents (1764), with ESR spectroscopy being used to detected and probe the nature of the copper environment. The *N*-sulfonylethylene bis(dithiocarbamate) ligand when anchored on macroporous polystyrene–divinylbenzene beads has been used for the selective removal of mercury(II), silver(I), and copper(II) from aqueous solutions, the overall selectivity being

$$Hg^{2+} \geq Ag^{+} > Cu^{2+} > Cd^{2+} > Fe^{3+} \sim Al^{3+} \sim Cr^{3+} > Ni^{2+} > Zn^{2+} \sim Co^{2+} > Mn^{2+} \gg Mg^{2+}$$

In other work, Guo and Khoo (1765) developed a method for the quantitative detection of cysteine in the 10^{-5}–10^{-3}-mol L^{-1} range using carbon paste electrodes chemically modified with $[Cu(S_2CNEt_2)_2]$.

ii. Molecular Precursors to Copper Sulfides and Related Materials. It has been known for some time, primarily as a result of TGA studies, that copper(II) bis(dithiocarbamate) complexes degrade under nitrogen to first give CuS and then Cu_2S at higher temperatures. Further, in some instances the early degradation product $[Cu(SCN)_2]$ is also observed. In contrast, carrying out the same thermal decomposition in air leads only to copper oxide and copper sulfate as the final products (593,1766). Given this behavior, these complexes have been

widely used as single-source precursors for the growth of semiconducting copper sulfide thin films (1766–1772). The degradation pathway can sometimes be a function of the nature of the dithiocarbamate substituents. For example, Nomura et al. (1766) established that while simple alkyl substituted complexes (R = Et, Bu, Hex, Oct) decompose to Cu_2S at temperatures up to 320°C, in contrast, hydroxy-substituted $[Cu\{S_2CNMe(CH_2CH_2OH)\}_2]$ displays different behavior. Here, formation of CuS occurs at ~230°C, being converted to Cu_2S at between 300 and 400°C. The same group later studied the decomposition of $[Cu(S_2CNEt_2)_2]$ in some detail, and showed that initial formation of CuS did occur, but this decomposed slowly to Cu_2S over 4–5 h.

The steric size and nature of the peripheral substituents on ancillary ligands can have a profound effect on the performance of the precursor under MOCVD conditions. Recently, O'Brien and co-workers (1772) showed in using $[Cu(S_2CNMeHex)_2]$ that crystalline plates of Cu_2S can be deposited within an hour, with the enhanced rate being attributed to its greater volatility. Further, using the same precursor, highly orientated thin films of non-stoichiometric cubic CuS have been grown using aerosol-assisted chemical vapor deposition. In order to determine the effect of changes to the ancillary groups on potential MOCVD performance, Welch and co-workers (317) probed the thermal and structural properties of a range of copper(II) bis(dithiocarbamate) complexes. Interestingly, they found that only modest gains in volatility resulted from increasing alkyl chain length, and while unsymmetrical substitution also gave improved volatility, this was at a cost of some loss in thermal stability. They also found that the volatility of the complexes showed little dependence on whether intermolecular C---S interactions were present in the solid state (see earlier), consistent with the view that all are monomeric in the gas phase (589,1674).

In other work in this area, thermal decomposition of $[Cu(S_2CNEt_2)_2]$ by remote plasma enhanced vapour deposition at low pressure (10^{-3}–10^{-1} Torr) and temperature (100–500°C) using helium as a carrier gas yields has been shown to give thin films of Cu_2S (1768), and the thermal decomposition kinetics of polymeric copper(II) complexes of bis(dithiocarboxy)piperazine in air have been followed by TGA and associated techniques; decomposition being slow at 240°C, but complete at 362°C, and follows first-order kinetics (1773). Further, Nomura et al. (1767) also demonstrated the preparation of Cu_2S thin films on glass substrates via the solution pyrolysis of $[Cu\{S_2CNMe(CH_2CH_2OH)\}_2]$ at 250–300°C in DMSO.

In related work, Nomura et al. (1774,1775) prepared bimetallic copper-indium complexes, such as $[Bu_{3-n}InCu(S{-}i\text{-}Pr)_n(S_2CNR_2)]$ (R = *i*-Pr, Bu) from the reactions of $[Bu_nIn(S{-}i\text{-}Pr)_{3-n}]$ with $[Cu(S_2CNR_2)_2]$; copper(II) was reduced to copper(I) in the process. The precise structures of these heterobimetallic complexes are unknown, but they are believed to have bridging thiolate and dithiocarbamate ligands. Importantly, they have been utilized toward the

preparation of thin films of copper–indium sulfides by MOCVD (1664,1775–1778). For example, heating $[Bu_2InCu(S{-}i\text{-}Pr)(S_2CN{-}i\text{-}Pr_2)]$ at 400°C and 0.7 Torr generates thin films of $CuInS_2$, while $[BuInCu(S{-}i\text{-}Pr)_2(S_2CNBu_2)]$ affords $CuIn_5S_8$ under similar conditions (1774,1776). Further, pyrolysis of $[Bu_2InCu(S{-}i\text{-}Pr)(S_2CNBu_2)]$ at 300–350°C in *p*-xylene also leads to deposition of $CuInS_2$ (1664).

iii. Biological Applications. Copper(II) bis(dithiocarbamate) complexes have a number of potential biological applications. For example, while dithiocarbamate salts (R = Me, Et) are potent inhibitors of a clonogenic response in human C34* bone marrow cells, addition of copper sulfate greatly potentiates the hematotoxicity, suggesting a more general role for copper in dithiocarbamate-induced hematotoxicity (1779).

Diethyldithiocarbamate has long been used as an inhibitor of copper–zinc superoxide dismutase (SOD) (1780,1781). The SOD-like activity of bis(dithiocarbamate) complexes derived from amino acids has been determined, with glutamine dithiocarbamate showing high activity (131). Warshawsky et al. (1676) also prepared and assessed a range of dithiocarbamates with oligoether chains (Fig. 238), which leads to >1000-fold increase in hydrophobicity versus diethyldithiocarbamate, with only a 2.3-fold decrease in SOD-like activity.

Related to this, Martin et al. (1782) investigated the ability of $[Cu(S_2CNC_4H_8O)_2]$ to act as a scavenger of the superoxide anion, which takes place through a SOD-like process. Since the complex is only poorly soluble in water, an inclusion compound was formed with β-cyclodextrin; the inclusion constant was determined spectrophotometrically, and suggested the formation of a stable 2:1 inclusion complex.

By using a $^{62}Zn/^{62}Cu$ generator for the production of the short-lived positron-emitting radionuclide, $^{62}Cu[Cu(S_2CNR_2)_2]$ (R = Me, Et), have been prepared and their biodistribution in mice has been studied. They showed a higher take up in the brain than that of a ^{62}Cu–glycine complex, which may be due to their stable nature and lipophilic character (1783).

Dithiocarbamates have also been widely used as fungicides. When released into the environment they degrade within days via acid-catalyzed hydrolysis. Recent work has shown that the presence of trace amounts of copper(II) salts can increase half lives to >2 weeks, irrespective of pH, and it has been suggested that if $Me_2NCS_2^-$ was complexed to copper(II) before release into natural waters, it may be more persistent (1784).

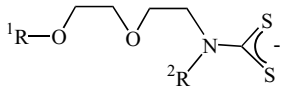

R^1 = Et; R^2 = Hex, Oct
R^1 = Bu; R^2 = Oct, Decyl, Dodecyl

Figure 238. Dithiocarbamates utilized by Warshawsky et al. (1676).

iv. Catalysis. Until recently, no catalysis had been carried out using copper dithiocarbamate complexes, however, now both copper(II) and copper(I) dithiocarbamate complexes have been shown to be extremely active in the nitrene-transfer reaction to alkenes, generating aziridines (1785). For example, $[Cu(S_2CNEt_2)_2]$ and $[Cu(S_2CNEt_2)]_4$ are active in the generation of aziridines from PhI=NTs and alkenes. Indeed, even the copper(III) complex $[Cu(S_2CNEt_2)_2][FeCl_4]$ is active, although more detailed work has shown a prereduction of the copper(III) center is required. While a range of copper complexes have previously been used as catalysts in this process, *hard* ligand donor atoms such as oxygen and nitrogen have been typically used and this work represents the first example of the *soft* donor supported copper center showing activity.

Over the past year, a number of copper dithiocarbamate complexes have been shown to be efficient catalysts for the atom-transfer radical polymerization (ATRP) (1786,1787) and reverse atom-transfer radical polymerization (1788,1789) of methyl methacrylate. Complexes used as catalysts to date are $[Cu(S_2CNEt_2)]_4$ (1786,1787) and $[CuCl(S_2CNEt_2)]_2$ [1788, 1789]. These methods permit the introduction of the photolabile diethyldithiocarbamate group into a polymeric chain (1790), and permit the preparation of block copolymers following later chain extension using fresh methyl methacrylate or styrene monomers (1788). Normal ATRP uses $[Cu(S_2CNEt_2)]_4$, together with tosylchloride and 2,2′-bpy, and generates polymers with quite low molecular weight distributions ($M_w/M_n < 1.10$) (1786,1787). The copper catalyst serves to initiate the living polymerization process via chloride abstraction from the tosylchloride, and a mechanistic scheme has been established (Fig. 239).

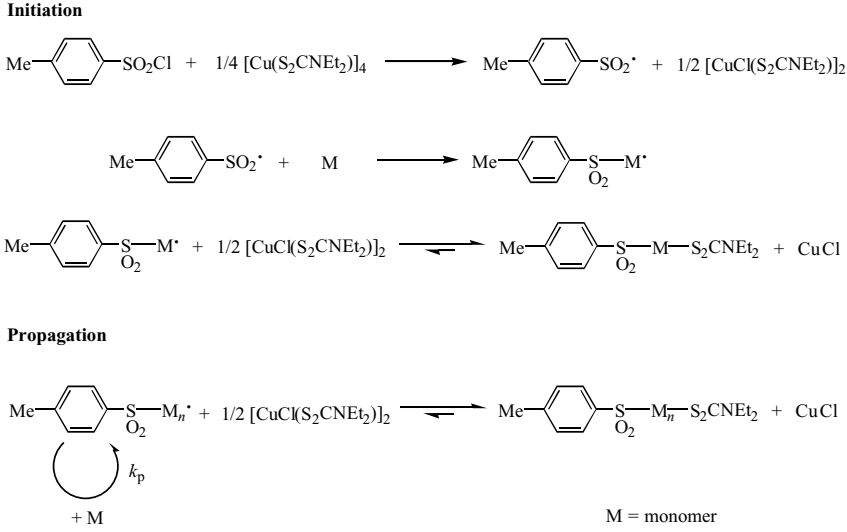

Figure 239. Proposed mechanism of the $[Cu(S_2CNEt_2)]_4$ catalyzed ATRP of methyl methacrylate.

Propagation

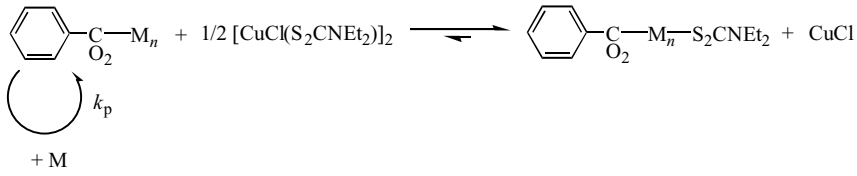

Figure 240. Proposed propagation step in the $[CuCl(S_2CNEt_2)]_2$ catalyzed reverse ATRP reaction.

Reverse ATRP using $[CuCl(S_2CNEt_2)]_2$ works in a similar fashion, with azodiisobutyronitrile (AIBN) (1788) or bezoyl peroxide (1789) being used to generate the active radicals for chain growth. Chloride abstraction from $[CuCl(S_2CNEt_2)]_2$ by the growing chain is used to regulate the concentration of active radical growth species (as shown in Fig. 240 for benzoyl peroxide), making the process a pseudo-living polymerization.

v. Other Applications. Bis(dithiocarbamate) complexes show a number of other potential applications. Some (R =Et; $R_2 = C_4H_8$, C_5H_{10}) have been used as photostabilizers in the photodegradation of poly(vinylchloride) (PVC). The initial photoproduct is believed to be $[Cu(S_2CNR_2)]_n$, which is then rapidly oxidized by the carbon–chlorine bonds to produce $[CuCl(S_2CNR_2)]_2$ and a cross-linked polymer (1790,1791).

The physical properties of bis(dithiocarbamate) complexes have also been exploited by Bruce and co-workers (1485,1668) to generate a series of paramagnetic mesomorphic liquid crystals, showing smectic phases S_c and crystal β mesophases. Electric spin resonance spectroscopy has shown the existence of a long-range exchange interaction at all temperatures, as established by the collapse of the hyperfine structure in the spectra of the condensed samples. Further, a comparison of the principal *g*-values in the solid state and in solution indicates that in the solid the molecules pack with their molecular axes parallel (1668).

The corrosion inhibition effect of a number of complexes, $[Cu(S_2CNR_2)_2]$ (R = Et; $R_2 = C_4H_8O$, C_5H_{10}), on copper in acids have been measured by weight loss and polarization studies. A layer of the dithiocarbamate complex is seen at the metal surface, its insoluble nature being responsible for the observed corrosion inhibition (1792).

Relatively few potential applications have been investigated or developed for other copper dithiocarbamate complexes. An exception is a recent report concerning the nonlinear responses of two hetrometallic selenide clusters: $[W(\mu\text{-}Se)_4\{Cu(S_2CNEt_2)\}_3][NEt_4]_2$ and $[W(\mu\text{-}Se)_4\{Cu(S_2CNMe_2)\}_4][NEt_4]_2$ (1745). The optical limiting effects were examined at a 0.5-Hz repetition rate,

the thresholds being 6.0 and 1.1 J cm^{-1}, respectively. The nonlinear responses of the clusters in DMF have been studied in picosecond time-resolved pump–probe experiments, and compared to that of C_{60} in toluene. The maximum nonlinear transmission loss for the pentanuclear cluster is much greater than that for the tetranuclear species, the latter being similar to C_{60}. The authors suggest that the dithiocarbamate ligands lead to extensive delocalization of electron density over the metal centers, such that the change in the extent of electron delocalization between the HOMOs and LUMOs in the cluster is more significant than with other, non-π-conjugated, ligands.

In other work, a diethyldithiocarbamate copper(II)-loaded zeolite has been prepared and characterized by a range of techniques (1793). However, only a small fraction of the copper ions bind the dithiocarbamate, probably those on the surface, as the large diethyldithiocarbamate anion cannot easily pass through the windows or pore openings of the channels into the cavities of the zeolite. The precise binding mode of the dithiocarbamate remains unknown, although ESR data show that the copper is still in the divalent state.

2. *Silver and Gold*

Gold dithiocarbamate complexes are common for oxidation states +1 and +3 and over the past 10 years a number of dimeric gold(II) complexes have been prepared containing bridging dithiocarbamate ligands. Silver(I) dithiocarbamate complexes are known, while claims have been made for silver(II) complexes, although they should be treated with a certain degree of caution. Silver also forms a large number of heterometallic dithiocarbamate cluster complexes in which it is not always easy to determine the oxidation state.

a. Silver(I) Complexes. Simple silver(I) dithiocarbamate complexes, $[Ag(S_2CNR_2)]_n$, have been known since the 1950s (1794), yet in the intervening years little further work had been carried out. Addition of cyclic dithiocarbamate salts to silver nitrate in ethanol–water affords a range of complexes, $[Ag(S_2CNC_4H_4)]_n$, $[Ag(S_2CNC_4H_8X)]_n$ (X = O, CH_2, NMe), and a 1,2,3,4-tetrahydroquinoline derivative (103,1795), while Singh et al. (59) reported the 4-aminophenazone complex. All are diamagnetic, non-electrolytes, being stable up to high temperatures, but their nuclearities are not discussed. Very recently, simple derivatives, $[Ag(S_2CNR_2)]_n$ (R = Me, Et, Bz), have been prepared from the reaction of thiuram disulfides with 1–3 equiv of silver fluoride (1796).

Early crystallographic studies revealed the hexameric nature (R = Et, Pr) (328,329) of silver(I) dithiocarbamate complexes in the solid state, although in solution they are believed to be in equilibrium with monomeric species (329). More recently, the diethyldithiocarbamate complex has been the subject of two further crystallographic studies (Fig. 241) (330,331). Delgado and Diez (329)

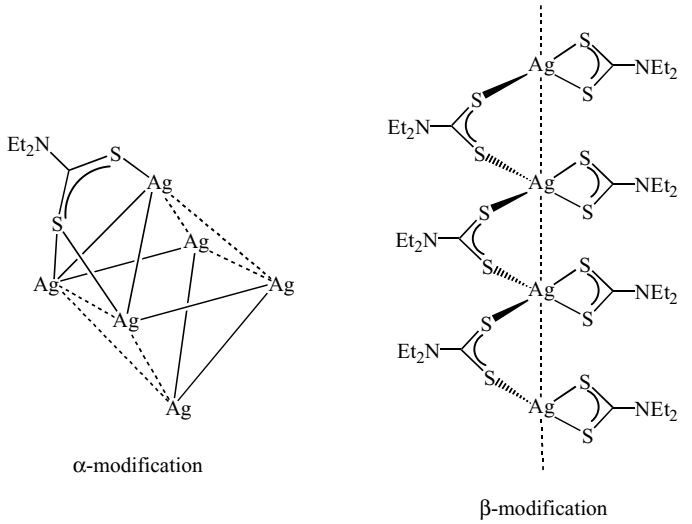

Figure 241. Crystallographic modifications of $[Ag(S_2CNEt_2)]_n$.

used powder data to characterize the previously known monoclinic α-modification (331). It is hexameric and consists of a distorted octahedron of silver atoms, with six comparatively short, and six long, silver–silver interactions. The dithiocarbamates cap six of the faces in an η^1,η^2-fashion, the remaining two faces, characterized by the long metal–metal interactions, remaining uncapped (329). In a second study, the new β-modification has been characterized, which shows a polymeric chain structure. Here, each metal ion is bound to three dithiocarbamate ligands, one acting as a chelate, the coordination geometry being a distorted tetrahedron. Each silver(I) center then makes one short (2.83 Å), and two long (3.44 Å), silver–silver interactions, which are repeated along the chain. The structure has been compared to the α-modification using a new type of topological mapping, which reveals similarities with a large number of other sterically restricted coordination compounds (330).

Few reactions of silver(I) dithiocarbamate complexes have been detailed. Burmeister and co-workers (1797) reported reactions of $[Ag(S_2CNEt_2)]_6$ with $(SCN)_2$ and $(SeCN)_2$. At $-78°C$, the former initially gives the partial substitution product $[Ag_6(S_2CNEt_2)_5(SCN)]$, the selenium analogue of which is the only product of $(SeCN)_2$ addition. However, when the reaction with $(SCN)_2$ was carried out at room temperature, the product was believed to be $[Ag_6(S_2CNEt_2)_6(SCN)_4]$, resulting from partial oxidation of the metal ions, and containing both silver(I) and silver(II) centers. The complex shows poor solubility in common organic solvents and characterization was made on the basis of

analytical, IR, and ESR data. Thus, the ν(CN) vibration at 1530 cm^{-1} is shifted to higher frequency than in the silver(I) complex, while a broad singlet is observed at 3000 G $(g|2.3)$ in the ESR spectrum.

Liu and co-workers (1798) prepared the diamagnetic silver(I) cluster $[Ag_{11}S(S_2CNEt_2)_9]$, from the reaction of silver nitrate with NaS_2CNEt_2 in the presence of either $[MS_4]^{2-}$ (M = Mo, W) or $[CuCl(PPh_3)_2]$ and 2-aminothiophenol (1799). Cubic and rhombahedral (1799) polymorphs have been crystallographically characterized and more recently, a selenium analogue has also been prepared and crystallographically characterized (1800). In all, the chalcogen lies inside a silver cage, binding to five silver ions in a trigonal-bipyramidal coordination mode, while the silver cluster has threefold symmetry through an Ag–E–Ag vector. Silver–silver distances in the order of 3 Å are shorter than twice the van der Waals radius of silver atoms (1.7 Å), indicating a weak metal–metal interaction (1800). Interestingly, ^1H NMR spectra of both complexes shows a single dithiocarbamate environment, however, three crystallographically distinct coordination modes are seen in the solid state; namely, terminal, triply, and quadruply bridging. The selenium complex is an isomorph of the rhombahedral form of the sulfide, and is best described as $[Ag_{11}(\mu^5\text{-Se})(\mu^3\text{-}S_2CNEt_2)_6(\mu^4\text{-}S_2CNEt_2)_3]$ (Fig. 242), with six triply bridging and three quadruply bridging dithiocarbamates. In contrast, the cubic polymorph has six quadruply and three triply bridging dithiocarbamate ligands.

A number of mononuclear silver(I) phosphine complexes have been prepared, including $[Ag(PPh_3)_2(S_2CNC_4H_8)]$ (**458**), which results from $[Ag(PPh_3)_2(\mu\text{-}O_2CMe)]_2$ and $NaS_2CNC_4H_8$ in ethanol (1801). Gimeno et al. prepared related ferrocenyl phosphine complexes $[Ag(PPhFc_2)_2(S_2CNEt_2)]$ (1802) and $[Ag(dppf)(S_2CNR_2)]$ (R = Me, Et) (1803), via similar methods; namely, the reactions of dithiocarbamate salts with $[Ag(OTf)(PPhFc_2)_2]$ and [Ag(dppf)

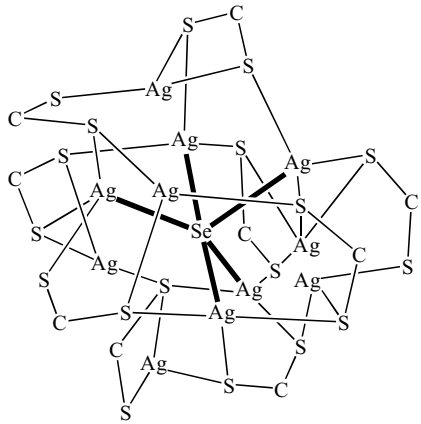

Figure 242. Representation of the cluster core of $[Ag_{11}(\mu^5\text{-Se})(\mu^3\text{-}S_2CNEt_2)_6(\mu^4\text{-}S_2CNEt_2)_3]$.

$(OClO_3)$], respectively. Crystallographic studies show that the silver(I) center adopts the expected distorted tetrahedral coordination environment (1801,1802).

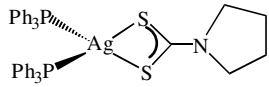

458

b. Silver(II) Complexes. While dimeric gold(II) dithiocarbamate complexes are well known, silver(II) dithiocarbamates remain an area of speculation. Early workers reported deep blue complexes, $[Ag(S_2CNR_2)_2]$, characterized primarily by ESR spectroscopy (188,1804–1806). However, in the intervening years little reference has been made to such complexes and no crystallographic data has been presented. Beinrohr et al. (1807) studied the addition of thiuram disulfides to $[Ag(S_2CNR_2)]_n$ (R = Et, Bu) in chloroform both by ESR spectroscopy and spectrophotometrically, proposing the formation of an equilibrium between the hexameric silver(I) and monomeric silver(II) complexes (Eq. 164).

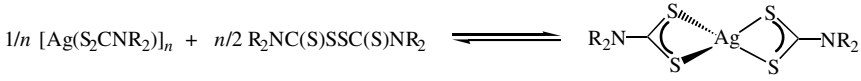

(164)

Further silver(II) bis(dithiocarbamate) complexes $[Ag(S_2CNR_2)_2]$ (R = Pr, *i*-Pr, Cy) and their Py adducts have purportedly been prepared in *N*-(4-methoxybenzlidene)-4′-butylaniline (MBBA) orientated in nematic glasses and organic solvents; the equilibrium between them and silver(I) species being studied (1808). Also, as detailed above, $[Ag_6(S_2CNEt_2)_6(SCN)_4]$ has been proposed to contain both silver(I) and silver(II) centers, the presence of the latter being based on ESR data (1797).

c. Mixed-Metal Clusters Containing Silver. Silver(I) ions bind to a wide-range of transition metal dithiocarbamate-stabilized centers leading to the formation of heterometallic clusters, in much the same way as previously discussed for copper(I). For example, Ebihara et al. (298,299) prepared polymeric and pentanuclear complexes upon mixing solutions of platinum bis(-dithiocarbamate) complexes and silver perchlorate (see Section IV.G.2.c), while Bond et al. (313) studied related reactions between $AgBF_4$ and group 9 (VIII) tris(dithiocarbamate) complexes, $[M(S_2CNR_2)_3]$ (M = Co, Rh, Ir). The latter yield trinuclear $[Ag\{M(S_2CNR_2)_3\}_2][BF_4]$, which can be isolated as stable solids, but are kinetically labile in solution. They have also studied these and related reactions by ESMS (540). The trinuclear mercury species $[Ag\{Hg(S_2CNR_2)_2\}_2]$, is also seen by this method, while in contrast, addition

of silver nitrate to $[M(S_2CNR_2)_2]$ (M = Ni, Zn, Pb) and $[Fe(S_2CNR_2)_3]$ results only in oxidation of the metal center (540).

Closely related silver–platinum complexes supported by ortho-metalated tri(*o*-tol)phosphine ligands have also been prepared from reactions of $[Pt(\eta^2\text{-}CH_2C_6H_4PAr_2)(S_2CNMe_2)]$ (Ar = *o*-tol) with silver perchlorate (see Section IV.G.2.c) (301). When silver or gold complexes $[M(PPh_3)(OClO_3)]$ (M = Ag, Au) are reacted with $[M'(\eta^2\text{-}CH_2C_6H_4PAr_2)(S_2CNMe_2)]$ (M' = Pd, Pt), dimeric dithiocarbamate-bridged species $[(PPh_3)MM'(\eta^2\text{-}CH_2C_6H_4PAr_2)(\mu\text{-}S_2CNMe_2)]$ result; characterized by relatively short metal–metal distances indicative of a significant interaction.

Similarly, the tetranuclear clusters $[Cp_2MoAg(\mu\text{-}H)_2(\mu\text{-}S_2CNR_2)]_2$ (R = Et, Ph) (**459**) formed from $[Cp_2MoH_2]$, dithiocarbamate salt, and silver tetrafluoroborate, contain a linear metal core characterized by short silver–silver [R = Et, 2.935 (2); R = Ph, 2.926(5) Å] and silver–molybdenum [R = Et, 2.998(3); R = Ph, 2.959(1) Å] vectors, the former being bridged by the two dithiocarbamates (300).

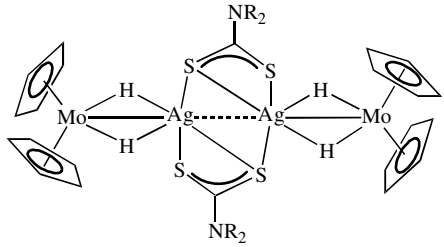

459

The isomorphous clusters $[M_2Ag_3S_2(\mu\text{-}S)_4(\mu^3\text{-}S)_2(\mu\text{-}S_2CNEt_2)][NEt_4]_2$ (M = Mo, W) (**460**) are formed from $[MS_4]^{2-}$, NaS_2CNEt_2, and silver nitrate. Both clusters have been characterized crystallographically and show no short heterometallic contacts, although the dithiocarbamate-bridged silver–silver interactions of 2.957(3) and 2.965(3) Å are indicative of a metal–metal bond (1809).

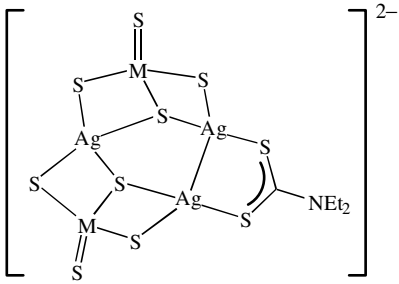

460

In further work, reactions of silver molybdate with dithiocarbamate salts are believed to give trinuclear products, $[Ag_2MoO_2(H_2O)_2(\mu\text{-}S_2CNR_2)_3]$ ($R = Et$; $R_2 = C_4H_8O$, C_5H_{10}), in which nonbonding metal–metal interactions are bridged by dithiocarbamate ligands, however, in the absence of structural data this is at best speculative (825). Magnetic measurements suggest they contain a molybdenum(V) center, while TGA studies show initial loss of two molecules of water and eventual formation of Ag_2S.

d. Gold(I) Complexes. Gold(I) dithiocarbamate complexes were first prepared by Åkerström (1810), and more recently a large number of new examples have been prepared, such as those with heterocyclic dithiocarbamate ligands (103, 251). All are dimeric (1811), the gold–gold vector being bridged by two dithiocarbamate ligands, as confirmed by a number of crystallographic studies (277–280, 284). They crystallize to form linear chains of gold(I) dimers (Fig. 243), characterized by alternating short (~2.5–2.8 Å) and long (~3.0–3.1 Å) gold–gold interactions. Two polymorphs of $[Au(\mu\text{-}S_2CNEt_2)]_2$ have been crystallographically characterized, with one (277) and two (278) independent molecules, respectively.

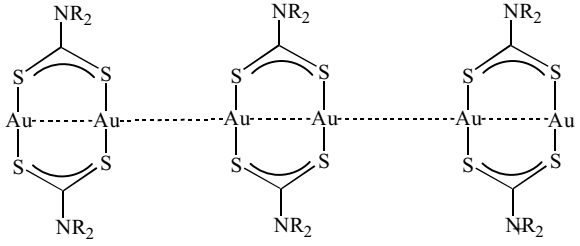

Figure 243. Linear-chain structure of gold(I) dimers in the solid state.

Laguna and co-workers (275) prepared related dimeric gold(I) complexes $[Au_2(\mu\text{-}S_2CNR_2)(\mu\text{-}CH_2PPh_2CH_2)]$ ($R = Me$, Et, Bz) in a number of ways, including the ligand redistribution reactions between $[Au(\mu\text{-}S_2CNR_2)]_2$ and $[Au(\mu\text{-}CH_2PPh_2CH_2)]_2$ (Eq. 165).

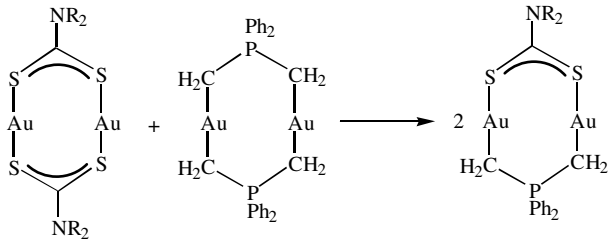

(165)

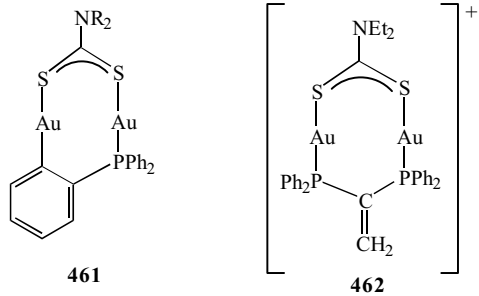

Figure 244. Examples of dimeric gold(I) complexes with a single dithiocarbamate bridge.

Ligand redistribution reactions involving $[Au(\mu\text{-}S_2CNR_2)]_2$ have also been utilized toward the synthesis of isomers of $[Au_2(\mu\text{-}S_2CNR_2)(\mu\text{-}Ph_2C_6H_3Me)]$ (**461**) (282) and $[Au_2(\mu\text{-}S_2CNEt_2)\{\mu\text{-}Ph_2PC(=CH_2)PPh_2\}][ClO_4]$ (**462**) (230) (Fig. 244); which crystallize in linear chains with alternating short (~2.82–2.87 Å) and long (~2.98–3.13 Å) metal–metal interactions (275,282). Diphosphine-bridged complexes $[Au_2(\mu\text{-}S_2CNEt_2)\{\mu\text{-}R_2P(CH_2)_nPPh_2\}]Cl$ (R = Me, Ph; $n = 1, 2$) have also been prepared upon addition of NaS_2CNEt_2 to $[Au_2Cl_2\{\mu\text{-}R_2P(CH_2)_nPPh_2\}]$, although the dmpe derivative is not very stable (1812). Concentration-dependent absorption spectra suggest that in solution they exist in equilibrium with monomers, while the temperature dependence of their ^{31}P NMR spectra has been attributed to the existence of molecular aggregation through intermolecular gold–gold contacts.

Monomeric gold(I) phosphine complexes $[Au(PPh_3)_2(S_2CNC_5H_{10})]$ (263) and $[Au(PPh_3)_2(S_2CN\text{—}i\text{-}Pr_2)]$ (262) have been crystallographically characterized; the metal center adopts a distorted tetrahedral coordination environment. Interestingly, while gold–sulfur interactions are similar in the latter [Au—S 2.714(2) and 2.681(2) Å], in $[Au(PPh_3)_2(S_2CNC_5H_{10})]$ they differ by almost 0.3 Å [Au—S 2.561(2) and 2.858(3) Å], and are attributed to an "allyl-like" interaction within the dithiocarbamate (see Section III.B) (263).

A monophosphine complex, $[Au(PPh_3)(S_2CNHBz)]$, has been proposed to result from $[AuCl(PPh_3)]$, benzylamine, and carbon disulfide (1520). The structure has not been elucidated, but it might be expected to contain a monodentate dithiocarbamate ligand and a linear two-coordinate gold(I) center. In support of this hypothesis, Ho and Tiekink (236,237) prepared $[Au(PR_3)(\eta^1\text{-}S_2CNEt_2)]$ (R = Cy, p-C_6H_4OMe) upon addition of NaS_2CNEt_2 to $[AuCl(PR_3)]$. Both have been structurally characterized, and the coordination geometry at gold is, as expected, approximately linear [S—Au—P 171.61(4) and 169.80(3)°]. The deviation results from the close approach (~3 Å) of the uncoordinated sulfur atom.

Faamau and Tiekink (238) also detailed the synthesis of a range of diphosphine complexes, $[Au_2(\eta^1\text{-}S_2CNR_2)_2\{\mu\text{-}Ph_2P(CH_2)_nPPh_2\}]$ (R = Et, Cy; $n = 1, 2, 3$), an example of which (R = Et, $n = 2$) (**463**) has been crystallographically characterized. It contains two linear gold(I) centers [S—Au—P 172.1(1), 174.1(1)°] bridged by the diphosphine. Each center is supported by a monodentate dithiocarbamate ligand, containing one short, 1.66(1)–1.68(1) Å, and one long, 1.71(1)–1.76(1) Å, carbon–sulfur bond.

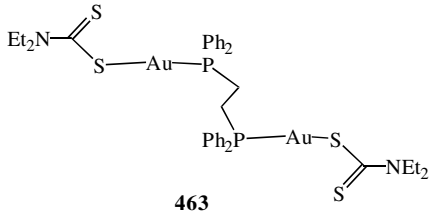

463

Laguna and co-workers (230) prepared related 1,1-bis(diphenylphosphino) ethane-bridged complexes, $[Au_2(\eta^1\text{-}S_2CNR_2)_2\{\mu\text{-}Ph_2PC(=CH_2)PPh_2\}]$ (R = Me, Et, Bz). Coordination at gold is also linear [S—Au—P 174.4(1)°], long and short carbon–sulfur bonds are seen, as are strong and weak gold–sulfur interactions [Au—S 2.319(4) and 2.949(4) Å]. Interestingly, the monodentate dithiocarbamates react further with group 11 (IB) salts to give cationic dithiocarbamate-bridged complexes, $[Au_2M(\mu\text{-}S_2CNR_2)_2\{\mu\text{-}Ph_2P(C{=}CH_2)PPh_2\}]^+$ (M = Cu, Ag, Au) (Eq. 166).

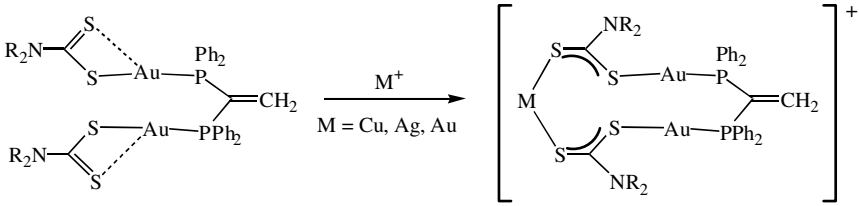

(166)

A number of other dimeric phosphine complexes have also been reported. Addition of NaS_2CNEt_2 to $[Au_2(\mu\text{-dppm})_2][BH_3CN]_2$ affords $[Au_2(\mu\text{-dppm})_2(\mu\text{-}S_2CNEt_2)][BH_3CN]$ (281), while related complexes $[Au_2\{\mu\text{-}Ph_2PC(=CH_2)PPh_2\}_2(\mu\text{-}S_2CNEt_2)][ClO_4]$ (**464**) and $[Au_2(PPh_3)_2\{\mu\text{-}Ph_2PC(=CH_2)PPh_2\}(\mu\text{-}S_2CNEt_2)][ClO_4]$ (**465**) (Fig. 245) result from addition of the relevant phosphine to $[Au_2\{\mu\text{-}Ph_2PC(=CH_2)PPh_2\}(\mu\text{-}S_2CNEt_2)][ClO_4]$ (230). The ν(C=N) bands in the IR spectra appear at $\sim$1480 cm^{-1}, a lower value than generally associated with dithiocarbamate ligands bridging gold centers. This

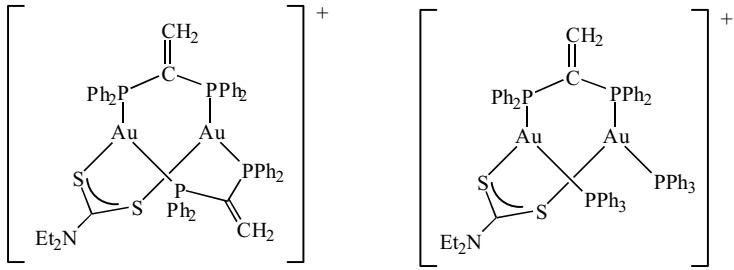

464 **465**

Figure 245. Examples of dimeric gold(I) 1,1-dppe complexes.

value is attributed to the tri-coordinate environment. The latter is confirmed in crystallographic studies on $[Au_2(\mu\text{-dppm})_2(\mu\text{-}S_2CNEt_2)][BH_3CN]$ (281) and **464**.

In a series of papers, Laguna and co-workers detailed the synthesis, structure, and reactivity of a number of trinuclear gold(I) phosphine complexes supported by bis(diphenylphosphinomethyl)phenylphosphine (dpmp) (283,1813), bis(diphenylphosphinoethyl)phenylphosphine (dpep) (1814), and 1,1,1-tris(diphenylphosphino)methane (triphos) (239). For example, addition of 3 equiv of NaS_2CNMe_2 to $[Au_3Cl_3(\mu^3\text{-triphos})]$ affords $[Au_3(\eta^1\text{-}S_2CNMe_2)_3(\mu^3\text{-triphos})]$, which contains three monodentate dithiocarbamate ligands, however, with 2 equiv, $[Au_3(\eta^1\text{-}S_2CNMe_2)(\mu\text{-}S_2CNMe_2)(\mu^3\text{-triphos})][ClO_4]$ can be isolated, with one bridging and one monodentate dithiocarbamate. The latter is synthetically useful as the monodentate dithiocarbamate can be easily replaced, for example, by chloride and pentafluorophenyl groups (Fig. 246) (239).

Crystallographic studies reveal a distorted linear arrangement of the gold(I) ions with metal–metal distances ranging from 2.9 to 3.4 Å. Very similar chemistry is observed with dpmp (283,1813) and dpep (1814). Interestingly, reaction of $[Au_3Cl_2(\eta^1\text{-}S_2COEt)(\mu^3\text{-dpmp})]$ with 1 equiv of dithiocarbamate salt yields $[Au_3Cl(\eta^1\text{-}S_2COEt)(\eta^1\text{-}S_2CNR_2)(\mu^3\text{-dpmp})]$ (R = Me, Bz), in which each gold(I) center has a different coordination environment (1813).

Air and moisture stable dmit-bridged gold(I) complexes (dmit = 1,3-dithiole-2-thione-4,5-dithiolate), $[Au_2(\mu\text{-}C_3S_5)(\mu\text{-}S_2CNR_2)]^-$ (R = Me, Et, Bz) (**466**) (Fig. 247), have been prepared upon addition of dithiocarbamate salts to $[Au_2(\mu\text{-}C_3S_5)(AsPh_3)]_n$ (1815), while Vincente et al. (216) described the preparation of anionic gold(I) complexes, $[Au(S_2CNHAr)_2][PPN]$ (PPN = bis(triphenylphosphine)iminium chloride) (**467**) (Fig. 247), formed upon insertion of isothiocyanates into the sulfur–hydrogen bonds of $[Au(SH)_2][PPN]$. The latter could not be isolated pure, however, those with strongly electron-withdrawing aryl groups (Ar = C_6F_5, *p*-$C_6H_4NO_2$) reacted further with $[Au(acac)_2]^-$ to give well-characterized dithiocarbimato complexes, $[Au_2(\mu\text{-}S_2CNAr)_2]^{2-}$ (216).

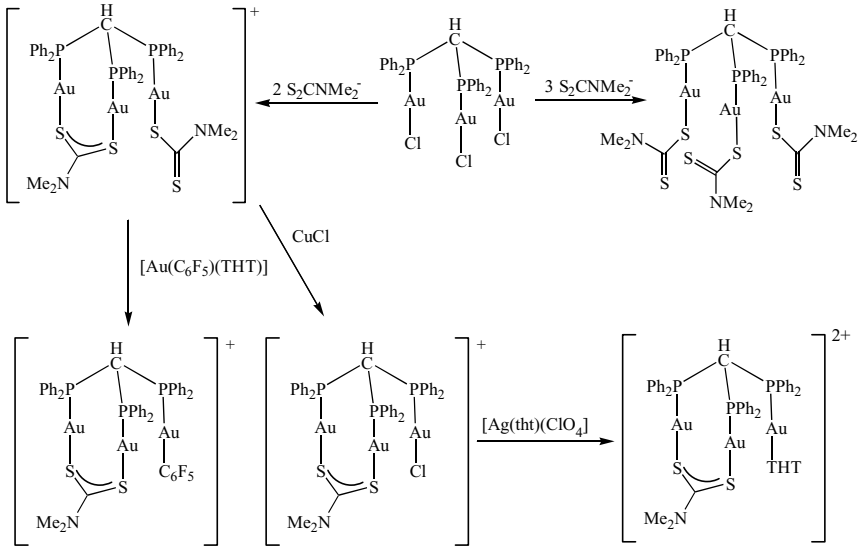

Figure 246. Synthetic routes to triphos-capped gold(I) trinuclear complexes.

e. Gold(II) Complexes. Prior to 1981, gold(II) dithiocarbamate complexes were virtually unknown. In early work, Vänngard and Åkerström (1805) observed a four-line ESR spectrum upon dissolution of $[Au(S_2CNR_2)_3]$ (R = Et, *i*-Pr) in benzene, suggesting the existence of a gold(II) center, while Bergendahl and Bergendahl (1816) observed similar behavior for the butyl derivative, which is explained in terms of a redox equilibrium (Eq. 167).

$$[Au(S_2CNR_2)_3] \rightleftharpoons [Au(S_2CNR_2)_2] + 1/2\ R_2NC(S)SSC(S)NR_2 \qquad (167)$$

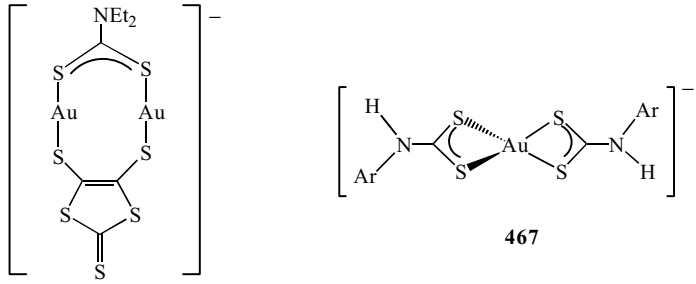

466 **467**

Figure 247. Examples of anionic gold(I) complexes.

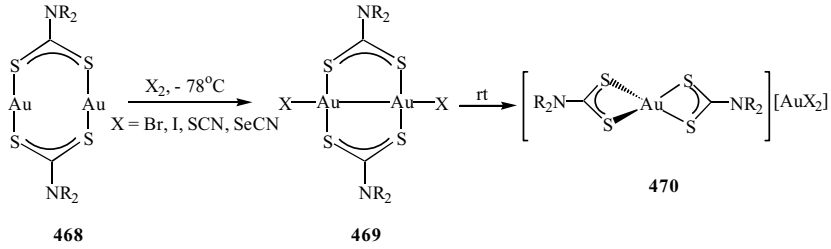

Figure 248. Synthesis and disproportionation of gold(II) complexes $[AuX(\mu\text{-}S_2CNR_2)]_2$.

In 1981, Burmeister and co-workers (1797) serendipitously discovered that low-temperature (−78°C) addition of halogens, Br_2 and I_2, or pseudo-halogens, $(SCN)_2$ and $(SeCN)_2$, to gold(I) dimers, $[Au(\mu\text{-}S_2CNR_2)]_2$ (R = Et, Bu) (**468**), yielded dark green gold(II) complexes $[AuX(\mu\text{-}S_2CNR_2)]_2$ (**469**). However, although the butyl complexes were more stable than the ethyl analogues, all underwent a disproportionation and ligand rearrangement upon warming to room temperature giving $[Au(S_2CNR_2)_2][AuX_2]$ (**470**) (Fig. 248). These yellow salts contain a gold(III) dithiocarbamate unit and are the sole product of the reactions of gold(I) dimers with iodine. Somewhat similarly, addition of a slight excess of NaS_2CNEt_2 to $[AuCl_4]^-$ has been reported to yield $[Au(S_2CNEt_2)_2]$, which upon storage affords the disproportionation product $[Au(S_2CNEt_2)_2]^+[Au(S_2CNEt_2)_2]^-$ (1817).

In 1994, Laguna and co-workers (276,1818) published two papers in which for the first time gold(II) dithiocarbamate complexes were crystallographically characterized. Addition of halogens to gold(I) dimers $[Au_2(\mu\text{-}S_2CNR_2)(\mu\text{-}CH_2PPh_2CH_2)]$ (R = Me, Et, Bz) was found to give $[Au_2X_2(\mu\text{-}S_2CNR_2)(\mu\text{-}CH_2PPh_2CH_2)]$ (X = Cl, Br, I) (Eq. 168). One example (R = Bz, X = Br) has been crystallographically characterized. It contains approximately square-planar gold(II) centers and an almost linear Br–Au–Au–Br vector. Further, the gold–gold interaction at 2.565(10) Å is very short and indicative of a substantial bonding interaction (276).

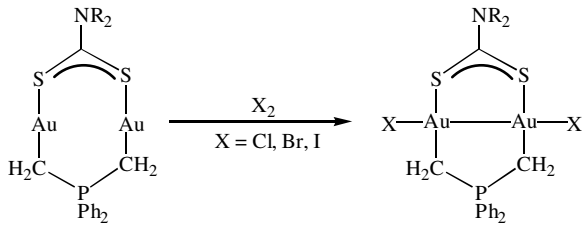

(168)

In a second approach, reaction of $[Au_2(\mu\text{-}CH_2PPh_2CH_2)_2(tht)_2][ClO_4]_2$ with 2 equiv of dithiocarbamate salt yielded $[Au_2(\mu\text{-}CH_2PPh_2CH_2)_2(\eta^1\text{-}S_2CNR_2)_2]^+$ ($R = Me$, Et; $R_2 = C_4H_8$); a crystallographic study revealing that the two dithiocarbamates were monodentate. In contrast, addition of dithiocarbamate salt to $[Au_2(\mu\text{-}CH_2PPh_2CH_2)_2(tht)Ar][ClO_4]$ ($Ar = C_6F_5$, 2,4,6-$C_6F_3H_2$) gave $[\{Au_2Ar(\mu\text{-}CH_2PPh_2CH_2)_2\}_2(\mu\text{-}S_2CNR_2)]$ (Eq. 169), in which the dithiocarbamate bridges the two dimeric gold(II) units (1818).

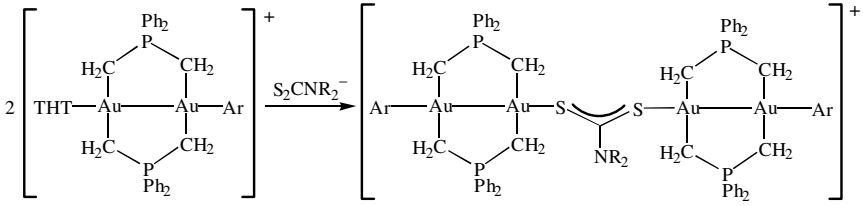

(169)

Interestingly, addition of 1 equiv of NaS_2CNBz_2 to $[Au_2(\mu\text{-}CH_2PPh_2CH_2)_2(tht)(PPh_3)]^{2+}$ appears to afford the substitution product $[Au_2(\mu\text{-}CH_2PPh_2CH_2)_2(\eta^1\text{-}S_2CNBz_2)(PPh_3)]^+$; however, it proved impossible to isolate this product due to it being in equilibrium with dicationic $[Au_2(\mu\text{-}CH_2PPh_2CH_2)_2(PPh_3)_2]^{2+}$ and neutral $[Au_2(\mu\text{-}CH_2PPh_2CH_2)_2(\eta^1\text{-}S_2CNBz_2)_2]$ (1819).

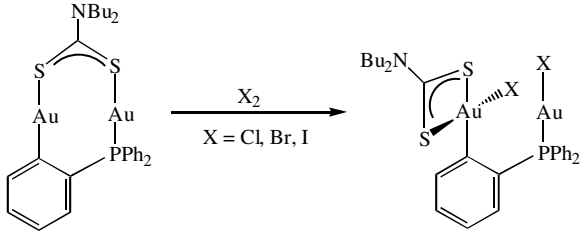

(170)

In a very recent report, oxidation of the gold(I) dimers $[Au_2(\mu\text{-}S_2CNBu_2)(\mu\text{-}Ph_2C_6H_3Me)]$ by halogens is reported to initially give very dark solutions believed to contain gold(II) species. However, these rapidly isomerize to yield mixed-valence gold(I)–gold(III) complexes $[Au_2X_2(S_2CNBu_2)(\mu\text{-}Ph_2C_6H_3Me)]$ ($X = Cl$, Br, I) (Eq. 170) (282). A crystal structure of the iodide shows the expected linear two-coordinate gold(I) center, while the gold(III) ion has a square-planar coordination environment [Au···Au 3.2201(3) Å]. This behavior is similar to that observed for $[Au(\mu\text{-}S_2CNEt_2)]_2$ (1820) and other gold(I) dimers (276). Thus, there is now a significant body of literature surrounding gold(II) dithiocarbamate chemistry, aspects of which have recently been reviewed (1821).

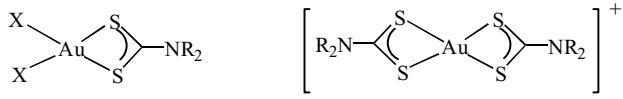

471 **472**

Figure 249. Examples of monomeric gold(III) complexes.

f. Gold(III) Complexes. Diamagnetic gold(III) complexes containing a square-planar metal center are relatively common. Simple examples include neutral $[AuX_2(S_2CNR_2)]$ (**471**) (103, 251, 1822–1826) and cationic $[Au(S_2CNR_2)_2]X$ (**472**) (Fig. 249) (103, 251, 421, 422, 1797, 1825), bis(dithiocarbamate) complexes. Addition of 1 equiv of dithiocarbamate to $[AuX_4]^-$ gives $[AuX_2(S_2CNR_2)]$ (251), as does addition of 2 equiv of bromine to $[Au(\mu\text{-}S_2CNR_2)]_2$ (1797). Further, $[Au(Mes)_2(S_2CNR_2)]$ (R = Me, Et, Bz) can be prepared from *cis*-$[AuCl_2(Mes)_2]$ (1822) and $[Au(C_6F_5)_2(S_2CNR_2)]$ (R = Me, Et, Bz) from $[Au(C_6F_5)_2(\mu\text{-Cl})]_2$ (1827).

A crystal structure of $[AuCl_2\{S_2CN(CH_2CH_2OH)_2\}]$ reveals that the molecules stack to give linear S···Au···S chains [Au···S 3.610(6) and 3.838(6) Å]. The bromide complex $[AuBr_2(S_2CNBu_2)]$ has been shown to form adducts with a wide range of organic molecules, of which the *trans*-stilbene and *trans, trans*-1,4-diphenyl-1,3-butadiene complexes have been crystallographically characterized. Interestingly, the gold centers show no specific intermolecular interactions either between themselves or the organic molecules (1823).

The dimethyl complex $[AuMe_2(S_2CNMePh)]$ has been prepared upon addition of the dithiocarbamate salt to $[AuMe_2(\mu\text{-I})]_2$ in dioxane (1826). Variable temperature ^1H NMR spectra show two gold–methyl resonances at room temperature that coalesce at 340 K allowing an activation barrier of 76 ± 4 kJ mol^{-1} to be derived for the restricted rotation about the carbon–nitrogen bond. Related organometallic complexes $[R_2Au(S_2CNMe_2)]$ and $[RAu(S_2CNMe_2)_2]$ (R = Me, CH_2CN, ferrocenyl, Ph, *p*-C_6H_4F, *p*-C_6H_4Br) have also been reportedly prepared upon addition of tetramethylthiuram disulfide to $[AuR(PPh_3)]$ (1828,1829). In contrast, addition of tetraethylthiuram disulfide reportedly yields only $[Au(\mu\text{-}S_2CNEt_2)]_2$ and $[Au(PPh_3)(S_2CNEt_2)]$ (1828). The same group also suggest that addition of tetraethylthiuram disulfide to the biaryl complex $[Au_2(PPh_3)_2(\mu\text{-}p\text{-}C_6H_4C_6H_4)]$ affords metallacyclic $[Au(S_2CNEt_2)\ (\eta^1,\eta^1\text{-}C_{12}H_8)]$ (Eq. 171) (1830).

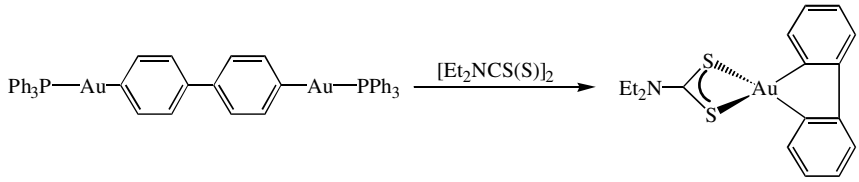

(171)

Anionic gold(III) mono(dithiocarbamate) complexes have been the subject of a single publication. Laguna and co-workers (1827) describe the reactions of dithiocarbamate salts (R = Me, Et, Bz) with $[Au(C_6F_5)_3(tht)]$, which give either mononuclear $[Au(C_6F_5)_3(\eta^1\text{-}S_2CNR_2)]^-$ or binuclear $[\{Au(C_6F_5)_3\}_2(\mu\text{-}S_2CNR_2)]^-$ complexes. Further, when binuclear $[Au(C_6F_5)_2(\mu\text{-}Cl)]_2$ was used as the gold source, neutral mononuclear complexes $[Au(C_6F_5)_2(S_2CNR_2)]$ resulted (Eq. 172); the dibenzyldithiocarbamate complex is crystallographically characterized.

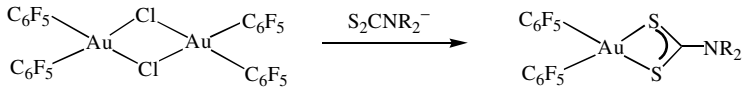

(172)

Cationic bis(dithiocarbamate) complexes $[Au(S_2CNR_2)_2]X$ have been prepared in a number of ways (421,422), including the further addition of dithiocarbamate to $[AuX_2(S_2CNR_2)]$ or reaction of silver(I) halides with thiuram disulfides (251). Reactions of $[AuX_3L]$ (X = Cl, Br, I; L = oxazoles or imidazoles) with tetramethylthiuram disulfide gave mixtures of $[AuX_2(S_2CNMe_2)]$ and $[Au(S_2CNMe_2)_2][X]$; ratios are dependent on the nature of both L and X (1825).

Crystallographic studies of ionic bis(dithiocarbamate) complexes all reveal a distorted square-planar gold(III) center (421, 422,1 825). In $[Au(S_2CNEt_2)_2][TcNCl_4]$, an interesting secondary interaction is seen, two anions and one cation assembling via coordination of a sulfur to the vacant coordination site at the technetium center [Tc···S 3.451(5)–3.568(5) Å] (Fig. 250), the second cation remains uncoordinated (421).

Cationic mono(dithiocarbamate) complexes include $[Au(S_2CNR_2)(\eta^2\text{-}C_6H_4C_5H_4N)]^+$ (R = Me, Et) (**473**), together with related complexes with substituted 2-phenyl pyridyl ligands (245) and $[Au(S_2CNR_2)(\eta^2\text{-}C_6H_4\ CH_2\ NMe_2)]^+$ (R = Me, Et) (**474**) (Fig. 251) (244). They contain the expected

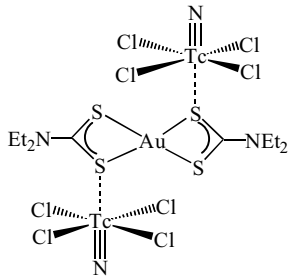

Figure 250. Part of the solid-state structure of $[Au(S_2CNEt_2)_2][TcNCl_4]$ showing secondary anion–cation interactions.

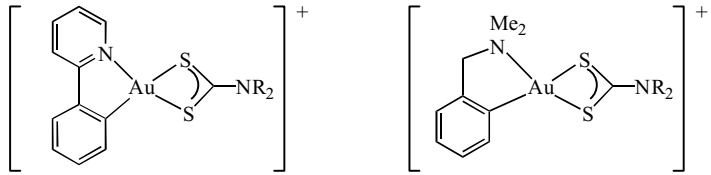

473 **474**

Figure 251. Examples of cationic, organometallic, gold(III) complexes with chelating ligands.

square-planar gold(III) center and can be prepared upon addition of 1 equiv of dithiocarbamate salt to $[AuCl_2(\eta^2\text{-}C_6H_4C_5H_4N)]$ or $[AuX_2(\eta^2\text{-}C_6H_4CH_2NMe_2)]$ (X = Cl, CN), respectively.

In both cases, addition of 2 equiv of dithiocarbamate salts yields neutral bis(dithiocarbamate) complexes $[Au(S_2CNR_2)_2(\eta^1\text{-}C_6H_4C_5H_4N)]$ (R = Me, Et) (245) and $[Au(S_2CNR_2)_2(\eta^1\text{-}C_6H_4CH_2NMe_2)]$ (R = Me, Et) (**475**) (Fig. 252) (244). A crystal structure of $[Au(S_2CNEt_2)_2(\eta^1\text{-}C_6H_4CH_2NMe_2)]$ reveals that one dithiocarbamate chelates, while the second is monodentate. In solution, however, the dithiocarbamates are equivalent in both types of complex, being attributed to the rapid interconversion of mono- and bidentate binding modes.

A similar situation is also found for $[Au(S_2CNEt_2)_2\{\eta^1\text{-}CH_2P(S)PPh_2\}]$, formed upon addition of tetraethylthiuram disulfide to $[Au(\mu\text{-}SPPh_2CH_2)]_2$ (Eq. 173) (248).

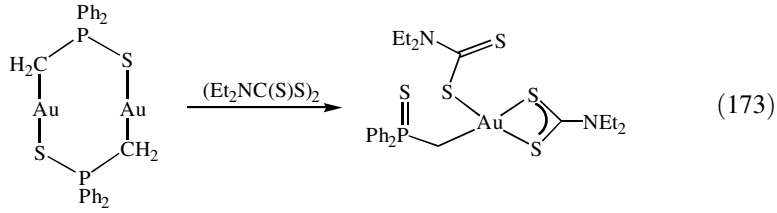

(173)

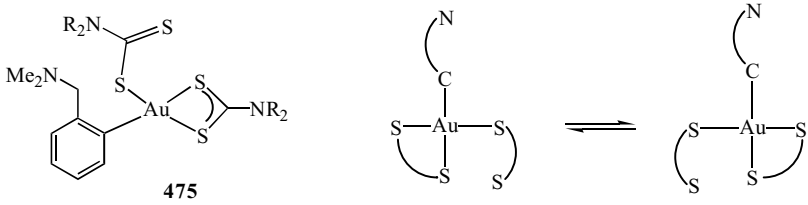

475

Figure 252. Proposed interconversion of dithiocarbamate ligands in $[Au(S_2CNR_2)_2(\eta^1\text{-}C_6H_4CH_2NMe_2)]$.

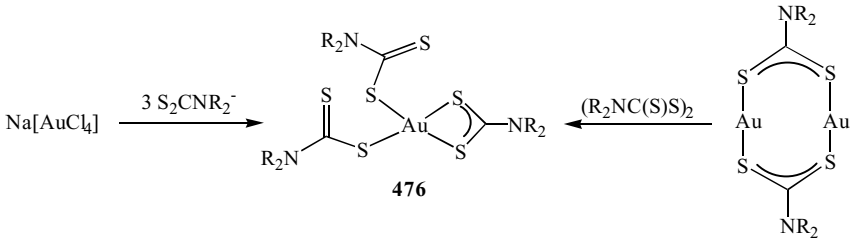

Figure 253. Synthetic routes to $[Au(S_2CNR_2)_3]$.

Gold(III) tris(dithiocarbamate) complexes $[Au(S_2CNR_2)_3]$ (**476**) result from addition of 3 equiv of dithiocarbamate salts to $Na[AuCl_4]$ or from the reaction of gold(I) dimers with thiuram disulfides (Fig. 253). A large number have been prepared with cyclic dithiocarbamates (251), as have α-amino acid derivatives (252). All are diamagnetic and some authors have suggested that the coordination geometry at gold is distorted trigonal prismatic (252); although a square-planar arrangement with one chelating and two monodentate dithiocarbamates, as found crystallographically for $[Au(S_2CNEt_2)_3]$ (249), seems more likely. Ahmed and Magee (250) studied the electrochemical reduction of tris(dithiocarbamate) complexes in propylene carbonate solution at a mercury electrode. All undergo an irreversible two-electron reduction, generating gold(I) complexes and 2 equiv of dithiocarbamate, which in turn serve to oxidize the mercury electrode.

Apart from those detailed above, few reactions have been carried out with gold dithiocarbamate complexes. Following on from the reaction of $[AuBr_2(S_2CNEt_2)]$ with *nido*-$[7,8\text{-}C_2B_9H_{11}]^{2-}$ reported by Wallbridge and coworkers (1831) to give $[Au(S_2CNEt_2)(1,2\text{-}C_2B_9H_{11})]$, reaction with *arachno*-$[B_9H_{14}]^-$ yields two products, $[4\text{-}Au(S_2CNEt_2)B_8H_{12}]$ and $[6,9\text{-}\{Au(S_2CNEt_2)\}_2B_8H_{10}]$ (Eq. 174). The latter has been crystallographically characterized and the gold dithiocarbamate units occupy open sites, which suggests that the mono-gold complex has a similar structure in which a gold dithiocarbamate unit is replaced by two hydrogens (1832).

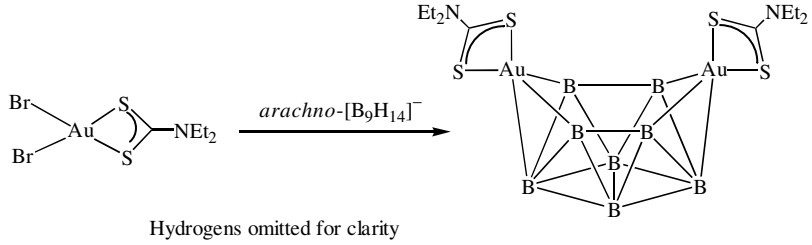

(174)

g. Applications. A number of quite different potential applications have been considered for silver dithiocarbamate complexes, with TGA and DSC studies revealing that they decompose to form Ag_2S (590,825), while in one instance, silver is generated in a single step at 220°C (1795).

In work toward the development of novel optical sensors for environmental analysis, optode membranes based on methylene bis(*i*-butyldithiocarbamate) showed a reversible response to both Ag^+ and Hg^{2+} together with extremely high selectivities versus a range of other cations. The detection limit for Ag^+ is $2.5 \times 10^{-9}\,M$ at pH 4.7 (1833). The development of a simple, yet sensitive, electrode sensor using the dithiocarbamate salt of pyrrolidine has also been reported; the dithiocarbamate ion-selective electrode based on a heterogeneous solid membrane of $[Ag(S_2CNC_4H_8)]/Ag_2S$/graphite is applied to the detection of the dissociation constant of dithiocarbamic acids (1834).

Other workers describe how addition of carbon disulfide to hepta-6-amino-6-deoxy-β-cyclodextrin in the presence of ammonia gas affords a mixture of partially substituted dithiocarbamate derivatives. When bound to a silver electrode, they are capable of discriminating between the three positional isomers of the nitrobenzoate ion and nitrophenol (as detected by cyclic voltammetry); an effect that is attributed to the different orientations of the nitro group with respect to the silver surface after inclusion in the cyclodextrin cavity (1835).

Gold complexes also find a range of potential applications. A monolayer of adsorbed dibutyldithiocarbamate can be generated on a gold electrode at 0.5 V, which is displaced as the thiuram disulfide upon exposure to hydroxide (1836). Ferrocenyl-substituted dithiocarbamates (Fig. 254) have also proved useful for the modification of gold and platinum microelectrodes and a monolayer of the redox active ferrocene centers is generated (1837).

Gold(I) dithiocarbamate complexes display luminescent behavior (279, 283, 1812–1814, 1838). For example, $[Au(\mu\text{-}S_2CNEt_2)]_2$ is luminescent in the solid state ($\lambda_{max} = 554$ nm) with an excited-state lifetime of 1.3 μS (1838) and has lead to possible applications for linear-chain gold(I) dimers as environmental sensors (279). For example, while colorless $[Au(\mu\text{-}S_2CNCy_2)]_2$ is not luminescent, exposure to a range of volatile organic compounds generates bright orange

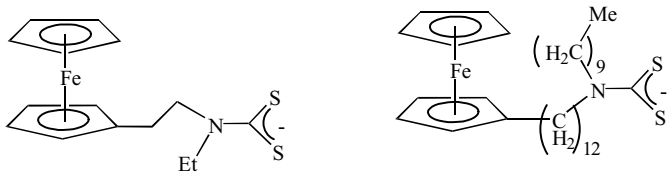

Figure 254. Examples of ferrocenyl substituted dithiocarbamates used to modify gold and platinum microelectrodes.

adducts, which show intense luminescence when exposed to UV light. This occurs for polar aprotic solvents such as acetone, acetonitrile, dichloromethane, and chloroform, but not for protic solvents such as alcohols. Further, the process is fully reversible, allowing the ''switching on'' of the luminescence (279). A crystal structure of the DMSO adduct of $[Au(\mu\text{-}S_2CNCy_2)]_2$ shows discrete dimers rotated by $\sim 90^\circ$ and stacked to form an infinite chain [Au—Au 2.7690(7); Au···Au 2.9617(7) Å]; the intermolecular gold–gold distance is the shortest observed to date in these systems.

Laguna and co-workers (283,1813,1814) also examined the optical properties of a number of trinuclear gold(I) phosphine complexes. At low temperature, most are luminescent and a red shift, related to the number of dithiocarbamate ligands present, is proposed to arise from gold(I)–gold(I) interactions that perturb the orbital energies involved in the LMCT transition (283).

In other work, Au^{3+} has been selected as a back-extracting agent for the determination of mercury in water and biological samples via an anionic stripping voltammetry method, as it has the highest extraction constant with diethyldithiocarbamate. Thus, $[Hg(S_2CNEt_2)_2]$ is initially generated and then transfers the dithiocarbamates to yield $[Au(S_2CNEt_3)_3]$ (1839). Other gold(III) tris(dithiocarbamate) complexes generated from α-amino acids show antibacterial activity against *streptococcus pneumoniae*, exhibiting greater activity than the reference compounds (252).

I. Group 12 (II B): Zinc, Cadmium, and Mercury

The dithiocarbamate chemistry of the group 12 (II B) elements is well developed, with applications in the areas of analytical chemistry, agriculture, rubber vulcanization, and as molecular precursors to metal sulfides. As expected, their chemistry is constrained to the +2 oxidation state and it is the bis(dithiocarbamate) complexes $[M(S_2CNR_2)_2]$, which are the most common, being first prepared in 1907 (2).

a. Bis(dithiocarbamate) Complexes. Bis(dithiocarbamate) complexes are easily prepared upon addition of 2 equiv of dithiocarbamate to M(II) salts in aqueous solution. In this way, a wide range of new examples have been prepared (49,1116,1121,1126,1426,1485,1667,1696,1773,1840–1849). These complexes include those derived from a range of cyclic amines (1116,1126,1773,1845, 1846), bidentate (1841,1849) and tridentate (1121,1844) amines, tetrahydroquinoline and isoquinoline (1842), and long-chain amines, to give complexes that display liquid-crystalline properties (1485,1486). The formation of $[Cd(S_2CNEt_2)_2]$ from cadmium(II) salts and NaS_2CNEt_2 has been studied potentiometrically using an amalgam electrode; stepwise stability constants of 1.0×10^4 and 1.4×10^7 mol^{-2} being determined for the two-step process (1850).

As detailed in earlier sections, Beer and co-workers (1469,1470) prepared a range of complexes in which two zinc bis(dithiocarbamate) centers are incorporated into macrocycles (Fig. 255). The terphenyl-based macrocycles **477** bind bidentate Lewis bases in their cavities (as discussed in Section IV.H.1.a), while **478** containing the well-known $[Ru(bpy)_3]^{2+}$ subunit has been utilized in anion-binding studies. The same group have also prepared a number of ferrocenyl-containing macrocycles **479–481**, containing up to six iron(II) centers, probing their electrochemical properties (see later) (1468).

Extensive structural studies have been carried out on zinc (212, 400, 536, 537, 1468, 1672, 1844, 1849, 1851–1862), cadmium (411, 1847, 1849, 1863–1866) and mercury (1867–1871) complexes, results prior to 1997 being summarized in a review (1872). Most simple zinc complexes form centrosymmetric dimers with one terminal and one bridging dithiocarbamate ligand per zinc center. On closer inspection, these dimeric complexes can be further divided into two structural types, differing with respect to the relative orientations of the bridging dithiocarbamates; being either on the same side (AA) or on the opposite side (BB) of the dimeric unit (Fig. 256). Another way of expressing this difference is to consider the central core of the molecule that consists of an eight-membered ring defined by the zinc ions and bridging dithiocarbamate ligands, which can adopt a boat or saddle conformation (AA), or a twisted-chair conformation (BB).

Structural motif (AA) is adopted by $[Zn(S_2CNMe_2)(\mu\text{-}S_2CNMe_2)]_2$ (1854, 1873), while the vast majority of other dimeric complexes are of type (BB), as exemplified by $[Zn(S_2CNEt_2)(\mu\text{-}S_2CNEt_2)]_2$ (1874). Within both types there are secondary zinc–sulfur interactions across the eight-membered ring of the order of 2.8–3.0 Å, as compared to the other zinc–sulfur interactions of ~2.3–2.5 Å (1872). If one takes these secondary zinc–sulfur interactions into account, the coordination geometry of the metal ions is best described as a highly distorted trigonal bipyramid, while even ignoring them, there is some significant distortion from the ideal tetrahedral geometry. One further feature of the eight-membered ring motif is the relatively short zinc–zinc distances of ~3.5–4.0 Å.

Recently, a number of zinc bis(dithiocarbamate) complexes have been shown to adopt monomeric structures (CC) in the solid state (1468,1851,1859). Beer and co-workers (1468) crystallographically characterized macrocycle **480** in which the two zinc centers are bound to two chelating dithiocarbamate ligands; the geometry about each zinc being approximately tetrahedral. The monomeric nature of the metal centers here is clearly a function of the constraints of the macrocycle. Three further recent studies have also revealed monomeric zinc bis(dithiocarbamate) complexes. These include $[Zn(S_2CNCy_2)_2]$ (1851) and $[Zn\{S_2CN(Bu)CH_2Ar\}_2]$ (**482**) (1859), presumably resulting from the increased steric nature of the large substituents, making dimer formation unfavorable.

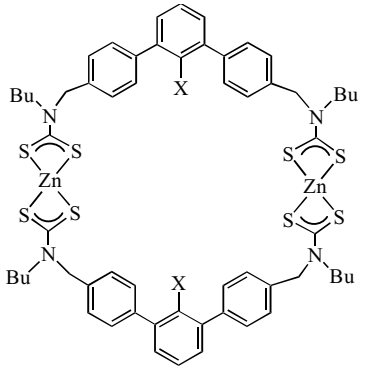

477

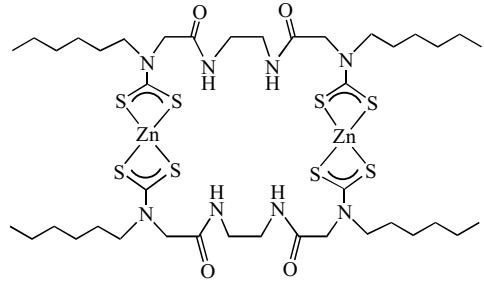

478

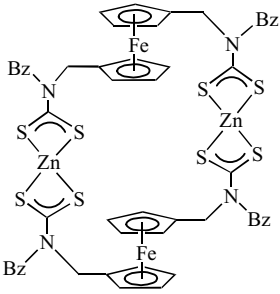

479

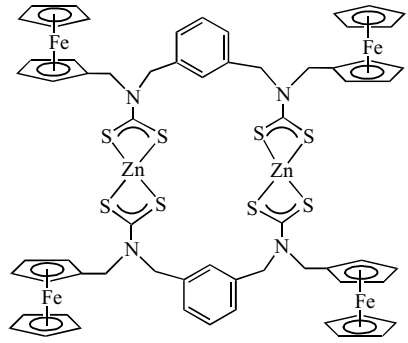

480

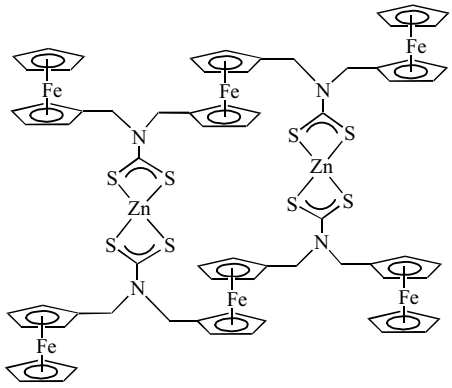

481

Figure 255. Example of zinc bis(dithiocarbamate) complexes prepared by Beer and co-workers (1468–1470).

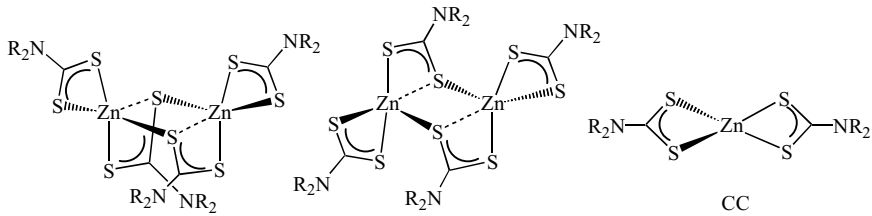

Figure 256. Solid-state conformations adopted by zinc bis(dithiocarbamate) complexes.

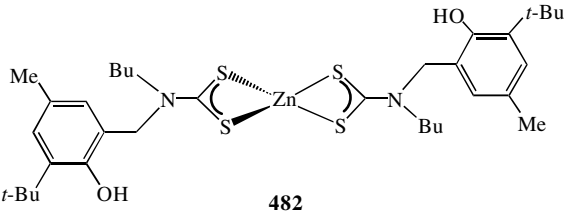

482

In another very recent publication, the crystallographic characterization of $[Zn(S_2CN{-}i\text{-}Bu_2)_2]$ has been reported (537). It shows the unusual feature of containing two independent molecules in the asymmetric unit, one being mononuclear, while the second is dimeric; highlighting the small energy differences that must exist between these different structural forms. Further, all six dithiocarbamate ligands are structurally inequivalent, which is consistent with the observation of six equal intensity signals in the ^{15}N CP/MAS NMR spectrum (537). This technique has been used in other examples to probe the structural characteristics of zinc bis(dithiocarbamate) complexes in the absence of crystallographic data (536).

Two polymeric zinc bis(dithiocarbamate) complexes have been crystallographically characterized (212, 1849). Adams and Huang (212) prepared $[Zn\{S_2CNH(CO_2Et)\}_2]$ from the reaction of $[EtO_2CN{=}CS_2C\{NH(CO_2Et)\}\{S_2CNH(CO_2Et)\}]$ with $[Zn(acac)_2]$. The five-coordinate zinc centers each bear one chelating dithiocarbamate, while a second bridges two zinc atoms via the sulfurs. The five-coordinate zinc manifold is completed by coordination of one of the oxygen atoms of the ester group.

In the second example, O'Brien et al. (1849) prepared $[M\{S_2CN(Me)CH_2CH_2CH_2NMe_2\}_2]$ ($M = Zn$, Cd) from trimethylpropane-1,3-diamine. The zinc complex **483** is polymeric. Each five-coordinate metal center carries two chelating dithiocarbamates and are linked via coordination of a pendant dimethylamino group. Interestingly, the analogous cadmium complex adopts a dimeric centrosymmetric structure in the solid state. Although these examples

are included here, in many respects they are best thought of as adducts of the bis(dithiocarbamates), which are discussed more fully below.

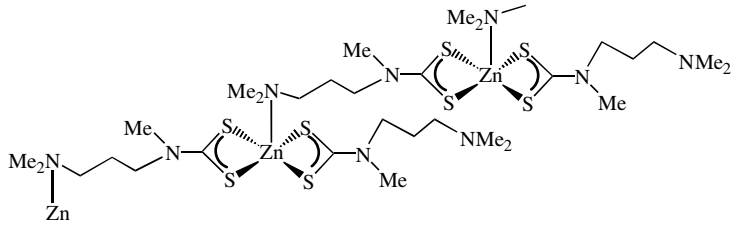

483

Despite the range of structural types adopted by zinc bis(dithiocarbamate) complexes in the solid state, they are probably monomeric in the gas phase. Certainly, a gas-phase electron diffraction study of $[Zn(S_2CNMe_2)_2]$ shows that this is the case. A distorted tetrahedral coordination geometry is found, and the formation of bridging rather than terminal dithiocarbamate ligands in the solid state is probably a consequence of the ring strain in the latter (1674).

Cadmium bis(dithiocarbamate) complexes, which are all dimeric, show similar structural features to their zinc analogues (411,1847,1863–1866, 1875,1876). For example, $[Cd(S_2CNBu_2)_2]$ adopts the structural motif (AA) with both dithiocarbamates on the same side of the ring (1847), as found previously for $[Cd(S_2CNMe_2)_2]$, while others such as $[Cd(S_2CNEt_2)_2]$ (411) generally adopt the motif (BB) in which bridging dithiocarbamates lie on opposite sides of the ring. As with the zinc complexes, metal–sulfur interactions occur across the ring, and at ~2.8 Å for the cadmium complexes, they represent a significant interaction. Thus, each cadmium ion can be considered to be five coordinate, and better structural representations are types (DD) and (EE), respectively (Fig. 257). Interestingly, in light of the momomeric nature of $[Zn(S_2\ CNCy_2)_2]$ (1851), the analogous cadmium complex $[Cd(S_2CNCy_2)_2]$ is dimeric (1864).

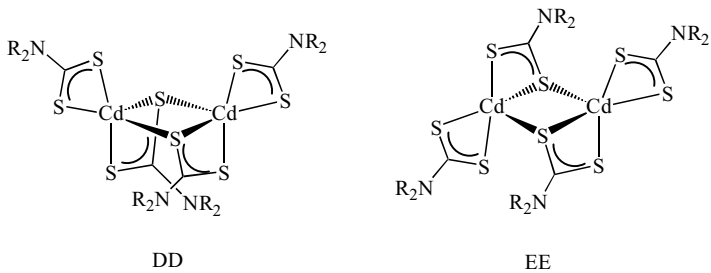

DD EE

Figure 257. Solid-state conformations adopted by cadmium bis(dithiocarbamate) complexes.

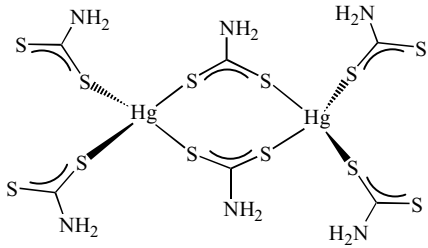

Figure 258. A portion of the structure of polymeric $[Hg(S_2CNH_2)_2]_n$ showing the formation of eight-membered rings.

Mercury bis(dithiocarbamate) complexes adopt five distinct structural forms in the solid state, ranging from isolated mononuclear units, to binuclear complexes and 2D arrays (1867–1871,1877–1879). The colorless parent complex $[Hg(S_2CNH_2)_2]$ is polymeric (Fig. 258) and consists of interconnected eight-membered rings, each containing two mercury atoms and two bridging dithiocarbamates. Connection of the dimeric subunits leads to a sheet-like structure of 8- and 16-membered rings, with each mercury atom adopting a distorted tetrahedral coordination environment. All the mercury–sulfur bonds fall within a relatively narrow range between 2.499(4) and 2.629(4) Å (1869).

A monomeric motif (CC) (Fig. 256), features distorted tetrahedral geometries and is found for $[Hg(S_2CN{-}i\text{-}Pr_2)_2]$ (1877), $[Hg(S_2CNCy_2)_2]$ (1879), $[Hg(S_2CN{-}i\text{-}Bu_2)_2]$ (1867), $[Hg\{S_2CN(i\text{-}Pr)Cy\}_2]$ (1867), and $[Hg(S_2CNC_4H_8)_2]$ (1878). In contrast, both $[Hg(S_2CNBu_2)_2]$ and $[Hg(S_2CNEtCy)_2]$ are dimeric in the solid state (1867), as is the 4-methylpiperidine complex $[Hg(S_2CNC_4H_8NMe)_2]$ (1870). All adopt a centrosymmetric structure (EE) with bridging dithiocarbamate ligands, which are similar to those found in $[Cd(S_2CNC_5H_{10})_2]$ (1875). The primary mercury–sulfur interactions in $[Hg(S_2CNC_4H_8NMe)_2]$ range between 2.450(2) and 2.669(1) Å, where the secondary interaction is 3.127(2) Å (1870).

Two polymorphs of $[Hg(S_2CNEt_2)_2]$ are known (423,424,1871). In the α-form (424,1871), a dimeric structure is found, akin to those of type (EE) discussed above. In contrast, in the β-form (423,424) the mercury atom is located on an inversion center and the two independent mercury–sulfur distances are quite different at 2.398(4) and 2.965(4) Å. This finding suggests that the primary coordination geometry about mercury can be considered as linear with respect to the two short interactions, while the other associations give rise to a distortion from linearity. There are also secondary intermolecular mercury–sulfur interactions, but these are quite long at 3.292(4) Å. The methyl analogue $[Hg(S_2CNMe_2)_2]$ also adopts this geometry [Hg–S 2.374(3) and 2.988(3) Å] (1868).

Polymorphism is also found for [Hg(S_2CN—*i*-Pr_2)$_2$] (1877,1880); recrystallization from acetone gives two types of crystal (α and β) where both are plate-like and yellow. The α-form contains only a monomer and the mercury center adopts a distorted tetrahedral coordination geometry [Hg—S 2.445(4) and 2.645(4) Å] (1875). In contrast, the β-form contains monomer and dimer molecules. The monomers in the two crystal types differ due to slight changes in the orientations of the methyl groups (1880), but are quite different from monomeric β-[Hg(S_2CNEt$_2$)$_2$] (discussed above) in which all four sulfur atoms are coplanar (423,424).

The adoption of these different structural types and the observation of polymorpism suggests that there is little energy difference between them. Cox and Tiekink (1867) studied the structural chemistry of this class of compounds in some detail. They suggest that it may be the need to maximize intermolecular interactions that is important in the structural type adopted. For example, when there is little or no steric barrier, then secondary mercury–sulfur interactions will give rise to dimeric or polymeric units.

A wide range of other studies have been carried out on group 12 (II B) bis(dithiocarbamate) complexes. The molecular structures of [M(S_2CNEt$_2$)$_2$] have been examined by PM3 and MMP2 methods (1881), and [Cd(S_2CNMe$_2$)$_2$] by PM3 and ab initio DFT methods (1882). For the ethyl complexes, as monomers their compressed tetrahedral structures are thought to be due to the highly strained four-membered rings (1881). In an attempt to trace the changes occurring to the metal coordination sphere of the complexes upon dissolution, the same authors studied the Raman spectra both in the solid state and in solution. In the solids, the zinc and cadmium complexes both showed band splittings that were attributed to intermolecular couplings in the dimeric structures, and as expected, these were not evident in the solution spectra (1881).

Others have also studied vibrational spectra (1494,1883). The IR spectrum of [Zn(S_2CNEt$_2$)$_2$] has been recorded in the solid state at temperatures between 20 and 120°C and in solution at 20°C. The decreased number of bands in solution and at higher temperatures is attributed to the loss of intermolecular contacts; thermal averaging takes place at ∼55°C in the solid state (1883).

Other theoretical contributions include bond valence sum analyses of metal ligand bond lengths in a range of zinc and cadmium bis(dithiocarbamate) complexes and their adducts by Ramalingam and co-workers (1884,1885). These studies confirm that the metal ion is in the +2 state, while for zinc they also show a lower bond valence sum for bis adducts attributed to the change in coordination geometry from tetrahedral to octahedral. In contrast, there is no obvious change for cadmium, its larger size alleviating strain involved in the transformation from four to six coordination (1885).

Cadmium bis(dithiocarbamate) complexes $[Cd(S_2CNR_2)_2]$ ($R = Et$; $R_2 = C_4H_8O$, C_5H_{10}) have been studied by MS, with molecular ions observed in all cases (1117). They have also been studied using ^{113}Cd NMR spectroscopy in both solution and the solid state, the latter allowing the metal coordination environment to be probed (1846,1847,1886–1888). For example, dimeric $[Cd(S_2CNEt_2)_2]$ resonates at δ 357 and with a line shape indicative of five coordination, while the pyrrolidine derivative $[Cd(S_2CNC_4H_8)_2]$ resonates at δ 280 with a highly symmetrical line shape. The latter is attributed to a tetrahedral environment, and suggests that this complex is monomeric (1887). Absorption spectra have also been measured for a range of cadmium complexes ($R = Et$, Pr, Bu, *i*-Pr, *i*-Bu; $R_2 = C_5H_{10}$); an alkyl group dependence on ξ and λ_{max} at $\sim$265 nm is noted (1889).

Bond and co-workers (163,607,1886,1890) studied the electrochemistry of group 12 (II B) bis(dithiocarbamate) complexes in some detail. At both platinum and mercury electrodes, zinc complexes are only reduced at very negative potentials giving elemental zinc or zinc amalgam, respectively; at the mercury electrode an additional process is also seen, involving dithiocarbamate exchange between zinc and mercury. A related exchange is the major process when cadmium complexes are reduced under similar conditions and no reductive chemistry is accessible at the platinum electrode. The oxidation chemistry at these electrodes is complex. At mercury, three reversible processes are observed. One is an exchange reaction between the metal(II) salts and the electrode mercury, which is mediated by the formation of a bimetallic cation, $[MHg(S_2CNR_2)_2]^{2+}$, while the remaining two processes are associated with the generated mercury complexes, $[Hg(S_2CNR_2)_2]$ (1890). For cadmium this exchange has been studied in some detail; ^{113}Cd NMR data confirms that exchange reactions are rapid on the NMR time scale (1886). In contrast, at a platinum electrode oxidation only occurs at much more positive potentials and yields the thiuram disulfide complexes $[M\{R_2NC(S)SS(S)CNR_2\}]^{2+}$ ($M = Zn$, Cd) (1890).

Beer and co-workers (1468) studied the electrochemistry of a number of zinc bis(dithiocarbamate) complexes, including ferrocene derivatives **479–481** (Fig. 255). The xylyl-bridged macrocycle **480** exhibits a single reversible oxidation wave for all four ferrocene groups ($E_{1/2} = 0.25$ V), and the ferrocene spacer groups in **479** are also oxidized reversibly in a single step ($E_{1/2} = 0.26$ V). In contrast, **481** shows two oxidation waves (as expected), but only a single return reduction wave—the reason is as yet unknown.

The electrochemistry of $[Hg(S_2CNR_2)_2]$ at mercury electrodes has been probed, with dithiocarbamate exchange occurring upon reduction (163, 607, 1891). Interestingly, two reversible one-electron oxidation processes are observed and this is believed to be associated with the oxidation of the mercury electrode producing cationic multinuclear mercury dithiocarbamate complexes

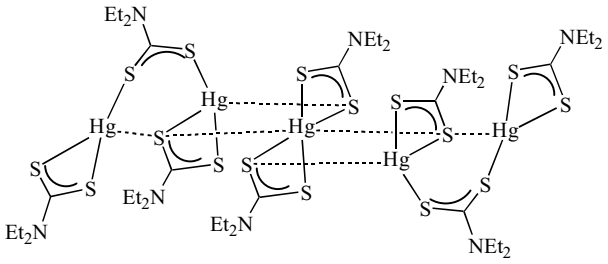

Figure 259. A portion of the structure of the polymeric cation $[Hg_5(S_2CNEt_2)_8]^{2+}$.

(607). Controlled potential electrolysis of $[Hg(S_2CNEt_2)_2]$ at 0.6 V gives a green solution, the ^{199}Hg NMR spectrum of which is consistent with the formulation $[Hg_3(S_2CNEt_2)_4]^{4+}$; a species is also generated at a platinum electrode. Evaporation of solutions containing this cation lead to the formation of crystals of $[Hg_5(S_2CNEt_2)_8][ClO_4]_2$, which were crystallographically characterized (163). The structure consists of a polymeric chain of repeating penta-mercury units, which are linked by pairs of dithiocarbamate ligands (Fig. 259). Within each Hg_5 subunit, four metal atoms are four coordinate and the other is six coordinate. The $[Hg_5(S_2CNEt_2)_8]^{2+}$ cation can be considered to be formed from $[Hg_3(S_2CNEt_2)_4]^{4+}$ and two bis(dithiocarbamate) units, and this is indeed what is generated upon redissolution of $[Hg_5(S_2CNEt_2)_8]^{2+}$ into dichloromethane.

Interestingly, the piperidene derived complex $[Hg(S_2CNC_5H_{10})_2]$ shows different oxidative behavior to that of the ethyl complex (1891). Oxidation at a mercury electrode affords $[Hg_2(S_2CNC_5H_{10})_3]^+$, the perchlorate salt of which has been structurally characterized. It consists of a polymeric chain of dimercury units, held together by two bridging η^1,η^2-dithiocarbamate ligands, which are linked to the next dimercury unit via a bridging η^1,η^1-dithiocarbamate ligand. Further, the two mercury centers in each binuclear unit are distinguished via the weak coordination of perchlorate to one of them [Hg—O 2.98(2) Å] (Fig. 260).

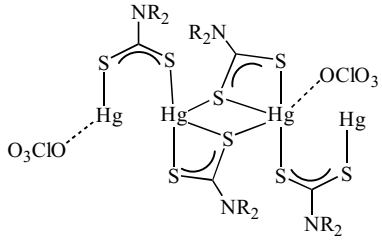

Figure 260. A portion of the structure of polymeric $[Hg_2(S_2CNC_5H_{10})_3][ClO_4]$.

These results are unusal in dithiocarbamate chemistry, in that a change in the nature of the dithiocarbamate substituent leads to a change in the stoichiometry of the complex formed. The authors have found that the dibenzyl and dicylcohexyl dithiocarbamate complexes behave like $[Hg(S_2CNEt_2)_2]$, while the morpholine dithiocarbamate complex behaves similar to that derived from piperidene. Thus it appears that it is the heterocyclic nature of the organic substituents that is responsible for the behavioral change (1891).

Bond and Scholz (606) calculated thermodynamic data for solid mercury bis(dithiocarbamate) complexes mechanically attached to the surface of a paraffin-impregnated graphite electrode. Two-electron reduction generates mercury and the soluble dithiocarbamate anions in a chemically reversible couple during the second and subsequent scans. The formal potential of the reaction has been measured, which enables the calculation of conventional stability constants (β_2) for 17 mercury complexes, and a previously unrecognized correlation between log β_2 and molecular weight is found (see Section III.G).

Dithiocarbamate exchange in mercury bis(dithiocarbamate) complexes has been shown by MS and ^{199}Hg NMR spectroscopy to be extremely fast in solution, possibly occurring via a dimeric intermediate (607). The exchange between $[Hg(S_2CNEt_2)_2]$ and $^{197}HgCl_2$ is also facile and occurs with a half-life of 63 min at 45°C (1892). Related work on the exchange between $[Zn(S_2CNEt_2)_2]$ and $^{65}ZnCl_2$ reveals a similar lability in this system (1893, 1894). The rate is dependent on the concentration of the dithiocarbamate complex, but not the free zinc(II) ion, leading the authors to propose a dissociative process as the rate-determining step (1894).

Somewhat related to these studies is the proposed formation of heterobimetallic complexes upon addition of MCl_2 (M = Co, Ni, Cu) to $[Zn(S_2CNR_2)_2]$ (R = Me, Cy; $R_2 = C_7H_{14}$) (1895). Precise product structures are unknown, but the authors propose the formation of either binuclear complexes in which either one MCl_2 unit is bound via sulfur coordination from two different dithiocarbamate ligands, or tetranuclear complexes, whereby two zinc bis(dithiocarbamate) centers are linked via two MCl_2 units.

b. Neutral Adducts of Bis(dithiocarbamate) Complexes. Both zinc and cadmium bis(dithiocarbamate) complexes form a range of five-coordinate adducts with nitrogen bases (Fig. 261); $[Zn(S_2CNMe_2)_2.py]$ is crystallographically characterized in the late 1960s (1896). More recent examples include zinc complexes adducted to Py (325, 492, 1489, 1699, 1897–1905), 2,2′- and 4,4′-bpy (551, 591, 1469, 1906–1917), 1,10-phen and derivatives (551, 1158, 1906–1908, 1910, 1918, 1919), imidazole (1920–1923), morpholine (1694, 1696), TMEDA (1903) and cadmium complexes to; Py (1845,1904), 2,2′- and 4,4′-bpy (1924–1927), 1,10-phen (1924–1926, 1928–1930), imidazole (1920), picolines, isoquinoline, and piperidene (1845), and *trans*-1,2-bis(4-pyridyl)ethylene

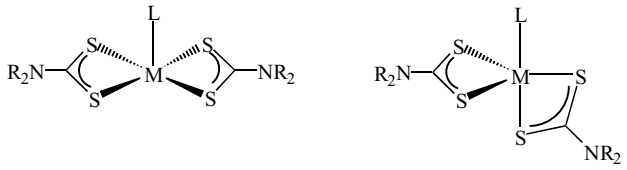

Figure 261. Extreme views of five-coordinate $[M(S_2CNR_2)_2L]$ (M = Zn, Cd) adducts.

(1931). Although less common, phosphine adducts of both metals are also accessible (1932, 1933).

These adducts are easily prepared upon addition of the Lewis base to the bis(dithiocarbamate) complex, which in many cases leads to disruption of the bi- or polynuclear structures found in the solid state (see above). In this context, this area of chemistry has interest in providing more suitable precursors for chemical vapor deposition studies (see Section IV.I.h.i).

A vast wealth of structural data has been accumulated (235, 258, 325, 552, 1158, 1469, 1489, 1694, 1878, 1897–1904, 1906–1922, 1924–1934). Pyridine adducts adopt a geometry that is intermediate between square pyramidal and trigonal bipyramidal. Ivanov et al. (1897, 1900, 1901, 1904, 1905, 1935) studied these complexes in considerable detail. As part of these studies they have prepared copper(II) doped adducts and studied them by ESR spectroscopy (1897, 1898, 1900, 1901, 1904, 1935). For some of the adducts, two structurally independent copper(II) sites have been detected leading to the proposal of an isomerism of the zinc(II) adducts. The nature of this isomerism is revealed by crystallographic, ESR, and solid-state NMR studies (1897). Thus, in the crystal structure of orthorhombic $[Zn(S_2CNEt_2)_2.Py]$, two structurally related but crystallographically independent molecules (α and β) are seen. The molecules differ primarily with respect to the conformation of the pyridine ligands, and thus might be considered as rotational isomers (rotamers), while geometric changes in bond lengths and angles are small. Rotational isomerism is seen also in $[Zn(S_2CNEt_2)_2(HNC_4H_8O)]$, with the nonplanar morpholine rings adopting different spatial orientations with respect to the four-membered chelates (1694).

Further complexity arises in the pyridine system, as O'Brien and co-workers (1898) reported a monoclinic polymorph (γ form), formed from the reaction of $[Zn(S_2CNEt_2)(S\text{-}2,4,6\text{-}Me_3C_6H_2)]$ with excess pyridine, and having slightly different bond lengths and angles from those in α and β $[Zn(S_2CNEt_2)_2.py]$. Ivanov and Antzutkin (1905) probed the interconversion of these polymorphs and the clathrated pyridine complex $[Zn(S_2CNEt_2)_2.py].Py$, which has also been structurally characterized (see below) (1900). By using natural abundance ^{15}N CP/MAS NMR, they provide evidence that the initial reaction of dimeric $[Zn(S_2CNEt_2)_2]_2$ with pyridine yields orthorhombic (α and β) $[Zn(S_2CNEt_2)_2.py]$. This complex in turn adds a second pyridine affording the clathrate

$[Zn(S_2CNEt_2)_2.py].Py$, which then loses pyridine to give the monoclinic γ form. Finally, the latter converts to α and β forms upon crystallization from a melt. This work is an illustration of chemical hysteresis, in which the structure of an adduct depends on the pathway of physicochemical conditions during the preparation of metastable compounds.

Ivanov et al. (1699) studied the pyridine adduct $[Zn(S_2CNMe_2)_2.py]$, and its benzene clathrate $[Zn(S_2CNMe_2)_2.py].0.5C_6H_6$, using ^{15}N CP/MAS NMR spectroscopy. For the former, a single ^{15}N dithiocarbamate resonance indicates that the molecule has significant symmetry, while the nonequivalence of the dithiocarbamates in the clathrate results in two separate signals. They have also studied adduct formation in the heterogeneous phase via this method and absorption of pyridine from the gas phase by a polycrystalline sample of $[Zn(S_2CNMe_2)_2]_2$ is accompanied by dissociation of the dimer molecules.

Beer et al. (492) recently reported the synthesis of a zinc–pyridine containing macrocycle **484** and cryptand **485**, based on a pyrrole framework (Fig. 262). A crystallographic study of the former shows that the macrocyclic loop is significantly twisted, having the effect of reducing the cavity size, which may have a bearing on the anion-receptor properties of such species.

In two further papers (325, 1489), Beer and co-workers described the synthesis and structural characteristics of nano-sized resorcarene-based molecules containing pyridine adducts of six zinc or cadmium bis(dithiocarbamate)

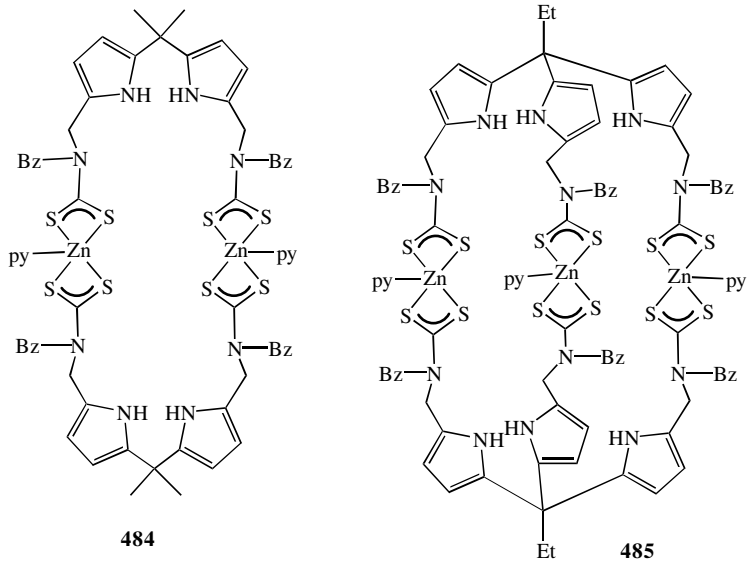

Figure 262. Pyrrole-based macrocycle and crytand prepared by Beer et al. (492).

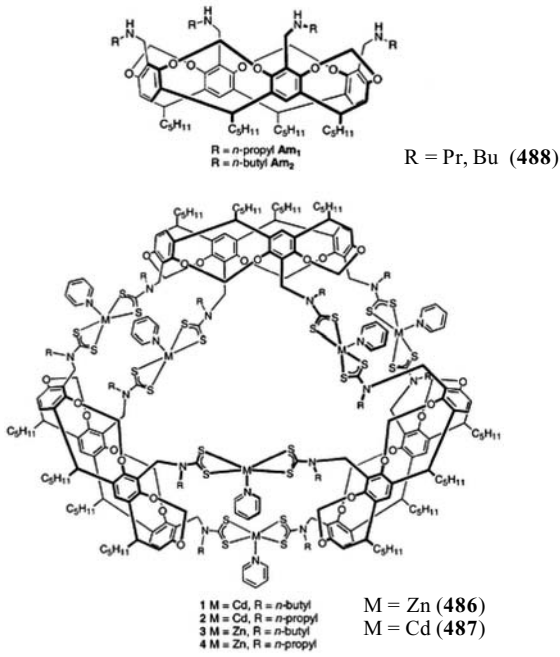

Figure 263. Resorcarene-based molecules prepared by Beer and co-workers (325, 1489).

centers (**486**–**487**) (Fig. 263). They are synthesized from the reactions of the resorcarene dithiocarbamates (**488**) with the corresponding metal(II) acetates, followed by crystallization from a pyridine–water mixture. All four isomorphous examples (**486**–**487**) have been characterized crystallographically (325, 1489).

These molecules consist of three resorcarene cups linked by the six divalent bis(dithiocarbamate) centers. The resorcarene ligands define the corners of a molecular equilateral triangle, with sides of ~19–20 Å, consisting of two parallel running sets of dithiocarbamate–metal–dithiocarbamate units. Packing the molecules in the solid state generates a ''molecular honeycomb''.

From space-filling CPK representations (Fig. 264) the cavity in **486**–**487** is circular with a diameter of ~16–17 Å, and therefore is suitable for binding spherical molecules like C_{60}. In the crystal structures the cavities are partially occupied by host ethanol molecules, however, when purple toluene or benzene solutions of C_{60} are added to colorless **486**–**487** they turn red-brown, indicative of a guest–host interaction. Probing the interaction using UV–vis spectroscopy shows that all guest–host interactions are of a 1:1 type, while it is also found that

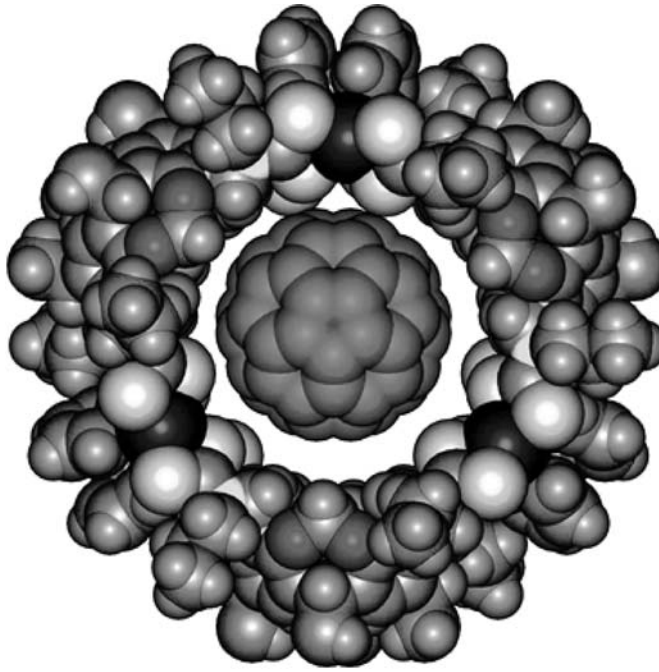

Figure 264. Space-filling diagram of **468**, **487** with host–C_{60} binding.

the cadmium complexes bind C_{60} more strongly than their zinc analogues despite their similar cavity dimensions (1489).

A range of other clathrated complexes have also been structurally characterized including $[Zn(S_2CNEt_2)_2.py].C_6H_6$ (1899), $[Zn(S_2CNEt_2)_2.py].2CCl_4$ (1901), $[Zn(S_2CNEt_2)_2.py].CH_2Cl_2$ (1902), $[Zn(S_2CNEt_2)_2.py].CHCl_3$ (1902) and $[Zn(S_2CNEt_2)_2.py].C_2H_4Cl_2$ (1904). In all, the unbound clathrated molecules occupy molecular channels and cavities within the structure. Solvent inclusion does result in some geometrical change at the metal center; for example, inclusion of carbon tetrachloride leads to an increase in the trigonal-bipyramidal character from 55 to 64% (1901). Some related clathrates of cadmium have also been prepared, but none have yet been crystallographically characterized (1904).

The bidentate ligand 4,4′-bpy has been extensively coordinated to zinc (1908, 1909, 1911–1913, 1915, 1917) and cadmium (1909, 1925). It can bind either to one or two zinc centers, as exemplified by the recent preparation and structural characterization of $[Zn(S_2CNPr_2)_2(4,4'\text{-bpy})]$ and $[\{Zn(S_2CNPr_2)_2\}_2(4,4'\text{-bpy})]$, respectively (Fig. 265) (1913). However, note that bidentate coordination is by

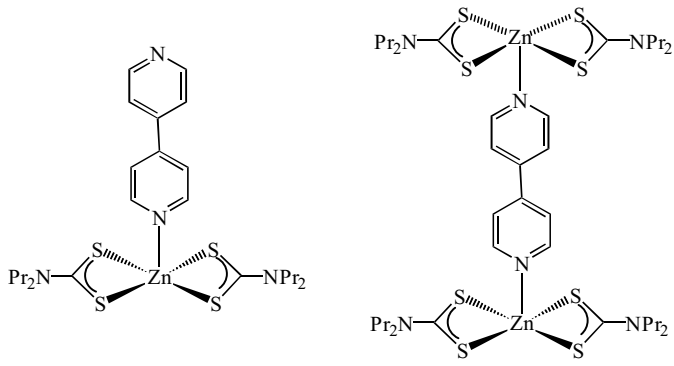

Figure 265. Examples of crystallographically characterized mono and dimeric 4,4′-bpy complexes.

far the more common, while in contrast imidazole acts only as a monodentate ligand in all cases (1920–1922).

Beer and co-workers (1469) bound 4,4′-bpy into the cavity of the large macrocyclic complex (**477**-H) (Fig. 255), forming an inclusion complex **489** (Fig. 266), whereby they believe it binds to both zinc centers. By using a ^{1}H NMR titration, they have been able to verify the 1:1 stoichiometry at higher guest concentrations, although at low concentrations some deviation is seen that may suggest that two hosts may associate with one guest when limited 4,4′-bpy is present.

Tetramethylethylene diamine also bridges between zinc centers as shown by the crystal structure of $[\{Zn(S_2CN{-}i\text{-}Pr_2)_2\}_2(Me_2NCH_2CH_2NMe_2)]$, the coordination geometry about the metal center not differing significantly from that in

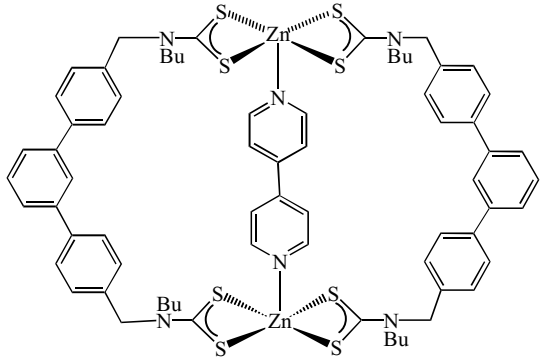

489

Figure 266. 4,4′-Bpy inclusion complex prepared by Beer and co-workers (1469).

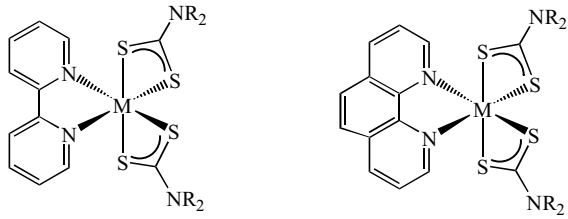

Figure 267. Octahedral 2,2′-bpy and 1,10-phen adducts of $[M(S_2CNR_2)_2]$ (M = Zn, Cd).

$[Zn(S_2CN{-}i\text{-}Pr_2)_2\}_2.Py]$. However, the relative bulkiness of the dimethyldiamino moiety does appear to inhibit close approach to zinc, the zinc–nitrogen bond at 2.137(5) Å being longer than that of 2.069(2) Å found in the pyridine adduct (1903).

Both 2,2′-bpy, 1,10-phen, and their derivatives bind to both zinc (551, 591, 1158, 1906–1909, 1914, 1918, 1919, 1923, 1936–1939) and cadmium (1924–1930) in a bidentate manner leading to the generation of six-coordinate centers, with a distorted octahedral geometry. An elongation of the zinc–sulfur bonds by ~0.2 Å when compared to simple bis(dithiocarbamate) complexes is probably due to steric rather than electronic factors (1906), although binding of the base does result in an increase of electron density on zinc as shown by electrochemical and XPS studies (551, 552).

Klevtsova and co-workers crystallographically characterized six 1,10-phen complexes, $[Zn(S_2CNR_2)_2(1,10\text{-phen})]$ (R = Me, Et, Pr, *i*-Pr, Bu, *i*-Bu), containing alkyl groups of different length and spatial structures (1918, 1936–1939). The molecules adopt various packing modes forming isolated dimers, ribbons (chains), columns, and layers resulting from the π-stacking of the 1,10-phen rings (R = Me, Et, *i*-Pr, Bu) or interactions between the rings and the carbon atoms of the alkyl chains (R = Pr, *i*-Bu). Lai and Tiekink have recently reported the crystallographic characterization of two 2,9-dimethyl-1,10-phenanthroline (1,10-phen*) complexes, $[Zn(S_2CNC_4H_8)_2(1,10\text{-phen*})]$ (**490**) (1919) and $[Cd(S_2CNEt_2)_2(1,10\text{-phen*})]$ (**491**) (Fig. 268) (1929). Interestingly, the latter displays the expected distorted octahedral coordination environment, while in the zinc complex, the dithiocarbamates bind only in a monodentate fashion, affording a distorted tetrahedral geometry.

In other reports, Tiekink and co-workers (1916) detailed the crystallographic characterization of $[\{Zn(S_2CNEt_2)_2\}_2(\mu\text{-}trans\text{-}NC_5H_4CH{=}CHC_5H_4N)]$, in which the two zinc centers are spanned by the *trans*-1,2-bis(4-pyridyl)ethylene ligand in the expected manner, and the related cadmium complex $[\{Cd(S_2CNEt_2)_2\}(\mu\text{-}trans\text{-}NC_5H_4CH{=}CHC_5H_4N)]_n$ (Fig. 269). The latter is polymeric, and adopts an octahedral coordination environment with a trans disposition of the adducts (1931).

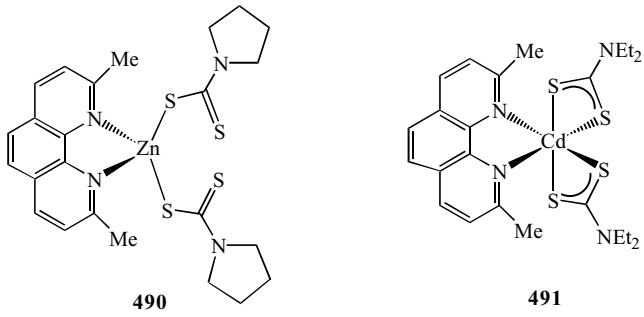

Figure 268. Crystallographically characterized 1,10-phen* adducts.

Phosphines also form adducts with both zinc and cadmium bis(dithiocarbamate) complexes, as exemplified by the synthesis and crystallographic characterization of $[Zn(S_2CNEt_2)_2(PMe_3)]$, $[Cd(S_2CNEt_2)_2(PEt_3)]$ (1932), $[\{Zn(S_2CNEt_2)_2\}_2(\mu\text{-depe})].2C_7H_8$ (1933), and $[\{Cd(S_2CNEt_2)_2\}_2(\mu\text{-dppf})]$ (1934). The coordination environment about the metal center is generally best described as trigonal pyramidal, with the phosphine occupying an equatorial site, although a considerable distortion toward square-based pyramidal is apparent. Detailed variable temperature ^{31}P and ^{113}Cd NMR studies show that in solution they undergo facile and reversible metal–phosphorus bond cleavage (1932, 1940). With PBu_3, this process is so facile that even at the lowest temperatures obtainable, only an exchange averaged position between the free phosphine and adduct is observed, while in contrast for the more basis PCy_3, a 1:1 adduct is clearly observed (1940).

Thermal gravimetric studies show that for the zinc complexes, phosphine loss occurs prior to their thermal decomposition to ZnS, while in contrast, $[Cd(S_2CNEt_2)_2(PEt_3)]$ exhibits a single weight loss to give polycrystalline

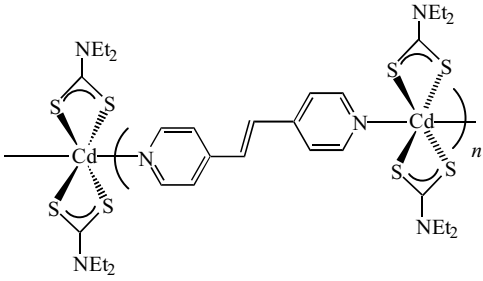

Figure 269. Portion of the polymeric structure of $[\{Cd(S_2CNEt_2)_2\}(\mu\text{-}trans\text{-}NC_5H_4CH{=}CHC_5H_4N)]_n$.

CdS. Mixed-metal complexes bridged by depe have also been prepared and decompose to give $Zn_{0.5}Cd_{0.5}S$ according to powder X-ray diffraction data (1932).

c. Anionic Adducts of Bis(dithiocarbamate) Complexes. Zinc bis (dithiocarbamate) complexes have previously been shown by McCleverty and co-workers (1941) to add a further equivalent of dithiocarbamate salt affording tris(dithiocarbamate) anions, $[Zn(S_2CNR_2)_3]^-$. A number of further reports by the same group detail extensions to this work with a range of mixed-ligand complexes being prepared (400, 1942), while analogous chemistry has also been found for cadmium (Fig. 270) (412, 413, 415). Crystallographic characterization of $[Zn(S_2CNMe_2)_3][NEt_4]$ reveals four short [2.299(2)–2.457(2) Å] and two long [3.115(3) and 3.151(3) Å] zinc–sulfur interactions. The former define a tetrahedral coordination environment, while taking into account the latter, it can be considered as a distorted trigonal prism (401, 1941).

Somewhat similar structural features are found for cadmium analogues (415), examples of which, $[Cd(S_2CNEt_2)_3][M(en)_3]$ (M = Cd, Zn), also have been prepared from the reaction of $[Cd(S_2CNEt_2)_2]$ with en alone (M = Cd), and in the presence of $[Zn(S_2CNEt_2)_2]$ (M = Zn) (412, 413). The larger size of cadmium leads to the coordination of all six sulfur atoms, although in two of the dithiocarbamates there is considerable asymmetry in the cadmium sulfur distances, which range from 2.548(4) to 3.030(5) Å. By taking these longer interactions into account, the coordination geometry is best described as distorted trigonal prismatic, the vertical edges of which are described by sulfur–sulfur interactions of 2.94(1)–3.00(2) Å (412).

Some reactivity studies have been carried out on the tris(dithiocarbamate) complexes. Like its zinc analogue, $[Cd(S_2CNEt_2)_3]^-$ reacts with sulfur in refluxing xylene to give a red oil, although at a much slower rate. This result may be a reflection of the greater kinetic stability of the cadmium complex, suggesting that the equilibrium with $[M(S_2CNR_2)_2]$ and $[S_2CNR_2]^-$ lies further

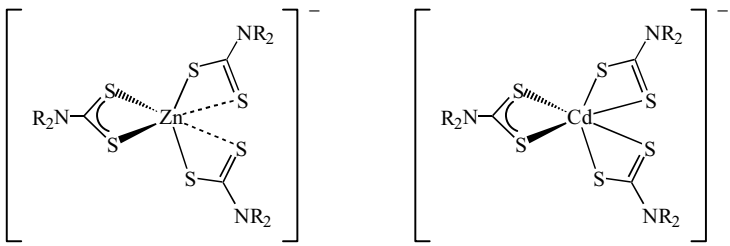

Figure 270. Structures of zinc and cadmium tris(dithiocarbamate) anions.

to the right-hand side for cadmium (Eq. 175) (415, 1941, 1943).

$$[M(S_2CNR_2)_2] + R_2CNS_2^- \rightleftharpoons [M(S_2CNR_2)_3]^- \qquad (175)$$

In an analogous fashion to the reactions with dithiocarbamate salts, $[M(S_2CNR_2)_2]$ (M = Zn, Cd) also react with other monoanionic chelate ligands to form related adducts. For example, reaction of $[Zn(S_2CNMe_2)_2]$ with acetate salts yields $[Zn(S_2CNMe_2)_2(O_2CR)]^-$ (R = Me, Et, Pr, Bu), although with more bulky acetates (e.g., R = Pr, hexyl, octyl) only the tris(dithiocarbamate) complex, $[Zn(S_2CNMe_2)_3]^-$, was isolated. Structural data for mononuclear acetate adducts $[Zn(S_2CNMe_2)_2(O_2CR)]^-$ is absent and attempted recrystallization of $[Zn(S_2CNMe_2)_2(O_2CMe)][NBu_4]$ from acetone–light petroleum affords dimeric $[\{Zn(S_2CNMe_2)_2\}_2(\mu\text{-}O_2CR)][NBu_4]$. The latter consists of two approximately square-pyramidal zinc centers bridged by the acetate group, with the oxygens occupying axial sites (1942). The isolation of this product suggests that like the tris(dithiocarbamate) complexes, the mixed-dithiocarbamate–acetate system can be described by a series of equilibria, the adventitious isolation of $[\{Zn(S_2CNMe_2)_2\}_2(\mu\text{-}O_2CR)][NBu_4]$ resulting from loss of an acetate to generate $[Zn(S_2CNMe_2)_2]$, which in turn reacts with more $[Zn(S_2CNMe_2)_2(O_2CR)]^-$ (Eq. 176).

$$2\,[Zn(S_2CNMe_2)_2(O_2CMe)]^- \rightleftharpoons \left[\begin{array}{c} Me_2N\text{–}C(S)(S)\text{–}Zn(S)(S)\text{–}C(S)(S)\text{–}NMe_2 \\ \qquad\qquad\qquad\qquad O \\ \qquad\qquad\qquad\qquad \| \\ \qquad\qquad\qquad\qquad C\text{–}Me \\ \qquad\qquad\qquad\qquad O \\ Me_2N\text{–}C(S)(S)\text{–}Zn(S)(S)\text{–}C(S)(S)\text{–}NMe_2 \end{array}\right]^- + MeCO_2^- \qquad (176)$$

Bis(dithiocarbamate) complexes $[Zn(S_2CNR_2)_2]$ (R = Me, Et, Bu; $R_2 = C_5H_{10}$) also react with benzothiazole-2-thiolate, and benzoxazole-2-thiolate generating anionic adducts $[Zn(S_2CNR_2)_2(C_7H_4NES)]^-$ (E = S, O). Likewise, the related mono(dithiocarbamate) complexes $[Zn(S_2CNR_2)(C_7H_4NES)_2]^-$ have been prepared from the reaction of dithiocarbamate salts with bis(thiolate) complexes. Examples of each type of benzothiazole-2-thiolate complex, namely, $[Zn(S_2CNMe_2)_2(C_7H_4NS_2)][NBu_4]$ (**492**) and $[Zn(S_2CNMe_2)(C_7H_4NS_2)_2][NBu_4]$ (**493**) (Fig. 271), have been characterized crystallographically. The former has a five-coordinate square-pyramidal zinc center, with the monodentate benzothiazole-2-thiolate ligand binding through nitrogen and occupying the

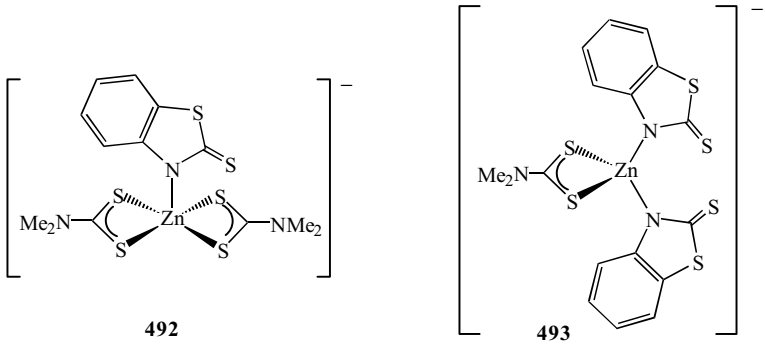

492 493

Figure 271. Zinc dithiocarbamate complexes containing the benzothiazole-2-thiolate ligand.

axial site, while the latter is four coordinate and approximately tetrahedral (401).

McCleverty et al. (415) also described the synthesis and characterization of analogous cadmium complexes $[Cd(S_2CNR_2)_3]^-$ (R = Me, Et, Bu), $[Cd(S_2CNEt_2)_2(O_2CMe)]^-$, and $[Cd(S_2CNEt_2)(C_7H_4NS_2)_2]^-$, although they were unable to isolate complexes of the type $[Cd(S_2CNR_2)_2(C_7H_4NS_2)]^-$. A crystallographic study of $[Cd(S_2CNEt_2)_3][NBu_4]$ revealed that, unlike the analogous zinc complexes, cadmium is six-coordinate, cadmium–sulfur bonds ranging from 2.655(3) to 2.755(3) Å, with the coordination geometry intermediate between octahedral and trigonal prismatic (415).

Perec and co-workers (414) reported the synthesis and characterization of xanthate adducts of zinc and cadmium, $[M(S_2CNR_2)_2(S_2COEt)]^-$ (M = Zn, R = Me; M = Cd, R = Me, Et), formed from the reaction of the bis(dithiocarbamate) complexes with xanthate salts in acetone. Crystallographic studies of both $[Zn(S_2CNMe_2)_2(S_2COEt)][NBu_4]$ (**494**) and $[Cd(S_2CNEt_2)_2(S_2COEt)][PPh_4]$ (**495**) (Fig. 272) have been carried out. The zinc complex is five coordinate with a monodentate xanthate and is nearer to a trigonal bipyramid than a square-based pyramid. In contrast, the xanthate ligand is bidentate at the

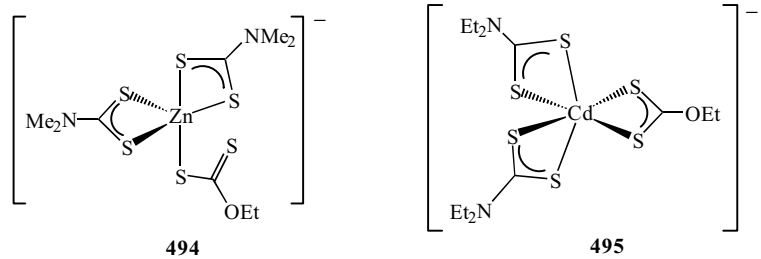

494 495

Figure 272. Examples of xanthate–bis(dithiocarbamate) complexes.

larger cadmium center where the coordination geometry is best described as a distorted trigonal prism and the two triangular units are rotated by $\sim 26^\circ$.

The same group have also reported that $[Zn(S_2CNMe_2)_2]$ and $[Cd(S_2CNEt_2)_2]$ both react with halides and isothiocyanate to give five-coordinate adducts $[M(S_2CNR_2)_2X]^-$ (X = Cl, Br, I, NCS). Both isothiocyanate adducts have been crystallographically characterized, the isothiocyanates binding through nitrogen and in the equatorial site of a distorted trigonal prism (1944). The cadmium halide complexes $[Cd(S_2CNEt_2)_2X][PPh_4]$ (X = Cl, Br) have also been crystallographically characterized showing a coordination geometry midway between square pyramidal and trigonal bipyramidal (1945).

d. Further Reactions of Zinc and Cadmium Bis(dithiocarbamate) Complexes. Ligand exchange reactions occur when $[Zn(S_2CNEt_2)_2]$ reacts with either $[Zn(mnt)_2]^{2-}$ (1946) or $[Zn(dmit)_2]^{2-}$ (1947) (mnt = 1,2-dicyanoethane-1,2-dithiolate; dmit = 1,3-dithiole-2-thione-4,5-dithiolate) generating distorted tetrahedral complexes $[Zn(S_2CNEt_2)(mnt)]^-$ (**496**) and $[Zn(S_2CNEt_2)(dmit)]^-$ (**497**) (Fig. 273), respectively. Related ligand-exchange reactions also occur at nickel(II) and copper(II) centers and are much faster at copper centers than at the other metals, while a second-order rate law determined for nickel has been interpreted in terms of a complicated reaction mechanism, which is started by a ligand dissociation step (1947).

Previously it was established that addition of halogens to bis(dithiocarbamate) complexes results in ligand-centered oxidation to generate thiuram disulfide complexes $[MX_2\{R_2NC(S)SS(S)CNR_2\}_2]$ (M = Zn, Cd, Hg) (Eq. 177) (1948). Ramalingam and co-workers (1949) have crystallographically characterized two examples of complexes of this type (M = Zn, Cd; $R_2 = C_5H_{10}$), while McCleverty et al. showed that while addition of iodine to $[Cd(S_2CNEt_2)_2]$ generates the thiuram disulfide complex, bromine addition in contrast affords $[S(SCNEt_2)_2][CdBr_4]$ (415).

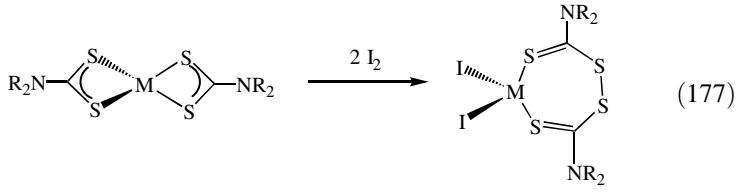

(177)

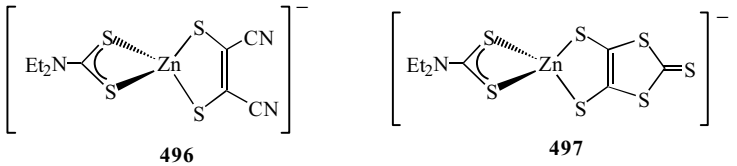

496 **497**

Figure 273. Anionic zinc dithiocarbamate complexes containing other dithiolate ligands.

More recent work has shown that the iodine reaction is highly dependent on the stoichiometry used. Thus, addition of 1 equiv of iodine affords polymeric $[Cd(\mu\text{-}I)(\mu\text{-}S_2CNEt_2)]_n$, together with tetraethylthiuram disulfide (Eq. 178) (1950). The same polymer, together with its zinc analogue, can also be prepared from addition of MI_2 (M = Zn, Cd) to the bis(dithiocarbamate) complexes in ethanol (1950, 1952). The cadmium complex has been characterized crystallographically, with metal centers alternatively bridged by two iodide and two dithiocarbamate ligands (1950–1952).

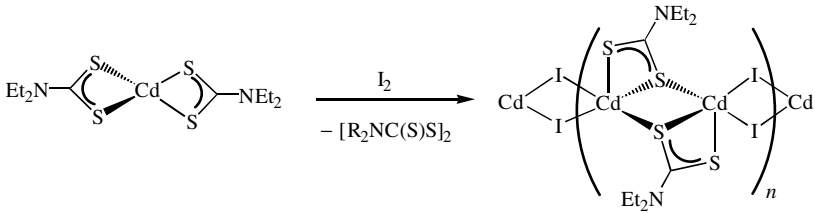

(178)

The reaction of isotopically labeled $[^{65}Zn(S_2CNEt_2)_2]$ with sodium azide, which ultimately affords zinc azide, has been probed mechanistically. The reaction is believed to occur via an associative pathway with $[Zn(S_2CNEt_2)_2(N_3)]^-$ being the first species generated, subsequent azide additions resulting in dithiocarbamate loss, possibly via a monodentate intermediate (1953).

e. Reactivity of Mercury Bis(dithiocarbamate) Complexes. The chemistry of mercury bis(dithiocarbamate) complexes is not as well developed as that of zinc and cadmium, however, a number of recent advances have been made. Addition of mercury(I) perchlorate to $[Hg(S_2CNR_2)_2]$ (R = Et, Bz; $R_2 = C_5H_{10}$) yields clusters $[Hg_3(S_2CNR_2)_4][ClO_4]_2$ (R = Me, Bz) and $[Hg_4(S_2CNC_5H_{10})_6][ClO_4]$ (1954) (see Section IV.I.1.a), which are analogous to those prepared upon electrochemical oxidation of $[Hg(S_2CNR_2)_2]$ (163, 1891). Variable temperature ^{199}Hg NMR spectra of 10^{-2} *M* solutions of the trinuclear species suggest that in solution they are better formulated as $[Hg_6(S_2CNR_2)_8]^{4+}$ (1954).

More recently, ESMS has been used to study the constitution of mercury and mixed-mercury–cadmium dithiocarbamate cations in dichloromethane and methanol. For mercury alone, a range of ions, $[Hg(S_2CNR_2)]^+/[Hg(S_2CNR_2)_2]_n$, are observed such as $[Hg_2(S_2CNR_2)_3]^+$ ($n = 1$), while addition of $[Hg(S_2CNR_2)_2]$ favors higher oligomers such as $[Hg_3(S_2CNR_2)_4]^+$ and $[Hg_5(S_2CNR_2)_8]^+$. Reaction of the mercury-rich dithiocarbamate cations with $[Cd(S_2CNR_2)_2]$ leads to global exchange of ligands and metals (547).

A number of mercury phosphine complexes have been described. Bond and co-workers (1940, 1955) demonstrated using ^{31}P and ^{199}Hg NMR that in

dichloromethane solution, phosphine adducts of the type $[Hg(S_2CNR_2)_2(PX_3)_n]$ (X = Bu, Cy; $n = 1, 2$) are formed. With PBu_3, both mono and bis adducts are in rapid equilibrium at room temperature, and it is only at ca−90°C that signals for individual species could be observed. For the more basic PCy_3, only the monoadduct $[Hg(S_2CNR_2)_2(PCy_3)]$ is seen. The precise nature of these adducts remains unknown. It may be that coordination of the bulky phosphine(s) results in the concomitant formation of monodentate dithiocarbamate(s), although on the basis of molecular weight measurements (R = Bu), polymeric species can be ruled out.

Electrochemical studies of $[Hg(S_2CNR_2)_2]$ (R = Et, Pr, Bu, cyclohexyl; $R_2 = C_5H_{10}$) at mercury electrodes in the presence of these phosphines give interesting results, including current reversal (cyclic voltammetry), negative differential current (differential pulse polarography), and current suppression (dc polarography), which seem to be associated with formation of $[Hg(S_2CNR_2)_2(PCy_3)_2]$ (1955).

Monitoring the reactions of $[Hg(S_2CNEt_2)_2]$ with phosphines by ESMS leads to the detection of cationic complexes $[Hg(S_2CNEt_2)(PR_3)]^+$ and $[Hg(S_2CNEt_2)(PR_3)_2]^+$ (546). Cations of this type have been isolated in some instances. Thus, reaction of $[Hg(S_2CNEt_2)_2]$ with PCy_3 in the presence of $[Hg(O_3SCF_3).dmso]$ affords $[Hg(S_2CNEt_2)(PCy_3)]^+$ as shown by ^{31}P and ^{199}Hg NMR spectroscopy. The latter reacts with more dithiocarbamate salt affording, $[Hg(S_2CNEt_2)_2(PCy_3)]$ (1956), and with more phosphine to generate $[Hg(S_2CNEt_2)(PCy_3)_2][CF_3SO_3]$ (**498**) (Fig. 274), which has been crystallographically characterized. The latter also reacts further with more dithiocarbamate salt to yield $[Hg(S_2CNEt_2)(PCy_3)_2][S_2CNEt_2]$, slow exchange of coordinated and uncoordinated dithiocarbamates is observed at low temperature (1956). The perchlorate salt $[Hg(S_2CNEt_2)(PCy_3)][ClO_4]$ (**499**) (Fig. 274) is generated from $[Hg(S_2CNEt_2)_2]$ and $[Hg(PCy_3)_2][ClO_4]_2$ in dichloromethane (1957). A crystal structure shows that the complex is actually dimeric, the mercury centers being bridged by two dithiocarbamate ligands that lie on the same side of the Hg_2S_2 square, each dithiocarbamate also carrys one phosphine and one perchlorate ligand. Further NMR studies suggest that in solution this may be in exchange equilibrium with an unbound perchlorate species (1957).

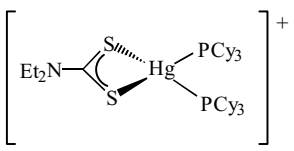

498

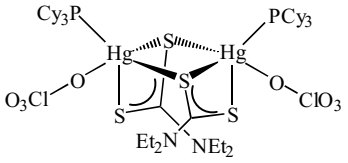

499

Figure 274. Crystallographically characterized mercury–tricyclohexyl phosphine complexes.

In a very recent contribution, Lai and Tiekink (235) isolated the mercury–chloride complex [HgCl(η^1-S_2CNEt_2)(1,10-phen*)] (**500**) from the reaction of [$Hg(S_2CNEt_2)_2$] and 1,10-phen*, which is presumed to result from the loss of a dithiocarbamate and chloride abstraction from the chloroform solvent. An X-ray crystal structure shows that the dithiocarbamate binds in a monodentate fashion, allowing the mercury center to adopt a highly distorted tetrahedral coordination geometry.

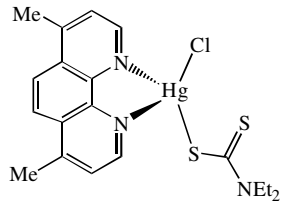

500

f. Alkyl and Aryl Complexes [$R'M(S_2CNR_2)$]. Organozinc dithiocarbamate complexes have been known for some years (1958) as have related mercury complexes (1959). They are easily formed upon insertion of carbon disulfide into metal amides. In this manner, O'Brien and co-workers (255, 1898) prepared a range of zinc and cadmium complexes, while others have prepared mercury complexes (1843). Tiekink and co-workers (257–259) also prepared [$PhHg(S_2CNR_2)$] ($R = Et$, Pr; $R_2 = C_4H_8$) upon reaction of PhHgCl and the appropriate dithiocarbamate salt.

A number of crystallographic studies have been carried out. They are generally dimeric, the tetrahedral metal centers being bridged by two dithiocarbamate ligands (255–259). For example, in [$PhHg(S_2CNPr_2)]_2$ (**23**), each mercury center is bound in an approximately linear fashion [C—Hg—S 166.76(10)°] to the phenyl group and one sulfur atom of the dithiocarbamate. The second sulfur binds less strongly [Hg—S 2.4033(9) and 2.9093(10) Å] and also forms a bridge to the second mercury center [Hg—S 3.1809(10) Å] (258).

An alternative synthesis of zinc and cadmium methyl complexes involves the ligand exchange between dimethyl reagents MMe_2 and bis(dithiocarbamate) complexes (1960–1962). By using the trimethylpropylenediamine dithiocarbamate ligand complex [$M\{S_2CNMe(CH_2CH_2CH_2NMe_2)\}_2$], a crystal structure of the resulting cadmium complex, [$CdMe\{S_2CNMe(CH_2CH_2CH_2NMe_2)\}$], shows that it is polymeric.

Few reactions of this class of complex have been carried out, but O'Brien and co-workers (1898) showed that addition of 2,4,6-trimethylthiophenol to [$MeZn(S_2CNEt_2)$] in toluene at 80°C affords [$Zn(S_2CNEt_2)$(S-2,4,6-$Me_3C_6H_2$)], the insolubility of which prevented full characterization.

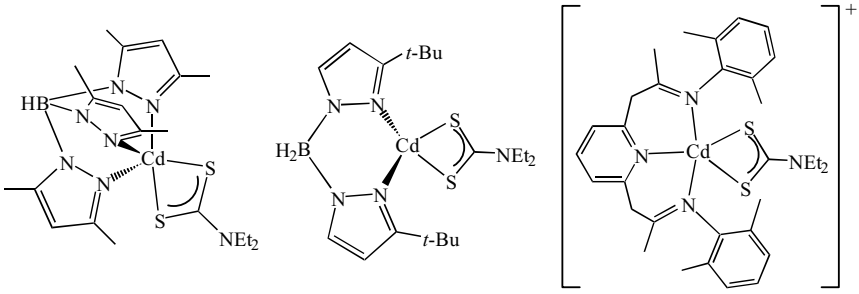

501 **502** **503**

Figure 275. Cadmium complexes with nitrogen-donor ligands prepared by Reger et al. (1964).

g. Other Dithiocarbamate Complexes. While mixed-ligand cyclopentadienyl–dithiocarbamate complexes remain unknown, Reger et al. (1963, 1964) reported the synthesis of related cadmium tris(pyrazolyl)borate complexes $[Cd(S_2CNEt_2)\{HB(3,5\text{-}Me_2pz)_3\}]$ (**501**) (Fig. 275) and $[Cd(S_2CNEt_2)\{HB(3\text{-}Rpz)_3\}]$ (R = Ph, *t*-Bu). These complexes are formed upon addition of equal amounts of NaS_2CNEt_2 and tris(pyrazolyl)borate salts to $CdCl_2$. The former has been crystallographically characterized. The dithiocarbamate ligand is anisobidentate at the five-coordinate cadmium center, having one long (axial), 2.708(2) Å, and one short, 2.540(2) Å, cadmium–sulfur interaction (1963); this situation is similar to that found in phosphine adducts (1932). The tris(pyrazolyl)borate is more symmetrically bound, the overall coordination geometry approximates a trigonal bipyramid, with the dithiocarbamate bridging axial and equatorial sites. Reger et al. (1964) also prepared closely related bis(pyrazolyl)borate (Bp), $[Cd(S_2CNEt_2)\{H_2B(3\text{-}t\text{-}BuBp)_2\}]$ (**502**), and 2,6-bis(2,6-dimethylphenylimino) (pydim), $[Cd(S_2CNEt_2)(\eta^3\text{-pydim})]Cl$ (**503**), complexes (Fig. 275).

Chieh (1965) reported that addition of tetraethylthiuram disulfide to $HgBr_2$ affords pale yellow crystals of the general formula $[Hg(S_2CNEt_2)_2.HgBr_2]$ (Fig. 276). A crystallographic study revealed it to be a polymer, consisting of

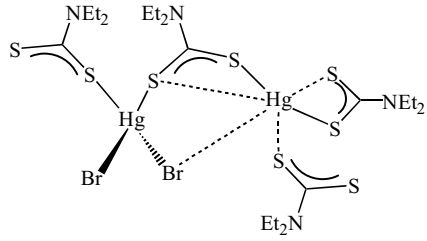

Figure 276. A portion of the polymeric structure of $[Hg(S_2CNEt_2)_2.HgBr_2]_n$.

alternating tetrahedral and linear two-coordinate mercury centers linked via a bridging dithiocarbamate.

A number of mixed-metal clusters containing mercury dithiocarbamate units have been prepared and crystallographically characterized. Addition of 2 equiv of $[Hg(S_2CNEt_2)_2]$ to $[Cp_2MH_2]$ (M = Mo, W) yields $[Cp_2M\{Hg(S_2CNEt_2)\}_2]$ (**504**) (Fig. 277) as one of the products; the same complexes is produced from $[Cp_2M(HgX)_2]$ upon addition of NaS_2CNEt_2. The molybdenum complex has been crystallographically characterized. The molybdenum is pseudo-tetrahedral and is bound directly to two mercury(I) centers, which are also ligated by a dithiocarbamate. This dithiocarbamate binds in an anisobidentate fashion with long, 2.94(3) Å, and short, 2.50(2) Å, mercury–sulfur interactions. The latter defines an approximately linear two-coordinate geometry at mercury with the molybdenum center (260). A series of related complexes, $[\{CpMo(CO)_2L\}_2\{Hg(\mu\text{-}S_2CNEt_2)\}_2]$ [L = CO, PPh_3, $P(OMe)_3$], containing mercury–molybdenum bonds, have been prepared and crystallographically characterized (L = CO) (**505**) (Fig. 277). The nature of the molybdenum–mercury bond has also been probed by IR and multinuclear NMR studies, both of which suggest that there is strong covalent character (1966).

In a further example, addition of $[Hg(S_2CNEt_2)_2]$ to $[Cp_2NbH_3]$ has been shown to afford the tetranuclear cluster $[Cp_2Nb\{Hg(S_2CNEt_2)\}_3]$ (**506**), which has again been characterized crystallographically. The four metal atoms define a rhombohedron, with mercury–niobium distances of between 2.777(3) and 2.808(3) Å, which are indicative of a significant covalent interaction, while the mercury–mercury bonds at 2.883(2) and 2.901(2) Å are slightly longer. Each mercury is chelated by a dithiocarbamate ligand, which again binds in an anisobidentate fashion. The short mercury–sulfur bonds, 2.513(8)–2.526(8) Å, lie in the plane of the metal atoms, while the longer interactions, 2.75(3)–2.919(10) Å, lie approximately perpendicular to it (261).

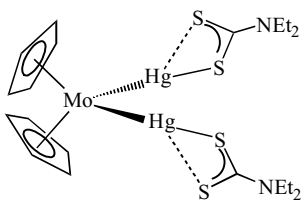

504

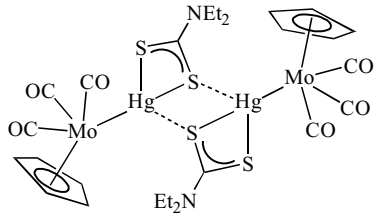

505

Figure 277. Examples of heterometallic mercury–molybdenum dithiocarbamate complexes.

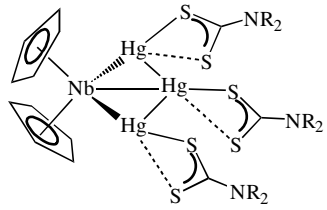

506

h. Applications. Traditional applications of group 12 (II B) bis(dithiocarbamate) complexes are in analytical chemistry, agriculture, and the rubber industry. More recently, advances have been made in their utilization as molecular precursors to technologically important metal sulfides, and the use of cadmium complexes in chelate therapy.

i. Molecular Precursors to ZnS and CdS. Both cadmium and zinc sulfide are important semiconductor materials. While they can easily be prepared from two-source MOCVD, single-source precursors offer a number of advantages including the ability to generate better quality films, while employing less hazardous materials. It is well known that solid-state pyrolysis of both zinc and cadmium bis(dithiocarbamate) complexes under an inert atmosphere generally afford the corresponding metal sulfides, although the phase and stoichiometry of the deposit depend strongly on the pyrolysis conditions (23, 1840, 1967). In this context, a wide range of zinc and cadmium bis(dithiocarbamate) complexes have been utilized as single-source MOVCD precursors toward binary sulfides ZnS, CdS, and also ternary systems such as $Cd_xZn_{1-x}S$ (1437, 1932). Aspects of this work have been reviewed (1968).

Group 12 (II B) bis(diethyldithiocarbamate) complexes, $[M(S_2CNEt_2)_2]$ ($M = Zn$, Cd), were first utilized toward the growth of thin films of ZnS and CdS by O'Brien and co-workers in 1989 (1969). Thin films were obtained at pressures of 10^{-4} Torr and between 370 and 420°C. The CdS films were polycrystalline and hexagonal on glass, but thin epitaxial layers were obtained on InP(100) and GaAs (100). The quality of ZnS films obtained by this method was lower than those of CdS.

Following this work, Wold and co-workers (1970) prepared thin films of ZnS by ultrasonically spraying a toluene solution of $[Zn(S_2CNEt_2)_2]$ onto silicon, sapphire, and GaAs substrates at 460–520°C. A highly orientated hexagonal structure was obtained on silicon and sapphire, while those on the cubic GaAs(100) showed a highly ordered cubic structure. The thermal decomposition pathway was also investigated by studying the volatile products using GC–MS. The results were consistent with earlier TGA experiments (1971), suggesting a

plausible pathway (Eqs. 179–180):

$$Zn(S_2CNEt_2)_2 \longrightarrow ZnS + EtNCS + Et_2NCS_2Et \quad (179)$$

$$Et_2NCS_2Et \longrightarrow Et_2NH + CS_2 + C_2H_4 \quad (180)$$

Nomura et al. (1972) also prepared highly orientated cubic ZnS on an Si(111) substrate using $[Zn(S_2CNEt_2)_2]$. They found that without a carrier gas, these films were thin and of poor morphology and crystallinity, while using nitrogen as a carrier gas gave much better films. Thin films of CdS have also been grown on different substrates using plasma enhanced chemical vapor deposition of the 1,10-phen adduct of $[Cd(S_2CNEt_2)_2]$, producing films with 90–95% transmittance of visible light and high resistivity (10^{12}–10^{13} Ω cm) (1971). Other neutral amine and phosphine adducts of $[Zn(S_2CNEt_2)_2]$ and $[Cd(S_2CNEt_2)_2]$ have also been used to prepare films (1768, 1920, 1925, 1932), as have anionic adducts such as $[M(S_2CNEt_2)_2(S_2COEt)]^-$ (414) and $[Cd(S_2CNEt_2)_3]^-$ (413). The latter give $Zn_{0.25}Cd_{0.75}S$ when $[Zn(en)_3][Cd(S_2CNEt_2)_3]$ was used (413).

In a series of recent contributions, Lamb and co-workers (1974–1976) studied in some detail the nature of the deposition of ZnS onto silicon surfaces from precursors $[Zn(S_2CNR_2)_2]$ (R = Me, Et). They found that during the initial growth period, a relatively high concentration of carbon is found at the interface, which decreases with increasing film thickness (1975). The films generated were comprised of a uniformly distributed array of columns ~300–500 nm wide, being attached to the surface via smaller columns of some 50–100 nm width (1976). They also noted that the orientation of crystallites occurred at an earlier stage than predicted and attributed this to the presence of impurities that may serve to influence the structural evolution of the film.

A major limitation of this approach is the physical properties of the diethyldithiocarbamate complexes, both having relatively high melting points; 175°C for $[Zn(S_2CNEt_2)_2]$ and 250°C for $[Cd(S_2CNEt_2)_2]$. Further, their volatility is marginal for MOCVD use, the vapor pressure of $[Zn(S_2CNEt_2)_2]$ is ~2 mTorr at 200°C (1977–1979).

O'Brien and co-workers (400) tackled this issue with the preparation of complexes with asymmetric dithiocarbamate ligands such as $[Zn(S_2CNMeR)_2]$ (R = Et, Pr, *i*-Pr, Bu), which are considerably more volatile than $[Zn(S_2CNEt_2)_2]$ (as surmised from TGA measurements). A further advantage of the substituent approach is data showing that the mean M—S bond dissociation energies (homolytic) for these complexes is a function of the substituents (see Table X) (page 138). For example, these vary in the order $[Zn(S_2CNEt_2)_2]$ (177.4 ± 3.4 kJ mol^{-1}) > $[Cd(S_2CNEt_2)_2]$ (167.3 ± 3.6 kJ mol^{-1}) > $[Hg(S_2CNEt_2)_2]$ (74.6 ± 3.6 kJ mol^{-1}); while the introduction of *i*-butyl groups gives significantly lower bond dissociation enthalpies for zinc and cadmium $[Zn(S_2CN—i\text{-}Bu_2)_2]$ (137 ± 4 kJ mol^{-1}) > $[Cd(S_2CN—i\text{-}Bu_2)_2]$ (118 ± 4 kJ mol^{-1}) (572–576). To

this end, $[Cd(S_2CNMeBu)_2]$ was found to be more volatile than $[Cd(S_2CNEt_2)_2]$. Both precursors give similar results in low pressure MOCVD experiments (1980).

A second approach adopted by O'Brien and co-workers (1841, 1849) is the preparation of bis(dithiocarbamate) complexes generated from trimethylethylene and trimethylpropylene diamines. The former gives fairly insoluble products that were not pursued, but the latter are soluble in toluene and benzene and were successfully used to deposit thin films of ZnS and CdS on glass, which gave better quality films than $[Cd(S_2CNEt_2)_2]$.

Nomura et al. (1981) used an equimolar mixture of [EtZn(S—*i*-Pr)] and $[Zn(S_2CNEt_2)_2]$ to deposit ZnS by a dip-dry method, while O'Brien's group also utilized alkyl complexes $[R'M(S_2CNR_2)]_2$ as precursors (255, 1962, 1982–1984). They are more volatile than the analogous bis(dithiocarbamate) complexes and many decompose cleanly under vacuum at 10^{-2} Torr, giving better quality films and higher growth rates than the parent bis(dithiocarbamate) complexes (1983). Their relative use as single-source precursors depends on the nature of both the alkyl and the dithiocarbamate groups. Thus, while $[MeCd(S_2CNEt_2)]_2$ gives cloudy and uneven CdS films on GaAs at 425°C, the neopentyl derivative affords crystalline and specular films (1961). The methyl zinc and cadmium complexes derived from trimethylpropylene diamine gave rapidly deposited, good quality, metal sulfide films (1984). A further advantage of this approach is the ease of synthesis of mixed-metal complexes such as $[NpZn_{0.5}Cd_{0.5}(S_2CNEt_2)]_2$, which has been used to deposit ternary metal sulfide films (1982); other examples have also been deposited from 2,2′-bpy adducts of mixed bis(dithiocarbamate) complexes (1768).

More recent work in this area has focused on the deposition of ZnS and CdS nanocrystallites using these single-source precursors, and this area has been reviewed (1985–1987). The first example of this approach was detailed in 1996 by Trindade and O'Brien (1988) who prepared nanoparticles of CdS from the thermal decomposition of $[Cd(S_2CNEt_2)_2]$ in refluxing 4-ethylpyridine solutions.

This method was later extended to the preparation of TOPO capped CdS, with both $[Cd(S_2CNEt_2)_2]$ and $[RCd(S_2CNEt_2)]_2$ (R = Me, Et, Np) acting as efficient precursors to CdS nanocrystallites. These can further be used to prepare novel composite materials upon addition of bridging diamine ligands such as pyrazine, 4,4′-bpy, and 2,2′-bipyrimidine (1989, 1990). Other TOPO-capped CdS nanoparticles have been prepared in a similar manner (1991, 1992), while TOPO-capped ZnS nanoparticles have been prepared from $[EtZn(S_2CNEt_2)]_2$ (1991, 1993) and $[Zn(S_2CNMeHex)_2]$ (1992).

A number of exciting recent developments have been made in this area. The asymmetric complex $[Cd\{S_2CNMe(C_{18}H_{37})\}_2]$ has been used for the generation of self-capped CdS quantum dots, simply prepared upon thermolysis in a

dynamic vacuum at between 150 and 300°C. Interestingly, the size of nanocrystals produced is temperature dependent. There is also a change in phase from cubic to hexagonal at 300°C (1994). Trindade et al. (1989) also reported a one-step synthesis of CdS nanoparticles on submicrometric silica particles (SiO_2@CdS) by simply decomposing cadmium bis(dithiocarbamate) in refluxing acetone. X-ray powder diffraction data is consistent with the formation of hexagonal CdS (1995).

Highly monodispersed CdSe—CdS core-shell nanoparticles have been prepared from the successive thermolysis of [$Cd(Se_2CNMeHex)_2$] and [$Cd(S_2CNMeHex)_2$] in TOPO (1960), as have manganese-doped ZnS and CdS quantum dots derived from [$M(S_2CNEt_2)_2$] and $MnCl_2$. The ZnS material gives emission in the orange region of the visible spectrum rather than the blue (1996, 1997).

In further work, Xie and co-workers reported the easy preparation of CdS nanowires via simple heating of [$Cd(S_2CNEt_2)_2$] in ethylenediamine at 117°C for 2 min. The precise role of the diamine is not yet understood, but no wire-like products were obtained when pyridine and diethylamine were used, suggesting that it may serve as a director for the growth of the intermediate inorganic Cd_2S_2 core (1998). Lieber and co-workers (1999) also prepared CdS and ZnS nanowires using [$M(S_2CNEt_2)_2$] as molecular precursors via a nanocluster-catalyzed approach. The nanowires in both cases were of high quality and the authors suggest that they may serve as well-defined nanowire components for the assembly of photonic devices.

The work described above has been largely confined to the synthesis of binary sulfides, however, it has been extended to ternary sulfides. Polycrystalline electroluminescent ZnS:Mn films have been obtained upon simultaneous pyrolysis of [$Zn(S_2CNEt_2)_2$] and [$Mn(S_2CNEt_2)_2$] at 200–300°C in a nonsealed system. Additional annealing lead to films with high luminance and luminous efficiency (2000), while copper-doped CdS has been prepared from [$Cd(S_2CNEt_2)_2$.CuI] (1768).

ii. Rubber Vulcanization. Zinc bis(dimethyldithiocarbamate), [$Zn(S_2CNMe_2)_2$] (Ziram), is a well-known accelerator, for the vulcanization of rubber. The process involves heating a mixture of sulfur, accelerator, and an unsaturated polymer, and results in the formation of sulfur bridges or cross-links between the individual polymer molecules, which give the rubber elasticity and durability (2001) (Fig. 278).

While [$Zn(S_2CNMe_2)_2$] has been shown to be a better accelerator than other dithiocarbamate complexes (2002), its role has not been fully understood. Traditionally, it has been thought to involve the formation of a polythiocarbamato intermediate, formed upon sulfur insertion into a zinc–sulfur bond, which in turn reacts with the rubber in a concerted fashion (Fig. 279). Over the past

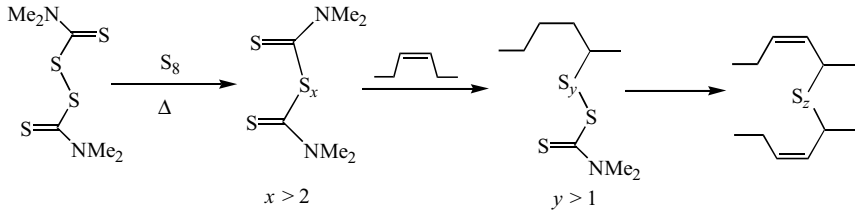

Figure 278. Process by which rubber is vulcanized.

10 years, work primarily by Reedijk and co-workers (2003–2007), McGill and co-workers (2008, 2009) along with others (2010, 2011) has served to shed light on the role of $[Zn(S_2CNMe_2)_2]$ in the vulcanization process, the main results of which are summarized in a recent review (2012).

The key first step appears to be the insertion of sulfur into one or more of the zinc–sulfur bonds of $[Zn(S_2CNMe_2)_2]$. However, while related zinc thiolate complexes, which are also accelerators, undergo this reaction to give crystallographically characterized trithiolate complexes (2013, 2014), no such stable analogues have been found for dithiocarbamates, and indeed well characterized monodentate trithiocarbamate ligands are unknown.

Reedijk and co-workers (2004) used the combined approach of density functional calculations and the matrix-assisted laser-desorption ionization (MALDI) MS approach in order to probe this important first step. The calculations suggested that the hypothetical sulfur-rich trithiocarbamate complex **507** was only some 59 kJ mol^{-1} higher in energy than trithiolate–zinc

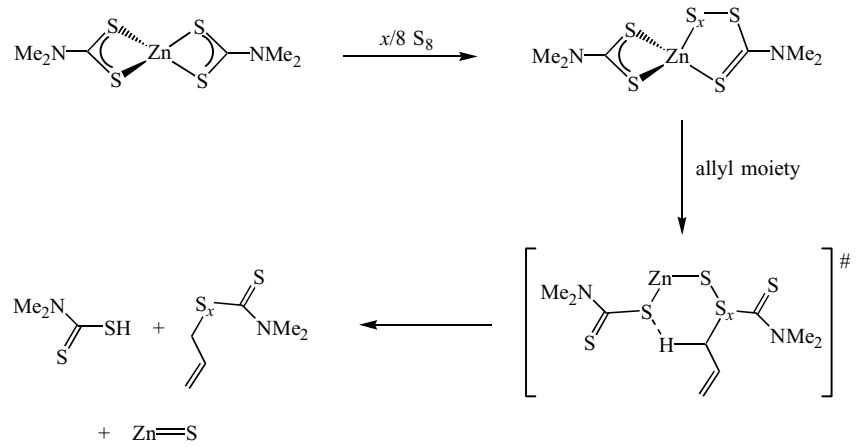

Figure 279. Proposed mode of action of $[Zn(S_2CNMe_2)_2]$ in rubber vulcanization.

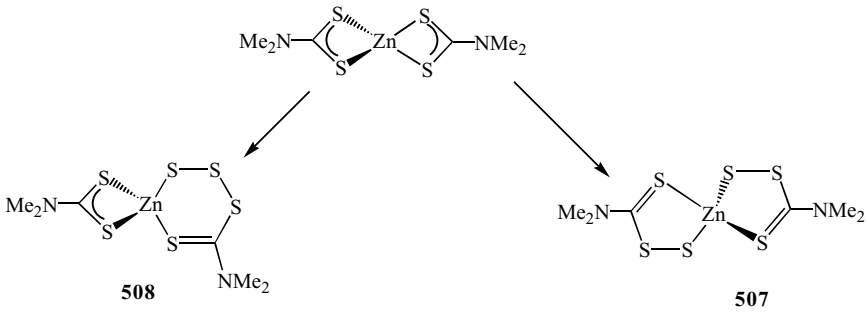

Figure 280. Possible routes for the insertion of sulfur into $[Zn(S_2CNMe_2)_2]$.

complexes, while somewhat surprisingly, the insertion of two sulfur atoms into a single zinc–sulfur bond to give **508** was more stable than **507** by 10 kJ mol^{-1} (Fig. 280). However, the key point is that given that vulcanization experiments are carried out at high temperatures (~140°C), then these relatively small differences suggest that sulfur-insertion should be accessible, although the products are presumably too reactive for isolation. The MS results provided further evidence for the generation of sulfur-inserted products, MALDI experiments with $[Zn(S_2CNMe_2)_2]$ and S_8 indicate the generation of polythiocarbamate species with up to eight inserted sulfur atoms.

Other work by this group has revealed that $[Zn(S_2CNMe_2)_2]$ homogeneously catalyzes a number of essential vulcanization reactions, including (1) the formation of trisulfidic cross-links—involving insertion of sulfur into the allylic carbon–hydrogen bonds via an ene-like reaction and generating a rubber-bound polythiothiol, (2) the equilibrated metathesis reaction of the resulting polythiothiols to give the initial sulfur cross-links, and (3) the desulfhydration of the polythiols producing sulfides and H_2S (2005). On the basis of this work, a catalytic cycle for the formation of cross-links and catalyst degradation has been proposed (Fig. 281).

In other work, McGill and co-workers (2008) investigated the effect of water and H_2S on the decomposition of $[Zn(S_2CNMe_2)_2]$ to give HS_2CNMe_2. The latter acts as a vulcanization accelerator in its own right in the absence of ZnO, while Rodríguez and Hummel (2011) provide evidence for ionic components in the vulcanization process by means of electric current measurements. Debnath and Basu (2010) investigated the role of zinc bis(dithiocarbamate) complexes in the presence of thiazole-based accelerators, and find the highest activity in the $[Zn(S_2CNBz_2)_2]$ and dibenzothiazyldisulfide accelerated system.

In further work relating to the role of $[Zn(S_2CNMe_2)_2]$ in the vulcanization process, Reedijk and co-workers (2006) reinvestigated the reaction of $[Zn(S_2CNMe_2)_2]$ with amines. With $CyNH_2$, 1,1,3-trisubstituted and 1,3-disubstituted thioureas are formed along with dimethylammonium dithiocarbamate, ZnS,

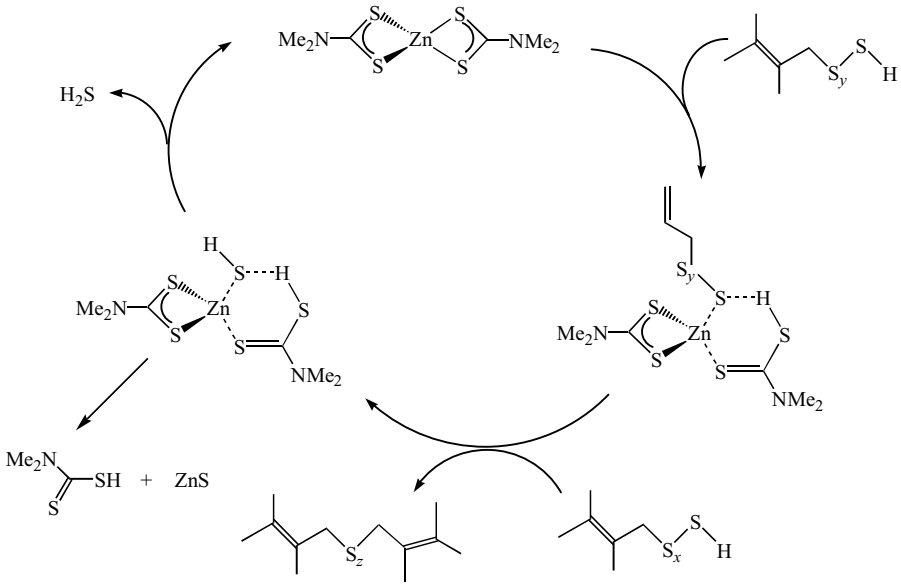

Figure 281. Proposed catalytic cycle for the vulcanization of rubber using $[Zn(S_2CNMe_2)_2]$.

and H_2S. A scheme is proposed in which an adduct is in equilibrium with an activated complex formed upon nucleophilic attack of the amine at the backbone carbon.

iii. Toxicological Studies. As previously detailed, $[Zn(S_2CNMe_2)_2]$ is used extensively in agriculture as a fungicide under the name ''Ziram'', and also as an accelerator for rubber vulcanization. In light of this finding, a number of toxicological studies have been carried out. Ziram has been shown to be extremely toxic to fish, chicken, or rat embryos (2015–2017). Further, resulting from its use as a vulcanization accelerator, it can also be present in domestic rubber goods such as gloves, clothing, and contraceptive sheaths, which has lead to a number of reports of contact dermatitis (2018, 2019).

The polymer ethylenebis(dithiocarbamate) zinc (Zineb) is used as a fungicide to protect fruit and vegetable crops from a wide range of foliar and other diseases (2020). Larramendy and co-workers (2021, 2022) carried out genotoxic evaluation on Chinese hamster ovary cells, and finds that even though it induces large DNA alterations *in vitro*, this does not necessarily mean that this compound should be considered clastogenic.

Sodium diethyldithiocarbamate (Imuthiol) has been shown to restore and regulate the number and activities of T-cells, and since zinc is essential for the formation of the immune system, a combination of them might be expected to have beneficial effcets. In this light, $[Zn(S_2CNEt_2)_2]$ has been tested, but was

found to be devoid of an immuno-enhancing influence on the responses to T-cell mitogens, and exerted a cytocidal effect on spleen lymphocytes (2023).

Diethyldithiocarbamate has been suggested to be an efficient chelator for acute cadmium intoxication, as its parenteral administration decreased mortality induced by parenteral cadmium, even at a protracted time after cadmium administration (2024, 2025). However, diethyldithiocarbamate was also found to enhance the brain deposition of injected (2026, 2027) or orally administered (2028) cadmium. Thus it is unsuitable for use as an antidote to acute cadmium intoxication. In search for an alternative, the groups of Jones and co-workers studied a wide range of dithiocarbamates for the *in vivo* mobilization of cadmium. This work showed a rapid reduction in liver cadmium levels after injection with water-soluble dithiocarbamate salts, with the anions gaining rapid access to intracellular hepatic sites (2027, 2029–2036). A large number have been tested, those derived from 4-carboxamidopiperidene-1-carbodithioate (**509**) (1846) and D-glucamine derivatives (**510**–**511**) (Fig. 282) (2030, 2036) have a good efficacy as an antidote for acute cadmium poisoning.

iv. Analytical Chemistry. Due to the agricultural importance of $[Zn(S_2CNMe_2)_2]$ (Ziram), a spectrophotometric determination has been reported (2037), as has a capillary electrophoretic separation and determination of Ziram and Zineb (2038), together with other analytical determinations (222, 2039).

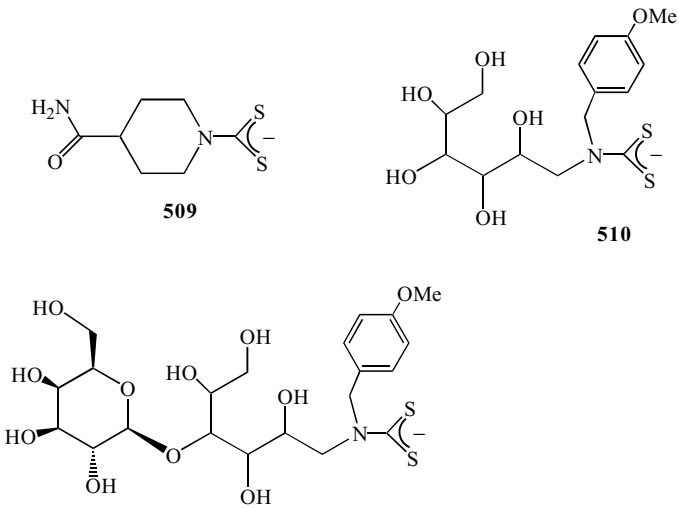

Figure 282. Water-soluble dithiocarbamate salts developed by Jones and co-workers (2027, 2029–2036) as possible antidotes for acute cadmium poisoning.

A simple and highly sensitive determination of palladium has also been developed based on the reaction between palladium(II) salts and [Zn(S_2CNBz_2)$_2$] in aqueous solution, although many other metal(II) salts interfere strongly (2040). Related to this, zinc silicate-bonded diethyldithiocarbamate has been prepared and utilized in the separation and preconcentration of some transition metal ions. This material shows a high selectivity for palladium(II) (2041), while the on-line mixing of industrial effluents with a buffered solution of water soluble [Zn{$S_2CN(CH_2CH_2OH)_2$}$_2$] leads to the formation of copper, cobalt, nickel, and cadmium complexes that can be monitored electrochemically (2042).

Mercury is a highly toxic element and its removal and analytical detection are important. Dithiocarbamate-incorporated monosized polystyrene-based microspheres (2 μm) have been prepared (2043) and used for the selective removal of mercury(II) from aqueous solutions. The absorption ability increases with pH (2044). Related to this, dithiocarbamate grafted onto dried silica gel have been shown to be highly effective for the removal of mercury from waste solutions containing various complexing agents (145).

An HPLC detection of $PhHgNO_3$ utilizes its reaction with NaS_2CNEt_2 in the presence of EDTA to generate diphenylmercury and [Hg(S_2CNEt_2)$_2$] (2045). A similar HPLC assay has been developed for Thimerosal, which acts as a topical antiseptic and antimicrobial preservative. It consists of reacting Thimerosal, [EtHg(1,2-$SC_6H_4CO_2$)]$^-$, with morpholine or piperidene dithiocarbamate to generate the neutral alkyl mercury complexes [EtHg($S_2CNC_4H_8X$)]$_2$ (X = O, CH_2) (2046).

v. Other Applications. In other potential applications, zinc bis(diamyldithiocarbamate) has been shown to be a better antioxidant for motor oils than zinc dithiophosphates (2047), and other bis(dithiocarbamate) complexes have been shown to have liquid-crystal properties (1485).

V. NONINNOCENT BEHAVIOR

Section IV emphasized the extraordinary versatility of dithiocarbamates to act as simple spectator ligands, and in the thousands of reports concerning them, this is by far their major role. However, in 1973 Ricard et al. (954, 955) showed the complex formed from the reaction of [Mo_2(μ-OAc)$_4$] and 4 equiv of NaS_2CNPr_2, while analyzing as [Mo_2(S_2CNPr_2)$_4$], was in fact the molybdenum(IV) dimer [Mo(μ-S)(S_2CNPr_2)(η^2-$SCNPr_2$)]$_2$ (Eq. 181). This complex clearly results from the cleavage of a carbon–sulfur bond, generating sulfido and thiocarboxamide ligands; a process that can be viewed as an

oxidative–addition, the oxidation state at molybdenum going from +2 to +4.

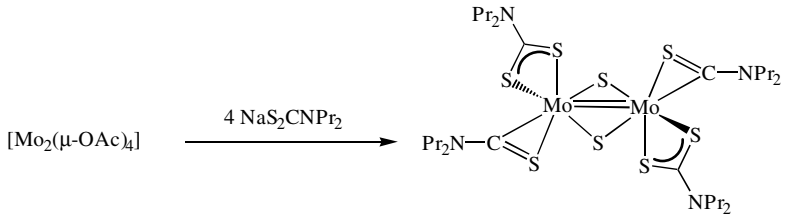

(181)

In the intervening 30 years, the noninnocent behavior of dithiocarbamates, while still remaining relatively rare, has become far more prevalent. A number of different types of noninnocent behavior have been found, although categorization in some instances is not simple. Further, the sulfur–carbon bond cleavage of dithiocarbamates has been widely utilized in the preparation of a wide range of metal sulfides from relatively volatile dithiocarbamate precursor complexes (see Sections IV.H.1.g.ii and IV.I.1.h.i), and the cleavage of carbon–sulfur bonds in dithiocarbamates appears to be far more prevalent than in related xanthate ligands (2048).

In the discussion below, a number of different types of noninnocent behavior have been identified and will be discussed within the following categories:

1. Sulfur–carbon bond cleavage to generate sulfido and thiocarboxamide ligands.
2. Double sulfur–carbon bond cleavage reactions.
3. Sulfur–carbon bond cleavage followed by addition of/to other constituents of the complex.
4. Addition of dithiocarbamates to unsaturated organic ligands.
5. Insertion of unsaturated moieties into metal–sulfur bond(s) of dithiocarbamates.

A. Cleavage of a Single Sulfur–Carbon Bond

As alluded to above, the oxidative–addition of a single sulfur–carbon bond can result in the formation of sulfido and thiocarboxamide ligands (Eq. 182).

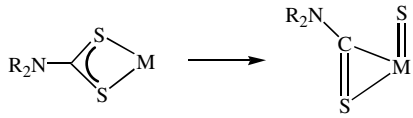

(182)

Since first being discovered in the early 1970s, it has become a relatively common transformation. For example, addition of 3 equiv of NaS_2CNEt_2 to the tetrahydrothiophene complexes $[M_2Cl_4L_2(\mu\text{-}Cl)(\mu\text{-tht})]$ (M = Nb, Ta) affords $[MS(S_2CNEt_2)_2(SCNEt_2)]$ in moderate yields (2049). Although the precise reaction mechanism is unknown, the authors propose the initial formation of dimeric metal(III) species with bridging dithiocarbamate ligands, which later undergo oxidative–addition (Eq. 183).

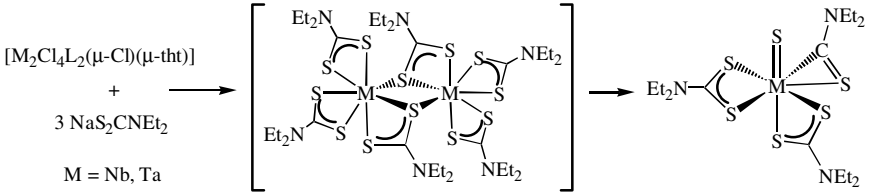

(183)

Templeton and co-workers (2050) reported that upon heating molybdenum(II) bis(alkyne) complexes, $[Mo(alkyne)_2(S_2CNR_2)_2]$ (R = Me, Et), with PEt_3, dimeric molybdenum(III) complexes carrying a thiocarboxamide ligand are generated (Eq. 184); the complex $[Mo_2(S_2CNMe_2)_3(\eta^2\text{-}SCNMe_2)(\mu\text{-}S)(\mu\text{-}Et\text{-}C_2Et)]$ is crystallographically characterized. The reaction can be considered to result from loss of alkyne, followed by oxidative–addition of the carbon–sulfur bond, with the molybdenum(IV) sulfido–thiocarboxamide complex generated reacting with a further equivalent of molybdenum(II) alkyne complex.

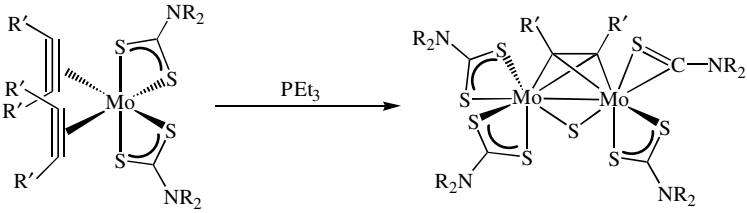

(184)

In a somewhat similar fashion, Jeffery and Went (2051, 2052) have reported that addition of $[Co_2(CO)_8]$ to tungsten(II) alkyne complexes, $[W(CO)(R^1C_2R^2)(S_2CNR_2)_2]$ (R = Me, Et; $R^1 = R^2 = H$, Me, Ph; $R^1 = H$, $R^2 = Ph$) (**512**), yields $[WCo_2(CO)_5(\mu^3\text{-}S)(\mu\text{-}R^1C_2R^2)(\eta^2\text{-}SCNR_2)(S_2CNR_2)]$ (**513**) as a result of sulfur–carbon bond cleavage. Here, the tungsten(IV) center generated as a result is "trapped" by the cobalt carbonyl, and the sulfido ligand ends up in a capping mode. These clusters undergo phosphine substitution and also lose carbon monoxide to give $[WCo_2(CO)_4(\mu^3\text{-}S)(R^1C_2R^2)(\mu^3\text{-}SCNR_2)(S_2CNR_2)]$ (**514**), a transformation that involves exchange of alkyne and thiocarboxamide ligands between bridging and terminal coordination modes (Fig. 283).

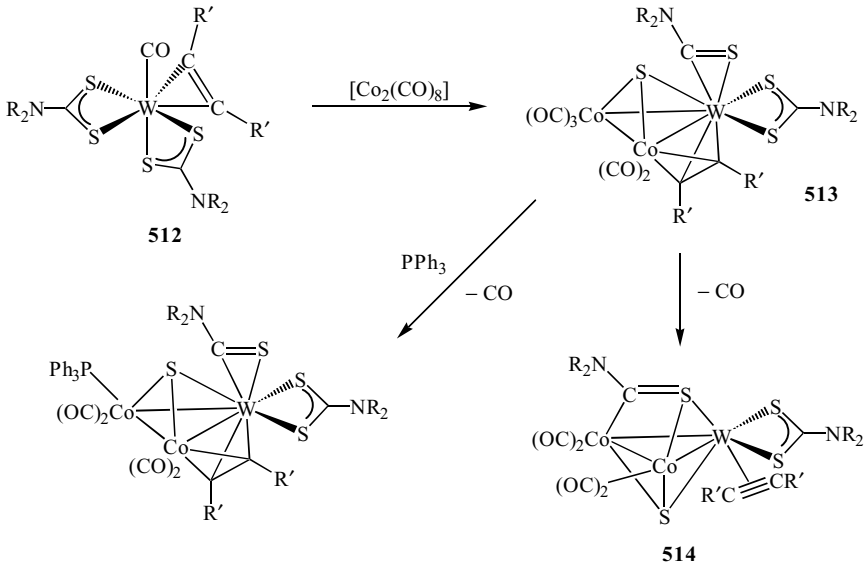

Figure 283. Synthesis and later reactions of $[WCo_2(CO)_5(\mu^3\text{-}S)(\mu\text{-}R'C_2R')(\eta^2\text{-}SCNR)(S_2CNR_2)]$.

Addition of cyclohexene sulfide to $[W(CO)(PhC_2Ph)(S_2CNR_2)_2]$ (R = Et, Me) (**515**) results in oxidation giving two tungsten(IV) sulfides, $[WS(PhC_2Ph)(S_2CNR_2)_2]$ and $[WS(PhC_2Ph)(S_2CNR_2)(SCNR_2)]$ (**516**) (Fig. 284) (1083). The latter is a thiocarboxamide complex that results from carbon–sulfur bond cleavage. It can also be made by addition of PEt_3 to $[WS(PhC_2Ph)(S_2CNR_2)_2]$ (**517**), suggesting that the unsaturated tungsten(II) species $[W(PhC_2Ph)(S_2CNR_2)_2]$ is the key intermediate (1084). This supposition is confirmed with the slow addition of PEt_3 to $[WS(PhC_2Ph)(S_2CNMe_2)_2]$ in the presence of *trans*-dicyanoethylene, which affords the alkene complex $[W(NCHC{=}CHCN)(PhC_2Ph)(S_2CNMe_2)_2]$ (1084).

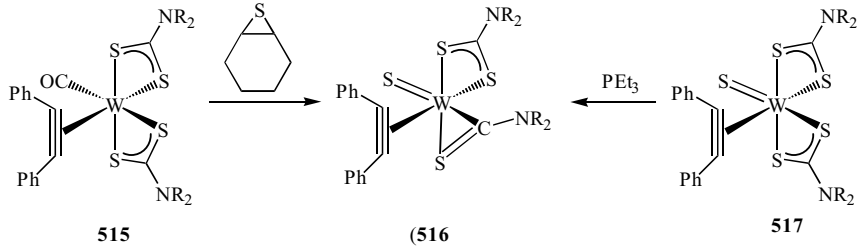

Figure 284. Synthetic pathways to $[WS(PhC_2Ph)(S_2CNR_2)(SCNR)]$.

Reactions of thiuram disulfides with $[Tp^*W(CO)_3]^-$ generate tetrasulfide complexes $[WS(\mu\text{-}S)(S_2CNR_2)]_2$ and in one case the intermediate $[Tp^*W(CO)_2(\mu\text{-}S)(S_2CNEt_2)_2(SCNEt_2)]$ (**518**), has been isolated. It is shown by a partial crystal structure to be a mixed-valence tungsten(II)–tungsten(IV) complex, resulting from a sulfur–carbon bond cleavage process together with the displacement of a tris(pyrazolyl)borate ligand (182).

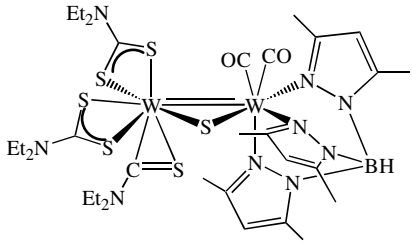

518

In the examples given above, the oxidative–addition of a single carbon–sulfur bond results in the generation of products containing both the thiocarboxamide and sulfido groups. However, in a number of instances the cleavage of a single carbon–sulfur bond can only be inferred from the isolation of *either* a thiocarboxamide or sulfido-containing product. For example, dithiocarbamate degradation occurs upon thermolysis of *trans*-$[ReCl_3(MeCN)(PPh_3)_2]$ (**519**) with a large excess of NaS_2CNEt_2 in acetone. The major product is $[Re(\eta^2\text{-}SCNEt_2)(S_2CNEt_2)_2(PPh_3)]$ (**520**) (Fig. 285). The fate of the sulfur atom remains unknown. This thiocarboxamide complex is readily oxidized to the rhenium(IV) complex $[Re(\eta^2\text{-}SCNEt_2)(S_2CNEt_2)_2(PPh_3)]^+$ (**521**) (Fig. 285), a process that is fully reversible. The perchlorate salt has been crystallographically characterized and shows a distorted pentagonal bipyramidal coordination geometry, with the phosphine occupying an axial site and the thiocarboxamide ligand lying in the equatorial plane (2053). Infrared characterization also proves useful; the $\nu(C{=}N)$ vibrations of the dithiocarbamates appears at 1570 cm^{-1}, while the thiocarboxamide is observed at 1510 cm^{-1}.

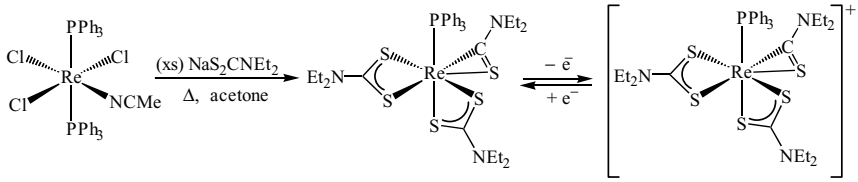

519 **520** **521**

Figure 285. Synthesis and redox chemistry to $[Re(\eta^2\text{-}CNEt_2)(S_2CNEt_2)_2(PPh_3)]$.

Pignolet and co-workers initially reported that photolysis of $[Ru(S_2CNR_2)_3]$ (R = Me, Et) in chloroform gave ruthenium(IV) complexes, $[RuCl(S_2CNR_2)_3]$ (1339), however, interestingly when the photolysis of $[Ru(S_2CNMe_2)_3]$ was carried out at 366 nm in the presence of a large excess of benzophenone, the thiocarboxamide complex $[RuCl(S_2CNMe_2)_2(\eta^2\text{-}SCNMe_2)]$ was formed in >90% yield (Eq. 185) (2054). A crystallographic study shows that all six methyl groups are inequivalent, which is confirmed by ^1H NMR at −40°C. At higher temperatures, however, spectral changes occur that are associated with restricted rotation about the carbon–nitrogen bonds.

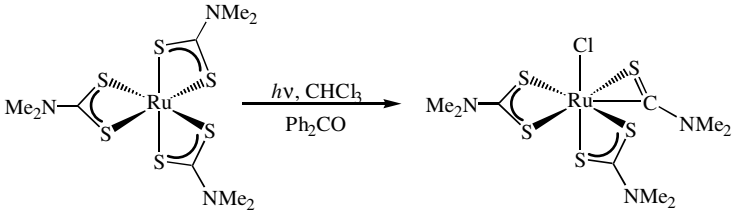

(185)

Abrahamson et al. 1066 reported that oxidation of $[CpW(CO)_3(\eta^1\text{-}S_2CNMe_2)]$ by iodine affords a mixture of two tungsten(IV) complexes, $[CpWI(CO)_2(S_2CNMe_2)]I$ and $[CpWI_2(\eta^2\text{-}SCNMe_2)]$ (Eq. 186), the latter resulting from sulfur extrusion. Some insight into the process is afforded with the identification of carbonylsulfide (COS) in the gas above the reaction, suggesting that the initially formed sulfido group may have later reacted with metal-bound carbon monoxide.

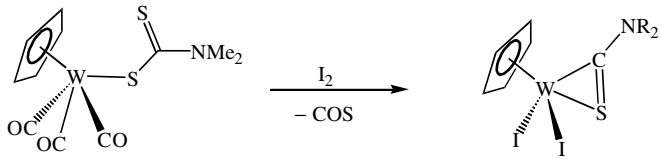

(186)

More commonly, it is the thiocarboxamide group that is lost, with only the sulfido ligand retained. In such instances, it is more debatable that the transformation occurring is a single carbon–sulfur bond cleavage, but this is often assumed. Thus, Cotton and co-workers (265) reported that reaction of tetraethylthiuram disulfide with $[W(CO)_3(MeCN)_3]$ in acetonitrile affords the green tungsten(IV) dimer, $[W(\mu\text{-}S)(\mu\text{-}S_2CNEt_2)(S_2CNEt_2)]_2$ (**522**). The metal–metal vector of 2.530(2) Å probably represents a tungsten–tungsten double bond. When the reaction is carried out in methanol a second species results, namely the tungsten(V) dimer $[W(\mu\text{-}S)(OMe)_2(S_2CNEt_2)]_2$ (**523**). Both

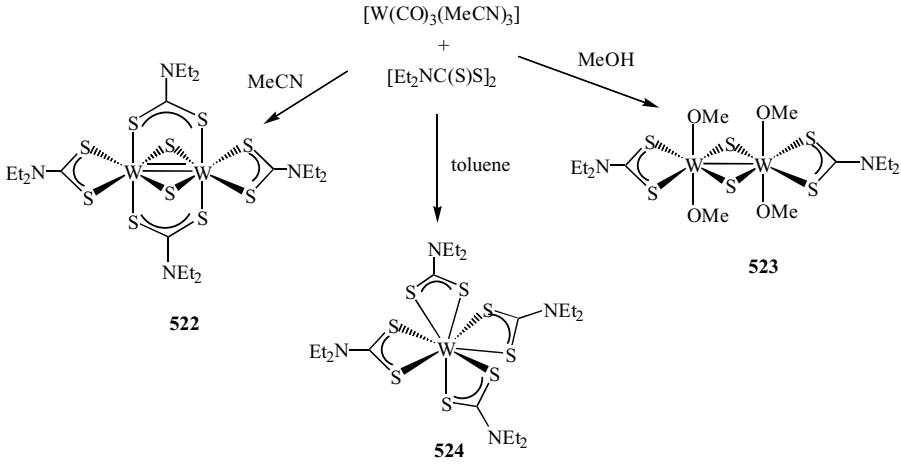

Figure 286. Products of the reaction of $[W(CO)_3(MeCN)_3]$ with tetraethylthiuram disulfide.

complexes appear to result from carbon–sulfur bond cleavage reactions, however, interestingly when the reaction is carried out in toluene at elevated temperatures only sulfur–sulfur cleavage is seen, affording mononuclear $[W(S_2CNEt_2)_4]$ (**524**) (Fig. 286).

Somewhat similarly, addition of 5 equiv of NaS_2CNEt_2 to $NbCl_5$ yields $[NbS(S_2CNEt_2)_3]$, while with $TaCl_5$ both yellow $[TaS(S_2CNEt_2)_3]$ and green $[TaS_2(S_2CNEt_2)_3]$ result (Eq. 187) (403). The latter may be the result of a double sulfur–carbon bond cleavage process (see below), however, it is known that the monosulfides $[MS(S_2CNEt_2)_3]$ (M = Ta, Nb) react with a range of sulfur sources to give the analogous disulfides, and this secondary reaction may be taking place here.

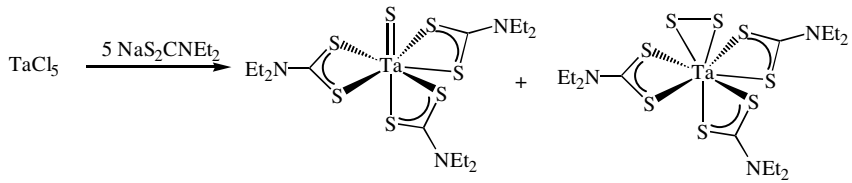

(187)

Very recently, Seymore and Brown (873) reported that one of the products of the reaction of $[TpOsNCl_2]$ with $[MoN(S_2CNEt_2)_3]$ is the thionitrosyl complex $[TpOs(NS)Cl_2]$ (Eq. 188); presumably formed from dithiocarbamate cleavage,

followed by addition of the sulfido group to nitrogen.

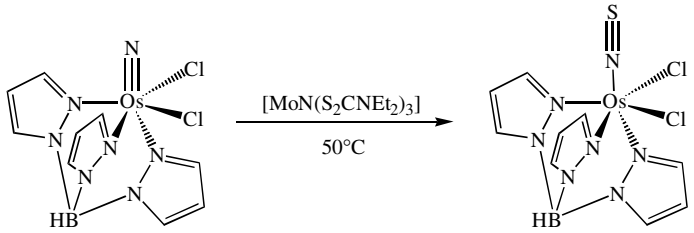

(188)

The related molybdenum thionitrosyl complex $[Mo(NS)(S_2CNEt_2)_3]$ has also been prepared in low yield as a result of a dithiocarbamate fragmentation process, after reaction of $[Mo(N\text{-}p\text{-}tol)_2Cl_2(dme)]$ with 2 equiv of $NH_4S_2CNEt_2$ (442). The precise nature of this process remains unknown, but the thionitrosyl ligand formally results from extrusion of the backbone carbon atom.

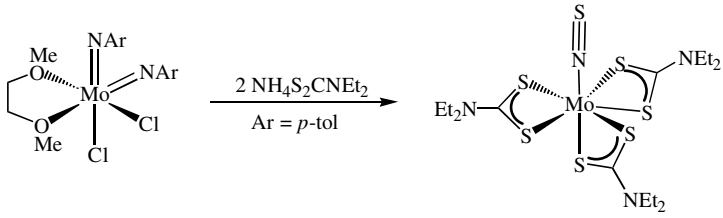

(189)

In another unusual transformation, a thiocarbonyl ligand is generated. Thus, heating $[ReCl_3(PPhMe_2)_3]$ with 5 equiv of dithiocarbamate salt in ethanol for 12 h gives $[Re(CS)(S_2CNEt_2)_3]$ (Eq. 190). The thiocarbonyl ligand clearly results from dithiocarbamate degradation, and interestingly the same reaction does not occur in acetone (456). The precise mode of formation remains unknown, but the thiocarbonyl is formally derived from cleavage of both a sulfur–carbon and nitrogen–carbon bond of the dithiocarbamate ligand.

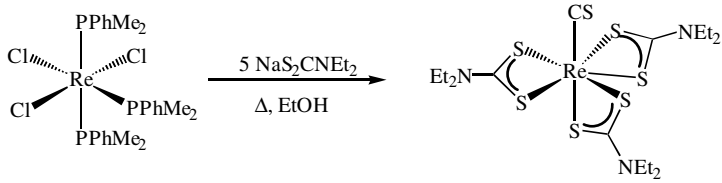

(190)

It is well known that reactions of $[Co(S_2CNR_2)_3]$ with chemical oxidants gives rise to a range of products. These products are dependent on the nature of the oxidant. An ESMS study of the products generated upon oxidation by

$NOBF_4$ revealed ions associated with the species $[Co_2(S_2CNR_2)_5S]^+$ and $[Co_2(S_2CNR_2)_5S_2]^+$. Neither the nature of sulfur coordination nor its source is known, although the authors suggest that the latter is the result of oxidation of thiuram disulfide (generated by dithiocarbamate oxidation) by NO^+ (303).

Facile sulfur–carbon cleavage of a dithiocarbamate at ruthenium(II) and osmium(II) centers is also implicated in the synthesis of thiophenylazopyridine complexes (**526**) from the analogous 2-chlorophenylazopyridine complexes (**525**) upon addition of NaS_2CNEt_2 in DMF (Eq. 191) (2055). An analogous transformation also occurs at the cobalt(III) center.

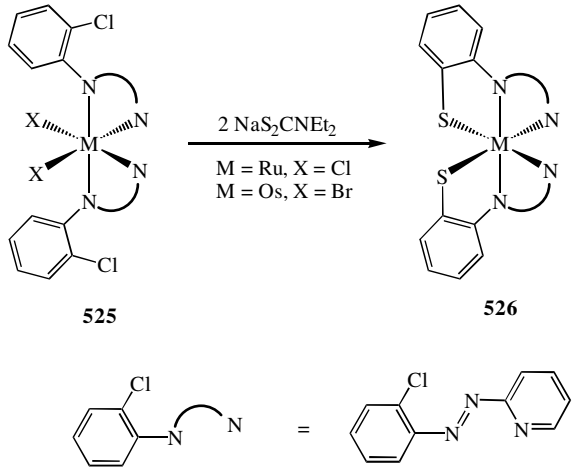

(191)

B. Double Sulfur–Carbon Bond Cleavage

The cleavage of both sulfur–carbon bonds of the dithiocarbamate ligand should in theory be a four-electron process, resulting in the formation of two sulfido groups and a single aminocarbyne ligand, although the resulting sulfido groups may further couple to give a disulfide ligand (Eq. 192).

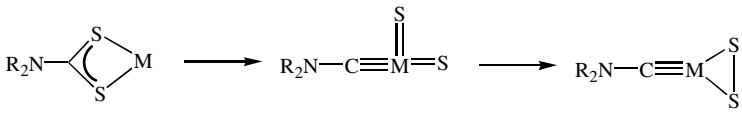

(192)

Given the oxidative nature of the process, it may be expected to occur primarily at low-valent centers. Over the past 10 years, a number of instances whereby this process has been shown or implied to occur have been reported. For example, heating *cis*-$[Ru(CO)_2(S_2CNEt_2)_2]$ with an excess of $[Ru_3(CO)_{12}]$ at 130°C

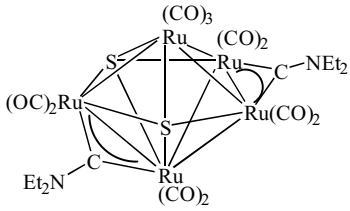

527

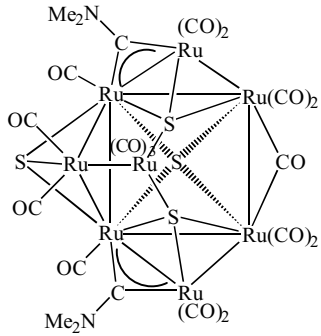

528

Figure 287. Products of the thermolysis of $[Ru(CO)_2(S_2CNR_2)_2]$ with $Ru_3(CO)_{12}$.

yields the novel pentanuclear cluster $[Ru_5(\mu^4\text{-}S)_2(\mu\text{-}CNEt_2)_2(CO)_{11}]$ (**527**), resulting from a double sulfur–carbon bond cleavage of the dithiocarbamates (1359). Further, with *cis*-$[Ru(CO)_2(S_2CNMe_2)_2]$, octanuclear $[Ru_8(\mu^4\text{-}S)_3(\mu^3\text{-}S)(\mu\text{-}CNMe_2)_2(CO)_{16}]$ (**528**) (Fig. 287) is the major product (169).

Precise details concerning the nature of these transformations remain unclear, however, they may well proceed via initial decarbonylation and formation of $[Ru(CO)(S_2CNR_2)(\mu\text{-}S_2CNR_2)]_2$. Further, conversion of the pentanuclear to the octanuclear cluster formally involves addition of "$Ru_3S_2(CO)_5$", and may arise via addition of $[Ru_3(\mu^3\text{-}S)_2(CO)_9]$, which is known to facilitate cluster expansion reactions. In support of both hypotheses, *cis*-$[Ru(CO)(PEt_3)(S_2CNEt_2)_2]$ reacts only slowly with $[Ru_3(CO)_{12}]$ giving $[Ru_3(\mu^3\text{-}S)_2(CO)_8(PEt_3)]$ as the major product (Eq. 193).

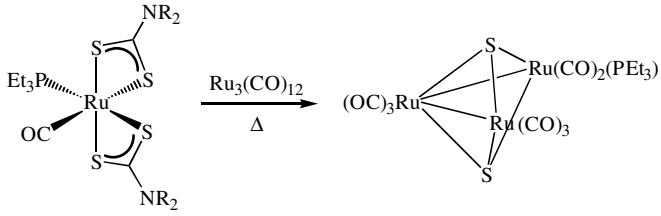

(193)

A recent related report shows that the reaction of $CoCl_2$, PPh_3, and NaS_2CNEt_2 in acetonitrile in the presence of zinc yields the trinuclear cluster $[Co_3Cl(PPh_3)_2(\mu^3\text{-}S)(\mu\text{-}CNEt_2)(\mu\text{-}SCNEt_2)_2]$ (Eq. 194). This complex formally results from one double, and two single, carbon–sulfur bond

cleavage processes (2056).

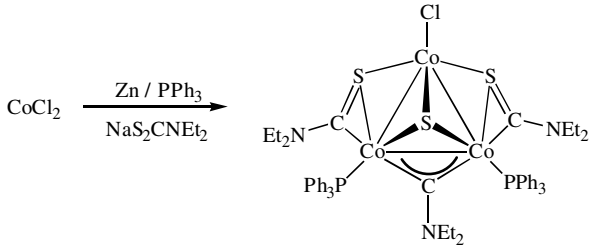

(194)

Lappert and co-workers (1074) showed that heating the tungsten(II) complex $[W(CO)_2(SnR_2)(S_2CNMe_2)_2]$ $[R = CH(SiMe_3)_2]$ (**529**) in benzene affords the mixed-valence tungsten(V)–tungsten(III) complex, $[W_2S(\mu\text{-}S)(\mu\text{-}Me_2NC{=}CNMe_2)(\eta^2\text{-}SCNMe_2)(\eta^2\text{-}S_2SnR_2)(S_2CNMe_2)]$ (**530**) (Fig. 288), bearing sulfido, thiocarboxamide, and bis(amino)alkyne ligands. The latter is unusual and presumably derives from the coupling of two aminocarbyne fragments, themselves generated upon a double sulfur–carbon bond cleavage process. Thus, the molecule contains the elements of both single- and double-bond cleavage events, while two of the sulfido groups have inserted into the stannylene. Interestingly, heating the corresponding diethyldithiocarbamate complex yields a blue diamagnetic product, $[W_2(\mu\text{-}S)(\mu\text{-}CNEt_2)(\mu\text{-}SSnR_2S)(S_2CNEt_2)_2]$ (**531**) (Fig. 288) (1075). Here again a double cleavage has occurred and two sulfido ligands have coupled with the stannylene, but now aminocarbyne coupling has not occurred.

While all of the transformations detailed above take place at low-valent metal centers, a double sulfur–carbon bond cleavage process has also been postulated to occur at the molybdenum(VI) center (527, 528, 839). Thus, thermolysis of organic isocyanates with $[MoO_2(S_2CNR_2)_2]$ affords imido–disulfide complexes, $[Mo(NR')(S_2)(S_2CNR_2)_2]$ (Fig. 289), in moderate yields. The fate of the aminocarbyne fragment remains unknown and further, since monosulfido

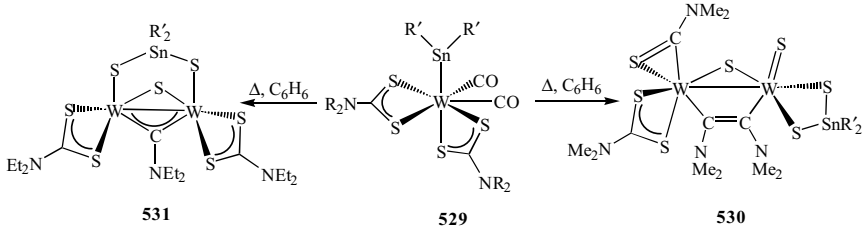

531 **529** **530**

Figure 288. Unusual dimeric products formed upon heating $[W(CO)_2(SnR'_2)(S_2CNR_2)_2]$.

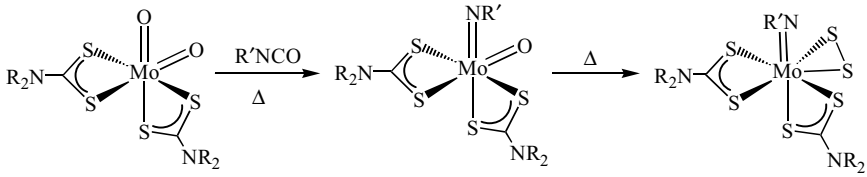

Figure 289. Formation of $[Mo(NR')(S_2)(S_2CNR_2)_2]$ upon thermolysis of $[MoO_2(S_2CNR_2)_2]$ and organic isocyanates.

complexes, $[MoS(NR')(S_2CNR_2)_2]$, also remain unknown, it is not clear that the process is necessarily a double sulfur–carbon bond cleavage process. The transformation is clearly not an oxidative–addition as the oxidation state of the metal remains unchanged throughout, however, some redox chemistry does take place. Other products are molybdenum(V) dimers and thiuram disulfides. Work designed to probe the nature of the transformation suggests that it is the oxo–imido species $[MoO(NR')(S_2CNR_2)_2]$, which are thermally unstable, as the analogous bis(imido) complexes $[Mo(NR')_2(S_2CNR_2)_2]$ show good stability at high temperatures.

Three recent publications by Goh et al. (240, 246, 247) concerning the behavior of dithiocarbamate ligands at chromium(II) cyclopentadienyl centers have shed considerable light of the carbon–sulfur bond scission process. When $[CpCr(CO)_3]_2$ and thiuram disulfides (R = Me, Et, *i*-Pr) are heated at 90°C, a number of products are also isolated, including $[Cp_6Cr_8S_8\{\eta^2{:}\eta^4\text{-}S_2(CNR_2)_2\}]$ (**532**), $[Cp_6Cr_8S_8(\eta^1{:}\eta^2\text{-}S_2CNR_2)_2]$ (**533**) (Fig. 290), $[Cr(S_2CNR_2)_3]$, $[Cp_2Cr_2(CO)_4(\mu\text{-}S)]$, and $[CpCr(\mu^3\text{-}S)]_4$. Some of these are the result of carbon–sulfur bond scission. Both octanuclear complexes contain two Cr_4S_4 cubane cores linked through the non-cyclopentadienyl complexed metal centers. In **533**, two

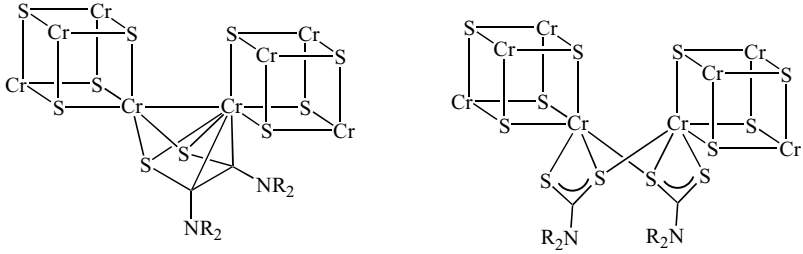

532 **533**

Figure 290. Cluster cores of fused cubane clusters formed upon thermolysis of $[CpCr(CO)_3]$ and thiuram disulfides.

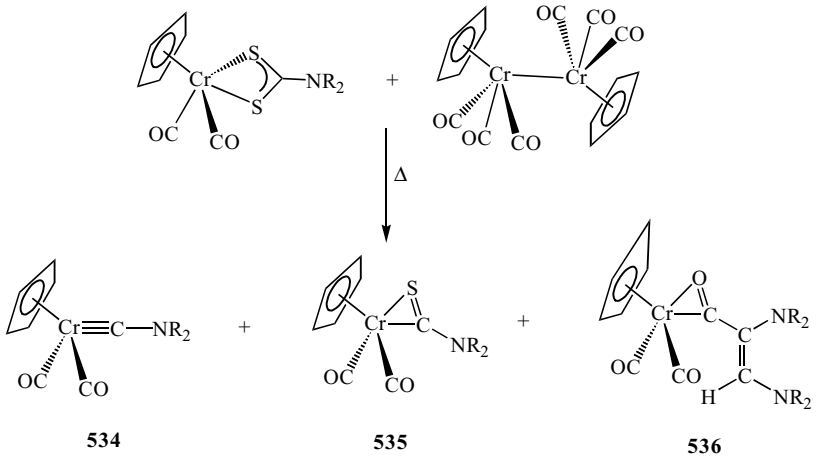

Figure 291. Mononuclear dithiocarbamate scission products of the reaction of $[CPCr(CO)_2(S_2CNR_2)]$ and $[CpCr(CO)_3]_2$.

dithiocarbamates bridge these chromium centers, while in **532** a new ligand formed from fusion of two thiocarboxamide ligands, acts as the bridge (240).

Further insight is gained into the dithiocarbamate scission process when $[CpCr(CO)_2(S_2CNR_2)]$ is heated with more $[CpCr(CO)_3]_2$. A number of products are obtained including **532**, and importantly, mononuclear thiocarboxamide $[CpCr(CO)_2(\eta^2\text{-}SCNR_2)]$ (**534**), aminocarbyne $[CpCr(CO)_2(CNR_2)]$ (**535**), and vinylacyl $[CpCr(CO)_2\{\eta^2\text{-}O{=}C\text{-}C(NR_2){=}CH(NR_2)\}]$ (**536**) complexes (Fig. 291) (247). The thiocarboxamide ligand is the product of a single sulfur–carbon bond scission of the dithiocarbamate, while the others result from a double-bond cleavage.

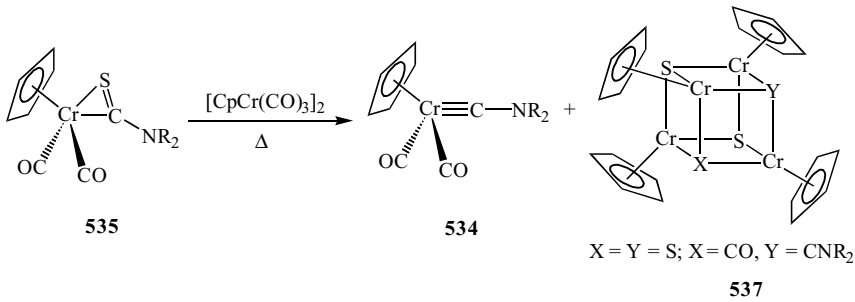

Figure 292. Products of the thermolysis of $[CpCr(CO)_2(SCNR_2)]$ with $[CpCr(CO)_3]_2$.

Perhaps most significantly, heating **535** with further $[CpCr(CO)_3]_2$ affords the aminocarbyne complex **534** together with the cubanes, $[CpCr(\mu^3\text{-}S)]_4$ and $[Cp_4Cr_4(\mu^3\text{-}S)_2(\mu^3\text{-}CO)(\mu^3\text{-}CNR_2)]$ (**537**), providing further evidence that the scission process occurs in a step-wise fashion (Fig. 292).

Heating $[CpCr(CO)_3]_2$ with $[Cr(S_2CNR_2)_3]$ also results in formation of aminocarbyne (**534**) and thiocarboxamide (**535**) complexes, leading the authors to conclude that it is the 17-electron organometallic radical $[CpCr(CO)_3]^{\cdot}$, that initiates the sulfur–carbon bond scission chemistry.

C. Sulfur–Carbon Bond Cleavage Followed by Addition of/to Other Constituents of the Complex

Two groups have reported novel products from the reaction of molybdenum disulfide complexes with the activated alkyne, dimethylacetylene dicarboxylate (dmad, $R' = CO_2Me$) (527, 724, 2057, 2058). Thermolysis with $[MoO(S_2)(S_2CN\,R_2)_2]$ (R = Me, Et) (2057) or $[Mo(S_2)(S_2CNEt_2)_3]$ (724) affords isomeric dithiolate complexes, orange $[Mo\{\eta^2\text{-}SC(CO_2Me){=}C(CO_2Me)S\}\{\eta^1,\eta^3\text{-}SC(CO_2Me){=}C(CO_2Me)SC(NR_2)\}(S_2CNR_2)]$ (**538**) and green $[Mo\{\eta^2\text{-}SC(CO_2Me){=}C(CO_2Me)S\}\{\eta^1,\eta^3\text{-}SC(CO_2Me){=}C(CO_2Me)C(NR_2)S\}(S_2CN\text{-}R_2)]$ (**539**) (Eq. 195), two examples of which have been crystallographically characterized (2057). They result from oxo loss, alkyne addition into the sulfur–sulfur bond, and the novel insertion of the alkyne into a dithiocarbamate ligand.

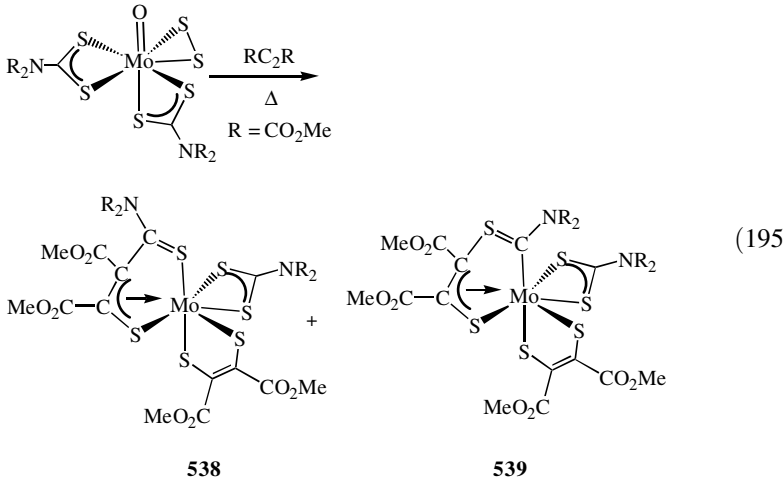

(195)

Similarly, with $[Mo(NPh)(S_2)(S_2CNEt_2)_2]$, the blue 1-thio-2-iminoene complex $[Mo\{\eta^2\text{-}PhNC(CO_2Me){=}C(CO_2Me)S\}\{\eta^1,\eta^3\text{-}SC(CO_2Me)C(CO_2Me)C(NEt_2)S\}(S_2CNEt_2)]$ (**540**) (Eq. 196) is the major product resulting from removal of one sulfur and alkyne addition across the remaining sulfur atom

and an imido ligand, together with alkyne insertion into a dithiocarbamate (2058).

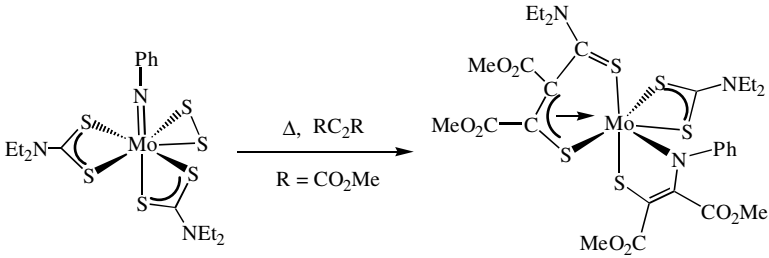

(196)

540

More recently, Young and co-workers (2059) reported related transformations at a tungsten center. Addition of certain alkynes to $[WS(S_2)(S_2CNR_2)_2]$ (R = Me, Et) (**541**) results in the formation of purple $[W\{\eta^2\text{-}SC(R')=C(R')S\}\{\eta^2,\eta^2\text{-}SC(R')=C(R')SC(NR_2)S\}(S_2CNR_2)]$ (**542**), by the addition of one alkyne across the disulfide unit, with a second linking the sulfido and dithiocarbamate ligands via the formation of two new sulfur–carbon bonds. This transformation is an addition of the dithiocarbamate to an unsaturated organic moiet (see below). Upon photolysis, a further transformation occurs to generate the green thiocarboxamide complexes, $[W\{\eta^2\text{-}SC(R')=C(R')S\}_2(SCNR_2)(S_2CNR_2)]$ (**543**), a result of the cleavage of a carbon–sulfur bond in the original dithiocarbamate ligand. While these complexes are relatively stable, upon dissolution in methanol a quantitative conversion to orange anionic species, $[W\{\eta^2\text{-}SC(R')=C(R')S\}_2(S_2CNR_2)]^-$, (**544**), occurs as a result of the loss of the thiocarboxamide group (Fig. 293).

Young and co-workers (1068) also noted that thermolysis of [Tp*W$(CO)_2(S_2CNEt_2)$] with dmad affords the unusual product [Tp*W$(\eta^2$-SCNEt)$\{SC(CO_2Me)C(CO_2Me)CO\}$] (Eq. 197), whereby the sulfido ligand formed as a result of carbon–sulfur bond scission has combined with both the alkyne and a molecule of carbon monoxide to give an unusual new organic ligand. It must, however, be noted that reactions with other alkynes do not give the same product types. Indeed, in no other case does carbon–sulfur bond cleavage occur, suggesting that not only does the electron-deficient nature of dmad serve to trap reactive scission products, but it may be required to be in the coordination sphere of the metal center in order to activate bond cleavage.

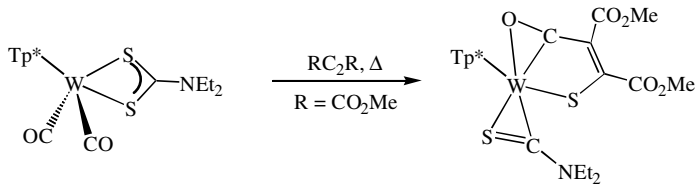

(197)

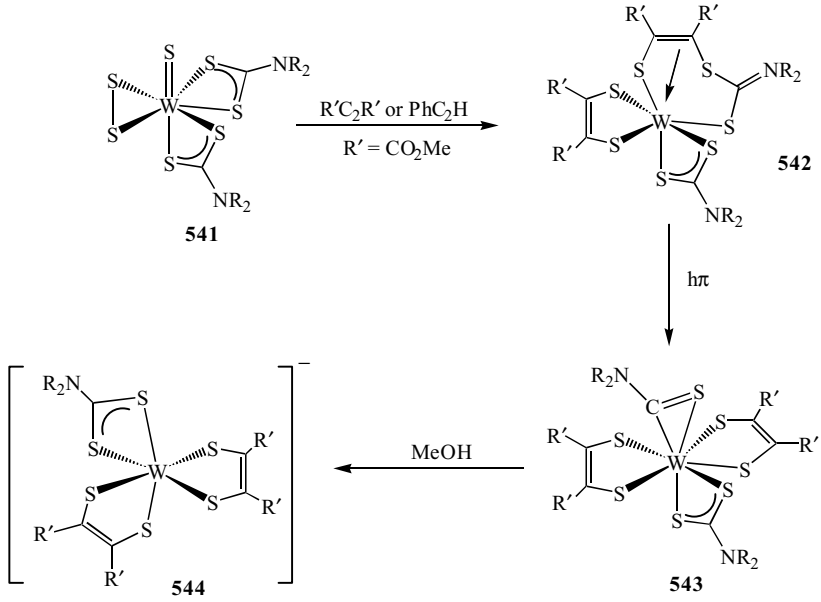

Figure 293. Stepwise formation and then loss of the thiocarboxamide ligand a tungsten center.

Even more unusual is the photolysis of $[W(PhC_2H)_2(S_2CNMe_2)_2]$ with excess phenylethyne. This gives the very unusual substituted cyclopentadienyl complex $[(\eta^5\text{-}1,3\text{-}Ph_2\text{-}4\text{-}NMe_2\text{-}C_5H_2)W(SCH{=}CPhS)(S_2CNMe_2)]$ (Eq. 198) in low yield (2060). Formation of the cyclopentadienyl and 1,2-dithiolene ligands is believed to be a result of a double carbon–sulfur bond cleavage generating an aminocarbyne and two sulfido ligands, followed by alkyne addition to both.

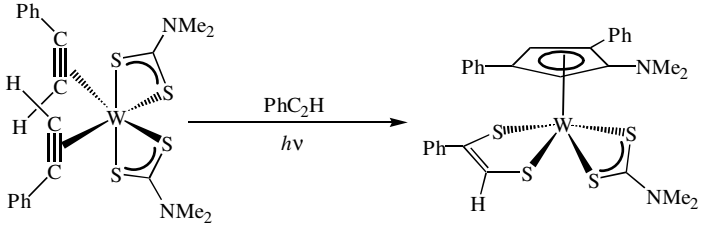

(198)

While addition of 2 equiv of sodium dithiocarbamate salts to $[WCl(CPh)(CO)_2py_2]$ also affords ketenyl complexes $[W(CO)\{PhCC(O)\}(S_2CNR_2)_2]^-$, with $[H_2NEt_2][S_2CNEt_2]$ a quite different reaction occurs. Remarkably, the thioaldehyde complex $[W(CO)(SCHPh)(SCNEt_2)(S_2CNEt_2)]$ is formed in 96%

yield (Eq. 199). Mechanistic details are unclear, however, it is proposed that an intermediate bearing two dithiocarbamate ligands (one monodentate) may have an alkylidyne ligand that is sufficiently basic to deprotonate the ammonium salt and give an alkylidene, which subsequently interacts with a dithiocarbamate to give thioaldehyde and thiocarboxamide ligands (1095).

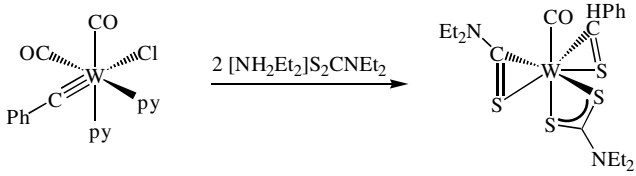

(199)

D. Addition of Intact Dithiocarbamates to Unsaturated Organic Ligands

Dithiocarbamates are moderate nucleophiles, and as such they might be expected to attack electrophilic metal-bound organic ligands to produce new hydrocarbyls as a result of the formation of a new carbon–sulfur bond. Indeed this is the case. The first example of such behavior was reported by McCleverty and Murray in 1979. They detailed an unusual transformation upon addition of dithiocarbamate salts to $[CpMo(\eta^3\text{-}C_3H_5)(CO)(NO)]^+$, with attack occurring at a terminal allyl-carbon to yield the novel addition products $[CpMo(CO)(NO)\{\eta^2\text{-}H_2C{=}CHCH_2SC(S)NR_2\}]$ (R = Me, Et, Bu) (Eq. 200). The methyl analogue was crystallographically characterized (2061).

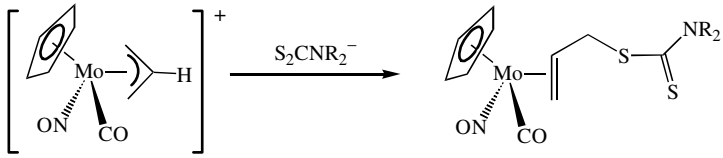

(200)

The formation of the new carbon–sulfur bond is often a reversible process. This is highlighted in the formation of vinylketenes, $[W(CO)(S_2CNR_2)_2\{\eta^2,\eta^2\text{-}O{=}C{=}C(Ph)CH{=}CHMe\}]$ (R = Me, Et, Ph) (**547**), from the allylidene complex $[W(CO)_2Br_2\{\eta^1,\eta^2\text{-}C(Ph)CH{=}CHMe\}(4\text{-picolene})]$ (**545**) and dithiocarbamate salts at 50°C (1096–1098). At lower temperatures four intermediates can be seen and spectroscopic studies indicate that each contains an η^1,η^3-allyldithiocarbamate ligand generated by dithiocarbamate addition to the tungsten–alkylidene bond. Indeed, in one case such a complex, namely, $[W(CO)_2(S_2CNEt_2)\{\eta^1,\eta^3\text{-}SC(NEt_2)SCPhCH{=}CHMe\}]$ (**546**), was isolated and crystallographically characterized (Fig. 294) (1096).

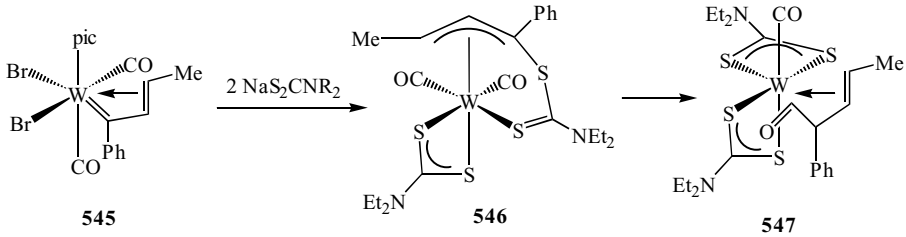

545 **546** **547**

Figure 294. Reversible sulfur–carbon bond formation and cleavage at a tungsten center.

Davidson (2062) showed that addition of dithiocarbamate salts to [CpMCl($R'C_2R'$)$_2$] (M = Mo, W; R′ = CF_3) (**548**) leads to the initial formation of η^2-vinyl complexes, [CpM($R'C_2R'$){η^2,η^3-C(R′)C(R′)SC(NR_2)S}] (**549**), a result of the addition of dithiocarbamate to the hexaflourobut-2-yne ligand. Upon heating the molybdenum complex, the carbon–sulfur bond is cleaved to yield the butadiene complex [CpMo(η^4-R_4C_4)(S_2CNR_2)] (**550**) as the major products. This complex is also formed upon addition of dithiocarbamate salts to [CpMoI(CO)(η^4-R_4C_4)] (**551**). Interestingly, a second minor product was also obtained, which was identified as the thiocarboxamide complex [CpMo{η^2,η^1-C(R′)C(R′)C(R′)C(R′)S}($SCNR_2$)] (**552**). This complex is formed in 90% yield upon photolysis of **549** and results from cleavage of a single carbon–sulfur bond and coupling of the alkyne with the newly generated hydrocarbyl group.

Another example of a reversible dithiocarbamate addition process has recently been described by Bordoni and co-workers (2063). Thus, reaction of [$Cp_2Fe_2(CO)_2$(μ-CS)(μ-CSMe)]$^+$ (**553**) with NaS_2CNMe_2 gives two products; dithiocarbene, [$Cp_2Fe_2(CO)$(μ-CS){μ-C(SMe)SC(NMe_2)S}] (**554**), and thiocarbyne, [Cp_2Fe_2(μ-CS)(μ-CSMe)(μ-S_2CNMe_2)] (**555**), with the former being quantitatively converted into the latter upon photolysis (Fig. 296).

Formation of the dithiocarbene probably results from the attack of the nucleophilic dithiocarbamate at the electrophilic thiocarbyne center followed by a secondary carbonyl substitution process. In support of this supposition, addition of NaS_2CNMe_2 to [$Cp_2Fe_2(CO)_2$(μ-CO){μ-C(CN)(SMe_2)}]$^+$ (**556**) has been shown to yield [$Cp_2Fe_2(CO)_2$(μ-CO){μ-C(CN)(S_2CNMe_2)}] (**557**), which upon photolysis gives [$Cp_2Fe_2(CO)$(μ-CO){μ-C(CN)(S_2CNMe_2)}] (**558**).

Over the past 10 years, Hill (1375, 1384, 1385, 2064) and Roper and co-workers (2065) detailed a number of instances in which novel metallacycles result from dithiocarbamate–hydrocarbyl coupling reactions at ruthenium, and to a lesser extent, osmium centers. Roper reported that addition of 2 equiv of NaS_2CNMe_2 to the chloro–carbene complex [$RuCl_2(CO)(PPh_3)_2$(CClR)] (RH = 2-C_4H_3NH) gave [Ru(CO)(PPh_3)(S_2CNMe_2){η^2-S=C(NMe_2)SCR}] (Eq. 201), in which one dithiocarbamate has attacked the carbene–carbon, displacing chloride and generating a stable 1-azafulvene complex (2065). The latter can

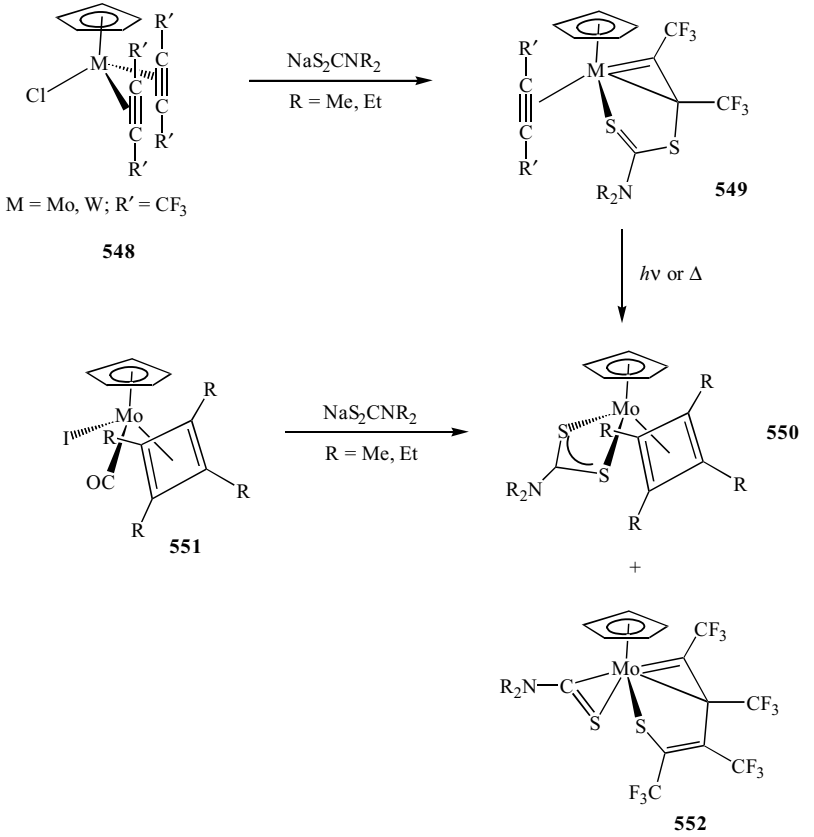

Figure 295. Reversible carbon–sulfur bond formation and cleavage at a molybdenum center together with the irreversible formation of a thiocarboxamide complex.

be reversibly protonated and irreversibly methylated at nitrogen.

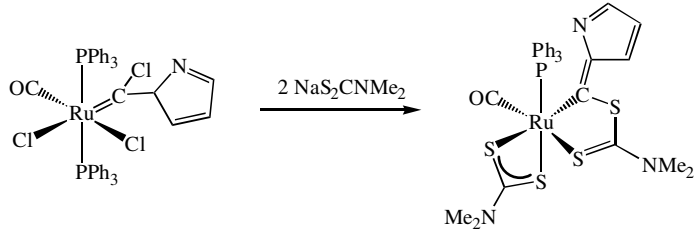

(201)

More recently, Hill showed that dithiocarbamate addition to related alkylidene $[MCl_2(CO)(PPh_3)_2(CHAr)]$ (M = Ru, Os; Ar = Ph, *p*-C_6H_4OMe) (**559**) or

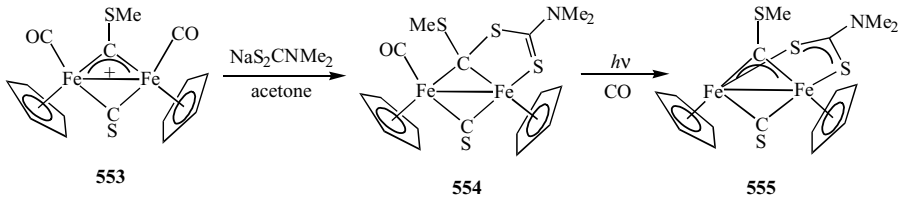

Figure 296. Reversible carbon–sulfur bond formation and cleavage at a di-iron center.

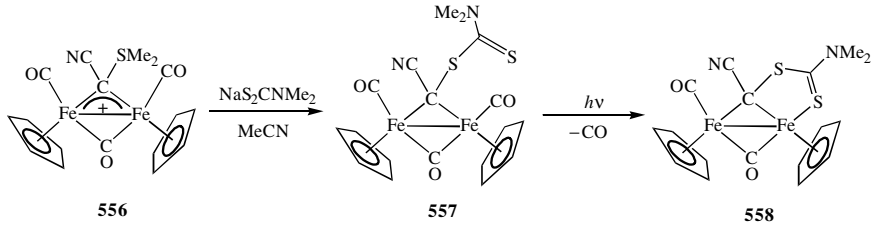

Figure 297. Nucleophilic attack of a dithiocarbamate at a metal-bound hydrocarbyl fragment.

alkylidyne $[MCl(CO)(PPh_3)_2(CAr)]$ (**560**) complexes yields metallacyclic $[M(CO)(PPh_3)(S_2CNR_2)\{\eta^2\text{-}S{=}C(NR_2)SCHAr\}]$ ($R = Et$; $R_2 = C_4H_8$) (**561**), again via attack at the alkylidene carbon (Fig. 298) (2064).

Coupling is not restricted to C_1 ligands. Hill has also shown that dithiocarbamate salts can couple to unsaturated C_2 and C_3 fragments at the ruthenium(II) center. For example, addition of $[Et_2NH_2][S_2CNEt_2]$ to the vinylidene complex $[TpRuCl(PPh_3)(C{=}C{=}CHAr)]$ ($Ar = p$-tol), affords $[TpRu(PPh_3)\{\eta^2\text{-}S{=}C(NEt_2)SC(=CHAr)\}]$ (Eq. 202). Here, attack takes place selectively at the

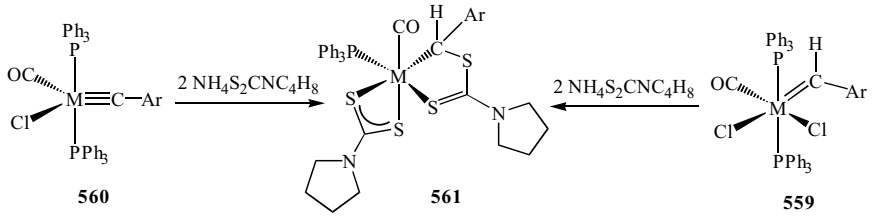

Figure 298. Formation of metallacyclic complexes upon dithiocarbamate addition to alkylidene or alkylidyne centers.

α-carbon (1375).

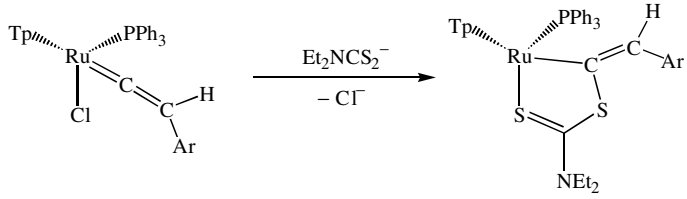

(202)

Similarly, NaS_2CNMe_2 attacks the α-carbon of the vinyl–carbene complex $[Ru(CO)(PPh_3)_2(S_2CNMe_2)(CHCH{=}CPh_2)]^+$, giving $[Ru(CO)(PPh_3)(S_2CNMe_2)\{\eta^2\text{-}S{=}C(NMe_2)SCH(CH{=}CPh_2)\}]$ (Eq. 203) (1385).

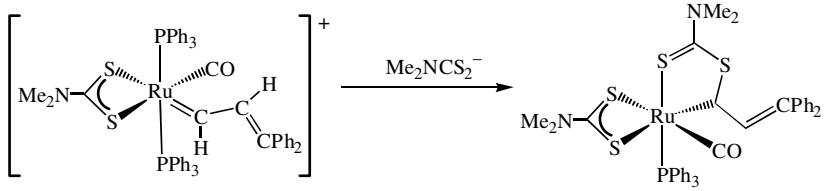

(203)

Attack at the α-carbon of diphenylallenylidene ligands is also facile (1375, 1384). Thus, reaction of NaS_2CNMe_2 with $[TpRuCl(PPh_3)(=C=C=CPh_2)]$ affords $[TpRu(PPh_3)\{\eta^2\text{-}S{=}C(NMe_2)SC(=C=CPh_2)\}]$ (Eq. 204). The regioselective nature of hydrocarbyl attack is not yet understood, but precoordination of the dithiocarbamate and steric control has been ruled out (1385).

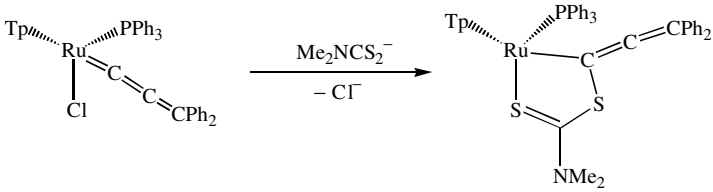

(204)

While the examples detailed above relate to dithiocarbamate addition to organic ligands, in a related but quite unique contribution, Greenwood and co-workers (2066) report that reaction of the metallaborane *nido*-[Pt(PPhMe_2)$B_{10}H_{12}$] with $[AuBr_2(S_2CNEt_2)]$ leads to formation of *nido*-[Pt(PPhMe_2)$B_{10}H_{11}(\mu\text{-}S_2CNEt_2)$] (**562**), in which the dithiocarbamate bridges across a platinum–boron vector.

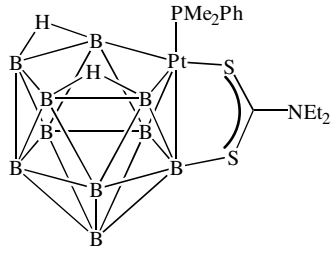

562

E. Insertion of Unsaturated Moieties into Metal–Sulfur Bond(s) of Dithiocarbamates

As discussed earlier (Section IV.I.1.h.ii), the insertion of sulfur into the zinc–sulfur bonds of $[Zn(S_2CNMe_2)_2]$ is proposed to be a key step in the rubber vulcanization process that utilizes this material. However, while the insertion of sulfur into the metal–sulfur bonds of related xanthate complexes is known, to date no such insertion has been noted for dithiocarbamates. However, the insertion of related isoelectronic fragments into the metal–sulfur bond(s) is known.

Insertion of an oxo fragment into a metal–sulfur bond in a dithiocarbamate complex has not been reported, although in one instance the product of such a transformation has been identified. Thus the oxygen-expanded complexes $[Cr(S_2CNR_2)_2\{OSCN(R_2)S\}]$ (**563**) (Fig. 299) have been formed along with $[Cr(S_2CNR_2)_3]$ from the reaction of dichromate and dithiocarbamate salts (746). A more recent report that this reaction produces a dimeric oxo-bridged complex would appear to be erroneous (747). Presumably, these oxygen-expanded ligands result from addition of the dithiocarbamate to the pre-formed metal oxide, and as such can be considered as examples of dithiocarbamate addition reactions, as detailed above. However, due to their relationship with other

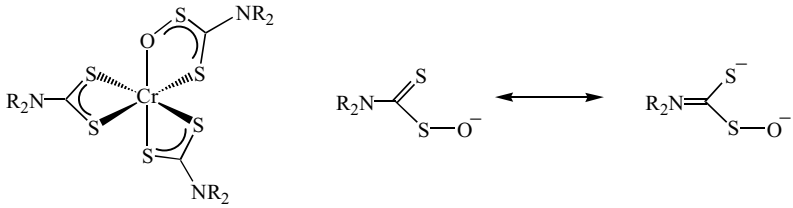

563

Figure 299. Oxygen-expanded chromium(III) complexes showing proposed resonance hybrids for the expanded ligand.

expanded ligands formed from insertion reactions, we consider them here. An early crystal structure of $[Cr(S_2CNEt_2)_2\{OSC(NEt_2)S\}]$ confirmed the nature of this expanded ligand, but contained a severe distortion, and in a later contribution a new refinement of the structure showed that the O,S-chelate was disordered over three sites (748).

An extensive electrochemical comparison of $[Cr(S_2CNR_2)_3]$ and $[Cr(S_2CNR_2)_2\{OSC(NR_2)S\}]$ has been carried out in order to examine the influence of oxygen insertion (746). Oxygen-inserted complexes are more easily oxidized and further, the cations exhibit enhanced stability, believed to result from the increased importance of the resonance state, $R_2N^+{=}CS(SO)^{2-}$.

Three further reports suggest that oxo insertion may be possible. Thus, the en complex $[Co(S_2CNMe_2)(en)_2][Sb_2(R,R\text{-tartrate})_2].5H_2O$ has been prepared, optically resolved, and crystallographically characterized. Interestingly, oxidation by hydrogen peroxide in acidic media is believed to afford $[Co\{\eta^2\text{-}S{=}C(NMe_2)S(=O)O\}(en)_2]^{2+}$ (Eq. 205), which results from insertion of one oxygen into a cobalt–sulfur bond and further oxidation of the sulfur atom involved. This result has not been confirmed crystallographically (1408).

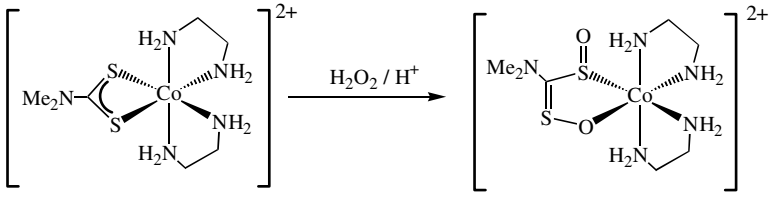

(205)

In the second, oxidation of $[Cu\{S_2CN(CH_2CH_2OH)_2\}_2]$ by hydrogen peroxide has been shown to yield copper sulfate as the final product. However, when the reaction with oxygen was monitored by ESR spectroscopy, new species were observed, which were proposed to result from oxidation of one and two sulfurs, respectively, of the dithiocarbamate ligand (1718). Further, $[Ni(S_2CNBu_2)_2]$ has been shown to strongly inhibit the light-induced fading of crystal violet lactone dye, which is an oxidative process involving peroxides. Allan et al. (1577) investigated reactions of $[Ni(S_2CNBu_2)_2]$ with organic peroxides, where the main transformation products are organosulfites and sulfur oxides, that were proposed to result from oxidation and insertion of the metal-bound dithiocarbamate ligands.

Multiple nitrene (NTs) insertion reactions have been found when $[Cu(S_2CNR_2)_2]$ react with the iodine(III) reagent, PhI=NTs (439,1785). The first products isolated are the bis(sulfido-amido) complexes, *trans*-$[Cu\{\eta^2\text{-}TsNSC(NR_2)S\}_2]$ (**564**), which undergo further insertion into the remaining copper–sulfur bonds to give zwitterionic bis(diamido) complexes, $[Cu\{\eta^2\text{-}TsNSC(NR_2)SNTs\}_2]$ (**565**) (Fig. 300).

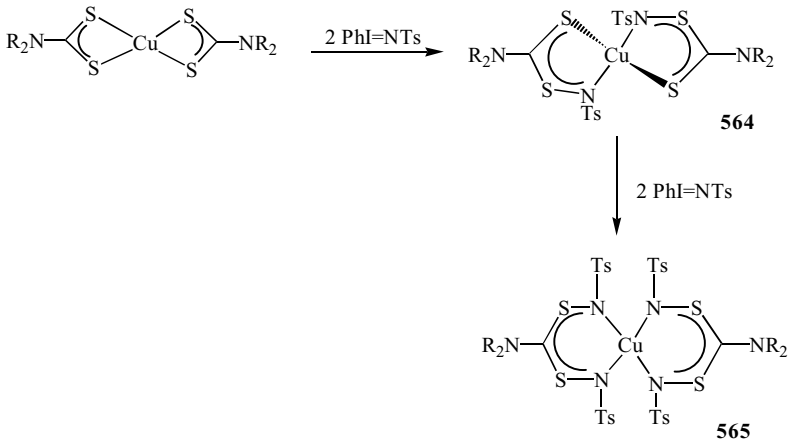

Figure 300. Multiple nitrene isertions into the copper–sulfur bonds of $[Cu(S_2CNR_2)_2]$.

The reaction is general for a range of different alkyl substituents, but perhaps significantly, the pyrrole derivative $[Cu(S_2CNC_4H_4)_2]$ is unreactive, probably because it cannot support the localization of positive charge at nitrogen (Fig. 301).

The same insertion reactions also occur at nickel, but fail with the heavier group 10 (VIII) elements. Insertion does not occur at iron tris(dithiocarbamate) complexes $[Fe(S_2CNR_2)_3]$, or at the related cobalt(III) species. However, reduction of the latter by zinc amalgam results in a color change from brown to slate-blue, associated with the transient formation of $[Co(S_2CNR_2)_2]$. Further addition of excess PhI=NTs at this stage affords $[Co\{\eta^2\text{-}TsNSC(NR_2)SNTs\}_2]$ (R = Me, Et, Pr, Bu) (Eq. 206). Thus these cobalt(II) products result from insertion of four NTs groups into the cobalt–sulfur bonds of the *in situ* generated

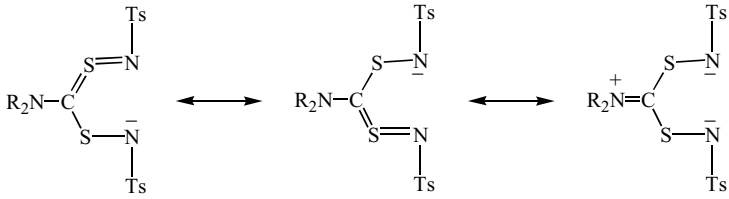

Figure 301. Possible resonance hybrids of bis(nitrene)-expanded ligands.

$[Co(S_2CNR_2)_2]$. Interestingly, no evidence of double insertion was noted (1427).

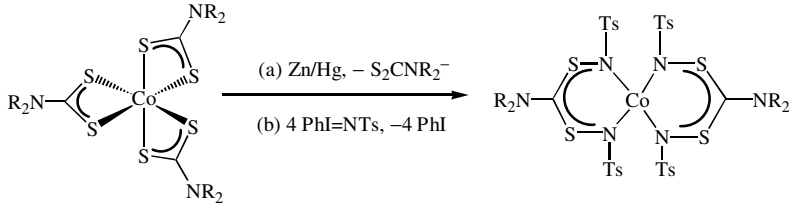

(206)

The mechanistic nature of these nitrene insertion reactions remains unknown. A number of possible routes can be considered (Fig. 302), including (1) direct insertion, (2) initial formation of a metal–nitrene (imido) complex followed by insertion, (3) initial addition of nitrene fragment to sulfur (i.e., oxidation of sulfur) followed by an isomeric rearrangement. On the basis that copper(II) nitrene complexes are unknown (although they have been implicated in the copper-catalyzed aziridination process) this route is ruled out and literature precedent suggests that route (3) is most likely.

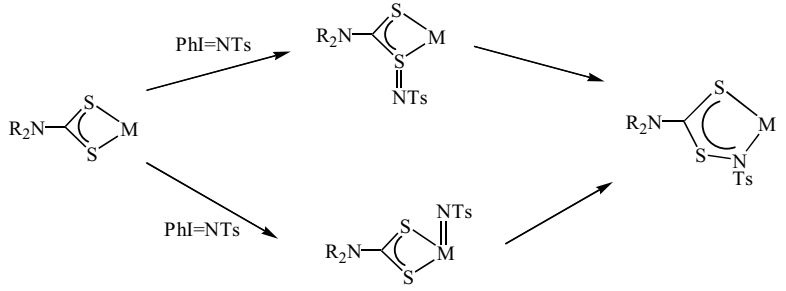

Figure 302. Possible routes to the generation of nitrene-expanded ligands.

The insertion of a methylene fragment into a cobalt–sulfur bond of $[CpCoI(S_2CNMe_2)]$ has been reported (2067). Thus, reaction with diazomethane affords two products, $[CpCoI\{\eta^2\text{-}CH_2SC(NMe_2)S\}]$ and $[CpCoI\{\eta^2\text{-}CH_2SC(=NMe_2)\}]$ (Eq. 207). The first results from an unprecedented insertion of a methylene group, while the second results from insertion followed by sulfur loss. The mode of formation of the latter is unknown, and attempts to extrude sulfur from $[CpCoI\{\eta^2\text{-}CH_2SC(NMe_2)S\}]$ were not successful.

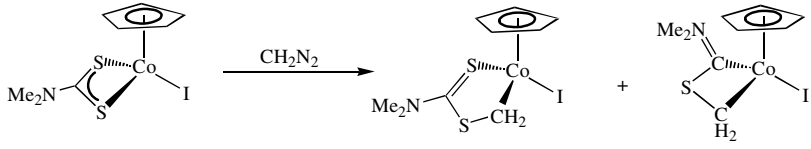

(207)

Very recently, Suzuki et al. (2068) reported the novel insertion of a nitrogen atom into an iridium–sulfur bond. Photolysis of the azide complexes [Cp*Ir(N_3)(S_2CNR_2)] (R = Me, Et) (**566**) at < 0°C results in the loss of nitrogen and formation of [Cp*Ir{η^2-NSC(NR_2)S}] (**567**), which at higher temperatures isomerize to the disulfur-ligated complexes [Cp*Ir{η^2-SNC(NR_2)S}] (**568**) (Fig. 303). A crystal structure of the former (R = Me) reveals a planar five-membered chelate ring, with a short iridium–nitrogen bond, suggestive of significant double-bond character, while the iridium–sulfur bond at 2.272(2) Å is also shorter than those found in [Ir(S_2CNEt_2)$_3$] (386). While the disulfur ligated isomer is monomeric in solution, crystallization leads to the isolation of a dimeric complex **569** (Fig. 303) in which the sulfur atoms bridge iridium centers. Here, the ring carbon–nitrogen bond is short [C—N 1.31(2) Å], while the iridium–sulfur bonds of 2.328(3)–2.370(3) Å are similar to those in tris(dithiocarbamate) complexes.

The thermal rearrangement involves a switch of the nitrogen and sulfurs in the chelate ring and can be formally considered as the insertion of a nitrogen atom into the carbon–sulfur bond of a dithiocarbamate. In order to probe this further a labeling study was carried out, with ^{15}N exchange occurring within

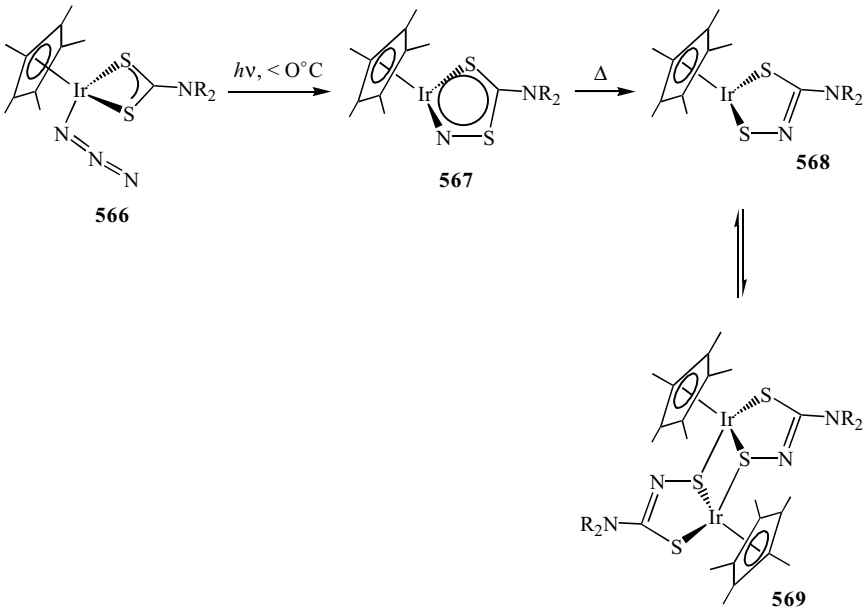

Figure 303. Formation and subsequent isomerization of nitrogen-expanded ligands.

hours at room temperature (Eq. 208).

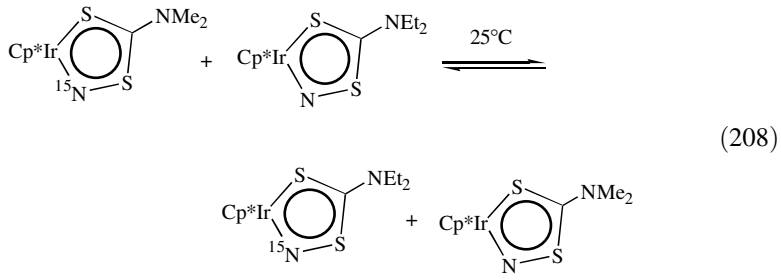

(208)

Interestingly, this ligand type is not new and was previously been described by Roesky and co-workers (209) from the reactions of TiX_4 (X = Cl, Br) with $Me_2NC(S)SN(SiMe_3)_2$, a result of the cleavage of both nitrogen–silicon bonds (Eq. 209).

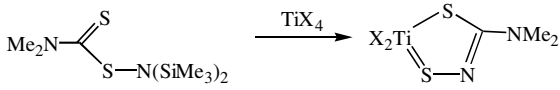

(209)

As alluded to earlier, the insertion of sulfur into the metal–sulfur bond of a dithiocarbamate, thus giving a mononuclear trithiocarbamate complex, remains elusive, as indeed do mononuclear trithiocarbamate complexes themselves, despite an early reference to such species (2069). The trithiocarbamate ligand has, however, been prepared and isolated in a bridging capacity. Thus, in a series of publications, Pignolet and co-workers (295,1379,1380) described the synthesis of diosmium complexes containing trithiocarbamate or selenodithiocarbamate ligands. For example, heating $[Os(S_2CNR_2)_3]$ (R = Me, Et) (**570**) with elemental sulfur in DMF yields trithiocarbamate complexes $[Os_2(S_2CNR_2)_3(\mu\text{-}S_5)(\mu\text{-}S_3CNR_2)]$ (**571**) and $[Os_2(S_2CNR_2)_3(\mu\text{-}S_3CNR_2)_2]^+$ (**572**). The former is converted into the latter upon reaction with thiuram disulfide, while reaction of $[Os_2(S_2CNR_2)_3(\mu\text{-}S_3CNR_2)_2]^+$ with phosphines or phosphites also yields small amounts of $[Os_2(S_2CNR_2)_3(\mu\text{-}S_2CNR_2)_2]^+$ (**573**) (Fig. 304) as a result of sulfur abstraction (1380).

The only pure product isolated from the reaction of $[Os(S_2CNMe_2)_3]$ and elemental selenium is $[Os_2(S_2CNMe_2)_3(\mu\text{-}SeS_2CNMe_2)_2]^+$ (Eq. 210), with the selenium atoms bridging the diosmium(III) center [Os—Os 2.836(1) Å] as

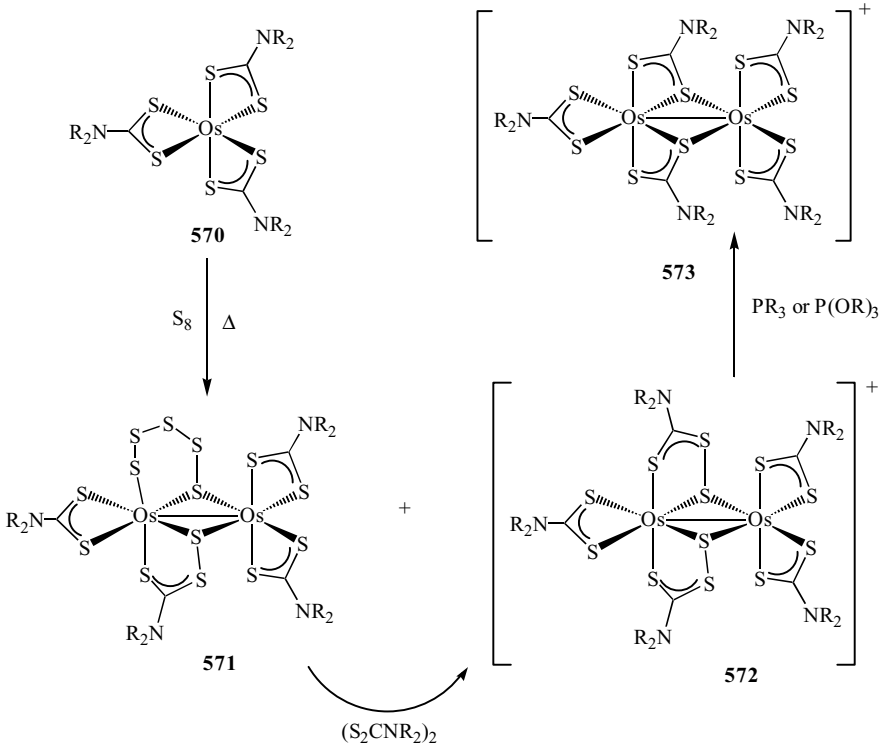

Figure 304. Formation and reactivity of bridging trithiocarbamate ligands at the diosmium center.

shown crystallographically (295).

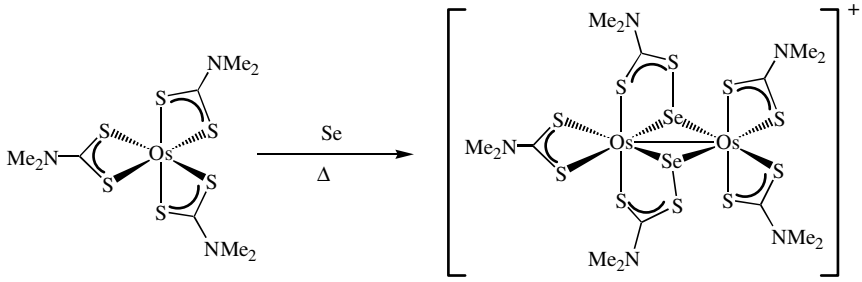

(210)

Related dirhenium trithiocarbamate complexes have also been prepared. For example, $[Re_2(\mu\text{-}S)(S_2CNR_2)_2]_2$ undergo a reversible one-electron oxidation

that in the presence of further thiuram disulfide gives rhenium(III) complexes, $[Re_2(\mu\text{-}S_3CNR_2)_2(S_2CNR_2)_3]^+$ (Eq. 211). Here the two trithiocarbamate ligands have been generated from sulfur–sulfur bond formation. Crystallographic characterization ($R = t$-Bu) again shows a short rhenium–rhenium bond of 2.573(2) Å, and reaction with $LiEt_3BH$ or H_2 results in regeneration of the starting material. The regioselectivity of this interconversion process has been investigated by labeling studies. These show that during trithiocarbamate formation, one dithiocarbamate unit from the thiuram disulfide ends up as either the trithiocarbamate or one of the equivalent pair of dithiocarbamates. In the back reaction, the same dithiocarbamate unit (or its symmetry equivalent) is eliminated and the authors favor the trithiocarbamate ligand as the reactive entity (185).

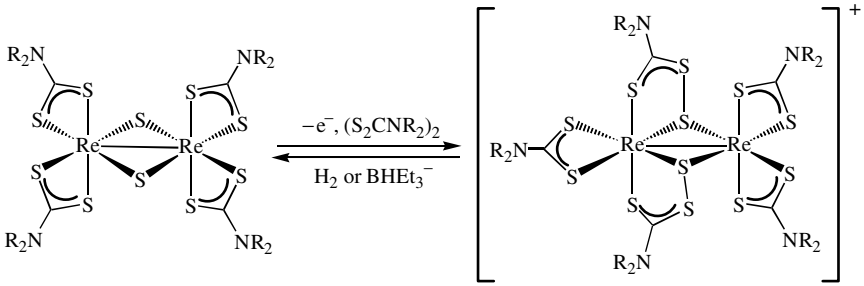

(211)

A selenium-expanded ligand has also been isolated and crystallographically characterized at a copper(I) center. Thus, $[Cu\{\eta^2\text{-}SeSC(NC_4H_8)S\}(\eta^1\text{-}S_2CNC_4H_8)][PPh_4]$ is one of a number of products of the reaction of $[Cu(S_2CNC_4H_8)]_n$ with $[PPh_4]_2[WSe_4]$ in DMF (Eq. 212) (1734). The selenium–sulfur interaction of 2.231(4) Å is indicative of a single bond, while there is also significant asymmetry in the carbon–sulfur bonds, suggesting the adoption of the resonance hybrid shown.

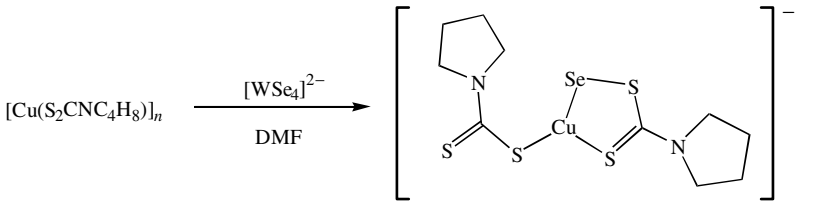

(212)

The insertion of carbonyl sulfide into a dithiocarbamate ligand has been noted in one instance. Thus, the molybdenum(II) dicarbonyl $[Mo(CO)_2(S_2CNEt_2)_2]$

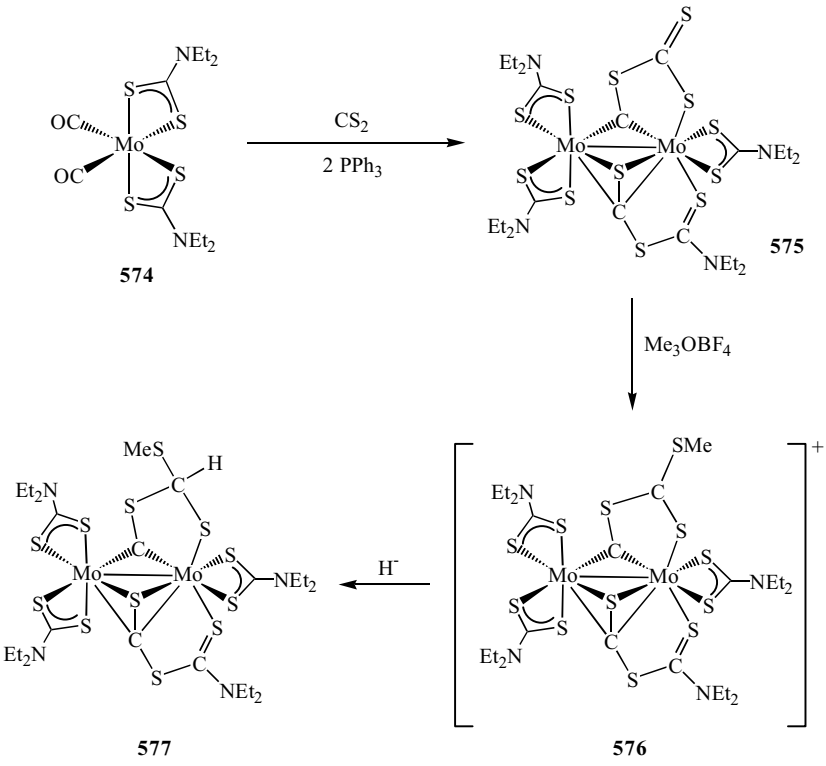

Figure 305. Insertion of carbonyl sulfide into a dithiocarbamate ligand and subsequent reactivity of the expanded-ligand complex.

(**574**) reacts with carbon disulfide in the presence of PPh_3 yielding an unusual molybdenum(III) complex, $[Mo_2(S_2CNMe_2)_3\{\mu,\eta^1\text{-}CSC(S)S\}\{\mu,\eta^1\text{-}SCSC(NEt_2)S\}]$ (**575**). This complex results from thiocarbonyl insertion into a dithiocarbamate and coupling of a thiocarbonyl and carbon disulfide at the dimolybdenum center (2070). The resulting trithiocarbonatocarbene ligand can be methylated at the unbound sulfur upon addition of $[Me_3O]BF_4$ to give **576**, which reacts further with hydride to give $[Mo_2(S_2CNMe_2)_3\{\mu,\eta^1\text{-}CSH(Me)C(S)S\}\{\mu,\eta^1\text{-}SCSC(NEt_2)S\}]$ (**577**) (Fig. 305).

In some instances, it is difficult to differentiate between the insertion of an unsaturated moiety into a metal–sulfur bond and addition of the dithiocarbamate to the group, as detailed in Section V.D. The reaction of $[CpFe(CO)_2(\eta^1\text{-}S_2CNR_2)]$ (**578**) with KCN in dry methanol provides a good example of this. Thus, the very air-sensitive metallacyclic complex $[CpFe(CO)\{\eta^2\text{-}SC(NR_2)SC(=N)\}]^-$ (**579**) results (Fig. 306). Overall the process involves

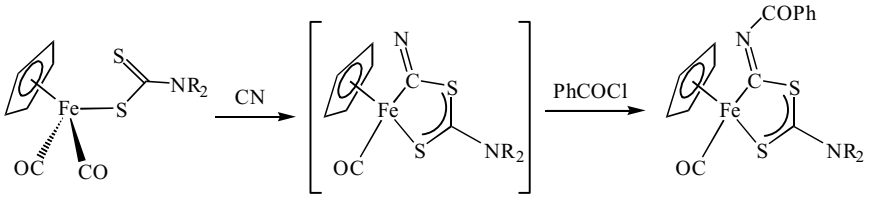

578 **579** **580**

Figure 306. Cyanide addition to a monodentate dithicarbamate ligand and subsequent reaction with PhC(O)Cl.

carbonyl loss, cyanide coordination, and carbon–sulfur bond formation, although it cannot easily be ascertained whether the cyanide is metal bound when this latter process takes place. In order to confirm the overall nature of the transformation, the authors quenched the reaction with PhCOCl to give crystallographically characterized [CpFe(CO){η^2-SC(NEt_2)SC(=NCOPh)}] (**580**) (Fig. 306) (1278,1283).

VI. SUMMARY AND OUTLOOK

Hopefully, this chapter has served to illustrate the tremendous diversity of the dithiocarbamate ligand. While it is over a century since the first transition metal dithiocarbamate complexes were prepared, exciting new developments are still being made, and we can look forward to more in the future.

It is difficult to predict where these may come, but the relative lack of applications of dithiocarbamate complexes in homogeneous catalysis seems somewhat surprising given their ability to stabilize metals in a range of oxidation states. This probably arises from the nonsterically demanding nature of the ligand and the relative instability of the carbon–sulfur bonds. The former could be addressed with ''smart'' dithiocarbamate ligands, with more than just the disulfur binding sites, and indeed in general the future for more exotic dithiocarbamate ligands looks promising. As Beer and co-workers (162,325,326,492,544,1468–1471,1489) recently shown, the melding of dithiocarbamates into supramolecular chemistry has generated an exciting new area of chemistry, which utilizes their well-defined coordination environments and redox properties, and hopefully such avenues will be developed to a greater extent.

While the dithiocarbamate is a sterically nondemanding ligand, electronic tuning can be easily made through judicious choice of substituents. It strikes me then as quite surprising that despite all the exotic chemistry developed around the dithiocarbamate-stabilized metal center, in the vast majority of cases it is just

the dimethyl and diethyl ligands that are used. Recently, Unoura and co-workers (1045) showed that the stability of tungsten(IV) dioxo complexes, $[WO_2(S_2CNR_2)_2]$, is strongly linked to the nature of the substituents, and it may be that inorganic chemists have missed out on some exciting new chemistry by simply considering the dithiocarbamate as an unimportant ancillary ligand.

Finally, if you are reading this in 15–20 years time with a view to adding to this series of reviews on dithiocarbamate chemistry—then good luck—you will certainly need it!

ACKNOWLEDGMENTS

Our research in this area has been supported by the EPSRC, AEA Technology and the University of London Central Research Fund. I would like to thank the staff of the Royal Society of Chemistry Library and Information Center and the British Library (Science Reading Room South) for their help in locating many of the references used in this chapter, especially those at the former who have worked tirelessly lugging up obscure manuscripts from the basement storage area. Hopefully, you won't see me for some time now!

ABBREVIATIONS

2,2′-bpy	2,2′-Bipyridine
3D	Three dimensional
313-NPPN	4,6-Diphenyl-4,6-diphosphanonane-1,9-diamine
4,4′-bpy	4,4′-Bipyridine
acac	Acetylacetenoate
AIBN	2,2′-Azobisisobutyronitrile
AMMEsar	8-Methyl-3,6,10,13,16,19-hexaazabicyclo[6.6.6] icosan-1-aminium
ATRP	Atom-transfer radical polymerization
ax	Axial
Bcat	Pyrocatecholatoboryl
bitt-3	Bis(dialkylimonium)trithiolane
Bz	Benzyl
[cat]	Catalyst
cod	1,5-Cyclooctadiene
cot	Cyclooctatetrene
Cp	Cyclopentadienyl
Cp*	Pentamethylcyclopentadienyl
CPI	Cerebral perfusion imaging

CTH	*rac*-5,5,7,12,12,14-Hexamethyl-1,4,8,11-tetraaza-cyclotetradecane
CV	Cyclic voltammetry
CVD	Chemical vapor deposition
cyclam	1,4,8,11-Tetraazacyclotetradecane
dcbH	4-CO_2H-4′-CO_2-2,2′-Bipyridine
DCE	*N*,*N*′-Bis(2-chloroethyl)ethylenediamine
Diars	*o*-Phenylene bis(dimethylarsine)
diNOsar	1,8-Dinitro-3,6,9,13,16,19-hexaazabicyclo[6.6.6]isosane
dmad	Dimethylacetylene dicarboxylate
dme	1,2-Dimethoxyethane
dmf	Dimethylformamide (ligand)
DMF	Dimethylformamide (solvent)
dmg	Dimethylglyoxime
dmit	1,3-Dithiole-2-thione-4,5-dithiolate
dmpe	Bis(dimethylphosphino)ethane
dmso	Dimethyl sulfoxide (ligand)
DMSO	Dimethyl sulfoxide (solvent)
dpa	2,2′-Dipyridylamine
dppm	Bis(diphenylphosphino)ethane
dppf	1,1′-Bis(diphenylphosphino)ferrocene
dppe	1,2-Bis(diphenylphosphino)ethane
1,1-dppe	1,1-Bis(diphenylphosphino)ethane
dpmp	Bis(diphenylphosphinomethyl)phenylphosphine
dpep	Bis(diphenylphosphinoethyl)phenylphosphine
DSC	Differential scanning calorimetry
ebdtc	Ethylenebis(dithiocarbamate)
edta	Ethylenediaminetetraacetic acid
EHMO	Extended Hückel molecular orbital
en	Ethylenediamine
ENDOR	Electron–nuclear double resonance
eq	Equatorial
ESMS	Electrospray mass spectrometry
ESR	Electron spin resonance
etpb	4-Ethyl-2,6,7-trioxa-1-phosphabicyclo[2.2.2]octane
FABMS	Fast atom bombardment mass spectrometry
Fc	$CpFeC_5H_4$
FON	Fractional oxidation number
gly	Glycine
H_4dmp	6,7-Dimethyl-5,6,7,8-tetrahydropterin

HOMO	Highest occupied molecular orbital
Hoxq	8-Hydroxyquinoline
HPLC	High-pressure liquid chromatography
Hpz^{An}	3(5)-*p*-Methoxyphenylpyrazole
GC	Gas chromatography
IR	Infrared
LMCT	Ligand–metal charge transfer
LMOG	Low-molecular mass organic gelators
LUMO	Lowest unoccupied molecular orbital
MALDI	Matrix-assisted laser-desorption ionization
MAS	Magic-angle spinning
mat	2-Methylaminothiazole
MBBA	*N*-(4-Methoxybenzlidene)-4′-butylaniline
Mes	Mesityl
MMA	Methylmethacrylate
mnt	1,2-Dicyanoethane-1,2-dithiolate
MS	Mass spectrometry
MOCVD	Molecular chemical vapor deposition
morph	Morpholine
M_w	Molecular weight
naphth	Naphthalenyl
NBD	Norbornadiene
NBS	*N*-Bromosuccinimide
NMR	Nuclear magnetic resonance
Np	Neopentyl
phen	1,10-Phenanthroline
1,10-phen*	2,9-Dimethyl-1,10-phenanthroline
pic	Picoline
pip	Piperidine
PMMA	Polymethylmethacrylate
prol	proline
PVC	Poly(vinyl chloride)
py	Pyridine (ligand)
Py	Pyridine (solvent)
pydim	2,6-Bis(2,6-dimethylphenylimino)
Rsal	Alkylsalicylaldiminate
rt	Room temperature
SERS	Surface-enhanced Raman scattering
SOD	Superoxide dismutase
SOMO	Singly occupied molecular orbital
tacn	1,4,7-Triazacyclononane
taiMe	1-Methyl-2-*p*-tolylazoimidazole

TCNE	Tetracyanoethylene
TCNQ	7,7,8,8-Tetracyano-*p*-quinodimethane
Tf	Triflate
TGA	Thermal gravimetric analysis
thf	Tetrahydrofuran (ligand)
THF	Tetrahydrofuran (solvent)
tht	Tetrahydrothiophene (ligand)
THT	Tetrahydrothiophene (solvent)
tmeda	Tetramethylethylenediamine
tol	Tolyl
TOPO	Trioctylphosphine
TOSS	Total side band suppression
Tp	Hydridotris(pyrazolyl)borate
Tp′	Hydridotris(3-methylpyrazolyl)borate
Tp*	Hydridotris(3,5-dimethylpyrazolyl)borate
tpyH	*o*-Pyridinethiol
triphos	1,1,1-Tris(diphenylphosphino)methane
Ts	Tosyl
UV	Ultraviolet
VE	Valence electrons
VT	Variable temperature
XAFS	X-ray absorption fine structure
XPS	X-ray photoelectron spectroscopy
xs	Excess

REFERENCES

1. H. Debus, *Ann. Chem. (Liebigs), 73*, 26 (1850).
2. M. Delépine, *Compt. Rend., 144*, 1125 (1907).
3. J. Stary, *The Solvent Extraction of Metal Chelates*, Pergamon Press, Oxford, 1964, pp. 155–168.
4. K.N. Kaul, A.K. Malik, B.S. Lark, and A.L.J. Rao, *Rev. Roum. Chim., 45*, 221 (2000).
5. P.C. Uden and I.E. Bigley, *Anal. Chim. Acta, 94*, 29 (1977).
6. G. Schwedt, *Chromatographica, 11*, 145 (1978).
7. J.W. O'Laughlin and T.P. O'Brien, *Anal. Lett. A, 11*, 829 (1978).
8. O. Liška, J. Lehotay, E. Brandšterová, G. Guichon, and H. Colin, *J. Chromatogr., 172*, 384 (1979).
9. J. Lehotay, O. Liška, E. Brandšterová, and G. Guichon, *J. Chromatogr., 172*, 379 (1979).
10. O. Liška, G. Guichon, and H. Colin, *J. Chromatogr., 171*, 145 (1979).
11. M.L. Riekkola, *Finn. Chem. Lett., 1980*, 83.
12. M.-L. Riekkola, *Mikrochim. Acta, 1*, 327 (1982).

13. http://www.tut.fi/plastics/tyreschool/moduulit/moduuli_4/hypertext_2/2/2_3.html
14. http://www.inchem.org/documents/jmpr/jmpmono/v070pr12.htm
15. http://www.inchem.org/documents/pds/pds/pest94_e.htm
16. D. Coucouvanis, *Prog. Inorg. Chem., 11*, 233 (1970).
17. D. Coucouvanis, *Prog. Inorg. Chem., 26*, 301 (1979).
18. J. Willemse, J.A. Cras, J.J. Steggerda, and C.P. Keijzers, *Struct. Bonding (Berlin), 28*, 83 (1976).
19. D.J. Halls, *Mikrochim. Acta, 1969*, 62.
20. A.M. Bond and R.L. Martin, *Coord. Chem. Rev., 54*, 23 (1984).
21. R.P. Burns, F.P. McCullough, and C.A. McAuliffe, *Adv. Inorg. Chem. Radiochem., 23*, 211 (1980).
22. J.O. Hill and R.J. Magee, *Rev. Inorg. Chem., 3*, 141 (1981).
23. A.K. Sharma, *Thermochim. Acta, 104*, 339 (1986).
24. V.F. Plyusnin, V.P. Grivin, and S.V. Larionov, *Coord. Chem. Rev., 159*, 121 (1997).
25. L.I. Victoriano, *Coord. Chem. Rev., 196*, 383 (2000).
26. S. Fujii and T. Yoshimura, *Coord. Chem. Rev., 198*, 89 (2000).
27. R.J. Magee and J.O. Hill, *Rev. Anal. Chem., 8*, 5 (1985).
28. R.J. Magee, *Rev. Anal. Chem., 1*, 335 (1973).
29. K. Gleu and R. Schwab, *Angew. Chem., 62*, 320 (1950).
30. M. Delépine, *Bull. Soc. Chim. Fr.*, 5 (1958).
31. R. Schubart, Dithiocarbamic acid and derivatives, in *Ullman's Encycolpedia of Industrial Chemistry, 6th ed., Wiley-VCH, 745*, 10 (2003).
32. G.D. Thorn and R.A. Ludwig, *The Dithiocarbamates and Related Compounds*, Elsevier, New York, 1962.
33. W. Dietzsch, D.L. Boyd, D.L. Uhrich, N.V. Duffy, and E. Sinn, *Inorg. Chim. Acta, 169*, 157 (1990).
34. P. Deplano, E.F. Trogu, F. Bigoli, E. Leporati, M.A. Pellinghelli, D.L. Perry, R.J. Saxton, and L.J. Wilson, *J. Chem. Soc., Dalton Trans.*, 25 (1983).
35. W. Dietzsch, D.L. Boyd, D.L. Uhrich, and N.V. Duffy, *Inorg. Chim. Acta, 121*, 19 (1986).
36. B.J. McCormick, R. Bereman, and D. Baird, *Coord. Chem. Rev., 54*, 99 (1984).
37. D.B. Dell' Amico, F. Calderazzo, L. Labella, F. Marchetti, and G. Pampaloni, *Inorg. Chem. Commun., 5*, 733 (2002).
38. J.R. Dilworth and N. Wheatley, *Coord. Chem. Rev., 199*, 89 (2000).
39. I. Haiduc and L.Y. Goh, *Coord. Chem. Rev., 224*, 151 (2002).
40. E.R.T. Tiekink and G. Winter, *Rev. Inorg. Chem., 12*, 183 (1992).
41. S.R. Rao, *Xanthates and Related Compounds,* Marcel Dekker, New York, 1971.
42. K. Tang, X. Jin, and Y. Tang, *Rev. Heteroatom Chem., 15*, 83 (1996).
43. A. Shaver, M. El-Khateeb, and A.-M. Lebuis, *Inorg. Chem., 40*, 5288 (2001).
44. C. Ives, E.L. Fillis, and J.R. Hagadorn, *J. Chem. Soc., Dalton Trans.*, 527 (2003).
45. T. Kitson, *Ed. Chem.*, 43 (1985).
46. G. Vefforazzi, W.F. Almeida, G.J. Burin, R.B. Jaeger, F.R. Puga, A.F. Rahde, F.G. Reyes, and S. Schvartsman, *Teratog. Carcinog. Mutag., 15*, 313 (1995).
47. M.F. Rabbi, A. Finnegan, L. Al-Hartli, S. Strong, and K.A. Roebuck, *J. Aquired Immune Defic. Syndr. Hum. Retrovirol., 19*, 321 (1998).

48. S.M. Long, V.E. Laubach, C.G. Tribble, A.K. Kaza, S.M. Fiser, D.C. Cassada, J.A. Kern, and I.L. Kron, *J. Surgical Res., 112*, 12 (2003).
49. K.S. Siddiqi and N. Nishat, *Synth. React. Inorg. Met.-Org. Chem., 30*, 1505 (2000).
50. J. Granell, M.L.H. Green, V.J. Lowe, S.R. Marder, P. Mountford, G.C. Saunders, and N.M. Walker, *J. Chem. Soc., Dalton Trans.*, 605 (1990).
51. S. Thirumaran, V. Venkatachalam, and K. Ramalingam, *Transition Met. Chem., 22*, 89 (1997).
52. O.P. Pandey, S.K Sengupta, and S.C. Tripathi, *Mon. Chem., 116*, 431 (1985).
53. S. Srivastava, V. Srivastava, K. Chaturvedi, O.P. Pandey, and S.K. Sengupta, *Thermochim. Acta, 240*, 101 (1994).
54. P. Auzeloux, J. Papon, T. Masnada, M. Borel, M.F. Moreau, A. Veyre, R. Pasqualini, and J.C. Madelmont, *J. Label. Compd. Radiopharm., 42*, 325 (1999).
55. A. Terzis, S. Filippakis, D. Mentzafos, V. Petrouleas, and A. Malliaris, *Inorg. Chem., 23*, 334 (1984).
56. A.A. Ensafi and S. Abbasi, *Anal. Sci., 16*, 377 (2000).
57. A. Golcu, M. Dolaz, and S. Serin, *Turk J. Chem., 25*, 485 (2001).
58. G.N. Kaludjerovic, V.M. Djinovic, S.R. Trifunovic, I.M. Hodzic, and T.J. Sabo, *J. Serb. Chem. Soc., 67*, 123 (2002).
59. H.B. Singh, S. Maheshwariand H. Tomer, *Thermochim. Acta, 64*, 47 (1983).
60. H.B. Singh, S. Maheshwari, S. Srivastava, and V. Rani, *Synth. React. Inorg. Met.-Org. Chem., 12*, 659 (1982).
61. R.A. Haines and S.M.F. Chan, *Inorg. Chem., 18*, 1495 (1979).
62. P.D. Beer, N.G. Berry, A.R. Cowley, E.J. Hayes, E.C. Oates, and W.W.H. Wong, *Chem. Commun.*, 2408 (2003).
63. F.Calderazzo, I.P. Mavani, D. Vitali, I. Bernal, J.D. Korp, and J.L. Atwood, *J. Organomet. Chem., 160*, 207 (1978).
64. F. Calderazzo, G. Dell'Amico, R. Netti, and M. Pasquali, *Inorg. Chem., 17*, 471 (1978).
65. K.J. Cavell, J.O. Hill, and R.J. Magee, *J. Inorg. Nucl. Chem., 41*, 1277 (1979).
66. K.J. Cavell, J.O. Hill, and R.J. Magee, *Thermochim. Acta, 33*, 377 (1979).
67. M.M. Jones, L.T. Burka, M.E. Hunter, M. Basinger, G. Campo, and A.D. Weaver, *J. Inorg. Nucl. Chem., 42*, 775 (1980).
68. E.A. Castro, R. Cortés, J.G. Santos, and J.C. Vega, J. Org. Chem., *47*, 3774 (1982).
69. E.A. Castro, S.A. Pena, J.G. Santos, and J.C. Vega, *J. Org. Chem., 49*, 863 (1984).
70. P. Vella and J. Zubieta, *J. Inorg. Nucl. Chem., 40*, 477 (1978).
71. E.J. Kupchick and P.J. Calabretta, *Inorg. Chem., 4*, 973 (1965).
72. R.D. Bereman and D. Nalewajek, *Inorg. Chem., 17*, 1085 (1978).
73. C.T. Vance and R.D. Bereman, *Inorg. Chim. Acta, 149*, 85 (1988).
74. A. Tavlaridis and R.Z. Neeb, *Z. Anal. Chem., 292*, 199 (1978).
75. A. Tavlaridis and R.Z. Neeb, *Z. Anal. Chem., 292*, 135 (1978).
76. K.J. Cavell, R.J. Magee, and J.O. Hill, *J. Inorg. Nucl. Chem., 41*, 1281 (1979).
77. J. Hrouzek, J. Krupcik, and I. Skacani, *Chem. Papers, 52*, 662 (1998).
78. K.E. Laintz, J.J. Yu, and C.M. Wai, *Anal. Chem., 64*, 311 (1992).
79. K. Kristsotakis and H.J. Tobschall, Frensius Z. Anal. Chem., *320*, 152 (1985).
80. S.K. Aggarwal, M. Kinter, M.R. Wills, J. Savory, and D.A. Herold, Anal. Chem., *61*, 1099 (1989).

81. M. Ashraf-Khorassani, M.T. Combsand L.T. Taylor, *Talanta, 44*, 755 (1997).
82. G.P. Foy and G.E. Pacey, *Talanta, 51*, 339 (2000).
83. L. Sucre and W. Jennings, *Anal. Lett., 13*, 497 (1980).
84. K.G. Moloy, *Inorg. Chem., 27*, 677 (1988).
85. G. Li, H. Tajima, and T. Ohtani, *J. Org. Chem., 62*, 4539 (1997).
86. C. C. Hadjikostas, G. A. Katsoulos, and S. K. Shakhatreh, *Inorg. Chim. Acta, 133*, 129 (1987).
87. A.N. Vasiliev and A.D. Polackov, *Molecules, 5*, 1014 (2000).
88. M. George and R.G. Weiss, *Langmuir, 19*, 8168 (2003).
89. M. George and R.G. Weiss, *J. Am. Chem. Soc., 123*, 10393 (2001).
90. M. George and R.G. Weiss, *Langmuir, 19*, 1017 (2003).
91. E. Humeres, N.A. Debacher, J.D. Franco, B.S. Lee, and A. Martendal, *J. Org. Chem., 67*, 3662 (2002).
92. B.B. Kaul and K.B. Pandeya, *J. Inorg. Nucl. Chem., 40*, 1035 (1978).
93. S.M. Losanitsch, *Berchte, 40*, 2970 (1907).
94. R.M. Ottenbrite, *J. Chem. Soc., Perkin Trans. 1*, 88 (1972).
95. B.B. Kaul and K.B. Pandeya, *J. Inorg. Nucl. Chem., 40*, 229 (1978).
96. H.S. Booth, *Inorg. Synth., 3*, 48 (1939).
97. A.W. Hofmann, *Berchte, 5*, 241 (1872).
98. L.C.A. Thompson and R.O. Moyer, *J. Inorg. Nucl. Chem., 27*, 2225 (1965).
99. A. Ya. Yakubovich and V.A. Klimova, *Zh. Obschei Khim. USSR, 34*, 1777 (1939).
100. W. Haas and T. Schwarz, *Mikrochim. Acta, 2*, 251 (1963).
101. H.L. Klöpping and G.J.M. van der Kerk, *Rec. Trav. Chim. Pays-Bas., 70*, 957 (1951).
102. T.C.W. Mak, K.S. Jasim, and C. Chieh, *Can. J. Chem., 62*, 808 (1984).
103. A.F. Fabretti, F. Forghieri, A. Giusti, C. Preti, and G. Tosi, *Spectrochim. Acta A, 40*, 343 (1984).
104. G. Hogarth and S. Faulkner, unpublished results.
105. D. Guérin, R. Carlier, and D. Lorcy, *J. Org. Chem., 65*, 6069 (2000).
106. D. Guérin, R. Carlier, M. Guerro, and D. Lorcy, *Tetrahedron, 59*, 5253 (2003).
107. R.N. Zagidullin, *Zh. Priklad. Khimii, 60*, 1829 (1987).
108. R.N. Zagidullin and P.O. Sterlitamaks, *Khim. Geterot. Soedin., 11*, 1524 (1989).
109. K.S. Siddiqi, F.M.A.M. Aqra, S.A. Shah, and S.A.A. Zaidi, *Synth. React. Inorg. Met.-Org. Chem., 23*, 685 (1993).
110. A. Ya Yakubovitch and V.A. Klimova, *J. Gen. Chem. U.S.S.R., Eng. Transl., 9*, 1777 (1939).
111. J. Dunderdale and T.I. Watkins, *Chem. Ind.(London)*, 174 (1956).
112. H. Nishimura and T. Kinugasa, *Chem. Pharm. Bull., 17*, 94 (1969).
113. A.F. McKay and W.B. Hatton, *J. Am. Chem. Soc., 78*, 1618 (1956).
114. A.W. Frank, *Appl. Spectrosc., 36*, 282 (1982).
115. N. Bellec, D. Lorcy, and A. Roberts, *Synthesis*, 1442 (1998).
116. Y.P. Tian, C.Y. Duan, Z.L. Lu, X.Z. You, H.K. Fun, and B.C. Yip, *Polyhedron, 15*, 1495 (1996).
117. G. Gattow and S. Lotz, *Z. Anorg. Allg. Chem., 531*, 101 (1985).
118. G. Gattow and S. Lotz, *Z. Anorg. Allg. Chem., 531*, 97 (1985).
119. A.I. El-Said, A.S.A. Zidan, M.S. El-Meligy, A.A.M. Aly, and O.F. Mohammed, *Transition Met. Chem., 26*, 13 (2001).

120. A.W. Frank, *Phosphorus, Sulfur Silicon Relat. Elem., 54*, 109 (1990).
121. B. Macías, M.V. Villa, E. Chicote, S. Martín-Velasco, A. Castiñeiras, and J. Borrás, *Polyhedron, 21*, 1899 (2002).
122. M. Castillo, J.J. Criado, B. Macías, and M.V. Vaquero, *Inorg. Chim. Acta, 124*, 127 (1986).
123. B. Macías, M.V. Villa, M. Martin-Simon, L. Rodriguez, and J. Licesio, *Transition Met. Chem., 24*, 533 (1999).
124. B. Macías, J.J. Craido, M.V. Villa, and M. Castillo, *Spec. Lett., 26*, 829 (1993).
125. B. Macías, P. Malet, R. Paradinas, V. Rives, and M.V.Villa, *Inorg. Chim. Acta, 288*, 127 (1999).
126. B. Macías, J.J. Criado, M.V. Villa, L.J. Rodriguez, and M. Castillo, *Polyhedron, 12*, 2791 (1993).
127. B. Macías, J.J. Criado, M.V. Villa, M.R. Iglesias, and M. Castillo, *Polyhedron, 12*, 501 (1993).
128. V. Lakshmanan, M.R.Udupa, and K.S. Nagaraja, *Polyhedron, 11*, 1387 (1992).
129. M. Castillo, A. Criado, R. Guzman, J.J. Criado, and B. Macías, *Transition Met. Chem., 12*, 225 (1987).
130. K. Sridharan and S. Muthuswamy, *J. Indian Chem. Soc., 70*, 833 (1993).
131. R. Cao, N. Travieso, A. Fragoso, R. Villalonga, A. Diaz, M.E. Martinez, J. Alpizar, and D.X. West, *J. Inorg. Biochem., 66*, 213 (1997).
132. S. Thirumaran and K. Ramalingam, *Transition Met. Chem., 25*, 60 (2000).
133. J.J. Criado, B. Macías, and M. Castillo, *Thermochim. Acta, 127*, 101 (1988).
134. J.J. Criado, R.L. Decegama, B. Macías, and M. Castillo, *Recl. Trav. Chim. Pays-Bas-J. R. Neth. Chem. Soc., 106*, 426 (1987).
135. M. Castillo, J.J. Criado, B. Macías, and M.V. Vaquero, *Transition Met. Chem., 11*, 476 (1986).
136. B. Macías, M.V. Villa, A. Mateos, and M. Paramo, *J. Coord. Chem., 46*, 71 (1998).
137. B. Macías, M.V. Villa, and M.R. Rodriguez-Gallego, *Transition Met. Chem., 20*, 347 (1995).
138. S. Wajda and K. Drabent, *Pol. J. Chem., 53*, 973 (1979).
139. S.-P. Huang, K.J. Franz, E.H. Arnold, J. Devenyi, and R.H. Fish, *Polyhedron, 15*, 4241 (1996).
140. P.C.H. Mitchell and M.G. Taylor, *Polyhedron,1*, 225 (1982).
141. R.S. Murthy and D.E. Ryan, *Anal. Chim. Acta, 140*, 163 (1982).
142. M.T. Suzuki and T. Yokoyama, *Polyhedron, 2*, 127 (1983).
143. B. Mathew and V. N. R. Pillai, *Eur. Polym. J., 30*, 61 (1994).
144. S.C. Lezzi and S. Cobianco, *J. Appl. Polym. Sci., 54*, 889.
145. K.A. Venkatesan, T.G. Srinivasan, and P.R.V. Rao, *Sep. Sci. Technol., 37*, 1417 (2002).
146. E. Humeres, E. De Souza, N.A. Debacher, and A.E. Aliev, *J. Phys. Org. Chem., 15*, 852 (2002).
147. I. Ymén, *Acta Crystallogr., Sect. C, 40*, 33 (1984).
148. Å. Oskarsson and I. Ymén, *Acta Crystallogr., Sect. C, 39*, 66 (1983).
149. I. Ymén, *Acta Crystallogr., Sect. B, 38*, 2671 (1982).
150. I. Ymén, *Acta Crystallogr., Sect. C, 39*, 874 (1983).
151. J. Albertsson, Å. Oskarsson, K. Stahl, C. Svensson, and I. Ymén, *Acta Crystallogr., Sect. B, 36*, 3072 (1980).
152. D.A. Cook, S.J. Coles, M.B. Hursthouse, and D.J. Price, *Z. Anorg. Allg. Chem., 629*, 192 (2003).
153. J.-P. Legros, D. Troy, and J. Galy, *Acta Crystallogr., Sect. C, 40*, 801 (1984).

154. V. Vrábel, Š. Gergely, J. Lojak, E. Kellö, and J. Garaj, *Acta Crystallogr., Sect. C, 43*, 2293 (1987).
155. S.P. Ewing, D. Lockshon, and W.P. Jencks, *J. Am. Chem. Soc., 102*, 3072 (1980).
156. E. Humeres, N.A. Debacher, M.M. de Sierra, J.D. Franco, and A. Schultz, *J. Org. Chem., 63*, 1598 (1998).
157. E. Humeres, N.A. Debacher, and M.M. de Sierra, *J. Org. Chem., 64*, 1807 (1999).
158. E.T.G. Cavalheiro and G.O. Chierice, *J. Braz. Chem. Soc., 8*, 53 (1997).
159. P.A. Antunes, S.T. Breviglieri, G.O. Chierice, and E.T.G. Cavalheiro, *J. Braz. Chem. Soc., 12*, 473 (2001).
160. F.F. Jian, D. Zhu, H.-K. Fun, K. Chinnakali, I.A. Razak, and X.You, *Acta Crystallogr. Sect. C, Cryst. Struct. Commun., 55,* 940 (1999).
161. L.B. Aubin, T.M. Wagner, J.D. Thoburn, B.S. Kesler, K.A. Hutchison, R.R. Schumaker, and J.P. Parakka, *Org. Lett., 3*, 3413 (2001).
162. V.F. Plyusnin, E.P. Kuznetzova, G.A. Bogdanchikov, V.P. Grivin, V.N. Kirichenko, and S.V. Larionov, *J. Photochem. Photobiol. A: Chem., 68*, 299 (1992).
163. A.M. Bond, R. Colton, A.F. Hollenkamp, B.F. Hoskins, and K. McGregor, *J. Am. Chem. Soc., 109*, 1969 (1987).
164. G. Crank and A. Mursyidi, *J. Photochem. Photobiol. A: Chem., 68*, 289 (1992).
165. M. Lieder, *Phosphorus, Sulfur Silicon Relat. Elem., 178*, 179 (2003).
166. H.L.M. van Gaal, J.W. Diesveld, F.W. Pijpers, and J.G.M. van der Linden, *Inorg. Chem., 18*, 3251 (1979).
167. T.S. Waraich, R.C. Gaur, K.B. Pandeya, and R.P. Singh, *J. Indian Chem. Soc., 59*, 103 (1982).
168. M. Mylrajan, *J. Mol. Struct., 348*, 257 (1995).
169. A.J.Deeming, C.Forth, and G. Hogarth, unpublished results.
170. L.I. Victoriano, *Polyhedron, 19*, 2269 (2000).
171. E.R.T. Tiekink, X.F. Yan, and C.G. Young, *Aust. J. Chem., 45*, 897 (1992).
172. T.R. Halbert, L.L. Hutchings, R.Rhodes, and E.I. Stiefel, *J. Am. Chem. Soc., 108,* 6437 (1986).
173. I. Cuadrado and M. Morán, *Transition Met. Chem., 11*, 375 (1986).
174. D.A. Brown, W.K. Glass, and K.S. Jasim, *Inorg. Chim. Acta, 45*, L97 (1980).
175. D.A. Brown, W.K. Glass, and K.S. Jasim, *Chemical Uses for Molybdenum*, Proceedings of the International Conference, 4th, 156, 1982.
176. T.C.W. Mak, K.S. Jasim, and C. Chieh, *Angew. Chem., Int. Ed. Engl., 23*, 391 (1984).
177. T.C.W. Mak, K.S. Jasim, and C. Chieh, *Inorg. Chem., 24,* 1587 (1985).
178. C.G. Young, S.A. Roberts, and J.H. Enemark, *Inorg. Chim. Acta, 114*, L7 (1986).
179. C.G. Young, S.A. Roberts, and J.H. Enemark, *Inorg. Chem., 25*, 3667 (1986).
180. W.-H. Pan, T.R. Halbert, L.L. Hutchings, and E.I. Stiefel, *J. Chem. Soc., Chem. Commun.*, 927 (1985).
181. C.G. Young, T.O. Kocaba, X.F.Yan, E.R.T. Tiekink, L. Wei, H.H. Murray, III, C.L. Coyle, and E.I.Stiefel, *Inorg. Chem., 33*, 6252 (1994).
182. C.G. Young, M.A. Bruck, P.A. Wexler, M.D. Carducci, and J.H. Enemark, *Inorg. Chem., 31*, 587 (1992).
183. C.G. Young, M.A. Bruck, and J.H. Enemark, *Inorg. Chem., 31*, 593 (1992).
184. L. Wei, T.R. Halbert, H.H., Murray, III, and E.I. Stiefel, *J. Am. Chem. Soc., 112*, 6431 (1990).

185. H.H. Murray, L. Wei, S.E. Sherman, M.A. Greaney, K.A. Eriksen, B. Carstensen, T.R. Halbert, and E.I. Stiefel, *Inorg. Chem., 34*, 841 (1995).
186. A.T. Casey and A.M. Vecchio, *J. Coord. Chem., 16*, 375 (1988).
187. A.T. Casey and A.M. Vecchio, *Transition Met. Chem., 11*, 366 (1986).
188. S. Åkerström, *Arkiv Kemi, 14*, 403 (1959).
189. T. Tetsumi, M. Sumi, M. Tanaka, and T. Shono, *Polyhedron, 5*, 703 (1986).
190. T. Tetsumi, M. Sumi, M. Tanaka, and T. Shono, *Polyhedron, 5*, 707 (1986).
191. B.I. Kharisov, L.M. Blanco, M.V. Salinas, and A.D. Garnovskii, *J. Coord. Chem., 47*, 135 (1999).
192. W. Wessel, W. Tyrra, and D. Naumann, *Z. Anorg. Allg. Chem., 627*, 1264 (2001).
193. D.C. Bradley and M.H. Gitlitz, *J. Chem. Soc., Chem. Commun.*, 289 (1965).
194. R. Rossi, A. Marchi, A. Duatti, L. Magon, U. Casellato, and R. Graziani, *J. Chem. Soc., Dalton Trans.*, 899 (1988).
195. R. Kumar and D.G. Tuck, *Inorg. Chim. Acta, 157*, 51 (1989).
196. A.M.M. Lanfredi, F. Ugozzoli, and A. Camus, *J. Chem. Crystallogr., 26*, 141 (1996).
197. O.R. Rodig, T. Brueckner, B.K. Hurlburt, R.K. Schlatzer, T.L. Venable, and E. Sinn, *J. Chem. Soc., Dalton Trans.*, 196 (1981).
198. K.-H. Yih, S.-C. Chen, Y.-C. Lin, G.H. Lee, and Y. Wang, *J. Organomet. Chem., 494*, 149 (1995).
199. H. Barrera and J. Suades, *Transition Met. Chem., 9*, 255 (1984).
200. R. Usón, J. Fornies, P. Espinet, and E. Lalinde, *J. Organomet. Chem., 334*, 399 (1987).
201. C. C. Hadjikostas, G. A. Katsoulos, M. P. Sigalas, and C. A. Tsipis, *Inorg. Chim. Acta, 163*, 173 (1989).
202. D.E. Schwarz and T.B. Rauchfuss, *Chem. Commun.*, 1123 (2000).
203. R.W. Light, L.D. Hutchins, R.T. Paine, and C.F. Campana, *Inorg. Chem., 19*, 3597 (1980).
204. S.I. Klein, A.E. Mauro, M.A. Momesso, C.C. Porta, R.H.A. Santos, and M.T.P. Gambardella, *Quim. Nova, 10*, 314 (1987).
205. N.V. Duffy and K. Stankiewicz, *ACS Nat. Meet., New Orleans, CHED666* (2003).
206. G. Faraglia, L. Sindellari, and S. Sitran, *Thermochim. Acta, 161*, 63 (1990).
207. G. Faraglia and S. Sitran, *Inorg. Chim. Acta, 176,* 67 (1990).
208. H.W. Roesky, B. Meller-Rehbein, and M. Noltemeyer, *Z. Naturforsch. Sect. B., 46*, 1117 (1991).
209. B. Meller-Rehbein, H.W. Roesky, and M. Noltemeyer, *Chem. Ber., 124*, 523 (1991).
210. L.S. Tan,G.V. Goeden, and B.L.Haymore, *Inorg. Chem., 22*, 1744 (1983).
211. R.D. Adams and M. Huang, *Organometallics, 15*, 2125 (1996).
212. R.D. Adams and M.S. Huang, *Polyhedron, 17*, 2759 (1998).
213. J. Li, D. Miguel, D. Morales, V. Riera, A. Aguirre-Pérez, and S. García-Granda, *J. Chem. Soc., Dalton Trans.*, 3264 (2003).
214. R.J. Angelici and R.G.W. Gingerich, *Organometallics, 2*, 89 (1983).
215. F. Sato, K. Nakamura, and M. Sato, *J. Organomet. Chem., 67*, 141 (1974).
216. J. Vincente, M.T. Chicote, M.D. Abrisqueta, P. González-Herrero, and R. Guerrero, *Gold Bull., 31*, 126 (1998).
217. I. Kovács, A.-M. Lebuis, and A. Shaver, *Organometallics, 20*, 35 (2001).

218. C. Bianchini, C.A. Ghilardi, A. Meli, S. Midollini, and A. Orlandini, *J. Organomet. Chem., 255*, C27 (1983).
219. C. Bianchini, C.A. Ghilardi, A. Meli, S. Midollini, and A. Orlandini, *Inorg. Chem., 24*, 932 (1985).
220. G. Ferguson, D. O'Connell, and T.R. Spalding, *Acta Crystallogr., Sect. C, 50*, 1432 (1994).
221. R. Rossi, A. Marchi, L. Magon, U. Casellato, and R. Graziani, *J. Chem. Res., 78*, 674 (1990).
222. R. Rossi, A. Marchi, A. Duatti, L. Magon, U. Casellato, and R. Graziani, *J. Chem. Soc., Dalton Trans.*, 2299 (1987).
223. J.P.Fackler, Jr., D. Coucouvanis, W.C. Seidel, R.C. Masek, and W. Holloway, *J. Chem. Soc., Chem. Commun.*, 924 (1967).
224. J.P.Fackler, Jr., and W.C. Seidel, *Inorg. Chem., 8*, 1631 (1969).
225. A. Vizi-Orosz and L. Markó, *Transition Met. Chem., 11*, 408 (1986).
226. C. Bianchini, C. Mealli, A. Meli, and G. Scapacci, *J. Chem. Soc., Dalton Trans.*, 799 (1982).
227. S.C. Sendlinger, J.R. Nicolson, E.B. Lobkovsky, J.C. Huffman, D. Rehder, and G. Christou, *Inorg. Chem., 32*, 204 (1993).
228. D.C. Bradley, I.F. Rendall, and K.D. Sales, *J. Chem. Soc., Dalton Trans.*, 2228 (1973).
229. K.-H. Yih, Y.-C. Lin, M.-C. Cheng, and Y. Wang, *J. Chem. Soc., Dalton Trans.*, 1305 (1995).
230. E.J. Fernandez, J.M. Lopez-de-Luzuriaga, M. Monge, E. Olmos, M.C. Gimeno, A. Laguna, and P.G. Jones, *Inorg. Chem., 37*, 5532 (1998).
231. A.M. Bond, R. Colton, D.A. Fiedler, J.E. Kevekordes, V. Tedesco, and T.F. Mann, *Inorg. Chem., 33*, 5761 (1994).
232. J.V. Dubrawski and R.D. Feltham, *Inorg. Chem., 19*, 355 (1980).
233. B.R. Cameron, M.C. Drakes, I.R. Baird, R.T. Skerlj, L. Santucci, and S.P. Fricker, *Inorg. Chem., 42*, 4102 (2003).
234. A. Coto, M.J. Tenorio, M.C. Puerta, and P. Valerga, *Organometallics, 17*, 4392 (1998).
235. C.S. Lai and E.R.T. Tiekink, *Appl. Organomet. Chem., 17*, 141 (2003).
236. S.Y.Ho and E. R. T. Tiekink, *Acta Crystallogr., Sect. E, 58*, m86 (2002).
237. S.Y. Ho and E. R. T. Tiekink, *Acta Crystallogr., Sect. E, 57*, m603 (2001).
238. J.W. Faamau and E.R.T. Tiekink, *J. Coord. Chem., 31*, 93 (1994).
239. E.J. Fernandez, J.M. Lopez-de-Luzuriaga, M. Monge, E. Olmos, A. Laguna, M.D. Villacampa, and P.G. Jones, *J. Clust. Sci., 11*, 153 (2000).
240. L.Y. Goh, Z. Weng, W.K. Leong, and P.H. Leung, *Organometallics, 21*, 4398 (2002).
241. M.F. Perpinan, L. Ballester, and A. Santos, *J. Organomet. Chem., 241*, 215 (1983).
242. M.F. Perpinan and A. Santos, *J. Organomet. Chem., 221*, 63 (1981).
243. E. Carmona, L. Contreras, M.L. Poveda, L.J. Sanchez, J.L. Atwood, and R.D. Rogers, *Organometallics, 10*, 61 (1991).
244. R.V. Parish, B.P. Howe, J.P. Wright, J. Mack, R.G. Pritchard, R.G. Buckley, A.M. Elsome, and S.P. Fricker, *Inorg. Chem., 35*, 1659 (1996).
245. R.V. Parish, J.P. Wright, and R.G. Pritchard, *J. Organomet. Chem., 596*, 165 (2000).
246. L.Y. Goh, Z. Weng, W.K. Leong, and P.H. Leung, *Angew. Chem., Int. Ed. Engl., 40*, 3236 (3236).
247. L.Y. Goh, Z. Weng, W.K. Leong, and P.H. Leung, *Organometallics, 21*, 4408 (2002).
248. H.H. Murray, G. Garzon, R.G. Raptis, A.M. Mazany, L.C. Porter, and J.P. Fackler Jr., *Inorg. Chem., 27*, 836 (1988).

249. J.H. Noordik, *Cryst. Struct. Commun., 2*, 81 (1973).

250. M. Ahmed and R.J. Magee, *Aust. J. Chem., 34*, 1861 (1981).

251. F. Forghieri, C. Preti, L. Tassi, and G. Tosi, *Polyhedron, 7*, 1231 (1988).

252. J.J. Criado, J.A. Lopezarias, B. Macías, L.R. Fernandezlago, and J.M. Salas, *Inorg. Chim. Acta, 193*, 229 (1992).

253. E.P. Cullen, J. Doherty, A.R. Manning, P. McArdle, and D. Cunningham, *J. Organomet. Chem., 348*, 109 (1988).

254. R. Colton, M.F. Mackay, and V. Tedesco, *Inorg. Chim. Acta, 207*, 227 (1993).

255. M.B. Hursthouse, M.A. Malik, M. Motevalli, and P. O'Brien, *Organometallics, 10*, 730 (1991).

256. M.A. Malik, P. O'Brien, and M. Motevalli, *Acta Crystallogr., Sect. C, 52*, 1931 (1996).

257. E.R.T. Tiekink, *J. Organomet. Chem., 322*, 1 (1987).

258. C.S. Lai and E.R.T. Tiekink, *Appl. Organomet. Chem., 17*, 194 (2003).

259. C. S.Lai and E. R. T. Tiekink, *Acta Crystallogr., Sect. E, 58*, m674 (2002).

260. M.M. Kubicki, R. Kergoat, J.E. Guerchais, R. Mercier, and J. Douglade, *J. Cryst. Mol. Struct., 11*, 43 (1981).

261. R. Kergoat, M.M. Kubicki, J.E. Guerchais, N.C. Norman, and A.G. Orpen, *J. Chem. Soc., Dalton Trans.*, 633 (1982).

262. F. Jian, L. Lu, X. Wang, S.S. Sundara Raj, I.A. Razak, and H.-K. Fun, *Acta Crystallogr., Sect. C, 56*, 939 (2000).

263. I.A. Razak, S. S. Sundara Raj, H.-K. Fun, F. Jian, F. Bei, X. Yang, L. Lu, and X. Wang, *Acta Crystallogr., Sect. C, 56*, 666 (2000).

264. S.-F. Lu, J.-Q. Huang, R.-M. Yu, X.-Y. Huang, Q.-J. Wu, Y. Peng, J. Chen, Z.-X. Huang, and D.-X. Wu, *Polyhedron, 20*, 2339 (2001).

265. A. Bino, F.A. Cotton, Z. Dori, and J.C. Sekutowski, *Inorg. Chem., 17*, 2946 (1978).

266. R. Cao, X.-J. Lei, M.-C. Hong, Z.-Y. Huang, and H.-Q. Liu, *Chinese J. Struct. Chem. (Jiegou Huaxue), 11*, 34 (1992).

267. A.M. Bradford, R.J. Puddephatt, G. Douglas, L. Manojlovic-Muir, and K.W. Muir, *Organometallics, 9*, 1579 (1990).

268. H.P. Zhu, Q.T. Liu, C.N. Chen, and D.X. Wu, *Inorg. Chim. Acta, 306*, 131 (2000).

269. Y.Deng, Q. Liu, Y. Yang, Y. Wang, Y. Cai, D. Wu, C. Chen, D. Liao, B. Kang, and J. Lu, *Inorg. Chem., 36,* 214 (1997).

270. J. Xu, J. Qian, Q. Wei, N. Hu, Z. Jin, and G. Wei, *Inorg. Chim. Acta, 164*, 55 (1989).

271. J.-Q. Xu, J.-S. Qian, Q. Wei, N.-H. Hu, Z.-S. Jin, and G.-C. Wei, *Huaxue Xuebao (Acta Chim. Sinica)(Chin.), 47*, 853 (1989).

272. S.-F. Lu, H.-B. Chen, J.-Q. Huang, Q.-J. Wu, Q.-L. Sun, J. Li, and J.-X. Lu, *Inorg. Chim. Acta, 232*, 43 (1995).

273. X. Lei, Z. Huang, M. Hong, Q. Liu and H.Liu, *Chinese J. Struct. Chem. (Jiegou Huaxue), 8*, 152 (1989).

274. Q. Liu, L. Huang, H. Liu, X. Lei, D. Wu, B. Kang, and J. Lu, *Inorg. Chem., 29*, 4131 (1990).

275. M. Bardají, N.G. Connelly, M.C. Gimeno, J. Jiménez, P.G. Jones, A. Laguna, and M.J. Laguna, *J. Chem. Soc., Dalton Trans.*, 1163 (1994).

276. M. Bardají, M.C. Gimeno, J. Jiménez, P.G. Jones, A. Laguna, and M.J. Laguna, *Organometallics, 13*, 3415 (1994).

277. D.D. Heinrich, R.J. Staples, and J.P.Fackler, Jr., *Inorg. Chim. Acta, 229*, 61 (1995).

278. M.-C. Hong, X.-J. Lei, Z.-Y. Huang, B.-S. Kang, F.-L. Jiang, and H.-Q. Liu, *Chin. Sci. Bull., 38*, 912 (1993).
279. M.A. Mansour, W.B. Connick, R.J. Lachicotte, H.J. Gysling, and R. Eisenberg, *J. Am. Chem. Soc., 120*, 1329 (1998).
280. P. Bishop, P. Marsh, A.K. Brisdon, B.J. Brisdon, and M.F. Mahon, *J. Chem. Soc., Dalton Trans.*, 675 (1998).
281. M.I. Khan, C. King, D.D. Heinrich, J.P. Fackler, Jr., and L.C. Porter, *Inorg. Chem., 28*, 2150 (1989).
282. S.K. Bhargva, F. Mohr, M.A. Bennett, L.L. Welling, and A.C. Willis, *Inorg. Chem., 40*, 4271 (2001).
283. M. Bardaji, A. Laguna, P.G. Jones, and A.K. Fischer, *Inorg. Chem., 39*, 3560 (2000).
284. D.D. Heinrich, J. Wang, and J.P. Fackler, Jr., *Acta Crystallogr., Sect. C, 46*, 1444 (1990).
285. A. Elduque, C. Finestra, J.A. Lopez, F.J. Lahoz, F. Merchan, L.A. Oro, and M.T. Pinillos, *Inorg. Chem., 37*, 824 (1998).
286. M. Cano, P. Ovejero, J.V. Heras, E. Pinilla, F.A. Ruiz, and A. Monge, *Polyhedron, 17*, 2115 (1998).
287. W.H. Leung, J.L.C. Chim, H.W. Hou, T.S.M. Hun, I.D. Williams, and W.T. Wong, *Inorg. Chem., 36*, 4432 (1997).
288. L.H. Pignolet and S.H. Wheeler, *Inorg. Chem., 19*, 935 (1980).
289. C. Landgrafe and W.S. Sheldrick, *J. Chem. Soc., Dalton Trans.*, 1885 (1994).
290. T. Furuhashi, M. Kawano, Y. Koide, R. Somazawa, and K. Matsumoto, *Inorg. Chem., 38*, 109 (1999).
291. H. Uemura, M. Kawano, T. Watanabe, T. Matsumoto, and K. Matsumoto*, Inorg. Chem., 31*, 5137 (1992).
292. W.-H. Leung, M.-C. Wu, J.L.C. Chim, and W.-T. Wong, *Inorg. Chem., 35*, 4801 (1996).
293. J.V. Kingston and G. Wilkinson, *J. Inorg. Nucl. Chem., 28*, 2709 (1966).
294. B.M. Mattson, J.R. Heiman, and L.H. Pignolet, *Inorg. Chem., 15*, 564 (1976).
295. L.J. Maheu, G.L. Miessler, J. Berry, M. Burow, and L.H. Pignolet, *Inorg. Chem., 22*, 405 (1983).
296. S.H. Wheeler and L.H. Pignolet, *Inorg. Chem., 19*, 972 (1980).
297. M. Ebihara, K. Tokoro, M. Maeda, M. Ogami, K. Imaeda, K. Sakurai, H. Masuda, and T. Kawamura, *J. Chem. Soc., Dalton Trans.*, 3621 (1994).
298. M. Ebihara, K. Tokoro, K. Imaeda, K. Sakurai, H. Masuda, and T. Kawamura, *J. Chem. Soc., Chem. Commun.*, 1591 (1992).
299. M. Ebihara, K. Sakurai, T. Kawamura, H. Katayama, H. Masuda, and T. Taga, *Chem. Lett.*, 415 (1990).
300. H. Brunner, A. Hollman, M. Zabel, and B. Nuber, *J. Organomet. Chem., 609*, 44 (2000).
301. J. Fornies, A. Martin, R. Navarro, V. Sicilia, P. Villarroya, and A.G. Orpen, *J. Chem. Soc., Dalton Trans.*, 3721 (1998).
302. J.A. Alden, A.M. Bond, R.Colton, R.G. Compton, J.C. Eklund, Y.A. Mah, P.J. Mahon, and V. Tedesco, *J. Electroanal. Chem., 447*, 155 (1998).
303. A.M. Bond, R. Colton, A. D'Agostino, J. Harvey, and J.C. Traeger, *Inorg. Chem., 32*, 3952 (1993).
304. R.G. Compton, J.C. Eklund, L. Nei, A.M. Bond, R. Colton, and Y.A. Mah, *J. Electroanal. Chem., 385*, 249 (1995).

305. A.M. Bond, R. Colton, Y. Ho, J.E. Moir, D.R. Mann, and R. Stott, *Inorg. Chem., 24*, 4402 (1985).
306. J.-P. Barbier, B.Mve Ondo, and R.P.Hugel, *J. Chem. Soc., Dalton Trans.*, 597 (1985).
307. A.M. Bond, A.R. Hendrickson, R.L. Martin, J.E. Moir, and D.R. Page, *Inorg. Chem., 22*, 3440 (1983).
308. M. Okuno, M. Kita, K. Kashiwabara, and J. Fujita, *Chem. Lett.*, 1643 (1989).
309. R.D. Webster, G.A. Heath, and A.M. Bond, *J. Chem. Soc., Dalton Trans.*, 3189 (2001).
310. A.M. Bond, R. Colton, and D.R. Mann, *Inorg. Chem., 28*, 54 (1989).
311. D.H.M.W. Thewissen and J.G.M. van der Linden, *Inorg. Chim. Acta, 52*, 225 (1981).
312. L.M. Engelhardt, P.C. Healy, B.W. Skelton, and A.H. White, *Aust. J. Chem., 42*, 885 (1989).
313. A.M. Bond, R. Colton, B.M. Gatehouse, and Y.A. Mah, *Inorg. Chim. Acta, 260*, 61 (1997).
314. A. Radha, M. Seshasayee, K. Radha, G. Aravamudan, and C. Subramanyam, *Acta Crystallogr. Sect. C, 41*, 1166 (1985).
315. E. Kello, V. Kettmann, and J. Garaj, *Collect. Czech. Chem. Commun., 49*, 2210 (1984).
316. F.F. Jian, Z.X.Wang, Z.P. Bai, X.Z. You, H.K. Fun, K. Chinnakali, and I.A. Razak, *Polyhedron, 18*, 3401 (1999).
317. S.C. Ngo, K.K. Banger, M.J. DelaRosa, P.J. Toscano, and J.T. Welch, *Polyhedron, 22*, 1575 (2003).
318. N.V. Pervukhina, N.V. Podberezskaya, L.A. Patrina, and S.V. Larionov, *J. Struct. Chem., 30*, 694 (1989).
319. G. Hogarth, A. Pateman, and S.P. Redmond, *Inorg. Chim. Acta, 306*, 232 (2000).
320. M.R. Caira, K.R. Koch, and C. Sacht, *Acta Crystallogr., Sect.C, 47*, 26 (1991).
321. A.L.Spek, *Cryst. Struct. Commun., 8*, 577 (1979).
322. A.L.Spek, *Cryst. Struct. Commun., 11*, 613 (1982).
323. K.L. Brown, *Cryst. Struct. Commun., 8*, 157 (1979).
324. G.M. Larin, G.A. Zvereva, P.A. Koz'min, T.B. Larina, and M.D.Surazhskaya, *Izv. Akad. Nauk SSSR, Neorg. Mater., 20*, 530 (1984).
325. O.D. Fox, M.G.B. Drew, and P.D. Beer, *Angew. Chem., Int. Ed. Engl., 39*, 136 (2000).
326. P.D. Beer, N. Berry, M.G.B. Drew, O.D. Fox, M.E. Padilla-Tosta, and S. Patell, *Chem. Commun.*, 199 (2001).
327. D. Cardell and G. Hogarth, unpublished results.
328. R. Hesse and L. Nilson, *Acta Chem. Scand., 23*, 825 (1969).
329. R. Hesse, *Arkiv. Kem., 20*, 481 (1963).
330. H. Anacker-Eickhoff, R. Hesse, P. Jennische, and A. Wahlberg, *Acta Chem. Scand. Ser. A, 36*, 251 (1982).
331. M.J.S. Delgado and L.M.P. Diez, *Anal. Quim., Ser. B, 81*, 255 (1985).
332. R.C. Aggarwal, B. Singh, and M.K. Singh, *J. Indian Chem. Soc., 59*, 269 (1982).
333. K.N. Johri, N.K. Kaushik, R.K. Bajaj, and A.K. Sharma, *Acta Chim. Hung., 113*, 325 (1983).
334. N.K. Singh, C. Kaw, and N. Singh, *Bull. Chem. Soc. Jpn, 64*, 1440 (1991).
335. G.S. Sodhi and J. Kaur, *Z. Naturforsch, Teil. B, 47*, 1297 (1992).
336. G. Exarchos and S.D. Robinson, *Polyhedron, 16*, 1573 (1997).
337. K. McGrouther, D.K. Weston, D. Fenby, B.H. Robinson, and J. Simpson, *J. Chem. Soc., Dalton Trans.*, 1957 (1999).

338. D.C. Calabro and J.L. Burmeister, *Inorg. Chim. Acta, 53*, L47 (1981).
339. R.D. Bereman, G.D. Shields, and D. Nalewajek, *Inorg. Chem., 17*, 3713 (1978).
340. S. Trofimenko, *J. Org. Chem., 33*, 890 (1968).
341. G.A. Ardizzoia, M. Angaroni, G. La Monica, M. Moret, and N. Masciocchi, *Inorg. Chim. Acta, 185*, 63 (1991).
342. S. Mukhopadhyay, U. Mukhopadhyay, T.C.W. Mak, and D. Ray, *Inorg. Chem., 40*, 1057 (2001).
343. T.H. Rakna, *Transition Met. Chem., 23*, 101 (1998).
344. P.K. Gogoi and D.P. Phukan, *Proc. Indian Acad. Sci., 102*, 725 (1990).
345. P.K. Gogoi and D.P. Phukan, *Indian J. Chem. Sect. A, 28*, 1070 (1989).
346. P.C. Christidis, *Acta Crystallogr., Sect. C, 42*, 781 (1986).
347. R. Kellner, P. Prokopowski, and H. Malissa, *Anal. Chim. Acta, 68*, 401 (1974).
348. R.D. Bereman and D. Nalewajek, *Inorg. Chem., 11*, 2687 (1977).
349. W.P. Anderson and D.M. Baird, *Inorg. Chem., 27*, 3240 (1988).
350. R.S. Herrick, S.J. Nieter-Burgmayer, and J.L. Templeton, *Inorg. Chem., 22*, 3275 (1983).
351. R.D.Bereman, M.R.Churchill, and D.Nalewajek, *Inorg. Chem., 18*, 3112 (1979).
352. R.D. Bereman and D. Nalewajek, *J. Inorg. Nucl. Chem., 40*, 1313 (1978).
353. R.S. Herrick and J.L. Templeton, *Inorg. Chem., 25*, 1270 (1986).
354. R.D. Bereman, D.M. Baird, C.T. Vance, J. Hutchinson, and J. Zubieta, *Inorg. Chem., 22,* 2316 (1983).
355. D.M. Baird, P.E. Fanwick, and T. Barwick, *Inorg. Chem., 24*, 3753 (1985).
356. A.G. El A'mma and R.S. Drago, *Inorg. Chem., 16*, 2975 (1977).
357. K. Stahl and I. Ymén, *Acta Chem.Scand. Ser.A - Phys. Inorg. Chem.,* 37, 729 (1983).
358. P.C. Healy, J.W. Connor, B.W. Skelton, and A.H. White, *Aust. J. Chem., 43*, 1083 (1990).
359. P.C. Healy, J.V. Hanna, N.V. Duffy, B.W. Skelton, and A.H. White, *Aust. J. Chem., 43*, 1335 (1990).
360. W. Dietzsch, N.V. Duffy, G.A. Katsoulos, and B. Olk, *Inorg. Chim. Acta, 184*, 89 (1991).
361. N. Juranic, *Coord. Chem. Rev., 96*, 253 (1989).
362. N. Juranic, *J. Chem. Phys., 74*, 3690 (1981).
363. C.E. Schäffer, *Proc. R. Soc. London, Ser. A, 297*, 96 (1967).
364. P.J. Heard, K. Kite, J.S. Nielsen, and D.A. Tocher, *J. Chem. Soc., Dalton Trans.*, 1349 (2000).
365. R.C. Fay, *Coord. Chem. Rev., 154*, 99 (1996).
366. R.C. Fay, J.R. Weir, and A.H. Bruder, *Inorg. Chem., 23*, 1079 (1984).
367. H.-M. Gau and R.C. Fay, *Inorg. Chem., 26*, 3701 (1987).
368. D.F. Lewis and R.C. Fay, *J. Am. Chem. Soc., 96*, 3843 (1974).
369. R.S. Herrick and J.L. Templeton, *Organometallics, 1*, 842 (1982).
370. C.G. Young, T.O. Kocaba, M. Sadek, R.T.C. Brownlee, and E.R.T. Tiekink, *Aust. J. Chem., 47*, 2075 (1994).
371. B.M. Mattson, A.E. Madera, and M.C. Palazzotto, *J. Coord. Chem., 13*, 321 (1984).
372. M. Moriyasu, Y. Hashimoto, and M. Endo, *Bull. Chem. Soc. Jpn., 56*, 1972 (1983).
373. A. Ariafard, M.D. Asli, H. Aghabozorg, H. Aghabozorg, and M. Monajjemi, *J. Mol. Struct. (Theochem), 636*, 49 (2003).
374. G.A. Katsoulos, M. Lalia-Kantouri, C.C. Hadjikostas, and P. Kokorotsikos, *Thermochim. Acta, 149*, 331 (1989).

375. G. A. Katsoulos, G. E. Manoussakis, and C. A. Tsipis, *Inorg. Chim. Acta, 30*, L295 (1978).
376. G. A. Katsoulos, G. E. Manoussakis, and C. A. Tsipis, *Polyhedron, 3*, 735 (1984).
377. G. A. Katsoulos, I. A. Tossidis, M. P. Sigalas, C. C. Hadjikostas, and E. Diemann, *Thermochim. Acta,158*, 23 (1990).
378. C. A. Tsipis, I. J. Meleziadis, D. P. Kessissoglou, and G. A. Katsoulos, *Inorg. Chim. Acta, 90*, L19 (1984).
379. C.A. Tsipis, D.P. Kessissoglou, and G.E. Manoussakis, *Inorg. Chim. Acta, 65*, L137 (1982).
380. P.C. Christidis and P.J. Rentzeperis, *Acta Crystallogr., Sect. B, 35*, 2543 (1979).
381. G. A. Katsoulos and C. A. Tsipis, *Inorg. Chim. Acta, 84*, 89 (1984).
382. S.H. Simonsen and J.W. Ho, *Acta Crystallogr., 6*, 430 (1953).
383. A.G. Orpen, L. Brammer, F.H. Allen, O. Kennard, D.G. Watson, and R. Taylor, *J. Chem. Soc., Dalton Trans.*, S1 (1989).
384. M. Colapietro, A. Vaciago, D.C. Bradley, M.B. Hursthouse, and I.F. Rendall, *J. Chem. Soc., Dalton Trans.*, 1052 (1972).
385. H.-P. Zhu, Y.-H. Deng, X.-Y. Huang, C.-N. Chen, and Q.-T. Liu, *Acta Crystallogr., Sect. C, 53,* 692 (1997).
386. C.L. Raston and A.H. White, *Aust. J. Chem., 30*, 2091 (1977).
387. R.L. Elliot, B.O. West, M.R. Snow, and E.R.T. Tiekink, *Acta Crystallogr., Sect.C, 42*, 763 (1986).
388. P.C. Healy and A.H. White, *J. Chem. Soc., Dalton Trans.*, 1883 (1972).
389. J.G. Leipoldt and P. Coppens, *Inorg. Chem., 12*, 2269 (1973).
390. T. Brennan and I. Bernal, *J. Phys. Chem., 73*, 443 (1969).
391. S. Merlino, *Acta Crystallogr., Sect. B, 24*, 1441 (1968).
392. D.-Y. Kong, Q. Zhu, Y.-Y. Xie, and X.-Y. Huang, *Chinese J. Struct. Chem. (Jiegou Huaxue), 17*, 337 (1998).
393. F.F. Jian, F.L. Beia, P.S. Zhao, X. Wang, H.K. Fun, and K. Chinnakali, *J. Coord. Chem., 55*, 429 (2002).
394. M. Bonamico, G. Dessy, C. Mariani, A. Vaciago, and L. Zambonelli, *Acta Crystallogr., 19*, 619 (1965).
395. M.N.I. Khan, J.P. Fackler, Jr., H.H.Murray, D.D. Heinrich, and C.Campana, *Acta Crystallogr., Sect. C, 43*, 1917 (1987).
396. R. Selvaraju, K. Panchanatheswaran, A. Thiruvalluvar, and V. Parthasarathi, *Acta Crystallogr., Sect. C, 51*, 606 (1995).
397. A.K. Mohamed, N. Auner, and M. Bolte, *Acta Crystallogr., Sect. E, 59*, m188 (2003).
398. M. Bonamico, G. Dessy, A. Mugnoli, A. Vaciago, and L. Zambonelli, *Acta Crystallogr., 19*, 886 (1965).
399. B.H. O'Connor, *Acta Crystallogr., 21*, 828 (1966).
400. M. Motevalli, P. O'Brien, J.R. Walsh, and I.M. Watson, *Polyhedron, 15*, 2801 (1996).
401. J.A. McCleverty, N.J. Morrison, N. Spencer, C.C. Ashworth, N.A. Bailey, M.R. Johnson, J.M.A. Smith, B.A. Tabbiner, and C.R. Taylor, *J. Chem. Soc., Dalton Trans.*, 1945 (1980).
402. A.H. Bruder, R.C. Fay, D.F. Lewis, and A.A. Sayler, *J. Am. Chem. Soc., 98*, 6932 (1976).
403. M.G.B. Drew, D.A. Rice, and D.M.Williams, *J. Chem. Soc., Dalton Trans.*, 1821 (1985).
404. J.G.M. van der Aalsvoort and P.T. Beurskens, *Cryst. Struct. Commun., 3*, 653 (1974).

405. J. Baldas, J. Bonnyman, P.M. Pojer, G.A. Williams, and M.F. Mackay, *J. Chem. Soc., Dalton Trans.*, 451 (1982).
406. L.H. Pignolet, *Inorg. Chem., 13*, 2051 (1974).
407. C.L. Raston and A.H. White, *J. Chem. Soc., Dalton Trans.*, 2425 (1975).
408. P.T. Beurskens, J.A. Cras, T.W. Hummelink, and J.H. Noordik, *J. Cryst. Mol. Struct., 1*, 253 (1971).
409. M. Maekawa, M. Munakata, T. Kuroda-Sowa, and M. Motokawa, *Anal. Sci., 10*, 977 (1994).
410. A. Domenicano, L. Torelli, A. Vaciago, and L. Zambonelli, *J. Chem. Soc. A*, 1351 (1968).
411. C.M. Dee and E.R.T. Tiekink, *Z. Kristallogr., 217*, 85 (2002).
412. S.M. Zemskova, L.A. Glinskaya, R.F. Klevtsova, M.A. Fedotov, and S.V. Larionov, *Zh.Strukt.-Khim., 40*, 340 (1999); *J. Struct. Chem., 40*, 284 (1999).
413. L.A. Glinskaya, S.M. Zemskova, R.F. Klevtsova, S.V. Larionov, and S.A. Gromilov, *Polyhedron, 11*, 2951 (1992).
414. R. Baggio A. Frigerio, E.B. Halac D. Vega, and M. Perec, *J. Chem. Soc., Dalton Trans.*, 1887 (1992).
415. J.A. McCleverty, S. Gill, R.S.Z. Kowalski, N.A. Bailey, H. Adams, K.W. Lumbard, and M.A. Murphy, *J. Chem. Soc., Dalton Trans.*, 493 (1982).
416. D.F. Lewis and R.C. Fay, *Inorg. Chem., 15*, 2219 (1976).
417. J.G. Wijnhoven, *Cryst. Struct. Commun., 2*, 637 (1973).
418. S.R. Fletcher and A.C. Skapski, *J. Chem. Soc., Dalton Trans.*, 486 (1974).
419. C.L. Raston and A.H. White, *J. Chem. Soc., Dalton Trans.*, 32 (1976).
420. A.T. Baker and M.T. Emett, *Aust. J. Chem., 45*, 429 (1992).
421. U. Abram, *Z. Anorg. Allg. Chem., 626*, 619 (2000).
422. M. Hong, Z. Huang, X. Lei, F. Jiang, and H. Liu, *Acta Crystallogr., Sect. C, 48*, 1101 (1992).
423. P.C. Healy and A.H. White, *J. Chem. Soc., Dalton Trans.*, 284 (1973).
424. H. Iwasaki, *Acta Crystallogr., B29*, 2115 (1973).
425. G. St. Nikolov, *J. Inorg. Nucl. Chem., 43*, 3131 (1981).
426. J.C. Dewan, D.L. Kepert, C.L. Raston, D. Taylor, A.H. White, and E.N. Maslen, *J. Chem. Soc., Dalton Trans.*, 2082 (1973).
427. F. Montilla, A. Pastor, A. Monge, E. Gutierrez-Puebla, and A.Galindo, *J. Chem. Soc., Dalton Trans.*, 2893 (1999).
428. Y. Do and R.R. Holm, *Inorg. Chim. Acta, 104*, 33 (1985).
429. J.R. Dilworth, R.A. Henderson, A. Hills, D.L. Hughes, C. MacDonald, A.N. Stephens, and D.R.M.Walton, *J. Chem. Soc., Dalton Trans.*, 1077 (1990).
430. X.F. Yan, L. Fox, E.R.T. Tiekink, and C.G. Young, *J. Chem. Soc., Dalton Trans.*, 1765 (1994).
431. E.J. Peterson, R.B. Von Dreele, and T.L. Brown, *Inorg. Chem., 17*, 1410 (1978).
432. M.G.B. Drew, D.M. Williams, and D.A. Rice, *Inorg. Chim. Acta, 89*, L19 (1984); M.G.B. Drew, D.A. Rice, and D.M. Williams, *J. Chem. Soc., Dalton Trans.*, 1821 (1985).
433. M.B. Hursthouse and M. Motevalli, *J. Chem. Soc., Dalton Trans.*, 1362 (1979).
434. S.B. Seymore and S.N. Brown, *Inorg. Chem., 40*, 6676 (2001).
435. J. Dirand, L. Richard, and R. Weiss, *Transition Met. Chem., 1*, 2 (1975).
436. M. Decoster, F. Conan, Y. Le Mest, J. Sala-Pala, A. Leblanc, P. Molinie, E. Faulques, and L. Toupet, *New J. Chem., 21*, 215 (1997).

437. M.W. Bishop, J. Chatt, J.R. Dilworth, B.D. Neaves, P. Dahlstrom, J. Hyde, and J. Zubieta, *J. Organomet. Chem., 213*, 109 (1981).
438. M. Minelli, M. Le Hoang, M. Kraus, G. Kucera, J. Loertscher, M. Reynolds, N. Timm, M.Y. Chiang, and D. Powell, *Inorg. Chem., 41*, 5954 (2002).
439. G. Hogarth and I. Richards, unpublished results.
440. G.A. Williams, and A.R.P. Smith, *Aust. J. Chem., 33*, 717 (1980).
441. P.C. Riveros, I.C. Perilla, A. Poveda, H.J. Keller, and H. Pritzkow, *Polyhedron, 19*, 2327 (2000).
442. T.A. Coffey, G.D. Forster, and G. Hogarth, *Acta Crystallogr., Sect.C, 52*, 2157 (1996).
443. T.F. Brennan and I. Bernal, *Inorg. Chim. Acta, 7*, 283 (1973).
444. J.A. Broomhead, N.S. Gill, B.C. Hammer, and M. Sterns, *J. Chem. Soc., Chem. Commun.*, 1234 (1982).
445. M.A. Halcrow, J.C. Huffman, and G. Christou, *Inorg. Chem., 33*, 3639 (1994).
446. N. Dupre, H.M.J. Hendriks, and J. Jordanov, *J. Chem. Soc., Dalton Trans.*, 1463 (1984).
447. U. Abram, S. Abram, and J.R. Dilworth, *Z. Anorg. Allg. Chem., 622*, 1257 (1996).
448. S. Ritter and U. Abram, *Z. Anorg. Allg. Chem., 620*, 1443 (1994).
449. D.V. Griffiths, S.J. Parrot, M. Togrou, J.R. Dilworth, Y. Zheng, S. Ritter, and U.Abram, *Z. Anorg. Allg. Chem., 624*, 1409 (1998).
450. L.H. Doerrer, A.J. Graham, and M.L.H. Green, *J. Chem. Soc., Dalton Trans.*, 3941 (1998).
451. S. Ritter and U. Abram, *Inorg. Chim. Acta, 231*, 245 (1995).
452. U. Abram, A. Hagenbach, A. Voigt, and R. Kirmse, *Z. Anorg. Allg. Chem., 627*, 955 (2001).
453. S. Ritter and U. Abram, *Z. Anorg. Allg. Chem., 622*, 965 (1996).
454. U. Abram, A. Voigt, and R. Kirmse, *Polyhedron, 19*, 1741 (2000).
455. J.R. Dilworth, P. Jobanputra, R.M. Thompson, C.M. Archer, J.D. Kelly, and W. Hiller, *Z. Naturforsch. Teil B, 46*, 449 (1991).
456. U. Abram and B. Lorenz, *Z. Naturforsch., Teil B, 48*, 771 (1993).
457. J. Baldas, J. Bonnyman, P.M. Pojer, G.A. Williams, and M.F. Mackay, *J. Chem. Soc., Dalton Trans.*, 1798 (1981).
458. C.L. Raston, A.H. White, and A.C. Willis, *J. Chem. Soc., Dalton Trans.*, 2429 (1975).
459. H. Iwasaki and K. Kobayashi, *Acta Crystallogr.,Sect. B, 36*, 1657 (1980).
460. N.V. Khitrich, I.I. Seifullina, and Z.A. Starikova, *Russ. J. Inorg. Chem., 47*, 80 (2002).
461. J. Lokaj, V. Kettmann, F. Pavelcik, V. Vrabel, and J. Garaj, *Collect. Czech. Chem. Commun., 47*, 2633 (1982).
462. G. Kartha and K.V. Krishnamurthy, *Proc. Indian Acad. Sci., Chem. Sci., 92*, 437 (1983).
463. T.C. Woon, M.F. Mackay, and M.J. O'Connor, *Inorg. Chim. Acta, 58*, 5 (1982).
464. J. Zhang, F. Jian, L. Lu, X. Yang, and X. Wang, *J. Chem. Cryst., 31*, 251 (2001).
465. R.J. Butcher and E. Sinn, *J. Am. Chem. Soc., 98*, 2440 (1976).
466. P.C. Healy and E. Sinn, *Inorg. Chem., 14*, 109 (1975).
467. D. Ondrusova, M. Koman, M. Pajtasova, and T. Glowiak, *Acta Crystallogr., Sect. E, 57*, m172 (2001).
468. G.F. Gasparri, M. Nardelli, and A. Villa, *Acta Crystallogr., 23*, 384 (1967).
469. S. Santos, Jr., S. Guilardi, J.A.L.C. Resende, M.M.M. Rubinger, M.R.L. Oliveira, and J. Ellena, *Acta Crystallogr., Sect. E, 59*, m77 (2003).
470. P.W.G. Newman and A.H. White, *J. Chem. Soc., Dalton Trans.*, 1460 (1972).

471. J. Kamenicek, R. Pastorek, F. Brezina, B. Kratochvil, and Z. Travnicek, *Collect. Czech. Chem. Commun., 55*, 1010 (1990).
472. C.L. Raston and A.H. White, *J. Chem. Soc., Dalton Trans.*, 1790 (1974).
473. J. Lokaj, J. Garaj, V. Kettmann, and V. Vrabel, *Collect. Czech. Chem. Commun., 45*, 2147 (1980).
474. A. Pignedoli and G. Peyronel, *Acta Crystallogr., Sect. B, 24*, 433 (1968).
475. G. Peyronel and A. Pignedoli, *Acta Crystallogr., 23*, 398 (1967).
476. F.-F. Jian, Z.-W. Wang, H.-K. Fun, Z.-P. Bai, Z.-Z. You, I.A. Razak, and K. Chinnakali, *Acta Crystallogr., Sect. C, 54*, IUC9800044 (1998).
477. A.V. Ivanov, E.V. Ivakhenko, W. Forsling, A.V. Gerasimenko, and B.V. Bukvetskii, *Zh. Neorg. Khim., 47*, 468 (2002).
478. J. Lokaj, V. Vrabel, and E. Kello, *Chem. Zvesti, 38*, 313 (1984).
479. C.L. Raston and A.H. White, *J. Chem. Soc., Dalton Trans.*, 523 (1976).
480. J. Kamenicek, R. Pastorek, B. Cvek, and J. Taraba, *Z. Kristallogr., 218*, 205 (2003).
481. M.J. Cox and E.R.T. Tiekink, *Z. Kristallogr., 214*, 242 (1999).
482. K. Ramalingam, K. Radha, G. Aravamudan, C. Mahadevan, C. Subramanyam, and M. Seshasayee, *Acta Crystallogr., Sect. C, 40*, 1838 (1984).
483. M.R. Sundberg and M.-L. Riekkola, *Inorg. Chim. Acta, 132*, 99 (1987).
484. J. Lokaj, F. Pavelcik, V. Kettmann, J. Masaryk, V. Vrabel, and J. Garaj, *Acta Crystallogr., Sect. B, 37*, 926 (1981).
485. P.W.G. Newman and C.L. Raston, *J. Chem. Soc., Dalton Trans.*, 1332 (1973).
486. L.M. Engelhardt, J.M. Patrick, and A.H.White, *Aust. J. Chem., 38*, 1413 (1985).
487. V. Vettmann, J. Garaj, and S. Kudela, *Collect. Czech. Chem. Commun., 43*, 1024 (1978).
488. A. Radha, M. Seshasayee, and G. Aravamudan, *Acta Crystallogr. Sect. C, 44*, 1378 (1988).
489. Z.A. Starikova, E.A. Shugam, V.M. Agre, and Yu.V. Oboznenko, *Kristollografiya, 17,* 111 (1972).
490. F.G. Herring, J.M. Park, S.J. Rettig, and J. Trotter, *Can. J. Chem., 57*, 2379 (1979).
491. S. Pan and Y. Wang, *Chin. J. Chem., 19*, 856 (2001).
492. P.D. Beer, A.G. Cheetham, M.G.B. Drew, O.D. Fox, E.J. Hayes, and T.D. Rolls, *J. Chem. Soc., Dalton Trans.*, 603 (2003).
493. Yu.L. Gol'dfarb, E.G. Ostapenko, V.G. Vinogradova, A.N. Zverev, A.V. Polyakov, A.I. Yanovsky, D.S. Yufit, and Yu.T. Struchkov, *Khim. Get. Soedin, SSSR*, 902 (1987).
494. J.M. Martin, P.W.G. Newman, B.W. Robinson, and A.H. White, *J. Chem. Soc., Dalton Trans.*, 2233 (1972).
495. D.L. Kepert, C.L. Raston, A.H. White, and D. Petridis, *J. Chem. Soc., Dalton Trans.*, 1921 (1980).
496. S.-F. Lu, J.-Q. Huang, H.-B. Chen, and Q.-J. Wu, *Huaxue Xuebao (Acta Chim. Sinica)(Chin.), 51*, 885 (1993).
497. S. Mitra, C.L. Raston, and A.H. White, *Aust. J. Chem., 31*, 547 (1978).
498. L.M. Engelhardt, P.C. Healy, R.I. Papasergio, and A.H. White, *Inorg. Chem., 24*, 382 (1985).
499. C.M. McGrath, C.J. O'Connor, C. Sangregorio, J.M.W. Seddon, E. Sinn, F.E. Sowrey, and N.A. Young, *Inorg. Chem. Commun., 2*, 536 (1999).
500. J. Albertsson, Å. Oskarsson, and M. Nygren, *Acta Crystallogr., Sect. B, 35*, 1473 (1979).
501. J. Albertsson, I. Elding, and Å. Oskarsson, *Acta Chem. Scand., Ser. A, 33*, 703 (1979).

502. J. Albertsson, Å. Oskarsson, K. Stahl, C. Svensson, and I. Ymén, *Acta Crystallogr.,Sect.B, 37*, 50 (1981).
503. J. Albertsson, Å. Oskarsson, and K. Stahl, *Acta Chem. Scand. Ser. A, 36*, 783 (1982).
504. C. Cartier, P. Thuery, M. Verdaguer, J. Zarembowitch, and A. Michalowicz, *J. de Phys., Coll., 8*, 563 (1986).
505. L.N. Mazalov, N.V. Bausk, S.B. Érenburg, and S.V. Larionov, *J. Struct. Chem., 42*, 784 (2001).
506. B.D. Shrivastava, S.K. Joshi, and K.B. Pandeya, *Physica B, 158*, 589 (1989).
507. W.T. Klooster, R. Piltz, and E. R. T. Tiekink, *Acta Crystallogr., Sect. A, 58*, C132 (2002).
508. J. Campo, J. Luzon, F. Palacio, G. De Fotis, J. Christophel, and E. Ressouche, *Appl. Phys. A., 74*, S923 (2002).
509. G. Antorrena, G. Le Caer, B. Malaman, F. Palacio, E. Ressouche, and J. Schweizer, *Physica B: Condensed Matter, 234*, 780 (1997).
510. C.R. Lee, L.Y. Tan, and Y. Wang, *J. Phys. Chem. Solids, 62*, 1613 (2001).
511. R. Kellner, *Anal. Chim. Acta, 63*, 277 (1973).
512. D. Oktavec, E. Beinrohr, B. Siles, J. Stefanec, and J. Garaj, *Czech. Collect. Chem. Commun., 45*, 1495 (1980).
513. R. Kellner and G. St. Nikolov, *J. Inorg. Nucl. Chem., 43*, 1183 (1981).
514. F. Bonati and R. Ugo, *J. Organomet. Chem., 10*, 257 (1967).
515. R. Kellner, G. St. Nikolov, and N. Trendafilova, *Inorg. Chim. Acta, 84*, 233 (1984).
516. K. Baghat and J. Mink, *Mikrochim. Acta, Suppl., 14*, 213 (1997).
517. H.O. Desseyn, A.C. Fabretti, F. Forghieri, and C. Preti, *Spectroc. Acta Pt. A-Molec. Biomolec. Spectrosc., 41*, 1105 (1985).
518. N. Trendafilova, G. Nikolov, H. Mikosch, G. Bauer, and R. Kellner, *Mikrochim. Acta, 2*, 391 (1987).
519. A.N. Chetty, P. Ramadevi, and G.R.K. Naidu, *J. Radioanal. Nucl. Chem. Lett., 117*, 347 (1987).
520. T. Gangaiah, P. Ramadevi, and G.R.K. Naidu, *J. Radioanal. Nucl. Chem. Lett., 117*, 299 (1987).
521. G. St. Nikolov and M.A. Atanasov, *J. Inorg. Nucl. Chem., 43*, 1201 (1981).
522. H. Mikosch, G. Bauer, R. Kellner, N.S. Trendafilova, and G. St. Nikolov, *J. Mol. Struct., 142*, 473 (1986).
523. R. Payne, R.J. Magee, and J. Liesegang, *J. Electron Spectrosc. Relat. Phenom., 35*, 113 (1985).
524. R. Keller, G. Nikolov, and N. Trendafilova, *Mikrochim. Acta, 2*, 247 (1983).
525. F.W. Pijpers, H.L.M. van Gaal, and J.G.M. van der Linden, *Anal. Chim. Acta, 112*, 199 (1979).
526. X.F. Yan and C.G. Young, *Aust. J. Chem., 44*, 361 (1991).
527. T.A. Coffey, G.D. Forster, and G. Hogarth, *J. Chem. Soc., Dalton Trans.*, 183 (1996).
528. T.A. Coffey, G.D. Forster, and G. Hogarth, *J. Chem. Soc., Chem. Commun.*, 1524 (1993).
529. N.V. Duffy, W.G. Movius, and D.L. Uhrich, *Inorg. Chim. Acta, 64*, L91 (1982).
530. N.V. Duffy, *Inorg. Chim. Acta, 47*, 31 (1981).
531. K. Drabent and L. Latosgrazynski, *Polyhedron, 4*, 1637 (1985).
532. S. Wajda, K. Drabent, and A. Ozarowski, *Inorg. Chim. Acta, 45*, L201 (1980).
533. A.V. Ivanov, T. Rodyna, and O.N. Antzutkin, *Polyhedron, 17*, 3101 (1998).
534. N.A. Law, W. Dietzsch, and N. V. Duffy, *Polyhedron, 22*, 3423 (2003).
535. N.V. Duffy and T.G. Appleton, *Inorg. Chim. Acta, 145*, 273 (1988).

536. A.V. Ivanov, E.V. Ivakhnenko, A.V. Gerasimenko, and W. Forshling, *Zh. Neorg. Khim., 48*, 52 (2003).
537. A.V. Ivanov, E.V. Ivakhnenko, W. Forshling, and A.V. Gerasimenko, *Doklady Chem., 390*, 162 (2003).
538. P. Barrie, T.A. Coffey, G.D. Forster, and G. Hogarth, *J. Chem. Soc., Dalton Trans.*, 4519 (1999).
539. J. Sachinidis and M.W. Grant, *Aust. J. Chem., 36*, 2019 (1983).
540. A.M. Bond, R. Colton, Y.A. Mah, and J.C. Traeger, *Inorg. Chem., 33*, 2548 (1994).
541. A.M. Bond, R. Colton, J.E. Moir, and D.R. Page, *Inorg. Chem., 24*, 1298 (1985).
542. D.F. Schoener, M.A. Olsen, P.G. Cummings, and C. Basic, *J. Mass Spectrom., 34*, 1069 (1999).
543. G. Faraglia, M.A. Fedrigo, and S. Sitran, *Transition Met. Chem., 27*, 200 (2002).
544. M.E. Padilla-Tosta, O.D. Fox, M.G.B. Drew, and P.D. Beer, *Angew. Chem., Int. Ed. Engl., 40*, 4235 (2001).
545. C.H. Jiang, T.S.A. Hor, Y.K. Yan, W. Henderson, and L.J. McCaffrey, *J. Chem. Soc., Dalton Trans.*, 3204 (2000).
546. A.M. Bond, R. Colton, J.C. Traeger, and J. Harvey, *Inorg. Chim. Acta, 228*, 193 (1995).
547. A.M. Bond, R. Colton, J.C. Traeger, and J. Harvey, *Inorg. Chim. Acta, 212*, 233 (1993).
548. R. Colton, J.C. Traeger, and V. Tedesco, *Inorg. Chim. Acta, 210*, 193 (1993).
549. P.M.T.M. van Attekum and J.M. Trooster, *J. Chem. Soc., Dalton Trans.*, 201 (1980).
550. G. Granozzi, A. Vittadini, L. Sindellari, and D. Ajo, *Inorg. Chem., 23*, 702 (1984).
551. S. Thirumaran, K. Ramalingam, G. Bocelli, and A. Cantoni, *Polyhedron, 18*, 925 (1999).
552. A. Manohar and K. Ramalingham, *Main Group Met. Chem., 24*, 789 (2001).
553. V. Venkatachalam, K. Ramalingam, R. Akilan, K. Sivakumar, K. Chinnakali, and H.K. Fun, *Polyhedron, 15*, 1289 (1996).
554. L.N. Mazalov, G.K. Parygina, E.S. Fomin, N.V. Bausk, S.B. Erenburg, S.M. Zemskova, and S.V. Larionov, *J. Struct. Chem., 39*, 923 (1998).
555. C. Furlani, G. Polzonetti, C. Preti, and G. Tosi, *Gazz. Chim. Ital., 113*, 609 (1983).
556. H. Chang and K.L. Cheng, *Spectrosc. Lett., 14*, 795 (1981).
557. G. Polzonetti, C. Preti, and G. Tosi, *Polyhedron, 5*, 1969 (1986).
558. P.K. Chan, D.C. Frost, and K. Venkateswaran, *Spectrosc. Lett., 19*, 1071 (1986).
559. J.O. Hill, R.J. Magee, and J. Liesegang, *Comm. Inorg. Chem., 5*, 1 (1985).
560. C. Furlani, G. Polzonetti, C. Preti, and G. Tosi, *Inorg. Chim. Acta, 73*, 105 (1983).
561. J. Liesegang and A.R. Lee, *J. Electron Spectrosc. Relat. Phenom., 35*, 101 (1985).
562. J.O. Hill, J.P. Murray, and K.C. Patil, *Rev. Inorg. Chem., 14*, 363 (1994).
563. J.O. Hill and R.P. Murray, *Rev. Inorg. Chem., 13*, 183 (1993).
564. S.K. Sengupta and S. Kumar, *Thermochim. Acta, 72*, 349 (1984).
565. G. D'Ascenzo and W.W. Wiendlant, *J. Inorg. Nucl. Chem., 32*, 2433 (1970).
566. G. D'Ascenzo and W.W. Wiendlant, *J. Therm. Anal., 1*, 423 (1969).
567. K.J. Cavell, J.O. Hill, and R.J. Magee, *Thermochim. Acta, 34*, 155 (1979).
568. K.J. Cavell, J.O. Hill, and R.J. Magee, *Thermochim. Acta, 33*, 383 (1979).
569. M.A.V. Ribeiro da Silva and A.M.M.V. Reis, *J. Chem. Thermodyn., 21*, 167 (1989).
570. M.A.V. Ribeiro da Silva and A.M.M.V. Reis, *J. Chem. Thermodyn., 21*, 423 (1989).
571. M.A.V. Ribeiro da Silva and A.M.M.V. Reis, *J. Chem. Thermodyn., 24*, 401 (1992).

572. S.C. Dias, M.D.A. Brasilino, C.D. Pinheiro, and A.G. Desouza, *Thermochim. Acta, 241*, 25 (1994).

573. M.A.V.Ribeiro da Silva, A.M.M.V. Reis, and R.I.M.C.P. Faria, *J. Chem. Thermodyn., 27*, 1365 (1995).

574. M.A.R.P. Carvalho, A.G. Souza, and C. Airoldi, *J. Chem. Soc., Dalton Trans.*, 1235 (1992).

575. A.G. Souza, J.H. Souza, and C. Airoldi, *J. Chem. Soc., Dalton Trans.*, 1751 (1991).

576. A.G. Souza, C.D. Pinheiro, L.C.R. Santos, and M.L.M. Melo, *Thermochim. Acta,* 231, 31 (1994).

577. J.R. Botelho, A.G. Souza, L.M. Nunes, A.P. Chagas, I.M. Garcia Dos Santos, M.M. Da Conceicao, and P.O. Dunstan, *J. Therm. Anal. Calorim., 67*, 413 (2002).

578. C. Airoldi, *J. Chem. Soc., Dalton Trans.*, 369 (1985).

579. K.J. Cavell, J.O. Hill, and R.J. Magee, *J. Chem. Soc., Dalton Trans.*, 763 (1980).

580. K.J. Cavell, J.O. Hill, and R.J. Magee, *J. Chem. Soc., Dalton Trans.*, 1638 (1980).

581. J.O. Hill and K.J. Cavell, *Thermochim. Acta, 223*, 187 (1993).

582. M.A.V. Ribeiro da Silva, A.M.M.V. Reis, and M.M.R Ferreira da Silva, *J. Chem. Thermodyn., 32*, 1319 (2000).

583. G.A. Souza, M.C.N. Machado, L. Helker-Carvalho, and M.F.S. Trindade, *J. Therm. Anal. Calorim., 59*, 633 (2000).

584. L.A. Kosareva and S.V. Larionov, *Russ. J. Inorg. Chem., 24*, 1578 (1979).

585. S.V. Sysoev, N.B. Morozova, G.I. Zharkova, I.K. Igumenov, R.P. Semyannikov, and V.M. Grankin, *J. Therm. Anal. Calorim., 53*, 87 (1998).

586. S.V. Larionov, L.A. Patrina, A.N. Shan'shin, I.M. Oglezneva, and E.M. Uskov, *Koord. Khim., 10*, 92 (1984).

587. C.S. Chamberlain and R.S. Drago, *Inorg. Chim. Acta, 32*, 75 (1979).

588. M. Ahmed and R.J. Magee, *Anal. Chim. Acta, 75*, 431 (1975).

589. M.-L. Riekkola, *Acta Chem. Scand. A, 37*, 691 (1983).

590. C. Bernal, E.A. Neves, and E.T.G. Cavalheiro, *Thermochim. Acta, 370*, 49 (2001).

591. J.A.A.I. Sales, A.G. Siuza, G.F.G. de Freitas, S. Prasad, M.F.S. Trindadae, L.H. Carvalho, and P.O. Dunstan, *Thermochim. Acta, 356*, 9 (2000).

592. S.T. Breviglieri, E.T.G. Cavalheiro, and G.O. Chierice, *Thermochim. Acta, 356*, 79 (2000).

593. E.D.T. Cavalheiro, M. Ionashiro, G. Marino, S.T. Breviglieri, and G.O. Chierice, *Transition Met. Chem., 25*, 69 (2000).

594. E.T.G. Cavalheiro, M. Ionashiro, G. Marino, S.T. Breviglieri, and G.O. Chierice, *J. Brazil Chem. Soc., 10*, 65 (1999).

595. B. Macías, J.J. Criado, M.V. Vaquero, and M.V. Villa, *Thermochim. Acta, 223*, 213 (1993).

596. I. Rogachev, V. Gusis, A. Gusis, J.L. Cortina, J. Gressel, and A. Warshawsky, *React. Funct. Polym., 42*, 243 (1999).

597. J. Sachinidis and M.W. Grant, *Aust. J. Chem., 34*, 2195 (1981).

598. K. Yamuna, V.V. Ramana, K.A. Emmanuel, and K. Saraswati, *Asian J. Chem., 4*, 387 (1992).

599. S.T. Breviglieri, E.T.G. Cavalheiro, and G.O. Chierice, *Polyhedron, 15*, 839 (1996).

600. J. Labuda, M. Skatulokova, M. Nemeth, and S. Gergely, *Chem. Zvesti, 38*, 597 (1984).

601. M.A. Doicheva and B.G. Jeliazkova, *Spectroc. Acta Pt. A, Molec. Biomolec. Spectrosc., 58*, 1181 (2002).

602. M. Moriyasu and Y. Hashimoto, *Bull. Chem. Soc. Jpn., 53*, 3590 (1980).

603. M. Moriyasu and Y. Hashimoto, *Bull. Chem. Soc. Jpn., 54*, 2470 (1981).
604. M. Moriyasu and Y. Hashimoto, *Bull. Chem. Soc. Jpn., 54*, 3374 (1981).
605. M. Moriyasu, Y. Hashimoto, and M. Endo, *Bull. Chem. Soc. Jpn., 54*, 3369 (1981).
606. A.M. Bond and F. Scholz, *J. Phys. Chem., 95*, 7460 (1991).
607. A.M. Bond, R. Colton, M.L. Dillon, J.E. Moir, and D.R. Page, *Inorg. Chem., 23*, 2883 (1984).
608. O.C. Dermer and W.C. Fernelius, *Z. Anorg. Allg. Chem., 221*, 83 (1934).
609. R.S.P. Coutts, P.C. Wailes, and J.V. Kingston, *J. Chem. Soc., Chem. Commun.*, 1170 (1968).
610. M.R. Chakrabarty, G.D. Ellis, and G.L. Campbell, *J. Inorg. Nucl. Chem., 40*, 354 (1978).
611. G.L. Campbell, G.D. Ellis, and M.R. Chakrabarty, *J. Inorg. Nucl. Chem., 43*, 2265 (1981).
612. S. Kumar and N.K. Kaushik, *Synth. React. Inorg. Met.-Org. Chem., 12*, 159 (1982).
613. S. Kumar and N.K. Kaushik, *Ind. J. Chem., Sect. A, 21,* 182 (1982).
614. K.S. Siddiqi, F.M.A.M. Aqra, S.A. Shah, and S.A.A. Zaidi, *Synth. React. Inorg. Met.-Org. Chem., 24*, 353 (1994).
615. M. Behnam-Dehkordy, B. Crociani, M. Nicolini, and R.L. Richards, *J. Organomet. Chem., 181*, 69 (1979).
616. K.S. Siddiqi, N.H. Khan, R.I. Kureshy, S. Tabassum, and S.A.A. Zaidi, *Ind. J. Chem. Sect. A, 26*, 70 (1987).
617. A.N. Bhat, R.C. Fay, D.F. Lewis, A.F. Lindmark, and S.H. Strauss, *Inorg. Chem., 13*, 886 (1974).
618. N.S.N. Jalil, *Synth. React. Inorg. Met.-Org. Chem., 19*, 1069 (1989).
619. H.S. Sangari, G.S. Sodhi, N.K. Kaushik, and R.P. Singh, *Synth. React. Inorg. Met.-Org. Chem., 11*, 373 (1981).
620. S. Bhargava, R. Bohra, and R.C. Mehrotra, *Transition Met. Chem., 16*, 622 (1991).
621. G.S. Sodhi and N.K. Kaushik, *Acta Chim. Acad. Sci.Hung., 111*, 207 (1982).
622. G.S. Sodhi and N.K. Kaushik, *Acta Chim. Acad. Sci.Hung., 108*, 389 (1981).
623. S. Bhattacharya, V.D. Gupta, K.Polborn, and H. Noth, *Ind. J. Chem., Sect. A, 33,* 1063 (1994).
624. Z.-Q.Wang, S.-W.Lu, H.-F.Guo and N.-H.Hu, *Chin. Chem. Lett., 2*, 865 (1991)
625. S. Kumar, G.S. Sodhi, and N.K. Kaushik, *Zh. Neorg. Khim., 28*, 357 (1983).
626. S. Kumar and N.K. Kaushik, *J. Inorg. Nucl. Chem., 43*, 2679 (1981).
627. V.V. Jain, V. Kumar, and B.S. Garg, *Inorg. Chim. Acta, 26*, 197 (1978).
628. K. Chandra, R.K. Tuli, B.S. Garg, and R.P. Singh, *J. Inorg. Nucl. Chem., 43*, 29 (1981).
629. Z.Wang, S. Lu, and H. Guo, *Wuji Huaxue Xuebao, 8*, 326 (1992).
630. V.K. Jian and B.S. Garg, *J. Inorg. Nucl. Chem., 40*, 239 (1978).
631. A. Bhatt, S.K. Sengupta, and O.P. Pandey, *Ind. J. Chem., Sect. A, 40*, 994 (2001).
632. Z.-Q. Wang, S.-W. Lu, and H.-F. Guo, *Synth. React. Inorg. Met.-Org. Chem., 21*, 1243 (1991).
633. S Kumar and N.K. Kaushik, *Acta Chim. Acad. Sci. Hung., 109*, 13 (1982).
634. R.K. Tuli, P. Soni, K. Chandra, R.K. Sharma, and B.S. Garg, *Transition Met. Chem., 5*, 145 (1980).
635. W.L. Steffen, H.K. Chun, and R.C. Fay, *Inorg. Chem., 17*, 3498 (1978).
636. Z.-Q. Wang, S.-W. Lu, H.-F.Guo, and N.-H. Hu, *Polyhedron, 11*, 39 (1992).
637. Z.-Q. Wang, S.-W. Lu, H.-F.Guo, and N.-H. Hu, *Chin. Chem. Lett., 2,* 863 (1991).
638. N.K. Kaushik, B. Bhushan, and G.R. Chhatwal, *Transition Met. Chem., 3*, 215 (1978).

639. H.S. Sangari, G.R. Chhatwal, N.K. Kaushik, and R.P. Singh, *Indian J. Chem., Sect. A, 20*, 185 (1981).
640. N.K. Kaushik, B. Bhushan, and G.R. Chhatwal, *Synth. React. Inorg. Met.-Org. Chem., 8*, 467 (1978).
641. N.K. Kaushik, B. Bhushan, and G.R. Chhatwal, *J. Inorg. Nucl. Chem., 42*, 457 (1980).
642. N.K. Kaushik, B. Bhushan, and G.R. Chhatwal, *Z. Naturforsch., Teil B, 34B*, 949 (1979).
643. N.K. Kaushik, M.S. Yadav, G.S. Sodhi, and B. Bhushan, *J. Indian Chem. Soc., 60*, 894 (1983).
644. H. Suzuki, T. Takiguchi, and Y. Kawasaki, *Bull. Chem. Soc. Jpn., 51*, 1764 (1978).
645. V.K. Jain, V. Kumar, and B.S. Garg, *Inorg. Chim. Acta, 26*, 197 (1978).
646. A.K. Sharma and N.K. Kaushik, *Acta Chim. Acad. Sci.Hung., 108*, 395 (1981).
647. M.E. Silver, O. Eisenstein, and R.C. Fay, *Inorg. Chem., 22,* 759 (1983).
648. Z.-Q. Wang, S.-W. Lu, H.-F.Guo, and N.-H. Hu, *Polyhedron, 11*, 1131 (1992).
649. A.F. Lindmark and R.C. Fay, *Inorg. Chem., 22*, 2000 (1983).
650. T.D. Tilley, *Organometallics, 4,* 1452 (1985).
651. D.A. Femec, T.L. Groy, and R.C. Fay, *Acta Crystallogr., Sect. C, 47*, 1811 (1991).
652. D.A. Femac, M.E. Silver, and R.C. Fay, *Inorg. Chem., 28*, 2789 (1989).
653. B. Bhushan, I.P. Mittal, G.R. Chhatwal, and N.K. Kaushik, *J. Inorg. Nucl. Chem., 41*, 159 (1979).
654. P.R. Shukla and S.K. Srivastava, *Indian J. Chem. Sect. A, 25*, 741 (1986).
655. P.R. Shukla and S.K. Srivastava, *Indian J. Chem., Sect. A, 26,* 352 (1987).
656. S. Kumar and N.K. Kaushik, *Inorg. Nucl. Chem. Lett., 16*, 389 (1980).
657. R.S. Sindhu, S. Tikku, A.K. Sharma, and S.K. Bansal, *Synth. React. Inorg. Met.-Org. Chem., 25*, 307 (1995).
658. A.K. Sharma and N.K. Kaushik*, Synth. React. Inorg. Met.-Org. Chem., 13*, 481 (1983).
659. R.K. Bajaj, N.K. Kaushik, K.N. Johri, and G.S. Sodhi, *J. Indian Chem. Soc., 64*, 55 (1987).
660. A.K. Sharma, G.S. Sodhi, and N.K. Kaushik, *Bull. Soc. Chim. France., Partie I-Physicochimie des Syst. Liq. Electrochemie Catal., Genie Chim.*, 52 (1983).
661. G.S. Sodhi, A.K. Sharma, and N.K. Kaushik, *Synth. React. Inorg. Met.-Org. Chem., 12*, 947 (1982).
662. A.K. Sharma and N.K. Kaushik, *Z. Naturforsch. Sect. B., 39*, 604 (1984).
663. B. Khera, A.K. Sharma, and N.K. Kaushik, *Polyhedron, 2*, 108 (1983).
664. G.S. Sodhi, S. Kumar, and N.K. Kaushik, *Acta Chim. Hung.- Models Chem., 114*, 329 (1983).
665. A.K. Sharma, B. Khera, and N.K. Kaushik, *Synth. React. Inorg. Met.-Org. Chem., 13*, 1059 (1983).
666. D.C. Bradley and M.H. Gitlitz, *J. Chem. Soc. A*, 1152 (1969).
667. F. Forghieri, G. Graziosi, C. Preti, and G. Tosi, *Transition Met. Chem., 8*, 372 (1983).
668. L.F. Larkworthy and M.W. O'Donoghue, *Inorg. Chim. Acta, 74*, 155 (1983).
669. L.C. Porter, S.G. Novick, and H.H.Murray, *J. Coord. Chem., 31,* 47 (1994).
670. H. Zhu, C. Chen, X. Zhang, Q. Liu, D. Liao, and L. Li, *Inorg. Chim. Acta, 328*, 96 (2002).
671. G. Soundararajan and M. Subbaiyan, *Indian J. Chem. Sect A-Inorg. Phys. Theor. Anal. Chem., 22*, 454 (1983).
672. R.D. Bereman and D. Nalewajek, *J. Inorg. Nucl. Chem., 40*, 1309 (1978).
673. D. Attanasio, C. Bellitto, A. Flamini, and G. Pennesi, *Inorg. Chem., 21*, 1461 (1982).

674. A.M. Bond, A.T. Casey, and J.R. Thackeray, *Inorg. Chem., 12*, 887 (1973).
675. A.T. Casey and J.R. Thackeray, *Aust. J. Chem., 27*, 757 (1974).
676. P. Ghosh, S. Ghosh, O.J. D'Cruz, and F.M. Uckun, *J. Inorg. Biochem., 72*, 89 (1998).
677. S. Kumar and N.K. Kaushik, *Gazz. Chim. Ital., 111*, 57 (1981).
678. H. Sakurai, H. Watanabe, H. Tamura, H. Yasui, R. Matsushita, and J. Takada, *Inorg. Chim. Acta, 283*, 175 (1998).
679. A.L. Doadrio, J. Sotelo, and A. Fernandez-Ruano, *Quim. Nova, 25*, 525 (2002).
680. M.T. Conconi, E. De Carlo, S. Vigolo, C. Grandi, G. Bandoli, N. Sicolo, G. Tamagno, P.P. Parnigotto, and G.G. Nussdorfer, *Hormone Metabol. Pharm. Sci., 35*, 402 (2003).
681. A.L. Doadrio Villarejo, C.V. Ragel, and A. Doadrio, *Anal. Real Acad. Farm., 50*, 727 (1984).
682. A. Jezierski and B. Jezowska-Trzebiatowska, *Bull. Acad. Pol. Sci., Ser. Sci. Chim., 33*, 85 (1985).
683. P.R. Shukla and S.K. Srivastava, *J. Indian Chem. Soc., 64*, 139 (1987).
684. K. Henrick, C.L. Raston, and A.H. White, *J. Chem. Soc., Dalton Trans.*, 26 (1976).
685. A.L.D. Villarejo, C.V. Ragel, and A. Doadrio, *Anal. Quimica Ser. B-Quim. Inorg. Quim., 82*, 234 (1986).
686. A.V. Ivanov, *Koord. Khimiya, 18*, 948 (1992).
687. A.V. Ivanov, P.M. Solozhenkin, Z.R. Baratova, and V.B. Klyashtornyi, *Dokl. Akad. Nauk SSSR, 315*, 396 (1990).
688. A.V. Ivanov, P.M. Solozhenkin, Z.R. Baratova, V.B. Klyashtornyi, and V.I.Uskov, *Dok. Akad. Nauk SSSR, 310*, 1387 (1990).
689. E.L. Jones, J.G. Reynolds, J.C. Huffman, and G. Christou, *Polyhedron, 10,* 1817 (1991).
690. J.G. Reynolds, E.L. Jones, J.C. Huffman, and G. Christou, *Polyhedron, 12*, 407 (1992).
691. N.E. Heimer and W.E.Cleland, Jr., *Acta Crystallogr., Sect. C, 46,* 2049 (1990).
692. D. Collison, F.E. Mabbs, K. Rigby, and W.E. Cleland, *J. Chem. Soc., Faraday Trans., 89*, 3695 (1993).
693. D.E. Wheeler, J.F. Wu, and E.A. Maatta, *Polyhedron, 17*, 969 (1998).
694. X.J. Lei, F.-L Jiang, D.-X. Wu, M.-C. Hong, Z.-Y. Huang, and H.-Q. Liu, *Chin. J. Chem. (Huaxue Xuebao)(Engl.), 11*, 40 (1993).
695. Y. Yang, L. Huang, Q. Liu, and B. Kang, *Acta Crystallogr., Sect. C, 47,* 2085 (1991).
696. M. Sokolov, A.Virovets, O. Oeckler, A. Simon, and V. Fedorov, *Inorg. Chim. Acta, 331*, 25 (2002).
697. H.P. Zhu, Q.T. Liu, Y.H. Deng, T.B. Wen, C.N. Chen, and D.X. Wu, *Inorg. Chim. Acta, 286*, 7 (1999).
698. Y. Yang, Q. Liu, and D. Wu, *Inorg. Chim. Acta, 208*, 85 (1993).
699. Q. Liu, Y. Yang, L. Huang, D. Wu, B. Kang, C. Chen, Y. Deng, and J. Lu, *Sci. Chin., B36*, 1425 (1995).
700. Y. Yang, Q.Y. Liu, L.G. Huang, B.S. Kang, and J.X. Lu, *J. Chem. Soc., Chem. Commun.*, 1512 (1992).
701. Y. Zhang, Q. Liu, Y. Deng, H. Zhu, C. Chen, D. Liao, and J. Cui, *Polyhedron, 18,* 3153 (1999).
702. Y. Deng, Q. Liu, C. Chen, Y. Wang, Y. Cai, D. Wu, B. Kang, D. Liao, and J. Cui, *Polyhedron, 16,* 4121 (1997).
703. H. Zhu, Q. Liu, X. Huang, T. Wen, C. Chen, and D. Wu, *Inorg. Chem., 37,* 2678 (1998).
704. Y. Yang and Q. Liu, *Acta Crystallogr., Sect. C, 49,* 1623 (1993).

705. Y. Yang, Q. Liu, L. Huang, B. Kang, and J. Lu, *J. Chem. Soc., Chem. Commun.*, 1512 (1992).
706. Q. Liu, Y. Yang, L. Huang, D. Wu, B. Kang, C. Chen, Y.Deng, and J. Lu, *Inorg. Chem., 34,* 1884 (1995).
707. F. Lin, R.L. Beddoes, D. Collison, C.D. Garner, and F.E. Mabbs, *J. Chem. Soc., Chem. Commun.*, 496 (1993).
708. K.S. Nagaraja, *Indian J. Chem. Sect A, 30*, 701 (1991).
709. A.S.A. Zidan, A.I. Elsaid, and A.A.M. Aly, *Synth. React. Inorg. Met.-Org. Chem., 22*, 1355 (1992).
710. A.T. Kotchevar, P. Ghosh, and F.M. Uckun, *J. Phys. Chem. B, 102*, 10925 (1998).
711. O.J. D'Cruz, P. Ghosh, and F.M. Uckun, *Mol. Hum. Reprod., 4*, 683 (1998).
712. O.J. D'Cruz, B. Waurzyniak, and F.A. Uckun, *Contaception, 64*, 177 (2001).
713. O.J. D'Cruz, P. Ghosh, and F.M. Uckun, *Biol. Reprod., 58*, 1515 (1998).
714. A.T. Casey, D.J. Mackey, R.L.Martin, and A.H. White, *Aust. J. Chem., 25*, 477 (1972).
715. S.M. Aliwi and S.M. Abdullah, *Polym. Int., 35*, 309 (1994).
716. S.P. Arya and K. Akora, *J. Indian Chem. Soc., 68,* 174 (1991).
717. R.A. Henderson, D.L. Hughes, and A.N. Stephens, *J. Chem. Soc., Dalton Trans.*, 1097 (1990).
718. J.A.M. Canich and F.A.Cotton, *Inorg. Chim. Acta, 159*, 163 (1989).
719. J.R.Weir and R.C. Fay, *Inorg. Chem., 25*, 2969 (1986).
720. P.R. Heckley and D.G. Holah, *Can. J. Chem., 49*, 1151 (1971).
721. A. Antinolo, F. Carrillo-Hermosilla, J. Fernandez-Baeza, S. Garcia-Yuste, A. Otero, E. Palomares, A.M. Rodriguez, and L.F. Sanchez-Barba, *J. Organomet. Chem., 603*, 194 (2000).
722. Y. Do, E.D. Simhon, and R.H. Holm, *Inorg. Chem., 22*, 3809 (1983).
723. E.J. Peterson, R.B. Von Dreele, and T.M. Brown, *Inorg. Chem., 17*, 1410 (1978).
724. P.J. Lim, R.W. Gable, and C.G. Young, *Inorg. Chim. Acta, 310*, 120 (2000).
725. F.P. O'Flaherty, R.A. Henderson, and D.L. Hughes, *J. Chem. Soc., Dalton Trans.*, 1087 (1990).
726. R.A. Henderson and K.E. Oglieve, *J. Chem. Soc., Dalton Trans.*, 1093 (1990).
727. R.A. Henderson, S.H. Morgan, and A.N. Stephens, *J. Chem. Soc., Dalton Trans.*, 1101 (1990).
728. R.A. Henderson, and S.H. Morgan, *J. Chem. Soc., Dalton Trans.*, 1107 (1990).
729. A.V. Virovets, N.V. PodberezskaYA, M.N. Sokolov, I.V. Korobkov, V.P. Fedin, and V.E. Fedorov, *J. Struct. Chem., 34*, 292 (1993).
730. A.V. Virovets, M.N. Sokolov, N.V. Podberezskaya, and V.E. Fedorov, *Zh. Strukt. Khim., 37*, 528 (1996).
731. M. Sokolov, A. Virovets, V. Nadolinnyi, K. Hegetschweiler, V. Fedin, N. Podberezskaya, and V. Fedorov, *Inorg. Chem., 33*, 3503 (1994).
732. M. Sokolov, H. Imoto, T. Saito, and V.Fedorov, *J. Chem. Soc., Dalton Trans.*, 85 (1999).
733. A.S. Batsanov, A.V. Churakov, J.A.K. Howard, A.K. Hughes, A.L. Johnson, A.J. Kingsley, I.S.Neretin, and K.Wade, *J. Chem. Soc., Dalton Trans.*, 3867 (1999).
734. J. Sala-Pala, J.L. Migot, J.E. Guerchais, L. Le Gall, and F. Grosjean, *J. Organomet. Chem., 248*, 299 (1983).
735. J. Fernandez-Baeza, F.A. Jalon, A. Otero, M.E.Rodrigo-Blanco, and M. Etienne, *J. Chem. Soc., Dalton Trans.*, 769 (1998).
736. M.N. Sokolov, O.A. Geras'ko, A.P. Majara, P.P. Semyannikov, V.M. Grankin, S.V. Belaya, and I.K. Igumenov, *Proc. Electrochem. Soc., 97*, 836 (1997).
737. K.B. Pandeya, T.S. Waraich, R.C. Gaur, and R.P. Singh, *Transition Met. Chem., 7*, 146 (1982).

738. C. Preti, G. Tosi, and P. Zannini, *J. Mol. Struct., 65*, 283 (1980).
739. A.C. Fabretti, C. Preti, L. Tassi, G. Tosi, and P. Zannini, *Aust. J. Chem., 39*, 605 (1986).
740. K.B. Pandeya and R. Singh, *Natl. Acad. Sci. Lett. India, 10*, 205 (1987).
741. I. Watanabe, M. Tanaka, S. Inada, and C.Hattori, *Anal. Sci., 9*, 891 (1993).
742. V. Kettmann, J. Garaj, and J. Majer, *Collect. Czech. Chem. Commun., 46*, 6 (1981).
743. J. Labuda, D.I. Bustin, and J. Mocak, *Chem. Zvesti, 37*, 273 (1983).
744. P. Vella and J. Zubieta, *J. Inorg. Nucl. Chem., 40*, 613 (1978).
745. G. Crisponi, P. Deplano, V. Nurchi, and E.F. Trogu, *Polyhedron, 3*, 1241 (1984).
746. A.M. Bond and G.G. Wallace, *Inorg. Chem., 23*, 1858 (1984).
747. G. Soundararajan, and M. Subbaiyan, *Indian J. Chem. Sect A, 22*, 1058 (1983).
748. R.L. Martin, J.M. Patrick, B.W. Skelton, D. Taylor, and A.H. White, *Aust. J. Chem., 35*, 2551 (1982).
749. G.M. Larin, M.K. Tuiebaev, G.A. Zvereva, V.V. Minin, and D.K. Kamysbaev, *Zh. Neorg. Khimii, 35*, 1515 (1990); *Russ. J. Inorg. Chem., 35*, 858 (1990).
750. B.S. Garg, R. Dixit, A.L. Singh, and R.K. Sharma, *J. Therm. Anal., 37*, 2541 (1991).
751. J. Labuda, J. Mocak, and D.I. Bustin, *Chem. Zvesti, 37*, 337 (1983).
752. S. Clamp, N.G. Connelly, G.E. Taylor, and T.S. Louttit, *J. Chem. Soc., Dalton Trans.*, 2162 (1980).
753. T.F. Brennan and I. Bernal, *Inorg. Chim. Acta, 7*, 283 (1973).
754. J.P. Fackler and D.G. Holah, *Inorg. Nucl. Chem. Lett., 2*, 251 (1966).
755. R. Lancashire and T.D. Smith, *J. Chem. Soc., Dalton Trans.*, 845 (1982).
756. A. Jezierski and B. Jezowska-Trzebiatowska, *Bull. Acad. Polon. Sci., Ser. Sci. Chim., 27*, 481 (1979).
757. M.R. Houchin and K. Mitsios, *Inorg. Chim. Acta, 64*, L147 (1982).
758. K.-H. Yih, G.-H. Lee, S.-L. Huang, and Y. Wang, *J. Organomet. Chem., 665*, 114 (2002).
759. M. Sperling, X.F. Yin, and B. Welz, *Analyst, 117*, 629 (1992).
760. J.H. Shofstahl, L. Keck, and J.K. Hardy, *Mikrochim. Acta, 2*, 67 (1989).
761. G.P. Foy and G.E. Pacey, *Talanta, 51*, 339 (2000).
762. M. Bittner and J.A.C. Broekaert, *Anal. Chim. Acta, 364*, 31 (1998).
763. S. Nielsen and E.H. Hansen, *Anal. Chim. Acta, 366*, 163 (1998).
764. I. Watanabe, *Bunseki Kagaku, 40*, T25 (1991).
765. A. Miyazaki and R.M. Barnes, *Anal. Chem., 53*, 364 (1981).
766. S.K. Aggarwal, M. Kinter, M.R. Wills, J. Savory, and D.A. Herold, *Anal. Chem., 62*, 111 (1990).
767. L. Malatesta, *Gazz. Chim. Ital., 69*, 752 (1939).
768. D.C. Bradley and M.H. Chisholm, *J. Chem. Soc. A*, 2741 (1971).
769. T.M. Brown and J.N. Smith, *J. Chem. Soc., Dalton Trans.*, 1614 (1972).
770. B. Zheng, J. Huang, H. Zhuang, and J. Lu, *Chinese J. Struct. Chem. (Jiegou Huaxue), 12,* 359 (1993).
771. Q. Fu, L. Wu, G. Zhang, and S. Chunting, *Wuji Huaxue Xuebao (Chinese J. Inorg. Chem.), 12*, 208-2 (1996).
772. M. Decoster, F. Conan, J.E. Guerchais, Y. Le Mest, J. Sala-Pala, J.C. Jeffery, E. Faulques, A. Leblanc, and P. Molinie, *Polyhedron, 14*, 1741 (1995).

773. L. Li, G.-D. Yang, G.-R. Zhang, Z.-K. Tang, G.-Q. He, X.-B Qu, C.-T. Sun, and Q.-J. Huang, *Chin. Sci. Bull.(Engl. Trans. Kexue Tongbao), 36*, 464 (1991).

774. S.C.Zhu, X.-X. Liu, L. Li, X.-F. Zheng, and W. Yue, *Chem. Res. Chin. Univ., 10*, 236 (1994).

775. C.G. Young, T.O. Kocaba, X.F. Yan, E.R.T. Tiekink, L.W. Wei, H.H. Murray, III, C.L. Coyle, and E.I. Stiefel, *Inorg. Chem., 33*, 6252 (1994).

776. C.D. Garner, N.C. Howlander, F.E. Mabbs, A.T. McPhail, R.W. Miller, and K.D. Onan, *J. Chem. Soc., Dalton Trans.*, 1582 (1978).

777. C.A. McAuliffe and B.J. Sayle, *Inorg. Chim. Acta, 30*, 35 (1978).

778. K.S. Jasim, C. Chieh, and T.C.W. Mak, *J. Crystallogr. Spectros. Res., 15*, 403 (1985).

779. S. Le Stang, F. Conan, J. Sala-Pala, Y. Le Mest, M.-T. Garland, R. Baggio, E. Faulques, *J. Chem. Soc., Dalton Trans.*, 489 (1998).

780. C.T. Sun, Y.B. Zhu, Q.H. Fu, X.X. Liu, and S.S. Yi, *Chin. Chem. Lett., 5*, 617 (1994).

781. T.C.W. Mak,S. P. So, C. Chieh, and K.S. Jasim, *J. Mol. Struct., 127*, 375 (1985).

782. K.S. Jasim, C. Chieh, and T.C.W. Mak, *Inorg. Chim. Acta, 116*, 37 (1986).

783. M.-C. Shao, G.-P. Li, Y.-C. Tang, D.-Y. Guo, P.-Z. Lu, and Y.-G. Fan, *Acta Crystallogr., Sect.A, 37*, C232 (1981).

784. S.M. Meicheng, L. Genpei, T. Youqi, L. Pinzhe, F. Yuguo, and G. Dongyao, *Sci. Sin., Ser.B (Engl.Ed.), 25*, 576 (1982).

785. Z. Zhang, F. Wang, and S. Li, *Huaxue Xuebao (Acta Chim. Sinica)(Chin.), 42,* 650 (1984).

786. S. Cheng and S. Chunting, *Gaodeng Xuexiao Huaxue Xuebao (Chem. J. Chin. Uni.), 5,* 541 (1984).

787. K.S. Jasim, G.B. Umbach, C. Chieh, and T.C.W. Mak, *J. Crystallogr. Spectrosc. Res., 15*, 271 (1985).

788. K.S. Jasim, C. Chieh, and T.C.W. Mak, *Angew. Chem., Int. Ed. Engl., 25*, 749 (1986).

789. F.W. Moore and M.L. Larson, *Inorg. Chem., 6*, 998 (1967).

790. R.N. Jowitt and P.C.H. Mitchell, *J. Chem. Soc. A*, 2632 (1969).

791. C.G. Young, *J. Chem. Educ., 72*, 751 (1995).

792. K.B. Pandeya and B.B. Kaul, *Synth. React. Inorg. Met.-Org. Chem., 12*, 259 (1982).

793. S.P. Sovilj, D. Mitic, and V.M. Leovac, *Asian J. Chem., 15*, 165 (2003).

794. K.B. Pandeya, T.S. Waraich, R.C. Gaur, and R.P. Singh, *J. Indian Chem. Soc., 59*, 213 (1982).

795. A. Nakamura, M. Nakayama, K. Sughihashi, and S. Otsuka, *Inorg. Chem., 18*, 394 (1979).

796. J.M. Berg and K.O. Hodgson, *Inorg. Chem., 19*, 2180 (1980).

797. A. Kopwillem, *Acta Chem. Scand., 26*, 2941 (1972).

798. K. Unoura, A. Yamazaki, A. Nagasawa, Y. Kato, and H. Itoh, *Inorg. Chim. Acta, 269*, 260 (1998).

799. K. Unoura, Y. Abiko, A. Yamazaki, Y. Kato, D.C. Coomber, G.D. Fallon, K. Nakahara, and A.M. Bond, *Inorg. Chim. Acta, 333*, 41 (2002); K. Unoura, A. Iwase, and H. Ogino, *J. Electroanal. Chem., 295*, 385 (1990).

800. M.W. Peterson and R.M. Richman, *Inorg. Chem., 21*, 2609 (1982).

801. K. Unoura, Y. Kato, K. Abe, A. Iwase, and H. Ogino, *Bull. Chem. Soc. Jpn., 64*, 3372 (1991).

802. K. Unoura, R. Kikuchi, A. Nagasawa, Y. Kato, and Y. Fukuda, *Inorg. Chim. Acta, 228*, 89 (1995).

803. H.H. Huang, W. Huang, H.X. Yang, P.L. Gao, and D.G. Han, *Polyhedron, 16*, 2163 (1997).

804. X. Lu and J. Sun, *Synth. React. Inorg. Met.-Org. Chem., 12*, 427 (1982).

805. H. Teruel, and A. Sierraalta, *Can. J. Chem., 77*, 1521 (1999).
806. G. Kim and S.W. Lee, *Bull. Kor. Chem. Soc., 19*, 1211 (1998).
807. H. Arzoumanian, C. Corao, H. Krentzien, R. Lopez, and H.Teruel, *J. Chem. Soc., Chem. Commun.*, 856 (1992).
808. A. Srivastava, Y.A. Ma, R. Pankayatselvan, W. Dinges, and K.M. Nicholas, *J. Chem. Soc., Chem. Commun.*, 853 (1992).
809. P. Nag, R. Bohra, R.C. Mehrotra, and R. Ratnani, *Synth. React. Inorg. Met.-Org. Chem., 32*, 1549 (2002).
810. C.G. Young, C.J. Boreham, and J.A. Broomhead, *J. Chem. Soc., Dalton Trans.*, 2135 (1983).
811. J.A. Broomhead, M. Sterns, and C.G. Young, *J. Chem. Soc., Chem. Commun.*, 1262 (1981).
812. J.A. Broomhead, M. Sterns, and C.G. Young, *Inorg. Chem., 23*, 729 (1984).
813. J.R. Dilworth, B.D. Neaves, C.J. Pickett, J. Chatt, and J.A. Zubieta, *Inorg. Chem., 22,* 3524 (1983).
814. H.L. Kaufmann, L. Liable-Sands, A.L. Rheingold, and S.J. Nieter-Burgmayer, *Inorg. Chem., 38*, 2592 (1999).
815. K.S. Nagaraja and M.R. Udupa, *Transition Met. Chem., 9*, 290 (1984).
816. W.E. Newton, J.W. McDonald, J.L. Corbin, L. Ricard, and R.Weiss, *Inorg. Chem., 19,* 1997 (1980).
817. E.A. Maatta, R.A.D. Wentworth, W.E. Newton, J.W. McDonald, and G.D. Watt, *J. Am. Chem. Soc., 100*, 1320 (1978).
818. E.A. Maatta and R.A.D. Wentworth, *Inorg. Chem., 18*, 524 (1979).
819. M.A. Bennett and I.W. Boyd, *J. Organomet. Chem., 290*, 165 (1985).
820. N. Le Berre, R. Kergoat, M.M. Kubicki, J.E. Guerchais, and P.L' Haridon, *J. Organomet. Chem., 389*, 61 (1990).
821. J.L. Templeton, P.B. Winston, and B.C. Ward, *J. Am. Chem. Soc., 103*, 7713 (1981).
822. E.A. Maatta and R.A.D. Wentworth, *Inorg. Chem., 17*, 922 (1978).
823. J.A. Smegal, I.K. Meier, and J. Schwartz, *J. Am. Chem. Soc., 108*, 1322 (1986).
824. T. Venkataraman and K.S. Nagaraja, *Polyhedron, 11*, 185 (1992).
825. K.S. Nagaraja, *Ind. J. Chem. Sect. A, 30*, 701 (1991).
826. D.J.A. Raj, C.J. Gem, C.R.S. Raj, and I.M. Mathai, *J. Indian Chem. Soc., 66*, 903 (1989).
827. T. Venkataraman and K.S. Nagaraja, *Indian J. Chem. Sect. A, 35*, 300 (1996).
828. J.D.A. Raj, K.S. Nagaraja, and M.R. Udupa, *Transition Met. Chem., 11*, 176 (1986).
829. F. Montilla, A. Pastor, and A. Galindo, *J. Organomet. Chem., 590*, 202 (1999).
830. D.D. Devore, E.A. Maatta, and F. Takusagawa, *Inorg. Chim. Acta, 112*, 87 (1986).
831. E.W. Harlan and R.H. Holm, *J. Am. Chem. Soc., 112*, 186 (1990).
832. E.A. Maatta and R.A.D. Wentworth, *Inorg. Chem., 18*, 2409 (1979).
833. C.Y. Chou, D.D. Devore, S.C. Huckett, E.A. Maatta, J.C. Huffman, and F. Takusagawa, *Polyhedron, 5*, 301 (1986).
834. D.D. Devore and E.A. Maatta, *Inorg.Chem., 24*, 2846 (1985).
835. R.L. Elliott, P. Kruger, K.S. Murray, and B.O. West, *Aust. J. Chem., 45*, 889 (1992).
836. T.A. Coffey, G.D. Forster, G. Hogarth, and A.Sella, *Polyhedron, 12*, 2741 (1993).
837. B.L. Haymore, E.A. Maatta, and R.A.D. Wentworth, *J. Am.Chem. Soc., 101*, 2063 (1979).
838. T.A. Coffey, G. Hogarth, and S.P. Redmond, *Inorg. Chim. Acta, 308*, 155 (2000).

839. G. Hogarth, T. Norman, and S.P. Redmond, *Polyhedron, 18*, 1221 (1999).

840. M. Minelli, R.L. Kuhlman, S.J. Shaffer, and M.Y. Chiang, *Inorg. Chem., 31*, 3891 (1992).

841. M. Minelli, M.R. Carson, D.W. Whisenhunt, Jr., and J.L. Hubbard, *Inorg. Chem., 29*, 442 (1990).

842. M. Minelli, M.R. Carson, D.W. Whisenhunt, Jr., W. Imhof, and G. Huttner, *Inorg. Chem., 29*, 4801 (1990).

843. E.A. Maatta, B.L. Haymore, and R.A.D. Wentworth, *Inorg. Chem., 19*, 1055 (1980).

844. D.N. Zaroubine, D.S. Holovko, and N.A. Ustynyuk, *Russ. Chem. Bullet., Int. Ed., 51*, 1075 (2002).

845. T.A. Coffey, G.D. Forster, and G. Hogarth, *Inorg. Chim. Acta, 274*, 243 (1998).

846. E.A. Maatta,and R.A.D. Wentworth, *Inorg. Chem., 19*, 2597 (1980).

847. A.C. Stergiou, S. Bladenopoulou, and C. Tsiamis, *Inorg. Chim. Acta, 217*, 61 (1994).

848. J. Chatt, B.A.L. Crichton, J.R. Dilworth, P. Dahlstrom, R. Gutkoska, and J.Zubieta, *Inorg. Chem., 21,* 2383 (1982).

849. M.W. Bishop, J. Chatt, J.R. Dilworth, M.B. Hursthouse, and M. Motevalli, *J. Chem. Soc., Dalton Trans.*, 1600 (1979).

850. M.W. Bishop, J. Chatt, J.R. Dilworth, M.B. Hursthouse, and M. Motevalli, *J. Chem. Soc., Dalton Trans.*, 1600 (1979).

851. J. Chatt, B.A.L. Crichton, J.R. Dilworth, P. Dahlstrom, R. Gutkoska, and J. Zubieta, *Inorg. Chem., 21,* 2383 (1982).

852. J.R. Dilworth, R.A. Henderson, P. Dahlstrom, T. Nicholson, and J.A. Zubieta, *J. Chem. Soc., Dalton Trans.*, 529 (1987).

853. J. Chatt, J.R. Dilworth, P.L. Dahlstrom, and J. Zubieta, *J. Chem. Soc., Chem. Commun.*, 786 (1980).

854. J.R. Dilworth, R.A. Henderson, P. Dahlstrom, T. Nicholson, and J.A. Zubieta, *J. Chem. Soc., Dalton Trans.*, 529 (1987).

855. J. Chatt, B.A.L. Crichton, J.R. Dilworth, P. Dahlstrom, R. Gutkoska, and J.A. Zubieta, *Transition Met. Chem., 4*, 271 (1979).

856. R. Mattes and H. Scholand, *Angew. Chem., Int. Ed. Engl., 22*, 245 (1983).

857. R. Mattes, H. Scholand, U. Mikloweit, and V. Schrenk, *Z. Naturforsch., Teil B, 42,* 589 (1987).

858. R. Mattes, H. Scholand, U. Mikloweit, and V. Schrenk, *Z. Naturforsch., Teil B, 42*, 599 (1987).

859. J.R. Dilworth and J.A. Zubieta, *Transition Met. Chem., 9*, 39 (1984).

860. R. Mattes, H. Scholand, U. Mikloweit, and V. Schrenk, *Chem. Ber., 120*, 783 (1987).

861. R. Mattes and H. Scholand, *Angew. Chem., Int. Ed. Engl., 23,* 382 (1984).

862. M.W. Bishop, J. Chatt, J.R. Dilworth, J.R. Hyde, S. Kim, K. Venkatasubramanian, and J. Zubieta, *Inorg.Chem.,17*, 2917 (1978).

863. C.P. Marabella, J.H. Enemark, W.E. Newton, and J.W. McDonald, *Inorg. Chem., 21*, 623 (1982).

864. M.W. Bishop, J. Chatt, and J.R. Dilworth, *J. Organomet. Chem., 73*, C59 (1974).

865. J. Chatt and J.R. Dilworth, *J. Less-Common Met., 36*, 513 (1974).

866. M.W. Bishop, G. Butler, J. Chatt, J.R. Dilworth, and G.J. Leigh, *J. Chem. Soc., Dalton Trans.*, 1843 (1979).

867. G. Butler, J. Chatt, G.J. Leigh, A.R.P. Smith, and G.A. Williams, *Inorg. Chim. Acta, 28*, L165 (1978).

868. G. Butler, J. Chatt, G.J. Leigh, A.R.P. Smith, and G.A. Williams, *Inorg. Chim. Acta, 28*, L165 (1978).
869. G. Butler, J. Chatt, W. Hussain, G.J. Leigh, and D.L. Hughes, *Inorg. Chim. Acta, 30*, L287 (1978).
870. K. Yamanouchi and J.H. Enemark, *Inorg. Chem., 17*, 1981 (1978).
871. J. Chatt and J. Dilworth, *J. Indian Chem. Soc., 54*, 13 (1977).
872. M.W. Bishop, J. Chatt, and J.R. Dilworth, *J. Chem. Soc., Dalton Trans.*, 1 (1979).
873. S.B. Seymore and S.N. Brown, *Inorg. Chem., 41*, 462 (2002).
874. K. Leonard, K. Plute, R.C. Haltiwanger, and M.R. Dubois, *Inorg. Chem., 18*, 3247 (1979).
875. J.W. McDonald and W.E. Newton, *Inorg. Chim. Acta, 44*, L81 (1980).
876. T.A. Coffey and G. Hogarth, *Polyhedron, 16*, 165 (1997).
877. S. Xiaoqing, Y. Huixing, and H. Degang, *Int. J. Chem. Kinet., 21*, 749 (1989).
878. S. Xiaoqing, Y. Huixing, and H. Degang, *Int. J. Chem. Kinet., 21*, 737 (1989).
879. A.M. Bond, J.A. Broomhead, and A.F. Hollenkamp, *Inorg. Chem., 27*, 978 (1988).
880. W. Adam, R.M. Bargon, S.G. Bosio, W.A. Schenk, and D. Stalke, *J. Org. Chem., 67*, 7037 (2002).
881. W. Adam, R.M. Bargon, and W.A. Schenk, *J. Am. Chem. Soc., 125*, 3871 (2003).
882. W. Adam and R.M. Bargon, *Chem. Commun.*, 1910 (2001).
883. D.S. Brown, C.F. Owens, B.G. Wilson, M.E. Welker, and A.L.Rheingold, *Organometallics, 10*, 871 (1991).
884. S. Asirvatham, M.A. Khan, and K.M. Nicholas, *Inorg. Chim. Acta, 305*, 221 (2000).
885. B.F.G. Johnson, A. Khair, C.G. Savory, R.H. Walter, K.H. Al-Obaidi, and T.J. Al-Hassam, *Transition Met. Chem., 3*, 81 (1978).
886. E.C. Alyea, G. Ferguson, and A. Somogyvari, *Inorg. Chem., 21*, 1372 (1982).
887. G. Ferguson and A. Somogyvari, *J. Crystallogr. Spectrosc. Res., 13*, 49 (1983).
888. J.A. Broomhead and J.R. Budge, *Aust. J. Chem., 32*, 1187 (1979).
889. W. De Oliveira, J.-L. Migot, M.B.G. De Lima, J. Sala-Pala, J.E. Guerchais, and J.-Y. Le Gall, *J. Organomet. Chem.,284*, 313 (1985).
890. J.A. Broomhead, J.R. Budge, and W. Grumley, *Inorg. Synth., 28*, 145 (1990).
891. M.F. Perpiñán, L. Ballester, A. Santos, A. Monge, C. Ruiz-Valero, and E. Gutièrrez, *Polyhedron, 6*, 1523 (1987).
892. S. Sarkar and P. Subramananian, *Inorg. Chim. Acta, 35*, L357 (1979).
893. J.R. Budge, J.A. Broomhead, and P.D.W. Boyd, *Inorg. Chem., 21*, 1031 (1982).
894. J.A. Broomhead and J.R. Budge, *Inorg. Chem., 17*, 2414 (1978).
895. J.A. Broomhead, J.R. Budge, W. Grumley, T.R. Norman, and M. Sterns, *Aust. J. Chem., 29*, 275 (1976).
896. K.H. Al-Obaidi and T.J. Al-Hassani, *Transition Met. Chem., 3*, 15 (1978).
897. K.-B. Shiu, S.-T. Lin, D.-W. Fung, T.-J. Chan, S.-M. Peng, M.-C. Cheng, and J.-L. Chou, *Inorg. Chem., 34*, 854 (1995).
898. K.-B. Shiu, S.-T. Lin, S.-M. Peng, and M.-C. Cheng, *Inorg. Chim. Acta, 229*, 153 (1995).
899. E. Carmona, E. Gutiérrez-Puebla, A. Monge, P.J. Pérez, and L.J. Sánchez, *Inorg. Chem., 28*, 2120 (1989).
900. H. Alper, F.W.B. Einstein, F.W. Hartstock, and R.H. Jones, *Organometallics, 6,* 829 (1987).

901. Y. Shi, G. Cheng, S. Lu, H. Guo, Q. Wu, X. Huang, and N. Hu, *J. Organomet. Chem., 455*, 115 (1993).
902. E. Roman, D. Catheline, and D. Astruc, *J. Organomet. Chem., 236*, 229 (1982).
903. H. Brunner and J. Wachter, *J. Organomet. Chem., 175*,, 285 (1979).
904. J.L. Davidson and F. Sence, *J. Organomet. Chem., 409*, 219 (1991).
905. J.L. Davidson, *J. Organomet. Chem., 186*, C19 (1980).
906. J.L. Davidson, *J. Chem. Soc., Chem. Commun.*, 113 (1980).
907. K.B. Shiu, J.Y. Lee, Y. Wang, and M.C. Cheng, *Inorg. Chem., 32*, 3565 (1993).
908. J.-H. Kim, M. Lamrani, J.-W. Hwang, and Y. Do, *Inorg. Chim. Acta, 283*, 145 (1998).
909. D.M. Baird and S.D. Croll, *Polyhedron, 5*, 1931 (1986).
910. M.V. Galakhov, P. Gomez-Sal, T. Pedraz, M.A. Pellinghelli, P. Royo, A. Tiripicchio, and A.V. de Miguel, *J. Organomet. Chem., 579*, 190 (1999).
911. C.C. Ramão and B. Royo, *J. Organomet. Chem., 663*, 78 (2002).
912. M.M. Hunt, W.G. Kita, B.E. Mann, and J.A. McCleverty, *J. Chem. Soc., Dalton Trans.*, 467 (1978).
913. M.M. Hunt, W.G. Kita, and J.A. McCleverty, *J. Chem. Soc., Dalton Trans.*, 474 (1978).
914. M.M. Hunt and J.A. McCleverty, *J. Chem. Soc., Dalton Trans.*, 480 (1978).
915. M.G.B. Drew, V. Felix, I.S. Goncalves, C.C. Romao, and B. Royo, *Organometallics, 17*, 5782 (1998).
916. C.G. Young, S.A. Roberts, R.B. Ortega, and J.H. Enemark, *J. Am. Chem. Soc., 109*, 2938, (1987).
917. N.E. Heimer and W.E. Cleland, Jr., *Acta Crystallogr., Sect.C, 47*, 56 (1991).
918. S.A. Roberts, C.G. Young, W.E. Cleland Jr., K. Yamanouchi, R.B. Ortega, and J.H. Enemark, *Inorg. Chem., 27,* 2647 (1988).
919. L.H. Doerrer, J.R. Galsworthy, M.L.H. Green, and M.A. Leech, *J. Chem. Soc., Dalton Trans.*, 2483 (1998).
920. R. Colton, G.R. Scollary, and I.B. Tomkins, *Aust. J. Chem., 21*, 15 (1968).
921. R. Colton and G.R. Scollary, *Aust. J. Chem., 21*, 1427 (1968).
922. G.L. Hillhouse and B.L. Haymore, *J. Am. Chem. Soc., 104*, 1537 (1982).
923. J.L. Templeton and S.J. Nieter-Burgmayer, *Organometallics, 1,* 1007 (1982).
924. J.L. Templeton and B.C. Ward, *J. Am. Chem. Soc., 102*, 6568 (1980).
925. J.L. Templeton, R.S. Herrick, C.A. Rusik, C.E. McKenna, J.W. McDonald, and W.E. Newton, *Inorg. Chem., 24*, 1383 (1985).
926. P.K. Baker, S.G. Fraser, and D.A. Kendrick, *J. Chem. Soc., Dalton Trans.*, 131 (1991).
927. E. Carmona, K. Doppert, J.M. Marin, M.L. Poveda, L. Sanchez, and R. Sanchezdelgado, *Inorg. Chem., 23*, 530 (1984).
928. S.J. Nieter-Burgmayer and J.L. Templeton, *Inorg. Chem., 24*, 2224 (1985).
929. B.A.L. Crichton, J.R. Dilworth, C.J. Pickett, and J. Chatt, *J. Chem. Soc., Dalton Trans.*, 892 (1981).
930. J.W. McDonald, W.E. Newton, C.T.C. Creedy, and J.L. Corbin, *J. Organomet. Chem., 92*, C25 (1975).
931. J.L. Templeton, R.S. Herrick, and J.R. Morrow, *Organometallics, 3*, 535 (1984).
932. F.M. Kerton, G.F. Mohmand, A. Tersteegen, M. Thiel, and M.J. Went, *J. Organomet. Chem., 519*, 177 (1996).

933. R.S. Herrick, D.M. Leazer, and J.L. Templeton, *Organometallics, 2*, 834 (1983).
934. J.R. Morrow, T.L. Tonker, and J.L. Templeton, *J. Am. Chem. Soc., 107*, 6956 (1985).
935. H.-B. Kraatz, M.J. Went, and J.C. Jeffery, *J. Organomet. Chem., 394*, 167 (1990).
936. J.R. Morrow, T.L. Tonker, and J.L. Templeton, *J. Am. Chem. Soc., 107*, 5004 (1985).
937. P.K. Baker and S.G. Fraser, *Transition Met. Chem., 11*, 273 (1986).
938. M. Al-Jahdali, P.K. Baker, and M.G.B. Drew, *J. Organomet. Chem., 622*, 228 (2001).
939. K.-B. Shiu, K.-H. Yih, S.-L. Wang, and F.-L. Liao, *J. Organomet. Chem., 420,* 359 (1991).
940. M.F. Perpiñán and A. Santos, *J. Organomet. Chem.,218*, 185 (1981).
941. K.-H. Yih, G.-H. Lee, S.-L. Huang, and Y. Wang, *Organometallics, 21*, 5767 (2002).
942. K.-H. Yih, G.-H. Lee, and Y. Wang, *J. Chin. Chem. Soc., 49*, 479 (2002).
943. L. Contreras, A. Monge, A. Pizzano, C. Ruiz, L. Sanchez, and E. Carmona, *Organometallics, 11*, 3971 (1992).
944. E. Carmona, L. Sanchez, M.L. Poveda, J.M. Marin, J.L. Atwood, and R.D.Rogers, *J. Chem. Soc., Chem. Commun.*, 161 (1983).
945. E. Carmona, L. Sanchez, J.M. Marin, M.L. Poveda, J.L. Atwood, R.D. Priester, R.D. Rogers, *J. Am. Chem. Soc., 106,* 3214 (1984).
946. G. Ujaque, F. Maseras, A. Lledos, L. Contreras, A. Pizzano, D. Rodewald, L. Sanchez, E. Carmona, A. Monge, and C. Ruiz, O*rganometallics, 18*, 3294 (1999).
947. K.-B. Shiu, S.-M. Peng, M.-C. Cheng, S.-L. Wang, and F.-L. Lioa, *J. Organomet. Chem., 461*, 111 (1993).
948. B.T. Zhuang, L.R. Huang, L.J. He, Y.Yang, and J.X. Lu, *Inorg. Chim. Acta, 145*, 225 (1988).
949. E. Alyea and A. Somogyvari, *Inorg. Chim. Acta, 83*, L49 (1984).
950. A.E. Sánchez-Peláez, M.F. Perpiñán, and A. Santos, *J. Organomet. Chem., 296*, 367 (1985).
951. B.T. Zhuang, P.H. Yu, L.G. Huang, L.J. He, and J.X. Lu, *Polyhedron, 13*, 125 (1994).
952. B. Zhuang, P. Chen, L. Huang, and J. Lu, *Polyhedron, 11,* 127 (1992).
953. R.D. Bereman, D.M. Baird, and C.G. Moreland, *Polyhedron, 2*, 59 (1983).
954. L. Ricard, J. Estienne, and R. Weiss, *Inorg. Chem., 12*, 2182 (1973).
955. L. Ricard, J. Estienne, and R. Weiss, *J. Chem. Soc., Chem. Commun.*, 906 (1972).
956. C. Sun, Q. Huang, S. Li, T. Wang, G. Zhang, X. Qu, Z. Tang, G. He, Y. Shen, Z. Jin, and G. Wei, *Chem. Res. Chin. Univ., 7*, 114 (1991).
957. R. Lozano, A. Moragues, and J. Roman, *Thermochim. Acta, 108*, 1 (1986).
958. T.O. Kocaba, C.G. Young, and E.R.T. Tiekink, *Inorg. Chim. Acta, 174*, 143 (1990).
959. F. Conan, J. Sala-Pala, M.T. Garland, and R. Baggio, *Inorg. Chim. Acta, 278*, 108 (1998).
960. K. Musha, S. Yamazaki, and S. Toda, *Nippon Kagaku Kaishi*, 1849 (1982).
961. K.S. Nagaraja and M.R. Udupa, *Transition Met. Chem., 11*, 217 (1986).
962. A. Muller, R.G. Bhattacharyya, N. Mohan, and B. Pfefferkorn, *Z. Anorg. Allg. Chem., 454*, 118 (1979).
963. S.-F. Lu, J.-Q. Huang, H.-B. Chen, and Q.-J. Wu, *Huaxue Xuebao (Acta Chim. Sinica)(Chin.), 51*, 885 (1993).
964. K.F. Miller, A.E. Bruce, J.L. Corbin, S. Wherland, and E.I. Stiefel, *J. Am. Chem. Soc., 102*, 5102 (1980).
965. K.S. Nagaraja and M.R. Udupa, *Transition Met. Chem., 8*, 191 (1983).
966. J.T. Huneke and J.H. Enemark, *Inorg. Chem., 17*, 3698 (1978).

967. K. Musha, Y. Ohashi, S. Yamazaki, S. Toda, and S. Tanaka, *Nippon Kagaku Kaishi*, 653 (1983).

968. K. Musha, N. Teramae, S. Yamazaki, S. Toda, and S. Tanaka, *Nippon Kagaku Kaishi*, 1889 (1984).

969. K. Musha, S.Yamazaki, and S. Toda, *Nippon Kagaku Kaishi*, 702 (1984).

970. W.E. Newton, J.W. McDonald, K. Yamanouchi, and J.H.Enemark, *Inorg. Chem., 18*, 1621 (1979).

971. R.C. Sharma and V.K. Srivastava, *J. Inst. Chem. (India), 69*, 18 (1997).

972. E.C. Alyea, G. Ferguson, M. Parvez, and A. Somogyvari, *Polyhedron, 4*, 783 (1985).

973. X.-Y. Huang, H.-B. Chen, and S.-F. Lu, *Chin. Chem. Lett., 4*, 1033 (1993).

974. N.C. Howlander, G.P. Haight, Jr., T.W. Hambley, M.R. Snow, and G.A. Lawrance, *Inorg. Chem., 23*, 1811 (1984).

975. J.T. Huneke and J.H. Enemark, *Inorg. Chem., 17*, 3698 (1978).

976. J.R. Dilworth, B.D. Neaves, P. Dahlstrom, J. Hyde, and J.A. Zubieta, *Transition Met. Chem., 7,* 257 (1982).

977. J.T. Huneke, K. Yamanouchi, and J.H. Enemark, *Inorg. Chem., 17*, 3695 (1978).

978. K. Unoura, T. Suzuki, A. Nagasawa, A. Yamazaki, and Y. Fukuda, *Inorg. Chim. Acta, 292*, 7 (1999).

979. A.L.D. Villarejo, M.P.Alonso, R. Lozano, and A. Doadrio, *Anal. Quimica Ser. B-Quimica Inorg. Quimica Anal., 79*, 195 (1983).

980. R.L. Thompson, S. Lee, S.J. Geib, and N.J. Cooper, *Inorg. Chem., 32*, 6067 (1993).

981. R. Ratnani, G. Srivastava, and R.C. Mehrotra, *Transition Met. Chem., 17*, 137 (1992).

982. C.D. Garner, N.C. Howlader, F.E. Mabbs, A.T. McPhail, and K.D. Onan, *J. Chem. Soc., Dalton Trans.*, 962 (1979).

983. T.A. Coffey, G.D. Forster, and G. Hogarth, *J. Chem. Soc., Dalton Trans.*, 2337 (1995).

984. K.L. Wall, K. Folting, J.C. Huffman, and R.A.D. Wentworth, *Inorg. Chem., 22,* 2366 (1983).

985. G.D. Forster and G.Hogarth, *J. Chem. Soc., Dalton Trans.*, 2539 (1993).

986. G.D. Forster and G.Hogarth, *Polyhedron, 14,* 1401 (1995).

987. V.P. Fedin, M.N. Sokolov, A.V. Virovets, N.V. Podberezskaya, and V. Ye. Fedorov, *Inorg. Chim. Acta, 194*, 195 (1992).

988. M.D. Meienberger, K. Hegetschweiler, H. Ruegger, and V. Gramlich, *Inorg. Chim. Acta, 213*, 157 (1993).

989. M.-F. Wang, G.-C. Guo, J.-S. Huang, H.-H. Zhuang, Q.-E. Zhang, and J.-X.Lu, *Chinese J. Struct. Chem. (Jiegou Huaxue), 13*, 221 (1994).

990. C.-Z. Lu, W. Tong, H.-H. Zhuang, and D.-M. Wu, *Chinese J. Struct. Chem.(Jiegou Huaxue), 12*, 124 (1993).

991. H.-P. Zhu, C.-N. Chen, Q.-T. Liu, and J.-T. Chen, *Acta Crystallogr., Sect.C, 54*, 1273 (1998).

992. H.-P. Zhu, Q.-T. Liu, C.-N. Chen, Y.-H. Deng, *Chinese J. Struct. Chem. (Jiegou Huaxue), 17*, 142 (1998).

993. M.J. Mayor-Lopez, J. Weber, K. Hegetschweiler, M.D. Meienberger, F. Joho, S. Leoni, R. Nesper, G.J. Reiss, W. Frank, B.A. Kolesov, V.P. Fedin, and V.E.Fedorov, I*norg. Chem., 37,* 2633 (1998).

994. H. Zimmermann, K. Hegetschweiler, T. Keller, V. Gramlich, H.W. Schmalle, W. Petter, and W. Schneider, *Inorg. Chem., 30*, 4336 (1991).

995. V.P. Fedin, M.N. Sokolov, O.A. Geras'ko, A.V. Virovets, N.V. Podberezskaya, and V. Ye. Fedorov, *Inorg. Chim. Acta, 192*, 153 (1992).
996. O.V. Volkov, T.M. Polyanskaya, E.A. Il'inchik, V.V. Volkov, K.G. Myakishev, and B.A. Kolesov, *Zh. Obshch. Khim., 69,* 607 (1999).
997. V.P. Fedin, A. Muller, H. Bogge, A. Armatage, M.N. Sokolov, S.S. Yarovoi, and V.E. Fedorov, *Zh. Neorg. Khim., 38*, 1677 (1993).
998. V.V. Volkov, E.A. Il'inchik, O.V. Volkov, G.S. Voronina, and K.G. Myakishev, *Russ. J. Coord. Chem., 24*, 844 (1998).
999. V.P. Fedin, M.N. Sokolov, O.A. Geras'ko, A.V. Virovets, N.V. Podberezskaya, and V.Ye. Fedorov, *Inorg. Chim. Acta, 187*, 81 (1991).
1000. V.P. Fedin, M.N. Sokolov, O.A. Geras'ko, A.V. Virovets, N.V. Podberezskaya, and V. Ye. Fedorov, *Inorg. Chim. Acta, 187*, 81 (1991).
1001. V.V. Volkov, K.G. Myakishev, and E.A. Il'inchik, *Russ. J. Coord. Chem., 27*, 398 (2001).
1002. M.J. Almond, M.G.B. Drew, H. Redman, and D.A. Rice, *Polyhedron, 19*, 2127 (2000).
1003. V.P. Fedin, M.N. Sokolov, A.V. Virovets, N.V. Podberezskaya, and V.Ye. Federov, *Polyhedron, 11*, 2395 (1992).
1004. V.P. Fedin, Yu.V. Mironov, M.N. Sokolov, A.V. Virovets, N.V. Podberezskaya, and V.E. Federov, *Zh. Neorg. Khim., 37*, 2205 (1992).
1005. W.-B. Yang, X. Lin, C.-Z. Lu, and H.-H. Zhuang, *Chin. J. Chem., 20*, 327 (2002).
1006. M.-D. Huang, S.-F. Lu, J.-Q. Huang, and J.-L. Huang, *Huaxue Xuebao (Acta Chim. Sinica) (Chin.), 47*, 121 (1989).
1007. S.-F. Lu, Z.-X. Huang, J.-Q. Huang, B. Zhang, J.-L. Hunag, *Chin. J. Chem. (Huaxue Xuebao)(Engl.), 10*, 52 (1992).
1008. Y.-S. Zhang, Q.-T. Liu, H.-P. Zhu, Y.-H. Chen, C.-N. Chen, *Chin. J. Chem., 18*, 188 (2000).
1009. Q.-T. Liu and L.-R. Huang, *Chinese J. Struct. Chem.(Jiegou Huaxue), 10*, 10 (1991).
1010. K. Tsuge, S. Mita, H. Fujita, H. Imoto, and T. Saito, *J. Cluster Sci., 7*, 407 (1996).
1011. Q. Liu. L. Huang, B. Kang, Y. Yang, and J. Lu, *Kexue Tongbao (Chin. Sci. Bull.)(Engl.), 32*, 898 (1987).
1012. Q. Liu. L. Huang, B. Kang, Y. Yang, and J. Lu, *Huaxue Xuebao (Acta Chim. Sinica)(Chin.), 45,* 133 (1987).
1013. Q. Liu, L. Huang, L. Wang, B. Kang, and J. Lu, *Chinese J. Struct. Chem. (Jiegou Huaxue), 2*, 291 (1983).
1014. Q. Liu, L. Huang, B. Kang, C. Liu, L. Wang, and J. Lu, *Huaxue Xuebao (Acta Chim. Sinica)(Chin.), 44*, 343 (1986).
1015. Q.-T. Liu, L.-R. Huang, Y. Yang, and J.-X. Lu, *Huaxue Xuebao (Acta Chim. Sinica)(Chin.), 46*, 1 (1988).
1016. Q.-T. Liu, L.-R. Huang, Y. Yang, and J.-X. Lu, *Huaxue Xuebao (Acta Chim. Sinica)(Chin.), 46*, 1075 (1988).
1017. M.-D. Huang, S.-F. Lu, J.-Q. Huang, and J.-L. Huang, *Acta Chim. Sinica, 47*, 121 (1989).
1018. Y. Peng, MS Thesis, Fujian Institute of Research on the Structure of Matter, Chinese Academy of Sciences, Fuzhon, 2000.
1019. T. Ikada, S. Kuwata, Y. Mizobe, and M. Hidai, *Inorg. Chem., 38*, 64 (1999).
1020. T. Ikada, Y. Mizobe, S. Kuwata, and M. Hidai, *Nippon Kagaku Kaishi*, 493 (2001).
1021. T. Ikada, Y. Mizobe, and M. Hidai, *Organometallics, 20*, 4441 (2001).
1022. T.R. Halbert, S.A. Cohen, and E.I. Stiefel, *Organometallics, 4*, 1689 (1985).

1023. T. Ikada, S. Kuwata, Y. Mizobe, and M. Hidai, *Inorg. Chem., 38*, 64 (1999).
1024. T. Ikada, S. Kuwata, Y. Mizobe, and M.Hidai, *Inorg. Chem., 37*, 5793 (1998).
1025. N. Ueyama, K. Kamabuchi, and A. Nakamura, *J. Chem. Soc., Dalton Trans.*, 635 (1985).
1026. G.D. Watt, J.W. McDonald, and W.E. Newton, *J.Less-Common Met., 54*, 415 (1977).
1027. S. Bhaduri and H. Khwaja, *J. Chem. Soc., Dalton Trans.*, 415 (1983).
1028. R.R. Kuntz, *J. Photochem. Photobiol. A-Chem., 108*, 215 (1997).
1029. M.G.B. Drew, N.J. Jutson, P.C.H. Mitchell, and S.A. Wass, *Polyhedron, 8*, 1817 (1989).
1030. K. Arai and Y. Yamamoto, *Tribol. Trans., 43*, 45 (2000).
1031. C. Grossiord, K. Varlot, J.M. Martin, T. Le Mogne, C. Esnouf, and K. Inoue, *Tribol. Int., 31*, 737 (1998).
1032. Y. Yamamoto and G.S. Gondo, *Tribol. Trans., 32*, 251 (1989).
1033. J. Graham, H. Spikes, and S. Koreck, *Tribol. Trans., 44*, 626 (2001).
1034. J. Graham, H. Spikes, and R. Jensen, *Tribol. Trans., 44*, 637 (2001).
1035. K.T. Miklozic, J. Graham, and H. Spikes, *Tribol. Lett., 11*, 71 (2001).
1036. S. Gondo and M. Konishi, *Wear, 120*, 51 (1987).
1037. I. Watanabe, M. Otake, M. Yoshimoto, K. Sakanishi, Y. Korai, and I. Mochida, *Fuel, 81*, 1515 (2002).
1038. J. Ye, M. Kano and Y. Yasuda, *Tribol. Lett., 13*, 41 (2002).
1039. M. Muraki and H. Wada, *Trib. Int., 35*, 857 (2002).
1040. M.R.Udupa and K.S. Nagaraja, *Thermochim. Acta, 56*, 241 (1982).
1041. Y.V. Rakitin and A.V. Ivanov, *Russ. Chem. Bull., 48*, 2073 (1999).
1042. V.V. Ramana, K. Santha, M.D. Ramaiah, and K. Saraswathi, *J. Indian Chem. Soc., 68*, 178 (1991).
1043. J.N. Smith and T.M. Brown, *Inorg. Nucl. Chem. Lett., 6*, 441 (1970).
1044. G.J.-J. Chen, J.W. McDonald, and W.E. Newton, *Inorg. Chim. Acta, 19*, L67 (1976).
1045. K. Unoura, M. Kondo, A. Nagasawa, M. Kanesato, H. Sakiyama, A. Oyama, H. Horiuchi, E. Nishida, and T. Kondo, *Inorg. Chim. Acta, 357*, 1265 (2004).
1046. S.D. Robinson and A. Sahajpal, *J. Organomet. Chem., 99*, C65 (1975).
1047. A. Nieuwpoort and J.J. Steggerda, *Recl. Trav. Chim. Pays-Bas, 95*, 250 (1976).
1048. D.A. Brown, W.K. Glass, H.J. Toma, and W.E. Waghorne, *J. Chem. Soc., Dalton Trans.*, 2531 (1987).
1049. V.P. Fedin, Yu.V. Mironov, A.V. Virovets, N.V. Podberezskaya, and V.Ye. Federov, *Polyhedron, 11*, 1959 (1992).
1050. V.P. Fedin, Yu.V. Mironov, A.V. Chernobrivets, A.V. Virovets, N.V. Podberezskaya, V.E. Fedorov, *Zh. Neorg. Khim., 37*, 1087 (1992).
1051. M.L. Ziegler, K. Blechschmitt, H. Bock, E. Guggolz, and R.P. Korswagen, *Z. Naturforsch., Teil B, 43*, 590 (1988).
1052. S. Yu and R.H. Holm, *Inorg. Chem., 28*, 4385 (1989).
1053. S. Lee, D.L. Staley, A.L. Rheingold, and N.J. Cooper, *Inorg. Chem., 29*, 4391 (1990).
1054. E. Carmona, L. Sachez, M.L. Proveda, R.A. Jones, and J.G. Hefner, *Polyhedron, 2*, 797 (1983).
1055. R. Lozano, E. Alarcón, A.L. Doadrio, and A. Doadrio, *Polyhedron, 3*, 25 (1984).
1056. R. Lozano, E. Alarcón, A. L. Doadrio, and A. Doadrio, *Polyhedron, 2*, 435 (1983).

1057. N.K. Kaushik, G.S. Sodhi, H.S. Sangari, and G.R. Chhatwal, *J. Inst. Chem. (India), 52*, 259 (1980).
1058. J.L. Templeton, B.C. Ward, G.J.-J. Chen, J.W. McDonald, and W.E. Newton, *Inorg. Chem., 20*, 1248 (1981).
1059. J.A. Broomhead, J.H. Enemark, B. Hammer, R.B. Ortega, and W. Pienkowski, *Aust. J. Chem., 40*, 381 (1987).
1060. M.R. Snow, E.R.T. Tiekink, and C.G. Young, *Inorg. Chim. Acta, 150*, 161 (1988).
1061. V.P. Fedin, Yu.V. Mironov, A.V. Virovets, N.V. Podberezskaya, V.Ye. Fedorov, and P.P. Semyannikov, *Polyhedron, 11*, 279 (1992).
1062. M.F. Mackay, P.J. Oliver, and C.G. Young, *Aust. J. Chem., 42*, 837 (1989).
1063. Y. Gea, M.A. Greaney, C.L. Coyle, and E.I. Stiefel, *J. Chem. Soc., Chem. Commun.*, 160 (1992).
1064. E.R.T. Tiekink, A.A. Eagle, and C.G. Young, *Aust. J. Chem., 53*, 779 (2000).
1065. G.X. Jin and M. Herberhold, *Transition Met. Chem., 24*, 317 (1999).
1066. H.B. Abrahamson, M.L. Freeman, M.B. Hossain, and D. Van der Helm, *Inorg. Chem., 23*, 2286 (1984).
1067. H.B. Abrahamson and M.L. Freeman, *Organometallics, 2*, 679 (1983).
1068. P.J. Lim, D.A. Slizys, J.M. White, C.G.Young, and E.R.T. Tiekink, *Organometallics, 22*, 4853 (2003).
1069. B.T. Zhuang, P.H. Yu, L.G. Huang, L.J. He, J.X. Lu, *Inorg. Chim. Acta, 177*, 239 (1990).
1070. A.E. Sánchez-Peláez, M.F. Perpiñán, E. Gutierrez-Puebla, and C. Ruiz-Valero, *J. Organomet. Chem., 384*, 79 (1990).
1071. J.L. Templeton and B.C. Ward, *Inorg. Chem., 19*, 1753 (1980).
1072. J.A. Broomhead and C.G. Young, *Aust. J. Chem., 35*, 277 (1982).
1073. J.L. Templeton and B.C. Ward, *J. Am. Chem. Soc., 103*, 3743 (1981).
1074. P.B. Hitchcock, M.F. Lappert, and M.J. McGeary, *J. Am. Chem. Soc., 112*, 5658 (1990).
1075. P.B. Hitchcock, M.F. Lappert, and M.J. McGeary, *Organometallics, 9*, 2645 (1990).
1076. L. Ricard, R. Weiss, W.E. Newton, J.-J. Chen, and J.W. McDonald, *J. Am. Chem. Soc., 100*, 1318 (1978).
1077. G.J.-J. Chen, R.O. Yelton, and J.W. McDonald, *Inorg. Chim. Acta, 22*, 249 (1977).
1078. B.C. Ward and J.L. Templeton, *J. Am. Chem. Soc., 102*, 1532 (1980).
1079. L. Carlton and J.L. Davidson, *J. Chem. Soc., Dalton Trans.*, 2071 (1988).
1080. P.K. Baker and K.R. Flower, *J. Organomet. Chem., 447*, 67 (1993).
1081. J.L. Templeton and B.C. Ward, *J. Am. Chem. Soc., 102*, 3288 (1980).
1082. A.K. Powell and M.J. Went, *J. Chem. Soc., Dalton Trans.*, 439 (1992).
1083. J.R. Morrow, T.L. Tonker, and J.L. Templeton, *Organometallics, 4*, 745 (1985).
1084. D.C. Brower, T.L. Tonker, J.R. Morrow, D.S. Rivers, and J.L. Templeton, *Organometallics, 5*, 1093 (1986).
1085. T.P. Curran, A.L. Grant, R.A. Lucht, J.C. Carter, and J. Affonso, *Organic Lett., 4*, 2917 (2002).
1086. P.K. Baker, G.A. Cartwright, P.D. Jackson, K.R. Flower, N. Galeotti, and L.M. Severs, *Polyhedron, 11*, 1043 (1992).
1087. P.K. Baker, K.R. Flower, and M.G.B. Drew, *Organometallics, 12*, 276 (1993).
1088. P.K. Baker, K.R. Flower, M.E. Harman, and M.B. Hursthouse, *J. Chem. Soc., Dalton Trans.*, 3169 (1990).

1089. E.M. Armstrong, P.K. Baker, K.R. Flower, and M.G.B. Drew, *J. Chem. Soc., Dalton Trans.*, 2535 (1990).

1090. P.K. Baker, M.G.B. Drew, and K.R. Flower, *J. Organomet. Chem., 391*, C12 (1990).

1091. P.K. Baker and K.R. Flower, *J.Organomet.Chem., 397*, 59 (1990).

1092. A. Mayr, R.T. Chang, T.Y. Lee, O.K. Cheung, M.A. Kjelsberg, G.A. McDermott, and D. Van Engen, *J. Organomet. Chem., 479*, 47 (1994).

1093. K.R. Birdwhistell, T.L. Tonker, and J.L. Templeton, *J. Am. Chem. Soc., 107*, 4474 (1985).

1094. L. Zhang, M.P. Gamasa, J. Gimeno, A. Galindo, C. Mealli, M. Lanfranchi, and A. Tiripicchio, *Organometallics, 16*, 4099 (1997).

1095. A. Mayr, G.A. Mc Dermott, A.M. Dorries, A.K. Holder, W.C. Fultz, and A.L.Rheingold, *J. Am. Chem. Soc., 108*, 310 (1986).

1096. M.F. Asaro, A. Mayr, B. Kahr, and D. Vanengen, *Inorg. Chim. Acta, 220*, 335 (1994).

1097. A. Mayr, M.F. Asaro, and T.J. Glines, *J. Am. Chem. Soc., 109*, 2215 (1987).

1098. M.F. Asaro, A. Mayr, B. Kahr, and D. Van Engen, *J. Am. Chem. Soc., 109*, 2215 (1987).

1099. E. Carmona L. Contreras, E. Gutierrezpuebla, A. Monge, and L.J. Sánchez, *Organometallics, 10*, 71 (1991).

1100. S.G. Feng, A.S.Gamble, and J.L. Templeton, *Organometallics, 8*, 2024 (1989).

1101. M.A. Bennett, I.W. Boyd, G.B. Robertson, and W.A. Wickramasinghe, *J. Organomet. Chem., 290*, 181 (1985).

1102. R. Lozano, J. Roman, F. De Jesús, and E. Alarcón, *Inorg. Chim. Acta, 186*, 231 (1991).

1103. R. Lozano, E. Alarcon, J. Roman, and A. Doadrio, *Polyhedron, 3*, 1021 (1984).

1104. R. Lozano, E. Alarcon, J. Roman, A.L. Doadrio, and A. Doadrio, *Anal. Quim. Ser. B-Quim. Inorg. Quim. Anal., 79*, 360 (1983).

1105. R. Lozano, E. Alarcon, A.L. Doadrio, and A. Doadrio, *Anal. Quim. Ser. B-Quim. Inorg. Quim. Anal., 79*, 37 (1983).

1106. M.G.B. Drew, R.J. Hobson, P.P.E.M. Mumba, D.A. Rice, and N. Turp, *J. Chem. Soc., Dalton Trans.*, 1163 (1987).

1107. R. Lozano, E. Alarcon, J. Roman, and A. Doadrio, *Rev. Chim. Miner., 21*, 177 (1984).

1108. R. Lozano, E. Alarcon, J. Roman, and A. Doadrio, *Acta Cientifica Venezolana, 36*, 214 (1985).

1109. R.C. Sharma and V.K. Srivastava, *J. Inst. Chem. (India), 69*, 16 (1997).

1110. R. Lozano, A.L. Doadrio, E, Alarcon, J. Roman, and A. Doadrio, *Rev. Chim. Miner., 20*, 109 (1983).

1111. S.A. Cohen and E.I. Stiefel, *Inorg. Chem., 24*, 4657 (1985).

1112. H. Seino, Y. Mizobe, and M. Hidai, *Bull. Chem. Soc. Jpn., 73*, 631 (2000).

1113. M.H. Chisholm, D.L. Clark, J.C. Huffman, and W.G.Van Der Sluys, *J. Am. Chem. Soc., 109*, 6817 (1987).

1114. L. Cambi and A. Cagnasso, *Atti Accad. Lincei, 14*, 71 (1931).

1115. B.S. Garg, A.L. Singh, and R. Dixit, *Transition Met. Chem., 13*, 351 (1988).

1116. A.C. Fabretti, G.C. Franchini, C. Preti, G. Tosi, and P. Zannini, *Transition Met. Chem., 10*, 284 (1985).

1117. G. Krishnan and C.P. Prabhakaran, *Polyhedron, 13*, 983 (1994).

1118. B.M. Ondo, J.P. Barbier, and R.P. Hugel, *Inorg. Chim. Acta, 77*, L211 (1983).

1119. B.K. Kanungo, B. Pradhan, D.V.R. Rao, *Indian J. Chem., Sect. A, 21*, 625 (1982).

1120. A. Jezierski, *J. Mol. Struct., 115*, 11 (1984).

1121. G.E. Manoussakis and C.A. Bolos, *Inorg. Chim. Acta, 108*, 215 (1985).
1122. P. Deplano, E.F. Trogu, F. Bigoli, and M.A. Pellinghelli, *J. Chem. Soc., Dalton Trans.*, 2407 (1987).
1123. B. Pradhan and D.V.R. Rao, *J. Indian Chem. Soc., 58*, 733 (1981).
1124. B.M. Ondo, J.P. Barbier, and R.P. Hugel, *J. Chem. Res. S*, 302 (1985).
1125. K.S. Siddiqi, M.A.A. Shah, and S.A.A. Zaidi, *Indian J. Chem. Sect A, Inorg. Phys. Theor. Anal. Chem., 22*, 812 (1983).
1126. H. Cesur, T.K. Yazicilar, B. Bati, and V.T. Yilmaz, *Synth. React. Inorg. Met.-Org. Chem., 31*, 1271 (2001).
1127. K.B. Pandeya, R. Singh, P.K. Mathur, and R.P. Singh, *Transition Met. Chem., 11*, 347 (1986).
1128. J. Doherty and A.R. Manning, *J. Organomet. Chem., 253*, 81 (1983).
1129. L. Busetto, A. Palazzi, and V. Foliadis, *Inorg. Chim. Acta, 40*, 147 (1980).
1130. L.V. Zavyalova, A.K. Savin, and G.S. Svechnikov, *Displays, 18*, 73 (1997).
1131. V.G. Bessergenev, V.I. Belyi, A.A. Rastorguev, E.N. Ivanova, Y.A. Kovalevskaya, V.A. Larionov, S.M. Zemskova, V.N. Kirichenko, V.A. Nadolinnyi, and S.A. Gromilov, *Thin Solid Films, 279*, 135 (1996).
1132. M.A. Scibioh, K. Swaminathan, and K.S. Nagaraja, *Bull. Electrochem., 14*, 164 (1998).
1133. E. Suresh, J. Pragasam, F.P. Xavier, and K.S. Nagaraja, *Int. J. Energy Res., 23*, 229 (1999).
1134. G. Meco, V. Bonifati, N. Vanacore, and E. Fabrizio, *Scand. J. Work Environ. Health, 20*, 301 (1994).
1135. H.B. Ferraz, P.H.F. Bertolucci, J.S. Pereira, J.G.C. Lima, and L.A.F. Andrade, *Neurology, 38*, 550 (1988).
1136. U. Abram, B. Lorenz, L. Kaden, and D. Scheller, *Polyhedron, 7*, 285 (1988).
1137. J. Baldas, J.F. Boas, S.F. Colmanet, and G.A. Williams, *J. Chem. Soc., Dalton Trans.*, 2845 (1992).
1138. J. Baldas, J.F. Boas, J. Bonnyman, S.F. Colmanet, and G.A. Williams, *J. Chem. Soc., Chem. Commun.*, 1163 (1990).
1139. A. Marchi, L. Marvelli, R. Rossi, L. Magon, L. Uccelli, V. Bertolasi, V. Ferretti, and F. Zanobini, *J. Chem. Soc., Dalton Trans.*, 1281 (1993).
1140. A. Boschi, L. Uccelli, C. Bolzati, A. Duatti, N. Sabba, E. Moretti, G. Di Domenico, G. Zavattini, F. Refosco, and M. Giganti, *J. Nucl. Med., 44*, 806 (2003).
1141. A. Boschi, C. Bolzati, L. Uccelli, A. Duatti, E. Benini, F. Refosco, F. Tisato, and A. Piffanelli, *Nucl. Med. Commun., 23*, 689 (2002).
1142. P.M. Pojer and J. Baldas, *Int. J. Nucl. Med. Biol., 8*, 112 (1981).
1143. J.H.Chiu, T.C. Chu, and P.S. Weng, *J. Radioanal. Nucl. Chem. Artic., 150*, 493 (1991).
1144. J.R. Ballinger, B. Gerson, and K.Y. Gulenchyn, *Nucl. Med. Biol., 16*, 721 (1989).
1145. U. Abram and H. Spies, *Inorg. Chim. Acta, 94*, L3 (1984).
1146. M.A. Stalteri, S.J. Parrott, V.A. Griffiths, J.R. Dilworth, and S.J. Mather, *Nucl. Med. Commun., 18*, 870 (1997).
1147. J.B. Zhang, X.B. Wang, G.X. Lu, and Z.G. Tang, *J. Label. Compd. Radiopharm., 43*, 693 (2000).
1148. R. Pasqualini, A. Duatti, E. Bellande, V. Comazzi, V. Brucato, D. Hoffschir, D. Fagret, and M. Comet, *J. Nucl. Med., 35*, 334 (1994).
1149. J.B. Zhang and X.B. Wang, *J. Radioanal. Nucl. Chem., 249*, 573 (2001).

1150. J.B. Zhang and X.B. Wang, *Appl. Radiat. Isot., 55*, 453 (2001).
1151. J.B. Zhang and X.B. Wang, *Chem. J. Chin. Univ., 22*, 1095 (2001).
1152. J.B. Zhang, X.B. Wang, G.X. Lu, and Z.G. Tang, *Appl. Radiat. Isot., 54*, 745 (2001).
1153. J.B. Zhang, X.B. Wang, and C.Y. Li, *J. Radioanal. Nucl. Chem., 254*, 99 (2002).
1154. J.R. Ballinger, K.Y. Gulenchyn, and M.N. Hassan, *Appl. Radiat. Isot., 40*, 547 (1989).
1155. J. Baldas and P.M. Pojer, *Int. J. Nucl. Med. Biol., 11*, 159 (1984).
1156. K. Takehana, G.A. Beller, M. Ruiz, F.D. Petruzella, D.D. Watson, and D.K.Glover, *J. Nucl. Med., 42*, 1388 (2001).
1157. J.B. Zhang, X.B. Wang, and C.Y. Li, *Nucl. Med. Biol., 29*, 665 (2002).
1158. J.B. Zhang, X.B. Wang, and C.Y. Li, *Appl. Radiat. Isot., 56*, 857 (2002).
1159. J.B. Zhang, X.B. Wang, and C.Y. Li, *Nucl. Med. Commun., 23*, 689 (2002).
1160. F.R. Colombo, Y. Torrente, R. Casati, R. Benti, S. Corti, S. Salani, M.G. D'Angelo, A. DeLiso, G. Scarlato, N. Bresolin, and P. Gerundini, *Nucl. Med. Biol., 28*, 935 (2001).
1161. J. Stach, S. Abram, and U. Abram, *J. Radioanal. Nucl. Chem. Lett., 128*, 131 (1988).
1162. J.R. Ballinger, B.Gerson, and K.Y. Gulenchyn, *Appl. Radiat. Isot., 38*, 665 (1987).
1163. C. Ghezzi, D. Fagret, C.C. Arvieux, J.P. Mathieu, R. Bontron, R. Pasqualini, J. Deleiris, and M. Comet, *J. Nucl. Med., 36*, 1069 (1995).
1164. D. Fagret, P.Y. Marie, F. Brunotte, M. Giganti, D. Leguludec, A.Bertrand, J.E. Wolf, A. Piffanelli, F. Chossat, D. Bekhechi, R. Pasqualini, J. Machecourt, and M.Comet, *J. Nucl. Med., 36*, 936 (1995).
1165. L. Uccelli, M. Giganti, A. Duatti, C. Bolzati, R. Pasqualini, C. Cittanti, P. Colamussi, and A. Piffanelli, *J. Nucl. Med., 36*, 2075 (1995).
1166. G. Johnson, I.L. Allton, K.N. Nguyen, J.M. Lauinger, D. Beju, R. Pasqualini, A. Duatti, and R.D. Okada, *J. Nucl. Cardiol., 3*, 42 (1996).
1167. G. Johnson, K.N. Nguyen, Z.L. Liu, P. Gao, R. Pasqualini, and R.D. Okada, *J. Nucl. Cardiol., 4*, 217 (1997).
1168. L. Riou, C. Ghezzi, O. Mouton, J.P. Mathieu, R. Pasqualini, M. Comet, and D. Fagret, *Circulation, 98*, 2591 (1998).
1169. T.A. Holly, J.A. Leppo, M.P. Gilmore, C.P. Reinhardt, and S.T. Dahlberg, *J. Nucl. Cardiol., 6*, 633 (1999).
1170. G. Vanzetto, D. Fagret, R. Pasqualini, J.P. Mathieu, F. Chossat, and J. Machecourt, *J. Nucl. Med., 41*, 141 (2000).
1171. F.D. Petruzella, M. Ruiz, P. Katsiyiannis, D.D. Watson, R. Pasqualini, G.A. Beller, and D.K. Glover, *J. Nucl. Cardiol., 7*, 123 (2000).
1172. F. Demaimay, L. Dazord, A. Roucoux, N. Noiret, H. Patin, and A. Moisan, *Nucl. Med. Biol., 24*, 701 (1997).
1173. P. Fang, B.-C. Wang, C.-Y. Wu, W.-X. Wan, N.-Y. Jiang, X. Zhou, and Z.-P. Chen, *J. Nucl. Med. Tech., 27*, 54 (1999).
1174. P. Fang, C. Wu, W. Wan, X. Zhou, Z. Chen, N. Jiang, *Nucl. Sci. Tech., 10*, 57 (1999).
1175. J. Baldas and J. Bonnyman, *Nucl. Med. Biol., 19*, 741 (1992).
1176. R.A. Bell, J.F. Britten, A. Guest, C.J.L. Lock, and J.F.Valiant, *J. Chem. Soc., Chem. Commun.*, 585 (1997).
1177. F.D. Rochon, R. Melanson, and P.C. Kong, *Inorg. Chim. Acta, 194*, 43 (1992).
1178. J. Baldas, J. Bonnyman, M.F. Mackay, and G.A. Williams, *Aust. J. Chem., 37*, 751 (1984).

1179. K.I. Okamoto, B.H. Chen, J.R. Kirchhoff, D.M. Ho, R.C. Elder, W.R. Heineman, E. Deutsch, and M.J. Heeg, *Polyhedron, 12*, 1559 (1993).
1180. A.S. Batsanov, Yu.T. Struchkov, B. Lorenz, and M. Wahren, *Z. Anorg. Allg. Chem., 510*, 117 (1984).
1181. R. Colton, R. Levitus, and G. Wilkinson, *J. Chem. Soc., Dalton Trans.*, 5275 (1960).
1182. J.F. Rowbottom and G. Wilkinson, *J. Chem. Soc., Dalton Trans.*, 826 (1972).
1183. A. Boschi, C. Bolzati, L. Uccelli, and A. Duatti, *Nucl. Med. Biol., 30*, 381 (2003).
1184. F. Demaimay, A. Roucoux, N. Noiret, and H. Patin, *J. Organomet. Chem., 575*, 145 (1999).
1185. G.N. Holder and M.W. Kanning, *Inorg. Chim. Acta, 197*, 67 (1992).
1186. U. Abram, *Z. Anorg. Allg. Chem., 625*, 839 (1999).
1187. U. Abram, *Inorg. Chem. Commun., 2*, 227 (1999).
1188. U. Abram, *Z. Anorg. Allg. Chem., 626*, 318 (2000).
1189. J.B. Stelzer, A. Hagenbach, and U. Abram, *Z. Anorg. Allg. Chem., 628*, 703 (2002).
1190. A. Ichimura, T. Kajino, and T. Kitagawa, *Inorg. Chim. Acta, 147*, 27 (1988).
1191. R. Mattes and H. Scholand, *Inorg. Chim. Acta, 116*, L39 (1986).
1192. J.R. Dilworth, D.V. Griffiths, S.J. Parrott, and Z.F. Zheng, *J. Chem. Soc., Dalton Trans.*, 2931 (1997).
1193. G.V. Goeden and B.L. Haymore, *Inorg. Chem., 22*, 157 (1983).
1194. J.B. Arterburn, K.V. Rao, D.M. Goreham, M.V. Valenzuela, M.S. Holguin, K.A. Hall, K.C. Ott, and J.C. Bryan, *Organometallics, 19*, 1789 (2000).
1195. K.N. Soe, A. Ichimura, and T. Kitagawa, *Inorg. Chim. Acta, 207*, 21 (1993).
1196. E.A. Maatta and C. Kim, *Inorg. Chem., 28*, 623 (1989).
1197. J.R. Dilworth, P. Jobanputra, S.J. Parrott, R.M. Thompson, D.C. Povey, and J.A. Zubieta, *Polyhedron, 11*, 147 (1992).
1198. H. Egold, U. Flörke, and S. Klose, *Acta Crystallogr. Sect. E, 58*, m116 (2002).
1199. E.A. Pasek and D.K. Straub, *Inorg. Chem., 11*, 259 (1972).
1200. L. Cambi and L. Szëgo, *Ber. Dtsch. Chem. Ges., 64*, 2591 (1931).
1201. H.L. Nigam, K.B. Pandeya, and R. Singh, *J. Indian Chem. Soc., 78*, 525 (2001).
1202. B. Leon and D.K. Straub, *Inorg. Chim. Acta, 156*, 13 (1989).
1203. K. Chandrasekhar and H.B. Burgi, *Acta Crystallogr. Sect. B, Struct. Commun., 40*, 387 (1984).
1204. P. Ganguli and S.K. Date, *Nat. Acad. Sci. Lett.-India, 5*, 55 (1982).
1205. N.V. Duffy and D.L. Uhrich, *Inorg. Chim. Acta, 63*, 5 (1982).
1206. M.S. Haddad, W.D. Federer, M.W. Lynch, and D.N. Hendrickson, *Inorg. Chem., 20*, 131 (1981).
1207. A. Malliaris and V. Papaefthimiou, *Inorg. Chem., 21*, 770 (1982).
1208. K.B. Pandeya, R. Singh, C. Prakash, and J.S. Baijal, *Inorg. Chem., 26*, 3216 (1987).
1209. K.B. Pandeya, R. Singh, C. Prakash, and J.S. Baijal, *Solid State Commun., 64*, 801 (1997).
1210. S. Singhal, C.L. Sharma, A.N. Garg, and K. Chandra, *Transition Met. Chem., 26*, 81 (2001).
1211. D.L. Boyd, N.V. Duffy, A. Felczan, E. Gelerinter, D.L. Uhrich, G.A. Katsoulos, and J.B. Zimmerman, *Inorg. Chim. Acta, 191*, 39 (1992).
1212. J.M. Fiddy, I. Hall, F. Grandjean, G.J. Long, and U. Russo, *J. Phys., Condes. Matter, 2*, 10091 (1990).
1213. S. Singhal, C.L. Sharma, A.N. Garg, and K. Chandra, *Polyhedron, 21*, 2489 (2001).

1214. S. Singhal, C.L. Sharma, A.N. Garg, and K. Chandra, *Transition Met. Chem., 26*, 81 (2001).
1215. D. Rininger, J.B. Zimmerman, N.V. Duffy, and D.L. Uhrich, *J. Inorg. Nucl. Chem., 42*, 689 (1980).
1216. K.B. Pandeya and R. Singh, *Inorg. Chim. Acta, 147*, 5 (1988).
1217. P. Ganguli, *Z. Naturforsch. A, 40*, 79 (1985).
1218. B. Hutchinson, P. Neill, A. Finkelstein, and J. Takemato, *Inorg. Chem., 20*, 2000 (1981).
1219. M. Sorai, *J. Inorg. Nucl. Chem., 40*, 1031 (1978).
1220. K.B. Pandeya and R. Singh, *Inorg. Chim. Acta, 147*, 5 (1988).
1221. N.E. Domracheva, S.A. Luchkina, and I.V. Ovchinnikov, *Koord. Khimiya, 21*, 26 (1995).
1222. S.A. Cotton, *Polyhedron, 13*, 2579 (1994).
1223. S. Yarish, N. V. Duffy, E. Gelerinter, W. Dietzsch, N. Law, and R. Kirmse, *Inorg. Chim. Acta, 217*, 101 (1994).
1224. E. Gelerinter, N.V. Duffy, S.S. Yarish, W. Dietzsch, and R. Kirmse, *Chem. Phys. Lett., 184*, 375 (1991).
1225. N.V. Duffy, T.E. Lockhart, E. Gelerinter, D. Todoroff, and D.L. Uhrich, *Inorg. Nucl. Chem. Lett., 17*, 1 (1981).
1226. K. Stahl, *Acta Crystallogr., Sect. B, 39*, 612 (1983).
1227. K. Stahl, *Inorg. Chim. Acta, 75*, 85 (1983).
1228. J. Albertsson and Å. Oskarsson, *Acta Crystallogr., 835*, 1473 (1979).
1229. C.A. Tsipis, C.C. Hadjikostas, and G.E. Manoussakis, *Inorg. Chim. Acta, 23*, 163 (1977).
1230. B.S. Garg, R. Dixit, and A.L. Singh, *J. Therm. Anal., 36*, 2567 (1990).
1231. R.B. Lanjewar and A.N. Garg, *Ind. J. Chem. Sect A-Inorg. Phys. Theor. Anal. Chem., 31*, 849 (1992).
1232. B.K. Kanungo, B. Pradhan, and D.V.R. Rao, *J. Indian Chem. Soc., 59*, 329 (1982).
1233. F.T. Esmadi and T.Z.A. Irshaidat, *Synth. React. Inorg. Met.-Org. Chem., 30*, 1347 (2000).
1234. C. Glidewell and I.L. Johnson, *Polyhedron, 7*, 1371 (1988).
1235. N. Sridevi and K.K.M. Yusuff, *Indian J. Chem., Sect. A, 39*, 933 (2000).
1236. B. Wu, M.R. Taylor, and L.L. Martin, *Acta Crystallogr., Sect. E, 59*, m1083 (2003).
1237. G.L. Miessler, E. Zoebisch, and L.H. Pignolet, *Inorg. Chem., 17*, 3636 (1978).
1238. J.M.Stegge, S.M. Woessner, and P.E. Hoggard, *Inorg. Chim. Acta, 250*, 385 (1996).
1239. V. Tamminen and E. Hjelt, *Suomen Kemi, 22B*, 39 (1950).
1240. G.A. Katsoulos, C.A. Tsipis, and F.D. Vakoulis, *Can. J. Chem., Rev. Can. Chim., 63*, 3249 (1985).
1241. B.M. Ondo, J.P. Barbier, and R.P. Hugel, *C. R. Acad. Sci. Ser. II, 301*, 225 (1985).
1242. G. Crisponi, P. Deplano, and E.F. Trogu, *J. Chem. Soc., Dalton Trans.*, 365 (1986).
1243. R.L. Martin and A.H. White, *Inorg. Chem., 6*, 712 (1967).
1244. D. Petridis, A. Kostikas, A. Simopoulos, and D. Niarchos, *Inorg. Chem., 21*, 766 (1982).
1245. B.E.A. Abadi, R.A. Palmer, and B.W. Fitzsimmons, *J. Crystallogr. Spect. Res., 18*, 35 (1988).
1246. V. Kettmann, F. Pavelcik, and J. Majer, *Collect. Czech. Chem. Commun., 46*, 2307 (1981).
1247. C.L. Raston, W.G. Sly, and A.H. White, *Aust. J. Chem., 33*, 221 (1980).
1248. P.C. Christidis, P.J. Rentzeperis, F. Vakoulis, and C.A. Tsipis, *Inorg. Chim. Acta, 83*, 87 (1984).
1249. S. Decurtins, C.B. Shoemaker, and H.H. Wickman, *Acta Crystallogr., Sect. C, 39*, 1218 (1983).
1250. M. Yoshikawa, M. Sorai, H. Suga, and S. Seki, *Chem. Phys. Lett., 77*, 54 (1981).

1251. S. Decurtins, F.V. Wells, K.C.-P. Sun and H.H. Wickham, *Chem. Phys. Lett., 89*, 79 (1982).
1252. B.E.A. Abadi, R.A. Palmer, and B.W. Fitzsimmons, *J. Crystallogr. Spectrosc. Res., 18*, 35 (1988).
1253. H.H. Wickman, A.M. Trozzolo, H.J. Williams, G.W. Hull, and F.R. Merritt, *Phys. Rev., 155*, 563 (1967).
1254. G.C. De Fotis, F. Palacio, and R.L. Carlin, *Physica B+C, Phys. Cond. Matter At. Mol. Plasma Phys. Optics, 95*, 380 (1978).
1255. G.C. De Fotis, F. Palacio, and R.L. Carlin, *Phys. Rev. B, Cond. Matter Mater. Phys., 20*, 2945 (1979).
1256. G.C. De Fotis and J.A. Cowen, *J. Chem. Phys., 73*, 2120 (1980).
1257. G.C. De Fotis and J.R. Laughlin, *J. Chem. Phys., 84*, 3346 (1986).
1258. G.C. De Fotis, M.L. Laccheo, and H.A. Katori, *Phys. Rev. B, Cond. Matt. Mater. Phys.*, 65 (2002).
1259. C.A. Tsipis, G.A. Katsoulos, E.G. Bakalbassis, and M.P. Sigalas, *Struct. Chem., 1*, 523 (1990).
1260. P. Ganguli and R.M. Iyer, *Z. Naturforsch. A, 36*, 1016 (1981).
1261. B.W. Fitzsimmons and A.R. Hume, *J. Chem. Soc., Dalton Trans.*, 1548 (1979).
1262. B. Sarte, J. Stanford, W.J. Laprice, D.L. Uhrich, T.E. Lockhart, E. Gelerinter, and N.V. Duffy, *Inorg. Chem., 17*, 3361 (1978).
1263. R.J. Butcher and E. Sinn, *Inorg. Chem., 19*, 3622 (1980).
1264. G.A. Brewer, R.J. Butcher, B. Letafat, and E. Sinn, *Inorg. Chem., 22*, 371 (1983).
1265. R. Kirmse, S. Saluschke, E. Moller, E.J. Reijerse, E. Gelerinter, and N.V. Duffy, *Angew. Chem., Int. Ed. Engl., 33*, 1497 (1994).
1266. Y. Katayama, N. Soh, K. Koide, and M. Maeda, *Chem. Lett.*, 1152 (2000).
1267. A.F. Vanin, X.P. Liu, A. Samouilov, R.A. Stukan, and J.L. Zweier, *Biochim. Biophys. Acta-Gen. Subj., 1474*, 365 (2000).
1268. Y. Kotake, T. Tanigawa, M. Tanigawa, I. Ueno, D.R. Allen, and C.S. Lai, *Biochim. Biophys. Acta, Gen. Subj., 1289*, 362 (1996).
1269. S. Fujii, T. Yoshimura, and H. Kamada, *Chem. Lett.*, 785 (1996).
1270. S.V. Paschenko, V.V. Khramtsov, M.P. Skatchkov, V.F. Plyusnin, and E. Bassenge, *Biochem. Biophys. Res. Commun., 225*, 577 (1996).
1271. Y. Xia, A.J. Cardounel, A.F. Vanin, and J.L. Zweier, *Free Radic. Biol. Med., 29*, 793 (2000).
1272. K. Tsuchiya, M. Yoshizumi, H. Houchi, and R.P. Mason, *J. Biol. Chem., 275*, 1551 (2000).
1273. P. Mordvintcev, A. Mülsch, R. Busse, and A. Vanin, *Anal. Biochem., 199*, 142 (1991).
1274. S. Fujii, K. Kobayashi, S. Tagawa, and T. Yoshimura, *J. Chem. Soc., Dalton Trans.*, 3310 (2000).
1275. I. Iliev and D. Shopov, *Polyhedron, 6*, 1497 (1987).
1276. M.H. DesBois, C.M. Nunn, A.H. Cowley, and D. Astruc, *Organometallics, 9*, 640 (1990).
1277. M.H. Delville Desbois, S. Mross, and D. Astruc, *Organometallics, 15*, 5598 (1996).
1278. E. Roman, D. Catheline, D. Astruc, P. Batail, L. Ouahab, and F.Varret, *J. Chem. Soc., Chem. Commun.*, 129 (1982).
1279. C. Amatore, J.N. Verpeaux, A. Madonik, M.H. Desbois, and D. Astruc, *J. Chem. Soc., Dalton Trans.*, 200 (1988).
1280. M.H. Desbois and D. Astruc, *Angew. Chem., Int. Edit. Engl., 28*, 460 (1989).

1281. M.-H. Delville-Desbois, S. Mross, D. Astruc, J. Linares, F. Varret, H. Rabaâ, A. Le Beuze, J.-Y. Saillard, R.D. Culp. D.A. Atwood, and A.H. Cowley, *J. Am. Chem. Soc., 118*, 4133 (1996).
1282. M.H. Delville, *Inorg. Chim. Acta, 291*, 1 (1999).
1283. D. Catheline, E. Roman, and D. Astruc, *Inorg. Chem., 23*, 4508 (1984).
1284. J.-N. Vepeaux, M.-H. Desbois, A. Madonik, C. Amatore, and D. Astruc, *Organometallics, 9*, 630 (1990).
1285. C. O'Conner, J.D. Gilbert, and G. Wilkinson, *J. Chem. Soc. A*, 84 (1969).
1286. L.H. Pignolet, R.A. Lewis, and R.H. Holm, *J. Am. Chem. Soc., 93*, 360 (1971).
1287. O. Ileperuma and R.D. Feltham, *Inorg. Chem., 14*, 3042 (1975).
1288. Y.H. Deng, T.B. Wen, Q.T. Liu, H.P. Zhu, C.N. Chen, and D.X. Wu, *Inorg. Chim. Acta, 293*, 95 (1999).
1289. H. Kunkely and A. Vogler, *Inorg. Chem. Commun., 5*, 730 (2002).
1290. P.K. Baker, K. Broadley, and N.G. Connelly, *J. Chem. Soc., Dalton Trans.*, 471 (1982).
1291. J. Tákacs and L. Markó, *Transition Met. Chem., 9*, 10 (1984).
1292. W.K. Dean, *J. Organomet. Chem., 133*, 195 (1977).
1293. S.K. Jha, B.H.S. Thimmappa, and P. Mathur, *Polyhedron, 5*, 2123 (1986).
1294. M.R. Houchin, *Inorg. Chim. Acta, 83*, 103 (1984).
1295. H. Kunkely and A. Vogler, *J. Photochem. Photobiol. A: Chem., 154*, 289 (2003).
1296. W.K. Dean and D.G. Van der Veer, *J. Organomet. Chem., 144*, 65 (1978).
1297. F.J. Lalor, L.H. Brookes, G. Ferguson, and M. Parvez, *J. Chem. Soc., Dalton Trans.*, 245 (1984).
1298. C.L. Raston, A.H. White, D. Petridis, and D.Taylor, *J. Chem. Soc., Dalton Trans.*, 1928 (1980).
1299. M.G. Kanatzidis, M. Ryan, D. Coucouvanis, A. Simopoulos, and A. Kostikas, *Inorg. Chem., 22*, 179 (1983).
1300. M.G. Kanatzidis, D. Coucouvanis, A. Simopoulos, A. Kostikas, and V. Papaefthymiou, *J. Am. Chem. Soc., 107*, 4925 (1985).
1301. Q.T. Liu, L.R. Huang, Y. Yang, and J.X. Lu, *Kexue Tongboa, 33*, 1633 (1988).
1302. Q. Liu, L. Huang, Y. Yang, and J. Lu, *Chin. J. Struct. Chem. (Jiegou Huaxue), 6*, 135 (1987).
1303. Y. Deng, Q. Liu, C. Chen, Y. Wang, Y. Cai, D. Wu, B. Kang, D. Liao, and J. Cui, *Polyhedron, 16*, 4121 (1997).
1304. D. Wu, X. Lei, Q. Liu, and H. Liu, *J. Struct. Chem., (Jiegou Huaxue), 12*, 163 (1993).
1305. A.K. Malik and A.L.J. Rao, *J. Agric. Food Chem., 48*, 4044 (2000).
1306. A.K. Malik, B.S. Seidel, and W. Faubel, *J. Chromat. A, 857*, 365(1999).
1307. A.K. Malik, A.L.J Rao, and B.K. Puri, *Environ. Anal. Chem., 44*, 159 (1991).
1308. A.K. Malik and A.L.J. Rao, *Talanta, 8*, 94 (1991).
1309. A.K. Malik and A.L.J. Rao, *Talanta, 44*, 177 (1997).
1310. A.K. Malik, *J. Agric. Food Chem., 48*, 5808 (2000).
1311. A.K. Malik, *J. Environ. Monit., 2*, 151 (2000).
1312. A.K. Malik, B.S. Seidel, and W. Faubel, *Pestic. Sci., 55*, 1000 (1999).
1313. A.K. Malik, J. Kapoor, and A.L.J. Rao, *Indian J. Chem. Sect A-Inorg. Phys. Theor. Anal.Chem., 32*, 180 (1993).
1314. A.K. Malik and A.L.J. Rao, *Pestic. Sci., 35*, 69 (1992).
1315. K. Saraswathi, M.D. Ramaiah, and V.V. Ramana, *J. Indian Chem. Soc., 68*, 116 (1991).
1316. O. Bergendorff and C. Hansson, *J. Agric. Food Chem., 50*, 1092 (2002).

1317. L.I. Victoriano, J.A. Gnecco, and H.V. Carbacho, *Polyhedron, 15*, 1315 (1996).
1318. H. Carbacho and J.A. Gnecco, *Bol. Soc. Chil. Quim., 34*, 27 (1989).
1319. X.-P.Chen and K.-Y.Qiu, *Chem. Commun.*, 1403 (2000).
1320. X.-P. Chen and K.-Y. Qiu, *Chem. Commun.*, 233 (2000).
1321. D.-Q. Qin, S.-H. Qin, and K.-Y. Qiu, *J. Poly. Sci: Part A; Poly. Chem., 39*, 3464 (2001).
1322. R.B. Lanjewar and A.N. Garg, *Polyhedron, 12*, 2619 (1993).
1323. D.K. Liu and S.G. Chang, *Environ, Sci. Tech., 22*, 1196 (1988).
1324. L. Cambi and L. Malatesta, *Rend. Lombardo Sci. Lettre*, A181, d1 (1938).
1325. L. Malatesta, *Gazz. Chim. Ital., 68*, 195 (1938).
1326. R.A. Bozis, *Univ.Microfilms*, 72–14,064 [*Chem.Abstr., 77*, 108887y (1972)].
1327. Z. Bartodej, *Chem. Listy, 48*, 1870 (1954).
1328. L.F. Shvydka, Yu.I. Usatenko, and F.M. Tulyipa, *Zh. Neorg. Khim., 18*, 756 (1973).
1329. S. Kumar and N.K. Kaushik, *Indian J. Chem., Sect. A., 20*, 512 (1981).
1330. B. Nalini and S.S. Narayanan, *Bull. Electrochem., 13*, 330 (1997).
1331. S. Kumar and N.K. Kaushik, *Acta Chim. Acad. Sci. Hung., 107*, 161 (1981).
1332. H.S. Sangari, G.S. Sodhi, and J. Kaur, *Thermochim. Acta, 171*, 49 (1990).
1333. H.S. Sangari, G.S. Sodhi, and J. Kaur, *Chem. Pap.-Chem. Zvesti, 51*, 280 (1997).
1334. S.H. Wheeler, B.M. Mattson, G.L.Miessler, and L.H. Pignolet, *Inorg. Chem., 17*, 340 (1978).
1335. R. Rameshand and K. Natarajan, *Synth. React. Inorg. Met.-Org. Chem., 26*, 1677 (1996).
1336. M. Arroyo, S. Bernes, L. Melendez, R.L. Richards, and H. Torrens, *Transition Met. Chem., 26*, 608 (2001).
1337. K. Araki, F.N. Rein, S.G. Camera, and H.E. Toma, *Transition Met. Chem., 17*, 535 (1992).
1338. I.R. Baird, B.R. Cameron, and R.T. Skerlj, *Inorg. Chim. Acta, 353*, 107 (2003).
1339. K.W. Given, B.M. Mattson, and L.H. Pignolet, *Inorg. Chem., 15*, 3152 (1976).
1340. C. Preti, G. Tosi, and P. Zannini, *Z. Anorg. Allg. Chem., 469*, 234 (1980)
1341. G.R. Clark, M.M.P. Ng, W.R. Roper, and L.J. Wright, *J. Organomet. Chem., 491*, 219 (1995).
1342. V. Chinnusamy and K. Natarajan, *Synth. React. Inorg. Met.-Org. Chem., 23*, 745 (1993).
1343. P.B. Critchlow and S.D. Robinson, *Inorg. Chem., 17*, 1902 (1978).
1344. P.B. Critchlow and S.D. Robinson, *J. Chem. Soc., Dalton Trans.*, 1367 (1975).
1345. M. Kawano, T. Watanabe, and K. Matsumoto, *Chem. Lett.*, 2389 (1992).
1346. H.G. Zheng, W.H. Leung, J.L.C. Chim, W. Lai, C.H. Lam, I.D. Williams, and W.T. Wong, *Inorg. Chim. Acta, 306*, 184 (2000).
1347. W.-H. Leung, E.Y.Y. Chan, T.C.Y. Lai, and W.-T. Wong, *J. Chem. Soc., Dalton Trans.*, 51 (2000).
1348. G. Exarchos, S.D. Robinson, and J.W. Steed, *Polyhedron, 20*, 2951 (2001).
1349. S. Pal and C. Sinha, *Transition Met. Chem., 27,* 218 (2002).
1350. S. Baitalik, S. Mohanta, and B. Adhikary, *Polyhedron, 16*, 983 (1997).
1351. R. Argazzi, C.A. Bignozzi, G.M. Hasselmann, and G.J. Meyer, *Inorg. Chem., 37*, 4533 (1998).
1352. A. Del Zotto, E. Rocchini, F. Pichierri, E. Zangrando, and P. Rigo, *Inorg. Chim. Acta, 299*, 180 (2000).
1353. A.M. Clark, C.E.F. Rickard, W.R. Roper, and L.J.Wright, *J.Organomet. Chem., 598*, 262 (2000).
1354. A.M. Clark, C.E.F. Rickard, W.R. Roper, and L.J.Wright, *Organometallics, 18*, 2813 (1999).

1355. A.M. Clark, C.E.F. Rickard, W.R. Roper, and L.J.Wright, *J. Organomet. Chem., 545*, 619 (1997).

1356. C.E.F. Rickard, W.R. Roper, A. Williamson, and L.J. Wright, *Organometallics, 17*, 4869 (1998).

1357. C.E.F. Rickard, W.R. Roper, T.J. Woodman, and L.J.Wright, *J. Chem. Soc., Chem. Commun.*, 837 (1999).

1358. C.E.F. Rickard, W.R. Roper, A. Williamson, and L.J. Wright, *Organometallics, 17*, 4869 (1998).

1359. A.J. Deeming and R. Vaish, *J. Organomet. Chem., 460*, C8 (1993).

1360. K.-B. Shiu, S.-J.Yu, Y. Wang, and G.-H. Lee, *J. Organomet. Chem., 650*, 37 (2002).

1361. D.J. Cole-Hamilton and T.A. Stephenson, *J. Chem. Soc., Dalton Trans.*, 739 (1974).

1362. M. Menon, A. Pramanik, N. Bag, and A. Chakravorty, *J. Chem. Soc., Dalton Trans.*, 1543 (1995).

1363. A.G. Alonso and L.B. Reventos, *J. Organomet. Chem., 338*, 249 (1988).

1364. X.L. Lu, S.Y. Ng, J.J. Vittal, G.K. Tan, L.Y. Goh, and T. S. A. Hor, *J. Organomet. Chem., 688*, 100 (2003).

1365. C. Preti, G. Tosi, and P. Zannini, *J. Inorg. Nucl. Chem., 41*, 485 (1979).

1366. A. Pramanik, N. Bag, and A. Chakravorty, *J. Chem. Soc., Dalton Trans.*, 237 (1993).

1367. T. Wilczewski, M. Bochenska, and J.F. Biernat, *J. Organomet. Chem., 215*, 87 (1981).

1368. L.B. Reventos and A.G. Alonso, *J. Organomet. Chem., 309*, 179 (1986).

1369. Q.J. McCubbin, F.J. Stoddart, T. Welton, A.J.P. White, and D.J. Williams, *Inorg. Chem., 37*, 3753 (1998).

1370. K.M. Rao, L. Mishra, and U.C. Agarwala, *Polyhedron, 6*, 1383 (1987).

1371. T. Wilczewski, *J. Organomet. Chem.,224*, C1 (1982).

1372. A.W. Cordes and M. Draganjac, *Acta Crystallogr., Sect.C, 44*, 363 (1988).

1373. N. Dodo, Y. Matsushima, M. Uno, K. Onitsuka, and S. Takahashi, *J. Chem. Soc., Dalton Trans.*, 35 (2000).

1374. Y. Mizobe, M. Hosomizu, and M. Hidai, *Inorg. Chim. Acta, 273*, 238 (1998).

1375. B. Buriez, I.D. Burns, A.F. Hill, A.J.P.White, D.J. Williams, and J.D.E.T. Wilton-Ely, *Organometallics, 18*, 1504 (1999).

1376. K.-B. Shiu, J.-Y. Chen, S.-J. Yu, S.-L. Wang, F.-L. Liao, Y. Wang, and G.-H. Lee, *J. Organomet. Chem., 648*, 193 (2002).

1377. K.W. Given, S.H. Wheeler, B.S. Jick, L.J. Maheu, and L.H. Pignolet, *Inorg. Chem., 18*, 1261 (1979).

1378. M. Kawano, H. Uemura, T. Watanabe, and K. Matsumoto, *J. Am. Chem. Soc., 115*, 2068 (1993).

1379. L.J. Maheu and L.H. Pignolet, *Inorg. Chem., 18*, 3626 (1979).

1380. L.J. Maheu and L.H. Pignolet, *J. Am. Chem. Soc., 102*, 6346 (1980).

1381. J.G. Toerienand P.H. Van Rooyen, *J. Chem. Soc., Dalton Trans.*, 1563 (1991).

1382. W.-R. Yao, Z.-H. Liu, and Q.-F. Zhang, *Acta Crystallogr., Sect. E, 59*, m303 (2003).

1383. A.F. Hill and J.D.E.T. Wilton-Ely, *J. Chem. Soc., Dalton Trans.*, 3501 (1998).

1384. B. Buriez, D.J. Cook, K.J. Harlow, A.F. Hill, T. Welton, A.J.P. White, D.J. Williams, and J.D.E.T. Wilton-Ely, *J. Organomet. Chem., 578*, 264 (1999).

1385. K.J. Harlow, A.F. Hill, T. Welton, A.J.P. White, and D.J.Williams, *Organometallics, 17*, 1916 (1998).

1386. B. Nalini and S.S. Narayanan, *Bull. Electrochem., 14*, 241 (1998).

1387. V. Shklover, T. Haibach, B. Bolliger, M. Hochstrasser, M. Erbudak, H.-U. Nissen, S.M. Zakeeruddin, M.K. Nazeeruddin, and M. Gratzel, *J. Solid State Chem., 132*, 60 (1997).

1388. M. Delépine and L. Compin, *Bull. Soc. Chim., 27*, 469 (1920).

1389. E. Kello, J. Lokaj, and V. Vrabel, *Collect. Czech. Chem. Commun., 57*, 332 (1992).

1390. B.B. Kaul and K.B. Pandeya, *Transition Met. Chem., 4*, 112 (1979).

1391. C.T. Eagle, D.G. Farrar, D.M. Gooden, A.B. Goodman, and S.W. Wyatt, *Chem. Educ.*, 4 (1999).

1392. T. Sabo, N. Juranic, V. Dondur, and M.B. Celap, *Thermochim. Acta, 213*, 293 (1993).

1393. M. Nakashima and S. Kida, *Bull. Chem. Soc. Jpn., 55*, 809 (1982).

1394. L.R. Gahan, J.G. Hughes, M.J. O'Connor, and P.J. Oliver, *Inorg. Chem., 18*, 933 (1979).

1395. N. Juranic, *Inorg. Chem., 22*, 521 (1983).

1396. A.M. Bond, R. Colton, D.R. Mann, and J.E. Moir, *Aust. J. Chem., 39*, 1385 (1986).

1397. A. Yamasaki, *J. Coord. Chem., 24*, 211 (1991).

1398. R.G. Compton, J.C. Eklund, A. Hallik, S. Kumbhat, L. Nei, A.M. Bond, R. Colton, and Y.A. Mah, *J. Chem. Soc., Dalton Trans.*, 1917 (1995).

1399. N.V. Khitrich and I.I. Seifullina, *Russ. J. Coord. Chem., 26*, 798 (2000).

1400. P.C. Healy, B.W. Skelton, and A.H. White, *J. Chem. Soc., Dalton Trans.*, 971 (1989).

1401. L.M. Engelhardt, P.C. Healy, R.M. Shephard, B.W. Skelton, and A.H. White, *Inorg. Chem., 27*, 2371 (1988).

1402. M. Kita, A. Okuyama, K. Kashiwabara, and J. Fujita, *Bull. Chem. Soc. Jpn., 63*, 1994 (1990).

1403. K. Kashiwabara, M. Watanabe, M. Kita, and T. Suzuki, *Bull. Chem. Soc. Jpn., 69*, 1947 (1996).

1404. K. Kashiwabara, N. Taguchi, H.D. Takagi, K. Nakajima, and T. Suzuki, *Polyhedron, 17*, 1817 (1998).

1405. M. Adachi, M. Kita, K. Kashiwabara, J. Fujita, N. Iitaka, S. Kurachi, S. Ohba, and D.-M. Jin, *Bull. Chem. Soc. Jpn., 65*, 2037 (1992).

1406. M. Kita, M. Okuno, K. Kashiwabara, and J. Fujita, *Bull. Chem. Soc. Jpn., 65*, 3042 (1992).

1407. H. Matsui, M. Kita, K. Kashiwabara, and J. Fujita, *Bull. Chem. Soc. Jpn., 66*, 1140 (1993).

1408. M. Kita, K. Yamanari, and Y. Shimura, *Bull. Chem. Soc. Jpn., 62*, 23 (1989).

1409. S.P. Sovilj and K. Babic-Samardzija, *Synth. React. Inorg. Met.-Org. Chem., 29*, 1655 (1999).

1410. S.P. Sovilj, G. Vukovic, K. Babic, T.J. Sabo, S. Macura, and N. Juranic, *J. Coord. Chem., 41*, 19 (1997).

1411. D.C. Ware, H.R. Palmer, F.B. Pruijn, R.E. Anderson, P.J. Brothers, W.A. Denny, and W.R. Wilson, *Anti-Cancer Drug Des., 13*, 81 (1998).

1412. K. Babic-Samardzija and S.P. Sovilj, *Asian J. Chem., 15*, 1207 (2003).

1413. V.M. Jovanovic, K. Babic-Samardzija, and S.P. Sovilj, *Electroanalysis, 13*, 1129 (2001).

1414. P. Deplano, E.F. Trogu, and A. Lai, *Inorg. Chim. Acta, 68*, 147 (1983).

1415. T. Suzuki, S. Kashiwamura, and K. Kashiwabara, *Bull. Chem. Soc. Jpn., 74*, 2349 (2001).

1416. T. Suzuki, S. Iwatuki, H.D. Takagi, and K. Kashiwabara, *Chem. Lett.*, 1068 (2001).

1417. S. Iwatsuki, S. Kashiwamura, K. Kashiwabara, T. Suzuki, and H.D. Takagi, *J. Chem. Soc., Dalton Trans.*, 2280 (2003).

1418. S. Iwatsuki, T. Suzuki, A. Hasegawa, S. Funahashi, K. Kashiwabara, and H.D.Takagi, *J. Chem. Soc., Dalton Trans.*, 3593 (2002).

1419. A.A. Achilleos, L.R.Gahan, T.W. Hambley, P.C. Healy, and D.M. Weedon, *Inorg. Chim. Acta, 157*, 209 (1989).
1420. L.R. Gahan, T.W. Hambley, and P.C. Healy, *Aust. J. Chem., 41*, 635 (1988).
1421. R.P. Wirth, L.L. Miller, and W.L. Gladfelter, *Organomet., 2*, 1649 (1983).
1422. H.T.V. Hoa and R.J. Magee, *J. Inorg. Nucl. Chem., 41*, 351 (1979).
1423. N.K. Kaushik, B. Bhushan, and A.K. Sharma, *Transition Met. Chem., 9*, 250 (1984).
1424. A.C. Fabretti, F. Forghieri, A. Giusti, C. Preti, and G. Tosi, *Inorg. Chim. Acta, 86*, 127 (1984).
1425. A. Benedetti, C. Preti, L. Tassi, G. Tosi, and P. Zannini, *J. Mol Struct., 129*, 107 (1985).
1426. A.O. Görgülü and A. Cukurovali, *Synth. React. Inorg. Met.-Org. Chem., 321*, 1033 (2002).
1427. G. Hogarth, A. Pateman, I. Richards, A. Sella, and J. Steed, unpublished results.
1428. J. Bultitude, L.F. Larkworthy, J. Mason, D.C. Povey, and B. Sandell, *Inorg. Chem., 23*, 3629 (1984).
1429. T. Khayamian, A.A. Ensafi, and B. Hemmateenejad, *Talanta, 49*, 587 (1999).
1430. E.F. Hilder, M. Macka, and P.R. Haddad, *Analyst, 123*, 2865 (1998).
1431. J.N. King and J.S. Fritz, *Anal. Chem., 59*, 703 (1987).
1432. Y. Shijo, K. Takada, and N. Uehara, *Anal. Sci., 9*, 315 (1993).
1433. O.W. Lau and S.Y. Ho, *Anal. Chim. Acta, 280*, 269 (1993).
1434. A. Meyer and R. Neeb, *Fres. Z. Anal. Chem., 313*, 221 (1982).
1435. S.K. Aggarwal, M. Kinter, and D.A. Herold, *J. Chromatogr., Biomed. Appl., 576*, 304 (1992).
1436. A. Godelitsas, D. Charistos, C. Tsipis, P. Misaelides, A. Filippidis, and M. Schindler, *Microporous Mesoporous Mater., 61*, 69 (2003).
1437. H. Cui, R.D. Pike, R. Kershaw, K. Dwight, and A. Wold, *J. Solid State Chem., 101*, 115 (1992).
1438. A.C. Fabretti, C. Preti, L. Tassi, G. Tosi, and P. Zannini, *Inorg. Chim. Acta, 137*, 73 (1987).
1439. A.M. Bond, R. Colton, and D.R. Mann, *Inorg. Chem., 29*, 4665 (1990).
1440. M. Ahmed and R.J. Magee, *Chemica Scripta, 26*, 643 (1986).
1441. G.K. Budnikov, O.N. Romanova, and E.P. Medyantseva, *J. Gen. Chem. USSR (Engl. Transl.), 57*, 1954 (1987).
1442. R. Robertson and T.A. Stephenson, *J. Chem. Soc., Dalton Trans.*, 486 (1978).
1443. M.J.H. Russell, C. White, A. Yates, and P.M. Maitlis, *J. Chem. Soc., Dalton Trans.*, 849 (1978).
1444. A.J. Blake, J.D. Fotheringham, and T.A. Stephenson, *Acta Crystallogr., Sect. C, 48*, 1485 (1992).
1445. A.J. Blake, J.D. Fotheringham, T.A. Stephenson, S.G. Hambling, and L. Sawyer, *Acta Crystallogr., Sect. C, 47*, 648 (1991).
1446. R.M. Bellabarba and G.C. Saunders, *J. Fluorine Chem., 112*, 139 (2001).
1447. Y. Wakatsuki, M. Maniwa, and H. Yamazaki, *Inorg. Chem., 29*, 4204 (1990).
1448. Y. Wakatsuki, M. Maniwa, and H. Yamazaki, *Anal. Sci., 6*, 787 (1990).
1449. K. Brandt and W.S. Sheldrick, *J. Chem. Soc., Dalton Trans.*, 1237 (1996).
1450. K. Brandt and W.S. Sheldrick, *Chem. Ber., 129*, 1199 (1996).
1451. G. Suardi, B.P. Cleary, S.B. Duckett, C. Sleigh, M. Rau, E.W. Reed, J.A.B. Lohman, and R. Eisenberg, *J. Am. Chem. Soc., 119*, 7716 (1997).
1452. H. Bauer and W. Beck, *J. Organomet. Chem., 308*, 73 (1986).
1453. W.K. Dean, *Cryst. Struct. Commun., 8*, 335 (1979).
1454. W.P. Bosman and A.L. Gal, *Cryst. Struct. Commun., 4*, 465 (1975).

1455. A.W. Gal, A.F.J.M. van der Ploeg, F.A. Vollenbroek, and W. Bosman, *J. Organomet. Chem., 96*, 123 (1975).
1456. J.V. Heras, M. Cano, M.A. Lobo, and P. Ovejero, *J. Organomet. Chem., 269*, 277 (1984).
1457. M. Cano, J.V. Heras, M.A. Lobo, P. Ovejero, J.A. Campo, E. Pinilla, and A. Monge, *Rhodium Express, 9*, 8 (1995).
1458. J.V. Heras, M. Cano, M.A. Lobo, and P. Ovejero, *J. Organomet. Chem., 332*, 213 (1987).
1459. L. Dahlenburg and M. Kühnlein, *Acta Crystallogr., Sect. C, 57*, 709 (2001).
1460. K.K. Pandey, D.T. Nehete, and R.B. Sharma, *Polyhedron, 9*, 2013 (1990).
1461. G. Exarchos and S.D. Robinson, *Polyhedron, 19*, 123 (2000).
1462. G. Matsubayashi, K. Kondo, and T. Tanaka, *Inorg. Chim. Acta, 69*, 167 (1983).
1463. D.G. Craciunescu, C. Molina, A. Doadrio Lopez, E. Parrondo Iglesias, A. Gomez, M. Sanchez de Leon, L. Fernandez de Simon, E. Gaston de Iriarte, and C. Ghirvu, *Anal. Real Acad. Farm., 53*, 205 (1987).
1464. D.G. Craciunescu, C. Molina, J.C. Doadrio-Villarejo, M.T. Gutierrez Rios, M.P. Alonso, E. Parrondo Iglesias, M.I. De Frutos, A. Doadrio Lopez, and E. Gaston de Iriarte, *Anal. Real Acad. Farm., 57*, 391 (1991).
1465. M. Huhn, W. Klaui, L. Ramacher, R. Herbstirmer, and E. Egert, *J. Organomet. Chem., 398*, 339 (1990).
1466. G.A. Bowmaker, P.D.W. Boyd, G.K. Campbell, J.M. Hope, and R.L. Martin, *Inorg. Chem., 21*, 1152 (1982).
1467. K. Oyaizu, K. Yamamoto, Y. Ishii, and E. Tsuchida, *Chem., Eur. J., 5*, 3193 (1999).
1468. S.-W. Lai, M.G.B. Drew, and P.D. Beer, *J. Organomet. Chem., 637–639*, 89 (2001).
1469. L.H. Uppadine, J.M. Weeks, and P.D. Beer, *J. Chem. Soc., Dalton Trans.*, 3367 (2001).
1470. N.G. Berry, M.D. Pratt, O.D. Fox, and P.D. Beer, *Supramol. Chem., 13*, 677 (2001).
1471. N.G. Berry, T.W. Shimell, and P.D. Beer, *J. Supramol. Chem., 2*, 89 (2002).
1472. R. Pastorek, F. Brezina, and Z. Sindelar, *Z. Chem., 28*, 223 (1988).
1473. R. Nomura and S. Nakamoto, *Trans. Mat. Res. Soc. Jpn., 26*, 483 (2001).
1474. P.K. Gogoi and D.P. Phukan, *J. Indian Chem. Soc., 68*, 377 (1991).
1475. K.B. Pandeya, T.S. Waraich, R.C. Gaur, and R.P. Singh, *J. Inorg. Nucl. Chem., 43*, 3159 (1981).
1476. A.A.M. Aly, M.M. Kamal, M.S. El-Meligy, and A.I. El-Said, *Z. Natuforsch. B., 42*, 233 (1987).
1477. U.M. Fayyaz and M.W. Grant, *Aust. J. Chem., 32*, 2159 (1979).
1478. V. Venkatachalam, K. Ramalingam, D. Natarajan, and N. Bhavani, *Synth. React. Inorg. Met.-Org. Chem., 26*, 735 (1996).
1479. B.S. Garg, R.K. Garg and M.J. Reddy, *Transition Met. Chem., 20*, 97 (1995).
1480. B. Prelesnik, K. Andjelkovic, T. Sabo, and S. Trifunovic, *Acta Crystallogr, Sect. C, 53*, 719 (1997).
1481. S.R. Trifunovic, Z. Markovic, D. Sladic, K. Andjelkovic, T. Sabo, and D. Minic, *J. Serb. Chem. Soc., 67*, 115 (2002).
1482. P.J. Nichols and M.W. Grant, *Aust. J. Chem., 32*, 1679 (1979).
1483. P.J. Nichols and M.W. Grant, *Aust. J. Chem., 31*, 2581 (1978).
1484. R. Chen, G. Deng, Q. Jiang, and R. Mu, *Wuli Huaxue Xuebao, 5*, 626 (1989).
1485. D.J. Price, M.A. Wali, and D.W. Bruce, *Polyhedron, 16*, 315 (1997).
1486. N. Hoshino-Miyajima, *J. Chem. Soc., Chem. Commun.*, 1442 (1993).
1487. A.G. Alonso and L.B. Reventos, *J. Chem. Soc., Dalton Trans.*, 537 (1988).

1488. C.F. Barrientos, H. Cabracho, J.C. Contreras, and C. Lagos, *J. Inorg. Nucl. Chem., 40*, 926 (1978).

1489. O.D. Fox, M.G.B. Drew, E.J.S. Wilkinson, and P.D. Beer, *Chem. Commun.*, 391 (2000).

1490. R. Thiruneelakandan, K. Ramalingam, A. Manohar, G. Bocelli, and L. Righi, *Z. Anorg. Allg. Chem., 628*, 685 (2002).

1491. M.V. Rajasekharan, G.V.R. Chandramouli, and P.T. Manoharan, *Chem. Phys. Lett., 162*, 110 (1989).

1492. E.J. Reijerse, M.L.H. Paulissen, and C.P. Keijzers, *J. Magn. Reson., 60*, 66 (1984).

1493. C. Nieke and J. Reinhold, *Theochem, 32*, 241 (1986).

1494. N.S. Trendafilova and G.S. Nikolov, *J. Mol. Struct., 115*, 439 (1984).

1495. D. Oktavec, B. Siles, J. Stefanec, E. Korgova, and J. Garaj, *Collect. Czech. Chem. Commun., 45*, 791 (1980).

1496. T.M. Grigolli, E.T.G. Cavalheiro, J.A.G. Neto, and G.O. Chierice, *J. Solution Chem., 23*, 813 (1994).

1497. H. Krebs, E.F. Weber, and H. Fassbender, *Z. Anorg. Allgem. Chem., 276*, 128 (1954).

1498. R.L. Carlin, J.S. Dubnoff, and W.T. Huntress, *Proc. Chem. Soc.*, 228 (1964).

1499. K. Ramalingam, V. Venkatachalam, M. Thilagavathi, and S.Thirumaran, *J. Indian Chem. Soc., 74*, 568 (1997).

1500. K.J. Cavell, J.O. Hill, and R.J. Magee, *J. Inorg. Nucl. Chem., 41*, 1379 (1979).

1501. F.P. Emmenegger, *Inorg. Chem., 28*, 2210 (1989).

1502. C. Preti, G. Tosi, and P. Zannini, *Transit. Met. Chem., 4*, 360 (1979).

1503. K.B. Callahan and E.J. Cichon, *Inorg. Chem., 20*, 1941 (1981).

1504. J. Willemse, J.A. Cras, W.P. Bosman, and J.J. Steggerda, *Rec. Trav. Chim. Pays-Bas 99*, 65 (1980).

1505. R. Pastorek, J. Kamenicek, F. Brezina, M. Hamrusova, Z. Sindelar, and J. Lasovsky, *Chem. Pap.-Chem. Zvesti, 47*, 210 (1993).

1506. R. Schierl, U. Nagel, and W. Beck, *Z. Naturforsch. B, 39*, 649 (1984).

1507. L.T. Chan, H.-W. Chen, J.P. Fackler, Jr., A.F. Masters, and W.-H. Pan, *Inorg.Chem., 21*, 4291 (1982).

1508. K. Ramalingam, G. Aravamudan, M. Seshasayee, and C. Subramanyam, *Acta Crystallogr.,-Sect.C, 40*, 965 (1984).

1509. K. Ramalingam, G. Aravamudan, and M. Seshasayee, *Inorg. Chim. Acta, 128*, 231 (1987).

1510. R. Pastorek, J. Kamenicek, Z. Travnicek, J. Husarek, and N. Duffy, *Polyhedron, 18*, 2879 (1999).

1511. R. Pastorek, Z. Travnicek, E. Kvapilova, Z. Sindelar, F. Brezina, and J. Marek, *Polyhedron, 18*, 151 (1999).

1512. J. Darkwa, E.Y. Osei-Twum, and L.A. Litorja, Jr., *Polyhedron, 18*, 1115 (1999).

1513. R. Pastorek, Z. Travnicek, Z. Sindelar, F. Brezina, and J. Marek, *Polyhedron, 15*, 3691 (1996).

1514. G. Sánchez, F. Ruiz, J.L. Serrano, M.C.R. de Arellano, and G. López, *Eur. J. Inorg. Chem.*, 2185 (2000).

1515. R. Pastorek, J. Kamenicek, F. Brezina, Z. Sindelar, E. Jehlarova, N.V. Duffy, and T. Glowiak, *Chem. Pap.-Chem. Zvesti, 48*, 317 (1994).

1516. C.A. Tsipis, D.P. Kessissoglou, and G.E. Manoussakis, *Chim. Chron. New Series, 11*, 235 (1982).

1517. C.A. Tsipis, D.P. Kessissoglou, and G.A. Katsoulos, *Chim. Chron. New Series, 14*, 195 (1985).
1518. C.A. Tsipis, D.P. Kessissoglou, and G.E. Manoussakis, *Inorg. Chim. Acta, 65*, L137 (1982).
1519. E. Carmona, F. Gonzalez, M.L. Poveda, J.M. Marin, and A. Martinez, *Anal. Quim. Ser.B, 78*, 51 (1982).
1520. R. Schierl, U. Nagel, and W. Beck, *Z. Naturforsch. B, 39*, 649 (1984).
1521. I.H. Anderson, A.J. Blake, and G.A. Heath, *Acta Crystallogr. Sect. C, 49*, 87 (1993).
1522. I.H. Anderson, A.J. Blake, and G.A. Heath, *Acta Crystallogr., Sect. C, 45*, 1430 (1989).
1523. V. Iliev and V. Alexiev, *Spectroc. Acta Pt. A-Molec. Biomolec. Spectr., 51*, 969 (1995).
1524. N. Rajendiran, K. Ramalingam, and R. Thiruneelakandan, *Ind. J. Chem. Sect A-Inorg. Phys. Theor. Anal. Chem., 40*, 1101 (2001).
1525. A.S.A. Zidan, *Synth. React. Inorg. Met.-Org. Chem., 31*, 457 (2001).
1526. F.T. Esmadi and T. Irshiadat, *Asian J. Chem., 13*, 603 (2001).
1527. V. Venkatachalam, K. Ramalingam, G. Bocelli, and A. Cantoni, *Inorg. Chim. Acta, 257*, 49 (1997).
1528. V. Venkatachalam, K. Ramalingam, T.C.W. Mak, and B.S. Luo, *Polyhedron, 15*, 1295 (1996).
1529. M.J. Tenorio, M.C. Puerta, and P. Valerga, *J. Chem. Soc., Dalton Trans.*, 1935 (1996).
1530. A. Manohar, V. Venkatachalam, K. Ramalingam, U. Casellato, and R. Graziani, *Polyhedron, 16*, 1971 (1997).
1531. R. Akilan, K. Sivakumar, V. Venkatachalam, K. Ramalingam, K. Chinnakali, and H.-K. Fun, *Acta Crystallogr., Sect. C, 51*, 368 (1995).
1532. R. Pastorek, Z. Travnicek, J. Marek, D. Dastych, and Z. Sindelar, *Polyhedron, 19*, 1713 (2000).
1533. R. Pastorek, Z. Travnicek, P. Ptosek, Z. Sindelar, F. Brezina, and J. Marek, *J. Coord. Chem., 44*, 247 (1998).
1534. A. Manohar, K. Ramalingam, R. Thiruneelakanden, G. Bocelli, and L. Righi, *Z. Anorg. Allg. Chem., 627*, 1103 (2001).
1535. A. Manohar, K. Ramalingam, G. Bocelli, and L. Righi, *Inorg. Chim. Acta, 314*, 172 (2001).
1536. R. Pastorek, J. Kamenicek, Z. Sindelar, and Z. Zak, *Pol. J. Chem., 75*, 363 (2001).
1537. R. Pastorek, J. Kamenicek, M. Pavlicek, J. Husarek, Z. Sindelar, and Z. Zak, *J. Coord. Chem., 55*, 1301 (2002).
1538. R. Pastorek, J. Kamenicek, J. Husarek, M. Pavlicek, Z. Sindelar, and Z. Zak, *Pol. J. Chem., 76*, 1545 (2002).
1539. B.A. Prakasam, K. Ramalingam, M. Saravanan, G. Bocelli, and A. Cantoni, *Polyhedron, 23*, 77 (2004).
1540. R. Pastorek, J. Kamenicek, J. Husarek, M. Pavlicek, Z. Sindelar, and Z. Zak, *Pol. J. Chem., 77*, 805 (2003).
1541. J.L. Serrano, L. Garcia, J. Perez, E. Perez, G. Sanchez, J. Garcia, G. Lopez, G. Garcia, and E. Molins, *Inorg. Chim. Acta, 355*, 33 (2003).
1542. D.L. Long, Q.H.Wang, and J.S. Huang, *Acta Crystallogr. Sect. C, 54*, 1251 (1998).
1543. G. Lopez, G. Sanchez, G. Garcia, J. Garcia, A. Sanmartin, and M.D. Santana, *Polyhedron, 10*, 2821 (1991).
1544. G.A. Bowmaker, P.D.W. Boyd, G.K. Campbell, and M. Zvagulis, *J. Chem. Soc., Dalton Trans.*, 1065 (1986).
1545. W. Kwoda, R.O. Moyer, and R. Lindsay, *J. Inorg. Nucl. Chem., 37*, 1889 (1975).
1546. R. Vicente, A. Escuer, J. Ribas, A. Dei, X. Solans, and T. Calvet, *Polyhedron, 9*, 1729 (1990).

1547. N.C. Norman, N.L. Pickett, W.D. Storr, N.M. Boag, and A.J. Goodby, *Polyhedron, 13*, 2525 (1994).

1548. R. Pastorek, Z. Travnicek, Z. Sindelar, and F. Brezina, *Transit. Met. Chem., 24*, 304 (1999).

1549. S. Babikanyisa and J. Darkwa, *Inorg. Chim. Acta, 256*, 15 (1997).

1550. K. Schulbert and R. Mattes, *Z. Naturforsch., Teil B, 49*, 770 (1994).

1551. J.R. Allan, J. Halfpenny, G.H.W. Milburn, T.A. Stephenson, and P.M. Veitch, *J.Chem.Res., 270*, 2601 (1986); *J. Chem. Res. S*, 270 (1986).

1552. F. Cecconi, C.A. Ghilardi, S. Midollini, and A. Orlandini, *Z. Naturforsch. B, 46*, 1161 (1991).

1553. H.C. Brinkhoff, *Recl.Trav.Chim.Pays-Bas, 90*, 377 (1971).

1554. H.C. Brinkhoff, J.A. Cras, J.J. Steggerda, and J. Willemse, *Recl. Trav. Chim. Pays-Bas, 88*, 633 (1969).

1555. J. Willemse and J.J. Steggerda, *J. Chem. Soc., Chem. Commun.*, 1123 (1969).

1556. J. Willemse, P.H.F.M. Rouwette, and J.A. Cras, *Inorg. Nucl. Chem. Lett., 8*, 389 (1972).

1557. B.M. Ondo, J.P. Barbier, and R.P. Hugel, *J. Chem. Res. S, 11*, 376 (1984).

1558. J.-P. Barbier, R.P. Hugel, and C. Kappenstein, *Inorg. Chim. Acta, 77*, L117 (1983).

1559. P. Eckstein and E. Hoyer, *Z. Anorg. Allg. Chem., 487*, 33 (1982).

1560. H. Hofbauerova, E. Beinrohr, and J. Mocak, *Chem. Zvesti, 41*, 441 (1987).

1561. S.O. Yaman, O.M. Onal, and H. Isci, *Z. Naturforsch., Teil B, 56*, 202 (2001).

1562. W. Chen, H. Li, Z.-J. Zhong, K. Zhang, and X.-Z. You, *Acta Crystallogr., Sect. C, 52*, 3030 (1996).

1563. J.P. Fackler, Jr., A. Avdeef, and R.G. Fischer, Jr., *J. Am. Chem. Soc., 95*, 774 (1973).

1564. D. Collison, C.D. Garner, C.M. McGrath, J.F.W. Mosselmans, E. Pidcock, M.D. Roper, B.G. Searle, J.M.W. Seddon, E. Sinn, and N.A. Young, *J. Chem. Soc., Dalton Trans.*, 4179 (1998).

1565. V.F. Plyusnin, V.P.Grivin, N.M. Bazhin, E.P. Kuznetzova, and S.V. Larionov, *J. Photochem. Photobiol. A: Chem., 74*, 121 (1993).

1566. V.F. Plyusnin, V.P.Grivin, N.M. Bazhin, E.P. Kuznetzova, and S.V. Larionov, *J. Photochem. Photobiol. A: Chem., 74*, 129 (1993).

1567. P. Eckstein, J. Stach, R. Kirmse, and E. Hoyer, *Z. Chem., 18*, 458 (1978).

1568. R. Pastorek, F. Brezina, and D. Krausova, *Z. Chem., 30*, 70 (1990).

1569. E. Beinrohr, A. Stasko, and J. Garaj, *Collect. Czech. Chem. Commun., 50*, 1648 (1985).

1570. Yu.V. Ivanov, V.F. Plyusnin, V.P. Grivin, and S.V. Larionov, *J. Photochem. Photobiol. A: Chem., 119*, 33 (1998).

1571. Yu.V. Ivanov, V.F. Plyusnin, V.P. Grivin, and S.V. Larionov, *Chem. Phys. Lett., 310*, 252 (1999).

1572. R. Nomura and H. Hayata, *Trans. Mater. Res. Soc. Jpn., 26*, 1282 (2001).

1573. P. O'Brien, J.H. Park, and J. Waters, *Thin Solid Films, 431*, 502 (2003).

1574. M. Lalia-Kantouri, G.A. Katsoulos, C.C. Hadjikostas, and P. Kokorotsikos, *J. Therm. Anal., 35*, 2411 (1989).

1575. N. Kuramoto and T. Kitao, *Dyes Pigment, 3*, 49 (1982).

1576. M.A. Caine, R.W. McCabe, L.C. Wang, R.G. Brown, and J.D. Hepworth, *Dyes Pigment, 52*, 55 (2002).

1577. N.S. Allan, N. Hughes, and P. Mahon, *J. Photochem., 37*, 379 (1987).

1578. J.G.M. van der Linden and A.H. Dix, *Inorg. Chim. Acta, 35*, 65 (1979).

1579. G. Cervantes, V. Moreno, E. Molins, and C. Miravitlles, *Metal-Based Drugs, 4,* 317 (1997).

1580. M.-L. Riekkola, T. Pakkanen, and L. Niinisto, *Acta Chem. Scand. Ser. A, 37*, 807 (1983).
1581. M.A. Malik, P. O'Brien, and N. Revaprasadu, *J. Mater. Chem., 12*, 92 (2002).
1582. A. Birri, B. Harvey, G. Hogarth, and E. Subasi, unpublished results.
1583. J.H.G. Rangel, S.F. Oliveira, J.G.P. Espínola, and A.G. Souza, *Thermochim. Acta, 328*, 187 (1999).
1584. G.C. Franchini, A. Giusti, C. Preti, L. Tassi, and P. Zannini, *Polyhedron, 4*, 1553 (1985).
1585. L. Marcheselli, C. Preti, M. Tagliazucchi, V. Cherchi, L. Sindellari, A. Furlani, A. Papaioannou, and V. Scarcia, *Eur. J. Med. Chem., 28*, 347 (1993).
1586. U. Casellato and R. Graziani, *Z. Krist.-New Cryst. Struct., 214*, 495 (1999).
1587. L. Sindellari, L. Trincia, M. Nicolini, M. Carrara, L. Cima, and S. Zampiron, *Inorg. Chim. Acta, 137*, 109 (1987).
1588. J.J. Criado, I. Fernandez, B. Macías, J.M. Salas, and M. Medarde, *Inorg. Chim. Acta, 174*, 67 (1990).
1589. J.J. Criado, A. Carrasco, B. Macías, J.M. Salas, M. Medarde, and M. Castillo, *Inorg. Chim. Acta, 160*, 37 (1989).
1590. K.A. Mitchell and C.M. Jensen, *Inorg. Chim. Acta, 265*, 103 (1997).
1591. D. Fregona, S. Tenconi, G. Faraglia, and S. Sitran, *Polyhedron, 16*, 3795 (1997).
1592. G. Faraglia, D. Longo, V. Cerchi, and S. Sitran, *Polyhedron, 14*, 1905 (1995).
1593. L.Z. Xu, P.S. Zhao, and S.S. Zhang, *Chin. J. Chem., 19*, 436 (2001).
1594. G.A. Heath, D.C.R. Hockless, and P.D. Prenzler, *Acta Crystallogr. Sect. C, 52*, 537 (1996).
1595. A.Z. Wang, X.L. Wu, and C.G. Fu, *Acta Chim. Sin., 44*, 1015 (1986).
1596. J.M.C. Alison and T.A. Stephenson, *J. Chem. Soc., Dalton Trans.*, 254 (1973).
1597. J.P. Fackler, Jr., L.D. Thompson, I.J.B. Lin, T.A. Stephenson, R.O. Gould, J.M.C. Alison, and A.J.F. Fraser, *Inorg. Chem., 21*, 2397 (1982).
1598. R. Colton, and V. Tedesco, *Inorg. Chim. Acta, 202*, 95 (1992).
1599. R. Colton, V. Tedesco, and J.C. Traeger, *Inorg. Chem., 31*, 3865 (1992).
1600. R. Colton and J. Ebner, *Inorg. Chem., 28*, 1559 (1989).
1601. E.G. Bakalbassis, G.A. Katsoulos, M.P. Sigalas, C.A. Tsipis, and C.E. Xanthopoulos, *Struct. Chem., 4*, 349 (1993).
1602. G. López, J. Ruiz, G. García, C. Vincente, J.M. Martí, and V. Rodríguez, *J. Organomet. Chem., 436*, 121 (1992).
1603. D.L. Reger, D.G. Garza, and L. Lebioda, *Organometallics, 10*, 902 (1991).
1604. D.L. Reger, D.G. Garza, and L. Lebioda, *Organometallics, 11*, 4285 (1992).
1605. D.L. Reger and J.E. Collins, *J. Organomet. Chem., 491*, 159 (1995).
1606. S. Narayan, V.K. Jain, and S. Chaudhury, *J. Organomet. Chem., 530*, 101 (1997).
1607. D.L. Reger and J.E. Collins, *Inorg. Chem., 34*, 2473 (1995).
1608. D.L. Reger, Y. Ding, D.G. Garza, and L. Lebioda, *J. Organomet. Chem., 452*, 263 (1993).
1609. V. Scarcia, A. Furlani, D. Fregona, G. Faraglia, and S. Sitran, *Polyhedron, 18*, 2827 (1999).
1610. G. Faraglia, D. Fregona, S. Sitran, L. Giovagnini, C. Marzano, F. Baccichetti, F. Casellato, and R. Graziani, *J. Inorg. Biochem., 83*, 31 (2001).
1611. V. Serban and I. Serban, *Rev. Roum. Chim., 39*, 165 (1994).
1612. D.A. Clemente, G. Faraglia, L. Sindellari, and L. Trincia, *J. Chem. Soc., Dalton Trans.*, 1823 (1987).

1613. L.T. Chan, H.-W. Chen, J.P. Fackler, Jr., A.F. Masters, and W.-H. Pan, *Inorg. Chem., 21*, 4291 (1982).

1614. S. Narayan, V.K. Jain, K. Panneerselvam, T.H. Lu, and S.-H. Tung, Shu-Fang, *Polyhedron, 18*, 1253 (1999).

1615. D.L. Reger, J.C. Baxter, and D.G. Garza, *Organometallics, 9*, 873 (1990).

1616. M. Nonoyama, K. Nakajima, and M. Kita, *Polyhedron, 14*, 1035 (1995).

1617. R. Roy, K. Bag, P.K. Santra, and C. Sinha, *Transition Met. Chem., 25*, 302 (2000).

1618. J. Fornies, A. Martin, R. Navarro, V. Sicilia, and P. Villarroya, *Organometallics, 15*, 1826 (1996).

1619. J.M. Bevilacqua and R. Eisenberg, *Inorg. Chem., 33*, 2913 (1994).

1620. S.H. Taylor and P.M. Maitlis, *J. Am. Chem. Soc., 100*, 4700 (1978).

1621. P.M. Bailey, S.H. Taylor, and P.M. Maitlis, *J. Am. Chem. Soc., 100*, 4711 (1978).

1622. M.C. Cornock, R.O. Gould, C.L. Jones, and T.A. Stephenson, *J. Chem. Soc., Dalton Trans.*, 496 (1977).

1623. D.M. Anderson, E.A.V. Ebsworth, T.A. Stephenson, and M.D. Walkinshaw, *J. Chem. Soc., Dalton Trans.*, 2343 (1982).

1624. D.M. Anderson, E.A.V. Ebsworth, T.A. Stephenson, and M.D. Walkinshaw, *Angew. Chem., Int. Ed. Engl., 20*, 290 (1981).

1625. L. Canovese, P. Uguagliati, F. Dibianca, and B. Crociani, *J. Organomet. Chem., 438*, 253 (1992).

1626. G. Exarchos, S.C. Nyburg, and S.D. Robinson, *Polyhedron, 17*, 1257 (1998).

1627. G. Exarchos, S.D. Robinson, and J.W. Steed, *Polyhedron, 19*, 1511 (2000).

1628. N. Jain, T.S. Srivastava, K. Satyamoorthy, and M.P. Chitnis, *J. Inorg. Biochem., 33*, 1 (1988).

1629. N. Jain and T.S. Srivastava, *Inorg. Chim. Acta, 128*, 151 (1987).

1630. H. Werner and W. Bertleff, *Chem. Ber., 115*, 1012 (1982).

1631. G. Sanchez, J.L. Serrano, J. García, G. López, J. Perez, and E. Molins, *Inorg. Chim. Acta, 287*, 37 (1999).

1632. D. Das and C. Sinha, *Transition Met. Chem., 23*, 309 (1998).

1633. J. Ruiz, V. Rodriguez, G. López, J. Casabo, E. Molins, and C. Miravitlles, *Organometallics, 18*, 1177 (1999).

1634. J.A.S. Duncan, D. Hedden, D.M. Roundhill, A.T. Stephenson, and M.D. Walkinshaw, *Angew. Chem., Int. Ed. Engl., 21*, 452 (1982).

1635. M.C. Cornock, R.C. Davis, D. Leaver, and T.A. Stephenson, *J. Organomet. Chem., 107*, C43 (1976).

1636. S.C. Nyburg, *Acta Crystallogr., Sect. B, 52*, 328 (1996).

1637. L.-K. Liu, Y.-S. Wen, I.J.B. Lin, J.S. Lai, and C.W. Liu, *Bull. Inst. Chem. Acad. Sin., 37*, 65 (1990).

1638. A.B. Goel, S. Goel, D. Van Der Veer, and C.G. Brinkley, *Inorg. Chim. Acta, 64*, L173 (1982).

1639. K. Hamamura, M. Kita, M. Nonoyama, and J. Fujita, *J. Organomet. Chem., 463*, 169 (1993).

1640. A.J. Blake, P. Kathirgamanathan, and M.J. Toohey, *Inorg. Chim. Acta, 303*, 137 (2000).

1641. M. Sokolov, H. Imoto, and T. Saito, *Inorg. Chem. Commun., 2*, 422 (1999).

1642. K. Sugimoto, T. Kuroda-Sowa, T. Goto, M. Maekawa, and M. Munakata, *Bull. Chem. Soc. Jpn., 73*, 651 (2000).

1643. J.R. Allan, G.H.W. Milburn, L. Sawyer, V.K. Shah, T.A. Stephenson, and P.M. Veitch, *Acta Crystallogr., Sect. C, 41*, 58 (1985).
1644. D.M. Anderson, A.J. Blake, J.D. Fotheringham, T.A. Stephenson, J.R. Allan, and P.M. Veitch, *Acta Crystallogr., Sect. C, 44*, 1305 (1988).
1645. A.J. Blake, J.D. Fotheringham, and T.A. Stephenson, *Acta Crystallogr., Sect. C, 46*, 1102 (1990).
1646. J.R. Allan, G.H.W. Milburn, T.A. Stephenson, and P.M. Veitch, *J. Chem. Res. S*, 215 (1983).
1647. P.M. Veitch, J.R. Allan, A.J. Blake, and M. Schroder, *J. Chem. Soc., Dalton Trans.*, 2853 (1987).
1648. D.L. Long, W.T. Wong, S. Shi, X.Q. Xin, and J.S. Huang, *J. Chem. Soc., Dalton Trans.*, 4361 (1997).
1649. D.-L. Long, D.-C. Yan, W.-D. Cheng, and J.-S. Huang, *Chinese J. Struct. Chem. (Jiegou Huaxue), 17*, 155 (1998).
1650. K. Utokoro, M. Ebihara, and T. Kawamura, *Acta Crystallogr. Sect. C, 51*, 2010 (1995).
1651. J. Fornies, A. Martin, V. Sicilia, and P. Villarroya, *Organometallics, 19*, 1107 (2000).
1652. L.R. Falvello, J. Fornies, A. Martin, R. Navarro, V. Sicilia, and P. Villarroya, *Inorg. Chem., 36*, 6166 (1997).
1653. J. Willemse, J.A. Cras, J.G. Wijnhoven, and P.T. Beurskens, *Recl. Trav. Chim. Pays-Bas, 92*, 1199 (1973).
1654. K. Saraswathi, A.V.S. Lakshmi, and V.V. Ramana, *J. Indian Chem. Soc., 69*, 795 (1992).
1655. D.K. Singh and N.K. Mishra, *Chromatographia, 31*, 300 (1991).
1656. A.K. Malik and A.L.J. Rao, *J. Chin. Chem. Soc., 39*, 235 (1992).
1657. R. Mital, N. Jain, and T.S. Srivastava, *Inorg. Chim. Acta, 166*, 135 (1989).
1658. H. Shimada, N. Sugimachi, T. Funakoshi, and S. Kojima, *Toxicol. Lett., 66*, 193 (1993).
1659. A. Trevisan, C. Marzano, P. Cristofori, M.B. Venturini, L. Giovagnini, and D. Fregona, *Arch. Toxicol., 76*, 262 (2002).
1660. D. Fregona, L. Giovagnini, L. Ronconi, C. Marzano, A. Trevisan, S. Sitran, B. Biondi, and F. Bordin, *J. Inorg. Biochem., 93*, 181 (2003).
1661. C. Marzano, A. Trevisan, L. Giovagnini, and D. Fregona, *Toxicol. Vitro, 16*, 413 (2002).
1662. L. Cambi and C. Coriselli, *Gazz. Chim. Ital., 66*, 779 (1936).
1663. P.T. Beurskens, J.A. Crass, and J.J. Steggerda, *Inorg. Chem., 7*, 810 (1968).
1664. R. Nomura, K. Kanaya, and H. Matsuda, *Chem. Lett.*, 1849 (1988).
1665. A.C. Fabretti, M. Ferrari, G.C. Franchini, A. Guisti, C. Preti, and G. Tosi, *Transition Met. Chem., 8*, 8 (1983).
1666. A. Mederos, A. Cachapa, R. Hernández-Molina, M.T. Armas, P. Gili, M. Sokolov, J. González-Platas, and F. Brito, *Inorg. Chem. Commun., 6*, 498 (2003).
1667. N. K. Kaushik, B. Bhushan, and A.K. Sharma, *Thermochim. Acta, 76*, 345 (1984).
1668. J.I. Martinez, D.W. Bruce, D.J. Price, and P.J. Alonso, *Liq. Crystallogr., 19*, 127 (1995).
1669. W.E. Hatfield, P. Singh, and F. Nepveu, *Inorg. Chem., 29*, 4214 (1990).
1670. J.-P. Lang, J.-M. Lu, G.-Q. Bian, J.-H. Cai, B.-S. Kang, and X.-Q. Xin, *Chin. J. Struct. Chem., 14*, 297 (1995).
1671. H. Iwasaki and K. Kobayashi, *Acta Crystallogr., Sect. B, 36*, 1655 (1980).
1672. F.F. Jian, T. Xue, K. Jiao, and S.S. Zhang, *Chin. J. Chem., 21*, 50 (2003).
1673. F.W.B. Einstein and J.S. Field, *Acta Crystallogr., Sect. B, 30*, 2929 (1974).

1674. K. Hagen, C.J. Holwill, and D.A. Rice, *Inorg. Chem., 28*, 3239 (1989).

1675. R. Kirmse, U. Abram, and R. Bottcher, *Chem. Phys. Lett., 90*, 9 (1982).

1676. A. Warshawsky, I. Rogachev, Y. Patil, A. Baszkin, L. Weiner, and J. Gressel, *Langmuir, 17*, 5621 (2001).

1677. P.D.W. Boyd, S. Mitra, C.L. Raston, G.L. Rowbottom, and A.H. White, *J. Chem. Soc., Dalton Trans.*, 13 (1981).

1678. J. Villa and W.E. Hatfield, *Inorg. Chem., 10*, 2038 (1971).

1679. J.A. Van Santen, A.J. Van Duyneveldt, and R.L. Carlin, *Inorg. Chem., 19*, 2152 (1980).

1680. Y. Suzuki, S. Fujii, T. Tominaga, T. Yoshimoto, T. Yoshimura, and H. Kamada, *Biochim. Biophys. Acta, Gen. Subj., 1335*, 242 (1997).

1681. W.J. Newton and B.J. Tabner, *J. Chem. Soc., Dalton Trans.*, 466 (1981).

1682. B.G. Jeliazkova, A. Dimitrova, and N.D. Yordanov, *Spectroc. Acta Pt. A, Molec. Biomolec. Spectrosc., 58*, 1163 (2002).

1683. G.H. Sarova and B.G. Jeliazkova, *Transition Met. Chem., 26*, 388 (2001).

1684. P.J.M. Geurts, P.C.P. Bouten, and A. Van der Avoird, *J. Chem. Phys., 73*, 1306 (1980).

1685. N.D. Yordanov, A. Dimitrova, and D. Roussanova, *Spectroc. Acta Pt. A, Molec. Biomolec. Spectr., 58*, 1155 (2002).

1686. A.V. Ivanov, P.M. Solozhenkin, and V.I. Mitrofanova, *Zh. Neorg. Khim., 42*, 256 (1997).

1687. A.V. Ivanov and V.B. Klyashtornyi, *Zh. Neorg. Khimii, 37*, 1597 (1992).

1688. A.V. Ivanov and P.M. Solozhenkin, *Zh. Neorg. Khimii, 35*, 1537 (1990).

1689. A.V. Ivanov and P.M. Solozhenkin, *Dokl. Akad. Nauk USSR, 311*, 392 (1990).

1690. A.V. Ivanov, V.I. Mitrofanova, and T.A. Rodina, *Zh. Neorg. Khimii, 42*, 644 (1997).

1691. A.V. Ivanov, P.M. Solozhenkin, M.Z. Khamkar, V.B. Klyashtornyi, and F.A. Shvengler, *Koord. Khimiya, 15*, 1223 (1989).

1692. P.M. Solozhenkin, F.A. Shvengler, N.I. Kopitsia, and A.V. Ivanov, *Dokl. Akad. Nauk USSR, 269*, 881 (1983).

1693. A.V. Ivanov, *Koord. Khimiya, 17*, 382 (1991).

1694. A.V. Ivanov, M. Kritikos, O.N. Antzutkin, and W. Forsling, *Inorg. Chim. Acta, 321*, 63 (2001).

1695. P.M. Solozhenkin, A.V. Ivanov, M.Z. Khamkar, and V.B. Klyashtornyi, *Zh. Neorg. Khimii, 32,* 2711 (1987); *Russ. J. Inorg. Chem., 32*, 1577 (1987).

1696. A.V. Ivanov, S.A. Leskova, M.A. Mel'nikova, T.A. Rodina, A. Lund, O.N. Antzutkin, and W. Forsling, *Russ. J. Chem., 48*, 415 (2003).

1697. P.M. Solozhenkin, V.F. Anufrienko, N.I. Kopitsia, V.A. Poluboiarov, F.A. Shvengler, and A.V. Ivanov, *Dokl. Akad. Nauk SSSR, 274*, 1420 (1984).

1698. A.V. Ivanov, P.M. Solozhenkin, and M.Z. Khamkar, *Koord. Khimiya, 14*, 754 (1988).

1699. A.V. Ivanov, I.A. Lutsenko, and W. Forsling, *Russ. J. Coord. Chem., 28*, 57 (2002).

1700. R. Kirmse, U. Abram, and R. Bottcher, *Chem. Phys. Lett., 88*, 98 (1982).

1701. A.R. Hendrickson, R.L. Martin, and N.M. Rohde, *Inorg. Chem., 15*, 2115 (1976).

1702. H.L. Nigam, K.B. Pandeya, I.P. Tripathi, P.R. Shukla, J. Prasad, and K. Srivastava, *J. Indian Chem. Soc., 69*, 536 (1992).

1703. B.G. Jeliazkova and N.D. Yordanov, *Inorg. Chim. Acta, 203*, 201 (1993).

1704. G.H. Sarova and B.G. Jeliazkova, *Transition Met. Chem., 26*, 388 (2001).

1705. V.I. Iliev, N.D. Yordanov, and D. Shopov, *Polyhedron, 3*, 291 (1984).

1706. V. Iliev, N.D. Yordanov, and D. Shopov, *Polyhedron, 3*, 297 (1984).

1707. R.N. Patel, S. Kumar, and K.B. Pandeya, *Indian J. Chem. Sect. A, Inorg. Bio-Inorg. Phys. Theor. Anal., 40*, 1104 (2001).
1708. G.M. Larin, G.A. Zvereva, V.V. Minin, and Y.V. Rakitin, *Bull. Acad. Sci. USSR, Chem. Sci., 37,* 2237 (1988).
1709. A. Diaz, M. Ortiz, I. Sanchez, R. Cao, A. Mederos, J. Sanchiz, and F. Brito, *J. Inorg. Biochem., 95*, 283 (2003).
1710. A.R. Hendrickson, R.L. Martin, and D. Taylor, *J. Chem. Soc., Chem. Commun.*, 843 (1975).
1711. L.I. Victoriano, H.B. Cortés, M.I.S. Yuseff, and L.C. Fuentealba, *J. Coord. Chem., 39*, 241 (1996).
1712. L.I. Victoriano and H. Cortés, *Bol. Soc. Chil. Quim., 41*, 5 (1996).
1713. B.G. Jeliazkova and M.A. Doicheva, *Polyhedron, 15*, 1277 (1996).
1714. B.G. Jeliazkova, M.A. Doicheva, and K. Miltchovska, *Polyhedron, 17*, 4553 (1998).
1715. M.A. Doicheva and B.G. Jeliazkova, *Spectroc. Acta Pt. A-Molec. Biomolec. Spectr., 54*, 2373 (1998).
1716. M. Doicheva and B. Jeliazkova, *Spectroc. Acta Pt. A-Molec. Biomolec. Spectr., 54*, 2385 (1998).
1717. K.K.M. Yusuff, K.M. Basheer, and M. Gopalan, *Polyhedron, 2*, 839 (1983).
1718. V.I. Iliev and N.D. Yordanov, *J. Mol. Liq., 28*, 137 (1984).
1719. B.G. Jeliazkova and G.C. Sarova, *Polyhedron, 16*, 3967 (1997).
1720. M. Lalia-Kantouri, M. Uddin, C.C. Hadjikostas, H. Papanikolas, G. Palios, S. Anagnostis, and V. Anesti, *Z. Anorg. Allg. Chem., 623*, 1983 (1997).
1721. B.G. Jeliazkova and G.C. Sarova, *Appl. Magn. Reson., 10*, 159 (1996).
1722. B.G. Jeliazkova, M.A. Doicheva, and L.B. Tosheva, *Appl. Magn. Reson., 10*, 151 (1996).
1723. K.B. Pandeya, T.S. Waraich, R.C. Gaur, and R.P. Singh, *Synth. React. Inorg. Met.-Org. Chem., 12*, 493 (1982).
1724. B.B. Kaul and K.B. Pandeya, *J. Inorg. Nucl. Chem., 43*, 1942 (1981).
1725. K.K.M. Yuseff and E.J. Mathew, *Synth. React. Inorg. Met.-Org. Chem., 22*, 575 (1992).
1726. L.I. Victoriano, *J. Chem. Educ., 79*, 1252 (2002).
1727. L. Victoriano, J. Granifo, and L. Parraguez, *Bol. Soc. Chil. Quim., 45*, 487 (2000).
1728. M.A. Willert-Porada, D.J. Burton, and N.C. Baenziger, *Chem. Commun., 1989*, 1633; R.E. Marsh, *Acta Crystallogr., Sect. B, 53*, 317 (1997).
1729. K. Anas, N. Sridevi, and K.K.M. Yusuff, *Indian J. Chem. Sect. A, Inorg. Bio-Inorg. Phys. Theor. Anal., 39*, 940 (2000).
1730. J.A. Cras, J. Willemse, A.W. Gal, and B.G.M.C. Hummelink-Peters, *Recl. Trav. Chim., 92*, 641 (1973).
1731. J. Willemse and J.A. Cras, *Recl. Trav. Chim. Pays-Bas, 91*, 1309 (1972).
1732. K.K.M. Yusuff and E.J. Mathew, *J. Coord. Chem., 26*, 133 (1992).
1733. L.I. Victoriano and H.B. Cortés, *J. Coord. Chem., 39*, 231 (1996).
1734. Q. Zhang, J. Chen, M. Hong, X. Xin, and H.-K. Fun, *Z. Naturforsch. Sect. B, 54*, 1313 (1999).
1735. A.L. Odom and C.C. Cummins, *Polyhedron, 17*, 675 (1998).
1736. L.Z. Xu, J.H. Lin, S.S. Zhang, K. Jiao, and F.F. Jian, *Pol. J. Chem., 75*, 755 (2001).
1737. S.-B. Huang and Y. Situ, *Jiegou Huaxue, 22*, 260 (2003).
1738. L.M. Engelhardt, P.C. Healy, B.W. Skelton, and A.H. White, *Aust. J. Chem., 41*, 839 (1988).
1739. X. Lei, Q. Liu, and H. Liu, *Chinese J. Struct. Chem. (Jiegou Huaxue), 7*, 99 (1988).

1740. Z. Huang, X. Lei, B. Kang, J. Liu, Q. Liu, M. Hong, and H. Liu, *Inorg. Chim. Acta, 169*, 25 (1990).

1741. M. Hong, Q. Zhang, R. Cao, D. Wu, J. Chen, W. Zhang, H. Liu, and J. Lu, *Inorg. Chem., 36*, 6251 (1997).

1742. H. Zhu, X. Huang, Y. Deng, D. Wu, C. Chen, and Q. Liu, *Inorg. Chim. Acta, 256*, 29 (1997).

1743. J.-N. Liu, X.-J. Lei, B.-S. Kang, Z.-Y. Huang, and M.-C. Hong, *Chinese J. Struct. Chem.(Jiegou Huaxue), 10*, 196 (1991).

1744. R. Cao, Q. Zhang, W. Su, M. Bao, Y. Zheng, and M. Hong, *Polyhedron, 18*, 333 (1999).

1745. Q.-F. Zhang, M.-T. Bao, M.-C. Hong, R. Cao, Y.-L. Song, and X.-Q. Xin, *J. Chem. Soc., Dalton Trans.*, 605 (2000).

1746. X.-J. Lei, Z.-Y. Huang, M.-C. Hong, Q.-T. Liu, and H.-Q. Liu, *Chinese J. Struct. Chem.(Jiegou Huaxue), 9*, 53 (1990).

1747. Y. Yang, Q. Liu, L. Huang, D. Wu, B. Kang, and J. Lu, *Inorg. Chem., 32*, 5431 (1993).

1748. Q. Liu, Y. Yang, L. Huang, D. Wu, B. Kang, C. Chen, Y. Deng, and J. Lu, *Inorg. Chem., 34*, 1884 (1995).

1749. X. Lei, Z. Huang, Q. Liu, M. Hong, and H. Liu, *Inorg. Chem., 28*, 4302 (1989).

1750. X. Lei, Z. Huang, M. Hong, Q. Liu, and H. Liu, *Inorg. Chim. Acta, 164*, 119 (1989).

1751. R. Cao, X. Lei, and H. Liu, *Acta Crystallogr., Sect. C, 47*, 876 (1991).

1752. H. Liu, R. Cao, X. Lei, D. Wu, G. Wei, Z. Huang, M. Hong, and B. Kang, *J. Chem. Soc., Dalton Trans.*, 1023 (1990).

1753. X.-J. Lei, R. Cao, M.-C. Hong, Z.-Y. Huang, and H. Liu, *Chin. J. Chem., 11*, 144 (1993).

1754. N. Singh, M. Mehrotra, and K. Rastogi, *J. Indian Chem. Soc., 58*, 1212 (1981).

1755. K. Hayashi, T. Sasaki, S. Tagashira, Y. Murakami, K. Kusumori, and Y. Morinaga, *Bunseki Kagaku, 36*, 450 (1987).

1756. R.M. Smith and T.G. Hurdley, *Anal. Chim. Acta, 166*, 271 (1984).

1757. T. Takada, Y. Okabe, and K. Nakano, *Bull. Chem. Soc. Jpn. 54*, 3589 (1981).

1758. T. Nomura, M. Kumagai, and A. Sato, *Anal. Chim. Acta, 343*, 209 (1997).

1759. A.M. Bond and G.G. Wallace, *Anal. Chem., 53*, 1209 (1981).

1760. J.H. Santos, A.M. Bond, J. Mocak, and T.J. Cardwell, *Anal. Chem., 66*, 1925 (1994).

1761. K. Tsukagoshi, K. Miyamoto, E. Saiko, R. Nakajima, T. Hara, and K. Fujinaga, *Anal. Sci., 13*, 639 (1997).

1762. K. Tsukagoshi, N. Okuzono, and R. Nakajima, *J. Chromatogr. A, 958*, 283 (2002).

1763. S. Cobianco, A. Lezzi, and R. Scotti, *React. Funct. Polym., 43*, 7 (2000).

1764. I.N. Marov, G.A. Evtikova, G.I. Malofeeva, O.M. Petrukhin, and T.V. Danilova, *Zh. Neorg. Khimii, 35*, 2573 (1990).

1765. S.X. Guo and S.B. Khoo, *Anal. Lett., 32*, 689 (1999).

1766. R. Nomura, K. Miyakawa, T. Toyosaki, and H. Matsuda, *Chem. Vap. Depos., 2*, 174 (1996).

1767. R. Nomura, K. Kanaya, and H. Matsuda, *Ind. Eng. Chem. Res., 28*, 877 (1989).

1768. Y.M. Rumyantsev, N.I. Fainer, M.L. Kosinova, B.M. Ayupov, and N.P. Sysoeva, *J. Phys. IV, 9*, 777 (1999).

1769. N.I. Fainer, Yu.M. Rumyantsev, M.L. Kosinova, G.S. Yur'ev, E.A. Maksimovskii, S.M. Zemskova, S.V. Sysoev, and F.A. Kuznetsov, *Inorg. Mater., 34*, 1049 (1998).

1770. N.I. Fainer, Yu. M. Rumyantsev, M.L. Kosinova, and F.A. Kuznetsov, *Electrochem. Soc. Proc., 97*, 1437 (1997).

1771. S.M. Zemskova, P.A. Stabnikov, S.V. Sysoev, and I.K. Igumenov, *Electrochem. Soc. Proc., 98*, 286 (1998).

1772. M. Kemmler, M. Lazell, P. O'Brien, D.J. Otway, J.H. Park, and J.R. Walsh, *J. Mater. Sci. Mater. Electron., 13*, 531 (2002).

1773. K.K. Aravindakshan and K. Muraleedharan, *J. Therm. Anal., 37*, 803 (1991).

1774. R. Nomura, Y. Seki, K. Konishi, and H. Matsuda, *App. Organomet. Chem., 6*, 685 (1992).

1775. R. Nomura, S. Fujii, K. Konishi, and H. Matsuda, *Polyhedron, 9*, 361 (1990).

1776. R. Nomura, Y. Seki, and H. Matsuda, *Thin Solid Films, 209*, 145 (1992).

1777. M. Kemmler, M. Lazell, P. O'Brien, and D.J. Otway, *Mat. Res. Soc., 606*, 147 (2000).

1778. S.M. Zemskova, S.V. Sysoev, L.A. Glinskaya, R.F. Klevtsova, S.A. Gromilov, and S.V. Larionov, *Electrochem. Soc. Proc., 97*, 1429 (1997).

1779. D.W. Pyatt, Y.Z. Yang, A. Le, W.S. Stillman, and R.D. Irons, *Biochem. Biophys. Res. Commun., 274*, 513 (2000).

1780. R. Heikkila, F. Cabbat, and G. Cohen, *J. Biol. Chem., 251*, 2182 (1976).

1781. M. Wiedau-Pazos, J.J. Goto, S. Rabizadeh, E.B. Gralla, J.A. Roe, M.K. Lee, J.S. Valentine, and D.E. Bredesen, *Science, 271*, 515 (1996).

1782. R. Martin, A. Fragoso, and R. Cao, *Supramol. Chem., 15*, 171 (2003).

1783. K. Matsumoto, Y. Fujibayashi, J. Konishi, and A. Yokoyama, *Radioisotopes, 39*, 482 (1990).

1784. K.W. Weissmahr and D.L. Sedlak, *Environ. Toxicol. Chem., 19*, 820 (2000).

1785. G. Hogarth, A. Pateman, and A. Sella, *Chem. Commun.*, 1029 (1997).

1786. P. Li and K.-Y. Qiu, *Macromol. Chem. Phys., 203*, 2305 (2002).

1787. P. Li and K.-Y. Qiu, *J. Polym. Sci. Pol. Chem., 40*, 2093 (2002).

1788. P. Li and K.-Y. Qiu, *Macromol. Rapid Commun., 23*, 1124 (2002).

1789. P. Li and K.-Y. Qiu, *Macromolecules, 35*, 8906 (2002).

1790. T. Otsu, *J. Polym. Sci., Part A: Polym. Chem., 38*, 2121 (2000).

1791. B.G. Jeliazkova, I. Petkov, G. Sarova, T. Deligeorgiev, and M. Evstatiev, *Polym. Degrad. Stabil., 51*, 301 (1996).

1792. V.P. Rao, T.A.S. Rao, and M.C. Ganorkar, *Bull. Electrochem., 10*, 83 (1994).

1793. A. Godelitsas, D. Charistos, J. Dwyer, C. Tsipis, A. Filippidis, A. Hatzidimitriou, and E. Pavlidou, *Microporous Mesoporous Mat., 33,* 77 (1999).

1794. S. Akerström, *Ark. Kemi, 14*, 413 (1959).

1795. R.H.K. Varma and C.P. Prabhakaran, *Indian J. Chem. Sect. A, Inorg. Phys. Theor. Anal. Chem., 28*, 1119 (1989).

1796. W. Tyrra, *J. Fluor. Chem., 109*, 189 (2001).

1797. D.C. Calabro, B.A. Harrison, G.T. Palmer, M.K. Moguel, R.L. Rebbert, and J.L.Burmeister, *Inorg. Chem., 20*, 4311 (1981).

1798. Z. Huang, X. Lei, M. Hong, and H. Liu, *Inorg. Chem., 31*, 2990 (1992).

1799. W. Su, M. Hong, F. Jiang, H. Liu, Z. Zhou, D. Wu, and T.C.W. Mak, *Polyhedron, 15*, 4047 (1996).

1800. Q.F. Zhang, R. Cao, M.C. Hong, W.P. Su, and H.Q. Liu, *Inorg. Chim. Acta, 277*, 171 (1998).

1801. A.H. Othman, H.-K. Fun, and K. Sivakumar, *Acta Crystallogr., Sect. C, 52*, 843 (1996).

1802. M.C. Gimeno, P.G. Jones, A. Laguna, and C. Sarroca, *Polyhedron, 17*, 3681 (1998).

1803. M.C. Gimeno, P.G. Jones, A. Laguna, and C. Sarroca, *J. Chem. Soc., Dalton Trans.*, 1473 (1995).

1804. R. Petterson and T. Vänngard, *Ark. Kemi, 17*, 249 (1960).
1805. T. Vänngard and S. Åkerström, *Nature (London), 184*, 183 (1959).
1806. N.S. Garif'yanov, B.M. Kozyrev, and E.I. Semenova, *Dokl. Akad. Nauk., SSSR, 170*, 1324 (1966).
1807. E. Beinrohr, J. Garaj, and J. Mocak, *J. Inorg. Nucl. Chem., 42*, 741 (1980).
1808. P. Chmielewski and A. Jezierski, *Polyhedron, 7*, 25 (1988).
1809. C.-C. Lin and Z.-X. Huang, *Chin. J. Struct. Chem.(Jiegou Huaxue), 9*, 58 (1990).
1810. S. Akerström, *Ark. Kemi, 14*, 387 (1959).
1811. R. Hesse and P. Jennische, *Acta Chem. Scand., 26*, 3855 (1972).
1812. S.S. Tang, C. Chang, I.J.B. Lin, L.Liou, and J. Wang, *Inorg. Chem., 36*, 2294 (1997).
1813. M. Bardají and A. Laguna, *Inorg. Chim. Acta, 318*, 38 (2001).
1814. M. Bardaji, A. Laguna, J. Vicente, and P.G. Jones, *Inorg. Chem., 40*, 2675 (2001).
1815. E. Cerrada, P.G. Jones, A. Laguna, and M. Laguna, *Inorg. Chim. Acta, 249*, 163 (1996).
1816. T.J. Bergendahl and E.M. Bergendahl, *Inorg. Chem., 11*, 638 (1972).
1817. L.V. Antonova, O.V. Mikhailov, V.K. Polovnyak, and A.E. Usachev, *Anal. Quim., 91*, 533 (1995).
1818. M. Bardají, A. Blascoa, J. Jiménez, P.G. Jones, A. Laguna, M. Laguna, and G.F. Merchán, *Inorg. Chim. Acta, 223*, 55 (1994).
1819. M.C. Gimeno, J. Jimenez, P.G. Jones, A. Laguna, M. Laguna, and R.V. Parish, *J. Organomet. Chem., 481*, 37 (1994).
1820. H. Kita, K. Itoh, K. Tanaka, and T. Tanaka, *Bull. Chem. Soc. Jpn., 51*, 3530 (1978).
1821. A. Laguna and M. Laguna, *Coord. Chem. Rev., 193–195*, 837 (1999).
1822. M. Contel, A.J. Edwards, J. Garrido, M.B. Hursthouse, M. Laguna, and R. Terroba, *J. Organomet. Chem., 607*, 129 (2000).
1823. F.T.H.M. Wijnhoven, W.P. Bosman, J. Willemse, and J.A. Cras, *Rec. Trav. Chim. Pays-Bas, 98*, 492 (1979).
1824. C.J.L. Lock, M.A. Turner, R.V. Parish, and G. Potter, *Acta Crystallogr., Sect. C, 44*, 2082 (1988).
1825. D.J. Radanovic, Z.D. Matovic, V.D. Miletic, L.P. Battaglia, S. Ianelli, I.A. Efimenko, and G. Ponticelli, *Transition Met. Chem., 21*, 169 (1996).
1826. C. Paparizos and J.P. Fackler, Jr., *Inorg. Chem., 19*, 2886 (1980).
1827. R. Uson, A. Laguna, M. Laguna, M.L. Castilla, P.G. Jones, and K. Meyerbase, *J. Organomet. Chem., 336*, 453 (1987).
1828. V.P. Dyadchenko, K.I. Grandberg, O.N. Kalinina, P.E. Krasik, O.Yu. Burtseva, M.A. Porai-Koshits, L.G. Kuz'mina, and E.G. Perevalova, *Metalloorg. Khim., 3*, 667 (1990).
1829. E.G. Perevalova, K.I. Grandberg, V.P. Dyadchenko, and O.N. Kalinina, *Koord. Khim., 14*, 1145 (1988).
1830. V.P. Dyadchenko, P.E. Krasik, K.I. Grandberg, L.G. Kuz'mina, N.V. Dvortsova, M.A. Porai-Koshits, and E.G. Perevalova, *Metalloorg. Khim., 3*, 1260 (1990).
1831. H.M. Colquhoun, T.J. Greenhough, and M.G.H. Wallbridge, *J. Chem. Soc., Dalton Trans.*, 303 (1978).
1832. M.A. Beckett, J.E. Crook, N.N. Greenwood, and J.D. Kennedy, *J. Chem. Soc., Dalton Trans.*, 1427 (1984).

1833. M. Lerchi, E. Reitter, W. Simon, E. Pretsch, D.A. Chowdhury, and S. Kamata, *Anal. Chem., 66*, 1713 (1994).

1834. S. Gomiscek, M. Veber, V. Francetic, and R. Durst, *J. Res. Nat. Bureau Stand., 93*, 496 (1988).

1835. E. Almirall, A. Fragoso, and R. Cao, *Electrochem. Commun., 1*, 10 (1999).

1836. R. Cordova, H. Gomez, F. Brovelli, P. Grez, G. Riveros, R. Schrebler, S.G. Real, and J.R. Vilche, *Bol. Soc. Chil. Quim., 42*, 175 (1997).

1837. C.D. Frisbie, I. Fritschfaules, E.W. Wollman, and M.S. Wrighton, *Thin Solid Films, 210*, 341 (1992).

1838. C. King, J.-C. Wang, Md.N.I. Khan, and J.P. Fackler, Jr., *Inorg. Chem., 28*, 2145 (1989).

1839. J.M. Lo and J.D. Lee, *Anal. Chem., 66*, 1242 (1994).

1840. S. Kumar and N.K. Kaushik, *J. Therm. Anal., 21*, 3 (1981).

1841. M.A. Malik, T. Saeed, and P. O'Brien, *Polyhedron, 12*, 1533 (1993).

1842. B.S. Garg, R.K.Garg, and M.J. Reddy, *Indian J. Chem. Sect A, Inorg. Phys. Theor. Anal. Chem.*, *32*, 697 (1993).

1843. A. Pages, J.S. Casas, A. Sanchez, J. Sordo, J. Bravo, and M. Gayoso, *J. Inorg. Biochem., 25*, 35 (1985).

1844. S. Thirumaran, V. Venkatachalam, A. Manohar, K. Ramalingam, G. Bocelli, and A. Cantoni, *J. Coord. Chem., 44*, 281 (1998).

1845. B.B. Mahapatra, S.K. Pujari, and A. Chiranjeevi, *J. Indian Chem. Soc., 58*, 714 (1981).

1846. S. Garcia-Fontan, P. Rodriguez-Seoane, J.S. Casas, J. Sordo, and M.M. Jones, *Inorg. Chim. Acta, 211*, 211 (1993).

1847. J.S. Casas, A. Sanchez, J. Bravo, S. Garcia-Fontan, E.E. Castellano, and M.M. Jones, *Inorg. Chim. Acta, 158*, 119 (1989).

1848. P. O'Brien, D.J. Otway, and J.R. Walsh, *Chem. Vap. Dep., 3*, 227 (1997).

1849. P. O'Brien, J.R. Walsh, I.M. Watson, M. Motevalli, and L.Henriksen, *J. Chem. Soc., Dalton Trans.*, 2491 (1996).

1850. I. Kani, *Turk. J. Chem., 19*, 224 (1995).

1851. M.J. Cox and E.R.T. Tiekink, *Z. Kristallogr., 214*, 184 (1999).

1852. E. Kellö, V. Vrábel, V. Kettmann, and J. Garaj, *Collect. Czech. Chem. Commun., 48*, 1272 (1983).

1853. N. Sreehari, B. Varghese, and P.T. Manoharan, *Inorg. Chem., 29*, 4011 (1990).

1854. K. Ramalingam, O.bin Shawkataly, H.-K. Fun, and I.A. Razak, *Z. Kristallogr., New Crystal Struct., 213*, 371 (1998).

1855. I. Baba, Y. Farina, A.H. Othman, I.A. Razak, H.K. Fun, and S.W. Ng, *Acta Crystallogr., Sect. E, 57*, m51 (2001).

1856. I. Baba, Y. Farina, K. Kassim, A. Hamid, A.H. Othman, I.A. Razak, H.K. Fun, and S.W. Ng, *Acta Crystallogr. Sect. E, 57*, m55 (2001).

1857. H. Miyamae, M. Ito, and H. Iwasaki, *Acta Crystallogr., Sect. B, 35*, 1480 (1979).

1858. V. Francetic and I. Leban, *Vestn. Slov. Kem. Drus., 26*, 113 (1979).

1859. G. Reck and R. Becker, *Acta Crystallogr., Sect. E, 59*, m234 (2003).

1860. I. Baba, L.H. Lee, Y. Farina, A.H. Othman, A.R. Ibrahim, A. Usman, H.K. Fun, and S.W. Ng, *Acta Crystallogr., Sect. E, 58*, m744 (2002).

1861. F.A. Almeida Paz, M.C. Neves, T. Trindade, and J. Klinowski, *Acta Crystallogr., Sect. E, 59*, m1067 (2003).

1862. W.G. Zhang, Y. Zhong, M.Y. Tan, N. Tang, and K.B. Yu, *Molecules, 8*, 411 (2003).
1863. F. Jian, Z. Wang, Z. Bai, X. You, H.-K. Fun, and K. Chinnakali, *J. Chem. Crystallogr., 29*, 227 (1999).
1864. M.J. Cox and E.R.T. Tiekink, *Z. Kristallogr., 214*, 670 (1999).
1865. F.-F. Jian, Z.-X. Wang, H.-K. Fun, Z.-P. Bai, and X.-Z. You, *Acta Crystallogr., Sect. C, 55*, 174 (1999).
1866. L.A. Glinskaya, S.M. Zemskova, and R.F. Klevtsova, *Zh. Strukt. Khim., 40*, 1206 (1999).
1867. M.J. Cox and E.R.T. Tiekink, *Z. Kristallogr., 214*, 571 (1999).
1868. M.J. Cox and E.R.T. Tiekink, *Z. Kristallogr., 212*, 542 (1997).
1869. C. Chieh and S.K. Cheung, *Can. J. Chem., Rev. Can. Chim., 59*, 2746 (1981).
1870. A. Benedetti, A.C. Fabretti, and C. Preti, *J. Crystallogr. Spectrosc. Res., 18*, 685 (1988).
1871. C.S. Mendoza, S. Kamata, and M. Kawaminami, *Anal. Sci., 13*, 517 (1997).
1872. M.J. Cox and E.R.T. Tiekink, *Rev. Inorg. Chem., 17*, 1 (1997).
1873. H.P. Klug, *Acta Crystallogr., 21*, 536 (1966).
1874. M. Bonamico, G. Mazzone, A. Vaciago, and L. Zambonelli, *Acta Crystallogr., 19*, 898 (1965).
1875. V.M. Agre and E.A. Shugam, *Kristallografiya, 17*, 256 (1972).
1876. L.A. Glinskaya, S.M. Zemskova, and R.F. Klevtsova, *J. Struct. Chem., 40*, 979 (2000).
1877. M. Ito and H. Iwasaki, *Acta Crystallogr., Sect. B, 35*, 2720 (1979).
1878. C.S. Lai and E.R.T. Tiekink, *Appl. Organomet. Chem., 17*, 143 (2003).
1879. M.J. Cox and E.R. Tiekink, *Main Group Met. Chem., 23*, 793 (2000).
1880. H. Iwasaki, M. Ito, and K. Kobayashi, *Chem. Lett.*, 1399 (1978).
1881. G. Bauer, G. St Nikolov, and N. Trendafilova, *J. Mol. Struct., 415*, 123 (1997).
1882. E.S. Fomin and L.N. Mazalov, *J. Struct. Chem., 41*, 934 (2000).
1883. N. Trendafilova and R. Kellner, *Spectroc. Acta Pt. A, Molec. Biomolec. Spectr., 47*, 1559 (1991).
1884. A. Manohar, K. Ramalingham, G. Bocelli, and A. Cantoni, *Pol. J. Chem., 75*, 147 (2001).
1885. S. Thirumaran, K. Ramalingam, G. Bocelli, and A. Cantoni, *Main Group Met. Chem., 22*, 423 (1999).
1886. A.M. Bond, R. Colton, M.L. Dillon, A.F. Hollenkamp and J.E. Moir, *Inorg. Chem., 24*, 1591 (1985).
1887. O.F.Z. Khan and P. O'Brien, *Polyhedron, 10*, 325 (1991).
1888. P.G. Mennit, M.P. Shatlock, V.J. Bartuska, and G.E. Maciel, *J. Phys. Chem., 85*, 2087 (1981).
1889. D. Oktavec, J. Lehotay, and V. Vrabel, *Chem. Papers, 55*, 233 (2001).
1890. A.M. Bond and A.F. Hollenkamp, *Inorg. Chem., 29*, 284 (1990).
1891. A.M. Bond, R. Colton, A.F. Hollenkamp, B.F. Hoskins, K. McGregor, and E.R.T. Tiekink, *Inorg. Chem., 30*, 192 (1991).
1892. P.R. Devi, P.V.V.P. Rao, K. Seshaiah, and G.R.K. Naidu, *J. Radioanal. Nucl. Chem. Lett., 105*, 309 (1986).
1893. T. Munivelu and G.R.K. Naidu, *Ind. J. Chem. Sect A-Inorg. Phys. Theor. Anal. Chem., 24*, 1050 (1985).
1894. A. Wyttenbach, *J. Inorg. Nucl. Chem., 43*, 1937 (1981).
1895. I.A. Mustafa, O.M. Al-Ramadany, and T.A.K. Al-Allaf, *Asian J. Chem., 13*, 745 (2001).
1896. K.A. Fraser and M.M. Harding, *Acta Crystallogr., 22*, 75 (1967).
1897. A.V. Ivanov, V.I. Mitrofanova, M. Kritikos, and O.N. Antzutkin, *Polyhedron, 18*, 2069 (1999).

1898. M.A. Malik, M. Motevalli, and P.O'Brien, *Polyhedron, 18*, 1259 (1999).

1899. A.V. Ivanov, M. Kritikos, A. Lund, O.N. Antsutkin, and T.A. Rodnina, *Zh. Neorg. Khim., 43*, 1482 (1998).

1900. A.V. Ivanov, M. Kritikos, O.N. Antsutkin, A. Lund, and V.I. Mitrofanova *Koord. Khim., 24*, 689 (1998).

1901. A.V. Ivanov, V. Forschling, O.N. Antsutkin, M. Kritikos, T.A. Rodnina, and I.A. Lutsenko, *Dokl. Akad. Nauk SSSR, 366*, 643 (1999).

1902. A.V. Ivanov, M. Kritikos, O.N. Antzutkin, V. Forshling, A. Lund, and I.A. Lutsenko, *Koord. Khim., 25*, 583 (1999).

1903. M.A. Malik, M. Motevalli, P. O'Brien, and J.R. Walsh, *Inorg. Chem., 36*, 1263 (1997).

1904. A.V. Ivanov, M. Kritikos, O.N. Antzutkin, and A. Lund, *Zh. Neorg. Khim., 44*, 1689 (1999).

1905. A.V. Ivanov and O.N. Antzutkin, *Polyhedron, 21*, 2727 (2002).

1906. A. Manohar, V. Venkatachalam, K. Ramalingam, S. Thirumaran, G. Bocelli, and A. Cantoni, *Main Group Met. Chem., 28*, 861 (1998).

1907. N.A. Bell, E. Johnson, L.A. March, S.D. Marsden, I.W. Nowell, and Y. Walker, *Inorg. Chim. Acta, 156*, 205 (1989).

1908. S.M. Zemskova, L.A. Glinskaya, R.F. Klevtsova, V.B. Durasov, S.A. Gromilov, and S.V. Larionov, *Zh. Strukt. Khim., 37*, 1114 (1996).

1909. S.M. Zemskova, L.A. Glinskaya, V.B. Durasov, R.F. Klevtsova, and S.V. Larionov, *Zh. Strukt. Khim., 34*, 157–5 (1993).

1910. S.V. Larionov, R.F. Klevtsova, V.G. Shchukin, L.A. Glinskaya, and S.M. Zemskova, *Koord. Khim., 25*, 743 (1999).

1911. X.-F. Chen, S.-H. Liu, X.-H. Zhu, J.J. Vittal, G.-K. Tan, and X.-Z. You, *Acta Crystallogr., Sect. C, 56*, 42 (2000).

1912. A. Manohar, K. Ramalingham, G. Bocelli, and L. Righi, *Inorg. Chim. Acta, 314*, 177 (2001).

1913. R.F. Klevtsova, L.A. Glinskaya, E.I. Berus, and S.V. Larionov, *J. Struct. Chem., 42*, 639 (2001).

1914. Q. Jie and E.R.T. Tiekink, *Main Group Met. Chem., 25*, 317 (2002).

1915. C.S. Lai and E.R.T. Tiekink, *Appl. Organomet. Chem., 17*, 253 (2003).

1916. C.S. Lai and E.R.T. Tiekink, *Appl. Organomet. Chem., 17*, 251 (2003).

1917. S.H. Liu, X.F. Chen, X.H. Zhu, C.Y. Duan, and X.Z. You, *J. Coord. Chem., 53*, 223 (2001).

1918. R.F. Klevtsova, L.A. Glinskaya, S.M. Zemskova, and S.V. Larionov, *Polyhedron, 18*, 3559 (1999).

1919. C.S. Lai and E.R.T. Tiekink, *Appl. Organomet. Chem., 17*, 255 (2003).

1920. S.M. Zemskova, L.A. Glinskaya, R.F. Klevtsova, and S.V. Larionov, *Zh. Neorg. Khim., 38*, 466 (1993).

1921. L.A. Glinskaya, S.M. Zemskova, R.F. Klevtsova, and S.V. Larionov, *Zh. Strukt. Khim., 37*, 176 (1996).

1922. D. Chen and L. Powers, *J. Inorg. Biochem., 58*, 245 (1995).

1923. C.S. Lai and E.R.T. Tiekink, *Appl. Organomet. Chem., 17*, 197 (2003).

1924. C. Airoldi, S.F. De Oliveira, S.G. Ruggiero, and J.R. Lechat, *Inorg. Chim. Acta, 174*, 103 (1990).

1925. S.M. Zemskova, G. Prashad, L.A. Glinskaya, R.F. Klevtsova, V.B. Durasov, S.V. Tkachev, S.A. Gromilov, and S.V. Larionov, *Zh. Neorg. Khim., 43*, 1644 (1998).

1926. L.A. Glinskaya, R.F. Klevtsova, and S.M. Zemskova, *Zh. Strukt. Khim., 33*, 91 (1992).

1927. A.V. Ivanchenko, S.A. Gromilov, S.M. Zemskova, and I.A. Baidina, *Zh. Strukt. Khim., 41*, 106 (2000).

1928. A.V. Ivanchenko, S.A. Gromilov, S.M. Zemskova, I.A. Baidina, and L.A. Glinskaya, *Zh. Strukt. Khim., 39*, 682 (1998).

1929. C.S. Lai and E.R.T. Tiekink, *Appl. Organomet. Chem., 17*, 139 (2003).

1930. T. Guo, C.S. Lai, X.J. Tan, C.S. Teo, and E. R. T. Tiekink, *Acta Crystallogr., Sect. E, 58*, m439 (2002).

1931. J. Chai, C.S. Lai, J. Yan, and E.R.T. Tiekink, *Appl. Organomet. Chem., 17*, 249 (2003).

1932. D. Zeng, M.J. Hampden-Smith, T.M. Alam, and A.L. Rheingold, *Polyhedron, 13*, 2715 (1994).

1933. D. Zeng, M.J. Hampden-Smith, and E.M. Larson, *Acta Crystallogr., Sect. C, 50*, 1000 (1994).

1934. C. M. Dee and E. R. T. Tiekink, *Acta Crystallogr., Sect. E, 58*, m136 (2002).

1935. A.V. Ivanov, P.M. Solozhenkin, and V.I. Mitrofanova, *Zh. Neorg. Khimii, 42*, 256 (1997).

1936. R.F. Klevtsova, L.A. Glinskaya, S.M. Zemskova, and S.V. Larionov, *Zh. Strukt. Khim., 40*, 77 (1999). *J. Struct. Chem., 40*, 64 (1999).

1937. S.M. Zemskova, L.A. Glinskaya, R.F. Klevtsova, S.A. Gromilov, V.B. Durasov, V.A. Nadolinnyii, and S.V. Larinov, *Zh. Strukt. Khim., 36*, 528 (1995).

1938. L.A. Glinskaya, R.F. Klevtsova, E.I. Berus, S.M. Zemskova, and S.V. Larionov, *Zh. Strukt. Khim., 39*, 688 (1998).

1939. R.F. Klevtsova, L.A. Glinskaya, S.M. Zemskova, and S.V. Larionov, *Zh. Strukt. Khim., 40*, 70 (1999). *J. Struct. Chem., 40*, 58 (1999).

1940. A.M. Bond, R. Colton, D. Dakternieks, M.L. Dillon, J. Hauenstein, and J.E. Moir, *Aust. J. Chem., 34*, 1393 (1981).

1941. C.C. Ashworth, N.A. Bailey, M. Johnson, J.A. McCleverty, N. Morrison, and B. Tabbiner, *J. Chem. Soc., Chem. Commun.*, 743 (1976).

1942. J.A. McCleverty, N. Spencer, N.A. Bailey, and S.L. Shackleton, *J. Chem. Soc., Dalton Trans.*, 1939 (1980).

1943. L.R. Gahan and M.J. O'Connor, *Inorg. Chim. Acta, 35*, 221 (1978).

1944. R. Baggio A. Frigerio, E.B. Halac D. Vega, and M. Perec, *J. Chem. Soc., Dalton Trans.*, 549 (1992).

1945. R. Baggio, M.T. Garland, and M. Perec, *Acta Crystallogr., Sect. C, 52*, 823 (1996).

1946. I. Leban, L. Golic, R. Kirmse, J. Stach, U. Abram, H.-J. Sieler, W. Dietzsch, H. Vergoossen, K.P. Keijzers, *Inorg. Chim. Acta, 112*, 107 (1986).

1947. W. Dietsch, S. Rauer, R.-M. Olk, R. Kirmse, K. Kohler, L. Golic, and B.Olk, *Inorg. Chim. Acta, 169*, 55 (1990).

1948. H.C. Brinkhoff, J.A. Cras, J.J. Steggerda, and J. Willemse, *Recl. Trav. Chem., 88*, 633 (1969).

1949. S. Thirumaran, K. Ramalingham, G. Bocelli, and A. Cantoni, *Polyhedron, 19*, 1279 (2000).

1950. A.-K. Duhme, S. Pohl, and H. Strasdeit, *Inorg. Chim. Acta, 175*, 5 (1990).

1951. L.A. Glinskaya, S.M. Zemskova, R.F. Klevtsova, S.A. Gromilov, and S.V.Larionov, *Zh. Neorg. Khim., 36*, 902 (1991).

1952. L.A. Glinskaya, S.M. Zemskova, R.F. Klevtsova, S.A. Gromilov, and S.V. Larionov, *Zh. Neorg. Khim., 36*, 902 (1991).

1953. M.T. Kostanski and W. Mendyk, *Polyhedron, 5*, 1143 (1986).

1954. A.M. Bond, A.F. Hollenkamp, R. Colton, and K. McGregor, *Inorg. Chim. Acta, 168*, 233 (1990).

1955. A.M. Bond, R. Colton, A.F. Hollenkamp, and J.E. Moir, *Inorg. Chem., 25*, 1519 (1986).
1956. B.F. Abrahams, D. Dakternieks, B.F. Hoskins, and G. Winter, *Aust. J. Chem., 41*, 757 (1988).
1957. B.F. Abrahams, D. Dakternieks, B.F. Hoskins, and G. Winter, *Inorg. Chim. Acta, 201*, 95 (1992).
1958. R.G. Noltes, *Rec. Trav. Chim., 84*, 126 (1965).
1959. C. Chieh and L.P.C. Leung, *Can. J. Chem., 54*, 3077 (1976).
1960. N. Revaprasadu, M.A. Malik, P. O'Brien, and G. Wakefield, *Chem. Commun.*, 1573 (1999).
1961. P. O'Brien, M.A. Malik, M.B. Hursthouse, and M. Motavelli, *J. Mater. Chem.*, 949 (1992).
1962. M.A. Malik, M. Motevalli, J.R. Walsh, and P. O'Brien, *Organometallics, 11*, 3136 (1992).
1963. D.L. Reger, S.M. Myers, S.S. Mason, A.L. Rheingold, B.S. Haggerty, and P.D. Ellis, *Inorg. Chem., 34*, 4996 (1995).
1964. D.L. Reger, T.D. Wright, and M.D. Smith, *Inorg. Chim. Acta, 334*, 1 (2002).
1965. C. Chieh, *Can. J. Chem., 56*, 564 (1978).
1966. M.M. Kubicki, R. Kergoat, J.-Y. Le Gall, J.E. Guerchais, J. Douglade, and R. Mercier, *Aust. J. Chem., 35*, 1543 (1982).
1967. R. Nomura, and H. Matsuda, *Trends Inorg. Chem., 2*, 79 (1991).
1968. P. O'Brien and S. Haggata, *Adv. Mater. Opt. Electron, 5*, 117 (1995).
1969. D.M. Frigo, O.F.Z. Khan, and P. O'Brien, *J. Cryst. Growth, 96*, 989 (1989).
1970. R.D. Pike, H. Cui, R. Kershaw, K. Dwight, A. Wold, T.N. Blanton, A.A. Wernberg, and H.J. Gysling, *Thin Solid Films, 224*, 221 (1993).
1971. M.A. Bernard, M.-M. Borel, and G. Lagouche, *Bull. Soc. Chim. Fr.*, 7066 (1969).
1972. R. Nomura, T. Murai, T. Toyosaki, and H. Matsuda, *Thin Solid Films, 271*, 4 (1995).
1973. N.I. Fainer, Y.M. Rumyantsev, E.G. Salman, M.L. Kosinova, G.S. Yurjev, N.P. Sysoeva, E.A. Maximovskii, S.V. Sysoev, and A.N. Golubenko, *Thin Solid Films, 286*, 122 (1996).
1974. E.Y.M. Lee, N.H. Tran, J.J. Russell, and R.N. Lamb, *J. Phys. Chem. B, 107*, 5208 (2003).
1975. N.H. Tran and R.N. Lamb, *J. Phys. Chem. B, 106*, 352 (2002).
1976. N.H. Tran, A.J. Hartmann, and R.N. Lamb, *J. Phys. Chem. B, 104*, 1150 (2000).
1977. B.L. Druz, Y.N. Evtukhov, V.A. Sazonov, and V.Z. Shemet, *Zh. Fiz. Khim., 64*, 1078 (1990).
1978. L. Druz, Yu.N. Evtukhov, and M.Ya. Rakhlin, *Metallorg. Khim., 1*, 645 (1988).
1979. L. Druz, Yu.N. Evtukhov, V.A. Sazonov, and V.Sh. Shemet, *Russ. J. Phys. Chem., 64*, 572 (1990).
1980. P. O'Brien, J.R. Walsh, I.M. Watson, L. Hart, and S.R.P. Silva, *J. Cryst. Growth, 167*, 133 (1996).
1981. R. Nomura, K. Konishi, S. Futenma, and H. Matsuda, *Appl. Organomet. Chem., 4*, 607 (1990).
1982. I. Abrahams, M.A. Malik, M. Motevalli, and P. O'Brien, *J. Organomet. Chem., 465*, 73 (1994).
1983. M.A. Malik and P. O'Brien, *Adv. Mater. Opt. Electron, 3*, 171 (1994).
1984. M.A. Malik, M. Motevalli, T. Saeed, and P. O'Brien, *Adv. Mater., 5*, 653 (1993).
1985. M. Green and P.O'Brien, *Chem. Commun.*, 2235 (1999).
1986. T. Trindade, P. O'Brien, and N.L. Pickett, *Chem. Mater., 13*, 3843 (2001).
1987. N.L. Pickett and P. O'Brien, *Chem. Record, 1*, 467 (2001).
1988. T. Trindade and P. O'Brien, *J. Mater. Chem., 6*, 343 (1996).
1989. T. Trindade, P. O,Brien, and X.M. Zhang, *Chem. Mater., 9*, 523 (1997).
1990. N. Revaprasadu, M.A. Malik, P. O'Brien, and G. Wakefield, *J. Mater. Res., 14*, 3237 (1999).

1991. B. Ludolph, M.A. Malik, P. O'Brien, and N. Revaprasadu, *Chem. Commun.*, 1849 (1998).

1992. M.A. Malik, N. Revaprasadu, and P. O'Brien, *Chem. Mater., 13*, 913 (2001).

1993. N. Revaprasadu, M.A. Malik, P. O'Brien, M.M. Zulu, and G. Wakefield, *J. Mater. Chem., 8*, 1885 (1998).

1994. M. Lazell and P.O'Brien, *Chem. Commun.*, 2041 (1999).

1995. O.C. Monteiro, A.C.C. Esteves, and T. Trindade, *Chem. Mater., 14*, 2900 (2002).

1996. M.A. Malik, P. O'Brien, and N. Revaprasadu, *J. Mater. Chem., 11*, 2382 (2001).

1997. N. Revaprasadu, M.A. Malik, and P. O'Brien, *Mater. Res. Soc. Symp. Proc., 536*, 353 (1999).

1998. P. Yan, Y. Xie, Y. Qian, and X. Liu, *Chem. Commun.*, 1293 (1999).

1999. C.J. Barrelet, Y. Wu, D.C. Bell, and C.M. Lieber, *J. Am. Chem. Soc., 125*, 11498 (2003).

2000. L.V. Zavyalova, A.K. Savin, and G.S. Svechnikov, *Displays, 18*, 73 (1997).

2001. P.J. Nieuwenhuizen, J. Reedijk, M. van Duin, and W. McGill, *Rubber Chem. Technol., Rubber Rev., 70*, 368 (1997).

2002. P. Versloot, J.G. Haasnoot, J. Reedijk, M. Van Duin, and J. Put, *Rubber Chem. Technol., 67*, 263 (1994).

2003. P. Versloot, M. van Duin, J.G. Haasnoot, J. Reedijk, and A.L. Spek, *J. Chem. Soc., Chem. Commun.*, 183 (1993).

2004. P.J. Nieuwenhuizen, A.W. Ehlers, J.W. Hofstraat, S.R. Janse, M.W.F. Nielen, J. Reedijk, and E.J. Baerends, *Chem. Eur. J., 4*, 1816 (1998).

2005. P.J. Nieuwenhuizen, A.W. Ehlers, J.G. Haasnoot, S.R. Janse, J. Reedijk, and E.J. Baerends, *J. Am. Chem. Soc., 121*, 163 (1999).

2006. A. Dirksen, P.J. Nieuwenhuizen, M. Hoogenraad, J.G. Haasnoot, and J. Reedijk, *J. Appl. Polym. Sci., 79*, 1074 (2001).

2007. P.J. Nieuwenhuizen, J.M. Van Veen, J.G. Haasnoot, and J. Reedijk, *Rubber Chem. Technol., 72*, 43 (1999).

2008. M. Shumane, M.H.S. Gradwell, and W.J. McGill, *J. Appl. Polym. Sci., 86*, 1516 (2002).

2009. M. Geyser and W.J. McGill, *J. Appl. Polym. Sci., 60*, 449 (1996).

2010. S.C. Debnath and D.K. Basu, *J. Appl. Polym. Sci., 52*, 597 (1994).

2011. F.J. Santos Rodríguez and K. Hummel, *J. Appl. Polym. Sci., 78*, 2206 (2000).

2012. P.J. Nieuwenhuizen, *Appl. Catal. A, 207*, 55 (2001).

2013. M. Bonamico, G. Dessy, V. Fares, and L. Scaramuzza, *J. Chem. Soc. A*, 3191 (1971).

2014. J.P. Fackler Jr., J.A. Fetchin, and D.C. Fries, *J. Am. Chem. Soc., 94*, 7323 (1972).

2015. C.J. Van Leeuwen, A. Espeldoom, and F. Mol, *Aquat. Toxicol., 9*, 129 (1986).

2016. C.J. Van Leeuwen, T. Helder, and W. Seinen, *Aquat. Toxicol., 9*, 147 (1986).

2017. D.O.E. Gebhardt and M.J. Van Logten, *Appl. Pharmacol., 13*, 316 (1968).

2018. I. Helander, and A. Makela, *Contact Dermatitis, 9*, 327 (1983).

2019. C. Zugerman, *Contact Dermatitis, 7*, 337 (1981).

2020. http://pmep.cce.cornell.edu/profiles/extoxnet/pyrethrins-ziram/zineb-ext.html

2021. S. Soloneski, M. González, E. Piaggio, M.A. Reigosa, and M.L. Larramendy, *Mut. Res., 514*, 201 (2002).

2022. S. Soloneski, M.A. Reigosa, and M.L. Larramendy, *Env. Mol. Mutagenesis, 40*, 57 (2002).

2023. G. Renoux, M. Renoux, and J.M. Guillaumin, *Int. J. Immunopharmacol., 10*, 489 (1988).

2024. G.R. Gale, A.B. Smith, and E.M. Walker, *Ann. Clin. Lab. Sci., 11*, 476 (1981).

2025. G.R. Gale, L.M. Atkins, and E.M. Walker, *Ann. Clin. Lab. Sci., 12*, 463 (1982).
2026. L.R. Cantilena, G. Irwin, S. Preskorn, and C.D. Klaassen, *Toxicol. Appl. Pharmacol., 63*, 338 (1982).
2027. S.G. Jones, M.A. Bassinger, M.M. Jones, and S.J. Gibbs, *Res. Commun. Chem. Pathol. Pharmacol., 38*, 271 (1982).
2028. O. Anderson and J.B. Nielsen, *Toxicology, 55*, 1 (1989).
2029. S.G. Jones, P.K. Singh, and M.M. Jones, *Chem. Res. Toxicol., 3*, 248 (1988).
2030. M.M. Jones, P.K. Singh, S.G. Jones, and M.A. Holscher, *Pharamcol. Toxicol., 68*, 115 (1991).
2031. P.K. Singh, C. Xu, M.M. Jones, K. Kostial, and M. Blanusa, *Chem. Res. Toxicol., 7*, 614 (1994).
2032. P.K. Singh, M.M. Jones, K. Kostial, M. Blanusa, and M. Piasek, *Chem. Res. Toxicol., 9*, 313 (1996).
2033. G.R. Gale, L.M. Atkins, E.M. Walker, Jr., A.B. Smith, and M.M. Jones, *Ann. Clin. Lab. Sci., 14*, 137 (1984).
2034. L.A. Shinobu, S.G. Jones, and M.M. Jones, *Acta Pharmacol. Toxicol., 54*, 189 (1984).
2035. M.M. Jones and M.G. Cherian, *Toxicology, 62*, 1 (1990).
2036. M.M. Jones, M.G. Cherian, P.K. Singh, M.A. Basinger, and S.G. Jones, *Toxicol. Appl. Pharmacol., 110*, 241 (1991).
2037. M.K. Deb, S. Chakravarty, and R.K. Mishra, *J. Indian Chem. Soc., 73*, 551 (1996).
2038. A.K. Malik and W. Faubel, *Talanta, 52*, 341 (2000).
2039. A.J. Nitowski, A.A. Nitowski, J.A. Lent, D.W. Bairley, and D Van Valkenburg, *J. Chomatogr. A, 781*, 541 (1997).
2040. V. Michaylova, B. Evtimova, and D. Nonova, *Anal. Chim. Acta, 207*, 373 (1988).
2041. D.K. Singh and N.K. Mishra, *Chromatographia, 31*, 300 (1991).
2042. A.M. Bond and T.P. Majewski, *Anal. Chem., 61*, 1494 (1989).
2043. E. Piskin, K. Kesenci, N. Satiroglu, and O. Genc, *J. Appl. Poly. Sci., 59*, 109 (1996).
2044. A. Denizli, K. Kesenci, Y. Arica, and E. Piskin, *React. Funct. Polym., 44*, 235 (2000).
2045. J.E. Parkin, *J. Liq. Chromatogr., 15*, 441 (1992).
2046. J.E. Parkin, *J. Chromatagr., 542*, 137 (1991).
2047. V.N. Bauman, I.V. Shkhiyants, A.B. Vipper, and P.I. Sanin, *Chem. Tech. Fuels Oils, 17*, 214 (1981).
2048. L. Contreras, R.F. Laínez, A. Pizzano, L. Sánchez, E. Carmona, A. Monge, and C. Ruiz, *Organometallics, 19*, 261 (2000).
2049. P.F. Gilletti, D.A. Femec, F.I. Keen, and T.M. Brown, *Inorg. Chem., 31*, 4008 (1992).
2050. R.S. Herrick, S.J. Nieter-Burgmayer, and J.L. Templeton, *J. Am. Chem. Soc., 105,* 2599 (1983).
2051. J.C. Jeffery and M.J. Went, *J. Chem. Soc., Chem. Commun.*, 1766 (1987).
2052. J.C. Jeffery and M.J. Went, *J. Chem. Soc., Dalton Trans.*, 567 (1990).
2053. A. Ichimura, Y. Yamamoto, T. Kajino, T. Kitagawa, H. Kuma, and Y. Kushi, *J. Chem. Soc., Chem. Commun.*, 1130 (1988).
2054. G.L. Miessler and L.H. Pignolet, *Inorg. Chem., 18*, 210 (1979).
2055. B.K. Santra and G.K. Lahiri, *J. Chem. Soc., Dalton Trans.*, 1613 (1998).
2056. X. Fan, R. Cao, M. Hong, W. Su, and D. Sun, *J. Chem. Soc., Dalton Trans.*, 2961 (2001).
2057. C.G. Young, X.F. Yan, B.L. Fox, and E.R.T. Tiekink, *J. Chem. Soc., Chem. Commun.*, 2579 (1994).

2058. G.D. Forster and G. Hogarth, *J. Chem. Soc., Dalton Trans.*, 2305 (1997).

2059. P.J. Lim, V.C. Cook, C.J. Doonan, C.G. Young, and E.R.T. Tiekink, *Organometallics, 19*, 5643 (2000).

2060. J.R. Morrow, J.L. Templeton, J.A. Bandy, C. Bannister, and C.K. Prout, *Inorg. Chem., 25*, 1923 (1986).

2061. J.A. McCleverty and A.J. Murray, *Transition Met. Chem., 4*, 273 (1979).

2062. J.L. Davidson, *J. Chem. Soc.,Dalton Trans.*, 2715 (1987).

2063. V.G. Albano, S. Bordoni, L. Busetto, A. Palazzi, P. Sabatino, and V. Zanotti, *J. Organomet. Chem., 659*, 15 (2002).

2064. D.J. Cook, K.J. Harlow, A.F. Hill, T. Welton, A.J.P. White, and D.J. Williams, *New J. Chem., 22*, 311 (1998).

2065. G.J. Irvine, C.E.F. Rickard, W.R. Roper, and L.J. Wright, *J. Organomet. Chem., 387*, C9 (1990).

2066. M.A. Beckett, N.N. Greenwood, J.D. Kennedy, and M. Thornton-Pett, *Polyhedron, 4*, 505 (1985).

2067. M. Kajitani, S. Adachi, I. Takiuchi, N.Nagao, T. Sugiyama, T. Akiyama, and A. Sugimori, *Chem. Lett.*, 731 (1995).

2068. T. Suzuki, A.G. DiPasquale, and J.M. Mayer, *J. Am. Chem. Soc., 125*, 10514 (2003).

2069. L.J. Maheu, Ph.D. Thesis, University of Minnesota, Minneapolis, MN, 1981—as quoted in Ref. 295.

2070. S.J. Nieter-Burgmayer and J.L. Templeton, *Inorg. Chem., 24*, 3939 (1985).

Subject Index

Progress in Inorganic Chemistry, Vol. 53 Edited by Kenneth D. Karlin

Cumulative Index, Volumes 1–53

Progress in Inorganic Chemistry, Vol. 53 Edited by Kenneth D. Karlin